ISSN 0582-4052　CODEN : SEBUAL
2012 年 8 月（増刊号）

生物物理

SEIBUTSU BUTSURI

SUPPLEMENT 1

Vol.52

第 50回年会講演予稿集

2012.9.22（土）～ 24（月）

名古屋大学・東山キャンパス

主催　日本生物物理学会

日本生物物理学会 THE BIOPHYSICAL SOCIETY OF JAPAN http://www.biophys.jp

Nikon

N-SIM

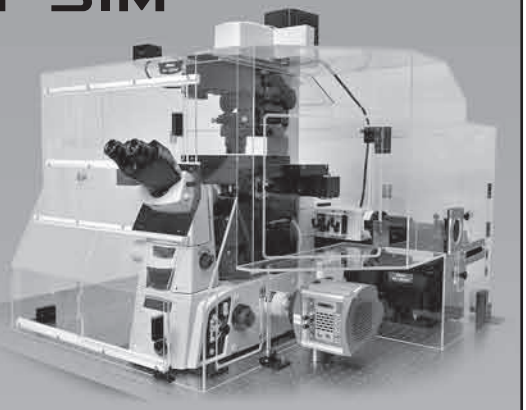

N-STORM

先進をゆく顕微鏡が、
生体/ライブセルイメージングの新時代を切り拓く。

微細な世界を見る技術が、また新たな次元に到達しました。
常に頂点を目指して挑戦し続けるニコンの高度な顕微鏡技術が、
生命科学の明日を揺り動かします。

A1R MP

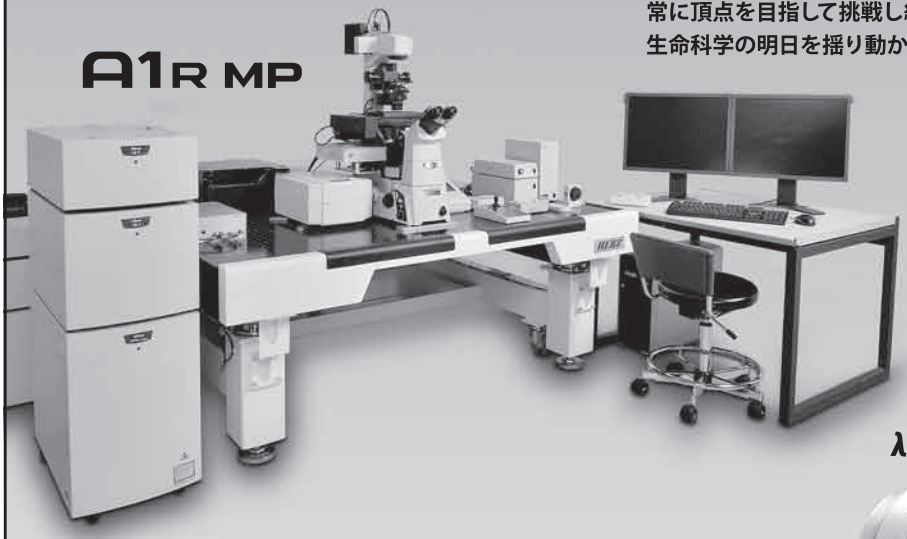

λS対物レンズ

超解像顕微鏡
N-SIM/N-STORM

- ●100nm以下の解像度で、0.6秒/枚*での連続画像取得が可能な「N-SIM」。
- ●従来製品の約10倍（約20nm）の分解能を実現した「N-STORM」。

*2D-SIM/TIRF-SIMモードで最速の場合。

高速多光子共焦点レーザー顕微鏡システム
A1R MP

- ●独自の高速スキャニング技術と高感度受光技術により、600μm以上の 深部からの画像を420枚/秒（512×32画素）で可視化します。

広帯域・高解像対物レンズ
λS対物レンズ

- ●超低屈折率を誇るニコン独自の薄膜技術、ナノクリスタルコートを採用。
- ●広範囲波長での高い透過率と同時に、広い色収差補正を実現しています。

販売元
株式会社ニコン／株式会社ニコン インステック

カタログ・パンフレット等のご請求は、(株)ニコンインステック　バイオサイエンス営業本部へ
100-0006 東京都千代田区有楽町1-12-1(新有楽町ビル4F)　電話(03)3216-9163
■本社カスタマーセンター（フリーダイヤル）0120-586-617　■ニコンインステックホームページ　**www.nikon-instruments.jp/instech/**

＜資料請求番号 S1-1＞

The 50th Annual Meeting of the Biophysical Society of Japan

日本生物物理学会第50回年会（2012年度）
ご案内

会　期： Date :	2012年9月22日（土）ー 24日（月） September 22（Sat）ー 24（Mon）, 2012
会　場： Venue :	名古屋大学 東山キャンパス （名古屋市千種区不老町） Higashiyama Campus, Nagoya University （Furo-cho, Chikusa-ku,Nagoya 464-8601）
年会実行委員長： Chair :	本間 道夫 （名古屋大学大学院 理学研究科） Michio Homma （Nagoya University）

名古屋城

HOMEPAGE

http://www.aeplan.co.jp/bsj2012/

※会期後は日本生物物理学会にデータを移行しますので、学会ホームページよりご覧ください。

編集・発行 ： 日本生物物理学会第50回年会実行委員会

日本生物物理学会第50回年会事務局
〒464-8602 名古屋市千種区不老町
名古屋大学大学院理学研究科 生命理学専攻 本間教授室
E-mail: ambsj50@bunshi4.bio.nagoya-u.ac.jp

日本生物物理学会第50回年会 実行委員会

年会実行委員長　　本間 道夫（名古屋大学大学院 理学研究科）

年会実行副委員長　　岡本 祐幸（名古屋大学大学院 理学研究科）

実行委員

庶務：	太田 元規	（名古屋大学大学院 情報科学研究科）
	秋山 修志	（自然科学研究機構 分子科学研究所）
広告財務：	曽我部 正博	（名古屋大学大学院 医学研究科）
	小嶋 誠司	（名古屋大学大学院 理学研究科）
プログラム：	笹井 理生	（名古屋大学大学院 工学研究科）
	成田 哲博	（名古屋大学大学院 理学研究科）
懇親会：	神山 勉	（名古屋大学大学院 理学研究科）
	須藤 雄気	（名古屋大学大学院 理学研究科）
実行委員：	石浦 正寛	（名古屋大学大学院 理学研究科）
	井上 圭一	（名古屋工業大学大学院 工学研究科 ）
	遠藤 斗志也	（名古屋大学大学院 理学研究科）
	大沼 清	（長岡技術科学大学）
	加藤 晃一	（自然科学研究機構 岡崎統合バイオサイエンスセンター）
	神取 秀樹	（名古屋工業大学大学院 工学研究科 ）
	木村 明洋	（名古屋大学大学院 理学研究科）
	桑島 邦博	（自然科学研究機構 岡崎統合バイオサイエンスセンター）
	佐藤 匡史	（名古屋市立大学大学院 薬学研究科）
	鈴木 直哉	（名古屋大学大学院 理学研究科）
	滝口 金吾	（名古屋大学大学院 理学研究科）
	辰巳 仁史	（名古屋大学大学院 医学研究科）
	千見寺 浄慈	（名古屋大学大学院 工学研究科）
	寺田 智樹	（名古屋大学・工学研究科）
	野口 巧	（名古屋大学大学院 理学研究科）
	廣明 秀一	（名古屋大学大学院 理学研究科）
	古谷 祐詞	（自然科学研究機構 分子科学研究所）
	前田 雄一郎	（名古屋大学大学院 理学研究科）
	槇 亙介	（名古屋大学大学院 理学研究科）
	松浦 能行	（名古屋大学大学院 理学研究科）
	美宅 成樹	（名古屋大学大学院 工学研究科）
	三野 広幸	（名古屋大学大学院 理学研究科）
	村上 緑	（名古屋大学大学院 理学研究科）
	倭 剛久	（名古屋大学大学院 理学研究科）
	横山 泰範	（名古屋大学大学院 工学研究科）

※順不同。敬称略。

The 50th Annual Meeting of the Biophysical Society of Japan

日本生物物理学会第50回年会（2012年度）

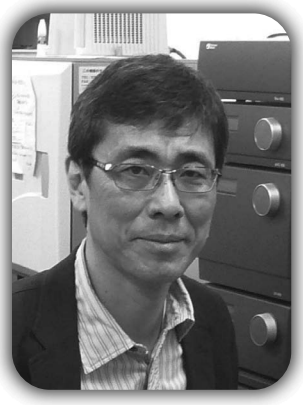

開催にあたって

第50回年会 実行委員長
本間 道夫
（名古屋大学大学院 理学研究科）

半世紀の第50回年会という節目の年会を、日本の生物物理発祥の地であると言える名古屋で、名古屋大学の東山キャンパス内の豊田講堂と大学院理学研究科の講義室などを使って開催させて頂きます。1962年に第一回の年会が行われ、第四回年会を名古屋で、大沢先生が豊田講堂で開催しています。50回年会は、7回目の名古屋での開催となります。前回が40回年会で垣谷先生が、その前の31回年会は、木島先生が、年会実行委員長をやられました。この2回の年会のお手伝いをして、汗を流したことを覚えています。私にとって、名古屋での3回目の年会を実行委員長として、生物物理学会のお手伝いができることを光栄に思っています。そして、半世紀の節目としての生物物理学会年会を名古屋で開催できることは、名古屋地区の生物物理メンバーにとって大きな喜びであります。運営委員のメンバーの力を合わせて、名古屋年会を少しでも良い発表ができ、サイエンスの交流が活発にできるような会にしたいと準備しています。

会場にお金をかけないということで、大学のキャンパスを使いました。そのため会場の制限から、ポスターと口頭発表を選択していただく方式にしました。希望が偏らないかと心配しましたが、予定した数にぴったりとあった数になりました。皆様の協力に感謝いたします。また、発表はすべて英語を原則とさせて頂きました。英語が苦手な自分が実行委員長をやるなら、日本語を原則にと思っていましたが、前回の兵庫年会では、発表がすべて口頭発表で、原則的には英語で行われても、全体的にはうまくいったと感じました。このことを知り合いに話したら、それは学会員のレベルが高いからできるのだというコメントを頂きました。メリットとデメリットはありますが、すべての面において国際化という流れの中では、英語が原則は正しい選択なのかもしれません。生物物理学会の大きさや会員の質に適した年会にするようにと、配慮するべきなのだと思います。

最後に、いろいろ至らない所もあるかと思いますが、年会の3日間を会員の皆様のお力添えで、乗り切りたいと思います。よろしく御願い致します。

会場のご案内

名古屋大学 東山キャンパス　Nagoya University　Higashiyama Campus

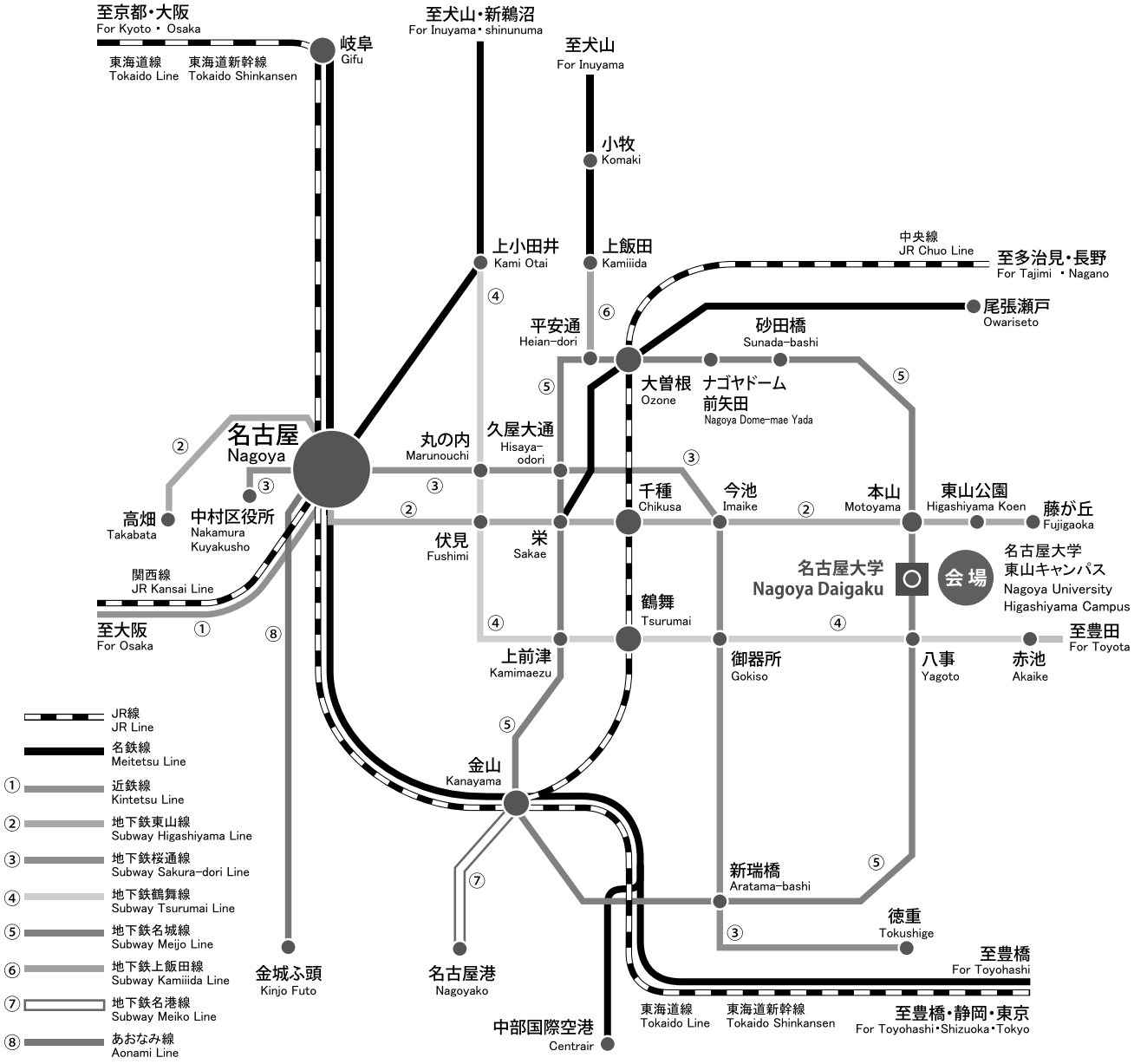

名古屋大学 東山キャンパスへは... 地下鉄 名城線 名古屋大学駅下車

To Nagoya University Higashiyama Campus

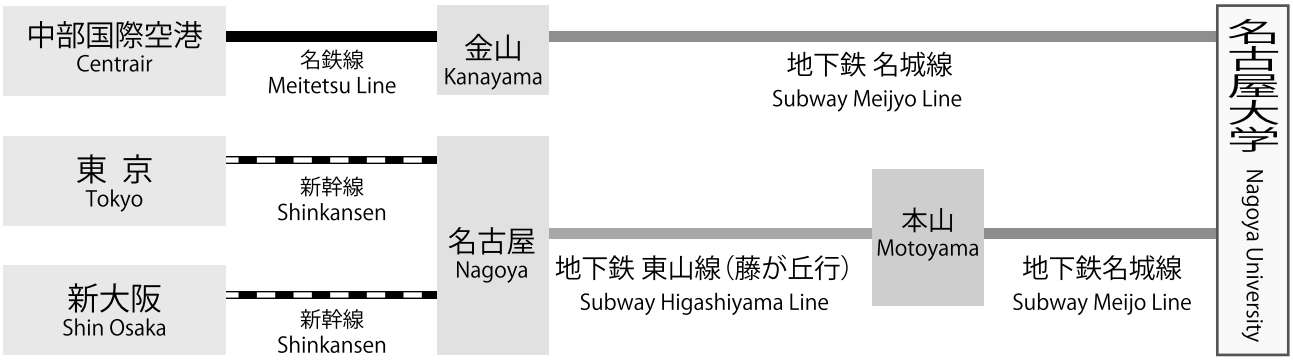

From Nagoya Station: Take the Subway Higashiyama Line to Motoyama Sta. (15 minutes), then transfer to the Subway Meijo Line to Nagoya Daigaku Sta. (Higashiyama Campus is just off the subway exit.).

From Centrair (Central Japan International Airport): Take the Meitetsu Line to Kanayama Sta. (30 min.), then transfer to the Subway Meijyo Line to Nagoya Daigaku Sta. (21 min.).

▌会場案内図

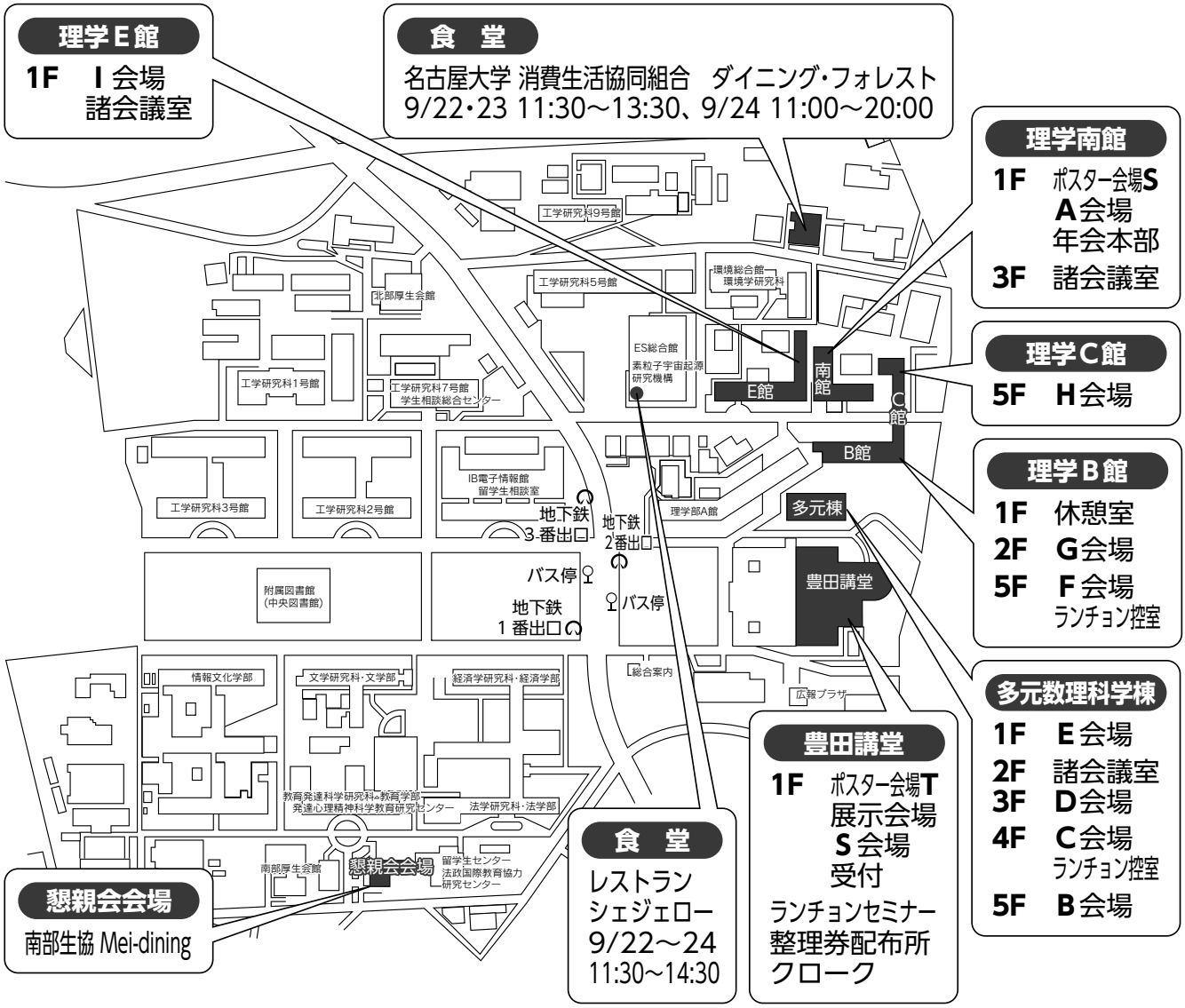

豊田講堂

【1F】ポスター会場T 展示会場 S会場 受付

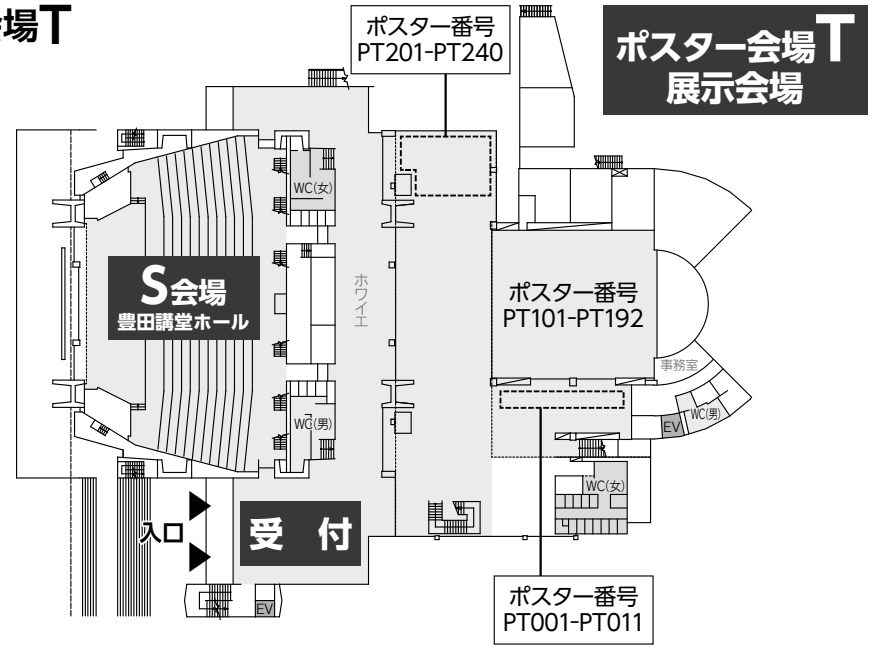

■ 会場案内図

理学南館

【1F】 A会場、年会本部、ポスター会場S

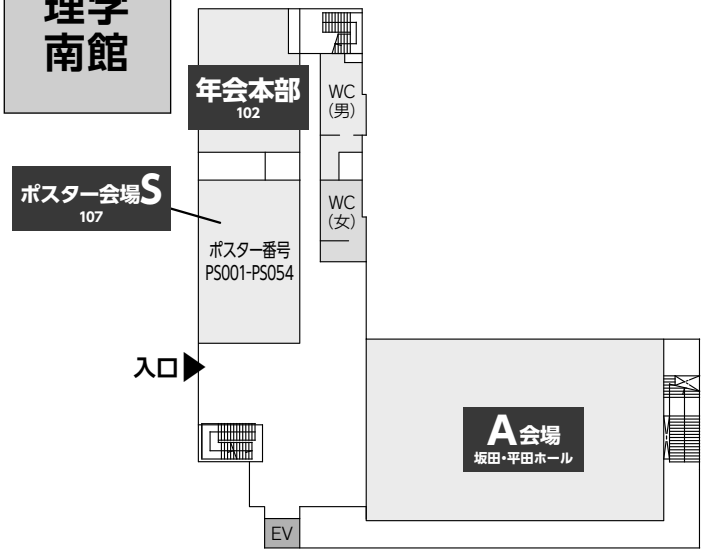

【3F】 諸会議室

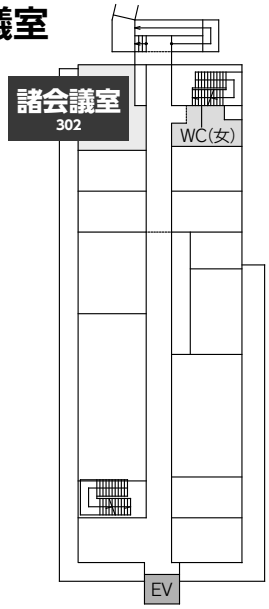

多元数理科学棟

【5F】 B会場

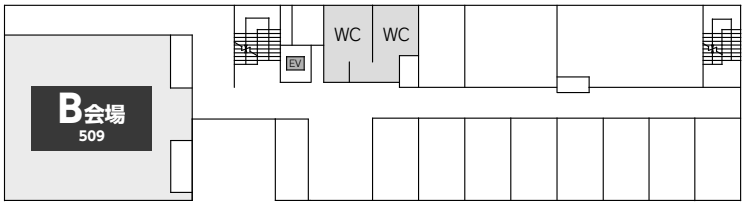

【4F】 C会場、ランチョン控室

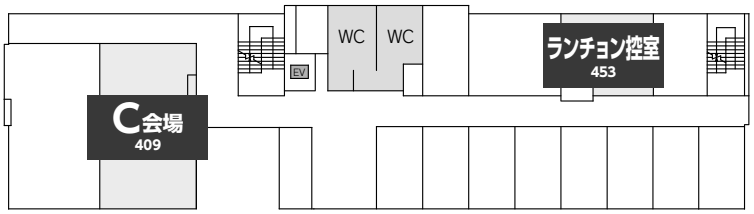

【3F】 D会場

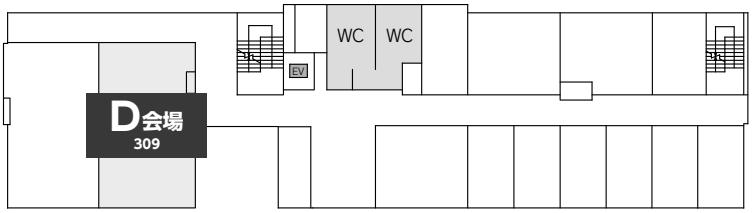

【2F】 諸会議室

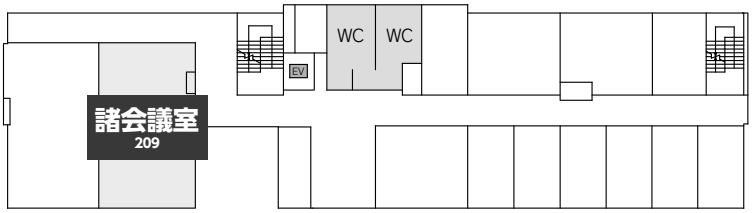

【1F】 E会場

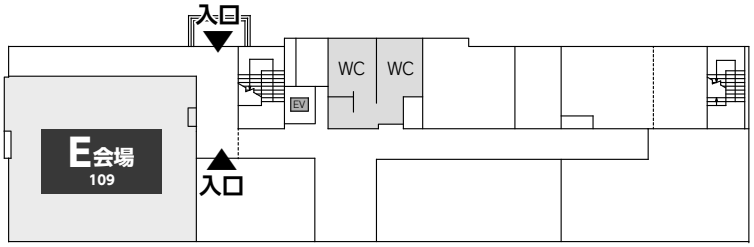

理学B館

【5F】F会場、ランチョン控室

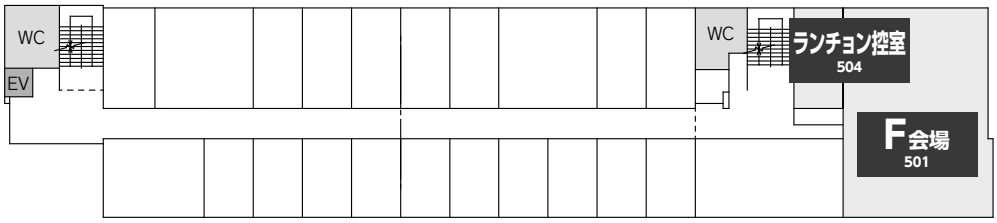

【2F】G会場

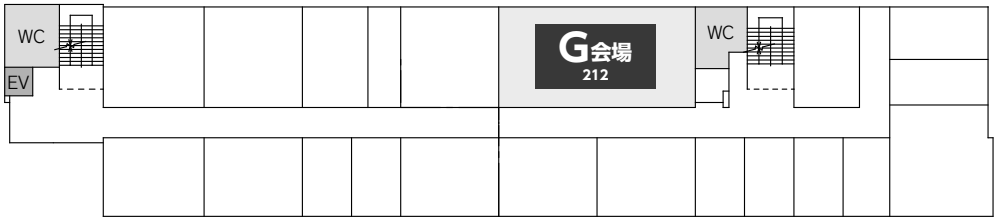

【1F】休憩室

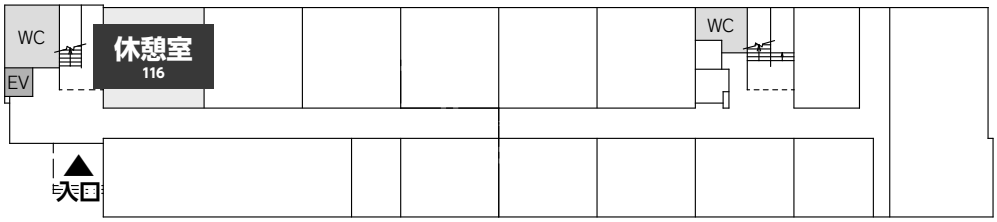

理学C館

【5F】H会場

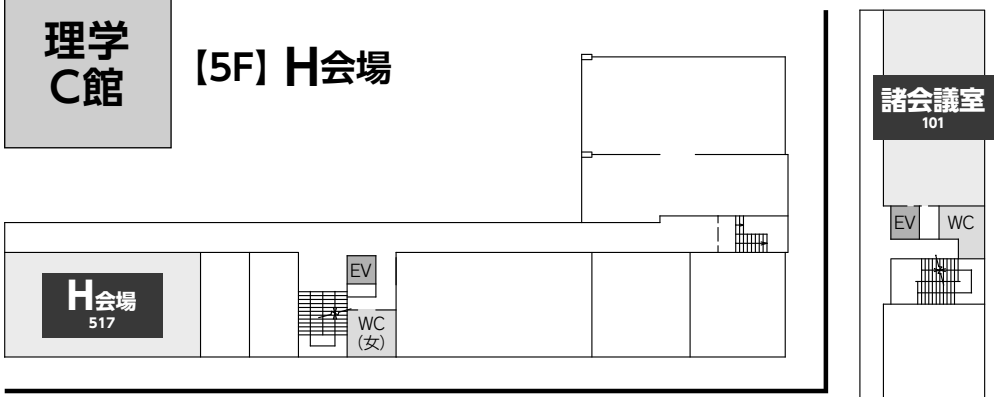

理学E館

【1F】I会場、諸会議室

■ 9月22日(土)　年会1日目　　【Day1】22th Sep.

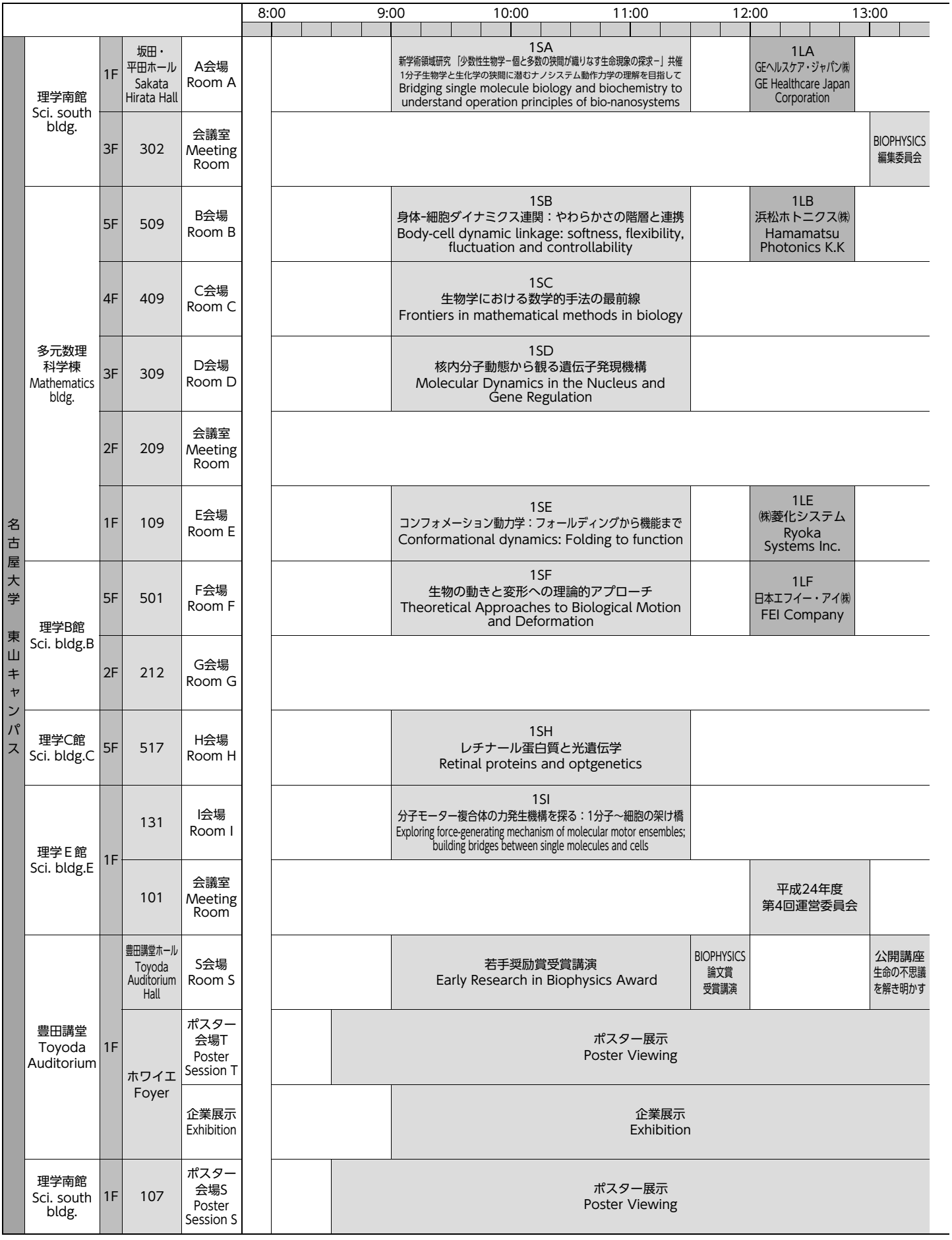

14:00 15:00 16:00 17:00 18:00 19:00 20:00 21:00

	1A 分子モーター I Molecular motors I				
		若手賞選考委員会			
	1B 蛋白質-構造機能相関 I Proteins: Structure & Function I				
	1C 蛋白質-計測、解析、エンジニアリング Proteins: Measurement, Analysis, Engineering				
	1D 発生・分化、神経 Development & Differentiation, Neuroscience				
	1E 蛋白質-物性 I Proteins: Property I	16:10	新旧合同委員会		
	1F 光生物-視覚、光受容 Photobiology: Vision & Photoreception I	16:10			
	1G 細胞生物的課題 I Cell biology I				
	1H バイオイメージング Bioimaging				
	1I 生命情報科学、 バイオエンジニアリング Bioinformatics & Bioengineering				
ポスター展示 Poster Viewing		ポスター発表 Poster Presentation 奇数／Odd number 16:30～17:30	ポスター発表 Poster Presentation 偶数／Even number 17:30～18:30	撤去 Removal	
企業展示 Exhibition					
ポスター展示 Poster Viewing		ポスター発表 Poster Presentation 奇数／Odd number 16:30～17:30	ポスター発表 Poster Presentation 偶数／Even number 17:30～18:30	撤去 Removal	

■ 9月23日(日)　年会2日目　　【Day2】23th Sep.

					8:00	9:00	10:00	11:00	12:00	13:00
名古屋大学　東山キャンパス	理学南館 Sci. south bldg.	1F	坂田・平田ホール Sakata Hirata Hall	A会場 Room A		2SA 海外招聘シンポジウム：生物物理学最前線 Invited symposium from abroad: Forefront of biophysics			分野別専門委員会	総会 Assembly
		3F	302	会議室 Meeting Room					若手の会会議	
	多元数理科学棟 Mathematics bldg.	5F	509	B会場 Room B		2SB 若手オーガナイズシンポジウム：生命科学の新しい地平を切り開く若手研究者たち Symposium organized by younger generation: Young scientists pioneering future life sciences			2LB オリンパス㈱ Olympus Corporation	
		4F	409	C会場 Room C		2SC 非平衡リビングマター：DNAから細胞骨格、細胞へ Living matter far from equilibrium: from DNA to cytoskeletons and cells				
		3F	309	D会場 Room D		2SD スーパーコンピューティング：分子ネットワークと細胞内ダイナミクス Supercomputing in Molecular Network to Cellular Dynamics				
		2F	209	会議室 Meeting Room			男女共同参画委員会			
		1F	109	E会場 Room E		2SE 新学術領域研究「運動超分子マシナリーが織りなす調和と多様性」共催 運動超分子マシナリーが織りなす調和と多様性 Harmonized supramolecular machinery for motility and its diversity			男女共同参画・若手問題シンポジウム Promoting Gernder Equality	
	理学B館 Sci. bldg.B	5F	501	F会場 Room F		2SF 生命システムのばらつきと情報処理 Inherent variability and information coding in biological systems			2LF Protein Data Bank Japan	
		2F	212	G会場 Room G		2SG 染色体場のダイナミクス Dynamics of chromatin as the physicochemical field for genetic activities				
	理学C館 Sci. bldg.C	5F	517	H会場 Room H		2SH 先端顕微計測が照らす生命の輝き Star of life shined by frontier microscopies			2LH スペクトリス㈱ マルバーン事業部 Malvern Japan Division of Spectris Co., Ltd.	
	理学E館 Sci. bldg.E	1F	131	I会場 Room I		2SI 一分子レベルで生体分子機械のエネルギーと機能効率を考える The art of energetic and functional efficiency in biomolecular machines on the single molecule level				
			101	会議室 Meeting Room						
	豊田講堂 Toyoda Auditorium	1F	豊田講堂ホール Toyoda Auditorium Hall	S会場 Room S						
			ホワイエ Foyer	ポスター会場T Poster Session T		ポスター展示 Poster Viewing				
				企業展示 Exhibition		企業展示 Exhibition				
	理学南館 Sci. south bldg.	1F	107	ポスター会場S Poster Session S		ポスター展示 Poster Viewing				

14:00 15:00 16:00 17:00 18:00 19:00 20:00 21:00

2A 分子モーター II: ダイニン Molecular motors II: Dynein	16:10				
2B 蛋白質-構造機能相関 II: 理論、凝集 Proteins: Structure & Function II: Theory, Aggregation					
2C 数理生物学 Mathematical biology					
2D 計測 Measurements	16:10				
2E 蛋白質-物性 II Protein: Property II					
2F 光生物-視覚、光受容 II Photobiology: Vision & Photoreception II	16:10				
2G 生体膜・人工膜 Biological & Artifical membrane					
2H 筋肉 Muscle					
2I 細胞生物学的課題 II: Prokaryotes Cell biology II: Prokaryotes					
ポスター展示 Poster Viewing		ポスター発表 Poster Presentation 奇数／Odd number 16:30～17:30	ポスター発表 Poster Presentation 偶数／Even number 17:30～18:30	撤去 Removal	
企業展示 Exhibition					
ポスター展示 Poster Viewing		ポスター発表 Poster Presentation 奇数／Odd number 16:30～17:30	ポスター発表 Poster Presentation 偶数／Even number 17:30～18:30	撤去 Removal	

懇親会
南部生協
Mei-dining

■ 9月24日(月)　年会3日目　　【Day3】 24th Sep.

					8:00	9:00	10:00	11:00	12:00	13:00
名古屋大学　東山キャンパス	理学南館 Sci. south bldg.	1F	坂田・平田ホール Sakata Hirata Hall	A会場 Room A			3A 分子モーター III: F1-ATPase、マイコプラズマ Molecular motors III: F1-ATPase, Mycoplasma	11:10	3LA ㈱ニコンインステック Nikon Instech Co.,Ltd.	
		3F	302	会議室 Meeting Room						
	多元数理科学棟 Mathematics bldg.	5F	509	B会場 Room B			3B 蛋白質-構造機能相関 III:動態、生体リズム Proteins: Structure & Function III: Dynamics, Circadian rhythm			
		4F	409	C会場 Room C			3C 核酸 Nucleic acids			
		3F	309	D会場 Room D			3D 光生物-光合成 Photobiology: Photosynthesis	11:10		
		2F	209	会議室 Meeting Room						
		1F	109	E会場 Room E			3E 蛋白質-構造 Proteins: Structure		科研費説明会	
	理学B館 Sci. bldg.B	5F	501	F会場 Room F			3F 膜蛋白質 Membrane proteins	11:10		
		2F	212	G会場 Room G			3G 生体膜・人工膜-構造・物性 Biological & Artifical membranes: Structure & Property			
	理学C館 Sci. bldg.C	5F	517	H会場 Room H			3H 細胞生物的課題 III:細胞骨格、細胞運動 Cell biology III:Cytoskeleton & Motility			
	理学E館 Sci. bldg.E	1F	131	I会場 Room I			3I ヘム蛋白質 Heme proteins	11:10		
			101	会議室 Meeting Room					平成24年度 第5回運営委員会	
	豊田講堂 Toyoda Auditorium	1F	豊田講堂ホール Toyoda Auditorium Hall	S会場 Room S						
			ホワイエ Foyer	ポスター会場T Poster Session T		ポスター展示 Poster Viewing				
				企業展示 Exhibition			企業展示 Exhibition			
	理学南館 Sci. south bldg.	1F	107	ポスター会場S Poster Session S		ポスター展示 Poster Viewing				

14:00 15:00 16:00 17:00 18:00 19:00 20:00 21:00

ポスター発表 Poster Presentation 奇数／Odd number 13:15～14:15	ポスター発表 Poster Presentation 偶数／Even number 14:15～15:15	撤去 Removal	
企業展示 Exhibition			
ポスター発表 Poster Presentation 奇数／Odd number 13:15～14:15	ポスター発表 Poster Presentation 偶数／Even number 14:15～15:15	撤去 Removal	

参加者へのご案内

1.　年会受付と参加登録

◇ 年会受付

場　　所:　豊田講堂 1 階 （フロア案内図をご参照ください）
受付時間:　9 月 22 日（土） 8:00-17:00
　　9 月 23 日（日） 8:00-17:00
　　9 月 24 日（月） 8:30-14:00

◆事前登録
事前登録が完了された方は、参加証および領収証が送付されますので、会場での受付は不要です。
当日は必ず参加証をご持参ください。

※ネームホルダーは当日配布しますので、会場内では必ずご着用ください。

注意 1)　事前登録は**年会参加登録費（参加費）**の振込後に完了します。振込がない場合、オンライン登録は無効となります。当日受付で当日参加費をお支払いください。

注意 2)　**日本生物物理学会会員は年度会費を納めていない場合、参加証が送付されません。**
年度会費未納者・新規入会受付デスクにて年度会費をお支払いください。

注意 3)　参加費・年度会費ともに振込済みで、参加証が事前送付されていない場合は、総合受付デスクまでお越しください。

◆当日登録
事前登録に完了していない方は当日登録をしていただきます。
当日受付にお越しの上、参加費を現金でお支払いください。

◇ 当日年会諸費用 （一覧表）

当日参加	会員				非会員		
	正会員	シニア会員	大学院生	学部学生	一般	大学院生	学部学生
当日参加費 Registration	¥8,000	¥5,000	¥5,000	¥0	¥10,000	¥5,000	¥0
懇親会費 Banquet	¥6,000	¥4,000	¥4,000	¥2,000	¥6,000	¥4,000	¥2,000

・ 学部学生の参加費は無料です。当日受付で学生証を提示してください。
参加証と年会予稿集をお渡しします。ただし、懇親会は有料です。

・ 若手招待講演者は、懇親会は招待です。既に懇親会参加費を振り込まれている場合は、総合受付で返却します。

◇ 参加証(名札)

参加証は会場内では必ずご着用ください。参加証のない方のご入場は固くお断りいたします。
事前送付された参加証は必ず会場にご持参ください。(ネームホルダーは会場内で配布します)

◇ 領収書の発行

参加証とともに領収書をお渡しいたしますが、別の形式の領収書が必要な場合、お渡しした領収書と引き換えに発行いたします。

◇ 講演予稿集

年会予稿集は日本生物物理学会会員に事前送付されます。残部がある場合に限り年会受付にて当日販売(3,500 円)を行います。プログラム(タイトル、発表者、所属)は予稿集発行日以後に、年会ホームページにて公開します。また年会終了後は、半年ほど経て、日本生物物理学会ホームページの年会の記録(http://www.biophys.jp/ann/ann02.html)から CiNii(国立情報学研究所の論文情報ナビゲータ)にリンクが張られ、CiNii の生物物理のページ(http://ci.nii.ac.jp/organ/journal/INT1000001547_jp.html)で予稿本文が公開されます。

◇ 年度会費の支払いと入会の手続き

日本生物物理学会の年度会費が未納の場合は、年会受付の年度会費未納者・新規入会受付デスクでお支払いください。また、日本生物物理学会への新規入会も受け付けます。

2. 会場内のサービス・施設

◇ クローク

場　　所:　豊田講堂入口

利用時間:　9 月 22 日(土)、23 日(日)　8:00-18:45
　　9 月 24 日(月)　8:30-15:30

※貴重品や傘、またコンピュータなどについては、破損、紛失などの責任は負いかねますので、各自でお持ちください。

※懇親会へ移動される際は荷物をお引き取りの上、懇親会会場に持参ください。

◇ 昼食

ランチョンセミナーならびに男女共同参画・若手問題シンポジウムでは、お弁当とお茶が無料で提供されます。積極的にご参加ください。また会期中以下の食堂をご利用できます。

◇名古屋大学消費生活協同組合　ダイニング・フォレスト
　　http://www.nucoop.jp/shop/list-sci.html#03
　　9 月 22 日(土)、23 日(日) 11:30-13:30
　　9 月 24 日(月)　　11:00-20:00
◇レストラン　シェジロー
　　http://chezjiroud.jp/
　　9 月 22 日(土)、23 日(日)、24 日(月)11:30-14:30

◇ 呼び出し

会場内での呼び出しは、緊急の場合を除いて一切行いません。参加者間の連絡用として、年会受付に伝言板を設置しますので、ご利用ください。

◇ 駐車場

会場には参加者用駐車場はございません。会場へは公共交通機関をご利用ください。

◇ 宿泊案内

宿泊に関しては年会ホームページ「宿泊について」をご参照ください。

◇ インターネットならびにドリンクコーナーのご案内

・インターネット:豊田講堂において無線LANがご利用になれます。
　　パスワード等については受付にてご確認ください。
・ドリンクコーナー:展示会場(豊田講堂)をご利用ください。

◇ 託児所

年会期間中は、託児所を設置いたします。詳しくは年会ホームページをご覧ください。

3.　年会行事・プログラム

◇ 総会

日本生物物理学会第 51 回定例総会を、年会 2 日目、9 月 23 日(日)12:50-13:50 に A 会場(理学南館 1 階坂田・平田ホール)で開催しますのでご出席ください。詳しくは開催通知をご覧ください。

◇ 若手招待講演

日本生物物理学会若手奨励賞の選考会である講演会を、年会 1 日目　9 月 22 日(土)9:00-11:30 に、S 会場(豊田講堂ホール)で開催します。

◇ BIOPHYSICS 論文賞受賞講演

BIOPHYSICS 論文賞受賞の講演会を、年会 1 日目　9 月 22 日(土)11:30-11:55 に、S 会場(豊田講堂ホール)で開催します。

◇ 懇親会

日時:　2012 年 9 月 23 日(日)19:00 - 21:00
会場:　名古屋大学 南部生協 1F Mei-dining
　　〒464-0814　名古屋市千種区不老町 1
　　Tel:052-734-6100
　　http://www.nucoop.jp/shop/list-south.html#04

懇親会の当日参加も受け付けます(会場前でも受け付けする予定です)。

◇ 男女共同参画・若手問題シンポジウム

日時:　2012 年 9 月 23 日(日)12:00 - 13:00
会場:　E 会場(多元数理科学棟-109)
昼食:　お弁当とお茶が無料で提供されます。

◇ 科研費説明会

日時:　2012 年 9 月 24 日(月)12:00 - 13:00
会場:　E 会場(多元数理科学棟-109)
昼食:　お弁当とお茶が無料で提供されます。

◇ ランチョンセミナー

昼食(お弁当とお茶、無料)をとりながらの協力企業によるセミナーに、ご参加ください。なお、お弁当の数に限りがあるため当日午前中に整理券を配布いたします。セミナー開始前に、会場入り口で整理券と引き換えにお弁当を受け取り、ご入場ください。

◆整理券の発券について

ランチョンセミナー整理券は配付デスクにて配付いたします

時間:会期中毎日　8:00-11:00(当日開催されるセミナー分のみ発券)

場所:豊田講堂 入口

※整理券はランチョンセミナー共催の企業、団体よりご提供頂く昼食の引換券になります。
昼食数はセミナーごとに異なりますので、発券は数が無くなり次第終了となります。

◆整理券の注意事項

<u>整理券は各日12:00を過ぎると無効になります。</u>

午前のプログラム終了後、ランチョンセミナー開始時間までにご来場ください。

上記有効時間までにご来場されない場合、整理券は無効となり、お弁当は整理券をお持ちでないセミナー参加者にご利用いただきますことをご了承ください。

◇ 機器・試薬・書籍等展示会

機器、試薬、ソフトウエア、書籍などの展示会を豊田講堂で行います。

◇ 公開講座

テーマ:　生命の不思議を解き明かす
日時:　9 月 22 日(土)　13:00-14:00
会場:　名古屋大学　豊田講堂ホール

お問い合わせ:　年会事務局までお願いします。
E-mail: ambsj50@bunshi4.bio.nagoya-u.ac.jp

4.　禁止事項

◇ 撮影・録音

会場内でのカメラ、ビデオ、携帯電話などによる撮影や講演音声の録音などを禁止します。

◇ 喫煙・飲食

学内は終日禁煙です。講演会場内での飲食はランチョンセミナー、男女共同参画・若手問題シンポジウム、各種委員会など食事が提供される場合を除いて禁止します。

◇ 携帯電話

シンポジウム、口頭発表、ポスター発表等の講演会場内での携帯電話による通話を禁止します。
講演会場内では電源をオフにするかマナーモードに設定し、呼び出し音が鳴らないようご注意ください。

5.　年会についての問い合わせ

◇ 会期中

年会本部 (Phone number reachable during the meeting)
Tel: 080-1158-8295

◇ 会期外

年会事務局

E-mail:ambsj50@bunshi4.bio.nagoya-u.ac.jp

参加登録・演題登録 システムサポートデスク

〒113-0033 東京都文京区本郷5-29-12-1304
中西印刷株式会社 東京事務所 内
TEL: 03-3816-0738 FAX: 03-3816-0766
E-mail: bsj@nacos.com

年会実行委員会サポート・展示・広告問い合わせ先

〒101-0051 東京都千代田区神田神保町 3-2-8 昭文館ビル 3F
株式会社エー・イー企画 展示会事業部
Tel: 03-3230-2744(代表) Fax: 03-3230-2479
実行委員会サポート関連: jbp2012@aeplan.co.jp
広告関連 E-mail: adinfo@aeplan.co.jp
展示関連 E-mail: e_jbp50@aeplan.co.jp

6. 発表者へのご案内

◇ 使用言語

シンポジウムおよび一般の口頭発表は、原則として、英語をお使いください。

◇ 映写機器

発表に使用できる映写機器は、液晶プロジェクターのみです。音声出力には対応しません。
会場にはコンピュータを用意しませんので、ご自身のノートパソコンを必ずご持参ください。

注意 1) 各自会場係員の指示に従い、コンピュータを会場に備え付けられた切り替え装置
(Video Switcher)に接続してください。

注意 2) 切り替え装置に繋がるコンピュータの映像出力端子は、
「ミニ D-sub15 ピン端子(メス)」*(3 列あるもの)のみです。
端子の形状が異なる場合(Macintosh 等)、変換アダプターをご持参ください。
*読み:みに D さぶ 15 ピンたんしメス

注意 3) 発表に使用するパワーポイントファイルが入った USB メモリーを念のためにお持ちください。

注意 4) バッテリー切れに備え、必ず電源アダプターをご持参ください。

◇ シンポジウム、若手招待講演の座長の方へ

受付: 座長の方はシンポジウム開始 15 分前までに各会場の「座長席」までおいでください。

進行: シンポジウムの進行と時間管理は座長に一任いたしますが、終了予定時間を越えないよう
ご注意ください。

◇ シンポジウム、若手招待講演の講演者の方へ

受付: 講演者の方は、シンポジウム開始の 15 分前までに各会場においでください。
ご持参いただいたノートパソコンを使用してスライドが正しく映写されることを確認ください。
スライド映写の確認は、あらかじめ理学 B 館 116(試写室 兼 休憩室)で行うことも可能です。
※モニターと接続し外部出力の確認のみです。機材オペレーターは常駐しておりません。

講演時間: 時間配分は座長に一任します。
若手招待講演の講演時間は、発表 10 分、討論 3 分、コンピュータの交換に 2 分です。

◇ 口頭発表の座長の方へ

受付: 口頭発表の座長の方は、担当されるセッション開始の 10 分前までに各会場の「座長席」まで
お越しください。会場には時間を計測するスタッフを置いています。

進行: 多くの講演者の発表を滞りなく進めるために、時間厳守をお願いいたします。

◇ 口頭発表の講演者の方へ

講演者は、各自の発表が含まれるセッションが始まる 10 分前までには会場においでください。
口頭発表の講演時間は、発表 9 分、質疑応答 3 分(交代時間含む)です。

発表者は各自コンピュータを持参し、会場に備え付けの液晶プロジェクターにより、図等をスクリーンに映写して発表します。使用ソフトはパワーポイント(米国マイクロソフト社)を標準とします。

画面の解像度は 1024×768 ピクセル(XGA)です。この環境下で発表データを作成ください。
これより大きい画面サイズでデータを作成すると、スクリーン映写時に画面をはみ出す等の不具合が起こる可能性がある旨ご理解ください。

またパソコンを切替機(セレクター)に繋ぎ、発表していただきますので、以下の時間に会場前の接続デスクにお越しください。

◇休憩時間以前(初日、2 日目:15 時以前、3 日目:10 時以前)に発表がある方
セッション開始 15 分前に会場前の接続デスクにお越しください。

◇休憩時間以降(初日、2 日目:15 時 10 分以降、3 日目:10 時 10 分以降)に発表がある方
休憩時間中に会場前の接続デスクにお越しください。

◇ ポスター発表の方へ

ポスターの貼付、展示、説明・討論、撤去:

		9 月 22 日(土)	9 月 23 日(日)	9 月 24 日(月)
展示		8:30-16:30	8:30-16:30	8:30-13:15
説明・討論	奇数番号	16:30-17:30	16:30-17:30	13:15-14:15
	偶数番号	17:30-18:30	17:30-18:30	14:15-15:15
撤去		18:45 までに撤去	18:45 までに撤去	15:30 までに撤去

1. ポスターは日替わりで貼り替えてください。
2. ポスターボードの大きさは、幅 90 cm、高さ 210 cm。貼付に必要な押しピンは会場に用意します。
3. 発表代表者の氏名には左肩に小さな○印を付けてください。
4. 撤去時間を過ぎて残ったポスターは年会事務局にて破棄しますので、ご了承ください。

◇ ポスター発表要項

ポスターは英語で作成してください。ただし、タイトル、所属、発表者名は、可能であれば日本語の併記もお願いいたします。

◇ 発表形式と演題番号(各抄録左上の番号)の見方

発表には、一般口頭発表(Short Talk)、シンポジウム発表(Symposium Talk)、若手招待講演(Early Research in Biophysics Award Candidate Presentations)、ポスター発表(Poster Presentation)があります。

一般口頭発表:(例)演題番号 2D1424
1 文字目は発表日(1: 9 月 22 日、2 :9 月 23 日、3: 9 月 24 日)、続くアルファベットは会場名(A〜I の合計 9 会場)、最後の 4 桁の数字は発表開始時刻を表します。上の例の発表は、9 月 23 日に D 会場で、14 時 24 分に始まる発表です。

シンポジウム発表:(例)1SA03
1 文字目は発表日(1:9 月 22 日、2:9 月 23 日)、次の S はシンポジウム発表であることを表します。
続くアルファベットは会場名、最後の 2 桁の数字は発表順を示します。

若手招待講演:(例)1YS1045
1 文字目は発表日(1:9 月 22 日)、2 文字目は Young (Scientists)、3 文字目は会場名(S)、
最後の 4 桁の数字は講演開始時刻です。

ポスター発表:(例 1)1PT001、(例 2)1PS001
1 文字目は発表日(1:9 月 22 日)、2 文字目は Poster、3 文字目は会場名(T:豊田講堂、S:南館)、
最後の 3 桁の数字はパネル番号を示します。

◇ Language

English

◇ Presentation equipments

Please bring your own laptop and connect it to our projector for your presentation.
We will not provide a sound output.

Attention1) Please connect the computer to a video switcher.

Attention2) The video output connector of presenter's laptop should be "miniD-sub15pin (female)". If the connector is not this type (for example, that of Macintosh computer), please bring an adaptor.

Attention3) Speaker is advised to bring his/her PowerPoint file in a USB memory.

◇ To Symposium Speakers

Please come to the symposium room 15 min before the start of the symposium, and check fitness of the connection between your PC and our projector. You can also check the connection in advance in the Sci. bldg. B 1F 116.

◇ Instructions for Short Talks

1. Speaker is requested to tell his/her arrival to the session room attendant.
2. Speaker will make a 12 min-presentation using his/her own computer.
   All session rooms will be equipped with a data projector and a lavaliere microphone.
3. PowerPoint® (Microsoft) is supposed to be used as a software.
4. Speaker will make a presentation through your computer, which must be connected to a video switcher. Please bring your computer with you to connecting desk in front of the presentation room by following times;

◇Those who are scheduled to make presentations before the break or before 15:00 for Day1 and Day2, before 10:00 for Day3, please bring your computer 15 minutes prior to your presentation.

◇Those who are scheduled to make presentations after the break or after 15:10 for Day1 and Day2, after 10:10 for Day3, please bring your computer during the break time.

◇ To Poster Presenters

		Day 1, Sep. 22	Day 2, Sep. 23	Day 3, Sep. 24
Poster Display		8:30–16:30	8:30–16:30	8:30–13:15
Poster Presentation	odd number	16:30–17:30	16:30–17:30	13:15–14:15
	even number	17:30–18:30	17:30–18:30	14:15–15:15

If you have any questions, please contact us by email (ambsj50@bunshi4.bio.nagoya-u.ac.jp).

◇ Instructions for Poster Presentations

Posters will be mounted at the poster room day by day.

Poster board size is 90 cm in width and 210 cm in height.

◇ Presentation Types and Decoding Presentation Numbers

Presentation types are Short Talk, Symposium Talk, Young Scientists Invited Talk and Poster.

Short Talks: (Ex.) abstract number, 2D1424

The 1st letter stands for the presentation day (1, 2 and 3 for Sat, Sun and Mon), the 2nd letter for the name of session room and the following 4 digits for the starting time of the presentation.

Symposium Talk: (Ex.) 1SQ03

The 1st letter stands for the presentation day (1 and 2 for Sat and Sun), the next 'S' for Symposium Talk, 3rd letter for the name of session room. Last 2 digits represent the order of the talk in each session.

Early Research in Biophysics Award Candidate Presentations: (Ex.) 1YS1045

The 1st letter stands for the presentation day (Sat), the 2nd letter Y for 'Young (Scientists)' and the 'S' for session room S. The last 4 digits stand for the starting time of the talk.

Poster Presentations: (Ex.) 1PT001, 1PS001

The first letter stands for the presentation day (1: August 22nd), the second letter P stands for Poster Presentation and the third letter stands for presentation rooms (T: Toyoda Auditorium, S: Sci. south bldg.). The last 3 digits numbers stand for the panel numbers.

7. 日本生物物理学会第 51 回定例総会開催通知

日時: 2012 年 9 月 23 日(日)12:50～13:50
場所: 名古屋大学東山キャンパス 理学南館 1 階 坂田・平田ホール(A 会場)
日本生物物理学会第51回定例総会を開催いたします。主な議題は下記の通りです。是非ご出席ください。
都合で出席できない方は委任状(葉書、切手貼付、本誌とじこみ)を総会開始前にご送付ください。
また、委任状は年会受付にも用意します。総会開始前に年会受付にご提出ください。

議長 年会実行委員長 本間道夫

総会議題

(1) 報告、承認事項
(会長 難波啓一)
平成 23 年度決算報告ならびに監査結果報告
平成 24 年度会計ならびに事業の中間報告、平成 24 年度の今後の計画
平成 25 年度次期会長および平成 25・26 年度役員選挙結果の報告
平成 25 年度予算案および事業計画

(2) その他

8. 運営委員会、各種委員会の案内

生物物理編集委員会	9 月 21 日(金)15:00～18:00	理学 E 館 1F E101
ホームページ編集委員会	9 月 21 日(金)16:00～18:00	理学南館 3F SS302
平成 24 年度第 4 回運営委員会	9 月 22 日(土)12:00～13:00	理学 E 館 1F E101
BIOPHYSICS 編集委員会	9 月 22 日(土)13:00～14:00	理学南館 3F SS302
若手賞選考委員会	9 月 22 日(土)16:30～17:30	理学南館 3F SS302
新旧合同委員会	9 月 22 日(土)18:00～19:00	多元数理科学棟 1F 109(E 会場)
男女共同参画委員会	9 月 23 日(日)10:30～12:00	多元数理科学棟 2F 209
若手の会会議	9 月 23 日(日)11:45～12:45	理学南館 3F SS302
分野別専門委員会	9 月 23 日(日)12:00～12:45	理学南館 1 階 坂田・平田ホール(A 会場)
平成 24 年度第 5 回運営委員会	9 月 24 日(月)12:00～13:00	理学 E 館 1F E101

謝 辞

本年会の開催・運営に当たり、以下の団体よりご援助いただきました。
関係者一同より御礼申し上げます。

新学術領域研究 「少数性生物学－個と多数の狭間が織りなす生命現象の探求－」
新学術領域研究 「運動超分子マシナリーが織りなす調和と多様性」
名古屋大学大学院 理学研究科

日本生物物理学会第 50 回年会
実行委員長 本間 道夫

「男女共同参画・若手問題シンポジウム」

「博士号を取得して多様なキャリアパスを手に入れる」
Alternative Careers after PhD Course

オーガナイザー：日本生物物理学会　男女共同参画・若手問題検討委員会
Organizers: Committee for Promoting Equal Participation of Men and Women and for Encouraging Young Researchers in the Biophysical Society of Japan

日時： 9 月 23 日（日）12:00～12:50（ランチョンセミナーの時間帯）
場所： E会場 （多元数理科学棟 1 階 109）
昼食： お弁当とお茶が無料で提供されます。ただし、数に限りがあります。
形式：講演会

講演者：当日発表。3名程度を予定

経済の悪化にともない、大学、研究機関および企業における新規雇用が極端に減り、若者が社会で活躍する場が非常に少なくなっています。大学で博士号を取得して研究者としてがんばっていこうと考えていたのに、思うように道を拓くことができないという話も、残念ながらよく聞くようになりました。このことで、若い方々が博士号を取得する道に進まなくなってきています。博士号取得者の減少は、長い目で見ると日本の科学技術力の低下につながり、悪循環に陥ってしまいます。

この状況を打開するために、日本社会における博士号取得者の評価を高めることも重要ですが、大学で博士号を取得したら、次は大学や研究所で研究をするものであるという固定観念を見直す必要もありそうです。博士号を取得した後に企業で活躍されている方はかなりおられます。また、政府や大学も、博士号取得後のキャリアに関する様々な取り組みを行ってきています。

そこで、生物物理学を含む理工系の分野において、博士号取得後にどのようなキャリアの可能性があるのかを、人材派遣会社から講師をお招きして紹介してもらうこととしました。その上で、博士号取得後にさまざまな経歴を歩んでこられた数名の方に、それぞれのご経歴について話していただくことを予定しております。これらのお話を聞きながら、フロアからのご意見や質問を受け、時間が許す限りディスカッションをしていきたいと考えております。特に博士前期および後期課程学生のなまの声が聞こえてくることを期待しています。

老若男女を問わず、ご関心のある方々の参加をお待ちしております。

日本生物物理学会第 50 回年会 公開講座

「生物物理学最前線」
―生命の不思議を解き明かすー

生命の不思議な営みは、生体分子が集まって個性のある働きをすることによって生まれます。そうした生体分子のなかでも、とりわけタンパク質は素晴らしい働きをしており、その仕組みを明らかにすることは、生物物理学の大きな目標のひとつです。この公開講座では、タンパク質の働きを理解するための最前線の研究をわかりやすく紹介します。
タンパク質の働きを理解するための重要なステップは、タンパク質の立体的な形を知ることですが、その新しい方法として、スーパーコンピューターや電子顕微鏡、電子線を用いた方法が注目されています、本公開講座では、この新しい分野で独創的な方法を考案し、世界をリードしてきた 2 人の研究者が講演をします。タンパク質の形を解き明かす技術の見事さとともに、タンパク質の形からわかる生命現象、生理現象の論理の見事さは、私たちを惹きつける魅力にあふれています。

日時: 2012 年(平成 24 年) 9 月 22 日(土) 13:00～14:00
場所: 名古屋大学 東山キャンパス 豊田講堂ホール(S 会場)
地下鉄名城線「名古屋大学」駅 2 番出口 徒歩すぐ
参加費 : 無料(どなたでも自由に参加できます)。
主催:日本生物物理学会第 50 回年会 実行委員会
共催:名古屋大学理学研究科

プログラム

13:00 開会
司会:笹井 理生 教授(名古屋大学 大学院工学研究科)

講演「スーパーコンピューターでタンパク質の形と働きを探る」
岡本 祐幸 教授(名古屋大学 大学院理学研究科)

準備中

講演「膜タンパク質の形と働きを観る」
藤吉 好則 教授(名古屋大学 大学院創薬科学研究科)

我々が見て、考えて、行動する場合に、神経細胞などの脂質膜の内にある膜タンパク質が重要な役割を果たしている。それらの働きを深く理解するために、電子顕微鏡を用いて、立体的な形＝構造を観たいと思う。しかし、強い電子線を照射すると生物試料は一瞬で黒焦げになってしまう。しかも、電子の通り道は高い真空状態に保たなければならない。それゆえ、室温の状態で生物試料を観察しようとすると、水分が飛んで干からびてしまい、電子線による損傷も受けてしまう。これらの問題を解決するために、液体ヘリウムでマイナス 270°C 近くまで冷却した状態で高い分解能の像を撮影できる電子顕微鏡が作られた。この様な装置を用いて、膜タンパク質の立体構造が解析されることで、それらの機能の詳細が理解できるようになった。「膜タンパク質の形と働きを観る」ことによって、ヒトの身体の機能を分子レベルから理解しようとする試みについて紹介したい。

おわりに
美宅 成樹 教授(名古屋大学 大学院工学研究科)

14:00 閉会

若手招待講演　Early Research in Biophysics Award

第 1 日目（9 月 22 日（土））／ Day 1 (Sep. 22, Sat.)

9:00〜11:30　S 会場：豊田講堂ホール／ Room S:

1YS　日本生物物理学会若手奨励賞選考会

Early Research in Biophysics Award Candidate Presentations

オーガナイザー：男女共同参画・若手問題検討委員会

Organizer: The Committee of Promoting Gender Equality and Young Scientists

---

In 2005, the Biophysical Society of Japan has founded Early Research in Biophysics Award to recognize distinguished research work by young members of the BSJ. In this eighth year, we received 41 highly qualified applications. After extremely competitive first round of screening based on written application forms, the following ten applicants were selected as the "young guest speakers." For the second round of the nomination, each young speaker will be asked to make a 10-minute presentation followed by 3-minute Q&A discussion. At the end of these rounds, up to five award winners will be selected. The award winners will be announced at the banquet in the evening of Sunday 23rd September, and the winners will deliver a short talk. We welcome all the BSJ members to attend the oral presentations on Saturday 22nd September at the Early Research in Biophysics Award Candidate Presentations and would like the members to foresee the future of biophysics in Japan through these speakers and their researches.

9:00　岩城　光宏　1PS049

1YS0900　生体分子モーターのストレインセンサー機構の発見とエネルギー変換への寄与の定量化

Discovery of strain-sensor mechanism in motor protein and the quantification for the energy conversion

○岩城　光宏[1,2,3]，藤田　恵介[2]，岩根　敦子[2]，マルクッチ ロレンツォ[2]，柳田　敏雄[1,2]（[1]理研・生命システム，[2]阪大・生命機能，[3]ハーバード・医）

Mitsuhiro Iwaki[1,2,3], Keisuke Fujita[2], Atsuko Iwane[2], Lorenzo Marcucci[2], Toshio Yanagida[1,2] ([1]QBiC, RIKEN, [2]Grad. Sch. Biosci., Osaka Univ., [3]Harvard Med. Sch.)

9:15　岡部　弘基　3PS010

1YS0915　生細胞内における温度分布のイメージング

Imaging of temperature distribution in a living cell

○岡部　弘基[1]，内山　聖一[1]，稲田　のりこ[2]，原田　慶恵[3]，船津　高志[1]（[1]東京大・院薬，[2]奈良先端大・バイオ，[3]京都大・iCeMs）

Kohki Okabe[1], Seiichi Uchiyama[1], Noriko Inada[2], Yoshie Harada[3], Takashi Funatsu[1] ([1]Grad. Sch. Pharm. Sci., Univ. Tokyo, [2]NAIST, [3]iCeMs, Kyoto Univ.)

9:30　加藤　英明　1PT128

1YS0930　光駆動性陽イオンチャネルであるチャネルロドプシンの結晶構造解析

Crystal Structure of a light-gated cation channel, channelrhodopsin

○加藤　英明[1]，Zhang Feng[2]，Yizhar Ofer[2]，Ramakrishnan Charu[2]，西澤　知宏[1]，平田　邦生[3]，伊藤　順平[4]，相田　雄亮[4]，塚崎　智也[1]，林　重彦[5]，Hegemann Peter[6]，Maturana Andres D.[4]，石谷　隆一郎[1]，Deisseroth Karl[2]，濡木　理[1]（[1]東大・院理・生化，[2]スタンフォード大・生命工学，[3]理研・播磨，[4]長岡技大・生命工学，[5]京大・院理・化学，[6]フンボルト大・実験物理・生物）

Hideaki E. Kato[1], Feng Zhang[2], Ofer Yizhar[2], Charu Ramakrishnan[2], Tomohiro Nishizawa[1], Kunio Hirata[3], Jumpei Ito[4], Yusuke Aita[4], Tomoya Tsukazaki[1], Shigehiko Hayashi[5], Peter Hegemann[6], Andres D. Maturana[4], Ryuichiro Ishitani[1], Karl Deisseroth[2], Osamu Nureki[1] ([1]Dept. of Biophys. and Biochem., Grad. Sch. of Sci., Univ. of Tokyo, [2]Dept. of Bioengineering, Stanford Univ., [3]Harima Inst., Riken, [4]Bioengineering Dept., Nagaoka Univ, of Tech., [5]Dept. of Chem., Grad. Sch. of Sci., Kyoto Univ., [6]Inst. of Biol., Experimental Biophys., Humboldt-Univ.)

9:45　島袋　勝弥　2PS020

1YS0945　Ascaris 精子をもちいたアメーバ運動装置の in vitro 再構成

Simultaneous reconstitution of MSP-based protrusion and retraction in the amoeboid sperm of Ascaris

○島袋　勝弥[1,2]，野田　直紀[3]，吉田　賢右[2,4]，Stewart Murray[5]，Roberts Thomas M.[6]（[1]宇部高専，[2]科技機構，[3]MBL，[4]京産大，[5]MRC，[6]フロリダ州立大学）

Katsuya Shimabukuro[1,2], Naoki Noda[3], Masasuke Yoshida[2,4], Murray Stewart[5], Thomas M. Roberts[6] ([1]Ube Nat. Colg. Tech., [2]ICORP, JST, [3]MBL, [4]Kyoto Sangyo Univ., [5]MRC, [6]Florida St. Univ.)

10:00　中村　照也　1PT129

1YS1000　DNA ポリメラーゼηによるホスホジエステル結合形成を観察する

Watching DNA polymerase η make a phosphodiester bond

○中村　照也[1]，Zhao Ye[2,3]，山縣　ゆり子[1]，Hua Yue-jin[3]，Yang Wei[2]（[1]熊本大・院薬，[2]NIDDK，NIH，[3]INAS，Zhejiang Univ.）

Teruya Nakamura[1], Ye Zhao[2,3], Yuriko Yamagata[1], Yue-jin Hua[3], Wei Yang[2] ([1]Grad. Sch. of Pharmaceut. Sci., Kumamoto Univ., [2]NIDDK,

NIH, [3]INAS, Zhejiang Univ.)

10:15　永田　崇　2PT190

1YS1015　クモにおけるピンぼけ像を用いた新規距離知覚メカニズム

A novel depth perception mechanism based on image defocus in a spider

○永田　崇[1]，小柳　光正[2]，塚本　寿夫[2]，佐伯　真二郎[3]，磯野　邦夫[3]，七田　芳則[4]，徳永　史夫[5]，木下　充代[1]，蟻川　謙太郎[1]，寺北　明久[2] ([1]総研大・先導研，[2]大阪市大・院理，[3]東北大・院情報科学，[4] 京都大・院理，[5]大阪大・院理)

Takashi Nagata[1], Mitsumasa Koyanagi[2], Hisao Tsukamoto[2], Shinjiro Saeki[3], Kunio Isono[3], Yoshinori Shichida[4], Fumio Tokunaga[5], Michiyo Kinoshita[1], Kentaro Arikawa[1], Akihisa Terakita[2] ([1]Dept Evol Stud Biol Sys, Sokendai-Hayama, [2]Grad. Sch. Sci., Osaka City Univ., [3]Grad. Sch. Information Sci., Tohoku Univ., [4]Grad. Sch. Sci., Kyoto Univ., [5]Grad. Sch. Sci., Osaka Univ.)

10:30　服部　素之　1PT103

1YS1030　P2X 受容体の ATP 認識機構およびチャネル活性化機構

Mechanism of ATP binding and channel activation in P2X receptors

○服部　素之[1]，Gouaux Eric[1,2] ([1]オレゴン健康科学大学ボラム研究所，[2]ハワード・ヒューズ医学研究所)

Motoyuki Hattori[1], Eric Gouaux[1,2] ([1]Vollum Institute, Oregon Health & Science University, [2]Howard Hughes Medical Institute)

10:45　濱田　勉　3PT153

1YS1045　脂質膜ヘテロ界面はナノ物質をサイズ依存的に識別する

Size-dependent selective localization of nano-particles on heterogeneous membrane surfaces

○濱田　勉，森田　雅宗，宮川　真紀代，高木　昌宏 (北陸先端科学技術大学院大学マテリアルサイエンス研究科)

Tsutomu Hamada, Masamune Morita, Makiyo Miyakawa, Masahiro Takagi (Japan Adv. Inst. of Sci. and Tech.)

11:00　原田　隆平　1PT201

1YS1100　細胞環境における蛋白質の構造安定性とダイナミクス

Protein stability and dynamics under cellular environments

○原田　隆平[1]，杉田　有治[1,2,3]，Michael Feig[3,4] ([1]理研 計算科学研究機構，[2]理研 基幹研究所，[3]理研 生命システム研究センター，[4]ミシガン州立大)

Ryuhei Harada[1], Yuji Sugita[1,2,3], Michael Feig[3,4] ([1]RIKEN AICS, [2]RIKEN ASI, [3]RIKEN QBiC, [4]Michgan state university)

11:15　渡邉　力也　1PS033

1YS1115　F_oF_1-ATP 合成酵素のプロトン駆動力による回転運動の直接観察

Direct observation of H^+-driven rotation of F_oF_1-ATP synthase

○渡邉　力也，田端　和仁，飯野　亮太，野地　博行 (東京大学大学院工学系研究科応用化学専攻)

Rikiya Watanabe, Kazuhito V. Tabata, Ryota Iino, Hiroyuki Noji (School of Engineering, The University of Tokyo)

（アイウエオ順）

「日本生物物理学会　第 1 回 BIOPHYSICS 論文賞受賞講演」

The 1st Award Seminar for outstanding BIOPHYSICS paper

オーガナイザー：日本生物物理学会 BIOPHYSICS 論文賞選考委員会
Organizers: Award committee for outstanding BIOPHYSICS paper

日時：9月22日（土）11：30ー11：55
場所：S 会場（豊田講堂ホール）
形式：講演会

第 1 回 BIOPHYSICS 論文賞受賞者
古澤　力　Chikara Furusawa
（理化学研究所・生命システム研究センター　Quantitative Biology Center, RIKEN）

自己複製する細胞内ダイナミクスにおける普遍統計則
Universal statistical laws in replicating cellular dynamics

In a cell, an huge number of organized chemical reactions are required to maintain its living state. Although analysis of detailed cellular processes is important for a complete description of cellular behavior, it is also necessary to search for universal laws with regard to the intracellular reactions common to all living systems and then to unravel the logic of life leading to such universal features. In this study, we found two fundamental laws concerning fluctuating cellular dynamics with recursive growth [1]. Firstly, the chemical abundances measured over many cells were found to obey a log-normal distribution. Secondly, the relationship between the average and standard deviation of the abundances was found to be linear. The ubiquity of these laws was explored both theoretically and experimentally. Using an abstract model with a catalytic reaction network, the laws were shown to exist near a critical state with efficient self-reproduction. Additionally, by measuring distributions of fluorescent proteins in bacteria cells, the ubiquity of log-normal distribution of protein abundances was confirmed. Several studies following the above findings, including analysis of the effect of such fluctuating expression dynamics on adaptation [2] and evolution [3], and the self-organizing mechanism of the critical state with a log-normal distribution of chemical abundance [4] will also be presented.

[1] Furusawa et al., Biophysics 1, 25–31 (2005)
[2] Furusawa and Kaneko, PLoS Comp. Biol. 4(1), e3 (2008)
[3] Kaneko and Furusawa, Jour. Theor. Biol. 240(1), 78–86 (2006)
[4] Furusawa and Kaneko, Phys. Rev. Lett. 108, 208103 (2012)

シンポジウム　Symposium

第 1 日目（9/22（土））／ Day1(Sep. 22, Sat.)

9:00~11:30　A 会場：理学南館 1 階 坂田・平田ホール／ Room A: Sci. south bldg. 1F Sakata Hirata Hall
新学術領域研究　「少数性生物学－個と多数の狭間が織りなす生命現象の探求－」共催
1SA　1 分子生物学と生化学の狭間に潜むナノシステム動作力学の理解を目指して
Bridging single molecule biology and biochemistry to understand operation principles of bio-nanosystems

オーガナイザー：石島　秋彦 (東北大), 永井　健治 (阪大)
Organizer: Akihiko Ishijima (Tohoku Univ.), Takeharu Nagai (Osaka Univ.)

Cooperative function/behavior in biological nanosystems consisting of small number of molecular elements is one of the most important aspects in biological phenomena. Although so many studies in terms of biochemistry and single molecule biology, which deal with Avogadro's number of molecules and single molecule, respectively, have been reported, there is almost no report showing elementary process of cooperative function/behavior among small number of molecules in living cells. In the symposium, we will focus on the methodology and biological phenomena to approach this issue and will discuss the prospect of biological nanosystems research.

はじめに
永井 健治 (阪大・産研)
Takeharu Nagai (ISIR, Osaka Univ.)

1SA-01　細胞内反応ネットワークと「少数性」問題～理論と計算によるアプローチ
Cracking Reaction Networks Involving "Minorities" in the Cell: Theoretical and Computational Approaches
冨樫 祐一 (神戸大・院システム)
Yuichi Togashi (Grad. Sch. Sys. Informat., Kobe Univ.)

1SA-02　1 分子デジタル ELISA
Single-Molecule Digital ELISA
野地 博行 (東大工・応用化学)
Hiroyuki Noji (Applied Chem. U-Tokyo)

1SA-03　遺伝子にコードされた発光型プローブ
Genetically encoded luminescent probes
永井 健治 (阪大・産研, JST・さきがけ)
Takeharu Nagai[1,2] ([1]ISIR, Osaka Univ., [2]PRESTO, JST)

1SA-04　**Coordinated reversal of flagellar motors on a single Escherichia coli cell**
石島 秋彦 (東北大学多元物質科学研究所)
Akihiko Ishijima (Tohoku University)

1SA-05　ヒトゲノム DNA の収納とそのダイナミクス
Human genome organization and dynamics
前島 一博 (国立遺伝学研究所構造遺伝学研究センター生体高分子研究室)
Kazuhiro Maeshima (Structural Biology Center, National Institute of Genetics)

1SA-06　哺乳類概日時計のシステム生物学・合成生物学
Systems and Synthetic Biology of Biological Timings
上田 泰己 (理化学研究所　発生・再生科学総合研究センター, 理化学研究所　生命システム研究センター)
Hiroki Ueda[1,2] ([1]RIKEN, CDB, [2]RIKEN, QBiC)

1SA-07　細菌べん毛形成の分子機構とその制御
Molecular mechanism of bacterial flagellar construction and its regulation
今田 勝巳 (阪大・院理・高分子)
Katsumi Imada[1], Tohru Minamino[2] ([1]Dept. Macromol. Sci., Grad. Sch. Sci., Osaka Univ., [2]Grad. Sch. Frontier BioSci., Osaka Univ.)

9:00~11:30　B 会場：多元数理科学棟 5 階 509 ／ Room B: Mathematics bldg. 5F 509

1SB　身体ー細胞ダイナミクス連関：やわらかさの階層と連携
Body-cell dynamic linkage: softness, flexibility, fluctuation and controllability

オーガナイザー：跡見　順子 (東大), 竹森　重 (東京慈恵医大)
Organizer: Yoriko Atomi (Univ. of Tokyo), Shigeru Takemori (Jikei Univ.)

After 3.11, we all need to acts with sense of responsibility and re-think the science. The aim of this symposium is to explore an innovative and sustainable biophysical research area based on the platform of human body and mind flexibility and free will inspired by Fumio-Osawa's finding that biological macro molecules such as F-actin in muscle is more flexible when its in action. Unique ideas to linking with flexibility such as exercise science, protein and DNA structural dynamis, extracellular matrix and also control of soft but unstable body under the gravity will be presented.

身体ー細胞ダイナミクス連関：やわらかさの階層と連携
跡見 順子 (東京大学アイソトープ総合センター)
Yoriko Atomi (Radioisotope Center The University of Tokyo)

1SB-01　DNA の硬さと柔らかさ：高次構造転移が生み出す時空間秩序
Synergy between Stiffness and Softness on DNA: Spatiotemporal Order Organized through the Higher-Order Structural Transition of DNA
武仲 能子 (産総研・ナノシステム)
Yoshiko Takenaka (Nanosystem Research Inst., AIST)

1SB-02　**Proteins as Mechano-Chemical Transducer**
赤坂 一之 (近畿大・先端研・ 高圧センター)
Kazuyuki Akasaka (Inst. Adv. Tech, Kinki UNIV.)

1SB-03　身体ー細胞能動 / 受動メカノケミカル連携：身体に生きる細胞のニッチとしての柔らかな細胞外基質環境が支配するやわらかさの階層と連携
Body-cell dynamic mechano-mechanical linkage: softness, flexibility, fluctuation and controllability derived from ECM environment as "niche for cells in our body"
跡見 順子 (東京大学アイソトープ総合センター)
Yoriko Atomi[1], Miho Shimizu[2], Eri Fujita[2], Tomoaki Atomi[3], Noboru Hirose[3], Katsuya Hasegawa[4] ([1]Radioisotope Center The University of Tokyo, [2]Dept. of Mechano-Informatics, Univ. of Tokyo, [3]Teikyo University of Science, [4]JAXA)

1SB-04　多分節立位を可能にした身体の冗長性：柔らかさの制御と破綻
Flexibility of human body with multi-segmental structure enabling bipedal standing
跡見 友章 (帝京科学大学, 首都大学東京大学院)
Tomoaki Atomi[1,2], Noboru Hirose[1], Miho Shimizu[3], Yoriko Atomi[3] ([1]Teikyo Univ. of Sci., [2]Grad. Sch., Univ. Tokyo Metropolitan, [3]Univ. of Tokyo)

1SB-05　人工制御した細胞基盤の柔らかさと細胞応答
Softness of the artificial cell niche and its active interplay of forces
清水 美穂 (東京大学大学院情報理工・知能機械)
Miho Shimizu[1], Yuki Katsurada[2], Toshiyuki Watanabe[2], Eri Fujita[1], Tomoaki Atomi[3], Noboru Hirose[3], Katsuya Hasegawa[4], Yoriko Atomi[5] ([1]Dept. of Mechano-Informatics, Univ. of Tokyo, [2]Tokyo Univ. of Agri. & Tech., [3]Teikyo University of Science, [4]JAXA, [5]Radioisotope Center The University of Tokyo)

1SB-06　培養基盤の硬さとの整合性が心筋拍動パターンを最適化する
Rigidity Matching between Cells and the Extracellular Matrix Leads to the Stabilization of Cardiac Conduction
Marcel Hoerning (神戸研究所 発生・再生科学総合研究センター フィジカルバイオロジー研究ユニット)
Marcel Hoerning (RIKEN, Center for Developmental Biology, Physical Biology Unit)

1SB-07　アクチン繊維のゆらぎを基盤とした生理機能
Physiological functions of an actin filament based on its fluctuation
本多 元 (長岡技術科学大学・生物系)
Hajime Honda (Dep. Bioeng. Nagaoka Uni. Tech.)

1SB-08　生命の神秘に迫る多次元アプローチ
Multidimensional Approaches to the Secrets of Life
竹森 重 (慈恵医大・分子生理)
Shigeru Takemori (Jikei Univ. Sch. Med.)

9:00~11:30　C 会場：多元数理科学棟 4 階 409 ／ Room C: Mathematics bldg. 4F 409

1SC　生物学における数学的手法の最前線
Frontiers in mathematical methods in biology

オーガナイザー：宇沢　達 (名大), 大平　徹 (名大)
Organizer: Tohru Uzawa (Nagoya Univ.), Toru Ohira (Nagoya Univ.)

In these lectures we explore frontiers of mathematical methods in biology. Phenomenon of varied time/space-scale will be examined, ranging from variations in enzyme concentrations, to bird-flocking.

1SC-01　特異極限解析：生物システムに現れるパターンを捉える
Singular limit analysis: Understanding of biological pattern formation
三村 泰昌 (明治大学大学院先端数理科学研究科)
Yasumasa Mimura (Graduate School of Advanced Mathematical Sciences, Meiji University)

1SC-02　鳥の群れの集団動力学
Collective dynamics of flocking
早川 美徳 (東北大学教育情報基盤センター)
Yoshinori Hayakawa (Center for Information Technology in Education)

1SC-03　バクテリアのコロニー形成―細胞の集団運動―
Colony Formation in Bacteria -Collective Movement of Cells-
松下 貢 (明治大学先端数理科学インスティテュート)
Mitsugu Matsushita (Meiji Institute for Advanced Study of Mathematical Sciences (MIMS), Meiji University)

1SC-04　生命ネットワークにおける動的ロバスト性の数理的解析
Mathematical analysis of dynamical robustness in biological networks
田中 剛平 (東京大学 生産技術研究所, 東京大学 情報理工学系研究科)
Gouhei Tanaka[1,2], Kai Morino[2], Kazuyuki Aihara[1,2] ([1]Institute of Industrial Science, The University of Tokyo, [2]Graduate School of Information Science and Technology, The University of Tokyo)

1SC-05　自律的酵素量制御による時間スケール調整；ホメオスタシスと記憶
Homeostasis and memory by autonomous regulation of time-scales through enzyme abundances
金子 邦彦 (東大総合文化)
Kunihiko Kaneko (University of Tokyo, Center for Complex-Systems Biology)

9:00~11:30　D 会場：多元数理科学棟 3 階 309 ／ Room D: Mathematics bldg. 3F 309

1SD　核内分子動態から観る遺伝子発現機構
Molecular Dynamics in the Nucleus and Gene Regulation

オーガナイザー：河野　秀俊 (日本原子力機構), 寺川　剛 (京大)
Organizer: Hidetoshi Kono (JAEA), Tsuyoshi Terakawa (Kyoto Univ.)

Advances in single molecule measurements and molecular imaging techniques enable us to directly observe molecular dynamics in the nucleus. The recent increase of computational power, which is demonstrated by the K super computer, now allows us to simulate behaviors of single molecules as well as complexes at different spatial and temporal resolutions. In this symposium, we will discuss how such molecular phenomena observed by experiment and simulation are associated with gene regulation.

1SD-01　**Characterization of Protein-DNA complexes dynamics related to Chromatin structure regulation using Single-Molecule Techniques**
韓 龍雲 (京都大学物質―細胞統合システム拠点)
Yong-Woon Han, Yoshie Harada (iCeMS, Kyoto University)

1SD-02　**The mechanism of nuclear protein searching on DNA: Coarse-Grained simulation study**
寺川 剛 (京都大学大学院)
Tsuyoshi Terakawa (Grad. Sch. Sci., Univ. Kyoto)

1SD-03　**Differences in dissociation free-energy profiles between cognite and non-cognite protein-DNA complexes**
米谷 佳晃 (日本原子力研究開発機構)

Yoshiteru Yonetani, Hidetoshi Kono (Japan Atomic Energy Agency)

1SD-04　線虫初期胚における染色体ダイナミクスの定量的解析
Quantitative analyses of chromosome dynamics in C. elegans early embryos
菅原 武志 (国立遺伝学研究所)
Takeshi Sugawara, Ritsuko Arai, Akatsuki Kimura (National Institute of Genetics)

1SD-05　蛍光相関分光法を用いた細胞内グルココルチコイド受容体の動態解析
Inside view of molecular dynamics of Glucocorticoid Receptor by using Fluorescence Cross Correlation Spectroscopy in living cell
金城 政孝 (北大 先端生命)
Masataka Kinjo (Faculty of Advanced Life Science, Hokkaido University)

9:00~11:30　E会場：多元数理科学棟 1 階 109 ／ Room E: Mathematics bldg. 1F 109
1SE　コンフォメーション動力学：フォールディングから機能まで
Conformational dynamics: Folding to function

オーガナイザー：高田　彰二 (京大), 笹井　理生 (名大)
Organizer: Shoji Takada (Kyoto Univ.), Masaki Sasai (Nagoya Univ.)

Proteins, and more generally biomolecules, are intrinsically flexible and change their conformations in multiscales both in time and space. In this symposium, we explore various recent studies on flexible conformational dynamics both in experiments and theories. We discuss recent studies on protein folding, molecular recognition, allosteric conformational change upon some reactions, and conformation-dependent aggregation.

1SE-01　蛋白質構造の整合性原理とその拡張
Consistency principle of protein conformation and its extension
笹井 理生 (名古屋大学, 岡崎統合バイオサイエンスセンター, KIAS)
Masaki Sasai[1,2,3] ([1]Nagoya University, [2]Okazaki Institute for Integrative Bioscience, [3]Korea Institute for Advanced Study)

1SE-02　**Dynamic mechanism for the transcription when responses to activators**
Wei Wang (National Lab. Solid State Microstructure and Dept. Phys., Nanjing Univ.)
Yaolai Wang, Feng Liu, **Wei Wang** (National Lab. Solid State Microstructure and Dept. Phys., Nanjing Univ.)

1SE-03　保存アミノ酸に着目したジンクフィンガーの構造と分子認識
New Functions of Zinc Fingers Revealed by Substitution of Conserved Residues
今西 未来 (京大・化研)
Miki Imanishi (ICR, Kyoto Univ.)

1SE-04　ドメインスワッピングによるシトクロム *c* の多量化
Oligomerization of cytochrome *c* by domain swapping
廣田 俊 (奈良先端科学技術大学院大学物質創成科学研究科)
Shun Hirota (Grad. Sch. Mat. Sci., Nara Inst. Sci. Tech.)

1SE-05　マルチドメインタンパク質のフォールディングとコンフォメーション動力学
Folding and conformational dynamics of multi-domain proteins
高田 彰二 (京大理生物物理)
Shoji Takada (Dept. Biophys, Kyoto Univ.)

9:00~11:30　F会場：理学 B 館 5 階 501 ／ Room F: Sci. bldg. B 5F 501
1SF　生物の動きと変形への理論的アプローチ
Theoretical Approaches to Biological Motion and Deformation

オーガナイザー：石原　秀至 (東大), 澤井　哲 (東大)
Organizer: Shuji Ishihara (Univ. of Tokyo), Satoshi Sawai (Univ. of Tokyo)

Motion and deformation observed in living cells emerge from their intrinsic active nature and interaction with the environment. Are there physical principles that could integrate and unify these rich and intriguing phenomena? One of key physical approaches is the framework of active matters that addresses cooperativity of motions at various length and timescales. The symposium will highlight recent progress in this direction with an emphasis on physical and theoretical approaches.

1SF-01　細胞の変形と運動：理論と実験の挑戦
Deformation and motion of cell: theoretical and experimental challenges
佐野 雅己 (東大院理)
Masaki Sano (Grad. Sch. Sci. U. Tokyo)

1SF-02　マウスの左右決定の過程に見られるノード繊毛の回転運動の同調
Synchronization of rotaional movement in mouse node cilia during left-right determination
高松 敦子 (早大・電気・情報生命)
Atsuko Takamatsu[1], Kyosuke Shinohara[2], Takuji Ishikawa[3], Hiroshi Hamada[2] ([1]Dept. Elec. Eng. and Biosci., Waseda Univ., [2]Grad. Sch. Frontier Biosci., Osaka Univ., [3]Dept. Bioeng. and Robotics, Tohoku Univ.)

1SF-03　鞭毛や繊毛の流体力学相互作用による同期：ミニマルアプローチ
Synchronization of flagella and cilia by hydrodynamic interactions: minimal approach
内田 就也 (東北大・理物理)
Nariya Uchida[1], Ramin Golestanian[2] ([1]Dept. Phys., Tohoku Univ., [2]Cent. Theor. Phys., Univ. of Oxford)

1SF-04　興奮性化学進行波に駆動される遊走細胞の形態ダイナミクスの数理モデル
Modeling morphological dynamics of migrating cells governed by self-organized excitable waves
石原 秀至 (東大・院総合文化)
Shuji Ishihara[1], Daisuke Taniguchi[1], Satoshi Sawai[1,2] ([1]Grad. Sch. Arts & Sciences, Univ. Tokyo, [2]JST PRESTO)

1SF-05　細胞の力学と、人工システムにおける自発運動
Mechanics of gels and spontaneous motion of droplets as biologically-motivated systems
義永 那津人 (東北大 WPI-AIMR)
Natsuhiko Yoshinaga (WPI-AIMR, Tohoku Univ.)

1SF-06　這行による移動運動の理解に向けて
Towards understanding the locomotion of animals by limbless crawling
小林 亮 (広島大学, 科学技術振興機構, CREST)
Ryo Kobayashi[1,4], Toshiya Kazama[1,4], Kentaro Ito[1,4], Yoshimi Tanaka[2], Toshiyuki Nakagaki[3,4] ([1]Hiroshima University, [2]Yokohama National University, [3]Future University Hakodate, [4]JST, CREST)

9:00~11:30　H 会場：理学 C 館 5 階 517 ／ Room H: Sci. bldg. C 5F 517

1SH　レチナール蛋白質と光遺伝学
Retinal proteins and optgenetics

オーガナイザー：神山　勉 (名大), 村上　緑 (名大)
Organizer: Tsutomu Kouyama (Nagoya Univ.), Midori Murakami (Nagoya Univ.)

Optogenetics, a new research field in which retinal proteins are utilized for functional analyses of the nervous systems, has recently attracted lots of attention. New technologies have been explored to express light-gated ion channels (channelrhodopsin) and light-driven ion pumps (halorhodopsin) in a specific region of the nervous system, making it possible to control nerve action potentials by light illumination at various wavelengths, or to regulate the intracellular concentrations of second messengers by light stimuli. In this symposium, current progresses in optogenetics will be reported.

1SH-01　ハロロドプシンの構造と分子機能
Structure and Molecular Function of Halorhodopsin
出村 誠 (北大・院先端生命)
Makoto Demura (Fac. Adv. Life Sci., Hokkaido Univ.)

1SH-02　**Structural basis for light-gated cation conductance by channelrhodopsin**
石谷 隆一郎 (東京大学大学院理学系研究科)
Osamu Nureki, **Ryuichiro Ishitani** (Graduate School of Science, The University of Tokyo)

1SH-03　チャネルロドプシンによる神経細胞ネットワーク素子の制御
Control of neural network devices by channelrhodopsin
宇理須 恒雄 (名古屋大学革新ナノバイオデバイス研究センター, 科学技術振興機構,CREST)
Tsuneo Urisu[1,2] ([1]Nagoya University, FIRST Research Center for Innovative Nanobiodevices, [2]Japan Science and Technology Agency, CREST)

1SH-04　オプトジェネティクスを用いた睡眠覚醒調節に関わる神経回路の動作原理解明
Optogenetics reveals function of neural network involved in the regulation of sleep/wakefulness

山中 章弘 (名古屋大学 環境医学研究所)
Akihiro Yamanaka (Research Institute of Environmental Medicine, Nagoya University)

1SH-05 レチナールタンパク質の進化と機能多様性
Evolution and functional diversity of animal opsin-based pigments
寺北 明久 (大阪市大・理)
Akihisa Terakita (Grad. Sch. Sci., Osaka City Univ.)

1SH-06 イカロドプシンの光活性化機構
Photo-activation mechanism of squid rhodopsin
村上 緑 (名大・院理・物理)
Midori Murakami, Tsutomu Kouyama (Grad. Sch. Sci., Nagoya Univ.)

1SH-07 GPCR の細胞内シグナル伝達を制御する構造特徴
Structural elements which control the signal transduction pathway of GPCRs
諏訪 牧子 (青学大 ・理工, 産総研 生命情報工)
Makiko Suwa[1,2], Minoru Sugihara[2] ([1]Colledge, Sci. Eng. AGU., [2]CBRC, AIST)

9:00~11:30 I会場：理学 E 館 1 階 131 ／ Room I: Sci. bldg. E 1F 131

1SI 分子モーター複合体の力発生機構を探る：1 分子～細胞の架け橋
Exploring force-generating mechanism of molecular motor ensembles; building bridges between single molecules and cells

オーガナイザー：茅　元司 (東大), 矢島　潤一郎 (東大)
Organizer: Motoshi Kaya (Univ. of Tokyo), Junichiro Yajima (Univ. of Tokyo)

Single molecule studies have been extensively developed for the last 20 years and revealed the force-generating mechanism of molecular motors, forming their ensembles to contribute to the force generation in various cellular activities. In this symposium, young frontier scientists, studying in two contrasting perspectives, molecular basis and cell basis approaches, will exchange their unique interpretations of the force-generating mechanism of various molecular motor (dynein, kinesin and myosin) ensembles in cells.

はじめに
茅 元司 (東大)
Motoshi Kaya (Univ. of Tokyo)

1SI-01 分子複合体フィラメントにおける骨格筋ミオシン 1 分子の力発生メカニズム
Force generation mechanism of single skeletal myosin molecules in myofilaments
茅 元司 (東京大学・院理物理, 科学技術振興機構・さきがけ)
Motoshi Kaya[1,2], Hideo Higuchi[1] ([1]Grad. Sch. Sci, Univ. Tokyo, [2]JST, PRESTO)

1SI-02 ダイニンモーター運動発生機構の構造的基盤
Structural basis of dynein motility
昆 隆英 (阪大・蛋白研)
Takahide Kon (Institute for Protein Research, Osaka Univ.)

1SI-03 **Microtubule corkscrewing motion driven by multiple non-processive motors**
矢島 潤一郎 (東京大学大学院総合文化研究科広域科学専攻生命環境科学系)
Junichiro Yajima (Department of Life Sciences, Graduate School of Arts and Sciences, The University of Tokyo)

1SI-04 微小管系分子モーターの複数分子による機能を計測する
Measuring ensemble functions of microtubule-based molecular motors
古田 健也 (情報通研, バイオ ICT)
Ken'ya Furuta (Bio ICT Lab, NICT)

1SI-05 **A cellular funicular: one active force generation drives two directional organelle movements**
木村 暁 (国立遺伝学研究所・細胞建築研究室, 総研大・遺伝学専攻)
Akatsuki Kimura[1,2] ([1]Cell Architecture Laboratory, National Institute of Genetics, [2]Dept. Genetics, SOKENDAI)

1SI-06 ミオシンの力生成・応答特性による上皮パターン形成
The emergence of epithelial pattern through force-generating and force-responding properties of myosin

杉村 薫 (京大・iCeMS)
Kaoru Sugimura[1], Shuji Ishihara[2] ([1]Kyoto Univ., [2]The Univ. of Tokyo)

第 2 日目（9/23（日））／ Day2(Sep. 23, Sun.)

9:00~11:30　A 会場：理学南館 1 階 坂田・平田ホール／ Room A: Sci. south bldg. 1F Sakata Hirata Hall
2SA　海外招聘シンポジウム：生物物理学最前線
Invited symposium from abroad: Forefront of biophysics

オーガナイザー：小嶋　誠司 (名大), 千見寺　浄慈 (名大)
Organizer: Seiji Kojima (Nagoya Univ.), George Chikenji (Nagoya Univ.)

The Biophysical Society of Japan will celebrate the 50th annual meeting this year. This symposium is planned as one of the anniversary events organized by the annual meeting organizing committee. In this symposium, we invite four speakers from abroad who have been recognized as their distinguished studies in the field of biophysics. We do not focus on the particular subject of biophysics, but instead we would like to include different topics with various techniques (structural analysis of proteins, (EM, X-ray), systems biology, single molecule biophysics). The aim of this symposium is to overview the forefront of the biophysics in the world, and to enjoy their outstanding studies by the omnibus style.

はじめに
小嶋 誠司 (名大)
Seiji Kojima (Nagoya Univ.)

2SA-01　**The Mechanism of Cytoplasmic Dynein Motility**
Ahmet Yildiz (University of California Berkeley)
Ahmet Yildiz (University of California Berkeley)

2SA-02　**Architecture of the Flagellar Switch Complex**
Brian R. Crane (Cornell University)
Brian R. Crane[1], R. Sircar[1], G. Gonzalez-Bonet[1], Koushik Paul[2], D. Blair[2] ([1]Cornell University, [2]University of Utah)

2SA-03　**Imaging Water at the Nanoscale and Protein in Water by TEM**
Paul T. Matsudaira (Department of Biological Science, National University of Singapore)
Paul T. Matsudaira (Department of Biological Science, National University of Singapore)

2SA-04　**Function dictates topology in biochemical networks**
Chao Tang (Peking University, University of California, San Francisco)
Chao Tang (Peking University, University of California, San Francisco)

9:00~11:30　B 会場：多元数理科学棟 5 階 509 ／ Room B: Mathematics bldg. 5F 509
2SB　若手オーガナイズシンポジウム：生命科学の新しい地平を切り開く若手研究者たち
Symposium organized by younger generation: Young scientists pioneering future life sciences

オーガナイザー：藤井　高志 (理研), 小山　昌子 (名大)
Organizer: Takashi Fujii (RIKEN), Masako Koyama (Nagoya Univ.)

In this symposium, young speakers actively working in diverse research fields introduce recent topics in their own research areas and talk about their progress and potential in addressing important biological questions.

2SB-01　遺伝子発現ノイズの起源
Examining origins of noise in gene expression
谷口 雄一 (理化学研究所生命システム研究センター)
Yuichi Taniguchi, Yutaka Ogawa, Masae Johmura (Quantitative Biology Center, RIKEN)

2SB-02　細胞環境下におけるタンパク質の NMR 計測
Protein NMR spectroscopy in the cellular environment
猪股 晃介 (独立行政法人理化学研究所生命システム研究センター)
Kohsuke Inomata[1], Shuhei Murayama[2], Shiro Futaki[3], Hidekazu Hiroaki[4], Yutaka Ito[5], Hidehito Tochio[2], Masahiro Shirakawa[2] ([1]Quantitative Biology Center, RIKEN, [2]Graduate School of Engineering, Kyoto University, [3]Institute for Chemical Research, Kyoto University, [4]Graduate School of Pharmaceutical Sciences, Nagoya University, [5]Graduate School

of Science and Engineering, Tokyo Metropolitan University)

2SB-03 高速原子間力顕微鏡による生体分子の構造ダイナミクスの直接観察
Direct observation of structural dynamics of biological molecules by high-speed atomic force microscopy
古寺 哲幸 (金沢大・理工・バイオ AFM 先端研究センター)
Noriyuki Kodera[1], Takayuki Uchihashi[1,2], Toshio Ando[1,2] ([1]Bio-AFM Frontier Research Center, Inst. Sci. & Eng., Kanazawa Univ., [2]Sch. Math. & Phys., Inst. Sci. & Eng., Kanazawa Univ.)

2SB-04 中心小体 9 回対称構造の謎を解く
Cracking the mystery of nine-ness: mechanisms of centriole formation
北川 大樹 (遺伝研・新分野創造センター)
Daiju Kitagawa (Nat. Inst. of Genetics, Cent. for Front. Res.)

2SB-05 低温電子顕微鏡法によるらせん複合体の高分解能構造解析
Recent advances in CryoEM high-resolution structural analysis for helical filaments
藤井 高志 (理化学研究所 生命システム研究センター)
Takashi Fujii (Qbic Riken)

2SB-06 **Kinetic and X-ray crystallographic studies of assembly/disassembly of the CRM1 nuclear export complex**
小山 昌子 (名古屋大・理・生命理学)
Masako Koyama[1], Natsuki Shirai[1], Yoshiyuki Matsuura[1,2] ([1]Grad. Sch. Sci., Nagoya Univ., [2]Strl. Biol. R. Ctr., Nagoya Univ.)

9:00~11:30 C 会場：多元数理科学棟 4 階 409 ／ Room C: Mathematics bldg. 4F 409
2SC 非平衡リビングマター：DNA から細胞骨格、細胞へ
Living matter far from equilibrium: from DNA to cytoskeletons and cells

オーガナイザー：島本 勇太 (ロックフェラー大), 前多 裕介 (京大)
Organizer: Yuta Shimamoto (The Rockefeller Univ.), Yusuke Maeda (Kyoto Univ.)

Essential understanding of complex biological systems requires revealing the underlying molecular processes and verifying how they follow the laws of physics. In this symposium we spotlight young researchers who see biological systems as living “matter” and are tackling fundamental problems in biology, using new tools and methodologies that allow for measuring quantitative physical parameters. Topics focus on the single and collective behavior of dynamic polymer systems, from genetic materials to cytoskeletal networks in cells. We believe that such collaborative interactions would facilitate deeper understanding of living systems as well as the development of physics for systems that are out of thermodynamic equilibrium.

2SC-01 有糸分裂紡錘体の構造形成と機能の物理的理解に向けて
Toward a physical understanding of spindle assembly and function
島本 勇太 (ロックフェラー大学)
Yuta Shimamoto (Rockefeller Univ.)

2SC-02 ダイニンに駆動されたマイクロチューブによる巨大渦の格子形成
Large-scale vortex lattice of microtubules driven by dyneins
永井 健 (東京大)
Ken Nagai[1], Yutaka Sumino[2], Kazuhiro Oiwa[3,4] ([1]Univ. Tokyo, [2]Aichi Univ. Edu., [3]NICT, [4]Univ. Hyogo)

2SC-03 **Non-Gaussian athermal fluctuations in active cytoskeletons**
水野 大介 (九州大学理学研究院)
Daisuke Mizuno (Kyushu University)

2SC-04 植物器官にみられるねじれた成長の弾性力学的および幾何学的な起原について
Elastic and geometric origin of the twisted growth of plant organs
和田 浩史 (立命館・物理)
Hirofumi Wada (Dep. Phys. Ritsumeikan Univ.)

2SC-05 **Visualizing Chromosome Structure with Superresolution Microscopy**
Peter Carlton (京都大学 物質ー細胞統合システム拠点 (iCeMS))
Peter Carlton (Kyoto University, iCeMS Institute)

2SC-06 DNA・RNA の輸送と選択：生命の起源への接近
Transport and selection for DNA and RNA: An approach to the origin of life

前多 裕介 (京大・白眉センター, 京大・理・物理, 科学技術振興機構さきがけ, ロックフェラー大)
Yusuke Maeda[1,2,3,4], Albert Libchaber[4] ([1]The Hakubi Center for Advanced Research, Kyoto Univ., [2]Dept. Phys., Grad. Sch. Sci., Kyoto Univ., [3]PRESTO, JST, [4]The Rockefeller Univ.)

9:00~11:30　D 会場：多元数理科学棟 3 階 309 ／ Room D: Mathematics bldg. 3F 309

2SD　スーパーコンピューティング：分子ネットワークと細胞内ダイナミクス
Supercomputing in Molecular Network to Cellular Dynamics

オーガナイザー：木寺　詔紀 (横市大), 杉田　有治 (理研)
Organizer: Akinori Kidera (Yokohama City Univ.), Yuji Sugita (RIKEN)

K computer (the ten Peta FLOPS supercomputer installed in Kobe) provides an enormous enhancement of the capability in computational life science. This symposium intends to bring forth the possibility of supercomputing in life science fully utilizing K computer. Particularly, it focuses on the multi-scale descriptions of molecular networks and cellular dynamics by integrating the molecular and the cellular simulation methods.

2SD-01　**Dynamics and stability of proteins in cellular environments**
Michael Feig (ミシガン州立大学)
Michael Feig (Michigan State University)

2SD-02　スーパーコンピュータは細胞生物学をどう変えるか
How supercomputing can help change cell biology
高橋 恒一 (理化学研究所 QBiC, 慶大・先端生命研, 阪大・生命機能)
Koichi Takahashi[1,2,3] ([1]RIKEN QBiC, [2]Keio Inst. Adv. Biosci., [3]Osaka Univ. Grad. Sch. Front. Biosci.)

2SD-03　細胞内の場を考慮したシミュレータ RICS の開発
Development of the cell simulator in consideration of space
横田 秀夫 (理研 基幹研, 理研 次世代生命体統合シミュレーション)
Hideo Yokota[1,2], Yasuhiro Sunaga[2], Sigeho Noda[3] ([1]ASI, Riken, [2]iSLIM, Riken, [3]ACCC, Riken)

2SD-04　「京」による大規模遺伝子ネットワーク推定
Large scale gene network estimation with K computer
玉田 嘉紀 (東京大・院情報理工)
Yoshinori Tamada[1], Teppei Shimamura[2], Rui Yamaguchi[2], Atsushi Niida[2], Ayumu Saito[2], Yuto Kataoka[1,2], Seiya Imoto[2], Masao Nagasaki[3], Satoru Miyano[1,4] ([1]Grad. Sch. Info. Sci. Tech., Univ. Tokyo, [2]Inst. Med. Sci., Univ. Tokyo, [3]Tohoku Med. Megabank, Tohoku Univ., [4]CSRP, RIKEN)

2SD-05　データ同化法にもとづくデータ統合・生体シミュレーション技術
Biological system modeling and data assimilation
吉田 亮 (情報・システム研究機構 統計数理研究所)
Ryo Yoshida (The Institute of Statistical Mathematics, Research Organization of Information and Systems)

9:00~11:30　E 会場：多元数理科学棟 1 階 109 ／ Room E: Mathematics bldg. 1F 109

新学術領域研究　「運動超分子マシナリーが織りなす調和と多様性」共催

2SE　運動超分子マシナリーが織りなす調和と多様性
Harmonized supramolecular machinery for motility and its diversity

オーガナイザー：宮田 真人 (阪市大), 南野　徹 (阪大)
Organizer: Makoto Miyata (Osaka City Univ.), Tohru Minamino (Osaka Univ.)

"Motility" observed inside and outside of cells has long been an important biophysical research subject. In the last decade, we have learned a lot about many motile systems, including conventional motor proteins and ATP synthetase and so on. However, the mechanisms of many motility systems are still unclear. In this symposium, we discuss the possibilities for new research subjects through six presentations.

はじめに
南野 徹 (阪大)
Tohru Minamino (Osaka Univ.)

2SE-01　細菌べん毛モーターの回転方向変換制御機構の解明
Elucidation of the directional switching mechanism of the bacterial flagellar motor

宮田 知子 (大阪大学大学院生命機能研究科)
Tomoko Miyata[1], Takayuki Kato[1], Takasi Fujii[1,2], Shuichi Nakamura[4], Yusuke Morimoto[1,2,3], Tohru Minamino[1], Hideyuki Matsunami[5], Keiichi Namba[1,2] ([1]Grad. Sch. Frontier Biosci., Osaka Univ., [2]QBiC, RIKEN, [3]Grad. Sch. Sci., Osaka Univ. Department of Applied Physics, [4]Tohoku Univ. School of Engineering, [5]OIST, Initial Research Project)

2SE-02 磁性細菌の超分子複合体ーマグネトソーム，細胞骨格そしてベン毛ーの構造的組織化
Structural Organization of Macromolecular assemblies -Magnetosome, Cytoskeleton and Flagella- in Magnetotactic Bacteria
福森 義宏 (金沢大学理工研究域)
Yoshihiro Fukumori, Azuma Taoka (College Sci. Eng., Kanazawa Univ.)

2SE-03 アクチンフィラメントの構造多型と機能分化
Structural polymorphism and functional differentiation of actin filaments
上田 太郎 (産総研・バイオメディカル)
Taro Q.P. Uyeda[1], Nobuhisa Umeki[1], Saku Kijima[2], Yusuke Nishikawa[3], Kiyotaka Tokuraku[3], Akira Nagasaki[1], Taro Q.P. Noguchi[2] ([1]Biomedical Res. Inst., AIST, [2]Miyakonojo Natl. Col. of Tech., [3]Muroran Inst. of Tech.)

2SE-04 マイコプラズマ滑走運動の謎にせまる
New foci to clarify *Mycoplasma* gliding
宮田 真人 (大阪市大・院理・生物地球)
Makoto Miyata (Grad. Sch. Sci., Osaka City Univ.)

2SE-05 バクテロイデスにおける分泌と滑走
Secretion and Gliding in Bacteroides
佐藤 啓子 (長崎大学医歯薬総合研究科)
Keiko Sato[1], Daisuke Nakane[1], Hirohumi Wada[2], Katsumi Imada[3], Mark J. McBride[4], Koji Nakayama[1] ([1]Graduate School of Biomedical Sciences, Nagasaki University, [2]Department of Physics Sciences, Ritsumeikan University, [3]Graduate School of Science, Osaka University, [4]Department of Biological Sciences, University of Wisconsin-Milwaukee)

2SE-06 **Molecular motor driven self-organization in Myxococcus xanthus**
Joshua W. Shaevitz (Princeton University, Departments of Physics and Genomics)
Joshua W. Shaevitz (Princeton University, Departments of Physics and Genomics)

総合討論
宮田 真人 (大阪市大・院理・生物地球)
Makoto Miyata (Grad. Sch. Sci., Osaka City Univ.)

9:00~11:30　F会場：理学B館5階501 ／ Room F: Sci. bldg. B 5F 501

2SF　生命システムのばらつきと情報処理
Inherent variability and information coding in biological systems

オーガナイザー：黒田　真也 (東大), 柴田　達夫 (理研)
Organizer: Shinya Kuroda (Univ. of Tokyo), Tatsuo Shibata (RIKEN)

Biological systems can process information and exert functions in the presence of inherent variability in expression levels and activity of molecules. Such variability generates diversity of biological functions including early embryonic development and wiring of neural circuits. In this symposium, inherent variability and information coding in biological systems will be discussed by having speakers from experimental and theoretical sides.

2SF-01 **Inconsistency between population and single cell growth rates revealed by dynamics cytometer**
若本 祐一 (東大・複雑系生命システム研究センター，JST さきがけ)
Yuichi Wakamoto[1] ([1]Research Center for Complex Systems Biology, Univ of Tokyo, [2]JST PRESTO)

2SF-02 **Information Processing via Noisy Biochemical Channels**
小林 徹也 (東京大学 生産技術研究所, 科学技術振興機構 さきがけ)
Tetsuya J. Kobayashi[1,2], Atsushi Kamimura[3,4] ([1]Institute of Industrial Science, the University of Tokyo, [2]JST PRESTO, [3]Graduate School of Arts and Sciences, The University of Tokyo, [4]JSPS)

2SF-03 ERK 経路の情報コード
Information coding of ERK signaling networks
黒田 真也 (東大・理・生物化学)
Shinya Kuroda, Shinsuke Uda, Takeshi Saito (Dept. Biophys. Biochem., Univ. Tokyo)

2SF-04 **Fluctuating signals in cellular signal transduction systems**
柴田 達夫 (理化学研究所 発生再生科学総合研究センター)
Tatsuo Shibata (RIKEN Center for Developmental BiologyE)

2SF-05 **Symmetry breaking in mouse development**
柊 卓志 (EMBL, iCeMS Kyoto University)
Takashi Hiiragi[1,2] ([1]EMBL, [2]iCeMS Kyoto University)

2SF-06 **Stochastic expression of cell adhesion molecules in individual neurons**
八木 健 (大阪大学, 科技振興機構)
Takeshi Yagi[1,2] ([1]Osaka University, [2]CREST-JST)

9:00~11:30　G 会場：理学 B 館 2 階 212 ／ Room G: Sci. bldg. B 2F 212

2SG　染色体場のダイナミクス
Dynamics of chromatin as the physicochemical field for genetic activities

オーガナイザー：徳永　万喜洋 (東工大), 木村　宏 (阪大)
Organizer: Makio Tokunaga (Tokyo Inst. of Tech.), Hiroshi Kimura (Osaka Univ.)

Spatial organization of DNA molecules within the nucleus contains potentially important, and yet mystifying genetic information. Such information includes physical properties, shapes, and spatio-temporal positioning of DNA and regulatory molecules, comprehensively providing the "physicochemical field" that ensures arranged storage, timely expression and faithful transmission of genetic materials. We will discuss the structure and function of DNA and protein complexes that are formed transiently and locally. Understanding of the physicochemical field will provide a tool to control and reconstitute various cellular functions.

2SG-01 生細胞における RNA ポリメラーゼ II による転写活性化の動態
Kinetics of RNA polymerase II transcription in living cells
木村 宏 (大阪大学生命機能研究科)
Hiroshi Kimura, Timothy J. Stasevich (Grad. Sch. Frontier Biosci., Osaka. Univ.)

2SG-02 染色体場の 1 分子イメージング定量解析
Quantitative analysis of single molecule imaging of the physicochemical field for genetic activities
十川 久美子 (東工大・院生命理工, 理研・免疫セ)
Kumiko Sakata-Sogawa[1,2], Makio Tokunaga[1,2] ([1]Grad. Sch. Biosci. Biotech., Tokyo Inst. Tech., [2]RCAI, RIKEN)

2SG-03 ヒストンバリアントによるヌクレオソームの構造多様性とダイナミクス
Structural versatility, dynamics, and functions of human nucleosomes containing histone variants
胡桃坂 仁志 (早稲田大学 理工学術院)
Hitoshi Kurumizaka (Waseda University, Faculty of Science and Engineering)

2SG-04 細胞のパターンをうみだす遺伝子回路の作製
Construction of genetic circuits underlying cell pattern formation
戎家 美紀 (京都大学生命科学系キャリアパス形成ユニット)
Miki Ebisuya (Career-Path Promotion Unit for Young Life Scientists, Kyoto Univ.)

2SG-05 細胞分裂と染色体分配のメカノバイオロジー
Mechanobiology of Cell Division and Chromosome Segregation
石渡 信一 (早大・理工, 早大・WABIOS)
Shin'ichi Ishiwata[1,2] ([1]Fac. Sci. Engn., Waseda Univ., [2]WABIOS, Waseda Univ.)

2SG-06 減数分裂特異的な非コード RNA が相同染色体の対合を促進する
Meiosis-specific non-coding RNA mediates robust pairing of homologous chromosomes in meiosis
平岡 泰 (大阪大学大学院生命機能研究科, 情報通信研究機構　未来 ICT 研究所)
Yasushi Hiraoka[1,2], Da-Qiao Ding[2], Tokuko Haraguchi[1,2] ([1]Graduate School of Frontier Biosciences, Osaka University, [2]Advanced ICT Research Institute Kobe, NICT)

9:00~11:30　H 会場：理学 C 館 5 階 517 ／ Room H: Sci. bldg. C 5F 517

2SH　先端顕微計測が照らす生命の輝き
Star of life shined by frontier microscopies

オーガナイザー：井上　圭一 (名工大), 今村　博臣 (京大)
Organizer: Keiichi Inoue (Nagoya Inst. of Tech.), Hiromi Imamura (Kyoto Univ.)

Microscopic techniques have continued to increase their presence in biological field as outstanding research methods to directly observe the spatiotemporal behaviors of various biological materials and phenomena in recent years. In this symposium, seven leading researchers will introduce their cutting-edge microscopic techniques and provide topics for discussing what will be possible with microscopic techniques in future biological science.

はじめに
今村 博臣 (京大)
Hiromi Imamura (Kyoto Univ.)

2SH-01　KcsA カリウムイオンチャネルの溶液条件変化応答 1 分子開閉ダイナミクスの解析
Analysis of Single Molecular Gating Dynamics of the KcsA Potassium Channels Responding to Rapid Changes of Solution Conditions
清水 啓史 (福井大・医・分子生理)
Hirofumi Shimizu[1], Masayuki Iwamoto[1], Antoine Royant[2,5], Stetten David von[5], Laurent Guerin[3], Yoshimitsu Aoki[4], Michael Wulff[5], Shigetoshi Oiki[1] ([1]Mol. Physiol. & Biophys., Univ. Fukui. Fac. Med. Sci., [2]CEA-CNRS-Universite Joseph Fourier, [3]Universite de Rennes 1, [4]Keio. Univ. Sci. & Tech. Elec., [5]ESRF)

2SH-02　中赤外波長領域の観察が可能な赤外超解像顕微鏡の開発と生体試料への応用
Development of a mid-IR super-resolution microscope and its application to biological samples
酒井 誠 (東工大・資源研)
Makoto Sakai (Tokyo Tech.)

2SH-03　白色レーザーを用いた CARS 分光イメージングによる生細胞の動態追跡
Tracing dynamical behavior of a single cell by CARS microspectroscopy using a white-light laser source
加納 英明 (筑波大 数理物質科学研究科)
Hideaki Kano[1], Masanari Okuno[2], Hiroki Segawa[2], Hiro-o Hamaguchi[3] ([1]Tsukuba Univ., [2]The Univ. of Tokyo, [3]National Chiao Tung Univ.)

2SH-04　イメージングマススペクトロメトリーによって初めて明らかになった、細胞内の脂質分布の分子種特異的な極性について
Imaging mass spectrometry revealed the polarized intracellular distribution of specific lipid molecular species
瀬藤 光利 (浜松医科大学解剖学講座)
Mitsutoshi Setou (Hamamatsu University School of Medicine Department of Cell Biology and Anatomy)

2SH-05　随意運動中のマウス運動野 2 光子イメージング
Two-photon imaging of the mouse motor cortex during voluntary skilled movement
松崎 政紀 (基礎生物学研究所, CREST, 総研大)
Riichiro Hira[1,2,3], Fuki Ohkubo[1,3,4], Katsuya Ozawa[2,3], Yoshikazu Isomura[3,5], Kazuo Kitamura[2,3], Masanobu Kano[2], Haruo Kasai[2], **Masanori Matsuzaki**[1,3,4] ([1]National Institute for Basic Biology, [2]Graduate School of Medicine, University of Tokyo, [3]CREST, [4]SOKENDAI, [5]Brain Science Institute, Tamagawa University)

2SH-06　**Chemiluminescence imaging of flow-induced ATP release at caveolae in vascular endothelial cells**
山本 希美子 (東京大学 大学院医学系研究科 医用生体工学講座 システム生理学)
Kimiko Yamamoto[1], Joji Ando[2] ([1]Laboratory of System Physiology, Department of Biomedical Engineering, Graduate School of Medicine, University of Tokyo, [2]Laboratory of Biomedical Engineering, School of Medicine, Dokkyo Medical University)

2SH-07　バイオイメージング技術
New Fluorescent Probes and New Perspectives in Bioscience
宮脇 敦史 (理化学研究所　脳科学総合研究センター)
Atsushi Miyawaki (Brain Science Institute, RIKEN)

おわりに
井上 圭一 (名工大)
Keiichi Inoue (Nagoya Inst. of Tech.)

9:00~11:30　I会場：理学E館 1 階 131 ／ Room I: Sci. bldg. E 1F 131

2SI　一分子レベルで生体分子機械のエネルギーと機能効率を考える
The art of energetic and functional efficiency in biomolecular machines on the single molecule level

オーガナイザー：鎌形　清人 (東北大), 藤芳　暁 (東工大), Chun Biu Li (北大)

Organizer: Kiyoto Kamagata (Tohoku Univ.), Satoru Fujiyoshi (Tokyo Inst. of Tech.), Chun Biu Li (Hokkaido Univ.)

How single or a few biomolecules perform functions with high energetic efficiency in a fluctuating environment is an intriguing question that concerns the understanding of the general designing and operational principles of biological nano-machineries. By bringing together both experimental and theoretical experts from interdisciplinary fields, this symposium aims to explore: 1) Novel experimental techniques to probe the energetic and functional efficiency on the single molecule level; 2) New theoretical frameworks and analysis methods in modeling and explaining the biophysical mechanisms to achieve energetic and functional efficiency; 3) Applications of these biological inspirations in building efficient nano-devices.

2SI-01　生物には効率が大事なのだろうか？

Is high efficiency necessary for organisms?

工藤 成史 (東北大・院応用物理)

Seishi Kudo (Dept. Applied Physics, Grad. Sch. Eng., Tohoku Univ.)

2SI-02　F_1-ATPase モーターの一分子エネルギー論

Single molecule energetics of F_1-ATPase motor

宗行 英朗 (中央大学理工学部物理学科)

Shoichi Toyabe[2], Takahiro Watanabe-Nakayama[3], Hiroshi Ueno[1], Tetsuaki Okamoto[4], Hiroshi Taketani[1], Seishi Kudo[5], **Eiro Muneyuki**[1] ([1]Dept. Phys., Faculty of Science and Engineering, Chuo Univ., [2]Faculty of Physics, LMU Munich, [3]Interdisciplinary Graduate School of Science and Engineering, Tokyo Inst. Tech., [4]Environment Preservation Center, Kanazawa Univ, [5]Dept. Appl. Phys., Sch. Eng., Tohoku Univ.)

2SI-03　**Observation of vibrational absorption of single proteins at few Kelvins**

藤芳 暁 (東工大 物理)

Satoru Fujiyoshi (Tokyo Tech.)

2SI-04　揺らぎの定理によるミトコンドリア輸送の駆動力測定

Estimation of driving force acting on a mitochondrion transported in a living cell: Application of the fluctuation theorem

林 久美子 (東北大工)

Kumiko Hayashi[1], Masaaki Sato[2], Kazunari Mouri[3], Chang-gi Pack[3], Kazunari Kaizu[4], Kouichi Takahashi[4], Yasushi Okada[4] ([1]Sch. Eng., Tohoku Univ., [2]IMRAM, Tohoku Univ., [3]ASI, RIKEN, [4]QBiC, RIKEN)

2SI-05　物質界面における構造と電荷移動を可視化する走査型プローブ顕微鏡法の開発

Development of scanning probe methods for investigating structures and charge transfers at material interfaces

木村 建次郎 (神戸大学 大学院理学研究科)

Kenjiro Kimura (Grad. Sch. of Sci., Kobe Univ.)

2SI-06　DNA 折り紙フレームを用いた一分子観察

Direct Observation of Single Molecular Event in DNA Origami Frame

杉山 弘 (京大院理, 京大物質一細胞)

Hiroshi Sugiyama[1,2] ([1]Grad. Sch. Sci. Kyoto Univ., [2]iCeMS)

口頭発表　Oral Presentation

第 1 日目（9 月 22 日（土））／ Day 1 (Sep. 22, Sat.)

14:00〜16:22　A 会場　理学南館 1 階 坂田・平田ホール／ Room A: Sci. south bldg. 1F Sakata Hirata Hall
分子モーター I
Molecular Motors I

1A1400　コイルドコイル ミオシンの脆弱部位と屈曲性の保存
Prediction of fragile points and conservation of bending ability of coiled coil myosin
Mieko Taniguchi[1], Hideki Tanizawa[2], Sigeki Mitaku[1] ([1]*Grad. Sch. Sci., Univ. Nagoya*, [2]*Inst. Wister, USA*)

1A1412　カーボンナノチューブ上におけるミオシン運動の温度応答
Thermal response of myosin motors on single carbon nanotubes
Mitsunori Nagata[1], Hiroshi Matsutaka[1], Takeru Okada[3], Akihiko Ishijima[2], Yuichi Inoue[2] ([1]*Grad. Sch. Life Sci., Tohoku Univ.*, [2]*IMRAM, Tohoku Univ.*, [3]*Institute of Fluid Science, Tohoku University*)

1A1424　生体分子モーターのためのステップ解析アルゴリズム
Powerful Algorithm for analyzing Stepping Motion of Biological Melecular Motors
Takeshi Nakagawa, Kazuo Sasaki (*Dept. of Applied Physics, Tohoku Univ.*)

1A1436　高時間分解能暗視野顕微鏡を用いたキネシン頭部の前方へのステップの観察
Direct observation of the forward stepping motion of kinesin-1 using dark-field microscopy with 50-μs temporal resolution
Hiroshi Isojima[1], Ryota Iino[2], Hiroyuki Noji[2], Michio Tomishige[1] ([1]*Dept. Appl. Phys., Sch. Eng., Univ. Tokyo*, [2]*Dept. Appl. Chem., Sch. Eng., Univ. Tokyo*)

1A1448　Front-head gating mechanism of kinesin-1 as studied by single molecule FRET observation of ATP binding
Yamato Niitani, Michio Tomishige (*Department of Applied Physics, School of Engineering, The University of Tokyo*)

休憩 15:00-15:10

1A1510　キネシン様モータータンパク質 Ncd の Power-stroke モデルの検証
The test on the power stroke model of Ncd
Masahiko Yamagishi, Yoko Toyoshima, Junichiro Yajima (*Dept. Life Sciences, Grad. Sch. Arts and Sciences, Univ. Tokyo*)

1A1522　細菌べん毛モーター固定子複合体 MotA/B チャネルの選択的透過メカニズム
Selective permeation mechanism through the channel of the stator complex MotA/B in the flagellar motor
Yasutaka Nishihara, Akio Kitao (*IMCB, Univ. of Tokyo*)

1A1534　Sodium Dynamics of the Bacterial Flagellar Motor
Chien-Jung Lo[1], Yoshiyuki Sowa[2], Teuta Pilizota[2], Richard Berry[2] ([1]*Department of Physics, Natioinal Central University, Taiwan*, [2]*Clarendon Laboratory, Department of Physics, University of Oxford*)

1A1546　Engineered disulfide crosslink in the the periplasmic region of PomB impaired function of the Na+-driven flagellar stator complex
Shiwei Zhu, Na Li, Seiji Kojima, Michio Homma (*Division of Biology Science, Graduate School of Science, Nagoya University*)

1A1558　高圧力が引き起こすべん毛繊維のダイナミック構造変化
Dynamic conformational changes of flagellar filament observed by high-pressure microscopy
Masayoshi Nishiyama[1], Yoshiyuki Sowa[2] ([1]*The Hakubi Center, Kyoto Univ.*, [2]*Hosei Univ.*)

1A1610　c-di-GMP 結合タンパク質 YcgR のホモログ PlzD の大量発現による *Vibrio alginolyticus* でのべん毛運動阻害
Flagellar motility inhibition by overexpression of PlzD, a YcgR homolog of c-di-GMP binding protein, in *Vibrio alginolyticus*
Takuro Yoneda, Wakako Morimoto, Seiji Kojima, Michio Homma (*Grad. Sci., Univ. Nagoya*)

14:00〜16:22　B 会場　多元数理科学棟 5 階 509 ／ Room B: Mathematics bldg. 5F 509
蛋白質-構造機能相関 I
Proteins: Structure & Function I

1B1400　“空隙”ー機能構造創出のための自然の戦略
Cavityーa Nature's strategy for functional sub states in proteins
Kazuyuki Akasaka (*Kinki UNIV., Inst. Adv. Tech.*)

1B1412　HD-exchange motion of free heptameric GroES studied by the use of TROSY and DMSO quenching followed by 2D NMR
Mahesh Chandak[1], Takashi Nakamura[1], Koki Makabe[2], Toshio Takenaka[1], Jin Chen[1], Koichi Kato[1], Kunihiro Kuwajima[1] ([1]*Okazaki Institute of Integrative Bioscience,National Institutes of Natural Sciences, The Graduate University for Advanced Studies (Sokendai)*, [2]*Graduate School of Science and Engineering,Yamagata University*)

1B1424　溶液 NMR を用いた Na^+駆動型べん毛モーターの固定子タンパク質 FliG の C 末端領域構造解析
Solution NMR analysis of FliG C-terminal domain derived from Na^+-driven motor of *Vibrio*
Mizuki Gohara[1], Rei Abe-Yoshizumi[1,2], Shiori Kobayashi[1], Yohei Miyanoiri[3], Yoshikazu Hattori[4], Chojiro Kojima[4], Masatsune Kainosho[3,5], Michio Homma[1] ([1]*Div. Bio. Sci., Grad. Sch. Sci., Nagoya Univ.*, [2]*Department of Frontier Materials, Nagoya Institute of Technology*, [3]*Structural Biology Research Center, Grad. Sch. Sci., Nagoya Univ.*, [4]*Institute for Protein Research, Osaka Univ.*, [5]*Center for Priority Areas, Tokyo Metropolitan Univ.*)

1B1436　酸化還元状態に依存してプロテインジスルフィドイソメラーゼの基質結合部位ドメインの空間配置が変化する仕組み

Molecular mechanism of redox-dependent domain rearrangement of the substrate-binding region of protein disulfide isomerase

Kouya Inagaki[1,2], Yoshinori Uekusa[1,2], Yukiko Kamiya[1,2], Tadashi Satoh[1], Koichi Kato[1,2] ([1]*Grad. Sch. Phar. Sci., Nagoya City Univ.*, [2]*Natl. Inst. Nat. Sci.*)

1B1448 Transferred cross-saturation 法を用いた EB1 の CH ドメインの微小管との結合界面の特定

Microtubule-binding sites of EB1 CH domain revealed by transferred cross-saturation experiments

Teppei Kanaba[1], Ryoko Maesaki[2], Tomoyuki Mori[2], Yutaka Ito[1], Toshio Hakoshima[2], Masaki Mishima[1] ([1]*Grad. Sch. of Sci. and Tech., TMU*, [2]*Grad. Sch.l of Biol. Sci., NAIST*)

休憩 15:00-15:10

1B1510 再構築型生体外タンパク質合成系を用いた分子シャペロンによる凝集抑制効果の大規模解析

Global analysis of aggregation-inhibotion effects of molecular chaperones using a reconstituted cell-free translation system

Tatsuya Niwa[1], Takuya Ueda[2], Hideki Taguchi[1] ([1]*Grad. Sch. of Biosci&Bioteh, Tokyo Institute of Technology*, [2]*Grad. Sch. of Frontier Sciences, The university of Tokyo*)

1B1522 DNA 界面での蛋白質の局所的構造変化

Local conformational changes of proteins in DNA interfaces

Tomoko Sunami, Hidetoshi Kono (*JAEA*)

1B1534 天然変性タンパク質の構造ゆらぎを生かした密度変化誘起型シグナル伝達過程

The possible advantage of structural disorder of intrinsically disordered pr oteins in the new type of signaling mechanism

Nobu C. Shirai[1,2], Macoto Kikuchi[1,2,3] ([1]*Graduate School of Science, Osaka University*, [2]*Cybermedia Center, Osaka University*, [3]*Graduate School of Frontier Biosciences, Osaka University*)

1B1546 分子動力学法による capping protein（CP）の動的構造の解析

Structural fluctuations of capping proteins analyzed by molecular dynamics simulations

Ryotaro Koike[1], Shuichi Takeda[2], Yuichiro Maeda[2], Motonori Ota[1] ([1]*Grad. Sch. Info. Sci., Nagoya Univ.*, [2]*Struct. Biol. Res. Center, Grad. Sch. of Sci., Nagoya Univ.*)

1B1558 シトクローム c 酸化酵素のプロトンポンプ機構に関する分子動力学シミュレーションによる研究

A Molecular Dynamics Study on Proton Pump Function of Cytochrome c Oxidase

Takefumi Yamashita (*Research Center for Advanced Science and Technology, University of Tokyo*)

1B1610 Substrate transport mechanisms in GatCAB: the smallest unidirectional valve in subnano scale

Jiyoung Kang[2], Shigehide Kuroyanagi[2], Yohsuke Hagiwara[2], Masaru Tateno[1] ([1]*Grad. Sch. Sci., Univ. Hyogo*, [2]*Grad. Sch. Pure and Appl. Sci., Univ. Tsukuba*)

14:00～16:22 C 会場 多元数理科学棟 4 階 409 ／ Room C: Mathematics bldg. 4F 409
蛋白質-計測，解析，エンジニアリング
Proteins: Measurement, Analysis, Engineering

1C1400 抗菌ペプチドを利用した病原体検出サンドイッチ発色検出技術の開発

New colorimetric sandwich assay for detection of pathogens by using antimicrobial peptides as detection probes

Chihiro Sakai[1], Eri Hojo[2], Taichi Nakazumi[1], Satoshi Tomisawa[1], Takashi Kikukawa[1], Yasuhiro Kumaki[1], Masakatsu Kamiya[1], Makoto Demura[1], Keiichi Kawano[1], Ryuji Ohtsuki[2], Taro Yonekita[2], Naoki Morishita[2], Takashi Matsumoto[2], Fumiki Morimatsu[2], **Tomoyasu Aizawa**[1] ([1]*Grad. Sch. Life Sci., Hokkaido Univ.*, [2]*R&D Center, Nippon Meat Packers Inc.*)

1C1412 VanX の溶菌活性を用いたルシフェラーゼのスクリーニングの簡略化

Toward a simplified screening method using a novel VanX cell lysis activity

Nan Wu[1], Tetsuya Kamioka[1], Shihori Sohya[1], Tomoki Matsuda[2], Takahisa Ikegami[3], Haruki Nakamura[3], Yutaka Kuroda[1] ([1]*Biotechnology and Department Life Science, Graduate School of Engineering, Tokyo University of Agriculture and Technology*, [2]*Research Institute for Electronic Science, Hokkaido University*, [3]*Institute for Protein Research, Osaka University*)

1C1424 Fluorescent Probe for the Direct Detection of Histone Deacetylase Activity

Koushik Dhara[1], Yuichiro Hori[1], Reisuke Baba[1], Kazuya Kikuchi[1,2] ([1]*Graduate School of Engineering, Osaka University*, [2]*Immunology Frontier Research Center, Osaka University*)

1C1436 RaPID システムによる Akt2 選択的環状ペプチド阻害剤の探索とその阻害ペプチドの生化学的活性の評価

Exploring cyclic peptide inhibitors against the Akt2 kinase by the RaPID system and evaluation of their biochemical properties

Yuuki Hayashi[1], Jumpei Morimoto[2], Hiroaki Suga[2] ([1]*Dept. Life Sci., Grad Sch. Arts and Life Sci., The Univ. Tokyo*, [2]*Dept. Chem., Grad Sch. Sci., The Univ. Tokyo*)

1C1448 低分子抗体の多機能化を可能とするピンポイント化学接合デザイン

Protein engineering for site-specific bioconjugation chemistry: Construction of multiple functional low-molecular antibodies

Mitsuo Umetsu, Asami Ueda, Takeshi Nakanishi, Kentaro Hashikami, Ryutaro Asano, Izumi Kumagai (*Department of Biomolecular Engineering, Graduate School of Engineering, Tohoku University*)

休憩 15:00-15:10

1C1510 ハイブリッドナノセルロームの構成要素としての CBM の機能解析

Hybrid nano-cellulosome: functional analysis of various cellulose binding module as component of artificial cellulosome

Hikaru Nakazawa[1], Do-myoung Kim[1], Takashi Matuyama[2], Nobuhiro Ishida[2], Akinori Ikeuchi[2], Izumi Kumagai[1], Mitsuo Umetsu[1] ([1]*Tohoku univ. tech.*, [2]*Toyota Central R&D lab*)

1C1522 エンド-1,3-β グルカナーゼの糖結合モジュール α-リピートに存在する Trp273 のラミナリン結合への寄与

Contribution of Trp273 in the α-repeat of the carbohydrate-binding module of endo-1,3-β-glucanase to laminarin binding

Tomonari Tamashiro[1], Yoichi Tanabe[1], Kenji Kanaori[2], Teikichi Ikura[3], Nobutoshi Ito[3], Masayuki Oda[1] ([1]*Grad. Sch. of Life and Environ. Sci., Kyoto Pref. Univ.*, [2]*Grad. Sch. of Sci. and Technol., Kyoto Inst. of Technol.*, [3]*Med. Res. Inst., Tokyo Med. and Dent. Univ.*)

1C1534 Construction of an in vitro gene screening system for membrane proteins

Haruka Soga[1], Satoshi Fujii[3], Tetsuya Yomo[2,3], Hajime

Watanabe[1], Tomoaki Matsuura[1,3] ([1]*Dept. Biotech., Grad. Sch. Eng., Osaka Univ.*, [2]*Dept. Bioinfo. Eng., Grad. Sch. IST, Osaka Univ.*, [3]*ERATO, JST.*)

1C1546 Orientation-controlled immobilization of pharaonis halorhodopsin onto gold revealed by SEIRAS

Hao Guo[1,2], Tetsunari Kimura[1,2,3], Yuji Furutani[1,2,4] ([1]*Department of Structural Molecular Science, the Graduate University for Advanced Studies*, [2]*Department of Life and Coordination-Complex Molecular Science, Institute for Molecular Science*, [3]*JST CREST*, [4]*JST PRESTO*)

1C1558 低収量生体分子の時間分解分光計測を目指した新規溶液交換・混合装置の開発

Development of novel rapid buffer-exchange system and microfluidic mixer for time-resolved spectroscopic study of low-yield biomolecules

Tetsunari Kimura[1,2,3], Yuji Furutani[1,2,4] ([1]*Inst. Mol. Sci.*, [2]*Dept. Struct. Mol. Sci., Sokendai*, [3]*CREST/JST*, [4]*PRESTO/JST*)

1C1610 溶液中の金属タンパク質の共鳴 X 線散乱法の開発

Development of resonant X-ray scattering method of metalloproteins in solutions

Mitsuhiro Hirai[1], Kazuki Takeuchi[1], Ryota Kimura[1], Noboru Ohta[2] ([1]*Grad. Sch. Eng., Gunma Univ.*, [2]*SPring-8*)

14:00〜16:22 D 会場 多元数理科学棟 3 階 309 ／ Room D: Mathematics bldg. 3F 309
発生，分化，神経
Development, Differentiation, Neuroscience

1D1400 マウス ES 細胞分化の単 1 細胞解析

Single-cell-based analysis of differentiation of mouse ES cells

Atsushi Maruyama[1], Yuichi Wakamoto[2,3], Shogo Nakamura[1], Tatsuo Michiue[2], Shin-ichi Sakai[4], Bayar Hexig[4], Toshihiro Akaike[4], **Kiyoshi Ohnuma**[1] ([1]*TRI, Nagaoka Univ of Tech*, [2]*Grad. Sch. Arts. & Sci., Univ. Tokyo*, [3]*Sakigake, JST*, [4]*Grad. Sch. Biosci. & Biotech., Tokyo Inst of Tech*)

1D1412 顕微ラマン分光法による分化因子刺激後の単一細胞ダイナミクスの計測

Measurements of Single Cell Dynamics upon Stimulation with a Differentiation Factor Using Raman Micro-Spectroscopy

Sota Takanezawa[1,2], Shin-ichi Morita[1], Yukihiro Ozaki[2], Yasushi Sako[1] ([1]*Cellular informatics Lab., RIKEN*, [2]*Grad. Sch. Sci. and Tech., Kwansei Gakuin Univ.*)

1D1424 1 分子定量計測技術を用いた *C. elegans* 受精卵における細胞極性のモデル化

Quantitative measurement and mathematical modeling of polarity-protein PAR-2 in *C. elegans* embryos

Yukinobu Arata[1], Tetsuya Kobayashi[2], Michio Hiroshima[1], Chan-gi Pack[1], Masashi Tachikawa[3], Kenichi Nakazato[3], Tatsuo Shibata[4], Yasushi Sako[1] ([1]*Cell. Info., ASI, Riken*, [2]*Inst. Ind. Sci., Univ. Tokyo*, [3]*Theo. Biol., ASI, Riken*, [4]*CDB, Riken*)

1D1436 形態形成中の組織の力学場を推定する

Estimating forces in the growing epithelial tissues

Shuji Ishihara[1,2], Kaoru Sugimura[3,4] ([1]*Grad. Sch. Arts & Sciences, Univ. Tokyo*, [2]*JST PRESTO*, [3]*iCeMS, Kyoto Univ.*, [4]*RIKEN BSI*)

1D1448 ショウジョウバエ形態形成におけるアポトーシスの能動的力学的寄与

Active Mechanical Role of Apoptosis in Tissue Dynamics during Drosophila Morphogenesis

Yusuke Toyama[1,2,3] ([1]*Dep. of Biol. Sci., National University of Singapore*, [2]*Mechanobiology Inst., National University of Singapore*, [3]*Temasek Life Sciences Lab.*)

1D1510 A model of cell-division stop for the limb regeneration

Hiroshi Yoshida (*Faculty of Math. Kyushu Univ.*)

1D1522 ラット培養神経回路網の長期発達過程における同期活動に関わる機能的分子の探索

Analysis of functional molecules underlying synchronous activity during long-term development of rat cultured neuronal networks

Daisuke Ito[1], Keiko Yokoyama[2], Kazutoshi Gohara[2] ([1]*Fac. Adv. Life Sci., Hokkaido Univ.*, [2]*Fac. Eng., Hokkaido Univ.*)

1D1534 モノアラガイの長期記憶におけるインスリンとグルコースの役割

Insulin and glucose for memory in a snail

Etsuro Ito[1], Ryuichi Okada[1], Mika Morikawa[1], Satoshi Takigami[2], Akiko Okuta[3], Manabu Sakakibara[2] ([1]*Kagawa School of Pharmaceutical Sciences, Tokushima Bunri University*, [2]*School of High-Technology for Human Welfare, Tokai University*, [3]*Graduate School of Science, Kyoto University*)

1D1546 光捕捉された神経細胞内シナプス小胞群の集合ダイナミクス

Assembling dynamics of optically trapped synaptic vesicles in neuronal cell

Yusuke Ueda[1,2], Suguru N. Kudoh[2], Takahisa Taguchi[1], Chie Hosokawa[1,2] ([1]*Health Res. Inst., AIST*, [2]*Grad. Sci. Eng., Kwansei Gakuin Univ.*)

1D1558 膜電位感受性色素・カルシウムイメージングに使える新しい超高速共焦点顕微鏡の開発

A new class of confocal microscope for a fast voltage-sensitive dye (VSD) and Ca^{2+} imaging

Takashi Tominaga, Yoko Tominaga (*Dept. Neurophysiol., Kagawa Sch Pharm Sci, Tokushima Buniri Univ*)

1D1610 De novo アセンブルによる軟体動物脳の全トランスクリプトーム解析

***De novo* sequencing and transcriptome analysis of the molluscan brain by deep RNA sequencing**

Hisayo Sadamoto[1], Hironobu Takahashi[2], Taketo Okada[1], Hiromichi Kenmoku[2], Yoshinori Asakawa[2] ([1]*Facul. Pharmaceut. Sci. Kagawa Camp, Univ. Tokushima Bunri*, [2]*Inst. Pharmacognosy, Univ. Tokushima Bunri*)

休憩 15:00-15:10

14:00〜16:10 E 会場 多元数理科学棟 1 階 109 ／ Room E: Mathematics bldg. 1F 109
蛋白質-物性 I
Proteins: Property I

1E1400 分子動力学シミュレーションによる Hsp90 と ADP の結合自由エネルギープロファイル

Free energy profile for binding of ADP to Hsp90 with molecular dynamics simulation

Kazutomo Kawaguchi, Hiroyuki Takagi, Masashi Iwayama, Megumi Nishimura, Hiroaki Saito, Hidemi Nagao (*Inst. Sci.*

Eng., Kanazawa Univ.)

1E1412 シャペロニン空洞内の変性タンパク質が受けるコンフォメーション制限

The conformational restriction of denatured protein encapsulated in the chaperonin cage

Fumihiro Motojima, Yuko Motojima-Miyazaki, Masasuke Yoshida (*Kyoto Sangyo Univ.*)

1E1424 小角 X 線散乱によるアミロイド線維形成の初期会合プロセスの解析

Investigation of initial assembling process of fibrillation by small angle X-ray scattering

Eri Chatani[1], Rintaro Inoue[2], Koji Nishida[2], Toshiji Kanaya[2], Masahide Yamamoto[3] ([1]*Dept. Chem., Grad. Sch. Sci., Kobe Univ.*, [2]*Inst. Chem. Res., Kyoto Univ.*, [3]*Kyoto Univ.*)

1E1436 Distinguishing crystal-like amyloid fibrils and glass-like amorphous aggregates from their kinetics of formation

Yuichi Yoshimura[1], Yuxi Lin[1], Hisashi Yagi[1], Young-Ho Lee[1], Hiroki Kitayama[1], Kazumasa Sakurai[1], Masatomo So[1], Hirotsugu Ogi[2], Hironobu Naiki[3], Yuji Goto[1] ([1]*Inst. Protein Res., Osaka Univ.*, [2]*Grad. Sch. Eng. Sci., Osaka Univ.*, [3]*Fac. Med. Sci., Univ. Fukui*)

1E1448 細胞濃度に近い無添加細胞抽出液の調製

A method to prepare cell extract near intracellular concentration without additional salts and buffers

Kei Fujiwara, Shin-ichiro M. Nomura (*Dept. Biorobot., Tohoku Univ.*)

休憩 15:00-15:10

1E1510 TMAO による分子クラウディング環境への蛋白質移相自由エネルギーの三次元描像

Three-Dimensional Imaging of the Protein Transfer Free Energy into the Molecular Crowding Condition with TMAO

Isseki Yu[1], Kyoko Nakada[1], Masataka Nagaoka[2] ([1]*Dep. of Cem. and Biol. Sci. Aoyama Gakuin Univ.*, [2]*Grad. School of Info. Sci., Nagoya Univ.*)

1E1522 シトクロム *c* に対する尿素効果の自由エネルギー解析

Free-energy analysis of urea effect on cytochrome *c*

Yasuhito Karino, Nobuyuki Matubayasi (*Inst. Chem. Res., Kyoto Univ.*)

1E1534 タンパク質の水和水の水素結合ダイナミクスとタンパク質ダイナミクスとの動的カップリング

Kinetics of hydrogen-bonding of protein hydration water and its dynamical coupling with protein dynamics

Hiroshi Nakagawa[1], Mikio Kataoka[1,2] ([1]*Japan Atomic Energy Agency, Quantum Beam Science Directorate*, [2]*Nara Institute of Science and Technology, Graduate School of Materials Science*)

1E1546 テラヘルツ時間領域分光を用いた天然および変性状態タンパク質における低振動スペクトルの水和および温度依存性の観測

Temperature and hydration effects of low-frequency spectra of native and denatured proteins studied by terahertz time-domain spectroscopy

Naoki Yamamoto[1], Atsuo Tamura[2], Keisuke Tominaga[1,2] ([1]*Molecular Photoscience Research Center, Kobe University*, [2]*Graduate School of Science, Kobe University*)

1E1558 誘電緩和分光法によるアルキルカルボン酸の水和特性

Hydration Properties of Alkyl Carboxylate Series by Dielectric Relaxation Spectroscopy

Yangtian Wang, George Mogami, Tetsuichi Wazawa, Nobuyuki Morimoto, Makoto Suzuki (*Grad. Sch. Eng., Tohoku. Univ*)

14:00〜16:10 F 会場 理学 B 館 5 階 501 ／ Room F: Sci. Bldg. B 5F 501
光生物-視覚，光受容 I
Photobiology: Vision & Photoreception I

1F1400 サル緑感受性視物質の全反射赤外分光解析

ATR-FTIR study of monkey green-sensitive visual pigment

Kota Katayama[1], Yuji Furutani[1,2], Hiroo Imai[3], Hideki Kandori[1] ([1]*Department of Frontier Materials, Nagoya Institute of Technology*, [2]*Department of Life and Coordination-Complex Molecular Science, Institute for Molecular Science*, [3]*Primate Research Institute, Kyoto University*)

1F1412 精製したタコロドプシンの SAXS 測定

SAXS measurements of purified octopus rhodopsin

Shingo Watanabe[1], Mitsuhiro Hirai[2], Tatsuo Iwasa[1,3] ([1]*CEDAR, Muroran IT*, [2]*Grad. Sch. Eng., Gunma Univ.*, [3]*Grad. Sch. Eng., Muroran IT*)

1F1424 ナノディスク試料を用いたロドプシンと錐体視物質によるトランスデューシン活性化効率の比較解析

Comparative analysis of transducin activation by rhodopsin and cone pigments in nanodiscs

Keiichi Kojima, Ryo Maeda, Yasushi Imamoto, Takahiro Yamashita, Yoshinori Shichida (*Dept. Biophys., Grad. Sch. Sci., Kyoto Univ.*)

1F1436 脊椎動物非視覚オプシン Opn5 とその類似光受容タンパク質の分子的性質の解析

Analysis of the molecular properties of vertebrate non-visual opsins, Opn5 and Opn5-like protein

Takahiro Yamashita[1], Hideyo Ohuchi[2], Sayuri Tomonari[3], Sari Fujita-Yanagibayashi[1], Kazumi Sakai[1], Sumihare Noji[3], Yoshinori Shichida[1] ([1]*Grad. Sch. Sci., Kyoto Univ.*, [2]*Grad. Sch. Med. Dent. Pharm. Sci., Okayama Univ.*, [3]*Inst. Technol. Sci., Univ. Tokushima Grad.Sch.*)

1F1448 グロイオバクターロドプシンの光反応ダイナミクスの分光研究

Spectroscopic study of photoreaction dynamics of *Groeobacter* rhodopsin

Kumiko Nagata, Keiichi Inoue, Hideki Kandori (*Nagoya Inst. Of Technol.*)

休憩 15:00-15:10

1F1510 ASR の Pro206 はレチナール構造と光反応を制御する

Pro206 of Anabaena sensory rhodopsin is responsible for the isomeric composition of retinal and photochromism

Yoshitaka Kato[1], Akira Kawanabe[2], Kwang-Hwan Jung[3], Hideki Kandori[1] ([1]*Grad. Sch. Eng., Nagoya Inst. Tech.*, [2]*Grad. Sch. Med., Osaka Univ.*, [3]*Sogang Univ. Korea*)

1F1522 Large deformation of helix F upon formation of the M intermediate of the azide-bound purple form of pharaonis halorhodopsin

Taichi Nakanishi[1], Soun Kanada[1], Midori Murakami[1], Kunio Ihara[2], Tsutomu Kouyama[1] ([1]*Grad. Sch, Sci., Univ. Nagoya*, [2]*Center for Gene Research., Univ. Nagoya*)

1F1534 センサリーロドプシン II-トランスデューサー複合体の比較シミュレーションにより明らかにされた基底状態と M 中間体の差異

Differences between the ground state and the M-intermediate of Sensory Rhodopsin II-Transducer complex revealed by comparative simulations

Koro Nishikata[1,3], Mitsunori Ikeguchi[1], Akinori Kidera[1,2]

(¹*Grad. Sch. of Nanobioscience, Yokohama City Univ.*, ²*Research Program for Computational Science, RIKEN*, ³*Bioinformatics And Systems Engineering division (BASE), RIKEN*)

1F1546 **Effect of potential on the photo reaction of Sensory rhodopsin II monolayer studied by Surface Enhanced IR absorption Spectroscopy**

Kenichi Ataka, Joachim Heberle (*Freie Universitaet Berlin, Fachbereich Physik*)

1F1558 **In-situ 光照射固体 NMR による光受容膜蛋白質の光活性状態の解明**

Light activated states of photoreceptor membrane proteins as revealed by in-situ photo-irradiated solid-state NMR

Akira Naito[1], Yuya Tomonaga[1], Tetsurou Hidaka[1], Yusuke Shibafuji[1], Yoshiteru Makino[1], Izuru Kawamura[1], Yuki Sudo[2], Akimori Wada[3], Takashi Okitsu[3], Naoki Kamo[4] (¹*Graduate School of Engineering, Yokohama National University*, ²*Graduate School of Science, Nagoya University*, ³*Kobe Pharmaceutical University*, ⁴*Matsuyama University*)

14:00～16:22　G 会場　理学 B 館 2 階 212 ／ Room G: Sci. bldg. B 2F 212
細胞生物的課題 I
Cell Biology I

1G1400 **Larger Intercellular Adhesion Strength Generates More Coherent and Directional Multicellular Movement - Measurement and Simulation**

Tsuyoshi Hirashima[1], Takanori Iino[2], Yoichiroh Hosokawa[2], Masaharu Nagayama[3,4] (¹*Anatomy and Developmental Biology, Faculty of Medicine, Kyoto University*, ²*Graduate School of Materials Science, Nara Institute of Science and Technology*, ³*Research Institute for Electronic Science, Hokkaido University*, ⁴*CREST, Japan Science and Technology Agency*)

1G1412 **GPI アンカー型タンパク質の短寿命ホモダイマーはラフト組織化・機能のための最小単位である**

Transient GPI-anchored protein homodimers are units for raft organization and function

Kenichi G. N. Suzuki[1], Rinshi S. Kasai[1], Koichiro M. Hirosawa[1], Yuri L. Nemoto[1], Munenori Ishibashi[1], Yoshihiro Miwa[2], Takahiro K. Fujiwara[1], Akihiro Kusumi[1] (¹*iCeMS, Kyoto Univ.*, ²*Dept. Pharmacol., Univ. Tsukuba*)

1G1424 **ナノ秒パルス高電界は新規細胞ストレスとして作用して翻訳抑制を引き起こす**

Nanosecond pulsed electric fields act as a novel cellular stress that induces translational suppression

Ken-ichi Yano, Keiko Morotomi-Yano (*Bioelectrics Res. Center, Kumamoto Univ.*)

1G1436 **弾性膜モデルを用いたゴルジ再集合過程シミュレーション**

Simulation study on Golgi reassembly process based on elastic membrane model

Masashi Tachikawa, Atsushi Mochizuki (*Theoretical Biology Laboratory, ASI, RIKEN*)

1G1448 **Analysis of cell behavior near silicon based micro-scale pore**

Yo Otsuka[1], Shinya Murakami[1], Manabu Sugimoto[1], Toshiyuki Mitsui[2] (¹*Grad. Sch. Sci., Aogaku Univ*, ²*Assoc. Sci., Aogaku Univ*)

休憩 15:00-15:10

1G1510 **重イオンマイクロビーム照射によるバイスタンダー応答で誘導されるシグナル伝達機構の解明**

Mechanisms of signal transduction activated by heavy-ion microbeam induced bystander responses

Masanori Tomita[1], Hideki Matsumoto[2], Tomoo Funayama[3], Yuichiro Yokota[3], Kensuke Otsuka[1], Munetoshi Maeda[1,4], Yasuhiko Kobayashi[3] (¹*Radiat. Safety Res. Cent., CRIEPI*, ²*Biomed. Imaging Res. Cent., Univ. Fukui*, ³*QuBS, JAEA*, ⁴*R&D, WERC*)

1G1522 **出芽酵母の遺伝子発現パターンの変化における染色体揺らぎの影響**

Effects of conformational fluctuation of chromosomes in budding yeast on the pattern of gene expression

Naoko Tokuda, Masaki Sasai (*Grad. Sch. Eng., Univ. Nagoya*)

1G1534 **人工自己複製システムのダーウィン進化**

Darwinian Evolution of artificial self-replication system

Norikazu Ichihashi[1,2], Tetsuya Yomo[1,2,3] (¹*JST ERATO*, ²*Graduate School of Information Science and Technology, Osaka University*, ³*Graduate School of Frontier Bioscience, Osaka University*)

1G1546 **多点蛍光相関分光を用いた時空間解析によるグルココルチコイド受容体の核移行解析**

Nuclear translocation analysis of glucocorticoid receptor by spatiotemporal analysis with multipoint fluorescence correlation spectroscopy

Johtaro Yamamoto, Masataka Kinjo (*Fuc. Adv. Life Sci., Hokkaido Univ.*)

1G1558 **細胞内 FRET イメージングによる情報処理タンパク質 RAF の構造と EGF 応答の相関解析**

Correlation between the molecular conformation and EGF response of RAF by FRET imaging in individual cells

Kayo Hibino[1], Masahiro Ueda[1], Yasushi Sako[2] (¹*RIKEN, QBiC*, ²*RIKEN, ASI*)

1G1610 **1 分子キネティクス解析により示された、ヘレギュリンと ErbB タンパク質のダイナミックに変化する相互作用**

Interaction between heregulin and ErbB proteins varies dynamically shown by single-molecule kinetic analysis in living cells

Michio Hiroshima[1,2], Yuko Saeki[3], Mariko Okada-Hatakeyama[3], Yasushi Sako[1] (¹*RIKEN ASI*, ²*RIKEN QBiC*, ³*RIKEN RCAI*)

14:00～16:22　H 会場　理学 C 館 5 階 517 ／ Room H: Sci. bldg. C 5F 517
バイオイメージング
Bioimaging

1H1400 **ラスター画像相互相関分光法（ccRICS）を用いた外来 DNA に対する細胞内防御機構の可視化**

Visualization of intracellular defense system against exogenous DNAs by using cross-correlation raster image correlation spectroscopy

Akira Sasaki, Masataka Kinjo (*Fac. Adv. Life Sci., Hokkaido Univ.*)

1H1412 **Non-invasive in vivo imaging of vesicle movement in neutrophils in mouse ear**

Kenji Kikushima, Sayaka Kita, Hideo Higuchi (*Dept of Phys,*

School of Science, The Univ. of Tokyo)

1H1424 **脂質二重膜を用いた T 細胞活性化の 1 分子イメージング解析**
Single molecule analysis of T cell activation with stimulatory lipid bilayers by live cell imaging
Yuma Ito[1,2], Hirofumi Oyama[1,2], Kumiko Sakata-Sogawa[1,2], Makio Tokunaga[1,2] ([1]*Grad. Sch. Biosci. Biotech., Tokyo Inst. Tech.*, [2]*RCAI, RIKEN*)

1H1436 **GTP 交換促進因子 Sos の生細胞一分子計測**
Single molecule imaging of guanine nucleotide exchange factor Sos in living cells
Yuki Nakamura[1,2] ([1]*RIKEN sako celluar informatics laboratory*, [2]*Osaka university Yanagida lab*)

1H1448 **リガンド結合したβ 2 アドレナリン受容体の短寿命ダイマーは三量体 G タンパク質のターンオーバーを加速する：2 色同時 1 分子観察による測定**
Single-molecule imaging revealed acceleration of trimeric G-protein turnover by transient dimerization of liganded β2adrenergic receptor
Rinshi Kasai[1], Takahiro Fujiwara[2], Akihiro Kusumi[1,2] ([1]*Inst. For Frontier Med. Sci., Kyoto Univ.*, [2]*WPI-iCeMS, Kyoto Univ.*)

休憩 15:00-15:10

1H1510 **光学顕微鏡と同時観察可能な高速 AFM**
High-speed AFM combined with optical microscopy
Shingo Fukuda, Takayuki Uchihashi, Toshio Ando (*Depertment of Mathmatics and Physics, Grad School of Natural Science and Technology Kanazawa Univ*)

1H1522 **High-speed AFM observation of intrinsically disordered proteins (NTAIL-GFP, PNT-GFP and SIC1-GFP)**
Sujit Kumar Dora[1], Kodera Noriyuki[1], David Bloquel[2], Johnny Habchi[2], Antoine Gruet[2], Sonia Longhi[2], Toshio Ando[1] ([1]*Bio AFM frontier research center, Institute of physics and mathematics, Kanazawa University*, [2]*AFMB Laboratory, University of Aix-Marseille*)

1H1534 **位相差電子顕微鏡用の帯電防止位相板**
Anti-charging Phase Plates for Phase Contrast Electron Microscopy
Kuniaki Nagayama[1], Toshiyuki Itoh[2], Yoko Kayama[2], Zenpei Saitoh[2], Yukinori Nagatani[1], Yoshihiro Arai[2], Masahiro Ohara[1], Noriko Kai[2], Kazuyoshi Murata[1] ([1]*National Institute for Physiological Sciences*, [2]*Terabase Inc.*)

1H1546 **500kV LinacTEM の開発**
Development of the 500kV Linac TEM
Yukinori Nagatani[1], Yoshihiro Arai[2], Takumi Sannomiya[3], Tadao Shirai[4], Ryuzo Aihara[2], Giichi Iijima[2], Kuniaki Nagayama[1] ([1]*National Inst. Physiological Sci.*, [2]*Terabase Inc.*, [3]*Tokyo Inst. Tech.*, [4]*RTS*)

1H1558 **光学顕微鏡とカソードルミネッセンス顕微鏡を用いたマルチモーダル細胞イメージング**
Multimodal cellular imaging with light microscopy and cathodoluminescence microscopy
Hirohiko Niioka[1], Taichi Furukawa[2], Masayoshi Ichimiya[3], Tomohiro Nagata[4], Masaaki Ashida[2], Tsutomu Araki[2], Mamoru Hashimoto[2] ([1]*Inst. for NanoSci. Design, Osaka Univ.*, [2]*Eng. Sci., Osaka Univ.*, [3]*Osaka Dental Univ.*, [4]*Tsukuba Institute for Super Materials, ULVAC Inc.*)

1H1610 **精製タンパク質の構造から in situ の構造まで：電顕を使用して**
From purified protein structures to in situ structures using EM
Naoyuli Miyazaki[1,2], Mineo Iseki[3], Koji Hasegawa[4], Akihiro Narita[5], Shinichi Adachi[6], Masakatsu Watanabe[7], **Kenji Iwasaki**[1] ([1]*Institute for Protein Research, Osaka University*, [2]*National Institute for Physiological Sciences*, [3]*Pharmaceutical sciences, Toho University*, [4]*AdvanceSoft Corp.*, [5]*Structural Biology Research Center, Nagoya University*, [6]*Institute of Materials Structure Science, High Energy Accelerator Research Organization (KEK)*, [7]*The Graduate School for the Creation of New Photonics Industries*)

14:00〜16:22 I 会場　理学 E 館 1 階 131 ／ Room I: Sci. bldg. E 1F 131
生命情報科学，バイオエンジニアリング
Bioinformatics & Bioengineering

1I1400 **Analyzing the conservation of the folding nucleuses among the Ferredoxin-like fold in their amino acids sequence**
Masanari Matsuoka, Takeshi Kikuchi (*Dept. Bioinf., Coll. Life Sci., Ritsumeikan Univ.*)

1I1412 **RNA とタンパク質の相互作用におけるタンパク質構造変化のデータベース解析**
Database analysis of the degree of protein conformational changes in RNA-protein interactions
Chihiro Kubota[1], Kei Yura[1,2,3] ([1]*Graduate School of Humanities and Sciences, Ochanomizu University*, [2]*Center for Informational Biology, Ochanomizu University*, [3]*Center of Simulation Sciences, Ochanomizu University*)

1I1424 **天然変性タンパク質のデータベース IDEAL の構築**
Construction of IDEAL database for the investigation of intrinsically disordered proteins
Takayuki Amemiya[1], Shigetaka Sakamoto[2], Yukiko Nobe[1], Seiko D. Murakami[1], Kazuo Hosoda[3], Ryotaro Koike[1], Hidekazu Hiroaki[4], Motonori Ota[1], Satoshi Fukuchi[3] ([1]*Grad. Schl of Info. Sci.*, [2]*HOLONICS Co., Ltd.*, [3]*Fac. Engr., Maebashi Ins. Tech.*, [4]*Grad. Schl of Pharm. Sci., Nagoya Univ.*)

1I1436 **Computational analysis of protean segments (ProSs) in intrinsically disordered proteins (IDPs)**
Divya Shaji[1], Takayuki Amemiya[1], Satoshi Fukuchi[2], Motonori Ota[1] ([1]*Graduate school of information science, Nagoya University, Japan*, [2]*Faculty of Engineering, Maebashi Institute of Technology, Japan*)

1I1448 **MODIC: a novel ab inito identification system of transcription factor binding motifs in genome DNA sequences**
Masaru Tateno[1], Ryo Nakaki[2], Jiyoung Kang[2] ([1]*Grad. Sch. Sci., Univ. Hyogo*, [2]*Grad. Sch. Pure and Appl. Sci., Univ. Tsukuba*)

休憩 15:00-15:10

1I1510 **Interaction of DNA molecules with nanopore studied by fluorescence microscopy**
Genki Ando[1], Kazuteru Yamada[2], Toshiyuki Mitsui[1,2] ([1]*Grad. Mat.Sci., Univ. Aoyama*, [2]*Phys., Univ. Aoyama*)

1I1522 **診断用 DNA 計算に向けた核酸応答型 DNA 合成システムの構築**
Construction of a nucleic-acid-responsive DNA synthesis system for diagnostic DNA-based computing
Ken Komiya, Asako Kobayashi, Masayuki Yamamura (*Interdis. Grad. Sch. of Sci. and Engi., Tokyo Tech.*)

1I1534 **DNA scaffold logic: logic operation on molecular inputs using**

FRET cascades

Takahiro Nishimura[1], Yusuke Ogura[1], Hirotsugu Yamamoto[2], Kenji Yamada[3], Jun Tanida[3] ([1]*Osaka University*, [2]*The University of Tokushima*, [3]*Osaka University*)

1I1546 **寄生虫による接着性宿主細胞への侵入過程観察のためのマイクロ加工デバイスの作製**

Observation of parasite invasion with the micro-fabricated device

Tetsuhiko Teshima[1], Hiroaki Onoe[1], Kaori Kuribayashi-Shigetomi[1], Hiroka Aonuma[2], Hirotaka Kanuka[2], Shoji Takeuchi[1] ([1]*The Institue of Industrial Science*, [2]*Jikei University School of Medicine*)

1I1558 **金属還元菌 *Shewanella* における微生物呼吸代謝の電気化学的制御**

Electrochemical regulation of bacterial respiratory activity of *Shewanella*, a dissimilatory metal reducing bacteria

Shoichi Matsuda[1], Huan Liu[3], Shuji Nakanishi[2], Kazuhito Hashimoto[1,2,3] ([1]*Grad. Sch. Engr., Univ. Tokyo*, [2]*RCAST, Univ. Tokyo*, [3]*ERATO/JST*)

1I1610 **Spatiotemporal control of cell motility in nano- to micro-scale topographical environment**

Hiromi Miyoshi[1], Hiroyoshi Aoki[1], Jungmyoung Ju[1], Sang Min Lee[2], Jong Soo Ko[2], Yutaka Yamagata[1] ([1]*ASI, RIKEN*, [2]*Grad. Sch. Mech. Eng., Pusan National Univ.*)

14:00～16:10　A会場　理学南館１階 坂田・平田ホール／ Room A: Sci. south bldg. 1F Sakata Hirata Hall
分子モーターII：ダイニン
Molecular Motors II: Dynein

2A1400　クライオ電子線トモグラフィーを用いた細胞中骨格タンパク質およびモータータンパク質の非侵襲的構造解析
Observation of intracellular cytoskeleton and motor protein in the non-invasive cells with electron cryo-tomography
Shinji Aramaki[1], Kazuhiro Aoyama[2,3], Kota Mayanagi[4], Takuo Yasunaga[1] ([1]*Dept. of Bioscience and Bioinformatics, Grad. School of Computer Sci. and Sys. Eng., Kyushu Inst. of Tech.*, [2]*FEI Company Japan Ltd., Application Lab.*, [3]*Grad. School of Frontier Biosciences, Osaka Univ.*, [4]*Medical Inst. of Bioregulation, Kyushu Univ.*)

2A1412　クライオ電子線トモグラフィーを用いたクラミドモナス軸糸外腕ダイニンにおけるメタロチオネイン標識 LC2 の検出
Detection of metallothionein-tagged LC2 on *chlamydomonas* axonemal ODA by electron cryo-tomography
Mingyue Jin[1,4], Haru-aki Yanagisawa[2], Kotaro Koyasako[1,4], Ritsu Kamiya[2], Kota Mayanagi[3,4], Takuo Yasunaga[1,4] ([1]*Dep. Biosci. Bioinf., Inst. Tech. Kyushu*, [2]*Dep. Biol. Sci., Grad. Sch. Sci., Univ. Tokyo*, [3]*Div. Struct. Biol., Med. Inst. Bioreg., Univ. Kyushu*, [4]*JST*)

2A1424　クライオ電子顕微鏡法とメタロチオネインラベルを用いた軸糸構造の解明
Elucidation of Axoneme architecture by cryo-electron microscopy and metallothionein labeling
Reiko Chijimatsu[1], Mingyue Jin[1,2], Takuo Yasunaga[1,2] ([1]*Kyushu Institute of Technology*, [2]*JST*)

2A1436　電子線トモグラフィー法により明らかになった、LIS1 による細胞質ダイニンの運動活性制御メカニズム
Regulation of cytoplasmic dynein-motility on microtubules by LIS1 revealed by electron-computed tomography
Shiori Toba[1], **Kotaro Koyasako**[2,3], Shinji Hirotsune[1], Takuo Yasunaga[2,3,4] ([1]*Dept. Genetic Disease Research, Osaka City Univ. Grad. Sch. of Medicine*, [2]*Dept. Bioscience & Bioinformatics, Faculty of Computer Science and Systems Engineering, Kyushu Inst. Tech.*, [3]*JST-SENTAN*, [4]*JST-CREST*)

2A1448　ヌクレオチド状態に依存したダイニン分子の形態変化
Nucleotide-dependent morphological change of cytoplasmic dynein
Muneyoshi Ichikawa, Kei Saito, Takayuki Torisawa, Keitaro Shibata, Yuta Watanabe, Tomonori Hata, Yoko Toyoshima (*Grad. Sch. of Arts & Sci., Univ. of Tokyo*)

休憩 15:00-15:10

2A1510　頭部間の直接的相互作用は細胞質ダイニンの連続的な運動に必要ない
A direct interaction between dynein two heads is not necessary for processive movements of dynein
Keitaro Shibata, Yui Utsumi, Takayuki Torisawa, Yoko Toyoshima (*Dept. Life Sci., Grad. Sch. Arts and Sci., Univ. Tokyo*)

2A1522　外部負荷存在下でのヒト細胞質ダイニンのメカノケミカルサイクル
The mechanochemical cycle of human cytoplasmic dynein under external force
Taketoshi Kambara[1], Yoshiaki Tani[1], Motoshi Kaya[1], Tomohiro Shima[2], Hideo Higuchi[1] ([1]*Grad. Sch. Sci., Univ. Tokyo*, [2]*QBiC, Riken*)

2A1534　Rotation of microtubules driven by *Tetrahymena* 22S outer arm dynein and its sub-particles
Shin Yamaguchi, Yoko Toyoshima, Junichiro Yajima (*Dept Life Sciences, Graduate School of Arts and Sciences, Univ. of Tokyo.*)

2A1546　哺乳類細胞質ダイニンが一方向性を獲得する機構について
The mechanism of the transition from diffusion to directed movement in mammalian cytoplasmic dynein
Takayuki Torisawa[1], Furuta Ken'ya[2], Muneyoshi Ichikawa[1], Yoko Toyoshima[1] ([1]*Dept Life Sciences, Graduate School of Arts and Sciences, the Univ of Tokyo*, [2]*Bio ICT lab, NICT*)

2A1558　骨格筋形成過程における細胞質ダイニンの分布変化
The dynamic change of the distribution of cytoplasmic dynein during skeletal muscle differentiation process
Takuya Kobayashi, Motoshi Kaya, Hideo Higuchi (*Department of physics, Graduate school of science, The university of Tokyo*)

2A1610　ダイニンアダプター Bicaudal-D2 の細胞周期依存的核膜局在の分子機構
Molecular mechanism of cell-cycle dependent nuclear envelope localization of Bicaudal-D2
Takashi Murayama, Hiroki Ota, Takashi Sakurai (*Dept. Pharmacol., Juntendo Univ. Sch. Med.*)

14:00～16:22　B会場　多元数理科学棟５階 509 ／ Room B: Mathematics bldg. 5F 509
蛋白質-構造機能相関II：理論，凝集
Proteins: Structure & Function II: Theory, Aggregation

2B1400　単一アミノ酸ポテンシャル力場の改良と短鎖ペプチドの構造予測への応用
Improvement of the Single Amino Acid Potential Force Field and the Application to Structure Prediction of Short Peptides
Michio Iwaoka, Kenichi Dedachi, Taku Shimosato, Toshiya Minezaki (*Tokai Univ*)

2B1412　オンサーガー・マハラップ作用を用いたペプチド系のパスサンプリング
Path sampling for small peptide systems using the Onsager-Machlup action method
Hiroshi Fujisaki[1,2], Yasuhiro Matsunaga[2], Akinori Kidera[2,3] ([1]*Nippon Medical School*, [2]*RIKEN*, [3]*Yokohama City University*)

2B1424　蛋白質系のシミュレーションの緩和モード解析
Relaxation mode analysis for simulations of protein systems
Ayori Mitsutake, Toshiki Nagai, Hiroshi Takano (*Keio Univ.*)

2B1436　A multi-body potential for normal mode analysis of protein structure
Bhaskar Dasgupta, Narutoshi Kamiya, Haruki Nakamura, Akira Kinjo (*Institute for Protein Research, Osaka University*)

2B1448　アクチン線維へのコフィリンの協同的結合の統計力学モデルの作成
A theoretical model of cooperative binding of cofilin to actin filaments
Shotaro Sakakibara[2], Kimihide Hayakawa[1], Hitoshi Tatsumi[2], Masahiro Sokabe[1,2] ([1]*FIRST Research Center for Innovative*

Nanobiodevice, Univ. Nagoya, [2]*Grad. Sch. Med., Univ. Nagoya*)

休憩 15:00-15:10

2B1510 **リゾチーム分子中のアミロド性ペプチド**
Amyloidogenic Peptides from Hen Lysozyme
Hideki Tachibana[1,3], Masao Fujisawa[1,3], Ryohei Kono[2,3], Minoru Kato[4] ([1]*Sch Biol-Oriented Sci Tech, Kinki Univ*, [2]*Wakayama Med Univ*, [3]*High Press Prot Res Center, Kinki Univ*, [4]*Coll Pharm Sci, Ritsumeikan Univ*)

2B1522 **Effects of raft components on the membrane-mediated aggregation of IAPP**
Kenji Sasahara (*Kobe University*)

2B1534 **タンパク質が生体内レドックス環境に依存して異なる凝集体を形成するメカニズムとその病理学的意義**
Redox environment is an intracellular factor to operate distinct pathways for protein aggregation
Yoshiaki Furukawa (*Dept. of Chemistry, Keio Univ.*)

2B1546 **銅シャペロンに依存しない SOD1 酵素の活性化制御メカニズム**
A copper chaperone-independent mechanism for activation of Cu, Zn-superoxide dismutase
Yasuyuki Sakurai, Yoshiaki Furukawa (*Dept. of Chem, Keio Univ.*)

2B1558 **タンパク質凝集体の形態を制御する「凝集後修飾」のメカニズム**
A mechanism controlling the morphologies of protein aggregates by "post-aggregation oxidation"
Yasushi Mitomi[1], Takao Nomura[1], Masaru Kurosawa[2], Nobuyuki Nukina[2], Yoshiaki Furukawa[1] ([1]*Dept. of Chem, Keio Univ.*, [2]*RIKEN Brain Science Institute*)

2B1610 **ジスルフィド結合の組換えによる不溶性 SOD1 オリゴマーの新たな形成メカニズム－筋萎縮性側索硬化症における分子病理変化**
Destabilization of SOD1 facilitates abnormal scrambling of its disulfide bond in the familial form of amyotrophic lateral sclerosis
Keisuke Toichi, Yoshiaki Furukawa (*Dept. of Chem, Keio Univ.*)

14:00～16:22 C 会場 多元数理科学棟 4 階 409 ／ Room C: Mathematics bldg. 4F 409
数理生物学
Mathematical Biology

2C1400 **A Brownian particle undergoing reversible binding in a surface: exact theoretical results and an application in single molecule biophysics**
Ziya Kalay (*Institute for Integrated Cell-Material Sciences, Kyoto University*)

2C1412 **Single-particle-level simulation reveals effects of molecular crowding on biochemical signaling response**
Kazunari Kaizu, Koichi Takahashi (*Laboratory for Biochemical Simulation, RIKEN Quantitative Biology Center (QBiC)*)

2C1424 **2 つのヒートショック反応系における反応機構の比較**
Conflicted dissociation constant in two reaction mechanisms for heat shock response
Masayo Inoue[1], Ala Trusina[2], Namiko Mitarai[2], Kim Sneppen[2] ([1]*CMC, Osaka Univ.*, [2]*CMOL, NBI*)

2C1436 **Mathematical analysis for vascular and spot patterns by auxin and PIN dynamics in plant development**
Yoshinori Hayakawa[1,2], Atsushi Mochizuki[1,2] ([1]*Tokyo Institute of Technology*, [2]*Wako Inst., Riken*)

2C1448 **Modeling wave propagation dynamics in MDCK wound healing assay**
Yusuke Sawabu[1], Masaharu Nagayama[2], Takashi Miura[3], Hiroyuki Kitahata[4] ([1]*Inst. of Nat. Sci. and Tech., Kanazawa Univ.*, [2]*Res. Inst. for Elect. Sci. Hokkaido Univ.*, [3]*Kyoto Univ. Grad. Sch. Of Med.*, [4]*Dept. of Phys., Chiba Univ., Grad. Sch. of Sci.*)

休憩 15:00-15:10

2C1510 **CA モデルによる多細胞性シアノバクテリアの形態形成ダイナミクスの解析**
Analysis of the internal dynamics for pattern formation in multi cellular cyanobacteria by CA model
Jun-ichi Ishihara[1,2], Masashi Tachikawa[2], Hideo Iwasaki[1], Atsushi Mochizuki[2] ([1]*Grad.Sci.Eng., Waseda Univ.*, [2]*Wako Inst., RIKEN*)

2C1522 **Modeling the mammalian circadian clock**
Craig Jolley, Hiroki Ueda (*RIKEN Center for Developmental Biology, Laboratory for Systems Biology*)

2C1534 **Determining the ratio of longitudinal to transverse conductivity in a cardiac tissue culture through application of FFP**
Marcel Hoerning[1], Seiji Tagaki[2], Kenichi Yoshikawa[3,4] ([1]*RIKEN, Center for Developmental Biology, Physical Biology Unit*, [2]*Hokkaido University, Research Institute for Electronic Science*, [3]*Doshisha University, Life and Medical Sciences*, [4]*Kyoto University, Department of Physics*)

2C1546 **気道上皮細胞における Cl^- 分泌の数理モデル**
Mathematical model of Cl^- secretion in airway epithelial cells
Kouhei Sasamoto[1], Naomi Niisato[2,3], Yoshinori Marunaka[2,3] ([1]*Undergraduate Student, Kyoto Prefectural Univ. Med.*, [2]*Molecular Cell Physiology, Kyoto Prefectural Univ. Med.*, [3]*Japan Institute for Food Education and Health, Heian Jogakuin (St. Agnes') Univ.*)

2C1558 **エラーカタストロフィーによる HIV-1 擬種集団の自壊過程に関する研究**
A Study on a Self-Destruction Process of a HIV-1 Quasispecies Population through the Error Catastrophe
Kouji Harada (*Toyohashi Univ. of Tech. Dept. of Comp. Sci. and Eng.*)

2C1610 **Characterization of Death and Division Process in Synthetic Bacterial Population with Antibiotic Treatment**
Takashi Nozoe[1], Reiko Okura[1], Yuichi Wakamoto[2,3] ([1]*Grad. Sch. Arts and Sci., Univ. Tokyo*, [2]*Research Center for Complex Systems Biology, Univ of Tokyo*, [3]*JST PRESTO*)

14:12～16:10 D 会場 多元数理科学棟 3 階 309 ／ Room D: Mathematics bldg. 3F 309
計測
Measurements

2D1412 **クライオ電子線トモグラフィーに対する超分解能技術**
Super-resolution cryo-electron tomography
Ryuzo Azuma[1,2], Takuo Yasunaga[1,2] ([1]*Grad. Sch. of Comp. Sc. & Eng., Dept. of Biosc. & Bioinfo., Kyushu Inst. of Tech.*, [2]*JST*)

2D1424 **定量位相顕微鏡による生細胞におけるナノスケールの形状変化の非染色ビデオレートイメージング**

Label-free and video-rate imaging of live cell membrane motion in the nanometer-scale by quantitative phase microscope

Toyohiko Yamauchi[1], Takashi Sakurai[2], Hidenao Iwai[1], Yutaka Yamashita[1] ([1]*Hamamatsu Photonics*, [2]*EIIRIS, Toyohashi Univ. of Tech.*)

2D1436 **ラマン分光を用いた超音波照射による細胞への影響の評価**

Evaluation of Ultrasound Irradiation effects on Cells by using Raman Spectroscopy

Manabu Sugimoto[1], Yo Otsuka[1], Shinya Murakami[1], Toshiyuki Mitsui[2] ([1]*Grad. Sci Eng., Aogaku Univ*, [2]*Assoc Prof, Aogaku Univ*)

2D1448 **脂肪酸と 7-ヒドロキシ-4-メチルクマリンを用いた質量と蛍光測定によるアンモニアの二次元検出**

Two dimensional ammonia sensing by measurement of mass and fluorescence using 7-hydroxy-4-methylcoumarin film and fatty acid

Yuta Ando, Masahiro Terashita, **Ryohei Matsueda**, Yutaka Tsujiuchi (*Department of Material Science and Engineering, Akita University*)

休憩 15:00-15:10

2D1510 **インビトロ心毒性予測のための心筋細胞ネットワークの時間的細胞外電位ゆらぎと空間的伝達速度ゆらぎの評価**

Evaluation of temporal fluctuation and spatial fluctuation on cardiomyocyte network for *in vitro* predictive cardiotoxicity measurement

Tomoyo Hamada, Fumimasa Nomura, Tomoyuki Kaneko, Kenji Yasuda (*Institute of Biomaterials and Bioengineering, Tokyo Medical and Dental University*)

2D1522 **SACLA における非結晶粒子の低温 X 線回折イメージング実験**

Cryogenic Coherent X-ray Diffraction Imaging of non-crystalline particles at SACLA

Masayoshi Nakasako[1,2], Yuki Takayama[1,2], Tomotaka Oroguchi[1,2], Yuki Sekiguchi[1,2], Masaki Yamamoto[2], Koji Yonekura[2], Takaaki Hikima[2], Saori Maki-Yonekura[2], Yukio Takahashi[3], Akihiro Suzuki[3], Sachihiro Matsunaga[4], Shoichi Kato[4], Takahiko Hoshi[5] ([1]*Department of Physics, Keio University*, [2]*RIKEN SPring-8 Center, RIKEN Harima Institute*, [3]*Department of Precision Science and Technology, Graduate School of Engineering, Osaka University*, [4]*Department of Applied Biological Science, Faculty of Science and Technology, Tokyo University of Science*, [5]*Kohzu Precision Co.,Ltd.*)

2D1534 **A protocol for structure analysis of non-crystalline particles with X-ray free electron laser**

Tomotaka Oroguchi, Masayoshi Nakasako (*Department of Physics, Faculty of Science and Technology, Keio University*)

2D1546 **イオンコンダクタンス顕微鏡による細胞膜揺らぎの測定**

Fluctuation of cell membrane investigated by ion conductance microscopy

Yusuke Mizutani[2], Satoshi Ichikawa[1], Zen Ishikura[1], **Takaharu Okajima**[1] ([1]*Grad. Sch. Inform. Sci. Tech., Hokkaido Univ.*, [2]*Grad. Sch. Life Sci., Hokkaido Univ.*)

2D1558 **Relationship between Intercellular Adhesion Strength and Communication Detected by Femtosecond Laser-induced Impulsive Force**

Takanori Iino[1], Man Hagiyama[2], Tadahide Furuno[3], Akihiko Ito[2], Yoichiroh Hosokawa[1] ([1]*Nara Institute of Science and Technology*, [2]*Kinki University*, [3]*Aichi Gakuin University*)

14:00〜16:22　E 会場　多元数理科学棟 1 階 109 ／ Room E: Mathematics bldg. 1F 109
蛋白質-物性 II
Proteins: Property II

2E1400 **AFM を用いたホロミオグロビンの一分子力学計測によるアンフォールディング経路の探索**

Mechanical unfolding pathways of holo-myoglobin explored by AFM-based single molecule force spectroscopy

Aya Yoshida, Masaru Kawakami (*Materials Sci, JAIST*)

2E1412 **走査型プローブ顕微鏡を用いた癌抑制因子 p53 の一分子構造解析**

Single-molecule structural analysis of tumor suppressor p53 using scanning probe microscopes

Seiya Takahashi[1], Yasuyuki Sainoo[1], Risa Kashima[2], Takashi Tokino[3], Tadahiro Komeda[1], Satoshi Takahashi[1], **Kiyoto Kamagata**[1] ([1]*IMRAM, Tohoku Univ.*, [2]*Univ. California*, [3]*Res. Inst. Front. Med., Sapporo Med. Univ. Sch. Med.*)

2E1424 **塩基性条件下でのヒトガレクチン 1 のβガラクトシド結合能力**

β-Galactoside-binding activity of human galectin-1 at basic pH

Hirotsugu Hiramatsu, Tomohide Nishino, Hideo Takeuchi (*Graduate School of Pharmaceutical Sciences, Tohoku University*)

2E1436 **A Molecular Mechanism of Induced-fit of U1A Protein**

Ikuo Kurisaki[1,2], Masayoshi Takayanagi[1,2], Masataka Nagaoka[1,2] ([1]*Grad. Sch. Info. Sci. Univ. Nagoya*, [2]*CREST, JST*)

2E1448 **Single mutation on a loop alters the key dynamics of the core, but not the average structure**

Akihiro Maeno[1], Sunilkumar P.N.[1], Yuji Wada[2], Eiji Ohmae[2], Shin-ichi Tate[2], Kazuyuki Akasaka[1] ([1]*HPPRC, Kinki Univ.*, [2]*Grad. Sch. Sci., Univ. Hiroshima*)

休憩 15:00-15:10

2E1510 **ヒト主要組織適合複合体の安定化に置ける揺らぎの重要性について**

The effect of flexibility on the stability of Human Leucocyte Antigen

Saeko Yanaka[1], Kenjji Sugase[2], Takamasa Ueno[3], Kouhei Tsumoto[1] ([1]*Med. Genome Sci., Grad. Sch. Frontier Sci., the Univ. of Tokyo*, [2]*Suntory Institue for Bioorganic research*, [3]*Center for AIDS Research, Kumamoto Univ.*)

2E1522 **Cavity-dependent dynamics of c-Myb R2R3 revealed by high-pressure fluorescence and NMR spectroscopy**

Satomi Inaba[1], Akihiro Maeno[2], Hisayuki Morii[3], Harumi Fukada[4], Kazuyuki Akasaka[2], Masayuki Oda[1] ([1]*Grad. Sch. of Life and Environ. Sci., Kyoto Pref. Univ.*, [2]*High Pressure Protein Res. Center, Kinki Univ.*, [3]*Biomed. Res. Inst., Natl. Inst. Adv. Ind. Sci. Technol.*, [4]*Grad. Sch. of Life and Environ. Sci., Osaka Pref. Univ.*)

2E1534 **単純化 BPTI に融合したペプチド系タグ配列を用いたアミノ酸溶解性の測定**

Analysis of amino acid contributions to protein solubility using short peptide tags fused to a simplified BPTI variant

Yutaka Kuroda[1], Alam, M. Khan[1], Mohammad, M. Islam[1,2] ([1]*Dept of Biotech and Life Sci, TUAT*, [2]*Dept of Mol Biol and Biochem, Chittagon University*)

2E1546 **Protein Aggregation Kinetics Using Short Amino acid**

Peptide Tags

Monsur A. Khan[1], Mohammad M. Islam[1,2], Yutaka Kuroda[1] ([1]*Tokyo University of Agriculture and Technology*, [2]*University of Chittagong, Bangladesh*)

2E1558 **Protein specific partial charges by Ab-initio fragment molecular orbital method for more accurate protein simulations**

Le Chang, Shoji Takada (*Grad. Sch. Sci., Kyoto Univ.*)

2E1610 **Regulatory Mechanism of the fluorescence emission from Green Fluorescent Protein Chromophore**

Jumpei Torii, Shoji Yamashita, Etsuko Nishimoto (*Institute of Biophysics, Faculty of Agriculture, Graduate school of Kyushu University*)

14:00〜16:10　F 会場　理学 B 館 5 階 501 ／ Room F: Sci. bldg. B 5F 501
光生物-視覚，光受容 II
Photobiology: Vision & Photoreception II

2F1400 **全原子量子化学計算によるレチナールタンパク質の吸収波長制御機構の解析**

Full-Quantum Chemical Calculations of the Absorption Maxima of Retinal Proteins

Tomohiko Hayashi[1], Azuma Matsuura[2], Hiroyuki Sato[2], Minoru Sakurai[1] ([1]*Center for Biological Resources and Informatics, Tokyo Institute of Technology*, [2]*Fujitsu Laboratories, Ltd.*)

2F1412 **プロテオロドプシンにおける細胞質側ループの変異がもたらす遠隔的波長制御メカニズム**

Mechanism of color change of proteorhodopsin by mutations at distant cytoplasmic loop

Yuya Ozaki[1], Rei Abe-Yoshizumi[1], Susumu Yoshizawa[2], Kazuhiro Kogure[2], Hideki Kandori[1] ([1]*Grad. Sch. Eng., Nagoya Inst. Tech*, [2]*AORI, Univ. Tokyo*)

2F1424 **キメラタンパク質を用いた Rhodobacter capsulatus 由来 Photoactive Yellow Protein の相互作用部位の解明**

Analysis of interaction sites on the Photoactive Yellow Protein of Rhodobacter capsulatus with chimeric proteins

Mayu Shimad, Yoichi Yamazaki, Hironari Kamikubo, Mariko Yamaguchi, Mikio Kataoka (*Grad. Sch. Mat. Sci., NAIST*)

2F1436 **FTIR study of Aureochrome that possesses LOV domain at the C-terminus**

Shota Ito[1], You Zhang[1], Tatsuya Iwata[2], Osamu Hisatomi[3], Fumio Takahashi[4], Hironao Kataoka[5], Hideki Kandori[1] ([1]*Nagoya Inst. Tech*, [2]*Ctr. Fost. Yng. Innov., Nagoya Inst. Tech*, [3]*Grad. Sch. Sci., Osaka Univ*, [4]*PRESTO, JST*, [5]*Botanical Gardens, Tohoku Univ*)

2F1448 **LOV ドメインを鋳型としたレドックス感受性蛍光タンパク質の開発**

Construction of LOV-based redox-sensitive fluorescent proteins

Yukiko Ono[1], Tatsuya Iwata[2], Hideki Kandori[1] ([1]*Nagoya Inst. Of Technol.*, [2]*Ctr. Fost. Yng. Innov. Res., Nagoya Inst. Tech.*,)

休憩 15:00-15:10

2F1510 **クラミドモナス由来の全長フォトトロピンが示す光反応ダイナミクスの時間分解検出**

Time-resolved study on photoreaction dynamics of full-length phototropin from Chlamydomonas reinhardtii

Yusuke Nakasone[1], Koji Okajima[2], Yusuke Aihara[3], Akira Nagatani[3], Satoru Tokutomi[2], Masahide Terazima[1] ([1]*Grad. Chem. Sci, Kyoto Univ.*, [2]*Grad. Sci, Osaka Prefecture Univ.*, [3]*Grad. Biol. Sci, Kyoto Univ.*)

2F1522 **N 末アミノ酸残基の有無は AppA BLUF ドメインの保存されたトリプトファン残基の位置に影響しない**

N-Terminal Truncation Does Not Affect the Location of a Conserved Tryptophan in the BLUF Domain of AppA from *Rhodobacter sphaeroide*

Masashi Unno[1], Yuuki Tsukiji[1], Kenshuke Kubota[1], Shinji Masuda[2,3] ([1]*Depart. Chem. Appl. Chem., Saga University*, [2]*Center for BioRes. & Inform., Tokyo Inst. Tech.*, [3]*PRSTO, JST*)

2F1534 **Substrate-Dependent Measurement Revealed Different Protein Conformations on Photoactivation and DNA Repair of E. coli CPD Photolyase**

I Made Mahaputra Wijaya[1], Yu Zhang[1], Junpei Yamamoto[2], Kenichi Hitomi[3], Shigenori Iwai[2], Elizabeth D. Getzoff[3], Hideki Kandori[1] ([1]*Nagoya Institute of Technology*, [2]*Osaka University*, [3]*The Scripps Research Institute, La Jolla, USA*)

2F1546 **アニオンラジカル型の(6-4)光回復酵素による DNA 修復**

Repair of damaged DNA by the anion radical form of (6-4) photolyase

Daichi Yamada[1], Yu Zhang[1], Tatsuya Iwata[2], Junpei Yamamoto[3], Kenichi Hitomi[4], Shigenori Iwai[3], Elizabeth Getzoff[4], Hideki Kandori[1] ([1]*Nagoya Inst. Tech.*, [2]*Ctr. Fost. Yng. Innov. Res., Nagoya Inst. Tech.*, [3]*Grad. Sch. Eng. Sci., Osaka Univ.*, [4]*The Scripps Res. Inst. USA*)

2F1558 **光センサータンパク質 UVR8 の解離・回復反応カイネティックスの測定**

The study of the dissociation and recovery reaction kinetics for photo-sensor protein UVR8

Takaaki Miyamori[1], Yusuke Nakasone[1], Kenichi Hitomi[2], John M. Christie[3], Elizabeth D. Getzoff[2], Masahide Terazima[1] ([1]*Grad. Sci. Chem., Univ. Kyoto*, [2]*Scripps Research Inst.*, [3]*Univ. Glasgow*)

14:00〜16:22　G 会場　理学 B 館 2 階 212 ／ Room G: Sci. bldg. B 2F 212
生体膜・人工膜
Biological & Artificial Membranes

2G1400 **膜融合におけるストーク構造からの変形：分子動力学シミュレーション**

Morphology change of fusion stalk studied by molecular dynamics simulation

Shuhei Kawamoto, Wataru Shinoda (*Nano. AIST*)

2G1412 **蛍光検出と電気計測による膜タンパク質計測に向けた脂質膜チャンバアレイ**

Lipid bilayer chamber array toward fluorescent and electrophysiological measurement of membrane proteins

Taishi Tonooka[1], Ryuji Kawano[2], Koji Sato[1], Toshihisa Osaki[2], Shoji Takeuchi[1] ([1]*Institute of Industrial Science, The University of Tokyo*, [2]*Kanagawa Academy of Science and Technology*)

2G1424 **蛋白質毒素ライセニンがスフィンゴミエリンを含む脂質膜中に誘起するポア形成： 単一 GUV 法による研究**

Single Giant Unilamellar Vesicle Method Reveals Lysenin-Induced Pore Formation in Lipid Membranes Containing

Sphingomyelin

Jahangir Md. Alam[1], Toshihide Kobayashi[2], Masahito Yamazaki[1] ([1]*Int. Biosci. Sec., Grad. Sch. Sci. Tech., Shizuoka University*, [2]*Lipid Bio. Lab., RIKEN*)

2G1436 人工細胞ベシクルにおける脂質ドメインへの化合物局在を介したドメインサイズと膜崩壊率の制御

Localization of bulky-molecules in raft-like domains on phase-separated liposomes: Control of domain size and bursting rate of liposome

Miho Yanagisawa[1], Damien Baigl[2], Kenichi Yoshikawa[3] ([1]*Grad. Sch. Sci., Kyushu Univ.*, [2]*Depart. Chem., Ecole Normale Superieure*, [3]*Depart. Biomed. Info., Doshisya Univ.*)

2G1448 PI4P と脂質膜曲率による Kes1 ステロール輸送活性の制御

Regulation of Kes1 sterol transport activity by PI4P and lipid membrane curvature

Hirokazu Yokoyama[1], Masaki Wakabayashi[1], Yasushi Ishihama[1], Minoru Nakano[2] ([1]*Graduate School of Pharmaceutical Sciences, Kyoto University*, [2]*Graduate School of Medicine and Pharmaceutical Sciences, University of Toyama*)

休憩 15:00-15:10

2G1510 リン脂質輸送タンパク質 Sec14 の脂質輸送メカニズムの解明

Elucidation of lipid transfer mechanism of phospholipid transfer protein Sec14

Chisato Takahashi[1], Makiko Yamada[1], Masaki Wakabayashi[1], Yasushi Ishihama[1], Minoru Nakano[2] ([1]*Grad. Sch. Pharm., Kyoto Univ.*, [2]*Grad.Sch.Pharm., Toyama Univ.*)

2G1522 ゲル、アミノ酸、水素化アモルファスシリコンを用いた光制御イオン伝導整流素子

Photo-controlled ion conductive rectification element using gel, amino acids and hydrogenated amorphous silicon film

Takaaki Ichikawa[1], **Hiroki Suzuki**[1], Ryohei Matsueda[1], Hiroshi Masumoto[2], Takashi Goto[3], Yutaka Tsujiuchi[1] ([1]*Department of Material Science and Engineering, Akita University*, [2]*Center for Interdisciplinary Research, Tohoku University*, [3]*Institute for Materials Research, Tohoku University*)

2G1534 高速 AFM による CFTR チャネルの動態観察

Single molecular observation of CFTR channels by high speed AFM

Hayato Yamashita[1], Kazuhiro Mio[2], Muneyo Mio[2], Takayuki Uchihashi[3], Masato Yasui[1], Toshio Ando[3], Yoshiro Sohma[1,4] ([1]*Pharmacol., Keio Univ. Med. Sch.*, [2]*AIST*, [3]*Dept of Physics, Kanazawa Univ.*, [4]*Dalton Cardiovas. Res. Cen., Univ. Missouri-Columbia*)

2G1546 KcsA チャネルの細胞内ドメインは不活性化に影響を与える

The KcsA channel cytoplasmic domain effects on the inactivation gating

Minako Hirano[1,2], Yukiko Onishi[2], Daichi Okuno[2], Toru Ide[1,2] ([1]*GPI*, [2]*RIKEN*)

2G1558 原子間力顕微鏡によるカリウムイオンチャネル KcsA の脂質膜中でのゲート開閉構造の直接観察

Direct Observation of Ion Entryway of Potassium Channel KcsA in Lipid Bilayer by Atomic Force Microscopy

Ayumi Sumino[1], Takashi Sumikama[2], Masayuki Iwamoto[2], Takahisa Dewa[1,3], Shigetoshi Oiki[2] ([1]*Grad. Sch. Eng., Nagoya Inst. Tech.*, [2]*Deprt. of Mol. Physiol. and Biophys., Univ. of Fukui Fac. Med. Sci.*, [3]*JST-PRESTO*)

2G1610 全反射赤外分光法による KcsA のイオン選択フィルターの振動解析

The Vibrational Analysis of the Selectivity Filter of KcsA by using ATR-FTIR Spectroscopy

Yuji Furutani[1,2], Hirofumi Shimizu[3], Yusuke Asai[1], Tetsuya Fukuda[1], Shigetoshi Oiki[3], Hideki Kandori[1] ([1]*Grad. Sch. Tech., Nagoya Inst. Tech.*, [2]*Inst. Mol. Sci.*, [3]*Facul. Med. Sci., Univ. Fukui*)

14:00〜16:22 H 会場 理学 C 館 5 階 517 ／ Room H: Sci. bldg. C 5F 517

筋肉
Muscle

2H1400 中性子散乱による心筋症関連トロポニン変異体のダイナミクス測定

Dynamics of cardiomyopathy-causing mutant of troponin observed by neutron scattering

Tatsuhito Matsuo[1], Francesca Natali[3], Giuseppe Zaccai[2,3], Satoru Fujiwara[1] ([1]*QuBS, JAEA*, [2]*CNRS*, [3]*ILL*)

2H1412 スピンラベル ESR 距離測定による細いフィラメントのアクチン、トロポミオシン、トロポニンの動的構造解析

Structural dynamics of actin, tropomyosin, and troponin in the thin filament as studied by distance measurements using spin-labeling ESR

Keisuke Ueda[1,2], Chenchao Zhao[1], Akie Yamamoto[1], Takayasu Somiya[1], Tomoki Aihara[1,3], Shoji Ueki[4], Masao Miki[5], **Toshiaki Arata**[1] ([1]*Grad. Sch. Sci., Osaka Univ.*, [2]*Inst. Prot. Res., Osaka Univ.*, [3]*Harima Inst., Riken*, [4]*Tokushima-Bunri Univ.*, [5]*Univ. Fukui*)

2H1424 アクチン周りのハイパーモバイル水の形成とその熱力学的考察

Formation of hyper-mobile water around actin and its thermodunamic considerations

Makoto Suzuki, George Mogami, Tetsuichi Wazawa, Asato Imao, Noriyoshi Ishida (*Tohoku Univ. Grad. Sch. Eng.*)

2H1436 アクチン様トレッドミリングモータが満たすべき最小条件

Minimum requirements for the actin-like treadmilling motor system

Akihiro Narita (*Grad. Sch. Sci., Nagoya Univ.*)

2H1448 3 次元トラッキングによる *in vitro* アクチンフィラメントモーティリティーアッセイ

Three-dimensional tracking of gliding actin filament in an *in vitro* motility assay

Tatsuya Naganawa, Togo Shimozawa, Tomoko Masaike, Takayuki Nishizaka (*Gakushuin Univ.*)

休憩 15:00-15:10

2H1510 Ca^{2+}に依存しない熱パルスによる心筋細胞の On-Off 制御

Ca^{2+}-independent on-off regulation of a cardiomyocyte by microscopic heat pulses

Kotaro Oyama[1], Akari Mizuno[1], Seine Shintani[1], Hideki Itoh[1], Takahiro Serizawa[1], Norio Fukuda[2], Madoka Suzuki[3,4], Shin'ichi Ishiwata[1,3,4] ([1]*Sch. Adv. Sci. Eng., Waseda Univ.*, [2]*Dept. Cell Physiol., Jikei Univ. Sch. Med.*, [3]*Org. Univ. Res. Initiatives, Waseda Univ.*, [4]*WABIOS, Waseda Univ.*)

2H1522 ミオシン分子の非線形弾性とフィラメントの弾性変形を考慮した筋収縮のシミュレーション

The Effects of Nonlinear Elasticity of Myosin Molecules on Muscle Contraction Studied by Numerical Simulation

Keita Miyamoto, Kazuo Sasaki (*Dept. Appl. Phys., Sch. Eng., Tohoku Univ.*)

2H1534 高塩濃度溶液中における熱変性したミオシン分子のミオシンフィラ

メントへの付着

Adhesion of heat-denatured myosin molecules to myosin filament at high salt concentration

Masato Shimada[1], Eisuke Takai[1], Daisuke Ejima[2], Kentaro Shiraki[1] ([1]*Facul. of Pure and Appl. Sci., Univ. of Tsukuba.*, [2]*Institute for Innovation, Ajinomoto Co. Inc.*)

2H1546　ラット幼若心筋細胞内サルコメア集団の自励振動(SPOC)特性

Auto-oscillation (SPOC) properties of sarcomeres in rat neonetal cardiomyocytes

Seine Shintani[1], Kotaro Oyama[1,2], Norio Fukuda[2], Shin'ichi Ishiwata[1,3] ([1]*Sch. Adv. Sci. Eng., Waseda Univ.*, [2]*Dept. Cell Physiol., Jikei Univ. Sch. Med.*, [3]*WABIOS, Waseda Univ.*)

2H1558　横紋筋サルコメアのフィラメント格子の安定性

Stability of Myofilament Lattice in Striated Muscle Sarcomere

Shigeru Takemori[1], Masako Kimura[2], Maki Yamaguchi[1], Tetsuo Ohno[1], Naoya Nakahara[1], Shunnya Yokomizo[3] ([1]*Jikei Univ. Sch. Med.*, [2]*Kagawa Nutrition Univ.*, [3]*Tokai Univ. Graduate Sch. Physical Education*)

2H1610　羽ばたくマルハナバチ中で拮抗する 2 種の飛翔筋の超高速 X 線回折像同時記録

Simultaneous ultrafast X-ray recordings of actions of two antagonistic flight muscles during wingbeat of live bumblebee

Hiroyuki Iwamoto, Naoto Yagi (*SPring-8, JASRI*)

14:00〜16:22　I 会場　理学 E 館 1 階 131 ／ Room I: Sci. bldg. E 1F 131
細胞生物的課題 II：Prokaryotes
Cell Biology II: Prokaryotes

2I1400　海洋性ビブリオ菌の周毛性べん毛形成の抑制に関与する DnaJ モチーフを持った新規遺伝子の解析

A novel gene of dnaJ family plays a role in the suppression of flagellation in Vibrio alginolyticus

Takehiko Nishigaki[1], Maya Kitaoka[1], Kunio Ihara[2], Noriko Nishioka[1], Seiji Kojima[1], Michio Honma[1] ([1]*Grad. Sch. Sci., Univ. Nagoya*, [2]*Gene., Univ. Nagoya*)

2I1412　バクテリアIV型線毛の粘着脱離動力学

Unbinding Dynamics of Type IV Pili

Tomonari Sumi[1,2], Rahul Marathe[2], Stefan Klumpp[2] ([1]*Dept. Comp. Sci. Eng., Toyohashi Univ. Tech.*, [2]*Dept. Theo. & Biosyst., Max Planck Inst. Colloids & Interfaces*)

2I1424　細菌べん毛特異的シャペロン FliT の C 末αヘリックの役割

Role of the C-terminal α-helix of FliT chaperone in the export of its cognate substrate FliD

Tohru Minamino[1], Miki Kinoshita[1,2], Noritaka Hara[1], Katsumi Imada[2], Keiichi Namba[1,3] ([1]*Grad. Sch. Frontier Biosci., Osaka Univ.*, [2]*Grad. Sch. Sci., Osaka Univ.*, [3]*QBiC RIKEN*)

2I1436　べん毛輸送装置近傍の局所 pH に対する FliI ATPase の効果

Effect of FliI ATPase on local pH around the bacterial flagellar protein export apparatus

Yusuke V. Morimoto[1,2], Nobunori Kami-ike[1], Tomoko Miyata[1], Keiichi Namba[1,2], Tohru Minamino[1] ([1]*Grad. Sch. Frontier Biosci., Osaka Univ.*, [2]*QBiC, RIKEN*)

2I1448　Na^+駆動型べん毛モーター固定子タンパク質 PomA の細胞質ループ領域の示差走査熱量測定を用いた性質検討

Characterization of cytoplasmic loop of PomA, Na^+-driven flagellar stator protein, using differential scanning calorimetry

Shiori Kobayashi[1], Rei Abe-Yoshizumi[1,2], Mizuki Gohara[1], Seiji Kojima[1], Michio Homma[1] ([1]*Division of Biological Science, Graduate School of Science, Nagoya University*, [2]*Department of Frontier Materials, Nagoya Institute of Technology*)

休憩 15:00-15:10

2I1510　プラグを欠失した Na^+駆動型べん毛モーター固定子複合体の精製・再構成系の構築

Purification and reconstitution of the plug-deleted Na^+-driven stator complex from *Vibrio alginolyticus*

Tetsuya Oba, Seiji Kojima, Michio Homma (*Division of Biological Science, Graduate school of science, Nagoya University*)

2I1522　蛍光相関分光法（FCS）を用いたべん毛モーターを構成するタンパク質間の相互作用解析

Analysis of interactions between rotor proteins of flagellar motor using Fluorescence Correlation Spectroscopy

Takaaki Kishi, Seiji Kojima, Michio Homma (*Division of Biological Science, Graduate School of Science, Nagoya University, Chikusa-ku, Nagoya, Japan.*)

2I1534　Na^+駆動型べん毛モーターの固定子と回転子間における荷電残基変異による協調作用の解析

Synergetic effects of the mutations of charged residues between the rotor and the stator in the Na^+-driven flagellar motor

Norihiro Takekawa, Seiji Kojima, Michio Homma (*Div. of Biol. Sci., Grad. Sch. of Sci., Nagoya Univ.*)

2I1546　光分解されたセリンへの大腸菌の応答計測

Measurement of cellular response of single *E. coli* to the photoreleased serine

Takashi Sagawa[1], Hajime Fukuoka[2], Yuichi Inoue[2], Hiroto Takahashi[2], Takahiro Muraoka[2], Kazushi Kinbara[2], Akihiko Isjijima[2] ([1]*Grad. Sch. Life Sci., Tohoku Univ.*, [2]*IMRAM, Tohoku Univ.*)

2I1558　CheZ 極局在の有無における大腸菌細胞内シグナル伝達の計測

Propagation of intracellular signaling molecule in the presence and absence of polar localization of CheZ in a single *E. coli* cell

Hajime Fukuoka[1], Takashi Sagawa[2], Yuichi Inoue[1], Hiroto Takahashi[1], Akihiko Ishijima[1] ([1]*IMRAM, Tohoku Univ.*, [2]*Grad. Sch. life Sci., Tohoku Univ.*)

2I1610　大腸菌の遊泳速度に及ぼすγ線照射の効果

Effect of gamma ray irradiation on the swimming speed of *Escherichia coli*

Eriko Fujimoto[1], Masakazu Furuta[2], Tatsuo Atsumi[3], **Mikio Kato**[2] ([1]*Osaka Prefecture University School of Science*, [2]*Osaka Prefecture University Graduate School of Science*, [3]*Gifu University of Medical Science*)

第３日目（９月 24 日（月））／ Day3(Sep. 24, Mon.)

9:12〜11:10　A 会場　理学南館 坂田・平田ホール／ Room A: Sci. south bldg. 1F Sakata Hirata Hall
分子モーター III：F1-ATPase, マイコプラズマ
Molecular Motors III: F1 ATPase and Mycoplasma

3A0912 **F_1-ATPase と繊毛軸糸の機能に関わる構造変化**
Motions in F_1-ATPase and ciliary axonemes that drive functions
Tomoko Masaike[1], Koji Ikegami[2], Rinako Nakayama[1], Mitsutoshi Setou[2], Takayuki Nishizaka[1] ([1]*Department of Physics, Gakushuin University*, [2]*Department of Cell Biology and Anatomy, Hamamatsu University School of Medicine*)

3A0924 **高速暗視野照明による金ナノロッドの方向検出システムを用いた F1-ATPase の回転の検出**
Detection of rotation of F1-ATPase using high-speed orientational detection of gold nanorod
Sawako Enoki[1,2], Ryota Iino[1,2], Hiroyuki Noji[1,2] ([1]*Grad. Sch. Engineering., Univ. Tokyo*, [2]*CREST*)

3A0936 **UTP を基質とした時の F1-ATPase の回転運動**
Characterization of UTP driven rotation of F1-ATPase
Hidenobu Arai, Rikiya Watanabe, Hiroyuki Noji (*Grad. applchem., Univ. Tokyo*)

3A0948 **Single Molecule Analysis of Inhibitory Pausing States of V_1-ATPase**
Naciye Esma Tirtom[1], Yoshihiro Nishikawa[2], Daichi Okuno[3], Masahiro Nakano[4], Ken Yokoyama[5], Hiroyuki Noji[1] ([1]*Department of Applied Chemistry, School of Engineering, University of Tokyo,* [2]*Dept. of Biotechnology, Osaka University,* [3]*RIKEN, Osaka, Japan*, [4]*The Institute of Scientific and Industrial Research,* [5]*Dept. of Biolmolecular Sciences, Kyoto Sangyo University*)

休憩 10:00-10:10

3A1010 **F_1-ATPase のトルク伝達における DELSEED ループの役割**
The role of DELSEED loop in torque-transmission of F_1-ATPase
Kazuma Koyasu[1], Rikiya Watanabe[1], Mizue Tanigawara[2], Hiroyuki Noji[1] ([1]*Department of Applied Chemistry, School of Engineering, The University of Tokyo*, [2]*Graduate School of Frontier Biosciences, Osaka University*)

3A1022 **F_1-ATPase の回転子γサブユニットに有限のトルク発生に必要な残基はない**
None of the rotor residues of F_1-ATPase are essential for torque generation
Ryohei Chiwata[1], Tomoya Kawakami[1], Ayako Kohori[1], Shou Furuike[2], Katsuyuki Shiroguchi[3], Kazuo Sutoh[1], Masasuke Yoshida[4], Kazuhiko Jr. Kinosita[1] ([1]*Dept. Physics, Fac. Sci. Eng., Waseda Univ.*, [2]*Fac. Physics, Osaka Med. Col.*, [3]*Dept. Chem. and Chem. Biol., Harvard Univ.*, [4]*Dept. of Mol. Biosci., Kyoto Sangyo Univ.*)

3A1034 **F1-ATPase のシリンダーから中心軸を引き抜く力の測定**
UNBINDING FORCE MEASUREMENTS OF THE SHAFT FROM THE CYLINDER OF F1-ATPase
Tatsuya Naito, Kaoru Okada, Tomoko Masaike, Takayuki Nishizaka (*Dept Phys, Gakushuin Univ.*)

3A1046 **リポソーム膜中に再構成した好熱菌由来 F_oF_1- ATP 合成酵素による ATP 駆動 H^+輸送の定量**
Quantification of ATP-driven H^+ transport by thermophilic *Bacillus* PS3 F_oF_1-ATP synthase reconstituted in a liposomal membrane
Yuzo Kasuya[1], Naoki Soga[1], Toshiharu Suzuki[2], Masasuke Yoshida[2], Kazuhiko Kinosita[1] ([1]*Dept. Phys., Facl. Sci. Eng., Waseda Univ.*, [2]*Dept. Mol. Bio., Facl. Life Sci., Kyoto Sangyo Univ.*)

3A1058 **マイコプラズマモービレゴーストのステップ検出**
Detection of steps of *Mycoplasma mobile* gliding ghost
Yoshiaki Kinosita[1], Daisuke Nakane[2,3], Kana Mizutani[1], Makoto Miyata[2], Takayuki Nishizaka[1] ([1]*Dept.phys., Gakushuin Univ*, [2]*Dept. Biol., Osaka City Univ*, [3]*Present address: Mol. Microbiol. and Immunol., Grad. Sch. Biomed. Sci., Nagasaki Univ*)

9:00〜11:22　B 会場　多元数理科学棟 5 階 509 ／ Room B: Mathematics bldg. 5F 509
蛋白質-構造機能相関 III：動態，生体リズム
Proteins: Structure & Function III: Dynamics and Circadian Rhythm

3B0900 **原核生物由来ナトリウムチャネルにおける C 末端 4 ヘリックスバンドルを用いたゲーティング制御**
The cytosolic C-terminal four-helix bundle regulates the gating of prokaryotic sodium channel
Katsumasa Irie, Takushi Shimomura, Yoshinori Fujiyoshi (*CeSPI., Univ. Nagoya*)

3B0912 **[NiFe]ヒドロゲナーゼ成熟化因子 HypE，HypF の X 線結晶構造解析**
X-ray structural analysis of HypE and HypF, maturation factors for [NiFe]-hydrogenases
Yasuhito Shomura[1,2], Yoshiki Higuchi[1,2] ([1]*Grad. Sch. Life Sci., Univ. Hyogo*, [2]*RIKEN/SPring-8 Center*)

3B0924 **Dynamic structural and antigen binding analyses of antibody single-chain Fvs**
Yusuke Tanaka[1], Hiroshi Sekiguchi[2], Yuji C. Sasaki[3], Takachika Azuma[4], Masayuki Oda[1] ([1]*Grad. Sch. of Life and Environ. Sci., Kyoto Pref. Univ.*, [2]*Jpn. Syn. Rad. Res. Inst.*, [3]*Grad. Sch. of Fron. and Sci., Univ. of Tokyo.*, [4]*Res. Ins. for Biol. Sci., Tokyo Univ. of Sci.*)

3B0936 **PYP の光構造変化の機械的な制御**
Mechanical control of light-induced protein conformational change of photoactive yellow protein
Yasushi Imamoto, Take Matsuyama, Yoshinori Shichida (*Grad. Sch. Sci., Kyoto Univ.*)

3B0948 **αカテニンによるアクトミオシン収縮の阻害**
Inhibition of actomyosin contractility by α-catenin, a component of adherens junctions
Shuya Ishii[1], Takashi Ohki[1], Hiroaki Kubota[1], Shin'ichi Ishiwata[1,2,3] ([1]*Dept. of Phys., Faculty of Sci. and Eng., Waseda Univ.*, [2]*Adv. Res. Inst. for Scie. and Eng., Waseda Univ.*, [3]*WABIOS, Waseda Univ.*)

休憩 10:00-10:10

3B1010 **ダイニンモータードメインの溶液中の分子動力学シミュレーション**
Molecular dynamics simulations of dynein motor domain in explicit water
Narutoshi Kamiya[1], Tadaaki Mashimo[2], Yu Takano[1], Takahide Kon[1], Genji Kurisu[1], Haruki Nakamura[1] ([1]*Institute for Protein Research, Osaka Univ.*, [2]*BIRC, AIST*)

3B1022 **A computational Investigation into the MHC-I Recognition Mechanism of MIR2 from Kaposi's Sarcoma-Associated Herpesvirus**
Pai-Chi Li[1,2], Naoyuki Miyashita[3], Satoshi Ishido[1], Yuji Sugita[2] ([1]*RIKEN Research Center for Allergy and Immunology*, [2]*RIKEN Advanced Science Institute*, [3]*RIKEN Quantitative Biology Center*)

3B1034 **タンパク質構造変化経路予測法の新規開発**
A Novel Method to simulate protein conformational change upon ligand binding
Koichi Tamura, Shigehiko Hayashi (*Grad. Sch. Sci., Univ. Kyoto*)

3B1046 **時計タンパク質 KaiA-KaiC 相互作用の ESR 解析**
Interactions between cyanobacterial clock proteins KaiA and KaiC revealed by ESR analysis
Kentaro Ishii[1], Toshiaki Arata[2], Masahiro Ishiura[1] ([1]*Center for gene research Nagoya Univ.*, [2]*Grad. Sch. of Science, Osaka Univ.*)

3B1058 **ATP を中間体とするシアノバクテリア概日時計蛋白質 KaiC の新規脱リン酸化機構**
Autodephosphorylation of cyanobacterial circadian clock protein KaiC occurs via formation of ATP as an intermediate
Taeko Ohkawa-Nishiwaki, Takao Kondo (*Div.Biol.Sci., Grad. Schl. Sci., Nagoya Univ.*)

3B1110 **シアノバクテリアの時計タンパク質 KaiC の ATPase に備わる分子内フィードバック制御**
Intramolecular feedback regulation of cyanobacterial KaiC ATPase
Atsushi Mukaiyama[1,2], Yasuhiro Onoue[1,2], Masato Osako[1,2], Takao Kondo[1,2], Shuji Akiyama[3] ([1]*Grad. Sch. of Sci., Nagoya Univ.*, [2]*CREST/JST*, [3]*IMS, SOKENDAI*)

9:00〜11:22 C 会場 多元数理科学棟 4 階 409 ／ Room C: Mathematics bldg. 4F 409
核酸
Nucleic Acids

3C0900 **DNA/RNA 結合タンパク質 TDP-43 が特異的な塩基配列を認識するメカニズム**
Tandem-like fusion of two heterologous RNA-recognition motifs in TDP-43 enhances the specificity to its target nucleotide sequence
Yo Suzuki, Yoshiaki Furukawa (*Dept. of Chem, Keio Univ.*)

3C0912 **不安定な二次構造をつくる DNA のハイブリダイゼーション速度**
Hybridization Rates of DNA Strands with Unstable Self-folded Secondary Structures
Hiroaki Hata[1], Akira Suyama[1,2] ([1]*Grad. Sch. Sci., Univ. Tokyo*, [2]*Grad. Sch. Arts and Sci., Univ. Tokyo*)

3C0924 **長鎖 DNA の 1 分子内折り畳みはカチオン性ポリマー凝縮剤の長さによってモードが変わる**
Folding of a Single Giant Duplex DNA Chain Expresses Contrastive Behaviors depending on the Length of Cationic Polymer
Tatsuo Akitaya[1], Norio Hazemoto[2], Toshio Kanbe[3], Makoto Demura[4], Hideaki Yamaguchi[1], Koji Kubo[5], Anatoly Zinchenko[5], Shizuaki Murata[5], Kenichi Yoshikawa[6] ([1]*Fac. Pharm., Meijo Univ.*, [2]*Grad. Sch. Pharm. Sci., Nagoya City Univ.*, [3]*Sch. Med., Nagoya Univ.*, [4]*Grad. Sch. Life Sci., Hokkaido Univ.*, [5]*Grad. Sch. Env. Study, Nagoya Univ.*, [6]*Grad. Sch. Life Med. Sci., Doshisha Univ.*)

3C0936 **カリウムイオン依存的な四重鎖構造形成によって活性がオンになるインテリジェントリボザイムの創製**
Development of intelligent ribozyme whose activity switches on in response to K^+ via quadruplex formation
Yudai Yamaoki[1,2], Tsukasa Mashima[1,2], Yu Sakurai[3], Yukari Hara[3], Takashi Nagata[1,2], Masato Katahira[1,2] ([1]*Inst. Adv. Energy, Kyoto Univ.*, [2]*Grad. Sch. Energy Sci., Kyoto Univ.*, [3]*Grad. Sch. Nanobio., Yokohama City Univ.*)

3C0948 **翻訳伸長におけるリボソームと tRNA の挙動－粗視化分子シミュレーションによる解析**
Dynamical motions of tRNA and ribosome complex during translation elongation studied by coarse-grained molecular simulations
Naoto Hori, Shoji Takada (*Grad. Sch. Sci., Kyoto Univ.*)

休憩 10:00-10:10

3C1010 **A structural basis for the antibiotic resistance conferred by an A1408G mutation in 16S rRNA**
Jiro Kondo (*Fac. Sci. Tech., Sophia University*)

3C1022 **Q β replicase を構成する翻訳因子の RNA 合成における役割**
Non-canonical functions of translational factors as RNA replication cofactors
Daijiro Takeshita, Kozo Tomita (*Biomed. Res. Inst., AIST*)

3C1034 **抗 HIV 宿主因子 APOBEC3G の位置依存的デアミネーション反応機構の解明**
Elucidation of the location-dependent deamination reaction mechanism of an anti-HIV factor, APOBEC3G
Ayako Furukawa[1,2], Kenji Sugase[2], Ryo Morishita[3], Taashi Nagata[1], Akifumi Takaori[4], Akihide Ryo[5], Masato Katahira[1] ([1]*Inst. of Adv. Energy, Kyoto Univ.*, [2]*Bioorg. Res. Inst., Suntory Found. Life Sci.*, [3]*CellFree Sci.*, [4]*Grad. Sch. Med., Kyoto Univ.*, [5]*Grad. Sch. Med., Yokohama City Univ.*)

3C1046 **大腸菌非六量体型 DNA ヘリカーゼ UvrD は多量体で DNA を巻き戻す**
Single-molecule visualization of a non-hexameric helicase reveals active roles of its oligomeric forms in DNA unwinding
Hiroaki Yokota, Yoshie Harada (*iCeMS, Kyoto Univ.*)

3C1058 **リボソーム-SecM 翻訳アレスト配列間相互作用の 1 分子顕微解析**
Single-molecule force measurement for the interaction between ribosome and SecM arrest sequence
Zhuohao Yang, Ryo Iizuka, Takashi Funatsu (*Grad. Sch. of Pharm. Sci., The Univ. of Tokyo*)

3C1110 **The probability of double-strand breaks in genome-sized DNA decreases markedly as the DNA concentration increases**
Shunsuke Shimobayashi[1], Takafumi Iwaki[2], Toshiaki Mori[3], Kenichi Yoshikawa[1,4] ([1]*Grad. Sch. of Sci., kyoto Univ.*, [2]*Fukui Inst., Kyoto Univ.*, [3]*Rad. Res. Cent., Osaka Pref. Univ.*, [4]*Grad. Sch. of Life and Med. Sci., Doshisha Univ.*)

9:00〜11:10　D 会場　多元数理科学棟 3 階 309 ／ Room D: Mathematics bldg. 3F 309
光生物-光合成
Photobiology: Photosynthesis

3D0900 **膜配向した PS II の ENDOR 法による Mn クラスター周辺のプロトンの位置の決定**
Determine the location of protons surrounding Mn cluster of PS II by proton matrix ENDOR using oriented PS II membrane
Hiroki Nagashima, Hiroyuki Mino (*Division of Material Science, Graduate School of Science, Nagoya University*)

3D0912 **Factors that differentiate the H-bond strengths of water near the Schiff bases in bacteriorhodopsin and *Anabaena* sensory rhodopsin**
Hiroshi Ishikita[1,2], Keisuke Saito[1], Hideki Kandori[3] ([1]*Career-Path, Kyoto U*, [2]*JST PRESTO*, [3]*Nagoya Inst Tech*)

3D0924 **BLUF ドメインの光反応における水素結合環境の変化**
Structural changes of hydrogen-bonding environment upon the photoreaction of the BLUF domains
Tatsuya Iwata[1], Shota Ito[2], Mineo Iseki[3], Masakatsu Watanabe[4], Hideki Kandori[2] ([1]*Cent. Fost. Young Innov. Res., NITech*, [2]*Dept. Front. Mater., NITech*, [3]*Faculty Pharm. Sci., Toho Univ.*, [4]*Grad. Sch. Creat. New Photo. Ind.*)

3D0936 **励起移動を記述する変分マスター方程式の改良および PSII への適用**
Improvement of variational master equation describing excitation energy transfer, and its application to PSII
Yuta Fujihashi, Akihiro Kimura (*Department of Physics, Graduate School of Science, Nagoya University*)

3D0948 **光化学系 II コア複合体での非光化学的消光の可能性**
Possible non-photochemical quenching mechanism within pohotosystem II core complex
Yutaka Shibata[1], Shunsuke Nishi[2], Keisuke Kawakami[3], Jian-Ren Shen[4], Thomas Renger[5] ([1]*Grad. Sch. Sci., Tohoku Univ.*, [2]*Grad. Sch. Sci., Nagoya Univ.*, [3]*Adv. Res. Inst., Osaka City Univ.*, [4]*Grad. Sch. Sci., Okayama Univ.*, [5]*JKU Linz*)

休憩 10:00-10:10

3D1010 **低温光化学系 II における多重光還元 $Mn_4CaO_5H_x$クラスター分布: 時間平均 XRD 構造の照射 X 線量依存性**
X-ray dose dependence of time-averaged XRD structure of multi-photoreduced $Mn_4CaO_5H_x$ clusters in photosystem II at low temperature
Masami Kusunoki (*Department of Physics, School of Science Technology, Meiji University*)

3D1022 **光化学系 II 酸素発生系 S_2状態における Mn 間磁気的相互作用の解明**
Determination of magnetic couplings of S_2 state Mn-cluster in Photosystem II studied by PELDOR measurement
Mizue Asada[1], Hiroki Nagashima[1], Faisal Hammad Mekky Koua[2], Jian-Ren Shen[2], Hiroyuki Mino[1] ([1]*Grad. Sch. Sci., Univ. Nagoya*, [2]*Grad. Sch. Natl. Sci. & Tech., Univ. Okayama*)

3D1034 **光化学系 II におけるキノン電子受容体の酸化還元電位制御機構**
Mechanism of controlling the redox potentials of the quinone electron acceptors in photosystem II
Ryota Ashizawa[1], Takuya Iwasa[1], Miwa Sugiura[2], Takumi Noguchi[1] ([1]*Division of Material Science, Graduate School of Science, Nagoya University*, [2]*Division of Material Science, Graduate School of Science, Nagoya University*)

3D1046 **光合成バクテリア反応中心の電子移動経路解析**
Electron Transfer Pathway Analysis in Bacterial Photosynthetic Reaction Center
Hirotaka Kitoh-Nishioka, Koji Ando (*Grad. Sch. Sci. Kyoto Univ.*)

3D1058 **光合成細菌 Rhodopseudomonas の遺伝子発現パターンの電気化学制御**
Electrochemical regulation of gene expression profiles of Rhodopseudomonas, a photosynthesis bacterium
Yue Lu[1], Syoichi Matsuda[1], Shuji Nakanishi[2], Kazuhito Hashimoto[1] ([1]*The Univesity of Tokyo, School of Engineering, Department of Applied Chemistry*, [2]*Research Center for Advanced Science and Technology*)

9:00〜11:22　E 会場　多元数理科学棟 1 階 109 ／ Room E: Mathematics bldg. 1F 109
蛋白質-構造
Proteins: Structure

3E0900 **核膜孔複合体構造変化による核移行制御機構の構造基盤**
Structural basis for nuclear import regulated by molecular rearrangements in the nuclear pore complex
Junya Kobayashi[1], Yoshiyuki Matsuura[1,2] ([1]*Div. Biol. Sci., Grad. Sch. Sci., Nagoya Univ.*, [2]*Strl. Biol. R. Ctr., Grad., Nagoya Univ.*)

3E0912 **NADH シトクロム b_5還元酵素超高分解能結晶構造解析による水素と外殻電子の観察**
Visualizing hydrogens and outer-shell electrons of NADH cytochrome b_5 reductase by ultra-high resolution crystallography
Kiyofumi Takaba[1], Kazuki Takeda[1], Masayuki Kosugi[1], Taro Tamada[2], Ryota Kuroki[2], Kunio Miki[1] ([1]*Grad. Sch. Sci., Univ. Kyoto*, [2]*JAEA*)

3E0924 **最新の各種固体 NMR 法を用いた絹の構造解析**
Silk Structure studied by Newly-developed Solid-state NMR
Keiko Okushita, Koji Yazawa, Akihiro Aoki, Tetsuo Asakura (*Grad. Sch. of Eng., Tokyo Univ. Agr. Tech.*)

3E0936 **Interaction of human calcitonin with curcumin as an inhibitor of fibrillation as revealed by NMR and docking simulation**
Ken Takeuchi[1], Hikari Watanabe[1], Javkhlantugs Namsrai[1], Hiroshi Hirota[2], Akira Naito[1] ([1]*Yokohama National University Graduate School of Engineering*, [2]*Riken*)

3E0948 **単粒子クライオ電子顕微鏡解析によるサポウイルスキャプシドの 8-Å 構造**
8-Å structure of sapovirus capsid by single particle electron cryomicroscopy
Naoyuki Miyazaki[1], David Taylor[1], Grant Houseman[2], Kosuke Murakami[2], Kuniaki Nagayama[1], Kazuhiko Katayama[2], Kazuyoshi Murata[1] ([1]*National Institute for Physiological Sciences*, [2]*National Institute of Infectious Diseases*)

休憩 10:00-10:10

3E1010 **Structural analysis of the 26S proteasome by cryo-electron microscopy and Single-Particle Analysis**

Zhuo Wang[1], Yasuo Okuma[1], Daisuke Kasuya[2], Kaoru Mitsuoka[3], Yasushi Saeki[4], Yasunaga Takuo[1] ([1]*Department of Bioscience and Bioinformatics, Faculty of Computer Science and Systems Engineering, Kyushu Institute of Technology*, [2]*Biomedicinal Information Research Center, Japan Biologycal Information Consortium (JBIC)*, [3]*Biomedicinal Information Research Center, National Institute of Advanced Industrial Science and Technology*, [4]*Laboratory of Protein Metabolism, Tokyo Metropolitan Institute of Medical Science*)

3E1022 大気圧電子顕微鏡（ASEM）によるタンパク質微結晶とマイコプラズマの液中観察

Direct electron microscopy of protein crystals and Mycoplasma cells in solution using the Atmospheric SEM

Yuusuke Maruyama[1], Tatsuhiko Ebihara[1], Daisuke Nakane[2], Hidetoshi Nishiyama[3], Takayuki Nishizaka[4], Miki Senda[5], Kazuhiro Mio[1], Mitsuo Suga[3], Toshiya Senda[1], Makoto Miyata[2], **Chikara Sato**[1] ([1]*AIST*, [2]*Univ. Osaka City*, [3]*JEOL*, [4]*Univ. Gakushuin*, [5]*JBIC*)

3E1034 粗視化 Go モデルを用いた Ferredoxine-like fold タンパクのフォールディング機構の解析

Analyses of folding processes on the Ferredokin-like fold proteins by means of a coarse grained Go model

Masatake Sugita, Takeshi Kikuchi (*Dept. Bioinf., Coll. Life Sci., Ritsumeikan Univ.*)

3E1046 異なる参照状態を用いた統計ポテンシャルによるタンパク質モデル構造の最適化

Optimization of protein model structures according to statistical potentials with different reference states

Matsuyuki Shirota[1,2], Kengo Kinoshita[1,2,3] ([1]*GSIS, Tohoku Univ.*, [2]*ToMMo, Tohoku Univ.*, [3]*IDAC, Tohoku Univ.*)

3E1058 クーロンレプリカ交換法を用いた A β フラグメントに関する研究

Studies on a Aβ fragment by the Coulomb replica-exchange method

Satoru Itoh[1,2], Hisashi Okumura[1,2] ([1]*Institute for Molecular Science*, [2]*The Graduate University for Advanced Studies*)

3E1110 レプリカ交換インターフェースプログラム(REIN)

Replica-exchange interface program (REIN)

Naoyuki Miyashita[1,2,3], Suyong Re[4], Yuji Sugita[1,2,3,4] ([1]*RIKEN QBiC*, [2]*RIKEN CSRC*, [3]*RIKEN AICS*, [4]*RIKEN ASI*)

9:00〜11:10 F 会場　理学 B 館 5 階 501 ／ Room F: Sci. bldg. B 5F 501

膜蛋白質
Membrane Proteins

3F0900 サポーテット膜を用いた膜タンパク質の顕微鏡下でのイオン輸送活性計測

Evaluation of ion-pump activity of membrane proteins reconstituted on supported membrane under optical microscope

Jyunan Ki, Rikiya Watanabe, Kazuhito Tabata, Hiroyuki Noji (*Department of Applied Chem., Univ. Tokyo*)

3F0912 Catalytic activity of MsbA reconstituted in nanodisc particles is modulated by remote interactions with the bilayer

Takeaki Kawai[1], Jose Caaveiro[1,2], Toyomasa Katagiri[3], Hisashi Tadakuma[1], Takuya Ueda[1], Kouhei Tsumoto[1,2,4] ([1]*Grad. Sch. of Front. Sci., Univ. of Tokyo*, [2]*Inst. Med. Sci., Univ. of Tokyo*, [3]*Inst. Gen. Res., Univ. of Tokushima*, [4]*Dep. Chem. Bio., Univ. of Tokyo*)

3F0924 線虫イネキシン 6 ギャップ結合チャネルの単離と機能特性

Isolation and characterization of C. elegans innexin-6 gap junction channels

Atsunori Oshima[1], Tomohiro Matsuzawa[2], Kouki Nishikawa[1], Yoshinori Fujiyoshi[1] ([1]*CeSPI, Nagoya Univ.*, [2]*Grad. Sch. of Sci., Kyoto Univ.*)

3F0936 ATR-FTIR 法を用いた KcsA 野生型と不活化しない変異体に対するカチオン誘起構造変化の赤外分光分析

Cation-induced structural changes in the WT and non-inactivating mutant KcsA studied by ATR-FTIR

Chikako Muramatsu[1], Masayo Iwaki[1], Tetsuya Fukuda[1], Yusuke Asai[1], Yuji Furutani[1,2], Hideki Kandori[1] ([1]*Grad. Sch. Tech., Nagoya Inst. Tech.*, [2]*Inst. Mol. Sci.,*)

3F0948 黄色ブドウ球菌の 2 成分性膜孔形成毒素の分子機構

Molecular basis of staphylococcal bi-component pore forming toxin

Yoshikazu Tanaka[1], Daichi Yamashita[2], Keitaro Yamashita[2], Yuka Kawai[2], Jun Kaneko[3], Noriko Tomita[4], Makoto Ohta[4], Yoshiyuki Kamio[5], Min Yao[1], Isao Tanaka[1] ([1]*Fac. of Adv. Life Sci., Hokkaido Univ.*, [2]*Grad. Schl. of Life Sci., Hokkaido Univ.*, [3]*Grad. Schl. of Agri. Sci., Tohoku Univ.*, [4]*Inst. of Fluid Sci., Tohoku Univ.*, [5]*Grad. Schl. of Life Sci., Tohoku Univ.*)

休憩 10:00-10:10

3F1010 分子動力学法によるグラミシジン A を含んだ脂質二重層膜の構造と圧力特性

Structure and lateral pressure profile of lipid bilayer containing gramicidin A by molecular dynamics simulation

Hiroaki Saito, Masashi Iwayama, Megumi Nishimura, Hiroyuki Takagi, Kazutomo Kawaguchi, Hidemi Nagao (*Kanazawa University*)

3F1022 代謝型グルタミン酸受容体の膜貫通領域における 1 アミノ酸変異がアゴニストをインバースアゴニストに変える

Single amino acid substitution in the transmembrane domain of metabotropic glutamate receptor changes an agonist into an inverse agonist

Masataka Yanagawa, Takahiro Yamashita, Yoshinori Shichida (*Department of Biophysics, Graduate School of Science, Kyoto University*)

3F1034 non-detergent sulfobetaine (NDSB)による G 蛋白質共役型受容体 (GPCR)の熱安定化

Thermal stabilization of G protein-coupled receptor by non-detergent sulfobetaines (NDSBs)

Toshihide Yamai, Layla Takahashi, Masato Nakajima, Naoki Yamashita, Takeshi Ishii, Shigeki Takeda, Kaori Wakamatsu (*Gunma Univ.*)

3F1046 固体 NMR を用いた熱および圧力により誘起されるバクテリオロドプシンの構造と運動性変化の解析

Thermal and Pressure induced structural and dynamics changes of bacteriorhodopsin as studied by solid-state NMR

Izuru Kawamura[1], Miyako Horigome[1], Hirohide Nishikawa[1], Kana Tajima[1], Takashi Okitsu[2], Akimori Wada[2], Satoru Tuzi[3], Tatsuo Iwasa[4], Akira Naito[1] ([1]*Grad. Sch. Eng., Yokohama Natl. Univ.*, [2]*Kobe Pharm. Univ.*, [3]*Univ. Hyogo*, [4]*Muroran Inst. Tech.*)

3F1058 OBSERVATION OF TRANSMEMBRANE PROTEIN BY HIGH SPEED ATOMIC FORCE MICROSCOPY: BACTERIORHODOPSIN D85S MUTANT, A CHLORIDE PUMP

Maxime Ewald[1], Mikihiro Shibata[2], Takayuki Uchihashi[1,3], Hideki Kandori[4], Toshio Ando[1,3] ([1]*School of Mathematics & Physics, Institute of Science & Engineering, Kanazawa*

University, [2]*Department of Neurobiology, Duke University Medical Center*, [3]*Bio-AFM Frontier Research Center, College of Science and Engineering, Kanazawa University*, [4]*Department of Frontier Materials, Nagoya Institute of Technology*)

9:00〜11:22 G 会場　理学 B 館 2 階 212 ／ Room G: Sci. bldg. B 2F 212
生体膜・人工膜-構造・物性
Biological & Artificial Membranes: Structure & Property

3G0900 **好熱性 *Meiothermus ruber* H328 株が産生放出する高耐性ケラチン分解性プロテアーゼ複合体のフリーズレプリカ電子顕微鏡観察**
Freeze-replica observation of keratinolytic protease complex produced and released from *Meiothermus ruber* H328
Kazunori Kawasaki[1], Maachi Kataoka[2], Keiji Nomura[2], Yasushi Shigeri[1], Kunihiko Watanabe[2] ([1]*AIST*, [2]*Grad. Sch. Kyoto Pref. Univ.*)

3G0912 **Effects of model peptides for late embryogenesis abundant (LEA) proteins on the thermal properties of liposomes**
Takao Furuki, Minoru Sakurai (*Center for Biol. Resources and Informatics, Tokyo Inst. Tech.*)

3G0924 **微細パターン化モデル生体膜における膜結合タンパク質の濃縮の空間的制御**
Spatially controlled accumulation of membrane-bound protein in a micro-patterned model biological membrane
Fumiko Okada[1], Kenichi Morigaki[1,2] ([1]*Grad. Sch. Agr., Univ. Kobe*, [2]*Res. Cent. Env. Genomi., Univ. Kobe*)

3G0936 **圧力摂動熱量法によるジミリストイルホスファチジルコリン二分子膜の緩和挙動の解明への試み**
An attempt to reveal the relaxation behavior of dimyristoylphosphatidylcholine bilayer by pressure perturbation calorimetry
Nobutake Tamai, Sayuri Kakibe, Saeko Tanaka, Masaki Goto, Hitoshi Matsuki (*Dept. Life System, Inst. Technol. & Sci., Univ. of Tokushima*)

3G0948 **リン脂質二重膜の圧力誘起指組み構造形成：疎水鎖長依存性と形成限界**
Pressure-induced interdigitation of phospholipid bilayer membranes: dependence of acyl-chain length and limitation of the formation
Hitoshi Matsuki, Masaki Goto, Nobutake Tamai (*Institute of Technology and Science, The University of Tokushima*)

休憩 10:00-10:10

3G1010 **均一でないリン脂質単分子膜における崩壊現象について**
Collapse of nonuniform phospholipid monolayers
Masahiro Hibino, Ken Hashimoto, Takuya Fujisawa (*Div. Appl. Sci., Muroran Inst. Technol.*)

3G1022 **脂質分子の電荷が引き起こす膜構造変化：2 次元相分離と 3 次元曲率**
Charge-induced transition in membrane mesoscopic structures: lateral domains and vesicular shapes
Hiroki Himeno, Tsutomu Hamada, Masahiro Takagi (*1Shool of Materials Science, Japan Advanced Institute of Science and Technology*)

3G1034 **油中水滴エマルション遠心沈降法を用いたミクロスフェア内包型ジャイアントベシクル**
Microsphere-containing giant vesicles prepared by water-in-oil emulsion centrifugation method
Yuno Natsume[1], Taro Toyota[1,2] ([1]*Grad. Art. Sci., Univ. Tokyo*, [2]*JST PRESTO*)

3G1046 **オイルフリー GUV に封入された分子演算システム RTRACS**
Molecular computing system RTRACS encapsulated in oil-free giant unilamellar vesicle
Koh-ichiroh Shohda, Tadashi Sugawara, Akira Suyama (*Grad. Sch. Arts Sci., Univ. Tokyo*)

3G1058 **低い pH が誘起する DOPS/MO 膜の液晶相からキュービック相への相転移の初期過程**
Initial Step of Low pH-Induced Lamellar to Bicontinuous Cubic Phase Transition in Dioleoylphosphatidylserine/Monoolein
Toshihiko Oka[1], Tomoki Takahashi[1], Taka-aki Tsuboi[1], Masahito Yamazaki[2] ([1]*Fac. Sci., Shizuoka Univ.*, [2]*Grad. Sch. Sci. Tech., Shizuoka Univ.*)

3G1110 **X 線及び電子線回折法を用いた皮膚角層の構造解析**
Breakthrough for Unresolved Structural Problems in Skin Function by Combined Use of X-ray and Electron Diffraction Methods
Hiromitsu Nakazawa[1], Ichiro Hatta[2], Satoru Kato[1] ([1]*Sch. Sci. Tech. kwansei Gakuin Univ.*, [2]*Nagoya Industrial Science Research Inst.*)

9:00〜11:22 H 会場　理学 C 館 5 階 517 ／ Room H: Sci. bldg. C 5F 517
細胞生物的課題 III：細胞骨格，細胞運動
Cell Biology III: Cytoskeleton & Motility

3H0900 **GTP 結合状態と GDP 結合状態の微小管分子構造における大きな構造変化**
Large Conformational Changes in Tubulin in the GTP- and GDP-States Microtubules Observed by Cryo Electron Microscopy
Hiroaki Yajima[1], Toshihiko Ogura[2], Ryo Nitta[1], Yasushi Okada[1], Chikara Sato[2], Nobutaka Hirokawa[1] ([1]*Grad. Sch. Med., Univ. Tokyo*, [2]*Biomedical Research Inst., AIST*)

3H0912 **紡錘体は一方の極から他方へ構造変化を伝搬することで対称形状を維持する**
Meiotic spindles maintain the symmetrical shape by propagating structural changes to the opposite side
Kazuya Suzuki[1], Jun Takagi[1], Takeshi Itabashi[1], Shin'ichi Ishiwata[1,2] ([1]*Dept. Phys., Adv Sci. Eng., Waseda Univ.*, [2]*WABIOS*)

3H0924 **高圧負荷によって誘導されるクラミドモナス非運動性変異株鞭毛の屈曲運動**
Resurrection of flagellar bending movements in *chlamydomonas* paralyzed mutants at high pressure
Toshiki Yagi[1], Masayoshi Nishiyama[2] ([1]*Grad. Sch. Medicine, Univ. Tokyo*, [2]*The Hakubi Center, Kyoto Univ.*)

3H0936 **走化性誘因物質の進行パルス刺激によって誘発された一方向細胞運動**
Directed cell migration induced by travelling waves of chemoattractant
Akihiko Nakajima[1], Satoshi Sawai[1,2] ([1]*Grad. Sch. Arts & Sci., Univ. Tokyo*, [2]*Res. Cent. for Complex Systems Biology, Univ. Tokyo*)

3H0948 **極性を持つアメーバ細胞の走化性運動に関する理論**
Theory on the chemotaxis of an amoeboid cell with the cell polarity
Tetsuya Hiraiwa, Tatsuo Shibata (*Kobe, Riken*)

休憩 10:00-10:10

3H1010 **Controlled cell migration with ultrasound**
Shinya Murakami[1], Yo Otsuka[1], Manabu Sugimoto[1], Toshiyuki Mitsui[2] ([1]*Grad. Sci. Eng., Aogaku Univ.*, [2]*Assoc Prof., Aogaku Univ.*)

3H1022 **筋肉と異なるストレスファイバーの収縮特性**
Contractile properties of stress fibers are distinct from those of muscles
Shinji Deguchi, Tsubasa Matsui, Daiki Komatsu, Masaaki Sato (*Tohoku University*)

3H1034 **Smooth muscle differentiation related transcription factor CRP2 directly regulates physical properties of actin filaments**
Takanori Kihara[1], Satoko Shinohara[1], Yasunobu Sugimoto[2], Jun Miyake[1] ([1]*Grad. Sch. Eng. Sci., Osaka Univ.*, [2]*Nagoya Univ. Synchrotron Radiat. Res. Center*)

3H1046 **細胞接着班における p130Cas と Src の動的相互作用を介した遊走制御機構の解明**
A distinct role for the dynamics of p130Cas at focal adhesion via interaction with Src in the regulation of cell migration
Hiroaki Machiyama[1,2], Hiroaki Hirata[1], Yasuhiro Sawada[1,2] ([1]*Mechanobiology Inst., Nat. Univ. Singapore*, [2]*Dept. Biol. Sci., Nat. Univ. Singapore*)

3H1058 **Spatiotemporal regulation of signaling by active cytoskeletal remodeling**
Bhaswati Bhattacharyya[1], Abhishek Chaudhuri[3], Kripa Gowrishankar[4], Satyajit Mayor[5], Madan Rao[4] ([1]*iCeMS, Kyoto University*, [2]*Rudolf Peierls Centre for Theoretical Physics, University of Oxford, UK*, [3]*Raman Research Institute, Bangalore, India*, [4]*NCBS-TIFR, Bangalore, India*)

3H1110 **Arp2/3 とアクチンを内包した油中液滴のフィロポディア様変形**
Filopodia-like protrusions in water-in-oil droplets induced by Arp2/3 and actin polymerization
Masataka Chiba[1], Makito Miyazaki[1], Takashi Ohki[1], Shin'ichi Ishiwata[1,2] ([1]*Dept. of Phys., Waseda Univ.*, [2]*WABIOS, Waseda Univ.*)

9:12～11:10 I会場 理学E館1階131 ／ Room I: Sci. bldg. E 1F 131
ヘム蛋白質
Heme Proteins

3I0912 **ヘモグロビンのアロステリック平衡のリアルな描像**
A realistic picture of allosteric equilibrium of hemoglobin
Naoya Shibayama[1], Sam-Yong Park[2] ([1]*Biophysics, Jichi Med. Univ.*, [2]*Protein Design Lab., Yokohama City Univ.*)

3I0924 **ヘムをヘム垂線のまわりに 90° 回転した時の共鳴ラマンスペクトル変化：ヘムオキシゲネース**
Effects of Heme Rotation around the Heme Normal by 90° on Resonance Raman Spectra of Heme Proteins; Observation for Heme Oxygenase
Sachiko Yanagisawa[1], Hiroshi Fujii[2], Saburo Neya[3], Takashi Ogura[1], Teizo Kitagawa[1] ([1]*University of Hyogo*, [2]*Okazaki Inst. Integrative Biosci.*, [3]*Chiba University*)

3I0936 **ヘムオキシゲナーゼにおける CO 光解離後の構造変化および CO の放出経路**
Protein motions and CO migration following CO photolysis in heme oxygenase
Masakazu Sugishima[1,2], Keith Moffat[2,3], Masato Noguchi[1] ([1]*Dept. Med. Biochem., Kurume Univ. Sch. Med.*, [2]*Dept. Biochem. & Mol. Biol., Univ. Chicago*, [3]*BioCARS, Univ. Chicago*)

3I0948 **多様な生物種によるヘムオキシゲナーゼ反応の微調整戦略：オキシヘムの安定化**
Strategy of a variety of organisms for the fine-tuning of heme oxygenase reactions: Stabilization of the oxyheme intermediate
Sayuri Takada, Taiko Migita (*Dep. Biol. Chem., Fac. Agr., Yamaguchi Univ.*)

休憩 10:00-10:10

3I1010 **Ultraviolet Resonance Raman Study on Indoleamine 2, 3-Dioxygenase**
Masayuki Hara[1], Sachiko Yanagisawa[1], Hiroshi Sugimoto[2], Yoshitsugu Shiro[2], Takashi Ogura[1] ([1]*Grad. Sch. Sci., Univ. Hyogo*, [2]*Harima Inst., Riken*)

3I1022 **An Intermediate Conformation of Cytochrome Oxidase in the Ligand-Free State Identified by Time-Resolved Resonance Raman Spectroscopy**
Izumi Ishigami, Takeshi Nishigaki, Kyoko Shinzawa-Itoh, Shinya Yoshikawa, Satoru Nakashima, **Takashi Ogura** (*Grad. Schl. Life Sci., U. Hyogo*)

3I1034 **ポンプ・プローブレーザーと同期したパルスフローシステムの開発とそれを用いたタンパク質の時間分解赤外分光解析**
Time-Resolved IR Analyses of Proteins Using a Novel Pulse Flow System Synchronized with Pump/Probe Lasers
Minoru Kubo[1], Satoru Nakashima[1], Masao Mochizuki[1], Kyoko Shinzawa-Itoh[2], Shinya Yoshikawa[1,2], Takashi Ogura[1,2] ([1]*Picobiology Inst., Grad. Sch. Life Sci., Univ. Hyogo*, [2]*Dept. Life Sci., Grad. Sch. Life Sci., Univ. Hyogo*)

3I1046 **チトクロム *c* 酸化酵素のヘム *a* 側鎖に由来する共鳴ラマン線の帰属**
The assignment of the resonance Raman bands of heme *a* peripheral substituents in cytochrome *c* oxidase
Miyuki Sakaguchi[1], Yukie Katayama[2], Hiroshi Fujii[3], Hideo Shimada[2], Takashi Ogura[1,2] ([1]*Grad. Sch. Life. Sci., Univ. Hyogo*, [2]*Picobiol. Inst., Grad. Sch. Life. Sci., Univ. Hyogo*, [3]*Okazaki Inst. Integr. Biosci.*)

3I1058 **シアン結合型構造から推察される一酸化窒素還元酵素の反応機構**
Functional Implications from Structural Characterization of CN-bound Nitric Oxide Reductase
Takehiko Tosha, Nozomi Sato, Norihiro Okada, Hiroshi Sugimoto, Yoshitsugu Shiro (*Harima Inst., RIKEN*)

一般口頭発表　座長一覧

建物名	フロア	会場名	部屋名	9月22日（土）	9月23日（日）	9月24日（月）
				14:00-16:30	14:00-16:30	9:00-11:30
理学南館	1階	A会場	坂田・平田ホール	1A 分子モーター I	2A 分子モーター II: ダイニン	3A 分子モーター III: F1-ATPase、マイコプラズマ
				富重 道雄（東大） 小嶋 誠司（名大）	吉川 雅英（東大） 昆 隆英（阪大）	野地 博行（東大） 西坂 崇之（学習院大）
多元数理科学棟	5階	B会場	509	1B 蛋白質-構造機能相関 I	2B 蛋白質-構造機能相関 II: 理論、凝集	3B 蛋白質-構造機能相関 III: 動態、生体リズム
				赤坂 一之（近大） 三島　正規（首都大）	古川 良明（慶大）　笹原 健二（神大）	神谷 成敏（阪大） 杉田 有治（理研）
	4階	C会場	409	1C 蛋白質-計測、解析、エンジニアリング	2C 数理生物学	3C 核酸
				古谷 祐詞（分子研） 黒田 裕（農工大）	柴田 達夫（理研） 西村 信一郎（広大）	古川 良明（慶大） 片平 正人（京大）
	3階	D会場	309	1D 発生・分化、神経	2D 計測	3D 光生物-光合成
				伊藤 悦朗（徳島文理大） 鈴木 直哉（名大）	安永 卓生（九工大） 佐甲 靖志（理研）	石北 央（京大） 柴田 穣（東北大）
	1階	E会場	109	1E 蛋白質-物性 I	2E 蛋白質-物性 II	3E 蛋白質-構造
				津本 浩平（東大） 元島 史尋（京産大）	槇 亙介（名大） 寺田 智樹（名大）	松浦 能行（名大） 佐藤 匡史（名市大）
理学B館	5階	F会場	501	1F 光生物-視覚、光受容 I	2F 光生物-視覚、光受容 II	3F 膜蛋白質
				村上 緑（名大） 今元 泰（京大）	海野 雅司（佐賀大） 佐々木 純（名工大）	内藤 晶（横浜国大） 神取 秀樹（名工大）
	2階	G会場	212	1G 細胞生物的課題 I	2G 生体膜・人工膜	3G 生体膜・人工膜-構造・物性
				楠見 明弘（京大） 望月 敦史（理研）	山崎 昌一（静大） 老木 成稔（福大）	豊田 太郎（東大） 松木 均（徳大）
理学C館	5階	H会場	517	1H バイオイメージング	2H 筋肉	3H 細胞生物的課題 III: 細胞骨格、細胞運動
				永山 國昭（生理研） 金城 政孝（北大）	石渡 信一（早大） 鈴木 誠（東北大）	辰巳 仁史（名大） 成田 哲博（名大）
理学E館	1階	I会場	131	1I 生命情報科学、バイオエンジニアリング	2I 細胞生物学的課題 II: Prokaryotes	3I ヘム蛋白質
				福地　佐斗志（前工大） 山村 雅幸（東工大）	難波 啓一（阪大） 石島 秋彦（東北大）	小倉 尚志（兵県大） 右田 たい子（山大）

1SA-01 細胞内反応ネットワークと「少数性」問題～理論と計算によるアプローチ

Cracking Reaction Networks Involving "Minorities" in the Cell: Theoretical and Computational Approaches

Yuichi Togashi (*Grad. Sch. Sys. Informat., Kobe Univ.*)

The activities of biological systems are maintained primarily by chemical reactions, and often modeled as reaction-diffusion systems represented by partial differential equations for the "concentrations" of chemicals. However, this classical scheme requires some preconditions. First, each reaction event is instantaneously completed and not affected by previous reactions. Secondly, the molecules diffuse freely and their excluded volume can be neglected. These conditions are however not always satisfied; many of enzymes are molecular machines whose reaction cycles and motions are coupled, and cells are highly crowded with macromolecules. Moreover, recent experiments have shown that there are a number of "minority" chemicals, existing only one or a few molecules per cell. For such rare species, the notion of continuous "concentrations" is no longer valid, and the classical scheme depending on it breaks down. Using simple autocatalytic models, we previously showed that the *molecular discreteness* in such rare chemicals, either discreteness in numbers (i.e. integerness) or spatial discreteness (i.e. finite space between molecules), may affect the reaction-diffusion behavior. Toward a theoretical framework to predict phenomena in the complex molecular networks in the cell, we have expanded the models for a number of chemical species. In some cases, the behavior strongly depends on the system size, which suggests importance of being moderately small. Relevance to cell behavior and possible experimental designs will be also discussed.

1SA-02 1 分子デジタル ELISA

Single-Molecule Digital ELISA

Hiroyuki Noji (*Applied Chem. U-Tokyo*)

I will introduce the single-molecule digital counting assay based on the array system of a million of water-in-oil droplets that we have recently developed (Lab on a chip 2010). Especially, I will focus the digital ELISA assay as one of application methods of the digital counting. The detection principle of the single-molecule digital counting is very simple; by encapsulating a single molecule of enzyme or enzyme-conjugated antibody in a micron-sized reactor, the catalytic product molecules are highly accumulated in the micron space. Individual chambers resultantly give detectable signal, fluorescence from reaction product molecules in general. By counting the number of chambers with evidently high fluorescent signal under an optical microscope, the number of target molecule is determined. As a model reaction, we conducted digital ELISA of the marker molecule of prostate tumor (PSA). The detection limit was revealed to be 2 aM that is million-times lower than that of conventional ELISA assay of PSA, demonstrating the extremely high sensitivity of digital counting assay. In the last part of the talk, I will also discuss about the prospective of the digital counting assay for single cells assay in addition to the integration to CMOS imaging sensor for palm-top digital counting devise.

1SA-03 遺伝子にコードされた発光型プローブ

Genetically encoded luminescent probes

Takeharu Nagai[1,2] ([1]*ISIR, Osaka Univ.*, [2]*PRESTO, JST*)

Optogenetic tools including ChR2, LOV domain, and CALI (chromophore-assisted light inactivation) allows us to operate biomolecule function upon light irradiation, by which we are now able to investigate protein of interest in terms of functional difference according to the existing area inside cells and expression stage with real time resolution. To understand what‘s going on after the light-switching of optogenetic tools, many researcher may want to visualize some other molecular dynamics and function by fluorescence imaging. However, excitation light for the imaging should mis-activate or mis-inactivate the optogenetic tools so that we cannot apply the fluorescence imaging in combination with the optogenetic technology. To overcome this problem, we have been developing genetically-encoded luminescent probes which are based on hybrid between a mutated chemiluminescent protein and a fluorescent protein variant. In the symposium, I will introduce our recent achievement such as development of color variant of bright luminescent protein, and the use of them in conjunction with the optogenetic technologies for understanding operation principles of bio-nanosystems.

1SA-04 Coordinated reversal of flagellar motors on a single Escherichia coli cell

Akihiko Ishijima (*Tohoku University*)

An E. coli cell transduces extracellular stimuli sensed by chemoreceptors to the intracellular signal molecule, which regulates the switching of the rotational direction of the flagellar motors in both direction changes. The switching is highly coordinated with a sub-second delay between motors in correlation with the distance of each motor from the chemoreceptor patch localized at a cell pole. This result suggested that a transient increase and decrease in the concentration of CheY-P caused by a spontaneous burst of its production by the chemoreceptor patch. The switching delay of the both switching was individually investigated. In wild-type cell, the switching delay clearly correlated with each motor’s relative distance from the receptor patch in both switching. However, in a mutant cell lacking CheAs, which is required for the polar localization of CheZ, in a CW-to-CCW switching, obvious switching delay was not observed. This result suggested that the polar localization of CheZ is critical for the directed propagation of the decrease of CheY-P concentration. Next, we used caged serine and developed a photoreleasing system of serine from the caged compounds. The response time was shortened by photorelease of serine. The measured response time appeared to increase with increment of distance between receptor patch and flagellar motor. This result suggested that the directed intracellular signal was propagated in cytoplasm from receptor patch to each flagellar motor with sub-seconds time scale.

1SA-05 ヒトゲノム DNA の収納とそのダイナミクス

Human genome organization and dynamics

Kazuhiro Maeshima (*Structural Biology Center, National Institute of Genetics*)

Human genome DNA of around 2 m in length is organized into a cell nucleus having a volume of only 1 picoliter. Each genome has only two sets of genes. In order to activate a certain gene, a protein factor, which is normally considered to be in a small number, has to search the whole genome and target the specific gene. In this process, genome organization must play an important role. In fact, how is the human genome DNA is organized into a nucleus? The DNA is wrapped around histones, forming a nucleosome structure. The nucleosome had been assumed to be folded into a 30-nm chromatin fiber and other helical folding structures. However, our recent cryo-microscopy (cryo-EM) and synchrotron X-ray scattering analyses have shown almost no visible 30-nm chromatin fibers or other regular structures in interphase nuclei and mitotic chromosomes. This suggests that chromosomes consist of irregularly folded nucleosome fibers. Thus, nucleosome fibers may be constantly moving and rearranging at the local level. Recently we observed these local nucleosome dynamics, which could be crucial for scanning genome information.

1SA-06 哺乳類概日時計のシステム生物学・合成生物学

Systems and Synthetic Biology of Biological Timings

Hiroki Ueda[1,2] ([1]*RIKEN, CDB*, [2]*RIKEN, QBiC*)

The logic of biological networks is difficult to elucidate without (1) comprehensive identification of network structure, (2) prediction and validation based on quantitative measurement and perturbation of network behavior, and (3) design and implementation of artificial networks of identified structure and observed dynamics.

Mammalian circadian clock system is such a complex and dynamic system consisting of complicatedly integrated regulatory loops and displaying the various dynamic behaviors including **i**) endogenous oscillation with about 24-hour period, **ii**) entrainment to the external environmental changes (temperature and light cycle), and **iii**) temperature compensation over the wide range of temperature. In this symposium, I will take a mammalian circadian clock as an example, and introduce the systems- and synthetic-biological approaches for understanding of biological timings.

References

1. Ueda, H.R. et al, *Nature* 418, 534-539 (2002).
2. Ueda, H.R. et al, *Nat. Genet*. 37, 187-92 (2005).
3. Sato T. K. et al, *Nat Genet*. 38, 312-9 (2006).
4. Ukai H. et al, *Nat Cell Biol*. 9, 1327-34 (2007).
5. Ukai-Tadenuma M. et al, *Nat Cell Biol*. 10, 1154-63 (2008).
6. Minami Y. et al, *PNAS* 106, 9890-5 (2009).
7. Isojima Y. et al, *PNAS* 106, 15744-49 (2009).

8. Masumoto KH. et al, *Curr Biol*.20(24),2199-206.(2010).
9. Ukai-Tadenuma M et al. *Cell* 144(2),268-81 (2011).
10. Hogenesch JB, Ueda HR. *Nature Rev. Genet*. 12(6),407-16 (2011).

1SA-07 細菌べん毛形成の分子機構とその制御

Molecular mechanism of bacterial flagellar construction and its regulation

Katsumi Imada[1], Tohru Minamino[2] ([1]*Dept. Macromol. Sci., Grad. Sch. Sci., Osaka Univ.*, [2]*Grad. Sch. Frontier BioSci., Osaka Univ.*)

The bacterial flagellum is a filamentous organelle made up of about 30 proteins with their copy numbers from a few to a few tens of thousands. Since the flagellum extends from the cytoplasm to the cell exterior, most of the component proteins are exported to the distal end of the growing flagellum through the flagellar type III protein export apparatus. The export apparatus is composed of the export gate made of six membrane proteins (FlhA, FlhB, FliO, FliP, FliQ, FliR) and three soluble proteins (FliH, FliI, FliJ), which assemble on and disassemble from the gate during the export cycle. Recent studies revealed that the export process is regulated by a small number of multifunctional substrate-specific chaperon proteins (FlgN, FliA, FliS, FliT). By forming a 1:1 complex with their substrates, they prevent their substrates from premature aggregation in the cytoplasm, and facilitate the export of the substrates through the direct interaction with the export apparatus. After release of their substrate, the free chaperons regulate flagellar protein expression. Thus the flagellar gene expression and flagellar assembly stage are linked by the export chaperones. In this symposium, we will show the role of chaperones on the flagellar construction process based on the recent biophysical, biochemical and genetic works and discuss the molecular mechanisms of the protein export and flagellar gene expression.

1SB-01 DNA の硬さと柔らかさ：高次構造転移が生み出す時空間秩序

Synergy between Stiffness and Softness on DNA: Spatiotemporal Order Organized through the Higher-Order Structural Transition of DNA

Yoshiko Takenaka (*Nanosystem Research Inst., AIST*)

Genomic DNA is a semi-flexible polymer chain, which has longer persistence length (~ 50 nm) than the diameter of a chain (~ 2 nm) and much longer total length (10^1μm to 1 cm) than the persistence length. That is, DNA behaves as a flexible chain over μm scale and a rigid chain in nm scale. Different from short oligomeric DNA, long DNA exhibits the property to undergo a discrete structural transition induced by the change in pH, temperature, concentration of polycation, ATP, RNA, etc. We call this kind of structural transition as higher-order structural transition of DNA. In the presentation, we propose a novel hypothesis to interpret the informational cascade from DNA to macroscopic spatio-temporal order in multi-cellular systems, based on the unique property of genome-sized DNA as a semi-flexible polymer.

We will present a hypothetical gene network model, in which the higher-order structural transition of DNA plays an essential role in regulating stable on-off switching and/or the oscillation of a large number of genes under the fluctuations in individual living cells. This model can explain the robust and broad transcriptional response in a genetic assembly against fluctuations.

We will also interpret the mechanism of the spatiotemporal pattern in somitogenesis. We will stress the importance of spatial discreetness, i.e., actual size of cells, on the reliable theoretical model. With this model, we can produce stationary patterns, which are similar to those of somitogenesis.

1SB-02 Proteins as Mechano-Chemical Transducer

Kazuyuki Akasaka (*Inst. Adv. Tech, Kinki UNIV.*)

"Human body has mechanisms for transducing mechanical stress (deformation and motion by force) into biochemical reactions, which is considered the basis for producing the dynamics of the body." stated Miyasaka et al. in Seikagaku (81, 494-501, 2009). They further stated that the mechanical stress would include 1) shearing, 2) hydrostatic pressure, 3) pulling, compressing and pushing, and 4) vibration. We have been studying structural, dynamic and thermodynamic properties of proteins on pressure-axis by NMR spectroscopy using hydrostatic pressure as variable. We have found that proteins are highly sensitive to pressure perturbation and change their equilibrium populations from the basic sub state often to an excited and functional sub state with increasing hydrostatic pressure (Akasaka K., Chemical Reviews 106: 1814-35, 2006). Experimentally, a uni-axial mechanical stress applied to a protein solution is used to produce a thermodynamically excited state of the protein with a higher chemical reactivity. Namely, [mechanical stress to a pump (uni-axial) ---hydrostatic pressure (isotropic) ---protein conformational transition (thermodynamics) ---activation of reactivity (chemical reaction, function)] Is s similar scheme as above found also in living systems? What is the relationship of the above scheme with the apparently non-uniform stress to human body like pulling, compressing, shearing and vibrating?

1SB-03 身体-細胞能動 / 受動メカノケミカル連携：身体に生きる細胞のニッチとしての柔らかな細胞外基質環境が支配するやわらかさの階層と連携

Body-cell dynamic mechano-mechanical linkage: softness, flexibility, fluctuation and controllability derived from ECM environment as "niche for cells in our body"

Yoriko Atomi[1], Miho Shimizu[2], Eri Fujita[2], Tomoaki Atomi[3], Noboru Hirose[3], Katsuya Hasegawa[4] ([1]*Radioisotope Center The University of Tokyo*, [2]*Dept. of Mechano-Informatics, Univ. of Tokyo*, [3]*Teikyo University of Science*, [4]*JAXA*)

After 3.11, we all need re-think the science based on the principle of living human system. Fumio-Osawa has already discerned that biological macro molecules such as F-actin in muscle is more flexible/fluctuate in action, suggesting that all physical activities may promote flexibility at the molecular levels. We human beings belong to eukaryote as multi-cellular organism. Sixty trillions cells in our body are soft and sticky compared with yeast cells, which have hard cell wall like plant. In addition, we should think about specificity of multicellular organism in our body, which cells can communicate each other with mechano-mechnical linkage and also using paracrine and autocrine, and/or secretion of ECM molecules. Acquiring controllability of the human body is essential to receive a benefit from cellular activity-dependent manner, which is a principle of life. Rapid progress of stem cell technology shed light on an importance of a special microenvironment termed the "niche" (ECM), a relation between the cells and our own body as a niche at macro-level is mysterious. Various phenomenological results from exercising/immobilized knee, unweighting/gravity loading muscle, heat loading muscle cells, and solubilized eggshell membrane treated skin which give us "Knowledge" of life and exercise sciences are included in this topic. Enhanced adaptability for wellbeing brought by soft and flexible fine-tuned extracellular matrix will link body-to-cell and solve many problems in aged society where people live with unstable body under the gravity.

1SB-04 多分節立位を可能にした身体の冗長性：柔らかさの制御と破綻

Flexibility of human body with multi-segmental structure enabling bipedal standing

Tomoaki Atomi[1,2], Noboru Hirose[1], Miho Shimizu[3], Yoriko Atomi[3] ([1]*Teikyo Univ. of Sci.*, [2]*Grad. Sch., Univ. Tokyo Metropolitan*, [3]*Univ. of Tokyo*)

Human body movements are restricted by the shape/structure of the human body parts, like bones, muscles, and joints. Structure-function relationship of the body is deduced from dynamic protein structures/ interactions at micro cellular level, and from bone shapes of the joint which affects how body moves at macro level. In principle, life has been evolved to the species survival and preservation. If we look at the individual humans, a system to control the gravity center of the body within an appropriate range away from a possible danger of falling down is essential for life survival. Gravity center of the body is affected by the shape of the segments primary consisting from bones, and soft tissue consisting of diarthrodial joint. Intrinsically unstable bipedal human being controls gravity center of the body at relatively higher position compare to four-legs animals. Possible compatibility of multi-segmentality and stability shows that close relation exists between regulation systems of physical movement and physical property of soft tissue, and gravity center of the body. The present study is focusing on body elasticity (material) and balance regulation (controllability) to the physical movement which affects the shape alterations of the body figure (eg. standing, crouch down, lay down, etc.).

1SB-05 人工制御した細胞基盤の柔らかさと細胞応答

Softness of the artificial cell niche and its active interplay of forces

Miho Shimizu[1], Yuki Katsurada[2], Toshiyuki Watanabe[2], Eri Fujita[1], Tomoaki Atomi[3], Noboru Hirose[3], Katsuya Hasegawa[4], Yoriko Atomi[5] ([1]*Dept. of Mechano-Informatics, Univ. of Tokyo*, [2]*Tokyo Univ. of Agri. & Tech.*, [3]*Teikyo University of Science*, [4]*JAXA*, [5]*Radioisotope Center The University of Tokyo*)

We, human beings are living on earth under 1G through interactive communication back-and-fourth between natural and artificial environment. By acquiring large adaptability, namely 'flexibility' at cellular level, we will survive super ageing society and extreme conditions such as natural disasters and climate changes within controllable range. Looking at micro-level, adherent cells reside in our body can 'feel' their environment such as stiffness of the ECM, known to determine the cell fate (Engler et al, 2006), and alter cell behavior. Therefore exploring the method for give a good ECM as niche of the cells will provide an ultimate strategy for human wellbeing. To do so, it is important to have a fine evaluation system at single cell level. In this study, we are using micro-needle arrays fabricated by two-photon initiated polymerization (TPIP) of polymer acryl amide gels that can detect an active interplay of forces between cells and their environment. Stiffness of the cell microenvironment can alter with several factors including gel components, hight and diameters, and coating materials of the micro-needle. Studies using rat L6 skeletal muscle cell tested for different protein coating condition and amount of small heat shock protein will be presented.

1SB-06 培養基盤の硬さとの整合性が心筋拍動パターンを最適化する

Rigidity Matching between Cells and the Extracellular Matrix Leads to the Stabilization of Cardiac Conduction

Marcel Hoerning (*RIKEN, Center for Developmental Biology, Physical Biology Unit*)

We show, though investigations in the spontaneous substrate-induced modulation of synchronized beating in cultured cardiomyocyte tissue, that when the rigidity of the cardiac cell culture environment matches that of the cardiac cells, the tissue functionality and entrainment dynamics enhances and lead to a closer approximation to native cell functionality [1]. Systematically studies on entrainment dynamics of spontaneous originated waves showed that the main entrainment-frequency increases with the increase in substrate rigidity, and the entrainment stability of spontaneous originated waves become maximized when the substrate rigidity and cell rigidity (~4 kiloPascals) matches. Further, independent studies on the calcium transient alternates (CTA) in high frequency-paced tissue showed an significant increase in the critical period. CTA is known to be responsible for life-threatening arrhythmia in a real beating heart. We explain our findings by the enhancement in the cell development that alters the cell morphology (actin skeleton, gap-junction distribution, etc.) on the one hand, and by optimization of force actuation and coupling between the cells and extracellular matrix. Our studies suggest that mimicking the extracellular environment in in vitro cultures can cause the tissue culture to more closely approximate native cell functionality, and may help improve reengineering heart tissues for regeneration of diseased hearts.

1SB-07 アクチン繊維のゆらぎを基盤とした生理機能

Physiological functions of an actin filament based on its fluctuation

Hajime Honda (*Dep. Bioeng. Nagaoka Uni. Tech.*)

Fluctuation of a trajectory of moving actin filaments appears to possess close relations to their velocity of sliding motion in vitro. The spatio-temporal fluctuation of wiggling filament strongly depends on both the chemical and the physical conditions imposed on it. We have been focusing on the transitions of mechanical fluctuations at low ATP concentrations where the filament begins to move from rigor states to a unidirectional manner. During sliding motion, single monomers embedded in a single filament supposed to be subjected to push-pull forces from neighboring monomers in addition to the driving forces from myosin molecule(s). Push-pull forces which should associated with the dynamic linkage between monomers, and the flexibility and the cooperativity along the filament. Detailed measurement of the wiggling of monomers within a filament seemed to insinuate that the spatial range of cooperativity spread not only along the filament but also perpendicular to it.

We have been investigating the mechanical fluctuation of actin filaments from the informational aspects; information in order to systematically control the velocity of both entire single and spatially distributed groups of filaments. Various types of dynamic behavior of actin filaments will be demonstrated in this symposium in association with their physiological functions.

1SB-08 生命の神秘に迫る多次元アプローチ

Multidimensional Approaches to the Secrets of Life

Shigeru Takemori (*Jikei Univ. Sch. Med.*)

To reveal the secrets of spirally streaming cream on coffee surface, diverse approaches at macroscopic to microscopic levels would certainly be necessary. In building our understanding of the spiral streaming, some findings intuitively seem significant in constructing a specific streaming pattern. We hope the present symposium under a key concept of flexibility in hierarchical dynamics has provided a good chance to brush up your intuition in your approach to the secret of life.

1SC-01 特異極限解析：生物システムに現れるパターンを捉える

Singular limit analysis: Understanding of biological pattern formation

Yasumasa Mimura (*Graduate School of Advanced Mathematical Sciences, Meiji University*)

Reaction-diffusion system is a model that describes patterns that arise in biological systems. Even though it is one of the most simple system of equations among non-linear partial differential equations, it nevertheless exhibits diverse temporal-spatial patterns. Singular limit analysis is a method developed to understand the occurrence of such patterns. In this lecture, we give an introduction to this method, illustrated with concrete examples.

1SC-02 鳥の群れの集団動力学

Collective dynamics of flocking

Yoshinori Hayakawa (*Center for Information Technology in Education*)

Flocking of birds exhibits varieties of collective behavior depending on species and conditions. To understand the physical properties of such collective dynamics as self-organization processes of self-propelling elements, we conducted quantitative field study on the structure of flocks and its spatiotemporal dynamics for two distinctive examples; skeins of white-fronted geese and swarm of starlings. In appropriate situations, large populations of geese exhibit dynamical rearrangements by repeated mergers and splits among the groups. We described such grouping process in terms of a mean-field model based on the Smoluchowski equation of coagulation with fragmentation and observationally plausible kernels. We also performed a spatiotemporal analysis of wave excitation in a long one-dimensional chain of airborne geese by measuring the phase velocity and the dispersion relation, which leads to a simple mathematical model similar to that of single-lane traffic flow. Cluster of starlings exhibits very different shapes and dynamics. By using a portable three-dimensional image analysis system to estimate the trajectories of each individual in the field, we determined the shape and the proportion of flocks of starlings and found a simple scaling relation. We also found that mutual rearrangement of individuals in a flock can be considered as a short-term diffusion process, which seems to be a stabilizing factor to tame intrinsic dynamical instabilities of the system.

1SC-03 バクテリアのコロニー形成―細胞の集団運動―

Colony Formation in Bacteria -Collective Movement of Cells-

Mitsugu Matsushita (*Meiji Institute for Advanced Study of Mathematical Sciences (MIMS), Meiji University*)

We present experimental results of colony formation in bacteria. Common bacterial species *Bacillus subtilis* is known to exhibit various colony patterns such as DLA, Eden, highly branched with smooth circular envelope and disk ones, depending on the environmental conditions, namely, substrate softness and nutrient concentration. We have extended experiments of colony formation to various species of bacteria such as *Proteus mirabilis*, and *Eschelichia coli*. The growth behavior really reminds us of the formation of human colonies such as villages, towns and cities. We have established the morphological diagram of colony patterns, and then examined and characterized both macroscopically and microscopically how they grow. The most impressive growth is the formation of concentric-ring colony formation. Our experimental results suggest that macroscopically the most important factor for its growth is the cell population density, i.e., that there seem to be higher threshold of the cell population density to start migrating and lower one to stop migrating. Recently we found that several other common bacterial species such as *Serratia marcescens* and even *Eschelichia coli* also exhibit repetitive growth of colonies under appropriate conditions. This suggests that this type of growth is common in the bacterial world.

1SC-04 生命ネットワークにおける動的ロバスト性の数理的解析

Mathematical analysis of dynamical robustness in biological networks

Gouhei Tanaka[1,2], Kai Morino[2], Kazuyuki Aihara[1,2] ([1]*Institute of Industrial Science, The University of Tokyo*, [2]*Graduate School of Information Science and Technology, The University of Tokyo*)

Biological systems are highly tolerant to some types of perturbations to which the systems are usually exposed. It is thought that this robustness has been acquired through an adaptation to the environment in the evolutionary process. However, they can be extremely fragile to other types of perturbations which rarely happen. Although this 'robust but fragile' property is an essential feature of biological systems, a mathematical theory to understand this property is yet to be fully established. A potent mathematical approach to examine structural robustness of biological networks has been developed in complex network theory. It has been revealed that heterogeneously connected networks (e.g. scale-free networks) are highly robust against random removal of nodes but extremely vulnerable to targeted removal of hubs. However, dynamics is not considered in this framework. Here we focus on another framework to deal with the robustness of dynamic activity in biological networks consisting of elements having intrinsic dynamics. When some elements are inactivated, the level of dynamic activity of the whole network is lowered. There is a critical ratio of inactivated elements, at which the network dynamics vanishes. By analyzing this phase transition, we show that heterogeneously connected networks are highly fragile to targeted inactivation of low-degree elements. This is in strong contrast to the property of structural robustness. Our result implies that the interplay between dynamics and structure plays an important role in network robustness.

1SC-05 自律的酵素量制御による時間スケール調整；ホメオスタシスと記憶

Homeostasis and memory by autonomous regulation of time-scales through enzyme abundances

Kunihiko Kaneko (*University of Tokyo, Center for Complex-Systems Biology*)

Biological systems generally consist of a variety of time scales. These timescales also change in time depending on their internal state, according to the change in abundances of enzyme that governs the reaction speed. Here we discuss that homoeostatic response and memory emerge as autonomous regulation of enzyme concentrations. First it is shown that slow relaxation process with some plateaus generally emerge in dynamics of catalytic reaction networks, where the negative correlation between the enzyme and substrate abundances is a key factor for such ‘glassy’ dynamics [1]. Second, we demonstrate that the enzyme-limited competition leads to a homeostasis in the system. To be specific, we study temperature compensation in period of circadian rhythm [2]: By considering a simple system consisting just of Kai proteins, the period of the rhythm is found to be kept constant against temperature change. The origin of this temperature compensation is attributed to enzyme-limited competition, where negative correlation between abundances of substrates and enzymes again plays an important role. Finally, another consequence of long-term dynamics by autonomous regulation of enzyme abundances is generation of cellular, epigenetic memory. After discussing this possibility, I will also illustrate relevance of epigenetic memory to adaptation [3] and differentiation, if I have time.

[1] A. Awazu and K. Kaneko “ “Glassy” Relaxation in Catalytic Reaction Networks” Phys.Rev. E, 80, 041931 (2009)

[2] T. S. Hatakeyama and K. Kaneko “Generic temperature compensation of biological clocks by autonomous regulation of catalyst concentration” PNAS, 109 (21) 8109-8114, 2012

[3] C. Furusawa and K. Kaneko, “Epigenetic feedback regulation accelerates adaptation and evolution” submitted.

1SD-01 Characterization of Protein-DNA complexes dynamics related to Chromatin structure regulation using Single-Molecule Techniques

Yong-Woon Han, Yoshie Harada (*iCeMS, Kyoto University*)

Eukaryotic gene expression is regulated by chromatin structures and/or DNA modification such as CpG methylation. The basic unit of eukaryotic chromatin structure is a nucleosome consisting of approximately 150 bp DNA wrapped in 1.7 superhelical turns around a histone octamer. The histone octamer consists of two copies each of H2A, H2B, H3 and H4. Posttranslational histone modifications such as acetylation, methylation, phosphorylation and ubiquitylation regulate chromatin structure, resulting in activation or repression of gene expression. On the other hand, CpG methylation represses gene expression and is essential for silencing of parasitic DNA, genomic imprinting and embryogenesis. During DNA replication, methylated CpGs are converted into hemi-methylated CpGs and newly replicated CpGs should be methylated to inherit methylation pattern. DNA methyltransferase 1 (Dnmt1) is the enzyme to methylate hemi-methylated CpG regions. Np95 is methylated CpG binding protein and interacts with Dnmt1, followed by recruitment of Dnmt1 to hemi-methylated CpG regions. SRA domain of Np95 is responsible for hemi-methylated CpG binding activity. We characterize the process of hemi-methylated CpG recognition by SRA domain using Single-Molecule technique, and in this symposium, we will show our present data.

1SD-02 The mechanism of nuclear protein searching on DNA: Coarse-Grained simulation study

Tsuyoshi Terakawa (*Grad. Sch. Sci., Univ. Kyoto*)

Various nuclear proteins search their specific binding sites on DNA and function at proper time and location. This process is important for gene expression regulation. Previous theoretical studies have revealed that combination of one-dimensional diffusion along the DNA chain and three-dimensional diffusion in the bulk solution makes it possible for these proteins to search its cognate binding site efficiently. Although this theory is based on an assumption that these proteins can quickly diffuse on DNA, the mechanism of the quick diffusion at molecular level has been elusive. In addition, it has been controversial whether the same mechanism is valid in nucleosomal environment in which histone proteins bind to DNA and possibly hinder the one-dimensional diffusion.

In order to approach such problems, we have developed coarse-grained model for protein-DNA complex where most of the parameters are derived from atomic structural information or atomic simulation results. Using this model, we conducted molecular dynamics simulations of several proteins (e.g. TF IIIA, p53, and PCNA) with DNA and got insights into the mechanism of one-dimensional diffusion on DNA. We also performed simulations of the proteins with DNA to which histone proteins bind. Then, we will discuss the validity of this mechanism in nucleosomal environment.

1SD-03 Differences in dissociation free-energy profiles between cognite and non-cognite protein-DNA complexes

Yoshiteru Yonetani, Hidetoshi Kono (*Japan Atomic Energy Agency*)

DNA-binding proteins recognize cognate and non-cognate DNA sequences with two different binding modes, in which proteins loosely bind to non-cognate DNA sequences, but to cognate sequences they tightly bind. Experimental structures of such complexes provides us an atomic view of the binding modes, however, it is not so simple to dissect which is cognate or non-cognate complexes by seeing the structures.

In this study, free-energy profiles for dissociation of a cognate and a non-cognate Lac repressor-DNA complexes were calculated to obtain energetic views by performing atomic-level molecular dynamics simulations. We implemented an algorithm of adaptive biasing force (ABF) [E. Darve, A. Pohorille, *J. Chem. Phys.* **128**, 144120 (2008)] into the AMBER software to calculate free energy changes in dissociation along a dissociation path. The results showed that the free energy profiles were clearly distinct between the cognate and non-cognate complexes. We found that this difference can be interpreted in terms of changes in the protein-DNA contacts and the number of interfacial hydration water. The calculated dissociation process here agrees with that suggested from an H/D exchange experiment. In the talk, we will discuss how gene regulatory proteins find their target sites on the DNA and what are determinants for distinguishing cognate and non-cognate targets.

1SD-04 線虫初期胚における染色体ダイナミクスの定量的解析

Quantitative analyses of chromosome dynamics in C. elegans early embryos

Takeshi Sugawara, Ritsuko Arai, Akatsuki Kimura (*National Institute of Genetics*)

During development and differentiation, it has been suggested that chromatin remodeling occurs and contributes to cell fate determination. However, there are few studies for chromatin dynamics during the course of development. We visualized and tracked chromatin loci in C. elegans early embryos. Based on the experimental data, we statistically analyzed dynamics of the chromatin locus, and then revealed quantitative features of chromatin dynamics for several developmental stages. We found several quantitative features that depend on

developmental stages and the size of the nuclei at the stages. In order to characterize chromatin dynamics further, we are focusing on the anomaly of chromatin diffusion. The anomalous diffusion should be caused by uncharacterized intra-nuclear structures that disrupt free diffusion of the chromatin locus. Therefore, we may be able to extract biological information about intra-nuclear structures.

1SD-05 蛍光相関分光法を用いた細胞内グルココルチコイド受容体の動態解析

Inside view of molecular dynamics of Glucocorticoid Receptor by using Fluorescence Cross Correlation Spectroscopy in living cell

Masataka Kinjo (*Faculty of Advanced Life Science, Hokkaido University*)

The glucocorticoid receptor (GR) is a ligand-inducible transcription factor belonging to the nuclear receptor superfamily. Upon ligand binding, GR translocates from cytoplasm to the nucleus, then associate as a dimer form with glucocorticoid response element (GRE) in a promoter region, or as a monomeric complex that operate with other transcription factors to induce transcription. Besides homodimer of GR can act as repressor by association to negative GRE, GR can tether other transcriptional factors, such as NFkB, as monomer. These complicated regulation can be unraveled by determination of affinity properties of GR and/or associated molecules in living cell.

Fluorescence correlation spectroscopy (FCS) provide two molecular properties such the diffusion time and the number of molecules in defined region. Then, molecular interaction is accessible from the changing of the diffusion time. FCS measurement revealed interaction between GR and DNA in nucleus could be modified by difference of ligand.

To understand more detailed of GR dynamics in nucleus, the dimerization process of GR that is occur before binding to GRE was evaluated by using Fluorescence Cross Correlation Spectroscopy (FCCS) measurement of transiently expressed mCherry tandem dimer (mChe2) and EGFP fused GR in living cell.

In our experiment, the positive cross correlation was obtained after addition of Dex. Then, Kd (dissociation constant) value of dimerization of GR wild type and mutant were estimated and compare in living cell.

1SE-01 蛋白質構造の整合性原理とその拡張

Consistency principle of protein conformation and its extension

Masaki Sasai[1,2,3] ([1]*Nagoya University*, [2]*Okazaki Institute for Integrative Bioscience*, [3]*Korea Institute for Advanced Study*)

Proteins are evolutionarily designed polymers which have the ability to fold into unique conformations (either as single molecules or as parts of molecular complexes). The design principle of proteins to facilitate such folding was summarized as "consistency principle" by N. Go in 1983. The validity of this principle was intensively examined in 1990s and 2000s, from the view point of the closely related "minimal frustration principle", and the power of those principles in analyses of folding pathways, structure prediction, and protein design has been proven. In this talk, we revisit the consistency principle and discuss its extension to analyze protein functioning. First, the consistency principle is represented in 2 or 3 dimensional space of order parameters of conformation change. In such multi-dimensional expression, competition among multiple folding pathways and coexistence of multiple intermediates can be analyzed, and the further application of the principle is discussed. Proteins have evolved, however, not to fold but to function, so that the functional necessities may lead to inconsistent interactions in proteins. We discuss the localized inconsistent (frustrated) regions in proteins, which are important in allosteric transformations and catalytic reactions. We show the chameleon model, which was introduced by T.P. Terada and colleagues, is the efficient tool to analyze the roles of inconsistency in proteins.

1SE-02 Dynamic mechanism for the transcription when responses to activators

Yaolai Wang, Feng Liu, **Wei Wang** (*National Lab. Solid State Microstructure and Dept. Phys., Nanjing Univ.*)

The transcription apparatus (TA) is a complex molecular machine, and involves complicated interactions between the enhancer and various proteins, and those between the related proteins themselves. The TA detects the time-varying concentrations of transcriptional activators and initiates mRNA transcripts at appropriate rates. We propose a dynamic model to describe how the TA can dynamically orchestrate reliable transcriptional response based on the general configurations of TA. We argue that there exists a relatively stable clamp-like space between the Mediator complex and the enhancer, and activators cycle rapidly in and out this space. The entry of activators into this space results in conformational transition in the Mediator complex, which gives rise to a facilitated circumstance where Pol IIs can initiate/re-initiate transcription rapidly. As a result, the activators' concentration can be encoded by a temporal occupancy rate which modulates the transcription. Furthermore, we build a stochastic model which reproduces and reconciles several experimental observations. These indicate that regulated transcription likely shares the same dynamic principles. [1] Y. L. Wang, F. Liu, and Wei Wang, "Dynamic mechanism for the transcription apparatus orchestrating reliable responses to activators", Scientific reports, 2: 422, DOI: 10.1038/srep00422

1SE-03 保存アミノ酸に着目したジンクフィンガーの構造と分子認識

New Functions of Zinc Fingers Revealed by Substitution of Conserved Residues

Miki Imanishi (*ICR, Kyoto Univ.*)

The C2H2-type zinc finger motif is among the most major DNA binding motifs in eukaryotes. Each finger folds into a globular structure by coordination of a zinc ion with the conserved two cysteine (C) and two histidine (H) residues in a tetrahedral fashion. This fold is stabilized by hydrophobic interactions formed by the conserved hydrophobic amino acid residues. Usually, multiple zinc finger motifs are connected by conserved linkers. Though the Zn(II) ligands, the hydrophobic amino acid residues, and the linker are highly conserved among the C2H2-type zinc fingers, their contribution to structure and functions is not clearly understood. Here, the highly conserved amino acid residues were mutated and the function was investigated. Mutation of the conserved hydrophobic amino acids clarified the relationship between formation of a hydrophobic core and DNA binding function. On the other hand, ligand substituted zinc fingers, in which cysteine residue(s) is substituted to histidine residue(s), showed hydrolytic ability. In addition, the Zn(II)-dependent DNA binding domain, CDH2-zinc finger, has been successfully created by reducing the Zn(II) binding affinity via ligand substitution of the second cysteine to aspartic acid. The linker alteration changed the DNA binding selectivity to discontinuous target sequences. The new functions of zinc fingers revealed by substitution of highly conserved residues will be discussed.

1SE-04 ドメインスワッピングによるシトクロム *c* の多量化

Oligomerization of cytochrome *c* by domain swapping

Shun Hirota (*Grad. Sch. Mat. Sci., Nara Inst. Sci. Tech.*)

Cytochrome *c* (cyt *c*) is a stable protein which functions in a monomeric state as an electron donor for cytochrome *c* oxidase. It is also released to the cytosol at the early stage of apoptosis. For nearly half a century, it has been known that cyt *c* forms polymers, but the polymerization mechanism remains unknown. We found that cyt *c* forms polymers by successive domain swapping, where the C-terminal helix is displaced from its original position in the monomer and Met-heme coordination is perturbed significantly [1]. In the crystal structures of dimeric and trimeric cyt *c*, the C-terminal helices are replaced by the corresponding domain of other cyt *c* molecules and Met80 is dissociated from the heme. The solution structures of dimeric, trimeric, and tetrameric cyt *c* were linear based on small-angle X-ray scattering measurements, where the trimeric linear structure shifted toward the cyclic structure by addition of PEG and $(NH_4)_2HPO_4$. The absorption and CD spectra of high order oligomers (~40mer) were similar to those of dimeric and trimeric cyt *c* but different from those of monomeric cyt *c*. For dimeric, trimeric, and tetrameric cyt *c*, the ΔH of the oligomer dissociation to monomers was estimated to be about -20 kcal/mol per protomer unit, where Met-heme coordination appears to contribute largely to ΔH. The present results suggest that cyt *c* polymerization occurs by successive domain swapping, which may be a common mechanism of protein polymerization.

1. S. Hirota *et al.*, Proc. Natl. Acad. Sci. USA, 107, 12854-12859 (2010).

1SE-05 マルチドメインタンパク質のフォールディングとコンフォメーション動力学

Folding and conformational dynamics of multi-domain proteins

Shoji Takada (*Dept. Biophys, Kyoto Univ.*)

Although folding reactions and fluctuations of small and single domain proteins have been relatively well understood by now, much less is clear for folding and functional dynamics of larger and multi-domain proteins. Here, we present our recent computational work on three case studies of large and/or multi-domain proteins. First, we discuss both folding and conformational dynamics of adenylate kinase, a model allosteric protein, which shows rather rich behaviors. Second, we discuss folding-coupled docking in a split GFP. Finally, importance of co-translational folding is addressed for a three-domain protein suf1 by computer simulations.

1SF-01 細胞の変形と運動：理論と実験の挑戦

Deformation and motion of cell: theoretical and experimental challenges

Masaki Sano (*Grad. Sch. Sci. U. Tokyo*)

Deformation and motion are indispensable features for the understanding of living systems. Recent development in theoretical approaches on deformation and motion of living systems will be discussed in this session. After taking a bird's eye view of these concepts, I will discuss on deformation and motion of single amoeba cell with regard to a mathematical modeling based on recent experimental findings.

Cell migration is a highly complex process that integrates many spatial and temporal cellular events. Motile bacteria and most eukaryotic cells can move in a directed manner or spontaneous fashion depending on the presence or absence of external cues. In general, motile cells are able to migrate spontaneously in a seemingly random manner even in the absence of external stimuli. It is this character that allows the cells to forage and explore their surroundings by balancing random and directed migrations. To understand how amoeboid cell crawls on the substrate by deforming its shape, we performed a multipole expansion analysis of traction force distribution exerted by individually migrating amoeboid *Dictyostelium* cells and looked at correlations to their motion. Interestingly enough, some new modes in traction force dynamics are found in this analysis. In addition to a familiar inchworm-like mode, we found other modes, i.e. squeezing-stretching mode and crawling mode. These modes are found to be fundamental modes in deformable objects that migrate on the substrate. Possible relations to a recent theoretical approach will be discussed.

1SF-02 マウスの左右決定の過程に見られるノード繊毛の回転運動の同調

Synchronization of rotaional movement in mouse node cilia during left-right determination

Atsuko Takamatsu[1], Kyosuke Shinohara[2], Takuji Ishikawa[3], Hiroshi Hamada[2] ([1]*Dept. Elec. Eng. and Biosci., Waseda Univ.*, [2]*Grad. Sch. Frontier Biosci., Osaka Univ.*, [3]*Dept. Bioeng. and Robotics, Tohoku Univ.*)

Animals have slight left-right (LR) asymmetry. The LR body axis in a mouse is considered to be established by unidirectional flow in a node cavity of mouse embryo. The unidirectional flow is generated by rotation of tilting monocilia. It has long been believed that rotation of the numerous cilia is necessary to trigger the LR determination. However, recently we found rotation of only two cilia is sufficient [1].

To investigate what the only two cilia can achieve, we focus on the relation of rotational movement between a pair of isolated two cilia in a mutant mouse. The cilia intervals are much larger than those for systems with densely arraigned cilia such as epithelium or swimming protozoan showing metachronal waves. Thus the establishment of the cooperative movement is considered to be difficult. However, we found the phase locking is easily observed in the mouse system.

To verify the existence of phase locking state theoretically, we applied the phase reduction theory combined with computational fluid dynamics under a hypothesis there is hydrodynamic interaction among cilia. Analysis results using the same parameter as those of the experimental condition such as cilia length, intervals, tilting angle, and etc. was compared. The results suggest the phase locking can be established via only hydrodynamic interaction even though the cilia arrangements are sparse. Finally the biological advantage of the phase locking will be discussed.

[1] K. Shinohara et al. (2012) Nat. Commun. 3, 622.

1SF-03 鞭毛や繊毛の流体力学相互作用による同期：ミニマルアプローチ

Synchronization of flagella and cilia by hydrodynamic interactions: minimal approach

Nariya Uchida[1], Ramin Golestanian[2] ([1]*Dept. Phys., Tohoku Univ.*, [2]*Cent. Theor. Phys., Univ. of Oxford*)

Unicellular organisms such as E. Coli and Paramecium swim in viscous environment using flagella or cilia. Coordinated motion of these active filaments, known as flagellar bundling and ciliary metachronal waves, are important for achieving efficient propulsion. The roles of long-range hydrodynamic interaction in their synchronized motion were addressed as early as in 1951 by G. I. Taylor, and are recently attracting increasing attention. While large-scale numerical simulations of the filament dynamics have been developed, the key mechanism of synchronization is still far from well understood. In this talk, we consider a couple of minimal models of hydrodynamic synchronization, in which the center-of-mass motion of cilia or flagella is represented by a rigid bead making a fixed trajectory. In the first model, the driving force acting on the bead is a periodic function of its phase, which generalizes the effective and recovery strokes of ciliary beating. For arbitrary trajectory shape, we derive sufficient and necessary conditions for two parallel rotors to synchronize. In the second model, each bead exerts a radial pumping force on the surrounding fluid, and at the same time is driven by a constant torque. The model exhibits various collective behavior such as defect coarsening, turbulent spiral waves, traveling waves, and order-disorder transition. We discuss the results from the perspective of coupled oscillators with long-range interactions.

1SF-04 興奮性化学進行波に駆動される遊走細胞の形態ダイナミクスの数理モデル

Modeling morphological dynamics of migrating cells governed by self-organized excitable waves

Shuji Ishihara[1], Daisuke Taniguchi[1], Satoshi Sawai[1,2] ([1]*Grad. Sch. Arts & Sciences, Univ. Tokyo*, [2]*JST PRESTO*)

Cell migration is one of the fundamental processes that support various biological functions such as immune response and development. In randomly moving cells, phosphatidylinositol (3, 4, 5)-trisphosphate (PIP3) and F-actin propagate as waves at the basal membrane that act to push out the cell border, and such chemical waves are responsible for the observed cyclic yet complex dynamics of cell migration. Although many of the molecular mechanisms underlying the process are known, how they give rise to these patterns is not well understood. Here, by using Dictyostelium discoideum as a model system, we address how the complex morphological change arises from the underlying molecular interactions. We present a theoretical description that integrates molecular processes inside cell and dynamics of cellular morphological change. In the model, excitability of the system is governed by positive feedback from PIP3 to PI3K activation that is mediated by actin polymerization. By incorporating membrane deformation into the model, we demonstrated how geometries of competing waves explain most of the observed dynamics of amoeboid morphology. The parameter dependence of the model, especially actin-mediated feedback strength, is compared with experimental observations for cells in which actin is perturbed.

1SF-05 細胞の力学と、人工システムにおける自発運動

Mechanics of gels and spontaneous motion of droplets as biologically-motivated systems

Natsuhiko Yoshinaga (*WPI-AIMR, Tohoku Univ.*)

In this talk, I will present two topics which would be hopefully merged in future: one is about mechanics of biological gels and the other is spontaneous motion of droplets. (i) Cross-linked actomyosin bundles retract when severed in vivo by laser ablation, or when isolated from the cell and micromanipulated in vitro in the presence of ATP. We identify the time scale for contraction as a viscoelastic time, where the viscosity is due to (internal) protein friction. The results are supported by an hydrodynamic model of a retracting bundle as a cylinder of isotropic, active matter, from which the order of magnitude of the active stress is estimated. (ii) I shall also show that spontaneous motion (also called as self-propulsion) of droplets driven by a surface tension gradient (Marangoni effect) coupled with internal and/or external patterns of chemicals. Such systems have been attracting attention in last decades for its potential application to biological problems such as cell motility. Recently several model experiments showing spontaneous motion have been proposed. The systems in these works consist of relatively simple ingredients, for instance, oil drops in water nevertheless the motion is as if the drops are alive. I will address why the particle moves without external force and why it breaks symmetry and chooses one direction.

1SF-06 這行による移動運動の理解に向けて

Towards understanding the locomotion of animals by limbless crawling

Ryo Kobayashi[1,4], Toshiya Kazama[1,4], Kentaro Ito[1,4], Yoshimi Tanaka[2], Toshiyuki Nakagaki[3,4] ([1]*Hiroshima University*, [2]*Yokohama National University*, [3]*Future University Hakodate*, [4]*JST, CREST*)

Limbless crawling is a fundamental form of animal locomotion adopted by a wide variety of species, including amoeba, earthworm, flatworm and snake. Limbless crawling can be classified into several types, which are amoeboid locomotion, one-dimensional peristaltic crawling (single lane and double lane), two-dimensional crawling and serpentine locomotion (lateral undulation, side winding, concertina). An interesting question from a biomechanics perspective is how limbless crawlers control their flexible bodies in order to realize directional migration.

In this paper, we mainly concentrate on the one-dimensional peristaltic crawling, which is driven by elongation-contraction waves propagating along the body axis. We will demonstrate that the model equation describing this type of locomotion is an one-dimensional diffusion equation with coefficients depending on the space and time variables. Simulations and theoretical analysis show that the proper control of friction with the substrate is essential for translating internal motion into directional migration. We also discuss about the two-dimensional crawling adopted by polyclad flatworms.

1SH-01 ハロロドプシンの構造と分子機能

Structure and Molecular Function of Halorhodopsin

Makoto Demura (*Fac. Adv. Life Sci., Hokkaido Univ.*)

Halorhodopsin acts as an inward-directed chloride pump. Recently, the electrical function of Natronomonas pharaonis HR (NpHR) has been applied to optogenetics, the technique of which has the potential to enhance the basic knowledge in neuroscience research and to inform the mechanisms and treatment of brain injury and disease. A detailed structural model of trimeric HsHR was built by Kolbe et al. in 2000 by means of X-ray crystallography. More recently, the trimeric NpHR-bacterioruberin complex has been isolated from the Natronomonas pharaonis strain KM-1 cells and its crystal structure has been also revealed by Kouyama group. The carotenoid bacterioruberin binds to crevices between adjacent NpHR subunits in the trimeric assembly and the central part of the trimer is filled with three lipid molecules. Although the crystal structures of HsHR and NpHR are very similar to each other, HsHR monomers in the homo-trimer are tilted relative to the monomers in the NpHR-bacterioruberin complex. In other words, there are two types of the trimeric HR assembly, a tilted homo-trimer and a trimeric complex with bacterioruberin. In the case of HR expressed in E. coli cell, NpHR forms a robust homo-trimer in a detergent DDM solution. Our results revealed that Phe150 was essential to form and stabilize the NpHR trimer in the DDM solution. Further analyses for examining the structural and functional significance of Phe150 mutant monomer and dimer in dark and light condition will be discussed.

1SH-02 Structural basis for light-gated cation conductance by channelrhodopsin

Osamu Nureki, **Ryuichiro Ishitani** (*Graduate School of Science, The University of Tokyo*)

Channelrhodopsins (ChRs) are light-gated cation channels derived from algae that have been found to provide experimental utility in the technology of optogenetics; for example, neurons expressing ChRs can be optically controlled with high temporal precision within systems as complex as freely moving mammals. Although ChRs have been broadly applied to neuroscience research, little is known about the molecular mechanism by which these remarkable and powerful proteins operate. Here we present the crystal structure of a ChR (C1C2 chimera between ChR1 and ChR2 from *Chlamydomonas reinhardtii*) at 2.3 Å resolution. The structure reveals the essential molecular architecture of ChR, including the retinal-binding pocket and the cation conducting pathway. Integration of structural and electrophysiological analyses provide insight into the molecular basis for the unusual operation of ChR, and pave the way for precise and principled design of ChR variants with novel properties. I will discuss the recent results of our study of the structure and variants of ChR.

1SH-03 チャネルロドプシンによる神経細胞ネットワーク素子の制御

Control of neural network devices by channelrhodopsin

Tsuneo Urisu[1,2] ([1]*Nagoya University, FIRST Research Center for Innovative Nanobiodevices*, [2]*Japan Science and Technology Agency, CREST*)

We have newly developed the incubation type planar patch clamp biosensor with PMMA (polymethyl methacrylate) substrate by using hot embossing, focused ion beam microfabrication and surface modification by extra cellular matrix. PMMA is an attractive material as the sensor chip of incubation type planar patch clamp from the view points of: low cost, easiness in various microstructure fabrications and surface chemical modifications and low dielectric constant compared with Si. Light-gated ion-channel protein is not only useful in the in vivo and in vitro neural network analysis, but also useful in the performance test of the newly developed ion-channel biosensor because of its high time and spacial resolutions and easiness of handling. We have evaluated the performance of the newly developed incubation type planar patch clamp biosensor with PMMA sensor chip by using the light-gated ion-channel protein, channelrhodopsin wide receiver, which was expressed on HEK293 cells. Observed laser-induced current profile almost completely agreed to those observed by pipette patch clamp. PMMA sensor chips showed faster response characteristics than Si sensor chip. Based on these results, we are now developing new high throughput screening devices with in vitro neural networks.

1SH-04 オプトジェネティクスを用いた睡眠覚醒調節に関わる神経回路の動作原理解明

Optogenetics reveals function of neural network involved in the regulation of sleep/wakefulness

Akihiro Yamanaka (*Research Institute of Environmental Medicine, Nagoya University*)

Orexin, also called hypocretin is a neuropeptide recently identified as a natural ligand for orphan G protein coupled receptor1. Orexin-producing neurons (orexin neurons) are located specifically in the hypothalamus but project their efferents throughout the brain. Intriguingly, the mice lacking prepro-orexin gene showed behavioral characteristics similar to human sleep disorder “Narcolepsy”, that is a fragmentation of sleep/wakefulness and sudden muscle weakness. Human clinical studies also showed that orexin neurons are specifically ablated in the narcoleptic patient’s brain. These results suggest that the orexin neurons play a critical role in the regulation of sleep/wakefulness. Previous studies using electrophysiology have identified potential neuronal pathways or networks connecting orexin neurons with other neurons which are known to be involved in sleep/ wakefulness regulation. However, it will be essential to analyze living animals for the purpose of elucidating how these neuronal networks regulate sleep/wakefulness, a physiological phenomenon only observed in living animals. To address this, we incorporated recently developed technique “optogenetics”, which allows us to control neuron activity by illuminating light locally in the brain. In this symposium, I will discuss physiological importance of the activity of orexin neurons in the maintenance of arousal using optogenetics.

1SH-05 レチナールタンパク質の進化と機能多様性

Evolution and functional diversity of animal opsin-based pigments

Akihisa Terakita (*Grad. Sch. Sci., Osaka City Univ.*)

Thousands of animal opsins have been identified so far and they are phylogenetically classified into several groups. Most opsin-based pigments other than vertebrate visual pigments have a nature of a bistable pigment, of which light-activated state is stable and reverts to the original dark state by subsequent light absorption. We have investigated functional properties of various bistable pigments. The phylogenetic classification of opsins roughly corresponds to the difference in molecular function of the opsin-based pigments. We identified two novel opsin-based pigments, which activate Go and Gs in scallop and jellyfish photoreceptor cells, respectively. Several lines of evidence including our findings revealed that visual pigments of most invertebrate (protostomes) such as insects and cephalopods as well as vertebrate OPN4 homologues (melanopsins) activate Gq. Recently, it was reported that vertebrate OPN5 (neuropsin) activates Gi (Yamashita et al., 2010; Kojima et al., 2011). Therefore, accumulated knowledge suggests that diverged bistable pigments may drive cyclic nucleotide cascade or phosphoinositide cascade. Interestingly, some of opsin moieties of bistable pigments can bind all-trans retinal, as a chromophore, probably related to non-visual function. Molecular characteristics including G-protein signaling, photoreaction and retinal binding of various opsin-based pigments will be compared, and potential availability of the

diversified opsins as an optogenetics tool also will be discussed.

1SH-06 イカロドプシンの光活性化機構

Photo-activation mechanism of squid rhodopsin

Midori Murakami, Tsutomu Kouyama (*Grad. Sch. Sci., Nagoya Univ.*)

Retinal proteins have proven useful in the field of optogenetics. For further extention of the optogenetics, it is important to elucidate the activation mechanisms of indicvidual retinal proteins. The visual pigment rhodopsin is a photo-sensor protein in retina. Upon absorption of light, rhodopsin undergoes the photocycle and, via several intermediates, forms a final photoproduct which stimulates the intracellular signaling pathway to excite visual cells. Photochemical reactions, conjugated G-protein types and activation efficiencies of G-protein of invertebrate and non-visual rhodopsins are different largely from those of vertebrate visual rhodopsin. To reveal the molecular mechanism of rhodopsin activation, we have performed crystallographic analysis of squid rhodopsin. Squid rhodopsin extracted from microvillar membrane was crystallized into a P62 crystal. Spectroscopic data of the P62 crystal showed that a series of intermediates can be trapped by adjusting illumination condition and temperature regulation. The difference electron density map derived from diffraction data of unphotolysed and illuminated crystals exhibits complementary positive and negative densities around retinal in the transition from dark-adapted state, via bathorhodopsin, to lumirhodopsin. These data suggest different structural changes during the early and middle part of the photocycle of squid rhodopsin from those of bovine rhodopsin. I will discuss its implications in activation mechanism of squid rhodopsin.

1SH-07 GPCR の細胞内シグナル伝達を制御する構造特徴

Structural elements which control the signal transduction pathway of GPCRs

Makiko Suwa[1,2], Minoru Sugihara[2] ([1]*Colledge, Sci. Eng. AGU.*, [2]*CBRC, AIST*)

Recent optogenetic technology intends to control the intracellular signal of G-protein coupled receptor (GPCR) by using light instead of chemical substances. This technology made a chimera in which cytoplasmic loops of a rhodopsin are exchanged to those of other GPCR (Raag, D, Airan *et al.*, *Nature*, 2009). We address a question of how specific partial structural elements of GPCRs contribute to control the signaling pathway (G-protein coupling selectivity) by performing combined quantum/molecular mechanical (QM/MM), molecular dynamics (MD) studies of rhodopsin structure and sequence analysis of GPCRs. We compared the structures of Bovine and Squid rhodopsin which bind to G proteins of different kinds, as a model case. In the retinal binding pockets of the two rhodopsins, the similar environment containing highly conserved aromatic residues was observed. However, in the inter-helical environment, the stability of hydrogen bonding network formed between highly conserved Trp274 (Trp265) and Tyr 315 (Tyr 306) in squid (bovine) was different. Moreover, two rhodopsins show the significant difference about the number of salt bridges formed on cytoplasmic side loops. We also indicate difference of simulated structure of cytoplasmic side of rhodopsin according to the interaction with different type (Gq, Gt, Gs) of G-protein. Paying attention to these regions distributions of hydrogen bonding residues and charged residues were summarized as profiles. And the correlation of profiles and G coupling selectivity was investigated.

1SI-01 分子複合体フィラメントにおける骨格筋ミオシン 1 分子の力発生メカニズム

Force generation mechanism of single skeletal myosin molecules in myofilaments

Motoshi Kaya[1,2], Hideo Higuchi[1] ([1]*Grad. Sch. Sci, Univ. Tokyo*, [2]*JST, PRESTO*)

Skeletal myosins are non-processive motors and form ensembles to generate a great amount of force during rapid muscle contractions. Hence in order to understand the force generation mechanism of single skeletal myosins, we have investigated the mechanical properties of myosins embedded in synthetic myosin-rod cofilaments. We previously found that the elasticity of skeletal myosins is non-linear, implying that the non-linear elasticity might be a complementary function to reduce the drag effect when myosins are negatively strained after the force generation. Recently, we further investigated displacements and forces produced by synthetic myosin-rod cofilaments, which are composed of ~20 myosin interacting molecules. The results show stepwise changes of displacement and, the individual step sizes continuously decrease as loads increase up to 30 pN. In such high force ranges, single myosins cannot resist external loads solely, implying the synchronization of force generations between several myosin molecules. Such a coupling of force generation between myosin motors might be achieved by synchronizing biochemical reactions through strain-dependent kinetics (e. g., ADP release rate). In this symposium, we will discuss the force generation mechanism of single skeletal myosins found uniquely in ensembles of motor.

1SI-02 ダイニンモーター運動発生機構の構造的基盤

Structural basis of dynein motility

Takahide Kon (*Institute for Protein Research, Osaka Univ.*)

Dyneins are microtubule-based motor complexes of 1,000-3,000 kDa that power a wide variety of biological processes within eukaryotic cells, including ciliary beating, cell division, cell migration, and intracellular trafficking. Compared to the other cytoskeletal motors, the molecular mechanism of dynein is still poorly understood, in part due to the lack of high-resolution structural information. Here we report the crystal structure of the 380-kDa motor domain of Dictyostelium cytoplasmic dynein at 2.8-Å resolution with approximately 90% of its amino acid residues traced. This atomic structure shows details of functional units constituting the motor domain, such as the ATP-hydrolyzing ring composed of six AAA+ modules, the long coiled-coil microtubule-binding stalk, and the force-generating rod-like linker. We visualizes four ADP molecules bound to the first four AAA+ modules of the ring, among which three are active ATP hydrolysis sites. Our analysis also uncovers the junctional structures between the ring and the two mechanical units, which should be critical for dynein's motor function. The structure, together with the results of our EM and functional analyses, provides a framework for understanding the mechanism of dynein-based motility.

1SI-03 Microtubule corkscrewing motion driven by multiple non-processive motors

Junichiro Yajima (*Department of Life Sciences, Graduate School of Arts and Sciences, The University of Tokyo*)

Microtubule-based molecular motors are engines for producing a mitotic bipolar spindle architecture and a coordinated beating of cilia. They work by converting scalar chemical energy into mechanical 3D vector motion along microtubules. Current models for their mechano-chemistry propose that three dimensional directed mechanical forces originates either in a directionally-biased selection of microtubule binding sites, or in a directional conformational change that follows microtubule binding. In this study, we are exploring these competing proposals using a 3D optical tracking microscope, which permits studies to be made on mechanical motions of motors that are masked in conventional 2D-tracking experiments. To do this, we quantified 3D-microtubule motion driven by ensembles of minimum motile unit of microtubule-based motors such as single-headed kinesin-1s, 5s, 6s, 10s, 14s and single-headed outer-arm dyneins. We found that microtubule corkscrewing motion driven by these motors have their own intrinsic pitches, handedness and directions which can be influenced by mutations or phosphorylations in the motor head, ATP concentrations and geometry on the glass surface. Our results indicate that motors are capable of exerting a directed force separately parallel to a longitudinal axis of microtubules and perpendicular to the axis of microtubules. The mechanochemical properties of individual motors might be related to conserved functions of their motor domains based on a directionally-biased selection of microtubule binding sites.

1SI-04 微小管系分子モーターの複数分子による機能を計測する

Measuring ensemble functions of microtubule-based molecular motors

Ken'ya Furuta (*Bio ICT Lab, NICT*)

Molecular motors usually work together in teams within the cell. However, studying coordination among these motors has posed a challenge. Here we present an experimental system that enables a bottom-up approach where a defined number of motors can be self-assembled on a DNA scaffold to form a linear array assembly with defined spacing. Using this system, we first quantified the motion and force production of assemblies composed of either kinesin-1 or kinesin-14, which are kinesin motors with different processivity. We found that, regardless of the motor type, the binding time of assemblies on microtubules depends on the spacing between motors, suggesting that cooperative microtubule binding is the key to improving multiple-motor based transport. Force measurement of these assemblies demonstrated that

nonprocessive motors can coordinate with each other to exert much larger force than can single motors, while processive motors are not able to effectively share an external load. Using numerical simulations, we reproduced the observed experimental behavior and hypothesized a formerly unexpected stepping mechanism of nonprocessive kinesins. We also present a minimal tug-of-war between defined numbers of kinesin and dynein, which resulted in highly stochastic, bidirectional movement in the absence of external regulators. These findings highlight the impact of physical motor-motor interactions on collective transport and thus provide a step toward bridging the gap between single molecules and ensemble function.

1SI-05 A cellular funicular: one active force generation drives two directional organelle movements

Akatsuki Kimura[1,2] ([1]*Cell Architecture Laboratory, National Institute of Genetics*, [2]*Dept. Genetics, SOKENDAI*)

Organelles inside cells move to position themselves at the right place at the right time. Such positioning is driven by active force generators, typically the molecular motors. Previous studies on organelle transport mainly focused on cases wherein a single active force generating mechanism is responsible for the movement of an organelle toward one direction. Alternatively, one active force generation mechanism in a cell may drive organelle movements in two directions at the same time, like a funicular. Our recent studies using Caenorhabditis elegans embryos [1,2] and embryonic mouse brain cells [3] suggest the existence of such funicular-like coupled movements of organelles inside cells. Hence, we propose the existence of a "cellular funicular," [4] in which one active force generation mechanism drives organelle movements in two opposite directions; this may apply to many intracellular movements, and therefore, it potentially comprises a common force generation mechanism inside the cell.

[1] Kimura K & Kimura A. Proc. Natl. Acad. Sci. USA 108, 137-142 (2011); [2] Kosodo, Suetsugu, Suda, Mimori-Kiyosue, Toida, Baba, Kimura A & Matsuzaki. EMBO J. 30, 1690-1704 (2011); [3] Niwayama, Shinohara & Kimura A. Proc. Natl. Acad. Sci. USA 108, 11900-11905 (2011); [4] Niwayama & Kimura A. Worm 1, 71-75 (2012)

1SI-06 ミオシンの力生成・応答特性による上皮パターン形成
The emergence of epithelial pattern through force-generating and force-responding properties of myosin

Kaoru Sugimura[1], Shuji Ishihara[2] ([1]*Kyoto Univ.*, [2]*The Univ. of Tokyo*)

In the course of animal development, tissues undergo a series of deformations. These processes are realized by the coordination of spatio-temporal profiles of activity of proteins and mechanical force that directly acts on cell shape. It has been shown that the non-uniform localization of the force-generating molecular machinery including myosin results in biased cellular forces that drive the cellular rearrangements underlying tissue morphogenesis. Along these lines, it was suggested that the stress field-dependent myosin redistribution consists of a positive feedback loop that accelerates such irreversible cell shape changes.
The present study determines that force-responsive property of myosin as well as its force-generating property is critical for morphogenesis. By using a novel force-estimation method, we characterize the relationship between the force distribution, myosin localization, and cell elongation in the Drosophila wing. Our force-estimation analysis and mechanical manipulation of tissues clarified that the proximal-distally biased intrinsic cortical tension is generated in order to resist the anisotropic extrinsic stretching force. Moreover, the emergent global balance between the intrinsic and extrinsic forces plays a pivotal role in the epithelial pattern formation: the maximum stress direction of a cell population provides the directional information to instruct the local alignment of hexagonal cells, leading to the global organization of the hexagonally packed, structurally stable wing.

2SA-01 The Mechanism of Cytoplasmic Dynein Motility

Ahmet Yildiz (*University of California Berkeley*)

Cytoplasmic dynein is a cytoskeletal motor driving minus-end directed motility along microtubules (MTs). In contrast to kinesins and myosins, the mechanism by which the two catalytic head domains interact and move relative to each other remains unresolved. By tracking the positions of both heads at nanometer resolution, we found that the heads remain widely separated and move independently along the microtubule. By engineering the mechanical and catalytic properties of the motor domain, we show that a rigid linkage between monomers and dimerization between N-terminal tail domains are not essential for processive movement. Instead, dynein processivity minimally requires the linker domain of one active monomer to be attached to an inert MT tether retaining only the MT-binding domain. The release of a dynein monomer from the MT can be mediated either by nucleotide binding or external load, however, force applied to the linker domain inhibits nucleotide dependent release. Force dependent release is significantly asymmetric, with faster release towards the minus-end. These results lead us to a detailed mechanistic model of dynein processivity, directionality and force generation.

2SA-02 Architecture of the Flagellar Switch Complex

Brian R. Crane[1], R. Sircar[1], G. Gonzalez-Bonet[1], Koushik Paul[2], D. Blair[2] ([1]*Cornell University*, [2]*University of Utah*)

The switch complex of the bacterial flagella motor comprises a large cytoplasmic rotor assembly that couples with the intramembrane proton motors to drive rotation and mediate switching of the flagellum. The switch complex of E. coli is composed of the proteins FliG, FliM and FliN, with FliG most directly involved in rotation. In Gram-positive bacteria FliN is replaced by a larger protein, FliY, which can also act as a phosphatase for the switching signal, phosphorylated CheY. Through a combination of biochemical, genetic, crystallographic and spin-labeling studies we have investigated the interactions and arrangement of key components within the switch complex. The stoichiometric mismatch between FliG (26 subunits) and FliM (34 subunits) is well explained by two distinct positions for FliM: one where it binds the FliG central domain and another where it binds the FliG C-terminal domain. This architecture provides a structural framework for addressing the mechanisms of motor rotation and direction switching. Recent data on conformational changes within the switch complex induced by phosphorylated CheY will also be discussed.

2SA-03 Imaging Water at the Nanoscale and Protein in Water by TEM

Paul T. Matsudaira (*Department of Biological Science, National University of Singapore*)

Interfacial water is the first layers of water molecules in immediate contact with a surface, whether solid, liquid, or gas and represent the "bound" water surrounding proteins and other macromolecules and structures in a cell. Since the cell is a "crowded" environment, interfacial water plays an important role in biological function. However, interfacial water does not display the hydrodynamic properties of bulk water. Studying interfacial water has been experimentally difficult and requires methods with resolution in the nm-scale. Recently, we have developed new methods for studying water and protein in water directly by imaging in the TEM. Key is the refinement of a microfabricated liquid cell, the dimensions of a TEM grid, which can protect liquids against the high vacuum of a TEM. Samples are viewed through 10 nm thick silicon nitride windows. In this device, we can study fluidics at the nanoscale and observe stick-slip motions of nm-diameter water droplets as well as significantly damped Brownian motion. Furthermore, when applied to protein, we can image macromolecular protein structures in liquid water and observe the dynamic motion of proteins that are not absorbed to the window of the liquid cell. We now show that the resolution is limited by radiation damage and the thickness of the silicon nitride windows. Our studies show that it is now possible to study directly dynamics of water and protein in water at the nm-scale by TEM.

2SA-04 Function dictates topology in biochemical networks

Chao Tang (*Peking University, University of California, San Francisco*)

A diverse set of biological functions in a diverse set of cells and organisms are performed by a myriad of biochemical networks. A major challenge in systems biology is to seek design principles or general rules that link network function and topology. I will present two case studies in which the network function limits the choice of the network topology to a very small set. One case concerns with the biochemical adaptation. We show that there are only two core topologies that can achieve perfect adaptation. The other case is the parasegments boundary formation in fruit fly development. The network topology for this patterning function has to be one of the few variants of a core topology. A function-topology map would guide us to comprehend natural biochemical networks, identifying key or missing nodes and links and suggesting the network's function. It can also provide us with a manual to synthesize artificial networks.

2SB-01　遺伝子発現ノイズの起源

Examining origins of noise in gene expression

Yuichi Taniguchi, Yutaka Ogawa, Masae Johmura (*Quantitative Biology Center, RIKEN*)

Protein and messenger RNA (mRNA) copy numbers vary from cell to cell in isogenic bacterial populations. However, these molecules often exist in low copy numbers and are difficult to detect in single cells. We carried out quantitative system-wide analyses of protein and mRNA expression in individual cells with single-molecule sensitivity using a newly constructed yellow fluorescent protein fusion library for *Escherichia coli*. We found that almost all protein number distributions can be described by the gamma distribution with two fitting parameters which, at low expression levels, have clear physical interpretations as the transcription rate and protein burst size. At high expression levels, the distributions are dominated by extrinsic noise. We found that a single cell's protein and mRNA copy numbers for any given gene are uncorrelated. In the symposium, we will present our recent challenges on mRNA dynamics, in addition to the work on single-cell proteome and transcriptome analyses.

2SB-02　細胞環境下におけるタンパク質の NMR 計測

Protein NMR spectroscopy in the cellular environment

Kohsuke Inomata[1], Shuhei Murayama[2], Shiro Futaki[3], Hidekazu Hiroaki[4], Yutaka Ito[5], Hidehito Tochio[2], Masahiro Shirakawa[2] ([1]*Quantitative Biology Center, RIKEN*, [2]*Graduate School of Engineering, Kyoto University*, [3]*Institute for Chemical Research, Kyoto University*, [4]*Graduate School of Pharmaceutical Sciences, Nagoya University*, [5]*Graduate School of Science and Engineering, Tokyo Metropolitan University*)

It has been known that protein structure and dynamics in the cellular environment can differ from in vitro. In-cell NMR can be a powerful method to compare this difference directly. In-cell NMR is an isotope-aided multi-dimensional NMR technique that enables observation of conformation and function of protein in living cells. However, application of in-cell NMR has been limited to E. coli or Xenopus laevis oocytes. To extend the applicability of in-cell NMR, we have established a method to obtain high-resolution multi-dimensional heteronuclear NMR spectra of proteins inside living human cells. Proteins were delivered to the cytosol by the pyrenebutyrate-mediated action of cell-penetrating peptides (CPPs) which were covalently linked to the proteins. Proteins were subsequently released from CPPs by endogenous enzymatic activity or autonomous reductive cleavage. In this presentation, we show and discuss our "in human cell NMR" results. In this course, we especially focus on protein folding stability in cells, because we observed a significant difference from in vitro. Moreover, we discuss protein folding stability and other forms of protein dynamics analyses under conditions that mimic the cellular environment such as macromolecular crowded solutions.

2SB-03　高速原子間力顕微鏡による生体分子の構造ダイナミクスの直接観察

Direct observation of structural dynamics of biological molecules by high-speed atomic force microscopy

Noriyuki Kodera[1], Takayuki Uchihashi[1,2], Toshio Ando[1,2] ([1]*Bio-AFM Frontier Research Center, Inst. Sci. & Eng., Kanazawa Univ.*, [2]*Sch. Math. & Phys., Inst. Sci. & Eng., Kanazawa Univ.*)

Biological molecules (protein molecules in particular) function by changing their structure. Thus, the direct observation of their structure dynamics is a straightforward approach to understanding how they operate to function. However, this observation has long been infeasible because of a lack of techniques that can meet all conditions required for it: single-nanometer resolution, high temporal resolution, aqueous environment, and low-invasiveness. To make the observation possible, we have been developing high-speed atomic force microscopy (HS-AFM), which has now reached its maturity [T. Ando, *Nanotechnology* (2012)]. HS-AFM opens up a new opportunity to directly visualizing the dynamic structure changes and processes of functioning biological molecules in physiological solutions at sub-second to sub-100 ms temporal and submolecular spatial resolution. Recently, the powerfulness of HS-AFM has continuously been demonstrated by the observations of several proteins. Unlike fluorescence microscopy, dynamic molecular events unselectively appear in detail in the AFM movies, facilitating our understanding of how they function. In the presentation, we will briefly overview the principle and performance of HS-AFM and then show molecular movies captured. Finally, future challenges of HS-AFM studies will be discussed.

2SB-04　中心小体 9 回対称構造の謎を解く

Cracking the mystery of nine-ness: mechanisms of centriole formation

Daiju Kitagawa (*Nat. Inst. of Genetics, Cent. for Front. Res.*)

Centrioles are critical for organizing cilia, flagella and centrosomes across eukaryotic evolution. Centrioles are barrel-shaped microtubule-containing structures characterized by a universal nine-fold radial symmetry. Initiation of centriole formation and establishment of its universal 9-fold symmetry require a structure called the cartwheel. In most species, the centriole is organized around a cartwheel that comprises a central hub from which nine spokes emanate outwards towards the microtubules. The mechanisms directing centriole formation are not understood and represent a fundamental open question in biology. Recently, we demonstrate that the evolutionarily conserved centriolar protein SAS-6 forms rod-shaped homodimers that self-interact through their N-terminal domains to form further oligomers. We establish that such oligomerization is essential for centriole formation in C. elegans and human cells. Moreover, by using X-ray crystallography and biophysical approaches, we generate a structural model of the related protein Bld12p from C. reinhardtii, in which nine homodimers assemble into a ring from which nine coiled-coil rod domains radiate outwards. Furthermore, we demonstrate that recombinant Bld12p self-assembles into structures akin to the central hub of the cartwheel, which serves as a scaffold for centriole formation. Overall, our findings establish a structural basis for the universal nine-fold symmetry of centrioles, thus contributing to solving a long-standing question in biology.

2SB-05　低温電子顕微鏡法によるらせん複合体の高分解能構造解析

Recent advances in CryoEM high-resolution structural analysis for helical filaments

Takashi Fujii (*Qbic Riken*)

CryoEM(cryo-electron microscopy) has made rapid advances in this decade and became one of core technologies for high-resolution structural analysis for biological macromolecules. Helical filaments such as F-actin and Microtubule without or with their associate proteins working as cytoskeleton and a central-hub of macromolecular interactions play important roles in numerous cellular processes. We have been working on CryoEM three-demensional reconstruction of the helical filaments, including the flagellar hook and rod, F-actin, the Type-III needle and the parM filament. Here, we report our recent developments in the high-resolution and high-throughput structural analysis for helical filaments.We have found the optimal conditions of ice thickeness and sample temparature in data collection and the removement of inelastic electron by Ω-type energy filter made drastic improvement on image contrast. We are now focusing on development of the automatic data collection, the automatic particle picking method and the accurate classification program to achieve atomic resolution.

2SB-06　Kinetic and X-ray crystallographic studies of assembly/disassembly of the CRM1 nuclear export complex

Masako Koyama[1], Natsuki Shirai[1], Yoshiyuki Matsuura[1,2] ([1]*Grad. Sch. Sci., Nagoya Univ.*, [2]*Strl. Biol. R. Ctr., Nagoya Univ.*)

CRM1 is the most versatile exportin that mediates nuclear export of a plethora of proteins and ribonucleoproteins bearing a leucine-rich nuclear export signal (NES). In the nucleus, cargo and RanGTP bind cooperatively to CRM1, forming a ternary nuclear export complex that translocates through nuclear pore complexes (NPCs) and then dissociates in the cytoplasm. Translocation through NPCs appears to be a reversible facilitated diffusive process that is mediated by weak interactions between CRM1 and nuclear pore proteins (nucleoporins) that contain characteristic FG sequence repeats. The assembly/disassembly of cargo-carrier complexes in the appropriate compartments not only imparts directionality, but also allows accumulation of cargo against a concentration gradient. Our kinetic study demonstrates that a cytoplasmic protein RanBP1 accelerates dissociation of cargo from CRM1 and RanGTP. A high-resolution structure of CRM1-RanBP1-RanGTP complex and its comparison with the structures of CRM1-NES-RanGTP complexes reveal that RanBP1 accelerates cargo release by inducing allosteric conformational changes in CRM1. Our kinetic study also shows that a nuclear protein Yrb2 accelerates binding of cargo to CRM1 in the presence of RanGTP. Yrb2 has a multi-domain structure containing nucleoporin-like FG repeats and a Ran-binding domain. A high-resolution structure of CRM1-Yrb2-RanGTP complex suggests that Yrb2

functions catalytically as a coordinating scaffold to increase the rate of nuclear export while preventing futile export of cargo-free CRM1.

2SC-01 有糸分裂紡錘体の構造形成と機能の物理的理解に向けて

Toward a physical understanding of spindle assembly and function

Yuta Shimamoto (*Rockefeller Univ.*)

The faithful segregation of chromosomes during cell division depends on a dynamic microtubule-based structure, the metaphase spindle. Although numerous molecular components responsible for spindle assembly and function have been revealed, it is still unclear how this micron-sized, multi-component cytoskeletal structure generates and responds to forces while maintaining its overall stability, as we have a poor understanding of its micromechanical properties. Here we combine the use of force-calibrated microneedles, high-resolution microscopy and biochemical perturbations to examine the vertebrate metaphase spindle's timescale- and orientation-dependent viscoelastic properties. We find that the metaphase spindle is mechanically anisotropic, and can deform either elastically (i.e., restore shape) or viscously (i.e., remodel and flow) depending on the timescale and orientation of applied force. We also find that spindle viscosity depends on the dynamics of microtubule crosslinking. Spindle elasticity can be linked to the rigidity of two subsets of polymers, kinetochore and non-kinetochore microtubules, which have different polymerization dynamics and stability. These data suggest a quantitative model for the micromechanics of this dynamic cytoskeletal architecture and provide insight into how structural and functional stability is maintained in the face of different forces, such as those that control spindle size and position, and can result from deformations associated with chromosome transport and stretch.

2SC-02 ダイニンに駆動されたマイクロチューブによる巨大渦の格子形成

Large-scale vortex lattice of microtubules driven by dyneins

Ken Nagai[1], Yutaka Sumino[2], Kazuhiro Oiwa[3,4] ([1]*Univ. Tokyo*, [2]*Aichi Univ. Edu.*, [3]*NICT*, [4]*Univ. Hyogo*)

Swarming behavior is well-known phenomena in living systems with various scales: e. g., flocks of birds and bioconvection. Many individuals move together through interaction between the others around itself.

Collective behaviors of microorganisms are often realized through chemical interaction between organisms. One example is spiral formation of dictyostelium cells mediated by cyclic AMP. The analysis using reaction diffusion equations also succeeded in pattern formation of colonies of bacillus subtilis on agar plate.

Not only chemical interaction but steric interaction, which is caused by collision, works between microorganisms. Theoretically, Vicsek et al. reported that it is possible to induce swarming only through steric directional interaction when the density of the self-propelled objects is high enough [1]. This type of nonequilibrium phase transition has been confirmed using granular materials experimentally [2]. We will report a novel type of swarming behavior induced by steric interaction using microtubule-dynein motility assay. Using this system, we found that periodic pattern of a finite size structure can be formed. Using the mathematical model based on the experimentally confirmed properties of microtubules, we found that the key properties for this phenomenon are the long correlation time of the motion of microtubules and nematic interaction between microtubules [3].

[1] T. Vicsek, et al., Phys. Rev. Lett. (1995).
[2] V. Narayan, et al., Science (2007).
[3] Y. Sumino, et al., Nature (2012).

2SC-03 Non-Gaussian athermal fluctuations in active cytoskeletons

Daisuke Mizuno (*Kyushu University*)

Dynamic networks designed to model the cell cytoskeleton can be reconstituted from filamentous actin, the motor protein myosin and a permanent cross-linker. They are driven out of equilibrium when the molecular motors are active. We have measured the fluctuations and response of probe particles in such "active gel" systems using active/passive simultaneous microrheology, and observed both a violation of fluctuation-dissipation theorem and significant stiffening of the networks due to the active tension. Here we further investigate the full distribution of athermal fluctuations, also known as the van Hove correlation function. The distribution exhibits a central Gauss-like region which we assume derives from the processive action of many but "not too many" independent motor proteins. Localized nature of displacement field surrounding the force dipoles which decays as 1/r2 ensures the ultraslow convergence to the central limit theorem. As a result, distribution is explained with truncated Levy-statistics rather than Gauss. We also found that athermal fluctuations are far from Gauss due to the extended exponential tails which we believe derived from randomly occurring motor detachments from actin networks. We extract an estimate of the velocity of motor heads and average run-length along the actin filaments. Recording the whole distribution rather than the second moment (mean-squared displacement) thus allowed us to differentiate between the effect of individual motors and the collective action of multiple motors.

2SC-04 植物器官にみられるねじれた成長の弾性力学的および幾何学的な起原について

Elastic and geometric origin of the twisted growth of plant organs

Hirofumi Wada (*Dep. Phys. Ritsumeikan Univ.*)

The molecular and cellular basis of the left−right asymmetry in plant morphogenesis is a fundamental issue in biology. A rapidly elongating root/hypocotyl of twisting mutants of Arabidopsis thaliana exhibits helical growth with its handedness opposite to that of underlying cortical microtubule arrays in epidermal cells. However, how such a hierarchical helical order emerges is currently unknown. We propose a model for investigating macroscopic chiral asymmetry in mutants. Our elastic model suggests that the observed helical pattern is a direct consequence of the simultaneous presence of anisotropic growth and tilting of cortical microtubule arrays. We predict the root helical pitch angle as a function of the microtubule helical angle, which is consistent with experimental measurements. The proposed model is versatile and will be potentially important to other biological systems ranging from protein fibrous structures to tree trunks.

2SC-05 Visualizing Chromosome Structure with Superresolution Microscopy

Peter Carlton (*Kyoto University, iCeMS Institute*)

The correct expression and inheritance of the genome is made possible in part by the cell's exquisite control and regulation of chromatin structure. While microscopy has been used to elucidate many aspects of chromatin structure, the diffraction limit of light has previously limited the amount of detail available to a resolution of ~250 nanometers. However, super-resolution microscopy techniques now allow the quantitative imaging of cellular structures at much higher detail. Three-Dimensional Structured Illumination Microscopy (3D-SIM) uses moire interference between the sample and a striped pattern of light to increase the resolution by a factor of two. We are using 3D-SIM to analyze the fine structure of meiotic chromosomes in C. elegans, as well as the covalent modification of histones in pluripotent cell chromatin. By visualizing the two lateral elements of the synaptonemal complex, separated from each other by a distance of ~150 nanometers, we can quantitatively analyze the progression of meiotic events to a finer extent than previously possible. I will discuss our use of 3D-SIM to analyze the phenotypes of meiotic mutants and to explore the function of the synaptonemal complex.

2SC-06 DNA・RNA の輸送と選択：生命の起源への接近

Transport and selection for DNA and RNA: An approach to the origin of life

Yusuke Maeda[1,2,3,4], Albert Libchaber[4] ([1]*The Hakubi Center for Advanced Research, Kyoto Univ.*, [2]*Dept. Phys., Grad. Sch. Sci., Kyoto Univ.*, [3]*PRESTO, JST*, [4]*The Rockefeller Univ.*)

Atoms and molecules move along a gradient of external fields as seen in electrophoresis, which is a motion of charged molecules relative to fluid along an electric field. One unexplored but relevant alternative is thermophoresis, the Soret effect, that makes a solute moves along a temperature gradient. In this talk we will present that thermophoresis has a great potential in biology, especially in the selection of molecules depending on their size and folding. Thermophoresis depletes a polyethylene (PEG) polymer of large concentrations from the hot region and builds a concentration gradient. In such a solution, solutes of small concentration experience thermophoresis and PEG concentration-dependent restoring forces. Under focused laser heating, DNA and RNA as solutes localize as a ring-like structure which diameter monotonically decreases with the size of polymer following a behavior analogous to gel electrophoresis [1]. Moreover, we show that the selection of small RNA depending on its stem-loop structure is also possible in a temperature gradient in a solution of PEG of large volume fraction. Thus

trapping and selection of molecules could be physically feasible in a simple way relying on temperature gradient. Selection of DNA and RNA via transport might be relevant to molecular evolution at the origin of life: Separation of RNA from the large library of RNA world might occur at the thermal vent of the deep ocean where large temperature gradient is present. [1] YT Maeda, A Buguin, A Libchaber (2011) Phys Rev Lett 107: 038301.

2SD-01 Dynamics and stability of proteins in cellular environments

Michael Feig (*Michigan State University*)

Biological cellular environments provide a complex biophysical environment with a high degree of macromolecular crowding and chemical heterogeneity. Its effect on biomolecular structure and dynamics remains only partially understood. Past studies of crowding have focused on the entropic volume exclusion effect but recent experimental data suggest that enthalpic effects that were largely neglected in previous work may be equally important. Here, results from recent computer simulations of protein and peptide systems in the presence of physicochemically realistic crowder environments are presented. The overall finding is a tendency towards destabilization of native protein structures and a significant reduction in diffusive motion. The role of direct protein-protein interactions vs. indirect modulation of solvent properties is discussed based on the simulation results.

2SD-02 スーパーコンピュータは細胞生物学をどう変えるか

How supercomputing can help change cell biology

Koichi Takahashi[1,2,3] ([1]*RIKEN QBiC*, [2]*Keio Inst. Adv. Biosci.*, [3]*Osaka Univ. Grad. Sch. Front. Biosci.*)

Predictive modeling of cellular behaviors bottom up from molecular interactions is a holy grail in computational systems biology. Although 'rigorous' chemical master equations exist since the midst of the 20th century, biochemical network simulations has been suffering from lack of quantitative bases. I argue that part of this lack of predictive power in systems biology is due to negligence of non-idealistic intracellular environments, including molecular crowding and spatial heterogeneity of proteins including localization and clustering in microdomains. Such an environment is beyond scopes of classical theories such as Einstein-Smoluchowski theory of molecular diffusion and Michaelis-Menten's enzymatic reaction kinetics. The advent of advanced laser micro-/spectro-scopy that can directly observe macromolecules in living cells made us realize the need of modeling at the level of individual molecules and their internal states, instead of electrical circuit-like reaction networks. To fulfill this computational need, we have been developing high-performance simulation platform E-Cell System Version 4 for supercomputing architectures that can potentially handle the enormous amount of computation required to reproduce macroscopic physiological responses of cellular systems from microscopic molecular events. We will also introduce our efforts in modeling various types of cellular signaling pathways including the epidermal growth factor response pathways in cellular environments using K-computer.

2SD-03 細胞内の場を考慮したシミュレータ RICS の開発

Development of the cell simulator in consideration of space

Hideo Yokota[1,2], Yasuhiro Sunaga[2], Sigeho Noda[3] ([1]*ASI, Riken*, [2]*iSLIM, Riken*, [3]*ACCC, Riken*)

Cells are the smallest life units, and the ultimate goal of the cell scale simulation team is to recreate intracellular and intercellular phenomena. However, intracellular phenomena have not, for the most part, been elucidated, and their clarification is a major objective in cell biology. It is currently impossible to develop a simulator that can recreate all complicated intracellular phenomena. Hence, the cell scale simulation team's objective is to simulate intracellular and extracellular phenomena that have been sufficiently elucidated by past research and for which mathematical models have been established. In addition, using the computational power of next-generation 10-petaflop supercomputers that are scheduled to be completed in 2012, we hopes to enable simulations that consider intracellular environments that heretofore could not have been calculated due to high computational costs. More concretely, intracellular spaces are viewed as grid coordinates with mesh-shaped positional information. In each grid, various intracellular phenomena are simulated to recreate intracellular environments, which are uneven environments containing spaces between organelles. Future advances in cell biology, mathematical model construction, and simulation technologies should markedly expand the scope of cell simulation. In the hope of contributing to the future development of cell simulation, a cell simulation platform that can analyze coupled phenomena by linking simulators for multiple phenomena (RICS) was developed.

2SD-04 「京」による大規模遺伝子ネットワーク推定

Large scale gene network estimation with K computer

Yoshinori Tamada[1], Teppei Shimamura[2], Rui Yamaguchi[2], Atsushi Niida[2], Ayumu Saito[2], Yuto Kataoka[1,2], Seiya Imoto[2], Masao Nagasaki[3], Satoru Miyano[1,4] ([1]*Grad. Sch. Info. Sci. Tech., Univ. Tokyo*, [2]*Inst. Med. Sci., Univ. Tokyo*, [3]*Tohoku Med. Megabank, Tohoku Univ.*, [4]*CSRP, RIKEN*)

We present large scale gene network estimation software called SiGN, which is currently developed for the Japanese flagship supercomputer "K computer." A gene network is a graphical representation of regulatory dependencies between genes. There are many algorithms to estimate gene networks from gene expression data. However, mainly due to their computational speed, the existing algorithms can be applied to only thousands of genes, which can cover only a few percent of the whole human genome. Using a supercomputer is a possible solution in order to speed up these algorithms. Without appropriate parallelization, however, we cannot receive benefits from its speed, due to is massively parallel architecture. In our group, we parallelized several gene network algorithms to overcome this problem to realize the human whole genome scale gene network estimation. SiGN consists of three different subprograms: SiGN-BN, SiGN-SSM and SiGN-L1. SiGN-BN estimates gene networks with static and dynamic Bayesian network models. SiGN-SSM implements a parameter estimation algorithm for the state space model which is suitable for modeling temporal systems of gene expressions. SiGN-L1 estimates gene networks with sparse learning techniques. These sub-programs can capture different aspects of gene expression data, which cannot be observed from a single gene network model. The estimated gene networks can be viewed and analyzed by Cell Illustrator Online and Systems Biology integrative Pipeline. The software will be available our web site at http://sign.hgc.jp/.

2SD-05 データ同化法にもとづくデータ統合・生体シミュレーション技術

Biological system modeling and data assimilation

Ryo Yoshida (*The Institute of Statistical Mathematics, Research Organization of Information and Systems*)

Modeling biochemical kinetic systems based on ordinary differential equations (ODEs) or algebraic equations has been practiced widely in metabolic engineering and many researches on systems biology. This has promoted in-depth understanding of action, design and control of the potentially complex dynamics. The system consists of a network of interacting biochemical species, which involves production, degradation, diffusion and binding of many substances. This study attempts, as the primary focus, to achieve a previously-unexplored task of the system model construction; robust biochemical networks are designed automatically according to the principle of Bayesian robustness. Certain types of biological systems are hypothesized to maintain robustness with respect to specific instances of systems perturbation and environmental uncertainty. The present Bayesian method is aimed at exploring a robust ODE network such that the model outputs fit given data robustly in response to artificially-created kinetic perturbations, damages, reaction failures and environmental uncertainty. The key idea lies in the use of the Dirichlet process mixture (DPM) as a prior distribution. Once system perturbations or kinetic parameter variations are modeled by the DPM prior, relevant robust systems can automatically be constructed while in the stochastic graph search process. We provide the general framework for the Bayesian robust networking, technical details on the Markov chain Monte Carlo algorithm, and demonstrations on some benchmark problems.

2SE-01 細菌べん毛モーターの回転方向変換制御機構の解明

Elucidation of the directional switching mechanism of the bacterial flagellar motor

Tomoko Miyata[1], Takayuki Kato[1], Takasi Fujii[1,2], Shuichi Nakamura[4], Yusuke Morimoto[1,2,3], Tohru Minamino[1], Hideyuki Matsunami[5], Keiichi Namba[1,2] ([1]*Grad. Sch. Frontier Biosci., Osaka Univ.*, [2]*QBiC, RIKEN*, [3]*Grad. Sch. Sci., Osaka Univ. Department of Applied Physics*, [4]*Tohoku Univ. School of Engineering*, [5]*OIST, Initial Research Project*)

Many bacteria swim by rotating flagella, which function as a helical propeller driven by a reversible rotary motor that are embedded in the cell membrane. The flagellum consists of three parts: the filament, the hook, and the basal body. The basal body houses machinery for rotation and directional switching as well as

for flagellar protein export, and its complex structure is composed of about 20 different proteins. The basal body contains at least five parts according to their functions: the rod, LP ring, MS ring, C ring, and type III protein export apparatus. The C ring is made of the switch complex proteins FliG, FliM, FliN, which controls counterclockwise-clockwise (CCW/CW) switching of the motor rotation and sits on the cytoplasmic face of the MS ring. To understand the switching mechanisms in detail, we analyzed the C ring structures of CCW-bias and CW-locked mutant motors by electron cryomicroscopy (cryoEM). The CCW-bias and CW-locked phenotypes arise from single point mutation (V135L) and the deletion of residues 169-171 (ΔPAA) in FliG, respectively. We purified the hook basal bodies from the both strains with fliC and clpP gene-disrupted, collected cryoEM images, and carried out image analysis. The fitting of the crystal structure of the switch proteins into the 3D map allowed us to build a partial swich complex model. We will report the structural change between the CCW and CW forms and the switching mecanism of flagellar motor rotation.

2SE-02 磁性細菌の超分子複合体ーマグネトソーム, 細胞骨格そしてベン毛ーの構造的組織化

Structural Organization of Macromolecular assemblies -Magnetosome, Cytoskeleton and Flagella- in Magnetotactic Bacteria

Yoshihiro Fukumori, Azuma Taoka (*College Sci. Eng., Kanazawa Univ.*)

Magnetotactic behavior in bacteria was discovered over 35 years ago by Richard P. Blakemore (Science, 190, 377-379, 1975). The discovery was based on the fact that certain motile, aquatic bacteria orient and migrate along magnetic field lines when subjected to a magnetic field of the order of the geomagnetic field, or greater. Furthermore, he reported that the magnetotactic bacteria have unique intracytoplasmic membrane vesicles named as magnetosome.
Magnetosomes comprise a chain of regular-sized bio-mineralized magnetite crystals, each of which is surrounded by a lipid bilayer membrane and organic components. Recently, we found that magnetosomes of *Magnetospirillum magneticum* AMB-1 are covered with TPR-protein MamA oligomers outside a lipid bilayer in near-native environments using atomic force microscopy. Furthermore, most magnetosomes are arranged intimately along novel cytoskeletal filaments composed of actin-like protein, MamK. Interestingly, one extremity of the MamK filaments is located at the cellular pole. Philippe and Wu have proposed that an MCP-like protein may interact with the MamK filaments (J. Mol. Biol., 400, 309-322, 2010). Based on these results, we will discuss structural organization of macromolecular assemblies, magnetosome, cytoskeleton and flagella in magnetotactic bacteria.

2SE-03 アクチンフィラメントの構造多型と機能分化

Structural polymorphism and functional differentiation of actin filaments

Taro Q. P. Uyeda[1], Nobuhisa Umeki[1], Saku Kijima[2], Yusuke Nishikawa[3], Kiyotaka Tokuraku[3], Akira Nagasaki[1], Taro Q.P. Noguchi[2] ([1]*Biomedical Res. Inst., AIST*, [2]*Miyakonojo Natl. Col. of Tech.*, [3]*Muroran Inst. of Tech.*)

Interaction with specific actin binding proteins (ABPs) is believed to define the function of the actin filaments. However, the story may not be that simple, because actin filaments are intrinsically polymorphic. Moreover, ABPs induce specific conformational changes of the filaments, often in a cooperative manner so that ABP-induced conformational changes that occurred in the bound actin subunit are propagated to neighbor subunits, presumably leading to cooperative binding of that ABP to the filaments. Along this line, we recently showed that cooperative binding of cofilin and HMM to actin filaments is mutually exclusive, so that when cofilin, HMM and actin filaments are mixed, some filaments bound only cofilin while others bound only HMM. Because cosedimentation assays showed that this does not involve competition for a binding site on actin, HMM and cofilin likely induce specific conformational changes in neighbor actin subunits to differentially modulate their affinities for cofilin, HMM and other ABPs. This property of actin filaments might have two biological implications. First, binding of a small number of a specific ABP molecules would initiate a domino effect to drive the conformation of the filament to one structure and consequently one function, amplifying and fixing the impact of biochemical signal or thermal fluctuation that induced the initial binding. Second, because actin filaments change the structure by stretching, they can function as mechanosensor to locally regulate ABPs and the function of the actin cytoskeleton.

2SE-04 マイコプラズマ滑走運動の謎にせまる

New foci to clarify *Mycoplasma* gliding

Makoto Miyata (*Grad. Sch. Sci., Osaka City Univ.*)

Many species of *Mycoplasma*, pathogenic bacteria form a membrane protrusion at a cell pole, and glide on host cell surfaces. Although the gliding is fast and smooth, the mechanism is not related to the conventional motor proteins or the known bacterial motility such as flagella or pili. We have studied mainly on the fastest species, *Mycoplasma mobile*, which glides up to 4.5 micron per s and 27 pN, and proposed a working model, “The movements generated by ATP hydrolysis inside cell transmits to a “leg” protein through a “crank” protein, resulting in the repeated catching, pulling, and releasing of sialic acids fixed on the surface (Miyata M. Annu Rev Microbiol. 2010 64: 519-37).” To obtain the better images of this gliding mechanism, we are now working on (i) fine and whole structures of gliding machinery, (ii) actual movements of legs in gliding, and (iii) coupling of ATP hydrolysis and leg behaviors.

2SE-05 バクテロイデスにおける分泌と滑走

Secretion and Gliding in Bacteroides

Keiko Sato[1], Daisuke Nakane[1], Hirofumi Wada[2], Katsumi Imada[3], Mark J. McBride[4], Koji Nakayama[1] ([1]*Graduate School of Biomedical Sciences, Nagasaki University*, [2]*Department of Physics Sciences, Ritsumeikan University*, [3]*Graduate School of Science, Osaka University*, [4]*Department of Biological Sciences, University of Wisconsin-Milwaukee*)

Flavobacterium johnsoniae is a Gram-negative bacterium in the phylum Bacteroidetes, which moves rapidly over surfaces at a speed of 1-3 μm/s. Bacteroidete gliding motility is thought to be different from any other motility systems, but the molecular mechanism is unknown. We recently found that SprB adhesin is responsible for the gliding motility of F. johnsoniae. Optical microscopic observation using the fluorescent labeling technique indicated that SprB adhesin molecules move along a “right-handed closed helical loop track” on the bacterial cell membrane, and this movement causes the cell rotation and translation. SprB adhesin is secreted by the Por secretion system (PorSS), whose gene is widely distributed in the phylum Bacteroidetes, even in nonmotile bacteria such as periodontal pathogen Porphyromonas gingivalis. The secretion substrates are recognized by their C-terminal signal domains composed of about 80 amino acid residues. Various proteins, such as chitinase and pathogenic cysteine proteinase, are secreted. Thus disruption of PorSS resulted not only in loss of secretion but also motility. In this symposium, we show the unique gliding motility and secretion system in Bacteroides, and discuss their relation.

2SE-06 Molecular motor driven self-organization in Myxococcus xanthus

Joshua W. Shaevitz (*Princeton University, Departments of Physics and Genomics*)

From wildebeest herds to bacterial biofilms and every scale in between, how individuals self-assemble into large, spatially complex groups is a key problem in understanding collective behavior, multicellularity and development. The coordinated motion of individuals at the cellular level can drive the formation of higher-scale structure is tissues, organisms and even populations. These phenomena arise statistically as cells modulate their direction and speed in response to both local and global cues. A full understanding of how collective behavior in cell populations arises has been difficult to achieve because we currently lack the ability to cross spatial scales and draw connections between sensory input, motor control and group formation. Experiments examining the effect of specific mutations on single cell movement and group morphology have identified many important molecular players but lack the ability to probe the behavior of individuals within groups or physical aspects of coordination. I will present some of my group's recent work studying force production, motion control and coordination on the molecular to the population scales using the model social bacterium Myxococcus xanthus, a fascinating organism that takes advantage of multi-cellular, coordinated motility to feed on colonies of bacteria in large, pack-like groups and to form giant, spore-filled fruiting bodies during starvation.

2SF-01 Inconsistency between population and single cell growth rates revealed by dynamics cytometer

Yuichi Wakamoto[1] ([1]*Research Center for Complex Systems Biology, Univ of Tokyo*, [2]*JST PRESTO*)

Any phenotypic states of single cells fluctuate in time-course, which produces spectra of phenotypes in cell populations. Although it is usually assumed that the mean inherent phenotypic state of single cells agree with the population average, heterogeneity of any phenotypic variables correlated with growth causes persistent natural selection within populations and the resultant inconsistency between single cell and population phenotypic states. Here we provide the first experimental evidence of inconsistency between growth rates of cell populations and inherent mean growth rates of single cells in constant environments using a newly developed single-cell measurement device, "dynamics cytometer". The results showed that growth rates of clonal cell populations of *Escherichia coli* under constant growth conditions were always greater than those of single cells. The extent of growth rate gain of cell populations quantitatively agreed with the prediction of simple growth model that assumes probabilistic age-dependent cell divisions. This model also successfully predicted the population age structures. Based on these results, we provide several mathematical relations that interconnect growth-associated parameters of single cells and populations. Our results provide clear evidence of inconsistency between single-cell and population properties, which indicate that the detailed information about single-cell dynamics is required to understand how population properties are shaped by inherently heterogeneous single cells.

2SF-02 Information Processing via Noisy Biochemical Channels

Tetsuya J. Kobayashi[1,2], Atsushi Kamimura[3,4] ([1]*Institute of Industrial Science, the University of Tokyo*, [2]*JST PRESTO*, [3]*Graduate School of Arts and Sciences, The University of Tokyo*, [4]*JSPS*)

Microscopic biochemical reactions are intrinsically noisy because of small number of molecules involved in the reactions. Biological systems, however, can behave reliable even though they are composed of such noisy reactions channels. From the information-theoretical viewpoint, the total amount of information transmitted via noisy channel bounds the reliability of outcome in response to the input to the systems. Maximization of information transfer, therefore, is crucial for reliable operation of biological systems. In this talk, we demonstrate that Bayesian computation implemented by biological reactions can contribute to the maximization of information transfer. The underlying mechanism for the efficient operation of the Bayesian computation is clarified as mapping of biologically irrelevant infinite dimensional trajectories onto biologically relevant intracellular states. The implication of our results will also be discussed. [1] T.J. Kobayashi, (2010), "Dynamic Bayesian Decision Making by Intracellular Kinetics," Phys. Rev. Lett., vol. 104, no. 228104. [2] T. J. Kobayashi, A. Kamimura, (2011). " Dynamics of Intracellular Information Decoding". Physical Biology, vol. 8, 055007. [3] T. J. Kobayashi, (2011), "Connection between noise-induced symmetry breaking and an information-decoding function for intracellular networks," Phys. Rev. Lett., vol. 106, no. 228101.

2SF-03 ERK 経路の情報コード
Information coding of ERK signaling networks

Shinya Kuroda, Shinsuke Uda, Takeshi Saito (*Dept. Biophys. Biochem., Univ. Tokyo*)

Cellular signaling network is capable of regulating multiple cellular functions depending on growth factors and cell lines. For example, in PC12 cells, EGF and NGF induce transient and sustained ERK activation, leading to cell proliferation and differentiation, respectively. This indicates that the same signaling network can encode multiplex signal information in temporal patterns. We made a system identification of temporal decoding of ERK activation by selective immediate early genes (IEGs) expression. We found that pulsatile ERK phosphorylation was decoded by selective expression of EGR1 rather than c-FOS, and conjunctive NGF and PACAP stimulation was decoded by synergistic JUNB expression through a switch-like response to c-FOS. Cellular signaling network can be regarded as a communication channel in the framework of Shannon's information theory. We can measure the distribution of phosphorylation of ERK and CREB and expression of IEGs products at a cell population level. We found that information transmission was generally more robust than averaged signal intensity despite pharmacological perturbations, and information transmission through unperturbed signaling pathways compensatorily increased in many signaling pathways. We propose that cells use information entropy as information, so that messages can be robustly transmitted despite noise and variation in molecular activities between individual cells. Information coding will be discussed as a general property of cellular signaling.

2SF-04 Fluctuating signals in cellular signal transduction systems

Tatsuo Shibata (*RIKEN Center for Developmental BiologyE*)

Many cellular processes respond to internal and external changes by using networks of interacting molecules. Because intracellular processes are stochastic processes, the signal transduction processes are inherently noisy. Such inherent noise may deteriorate or improve the performance of signal transduction systems. For example, it has been shown theoretically that the accuracy of eukaryotic chemotaxis is limited by stochastic fluctuations in the signaling processes of receptor on the plasma membrane. Large fluctuations are also observed in intracellular signaling processes. Such intracellular fluctuations are often produced by intrinsic mechanism mostly independent of extracellular stimuli. This implies that the fluctuations are necessary for the functions of signaling processes. For instance, a large fluctuation may generate an intracellular signal, which can be biased or carry an extracellular signals. In this presentation, I will discuss the roles of such fluctuations on intracellular processes.

2SF-05 Symmetry breaking in mouse development

Takashi Hiiragi[1,2] ([1]*EMBL*, [2]*iCeMS Kyoto University*)

A fundamental question in biology is the mechanism by which the embryonic asymmetry is established during development. The primary interest of my lab lies in the principles underlying the lineage establishment in mouse development. We have developed live-imaging for pre-implantation embryos, demonstrating unexpectedly high dynamicity during blastocyst morphogenesis. Our studies characterized unique principles of mouse embryonic patterning: localized determinants play no role in generating asymmetry; mechanical context plays a key role; stochastic processes generate dynamic heterogeneity. Collectively, an attractive hypothesis is that early mammalian embryogenesis may be a stochastic process in a particular structural context that leads to self-organization. These features suggest that, in order to fully understand the underlying mechanisms, it will be essential to address how the diverse inputs acting on every individual cells are integrated in the embryo at the systems level. Thus we have recently developed necessary tools and multi-disciplinary strategies: Venus-trap reporter mouse that visualize molecular dynamics; gene expression profile of every single cell; computer simulation of the blastocyst morphogenesis. In particular we have successfully established 9 Venus-trap lines active specifically in one of the initial lineages. This allows high-resolution 4D-imaging and tracking of dynamic lineage segregation, and characterizes the emergence and resolution of molecular heterogeneity. Recent results will be discussed.

2SF-06 Stochastic expression of cell adhesion molecules in individual neurons

Takeshi Yagi[1,2] ([1]*Osaka University*, [2]*CREST-JST*)

The brain contains an enormous, but finite, number of neurons. The ability of this limited number of neurons to produce nearly limitless neural information over a lifetime is typically explained by combinatorial explosion; that is, by the exponential amplification of each neuron's contribution through its incorporation into "cell assemblies" and neural networks. In development, each neuron expresses diverse cellular recognition molecules that permit the formation of the appropriate neural cell assemblies to elicit various brain functions. The mechanism for generating neural networks must involve molecular codes that give neurons individuality and allow them to recognize one another and join appropriate networks. The extensive molecular diversity of cell-surface proteins on neurons is likely to contribute to their individual identities. The clustered protocadherin (Pcdh) is a large subfamily within the diverse cadherin superfamily. The Pcdh genes are encoded in tandem by three gene clusters, and are present in all known vertebrate genomes. The set of Pcdh genes is expressed in a stochastic and combinatorial manner in each neuron. Here I present neuronal individuality based on the stochastic and combinatorial expression of Pcdh isoforms in individual neurons. Their molecular and biological features suggest that the diverse Pcdh molecules provide the molecular code by which neuronal individuality and cell assembly permit the combinatorial explosion of networks that supports enormous processing capability and plasticity of the brain.

2SG-01 生細胞における RNA ポリメラーゼ II による転写活性化の動態

Kinetics of RNA polymerase II transcription in living cells

Hiroshi Kimura, Timothy J. Stasevich (*Grad. Sch. Frontier Biosci., Osaka Univ.*)

RNA polymerase II (RNA pol II) is a multisubunit enzyme responsible for transcription of most genes in eukaryotes. To understand how transcription is regulated in living cells, the kinetics of RNA polymerase II have been measured by photobleaching-based techniques like FRAP. However, it has been difficult to accurately differentiate the multiple kinetic steps, such as the preinitiation complex assembly, the initiation and elongation, from a single FRAP curve. We now applied the Fab-based live endogenous modification labeling method, which is a recently developed technique for monitoring post-translational modification, to RNA polymerase II. The largest subunit of RNA pol II harbors YSPTSPS heptapeptide repeats at the C-terminal domain (CTD). Upon gene activation, RNA polymerase II is assembled into the preinitiation complex as unphosphorylated form, and becomes phosphorylated at Ser5 and Ser2 in the CTD during the initiation and elongation steps, respectively. By timing the recruitment of these different phosphorylation marks to a gene array upon the stimulation of transcription and by fitting the data to a mathematical model, it was able to differentiate the initiation kinetics from the recruitment and elongation kinetics. Our observations suggested that transcription on the array is quite efficient and that the elongation efficiency is correlated with the preexisting histone H3 acetylation level.

2SG-02 染色体場の 1 分子イメージング定量解析

Quantitative analysis of single molecule imaging of the physicochemical field for genetic activities

Kumiko Sakata-Sogawa[1,2], Makio Tokunaga[1,2] ([1]*Grad. Sch. Biosci. Biotech., Tokyo Inst. Tech.*, [2]*RCAI, RIKEN*)

Single cells in a living eukaryotic organism harbor the identical genetic information in the chromatin. The expression of each gene is regulated in both spatial and temporal manner. The dynamic regulation results in specificity and diversity of the cells and determines the characteristics of the individual organism. The nucleus accommodates the field not only to store the genetic information but also to orchestrate the regulation of the genetic activities. The functional compartmentation of the nucleus plays an important role in the regulation of the genetic activities. However the information about the organization and the architecture of the compartment of the nucleus is limited. Actin and actin related protein (Arps) are known to work as components of chromatin-remodeling complex. Our recent results of single molecule imaging analysis provide that transcriptional activation causes dissociation of Arp4, subfamily of Arp, from the target sites, indicating that Arp4 is involved in transcription control. In addition to the function, recent reports demonstrate their important function in the nuclear compartment. Furthermore actin is reported to bind RNA polymerase II and the binding may be required for the active forms of the enzyme. This talk will describe the recent results in our group regarding to the physicochemical field for genetic activities.

2SG-03 ヒストンバリアントによるヌクレオソームの構造多様性とダイナミクス

Structural versatility, dynamics, and functions of human nucleosomes containing histone variants

Hitoshi Kurumizaka (*Waseda University, Faculty of Science and Engineering*)

In eukaryotes, genomic DNA is packaged into chromatin, in which nucleosome is the fundamental repeating unit. Core histones, H2A, H2B, H3, and H4, are the protein components of nucleosomes, and histones H2A, H2B and H3, but not histone H4, have nonallelic isoforms called histone variants. The histone variants may have distinct functions in formation of specific chromosome regions and/or in regulation of transcription, replication, recombination, and repair of DNA. However, contributions of histone variants in these processes are poorly understood. To reveal the structural basis of functional chromatin architecture, we have solved crystal structures of human nucleosomes containing histone H2A, H2B, and H3 variants, including the centromere-specific histone H3 variant, CENP-A. We also performed biochemical and biophysical analyses of mono- and poly-nucleosomes containing these histone variants. In this symposium, I will show the current results of our structural and functional analyses of human nucleosomes containing histone variants, and discuss about their contribution in functional chromatin architecture.

2SG-04 細胞のパターンをうみだす遺伝子回路の作製

Construction of genetic circuits underlying cell pattern formation

Miki Ebisuya (*Career-Path Promotion Unit for Young Life Scientists, Kyoto Univ.*)

Our objective is to understand the mechanism and dynamics of biological phenomena by constructing genetic circuits. We are particularly interested in formation of cell patterns that are driven by Notch signaling, such as a signal propagation pattern and a salt-and-pepper pattern. Recently, we have constructed a genetic circuit that generates the signal propagation pattern, (in which a gene expression signal propagates within a cell population), in mammalian cultured cells. In our genetic circuit, binding of Delta (the ligand) to Notch (the receptor) promotes transcription of Delta. A cell that produces Delta forces its adjacent cells to produce a more amount of Delta. Namely, we constructed a positive feedback loop between the adjacent cells. To amplify the responses of Notch to Delta, we added a transcriptional cascade as well as a Notch modulator, Lunatic fringe (Lfng), to the cell-cell positive feedback loop. We found that when the genetic circuit satisfied conditions for cell-population level bistability, the expression signal of Delta propagated from one cell to its neighboring cells. These results demonstrate the mechanistic sufficiency of the cell-cell positive feedback loop to generate signal propagation.

2SG-05 細胞分裂と染色体分配のメカノバイオロジー

Mechanobiology of Cell Division and Chromosome Segregation

Shin'ichi Ishiwata[1,2] ([1]*Fac. Sci. Engn., Waseda Univ.*, [2]*WABIOS, Waseda Univ.*)

We have been studying the effects of mechanical perturbation on cell division and chromosome segregation, by using a microscopic manipulation technique. Here, I will present our recent results on the effects of mechanical impulse (MI) on the timing of chromosome segregation in HeLa cells (Itabashi, 2012), showing that the MI, applied perpendicular to the pole-to-pole axis of a spindle, accelerates the chromosome segregation, whereas the MI applied along the pole-to-pole axis decelerates it. I will discuss how the mechano-chemical processes regulate the timing of spindle check point. We are interested in the structural and functional hierarchy of the cell division system. Next, I will introduce the visco-elastic properties and the response to the external mechanical perturbation of meiotic spindle self-organized in Xenopus laevis egg extracts (Itabashi, 2009). The spindle behaves as an elastic body in response to small compression, whereas larger compression results in plastic deformation, but the spindle adapts to this change, establishing a stable architecture at different sizes. Finally, I will report that the microtubule-depolymerizing activity of MCAK is accompanied by the force generation at both microtubule ends (Oguchi, 2011). The results provide a simple model for the regulation of chromosome segregation through a “side-sliding, end-catching” mechanism. We propose that the force balanced by molecular motors and polymerization-depolymerization dynamics of microtubules is essential for the dynamic stability of spindles.

2SG-06 減数分裂特異的な非コード RNA が相同染色体の対合を促進する

Meiosis-specific non-coding RNA mediates robust pairing of homologous chromosomes in meiosis

Yasushi Hiraoka[1,2], Da-Qiao Ding[2], Tokuko Haraguchi[1,2] ([1]*Graduate School of Frontier Biosciences, Osaka University*, [2]*Advanced ICT Research Institute Kobe, NICT*)

Pairing and recombination of homologous chromosomes are essential for ensuring reductional segregation in meiosis. However, the mechanisms by which chromosomes recognize their homologous partners are poorly understood. Here we report that the sme2 gene encodes a meiosis-specific non-coding RNA that mediates homologous recognition in the fission yeast *Schizosaccharomyces pombe*. The *sme2* gene locus shows extraordinarily robust pairing from early in meiotic prophase. The *sme2* RNA transcripts accumulate at their respective gene loci, and greatly enhances pairing of homologous loci: deletion of the *sme2* sequence eliminates this robust pairing while transposition to other chromosomal sites confers the robust pairing at those sites. Thus, we propose that RNA transcripts retained on the chromosome play an active role in recognition of homologous chromosomes for pairing.

2SH-01 KcsA カリウムイオンチャネルの溶液条件変化応答 1 分子開閉ダイナミクスの解析

Analysis of Single Molecular Gating Dynamics of the KcsA Potassium Channels Responding to Rapid Changes of Solution Conditions

Hirofumi Shimizu[1], Masayuki Iwamoto[1], Antoine Royant[2,5], Stetten David von[5], Laurent Guerin[3], Yoshimitsu Aoki[4], Michael Wulff[5], Shigetoshi Oiki[1] ([1]*Mol. Physiol. & Biophys., Univ. Fukui. Fac. Med. Sci.*, [2]*CEA-CNRS-Universite Joseph Fourier*, [3]*Universite de Rennes 1*, [4]*Keio. Univ. Sci. & Tech. Elec.*, [5]*ESRF*)

Recently, we succeeded in recording single molecular gating transitions of KcsA potassium channel from closed to open state with the modified diffracted X-ray tracking (DXT) method. In the conventional method the motions were recorded at video rate under equilibrium conditions. To reveal a whole picture of the gating dynamics we introduced a fast measurement system, pH jump measurement system, optimized X-ray for the method, and an efficient spot tracking program. The channel was fixed on a glass plate at the extracellular part and a gold nanocrystal was attached to the intracellular end of the channel molecule as a probe. The sample was irradiated with an optimized white-beam from a synchrotron and the motions of the Laue diffraction spots from the nanocrystal were tracked on a CMOS detector at the speed of 5000 frames/s. Solution pH condition was jumped during the measurements from neutral to acidic pH by laser-photolysis of caged proton, which can trigger the gating motions of pH-gated KcsA channel. The diffraction spots in the sequential image data were extracted and tracked by a developed data analysis program. The trajectories of the diffraction spots were translated into movements of the channel. With this modified DXT method we succeeded in revealing the different dynamic status of the channel depending on the change of pH condition and the gating transitions starting from the closed state with a larger spatial range at the speed of 5000 frames/s which is comparable to the speed of single channel current recordings.

2SH-02 中赤外波長領域の観察が可能な赤外超解像顕微鏡の開発と生体試料への応用

Development of a mid-IR super-resolution microscope and its application to biological samples

Makoto Sakai (*Tokyo Tech.*)

Infrared (IR) microscope is a powerful tool to measure molecular images of biological samples based on molecular information. However, microscopic objects such as biological cells cannot be measured by conventional IR microscope, because of its low spatial resolution about 10 μm. This is a serious problem for a microscope.

To overcome this problem, we have developed a novel type of IR super-resolution microscope based on vibrational sum-frequency generation (VSFG) detection. VSFG is a non-linear optical process and we irradiate visible and IR beams on the sample. If IR beam is resonant to vibrational mode of target molecule, VSFG signal photon will strongly generate. Therefore, we can detect IR absorption of the molecule by monitoring VSFG. In addition, IR absorption can be also imaged at the diffraction limit of visible light (several 100 nm) because VSFG signal has visible wavelength. By using this method, we succeeded in obtaining IR super-resolution images of biological cells such as onion root cells and human lung cancer cells in the 3 μm IR region. The spatial resolution is approximately 1 μm, that is smaller than the diffraction limit of IR light.

In this study, we improved an observational wavelength range of it up to the 6-9 μm mid-IR region to observe amide bands, and applied this IR microscope to the biological samples such as sugar crystals, amino acids, and human hairs. In the presentation, the result of IR super-resolution micro-spectroscopy of human hairs will be discussed in detail.

2SH-03 白色レーザーを用いた CARS 分光イメージングによる生細胞の動態追跡

Tracing dynamical behavior of a single cell by CARS microspectroscopy using a white-light laser source

Hideaki Kano[1], Masanari Okuno[2], Hiroki Segawa[2], Hiro-o Hamaguchi[3] ([1]*Tsukuba Univ.*, [2]*The Univ. of Tokyo*, [3]*National Chiao Tung Univ.*)

The mechanism of a solubilization process of living organisms with surfactants has so far been attributed to the surface adsorption and subsequent disruption of cellular membranes. In this study, we applied quantitative CARS microspectroscopy to investigate the molecular dynamics of surfactant molecules and intracellular molecules in living cells after the exposure of surfactant with low concentration (0.1 w%). By using an isotope labeled surfactant with CD bonds, the dynamic behavior of the surfactant in living cells was clearly observed. The simultaneous CARS imaging of the cell itself and surfactant molecules can address the details of the solubilization process with the surfactant. We observed the accumulation of the surfactant molecules inside a living cell and a subsequent sudden leak of cytosolic components such as proteins. This indicates the surfactant uptake prior to the solubilization of the cells. Our observation revealed that the surfactant molecules are accumulated in the lipid rich part of the cells probably due to the similarity of the composition. Quantitative CARS microspectroscopy enables us to estimate the molecular concentration of the surfactant molecules accumulated in a cell quantitatively. We also investigated the drag response to the surfactant uptake dynamics. As the result of the inhibition of tubulin polymerization, the surfactant uptake rate was significantly lowered. This suggests that intracellular membrane trafficking contributes to the surfactant uptake mechanism.

2SH-04 イメージングマススペクトロメトリーによって初めて明らかになった、細胞内の脂質分布の分子種特異的な極性について

Imaging mass spectrometry revealed the polarized intracellular distribution of specific lipid molecular species

Mitsutoshi Setou (*Hamamatsu University School of Medicine Department of Cell Biology and Anatomy*)

Fluid mosaic model of cell membrane tells that fluid part phospholipids flow like liquid. This model predicts the evenly distributed phospholipids in cell membrane. However, the distribution of phospholipids was not well investigated experimentally at intracellular level because it was very difficult to visualize the distribution of distinct lipid molecular species regarding its variety of length of fatty acids. We applied high resolution imaging mass spectrometry on cultured neuron to visualize the gradient of phospholipids along the axon. Surprisingly, the distribution is distinct between the molecular species of phospholipids along the cellular polarity. We focus on the distribution of Arachidonic acid (AA)-containing PC (AA-PC), which we found to be enriched within the axon and is distributed across a proximal-to-distal gradient. Inhibitors of actin dynamics (cytochalasin D and phallacidin) disrupted this gradient, while microtubule dynamics inhibitors did not. A possible model of this newly found phenomena will be presented and discussed.

2SH-05 随意運動中のマウス運動野 2 光子イメージング

Two-photon imaging of the mouse motor cortex during voluntary skilled movement

Riichiro Hira[1,2,3], Fuki Ohkubo[1,3,4], Katsuya Ozawa[2,3], Yoshikazu Isomura[3,5], Kazuo Kitamura[2,3], Masanobu Kano[2], Haruo Kasai[2], **Masanori Matsuzaki**[1,3,4] ([1]*National Institute for Basic Biology*, [2]*Graduate School of Medicine, University of Tokyo*, [3]*CREST*, [4]*SOKENDAI*, [5]*Brain Science Institute, Tamagawa University*)

Motor cortical neurons are activated at multiple stages during voluntary skilled movement. However, the fine-scale organization of these activities remains poorly understood. To address this issue, we developed a self-initiated lever-pull task using a forelimb for two-photon calcium imaging of the mouse cortex in vivo. In layer 2/3 of two forelimb motor areas, the rostral forelimb area and caudal forelimb area, we identified several types of cortical cells according to their temporal activity patterns. We found that the trial-to-trial variability of the activity of individual cells is associated with that of other cells. This variability is not independent among neurons; rather, pairs of neurons covary their activities, depending on their spatial distribution and the extent of their firing rates. Our results suggest that sequential reconfiguration of functional ensembles with different correlation structures occurs in the motor cortical microcircuit.

2SH-06 Chemiluminescence imaging of flow-induced ATP release at caveolae in vascular endothelial cells

Kimiko Yamamoto[1], Joji Ando[2] ([1]*Laboratory of System Physiology, Department of Biomedical Engineering, Graduate School of Medicine, University of Tokyo*, [2]*Laboratory of Biomedical Engineering, School of Medicine, Dokkyo Medical University*)

Endothelial cells (ECs) alter their functions in response to hemodynamic shear

stress, and although their responses play important roles in vascular tone control, angiogenesis, and atherogenesis, how ECs recognize shear stress and transmit signals into the cell interior is poorly understood. Our previous studies demonstrated that calcium signaling is crucial to shear-stress mechanotransduction. Shear stress evokes a rapid, dose-dependent increase in intracellular calcium concentration caused by an influx of extracellular calcium via ATP-operated P2X4 ion channels. P2X4 activation requires the presence of endogenous ATP released by ECs, but the mechanism of the ATP release remains unknown. To analyze the dynamics of ATP release, we visualized ATP release at the cell surface by using cell-surface attached luciferase and a CCD camera. When exposed to shear stress, cultured ECs simultaneously released ATP in both, a highly concentrated, localized manner and a diffuse manner. The hot spots of ATP release occurred at caveolin-1-rich regions of the cell membrane and were blocked by caveolin-1 knockdown with siRNA, indicating involvement of caveolae in the localized ATP release. Immediately after this localized ATP release, an increase in intracellular calcium concentration and subsequent calcium wave occurred at the same site as the localized ATP release, suggesting that the ATP released at caveolae activates nearby P2X4 ion channels, which triggers shear stress calcium signaling in ECs.

2SH-07 バイオイメージング技術

New Fluorescent Probes and New Perspectives in Bioscience

Atsushi Miyawaki (*Brain Science Institute, RIKEN*)

The behavior of biochemical molecules moving around in cells makes me think of a school of whales wandering in the ocean, captured by the Argus system on the artificial satellite. When bringing a whale back into the sea — with a transmitter on its dorsal fin, every staff member hopes that it will return safely to a school of its species. A transmitter is now minute in size, but it was not this way before. There used to be some concern that a whale fitted with a transmitter could be given the cold shoulder and thus ostracized by other whales for "wearing something annoying." How is whale's wandering related to the tide or a shoal of small fish? What kind of interaction is there among different species of whales? We human beings have attempted to fully understand this fellow creature in the sea both during and since the age of whale fishing.

In a live cell imaging experiment, a fluorescent probe replaces a transmitter. We label a fluorescent probe on a specific region of a biological molecule and bring it back into a cell. We can then visualize how the biological molecule behaves in response to external stimulation. Since fluorescence is a physical phenomenon, we can extract various kinds of information by making full use of its characteristics. For example, the excited energy of a fluorescent molecule donor transfers to an acceptor relative to the distance and orientation between the two fluorophores. This phenomenon can be used to identify interaction between biological molecules or structural change in biological molecules. Besides, we can apply all other characteristics of fluorescence, such as polarization, quenching, photobleaching, photoconversion, and photochromism, in experimentation.

Cruising inside cells in a supermicro corps, gliding down in a microtubule like a roller coaster, pushing our ways through a jungle of chromatin while hoisting a flag of nuclear localization signal — we are reminded to retain a playful and adventurous perspective at all times. What matters is mobilizing all capabilities of science and giving full play to our imagination. We believe that such serendipitous findings can arise out of such a sportive mind, a frame of mind that prevails when enjoying whale-watching.

2SI-01 生物には効率が大事なのだろうか？

Is high efficiency necessary for organisms?

Seishi Kudo (*Dept. Applied Physics, Grad. Sch. Eng., Tohoku Univ.*)

I have wondered whether organisms have pursued energetic efficiency. A little while ago, I simultaneously measured swimming speed and flagellar rotation rate of bacteria. Obtained ratio of swimming speed to flagellar rotation rate, which indicates how long a cell progresses during one flagellar rotation, was 7% of flagellar helical pitch for singly flagellated Vibrio alginolyticus. That for peritrichously flagellated Salmonella typhimurium was 11% of the pitch. These data show that flagellar screw propeller slips almost 90% during swimming. Energetic efficiency of the screw propeller is only a few percent. Though the efficiency of the flagellar motor has been reported to be nearly 100%, it seems to have little meaning. Energetic efficiency may not be the most important assessment function for organisms. In the case of bacteria, they do not seem to have pursued the most efficient shape of the screw propellers. Instead, they chose minor changes of morphology of the flagellar filaments which they happened to get during the evolutional history. To better understand the biological system, it may be necessary to evaluate the total cost which includes not only short-term cost of energy but also long-term cost of development.

2SI-02 F_1-ATPase モーターの一分子エネルギー論

Single molecule energetics of F_1-ATPase motor

Shoichi Toyabe[2], Takahiro Watanabe-Nakayama[3], Hiroshi Ueno[1], Tetsuaki Okamoto[4], Hiroshi Taketani[1], Seishi Kudo[5], **Eiro Muneyuki**[1] ([1]*Dept. Phys., Faculty of Science and Engineering, Chuo Univ.*, [2]*Faculty of Physics, LMU Munich*, [3]*Interdisciplinary Graduate School of Science and Engineering, Tokyo Inst. Tech.*, [4]*Environment Preservation Center, Kanazawa Univ*, [5]*Dept. Appl. Phys., Sch. Eng., Tohoku Univ.*)

Since the first single molecule observation of the rotation of F_1-ATPase (Noji et al. Nature 1997), the mechanism of the rotation has been intensively investigated. However, study in the energetics of the rotation has been somewhat hampered due to the lack of the method to apply external torque. Using the electrorotation method, we applied precisely controlled torque on the rotational probe and examined the stall torque as a function of the free energy of ATP hydrolysis (ΔG_{ATP}) (Toyabe et al. PNAS 2011). The maximum work calculated from the stall torque coincided well with ΔG_{ATP} under wide conditions, indicating that the coupling of ATP hydrolysis/synthesis and step rotation was quite tight. Distant from the stall conditions, applying Harada-Sasa equality, we found that the difference between ΔG_{ATP} and work against the external torque dissipated through the nonequilibrium fluctuation and steady motion in the rotational degree of freedom (Toyabe et al. PRL 2010). Furthermore, we could successfully reconstitute state-specific free energy potential from single molecule trajectories (Toyabe et al. epl 2012). We could also estimate the point where the chemical state switches and found that the state transition occurred where the free energy potentials intersected. This finding gives a phenomenological interpretation for the high efficiency of F_1-ATPase motor.

2SI-03 Observation of vibrational absorption of single proteins at few Kelvins

Satoru Fujiyoshi (*Tokyo Tech.*)

Single-protein fluorescence spectroscopy at few K was applied to study individual structures and conformational dynamics of proteins. The method is attractive as well in the mid-infrared (MIR) wavelength region, information on the three dimensional structure of the backbone of individual proteins would be provided if vibrational infrared-absorption spectroscopy was applied to single proteins. However, detection of infrared absorption of a backbone vibration of a single protein has not yet been achieved. Here we report that MIR irradiation modified temporal behavior at 1.5 K of the fluorescence-excitation spectrum in the near-infrared region of single bacteriochlorophyll a molecules bound as a B800 pigment to the light harvesting 2 complex. Out of over 1000 vibrational modes that absorbed MIR light, measurement of MIR-frequency dependence of the modification revealed MIR-absorption spectrum of the vibration that induces change of a hydrogen-bond at the pigment-binding site.

2SI-04 揺らぎの定理によるミトコンドリア輸送の駆動力測定

Estimation of driving force acting on a mitochondrion transported in a living cell: Application of the fluctuation theorem

Kumiko Hayashi[1], Masaaki Sato[2], Kazunari Mouri[3], Chang-gi Pack[3], Kazunari Kaizu[4], Kouichi Takahashi[4], Yasushi Okada[4] ([1]*Sch. Eng., Tohoku Univ.*, [2]*IMRAM, Tohoku Univ.*, [3]*ASI, RIKEN*, [4]*QBiC, RIKEN*)

Technological development in both the manipulation and observation of nano- and micro- sized objects has led to a new understanding of thermodynamics and statistical mechanics in small systems such as colloidal particles and proteins, moving subject to thermal fluctuation. For example, while the second law of thermodynamics predicts that an entropy production should be increased, it became an apparent after the discovery of statistical mechanics that it can have instantaneously negative values. Probability of measuring negative values of entropy production is related to that of measuring positive values by the fluctuation theorem (FT). FT has several important consequences such as the Jarzynski equality and the Crooks fluctuation theorem. They are useful to compute the free energy difference between two equilibrium states, and were experimentally tested in RNA hairpin systems. Recently, another kind of FT has been suggested to be useful for measuring the driving forces of motor proteins. This force measurement method using fluctuations was applied to the single-molecule experiment on F1-ATPase. In this talk, we extended the applicability

of FT, as the force measurement method, to estimate driving force acting on an organelle transported by motor proteins in a living cell. Among organelle, we experimentally studied mitochondria transported by linear motor proteins such as kinesin and dynein in PC12 cells. The result was compared with the simulation developed by the E-Cell system, which is a software platform for modeling cells.

2SI-05 物質界面における構造と電荷移動を可視化する走査型プローブ顕微鏡法の開発

Development of scanning probe methods for investigating structures and charge transfers at material interfaces

Kenjiro Kimura (*Grad. Sch. of Sci., Kobe Univ.*)

It is essential for understanding the working mechanism of functional bio-materials in liquid to study their structures including solvation with higher spatial resolution. Recently, we have developed a molecular-scale solvation imaging method using frequency-modulation atomic force microscope with atomic resolution in liquid. In this method, the atomic force microscope tip is three-dimensionally scanned at solid- liquid interface, and distributions of applied forces toward the tip, related to the structures of solid surface and its solvation, are imaged. Using this method, we have revealed solvation structures around various materials such as minerals, polymer films, organic monolayers and bio-molecules and relationships with their solid surface structures. More recently, we have developed a subsurface magnetic field imaging method for understanding the locations of charge transfers inside materials. In this method, highly-sensitive magnetic field sensor is two-dimensionally scanned above materials, and a couple of magnetic field images are acquired at different heights from the material surface. Then, basic equation of electro-magnetic field is solved using two images as its boundary conditions, and two-dimensional magnetic field around the locations of charge transfers inside materials is reconstructed with sensor-size spatial resolution.

2SI-06 DNA 折り紙フレームを用いた一分子観察

Direct Observation of Single Molecular Event in DNA Origami Frame

Hiroshi Sugiyama[1,2] ([1]*Grad. Sch. Sci. Kyoto Univ.*, [2]*iCeMS*)

The DNA origami method developed for the preparation of fully addressable two-dimensional (2-D) structures has been utilized for the selective positioning of the functional molecules and nanoparticles and for the design of various 3-D architectures. Here we report the design of ”DNA frame” using the DNA origami method to examine enzymatic action. We newly developed the tension-controlled dsDNA substrates in the DNA frame and showed the importance of DNA strand relaxation in allowing double helix bending during enzymatic reaction. In our DNA frame, tensed and relaxed dsDNA can be created by bridging the defined length of dsDNA in the DNA scaffold. The relaxed strand can accommodate the enzymes to bind and bend the target sequences. On the other hand, the tensed strand allows binding of these enzymes, while this strand is a poor substrate for bending, resulting in the lower reaction efficiency. In addition, the DNA frame is valuable for analyzing the motion of the enzyme because of the defined coordinated space. The exact location and displacement of the enzyme in the reaction on the dsDNA can be monitored and analyzed. Therefore, the time-resolved reaction coordination between the enzymes and substrate can be estimated at meso-scale spatial resolution. In this presentation direct observation of DNA modifying enzymes such as DNA methylase (M. EcoRI), 8-oxoguanine glycosylase (hOgg1), T4 pyrimidine dimer glycosylase (PDG), and recombinase (Cre recombinase) as well as DNA structural change will be discussed.

1A1400 コイルドコイル ミオシンの脆弱部位と屈曲性の保存

Prediction of fragile points and conservation of bending ability of coiled coil myosin

Mieko Taniguchi[1], Hideki Tanizawa[2], Sigeki Mitaku[1] ([1]*Grad. Sch. Sci., Univ. Nagoya*, [2]*Inst. Wister, USA*)

Myosin is a mechano-chemical motor that converts the chemical energy of ATP hydorolysis into mechanical energy. Myosin has two heads and a long tail. Recently a prediction system has developed for identification of heptad break points and fragile points due to the hydrophilic core or hydrophobic outfield region in the coiled coil. Here we identified the skeletal myosin rod using this prediction system. The results showed that the rod has 8 heptad break points and 10 fragile points. To compare their values from prediction, we precisely analyzed their bending positions of the rods using AFM. As a result, we found that typical bending positions with high bending angles in the rod were tightly correlated to their fragile points and heptad break points.
Finally we would like to report about sequence homology between their heptad break points in 22 myosins from different sources.

1A1412 カーボンナノチューブ上におけるミオシン運動の温度応答

Thermal response of myosin motors on single carbon nanotubes

Mitsunori Nagata[1], Hiroshi Matsutaka[1], Takeru Okada[3], Akihiko Ishijima[2], Yuichi Inoue[2] ([1]*Grad. Sch. Life Sci., Tohoku Univ.*, [2]*IMRAM, Tohoku Univ.*, [3]*Institute of Fluid Science, Tohoku University*)

We demonstrated that single carbon nanotubes (CNTs) can be used as a new heat conductor to induce temperature change for skeletal muscle myosin (Annual meeting, 2011). However, dynamic range and local gradient of the induced temperature were not well characterized. Toward an application of various proteins including motor proteins, thermal response of myosin motors on single CNT was examined.
Multiwall CNTs (~170 nm diameter, ~10 μm length) were coated with skeletal myosin to observe sliding of fluorescently-labeled actin filaments in the presence of 2 mM ATP. During the sliding, an endpoint of the CNT was temporarily heated with a laser irradiation (645 nm, φ ~2 μm, ~0.2 s) to supply external heat.
By the local heating with laser, the sliding speed linearly increased to ~12 μm/s with increasing laser power up to 2.7 mW, indicating temperature jump of ~15°C at myosin. However, laser irradiation of 3.7 mW reduced the sliding speed, suggesting the denaturation of myosin at > 40°C.
Our results show that CNTs work as a heat conductor to induce temperature jump over 20° C for myosin. Distribution of the speed along a CNT and simulation with finite element method suggest the temperature gradient along CNT (~10 mu;m) and perpendicular to CNT (sub mu;m). Possibility of the local temperature and future applications would be discussed in the meeting.

1A1424 生体分子モーターのためのステップ解析アルゴリズム

Powerful Algorithm for analyzing Stepping Motion of Biological Melecular Motors

Takeshi Nakagawa, Kazuo Sasaki (*Dept. of Applied Physics, Tohoku Univ.*)

Many of biological molecular motors move stochastically along a linear track in a stepwise manner. The algorithms extracting step sizes and dwell times from the noisy experimental data proposed by Kerssemakers et al. [Nature 442, 709 (2006)] and by Kalafut et al. [Comput. Phys. Comm. 179, 716 (2008)], among others, seem excellent in that they do not require assumptions on the underlying mechanism of the stepping motion or user supplied parameters. We evaluated the performance of these algorithms using benchmark data under various conditions, and found that the Kerssemakers algorithm becomes considerably worse as the noise level increases and that the Kalafut algorithm shows better performance than the Kerssemakers algorithm under almost all conditions.
We propose a new step finding algorithm, which turned out to work better than the Kalafut algorithm for benchmark data with noise level smaller than about 3/8 of the step size and work equally well with the Kalafut algorithm for data with larger noise level. Our method adopts the first stage of the Kerssemakers algorithm to fit a step function to the data by the least-square method. Each candidate step is accepted or rejected based on the two-sample Student's *t*-test. The significance level for the test is automatically determined depending on the number of data points in the two dwells adjoining the step. We will explain the details of our method and compare its performance with the other algorithms at the meeting.

1A1436 高時間分解能暗視野顕微鏡を用いたキネシン頭部の前方へのステップの観察

Direct observation of the forward stepping motion of kinesin-1 using dark-field microscopy with 50-μs temporal resolution

Hiroshi Isojima[1], Ryota Iino[2], Hiroyuki Noji[2], Michio Tomishige[1] ([1]*Dept. Appl. Phys., Sch. Eng., Univ. Tokyo*, [2]*Dept. Appl. Chem., Sch. Eng., Univ. Tokyo*)

Kinesin-1 moves along microtubule by alternately moving two motor domains, in which the trailing head detaches and displaces toward the 16-nm forward tubulin-binding site upon ATP binding to the partner head. However, the detailed process and the mechanism of the forward stepping motion are still unknown, mainly due to the lack of temporal resolution of the single-molecule measurements. Here we employed dark-field microscopy with perforated mirror, and observed the movement of one of kinesin heads labeled with 40-nm gold nano-particle (GNP) with ~4 nm spatial and ~50 μs temporal resolutions. In the presence of saturating ATP, the GNPs showed ~16 nm discrete steps toward the microtubule long axis, which is consistent with the previous observations. However, our measurements also revealed that the GNP displaced ~20 nm rightward, perpendicular to the microtubule axis, accompanied with a significant increase in the fluctuation of GNP. The rightward asymmetry is consistent with the kinesin's structure that the proximal end of the neck linker is located right side of the head. Then GNPs showed rapid left-forward displacement followed by decrease in the fluctuation, although we could not detect clear sub-step. The duration of the highly fluctuating period increased as the ATP concentration was decreased, indicating that the period represents ATP-waiting state. These results support the biased binding mechanism in which the tethered head freely diffuses and is selectively captured at the forward tubulin-binding site.

1A1448 Front-head gating mechanism of kinesin-1 as studied by single molecule FRET observation of ATP binding

Yamato Niitani, Michio Tomishige (*Department of Applied Physics, School of Engineering, The University of Tokyo*)

Kinesin is a dimeric motor protein that moves along microtubule in a hand-over-hand manner. To walk in a coordinated fashion, kinesin's two motor domains (heads) should alternately move and hydrolyze ATP, however the underlying mechanism is still controversial. At the last meeting, we presented results using disulfide-crosslinking showing that ATP hydrolysis cycle of momomeric kinesin can be differently regulated depending on the direction of the neck linker extension. Here we investigated the effect of neck linker tension on the head of dimeric kinesin by directly observing ATP binding/dissociation to/from the leading head using single molecule FRET. We employed heterodimeric kinesin that is composed of a wild-type head and a mutant head that binds ATP but hydrolyzes it very slowly. This heterodimer has been shown to predominantly take two-head-bound state where the wild-type head is the leading. Then we introduced donor fluorophore to the wild-type head near the nucleotide-binding pocket and observed FRET in the presence of Alea-647 labeled ATP. We observed robust binding of ATP to the trailing head (low FRET state) but rarely observed binding to the leading head (high FRET state). When we extended the neck linker of the heterodimer by inserting poly-Gly after the neck linker, we observed frequent, transient binding of ATP to the leading head. These results support the front-head gating mechanism that the backward tension posed to the neck linker suppresses ATP binding to the leading head.

1A1510 キネシン様モータータンパク質 Ncd の Power-stroke モデルの検証

The test on the power stroke model of Ncd

Masahiko Yamagishi, Yoko Toyoshima, Junichiro Yajima (*Dept. Life Sciences, Grad. Sch. Arts and Sciences, Univ. Tokyo*)

Drosophila kinesin-14, Ncd, moves toward the minus-end of microtubules. Ncd has a neck region between the motor domain, the catalytic core of ATPase, and the stalk domain, dimerizing region. The neck is composed of a rigid coiled-coil structure. The widely accepted model of its force-producing mechanism is the power-stroke model in which Ncd strokes its neck region as a lever-arm around the motor domain as a pivot in the direction to the minus-end of microtubules. Therefore, the power-stroke model needs the rigid coiled-coil structure. Here, to test the power-stroke model, we have engineered Ncd that was fused to gelsolin at the C-terminus as a tag to fix to the glass surface. These Ncds are able to be linked

to the surface via their C-terminus, leaving the N-terminal coiled-coil structure hanging free. These C-linked Ncds drove microtubule sliding at similar rates to N-linked Ncds, thereby ruling out models in which the rigid coiled-coil structure is the only element able to exert or transmit force. Instead, our findings indicate another force-generating mechanism that shifts both the N & C terminus of the head, so that force can almost equally well be exerted by either the N or C terminus of the head. It was previously reported that a chimera Ncd whose C-terminus was replaced with kinesin-1 neck was able to move when it was attached to the glass at its C-terminus, so the kinesin-1 neck was regarded as a critical part. But our result shows that the kinesin-1 neck is not necessary.

1A1522 細菌べん毛モーター固定子複合体 MotA/B チャネルの選択的透過メカニズム

Selective permeation mechanism through the channel of the stator complex MotA/B in the flagellar motor

Yasutaka Nishihara, Akio Kitao (*IMCB, Univ. of Tokyo*)

Bacterial flagellar motor is composed of a rotor and stators. *Escherichia coli* have proton-driven motor embedded in the membrane and the stator consists of MotA and MotB proteins. Experimental studies have suggested that the stator is a torque-generating unit and that binding of protons across the membrane to Asp32 of MotB induces changes of the stator structure and the interaction of MotA with the rotor. However, atomic-level structure of the transmembrane (TM) regions of the stator has not been determined yet and the detailed mechanism of torque generation is still unclear. In this study, we constructed the structure of TM regions of the stator using molecular modeling and calculated free energy profiles for ion permeation through the channel of the stator. For the modeling, the distance restraints derived from disulfide cross-linking experimental data were employed in simulated annealing and molecular dynamics (MD) calculations. The free energy profiles for the permeation of water molecule, hydronium ion and sodium ion were calculated with the steered MD calculations. These profiles show that water molecule should overcome a high free energy barrier (< 7 kcal/mol) whereas no high free energy barrier was found in the hydronium ion permeation. We identified that difference of interaction between the permeated molecules and main chain is the origin of the selectivity.

1A1534 Sodium Dynamics of the Bacterial Flagellar Motor

Chien-Jung Lo[1], Yoshiyuki Sowa[2], Teuta Pilizota[2], Richard Berry[2] ([1]*Department of Physics, Natioinal Central University, Taiwan*, [2]*Clarendon Laboratory, Department of Physics, University of Oxford*)

Many species of bacteria swim by means of flagella, the long helical filaments connected to rotary molecular motors embedded in the cell membrane. Motors can run up to several hundred hertz. The motor is powered by the transmembrane ion-motive force: a combination of electrical voltage (Vm) and chemical potential. To explore the fundamental mechanism of this powerful molecular machine, we measured the torque-speed curves of sodium-driven chimeric flagellar motor in Escherichia coli. We test the motor speed in 25 different sodium-motive-force conditions. Similar to other report, the general shape of torque-speed cure is concave down with negative slop. The shape is less sensitive to the membrane voltage but very sensitive to the sodium concentration. The knee and the zero-torque speed depended on sodium concentration and the stall torque depended on the total sodium-motive- force. In high load conditions, the motor operates close to thermodynamic equilibrium with high efficiency. By energy balance, the ion number required to drive the motor in high load in different smf are 37 ± 2 ion/rev. We also build a 4-state kinetic model to fit the data. Using Monte Carlo Optimization, we found the model parameters to fit the experimental data. We found the ion binding in low sodium concentration and the ion transition through stators are the rate limiting steps. The fitted parameters indicate that the motor mechanism is 'power-stroke' and ion transit is channel-like rather than carrier-like.

1A1546 Engineered disulfide crosslink in the the periplasmic region of PomB impaired function of the Na+-driven flagellar stator complex

Shiwei Zhu, Na Li, Seiji Kojima, Michio Homma (*Division of Biology Science, Graduate School of Science, Nagoya University*)

In the functioning bacterial flagellar motor, multiple stator units composed of PomA and PomB must be incorporated into the motor at the appropriate places around the rotor. When assembled, stator units are anchored at the peptidoglycan layer through the periplasmic region of the B subunit. Crystal structures of this region have been recently solved, and it was proposed that the large conformational changes in this region are required for activation and assembly of the stator complex. To test this model, here we employed the disulfide crosslinking approach. If the large conformational changes are induced during the assembly of stator, then an intramolecular disulfide bridge that is engineered to covalently link between two movable elements may inhibit stator function. Based on structural information of the periplasmic region of PomB (PomBC), cysteine replacements were introduced into the cysteine-less PomB protein. We found that mutant strains with single cysteine replacement remain motile, but when we introduced several pairs of cysteine, one in the α1 helix (154-169) and another in the core domain (C-terminal region from residue 170) of PomBC, pairs of M157C-I186C, L160C-I186C, I164C-L217C and L168C-Q213C inhibited the function of the Cysteine-less PomB. However, after treating with DTT, all of them restored the motility less than 1 hour. Thus, we speculated that the crosslink due to the disulfide bridge formed by one pair of cysteine inhibits the conformational change in the periplamic region of PomB. (1529/1560)

1A1558 高圧力が引き起こすべん毛繊維のダイナミック構造変化

Dynamic conformational changes of flagellar filament observed by high-pressure microscopy

Masayoshi Nishiyama[1], Yoshiyuki Sowa[2] ([1]*The Hakubi Center, Kyoto Univ.*, [2]*Hosei Univ.*)

The bacterial flagellar motor is a molecular machine that rotates a flagellum in both directions. CCW rotation allows the left-handed helical filaments to form a bundle that propels the cell smoothly, whereas CW rotation of a filament leads to change the shape of filament in right-handed helix and break the bundle, and inhibits smooth swimming of the cell, called a tumble. The switching in the helical structure is thought to be caused by directional mechanical actions arising from abrupt change of exerted torque by the motor rotation. Here, we show that application of pressure can also change the helical structure of flagellar filaments. The flagellar filaments in *E. coli* cells were fluorescently labeled, and then the images were acquired by using an improved high-pressure microscope. We measured the diameter and pitch of the individual filaments and then classified them into 11 possible waveforms which are predicted from structural data. At 0.1MPa (ambient pressure), all flagellar filaments form left-handed helical structure (normal form). At 40 MPa, we found not only left-, but also right-handed structures such as coiled-coil and curly I (or II). At 80 MPa, only the right-handed structures existed. After the pressure was released, most filaments returned to the initial left-handed structures. The application of pressure is thought to enhance the structural fluctuation and/or association of water molecules with the exposed regions of flagellin molecules, and results in switching the helical from left- to right-handed structure.

1A1610 c-di-GMP 結合タンパク質 YcgR のホモログ PlzD の大量発現による *Vibrio alginolyticus* でのべん毛運動阻害

Flagellar motility inhibition by overexpression of PlzD, a YcgR homolog of c-di-GMP binding protein, in *Vibrio alginolyticus*

Takuro Yoneda, Wakako Morimoto, Seiji Kojima, Michio Homma (*Grad. Sci., Univ. Nagoya*)

Bacterial flagellum is a locomotive apparatus which is needed to swim or to swarm. At the base of each flagellum, there exists a membrane-embedded motor. The ion flux through the stator couples to the rotor-stator interaction that generates torques. Recently it was found that YcgR inhibits motility in the presence of cyclic diguanylate (c-di-GMP) in *E. coli*. Its N-terminal YcgR/PilZN domain is considered to be required to interact with flagellar basal protein(s) and C-terminal PilZ domain is a receptor for c-di-GMP. It was reported that PlzD of *Vibrio chorelae*, a homolog of YcgR, affected the flagellar motility under a poor nutrient condition. In this study, we cloned PlzD from *Vibrio alginolyticus*. *V. alginolyticus* PlzD conserves all 5 residues required for binding to c-di-GMP for PlzD of *Vibrio chorelae*. PlzD inhibited motility in nutrient-poor plate and EGFP-PlzD was localized at cell pole. N-terminally-truncated PlzD shows weaker motility inhibition than wild type PlzD, and EGFP-PlzD$_{\Delta 1\text{-}35}$ exhibits no fluorescent localization. Based on these results, we speculate that N-terminal region of PlzD is important for interact flagellar basal protein(s) and that PlzD can assemble around flagellar basal body. PlzD as well as YcgR repress motility significantly in *E. coli* MS1467 strain (ΔyhjHΔycgR). This indicates that PlzD can function in *E. coli* and may suggest a conformational similarity between N-terminal region of PlzD and YcgR though the sequence homology is very low.

1B1400 “空隙”ー機能構造創出のための自然の戦略

Cavityーa Nature’s strategy for functional sub states in proteins

Kazuyuki Akasaka (*Kinki UNIV., Inst. Adv. Tech.*)

How Nature can provide proteins with the dynamics and sub states required for their specific needs for function is a fundamental question in protein science and evolution. To address the question, here we focus on cavities. Cavity is synonymous to void in folded proteins, often discernible as atom defect in crystal structures of proteins. Although cavity has long been known as a factor that affects thermal stability and compressibility of proteins (Gekko and Hasegawa, Biochemistry 1986), its specific role in protein dynamics and function remains unclear. In recent years, the question is pursued intently on pressure axis using NMR or X-ray crystallography in functional proteins including hen lysozyme, cMyb protein and OspA among others (1-3). The studies start revealing crucial roles of cavities in providing functional dynamics and sub states, and further suggest their roles in evolution.

References
1. Kamatari et al., Biophys. Chem.156, 24-30 (2011).
2. Sunilkumar P N et al., Biophys. J. 102, L8-L10 (2012).
3. Kitahara et al., Biophys. J. 102, 916-926 (2012).

1B1412 HD-exchange motion of free heptameric GroES studied by the use of TROSY and DMSO quenching followed by 2D NMR

Mahesh Chandak[1], Takashi Nakamura[1], Koki Makabe[2], Toshio Takenaka[1], Jin Chen[1], Koichi Kato[1], Kunihiro Kuwajima[1] (*[1]Okazaki Institute of Integrative Bioscience,National Institutes of Natural Sciences,The Graduate University for Advanced Studies (Sokendai)*, *[2]Graduate School of Science and Engineering,Yamagata University*)

The GroEL-GroES is a chaperonin complex which assists target proteins to fold into native state. To understand structural and functional relationship of GroES-GroEL complex, we studied the dynamic structural fluctuations of free heptameric GroES by the use of hydrogen/deuterium (H/D) exchange and 2DNMR techniques. H/D exchange analysis is used to trace the rate at which protein backbone amides undergo chemical exchange with deuterated solvent. NMR spectroscopy is used to study proteins having molecular weight up to 50KDa. However, as the molecular weight of the GroES complex is 70KDa, we cannot get well resolved NMR spectrum. So, we need a modified strategy to study this complex. In this study, we report the dynamic structural fluctuations of free heptameric GroES by the use of H/D exchange technique followed by: 1) Transverse relaxation optimized spectroscopy (TROSY) and 2) DMSO quenching with 2DNMR. In our study, we observed rapid exchange rate of backbone amide residues in a mobile loop region. During the GroES-GroEL complex formation, this mobile loop region forms contact with GroEL complex. Therefore, this result indicates that mobile loop is very flexible in free heptameric GroES.

1B1424 溶液 NMR を用いた Na^+駆動型べん毛モーターの固定子タンパク質 FliG の C 末端領域構造解析

Solution NMR analysis of FliG C-terminal domain derived from Na^+-driven motor of *Vibrio*

Mizuki Gohara[1], Rei Abe-Yoshizumi[1,2], Shiori Kobayashi[1], Yohei Miyanoiri[3], Yoshikazu Hattori[4], Chojiro Kojima[4], Masatsune Kainosho[3,5], Michio Homma[1] (*[1]Div. Bio. Sci., Grad. Sch. Sci., Nagoya Univ.*, *[2]Department of Frontier Materials, Nagoya Institute of Technology*, *[3]Structural Biology Research Center, Grad. Sch. Sci., Nagoya Univ.*, *[4]Institute for Protein Research, Osaka Univ.*, *[5]Center for Priority Areas, Tokyo Metropolitan Univ.*)

In the bacterial flagellar motor, torque is generated by interactions between the rotor and the stator. In the rotor, a C ring component, FliG, mainly participates in torque generation, primarily through its C-terminal domain. In the H^+-driven motor of *Escherichia coli*, mutational analyses revealed that the rotor-stator interaction is mediated by charged residues between the FliG C-terminal domain and the MotA cytoplasmic loop region. However, in the Na^+-driven motor of *Vibrio*, the effects of mutations of the charged residues on the motility were very weak. Therefore, the mechanism of torque generation in the Na^+-driven motor remains unknown. To investigate the interaction between FliG and the MotA ortholog PomA in the Na^+-driven motor, we performed solution NMR analyses. We previously reported that drastically improved ^{1}H-^{15}N TROSY-HSQC spectra were obtained with the N-terminally truncated FliG variant, G214-FliG ($FliG_C$). We’d now like to discuss the result of the 3D ^{1}H-^{13}C-^{15}N NMR measurements and the on-going sequential signal assignments. Furthermore, we tried to create PomA fragments containing the cytoplasmic loop region, with which FliG is supposed to interact. We found that overexpression of the PomA fragment impedes the motility. We are currently trying to measure NMR spectra of $FliG_C$ in the presence and absence of PomA fragments, and further results will be discussed at the meeting.

1B1436 酸化還元状態に依存してプロテインジスルフィドイソメラーゼの基質結合部位ドメインの空間配置が変化する仕組み

Molecular mechanism of redox-dependent domain rearrangement of the substrate-binding region of protein disulfide isomerase

Kouya Inagaki[1,2], Yoshinori Uekusa[1,2], Yukiko Kamiya[1,2], Tadashi Satoh[1], Koichi Kato[1,2] (*[1]Grad. Sch. Phar. Sci., Nagoya City Univ.*, *[2]Natl. Inst. Nat. Sci.*)

Protein disulfide isomerase (PDI), a major protein in the endoplasmic reticulum, operates as an essential folding catalyst and molecular chaperone for disulfide-containing protein substrates. We have previously reported that b’ and a’ domains of PDI exhibit an intramolecular domain rearrangement depending on the redox state of the active site cysteine pair in a’ domain, which is coupled with the shielding and exposure of substrate-binding hydrophobic surface spanning across these domains. To gain insights into the molecular mechanism of this domain rearrangement, we prepared mutated PDI-b’ a’ in which a cysteine pair was substituted for serine or alanine. By using fluorescent hydrophobic probe, we revealed that the serine- and alanine-substituted mutants mimicked the reduced and oxidized forms of wild-type protein, respectively, in terms of exposure of hydrophobic surface. By nuclear Overhauser effect experiments of NMR spectroscopy, we demonstrated that the side chain of the tryptophan residue located adjacent to the a’ active site was in contact with the b’ domain in the reduced form and serine-substituted mutant, whereas the tryptophan side chain was accommodated in the active site in the oxidized state and the corresponding site of the alanine-substituted mutant. Based on these results along with those obtained by X-ray crystallographic analyses, we proposed a mechanistic model of the domain rearrangement triggered by redox-dependent flipping of the tryptophan side chain.

1B1448 Transferred cross-saturation 法を用いた EB1 の CH ドメインの微小管との結合界面の特定

Microtubule-binding sites of EB1 CH domain revealed by transferred cross-saturation experiments

Teppei Kanaba[1], Ryoko Maesaki[2], Tomoyuki Mori[2], Yutaka Ito[1], Toshio Hakoshima[2], Masaki Mishima[1] (*[1]Grad. Sch. of Sci. and Tech., TMU*, *[2]Grad. Sch.l of Biol. Sci., NAIST*)

End-binding 1 (EB1) is a member of plus end tracking proteins which bind to microtubule (MT) plus end and regulate MT dynamics. EB1 binds to microtubule lattice with its N-terminal CH domain and stabilizes MT. EB1 is thought to be autoinhibited by the interaction between CH domain and C-terminal domain. Despite the importance of the EB1-MT interaction in regulation of MT dynamics, the molecular details of the EB1 autoinhibition remain unclear.

By comparison between CH domain K59E mutant (low affinity interactor) data and a competition data, we identified the binding interface of CH domain with polymerized tubulin by transferred cross-saturation (TCS) experiments. In addition, by chemical shift perturbation experiments, we identified the binding interface between EB1 CH domain and C-terminal domain. Interestingly, we found that the MT-binding sites and C-terminal domain binding sites of CH domain are closely located, indicating that the MT-binding sites are masked by the interaction between the C-terminal domain in an autoinhibited state. Our chemical shift perturbation experiments suggest that the CH domain binding region of C-terminal domain is almost identical to the SxIP motif of APC and CAP-Gly domain of p150 ^{glued} binding region. Autoinhibition may therefore be regulated through competition binding by such binding partners.

1B1510 再構築型生体外タンパク質合成系を用いた分子シャペロンによる凝集抑制効果の大規模解析

Global analysis of aggregation-inhibotion effects of molecular chaperones using a reconstituted cell-free translation system

Tatsuya Niwa[1], Takuya Ueda[2], Hideki Taguchi[1] (*[1]Grad. Sch. of Biosci&Bioteh, Tokyo Institute of Technology*, *[2]Grad. Sch. of Frontier Sciences, The university of Tokyo*)

Protein folding is often hampered by protein aggregation, which can be prevented by a variety of chaperones in the cell. A dataset that evaluates which chaperones are effective for aggregation-prone proteins would provide an invaluable resource not only for understanding the roles of chaperones, but also for broader applications in protein science and engineering. Previously, we conducted comprehensive aggregation analysis of more than 3,000 Escherichia coli proteins by using a reconstituted cell-free translation system (PURE system), which does not contain any chaperones (Niwa et al., PNAS, 2009). A histogram of the solubilities revealed a clear bimodal distribution, implying that the many aggregation-prone proteins require chaperones to fold correctly.
Then, we comprehensively evaluated the effects of the major E. coli chaperones, trigger factor, DnaK/DnaJ/GrpE, and GroEL/GroES, on ~800 aggregation-prone cytosolic E. coli proteins, using the PURE system. Statistical analyses revealed the robustness and the intriguing properties of chaperones. The DnaK and GroEL systems drastically increased the solubilities of hundreds of proteins with weak biases, whereas trigger factor had only a marginal effect on solubility. The combined addition of the chaperones was effective for a subset of proteins that were not rescued by any single chaperone system, supporting the synergistic effect of these chaperones. The resource can be used to investigate the properties of proteins of interest in terms of their solubilities and chaperone effects.

1B1522 DNA 界面での蛋白質の局所的構造変化

Local conformational changes of proteins in DNA interfaces

Tomoko Sunami, Hidetoshi Kono (*JAEA*)

To better understand the conformational changes of proteins upon DNA binding, we carried out quantitative analyses. We first described the proteins using a structural alphabet library of backbone geometries created by Kolodony et al. and then detected the conformational changes as changes in alphabets between DNA-free and bound forms. We first divided protein surface into two regions, DNA interface and protein surface which exclude the DNA interface and carried out analyses. The results show that 1) the conformational changes at DNA interfaces are more frequent than those at the other surfaces; 2) DNA interfaces have more conformational variation even in the DNA-free form. The latter suggests that intrinsic, conformational flexibility of DNA interface seems to be important to adjust their conformations to DNA. In amino acid propensities, conformationally changed regions in DNA interfaces as well as those in the other protein surfaces show that hydrophilic and glycine residues are more preferred compared with conformation-unchanged regions. This trend is also found in the propensity for disordered regions, suggesting that the intrinsic flexibility be of importance not only for DNA binding but also for interacting with other molecules. Comparison of the distributions of structural alphabets between DNA interfaces and the other surfaces shows that some specific alphabets appear more often in DNA interfaces. This suggests that these local conformations may be adjustable to DNA structure with a low energy cost.

1B1534 天然変性タンパク質の構造ゆらぎを生かした密度変化誘起型シグナル伝達過程

The possible advantage of structural disorder of intrinsically disordered pr oteins in the new type of signaling mechanism

Nobu C. Shirai[1,2], Macoto Kikuchi[1,2,3] ([1]*Graduate School of Science, Osaka University*, [2]*Cybermedia Center, Osaka University*, [3]*Graduate School of Frontier Biosciences, Osaka University*)

There are questions about intrinsically disordered proteins (IDPs), why higher organisms have much more IDPs and what the advantages of structural disorder of IDPs are. To investigate these questions, we construct a lattice gas model of IDPs and their targets based on the following assumption about structural disorder of IDPs: structural disorder of IDPs can be represented by effective volume and internal entropy under crowded condition of a cell. Based on the result of the Monte Carlo simulation, we propose a new type of signaling mechanism, which we call density-regulated signaling mechanism. By the use of the mechanism, a cell can regulate the number fraction of bound-state IDPs, which is considered as signal intensity, by increasing or decreasing the density of total biomolecules. We find that IDPs must have sufficiently large internal entropy in order to realize an all-or-none signaling switch. We conclude that the all-or-none signaling switch is an advantage of structural disorder of IDPs.

1B1546 分子動力学法による capping protein（CP）の動的構造の解析

Structural fluctuations of capping proteins analyzed by molecular dynamics simulations

Ryotaro Koike[1], Shuichi Takeda[2], Yuichiro Maeda[2], Motonori Ota[1] ([1]*Grad. Sch. Info. Sci., Nagoya Univ.*, [2]*Struct. Biol. Res. Center, Grad. Sch. of Sci., Nagoya Univ.*)

Capping protein (CP) binds to the barbed end of an actin filament and inhibits the further polymerization of actin monomers onto the filament. The polymerization inhibition of CP is regulated by two distinct proteins, V-1 and CARMIL, through their interactions with CP. The regulation mechanisms of the two are quite different; V-1 sterically inhibits the binding of CP to actin filament, and allosterically does CARMIL. Moreover, CARMIL can dissociate bound CP from actin filament or V-1. The crystal structure of CP/V-1 complex locates the V-1 binding site on CP, and reveals that V-1 sterically hinders the interaction between CP and filament. On the other hand, the regulation mechanism of CARMIL has not been unveiled. The crystal structure of CP/CARMIL complex indicates that the CARMIL binding site on CP is distant from the binding site for filament or V-1, and the binding of CARMIL to CP induces an insignificant structural change in the V-1 binding site of CP. To unveil the regulation mechanism of CARMIL, we focused on structural fluctuation of CP because CARMIL can influence an essential motion in CP. We applied AMBER, a program for molecular dynamic simulation, to structures of free CP, CP/CARMIL and CP/V-1 complexes and examined their dynamic properties. We discuss the properties and their differences.

1B1558 シトクローム c 酸化酵素のプロトンポンプ機構に関する分子動力学シミュレーションによる研究

A Molecular Dynamics Study on Proton Pump Function of Cytochrome c Oxidase

Takefumi Yamashita (*Research Center for Advanced Science and Technology, University of Tokyo*)

The proton-pumping mechanism of cytochrome c oxidase (CcO) has received broad attention not only as a biological function but also as a physical energy conversion. Coupling the electron transfer to reduce a trapped oxygen molecule to a water molecule, CcO transports protons across the mitochondrial membrane to form electrochemical gradient, which is essential to produce ATP. In this work, we aim to clarify how the electron transfer can control the proton transport in the non-polar cavity, which is expected to be important since this region is surrounded by the two heme groups. In order to simulate the proton transport in CcO realistically, the multi-state empirical valence bond (MS-EVB) model is adopted here. We evaluated free energy profiles for several oxidation states to see electron transfer effects. The results clearly suggest that the reduction of heme a opens the gate of the proton exit channel. More detailed results will be discussed in this presentation.

1B1610 Substrate transport mechanisms in GatCAB: the smallest unidirectional valve in subnano scale

Jiyoung Kang[2], Shigehide Kuroyanagi[2], Yohsuke Hagiwara[2], Masaru Tateno[1] ([1]*Grad. Sch. Sci., Univ. Hyogo*, [2]*Grad. Sch. Pure and Appl. Sci., Univ. Tsukuba*)

Glutamine amidotransferase CAB (GatCAB) is a crucial enzyme involved in translational fidelity, catalyzing the glutaminase reaction to yield ammonia (NH_3 or NH_4^+) from glutamine and the transamidase reaction to convert the phosphorylated Glu-tRNA^{Gln} to Gln-tRNA^{Gln}. In the crystal structure of GatCAB, these two catalytic centers are far apart, and the presence of a hydrophilic channel to dislocate the produced NH_3/NH_4^+ was proposed. We investigated the transport mechanisms of GatCAB by large time scale (~1.1 μs) molecular dynamics (MD) simulations and free energy (PMF) calculations. As a result of the analysis, we found that the entrance of the previously-proposed channel is closed, as observed in the crystal structure. Instead, a novel hydrophobic channel was identified; its entrance opened and closed repeatedly, and thus acted as a gate. The calculated free energy (PMF) difference revealed the significant preference of the newly-identified gate/channel for NH_3 transport (~104-fold). In contrast, NH_4^+ tightly hydrogen-bonded with hydrophilic residues for both channels, which hindered efficient transport. The opening of this gate was modulated by Phe206, which acted as a “valve”. Note that for the backward flow of NH_3, the opening of the gate was hindered by Ala207, which acted as a mechanistic “stopper” against the motion of the “valve”. Thus, this can be considered as the smallest unidirectional valve inside proteins.
[1] J. Kang, S. Kuroyanagi, Y. Hagiwara, T. Akisada, and M. Tateno: *J. Chem. Theory Comp.* **8** (2012) 649.

1C1400 抗菌ペプチドを利用した病原体検出サンドイッチ発色検出技術の開発

New colorimetric sandwich assay for detection of pathogens by using antimicrobial peptides as detection probes

Chihiro Sakai[1], Eri Hojo[2], Taichi Nakazumi[1], Satoshi Tomisawa[1], Takashi Kikukawa[1], Yasuhiro Kumaki[1], Masakatsu Kamiya[1], Makoto Demura[1], Keiichi Kawano[1], Ryuji Ohtsuki[2], Taro Yonekita[2], Naoki Morishita[2], Takashi Matsumoto[2], Fumiki Morimatsu[2], **Tomoyasu Aizawa**[1] ([1]*Grad. Sch. Life Sci., Hokkaido Univ.*, [2]*R&D Center, Nippon Meat Packers Inc.*)

Antibody-based assays such as an enzyme-linked immunosorbent assay (ELISA) are important techniques for rapid and efficient detection and identification of pathogens. These methods are widely used in many applications because the antibodies for specific antigenic sites on target pathogens can be used to be distinguished very closely related species. However, in the case of some target pathogens, it is very difficult to develop antibodies with both high sensitivity and high specificity and practical pathogen detection systems.
In this study, we used antimicrobial peptides (AMPs) as candidates for alternative detection molecule, expecting that AMPs can bind to pathogens with greater density than antibodies because of the size. In the general sandwich ELISA with immobilized antibodies and biotin-labeled antibodies for colorimetric detection by using streptavidin conjugated horseradish peroxidase, we replaced the biotin-labeled antibodies with the biotin-labeled AMPs as probes for detection. As the results of screening of AMPs, we found that some AMPs, such as cecropin P1 and magainin 2, are suitable for the detection molecules in our sandwich assay system. After optimization of well plate materials and blocking reagents, our new system could be used for detection of *Salmonella* with high detection sensitivity and specificity.

1C1412 VanX の溶菌活性を用いたルシフェラーゼのスクリーニングの簡略化

Toward a simplified screening method using a novel VanX cell lysis activity

Nan Wu[1], Tetsuya Kamioka[1], Shihori Sohya[1], Tomoki Matsuda[2], Takahisa Ikegami[3], Haruki Nakamura[3], Yutaka Kuroda[1] ([1]*Biotechnology and Department Life Science, Graduate School of Engineering, Tokyo University of Agriculture and Technology*, [2]*Research Institute for Electronic Science, Hokkaido University*, [3]*Institute for Protein Research, Osaka University*)

VanX belongs to the VanA gene cluster that provides Vancomycin resistance. VanX hydrolyzes the D-Ala-D-Ala dipeptide which eventually blocks the cell wall formation (D-Ala-D-Ala dipeptide usually fuse to the C-terminal of the murein monomer, and induce the synthesis of murein chain forming the cell wall). Recently, we expressed VanX as a single gene in E.coli, and found that it has a strong cell lysis activity. Here, we report attempts to use this novel cell lysis activity to purify recombinant proteins from E.coli without mechanical or chemical breakage of the cell wall. As a target protein, we used Gaussia Luciferase, which is a bioluminescent protein containing 10 cysteines forming 5 dissulfide bridges and is expected to provide an efficient reporter protein. Our strategy is to co-express the target protein, GLuc, with VanX, so that cell autolysis occurs, and release Gluc into the culture medium. We thus expressed VanX and GLuc using, respectively, pET26 and pET21(Novagen) in JM109 (DE3) plysS E.coli cells. Upon addition of luciferin directly into the culture medium, the sample emitted a strong blue light indicating that VanX lysed the E.coli cells and that GLuc was released into the medium in a native form. Cell lysis by VanX may thus provide a versatile method for recovering protein from E.coli without a need for mechanical, chemical cell breakage or the introduction of a secretion signal sequence. We are now applying this method to the screening of GLuc with new bioluminescent properties.

1C1424 Fluorescent Probe for the Direct Detection of Histone Deacetylase Activity

Koushik Dhara[1], Yuichiro Hori[1], Reisuke Baba[1], Kazuya Kikuchi[1,2] ([1]*Graduate School of Engineering, Osaka University*, [2]*Immunology Frontier Research Center, Osaka University*)

Histone deacetylases (HDACs) are important enzymes for the transcriptional regulation of gene expression in eukaryotic cells. The reversible acetylation of lysine residues near the N-terminal of nucleosomal histones by HDACs and histone acetyltransferases (HATs) regulates chromatin structure and transcriptional activity. HDAC enzymes are the major targets of drug development and many of the reports indicate that HDACs have been found to be major targets for the various diseases such as cancer, neurological diseases and metabolic diseases. Therefore, in terms of medical science as well as basic biology, the detection of the HDACs enzyme activities is a key for emerging drugs and the elucidation of epigenetic mechanism and various biological phenomena. Although in vitro assays for HDACs are known, the methods do not allow the direct and real-time detection of the enzymatic activities. To the best of our knowledge, there is no report of fluorescent probes that allow the real time determination of HDAC activity. To overcome the problem, we design a novel fluorescent probe for the direct detection of HDAC activity. Time-dependent enhancement of the fluorescent intensity was observed in the enzyme reaction with SIRT1. Deacetylated product of the probe upon enzyme reaction was monitored by HPLC analysis. The probe showed excellent stability for a long time in the aqueous buffer. This new probe constitutes a great innovation in the field of HDAC sensing assays in a direct manner.

1C1436 RaPID システムによる Akt2 選択的環状ペプチド阻害剤の探索とその阻害ペプチドの生化学的活性の評価

Exploring cyclic peptide inhibitors against the Akt2 kinase by the RaPID system and evaluation of their biochemical properties

Yuuki Hayashi[1], Jumpei Morimoto[2], Hiroaki Suga[2] ([1]*Dept. Life Sci., Grad Sch. Arts and Life Sci., The Univ. Tokyo*, [2]*Dept. Chem., Grad Sch. Sci., The Univ. Tokyo*)

Human Akt isoforms, Akt1, Akt2, and Akt3, are serine/threonine kinases that regulate cell signal transductions. Since dysregulation of Akt activity often causes various carcinomas, Akt has been targeted for drug discovery. Because most of Akt inhibitors target the substrate binding sites in kinase domain, which is highly conserved over various kinases, the inhibitors act against both Akt isoforms and non-Akt kinases, and might cause side effects through the undesired inhibitions. Therefore it remains challenging to achieve high isoform-selectivity and potency simultaneously against a specific isoform. Here, we explored cyclic peptide inhibitors against the kinase activity of Akt2 isoform using the RaPID (Random nonstandard Peptide Intecrated Discovery) system that allows us to 'rapidly' select high-affinity binders for Akt2 from cyclic peptide libraries with a huge diversity (~10^{13} sequences). As a result, we succeeded in selecting three peptides, Pakti-L1, -L2 and -L3, that inhibit Akt2 kinase activity with ~100 nM of IC_{50} values but less inhibit the kinase activity of PKA and SGK. Interestingly, despite the absence of selection pressure to eliminate other isoform-binders, Pakti-L1 shows 250- and 40-fold higher specific inhibition against the Akt2 isoform compared to the Akt1 and Akt3 isoforms, respectively. Akt isoforms share the same amino acid sequence in the substrate binding sites, it suggests that Pakti-L1 binds outside of the substrate binding sites in the Akt2 and allosterically inhibits the Akt2 kinase activity.

1C1448 低分子抗体の多機能化を可能とするピンポイント化学接合デザイン

Protein engineering for site-specific bioconjugation chemistry: Construction of multiple functional low-molecular antibodies

Mitsuo Umetsu, Asami Ueda, Takeshi Nakanishi, Kentaro Hashikami, Ryutaro Asano, Izumi Kumagai (*Department of Biomolecular Engineering, Graduate School of Engineering, Tohoku University*)

IgG-type antibodies are usually produced in mammalian cell expression systems, but the construction of a stable and large-scale production process in mammalian systems is laborious, timeconsuming, and expensive. In contrast, antibody fragments, such as single-chain Fv (scFv) and Fab fragments, can be prepared in bacterial secretory expression systems; however, the downsizing of antibodies has some benefits in protein expression processes, while it results in low affinity for antigen-displayed cell surfaces by the degrease of antigen-binding valence. Here, we propose a new construction of low molecular multivalent/bispecific antibody by conjugation of protein engineering and chemical conjugation engineering. In this method, all the lysine residues in scFv fragment are first mutated to alternative amino acid residues by utilizing bioinformatics and molecular evolution technique to prepare the scFv with only one lysine residue at a specific position by bacterial expression. After the design of the lysine-mutated scFv fragment, the two scFv fragments are chemically conjugated via a dicarboxylic organic linker that make amide binding with the lysine in scFv; consequently, homogeneous bivalent/bispecific antibody can be generated. Here, we show the construction of bispecific low molecular antibody with affinity for epidermal growth factor receptor on tumor and for CD3 receptor on lymphocyte cell.

1C1510 ハイブリッドナノセルロームの構成要素としての CBM の機能解析

Hybrid nano-cellulosome: functional analysis of various cellulose binding module as component of artificial cellulosome

Hikaru Nakazawa[1], Do-myoung Kim[1], Takashi Matuyama[2], Nobuhiro Ishida[2], Akinori Ikeuchi[2], Izumi Kumagai[1], Mitsuo Umetsu[1] ([1]*Tohoku univ. tech.*, [2]*Toyota Central R&D lab*)

Cellulose is naturally occurring plant cell wall constituent and most abundant polysaccharides on earth. An economically viable process for converting this biomass to fermentable sugar is a prerequisite for the development of cellulosic biomass-based bio-refineries for the production of food, feed, chemicals and fuels. Cellulose can be converted to fermentable sugar by microbial cellulose degrading enzymes, so called cellulase. Cellulases are generally modular proteins with an independent catalytic domain (CD) and a carbohydrate-binding module (CBM) and in some bacteria, CDs with different functions are clustered on a giant scaffold protein containing CBM, via coheisin-dockerin interaction to efficient degradation, so called cellulosome.
Recently, we proposed a new design of artificial cellulosome to enhance cellulase activity with streptavidin or streptavidin modified CdSe quantum dot as a scaffold via biotin-avidin interaction.Activity of the cluster enzyme with two kind of CBD indicated that depend on combination of scaffold and CBD. Thus, selection of the promising CBM is important in this artificial cellulosome format for efficient cellulose degradation. Currently, cellulose binding module was belonging to carbohydolate binding module family (CBMF) 1-4, 6, 8-11, 17, 30, 37, 44, 46, 49, 63, 64, and NC.
In this study, we carried out to express CBM from each CBM family in *Escherichia coli* and evaluated the kinetic parameter in cellulose binding and the activity of the clustering enzyme with CD and these CBM on scaffold.

1C1522 エンド-1,3-βグルカナーゼの糖結合モジュールα-リピートに存在する Trp273 のラミナリン結合への寄与

Contribution of Trp273 in the α-repeat of the carbohydrate-binding module of endo-1,3-β-glucanase to laminarin binding

Tomonari Tamashiro[1], Yoichi Tanabe[1], Kenji Kanaori[2], Teikichi Ikura[3], Nobutoshi Ito[3], Masayuki Oda[1] ([1]*Grad. Sch. of Life and Environ. Sci., Kyoto Pref. Univ.*, [2]*Grad. Sch. of Sci. and Technol., Kyoto Inst. of Technol.*, [3]*Med. Res. Inst., Tokyo Med. and Dent. Univ.*)

Endo-1,3-β-glucanase from *Cellulosimicrobium cellulans* DK-1, is composed of catalytic domain and carbohydrate-binding module (CBM), both of which are connected by a Gly/Ser-rich linker. The CBM, CBM-DK, is classified as CBM family 13, which would have a β-trefoil fold displaying the pseudo-3-fold symmetry arising from imperfect tandem α-, β-, and γ-repeats. Among the three repeats, we recently showed that α-repeat mainly contributes to the carbohydrate binding (Glycoconj. J. 29, 77, 2012). In this study, we focused on Trp273 in α-repeat, which has critical role for the binding, together with Asp270. We overexpressed CBM-DK, corresponding to Gly257-Leu383, and its mutants, W273A and W273S, in *E. coli* with N-terminal His-tag, and purified them using Ni-NTA affinity chromatography. The interactions with β-1, 3-glucans, laminarin and laminarioligosaccharides, were analyzed using surface plasmon resonance biosensor and isothermal titration calorimetry (ITC). The binding affinities to laminarin determined using ITC were 1.3×10^6 M^{-1} for CBM-DK wild-type, 3.7×10^4 M^{-1} for W273A, and 1.5×10^4 M^{-1} for W273S. Trp273 could participate in the carbohydrate binding through a hydrophobic interaction. This seems to be correlated with the facts that W273A mutant could be concentrated using the membrane filter system, while CBM-DK wild-type could not. We prepared ^{15}N-uniform labeled W273A sample for NMR experiments. In the presentations, we will discuss the structural properties of CBM-DK and its complex with laminarioligosaccharide.

1C1534 Construction of an in vitro gene screening system for membrane proteins

Haruka Soga[1], Satoshi Fujii[3], Tetsuya Yomo[2,3], Hajime Watanabe[1], Tomoaki Matsuura[1,3] ([1]*Dept. Biotech., Grad. Sch. Eng., Osaka Univ.*, [2]*Dept. Bioinfo. Eng., Grad. Sch. IST, Osaka Univ.*, [3]*ERATO, JST.*)

In vitro molecular evolution is a method to screen for proteins with desired properties by mimicking the Darwinian evolution entirely in vitro. So far, various methods including ribosome display, mRNA display and in vitro compartmentalization have been developed, and successfully used to evolve the function of soluble proteins, however, none of these methods can deal with integral membrane proteins. Here, we report the development of a technology for in vitro selection and evolution of membrane proteins. It uses synthesis of membrane proteins by in vitro transcription-translation system (the PURE system) within giant unilamellar vesicles (GUV). The gene encoding the membrane protein is encapsulated in GUV at a single molecular level together with the PURE system. Subsequently, the membrane protein is synthesized and inserted into the lipid bilayer. The GUVs that display the membrane protein with desired properties (affinity to the ligand or high transporter activity) are screened. We show using EmrE, a multidrug transporter from Escherichia coli, as a model protein that this protein can be synthesized from a single DNA molecule inside and get localized on the surface of the GUV. Furthermore, the synthesized EmrE transported ethidium bromide in response to the proton gradient. Finally, we show the results of an enrichment experiment, where EmrE gene is enriched from a mixture with others.

1C1546 Orientation-controlled immobilization of pharaonis halorhodopsin onto gold revealed by SEIRAS

Hao Guo[1,2], Tetsunari Kimura[1,2,3], Yuji Furutani[1,2,4] ([1]*Department of Structural Molecular Science, the Graduate University for Advanced Studies*, [2]*Department of Life and Coordination-Complex Molecular Science, Institute for Molecular Science*, [3]*JST CREST*, [4]*JST PRESTO*)

Despite membrane proteins play an essential role in the proper functioning of the cell, the knowledge of their molecular mechanisms remains limited. Protein immobilization with a desired orientation is a valuable approach to mimic a natural membrane environment. However, there is no clear experimental evidence to validate the effectiveness of the orientational control. Here we report the immobilization of pharaonis halorhodopsin (pHR), a light-driven chloride pump in bacterial cell membrane, onto gold by the affinity of a histidine-tag (His-tag) to a nickel chelating nitrilotriacetic acid surface. Control of the orientation was performed by the adsorption of pHR via the 6×His-tag introduced into either the N- or the C-terminus. Use of the optical near-field effect of surface-enhanced infrared absorption spectroscopy (SEIRAS), difference between these two surface orientations can be distinguished. Deconvolution and curve fitting of the SEIRA spectra of bound pHR suggest that more antiparallel β-sheet structure is detected in the case of N-terminus binding. To directly corroborate our results, the binding experiments have been repeated under identical conditions using β-sheet deleted pHR mutants. The results show that the mutated pHRs display a significant decrease of the characteristic peak of antiparallel β-sheet structure. Thus, the full control of the orientation of pHR on gold is distinctly confirmed by SEIRAS.

1C1558 低収量生体分子の時間分解分光計測を目指した新規溶液交換・混合装置の開発

Development of novel rapid buffer-exchange system and microfluidic mixer for time-resolved spectroscopic study of low-yield biomolecules

Tetsunari Kimura[1,2,3], Yuji Furutani[1,2,4] ([1]*Inst. Mol. Sci.*, [2]*Dept. Struct. Mol. Sci., Sokendai*, [3]*CREST/JST*, [4]*PRESTO/JST*)

The real-time observation of structural changes in reacting biomolecules is one of the best approaches to clarify their molecular mechanisms. Rapid buffer-exchange and rapid solution-mixing techniques, which suddenly change the buffer conditions, have been widely used to trigger the reaction. The additional advantage of these techniques is an easy integration into many spectroscopic methods. However, the high consumption of samples has limited their application to low-yield and rare biomolecules. In this presentation, our recent efforts to develop two novel systems, which require much less amount of sample than conventional systems, and our trials to investigate the structural changes of biomolecules, especially membrane proteins, will be reported.
1) Rapid buffer-exchange system combined with ATR-FTIR spectroscopy. Measurements of difference FTIR spectra are very powerful to investigate the structural changes, because only the vibrational modes that are affected by buffer-exchange can be observed. We developed a novel rapid buffer-exchange system, which can exchange buffer within tens of millisecond at slowest, and the structural changes of the samples physically adsorbed on ATR crystal are followed.
2) Microfluidic mixer combined with fluorescence spectroscopy. Laminar-flow fluid mixer composed of tens of micrometer channels is designed and fabricated by using the photolithography and PDMS patterning techniques. The mixer is combined with fluorescence spectroscopy, which is also sensitive to the structure.

1C1610 溶液中の金属タンパク質の共鳴 X 線散乱法の開発

Development of resonant X-ray scattering method of metalloproteins in solutions

Mitsuhiro Hirai[1], Kazuki Takeuchi[1], Ryota Kimura[1], Noboru Ohta[2] ([1]*Grad. Sch. Eng., Gunma Univ.*, [2]*SPring-8*)

Small-angle X-ray scattering technique of solutions is a useful method for observing in-situ structural information of solute particles such as radii of gyration and size distributions by analyzing data sets in small-angle scattering regions. In addition, recent improvements in X-ray beam brightness and detection at third-generation synchrotron sources enables us to obtain high-statistic data with a wide real-space resolution ranging from ~0.2 nm to ~250 nm, even in standard experimental set-ups. Due to such improvements, we successfully discussed about whole hierarchal structures of proteins [1] and lipid aggregates [2] and those transition phenomena in detail.
However, another characteristic of synchrotron sources, namely selectivity of incident X-ray energy, has been rarely used for solution scattering of proteins. Therefore, we have tried to apply resonant (anomalous dispersion) small- and wide-angle X-ray scattering (A-SWAXS) to determine internal structures of metallo-proteins in solutions.
As metallo-proteins, myoglobin (MY) from horse skeletal muscle, hemoglobin (HM) form bovine blood, ferritin from horse spleen, and hen-egg white lysozyme with Hg-atom isomorphous replacements were used. A-SWAXS measurements were performed by using the BL40B2 spectrometer at SPring-8. The detailed results and discussion will be given.
[References]
1. M. Hirai, et al., Thermochimica Acta, 532 (2012) 15.; J. Appl. Cryst., 40 (2007) s184.; Biochemistry, 43 (2004) 9036.
2. T. Onai, and M. Hirai. J. Phys. Conf. Ser., 247 (2010) 012018.

1D1400 マウス ES 細胞分化の単 1 細胞解析

Single-cell-based analysis of differentiation of mouse ES cells

Atsushi Maruyama[1], Yuichi Wakamoto[2,3], Shogo Nakamura[1], Tatsuo Michiue[2], Shin-ichi Sakai[4], Bayar Hexig[4], Toshihiro Akaike[4], **Kiyoshi Ohnuma**[1] ([1]*TRI, Nagaoka Univ of Tech*, [2]*Grad. Sch. Arts. & Sci., Univ. Tokyo*, [3]*Sakigake, JST*, [4]*Grad. Sch. Biosci. & Biotech., Tokyo Inst of Tech*)

A mechanism that provides stability during embryonic development remains to be uncovered. Embryonic stem (ES) cells are a good model for developing such a mechanism because they can be differentiated into all kinds of cells in the body. At the last annual meeting, we reported a system to observe a single-ES cell reaction to culture medium stimulation. The system consists of four parts: Nanog-GFP reporter ES cells, which can be observed cell state by imaging, a culture medium without any unknown factors, a specially coated culture dish that enabled us to dissociate cells without aggregation, and time-lapse microscopy.
In this meeting, we will report the results of single-cell analysis of ES cell differentiation. We monitored life-and-death, proliferation, and differentiation of a single ES cell during differentiation for a few days. We created individual histories or lineage trees to analyze temporal sequences of all reproduction events and phenotypic changes in individual cells. We also performed sibling analysis to compare cell pairs derived from common mother cells. Single-cell level observation of the stimulation response of ES cells will deepen our understanding of developmental stability.

1D1412 顕微ラマン分光法による分化因子刺激後の単一細胞ダイナミクスの計測

Measurements of Single Cell Dynamics upon Stimulation with a Differentiation Factor Using Raman Micro-Spectroscopy

Sota Takanezawa[1,2], Shin-ichi Morita[1], Yukihiro Ozaki[2], Yasushi Sako[1] ([1]*Cellular informatics Lab., RIKEN*, [2]*Grad. Sch. Sci. and Tech., Kwansei Gakuin Univ.*)

Many extracellular factors are known to induce cell differentiation. It is important to note that the response to these factors is variable even among a clonal population of cells. The variance of cellular response could be caused by the difference of cellular states relating to the chemical composition in each cell. A general method for detecting the cellular state is required to understand diversity and individuality of cells in the differentiation pathway. Actually, specific genes, proteins, and metabolic products are used to define the cellular state, but these markers should be pre-determined for each specific case. In this study, we confirmed whether the Raman micro-spectroscopy is effective to detect the state dynamics of single living cells upon stimulation with a differentiation factor. Raman micro-spectroscopy is applicable in a single living cell, and shows several advantages: i) providing information about composition and dynamics of cellular contents, ii) non–destructive and non–labeling analytical technique, iii) the high spatial resolution. MCF–7, a breast cancer cell line, was used for a model cell. MCF-7 is differentiated by heregulin (HRG) into mammalian grand–like cells. The time–course Raman spectra changes were measured in total 56 cells with and without HRG stimulation for 2hr with a 20–min interval. For comprehensive understanding of the time–courses, a principal component analysis (PCA) was carried out. In the result of PCA, dynamics of stimulated cells were more diverse than those without stimulation.

1D1424 1 分子定量計測技術を用いた *C. elegans* 受精卵における細胞極性のモデル化

Quantitative measurement and mathematical modeling of polarity-protein PAR-2 in *C. elegans* embryos

Yukinobu Arata[1], Tetsuya Kobayashi[2], Michio Hiroshima[1], Chan-gi Pack[1], Masashi Tachikawa[3], Kenichi Nakazato[3], Tatsuo Shibata[4], Yasushi Sako[1] ([1]*Cell. Info., ASI, Riken*, [2]*Inst. Ind. Sci., Univ. Tokyo*, [3]*Theo. Biol., ASI, Riken*, [4]*CDB, Riken*)

Cell polarization is a fundamental mechanism for cell migration, cell morphogenesis, and asymmetric cell division in animal development. In asymmetric cell division of *C. elegans* zygote, the asymmetric localization of polarity proteins is developed by a mutual exclusion mechanism through phosphorylation. Despite accumulated molecular knowledge, it remains unknown how intracellular biochemical reaction rates are balanced to maintain asymmetric localization. We succeeded to study dynamics and measure concentration of PAR-2 proteins in living *C. elegans* embryos using total internal reflection microscopy and fluorescence correlation spectroscopy. Cortical PAR-2 proteins were present as a mixture of monomer and oligomer. The abundance ratio of high-degree oligomer increased along the anterior-posterior axis. Combined with our molecular genetics analyses, we conclude that dissociation rate from cortex is regulated through the PAR-2 oligmerization. Next, we determined association rate from cytoplasm to cortex. The association rate was higher in the posterior cortical region where cortical PAR protein accumulated, suggesting that the association rate is under the control by the feedback from cortical PAR-2 proteins. Using reaction-diffusion model determined by experimentally-obtained parameters, we reproduced asymmetric localization of PAR-2 proteins in silico. In this conference, I will talk about novel molecular mechanisms and results of model analysis for cell polarization.

1D1436 形態形成中の組織の力学場を推定する

Estimating forces in the growing epithelial tissues

Shuji Ishihara[1,2], Kaoru Sugimura[3,4] ([1]*Grad. Sch. Arts & Sciences, Univ. Tokyo*, [2]*JST PRESTO*, [3]*iCeMS, Kyoto Univ.*, [4]*RIKEN BSI*)

How do mechanical forces trigger a series of deformations to shape an adult body during morphogenesis? Though recent studies have clarified how geometrical changes of cells are coordinated via the activity and/or localization of force-generating molecular machineries within a cell, comprehensive understandings of how global balance of forces control the tissue deformation has been still elusive. One reason is lack of direct and noninvasive measurement to quantify the forces in the cell population inside the animal body. In this study, we developed a theoretical framework for estimating the pressure of each cell, the tension of each cell adhesion surface and stress tensor of a group of cells, by adopting Bayesian scheme of inverse problem. Responses to laser cutting and myosin distribution agreed with the estimated tensions. By applying our method for growing Drosophila wing, we studied how myosin-mediated cell surface tensions resist against external stretching forces. Further, we showed how arising balance of forces in the tissue drives hexagonal cell packing that is responsible for stable structure of the wing. Our force estimation method will become a powerful tool in analyzing how information for orchestrating cellular behaviors during morphogenesis is encoded in distributions of forces within a tissue.

1D1448 ショウジョウバエ形態形成におけるアポトーシスの能動的力学的寄与

Active Mechanical Role of Apoptosis in Tissue Dynamics during Drosophila Morphogenesis

Yusuke Toyama[1,2,3] ([1]*Dep. of Biol. Sci., National University of Singapore*, [2]*Mechanobiology Inst., National University of Singapore*, [3]*Temasek Life Sciences Lab.*)

During the long journey from egg to adult, the number of cells is finely controlled as the cells collect into distinct tissues that undergo patterned

movements to form the adult body. Apoptosis is the process that eliminates cells which are no longer biologically necessary. During the apoptotic process, the dying cell is squeezed out from the tissue by mechanical forces produced within the cell and by forces produced within the neighboring cells. We experimentally demonstrated that the forces that squeezed out the apoptotic cell also contributed to tissue movements during development in Drosophila. This active mechanical role is not classically attributed to apoptosis.

1D1510 A model of cell-division stop for the limb regeneration

Hiroshi Yoshida (*Faculty of Math. Kyushu Univ.*)

Cell-division stop is essential for the limb regeneration. The steepness hypothesis was submitted as a model that explains regulation of the cell-division stop under an assumption of a gradient across cells. The *Dachsous/Fat* heterodimers are now considered to substantiate the steepness hypothesis and to be involved in regeneration in insect legs. Little is, however, known about the way *Dachsous* and *Fat* molecules are distributed during cell division. Extending the steepness hypothesis, we here show that some condition of the distribution ratio provides the cell with cell-division stop, enabling regeneration. We found that the obtained condition provides a molecular-based explanation for a variety of limb regeneration such as distal outgrowth and intercalary regeneration. It has been revealed that the condition can explain several results of experiments using regeneration-dependent RNAi in cricket legs. We anticipate our result to provide a unified view of regeneration based on molecules within the cell.

1D1522 ラット培養神経回路網の長期発達過程における同期活動に関わる機能的分子の探索

Analysis of functional molecules underlying synchronous activity during long-term development of rat cultured neuronal networks

Daisuke Ito[1], Keiko Yokoyama[2], Kazutoshi Gohara[2] ([1]*Fac. Adv. Life Sci., Hokkaido Univ.*, [2]*Fac. Eng., Hokkaido Univ.*)

Synchronous activity is a remarkable phenomenon in the electrical activity of neuronal networks and is thought to be involved in the higher function of the nervous system, such as memory and learning. Studies using multi-electrode arrays (MEAs) have revealed that cultured neuronal networks reconstructed in vitro show synchronized bursts (SBs). However, the molecular mechanisms underlying the generation of SBs during long-term development remain unclear. In order to clarify the mechanisms of this phenomenon at a molecular level, we analyzed the gene expression involved in the changes in network activity. We cultured rat cortical neurons for 1 month, and the spontaneous electrical activity was recorded using MEAs. SBs were observed starting at approximately 2 weeks and the rate increased gradually during the culture periods. Reverse transcription PCR analysis revealed that the housekeeping gene and transcription factor gene creb were found to be consistently expressed during the culture period. However, the immediate early gene arc was not identified at 1-7 days in vitro (DIV), but the expression level increased up to 28 DIV. This increase in the expression of arc resembled the increase in the SB rate. These results suggest that the generation of SBs is correlated with the increase in immediate early gene expression during the culture periods. Based on these preliminary results, we have begun to quantify the expression level of arc and investigate the expression of other genes and proteins involved in network activity.

1D1534 モノアラガイの長期記憶におけるインスリンとグルコースの役割

Insulin and glucose for memory in a snail

Etsuro Ito[1], Ryuichi Okada[1], Mika Morikawa[1], Satoshi Takigami[2], Akiko Okuta[3], Manabu Sakakibara[2] ([1]*Kagawa School of Pharmaceutical Sciences, Tokushima Bunri University*, [2]*School of High-Technology for Human Welfare, Tokai University*, [3]*Graduate School of Science, Kyoto University*)

The pond snail *Lymnaea stagnalis* is capable of learning taste aversion and consolidating this learning into long-term memory (LTM) that is called conditioned taste aversion (CTA). First, we examined the role of insulin in the LTM formation of CTA. When we applied insulin to the brain, we observed a long-term change in synaptic efficacy (i. e., enhancement) of the synaptic connection between some neurons. This synaptic enhancement was blocked by application of an insulin receptor antibody to the brain. Injection of the insulin receptor antibody into the snail before CTA training, while not blocking the acquisition of taste aversion learning, blocked the memory consolidation process, thus LTM was not observed. Second, we examined the relationship among learning ability, starvation period and hemolymph glucose concentration, and tested the effect of insulin on the learning score. One-day mild starvation improves the learning score and keeps good LTM. When we injected glucose into the abdominal cavity of mild starved snails for a short period, the snails showed worse scores than the case of no injection. Further, when insulin was injected into snails with a complete bellyful of food, the glucose concentration decreased and the learning score and LTM were improved. These results showed that learning ability depends on the starvation period and the glucose concentration and that learning ability must be controlled by manipulation of glucose concentration and injection of insulin in CTA learning of *Lymnaea*.

1D1546 光捕捉された神経細胞内シナプス小胞群の集合ダイナミクス

Assembling dynamics of optically trapped synaptic vesicles in neuronal cell

Yusuke Ueda[1,2], Suguru N. Kudoh[2], Takahisa Taguchi[1], Chie Hosokawa[1,2] ([1]*Health Res. Inst., AIST*, [2]*Grad. Sci. Eng., Kwansei Gakuin Univ.*)

The turnover of synaptic vesicles in presynaptic terminals of neurons is essential for information processing within the brain. For aiming artificial control toward modulating the synaptic transmission in a neuronal network with optical tweezers, we investigated assembling dynamics of optically trapped synaptic vesicles in neuronal cells by fluorescence analysis. When a 1064-nm trapping laser beam is focused on synapses of a neuronal cell labeled with a fluorescent endocytic marker, the fluorescence intensity increased gradually with the laser irradiation time, suggesting that optical trapping force causes vesicles assembly at the focus. The synaptic vesicle dynamics in an optical trap was evaluated by fluorescence correlation spectroscopy. The decay time of fluorescence autocorrelation curves increased with the trapping laser power and the laser irradiation time, indicating that vesicle motion was restrained at the focus due to optical trapping force. Moreover, the decay time of autocorrelation curves was decreased after applying the phosphatase inhibitor okadaic acid causes vesicles to diffuse freely and the degree of decrement was related to the trapping laser power, which will be presented and discussed.

1D1558 膜電位感受性色素・カルシウムイメージングに使える新しい超高速共焦点顕微鏡の開発

A new class of confocal microscope for a fast voltage-sensitive dye (VSD) and Ca^{2+} imaging

Takashi Tominaga, Yoko Tominaga (*Dept. Neurophysiol., Kagawa Sch Pharm Sci, Tokushima Buniri Univ*)

Monitoring neuronal activities using imaging devices is central to our understanding of brain microcircuit functions. Recent progresses in imaging devices together with the rapidness of VSD response have allowed us to follow the sub-millisecond timescale of neuronal activities by VSD imaging. Confocal microscopy provides a more efficient S/N ratio in terms of spatial resolution and thus could be used to obtain better S/N ratios from the VSD signal. However, sampling rates have been difficult to achieve in millisecond timescales. Here we describe the basic configuration of a new no-scanning type of confocal microcopy designed for VSD imaging. The confocal optics was designed to fit a standard camera adaptor of an eqi-fluorescent microscope (e. g., BX51WI, Olympus). The images of the subject placed under the objective lens (20x/0.95, Olympus) were projected onto a 100 × 100 pinhole array placed at a conjugation point. An excitation light reflected by a standard mirror unit was projected onto the pinhole array and illuminated onto the subject. Fluorescence emitted from the subject was then converted into an image using the MOS-type 100 × 100 pixel imager (MiCAM Ultima, Brainvision). The pinhole array and pixel imager correspond with each other in terms of pixels. Since the pinhole array is at a fixed position, there are no mechanical disturbances. We tested the microscope by imaging a rat hippocampal slice preparation by bulk and single cell VSD staining of the slices, and bulk staining with a Ca^{2+} indicator.

1D1610 De novo アセンブルによる軟体動物脳の全トランスクリプトーム解析

De novo sequencing and transcriptome analysis of the molluscan brain by deep RNA sequencing

Hisayo Sadamoto[1], Hironobu Takahashi[2], Taketo Okada[1], Hiromichi Kenmoku[2], Yoshinori Asakawa[2] ([1]*Facul. Pharmaceut. Sci. Kagawa Camp, Univ. Tokushima Bunri*, [2]*Inst. Pharmacognosy, Univ. Tokushima Bunri*)

The pond snail *Lymnaea stagnalis* is among several mollusc species that have been well investigated due to the simplicity of their nervous systems and large

identifiable neurons. Nonetheless, despite the continued attention given to the physiological characteristics of its nervous system, the genetic information of the *Lymnaea* central nervous system (CNS) has not yet been fully explored. The absence of genetic information is a large disadvantage for transcriptome sequencing because it makes transcriptome assembly difficult. We here performed transcriptome sequencing for *Lymnaea* CNS using an Illumina Genome Analyzer IIx platform and obtained 81.9 M of 100 base pair (bp) single end reads. For *de novo* assembly, five programs were used: ABySS, Velvet, OASES, Trinity and Rnnotator. Based on a comparison of the assemblies, we chose the Rnnotator dataset for the following blast searches and gene ontology analyses. The present dataset, 116, 355 contigs of *Lymnaea* transcriptome shotgun assembly (TSA), contained longer sequences and was much larger compared to the previously reported *Lymnaea* expression sequence tag (EST) established by classical Sanger sequencing. The TSA sequences were subjected to blast analyses against several protein databases and other molluscan EST data. As a result, the richness of the present TSA data allowed us to identify a large number of new transcripts in *Lymnaea* and molluscan species.

1E1400 分子動力学シミュレーションによる Hsp90 と ADP の結合自由エネルギープロファイル

Free energy profile for binding of ADP to Hsp90 with molecular dynamics simulation

Kazutomo Kawaguchi, Hiroyuki Takagi, Masashi Iwayama, Megumi Nishimura, Hiroaki Saito, Hidemi Nagao (*Inst. Sci. Eng., Kanazawa Univ.*)

Binding of a ligand molecule to a protein plays a key role in the function of many proteins. The functional cycle of proteins is driven by the binding of some of the ligand molecules, and is inhibited by the binding of some of the other ligand molecules. Hsp90 (Heat Shock Protein 90) is one of a group of molecular chaperones required for protein folding, maturation and trafficking of client proteins. Recent studies have shown that Hsp90 is associated with many pathologies: cancer, virus infectious diseases, protein folding disorders and neurological diseases. Hsp90 is an attractive target for the therapies of many pathologies. The functional cycle of Hsp90 is driven by ATP binding and hydrolysis to ADP. However, the processes of binding and hydrolysis of ATP and dissociation of ADP are not revealed at atomic resolution. The purpose of our study is to elucidate the free energy profile for binding of ADP to Hsp90. We performed all-atom molecular dynamics (MD) simulations of Hsp90 with ADP. The initial structure used in our simulations is the X-ray crystallographic structure of the N-terminal domain of human Hsp90 in complex with ADP (PDB code: 1byq). We calculated the free energy profile for binding of ADP to Hsp90 using the thermodynamic integration method. We will report the results of the free energy calculation.

1E1412 シャペロニン空洞内の変性タンパク質が受けるコンフォメーション制限

The conformational restriction of denatured protein encapsulated in the chaperonin cage

Fumihiro Motojima, Yuko Motojima-Miyazaki, Masasuke Yoshida (*Kyoto Sangyo Univ.*)

Chaperonin assists protein folding in its closed cage. Recently, in addition to the isolation of protein into the cage to reduce a risk of aggregation, it has been proposed that the folding rate of denatured protein is accelerated by the restriction of conformational space in the cage. Hartl's group suggested that the formation of disulfide-bond in the slow folding mutant of maltose binding protein (DMMBP) resulting in more rapid folding as wild-type MBP mimics the conformational restriction in the chaperonin cage. However, on the contrary, our recent results showed that denatured protein encapsulated in the cage is not completely isolated and can even escape out of the cage.

In the last meeting, we reported that blue fluorescence protein starts its folding from more unfolded state than its spontaneous folding, using FRET to observe its conformational change. Here, we applied same technique to maltose binding protein (MBP) and its slow folding mutant (DMMBP). If Hartl's notion is true, the distance between cysteine residues of MBP that used for disulfide-bond formation should be smaller than that of DMMBP. However, their distance changes during folding are almost same. Therefore, the folding acceleration of DMMBP in the chaperonin cage is not caused by disulfide-bond-like conformational restriction, and thus our proposition of unfolding effect in the cage is more probable. We will report the comprehensive study of the conformational effect in the chaperonin cage on MBP and DMMBP at this session.

1E1424 小角 X 線散乱によるアミロイド線維形成の初期会合プロセスの解析

Investigation of initial assembling process of fibrillation by small angle X-ray scattering

Eri Chatani[1], Rintaro Inoue[2], Koji Nishida[2], Toshiji Kanaya[2], Masahide Yamamoto[3] ([1]*Dept. Chem., Grad. Sch. Sci., Kobe Univ.*, [2]*Inst. Chem. Res., Kyoto Univ.*, [3]*Kyoto Univ.*)

Amyloid fibrils are supramolecular assemblies associated with many degenerative diseases including Alzheimer's, prion, and Huntington's diseases. It has been proposed that several smaller aggregates such as oligomers and protofibrils are involved in the fibrillation process, but little is known about a detailed picture how these species contribute to form the mature amyloid fibrils with a rigid cross-β structure. To explore this issue, we have performed time-resolved small angle X-ray scattering (SAXS) measurements of insulin fibrillation combined with analyses of thioflavin T fluorescence and secondary structure. The SAXS data were monitored every 9 seconds immediately after the initiation of fibrillation reaction inside a quartz cell.

As a result, we have found that insulin molecules transform into a characteristic oligomeric structure in the very early stage of lag phase. After the accumulation of oligomers, the scattering curves further increased, implying the assembling process of oligomers into mature fibrils. Interestingly, a distinct type of oligomers in terms of size, cross-β content, and thioflavin T fluorescence intensity was observed when fibrillation reaction was performed at a high salt concentration, suggesting the presence of diverse oligomeric structures that may contribute to a variety of fibrillation pathways and furthermore, the manifestation of polymorphism of mature amyloid fibrils.

1E1436 Distinguishing crystal-like amyloid fibrils and glass-like amorphous aggregates from their kinetics of formation

Yuichi Yoshimura[1], Yuxi Lin[1], Hisashi Yagi[1], Young-Ho Lee[1], Hiroki Kitayama[1], Kazumasa Sakurai[1], Masatomo So[1], Hirotsugu Ogi[2], Hironobu Naiki[3], Yuji Goto[1] ([1]*Inst. Protein Res., Osaka Univ.*, [2]*Grad. Sch. Eng. Sci., Osaka Univ.*, [3]*Fac. Med. Sci., Univ. Fukui*)

Amyloid fibrils and amorphous aggregates are two types of aberrant aggregates associated with protein misfolding diseases. Although they differ in morphology, the two forms are often treated indiscriminately. β2-Microglobulin (β2m), a protein responsible for dialysis-related amyloidosis, forms amyloid fibrils or amorphous aggregates depending on the NaCl concentration at pH 2.5. We compared the kinetics of their formation, which was monitored by measuring thioflavin T (ThT) fluorescence, light scattering, and 8-anilino-1-naphthalenesulfonate (ANS) fluorescence. ThT fluorescence specifically monitors amyloid fibrillation, whereas light scattering and ANS fluorescence monitor both amyloid fibrillation and amorphous aggregation. The amyloid fibrils formed via a nucleation-dependent mechanism in a supersaturated solution, analogous to crystallization. The lag phase of fibrillation was reduced upon agitation with stirring or ultrasonic irradiation, and disappeared by seeding with preformed fibrils. In contrast, the glass-like amorphous aggregates formed rapidly without a lag phase. Neither agitation nor stirring accelerated the amorphous aggregation. Thus, by monitoring the kinetics, we can distinguish between crystal-like amyloid fibrils and glass-like amorphous aggregates. Solubility and supersaturation will be key factors for further understanding the aberrant aggregation of proteins.

1E1448 細胞濃度に近い無添加細胞抽出液の調製

A method to prepare cell extract near intracellular concentration without additional salts and buffers

Kei Fujiwara, Shin-ichiro M. Nomura (*Dept. Biorobot., Tohoku Univ.*)

For the aim to elucidate essential processes for synthesizing cells, we have established a method to prepare additive-free cell extract having high concentration like cells. At first, essentiality of buffers and salts for preparing functional cell-free translation extract was verified. Exponential growth cells of *Escherichia coli* were washed with double distilled water (DDW) at twice, and were dissolved with DDW. After freezing, the cells were disrupted by sonication. S30 fraction of the obtained cell extract (DDW-S30) showed sufficient activity for cell-free protein production of GFP and luciferase.

Next, a gradual evaporating method to accumulate biological components has been established. Here, we used vacuum desiccator to accumulate samples. Total volume decreased 20 μl per hour on average, and 4.5-fold concentration of BSA was obtained thorough the methods. The methods also achieved

accumulation of GFP, alkaline phosphatase (PAP), and diluted PURE system with active forms. Especially, accumulation rate of PAP reached 25-fold. The methods also succeeded to accumulate DDW-S30. The accumulated DDW-S30 showed 180 mg/ml protein concentration, which expected to contain ca. 260 mg/ml of macromolecules, and showed equivalent activity of cell-free protein production to the DDW-S30 before accumulation. Such an accumulated DDW-S30 has a potential to be a material for revealing the difference between cells and materials, and is expected to contribute synthesizing cells from cell extract in future.

1E1510 TMAO による分子クラウディング環境への蛋白質移相自由エネルギーの三次元描像

Three-Dimensional Imaging of the Protein Transfer Free Energy into the Molecular Crowding Condition with TMAO

Isseki Yu[1], Kyoko Nakada[1], Masataka Nagaoka[2] ([1]*Dep. of Cem. and Biol. Sci. Aoyama Gakuin Univ.*, [2]*Grad. School of Info. Sci., Nagoya Univ.*)

Some of the living organisms in the extreme environments contain various organic cosolvents (osmolytes) in their cells. These osmolytes protect the conformation and the function of biomolecules from environmental stresses, such as high temperature or high pressure.
In this study, cytoplasmic conditions of the extremophiles were mimicked by aqueous solution of 2.2M TMAO (trymethilamine N-oxide: osmolyte found in deep sea fishes). The volume fraction of the TMAO as crowder was set to mimic the typical molecular crowding condition in the cytoplasm. Under such conditions, transfer free energy (TFE: the change in Gibbs energy of the solute when it transfers from the solvent phase into a different phase) of apomyoglobin were calculated by Kirkwood-Buff (KB) theory using the atomic configurations of the solvent molecules generated by MD simulations. The simulated TFE and the preferential interaction parameter correlated favorably with experimental values.
Furthermore, 3-dimensional distribution of the TFE were revealed with our developed space-time deconvolution techniques of the KB integrals. The results indicated that the positive TFE regions have planer shapes, and are continuously distributed along the surface of protein. In contrast, the negative TFE regions have spherical shapes and are scattered mainly around the side-chains [1]. The correlation between TFE distribution and the chemical or geometric property of the protein surface will be discussed.
[1] Yu, I; Nakada, K.; Nagaoka, M., J. Phys. Chem. B, 2012, 116, 4080-4088.

1E1522 シトクロム *c* に対する尿素効果の自由エネルギー解析

Free-energy analysis of urea effect on cytochrome *c*

Yasuhito Karino, Nobuyuki Matubayasi (*Inst. Chem. Res., Kyoto Univ.*)

Urea is a widely used denaturant for protein. The mechanism of the denaturation has not been clearly determined though its effect has been discussed in both experimental and theoretical studies. At the moment, the driving force of denaturation is explained by the following two mechanisms. One is the direct mechanism. In the direct mechanism, the denaturation is caused by the direct interaction between protein and urea. Urea is considered to interact with hydrophilic residues and backbone via the electrostatic interactions, and with large, heavy residues via the van der Waals interactions. The other is the indirect mechanism. In the indirect mechanism, urea disturbs the water structure such as hydrogen bonding, and the hydrophobic core is exposed to the solvent. The calculation of salvation free energy may provide a key for elucidating the urea effect if the contributions of water and urea are obtained individually. In this study, we calculated the solvation free energies of cytochrome *c* immersed in pure water and that in urea solution by using the molecular dynamics simulation coupled with the method of energy representation. The transfer free energy is always negative, and the transfer free energy from pure water to urea solution is found to be strongly correlated to the van der Waals interaction between solute and solvent molecules. The result supports the “direct” mechanism and the dominance of the van der Waals interaction in the urea effect on protein.

1E1534 タンパク質の水和水の水素結合ダイナミクスとタンパク質ダイナミクスとの動的カップリング

Kinetics of hydrogen-bonding of protein hydration water and its dynamical coupling with protein dynamics

Hiroshi Nakagawa[1], Mikio Kataoka[1,2] ([1]*Japan Atomic Energy Agency, Quantum Beam Science Directorate*, [2]*Nara Institute of Science and Technology, Graduate School of Materials Science*)

Unique physical properties of water are originated from the hydrogen bond. The hydrogen bond determines the spatial network patterns and water dynamics. Hydration water around the molecules, such as ions, polymers and bio-molecules, has quite different physical properties from bulk water. The protein hydration affects the biological function of the protein. Here, by using the molecular dynamics simulation, we show that the hydrogen bond kinetics of the protein hydration water is strongly affected by the local bonding patterns near the tagged hydrogen bond and that percolation of hydration water on the protein surface essentially determines the cooperative hydrogen bond forming and breaking dynamics. These dynamical characters of hydration water are quite different from those of the bulk water. The hydrogen bond kinetics between hydration water is correlated with the kinetics between the protein and hydration water, suggesting the dynamical coupling between them. The percolation of hydrogen bond network would contribute to the physical properties of protein hydration water. This hydration water dynamics induces the protein dynamical transition observed by neutron inelastic scattering. The dynamical coupling between hydration water and protein should be essential for protein thermal fluctuation and functionality.

1E1546 テラヘルツ時間領域分光を用いた天然および変性状態タンパク質における低振動スペクトルの水和および温度依存性の観測

Temperature and hydration effects of low-frequency spectra of native and denatured proteins studied by terahertz time-domain spectroscopy

Naoki Yamamoto[1], Atsuo Tamura[2], Keisuke Tominaga[1,2] ([1]*Molecular Photoscience Research Center, Kobe University*, [2]*Graduate School of Science, Kobe University*)

Theoretical calculations have shown that in the pico-second region proteins exhibit collective vibrational motions. These modes can be referred as low-frequency modes, since these modes usually appear in several wavenumber regions, or terahertz frequency regions. It is known that these motions are usually well correlated with large conformational changes that are necessary for protein functional expression. Until now a lot of studies focusing on hydration and temperature dependences on protein dynamics have been done by using a large number of spectroscopic methods since these parameters are deeply connected to the protein function. Though it has been proved that “dynamical transition” is universally observed at around 200 K, little is known about the effect of hydration. In this study we measured low-frequency dynamics of native and chemically denatured lysozyme to understand the effect of hydration by using terahertz time-domain spectroscopy. Difference spectra between dried and hydrated states indicate that above the dynamical transition temperature the low-frequency dynamics were activated. In contrast, the differential spectra below the dynamical transition point show complicated features. Below 25 cm^{-1} absorption coefficients of the difference spectra are negative, and above this wavenumber the values increase as the wavenumber increasing. We discuss about the interpretation of these observations and differences between the native and denatured states.

1E1558 誘電緩和分光法によるアルキルカルボン酸の水和特性

Hydration Properties of Alkyl Carboxylate Series by Dielectric Relaxation Spectroscopy

Yangtian Wang, George Mogami, Tetsuichi Wazawa, Nobuyuki Morimoto, Makoto Suzuki (*Grad. Sch. Eng., Tohoku. Univ*)

We measured hydration properties of sodium carboxylate series A: C_nH_{2n+1} COONa (n=1-5), and B: $C_4H_{8-m}(COONa)_m$ (m=2-4) in a low concentration range (<0.09 M) at 20.0 ± 0.01 °C by dielectric relaxation (DR) spectroscopy in the frequency range 0.2-26 GHz. The DR spectra were decomposed into several Debye components and the bulk water component by Hanai mixture theory. Their DR parameters were determined by least fitting. As results, a Debye component with a DR frequency (f_c) of ~18 GHz, which is higher than bulk frequency (17.0 GHz at 20 °C) hence assigned as hyper-mobile water (HMW), and another component with lower f_c (5.3-8.5 GHz) assigned as constrained water (CW) were found around solutes of series B, while only the 5.3-8.5 GHz component (CW) was found around series A. An error propagation analysis assured the resolution of f_c ~0.5 GHz, supporting the existence of these components distinguished from the bulk water component. By fixed volume analysis, we found that: 1) with increasing the length of hydrophobic alkyl group, CW increased while bulk water decreased; 2) with increasing the number of carboxylic group, HMW increased and bulk water decreased. Also, both HMW and CW were found around $HCOON_a$ (0.06M) at 10.0 ± 0.01 °C. In

addition, DR measurements of CH_3COONa at different temperatures (5, 10, 15 and 20 °C) were carried out. The results showed that a decrease of temperature gave rise to an increase of CW. The Gibbs free energy of formation of hydration water and the protonation effect of carboxyl group will be discussed at meeting.

1F1400 サル緑感受性視物質の全反射赤外分光解析

ATR-FTIR study of monkey green-sensitive visual pigment

Kota Katayama[1], Yuji Furutani[1,2], Hiroo Imai[3], Hideki Kandori[1] ([1]*Department of Frontier Materials, Nagoya Institute of Technology*, [2]*Department of Life and Coordination-Complex Molecular Science, Institute for Molecular Science*, [3]*Primate Research Institute, Kyoto University*)

Our color vision is based on three different proteins absorbing blue, green and red lights using the same chromophore, an 11-cis retinal. Because of the difficulty in sample preparation, there have been little structural studies on color visual pigments. We thus started low-temperature FTIR analysis of monkey green (MG) and red (MR) sensitive pigments, from which we revealed important structural differences such as green-specific amide-I vibration, red-specific X-H stretch, and unique protein bound waters1, 2. It is also known that binding of a chloride ion contributes to the spectral red-shift in primate green and red pigments, but no structural studies have been performed. Here we apply attenuated total reflection (ATR) FTIR spectroscopy to MG to gain structural information of the chloride binding site. MG proteins are attached to the ATR cell, and difference FTIR spectra are measured between two anions among Cl^-, Br^-, NO_3^- and I^- at room temperature. The Cl^- minus Br^- difference spectra coincide with the baseline, which is entirely different from those of a light-driven chloride pump halorhodopsin. In contrast, clear difference spectra are obtained between Cl^- and I^-, or Cl^- and NO_3^-. Isotope shift for $^{15}NO_3^-$ implies direct nitrate binding to MG, and chloride binding accompanies formation of β-sheet and protonation of a carboxylate. We propose a model for the chloride binding site on the basis of the present results.

[1] Katayama et al. *Angew. Chem. Int. Ed.* 49, 891 (2010).
[2] Katayama et al. *Biochemistry* 51, 1126 (2012).

1F1412 精製したタコロドプシンの SAXS 測定

SAXS measurements of purified octopus rhodopsin

Shingo Watanabe[1], Mitsuhiro Hirai[2], Tatsuo Iwasa[1,3] ([1]*CEDAR, Muroran IT*, [2]*Grad. Sch. Eng., Gunma Univ.*, [3]*Grad. Sch. Eng., Muroran IT*)

Photo-activated rhodopsin (Rh) couples with G-protein, triggers an enzymatic cascade and finally causes the depolarization of an invertebrate photoreceptor cell. In order to investigate the photo-induced conformational changes of Rh, the SAXS measurements were performed with solubilized octopus microvillar (MV) membrane last year and showed that the irradiation of the sample with blue light caused an increase in the particle size. In the present study, we performed SAXS measurements using purified octopus Rh to survey the origin of the change in the particle size. Rhodopsin purified by conA-sepharose column was irradiated with blue light (510 nm) to convert it into acid meta-Rh. The acid meta-Rh was then reverted to Rh by orange light irradiation (>560 nm). The gyration radii of the purified Rh, that of blue light irradiated products (acid meta-Rh), and that of the further orange light irradiated products (reverted Rh) were the same within the experimental error, about ca. 40 Å. The size was smaller than that estimated from the solubilized MV experiment. The results suggest that the increase in the particle size observed with solubilized MV may be resulted from the presence of the other proteins.

1F1424 ナノディスク試料を用いたロドプシンと錐体視物質によるトランスデューシン活性化効率の比較解析

Comparative analysis of transducin activation by rhodopsin and cone pigments in nanodiscs

Keiichi Kojima, Ryo Maeda, Yasushi Imamoto, Takahiro Yamashita, Yoshinori Shichida (*Dept. Biophys., Grad. Sch. Sci., Kyoto Univ.*)

Most vertebrate eyes have two types of photoreceptor cells, rods and cones. Both cells have similar phototransduction systems, but cones show faster and less sensitive photoresponses, suggesting that the photoresponses are characterized by the different molecular properties of functional proteins between these cells. In order to elucidate the difference in responses, we focused on the activation process of transducin (Gt) by photoactivated rhodopsin and cone pigment, which is the first step of signal transduction cascades and likely to directly affect the signal amplifications. In the previous works, we investigated them by using the detergent-solubilized pigments. However, detergent possibly affects the interaction between photoactivated pigments and Gt. In this study, we prepared nanodiscs containing bovine rhodopsin and chicken green-sensitive cone pigment to conduct the spectroscopic measurement in the detergent-free system. We have reported that the photobleaching processes of rhodopsin and chicken green in nanodiscs were similar to those in the membrane unlike those in detergent (Kojima et al., Annual Meeting of Biophysical Society of Japan, 2011). We first showed that total amount of activated Gt by photobleached rhodopsin was much greater than that by chicken green. On the other hand, the initial rate of Gt activation by rhodopsin was only a little greater. Based on these results, we will discuss the difference in Gt activation by rhodopsin and cone pigments, and its contribution to the natures of photoreceptor cells.

1F1436 脊椎動物非視覚オプシン Opn5 とその類似光受容タンパク質の分子的性質の解析

Analysis of the molecular properties of vertebrate non-visual opsins, Opn5 and Opn5-like protein

Takahiro Yamashita[1], Hideyo Ohuchi[2], Sayuri Tomonari[3], Sari Fujita-Yanagibayashi[1], Kazumi Sakai[1], Sumihare Noji[3], Yoshinori Shichida[1] ([1]*Grad. Sch. Sci., Kyoto Univ.*, [2]*Grad. Sch. Med. Dent. Pharm. Sci., Okayama Univ.*, [3]*Inst. Technol. Sci., Univ. Tokushima Grad.Sch.*)

Opsins are the universal photoreceptive molecules that underlie the molecular basis of visual and non-visual photoreceptions in animals and are classified into seven distinct groups based on their amino acid sequences. Opn5 (neuropsin) was first identified in mouse and human genomes and was found to be expressed in retina and brain. However, there was little information about the molecular properties and the physiological functions of Opn5.

Vertebrate Opn5 genes are diversified into three subtypes. Most mammals have only one Opn5 gene, Opn5m, and many non-mammalian vertebrates have additional two subtypes, Opn5-like1 and -like2 (L1 and L2). We previously revealed that chicken Opn5m is sensitive to UV light and functions as a Gi-coupled receptor. The distribution of Opn5m in the retina, pineal gland and paraventricular organ of the hypothalamus was detected by the specific antibody. Thus Opn5m is related with multiple photoreceptions in chicken [1]. Recently, we successfully obtained the active protein of chicken Opn5L2 and found that Opn5L2 also works as a Gi-coupled UV-sensitive opsin. In addition, we detected the expression of Opn5L2 within the retina, brain, and, unexpectedly, adrenal gland of chicken [2]. Based on the analyses of chicken Opn5 proteins, we discuss the relationship between the molecular properties and the physiological function of Opn5.

[1] Yamashita et al., (2010) PNAS 107, 22084-22089. [2] Ohuchi et al, (2012) PLoS One 7, e31534.

1F1448 グロイオバクターロドプシンの光反応ダイナミクスの分光研究

Spectroscopic study of photoreaction dynamics of *Groeobacter* rhodopsin

Kumiko Nagata, Keiichi Inoue, Hideki Kandori (*Nagoya Inst. Of Technol.*)

Groeobacter rhodopsin (GR) is a member of microbial rhodopsins found in the genome of cyanobacterium PCC7421. GR pumps protons like bacteriorhodopsin (BR) and proteorhodopsin (PR), but the detailed pumping mechanism and structural changes during the photocycle are not well understood. Therefore, we started studying the dynamics of structural change of GR. Here we conducted transient absorption (TA) and transient grating (TG) measurements of GR. GR proteins were expressed in *E. coli*, and TA and TG methods were applied to the purified proteins in detergent. TG measurements showed that GR and the O intermediate form trimer at 300 mM NaCl conditions, while a portion of the O intermediates has larger volume than the others. TG signals were dramatically changed at higher salt conditions such as 4 M NaCl. First, a new component was found after the production of the O intermediate, which was assigned as the component to proton uptake. We performed the quantitative TG measurements and determined $\Phi \Delta V_{H+} = 36$ cm^3/mol. At 4 M NaCl, diffusion rate of the O intermediate was slower than that of GR, indicating that large conformational changes occur in the O intermediate. From the diffusion coefficient, we estimated the size of the oligomer to be about 7 molecules. The results of gel filtration chromatography and circular dichroism (CD) analysis were consistent with those of TG. The observed large conformational changes in the O intermediate will be discussed in relation to the proton-pumping function.

1F1510 ASR の Pro206 はレチナール構造と光反応を制御する

Pro206 of Anabaena sensory rhodopsin is responsible for the isomeric composition of retinal and photochromism

Yoshitaka Kato[1], Akira Kawanabe[2], Kwang-Hwan Jung[3], Hideki Kandori[1] ([1]*Grad. Sch. Eng., Nagoya Inst. Tech.*, [2]*Grad. Sch. Med., Osaka Univ.*, [3]*Sogang Univ. Korea*)

Anabaena Sensory Rhodopsin (ASR) is a microbial rhodopsin found in *Anabaena* (*Nostoc*) sp. PCC7120, a freshwater cyanobacterium. ASR is believed to function as a photochromism sensor. Microbial rhodopsins possess all-trans and 13-cis retinal as the chromophore, but only the former is important for function. In bacteriorhodopsin (BR), the stable photoproduct at the end of the functional cycle of the all-trans form is 100% all-trans. Nevertheless, we found that the photoreaction of ASR is completely photochromic; the stable photoproduct of the all-trans form is 100% 13-cis, and that of the 13-cis form is 100% all-trans [1]. It is intriguing that BR and ASR exhibit similar protein architecture, but photoreactions are entirely different.

One of key amino acids may be Pro206 of ASR, because the corresponding amino acid of other microbial rhodopsins is Asp (Asp212 in BR). In the present study, we replaced Pro206 of ASR into 19 amino acids and examined their moleculer properties. Interestingly, all mutants were properly expressed and folded, including P206R and P206K. HPLC analysis shows that the isomeric composition between all-trans and 13-cis forms is highly amino-acid dependent, and some mutants contain 9-cis and 11-cis forms under light conditions. P206D contains 13-cis retinal dominantly under both dark and light conditions. We thus conclude that Pro206 is a responsible residue for the photochromic reaction in ASR, and the mechanism will be discussed.

[1] Kawanabe et al. *J. Am. Chem. Soc. 129,* 8644 (2007).

1F1522 Large deformation of helix F upon formation of the M intermediate of the azide-bound purple form of pharaonis halorhodopsin

Taichi Nakanishi[1], Soun Kanada[1], Midori Murakami[1], Kunio Ihara[2], Tsutomu Kouyama[1] ([1]*Grad. Sch, Sci., Univ. Nagoya*, [2]*Center for Gene Research., Univ. Nagoya*)

Halorhodopsin(HR) utilizes light energy to transport chloride ions from the extracellular side to the cytoplasmic side. When the chloride ion bound to the active site is replaced with an azide ion, it acquires the ability to transport protons. To clarify this proton pumping mechanism, we investigated light-induced structural changes in pharaonis halorhodopsin (pHR) using the C2 crystal that was prepared in the presence of chloride ion. When the C2 crystal was soaked in a solution containing azide ion, the chloride ion and one water molecule in a cavity between the Schiff base and Thr126 were replaced with an azide ion. When the azide-bound purple form of pHR was exposed to orange light, an M-like yellow species containing 13-cis retinal was generated efficiently in one of the three subunits in the asymmetric unit. This subunit has the EF loop facing a free space, so that a profound outward movement of the cytoplasmic half of helix F was induced upon formation of the M state. This structural change was accompanied by a large swing of the phenyl ring of Phe259 in helix G, creating a large cavity in the cytoplasmic side of the retinal Schiff base, where a linear cluster of water molecules were incorporated. Simultaneously, the middle moiety of helix C distorted largely, leading to a significant shrinkage of the primary anion binding site (site I). As a result, the azide ion that was initially located in site I was forced to move to a large cavity created by a flip-flop motion of the side chain of Glu234 in the anion uptake channel.

1F1534 センサリーロドプシン II-トランスデューサー複合体の比較シミュレーションにより明らかにされた基底状態と M 中間体の差異

Differences between the ground state and the M-intermediate of Sensory Rhodopsin II-Transducer complex revealed by comparative simulations

Koro Nishikata[1,3], Mitsunori Ikeguchi[1], Akinori Kidera[1,2] ([1]*Grad. Sch. of Nanobioscience, Yokohama City Univ.*, [2]*Research Program for Computational Science, RIKEN*, [3]*Bioinformatics And Systems Engineering division (BASE), RIKEN*)

The complex of sensory rhodopsin II (SRII) and its cognate transducer HtrII (SRII:HtrII/2:2) is a photosensor associated with negative phototaxis in extreme halophiles. To examine how photoexcitation of SRII influences the overall structure of the complex, we performed comparative molecular dynamics simulations of the complex of SRII and truncated HtrII (residues: 1-136) from *N. pharaonis* of two photochemical states, the ground state and the M-intermediate, in explicit solvent and lipid bilayer. The simulation systems consist of each crystal structure appended with the models of the missing residues and the N-terminal HAMP domain. The simulation results showed significant increases in the structural differences compared to the two crystal structures: the outward bending motions of F-helix of SRII and the rotation of the C-terminal region of TM2 helix. The most remarkable change was found in the overall orientation of the two SRII molecules: the cytoplasmic side was closed in the ground state and open in the M-intermediate. This change was attributed to the differences in the side-chain packing of the 4-helix bundle of the HtrII dimmer. We will discuss the results in detail with additional simulations of the complex without the HAMP domain. Finally, we will propose a hypothesis for the signal transduction mechanism of SRII-HtrII system.

1F1546 Effect of potential on the photo reaction of Sensory rhodopsin II monolayer studied by Surface Enhanced IR absorption Spectroscopy

Kenichi Ataka, Joachim Heberle (*Freie Universitaet Berlin, Fachbereich Physik*)

Membrane potential is one of important factors that set out the function of many membrane proteins. Although an importance of this factor is widely accepted, experimental method that can access directly to the effect is limited. Here, we introduce a method tackling this problem, in which exploit a membrane protein monolayer tethered on a metal solid-support and surface enhanced infrared absorption spectroscopy (SEIRAS). To reproduce highly orientated protein layer as mimic of the cellular membrane, we employed a tactic that the membrane protein bind through recombinant histidine tags with Ni-NTA self-assembled monolayer modified solid support. After orientated binding of the protein to the surface, full functional integrity is regained by embedding into a lipid layer. SEIRAS provides specific enhancement of the signal from the tethered membrane protein, in which is difficult to detect by conventional IR technique due to a scarce amount of monolayer as few as pico-mol/cm2. Advantage of SEIRAS becomes most beneficial when the functional studies of the tethered membrane proteins are performed by the application of external stimuli (light, voltage, chemicals etc.) to initiate the reaction. Functional difference spectroscopy between initial non-active and active state can extract the contributions from functional groups that are involved in the reaction. Application on the study of a photo-cycle reaction of sensory rhodopsin II under potential control will be discussed.

1F1558 In-situ 光照射固体 NMR による光受容膜蛋白質の光活性状態の解明

Light activated states of photoreceptor membrane proteins as revealed by in-situ photo-irradiated solid-state NMR

Akira Naito[1], Yuya Tomonaga[1], Tetsurou Hidaka[1], Yusuke Shibafuji[1], Yoshiteru Makino[1], Izuru Kawamura[1], Yuki Sudo[2], Akimori Wada[3], Takashi Okitsu[3], Naoki Kamo[4] ([1]*Graduate School of Engineering, Yokohama National University*, [2]*Graduate School of Science, Nagoya University*, [3]*Kobe Pharmaceutical University*, [4]*Matsuyama University*)

Pharaonis phoborhodopsin (*pp*R or sensory rhodopsin II) is a negative phototaxis receptor of *Natronomonus* pharaonis and forms a 2:2 complex with the cognate transducer (*p*HtrII), which transmits the photosignal into cytoplasm. Light absorption of *pp*R initiates *trans-cis* photo-isomerization of the retinal chromophore followed by cyclic chemical reaction consisting of several intermediates (K, L, M and O). The M intermediate is thought to be an active state for signal transduction. We have successfully observed the M intermediate by using photo-irradiated solid-state NMR, because the life time of the M-intermediate is much longer than the other intermediates. ^{13}C NMR signal from [20-^{13}C] retinal-*pp*R and *pp*R/*p*HtrII revealed that multiple M-intermediates (M1, M2 and M3) with 13-*cis*, 15-*anti* retinal configurations coexisted under the photo-irradiated condition. Further, since the life time of M3 state was much longer than those of the other M states, the M3 state could be distinguished from the other M states. Carbonyl carbon signals of [1-^{13}C] Tyr174 in ppR also showed that multiple structures coexisted in the protein side. Light induced structural changes were further observed in [3-^{13}C]Ala-*p*HtrII/*pp*R complexes. Particularly, helix structure of the interfacial region in *p*HtrII changed significantly. Detailed structure of photo-intermediate in photo-receptor membrane proteins is now possible to gain insight into the signal transduction mechanism by using in-situ photo-irradiated solid-state NMR.

1G1400 Larger Intercellular Adhesion Strength Generates More Coherent and Directional Multicellular Movement - Measurement and Simulation

Tsuyoshi Hirashima[1], Takanori Iino[2], Yoichiroh Hosokawa[2], Masaharu Nagayama[3,4] ([1]*Anatomy and Developmental Biology, Faculty of Medicine, Kyoto University*, [2]*Graduate School of Materials Science, Nara Institute of Science and Technology*, [3]*Research Institute for Electronic Science, Hokkaido University*, [4]*CREST, Japan Science and Technology Agency*)

Collective cell movement is an essential process in many events of all animals, including wound healing and embryonic development although our understanding of what attributes the emergence of collective cell movement is far from complete. We examined cellular behaviors in a monolayer sheet of a skin cell under culture conditions with different Ca2+ concentration, and observed that the frontal line of sheet moved faster in higher Ca2+ concentration. The particle image velocimetry analysis for the movement of skin cell revealed that the cells in the leading front region moved faster and those in the rear moved slower for the treatment of higher Ca2+ concentration although there were no differences in the average speed of whole cell movement for any Ca2+ treatments. We also found that the movement of cells became more directional with longer spatial correlation in proportional to the treated Ca2+ concentration. To know influences in the cellular level to the variation of treated Ca2+ concentration, we quantitatively measured cellular behaviors such as cell division rate and the strength of intercellular adhesion, and found that the strength of intercellular adhesion more increases in higher Ca2+ concentration. Integrating the quantitative data into a computational model, we reproduced the coherent and directional multi-cellular behavior, indicating that the collective cell behavior of skin cell can be induced only by the strength of intercellular adhesion.

1G1412 GPI アンカー型タンパク質の短寿命ホモダイマーはラフト組織化・機能のための最小単位である

Transient GPI-anchored protein homodimers are units for raft organization and function

Kenichi G. N. Suzuki[1], Rinshi S. Kasai[1], Koichiro M. Hirosawa[1], Yuri L. Nemoto[1], Munenori Ishibashi[1], Yoshihiro Miwa[2], Takahiro K. Fujiwara[1], Akihiro Kusumi[1] ([1]*iCeMS, Kyoto Univ.*, [2]*Dept. Pharmacol., Univ. Tsukuba*)

Advanced single-molecule fluorescent imaging was applied to study the dynamic organization of raft-associated glycosylphosphatidylinositol-anchored protein (GPI-APs) in the plasma membrane and their stimulation-induced changes. In resting cells, virtually all of the GPI-APs are mobile and continually form transient (~200 ms) homodimers through ectodomain protein interactions, stabilized by the presence of the GPI-anchoring chain and cholesterol (termed homodimer rafts). Heterodimers do not form, suggesting a fundamental role for the specific ectodomain protein interaction. Under higher physiological expression conditions, homodimers coalesce to form hetero- and homo-GPI-AP oligomer rafts by raft-based lipid interactions. Upon ligation, CD59 formed stable oligomer rafts, containing up to four CD59 molecules, which triggered intracellular Ca^{2+} responses that were dependent on GPI-anchorage and cholesterol, suggesting a key role played by transient homodimer rafts. Transient homodimer rafts are likely one of the basic units for the organization and function of raft domains containing GPI-APs.

1G1424 ナノ秒パルス高電界は新規細胞ストレスとして作用して翻訳抑制を引き起こす

Nanosecond pulsed electric fields act as a novel cellular stress that induces translational suppression

Ken-ichi Yano, Keiko Morotomi-Yano (*Bioelectrics Res. Center, Kumamoto Univ.*)

Pulsed electric fields (PEFs) of millisecond durations are widely used for DNA electroporation. Recent advances in electrical engineering enable the generation of ultrashort PEFs (nanosecond PEFs, nsPEFs). Contrary to conventional PEFs for DNA electroporation, nsPEFs can directly reach intracellular components without membrane destruction and efficiently induce apoptosis. Although nsPEFs are now recognized as a unique tool in life sciences, the molecular mechanism of nsPEF action remains largely unclear. In this study, we revealed that nsPEFs act as a novel cellular stress. Exposure of HeLa S3 cells to nsPEFs quickly induced eIF2α phosphorylation, which is a common hallmark of stress responses, and elicited concomitant translational suppression. We analyzed upstream stress-responsive kinases and observed that nsPEFs activate PERK and GCN2, but not PKR. Experiments using PERK- and GCN2-knockout cells demonstrated dual contribution of PERK and GCN2 to nsPEF-induced eIF2α phosphorylation. Moreover, nsPEF exposure yielded the elevated GADD34 expression, which is known to function as a negative feedback control for eIF2α phosphorylation. RT-PCR analysis of a set of stress-inducible genes demonstrated that cellular responses to nsPEFs are distinct from those induced by previously known forms of cellular stress, such as ER stress, UV, and heat. Taken together, these results provide new mechanistic insights into nsPEF action and implicate the therapeutic potential of nsPEFs for stress response-associated diseases.

1G1436 弾性膜モデルを用いたゴルジ再集合過程シミュレーション

Simulation study on Golgi reassembly process based on elastic membrane model

Masashi Tachikawa, Atsushi Mochizuki (*Theoretical Biology Laboratory, ASI, RIKEN*)

Golgi apparatus is a cellular organelle which processes proteins, and sorts them for delivery to various destinations. Golgi apparatus shows characteristic shape; a stack of flattened cisternae made of lipid membrane. In the mitotic phase, it disperses into small vesicles, and they reassemble to form the characteristic shape in individual daughter cells. No plausible mechanism has been proposed to explain the characteristic shape.

In this study, we reconstruct a Golgi reassembly process by computer simulations and propose a possible mechanism to produce the characteristic Golgi shape. The relation between local shapes of lipid membrane and its deformation is well characterized by elastic membrane theory. Based on it, we constructed a bio-membrane simulator. An arbitrary shape of membrane surface is approximately represented by a polygon, and the shape deformation is simulated using Monte Carlo method. Effects of membrane-associated molecules, such as deformability change, adhesion and membrane fusion, are also considered.

Without any additional assumption, sponge-like structures are emerged through the simulations. It indicates that the Golgi-like layered structure is not formed by itself. We then considered several assumptions for the occurrence of the membrane fusion, and found that if the fusion occurs only between convex membranes, a Golgi-like layered structure is observed. This fusion modification can be realized when the distribution of fusion-promoting proteins depends on membrane curvature.

1G1448 Analysis of cell behavior near silicon based micro-scale pore

Yo Otsuka[1], Shinya Murakami[1], Manabu Sugimoto[1], Toshiyuki Mitsui[2] ([1]*Grad. Sch. Sci., Aogaku Univ*, [2]*Assoc.Sci., Aogaku Univ*)

The propose of our study is to understand of the cell behavior under various conditions for example, concentration gradients created by silicon based micro-scale pores. In bone remodeling and fracture treatment, recruitment to sites for bone formation of osteoblasts secrete bone matrix is crucial. If we are able to control the cell recruitment, it may be possible to promote the bone formation on specific site. For this recruitment, we have created concentration gradients of certain substances in μm-range by using micro-scale pores milled on a free standing SiN membrane, and analyzed the possible control cell differentiation and behavior. In addition, we have assembled the instrument to culture cell under the microscopy and to observe to analyze cell behavior in real time. By using this instrument, the concentration gradient of FBS induced by the 5 μm diameter pore enhances the Osteoblast motions toward the pore mouth. In this conference, we describe the method to create concentration gradients by using the micro-scale pores and the possibility to control of cell recruitment.

1G1510 重イオンマイクロビーム照射によるバイスタンダー応答で誘導されるシグナル伝達機構の解明

Mechanisms of signal transduction activated by heavy-ion microbeam induced bystander responses

Masanori Tomita[1], Hideki Matsumoto[2], Tomoo Funayama[3], Yuichiro Yokota[3], Kensuke Otsuka[1], Munetoshi Maeda[1,4], Yasuhiko Kobayashi[3] ([1]*Radiat. Safety Res. Cent., CRIEPI*, [2]*Biomed. Imaging Res. Cent., Univ. Fukui*, [3]*QuBS, JAEA*, [4]*R&D, WERC*)

Radiation-induced bystander responses are defined as responses in cells that have not been directly traversed by radiations but are in the neighborhood of cells that have been directly traversed by them. Bystander responses induced by low doses of heavy-ion beams are an important problem in cancer therapy. In

the present study, we aim to clarify the bystander signal transductions activated by heavy-ion microbeam irradiation. After forming 5 colonies, which composed by the targeted colony in center and four untargeted colonies around it, on a dish using normal human fibroblast WI-38 cells, a cell in the targeted colony was irradiated with Ar-ion microbeams. Focus formation of DNA repair proteins was examined in the cells in the untargeted colonies. Next, 5 cells within the confluent culture were irradiated with the Ar-ion microbeams. Phosphorylation of NF-κB in the bystander cells was observed 3 h after irradiation, but was not 6 h. Phosphorylation of Akt was not only observed 3 h but also 6 h after irradiation. On the other hand, accumulation of COX-2 was observed only 6 h after irradiation. In addition, accumulation of COX-2 was not detected in the broadbeam irradiated cells, whereas phosphorylation of NF-κB and Akt were observed. Bystander responses induced by Ar-ion microbeam irradiation were at least partially suppressed by pretreatment with a scavenger of nitric oxide (NO). These results suggested that NF-κB-dependent signaling pathway involving Akt and COX-2 play an important role in the NO-mediated bystander response.

1G1522 出芽酵母の遺伝子発現パターンの変化における染色体揺らぎの影響

Effects of conformational fluctuation of chromosomes in budding yeast on the pattern of gene expression

Naoko Tokuda, Masaki Sasai (*Grad. Sch. Eng., Univ. Nagoya*)

Recently, conformation of all chromosomes in the interphase nucleus of budding yeast has been inferred from the Chromosome Conformation Capture-on-Chip (4C) data (Duan et al., Nature (2010)). However, it has not yet been ascertained how the conformational fluctuation around their mean structures affects the regulation of gene expression. To clarify this issue, we developed a dynamical structural model of interphase chromosomes in budding yeast (Tokuda et al., Biophys. J. (2012)). In the present paper, the effects of the conformational fluctuation on the pattern of gene expression will be examined by using this coarse-grained chromosome model. Specifically, I will discuss the observed difference in the pattern of gene expression between the *yku70 esc1* mutant which abrogates telomere anchoring and the wild-type strain (Taddei et al., Genome Res. (2009)). In the data of Taddei et al., 32 genes are expressed at higher levels and 28 genes are expressed at lower levels in the *yku70 esc1* mutant than in the wild-type strain. We examine the reason of this misregulation by comparing the fluctuation of the chromosome conformation in the case that telomeres are not anchored to the nuclear periphery with that in the anchored case.

1G1534 人工自己複製システムのダーウィン進化

Darwinian Evolution of artificial self-replication system

Norikazu Ichihashi[1,2], Tetsuya Yomo[1,2,3] ([1]*JST ERATO*, [2]*Graduate School of Information Science and Technology, Osaka University*, [3]*Graduate School of Frontier Bioscience, Osaka University*)

Darwinian evolution, the consequence of variation and natural selection, has played a central role in the emergence of the complexity of living organisms. To understand requirements for Darwinian evolution, we have constructed an artificial self-replication system which capable of Darwinian evolution from non-living molecules. We used an RNA encoding an RNA-dependent RNA polymerase as a genetic molecule and mixed it with a reconstituted cell-free translation system. The RNA polymerase was translated from the RNA, and translated polymerase, in turn, replicated the original RNA. During this self-replication process, mutations are spontaneously introduced by replication error. In addition, to link the genotype to the phenotype, we encapsulated the reaction into a micro-scale water-in-oil emulsion.

After about 180 rounds of repeated self-replication, the self-replication activity increased gradually and finally reached 100-fold. Mutations were randomly introduced into RNA, some of which became fixed in the population. The final RNA has higher replication rate and higher competence against parasitic replicator. These result demonstrated that in our system, more self-replicable RNA has evolved as a consequence of spontaneously mutation and natural selection. This artificial self-replication system would be a novel platform to experimentally investigate the possible evolutionary process of complex nature of living organisms

---

1G1546 多点蛍光相関分光を用いた時空間解析によるグルココルチコイド受容体の核移行解析

Nuclear translocation analysis of glucocorticoid receptor by spatiotemporal analysis with multipoint fluorescence correlation spectroscopy

Johtaro Yamamoto, Masataka Kinjo (*Fuc. Adv. Life Sci., Hokkaido Univ.*)

Glucocorticoid receptor (GR) is one of the nuclear receptors that localizes in cytosol without ligand binding. Once the GR binds with their ligand, the GR starts to translocate to nuclear. Finally, the GR binds to DNA as dimers, and regulates transcriptions of various genes. The nuclear translocation property of GR is unclear yet though the dexamethasone, a ligand of GR, is widely used such as steroidal anti-inflammatory drug.

In this work, the nuclear translocation rate of GR was analyzed in living cells using a multipoint fluorescence correlation spectroscopy (MP-FCS) with single molecule sensitivity. The system realizes simultaneous measurement of fluorescence fluctuation emitted from EGFP-GR at up to three dimensionally arbitrary seven points in living cells. The auto-correlation functions of these fluorescence signals provide the concentrations of EGFP-GR and its diffusion constants. In addition, the spatiotemporal cross-correlation functions provide the traveling time of EGFP-GR between two measurement points. Analyzing the correlation functions between a point in cytosol and in nucleus, the nuclear translocation rates of GR were obtained. The result was much slower than the expected result of free diffusion, and this can be considered the result caused by that the nuclear translocation of GR is an energy consuming process. We expect the MP-FCS system can reveal a part of active transport mechanism. In our presentation, we will investigate the effect of some mutation of GR on the nuclear translocation rate.

1G1558 細胞内 FRET イメージングによる情報処理タンパク質 RAF の構造と EGF 応答の相関解析

Correlation between the molecular conformation and EGF response of RAF by FRET imaging in individual cells

Kayo Hibino[1], Masahiro Ueda[1], Yasushi Sako[2] ([1]*RIKEN, QBiC*, [2]*RIKEN, ASI*)

RAS-RAF signaling regulates various cellular responses including proliferation, differentiation, and carcinogenesis. After the stimulation of cells with epidermal growth factor (EGF), the activated RAS recruits RAF from the cytoplasm to the plasma membrane. At the membrane, RAF is activated through phosphorylations by undetermined kinases and signals to downstream. Thus, the redistribution of RAF in ensemble molecules is important in the cell-fate determination, however, this responsiveness to EGF differed in individual cells, even though the cells were synchronized each other by serum starvation and stimulated with the saturation amount of EGF.

By using FRET-based probe of RAF, we found that the EGF response correlated with the ensemble conformation of RAF in individual resting cells. The cells with an open-bias form of RAF responded to EGF and showed the redistributions of RAF remarkably, whereas the cells with closed form of RAF hardly responded to EGF and did not show the redistribution of RAF.

By analyses of RAF with particular phosphorylation status or mutations of phosphorylation-sites, we found that the conformation of RAF in resting cells was modulated by the phosphorylation status of RAF. This result suggests that the phosphorylation status of RAF differs in individual resting cells, which correlates with the EGF response in the RAS-RAF signaling. The phosphorylation status of RAF could be affected by the cellular memory of the past extracellular environment and the intracellular reactions.

1G1610 1 分子キネティクス解析により示された、ヘレギュリンと ErbB タンパク質のダイナミックに変化する相互作用

Interaction between heregulin and ErbB proteins varies dynamically shown by single-molecule kinetic analysis in living cells

Michio Hiroshima[1,2], Yuko Saeki[3], Mariko Okada-Hatakeyama[3], Yasushi Sako[1] ([1]*RIKEN ASI*, [2]*RIKEN QBiC*, [3]*RIKEN RCAI*)

Cell fate of the MCF7 human breast adenocarcinoma cells is determined by the ligand-specific manner. When MCF7 cells are stimulated by epidermal growth factor (EGF) or heregulin (HRG), proliferation or differentiation is induced, respectively. Both EGF and HRG receptors are ErbB receptor tyrosine kinases that transduce ligand signals to the cytoplasmic proteins thorough homo- and hetero-dimerization. The ErbB family proteins consists of four members, ErbB1 to B4, and EGF mainly associates with ErbB1, whereas HRG with B3 and B4. By single-molecule measurement on interactions between dye-conjugated HRG and the receptors in living MCF7 cells, we obtained kinetic parameters of both ligand association and dissociation. The ligand-receptor association pathways of ErbB3/4 were almost the same as that of ErbB1. A receptor predimer accelerated the formation of a doubly-liganded signaling dimer through an intermediate formation between the first and the second HRG bindings. On the

other hand, the first dissociation of HRG from the doubly-liganded dimers was rapid, but the other HRG from the singly-liganded dimers was slow. The dynamic change between the association and dissociation kinetics that produced different affinity sites of HRG on the cell surface lead to concave-up shape of the Scatchard plot. The biphasic kinetics indicated the existence of negative cooperativity in the ligand-receptor interaction and enables the ErbB system to detect the extracellular HRG signals rapidly and sensitively.

1H1400 ラスター画像相互相関分光法（ccRICS）を用いた外来 DNA に対する細胞内防御機構の可視化

Visualization of intracellular defense system against exogenous DNAs by using cross-correlation raster image correlation spectroscopy

Akira Sasaki, Masataka Kinjo (*Fac. Adv. Life Sci., Hokkaido Univ.*)

Gene delivery systems with artificial vectors are widely used in the research field of cell biology and also in the clinical field as gene therapy to promote exogenous gene expression or inhibit production of a target protein. It is presumed that the translocation of transfected DNA to nucleus competes with degradation by cytoplasmic nucleases as the intracellular defense system against exogenous DNAs, such as viral genes. Previously, the size and structure of degraded DNAs were monitored by fluorescence cross-correlation spectroscopy (FCCS) in solution and in the cytoplasm of living cells [1]. The result showed that the exonuclease activity affected the transfection efficiency, and the level of exonuclease activity in cytoplasm was different depending on the cell line. However, such FCCS measured only one point at a time. To overcome this drawback of FCCS measurement, raster image correlation spectroscopy (RICS) and cross-correlation RICS (ccRICS) are employed to investigate when and where nucleases work in living cells. As the probe of DNA degradation, dual fluorescent labeled linear DNA was synthesized. RICS enabled the mapping of degradation state of the DNA probe in living cells. In this report, the proof of principle study of the measurement system by observation of the DNA probe in solution and in living cells will be discussed. This work will contribute in understanding the fate of exogenous DNA, which is critical in development of efficient vectors.

[1] Sasaki A and Kinjo M., *J . Control. Release* 143(1):104-111 (2010)

1H1412 Non-invasive in vivo imaging of vesicle movement in neutrophils in mouse ear

Kenji Kikushima, Sayaka Kita, Hideo Higuchi (*Dept of Phys, School of Science, The Univ. of Tokyo*)

Neutrophils play an essential role in innate immune response. Observation of neutrophil under non-invasive conditions has been an important problem to be solved. Quantum dots (QDs) are semiconductor nanoparticles that show good photostability and strong fluorescence compared to conventional dyes. Here, we succeeded to observe QD-labeled neutrophils in mouse ear under non-invasive conditions up to 100 um below the surface of skin. Neutrophils began to extravasate from blood vessels upon inflammation, and locomote in interstitial space. Most intriguingly, QDs were uptaken into the neutrophils and vesicle movements inside the cells were able to be seen. Movement of these vesicles was tracked at 80 frames/sec with 15 nm accuracy or in 3D space. While vesicles in the neutrophil on the vascular wall did not show any directional movements, vesicles in the neutrophil locomoting in the tissue were transported actively. Movements of these vesicles were independent each other even in the same cell, and some of them underwent as “diffuse-and-go” manner. The speed of the vesicle at “go” phase achieved about 4 um/sec, which was about three times faster than the velocity of a molecular motor such as kinesin or dynein in vitro. The high speed transport of the vesicle should be important for the ability of neutrophil to kill various microbes.

1H1424 脂質二重膜を用いた T 細胞活性化の 1 分子イメージング解析

Single molecule analysis of T cell activation with stimulatory lipid bilayers by live cell imaging

Yuma Ito[1,2], Hirofumi Oyama[1,2], Kumiko Sakata-Sogawa[1,2], Makio Tokunaga[1,2] ([1]*Grad. Sch. Biosci. Biotech., Tokyo Inst. Tech.*, [2]*RCAI, RIKEN*)

T cells are activated when the T cell receptor (TCR) binds to a peptide-MHC complex. TCRs form microclusters with T cell signaling molecules on the activated T cell surface. Although it is necessary for the initialization of adaptive immune responses, the formation mechanism of the microclusters remains unclear. To observe the dynamics of TCR on the living T cell surface, we have developed a model system on planer lipid bilayers with stimulatory antibodies. With this system we can visualize the dynamic formation of TCR microclusters at the single-molecule level.

Using this system, here we compared the dynamics of TCR on the stimulated and resting T cell surface. We analyzed two-dimensional motions of fluorescently labeled TCR. On the activated T cell surface, the diffusion coefficient of TCR was one fourth of that of CD45 (the receptor-like protein tyrosine phosphatase outside of microclusters). It indicates the interaction of TCR molecules with TCR microclusters. Contrary to expectation, TCR molecules formed clusters also in resting T cells before activation. We calculated the number of TCR molecules in the clusters using the fluorescence intensity of single TCR molecules. The clusters contained 18 ± 6 molecules of TCR. The clusters moved diffusively at whole regions on the cell surfaces, and frequently divided and fused each other. The present result raises the possibility that the TCR can exist as nano-scale clusters even in resting T cells before activation and gives a fresh insight into the mechanism of T cell signaling.

1H1436 GTP 交換促進因子 Sos の生細胞一分子計測

Single molecule imaging of guanine nucleotide exchange factor Sos in living cells

Yuki Nakamura[1,2] ([1]*RIKEN sako celluar informatics laboratory*, [2]*Osaka university Yanagida lab*)

The small GTPase Ras is one of the essential regulators for controlling cell differentiation and proliferation. Ras activation is induced on the plasma membrane by the exchange of bound GDP for GTP. The guanine nucleotide exchange factor son of sevenless (Sos) regulates this GDP/GTP exchange on Ras. Upon stimulation with various extracellular factors including epidermal growth factor EGF, Sos translocates from the cytoplasm to the plasma membrane. However, spatio-temporal dynamics of the translocation and the regulation of Ras activation have not been known for the full length of Sos molecule.

In this study, we observed single molecules of GFP-tagged Sos in living HeLa cells using total internal reflection fluorescence microscopy. We found an increase of the amount of Sos molecules on the plasma membrane upon EGF-stimulation, which had not been detected by ensemble molecule imaging in the previous studies. In addition to the increase of the on rate, duration of the membrane association for each single molecule increased after the stimulation. As the result, even though the time-course and amount of Sos translocation were varied among cells, on average, an increase of the molecular density by a factor of 2.5 was observed 5 min after the stimulation. Although, before stimulation, a small number of Sos molecules localized on the plasma membrane with short durations, our result suggested that Sos molecules, associated with the membrane for long durations, are responsible for Ras-activation.

1H1448 リガンド結合したβ 2 アドレナリン受容体の短寿命ダイマーは三量体 G タンパク質のターンオーバーを加速する：2 色同時 1 分子観察による測定

Single-molecule imaging revealed acceleration of trimeric G-protein turnover by transient dimerization of liganded β2adrenergic receptor

Rinshi Kasai[1], Takahiro Fujiwara[2], Akihiro Kusumi[1,2] ([1]*Inst. For Frontier Med. Sci., Kyoto Univ.*, [2]*WPI-iCeMS, Kyoto Univ.*)

Previously, we for the first time succeeded in fully characterizing the dynamic dimer-monomer equilibrium of GPCRs, formyl peptide receptor and beta2 adrenergic receptor (AR) (Kasai, 2011 JCB & BPS meeting), including the dimer lifetime of ~100 ms for both molecules. To examine the physiological functions of the transient GPCR dimers, we performed simultaneous dual-color single-molecule imaging of trimeric G-protein, Gs (Gs-mGFP), and fluorescently-labeled AR in the living cell plasma membrane under physiological conditions. Arrivals of Gs at the AR monomers and dimers and Gs departures from them were observed at the single-molecule level, allowing us to determine the residency time of Gs on the transient AR monomers and dimers. Due to much higher expression levels of endogenous Gs, the Gs-mGFP residency time (or Gs off rate) is likely to be the rate limiting step for the Gs turnover at the AR and thus for the Gs activation at the bulk level. We found that, even before stimulation, G-protein is recruited to AR and its residency times on transient AR monomers and dimers were about the same. Ligation reduced the G-protein residency times on both transient monomers and dimers, but the effect was more on that on dimers, suggesting that transient dimerization of liganded AR accelerates Gs turnover.

1H1510 光学顕微鏡と同時観察可能な高速 AFM

High-speed AFM combined with optical microscopy

Shingo Fukuda, Takayuki Uchihashi, Toshio Ando (*Depertment of Mathmatics and Physics, Grad School of Natural Science and Technology Kanazawa Univ*)

High-speed-atomic-force-microscopy (HS-AFM) can directly visualize dynamic processes of single protein molecules at work. This new microscopy has recently been proven to be capable of obtaining previously inaccessible information. 1-3). It now can be routinely applied to various isolated biomolecules. The next stage towards the evolution of HS-AFM would be the incorporation of functions by which we can gain multiple aspects of data inaccessible only with HS-AFM. In fact, with the current HS-AFM setup, it is hard to observe large objects such as live cells because the maximum scan range is limited to a few μm. Therefore it is difficult to position the AFM tip on a specific area of a large sample. In addition, very small molecules such as nucleotides cannot be seen, prohibiting us from observing, for example, the dynamic events of nucleotide binding and dissociation. On the other hand, optical microscopy has a wide view and enables us to visualize small molecules by the attachment of fluophores to them.

Thus, we have now been developing a HS-AFM system which can be mounted on a conventional optical microscope. For this combined system, we have developed a compact optical detection system, a laser tracking device, and others. We are now using this combined HS-AFM/optical microscopy setup to observe dynamics of live cells and single molecules.

1. M. Shibata et al., Nature Nanotechnology 5, 208-212 (2010).
2. N. Kodera, D. Yamamoto et al., Nature 468, 72-76 (2010).
3. T. Uchihashi, R. Iino et al., Science 333, 755-758 (2011).

1H1522 High-speed AFM observation of intrinsically disordered proteins (NTAIL-GFP, PNT-GFP and SIC1-GFP)

Sujit Kumar Dora[1], Kodera Noriyuki[1], David Bloquel[2], Johnny Habchi[2], Antoine Gruet[2], Sonia Longhi[2], Toshio Ando[1] ([1]*Bio AFM frontier research center, Institute of physics and mathematics, Kanazawa University*, [2]*AFMB Laboratory, University of Aix-Marseille*)

Intrinsically disordered proteins (IDPs) are functional proteins either fully or partly lacking stable secondary and tertiary structures under physiological conditions. They are involved in important biological functions such as transcription, translation, and cellular signal transduction. Despite the important roles of ID regions, effective methods to observe their structures were practically not available until the advent of high-speed AFM (HS-AFM). In this report, HS-AFM is employed to study the structure of three different ID proteins: two measles virus protein (NTAIL and PNT) and a yeast protein SIC1, all fused to green fluorescent protein (GFP). Successive AFM images of these proteins on mica surface captured at 10 frames per second clearly show the presence of two globular parts (small globule of ~1.5 nm diameter and large globule of ~4 nm diameter) interconnected by ID regions. The measured end-to-end distances of these ID regions are in excellent agreement with the respective theoretical values predicted under the assumption that the microscopic persistence length is the same (~1.2 nm) irrespective of different ID regions. Thus, the value of the microscopic persistence length is a finger print of the conformation of ID regions. Further, the height distribution of globular parts indicates the large globule (~4nm) to be GFP. The reason for the existence of small globular parts is still unknown.

1H1534 位相差電子顕微鏡用の帯電防止位相板

Anti-charging Phase Plates for Phase Contrast Electron Microscopy

Kuniaki Nagayama[1], Toshiyuki Itoh[2], Yoko Kayama[2], Zenpei Saitoh[2], Yukinori Nagatani[1], Yoshihiro Arai[2], Masahiro Ohara[1], Noriko Kai[2], Kazuyoshi Murata[1] ([1]*National Institute for Physiological Sciences*, [2]*Terabase Inc.*)

Phase contrast electron microscopy (EM) has a particular advantage when applied to biological samples that are made of light elements of which electron scattering is weak. A thin-film type of phase plates made of amorphous carbon has been applied to various biological samples with an expected performance of high contrast. Nevertheless the phase plate EM has not gotten a foothold in the EM community mainly due to the tedious handling of the plate. The success of biological applications have actually been supported by a mass-consumption of phase plate to redeem its short-life owing to the trouble of phase plate charging. Charging has always been the biggest obstacle to the phase plate development. Such a charging as originated from external causes, namely contaminant charging, has been cleaned up by a treatment of wrapping contaminants with carbon. But charging of carbon material itself after a high electron dose as revealed as an aging effect, also known as "Berriman effect", has remained to be fixed at last. To overcome the internal cause, the best way is known to add high conductivity to the carbon film by converting the carbon material from amorphous to graphite one, which is robust to the electron dose and highly conductive. We have tried several approaches to improve the conductivity and developed anti-charging phase plates which guarantee better handling. We report the mechanism behind the charging, an image deterioration model due to charging, anti-charging technologies and applications to biological samples.

1H1546 500kV LinacTEM の開発

Development of the 500kV Linac TEM

Yukinori Nagatani[1], Yoshihiro Arai[2], Takumi Sannomiya[3], Tadao Shirai[4], Ryuzo Aihara[2], Giichi Iijima[2], Kuniaki Nagayama[1] ([1]*National Inst. Physiological Sci.*, [2]*Terabase Inc.*, [3]*Tokyo Inst. Tech.*, [4]*RTS*)

High Voltage Electron Microscopy (HVEM) is providing a powerful mean to observe thick (>1 um) samples with nanometer resolutions in biology. The deep penetration of the high voltage electron beam (> 0.5MV) is useful to reconstruct 3-dimensional structures of biological samples. HVEM is, however, quite huge and expensive, of which cost exceeds 10 - 20 million dollars, because it is equipped with a high voltage DC accelerator which should be stored into a high pressure SF6-gas tank. We have constructed a novel kind of HVEM, which is designed to avoid the costly high voltage DC accelerator, 500kV Linac TEM, in the National Institute for Physiological Sciences. The Linac (linear accelerator) technologies have no need for the DC accelerator but need only for a smaller-scaled RF accelerator. Thus the total HVEM system demands a cost smaller than 6 million dollars and a height smaller than 4 meters. The idea applying the linac to HVEM is not new but the technical requirements as an EM system such as high stability (dE/E <10^-5) of the beam energy and fine emittance (<1 mrad) of the beam, both of which are beyond the current accelerator technologies, have been blocking its implementation. To satisfy the requirements, we have developed a system including a 10^-5 stabilized RF power supply of 30kW/2.45GHz and 250 femtoseconds beam choppers with a low energy spread and a fine emittance. We propose a project of the 5MV HVEM, by superconducting accelerators, which is to realize the 3-dimensional nanoscale imaging of a whole cell.

1H1558 光学顕微鏡とカソードルミネッセンス顕微鏡を用いたマルチモーダル細胞イメージング

Multimodal cellular imaging with light microscopy and cathodoluminescence microscopy

Hirohiko Niioka[1], Taichi Furukawa[2], Masayoshi Ichimiya[3], Tomohiro Nagata[4], Masaaki Ashida[2], Tsutomu Araki[2], Mamoru Hashimoto[2] ([1]*Inst. for NanoSci. Design, Osaka Univ.*, [2]*Eng. Sci., Osaka Univ.*, [3]*Osaka Dental Univ.*, [4]*Tsukuba Institute for Super Materials, ULVAC Inc.*)

Correlative light and electron microscopy (CLEM) allows us to observe molecular distribution with the combination of light microscopy (LM) and electron microscopy. Quantum dots are used for multi-labeling and the same molecules were observed with LM via color and TEM directly [1, 2]. However, TEM provides monochrome image and we cannot see the colors but check the size and shape of quantum dots to determine the molecular species in TEM images.

Cathodoluminescence microscopy (CLM) has a potential to enable color imaging of individual biomolecules with using nanophosphor labeling [3]. Cathodoluminescence (CL) is the emission of light from a material as a result of bombardment by a beam of accelerated electrons and because of electron beam excitation the spatial resolution of CLM reaches 10 nm order.

Rare-earth doped nanophosphors emit light via both UV and electron beam excitation. We prepared Eu doped nanophosphors and observed the phosphors in HeLa cells with LM and CLM. For LM imaging 254 nm light line of mercury lamp was used. The emission wavelength of the phosphors is around 614 nm, therefore the effect of autofluorescence is negligible. The phosphors in the cells were observed by CLM with high-spatial resolution after thin-sectioning of the cells. This technique is, so to say, correlative light and CL microscopy.

[1] B. N. G. Giepman et al., Nat. Meth, 2, 743 (2005). [2] C. V. Rijnsoever et al., Nat. Meth, 5, 973 (2008). [3] H. Niioka et al., APEX 4, 112402 (2011).

1H1610 精製タンパク質の構造から in situ の構造まで：電顕を使用して

From purified protein structures to in situ structures using EM

Naoyuli Miyazaki[1,2], Mineo Iseki[3], Koji Hasegawa[4], Akihiro Narita[5], Shinichi Adachi[6], Masakatsu Watanabe[7], **Kenji Iwasaki**[1] ([1]*Institute for Protein Research, Osaka University*, [2]*National Institute for Physiological Sciences*, [3]*Pharmaceutical sciences, Toho University*, [4]*AdvanceSoft Corp.*, [5]*Structural Biology Research Center, Nagoya University*, [6]*Institute of Materials Structure Science, High Energy Accelerator Research Organization (KEK)*, [7]*The Graduate School for the Creation of New Photonics Industries*)

The fullness of electron microscopy (EM) imaging techniques is not comprised only of single particle reconstruction methods for obtaining the molecular structure of purified symmetrical proteins at a middle range resolution. For instance, one additional EM imaging technique is CEMOVIS (Cryo-Electron Microscopy of Vitreous Sections), which unlike other methods enables us to visualize sections of hydrated cells or tissues with cryo-EM. Conventional plastic sectioning requires chemical cross-linking, dehydration and resin embedding. These processes undoubtedly denature molecules, and any unlinked molecules are lost through the dehydration process. Finally, we observe specimens stained with heavy metal for high contrast. Contrary to these, in the case of CEMOVIS, a sample is frozen in a high-pressure freezing machine such as the Leica EM PACT2 and directly cut into vitreous cryo-sections by cryo-microtome. In this way, we can also observe the phase contrast in vitrified samples by cryo-EM, which conveys the signals coming from the molecules in the proteins themselves as opposed to contrast attributed to the heavy metals in plastic sections. Here, we revealed the paracrystal structure of the photo-sensing organelle composed mainly of photoactivated adenylyl cyclase (PAC) in Euglena using CEMOVIS. We also succeeded in showing the tetrameric structure of PAC using single particle reconstruction in addition to the homology modeling of PAC. Merging these collective results, the arrangement of PAC in situ has been successfully shown.

1I1400 Analyzing the conservation of the folding nucleuses among the Ferredoxin-like fold in their amino acids sequence

Masanari Matsuoka, Takeshi Kikuchi (*Dept. Bioinf., Coll. Life Sci., Ritsumeikan Univ.*)

While there are many studies focused on how the proteins fold by means of Molecular Dynamics or Go-like Model simulations, we may extract this information regarding the folding processes only from their amino acids sequences, because all information on the 3D structures should be coded in them. We have been trying to extract this kind of information based on the amino acids sequences using inter-residue average distance statistics. In this analysis, we construct the predicted contact map (Average Distance Map) and analyze them to extract possible structural domains or folding nucleuses. Our previous results for four proteins of Ferredoxin-like fold showed good agreements with experimental data. Thus, in this study, we extend this analysis to their homologues and observe the relationship between the conservation of the folding nucleuses and their sequence similarities. The detailed results will be discussed at the following conference.

1I1412 RNA とタンパク質の相互作用におけるタンパク質構造変化のデータベース解析

Database analysis of the degree of protein conformational changes in RNA-protein interactions

Chihiro Kubota[1], Kei Yura[1,2,3] ([1]*Graduate School of Humanities and Sciences, Ochanomizu University*, [2]*Center for Informational Biology, Ochanomizu University*, [3]*Center of Simulation Sciences, Ochanomizu University*)

Conformational changes in the interactions between proteins and other molecules are one of the basic issues in predicting the docking structures. Previously, we have developed a method to predict RNA interface residues on proteins with relatively high accuracy and started applying the method to build structures of RNA-binding proteins with the target RNA molecule. To build an accurate model structures, the knowledge for the effect of conformational changes in proteins is required. We, therefore, studied the degree of conformational changes in RNA-binding proteins, when the proteins bind RNA molecules. Three-dimensional structures of proteins determined with RNA molecules were selected from Protein Data Bank (PDB). Proteins which have more than 90% sequence identity to the RNA-binding proteins, and of which structures were determined without an RNA molecule, were also selected. By sorting out the selected protein structures, we made a list of 108 RNA-binding proteins with RNA bound and RNA non-bound forms. Of them, 77% has RMSD of alpha carbons no more than 2.0Å, when RNA bound and non-bound forms were superimposed. Protein pairs with the RMSD more than 2.0Å showed an overall tendency to slightly shrink into a cleft for an RNA molecule without a huge conformational change, when the protein binds to it. Except for the intrinsically disordered regions, the conformational changes in proteins were found to be slight. These findings suggest that conformational changes of the proteins should play a minor role in RNA-protein interactions.

1I1424 天然変性タンパク質のデータベース IDEAL の構築

Construction of IDEAL database for the investigation of intrinsically disordered proteins

Takayuki Amemiya[1], Shigetaka Sakamoto[2], Yukiko Nobe[1], Seiko D. Murakami[1], Kazuo Hosoda[3], Ryotaro Koike[1], Hidekazu Hiroaki[4], Motonori Ota[1], Satoshi Fukuchi[3] ([1]*Grad. Schl of Info. Sci.*, [2]*HOLONICS Co., Ltd.*, [3]*Fac. Engr., Maebashi Ins. Tech.*, [4]*Grad. Schl of Pharm. Sci., Nagoya Univ.*)

Considerable regions of eukaryotic proteins are thought to be intrinsically disordered, which lack a globular three dimensional (3D) structure in physiological conditions. The intrinsically disordered proteins (IDPs) play important roles in signal transduction and transcriptional regulation. The characteristics of IDPs are contrary to the traditional view of structural biology, where a stable 3D structure is necessary for protein function. In the past 10 years, many studies of IDPs have been carried out to contribute the accumulated experimental information. A well-designed database of IDPs is demanded for summarizing this information. We have developed a new database, IDEAL (IDPs with Extensive Annotations and Literature, http://www.ideal.force.cs.is.nagoya-u.ac.jp/IDEAL/), which collects experimentally verified intrinsically disordered regions (IDRs). Now, we are annotating mainly human nucleus proteins. We defined the protean segments (ProSs) as coupled folding and binding regions which are IDRs acting as recognition elements of their partner proteins. We have provided 209 entries including 97 entries with ProSs. In the presentation, we will demonstrate how to use IDEAL and present some examples of collected IDPs.

1I1436 Computational analysis of protean segments (ProSs) in intrinsically disordered proteins (IDPs)

Divya Shaji[1], Takayuki Amemiya[1], Satoshi Fukuchi[2], Motonori Ota[1] ([1]*Graduate school of information science,Nagoya University, Japan*, [2]*Faculty of Engineering, Maebashi Institute of Technology, Japan*)

Intrinsically disordered proteins (IDPs) are proteins that lack a stable, tertiary structure. Many regions of disordered proteins undergo disorder to order transitions upon binding to their protein or nucleic acid partners, known as coupled folding and binding mechanism. We call these regions Protean segments (ProSs). In this study, we analyzed the amino acid composition of ProSs. A non-redundant dataset of ProSs were extracted from IDEAL, a database with collection of experimentally verified intrinsically disordered proteins. The amino acid composition of ProSs was compared to those of ordered and disordered datasets. We created these datasets based on SCOP (SCOP25). The results of this analysis demonstrate that ProSs are similar in composition to disordered residues than to ordered residues. Next, we compared the composition of ProSs with those of interior and surface residues. For this analysis, we extracted a dataset of non-redundant monomeric structures from PDB. We calculated the relative accessible surface area (rASA) of residues by using Naccess program and classified the residues with greater than 25% of rASA as surface and the residues with less than 25% as interior. The results of this analysis indicate that ProSs are similar in composition to surface residues. Based on these results, we will discuss the physicochemical properties of ProSs.

1I1448 MODIC: a novel ab inito identification system of transcription factor binding motifs in genome DNA sequences

Masaru Tateno[1], Ryo Nakaki[2], Jiyoung Kang[2] ([1]*Grad. Sch. Sci., Univ. Hyogo*, [2]*Grad. Sch. Pure and Appl. Sci., Univ. Tsukuba*)

We developed a novel program, MODIC, to identify transcription factor binding motifs (TFBMs) in genome DNA sequences, which involves a new algorithm for identification of gaps in TFBMs. In MODIC, we defined a new information entropy to conduct the statistical comparison of two types of frequency distributions with respect to the TFBM candidates in the target DNA sequences and the non-candidates in the background sequence, with the latter generated by

utilizing the intergenic sequences. Our identification algorithm is based on the maximum information entropy principle, employing the above-mentioned information entropy. We tested our system employing several sets of ChIP-seq data concerning mammalian genomes as well as yeast ChIP-chip data, and it was revealed that the result of MODIC is the best among the available programs (MDscan, MEME, Weeder, DME, and BioProspector) [1]. Our system does not need any other biological information except for gene positions, and does not need tuning of the parameter set for each TFBM and pre-treatment/editing of the target DNA sequences. Thus, MODIC is also expected to be applicable to genome DNA sequences to accurately identify unknown TFBMs as well as known ones.

[1] Nakaki, R., Kang, J., and Tateno, M., *Nucleic Acids Research*, in press.

1I1510 Interaction of DNA molecules with nanopore studied by fluorescence microscopy

Genki Ando[1], Kazuteru Yamada[2], Toshiyuki Mitsui[1,2] ([1]*Grad. Mat.Sci., Univ. Aoyama*, [2]*Phys., Univ. Aoyama*)

Silicon based solid state nanopore devises have shown the capability to monitor the translocation of single DNA molecule and expected for future low-cost DNA sequencing at a single molecule level. However, relatively long DNA molecules, for example Lambda-phage DNA near 16.3 μm in length can easily clogatnanopore and end the translocation experiments because the clogging DNA molecules at nanopore strongly interact with the other DNA's and cannot be removed by reversing the polarity of external bias voltages across the nanopore membrane. We have studied these clogging events carefully by using by fluorescence microscopy. We have found the chances for single DNA clogging at pore under the various experimental conditions. We have also investigated the possibility to remove the clogging DNA by pulsing electric fields at nanopore. Recent trends of nanopore related researches are the translocation experiments through electricallymodifiednanopores. We also fabricated nanopores with gold gate and observed the effects of pulsing gate voltages on clogging DNA molecules at pore. Finally, we will discuss the mechanism of the DNA clogging and the clogging DNA removal from nanopore.

1I1522 診断用 DNA 計算に向けた核酸応答型 DNA 合成システムの構築
Construction of a nucleic-acid-responsive DNA synthesis system for diagnostic DNA-based computing

Ken Komiya, Asako Kobayashi, Masayuki Yamamura (*Interdis. Grad. Sch. of Sci. and Engi., Tokyo Tech.*)

The ability of a single-stranded DNA (ssDNA) to bind specifically to its complement makes DNA a useful switch for synthetic biomolecular systems, consisting of various reactions triggered by DNA hybridization, and allows cascading of such DNA-based reactions for the purpose of information processing. We previously reported a DNA state machine that implements successive state transitions via the cascaded DNA synthesis, according to a computational program encoded with a single ssDNA. This DNA-based computing system is highly versatile in principle, and thus, is expected to be applied to computational, biological and medical tasks. However, for achieving information processing on molecular distribution, including RNA transcription pattern, simple cascading of DNA-based reactions is not enough. Additional machinery to convert information of distribution into the form suitable for sequential processing of the DNA state machine is required.

In the present study, we propose a nucleic-acid-responsive DNA synthesis system that generates distinct ssDNA species at sufficient intervals in response to different nucleic acid species. Conversion of nucleic acids distribution is implemented via toehold-mediated strand exchange reaction, followed by ssDNA generation reaction utilizing a DNA polymerase and a nicking endonuclease. The proposed system could be applied to diagnostic DNA-based computing, where biomolecules autonomously determine the pathological state of their surrounding environment based on distribution of nucleic acid biomarkers.

1I1534 DNA scaffold logic: logic operation on molecular inputs using FRET cascades

Takahiro Nishimura[1], Yusuke Ogura[1], Hirotsugu Yamamoto[2], Kenji Yamada[3], Jun Tanida[3] ([1]*Osaka University*, [2]*The University of Tokushima*, [3]*Osaka University*)

DNA logic circuits handling molecular information based on DNA reactions are useful in biological applications. To construct scalable DNA logic circuits with simple DNA reactions, we propose an effective method called DNA scaffold logic. In the DNA scaffold logic, a logic operation on molecular inputs is achieved by formation of FRET paths on a DNA scaffold and the result is obtained as the cascaded FRET signal. FRET signaling contributes to simplify the DNA reactions for logic operations, to concentrate the signal path into a nanometer region, and to accelerate the response time of molecule-based logic circuits. The FRET signaling path is regulated according to the input molecules. If a set of input molecules satisfies the given logic condition, the FRET path is formed and the fluorescence molecule emitting the output signal is excited. Experimentally, we demonstrated a complete set of Boolean logic functions (AND, OR, NOT) and logic expressions represented by several Boolean functions by using multi-step FRET. In numerical simulation, we confirmed that additional time for increasing extra layers approaches asymptotically to zero. This result suggests that the method is useful for construction of multi-layered circuits with fast response.

1I1546 寄生虫による接着性宿主細胞への侵入過程観察のためのマイクロ加工デバイスの作製
Observation of parasite invasion with the micro-fabricated device

Tetsuhiko Teshima[1], Hiroaki Onoe[1], Kaori Kuribayashi-Shigetomi[1], Hiroka Aonuma[2], Hirotaka Kanuka[2], Shoji Takeuchi[1] ([1]*The Institue of Industrial Science*, [2]*Jikei University School of Medicine*)

Cytological studies for infectious microorganism have garnered much attention for detailed analysis of their behavior and function. Especially, it is important to observe the invasion of obligate intracellular pathogens, which gives us much information about morphological changes and expressed protein. With conventional methods, however, it is difficult to capture pathogen invasion into adherent cells and to confirm whether parasites are located inside cells or not. In this study, we propose microflap system to realize multiple-angle observation of adherent cells in order to detect boundary membrane of parasites and host cells. Fabricated devices are composed of alginate hydrogel, Parylene, Chromium and Permalloy layer. After removing the alginate layer, the microflaps were released from glass substrates and responded to magnetic field. Permalloy layer generates lifting torque, so that inclination angles increased with increasing external magnetic fields. As a model of microbial infection, we used a parasite, Toxoplasma gondii, and its host HFF cells. During changing the inclination, cells remained attached to the surface of microflaps and cellular membrane could be clearly observed. Parasites approached to HFF cells and microflaps were inclined in the desired orientation. We could optimize the angle and observe time-scale invasion. Thus, we clearly observed how parasites invaded through membrane and judged completed infection. This method is widely applicable to the analysis of interaction between infectious microbes and host cells.

1I1558 金属還元菌 *Shewanella* における微生物呼吸代謝の電気化学的制御
Electrochemical regulation of bacterial respiratory activity of *Shewanella*, a dissimilatory metal reducing bacteria

Shoichi Matsuda[1], Huan Liu[3], Shuji Nakanishi[2], Kazuhito Hashimoto[1,2,3] ([1]*Grad. Sch. Engr., Univ. Tokyo*, [2]*RCAST, Univ. Tokyo*, [3]*ERATO/JST*)

Dissimilatory metal reducing bacteria, *Shewanella* is well known to express c-type cytochromes abundantly on the outer membrane. The bacteria facilitates efficient electron transfer through the outer membrane cytochromes(OMCs) by extracellular electron transfer mechanism. Interestingly, they can utilize solid-state metal oxides as sole electron acceptor for the respiration. The bacterial respiratory activity can be investigated electrochemically by providing an electrode of an appropriate potential as the sole electron acceptor, which allows the capture of respiratory electrons and reversible tuning of the electron energy level of the solid-state electron acceptor. We investigated the electrode potential dependence of the microbial respiratory activity with/without malonic acid, a chemical inhibitor for TCA cycle. At the negative potential region where OMCs exist as the reduced state, microbial current was drastically decreased by the addition of the TCA cycle inhibitor. In contrast, at the positive potential region where OMCs exist as the oxidized state, the addition of the inhibitor had no effect on the microbial current. These results indicated that TCA cycle activity of *Shewanella* changed depending on the redox state of OMCs. Thus, it was revealed that TCA cycle activity of Shewanella can be electrochemically gated.

1I1610 Spatiotemporal control of cell motility in nano- to micro-scale topographical environment

Hiromi Miyoshi[1], Hiroyoshi Aoki[1], Jungmyoung Ju[1], Sang Min Lee[2], Jong Soo Ko[2], Yutaka Yamagata[1] ([1]*ASI, RIKEN*, [2]*Grad. Sch. Mech. Eng., Pusan National Univ.*)

The extracellular matrix (ECM) topography is known to affect various cell functions, such as cell motility and proliferation. The ECM consists of hierarchical organization over different length scales from nanometers to hundreds of micrometers. However, in most of the previous studies, the effects of the ECM topography on the cell functions have been analyzed only focusing on a specific scale in each study. Our aim here is to clarify how cells sense the hierarchical inputs from the ECM topography and determine motile behavior by a systematic analysis using micro/nano-topographical extracellular environments. Silicon micropillar array and polyacrylonitrile nanofibrous structures were used as the extracellular environments. Fibroblasts having bundled actin filaments and discrete cell-substrate adhesions, and fish epidermal keratocytes having actin meshwork and continuous adhesions were used for the analysis. In the micropillar array, cells had a tendency to wrap the pillars. Keratocytes extended very few protrusion, whereas, fibroblasts formed lamellar and filopodial protrusions into the gaps between the pillars. In the nanofibrous structures, both fibroblasts and keratocytes extended protrusions along the nanofibers. We assumed that the cell motile behavior depending on the scale of the extracellular environments will comes from the dynamic flexibility of the actin cytoskeleton, including actin network bending, actin reorganization, and the dynamic connection between the actin network and adhesion complex.

2A1400　クライオ電子線トモグラフィーを用いた細胞中骨格タンパク質およびモータータンパク質の非侵襲的構造解析

Observation of intracellular cytoskeleton and motor protein in the non-invasive cells with electron cryo-tomography

Shinji Aramaki[1], Kazuhiro Aoyama[2,3], Kota Mayanagi[4], Takuo Yasunaga[1] ([1]*Dept. of Bioscience and Bioinformatics, Grad. School of Computer Sci. and Sys. Eng., Kyushu Inst. of Tech.*, [2]*FEI Company Japan Ltd., Application Lab.*, [3]*Grad. School of Frontier Biosciences, Osaka Univ.*, [4]*Medical Inst. of Bioregulation, Kyushu Univ.*)

Most life is composed of protein, and water, and their localizations change depending on functions, types, and environments. Usually proteins are produced near nucleus. However, their localization is very highly regulated. It is realized by not only diffusion which is passive transportation but also active transportation. Actin, and microtubules called cytoskeleton, and myosin, kinesin, and dynein called motor proteins are known as important players of the intracellular transportation.

In these days motility of motor proteins and interaction between motor proteins, and cytoskeleton proteins have been revealed by *in vivo* single-molecule analysis. Moreover actin filament and motor domain of cytoplasmic dynein are difficult to structural analysis due to large their molecular complex size and so their structural understandings has not suggested *in vivo* interaction between motor proteins and cytoskeletons. Hence we set out to reveal structure of intracellular transportation.

We observed ultrastructure of the intracellular architecture by electron cryo-tomography, which can realize observation of intact cell as three-dimensional objects, because cells are vitrified by quickly freezing by liquid ethane, and so samples are not affected by chemical regents. Hence, it would give us intracellular structural images without any artifacts. This powerful technique will give us a major breakthrough of elucidating intracellular protein-protein interactions.

2A1412　クライオ電子線トモグラフィーを用いたクラミドモナス軸糸外腕ダイニンにおけるメタロチオネイン標識 LC2 の検出

Detection of metallothionein-tagged LC2 on *chlamydomonas* axonemal ODA by electron cryo-tomography

Mingyue Jin[1,4], Haru-aki Yanagisawa[2], Kotaro Koyasako[1,4], Ritsu Kamiya[2], Kota Mayanagi[3,4], Takuo Yasunaga[1,4] ([1]*Dep. Biosci. Bioinf., Inst. Tech. Kyushu*, [2]*Dep. Biol. Sci., Grad. Sch. Sci., Univ. Tokyo*, [3]*Div. Struct. Biol., Med. Inst. Bioreg., Univ. Kyushu*, [4]*JST*)

Axonemal structures including dynein molecules have been reported at relatively high resolution. However, due to the limitation of cryo-EM, individual dynein subunits could not discriminate in all reported axonemal outer dynein arm (ODA) structures. Thus, our group has introduced a genetic tag of murine metallothionein (mMT2), a heavy metal binding protein. To improve the expression level, mMT2 was exchanged to *C. reinhardtii* codon usage and reborn as CrMT2. We fused CrMT2 to ODA subunits, light chain 2 (LC2), which is known to be an essential element for ODA's assembly on the axoneme. In this study, we successfully expressed CrMT2-tagged LC2 to rescue ODAs on the axoneme. LC2-2xCrMT2-expressed or wild type axonemes were treated with $CdCl_2$ and their 3D structures were obtained by cryo-ET. Unlike wild type, linearly aligned punctate high densities were found in LC2-2xCrMT2 transformed axonemes alone. In addition, these high densities have a 24-nm periodicity identical to that of wild type ODA molecules on the axoneme. We concluded that individual punctate high densities identified on the CrMT2-tagged axoneme must be from Cd-CrMT2. Furthermore, the Cd-CrMT2 location on the ODA was measured from three orientations. Based on these data, we decided precise LC2 localization in the axonemal ODA. This is the first time to visualize a genetic heavy metal labels on the axoneme by cryo-ET. Taken together, the CrMT2 adapted to C. reinhardtii will be a promising method to detect subunits of huge protein complex *in situ*.

2A1424　クライオ電子顕微鏡法とメタロチオネインラベルを用いた軸糸構造の解明

Elucidation of Axoneme architecture by cryo-electron microscopy and metallothionein labeling

Reiko Chijimatsu[1], Mingyue Jin[1,2], Takuo Yasunaga[1,2] ([1]*Kyushu Institute of Technology*, [2]*JST*)

Motile cilia/flagella are driven by dynein motor proteins that form the inner and outer rows of arms attached to the outer doublet microtubules. *Chlamydomonas* outer arm dynein has three heavy chain motor units (α, β, γ). Previous works reported that γ heavy chain contains LC4 like calmodulin, but its detailed location are unknown. Thus we used cryo-EM and single particle analysis to identify LC4's detailed location.

The *Chlamydomonas* strains used in this study are wild type and *F11* whose LC4 is fused to Mt (heavy metal-binding protein). Cells were cultured in TAP medium with a light/dark cycle of 12h before crude dynein was extracted from cells. Crude dynein was set on ice with 10μM Cd^{2+} overnight and dialyzed in two types of ionic strength (0.6M KCl, 50mM K-acetate) before quick freezing and observations. We also prepared crude dynein from *F11* and confirmed that it had Mt-fused one, by electrophoresis. We observed two samples, crude dynein prepared from wild-type and *F11* and compared them. As a result, when we observed crude dynein extract prepared from *F11*, high density was observed near dynein heavy chain-like particles. We thus conclude that this high density is Mt binding Cd and the position of LC4 should be determined. Interestingly, in only lower ionic strength (50mM K-acetate), the filamentous protein on 24nm cycle was observed. Due to the periodicity, this protein can be important for axoneme assembly. We'll identify the location of LC4 precisely and what is the filamentous protein above-mentioned.

2A1436　電子線トモグラフィー法により明らかになった、LIS1 による細胞質ダイニンの運動活性制御メカニズム

Regulation of cytoplasmic dynein-motility on microtubules by LIS1 revealed by electron-computed tomography

Shiori Toba[1], **Kotaro Koyasako**[2,3], Shinji Hirotsune[1], Takuo Yasunaga[2,3,4] ([1]*Dept. Genetic Disease Research, Osaka City Univ. Grad. Sch. of Medicine*, [2]*Dept. Bioscience & Bioinformatics, Faculty of Computer Science and Systems Engineering, Kyushu Inst. Tech.*, [3]*JST-SENTAN*, [4]*JST-CREST*)

Cytoplasmic dynein is a microtubule-based and minus end-directed motor protein. Striking feature of the dynein is that its carries out diverse transport activities through interactions with the numerous accessory molecules. LIS1 is one of those dynein-associated proteins, and its regulatory role on the dynein has been intensively investigated. Although the dynein is critically regulated by LIS1, the underlying mechanism remains largely unknown.

Here, we have uncovered three dimensional structure of the dynein bound to microtubules and nucleotide-induced structural changes by electron-computed tomography (ECT) analysis. The typical features of the dynein motor domain such as a ring-like structure were successfully visualized from ECT of single particle. ECT allows us to interpret the flexible and huge structure of the dynein-microtubule complex reflecting working conditions in cells.

Furthermore, we disclosed the orientation of the two motor domains of the dynein and the underlying molecular mechanism by which LIS1 regulates dynein motility. Surprisingly, LIS1 handcuffs the structure of dynein in a no nucleotide state regardless of nucleotide conditions through its simultaneous binding to two motor domains. These structural characterizations were further confirmed by cryo-electron microscopy coupled with hierarchical cluster analysis and terminal specific gold particle-labeling of LIS1. We propose that the dynein-LIS1 complex is used as an immotile fastener of microtubules, which is essential for dynein-dependent cellular function.

2A1448　ヌクレオチド状態に依存したダイニン分子の形態変化

Nucleotide-dependent morphological change of cytoplasmic dynein

Muneyoshi Ichikawa, Kei Saito, Takayuki Torisawa, Keitaro Shibata, Yuta Watanabe, Tomonori Hata, Yoko Toyoshima (*Grad. Sch. of Arts & Sci., Univ. of Tokyo*)

Cytoplasmic dynein moves on microtubules toward the minus-end by the ATP hydrolysis-driven structural change and is involved in diverse cellular activities, including cell division, cargo transport, and neural development. Cytoplasmic dynein is a homodimer of two heavy chains and forms a two-headed structure.

The structure of head domain of cytoplasmic dynein has been extensively studied. Previous electron microscopy and FRET analysis have revealed the structural change of the linker orientation relative to the AAA ring depending on the nucleotide state. However, the structural basis of how dynein molecule uses two heads during the walk is still unveiled.

Here, we examined the structural change of full length cytoplasmic dynein in an electron microscopy. Negatively stained porcine brain dynein molecules appeared in both open (Y-shaped) and closed (φ -shaped) structures as previously reported (Amos 1989). The two heads were separated in Y-shaped

structure, and the two heads were stacked together in φ-shaped structure. In the presence of AMPPNP, Y-shaped dynein was predominant (Y-shaped, 62.7% / φ-shaped, 24.6%). In contrast, in an ADP-Vi condition, which mimics the ADP-Pi state of the catalytic cycle, dynein molecule tended to form a closed conformation (Y-shaped, 26.0% / φ-shaped, 53.4%). We constructed His-tagged recombinant human dynein heavy chains and performed a site-specific Ni-NTA-gold labeling. Combined with single particle analysis, the orientation of the two heads in φ-shaped structure will be discussed.

2A1510 頭部間の直接的相互作用は細胞質ダイニンの連続的な運動に必要ない

A direct interaction between dynein two heads is not necessary for processive movements of dynein

Keitaro Shibata, Yui Utsumi, Takayuki Torisawa, Yoko Toyoshima (*Dept. Life Sci., Grad. Sch. Arts and Sci., Univ. Tokyo*)

Cytoplasmic dynein is a two-headed motor protein which moves toward the minus end of microtubules. Recently, the crystal structure of dynein motor domain has been reported and understanding of the motor machinery has progressed. However, how dynein uses two heads during its processive movement on microtubules is not clear yet.

Previously, we reported that dynein moved on zinc-induced tubulin polymers (zinc-sheets) which include only one protofilament to be utilized by dynein movement, suggesting that dynein moves on zinc-sheets by inchworm mechanism.

Here, to elucidate whether a direct interaction between the two heads is necessary for its processive movement, we prepared an artificial dimer: the dynein motor domains are dimerized by an anti-parallel actinin rod known to have a high persistence length. EM images of this actinin-dimers revealed that the two heads keep a distance of ~25 nm by the rigid rod. A single molecules of the actinin-dimer moved both on microtubules and on zinc-sheets processively. Our results suggest that a direct interaction between dynein two heads is not necessary for the processive movement of dynein.

2A1522 外部負荷存在下でのヒト細胞質ダイニンのメカノケミカルサイクル

The mechanochemical cycle of human cytoplasmic dynein under external force

Taketoshi Kambara[1], Yoshiaki Tani[1], Motoshi Kaya[1], Tomohiro Shima[2], Hideo Higuchi[1] ([1]*Grad. Sch. Sci., Univ. Tokyo*, [2]*QBiC, Riken*)

Dynein is a molecular motor that moves toward the minus-end of microtubules. Cytoplasmic dynein play roles in positioning the Golgi complex and other organelles in cells, movement of chromosomes, and positioning the mitotic spindles during mitosis. Here, we used optical trapping to show the single molecule properties and the effect of load on the mechanochemical cycle of human cytoplasmic dynein. We expressed truncated C-terminal motor domain of dynein using baculovirus expression system. The double-headed motor domain was responsible for producing a high force of ~6 pN with a predominant step size of 8 nm. An unbinding force of single-headed dynein was measured in various nucleotide conditions. Dynein with the biotin-tag was attached to avidin-coated polystyrene beads, and the bead was trapped by optical tweezers. The external load was imposed by moving the stage. An unbinding force measurement indicates that dynein-microtubule binding is weak for the ADP/vanadate state and strong for the nucleotide-free, AMPPNP and ADP states. The unbinding force was weaker when dynein was pushed toward the minus end of microtubule in the strongly bound state, while it was independent of loading direction in the weakly bound state. Analysis with a model revealed that the dissociation rate of dynein from microtubules increases as the force increases. Our results suggest that force plays an important role in the mechanochemical cycle of dynein to ensure the increasing of a probability for rear-head detachment with strain.

2A1534 Rotation of microtubules driven by *Tetrahymena* 22S outer arm dynein and its sub-particles

Shin Yamaguchi, Yoko Toyoshima, Junichiro Yajima (*Dept Life Sciences, Graduate School of Arts and Sciences, Univ. of Tokyo.*)

Axonemal dynein is the molecular motor that provides motive force in cilia. *Tetrahymena* 22S outer arm dynein, which is localized between the outer-doublet microtubules (MTs), consists of three different heavy chains, termed α, β and γ, and is decomposed into two-headed βγ sub-particle and one-headed α sub-particle by chymotryptic digestion. Previous study showed that these sub-particles had motility, yet it has not been clear how the three-headed structure of 22S dynein affected its force generation. To decipher the contribution of each heads to the 22S dynein activity, we examined the motility of the 22S dynein and its sub-particles, using three-dimensional tracking of a quantum dot attached to MTs in an *in vitro* motility assay. As a result, we found that surface-attached 22S dynein and its sub-particles drove not only on-axis MT sliding, but also clockwise MT rotation around its axis. We estimated rotational pitch by fitting the *xy*-position of a quantum dot with a sine function. The pitch of 22S dynein and βγ sub-particle had different ATP dependency, whereas the pitch of α sub-particle was constant. At 10 μM ATP, each dyneins showed almost same pitch. These corkscrewing motions of MTs have not been seen for both 22S dynein and its sub-particles, and it demonstrates that these dyneins produce torsional forces as well as axial sliding forces. Our results suggest that torque generation by the three-headed 22S dynein is not due to the cooperation between each of the three heads, but due to the intrinsic property of individual heads.

2A1546 哺乳類細胞質ダイニンが一方向性を獲得する機構について

The mechanism of the transition from diffusion to directed movement in mammalian cytoplasmic dynein

Takayuki Torisawa[1], Furuta Ken'ya[2], Muneyoshi Ichikawa[1], Yoko Toyoshima[1] ([1]*Dept Life Sciences, Graduate School of Arts and Sciences, the Univ of Tokyo*, [2]*Bio ICT lab, NICT*)

Cytoplasmic dynein is a minus-end-directed molecular motor involving in various cellular functions. Mammalian cytoplasmic dynein has been reported to exhibit unidirectional movements for several micrometers in vivo (Kobayashi, 2009). However, some in vitro studies have reported that single molecules of cytoplasmic dynein/dynactin complex showed diffusive movements along microtubules (Ross, 2006; Miura, 2010), and a recent study has demonstrated that an mRNP complex bound by a few dyneins displayed diffusive movement (Amrute-Nayak, 2012). To reveal the mechanism of the transition from diffusion to directed movement in cytoplasmic dynein, we designed recombinant dyneins using HEK293 cell expressing system. An artificially dimerized, tail-truncated human cytoplasmic dynein 1 (GST+380 kD) showed unidirectional movement, whereas full-length dyneins purified from the same system diffused along microtubules. Furthermore, using several other recombinant dyneins that have different head-to-head distances between two motor head, we discovered that the dynein with longer head-to-head distance contained larger diffusive component. We also observed that multiple full-length dyneins bound to Qdot moved unidirectionally along microtubules, while single dyneins carrying Qdot exhibited diffusive movement. These observations imply that the directed movement of dynein is influenced strongly by the head-to-head distances and the motor number, leading to the possibility of dynein regulation by these factors in the cell.

2A1558 骨格筋形成過程における細胞質ダイニンの分布変化

The dynamic change of the distribution of cytoplasmic dynein during skeletal muscle differentiation process

Takuya Kobayashi, Motoshi Kaya, Hideo Higuchi (*Department of physics, Graduate school of science, The university of Tokyo*)

Skeletal muscles are thought to be rigid structure, but it must be always maintained. In non-muscle cells, cytoplasmic dynein is bearing important roles for intracellular maintenance. However, the roles of dynein are not understood in skeletal muscles. In order to understand the role of cytoplasmic dynein, we developed the in vivo fluorescence imaging of mouse skeletal muscle which molecular structures are visualized by using the gene transfer of GFP-fused proteins. Microtubules and cytoplasmic dyneins in in vivo muscles were successfully visualized by expressing GFP-Tubulin and dynein IC74-GFP with confocal microscope. The distribution and dynamics of vesicles transported by cytoplasmic dyneins in living muscle differed from non-muscle cells, and these vesicles did not move along the microtubule in living muscle. Meanwhile, dynein IC74-GFP were stably expressed in the myoblast cell line C2C12 and, vesicle transports were observed in myoblast cell and myotube. The dynein binding vesicles in the myoblast stage distributed as similar as in non-muscle cells. However, in myotube, the vesicles mainly moved along longitudinal axis and the speed of the vesicles was decreased to 20% of myoblast stage. Thus, the distribution and dynamics of vesicle transport by cytoplasmic dyneins remarkably changed during the muscle differentiate process.

2A1610 ダイニンアダプター Bicaudal-D2 の細胞周期依存的核膜局在の分子機構

Molecular mechanism of cell-cycle dependent nuclear envelope localization of Bicaudal-D2

Takashi Murayama, Hiroki Ota, Takashi Sakurai (*Dept. Pharmacol., Juntendo Univ. Sch. Med.*)

Bicaudal-D is an evolutionarily conserved dynein adaptor and involved in Rab6-dependent cargo transport. In mammals, there are two subtypes of Bicaudal-D, i. e., BICD1 and BICD2. Recent study has shown that BICD2, but not BICD1, is localized to the nuclear envelope (NE) in a G2-specific manner via interaction with RanBP2, a protein of nuclear pore complexes, and may play an important role in nuclear positioning during mitotic entry. However, it remains unclear (1) how G2-specific NE localization of BICD2 is regulated and (2) why BICD1 is NOT localized to NE. To address these questions, we expressed various truncated and chimeric BICD1/BICD2 mutants and tested their NE localization in HeLa cells. Bicaudal-D has three coiled-coil domains (CC1-CC3) and linkers (L1 and L2) between them. BICD2 is reported to interact with RanBP2 at the C-terminal CC3 domain. Consistent with the previous study, full-length BICD2 was localized to NE only in G2 phase (cyclin B1 positive), whereas full-length BICD1 was not localized to NE throughout the cell cycle. BICD2 lacking the N-terminal CC1 domain showed NE localization in both G2 and non-G2 (cyclin B1 negative) phases. Surprisingly, BICD1 lacking CC1 was also localized to NE in both G2 and non-G2 phases. The BICD1 chimeric mutant having CC1 and L1 of BICD2 showed G2-specific NE localization. These findings suggest that CC1 functions as inhibitory domain for NE localization and CC1 and L1 domains confer G2-specific disinhibiton of CC1 in BICD2.

2B1400 単一アミノ酸ポテンシャル力場の改良と短鎖ペプチドの構造予測への応用

Improvement of the Single Amino Acid Potential Force Field and the Application to Structure Prediction of Short Peptides

Michio Iwaoka, Kenichi Dedachi, Taku Shimosato, Toshiya Minezaki (*Tokai Univ*)

The Ramachandran-type potential energy surfaces calculated for single amino acid units in water are in good agreement with the statistical structures of the corresponding amino acid residues in proteins. Based on this interesting property of proteins, we recently developed a new all-atom force field called the Single Amino Acid Potential force field (SAAPFF) for molecular simulation for polypeptide molecules. In this paper, we report on improvement of the SAAPFF and the application to structure prediction of short peptides. The classical canonical Monte Carlo simulation was carried out by using the improved SAAPFF for Met-enkephalin, a short peptide with five amino acid residues, and chignolin, a small protein with ten amino acid residues. Diverse structures were obtained for Met-enkephalin at 300 K in water, while three representative folded structures, one corresponding to the native-like structure with three native hydrogen bonds, were obtained for chignolin. The results were compared to the molecular dynamics simulations using a conventional AMBER force field with the Generalized Born solvent model. The SAAPFF was found to be useful for conformational sampling for short peptides. In addition, a protocol of the SAAP-MC simulation followed by structural clustering and ab initio calculation was suggested to be an effective strategy toward prediction of the native folded structure.

2B1412 オンサーガー・マハラップ作用を用いたペプチド系のパスサンプリング

Path sampling for small peptide systems using the Onsager-Machlup action method

Hiroshi Fujisaki[1,2], Yasuhiro Matsunaga[2], Akinori Kidera[2,3] ([1]*Nippon Medical School*, [2]*RIKEN*, [3]*Yokohama City University*)

Proteins often accompany conformational changes when they function in cells, and its characterization is one of the most important subjects in biophysics. The ability of theoretical and computational methods based on molecular dynamics simulation has been increasing mainly due to the advance of hardware, it is, however, still not feasible to simulate and clarify a biological role of conformational changes of large proteins. To address this time-scale problem from a different point of view, we proposed to use a statistical approach based on the Onsager-Machlup (OM) action (J. Chem. Phys. **132**, 2010, 134101), where a path, not a configuration, is the most fundamental object to be studied, and its distribution is described by a path-integral representation using the OM action. In the present study, we apply this formalism to small peptide systems, including alanine dipeptide, chignolin, and WW domain, in implicit solvent where a hessian matrix is implicitly evaluated using the numerical scheme due to Vanden-Eijnden and Heynman (J. Chem. Phys. **128**, 2008, 061103). To facilitate path sampling, we further combine the OM method with our replica exchange strategy (Fujisaki, Shiga, Kidera, in preparation), and analyze the resulting huge path space in terms of transition rates and transition state ensembles.

2B1424 蛋白質系のシミュレーションの緩和モード解析

Relaxation mode analysis for simulations of protein systems

Ayori Mitsutake, Toshiki Nagai, Hiroshi Takano (*Keio Univ.*)

Classical molecular dynamics simulations are a popular method for describing the structure, dynamics, and function of biomolecules in microscopic detail. As longer and larger MD simulations are performed, it is more important to develop methods to extract the “essential”modes from the trajectory. Relaxation mode analysis (RMA) has been developed to investigate “dynamic” properties of homopolymer systems while principal component analysis (PCA) is one of the popular methods for analyzing the static properties of fluctuations of structures. In the case of liner polymers, the relaxation phenomena have been studied systematically in terms of the relaxation modes and rates by using RMA. We have applied RMA to a biomolecular system (J. Chem. Phys. 135, 164102 (2011)). As a biomolecular system, we choose the system of Met-enkephalin in gas phase because it is known to have several meta-stable or stable conformations and is therefore suited for the verification of the validity of RMA. We perform a Monte Carlo simulation of the system and apply PCA and RMA. Here, we show the effectiveness of RMA by comparing these results with RMA and PCA.

2B1436 A multi-body potential for normal mode analysis of protein structure

Bhaskar Dasgupta, Narutoshi Kamiya, Haruki Nakamura, Akira Kinjo (*Institute for Protein Research, Osaka University*)

To describe native protein dynamics normal mode analysis (NMA) of an elastic network model (ENM) is widely accepted. In ENM, the energy of a native protein is modeled as a sum of energy of all pairs of atoms, each connected by a Hookean spring. However, in this model protein-solvent interactions are ignored. Therefore, solvent-exposed atoms sometimes exhibit unrealistically high fluctuations. To model the effect of solvent on protein here we propose differential contact number model (DCNM), which is based on the physical intuition of phase separation between hydrophobic and hydrophilic atoms. The hydrophobicity of an atom is defined in terms of contact number of an atom. In the objective energy function the difference in the contact numbers of neighboring atoms are restrained to their native value. To evaluate the DCNM against the ENM, we compared the dynamics of 19 pairs of proteins, each of which shows a conformational change between open and closed forms. We observed that the DCNM yields high fluctuation for a less number of atoms than the ENM. From the first 30 modes we observed that the DCNM exhibited greater overlap with the conformational change than the ENM and on average the modes obtained from the DCNM are more collective than the ENM.

2B1448 アクチン線維へのコフィリンの協同的結合の統計力学モデルの作成

A theoretical model of cooperative binding of cofilin to actin filaments

Shotaro Sakakibara[2], Kimihide Hayakawa[1], Hitoshi Tatsumi[2], Masahiro Sokabe[1,2] ([1]*FIRST Research Center for Innovative Nanobiodevice, Univ. Nagoya*, [2]*Grad. Sch. Med., Univ. Nagoya*)

Actin dynamics is regulated by a large number of actin binding proteins. Cofilin, one of these actin binding proteins, severs actin filaments and presumably plays a central role in the regulation of the actin dynamics. Biochemical and electron microscopic studies suggest that cofilin binds to the actin filament in a cooperative manner, and electron microscopic analyses have revealed that the twist of the actin filament is increased when the filament is fully decorated by cofilin. Here, we propose a simple theoretical model inspired from the Ising model in statistical physics. The model assumes that the actin filament is an array of actin protomers, and that each protomer has only two states “0” or “1”, where “0” denotes the non-twisted state and “1” the twisted-state. The model also assumes that binding of a cofilin to an actin protomer (i th) induces changes in the state (from 0 to 1) in the neighboring actin protomers (i-1 th and i+1th), resulting in an acceleration of cofilin binding to these protomers. By fitting the theoretical curve calculated with this model to the experimentally obtained relationship (percentage of cofilin binding protomers in actin filaments vs.

cofilin concentration), we estimated the binding energy of cofilin to actin filaments at ca -7 kT and the energy required for twisting the neighboring protomer at ca 3.5 kT.

2B1510 リゾチーム分子中のアミロド性ペプチド

Amyloidogenic Peptides from Hen Lysozyme

Hideki Tachibana[1,3], Masao Fujisawa[1,3], Ryohei Kono[2,3], Minoru Kato[4] ([1]*Sch Biol-Oriented Sci Tech, Kinki Univ*, [2]*Wakayama Med Univ*, [3]*High Press Prot Res Center, Kinki Univ*, [4]*Coll Pharm Sci, Ritsumeikan Univ*)

Amyloid protofibril-like assembly spontaneously forms from hen lysozyme disulfide-deficient variant protein termed 0SS. Four peptide regions protected from the access of solvent in the 0SS fibrillar state have been identified with NMR-detected hydrogen/deuterium exchange measurements. These regions have high predicted beta-aggregation propensity, and most probably constitute the core of 0SS fibril. Here, the fibrillation of one of these peptides,Y52-R61, was investigated in detail. When monitored with thioflavine T fluorescence the Y52-R61 peptide facilely form amlyoid fibrils under mildly acidic solution conditions, but not under neutral or alkaline conditions, which indicates that the presence of small amount of excess positive charge facilitates amyloid-fibrillation of this peptide. Atomic force microscopy observation showed that the Y52-R61 peptide fibrils were thin at the initial stage of fibrillation when obtained from dilute peptide solutions, and grew thick with prolonged incubation period by bundle formation. MMPBSA calculation on two molecules of the Y52-R61 peptides showed that an anti-parallel beta structure is more stable than a parallel one by about 40 kJ, which agrees with our previous finding with IR measurement that the anti-parallel beta structure predominantly exists in the 0SS amyloid-like fibrils.

2B1522 Effects of raft components on the membrane-mediated aggregation of IAPP

Kenji Sasahara (*Kobe University*)

Human islet amyloid polypeptide (IAPP) is a 37-resudue peptide which is the major constituent of amyloid fibrils deposited in the pancreatic islets with type II diabetes mellitus (T2DM). IAPP is synthesized in pancreatic beta-cells and co-secreted with insulin. Numerous studies have shown that the interactions between IAPP and lipid membranes play an important role in the pathogenesis of T2DM, in which the lipid membranes of beta-cell are the target of IAPP toxicity. Despite recent efforts toward biophysical characterization of the IAPP-lipid interactions, the effects of IAPP aggregation on the physiological properties and organization of lipid membranes have not been well characterized, which is of critical importance in further understanding of the pathogenesis of T2DM. In the present study, amyloid aggregation of IAPP was induced on the supported lipid bilayers (DOPC/DOPS/raft components) to investigate the effects of raft components on its aggregate formation and the associated membrane damage. Microscopic observations indicated that IAPP aggregation is significantly accelerated on the membrane including the raft components, and that the aggregates are subsequently converted to the needle-like fibrillar aggregates during the prolonged incubation, which is promoted for the rafts-containing membranes. Furthermore, the conversion of IAPP to fibrillar forms was microscopically found associated with the membrane damage.

2B1534 タンパク質が生体内レドックス環境に依存して異なる凝集体を形成するメカニズムとその病理学的意義

Redox environment is an intracellular factor to operate distinct pathways for protein aggregation

Yoshiaki Furukawa (*Dept. of Chemistry, Keio Univ.*)

Redox control of the thiol-disulfide status is critical for functioning of many proteins, and Cu,Zn-superoxide dismutase (SOD1) is one of such proteins in which formation of an intramolecular disulfide bond is required for folding into its native structure. Indeed, abnormal reduction of a disulfide bond in SOD1 triggers the formation of insoluble aggregates in vitro. In addition, aggregation of mutant SOD1 proteins is a pathological hallmark in a familial form of amyotrophic lateral sclerosis (fALS); therefore, a thiol-disulfide status of SOD1 should be correctly regulated inside cells. Given that SOD1 exists in various intracellular organelles, however, it remains obscure how their distinct redox environment affects misfolding pathways of SOD1. To investigate effects of intracellular redox environment on SOD1 misfolding, fALS-mutant SOD1s were expressed in E. coli, BL21 and SHuffleTM. BL21 offers strongly reducing environment of the cytoplasm, while the cytoplasm in SHuffleTM is more oxidizing by deleting cytoplasmic reductases keeping cysteines in their thiol state. In both cells, fALS-mutant SOD1s were obtained as insoluble pellets but with distinct properties; a disulfide bond of SOD1 was either completely reduced in BL21 or abnormally formed between SOD1 molecules in SHuffleTM. Depending upon the intracellular redox environment where SOD1 resides, therefore, fALS-mutant SOD1 is considered to be misfolded into aggregates with distinct properties, which would be relevant in the pathological heterogeneity in fALS cases.

2B1546 銅シャペロンに依存しない SOD1 酵素の活性化制御メカニズム

A copper chaperone-independent mechanism for activation of Cu, Zn-superoxide dismutase

Yasuyuki Sakurai, Yoshiaki Furukawa (*Dept. of Chem, Keio Univ.*)

Cu,Zn-superoxide dismutase (SOD1) is an antioxidant enzyme that removes superoxide anion radicals, and is widely conserved among aerobic organisms. In order for SOD1 to gain catalytic activity, two post-translational processes are known to be necessary: binding of a copper ion and formation of an intramolecular disulfide bond. In eukaryotes, the copper chaperone CCS plays a pivotal role in the activation of cytoplasmic SOD1 by delivering the catalytic copper ion and introducing the intramolecular disulfide bond to SOD1. A *ccs*-knockout mouse, however, exhibits residual SOD1 activity, implying that a CCS-independent pathway is also operative for SOD1 activation.

To get insight into the mechanism of this CCS-independent pathway, we have focused upon the activation of *Escherichia coli* periplasmic SOD1 (SODC), which occurs independently of CCS, as the *E. coli* genome contains no CCS homologue. We have confirmed that an intramolecular disulfide bond as well as a bound copper ion is essential for catalytic activity of SODC and also found that the canonical binding of copper/zinc ions in SODC requires the formation of a disulfide bond. During the activation of SODC in *E. coli* cells, therefore, metal binding is considered to be preceded by formation of a disulfide bond. This mechanism appears to fit well with the oxidizing environment of the bacterial periplasm. We thus propose a regulatory role of the disulfide formation both in the CCS-dependent and independent activation of SOD1 enzymes.

2B1558 タンパク質凝集体の形態を制御する「凝集後修飾」のメカニズム

A mechanism controlling the morphologies of protein aggregates by "post-aggregation oxidation"

Yasushi Mitomi[1], Takao Nomura[1], Masaru Kurosawa[2], Nobuyuki Nukina[2], Yoshiaki Furukawa[1] ([1]*Dept. of Chem, Keio Univ.*, [2]*RIKEN Brain Science Institute*)

Misfolding of a protein molecule often leads to the formation of insoluble aggregates and is also characterized as a pathological hallmark in neurodegenerative diseases. One of the important factors regulating the aggregation of proteins is a post-translational modification; indeed, abnormal modifications are often identified in the aggregate-consisting proteins. Actually, however, it remains quite obscure when and how proteins are modified in the course of the aggregation.

To reveal an unprecedented role of modifications in protein aggregation, we focus upon a protein, huntingtin (HTT), which has been known to form insoluble aggregates in a neurodegenerative disorder, Huntington disease (HD). By examining aggregation of recombinant HTT proteins, we have for the first time identified oxidation of a Met residue in HTT during the aggregation *in vitro*. The Met residue has also been found to oxidize in pathological HTT aggregates purified from HD-model mice. A trace amount of contaminated copper ions as well as a physiological concentration of hydrogen peroxide oxidized a Met residue in HTT, and more interestingly, this Met oxidation occurred only in the aggregated HTT but not in the soluble state. Furthermore, we have found that the Met oxidation creates additional interactions among HTT aggregates and alters those overall morphologies. Protein aggregates can thus be a target of oxidative modifications, and we propose that such a "post-aggregation" modification is a relevant factor to regulate properties of protein aggregates.

2B1610 ジスルフィド結合の組換えによる不溶性 SOD1 オリゴマーの新たな形成メカニズムー筋萎縮性側索硬化症における分子病理変化

Destabilization of SOD1 facilitates abnormal scrambling of its disulfide bond in the familial form of amyotrophic lateral sclerosis

Keisuke Toichi, Yoshiaki Furukawa (*Dept. of Chem, Keio Univ.*)

Dominant mutations in Cu,Zn-superoxide dismutase (SOD1) are a cause of a familial form of amyotrophic lateral sclerosis (fALS). Wild-type SOD1 possesses four Cys residues of total, among which Cys 57 and 146 form a highly conserved intra-molecular disulfide bond. In contrast, mutant SOD1 proteins in fALS-model mice have been known to be cross-linked via inter-molecular disulfide bonds and form insoluble oligomers. A thiol-disulfide status in SOD1 will thus play a regulatory role in determining its folding/misfolding pathways; however, it remains unknown how pathogenic mutations affect the thiol-disulfide status in SOD1.
Here, we show that the structural destabilization of SOD1 scrambles a disulfide bond among four Cys residues in an SOD1 molecule. Destabilization of wild-type SOD1 with a chaotropic reagent produced an SOD1 protein with alternative electrophoretic mobility, and a peptide-mapping analysis using MALDI-TOF mass spectrometry revealed that a disulfide bond was shuffled among four Cys residues in SOD1. Furthermore, we have found that fALS-linked mutations facilitate the disulfide-scrambling process and also reproduce the formation of insoluble oligomers cross-linked via inter-molecular disulfide bonds. Based upon our results, therefore, scrambling of the conserved disulfide bond in SOD1 will be a key molecular event to describe the pathological changes of mutant SOD1 in fALS cases.

2C1400 A Brownian particle undergoing reversible binding in a surface: exact theoretical results and an application in single molecule biophysics

Ziya Kalay (*Institute for Integrated Cell-Material Sciences, Kyoto University*)

Despite the apparent need to study reversible reactions between molecules confined to a two-dimensional space such as the cell membrane, exact solutions of the diffusion equation, or Green's functions, have not been reported. Here we present exact analytical Green's functions for a Brownian particle reversibly reacting with a fixed reaction center in a finite two-dimensional region with reflecting or absorbing boundaries, considering either a spherically symmetric initial distribution or a particle that is initially bound. We show that these Green's functions can be used to predict the effect of measurement uncertainties on the outcome of single-particle/molecule-tracking experiments in which molecular interactions are investigated. Hence, we bridge the gap between previously known solutions in one dimension and three dimensions, and provide an example of how theoretical results can be used to predict experimentally accessible quantities in single molecule biophysics.

2C1412 Single-particle-level simulation reveals effects of molecular crowding on biochemical signaling response

Kazunari Kaizu, Koichi Takahashi (*Laboratory for Biochemical Simulation, RIKEN Quantitative Biology Center (QBiC)*)

Signal transduction pathway is a sophisticated information processing system consisting of biochemical reactions. Although the reactions occur in a cell which is significantly different from ideal conditions assumed in conventional biochemical theories, effect of “cellular environment”, such as clustering, compartmentalization and macromolecular crowding, on biochemical reaction networks is poorly understood. In this study, molecular crowding effects on dynamics of biochemical reactions and signal transduction pathways were quantitatively determined by particle-level simulations. We have previously shown that re-binding of kinases to substrates can remarkably increase the processivity of dual-phosphorylation reactions and change the response characteristics. To quantify the significance *in vivo*, we simulated diffusion-controlled reactions in crowded medium and measured re-binding probabilities at the single-particle level. As a result, re-binding was highly enhanced by molecular crowding and its time dependence was nonlinearly changed at microscopic level even though the kinetics at macroscopic level followed the conventional equations in dilute media. The rate law revised on the basis of these calculations enables the quantitative modeling and analysis of biochemical networks in intracellular environments with crowding. In particular, the results were applied to the MEK-ERK system and validated with experimental measurements.

2C1424 2 つのヒートショック反応系における 反応機構の比較
Conflicted dissociation constant in two reaction mechanisms for heat shock response

Masayo Inoue[1], Ala Trusina[2], Namiko Mitarai[2], Kim Sneppen[2] ([1]*CMC, Osaka Univ.*, [2]*CMOL, NBI*)

Cellular homeostasis is essential for proper protein folding and function. Heat shock, sudden increase of temperature, causes protein unfolding and misfolding and can result in cell death. To counteract the heat shock, cells upregulate production of chaperons and proteases.
The heat shock response is one of the stress responses observed in most living-things. Interestingly, the protein sequence of most chaperones and proteases are well conserved from bacteria to humans. It is, however, unclear if the features of heat shock response are also preserved at the level of the regulatory network.
In this study, we focus on two different mechanisms for heat shock response widely observed in microorganisms. The production rate of chaperon is regulated with a negative feedback loop in each system, however, the direction of regulations is opposite, i.e., the production of chaperon is activated in one system but inhibited in the other.
In this study, we constructed a model for each system and obtained a reasonable response in the production rate of chaperon. We also showed that a corresponding parameter have to satisfy a conflicted condition. This condition based on the difference of activation/inhibition direction in the regulation mechanisms.

2C1436 Mathematical analysis for vascular and spot patterns by auxin and PIN dynamics in plant development

Yoshinori Hayakawa[1,2], Atsushi Mochizuki[1,2] ([1]*Tokyo Institute of Technology*, [2]*Wako Inst., Riken*)

Inhomogeneous distribution of auxin is essential factor in various differentiation processes of plant development. Auxin distribution is generated by auxin efflux carrier protein called PINFORMED (PIN) and the interaction between these molecules has been discussed for long time. However, the mechanism of the dynamics generated by relationship between auxin and PIN are still unknown. In this study, we analyzed pattern formation of auxin distribution mediated by polarization of PIN using mathematical methods. We developed several different models for interaction between auxin and PIN on 2-dimentional hexagonal cellular lattice, (1) Auxin flux model, (2) Auxin-dependent PIN degradation model and so on.
We analyzed these models by numerical simulation using different parameter values and initial patterns. We found that there are three different types of dynamical behaviors from the view of pattern formation, (a) Homogeneous, (b) Passage and (c) Spot formation. In numerical simulation, these patterns appear in different parameter and initial conditions. We introduce mathematical analysis using approximation of 1-dimensional periodic space. We analyzed stabilities of three patterns (a) to (c), and determined condition of parameters for generating these patterns. These results suggest possibility that plants use different mechanisms of interaction between auxin and PIN for passage and spot formation. We are examining other different types of interaction between auxin and PIN orientation.

2C1448 Modeling wave propagation dynamics in MDCK wound healing assay

Yusuke Sawabu[1], Masaharu Nagayama[2], Takashi Miura[3], Hiroyuki Kitahata[4] ([1]*Inst. of Nat. Sci. and Tech., Kanazawa Univ.*, [2]*Res. Inst. for Elect. Sci. Hokkaido Univ.*, [3]*Kyoto Univ. Grad. Sch. Of Med.*, [4]*Dept. of Phys., Chiba Univ., Grad. Sch. of Sci.*)

Wound healing assay is frequently utilized as an example of collective cell migration. We observe wave-like movement of cells in scratch assay of confluent MDCK cell sheet. A region of fast-moving cells, which is 10-20 cells wide, moved backward from the wound front, which is similar to propagation of a compression wave in a elastic body or a traffic jam. At first we formulate a one-dimensional model which assumes that the velocity of a cell is proportional to the distance between neighboring cell, but the model did not reproduce the wave propagation phenomenon. We could mathematically show that under such assumption no parameter set can reproduce the wave propagation. Next we formulate a one dimensional model which assumes that the polarity of each cell changes according to the distance between neighboring cells, and cells move according to the cell polarity. This model successfully reproduced the wave propagation phenomenon during the wound healing assay. We also formulate two-dimensional system which utilize the same type of cell-cell interaction. Connection between these cells are defined in the beginning using Voronoi diagram, which do not change during simulation. we confirmed two-dimensional wave propagation observed in one-dimentional system. Experiments are underway to quantitatively measure the interaction between the cells.

2C1510 CA モデルによる多細胞性シアノバクテリアの形態形成ダイナミクスの解析

Analysis of the internal dynamics for pattern formation in multi cellular cyanobacteria by CA model

Jun-ichi Ishihara[1,2], Masashi Tachikawa[2], Hideo Iwasaki[1], Atsushi Mochizuki[2] ([1]*Grad.Sci.Eng., Waseda Univ.*, [2]*Wako Inst., RIKEN*)

The multicellular cyanobacteria, Anabaena sp. PCC 7120, differentiates cells named heterocysts for nitrogen fixation at every ~10 cells under nitrogen-deprived culture. This is known as one of the simplest pattern formation, but a detailed mechanism has not yet been validated theoretically.
To address this question, we made a 1-dimensional cellular automaton (CA) model for the pattern formation, including stochastic cell cycle processing, cell division and differentiation. And a differentiated cell suppresses differentiation of neighboring cells. In the CA model, we considered that the division and/or differentiation probability may depend on time after cell birth, “cell age”. Some parameters were quantitatively determined from cell-lineage analysis made by our group.
To evaluate our models, we compared the distribution of heterocyst interval between experimental data under microscope and computer simulation data by CA models. As a result, respective features in steady-state of simulation data agreed with that of the experimental data if cell division and differentiation depended on cell age in CA model. These result suggested that the probability of cell differentiation and division connected to cell age was very important condition. Moreover, pattern formation in transitional state of experimental data agreed with that of simulation data if cell differentiated independently of cell age in CA model.
We also succeeded in solving the distribution of heterocyst interval of CA model by Marcov process including cell age transition.

2C1522 Modeling the mammalian circadian clock

Craig Jolley, Hiroki Ueda (*RIKEN Center for Developmental Biology, Laboratory for Systems Biology*)

Life generally runs on a schedule. The earth's rotation creates daily changes in light, temperature, and other environmental conditions, and many organisms respond to this by synchronizing their behavior and physiology with the day/night rhythm. We have developed a simplified model of the circadian clock system in mammals that captures many of its key features and can be parameterized by fitting to cellular-level measurements of biological rhythms. By using Monte Carlo sampling of the parameter-fitting landscape, we have been able to create an ensemble of data-fitted models and use tools from statistical mechanics to assess the system's robustness to parameter variations. We are currently using this model to explore the effects of external perturbations on the cellular clock, which can be important for tissue-level synchronization and entrainment to environmental signals.

2C1534 Determining the ratio of longitudinal to transverse conductivity in a cardiac tissue culture through application of FFP

Marcel Hoerning[1], Seiji Tagaki[2], Kenichi Yoshikawa[3,4] ([1]*RIKEN, Center for Developmental Biology, Physical Biology Unit*, [2]*Hokkaido University, Research Institute for Electronic Science*, [3]*Doshisha University, Life and Medical Sciences*, [4]*Kyoto University, Department of Physics*)

Tachycardia and fibrillation are potentially fatal arrhythmias associated with the formation of rotating spiral waves in the heart. Low-energy far-field pacing (FFP) has recently been proposed as a superior therapy, and it has been found that the formation of such sites can lead to the termination of undesired states in the heart and the restoration of normal beating. In this study, we investigate a particular aspect of this method. Here, we seek to determine how the activation site density depends on the applied electric field through in vitro experiments carried out on neonatal rat cardiac tissue cultures. The results indicate that the activation site density increases exponentially as a function of the intracellular conductivity and the level of cell isotropy. Additionally, we report numerical results obtained from bidomain simulations that are quantitatively consistent with our experimental results. Also, we derive an intuitive analytical framework that describes the activation site density and provides useful information for determining the ratio of longitudinal to transverse conductivity in a cardiac tissue culture. The obtained results should be useful in the development of an actual therapeutic method based on low-energy far-field pacing. In addition, they provide a deeper understanding of the intrinsic properties of cardiac cells.

2C1546 気道上皮細胞における Cl^- 分泌の数理モデル

Mathematical model of Cl^- secretion in airway epithelial cells

Kouhei Sasamoto[1], Naomi Niisato[2,3], Yoshinori Marunaka[2,3] ([1]*Undergraduate Student, Kyoto Prefectural Univ. Med.*, [2]*Molecular Cell Physiology, Kyoto Prefectural Univ. Med.*, [3]*Japan Institute for Food Education and Health, Heian Jogakuin (St. Agnes') Univ.*)

Transcellular Cl^- secretion in airway epithelial cells followed by paracellular Na+ secretion from the basolateral space to the apical one increases osmotic pressure in the apical space, which induces water secretion. Therefore, transcellular Cl^- secretion plays a crucial role in prevention form infection of bacteria and virus etc, by producing water secretion into the apical space covering airway epithelial cells.
Even using various techniques, we could not exactly get ideas how transcellular Cl^- secretion varies in its magnitude and time course due to modification of activity of Cl^- channels and transporters located at the apical and basolateral membranes. In the present study, we try to clarify how transcellular Cl^- secretion varies in its magnitude and time course when activity of Cl^- channels and transporters located at the apical and basolateral membranes changes using mathematical simulation with three parameters.
(1) the entry step; Cl^- into the intracellular space across the basolateral membrane
(2) the secretion step; Cl^- from the intracellular space across the apical membrane
(3) the recycle step; Cl^- across the basolateral membrane
This novel method reported in the present study provides us how activity of Cl^- channels and transporters located at the apical and basolateral membranes changes and understandings on roles of intracellular signaling in transcellular Cl^- secretion.

2C1558 エラーカタストロフィーによる HIV-1 擬種集団の自壊過程に関する研究

A Study on a Self-Destruction Process of a HIV-1 Quasispecies Population through the Error Catastrophe

Kouji Harada (*Toyohashi Univ. of Tech. Dept. of Comp. Sci. and Eng.*)

The present study examines possibility of a new AIDS treatment without using anti-HIV-1 drugs to avoid drug resistance. It is well-known that HIV-1 is frequently-mutated. Our idea for the new treatment is by inducing excess mutations to HIV-1 genome, to drive HIV-1 population to self-destruction. Namely, we will use the HIV-1's remarkable character of its mutating at high rate as an underhanded way. Our study proposes a novel HIV-1 mathematical model considered viral kinetic processes such as mutation, replication, infection and an action of a mutagen to control HIV-1 mutation rate. In terms of HIV-1 population, our model considers a quasi species formed by four different traits. Fast and slow replicators and either type can take viable and defective form. Through some numerical simulations of the model we will present that increasing HIV-1 mutation rate causes HIV-1 population to the error catastrophe.

2C1610 Characterization of Death and Division Process in Synthetic Bacterial Population with Antibiotic Treatment

Takashi Nozoe[1], Reiko Okura[1], Yuichi Wakamoto[2,3] ([1]*Grad. Sch. Arts and Sci., Univ. Tokyo*, [2]*Research Center for Complex Systems Biology, Univ of Tokyo*, [3]*JST PRESTO*)

We previously succeeded in observing non-genetic adaptation in antibiotic exposure by using a synthetic E. coli strain, expressing antibiotic resistant gene as fusion with fluorescent protein. Generally, phenotypic adaptation requires cell-to-cell variation of fitness, which is defined as difference between division rate and death rate. So, there are three possibilities on how phenotypic adaptation occurs in lethal environment; (i) growth rate varies among cells while death rate not, (ii) death rate varies while division rate not, and (iii) both rates vary. To test which scenario would be probable, we estimated, as a first step, temporal transitions in division frequency and death frequency, which were defined against a whole population. Time-lapse observation on a microfluidics device enabled us to directly observe growth, division and death in antibiotic exposure at single-cell level, followed by acquisition of time-series of division and death events. Consequently, it was clarified that death frequency decreased in antibiotic exposure while division frequency was almost constant

at lower frequency than before antibiotic addition. These results could support that fluctuation of the antibiotic resistant gene expression level might cause cell-to-cell variation of death rate in antibiotic exposure whereas division rate might be independent of the expression level of the resistant gene. This consideration would be useful for further analysis of the relation between gene expression noise and phenotypic adaptation.

2D1412 クライオ電子線トモグラフィーに対する超分解能技術

Super-resolution cryo-electron tomography

Ryuzo Azuma[1,2], Takuo Yasunaga[1,2] ([1]*Grad. Sch. of Comp. Sc. & Eng., Dept. of Biosc. & Bioinfo., Kyushu Inst. of Tech.*, [2]*JST*)

We have been investigating a tomographic method that enables a 3D visualization of computationally reconstructed object from electron micrographs of biological samples prepared under cryo-conditions that severely require low amount of total electron dose. The key issue was to resolve phase and amplitude (P/A) moieties separately from intensities of these electron micrographs, thereby complement missing information from finite tilt series sampling. This problem was also concerned with how to manage super-resolution (SR) issues arising from discretized data structures recorded as 2D-pixels. We are now tackling these problems from the respects of recovering z-axis resolution technique as proposed by Hoppe, combined with the “mechanical” tilting (not by beam tilting [1].) Also we incorporate iterative restoration of the P/A parts, by referring to the method of Grechberg and Saxton [2]. The SR issue turned out to crucially dependent on the method of phase image reconstruction from its auto-correlations [3], provided that the development of 3D-version under investigation was successful. Also the Histogram matching and modified Sayre methods may help to improve the performance of SR technique [3]. The basic concept, theory, and characterization by simulations will be presented. Also we acknowledge the method will be implemented as a software tool participated in Eos program package.

[1] W. Hoppe, *Z. Naturforsch*, A26, 1155 (1971.)
[2] R. W. Grechberg & W. O. Saxton, *Optik*, 35(2), 237-46 (1972.)
[3] V. Elser, *J Opt Soc Am A*, 20(1) (2003.)

2D1424 定量位相顕微鏡による生細胞におけるナノスケールの形状変化の非染色ビデオレートイメージング

Label-free and video-rate imaging of live cell membrane motion in the nanometer-scale by quantitative phase microscope

Toyohiko Yamauchi[1], Takashi Sakurai[2], Hidenao Iwai[1], Yutaka Yamashita[1] ([1]*Hamamatsu Photonics*, [2]*EIIRIS, Toyohashi Univ. of Tech.*)

Video-rate surface topography of live cultured cells was realized by our newly developed microscope called "quantitative phase microscopy"(QPM). QPM is an optical interference microscope which shines white light onto the cells, probes weak reflection light from cell membrane and visualizes three-dimensional morphology of cell surface. QPM, which utilizes optical phase-resolved interferometric technique, is able to quantify nanometer-scale vertical displacement of the reflecting interface, such as cell membrane.

As a preliminary application study, we compared spontaneous membrane motions of HeLa cells (derived from cervix cancer) and INS-1 cells (derived from rat insulinoma). Both samples were measured at two different temperatures (36 °C and 24 °C). Surface topography of every cell was obtained at 21 frames/sec. and the vertical motions of the cell membrane were analyzed by the mean-square-displacement (MSD). We have also demonstrated a time-lapse (2 sec. intervals) measurement for 10 minutes and even after the measurement, the cells lost no activity in terms of the amplitude of their spontaneous membrane motion. The HeLa and INS-1 cells showed significant difference in terms of membrane motion. For example, MSD(τ=10sec) = 630 nm^2 in HeLa cells while MSD(τ=10sec) = 3200 nm^2 in INS-1 cells (both at 36 °C). We believe that our low-invasive and three-dimensional microscopic technology could be a unique tool for further biophysical studies.

2D1436 ラマン分光を用いた超音波照射による細胞への影響の評価

Evaluation of Ultrasound Irradiation effects on Cells by using Raman Spectroscopy

Manabu Sugimoto[1], Yo Otsuka[1], Shinya Murakami[1], Toshiyuki Mitsui[2] ([1]*Grad. Sci Eng., Aogaku Univ*, [2]*Assoc Prof, Aogaku Univ*)

We evaluate the effects of ultrasound irradiation on the cell’s interior by using Raman spectroscopy. Recently, the ultrasound irradiation is known to promote a born growth and used for the treatment of born fracture healing. In cell unit, ultrasound irradiation is also known to accelerate the cell differentiation. However, the mechanism of these fracture healing and cell differentiation are not known. Therefore, we have observed the alteration of the cell interior in vivo where ultrasound is irradiated by using Raman spectroscopy. In this study, we have fabricated the “ultrasound probe” for our experiment. This needle shape probe allows us to measure the effects of ultrasound irradiation on one cell unit and control the ultrasound intensity near 24mW/cm2 with its frequency at 1.5 MHz. We will discuss the results of the alterations of the cell and their analysis of Raman spectrum measurements before and after the ultrasound irradiations on the cell.

2D1448 脂肪酸と 7-ヒドロキシ-4-メチルクマリンを用いた質量と蛍光測定によるアンモニアの二次元検出

Two dimensional ammonia sensing by measurement of mass and fluorescence using 7-hydroxy-4-methylcoumarin film and fatty acid

Yuta Ando, Masahiro Terashita, **Ryohei Matsueda**, Yutaka Tsujiuchi (*Department of Material Science and Engineering, Akita University*)

Two-dimensional sensing method for highly detecting of an organic compound in atmosphere is demonstrated in this report. As a simple model case, an ammonia sensing is exhibited, by measurement of mass with QCM sensor system and measurement of fluorescent spectrum of composite film of 7-hydroxy-4-methylcoumarin and fatty acid on a QCM Sensor unit. The fluorescent dye used here, 7-hydroxy-4-methylcoumarin, has an appropriate pH dependency of changing its emission light wavelength. Therefore, in this study, detecting of ammonia by measuring of emitted light at different wavelength is conducted. And mass change measurement is also conducted. In the previous conference, our first attempt of construction of ammonia sensor, using two types of phospholipid, dimyristoyl-phosphatidylcoline (DMPC) or soya PC (phosphatidylcholine contained in soya beans), comparison for applying them to the composite film with 7-hydroxy-4-methylcoumarin was reported. In this report, we demonstrated an improved attempt using different mol cular combination in the composite film on sensor unit. A set of reproducible results will be exhibited that the ammonia sensing with high precision that has not been observed before.

2D1510 インビトロ心毒性予測のための心筋細胞ネットワークの時間的細胞外電位ゆらぎと空間的伝達速度ゆらぎの評価

Evaluation of temporal fluctuation and spatial fluctuation on cardiomyocyte network for *in vitro* predictive cardiotoxicity measurement

Tomoyo Hamada, Fumimasa Nomura, Tomoyuki Kaneko, Kenji Yasuda (*Institute of Biomaterials and Bioengineering, Tokyo Medical and Dental University*)

Current guidelines for drug safety recommend the preclinical studies to to predict lethal arrhythmia potential especially torsade de pointes (TdPs) by measuring the *in vivo* drug-induced QT interval prolongation. However, recent studies show that those guidelines have limitations because they do not cover the pro-arryhthmic potential of drugs induced fatal ventricular tachycardia (VT) or fibrillation (VF) in the absence of QT prolongation. Hence, we have examined the most effective risk index to be able to replace from conventional QT prolongation. First, the temporal fluctuation of the field potential duration (FPD) of human embryonic stem (hES) cell derived cardiomyocyte clusters in on-chip microelectrode array (MEA) system was measured, and increased by the positive compounds even though in the absence of QT prolongation, but not by the negative compounds. Next, the spatial fluctuation of the conduction velocity (CV) in the lined-up hES cardiomyocyte network on a MEA chip by using agarose-microchambers was measured, and showed that the spatial fluctuation of CV was increased even by terfenadine, which was difficult to detect the risk in the traditional *in vitro* assays. The results suggest that both the temporal fluctuation of FPD and the spatial fluctuation of CV are good indices to evaluate the potential risks of pro-arrythmia including VT/VF and further for understanding the mechanism of pro-arrhythmia.

2D1522 SACLA における非結晶粒子の低温 X 線回折イメージング実験

Cryogenic Coherent X-ray Diffraction Imaging of non-crystalline particles at SACLA

Masayoshi Nakasako[1,2], Yuki Takayama[1,2], Tomotaka Oroguchi[1,2], Yuki Sekiguchi[1,2], Masaki Yamamoto[2], Koji Yonekura[2], Takaaki Hikima[2], Saori Maki-Yonekura[2], Yukio Takahashi[3], Akihiro Suzuki[3], Sachihiro Matsunaga[4], Shoichi Kato[4], Takahiko Hoshi[5] ([1]*Department of Physics, Keio University*, [2]*RIKEN SPring-8 Center, RIKEN Harima Institute*, [3]*Department of Precision Science and Technology, Graduate School of Engineering, Osaka University*, [4]*Department of Applied Biological Science, Faculty of Science and Technology, Tokyo University of Science*, [5]*Kohzu Precision Co.,Ltd.*)

Coherent X-ray diffraction imaging (CXDI) experiments of non-crystalline particles were performed at 66 K using our diffraction apparatus, named KOTOBUKI, at BL3 of SACLA on March and April. In the preparation of samples, suspension of non-crystalline particles at high concentration was dropped on thin silicon-nitride or carbon membrane using a humidity controlled sample preparation chamber. Samples were set in the liquid nitrogen pot inside the diffractometer and moved synchronously with the XFEL pulse. The hit-rate of XFEL pulse to sample particles was 40-60%. Diffraction patterns from nano-materials with the maximum dimensions of 100-300 nm were retrieved by using only the combinational use of hybrid-input-output and shrink-wrap algorithms.

2D1534 A protocol for structure analysis of non-crystalline particles with X-ray free electron laser

Tomotaka Oroguchi, Masayoshi Nakasako (*Department of Physics, Faculty of Science and Technology, Keio University*)

X-ray free electron laser facilities provides coherent and intense X-ray pulse in the range of 10^{11}-10^{12} photons/μm^2/pulse. Taking the cross section in Thomson scattering into consideration, the X-ray intensity is still smaller than that requested to carry out single molecular diffraction experiments for biological supramolecular assemblies such as ribosome that has a molecular mass of a few mega Dalton. Therefore, the single particle structure analyses of proteins with the molecular mass are still formidable task. Here we propose a protocol to visualize the structure of molecular assemblies with a molecular mass of more than a few mega Dalton by the combinational application of the coherent X-ray diffraction imaging method and the three-dimensional reconstruction algorithm. The details and limitations of the protocol are going to be reported based on the simulation for the structure analysis at 0.8 nm for 50S ribosome particles embedded in vitreous ice plates of $500 \times 500 \times 50$ nm^3.

2D1546 イオンコンダクタンス顕微鏡による細胞膜揺らぎの測定

Fluctuation of cell membrane investigated by ion conductance microscopy

Yusuke Mizutani[2], Satoshi Ichikawa[1], Zen Ishikura[1], **Takaharu Okajima**[1] ([1]*Grad. Sch. Inform. Sci. Tech., Hokkaido Univ.*, [2]*Grad. Sch. Life Sci., Hokkaido Univ.*)

The cell membrane thermally fluctuates and actively moves. Since the membrane contains various types of membrane proteins and interacts the cytoskeleton such as actin filaments, understanding the dynamic behaviors of the cell membrane is key to elucidate how various cell functions are regulated. In this study, we report the direct measurement of the fluctuation of living cell membrane by scanning ion conductance microscopy (SICM). As an electrically charged micropipette tip approaches a sample surface in an oppositely charged bath of electrolyte, the ion current steeply decreases in proximity to the surface [1]. Therefore, the SICM has a potential to precisely measure the position of the surface in a noncontact region. We used a commercial ICM system (XE-Bio, Park Systems, Korea) combined an inverted optical microscopy (Ti-U, Nikon) to map the spatiotemporal ion current of epithelial MDCK cells which were confluent on culture dish. It was observed that the ion current-distance curves largely changed depending on cell modifications such as a disruption of cytoskeleton and a chemical fixation of cell. We found that the disruption of actin filaments facilitated a change in the fluctuation of cell membrane. The averaged amplitude of cell membrane fluctuation could be estimated in different cell samples. [1] P. K. Hansma et al., Science 243, 641-643 (1989). Y. E. Korchev et al., Biophys. J 73, 653-658, (1997). Y. E. Korchev et al., Biophys. J, 78, 451-457, (2000).

2D1558 Relationship between Intercellular Adhesion Strength and Communication Detected by Femtosecond Laser-induced Impulsive Force

Takanori Iino[1], Man Hagiyama[2], Tadahide Furuno[3], Akihiko Ito[2], Yoichiroh Hosokawa[1] ([1]*Nara Institute of Science and Technology*, [2]*Kinki University*, [3]*Aichi Gakuin University*)

We have indicated that femtosecond laser-induced impulsive force can be available as an external force to break the cell adhesion[1]. Furthermore, we have developed a method to estimate the intercellular adhesion strength using femtosecond laser-induced impulsive force and atomic force microscopy[1,2]. Now, we are interested in a relationship between the adhesion strength and intercellular communication. In this work, we investigated the communication between a neuron and a mast cell as propagation of Ca^{2+} wave between them, simultaneously with the intercellular adhesion strength.
Mast cells (from mouse) and neurons resulting from differentiation induction of neuroblastoma (Neuro2a) were prepared. By depositing the mast cells on the neurons and culturing them together (co-culture), the mast cells were adhered to the neurites. After they were co-cultured for 16 hrs, the communication between the neuron and the mast cell was investigated to monitor the propagation of Ca^{2+} wave, in which the neuron was activated by loading the impulsive force to focus the femtosecond laser (780 nm, 250 fs) near the neuron through an objective lens (10x, NA=0.25). After that, the intercellular adhesion strength was estimated as described previously[1]. In the presentation, the relationship will be discussed on the basis of these results.
[1] I. Takanori et. al., The 48th Annual Meeting, 3p211 (2010).
[2] H. Yoichiroh et al., Proc. Natl. Acad. Sci. USA, 108, 1777 (2011).

2E1400 AFM を用いたホロミオグロビンの一分子力学計測によるアンフォールディング経路の探索

Mechanical unfolding pathways of holo-myoglobin explored by AFM-based single molecule force spectroscopy

Aya Yoshida, Masaru Kawakami (*Materials Sci, JAIST*)

We have applied Single Molecule Force Spectroscopy (SMFS) using atomic force microscopy (AFM) technique to characterize the unfolding pathway of myoglobin. A recombinant chimera polyprotein of holo-myoglobin with titin I27 [$(I27)_7$-Mb-$(I27)_2$] was engineered, in which a Heptameric I27 concatamer serves as a molecular handle for the manipulation of the polyprotein by an AFM cantilever *via* non-specific adhesion. SMFS results showed that the mechanical unfolding of myoglobin occurs at forces well below that of I27. This observation agrees with the previous reports that all α-helical proteins are mechanically weaker than their all β-sheet counterparts. Close inspection of each unfolding force curve of myoglobin revealed that the mechanical unfolding trajectory of myoglobin can be categorized into several patterns. One pattern contains only one unfolding peak with a full-molecular length elongation upon unfolding, indicating a catastrophic unfolding, i.e. myoglobin molecules unfold in all-or-none fashion. Other patterns include complex force peaks following the first major unfolding peak. They appeared with diversity of unfolding force and elongation length, suggesting that mechanical unfolding of myoglobin occurs in a three-(or more) state fashion through mechanically stable intermediate(s). These results indicate that the mechanical unfolding of myoglobin has multiple complex pathways, due to the bound heme molecule which is mechanically stabilizing the tertiary structure of myoglobin.

2E1412 走査型プローブ顕微鏡を用いた癌抑制因子 p53 の一分子構造解析

Single-molecule structural analysis of tumor suppressor p53 using scanning probe microscopes

Seiya Takahashi[1], Yasuyuki Sainoo[1], Risa Kashima[2], Takashi Tokino[3], Tadahiro Komeda[1], Satoshi Takahashi[1], **Kiyoto Kamagata**[1] ([1]*IMRAM, Tohoku Univ.*, [2]*Univ. California*, [3]*Res. Inst. Front. Med., Sapporo Med. Univ. Sch. Med.*)

p53 binds specific sites of DNA tightly with hopping and/or sliding motions along the DNA, which is the initial stage of transcriptional regulation of target genes. However, the detailed mechanism of the DNA-binding based on the structural and dynamical characterization of p53 remains unclear. A single-molecule characterization is required to further understand the DNA-binding mechanism, because ensemble experimental methods cannot determine heterogeneity of its structure with flexible disordered regions. Here, we performed structural analysis of p53 at a single-molecule level using two scanning probe microscopys; atomic force microscopy (AFM) and scanning tunnel microscopy (STM). p53 molecules were attached to gold surface, and then individual molecules on the surface were characterized under a dry condition using AFM. The volume histogram of these molecules showed the existence of monomers and oligomers such as dimers, tetramers and higher-

order aggregations. These structures were determined at a nanometer resolution. In the tetramer, small spheres were observed, which were spatially separated each other. Because their size is similar to that of the DNA binding domain, they were assigned to the DNA binding domains connected to a tetramerization domain with flexible linkers. Furthermore, we confirmed that p53 molecules on the surface can be imaged using STM. We will discuss the result of further statistical analysis of single-molecule structures and the conformational change against specific and non-specific binding to DNA.

2E1424 塩基性条件下でのヒトガレクチン 1 のβガラクトシド結合能力
β-Galactoside-binding activity of human galectin-1 at basic pH

Hirotsugu Hiramatsu, Tomohide Nishino, Hideo Takeuchi (*Graduate School of Pharmaceutical Sciences, Tohoku University*)

Human galectin-1 (hGal-1) is a soluble, β-galactoside-binding lectin. hGal-1 takes part in physiological functions such as cell adhesion and intercellular signal transduction by binding glycoconjugates on cell surfaces. In this study, the β-galactoside-binding (lectin) activity of hGal-1 was evaluated from the hGal-1 fraction bound to lactose gel (Y) and the lactose-binding constant in solution (Kb) at pH 7-10 by using fluorescence spectroscopy. Y showed dependence on the hGal-1 concentration, NaCl concentration, and pH. Y decreased at pH >7.5 in the absence of NaCl, while it was constant in the presence of 150 mM NaCl. On the other hand, Kb was found to be independent of pH and the NaCl concentration. Analysis of the S-H Raman band intensity at varied pH suggested that the average pKa of six Cys residues of hGal-1 was 9.6 ± 0.1. The apparent pH dependence of Y is explained by Coulombic repulsion among hGal-1 molecules on the lactose gel surface. At basic pH, the Cys (and other) residues of hGal-1 will be deprotonated to gain negative charges, which would prevent hGal-1 from binding to the gel excessively. The Coulombic effect is supported by the lack of the pH dependence in the presence of 150 mM NaCl. In conclusion, the lactose-binding ability of hGal-1 does not decrease at basic pH, despite that the amount of hGal-1 bound to the gel decreases at basic pH in the absence of NaCl. This result suggests that Y is not a good indicator of the lectin activity of galectins, which contain many Cys residues.

2E1436 A Molecular Mechanism of Induced-fit of U1A Protein

Ikuo Kurisaki[1,2], Masayoshi Takayanagi[1,2], Masataka Nagaoka[1,2] ([1]*Grad. Sch. Info. Sci. Univ. Nagoya*, [2]*CREST, JST*)

The induced-fit mechanism of U1A protein upon RNA-binding has been a paradigm of protein-RNA molecular recognition. However, the molecular mechanism still remains not fully understood in atomic level. To address the problem, we performed molecular dynamics (MD) simulations starting with apo-U1A and U1A-RNA complex structure. We compared the conformation distribution between apo-U1A and U1A-RNA system. The result indicates that the RNA-binding to U1A maintains the RNA-binding form of U1A. Among snapshot structures in apo-U1A system, we obtained a plausible intermediate structure at the initial step of induced-fit, termed the open-unfolded form [1]. This finding is consistent with previous conjectures for intermediate structure upon induced-fit [2,3]; (1) the C-terminal region partially unfolds and (2) the C-terminal region reorients under the inter-molecular electrostatic interaction. We performed the MD simulations starting from the complex of U1A in the open-unfolded form and RNA, resulting in the structure relaxation of U1A into the RNA-binding form [4]. The obtained results can be promising clues to clarify the molecular mechanism of induced-fit of U1A at the atomic level, leading to establishment of a full understanding of the protein-RNA molecular recognition mechanism.

[1] Kurisaki, Takayanagi and Nagaoka, J. Phys. Chem. Lett., submitted for publication.
[2] Tang and Nilsson, J. Biophys., 77(3), 1284-1305 (1999)
[3] Williamson, Nat. Struct. Biol., 7(10), 834-837 (2000)
[4] Kurisaki, Takayanagi and Nagaoka, in preparation.

2E1448 Single mutation on a loop alters the key dynamics of the core, but not the average structure

Akihiro Maeno[1], Sunilkumar P.N.[1], Yuji Wada[2], Eiji Ohmae[2], Shin-ichi Tate[2], Kazuyuki Akasaka[1] ([1]*HPPRC, Kinki Univ.*, [2]*Grad. Sch. Sci., Univ. Hiroshima*)

Evolution of a protein occurs often by mutations on the peripheral region of the protein structure, which cause functional changes. To find the molecular origin of the surface mutation on protein function, we studied the effect of a single mutation in a loop in E-coli DHFR, G67V, on the structure and dynamics in a site-specific manner by using NMR spectroscopy on the ^{15}N-uniformly labeled wild-type and the G67V mutant.

In a binary complex, DHFR: folate, the G67V mutation caused structural changes only localized around the mutation site, but caused no change in the average structure in the rest of the protein, the major core part including the active sites. On the other hand, the G67V mutation showed definite changes in conformational fluctuation in the remote core region of the protein including the active sites. In accord with the finding, distinct changes were observed in spin relaxation dispersion in the G67V mutant in the ternary complex, DHFR: NADPH:folate, which explains the observation that the hydride transfer rate is decreased by the same mutation. The present finding shows that a surface mutation, causing practically no change in the average structure of the protein, can cause a change in the crucial dynamics for function. The result may explain why surface mutations prevail in protein evolution.

2E1510 ヒト主要組織適合複合体の安定化に置ける揺らぎの重要性について
The effect of flexibility on the stability of Human Leucocyte Antigen

Saeko Yanaka[1], Kenjji Sugase[2], Takamasa Ueno[3], Kouhei Tsumoto[1] ([1]*Med. Genome Sci., Grad. Sch. Frontier Sci., the Univ. of Tokyo*, [2]*Suntory Institue for Bioorganic research*, [3]*Center for AIDS Research, Kumamoto Univ.*)

In the first step of human infection defense, human leucocyte antigens (HLA) present foreign peptides, which are recognized by cytotoxic T lymphocytes (CTL), resulting in the activation of CTLs to kill infected cells. Previous CD experiments have revealed that the thermal stability of HLA in cells is closely related to the CTL activity, and considerably depends upon the presented peptides. Although many crystal structures of HLA with different peptides have been determined, they are almost identical to each other. DSC experiments have shown that denaturation enthalpy cannot explain the HLA stability, while suggesting the structural difference in solution. Therefore, the stabilization mechanism of HLA is still unclear. Here we have studied the stabilization mechanism from the viewpoint of flexibility, using NMR relaxation dispersion spectroscopy. We focused on two HLAs presenting peptides, VY8-5A, and RY11-8A, which have the same sequence except that RY11-8A has three additional amino acids in the N-terminus. VY8-5A is known to activate CTL much longer than RY11-8A. In previous CD measurements it is shown that HLA in complex with VY8-5A has a higher temperature midpoint. NMR relaxation dispersion experiments revealed that the peptide recognition site in HLA is fluctuating in solution. Interestingly, HLA with VY8-5A, which is more thermostable, is more flexible, and is prone to form low-populated minor conformation. This suggests that the flexibility is critical for the HLA stability.

2E1522 Cavity-dependent dynamics of c-Myb R2R3 revealed by high-pressure fluorescence and NMR spectroscopy

Satomi Inaba[1], Akihiro Maeno[2], Hisayuki Morii[3], Harumi Fukada[4], Kazuyuki Akasaka[2], Masayuki Oda[1] ([1]*Grad. Sch. of Life and Environ. Sci., Kyoto Pref. Univ.*, [2]*High Pressure Protein Res. Center, Kinki Univ.*, [3]*Biomed. Res. Inst., Natl. Inst. Adv. Ind. Sci. Technol.*, [4]*Grad. Sch. of Life and Environ. Sci., Osaka Pref. Univ.*)

The c-Myb DNA-binding domain consists of three imperfect tandem repeats (designed R1, R2, and R3), and the last two repeats, R2 and R3, are necessary for the specific DNA-binding. Each repeat has three conserved Trp residues, which are involved in the hydrophobic core. The ternary structure of each repeat is similar, but R2 has a larger internal cavity. The cavity-filling mutation, V103L, reduced the specific DNA-binding, simultaneously reducing its conformational fluctuation and hydration, indicating that the cavity-dependent dynamics is closely related to the function. In this work, we studied the cavity-dependent dynamics of c-Myb R2R3 in more detail, using high-pressure Trp fluorescence (up to 700 MPa) and high-pressure ^{1}H one-dimensional and ^{15}N/^{1}H two-dimensional NMR spectroscopy (up to 250 MPa), along with differential scanning calorimetry. The maximum fluorescence emission of the wild-type R2R3 shifted from 332 to 346 nm at 700 MPa, while the cavity-filling mutant, V103L, shifted from 332 to 340 nm, showing that the cavity significantly contributes to the hydration, while the full unfolding of R2R3 was not yet attained even at 700 MPa. The high-pressure NMR experiments reveal more details of the cavity-dependent dynamics and stability of R2R3, in particular the different behavior and cooperativity of the two repeats, R2 and R3.

2E1534 単純化 BPTI に融合したペプチド系タグ配列を用いたアミノ酸溶解性の測定

Analysis of amino acid contributions to protein solubility using short peptide tags fused to a simplified BPTI variant

Yutaka Kuroda[1], Alam, M. Khan[1], Mohammad, M. Islam[1,2] ([1]*Dept of Biotech and Life Sci, TUAT*, [2]*Dept of Mol Biol and Biochem, Chittagon University*)

Protein solubility is usually characterized in terms of a hydrophobicity scale, which refers to the free energy of transfer of a molecule from an aqueous to a nonpolar solution and is not a "solubility propensity scale" per se. Using a "host-guest" approach, we measured the effects of short poly-amino-acid tags (guests) on the solubility of a host protein, a simplified bovine pancreatic trypsin inhibitor (BPTI), to which they were fused at the C-terminus. We analyzed 10 amino acid types, representing the full range of biophysical properties (acidic, basic, polar, and hydrophobic). As anticipated, positively charged residues significantly increased the solubility of the model protein, at both pH 4.7 and 8.7, whereas very hydrophobic poly-Ile markedly reduced the solubility of BPTI. Poly-Asp and poly-Glu barely affected BPTI solubility at pH 4.7, but induced an eight to ten-fold increase at pH 8.7, attributable to the ionization of their side chains. Although Pro is the most soluble amino acid, poly-Pro did not affect the protein's solubility. The effects of the other tags on BPTI solubility ranged from none to an eight-fold increase. These observations suggest that a solubility propensity scale could eventually allow the calculation of a polypeptide's relative solubility from its amino acid sequence.

2E1546 **Protein Aggregation Kinetics Using Short Amino acid Peptide Tags**

Monsur A. Khan[1], Mohammad M. Islam[1,2], Yutaka Kuroda[1] ([1]*Tokyo University of Agriculture and Technology*, [2]*University of Chittagong, Bangladesh*)

Protein aggregation is becoming an important issue in protein chemistry ranging from truly academic to biotechnological applications. Understanding the solubility and/or aggregation tendency is a prerequisite for proper use of a protein. Here we report the aggregation kinetics of protein using short artificial poly peptide tags containing five amino acids added to the C terminus of a simplified bovine pancreatic trypsin inhibitor (BPTI) variant. We measured the concentration of the sample of BPTI variants in supernatant after different incubation period (20min, 6hrs, 12hrs, 24hrs and 48hrs) and starting with different initial protein concentrations ranging form 0.25mg/ml to 20.0mg/ml. We observed that precipitation occurs promptly when BPTI was dissolved at a concentration above a maximum protein concentration, which we named “maximum transient solubility (MTS)”. Samples with protein concentration below the MTS but above a lower critical concentration, which we named “maximum mid-term solubility (MMTS)”, decreased upon long incubation period. On the other hand, samples with concentrations lower than the MMTS remained unchanged up to 48hrs of incubation. These results provide insights into the understanding of protein aggregation kinetics.

2E1558 **Protein specific partial charges by Ab-initio fragment molecular orbital method for more accurate protein simulations**

Le Chang, Shoji Takada (*Grad. Sch. Sci., Kyoto Univ.*)

Reliability of atomistic molecular dynamics simulations largely depends on accuracy of the force fields used. Among force field parameters, partial charges are one of the most important and hard-to-decide parameters. Normally, partial charges are determined for small building-blocks, often single amino acids, and they are used in proteins for simplicity. However, chemical moiety of an amino acid depends on its environment and even the same type of amino acid can have different electronic states. Thus, if one can determine partial charges for each atom in the target protein environment, they could be more accurate.
In the past, it was impossible to solve the electronic Schrödinger equations for large biomolecules. Recently, the fragment molecular orbital (FMO) method makes the ab-initio quantum mechanical calculation for the energy of protein size system possible. In this work, the partial atomic charges for protein native conformation is obtained from FMO calculation. From the new partial atomic charges, we observe some interesting features of the protein electrostatic characteristics. Besides, the binding free energies of some ligands to proteins are calculated from the molecular dynamic simulations using new partial atomic charges. The free energies of protein-ligand binding based on the new partial atomic charges are compared for several ligands with those by the standard AMBER force field, giving some promising results.

2E1610 **Regulatory Mechanism of the fluorescence emission from Green Fluorescent Protein Chromophore**

Jumpei Torii, Shoji Yamashita, Etsuko Nishimoto (*Institute of Biophysics, Faculty of Agriculture, Graduate school of Kyushu University*)

Green fluorescent protein (GFP) has been widely used in the biological studies as a marker of gene expressions, protein localizations, and protein-protein interactions. The chromophore of GFP shows high quantum efficiency (80%), its radiation mechanism however is yet unclarified. In this study the fluorescence intensity of p-hydroxybenzylidene dimethylimidazolinone (p-HBDI) as an analogue of GFP chromophore was measured at both 296 K and 77 K. While p-HBDI showed strong fluorescence at 77 K, little fluorescence was observed at 296 K. This result suggests that twisting motion of p-HBDI in the singlet excited state competes with fluorescence emission. To estimate the activation energy of this motion, which is speculated to cause the photo induced E-Z isomerisation of p-HBDI and its fluorescence quenching at the same time, the quantum yield of S65T-GFP was measured in the temperature ranging from 296 K to 340 K. In the lower temperature range, higher activation energy was observed than in the higher temperature range. This result indicates that when GFP folds properly, twisting motion of GFP chromophore is suppressed because of its high activation energy, however this barrier gradually diminishes with the relaxation of tertiary structure, which results in fluorescence quenching. For further investigation into the radiation mechanism of GFP chromophore, temperature and viscosity dependence of p-HBDI fluorescence intensity, CD spectrum of S65T-GFP, and the fluorescence lifetimes of both p-HBDI and S65T-GFP were measured respectively.

2F1400 **全原子量子化学計算によるレチナールタンパク質の吸収波長制御機構の解析**

Full-Quantum Chemical Calculations of the Absorption Maxima of Retinal Proteins

Tomohiko Hayashi[1], Azuma Matsuura[2], Hiroyuki Sato[2], Minoru Sakurai[1] ([1]*Center for Biological Resources and Informatics, Tokyo Institute of Technology*, [2]*Fujitsu Laboratories, Ltd.*)

A retinal protein consists of a seven-transmembrane protein (called “opsin”) and a retinal chromophore covalently bound to a Lys residue via protonated Schiff base linkage. The absorprion maxima (λ_{max}) of the chromophore is 610 nm in the gas phase but blue-shifts by 42~102 nm in the opsin. Such a shift is hence referred to as the “opsin shift”. The elucidation of the origin of the opsin shift has been an important subject not only in photobiology but also computational chemistry in recent decades. Although there have been reported a variety of quantum chemical calculations on the opsin shift, its precise physical origin is still a challenging open question. In this study, the λ max values of the bacteriorhodopsin (bR) and *pharaonis* phoborhodopsin (*pp*R) are calculated using our recently developed method that enables us to treat the whole protein quantum-chemically. We show that such a full quantum chemical calculation reproduce the opsin shift with an error of less than ± 0.04 eV. To decompose the opsin shift into the contributions from each amino acid, we also apply the same calculation for 226 different bR Gly mutants and 217 different ppR Gly mutants. Finally, we discuss the origin of the opsin shift from the following four factors, 1) contribution of the structural change of the chromophore accompanied by its transfer from the gas state to the protein interior, 2) contribution of each amino acid, 3) contribution from the backbone structure of the protein and 4) their synergistic effect.

2F1412 **プロテオロドプシンにおける細胞質側ループの変異がもたらす遠隔的波長制御メカニズム**

Mechanism of color change of proteorhodopsin by mutations at distant cytoplasmic loop

Yuya Ozaki[1], Rei Abe-Yoshizumi[1], Susumu Yoshizawa[2], Kazuhiro Kogure[2], Hideki Kandori[1] ([1]*Grad. Sch. Eng., Nagoya Inst. Tech*, [2]*AORI, Univ. Tokyo*)

It has been believed that the amino acids near the retinal chromophore are only responsible for color tuning of rhodopsins. However, we found that replacement of Ala178 with Arg in the E-F loop of green-absorbing proteorhodopsin (GPR) exhibits spectral red-shift and the pKa increase of the Schiff base counterion[1], which was not observed for bacteriorhodopsin (BR) [2]. Distant mutation effect was also observed for Ala115 in the C-D loop of GPR. It is likely that the loop regions contain unique structure in GPR, disruption of which causes large-scale rearrangement of α-helices.

Here we studied similar mutation effect for blue-absorbing PR (BPR). Thousands of PR are classified into GPR (λ_{max}~520 nm) and BPR (λ_{max}~490 nm). GPR and BPR possess Leu and Gln at position 105, and L/Q GPR and Q/L BPR absorb blue and green lights, respectively (L/Q switch) [3]. In case of BPR, distant mutation effect was only observed for the C-D loop, not E-F loop, suggesting that large-scale structural rearrangement is absent for the E-F loop of BPR. In case of GPR, distant mutation effects of the C-D and E-F loops were not additive, suggesting that common structure around the retinal chromophore is formed. Molecular mechanism of mutation effect in the cytoplasmic loops will be discussed on the basis of the present results.

1. Yoshitsugu et al. *Angew. Chem. Int. Ed*. **47**, 3923 (2008).
2. Yoshitsugu et al. *Biochemistry*. **48**, 4324 (2009).
3. Man et al. *EMBO J*. **22**. 1725 (2007).

2F1424 キメラタンパク質を用いた Rhodobacter capsulatus 由来 Photoactive Yellow Protein の相互作用部位の解明

Analysis of interaction sites on the Photoactive Yellow Protein of Rhodobacter capsulatus with chimeric proteins

Mayu Shimad, Yoichi Yamazaki, Hironari Kamikubo, Mariko Yamaguchi, Mikio Kataoka (*Grad. Sch. Mat. Sci., NAIST*)

Photoactive Yellow Protein (PYP) is a photoreceptor protein that absorbs blue light with p-coumaric acid as a chromophore. We identified the target protein of PYP named PBP from Rhodobacter capsulatus (Rc-PYP). PBP interacts with Rc-PYP in light dependent manner. This is the only target protein of PYP homologues revealed so far. Rc-PYP shows no substantial conformation changes upon absorption of light. The observation raised a serious question how PBP recognizes the photolyzed state of Rc-PYP. In order to clarify the mechanism of light dependent interaction of PBP with Rc-PYP, we aimed to identify the interaction sites on Rc-PYP by using chimeric mutants between Rc-PYP and Halorhodspira halophila PYP (Hh-PYP). Rc-PYP and Hh-PYP are separated into four segments considering secondary structure and amino acid conservation. The first block contains N-terminal 30 residues, the second block contains 31st -57th residues, the third block contains 58th - 86th and the fourth block contains remaining residues. Chimeric proteins were designed to replace some of four segments into a parent protein. Binding ability of PBP was verified spectroscopically, since the complex formation brings distinguishable spectral shift. The complex formation was also examined by photocycle kinetics the size exclusion chromatography. As a result, chimeric proteins having the second block of Hh-PYP depressed binding ability. While chimeric proteins having the other block(s) of Hh-PYP did not bind PBP. The further analyses are required to identify interaction sites.

2F1436 FTIR study of Aureochrome that possesses LOV domain at the C-terminus

Shota Ito[1], You Zhang[1], Tatsuya Iwata[2], Osamu Hisatomi[3], Fumio Takahashi[4], Hironao Kataoka[5], Hideki Kandori[1] ([1]*Nagoya Inst. Tech*, [2]*Ctr. Fost. Yng. Innov., Nagoya Inst. Tech*, [3]*Grad. Sch. Sci., Osaka Univ*, [4]*PRESTO, JST*, [5]*Botanical Gardens, Tohoku Univ*)

LOV domain is a blue-light sensor that binds an FMN. In many blue-light sensors, LOV domain is located at the N-terminal side. For example, phototropin possesses two LOV domains at the N-terminal side and regulates serine-threonine kinase domain at the C-terminal side[1]. By means of light-induced difference FTIR spectroscopy, we have studied photoactivation mechanism of LOV domains in phototropin[2].Aureochrome, a novel photosensor protein from *Vaucheria frigida*,possesses a LOV domain at the C-terminus, while bZIP domain is located at the N-terminal side[3].It is reported that the bZIP domain of aureochrome can recognize a DNA sequence (TGACGT), when its LOV domain is photoactivated. An interesting question is how signal transductions in LOV domains differ between the N- and C-termini?
In this study, we measured light-induced structural changes of aureochrome (bZip-LOV) by low-temperature FTIR spectroscopy, where temperature-dependent structural changes were observed at 150, 200 and 295 K. The obtained spectra were compared with those of an isolated LOV domain, and those with DNA. We also measured the mutants of Phe298 and Gln317, which are located at the β-sheet near the FMN and identified as the important residues for the structural changes of LOV domain in phototropins[2]. Molecular mechanism of the light-switch in aureochrome will be discussed.

1. Briggs, R, W., et al. *Trends Plant Sci*. **7**, 204-210 (2002).
2. Iwata, T., et al. *BIOPHYSICS* **7**, 89-98 (2011).
3. Takahashi, F., et al. *Proc. Natl. Acid. Sci. USA* **104**, 19625-19630 (2007).

2F1448 LOV ドメインを鋳型としたレドックス感受性蛍光タンパク質の開発

Construction of LOV-based redox-sensitive fluorescent proteins

Yukiko Ono[1], Tatsuya Iwata[2], Hideki Kandori[1] ([1]*Nagoya Inst. Of Technol.*, [2]*Ctr. Fost. Yng. Innov. Res., Nagoya Inst. Tech.,*)

LOV domain is a blue-light sensor domain that was first found in phototropin. LOV domain binds a flavin mononucleotide (FMN) as a chromophore, and its sensor function is initiated by the adduct formation with an S-H group of Cys. It was proposed that the C/A-based mutant LOV domains (iLOV) could be better fluorescent probe than GFP because of smaller size [1]. In such case, highly fluorescent iLOV proteins are desired, where the oxidized FMN emits green light. It should be however noted that FMN is a redox active cofactor, and photoreduction of the oxidized form causes florescence quenching. In other words, this fact suggests that redox-sensitive fluorescent proteins may be designed from the C/A mutants of LOV domains. The purpose of this research is to construct redox-sensitive probes using random mutagenesis into Arabidopsis phot2-LOV2 C426A mutant. The candidate plasmids were transformed into JM109 E. coli cells. The bacteria were grown in liquid media in the dark, and the fluorescence quenching by light illumination was used as a screening method to find desired proteins. Consequently, we found a mutant showing faster photoreduction and lower fluorescence level compared to C426A. Another mutant showed slower photoreduction than C426A. Interestingly, the mutated amino acid residues were distant from FMN. Highly redox-sensitive fluorescent proteins are searched by this method, and the molecular properties of the obtained mutant proteins will be discussed.

[1] Chapman S et al. PNAS USA 105, 20038 (2008)

2F1510 クラミドモナス由来の全長フォトトロピンが示す光反応ダイナミクスの時間分解検出

Time-resolved study on photoreaction dynamics of full-length phototropin from Chlamydomonas reinhardtii

Yusuke Nakasone[1], Koji Okajima[2], Yusuke Aihara[3], Akira Nagatani[3], Satoru Tokutomi[2], Masahide Terazima[1] ([1]*Grad. Chem. Sci, Kyoto Univ.*, [2]*Grad. Sci, Osaka Prefecture Univ.*, [3]*Grad. Biol. Sci, Kyoto Univ.*)

Phototropin (phot) is a blue-light dependent kinase which regulates phototropism of higher plants. It contains two LOV domains (LOV1 and LOV2) as light sensor domains and adduct formations between their chromophores and Cys residues upon light illumination are essential for the signal transduction. So far, biophysical studies of phot has been restricted to shorter fragments such as the LOV domains, LOV2-linker, and the LOV1-LOV2 tandem protein, because of the difficulty of purification of the full-length protein. Kinase activation of phot has been studied in vitro by autophosphorylation assays, which, however, did not provide any information about the signal transfer to the kinase after the activation of LOV domains. In this study, we used full-length Chlamydomonas phototropin (Cr-phot), which regulates sexual differentiation. In order to understand the mechanism of the kinase activation, we have investigated the reaction dynamics of full-length Cr-phot by using the transient grating (TG) method. The TG signal showed that the adduct formation was completed within few microseconds, which is similar to the case of shorter constructs. Additionally, we have detected global conformational changes of protein moiety in milliseconds time scale as a decrease of diffusion coefficient. CD measurements also showed that the secondary structure was partially changed upon light illumination. We will discuss the photochemistry of intact protein on the basis of these findings.

2F1522 N 末アミノ酸残基の有無は AppA BLUF ドメインの保存されたトリプトファン残基の位置に影響しない

N-Terminal Truncation Does Not Affect the Location of a Conserved Tryptophan in the BLUF Domain of AppA from *Rhodobacter sphaeroide*

Masashi Unno[1], Yuuki Tsukiji[1], Kenshuke Kubota[1], Shinji Masuda[2,3] ([1]*Depart. Chem. Appl. Chem., Saga University*, [2]*Center for BioRes. & Inform., Tokyo Inst. Tech.*, [3]*PRSTO, JST*)

The flavin-binding BLUF domains are a class of blue-light receptors, and AppA is a representative of this family. Although the crystal and solution structures of several BLUF domains have already been obtained, there is a key uncertainty

regarding the position of a functionally important tryptophan (Trp104 in AppA). In the first crystal structure of an N-terminally truncated BLUF domain of AppA133 (residues 17-133), Trp104 was found in close proximity to flavin (Trp_{in}), whereas in a subsequent structure with an intact N-terminus AppA126 (residues 1-126), Trp104 was exposed to the solvent (Trp_{out}). A recent study compared spectroscopic properties of AppA126 and AppA133 and claimed that the Trp_{in} conformation is an artifact of N-terminal truncation in AppA133. In this study, we compared the flavin vibrational spectra of AppA126 and AppA133 by using near-infrared excited Raman spectroscopy. In addition, the conformations as well as the environments of Trp104 were directly monitored by ultraviolet resonance Raman spectroscopy. These studies demonstrate that the N-terminal truncation does not induce the conformational switch between Trp_{in} and Trp_{out}.

2F1534 Substrate-Dependent Measurement Revealed Different Protein Conformations on Photoactivation and DNA Repair of E. coli CPD Photolyase

I Made Mahaputra Wijaya[1], Yu Zhang[1], Junpei Yamamoto[2], Kenichi Hitomi[3], Shigenori Iwai[2], Elizabeth D. Getzoff[3], Hideki Kandori[1] ([1]*Nagoya Institute of Technology*, [2]*Osaka University*, [3]*The Scripps Research Institute, La Jolla, USA*)

Photolyases (PHRs) are flavoproteins that repair UV-induced damaged DNA by the use of near UV/blue light. PHR that repair cyclobutane pyrimidine dimers (CPDs) and (6-4) photoproducts are called CPD-PHR and (6-4) PHR, respectively. In order to study protein-mediated chemical reactions on PHRs, light-induced difference FTIR spectroscopy was applied. Previously, we have successfully measured FTIR difference spectra of the light-induced activation and DNA repair of *X. laevis* (6-4) PHR [1] and *E. coli* CPD-PHR [2].
CPD-PHR can repair not only cyclobutane thymine dimer, but also cyclobutane cytidine dimer and dimers from combination thymine-cytidine and vice versa. In the present study, we introduced those different dimer compositions as DNA substrates and observed FTIR light-induced activation and DNA repair spectra of CPD-PHR. From these substrate-dependent measurements, we successfully observed different signals of peptide backbone, α-helices, and β-sheets of the enzyme, suggesting different protein conformations occurred during photoactivation and photorepair, which depend on the substrates. In addition, we also successfully observed difference spectra on binding of each different substrate to CPD-PHR enzyme. Enzyme conformations difference of photoactivation, photorepair, and substrate-enzyme binding will be discussed on the basis of the spectral comparison among each substrate.

[1] Zhang et al. Biochemistry 50, 3591 (2011)
[2] Wijaya et al. to be submitted

2F1546 アニオンラジカル型の(6-4)光回復酵素による DNA 修復

Repair of damaged DNA by the anion radical form of (6-4) photolyase

Daichi Yamada[1], Yu Zhang[1], Tatsuya Iwata[2], Junpei Yamamoto[3], Kenichi Hitomi[4], Shigenori Iwai[3], Elizabeth Getzoff[4], Hideki Kandori[1] ([1]*Nagoya Inst. Tech.*, [2]*Ctr. Fost. Yng. Innov. Res., Nagoya Inst. Tech.*, [3]*Grad. Sch. Eng. Sci., Osaka Univ.*, [4]*The Scripps Res. Inst. USA*)

Photolyases (PHRs) are repair enzymes of UV–damaged DNA by utilizing near–UV/blue lights, which maintain genetic integrity by reverting UV–induced photoproducts into normal bases. The FAD chromophore of PHRs has four different redox states: oxidized (FAD^{ox}), anion radical ($FAD^{\cdot-}$), neutral radical ($FADH^{\cdot}$) and fully reduced ($FADH^{-}$) forms, and the enzymatically active state of PHR is $FADH^{-}$. Mechanism of photoactivation from FAD^{ox} to $FADH^{-}$ by proton–transfer coupled electron transfer through $FAD^{\cdot-}$ and $FADH^{\cdot}$ is intriguing, and we recently obtained difference FTIR spectra among four redox states of *Xenopus* (6–4) PHR by selecting temperature and illumination conditions [1]. According to the FTIR analysis, the protein structure of the $FAD^{\cdot-}$ form trapped at 200 K is very similar to that of the $FADH^{-}$ form, suggesting that $FAD^{\cdot-}$ might have the DNA repair activity. To test this hypothesis, we attempted to stabilize the $FAD^{\cdot-}$ state at room temperature, by introducing the N392C mutant that mimics insect cryptochromes and cyanobacterial cryptochrome mutant [2, 3]. The $FAD^{\cdot-}$ form is observed even at room temperature, and FTIR spectroscopy detects possible photorepair signals of (6–4) photoproduct by the $FAD^{\cdot-}$ form. Activation and repair mechanism of the N392C mutation of (6–4) PHR will be discussed on the basis of the present spectroscopic observations.

[1] Yamada D. et al, submitted.
[2] Kao Y.-T. et al, *J. Am. Chem. Soc.* 130, 7695–7701 (2008).
[3] Iwata T. et al, *Biochemistry* 49, 8882–8891 (2010).

2F1558 光センサータンパク質 UVR8 の解離・回復反応カイネティックスの測定

The study of the dissociation and recovery reaction kinetics for photo-sensor protein UVR8

Takaaki Miyamori[1], Yusuke Nakasone[1], Kenichi Hitomi[2], John M. Christie[3], Elizabeth D. Getzoff[2], Masahide Terazima[1] ([1]*Grad. Sci. Chem., Univ. Kyoto*, [2]*Scripps Research Inst.*, [3]*Univ. Glasgow*)

Plants can perceive and respond to UV-B in order to protect them from UV-light. UVR8 from Arabidopsis has been found as a UV-light sensor protein, which mediates gene expression responses to establish the UV protection. Dimers of UVR8 are dominant under dark condition in the living cells. Doubly hydrogen-bonded salt bridges, which link R286 with D107 and R146 with E182 is thought to make the dimer stable. Upon UV-B light illumination, the dimer dissociates into the monomer, and this dissociation reaction is believed to be important for the biological function. Generally, light sensor proteins possess specific chromophore molecules to absorb light and initiate photochemical reactions for signal transduction. Interestingly, however, the UVR8 protein employs Trp residues, particularly W285 to sense the environmental light condition instead of having such specific chromophores. We investigate the kinetics of its dissociation reaction by the time-resolved transient grating method (TG method). In order to examine the importance of above key residues (R286, R146, W285), we performed the same kinetic measurements for the following mutants; R146A/R286A and W285F. Furthermore, the dark recovery reaction (dimerization) was studied by the circular dichroism method (CD method).

2G1400 膜融合におけるストーク構造からの変形：分子動力学シミュレーション

Morphology change of fusion stalk studied by molecular dynamics simulation

Shuhei Kawamoto, Wataru Shinoda (*Nano. AIST*)

The life cycle of living organisms involves membrane fusion. In eukaryotes, membrane fusion is ubiquitous. As a plausible fusion pathway, the stalk-pore pathway has been identified and explored theoretically. However, stability of transiently appeared morphologies and driving force of the morphology change are not clear yet. We have investigated the fusion pore formation process from the stalk structure by coarse-grained molecular dynamics simulations. We found that the stalk was stabilized when the lipid membranes contain phosphatidylethanolamine (PE), which are more likely found around the stalk. By applying tension selectively on the proximal leaflet, we observed the progress of pore formation. The energy required for the fusion pore formation is estimated as about 50 k_BT, which is close to that obtained from the previous theoretical study.

2G1412 蛍光検出と電気計測による膜タンパク質計測に向けた脂質膜チャンバアレイ

Lipid bilayer chamber array toward fluorescent and electrophysiological measurement of membrane proteins

Taishi Tonooka[1], Ryuji Kawano[2], Koji Sato[1], Toshihisa Osaki[2], Shoji Takeuchi[1] ([1]*Institute of Industrial Science, The University of Tokyo*, [2]*Kanagawa Academy of Science and Technology*)

Artificial lipid bilayer chamber, which is a small chamber sealed with lipid bilayer, is an attractive tool for membrane protein analysis because of its purity. Previous studies of artificial lipid bilayer chambers for membrane protein analysis had been focused on two main streams: one was for fluorescent measurement, the other for electrophysiological measurement. Recently, the devices for two-way measurement of fluorescent imaging and electrophysiological recording have been developed. These devices allow us to combine the information of channel conformational change resulting in electrical signals and molecular interaction between channels and ligands. Therefore, they have potential to demonstrate novel membrane protein properties. Here, we propose an array system leading to multi-channel two-way measurement as a next challenge for high-throughput membrane protein analysis. In this study, we successfully demonstrated the function of the pore-forming membrane protein, α-hemolysin, by electrophysiological measurement, and succeeded in Ca^{2+} ion concentration measurement in the chambers by using Ca^{2+} ion fluorescent indicators. We believe that this technique will be a strong tool for basic research or drug screening of membrane proteins.

2G1424 蛋白質毒素ライセニンがスフィンゴミエリンを含む脂質膜中に誘起するポア形成： 単一 GUV 法による研究

Single Giant Unilamellar Vesicle Method Reveals Lysenin-Induced Pore Formation in Lipid Membranes Containing Sphingomyelin

Jahangir Md. Alam[1], Toshihide Kobayashi[2], Masahito Yamazaki[1] ([1]*Int. Biosci. Sec., Grad. Sch. Sci. Tech., Shizuoka University*, [2]*Lipid Bio. Lab., RIKEN*)

Lysenin is a sphingomyelin (SM) -binding pore-forming toxin. To reveal the interaction of lysenin with lipid membranes, we investigated lysenin-induced membrane permeation of a fluorescent probe, calcein, through dioleoylphosphatidylcholine (DOPC) /SM, DOPC/SM/cholesterol (chol), and SM/chol membranes, using the single giant unilamellar vesicle (GUV) method[1]. The membrane permeability coefficient of calcein increased over time to reach a maximum, steady value, P^s, which persisted for a long time (100-500 s), indicating that pore concentration increases over time and finally reaches its steady value. The P^s values increased as the SM/lysenin ratio decreased, and at low concentrations of lysenin the P^s values of SM/DOPC/chol (42/30/28) -GUVs were much larger than those of SM/DOPC (58/42) -GUVs. The dependence of P^s on the SM/lysenin ratio for these membranes was almost the same as that of the fraction of sodium dodecyl sulphate (SDS)-resistant lysenin oligomers. On the other hand, lysenin formed pores in GUVs of SM/chol (60/40) membrane in homogeneous liquid-ordered phase, indicating that the phase boundary is not necessary for the pore formation. The P^s values of SM/chol (60/40)-GUVs were smaller than those of SM/DOPC/chol (42/30/28)-GUVs even though the SDS-resistant oligomer fractions was similar for both the membranes, suggesting that there are irreversible oligomers (or pre-pores) before conversion to pores. Based on these results, we discuss the elementary processes of lysenin-induced pore formation.

1. *Biochemistry, in press*

2G1436 人工細胞ベシクルにおける脂質ドメインへの化合物局在を介したドメインサイズと膜崩壊率の制御

Localization of bulky-molecules in raft-like domains on phase-separated liposomes: Control of domain size and bursting rate of liposome

Miho Yanagisawa[1], Damien Baigl[2], Kenichi Yoshikawa[3] ([1]*Grad. Sch. Sci., Kyushu Univ.*, [2]*Depart. Chem., Ecole Normale Superieure*, [3]*Depart. Biomed. Info., Doshisya Univ.*)

It is established that the cell-sized liposomes composed of a saturated lipid DPPC, an unsaturated lipid DOPC, and cholesterol (Chol) show phase separation below the transition temperature, and form domain structures like lipids rafts [1]. These micro-domains grow up to mono-domain, so as to minimize interfacial instability. By applying the phase separation of lipids, we report two control methods, i.e., a size-control of domains by the addition of poly(ethylene glycol)-conjugated Chol (PEG-Chol) [2], and a rate-control of UV-induced bursting of liposomes by the addition of Azo-TAB molecules [3]. As for the domain-size control, dispersed micro-domains <1μm were observed in the presence of PEG-Chol above a critical composition. The transition from global- to micro-segregation is interpreted in terms of the competition between steric repulsive interaction between the bulky-head groups of PEG-Chol and the cost in line energy along the domain boundaries. On the other hand, the addition of Azo-TAB into the membrane expands it and induces bursting of liposomes due to the UV irradiation. Furthermore, the bursting rate was controlled by the area fraction of domains rich in DPPC. These achievements lead us to further understanding the lipid raft structure from physicochemical view.

[1] M. Yanagisawa et al., 2007 Biophys. J. 92:115.
[2] M. Yanagisawa, et al., 2012 Soft matter, 8:488.
[3] A. Diguet, et al., 2012 J. Am. Chem. Soc., 134:4898.

2G1448 PI4P と脂質膜曲率による Kes1 ステロール輸送活性の制御

Regulation of Kes1 sterol transport activity by PI4P and lipid membrane curvature

Hirokazu Yokoyama[1], Masaki Wakabayashi[1], Yasushi Ishihama[1], Minoru Nakano[2] ([1]*Graduate School of Pharmaceutical Sciences, Kyoto University*, [2]*Graduate School of Medicine and Pharmaceutical Sciences, University of Toyama*)

Kes1 is one of seven members of the yeast Oxysterol binding protein homolog (Osh) family. This protein transfers sterols between plasma membrane and the Golgi, and regulates Golgi secretory function. However, these detailed mechanisms have not been well understood. In this work, we investigated the effect of lipid membrane state (lipid composition and membrane curvature) on Kes1 activities (sterol extraction and transport) by fluorescence resonance energy transfer. Especially we focused on phosphatidylinositol 4-phosphate (PI4P) because PI4P is considered to stimulate Kes1 sterol transport activity. Effects of membrane curvature were evaluated by using liposomes with different size. For planar membranes, while two anionic lipids, phosphatidylinositol and phosphatidylserine, had little effect on the Kes1 activities, PI4P was found to affect on the Kes1 activities depending on PI4P amount: Although a small amount (1 mol%) of PI4P stimulated sterol extraction and transport by Kes1, larger amount (~10 mol%) of PI4P inhibited the Kes1 activities. This sterol extraction inhibitory effect of PI4P was dependent on the membrane curvature. That is, even 1 mol% of PI4P inhibited the sterol extraction from highly curved membranes, suggesting that the membrane curvature regulates the effect of PI4P. These findings suggest a possibility that PI4P and the membrane curvature are regulating factors of Kes1 biological function.

2G1510 リン脂質輸送タンパク質 Sec14 の脂質輸送メカニズムの解明

Elucidation of lipid transfer mechanism of phospholipid transfer protein Sec14

Chisato Takahashi[1], Makiko Yamada[1], Masaki Wakabayashi[1], Yasushi Ishihama[1], Minoru Nakano[2] ([1]*Grad. Sch. Pharm., Kyoto Univ.*, [2]*Grad. Sch. Pharm., Toyama Univ.*)

Sec14, a major yeast phosphatidylinositol/phosphatidylcholine transfer protein (PITP) regulates lipid membrane trafficking from the trans-Golgi network. However, its detailed mechanism remains to be elucidated. In this work, we investigated PITP-membrane interactions by surface plasmon resonance (SPR) and fluorescence spectroscopy. Sec14 WT and two mutants, which have been designed to ablate their phosphatidylcholine (PC)-binding ability (Sec14 II) and phosphatidylinositol (PI)-binding ability (Sec14 AD) were used and compared. In the fluorescence spectroscopy, capture of pyrene-labelled PC by PITPs from large unilamellar vesicles (LUVs) was detected by the decrease in the pyrene excimer/monomer intensity ratio. The results showed that Sec14 WT and its mutants, including PC-binding mutant (Sec14 II), have PC transfer activity. In the presence of PI, however, PC transfer activity for Sec14 II was reduced, suggesting that Sec14 II has higher affinity for PI.

Binding behavior of PITPs to immobilized LUVs was evaluated by SPR method. Sec14 II exhibited higher binding to PC membrane than Sec14 WT and AD, which have intact PC binding pocket. On the other hand, membrane binding of Sec14 II was decreased in the presence of PI, Ligand for this mutant. These findings that Sec14 represents reduced affinity to the membranes that contain ligands for the protein suggest the ingenious lipid transfer mechanism, by which Sec14 dissociates from the membrane when it captures PC or PI in appropriate position of the binding pocket.

2G1522 ゲル、アミノ酸、水素化アモルファスシリコンを用いた光制御イオン伝導整流素子

Photo-controlled ion conductive rectification element using gel, amino acids and hydrogenated amorphous silicon film

Takaaki Ichikawa[1], **Hiroki Suzuki**[1], Ryohei Matsueda[1], Hiroshi Masumoto[2], Takashi Goto[3], Yutaka Tsujiuchi[1] ([1]*Department of Material Science and Engineering, Akita University*, [2]*Center for Interdisciplinary Research, Tohoku University*, [3]*Institute for Materials Research, Tohoku University*)

Ionic conduction, in solution as well as in intermediate states between a liquid and a solid, such as gels, is a phenomenon key to inter-conversion between light energy, chemical energy, and electric energy. As such, this phenomenon is essential for devices that store, generate, and convert electric energy, including batteries, photovoltaics, capacitors, and actuators. While not dismissing these applications, this article focuses on ionic conduction in nontoxic materials to discuss the creation of elements coated with multi-layer functional thin-films using a combination of different technologies, such as the rectification property of ionic conduction, photo-induction control, and the use of wavelength conversion materials, and the potential application of these materials to biological tissue. Amino acid is the elementally element of bio molecule, has potential of diversity to electro chemical device. Our group has been working with amino acids dispersed in agarose gel, and with semi-conductive material, hydrogenated amorphous silicon (a-Si: H) film. In previous report, ion

conductive behavior of neutral, acidic, or basic amino acid dispersed in agarose gel are characterized. In this conference, we report an attempt of measuring a photo-controlled effect of a-Si:H film on ion conducting behavior of bio-molecules in detail, comparing several hydrogen concentrations that used in process gas for preparation of a-Si:H.

2G1534 高速 AFM による CFTR チャネルの動態観察

Single molecular observation of CFTR channels by high speed AFM

Hayato Yamashita[1], Kazuhiro Mio[2], Muneyo Mio[2], Takayuki Uchihashi[3], Masato Yasui[1], Toshio Ando[3], Yoshiro Sohma[1,4] ([1]*Pharmacol., Keio Univ. Med. Sch.*, [2]*AIST*, [3]*Dept of Physics, Kanazawa Univ.*, [4]*Dalton Cardiovas. Res. Cen., Univ. Missouri-Columbia*)

Cystic Fibrosis Transmembrane conductance Regulator (CFTR) chloride channel, a member of ABC transporter superfamily, gates following ATP-dependent conformational changes of the nucleotide binding domains. Mutations in the CFTR gene cause cystic fibrosis in which salt, water and protein transports are defective in various tissues. Channel function of CFTR has been mainly studied by measuring ionic current going through the pore using the patch-clamp technique, which has given us many important findings about CFTR dysfunction. On the other hand, recent advances in X-ray crystallography provide atomic-level structures for several bacterial and mammalian ABC transports. However, neither the electro-physiology nor the crystal structure can give us the information about the molecular dynamic processes of CFTR proteins.
In this study, we applied the high speed atomic force microscopy (HS-AFM) to image dynamic structural changes and interactions occurring in individual CFTR molecules. The HS-AFM visualized a dimeric formation of DMM-solubilized, purified WT-CFTR molecules attached on the stage over sideways. Next we attempted to observe the PKA-dependent phosphorylation process of Regulatory (R)-domain in CFTR. With applying a solution containing PKA catalytic subunits, we confirmed many small molecules appeared around CFTR and occasionally bound to the bottom of CFTR molecules where R-domain was supposed to be located. Now we are attempting to visualize the phosphorylation-induced conformational change of the CFTR R-domain.

2G1546 KcsA チャネルの細胞内ドメインは不活性化に影響を与える

The KcsA channel cytoplasmic domain effects on the inactivation gating

Minako Hirano[1,2], Yukiko Onishi[2], Daichi Okuno[2], Toru Ide[1,2] ([1]*GPI*, [2]*RIKEN*)

The KcsA channel is a representative potassium channel that is activated by changes in pH. Recently, we found that the cytoplasmic domain (CPD) acts as a pH-sensor by observing significant confirmation changes there in response to pH. These changes can influence the opening and closing of the KcsA channel. A selectivity filter region within the KcsA channel is also known to regulate gating by forming activation and inactivation states. However, it is not clear how the CPD and the selectivity filter region coordinate. We therefore made a mutant channel that has the wild-type filter and a CPD with all its negative charges neutralized. We found that this mutant had high activity independent of pH and no inactivation gating, indicating removal of negative charges in the CPD causes removal of inactivation. These results suggest that the CPD primarily regulates activation gating, and conformational changes of the CPD effects on the inactivation gating.

2G1558 原子間力顕微鏡によるカリウムイオンチャネル KcsA の脂質膜中でのゲート開閉構造の直接観察

Direct Observation of Ion Entryway of Potassium Channel KcsA in Lipid Bilayer by Atomic Force Microscopy

Ayumi Sumino[1], Takashi Sumikama[2], Masayuki Iwamoto[2], Takahisa Dewa[1,3], Shigetoshi Oiki[2] ([1]*Grad. Sch. Eng., Nagoya Inst. Tech.*, [2]*Deprt. of Mol. Physiol. and Biophys., Univ. of Fukui Fac. Med. Sci.*, [3]*JST-PRESTO*)

The crystallography has provided high resolution structure of channel proteins, whereas they are mostly in the absence of the lipid bilayer, and even some parts are remained unsolved. For the open conformation of the KcsA potassium channel, structure of the intracellular entryway is still elusive, even though it is critical to understand the ion permeation mechanism. Here, we examined the native transmembrane structure of the KcsA channel embedded in the membrane using atomic force microscopy (AFM). To observe the ion entryway from the intracellular side, the cytoplasmic domain (CPD) was truncated. In the open conformation, the individual subunits in the tetramer with the pore open at the center were resolved. The measured longitudinal length is longer than that of crystallography, which indicates that AFM successfully captured the unresolved structure of the terminal parts. The crystallographycally-missed terminal helix (bulge helix) was grafted to the pore entrance using the molecular dynamics simulation, which demonstrated that the bulge helices fluctuate vigorously. The single-channel currents for the CPD-truncated channel exhibited fluctuating currents, indicating that the helices chop up the steady ionic currents. In this study an integrated approach, involving AFM measurements, MD simulation and single-channel current recordings, revealed the dynamic feature of the ion entryway of the KcsA channel.

2G1610 全反射赤外分光法による KcsA のイオン選択フィルターの振動解析

The Vibrational Analysis of the Selectivity Filter of KcsA by using ATR-FTIR Spectroscopy

Yuji Furutani[1,2], Hirofumi Shimizu[3], Yusuke Asai[1], Tetsuya Fukuda[1], Shigetoshi Oiki[3], Hideki Kandori[1] ([1]*Grad. Sch. Tech., Nagoya Inst. Tech.*, [2]*Inst. Mol. Sci.*, [3]*Facul. Med. Sci., Univ. Fukui*)

KcsA is a potassium ion channel, which selectively permeates K^+ ions. The X-ray structure of KcsA showed that the carbonyl oxygens of the selectivity filter (TVGYG) interacts with K^+ or Na^+ ions. Distribution of ions in the selectivity filter and interactions between ions and carbonyl oxygens are crucial to understand the role of the selective filter in KcsA channel. To address this question, we used attenuated total reflection Fourier-transform infrared (ATR-FTIR) spectroscopy which has been recently utilized for the study of the ion-protein interaction[1].
Two solutions containing potassium (x mM; x =3, 10, 20, 50, 200) and sodium (200-x mM) cations or only sodium cation (200 mM) were alternately flowed through the KcsA/liposome samples on the ATR cell, which provided ion-exchange induced difference FTIR spectra at pH 7. The up-shift of the amide I vibration upon binding of potassium ions were observed, which means that the carbonyl groups in the amide groups in the KcsA(K^+) has weaker interactions than those in the KcsA(Na^+). From the spectral comparison of the wild-type and the Y78F mutant proteins, we concluded that the amide-I vibrations originate from the C=O groups in the selectivity filter[2].
(1) Y. Furutani, T. Murata, H. Kandori, J. Am. Chem. Soc. 133 (9), 2860-3, 2011.
(2) Y. Furutani, H. Shimizu, Y. Asai, T. Fukuda, S. Oiki, H. Kandori, submitted.

2H1400 中性子散乱による心筋症関連トロポニン変異体のダイナミクス測定

Dynamics of cardiomyopathy-causing mutant of troponin observed by neutron scattering

Tatsuhito Matsuo[1], Francesca Natali[3], Giuseppe Zaccai[2,3], Satoru Fujiwara[1] ([1]*QuBS, JAEA*, [2]*CNRS*, [3]*ILL*)

Troponin (Tn) is a protein that consists of three subunits (C, I, and T) and regulates the muscle contraction depending on the intracellular Ca^{2+} concentration. K247R mutation of TnT is known to cause the familial hypertrophic cardiomyopathy. For understanding the molecular mechanism of pathogenesis of cardiomyopathy, it is important to elucidate the relationship between differences in dynamics (thermal fluctuations of a protein) and function of troponin caused by mutation because dynamics of a protein is crucial for its function.
To detect possible changes in dynamics of troponin caused by mutation, elastic incoherent neutron scattering experiments were carried out on solution samples of the wild type (80 mg/ml), and K247R mutant (40 mg/ml) in the D_2O buffer containing Ca^{2+}, at the thermal neutron backscattering spectrometer IN13 in the Institut Laue-Langevin (Grenoble, France), at temperatures between 280 K and 292 K with an interval of 3 K.
Root mean square displacements (rmsd) of hydrogen atoms in the protein were obtained from the spectra at each temperature. From the slope of the rmsd with respect to the temperature, force constants (<k>), which reflect the resilience of the protein, were calculated. The <k> values for the wild type and K247R mutant were 0.077 ± 0.035 N/m and 0.046 ± 0.026 N/m (mean $\pm$ s.d.), respectively. This suggests that the disease-causing mutant is more flexible than the wild type. The large flexibility might modulate Ca^{2+} signal transmission mechanism, leading to the functional aberration.

2H1412 スピンラベル ESR 距離測定による細いフィラメントのアクチン、トロポミオシン、トロポニンの動的構造解析

Structural dynamics of actin, tropomyosin, and troponin in the thin filament as studied by distance measurements using spin-labeling ESR

Keisuke Ueda[1,2], Chenchao Zhao[1], Akie Yamamoto[1], Takayasu Somiya[1], Tomoki Aihara[1,3], Shoji Ueki[4], Masao Miki[5], **Toshiaki Arata**[1] ([1]*Grad. Sch. Sci., Osaka Univ.*, [2]*Inst. Prot. Res., Osaka Univ.*, [3]*Harima Inst., Riken*, [4]*Tokushima-Bunri Univ.*, [5]*Univ. Fukui*)

We can measure the distance between spin labels on protein complex on nanometer scale by cw and pulse ESR (1-3). Using pulse ESR for reconstituted thin filament we previously found that the regulatory-switch region of TnI moves by ~4 nm between TnC and presumably actin (4). The heart beating is controled by phosphorylation of cTnI. Recently we measured the interspin distance between cTnC and regulatory-switch region of cTnI by cw-ESR, and found that cTnI binding to cTnC was loosened by PKA or PKC phosphorylation which may cause Ca^{2+} desensitization. We next examined how tropomyosin (Tm) and actin undergo structural changes in the thin filament in response to Ca^{2+}. The side-chain mobility of a spin label on the 1-284 a.a. of Tm showed unexpectedly no Ca^{2+} effect (5). The distance between Cys374 and Mn^{2+} within actin monomer also increased by ~0.2 nm when actin filament was decorated with Tm-Tn with and without Ca^{2+}. Then, ^{14}N-based spin label bound to Cys374 of each actin whereas ^{15}N-label bound to a cysteine at several positions of Tm. Distance was successfully determined by fitting the cw-spectrum obtained after ^{14}N-label spectrum of excess actin was cancelled out for distinct spectral characteristics of ^{14}N- and ^{15}N-labels. Ca^{2+} effects on the distance were restricted at the N-C joints of Tm. More spin-labeling points are needed for final conclusion. 1.Ueki et al. Biochem. 44 411('05). 2. Nakamura et al. JMB 348 127('05). 3. Abe et al. AMR 42 473('12). 4. Aihara et al. JBC 285 10671('10). 5. Ueda et al. Biophys J 100 2432('11).

2H1424 アクチン周りのハイパーモバイル水の形成とその熱力学的考察

Formation of hyper-mobile water around actin and its thermodunamic considerations

Makoto Suzuki, George Mogami, Tetsuichi Wazawa, Asato Imao, Noriyoshi Ishida (*Tohoku Univ. Grad. Sch. Eng.*)

This paper introduces recent studies on the hyper-mobile water around actin in G- and F- forms. Microwave dielectric relaxation spectroscopy (DRS). The DRS measurements showed that F-actin exhibits dual hydration properties as a structure-maker and a structure-breaker. Thus, in addition to the water molecules with lowered rotational mobility that form a constrained hydration shell around the F-actin, there exist water molecules with rotational relaxation frequencies higher than those of bulk water, which are here referred to as hyper-mobile water (HMW). HMW was detected in G-actin solution, and significantly increased upon polymerization into F-actin. Formation of HMW was investigated by measuring the temperature dependence of the dispersion amplitudes of HMW and constrained water. The van't Hoff enthalpies of those water from the bulk were estimated. The results indicate that formation of HMW is endothermic and that of constrained water is exothermic. Isothermal titration calorimetry experiments were performed to measure the exothermic heat of depolymerization of F-actin in G-buffer. These results will be reported at the meeting.

2H1436 アクチン様トレッドミリングモータが満たすべき最小条件

Minimum requirements for the actin-like treadmilling motor system

Akihiro Narita (*Grad. Sch. Sci., Nagoya Univ.*)

Actin is one of the most abundant proteins in eukaryote cells, which forms a double stranded filament. The actin filament is not only a main component of the cytoskeleton, but also acts as a motor protein which moves toward one specific end, the barbed end, driven by polymerization at the barbed end and depolymerization at the other end, the pointed end, without any associated proteins. This motor activity is referred to as "treadmilling" and it represents the simplest motor system known, consisting of only one 42 kDa protein, actin. The mechanisms of molecular motors are not fully understood, although many motors have been identified, including myosins, kinesins, dyneins and F1-ATPase. Therefore, knowing the minimum requirements of the actin-like motor system may help us to understand not only actin-like motors but also many other motors. We clarified there are three requirements for the treadmilling motor system by computer simulations: 1) Nucleotide binding and ATPase activity in the filament; (2) Polarity in the rates of polymerization and depolymerization between the two ends; and (3) The dependence of the subunit-subunit interactions on the bound nucleotide. These requirements are simple and this knowledge should facilitate the development of artificial molecular motor systems in the future.

2H1448 3 次元トラッキングによる *in vitro* アクチンフィラメントモーティリティーアッセイ

Three-dimensional tracking of gliding actin filament in an *in vitro* motility assay

Tatsuya Naganawa, Togo Shimozawa, Tomoko Masaike, Takayuki Nishizaka (*Gakushuin Univ.*)

In an *in vitro* motility assay of actin filament (AF) and skeletal myosin system, it has been reported that the AF rotated around filament axis during its sliding motion. However, the previous two researches had reported the rotation in oposite direction by each detection method and assay system (Nishizaka *et al.*, *Nature*; 1993; Beausang *et al*., *Biophys J.*, 2008). Thus, the mechanisms of the AF rotational motion have been controversial. On the other hand, microtubule rotation accompanied with sliding motion was revealed by three-dimensional Prismatic Optical Tracking, termed tPOT (Yajima *et al.*, *Nat. Struct.Mol.Biol.*, 2008). Applying tPOT to AF sliding assay expects to contribute for further information about the AF rotation machanisms.

Actin and heavy meromyosin were purified from rabbit skeletal muscles. To apply tPOT to AF gliding assay, avidin conjugated quatum-dots (QD) were sparsely attached to the AF containing ~10 % of Cys-374 biotinylated actin (QD-AF), and the QD-AF was stablized and visualized by rhodamine phalloidin (RhPh).

Similar sliding velocities of QD-AF (6.3 μm s^{-1}, n = 8) and AF labeled with only RhPh (6.2 μm s^{-1} , n = 5) (ATP 2 mM , 25 °C) suggested that the attached QD did not disturb intact sliding motion. We measured three-dimesional discplacement of QD in sliding QD-AF in various conditions, and the possible mechanisms of the AF rotation will be discussed at the meeting.

2H1510 Ca^{2+}に依存しない熱パルスによる心筋細胞の On-Off 制御

Ca^{2+}-independent on-off regulation of a cardiomyocyte by microscopic heat pulses

Kotaro Oyama[1], Akari Mizuno[1], Seine Shintani[1], Hideki Itoh[1], Takahiro Serizawa[1], Norio Fukuda[2], Madoka Suzuki[3,4], Shin'ichi Ishiwata[1,3,4] ([1]*Sch. Adv. Sci. Eng., Waseda Univ.*, [2]*Dept. Cell Physiol., Jikei Univ. Sch. Med.*, [3]*Org. Univ. Res. Initiatives, Waseda Univ.*, [4]*WABIOS, Waseda Univ.*)

Laser irradiation on neural and cardiac tissues has developed into a novel technique of non-invasive stimulation. The physical parameters that induce contraction of cardiomyocytes and a heart are under discussion, because the laser irradiation triggers various reactions, such as photochemical and photothermal. Here we focused on the laser-induced local temperature changes. We demonstrated previously that a microscopic heat pulse (ΔT = 0.2°C for 2 sec) induces a Ca^{2+} burst in cancer cells (HeLa cells) at body temperature (Tseeb, V., et al., *HFSP J.* , 2009). The mechanism is thought to be similar to that of rapid cooling contracture of skeletal and cardiac muscles. In this study, we show that a microscopic heat pulse (ΔT = 5°C for 0.5 sec) generated by a focused infrared laser induces the contraction of rat adult cardiomyocyte at basal temperature of 36°C. ΔT required to induce the contraction of cardiomyocyte at 36°C was lower than at 25°C. Contrary to a regular muscle contraction, Ca^{2+} transients were not detected during the contraction. Also, we induced the contraction of skinned cardiomyocytes by heat pulse in Ca^{2+}-free solution. These results indicate that a heat pulse regulates the contraction without the involvement of Ca^{2+} dynamics, i.e., the microheating stimulation skips several steps relating to Ca^{2+} signaling in the excitation-contraction coupling and directly activates actomyosin interaction. Our method may be useful for stimulating the beating of failing hearts without exacerbating abnormal Ca^{2+} dynamics.

2H1522 ミオシン分子の非線形弾性とフィラメントの弾性変形を考慮した筋収縮のシミュレーション

The Effects of Nonlinear Elasticity of Myosin Molecules on Muscle Contraction Studied by Numerical Simulation

Keita Miyamoto, Kazuo Sasaki (*Dept. Appl. Phys., Sch. Eng., Tohoku Univ.*)

The elasticity of myosin molecules is responsible for the force (tension) generation in muscle contraction. In traditional theories of muscle contraction, researchers have assumed that the displacement of a myosin head relative to the myosin filament is proportional to the force applied to the head along the filament. However, a recent experiment by Kaya and Higuchi [M. Kaya and H.

Higuchi, Science 329, 686 (2010)] clearly showed that the elasticity of myosin is strongly nonlinear. In a previous work (Biophysical Society Meeting in Himeji, 2011) we studied the quick response of tension to the length change of a muscle fiber and the force-velocity relation in isotonic contraction based on the theory proposed by Duke [T.A.J. Duke, Proc. Natl. Acad. Sci. USA 96, 2770 (1999)] with the linear elasticity of myosin replaced by a nonlinear elasticity. It turned out that we have to set the (nonlinear) elastic constant of myosin molecule to about one forth of the value obtained by Kaya and Higuchi to account for the experimental results. A plausible reason for the discrepancy is that actin and myosin filaments are treated as rigid rods in our model as in the Duke model. In the present work, we will carry out numerical simulations taking account of the elasticity of actin and myosin filaments as well as the nonlinear elasticity of myosin molecules to reveal whether we can resolve the inconsistency between the values of elastic constant in the simulation and the experiment.

2H1534 高塩濃度溶液中における熱変性したミオシン分子のミオシンフィラメントへの付着

Adhesion of heat-denatured myosin molecules to myosin filament at high salt concentration

Masato Shimada[1], Eisuke Takai[1], Daisuke Ejima[2], Kentaro Shiraki[1] ([1]*Facul. of Pure and Appl. Sci., Univ. of Tsukuba.*, [2]*Institute for Innovation, Ajinomoto Co. Inc.*)

Myosin filament is formed from myosin molecules mainly by electrostatic interaction. Thus, myosin filament disassociates in salt solutions at above 0.3 M. However, it may be questioned whether the interaction is completely damped out even at the high salt concentration. To explore the question, we investigated the myosin filaments at various salt concentrations by dynamic light scattering (DLS) and transmission electron microscopy (TEM). Myosin from porcine was well dissolved in 1.0 M NaCl solution. Then the myosin solution was diluted to various salts concentration. The myosin filament with hydrodynamic radius of 200 nm was dissolved to myosin molecules with that of 60 nm monitored by DLS, which was not fully disassociated with increasing temperature and salt concentration. The size of myosin filament gradually increased with heating at above 55 °C . Interestingly, the heat-denature myosin molecules adhere onto myosin filaments observed by TEM. These data suggest that the adhesion above the denaturation temperature of myosin decreased with increasing salt concentration through hydrophobic interaction. This experimental system could quantitatively analyze the kinetics of myosin filament-myosin molecule interaction.

2H1546 ラット幼若心筋細胞内サルコメア集団の自励振動(SPOC)特性

Auto-oscillation (SPOC) properties of sarcomeres in rat neonetal cardiomyocytes

Seine Shintani[1], Kotaro Oyama[1,2], Norio Fukuda[2], Shin'ichi Ishiwata[1,3] ([1]*Sch. Adv. Sci. Eng., Waseda Univ.*, [2]*Dept. Cell Physiol., Jikei Univ. Sch. Med.*, [3]*WABIOS, Waseda Univ.*)

Auto-oscillations of sarcomere length (SL) occur at intermediate activation conditions in cardiac and skeletal muscles. The waveform of sarcomeric auto-oscillation usually consists of slow shortening and quick lengthening. We have termed this phenomenon SPOC. SPOC has properties of auto-oscillation at single sarcomere level and synchronous dynamics of sarcomeres, e.g., propagation of SPOC wave. Therefore, observation of SPOC allows us to understand the dynamic properties of sarcomeres. In order to fully understand the molecular mechanism of SPOC, we examined neonatal rat cardiomyocytes expressing GFP-α-actinin and visualized the motions of sarcomeres. First, we successfully induced SPOC in the neonatal myocytes with the intact inner-membrane system following treatment with ionomycin by controlling the cytoplasmic Ca^{2+} concentrations. And we have termed this phenomenon Cell-SPOC. Our analysis of the Cell-SPOC revealed that the SPOC period of SL oscillations (in the range of 0.2 s to 1 s) increased with the increase in the amplitude of SL oscillations. As the amplitude became smaller, the shortening velocity tended to become larger, especially in the range of 0.2 to 0.5 s of the SPOC period. We also found that the oscillation properties of the Cell-SPOC and those of intact cells activated by electrical stimulation became similar as the oscillation period approaches to 0.2 s from 1 s. Based on these results, we will discuss the similarities and differences between the Cell-SPOC and the oscillations of intact cells.

2H1558 横紋筋サルコメアのフィラメント格子の安定性

Stability of Myofilament Lattice in Striated Muscle Sarcomere

Shigeru Takemori[1], Masako Kimura[2], Maki Yamaguchi[1], Tetsuo Ohno[1], Naoya Nakahara[1], Shunnya Yokomizo[3] ([1]*Jikei Univ. Sch. Med.*, [2]*Kagawa Nutrition Univ.*, [3]*Tokai Univ. Graduate Sch. Physical Education*)

Removal of cell membrane from striated muscle cells to prepare skinned muscle specimens not only increases inter-myofilament spacing but also destabilize lattice structure of myofilaments. Takemori et al (2007) revealed that this destabilization is accompanied by diffusion of macromolecular solutes out of inter-myofibrillar space. Therefore, we expected that exogenous macromolecules that penetrate into inter-myofibrillar space may recover the stability. Adopting a set of myosin layer lines on the two dimensional X-ray diffraction patterns (obtained at BL-6A of KEK and at BL-45XU of SPring8) as one of the indicators of lattice stability, we found that 3% polyethylene glycol molecules (M_w less than 3, 360) that penetrate into myofilament lattice restore myosin layer lines of skinned specimens of striated (rabbit skeletal and rat cardiac) muscles. Polyethylene glycol also dehydrated the skinned specimens to restore physiological inter-filament spacing. Since the dehydrating effect mainly depends on the concentration of hydrophobic -CH_2- unit in the solution (Kimura and Takemori, 2008), we consider this stabilizing effect of polyethylene glycol to support our hypothesis that construction of myofilament lattice involves structured water that serves as free-energy sink for contractile interaction. From this view point, cause of differential radial stiffness of relaxed and rigor muscle specimens are reconsidered.

2H1610 羽ばたくマルハナバチ中で拮抗する 2 種の飛翔筋の超高速 X 線回折像同時記録

Simultaneous ultrafast X-ray recordings of actions of two antagonistic flight muscles during wingbeat of live bumblebee

Hiroyuki Iwamoto, Naoto Yagi (*SPring-8, JASRI*)

In bees and other insects, their flight muscles drive their wings indirectly by deforming the thoracic exoskeleton (indirect flight muscle). The deformation is caused by alternating force generation by two antagonistic flight muscles (dorsal longitudinal muscle, DLM, and dorsoventral muscle, DVM). Here we studied how the actions of these two antagonistic muscles are coordinated by simultaneously recording the X-ray diffraction patterns from these muscles during wingbeat. Intense X-ray beams from the BL40XU high-flux beamline of SPring-8 were irradiated from the side of the thorax of a live bumblebee, where the two antagonistic muscles cross. The diffraction patterns were recorded at 5,000 frames/s by using a fast CMOS video camera. A second fast CMOS video camera recorded its wingbeat. The frames of the two video cameras were synchronized in a master-slave connection. Besides the strong equatorial reflections, the 1st myosin meridional reflection (1MM) and the 2nd troponin off-meridional reflection (2TN, reporting myosin binding to actin) were clearly recognized for both DLM and DVM after summing the frames for ~5 wingbeat cycles. The intensities of these reflections, as well as the lattice spacing (d10), changed basically in an anti-phase fashion for DLM and DVM but not always in a sinusoidal manner as generally assumed. Further analyses are underway and they will give more detailed information about the timing of action of the two antagonistic flight muscles during wingbeat.

2I1400 海洋性ビブリオ菌の周毛性べん毛形成の抑制に関与する DnaJ モチーフを持った新規遺伝子の解析

A novel gene of dnaJ family plays a role in the suppression of flagellation in Vibrio alginolyticus

Takehiko Nishigaki[1], Maya Kitaoka[1], Kunio Ihara[2], Noriko Nishioka[1], Seiji Kojima[1], Michio Honma[1] ([1]*Grad. Sch. Sci., Univ. Nagoya*, [2]*Gene., Univ. Nagoya*)

Bacterial flagella are formed in various numbers and locations in different kinds of bacteria. A Vibrio alginolyticus strain VIO5 that lacks lateral flagella and possesses wild-type flagella, has a single polar flagellum by expressing FlhF and FlhG. FlhF positively regulates the number and location of flagella, while FlhG does so negatively. The ΔflhFG strain, derived from VIO5, has mostly no flagellum, but a small population of the ΔflhFG cells have some peritrichous flagella and only slightly form the motility ring on the soft-agar plate. In our laboratory, the suppressor mutant recovering motility on the soft-agar plate was isolated from the ΔflhFG strain (named ΔflhFG-sup). The ΔflhFG-sup cells were peritrichously flagellated. We identified the sup mutation by whole genome sequence, on the unknown gene which has a DnaJ motif and was specific in Vibrio. We named this gene sflA (suppressor of ΔflhFG). We showed that the ΔflhFG strain expressing mutant SflA from plasmid recovered motility and biosynthesis of flagellin, and the ΔflhFG-sup strain expressing

wild-type SflA from plasmid repressed motility and biosynthesis of flagellin. In addition, the Δ flhFG Δ sflA triple deletion mutant represented the same phenotype as the ΔflhFG-sup strain. Thus, we concluded that mutation in sflA is responsible for suppressor phenotype of the ΔflhFG-sup strain. We propose that sflA was a novel gene involved in the flagellation of V. alginolyticus.

2I1412 バクテリアⅣ型線毛の粘着脱離動力学

Unbinding Dynamics of Type IV Pili

Tomonari Sumi[1,2], Rahul Marathe[2], Stefan Klumpp[2] ([1]*Dept. Comp. Sci. Eng., Toyohashi Univ. Tech.*, [2]*Dept. Theo. & Bio-syst., Max Planck Inst. Colloids & Interfaces*)

Type IV pilus is a highly dynamic fiber supporting adhesion, surface motility, and gene transfer. To the best of our knowledge, type IV pilus is the strongest linear motor that generates considerable strong force larger than 100pN. In this study, we present a simple stochastic model for rupture dynamics of pilus binding to a bead manipulated by laser tweezers. Theoretical analysis of single-molecular observation data reveals that bacteria use a switching mechanism between high velocity retraction and low velocity one to reduce mean rupture rate of pilus binding to a bead under higher external forces. We show that the auto-regulation-like system that seems to be effectively working as a tension control mechanism can be constructed by introducing two independent competing motors for pilus retraction and elongation without feedback control of the tension.

2I1424 細菌べん毛特異的シャペロン FliT の C 末αヘリックの役割

Role of the C-terminal α-helix of FliT chaperone in the export of its cognate substrate FliD

Tohru Minamino[1], Miki Kinoshita[1,2], Noritaka Hara[1], Katsumi Imada[2], Keiichi Namba[1,3] ([1]*Grad. Sch. Frontier Biosci., Osaka Univ.*, [2]*Grad. Sch. Sci., Osaka Univ.*, [3]*QBiC RIKEN*)

For construction of the bacterial flagellum, which is responsible for motility, most of the flagellar proteins are exported into the distal end of the growing structure by the flagellar export apparatus. The export apparatus consists of an export gate complex made of six membrane proteins and a water-soluble ATPase complex consisting of FliH, FliI, and FliJ.
FliT, which is a substrate-chaperone responsible for the filament-capping protein FliD, consists of four α-helices, α1, α2, α3 and α4. The core of the molecule is formed by an anti-parallel α-helical bundle composed of α1, α2 and α 3. The FliT-FliD complex binds to the FliI ATPase complex through interactions of the core domain of FliT with FliD, FliI and FliJ in the cytoplasm and then is transferred from the ATPase complex to the export gate. It has been shown that the C-terminal α4 helix binds to a hydrophobic cleft formed by the α2 and α3 helices to regulate the binding affinity of FliT for FliI and FliJ. But it remains unknown how FliD enters the gate.
To clarify a specific role of the C-terminal α4 helix of FliT in protein export, we investigated how the FliT-FliD complex interacts with the export gate. We show that an interaction between FliT and an export gate protein FlhA is required for efficient FliD export. We also show that a highly conserved Tyr106 residue in the α4 helix of FliT is critical for the interaction with FlhA. These results suggest that the FliT-FlhA interaction efficiently transfers FliD to the export gate to promote its protein export.

2I1436 べん毛輸送装置近傍の局所 pH に対する FliI ATPase の効果

Effect of FliI ATPase on local pH around the bacterial flagellar protein export apparatus

Yusuke V. Morimoto[1,2], Nobunori Kami-ike[1], Tomoko Miyata[1], Keiichi Namba[1,2], Tohru Minamino[1] ([1]*Grad. Sch. Frontier Biosci., Osaka Univ.*, [2]*QBiC, RIKEN*)

Membrane-imbedded molecular machines utilize proton motive force (PMF) across the biological membrane for their biological activities. The bacterial flagellum is a biological nanomachine consisting of a rotary motor and a filamentous helical propeller. Most of flagellar proteins are transported to the distal end of the growing structure for their self-assembly by the flagellar protein export apparatus. The export apparatus consists of a water-soluble ATPase complex consisting of FliH, FliI, and FliJ, and a membrane-imbedded export gate. Recently, it has been shown that the export gate is a proton-protein antiporter that uses the two components of PMF, $\Delta\psi$ and ΔpH for different steps of the protein export process, and a specific interaction between the ATPase complex and the gate switches the export gate into a highly efficient $\Delta\psi$-driven export apparatus, but it remains unknown how it occurs.
To clarify the energy transduction mechanism used in flagellar protein export, we measured local pH around the export apparatus of wild-type cells and a FliH-FliI bypass mutant using a ratiometric pH indicator, pHluorin(M153R), fused to FliG, a rotor component of the flagellar motor. The local pH near the export gate of wild-type cells was significantly lower than that of the bypass mutant. The FliI catalytic mutations increased the local pH to the FliH-FliI bypass mutant level. These results suggest that ATP hydrolysis by FliI ATPase is closely linked to proton translocation through the export gate.

2I1448 Na^+駆動型べん毛モーター固定子タンパク質 PomA の細胞質ループ領域の示差走査熱量測定を用いた性質検討

Characterization of cytoplasmic loop of PomA, Na^+-driven flagellar stator protein, using differential scanning calorimetry

Shiori Kobayashi[1], Rei Abe-Yoshizumi[1,2], Mizuki Gohara[1], Seiji Kojima[1], Michio Homma[1] ([1]*Division of Biological Science, Graduate School of Science, Nagoya University*, [2]*Department of Frontier Materials, Nagoya Institute of Technology*)

Vibrio alginolyticus has a single polar flagellum that is driven by rotary motor powered by the Na^+-motive force. The motor is consisted of the stator and the rotor, and it is believed that the interaction between stator and rotor that coupled with ion-flux through the stator generates torque. From previous our study, we demonstrated that the structure of C-terminal domain of FliG is important for interaction between stator and rotor using differential scanning calorimetry (DSC). Next, we focused on the stator protein PomA, which is thought to interact with rotor protein FliG in *Vibrio*. It has been shown that the cytoplasmic loop domain of either H^+-driven *E. coli* MotA or Na^+-driven *Vibrio* PomA is closely participated in the rotor-stator interaction. To characterize this domain of Na^+ -driven *Vibrio* PomA (PomA-loop), we tried to over-produce the recombinant PomA-loop with His-tag in *E. coli* and purify it by affinity chromatography, but it was insoluble. So, we made a fusion with a small soluble tag (GB1) and we could handle and characterize the soluble recombinant protein of PomA (Q54-D148 or Q54-E253) fused with GB1. We characterized the purified proteins by DSC and compared the thermal stability between the PomA fragments. Furthermore, we are planning to introduce mutations in the PomA cytoplasmic region which are predicted to affect the interaction between stator and rotor and to measure the mutant proteins by DSC. We want to discuss the thermodynamic property of the cytoplasmic loop.

2I1510 プラグを欠失した Na^+駆動型べん毛モーター固定子複合体の精製・再構成系の構築

Purification and reconstitution of the plug-deleted Na^+-driven stator complex from *Vibrio alginolyticus*

Tetsuya Oba, Seiji Kojima, Michio Homma (*Division of Biological Science, Graduate school of science,Nagoya University*)

The polar flagellar motor of *Vibrio alginolyticus* is driven by Na^+ motive force. This motor couples Na^+ influx through the stator to torque generation. It has been known that PomA, PomB, MotX and MotY are required for rotation of the *Vibrio* motor. PomA and PomB are integral membrane proteins that form the $PomA_4/PomB_2$ stator complex, and MotX and MotY are periplasmic proteins associated with the basal body to form the T ring structure. The PomA/B complex functions as Na^+ channel in the stator. However, quantitative analysis of Na^+ permeation through the PomA/PomB complex is technically challenging because of the difficulty to purify and reconstitute intact complex. Recently, we investigated the plug region of PomB that participates in Na^+ flux regulation. When the stator with plug-deleted PomB ($PomA/B_{\Delta L}$) was over-expressed the growth rate of cells was decreased without motility impairment. We speculated that plug-deleted PomA/B complex mimics open state of the stator channel, so that massive Na+ influx caused growth impairment. Therefore, we attempted to overproduce and purify the open-state mimicking $PomA/B_{\Delta L}$ complex and then reconstitute it to proteoliposome. Using the detergent Cymal-5, we could isolate relatively pure complex with appropriate molecular size. Currently we are trying to establish the method to reconstitute the purified complex into liposome and by using radioactive Na^+ ($^{22}Na^+$), to detect Na^+ uptake activity of $PomA/PomB_{\Delta L}$ complex.

2I1522 蛍光相関分光法（FCS）を用いたべん毛モーターを構成するタンパク質間の相互作用解析

Analysis of interactions between rotor proteins of flagellar

motor using Fluorescence Correlation Spectroscopy

Takaaki Kishi, Seiji Kojima, Michio Homma (*Division of Biological Science, Graduate School of Science, Nagoya University, Chikusa-ku, Nagoya, Japan.*)

Vibrio alginolyticus has a single polar flagellum responsible for motility by utilizing sodium motive force. The flagellar motor consists of rotor and stator. It is thought that rotor-stator interaction that couples to Na^+ flux through the stator generates torque. However, the direct interaction between rotor and stator has not been detected clearly in vitro yet, presumably because such an interaction is weak and transient. Here, to establish a new method to detect interactions between rotor and stator, we used Fluorescence Correlation Spectroscopy (FCS). FCS can measure diffusion time of the fluorescently labeled particles in the confocal area. If a protein is bound to the labeled one, then diffusion time increases, so that we can detect protein-protein interactions. Last year we have found that some kinds of detergents still allowed us to detect membrane protein interactions by the FCS analyses. Also, the purification method of the PomA/PomB stator complex that lacks the linker region of PomB (named PomA/BΔL) was established. Using PomA/BΔL and the rotor protein FliG, we tried to detect the direct interaction between rotor and stator by FCS. FliF, a component of rotor, form the MS ring structure and serve as a platform of rotor. To detect FliG-PomA interaction, MS ring might be necessary to mimic the in vivo rotor structure. However overproduction of *Vibrio* FliF alone in *E. coli* did not produce MS ring. Now we co-express FliF with the flagellar export apparatus FlhA to facilitate formation of MS ring.

2I1534 Na^+駆動型べん毛モーターの固定子と回転子間における荷電残基変異による協調作用の解析

Synergetic effects of the mutations of charged residues between the rotor and the stator in the Na^+-driven flagellar motor

Norihiro Takekawa, Seiji Kojima, Michio Homma (*Div. of Biol. Sci., Grad. Sch. of Sci., Nagoya Univ.*)

Some bacteria have flagella for their motility. At the base of the flagellum, there exists the reversible rotary motor. The flagellar motor is consisted of two parts, rotor and stator. Essential components for torque generation in the rotor is located at the C-ring composed of FliG, FliM, and FliN, and the stator is composed of the membrane proteins MotA and MotB in H^+-driven flagellar motor and PomA and PomB in Na^+-driven flagellar motor that forms ion channel structure. In the H^+-driven motor of *E. coli*, the interaction between conserved charged residues of FliG and MotA is important for generation of the torque of the motor. However, the importance of such interactions had been unclear in the Na^+-driven motor. In this study, we systematically made mutants whose charged residues of FliG and PomA were replaced to uncharged or charge-reversed ones, and examined motility of those mutants. We found that some FliG/PomA double mutations gave the synergetic effects or suppression on the motor rotation. Our results suggest that interactions between charged residues of FliG (K284, R301, D308, and D309) and those of PomA (R88, K89, E96, and E97) are important for force generation of Na^+-driven flagellar motor. Especially the suppression effect between FliG-K284E and PomA-E97K was only seen in the Na^+-driven motor, may show more robust rotor-stator interface due to the Na^+-type specific interaction as suggested in the previous study.

2I1546 光分解されたセリンへの大腸菌の応答計測

Measurement of cellular response of single *E. coli* to the photoreleased serine

Takashi Sagawa[1], Hajime Fukuoka[2], Yuichi Inoue[2], Hiroto Takahashi[2], Takahiro Muraoka[2], Kazushi Kinbara[2], Akihiko Isjijima[2] ([1]*Grad. Sch. Life Sci., Tohoku Univ.*, [2]*IMRAM, Tohoku Univ.*)

A rotational direction of flagellar motors of *E.coli* is regulated by binding of intracellular signaling protein, CheY-P. By the recognition of serine, intracellular concentration of the CheY-P is decreased and the rotational direction of the motor is kept in CCW direction.

In this study, we investigated the cellular response of the *E.coli* to the locally applied chemotactic signal, using caged-serine. By photoreleased serine, the motor was switched back to CCW direction within sub-second delay and continued the CCW rotation for several seconds. From the sub-second delay and the CCW duration, the upward and downward concentration of serine was estimated, respectively. The upward concentration of serine was higher than that of downward. This result suggested that it is necessarily to refill the CheY-P to recover the signal transduction.

To investigate the detail of response of motors to the concentration of CheY-P, dual motor analysis was preceded. When the rotational direction of motor near receptor changed CCW to CW, serine was photoreleased. The motor near receptor was switched back to CCW direction within sub-second delay. However, the motor far from the receptor kept CCW rotation. Therefore, the signaling of CheY-P molecules could not reach to the end of the cell by the inhibition of CheY-P production.

These results suggested that the signaling molecules diffused from chemoreceptors and the sufficient concentration change of CheY-P in entire cell should be required to transmit the signal from the receptor to the end of the cell.

2I1558 CheZ 極局在の有無における大腸菌細胞内シグナル伝達の計測

Propagation of intracellular signaling molecule in the presence and absence of polar localization of CheZ in a single *E. coli* cell

Hajime Fukuoka[1], Takashi Sagawa[2], Yuichi Inoue[1], Hiroto Takahashi[1], Akihiko Ishijima[1] ([1]*IMRAM, Tohoku Univ.*, [2]*Grad. Sch. life Sci., Tohoku Univ.*)

In chemotaxis system, the extracellular signals are detected by receptors and are transduced to an intracellular signaling molecule, phospholylated CheY (CheY-P), at the cell pole. The binding of CheY-P to the flagellar motor switches rotational direction of it from counterclockwise (CCW) to clockwise (CW). By measuring switching delay between 2 motors, we previously proposed an increase and decrease in the CheY-P concentration are propagated wave-likely from receptor patch to the opposite cell pole. However, it is not understood how such dynamic propagation is generated. In this study, to understand the signaling process by CheY-P, we measured the switching delay of CCW-to-CW and CW-to-CCW switching individually with and without polar localization of CheZ, which dephosphorylates CheY-P. For the measurement in the absence of CheZ localization, we constructed a mutant cell lacking $CheA_{short}$, which binds CheZ in receptor patch. Regardless of CheZ localization, the switching delay correlated with the relative positions of 2 motors from receptors in CCW-to-CW switching. However, in CW-to-CCW switching, switching delay correlated with the positions of 2 motors only in the presence of CheZ localization. These results indicate the polar localization of CheZ is critical for the directed propagation of the decrease of CheY-P concentration. Now we are measuring chemotactic response in the presence and absence of CheZ localization to understand the role of its localization in chemotaxis. We would like to discuss our results in annual meeting.

2I1610 大腸菌の遊泳速度に及ぼすγ線照射の効果

Effect of gamma ray irradiation on the swimming speed of *Escherichia coli*

Eriko Fujimoto[1], Masakazu Furuta[2], Tatsuo Atsumi[3], **Mikio Kato**[2] ([1]*Osaka Prefecture University School of Science*, [2]*Osaka Prefecture University Graduate School of Science*, [3]*Gifu University of Medical Science*)

The effects of ionizing radiation on bacteria are generally evaluated using a dose-dependent survival ratio based on the colony-forming ability and mutation rate of the cells. To date, the mutagenic damage to cellular DNA induced by radiation has been extensively investigated, primarily by using methodologies that estimate the degree of DNA damage in specimens following bulk irradiation. However, the effects of irradiation on cellular machinery in situ remain unclear.

Recently, we applied a micrometer-sized proton beam, generated by a Pelletron accelerator through a tapered glass capillary, to a single cell of *Escherichia coli* in liquid media to evaluate the effect of irradiation on the flagellar motor and cell division. We observed an unexpected robustness of the bacterial flagellar motor against irradiation from a high-energy (2 MeV) proton beam; the average ion fluence required to stop the flagellar motor of the tethered cells was 2.0×10^{12} protons/cm^2 (approximately 60 kGy).

In the present study, we applied a γ ray from ^{60}Co (up to 8 kGy) to *E. coli* cells in liquid media, and measured their swimming speed using a microscope. The results indicated that the swimming speed remained unaltered after the lethal gamma ray dose was administered to the cells; however, the ratio of the cells adhering to the glass substrate (not swimming freely) increased by the irradiation. Moreover, the inhibition of protein synthesis by kanamycin did not alter the swimming speed, but increased the ratio of the stuck cells.

3A0912 F_1-ATPase と繊毛軸糸の機能に関わる構造変化

Motions in F_1-ATPase and ciliary axonemes that drive functions

Tomoko Masaike[1], Koji Ikegami[2], Rinako Nakayama[1], Mitsutoshi Setou[2], Takayuki Nishizaka[1] ([1]*Department of Physics, Gakushuin University*, [2]*Department of Cell Biology and Anatomy, Hamamatsu University School of Medicine*)

Our goal is to visualise how motions and functions of components are coupled in various hierarchy levels of biological systems under optical microscopes.
As a model of enzymes, we chose F_1-ATPase. Cooperative ATPase activity at three catalytic β subunits is known to be greatly accelerated by the presence of the central shaft subunit γ. To investigate involvement of physical rotation of γ in conformational states of β, orientation of the C-terminal helix of β was measured using advanced TIRF microscopy, while γ was forcibly rotated using magnetic tweezers. We found that conformational changes of β are dependent on both orientation of γ and direction of its rotation. Thus the interplay between β and γ indeed contributes to conformational states and thus chemical states of the enzyme during efficient rotary catalysis.
The next target is an organelle. A fluorescent bead was attached to the axonemal tip of a tracheal cilium of a mouse, and beating motions were recorded under a three-dimensional tracking microscopy. We obtained 3-D coordinates of trajectories and fitted them with spherical shells. We found multiple phases of velocities along the spherical shells during strokes. Moreover, counterclockwise rotational motions and a difference of height between effective and recovery strokes were quantitatively indicated. Cilia may follow different trajectories in synchronised effective and recovery strokes to avoid drag of the opposite stroke and maintain effective fluid flow for elimination of harmful materials.

3A0924 高速暗視野照明による金ナノロッドの方向検出システムを用いた F1-ATPase の回転の検出

Detection of rotation of F1-ATPase using high-speed orientational detection of gold nanorod

Sawako Enoki[1,2], Ryota Iino[1,2], Hiroyuki Noji[1,2] ([1]*Grad. Sch. Engineering., Univ. Tokyo*, [2]*CREST*)

The scattered light from single gold nanorod is strongly polarized along the axis of the rod and can be used for the detection of its orientation. For the orientational detection, the gold nanorod would be a better probe than a fluorescent dye, because its high scattering intensity made it possible the detection at high rate for a long time without photobleaching. Furthermore, gold nanorod would be better than gold nanoparticle, because the orientational change that causes only very small lateral displacement of the attached probe can be detected. At last annual meeting, we reported two dark-field imaging systems based on objective-type evanescent and backscattering illuminations to detect the orientation of nanorod by analyzing the scattering intensities. Here, we tried defocus imaging of scattering of gold nanorod based on objective-type backscattering illumination. We tested defocus imaging of nanorod by observing the rotation of molecular rotary motor, F_1-ATPase. By analyzing the scattering pattern from gold nanorod, we could detect the orientation of the gold nanorod quantitatively at high speed (10 μs) and at high angle resolution. There are several advantages for defocus imaging compared to previously reported imaging systems. The angle can be directly determined from the image and angle range was wide (0-360 degree), while those of previously reported systems are narrow (0-90 degree). We will apply this imaging system to observation of domain motion of proteins.

3A0936 UTP を基質とした時の F1-ATPase の回転運動

Characterization of UTP driven rotation of F1-ATPase

Hidenobu Arai, Rikiya Watanabe, Hiroyuki Noji (*Grad. applchem., Univ. Tokyo*)

F_1-ATPase (F_1) is a rotary motor protein driven by ATP hydrolysis. In our early work, we examined the competency of various nucleotides to drive the rotation of F_1. While ATP, GTP, and ITP have been shown to support the rotation, we have not found evidence of UTP-driven rotation despite of the hydrolyzablity of UTP. In this study, we again attempted to verify the incompetency of UTP to drive the rotation by using very pure UTP that did not contain detectable ATP (<0.0025 %). At various UTP concentrations, we observed the anticlockwise rotation of F_1. From the Michaelis-Menten analysis, the rate constant of UTP binding was determined as 10^4 $M^{-1}s^{-1}$, which is 1,000 times smaller than that of ATP. Thus, the rotation is not attributable to the possible ATP contamination, showing that UTP drives the rotation of F_1. We measured the rotary torque of UTP rotation from the viscous coefficient (Γ)and the angular velocity of the rotation probe (ω); N=Γω. The estimated torque was around 40 pNnm as same as the ATP-driven rotation. To confirm this, we also conduced a buffer exchange experiment from ATP to UTP to compare the angular velocity of individual F_1 molecules in the presence of ATP or UTP. No obvious difference was found. These results showed that F1 efficiently convets the hydrolysis energy of UTP into mechanical wok even though UTP is a very low affinity substrate. The present work suggests that the base moiety of nucleotides is dispensable for the chemomechanical coupling of F_1.

3A0948 Single Molecule Analysis of Inhibitory Pausing States of V_1-ATPase

Naciye Esma Tirtom[1], Yoshihiro Nishikawa[2], Daichi Okuno[3], Masahiro Nakano[4], Ken Yokoyama[5], Hiroyuki Noji[1] ([1]*Department of Applied Chemistry, School of Engineering, University of Tokyo,* [2]*Dept. of Biotechnology, Osaka University,* [3]*RIKEN, Osaka, Japan*, [4]*The Institute of Scientific and Industrial Research,* [5]*Dept. of Biolmolecular Sciences, Kyoto Sangyo University*)

V_1-ATPase, the hydrophilic domain of V-ATPase, is a rotary motor fueled by ATP hydrolysis. Some biochemical studies indicated a strongly-inhibited state of V_1-ATPase, which we analyzed in detail at single molecule level, in this study. Here we showed that Thermus thermophilus V_1-ATPase had two types of inhibitory pauses interrupting continuous rotation: a short pause (SP, 4.2 s) that occurred frequently during rotation and a long inhibitory pause (LP, >30 min) that terminated all active rotation.Both pauses occurred at the same angle with ATP binding and hydrolysis. Kinetic analysis revealed that the time constants of inactivation into and activation from SP were too short to correspond to biochemically predicted ADP inhibition, suggesting that SP is a newly identified inhibitory state of V_1. The time constant of inactivation into LP was 17 min, consistent with one of the two time constants governing the inactivation process observed in bulk ATPase assay. When forcibly rotated in forward direction by using magnetic field, V_1 in LP resumed active rotation. Solution ADP suppressed the probability of mechanical activation, suggesting that mechanical rotation enhanced inhibitory ADP release. These features were highly consistent with mechanical activation of ADP-inhibited F_1, suggesting that LP represents the ADP-inhibited state of V_1. Mechanical activation largely depended on the direction and angular displacement of forced rotation, implying that V_1-ATPase rotation modulates the off rate of ADP.

3A1010 F_1-ATPase のトルク伝達における DELSEED ループの役割

The role of DELSEED loop in torque-transmission of F_1-ATPase

Kazuma Koyasu[1], Rikiya Watanabe[1], Mizue Tanigawara[2], Hiroyuki Noji[1] ([1]*Department of Applied Chemistry, School of Engineering, The University of Tokyo*, [2]*Graduate School of Frontier Biosciences, Osaka University*)

F_1-ATPase is an ATP-driven rotary motor that generates torque at the stator-rotor interface. The torque-generating unit, β, largely changes its conformation, by swinging the *C*-terminal domain inwardly upon ATP binding. The protruding loop of the *C*-terminal domain, so called DELSEED loop (D-loop) forms a large contact interface with the rotor subunit. From these observations, D-loop has been supposed to have a crucial role in the torque transmission of F_1. In our recent work, we analyzed the rotation behaviors of the mutant F_1 of which D-loop residues were all substituted to glycine in order to disrupt the specific interaction with the rotor and rigidity of the loop (Tanigawara *et al.* submitted). Surprisingly, the mutant has shown active rotation although it halved the torque. In the present study, we attempted to identify which reaction step is impaired by the glycine substitution. For this purpose, we measured the angular dependency of the equilibrium constant and reaction rate of ATP binding and hydrolysis steps by conducting the single-molecule stall-release experiment (Watanabe *et al.* NCB 2012). It was shown that the angular dependency of ATP binding was reduced to 60% while that of hydrolysis was not changed. These results suggest that D-loop has a crucial role in the force transmission from the catalytic reaction center to the rotor subunit in ATP-binding process but not in hydrolysis step.

3A1022 F_1-ATPase の回転子γサブユニットに有限のトルク発生に必要な残基はない

None of the rotor residues of F_1-ATPase are essential for torque generation

Ryohei Chiwata[1], Tomoya Kawakami[1], Ayako Kohori[1], Shou Furuike[2], Katsuyuki Shiroguchi[3], Kazuo Sutoh[1], Masasuke Yoshida[4], Kazuhiko Jr. Kinosita[1] ([1]*Dept. Physics, Fac. Sci. Eng., Waseda Univ.*, [2]*Fac. Physics, Osaka Med. Col.*, [3]*Dept. Chem. and Chem. Biol., Harvard Univ.*, [4]*Dept. of Mol. Biosci., Kyoto Sangyo Univ.*)

F_1-ATPase is a rotary motor in which the central γ subunit rotates inside a stator ring made of $\alpha_3\beta_3$ subunits. ATP hydrolysis in the β subunits generates torque for γ rotation by a mechanism not fully understood. The γ rotor consists of a globular domain that protrudes from the stator and a slender shaft that penetrates the $\alpha_3\beta_3$ ring. The shaft is an anti-parallel coiled coil of the N- and C- terminal helices of γ. Previously we have deleted either or both of these terminal helices genetically. Surprisingly, all mutants rotated in the correct direction, showing that the shaft portion is dispensable. Here we inquire if the rest of the γ rotor, the globular protrusion that accounts for ~70 % of the γ residues, is also dispensable. Keeping the N- and C-terminal helices that constitute the shaft, we have replaced the middle ~200 residues with a short helix-turn-helix motif borrowed from a different protein. Furthermore, 14 residues of the remaining N- and C- terminal helices have been replaced with unrelated residues such that the resulting construct and the previous shaft-truncated mutants (ΔC36 and ΔN29) that generated ~half the wild-type torque do not share common residues. This construct retained a high ATPase activity and rotated fast in the correct direction, generating a sizable torque. We conclude that none of the residues of the rotor are needed for the generation of finite torque.

3A1034 F1-ATPase のシリンダーから中心軸を引き抜く力の測定

UNBINDING FORCE MEASUREMENTS OF THE SHAFT FROM THE CYLINDER OF F1-ATPase

Tatsuya Naito, Kaoru Okada, Tomoko Masaike, Takayuki Nishizaka (*Dept Phys, Gakushuin Univ.*)

F_1-ATPase is a rotary motor protein in which the central γ subunit rotates inside the cylinder made of $\alpha_3\beta_3$ subunits. We investigated interactions between γ and the cylinder by unbinding γ in the direction of the optical axis. Three-dimensional single-particle tracking using a wedge prism has been combined with optical tweezers to quantify molecular scale 3-D force in F_1-ATPase. We placed the trap center 200-300 nm above a bead attached to γ, and the spring constant of the trap was increased by adjusting laser power. Here we report improvements of the experimental setup. First we adjusted the height of the trapping center every time just before unbinding to accommodate the trapping force within the range that it is proportional to the displacement. Second we attempted to ensure that γ is actually dismantled from the cylinder: Specific biotin-avidin binding of γ and beads were confirmed. Moreover the glass surface was modified with Ni-NTA to achieve specific binding of F_1-ATPase. Then we set up a system to check whether the fluorescently labeled cylinder remained on the glass surface after unbinding. As a result, the average unbinding force was 7.7 ± 5.0 pN (n=30) at 100 nM ATP. In the course of the experiment, we noticed that the sample plane apparently displaced in the Z-direction as laser power was increased. We plan to show differences in unbinding force depending on chemical states during catalysis.

3A1046 リポソーム膜中に再構成した好熱菌由来 F_oF_1- ATP 合成酵素による ATP 駆動 H^+輸送の定量

Quantification of ATP-driven H^+ transport by thermophilic *Bacillus* PS3 F_oF_1-ATP synthase reconstituted in a liposomal membrane

Yuzo Kasuya[1], Naoki Soga[1], Toshiharu Suzuki[2], Masasuke Yoshida[2], Kazuhiko Kinosita[1] ([1]*Dept. Phys., Facl. Sci. Eng., Waseda Univ.*, [2]*Dept. Mol. Bio., Facl. Life Sci., Kyoto Sangyo Univ.*)

F_oF_1 ATP synthase is composed of a water-soluble F_1 that has three catalytic sites for ATP synthesis/hydrolysis and a membrane embedded F_o that acts as a H^+ channel. The F_oF_1 synthesizes ATP using H^+ transport through the F_o and pumps H^+ reverse direction using ATP hydrolysis. ATP hydrolysis and resultant subunit rotation in F_1 have been well characterized by various single molecule techniques. The transport of H^+ through F_o, in contrast, has been difficult to observe in single molecules, and bulk assays have in most cases qualitative rather than quantitative.

Here, we measured the H^+ pump activity of F_oF_1 from thermophilic *Bacillus* PS3 (TF_oF_1) by an ensemble assay in a spectrophotometer and a single-liposome assay under a microscope. To visualize the H^+ transport through the TF_oF_1 into liposomes driven by ATP hydrolysis, a fluorescent dye pH-rodo, of which the fluorescence intensity increases upon lowering of pH, was conjugated to the phospholipids. The dye-labeled liposomes containing ~one TF_oF_1 on average responded to the addition of ATP by gradually increasing the fluorescence. We estimated the initial H^+ pump activity of TF_oF_1 by calibrating the buffering capacity; V_{max} was in the order of 600 H^+ sec^{-1} in ensemble and 800 H^+ sec^{-1} in single-liposome assays, with K_m for ATP of 20 μM in both assays for the starting pH of 8.0 and at room temperature. Now we are still trying to determine the H^+ pump activity more precise.

3A1058 マイコプラズマモービレゴーストのステップ検出

Detection of steps of *Mycoplasma mobile* gliding ghost

Yoshiaki Kinosita[1], Daisuke Nakane[2,3], Kana Mizutani[1], Makoto Miyata[2], Takayuki Nishizaka[1] ([1]*Dept. phys., Gakushuin Univ*, [2]*Dept. Biol., Osaka City Univ*, [3]*Present address: Mol. Microbiol. and Immunol., Grad. Sch. Biomed. Sci.,Nagasaki Univ*)

Mycoplasma mobile is a pathogenic flask-shaped bacterium about 0.8 μm long and has prominent gliding activity, on the glass surface coated with sialic acids at velocities of 2.5 μm/sec. Previous studies showed that the gliding motion is driven by many legs which repeatedly catch and release sialic acids on the glass surface, accompanied by ATP hydrolysis. To comprehend a unique mechanism of the gliding machinery, the step size and the kinetics per one ATPase cycle should be clarified. Nakane *et al.* have shown that the living *M. mobile* takes 85-nm step during gliding. Next challenge is to elucidate the kinetics of ATP hydrolysis in the stepwise motion. Here we performed the improved motility assay by using "gliding ghosts" of which the cell membrane was permeabilized by triton X-100. The ghosts allow us to control the gliding speed by modifying ATP concentrations in solution. The cell membrane was stained with Cy3 so that we could observe the gliding motility at the time resolution of 2 ms without a huge probe . Furthermore, to reduce the number of the legs contributing the gliding motility, free sialic acids was added to the assay buffer. Through these improvements we successfully observed the stepwise motion of the ghosts. A pairwise distance analysis showed that the *M. mobile* gliding ghosts took 60-100 nm steps, which are consistent with that of the living cell. Michaelis-Menten constant and V_{max} were 59 μM and 2.5 μm/sec.Now we are analyzing the dwell time.

3B0900 原核生物由来ナトリウムチャネルにおける C 末端 4 ヘリックスバンドルを用いたゲーティング制御

The cytosolic C-terminal four-helix bundle regulates the gating of prokaryotic sodium channel

Katsumasa Irie, Takushi Shimomura, Yoshinori Fujiyoshi (*CeSPI., Univ. Nagoya*)

Voltage-gated sodium channels play essential roles in many important physiological processes, including electric signalling and muscle contraction. Therefore their activation and inactivation are needed to be strictly regulated. Here, we show that the cytosolic C-terminal region of NavSulP, a prokaryotic voltage-gated sodium channel cloned from *Sulfitobacter pontiacus*, accelerates the inactivation rate and keeps the voltage dependent activation positively. The crystal structure of the C-terminal region of NavSulP grafted into the C-terminus of NaK channel at 3.2 Å resolution revealed that the C-terminal region forms a four-helix bundle. Point mutations of the residues of the four-helix bundle destabilised channel tetramer and reduced the inactivation rate. The four-helix bundle was directly connected to the inner helix of the pore domain. The increase of the rigidity of the inner helix with the glycine-to-alanine mutation also reduced the inactivation rate, but did not destabilize the tetrameric channel. Moreover, all of these mutants shifted the voltage dependent activation negatively, which indicates that the four-helix bundle suppress the opening of the pore domain. These findings suggest that the NavSulP four-helix bundle plays important roles not only in stabilising the tetramer, but also in regulating the channel gating by the restriction of the conformational change of the inner helix. The four-helix bundle could reduce excess ion flux after activation and also suppress accidental ion flux even in the resting state.

3B0912 [NiFe]ヒドロゲナーゼ成熟化因子 HypE，HypF の X 線結晶構造解析

X-ray structural analysis of HypE and HypF, maturation factors for [NiFe]-hydrogenases

Yasuhito Shomura[1,2], Yoshiki Higuchi[1,2] ([1]*Grad. Sch. Life Sci., Univ. Hyogo*, [2]*RIKEN/SPring-8 Center*)

As a remarkable structural feature of hydrogenase active sites, [NiFe] -hydrogenases harbor one carbonyl and two cyano ligands, where HypE and

HypF are involved in the biosynthesis of the nitrile group as a precursor of the cyano groups. HypF catalyzes *S*-carbamoylation of the C-terminal cysteine of HypE via three steps using carbamoylphosphate and ATP, producing two unstable intermediates: carbamate and carbamoyladenylate. It remains unclear how the consecutive reactions occur without the loss of unstable intermediates during the proposed reaction scheme. We have recently determined the crystal structures of full-length HypF both alone and in complex with HypE at resolutions of 2.0 and 2.6 Å, respectively. Three catalytic sites of the structures of the HypF nucleotide- and phosphate-bound forms have been identified, with each site connected via channels inside the protein. This finding suggests that the first two consecutive reactions occur without the release of carbamate or carbamoyladenylate from the enzyme. The structure of HypF in complex with HypE revealed that HypF can associate with HypE without disturbing its homodimeric interaction and that the binding manner allows the C-terminal Cys351 of HypE to access the *S*-carbamoylation active site in HypF, suggesting that the third step can also proceed without the release of carbamoyladenylate.

3B0924 Dynamic structural and antigen binding analyses of antibody single-chain Fvs

Yusuke Tanaka[1], Hiroshi Sekiguchi[2], Yuji C. Sasaki[3], Takachika Azuma[4], Masayuki Oda[1] ([1]*Grad. Sch. of Life and Environ. Sci., Kyoto Pref. Univ.*, [2]*Jpn. Syn. Rad. Res. Inst.*, [3]*Grad. Sch. of Fron. and Sci., Univ. of Tokyo.*, [4]*Res. Ins. for Biol. Sci., Tokyo Univ. of Sci.*)

We generated single-chain Fvs (scFvs) of anti-(4-hydroxy-3-nitrophenyl)acetyl (NP) antibodies, N1G9 and C6, which are germline and affinity maturated IgG1 antibodies, to analyze the change of structural fluctuation upon the antigen binding and through the affinity maturation. We overexpressed the scFvs in *E. coli*, and refolded by stepwise-dialysis method, followed by purification using NP-conjugated column. The scFv-antigen interactions were analyzed using surface plasmon resonance biosensor, Biacore, in which NP conjugated proteins were immobilized on sensor chip. The equilibrium association constant of C6 scFv for NP was about 10 times higher than that of N1G9 scFv, mainly due to the decreased dissociation rate constant. The kinetic parameters were similar to those of corresponding Fab and intact antibody, indicating that the scFvs are refolded correctly. The structural fluctuations of scFvs were measured using diffracted X-ray tracking (DXT) system at single-molecule level. Upon the binding of NP-ε-amino caproicacid, the fluctuations were decreased in either N1G9 or C6 scFv, indicating that the antigen binding stabilizes the scFv structure. In comparison of N1G9 and C6 scFvs in the absence of antigen, the fluctuation of C6 was lower than that of N1G9, which could be correlated with the different antigen binding mechanism such as “induced-fit” and “lock-and-key” types. On the advantage of scFv, whose amino acid could be mutated, we try to obtain more quantitative and site-specific information.

3B0936 PYP の光構造変化の機械的な制御

Mechanical control of light-induced protein conformational change of photoactive yellow protein

Yasushi Imamoto, Take Matsuyama, Yoshinori Shichida (*Grad. Sch. Sci., Kyoto Univ.*)

Proteins are formed from polypeptides by folding into the specific conformations, by which the physiological roles of the proteins are determined. The structure of the protein closely correlates with the physiological activity, and the activity of the protein is regulated by conformational change. For example, the receptor proteins alter their conformations in response to the stimuli to activate the cellular transduction system. Thus, if the protein conformation is artificially regulated, one would control the protein activity. Here we tried to establish the technique to regulate the protein activity by changing the conformation.

Photoactive yellow protein (PYP), a bacterial blue-light sensor protein, was used as the model protein. Two amino acid residues present in the surface of PYP molecule were replaced by cysteines and crosslinked by an azobenzene linker, whose length is reversibly changed by trans/cis photoisomerization. We found that the velocity of photocycle was varied by 10-100 times by the isomerization of azobenzene when Met100 loop and pCA loop were crosslinked. Since the global protein conformational change involving Met100 loop takes place in the photocycle, it is likely that the protein conformational changes were perturbed by the isomerization of azobenzene linker. This technique is possibly applied to switch the enzymatic activity of the protein by light.

3B0948 αカテニンによるアクトミオシン収縮の阻害

Inhibition of actomyosin contractility by α-catenin, a component of adherens junctions

Shuya Ishii[1], Takashi Ohki[1], Hiroaki Kubota[1], Shin'ichi Ishiwata[1,2,3] ([1]*Dept. of Phys., Faculty of Sci. and Eng., Waseda Univ.*, [2]*Adv. Res. Inst. for Scie. and Eng., Waseda Univ.*, [3]*WABIOS,Waseda Univ.*)

α-catenin is known as a linker protein between cell adhesion and the actin cytoskeleton. It has been believed that monomer of α-catenin forms a complex with β-catenin and E-cadherin in cell-cell adherens junctions and plays an essential role as an anchor, directly or indirectly, of E-cadherin-mediated adherens junctions and cytoskeletal F-actin networks. Dimer of α-catenin, which is formed by the dissociation from the complex, binds to F-actin with μM affinity and bundles it, locally inhibiting the Arp2/3 complex. This reorganization of actin dynamics decreases membrane activity at sites of cell-cell contact and stabilizes cadherin-mediated cell-cell adhesion. In addition, inhibition studies of myosin ATPase activity suggested that the intracellular actomyosin contractile force also contributes to the assembly and extension of adherens junctions. In present study, we report that α-catenin inhibits actomyosin contraction in the dose-dependent manner, which was characterized by an in vitro F-actin gliding assay with myosin II HMM. Furthermore, no direct significant association between α-catenin and myosin II was observed in immunoprecipitation assay, indicating that α-catenin may compete with myosin II for binding to actin, resulting in a decrease in the number of myosin heads able to propel actin filaments, or may indirectly, through an actin filament, inhibit myosin activity. Herein, we will discuss how α-catenin inhibits actomyosin contraction and the implications of that in maintaining adherens junctions.

3B1010 ダイニンモータードメインの溶液中の分子動力学シミュレーション

Molecular dynamics simulations of dynein motor domain in explicit water

Narutoshi Kamiya[1], Tadaaki Mashimo[2], Yu Takano[1], Takahide Kon[1], Genji Kurisu[1], Haruki Nakamura[1] ([1]*Institute for Protein Research, Osaka Univ.*, [2]*BIRC, AIST*)

Dyneins are large microtubule motor proteins that play important roles in various biological movements. Cytoplasmic dynein is responsible for cell division, cell migration and other basic cellular functions. The motor domain of dynein consists of a ring-shaped six ATPases called AAA^+ modules. Recently, an ADP-bound high-resolution structures of cytoplasmic dynein have revealed the organization of the motor domain that comprises the AAA^+ ring, the linker, stalk/strut and C sequence (PDB IDs = 3vkh, 3vkg). However, the high-resolution structure of an ATP-bound dynein remains unclear. Here, we carried out molecular dynamics (MD) simulations of both ADP and ATP-bound forms to examine their structures and dynamics.

We built initial structures for MD as following. A higher resolution structure (3vkg), which is a truncation mutant, was chosen. Then, we modeled missing residues and added a truncated domain from the wild type structure (3vkh). Four ADP molecules were placed to their original positions in the ADP bound form. One of the ADP molecules, bound to the main ATPase site (AAA1), was replaced to ATP in the ATP bound form. A rectangular water box was placed around dynein. Finally, the systems consisted of approximately one million atoms. Electrostatic interactions were treated with zero-dipole summation method, and their computation was accelerated by using GPGPU.

We will discuss the effect of ATP on the structure and dynamics of dynein by comparing the trajectories between the ADP- and ATP-bound forms.

3B1022 A computational Investigation into the MHC-I Recognition Mechanism of MIR2 from Kaposi's Sarcoma-Associated Herpesvirus

Pai-Chi Li[1,2], Naoyuki Miyashita[3], Satoshi Ishido[1], Yuji Sugita[2] ([1]*RIKEN Research Center for Allergy and Immunology*, [2]*RIKEN Advanced Science Institute*, [3]*RIKEN Quantitative Biology Center*)

Kaposi's sarcoma-associated herpesvirus, a human tumor virus, encodes two membrane-bound E3 ubiquitin ligases, modulator of immune recognition 1 (MIR1) and MIR2, to evade host immune system through the ubiquitination-mediated endocytosis and lysosomal degradation of the proteins involved in immune recognition. MIR2 downregulates the surface expression of MHC I (major histocompatibilty complex class I), co-stimulatory proteins (B7-2, ICAM-1), and platelet endothelial cell adhesion molecule 1 (PECAM-1). Recent

experiments results have shown that the palmitoylation of MIR2 Cys146 is essential for MHC I and PECAM-1 downregulation. This observation raises questions about the function of palmitoyl Cys146 (Cyp146), such as Cyp146 is whether located at the MIR2/MHC-1 and MIR2/PECAM-1 contact interfaces. To gain insight into the molecular basis of MHC-1 recognition by MIR2 and the role of Cyp146 of MIR2, we performed a series of molecular dynamic simulations. We first performed the replica-exchange molecular dynamics simulations in an implicit membrane/solvent environment to predict the structure of the transmembrane region of MIR2, then simulated the interaction between MHC-1 and MIR2. We then estimated the association energy of MIR2/MHC-1 complex by performing all-atom molecular dynamics simulations in the explicit membrane/solvent environment. Finally, the recognition mechanism for MIR2/MHC-1 is proposed and compared with that for MIR2/B7-2.

3B1034 タンパク質構造変化経路予測法の新規開発

A Novel Method to simulate protein conformational change upon ligand binding

Koichi Tamura, Shigehiko Hayashi (*Grad. Sch. Sci., Univ. Kyoto*)

Proteins undergo large conformational change when they interact with ligands. Whereas all-atom molecular dynamics simulations offer detailed description of the systems, its capability is limited to several hundreds of nanoseconds timescale, much lower than the actual timescale of the transitions. To enforce conformational change within the accessible simulation timescale, one can employ external forces to bring systems to end states. Especially, force probing, or steered molecular dynamics(SMD) and targeted molecular dynamics(TMD) technique is often applied to investigate the transition paths. In SMD, one have to determine direction of the applied forces somewhat intuitively, making it difficult to use the method within complex system. TMD requires explicit end state's knowledge to construct biasing forces, which indicates it's non-predictive nature. Thus, both methods have some deficiencies. In this work, we present a novel method, which based on the linear response theory, to study protein's complex conformational change upon ligand binding. The new method, which we call linear responce path following(LRPF), has some features not contained in the method described above; external forces are calculated nonintuitively, and it doesn't require any end state's information. The technique was succeffuly applied to comformational change of yeast calmodulin N terminal domain. The detailed transition pathway is discussed.

3B1046 時計タンパク質 KaiA-KaiC 相互作用の ESR 解析

Interactions between cyanobacterial clock proteins KaiA and KaiC revealed by ESR analysis

Kentaro Ishii[1], Toshiaki Arata[2], Masahiro Ishiura[1] ([1]*Center for gene research Nagoya Univ.*, [2]*Grad. Sch. of Science, Osaka Univ.*)

The circadian clock is an endogenous biological mechanism that generates daily cycles in gene expression, physiological, and behavioral activities (circadian rhythms). Many organisms from cyanobacteria to eukaryotes have circadian clocks, which enable the organisms to predict environmental alterations during the day. Cyanobacteria are the simplest organisms that have the circadian clock. The cyanobacterial circadian clock can be reconstituted in vitro from three clock proteins, KaiA, KaiB and KaiC, in the presence of ATP. A series of reactions and interactions among Kai proteins generate circadian oscillations such as oscillations in the phosphorylation level and ATPase activity of KaiC and complex formation among Kai proteins. Here, we investigated interactions between KaiA and KaiC by the spin labeling-electron spin resonance (SDSL-ESR) method. SDSL-ESR spectroscopy can provide information on the location and environment of an individual residue within a protein. We labeled each cystein (Cys) residue of Cys-substituted mutants of KaiC and KaiA derived from the thermophilic cyanobacterium Thermosynechococcus elongatus with spin labels, performed ESR analyses, and identified specific residues involved in KaiA-KaiC interactions. We also found that KaiA induces structural changes in the base part of the C-terminal tail of KaiC on its interaction with KaiC.

3B1058 ATP を中間体とするシアノバクテリア概日時計蛋白質 KaiC の新規脱リン酸化機構

Autodephosphorylation of cyanobacterial circadian clock protein KaiC occurs via formation of ATP as an intermediate

Taeko Ohkawa-Nishiwaki, Takao Kondo (*Div. Biol. Sci., Grad. Schl. Sci., Nagoya Univ.*)

The cyanobacterial circadian oscillator can be reconstituted *in vitro*; mixing three clock proteins KaiA, KaiB, and KaiC with ATP results in an oscillation of KaiC phosphorylation with a periodicity of approximately 24 h. The hexameric ATPase KaiC hydrolyzes ATP bound at subunit interfaces. KaiC also exhibits autokinase and autophosphatase activities, the latter of which is particularly noteworthy because KaiC is phylogenetically distinct from typical protein phosphatases. To examine this activity, we performed autodephosphorylation assays using ^{32}P-labeled KaiC. We detected the transient formation of [^{32}P]ATP preceding the accumulation of ^{32}Pi. Together with kinetic analyses, our data demonstrate that KaiC undergoes dephosphorylation via a mechanism that differs from those of conventional protein phosphatases. A phosphate group at a phosphorylation site is first transferred to KaiC-bound ADP to form ATP as an intermediate, which can be regarded as a reversal of the autophosphorylation reaction. Subsequently, the ATP molecule is hydrolyzed to form inorganic phosphate. The ATPase activity of KaiC has two critical roles for autodephosphorylation: one is the degradation of the intermediate, and the other is providing ADP, a phosphate acceptor for the reversal of the autokinase reaction. We propose that KaiC phosphorylation rhythm is sustained by periodical shift in the equilibrium of the intersubunit phosphate transfer reaction between KaiC-bound nucleotides and phosphorylation sites.

3B1110 シアノバクテリアの時計タンパク質 KaiC の ATPase に備わる分子内フィードバック制御

Intramolecular feedback regulation of cyanobacterial KaiC ATPase

Atsushi Mukaiyama[1,2], Yasuhiro Onoue[1,2], Masato Osako[1,2], Takao Kondo[1,2], Shuji Akiyama[3] ([1]*Grad. Sch. of Sci., Nagoya Univ.*, [2]*CREST/JST*, [3]*IMS, SOKENDAI*)

Circadian clock is an endogenous timing device in various organisms to adapt their biochemical and physiological processes to daily alterations in external environments. In cyanobacterium *Synechococcus elongatus* PCC 7942, circadian clock is composed of three proteins termed KaiA, KaiB, and KaiC. KaiA stimulates the auto-phosphorylation of KaiC, whereas KaiB attenuates the effect of KaiA, resulting in the auto-dephosphorylation of KaiC. In vitro incubation of the three Kai proteins with ATP generates phosphorylation cycle of KaiC with a period of approximately 24h.

Previous studies demonstrate that the frequency of the phosphorylation cycle is shown to be linearly correlated with ATPase activity of KaiC alone. In addition, our biophysical analyses have shown a conformational ticking of KaiC in solution, which reveals that KaiC expands and contracts its C-terminal ring during circadian oscillation in order to assemble/disassemble with KaiA and KaiB. These observations suggest that KaiC plays a key role as a circadian pacemaker.

ATPase activity of KaiC is extremely low compared to those for other ATPases, and temperature-compensated. Low and temperature-compensated ATPase activity seems to be under negative feedback regulation, but experimental evidences were not sufficient to support this hypothesis. For this purpose, we developed a method to examine the negative feedback regulation of KaiC ATPase. We present the results obtained by this method.

3C0900 DNA/RNA 結合タンパク質 TDP-43 が特異的な塩基配列を認識するメカニズム

Tandem-like fusion of two heterologous RNA-recognition motifs in TDP-43 enhances the specificity to its target nucleotide sequence

Yo Suzuki, Yoshiaki Furukawa (*Dept. of Chem, Keio Univ.*)

The RNA-recognition motif (RRM) is the most abundant RNA-binding domain in higher vertebrates and present in about 1 % of human genes. Typically, RRM consists of six strongly conserved secondary structures, βαββαβ, in which the four β-strands form a single anti-parallel β-sheet and the two α-helices pack tightly on one side of it. Interestingly, in spite of such a simple structural organization of RRM, each protein achieves its distinct specificity toward the target nucleotide sequence. Given that most of RRM-containing proteins comprise tandem copies of RRM, such multiplicities of RRM in a single protein may enhance the binding affinity and/or the specificity to the target RNAs; however, roles of multiple RRMs in the binding of nucleotides remain obscure.

To find functional cooperativity among multiple RRMs in the protein, we have noted a DNA/RNA-binding protein, TDP-43, which contains two tandem copies of RRM (RRM1 and RRM2). In addition to RRM1 and RRM2 in isolate, a TDP-43 fragment spanning from RRM1 and RRM2 (RRM1-2) was prepared. A

convenient method to evaluate the DNA/RNA binding of those RRMs was first developed; thereby, ability to bind DNA/RNA was detected in RRM1 and RRM1-2 but was completely absent in RRM2. Compared to RRM1 alone, furthermore, RRM1-2 was found to more exclusively bind the TG-repeated single-stranded DNA among other repeated sequences. We will thus discuss an unprecedented mechanism of how tandem-like organization of multiple RRMs contributes to the specific recognition of the target nucleotides.

3C0912 不安定な二次構造をつくるDNAのハイブリダイゼーション速度

Hybridization Rates of DNA Strands with Unstable Self-folded Secondary Structures

Hiroaki Hata[1], Akira Suyama[1,2] ([1]*Grad. Sch. Sci., Univ. Tokyo*, [2]*Grad. Sch. Arts and Sci., Univ. Tokyo*)

In this work, we investigated the effects of self-folding and single-strand base-stacking of ssDNA strands on hybridization rates. Hybridization rates of 47 pairs of complementary DNA strands were measured by using DNA microarrays. These DNA sequences have a uniform length, a uniform melting temperature and unstable self-folded structures. We found that the upper-bound of apparent hybridization rates proportionally increased with the probability of both complementary ssDNA strands being in random coil, while for the most sequences with the similar random coil probability the hybridization rate varied significantly from sequence to sequence. The large variation of hybridization rates was found to be related with the strength (S_{sbs}) of single-strand base-stacking formation in ssDNA. The hybridization rates for sequences with larger S_{sbs} were more reduced compared to the upper-bound. From the experimental results, we have constructed a hybridization reaction model describing that self-folded and base-stacked states of ssDNA reduce hybridization rates.

3C0924 長鎖DNAの1分子内折り畳みはカチオン性ポリマー凝縮剤の長さによってモードが変わる

Folding of a Single Giant Duplex DNA Chain Expresses Contrastive Behaviors depending on the Length of Cationic Polymer

Tatsuo Akitaya[1], Norio Hazemoto[2], Toshio Kanbe[3], Makoto Demura[4], Hideaki Yamaguchi[1], Koji Kubo[5], Anatoly Zinchenko[5], Shizuaki Murata[5], Kenichi Yoshikawa[6] ([1]*Fac. Pharm., Meijo Univ.*, [2]*Grad. Sch. Pharm. Sci., Nagoya City Univ.*, [3]*Sch. Med., Nagoya Univ.*, [4]*Grad. Sch. Life Sci., Hokkaido Univ.*, [5]*Grad. Sch. Env. Study, Nagoya Univ.*, [6]*Grad. Sch. Life Med. Sci., Doshisha Univ.*)

Folding transitions typically take place on duplex DNA that is sufficiently longer than the persistent length of about 50 nm, that is, 150 base pairs. On folding transition of a long duplex DNA chain induced by poly-L-lysine (PLL), we found that weak interaction induces an ON/OFF switch, whereas strong interaction causes gradual change. T4 bacteriophage genomic DNA composed of 166 kbp with a contour length of 57 μm was used for fluorescence microscopy. Tetramer and 100-mer PLL were mixed with T4 DNA solution and observed the effect on folding of a single giant DNA chain, respectively. To visualize DNA, DAPI was used to stain DNA molecules. The large-scale structure of T4 bacteriophage DNA in aqueous solution was directly observed with fluorescence microscopy. Fluorescence images were recorded on DVD through a high-sensitivity EB-CCD camera (Hamamatsu Photonics). The effects of coexisting salts on the folding of T4 DNA induced with tetramer and 100-mer PLL, concerning with an ON/OFF manner of folding and precise structure of condensed DNA. Coexisting salt inhibited the ON/OFF folding of T4 genomic DNA chain by tetramer PLL, but enhanced continuous folding by 100-mer PLL. Precise structure of folded structure was analyzed with TEM and ζ-potential. Folding analysis were also demonstrated for nonspecific DNA-binding protein HMG-1, 2 and specific protein STPR. Mechanisms and biological behavior of discrete (ON/OFF) / continuous change in large-scale structure of genomic DNA will be discussed.

3C0936 カリウムイオン依存的な四重鎖構造形成によって活性がオンになるインテリジェントリボザイムの創製

Development of intelligent ribozyme whose activity switches on in response to K^+ via quadruplex formation

Yudai Yamaoki[1,2], Tsukasa Mashima[1,2], Yu Sakurai[3], Yukari Hara[3], Takashi Nagata[1,2], Masato Katahira[1,2] ([1]*Inst. Adv. Energy, Kyoto Univ.*, [2]*Grad. Sch. Energy Sci., Kyoto Univ.*, [3]*Grad. Sch. Nanobio., Yokohama City Univ.*)

R11, an RNA that has r (GGAGGAGGAGG) sequence, forms a compact parallel quadruplex structure in response to increased K^+ concentration. We divided hammerhead ribozyme (HR) into the 5´ and 3´ portions (5´ HR and 3´ HR) within its catalytic core and inserted this R11 via linkers composed of uracil residues. The idea is to render a switch to a HR so that it turns on its catalytic activity upon increase of K^+ concentration. This molecular would be inactive outside the cell (~5 mM K^+) but turns on its activity by entering the cell (~100 mM K^+). Our first designed ribozyme, however, had some small but non-negligible activity under low K^+ concentration. The purpose of this study is to further suppress the ribozyme activity at low K^+ concentration, bring out highest possible activity at high K^+ concentration, and make the on/off difference more distinct.

First, we optimized the lengths of the uracil linkers. Among the designed ribozymes, '5´HR-UUU-R11-UU-3´HR' exhibited the highest activity under high K^+ concentration. Its activity was enhanced by ca. 4-fold as K^+ concentration was increased. Next, we introduced the complementary strand (CS) against the R11 and examined the correlation between its length and the activity. Presence of 5-mer CS showed ca. 0.3-fold lower activity than without the CS at low K^+ concentration. As a result it turned out that the enhancement of the activity by increasing K^+ concentration reached as high as ca. 6-fold.

3C0948 翻訳伸長におけるリボソームとtRNAの挙動－粗視化分子シミュレーションによる解析

Dynamical motions of tRNA and ribosome complex during translation elongation studied by coarse-grained molecular simulations

Naoto Hori, Shoji Takada (*Grad. Sch. Sci., Kyoto Univ.*)

In the final step of the translation-elongation cycle, the complex of two tRNA and mRNA molecules need to be advanced by exactly one codon in the ribosome. To realize this movement, the two ribosomal subunits are thought to be largely rearranged by the so-called ratchet-like rotation. Experiments have also shown that the tRNAs form hybrid state and cofactor EF-G is essential to efficient translocation. Although many experiments, including high-resolution structural studies, have been performed, the entire mechanism is still unclear and we were motivated to examine how these multiple factors involved in the translocation.

To reveal the molecular mechanisms, we performed coarse-grained (CG) molecular dynamics (MD) simulations. In the CG model, each nucleotide is represented as three beads and interactions are modeled with a structure-based potential, parameters of which were determined by fluctuation matching method to achieve higher accuracy. First we investigated the difference of tRNA motions between before and after the subunit rotation. In simulations, upper parts of both A-site and P-site tRNAs fluctuate between canonical(A/A and P/P) and hybrid(A/P and P/E) states. Both MD trajectories and free energy profile obtained by umbrella sampling show that the hybrid states are more stabilized in the rotated conformation. Next we further focused on relations among the inter-subunit motion, fluctuation of the tRNAs, conformational change of EF-G, and tRNA-mRNA movement.

3C1010 A structural basis for the antibiotic resistance conferred by an A1408G mutation in 16S rRNA

Jiro Kondo (*Fac. Sci. Tech., Sophia University*)

Antibiotic resistance continues to be a major public health threat. An A1408G mutation at the A site of 16S rRNA confers high-level resistance to aminoglycosides with a 6'-NH3+ group on ring I, but moderate resistance to those with a 6'-OH group such as geneticin. In order to gain insights into the antibiotic resistance, crystal structures of the mutant A site with and without geneticin have been solved in the present study. As observed in the wild-type bacterial A site, geneticin specifically binds to and stabilizes an "on" state of the mutant A site. Its ring I with a 6'-OH group forms a pseudo pair with G1408. Obviously, ring I with a 6'- NH3+ group cannot form the identical pseudo pair, because the NH3+ group repels N1-H or N2-H of G1408. In the absence of geneticin, the mutant A site takes an "off" state, which is identical to one of several "off" state conformations reported for the wild-type A site. The structural similarities observed for both the "off" and "on" states of the wild-type and A1408G-mutant A sites suggest that the A1408G mutation does not drastically disturb the function of the A site, where a cognate tRNA is discriminated from near-cognate tRNAs. Indeed, it has been reported that the A1408G mutation confers only a little reduction of the fitness of bacteria in the absence of antibiotics.

3C1022 Qβ replicase を構成する翻訳因子の RNA 合成における役割

Non-canonical functions of translational factors as RNA replication cofactors

Daijiro Takeshita, Kozo Tomita (*Biomed. Res. Inst., AIST*)

Qβ virus infects *E. coli* and replicates its genomic RNA by Qβ replicase, a tetrameric protein complex of the virus-encoded catalytic RdRp (β-subunit), and the host-donated translational elongation factors EF-Tu, EF-Ts and ribosomal protein S1. The core Qβ replicase, comprising the β-subunit, EF-Tu and EF-Ts, has RNA polymerization activity. The functions of EF-Tu and EF-Ts in Qβ replicase for RNA polymerization, beyond their established functions in protein synthesis, have remained elusive. We present six structures of the core Qβ replicase complexed with RNAs, either with or without nucleotides (and/or nucleotide analogs). The structures represent the initiation stage and five elongation stages of RNA polymerization. At the initiation stage, the 3'-terminal adenosine of the template RNA is required for *de novo* initiation, and acts as a platform for the construction of a stable initiation complex. Thus, Qβ virus acquired a nucleic acid element at the 3'-end of its genomic RNA for efficient replication of its own genome. At the elongation stages, EF-Tu in Qβ replicase assists in the separation of the dsRNA of the template and the growing RNAs, and acts as a modulator for processive RNA polymerization. Separation of the dsRNA formed by the template and the growing RNA is required for the exponential amplification the own genomic RNA in infected cells. The present study has now revealed the novel function of translational factors as RNA replication cofactors, beyond their established function in protein synthesis.

3C1034 抗 HIV 宿主因子 APOBEC3G の位置依存的デアミネーション反応機構の解明

Elucidation of the location-dependent deamination reaction mechanism of an anti-HIV factor, APOBEC3G

Ayako Furukawa[1,2], Kenji Sugase[2], Ryo Morishita[3], Taashi Nagata[1], Akifumi Takaori[4], Akihide Ryo[5], Masato Katahira[1] ([1]*Inst. of Adv. Energy, Kyoto Univ.*, [2]*Bioorg. Res. Inst., Suntory Found. Life Sci.*, [3]*CellFree Sci.*, [4]*Grad. Sch. Med., Kyoto Univ.*, [5]*Grad. Sch. Med., Yokohama City Univ.*)

APOBEC3G (A3G) deaminates cytidines in the minus-strand of the HIV DNA so that the HIV replication can ultimately be inhibited. A3G preferentially deaminates the third cytidine residue of a CCC sequence in a single-strand DNA (ssDNA). In order to obtain insight into the mechanism of the deamination reaction by A3G, we developed a real-time NMR method that can analyze the cytidine deamination reaction quantitatively. We chased the intensity changes of the cytidine peaks to be deaminated after addition of A3G to ssDNA solution. The real-time NMR experiments revealed that the deamination rates were faster for cytidines located closer to the 5' end than the 3' end, indicating that the A3G deamination reaction depends on the CCC-location.

Subsequently, to understand how A3G exerts the location-dependent deamination activity, we fitted the real-time NMR data to newly constructed kinetic models. In the model 1, A3G catalyzes at the same rates, but slides at two different rates, k_{s1} and k_{s2}, in back and forth. In the model 2, A3G slides on an ssDNA back and forth with the same sliding rate, but catalyzes at two different rates k_{cat1} and k_{cat2}, corresponding to the catalytic reactions in which A3G enters to CCC from 3' and 5', respectively. The experimental data fit well to the both models, and the quality of fitting was identical to each other. However, model 2 yielded biologically more reasonable k_{cat} values than model 1. Therefore, we concluded that the location-dependent deamination activity can be explained by model 2.

3C1046 大腸菌非六量体型 DNA ヘリカーゼ UvrD は多量体で DNA を巻き戻す

Single-molecule visualization of a non-hexameric helicase reveals active roles of its oligomeric forms in DNA unwinding

Hiroaki Yokota, Yoshie Harada (*iCeMS, Kyoto Univ.*)

Escherichia coli UvrD protein is a non-hexameric superfamily I DNA helicase which plays a crucial role in nucleotide excision repair and methyl-directed mismatch repair. We reported that the helicase takes the form of a dimer or a trimer when bound to duplex DNA with a ssDNA tail (12, 20 or 40 nt) in the absence of nucleotide or in the presence of ATPγS. Here we have extended the previous study to provide a clear answer to the question whether the helicase unwinds DNA in the form of a monomer or an oligomer in the presence of ATP, we performed simultaneous single-molecule visualization of DNA unwinding events driven by the helicase and association/dissociation events between the helicase and DNA. Kinetic analysis of the data suggests that DNA unwinding can be completed in a few seconds after two or more helicases are bound to DNA, which strongly supports the model that an oligomer is the active form of the helicase. In addition, the analysis reveals that both of the dissociation and association rates increase as the number of helicases that are bound to DNA increases. Thus, we can draw a new kinetic scheme of the DNA–helicase interaction in which not only a dimeric helicase but also a trimeric helicase can unwind DNA.

3C1058 リボソーム-SecM 翻訳アレスト配列間相互作用の 1 分子顕微解析

Single-molecule force measurement for the interaction between ribosome and SecM arrest sequence

Zhuohao Yang, Ryo Iizuka, Takashi Funatsu (*Grad. Sch. of Pharm. Sci., The Univ. of Tokyo*)

The SecM protein contains an arrest sequence at the C-terminus, which interacts with the ribosomal tunnel to induce the translation arrest. It is thought that the nascent SecM chain out of the ribosomal exit tunnel is pulled by the protein export machinery to release the translation arrest. However, this has never been fully substantiated. Then, we tried to release the translation arrest by pulling the arrested complex with optical tweezers.

The biotinylated HaloTag protein containing SecM arrest sequence at the C-terminus was synthesized using PURE system and C68 ribosome to prepare arrested ribosome-HaloTag complex. The complex was immobilized onto the glass surface via biotin-streptavidin linkage. An oligonucleotide labeled with digoxigenin was designated to hybridize to the extension loop on 30S subunit of C68 ribosome. A bead coated with anti-digoxigenin antibody was conjugated to the oligonucleotide, and used for optical trapping of the ribosomal complex. First, we measured the rupture force for the interaction between ribosome and the arrest sequence by moving the piezo stage at a constant rate. The rupture force was estimated to be 20 pN. On the other hand, the rupture force of the arrested ribosome-HaloTag complex on mRNA lacking stop codon showed 22 pN. These results suggest that <20 pN of external force is required to release the translation arrest. Now, we are examining the relationship between the lifetime of translation arrest and the applying force to evaluate the interaction between ribosome and SecM arrest sequence.

3C1110 The probability of double-strand breaks in genome-sized DNA decreases markedly as the DNA concentration increases

Shunsuke Shimobayashi[1], Takafumi Iwaki[2], Toshiaki Mori[3], Kenichi Yoshikawa[1,4] ([1]*Grad. Sch. of Sci., kyoto Univ.*, [2]*Fukui Inst., Kyoto Univ.*, [3]*Rad. Res. Cent., Osaka Pref. Univ.*, [4]*Grad. Sch. of Life and Med. Sci., Doshisha Univ.*)

DNA double-strand breaks (DSBs) represent a serious source of damage for all living things. Despite this fact, the processes that lead to their production have not yet been clearly understood, and there is no established theory that can account for the statistics of their production, in particular, the number of DSBs per base pair per unit Gy, here denoted by P_1. This is the most important parameter for evaluating the degree of risk posed by DSBs. Here, using the single-molecule observation method with giant DNAmolecules (166 kbp), we evaluate the number of DSBs caused by gamma-ray irradiation. We find that P_1 is nearly inversely proportional to the DNA concentration above a certain threshold DNA concentration. A simple model that accounts for the marked decrease of P_1. shows that it is necessary to consider the characteristics of giant DNA molecules as semiflexible polymers to understand the mechanism of DSBs.

3D0900 膜配向した PS II の ENDOR 法による Mn クラスター周辺のプロトンの位置の決定

Determine the location of protons surrounding Mn cluster of PS II by proton matrix ENDOR using oriented PS II membrane

Hiroki Nagashima, Hiroyuki Mino (*Division of Material Science, Graduate School of Science, Nagoya University*)

In oxygenic photosynthesis, light driven water-splitting is catalyzed by the Mn Cluster (Mn_4O^5Ca) in photosystem II (PS II). There are five different redox states, labeled S_n (n=0-4). By absorbing one photon, S state advanced higher oxidation state. Molecular oxygen is released during the transition of S_4 to S_0 states. Recently, the crystal structure of PS II was revealed with 1.9 &Aring

resolutions, including the location of the water molecules, amino acid and oxygen atoms coordinated to Mn cluster.
S_2 multiline signal is the well-characterized EPR signal, arising from Mn cluster. In this work, S_2 multiline signal was investigated by proton matrix ENDOR. Six pairs of ENDOR signals have been reported previously. In order to determine the locations of protons proximity to Mn cluster, the oriented PS II membranes were used for the measurements. The hyperfine splitting with 4.0 MHz changed to that with 3.6 MHz at the angle of 0°C between membrane normal $\boldsymbol{n}$ and the external magnetic field $\boldsymbol{H_0}$. In addition, the new hyperfine splitting with 1.7 MHz was detected. These signals were simulated by the dipole interactions between the electron spin on each Mn and nuclear spin of surrounding protons. Based on X-ray crystal structure, the locations of the protons for these ENDOR signals were assigned.

3D0912 Factors that differentiate the H-bond strengths of water near the Schiff bases in bacteriorhodopsin and *Anabaena* sensory rhodopsin

Hiroshi Ishikita[1,2], Keisuke Saito[1], Hideki Kandori[3] ([1]*Career-Path, Kyoto U*, [2]*JST PRESTO*, [3]*Nagoya Inst Tech*)

Bacteriorhodopsin (BR) functions as a light-driven proton pump, whereas *Anabaena sensory rhodopsin* (ASR) is believed to function as a photosensor, despite the high similarity in their protein sequences. In Fourier transform infrared (FTIR) spectroscopic studies, the lowest O-D stretch for D_2O was observed at ~2200 cm^{-1} in BR but was significantly higher in ASR (>2500 cm^{-1}), which was previously attributed to a water molecule near the Schiff base (W402) that is H-bonded to Asp85 in BR and Asp75 in ASR. We investigated the factors that differentiate the lowest O-D stretches of W402 in BR and ASR. Quantum mechanical/molecular mechanical (QM/MM) calculations reproduced the H-bond geometries of the crystal structures and the calculated O-D stretching frequencies were corroborated by the FTIR band assignments. The potential-energy profiles indicate that the smaller O-D stretching frequency in BR originates from the significantly higher pK_a(Asp85) in BR relative to the pK_a(Asp75) in ASR, which were calculated to be 1.5 and -5.1, respectively. The difference is mostly due to the influences of Ala53, Arg82, Glu194-Glu204, and Asp212 on pK_a(Asp85) in BR, and the corresponding residues Ser47, Arg72, Ser188-Asp198, and Pro206 on pK_a(Asp75) in ASR. Because these residues participate in proton transfer pathways in BR but not in ASR, the presence of a strongly H-bonded water molecule near the Schiff base ultimately results from the proton-pumping activity in BR.

3D0924 BLUF ドメインの光反応における水素結合環境の変化
Structural changes of hydrogen-bonding environment upon the photoreaction of the BLUF domains

Tatsuya Iwata[1], Shota Ito[2], Mineo Iseki[3], Masakatsu Watanabe[4], Hideki Kandori[2] ([1]*Cent. Fost. Young Innov. Res., NITech*, [2]*Dept. Front. Mater., NITech*, [3]*Faculty Pharm. Sci., Toho Univ.*, [4]*Grad. Sch. Creat. New Photo. Ind.*)

Of flavin-binding photoreceptors, BLUF (sensor of blue-light using FAD) domain shows a unique photoreaction: no apparent change in the chemical structure of FAD between unphotolyzed and red-shifted intermediate states. It has been reported that the conserved glutamine and tyrosine residues nearby FAD play crucial roles in the formation of the intermediate state. Hydrogen-bonding environment of FAD and amino acid residues are important for the photoreaction of BLUF. To investigate the hydrogen-bonding environment of FAD and these residues, we measured the BLUF domain of AppA from *Rhodobacter sphaeroides* (AppA-BLUF) by FTIR spectroscopy.
In the deuterated samples, the bands at 2416 (-) and 2029 (+) cm^{-1} were influenced by the Tyr-D_4 and ^{13}C -labeled AppA-BLUF. Thus, we concluded that these signals originate form O-D stretch of Tyr21 in the unphotolyzed and intermediate states, respectively. The corresponding frequencies of O-H stretches are ~3300 and ~2800 cm^{-1}. O-H group of Tyr21 forms moderate hydrogen bond in the unphotolyzed state and forms stronger hydrogen bond in the red-shifted intermediate state.
Measurement of ^{13}C-labeled, ^{13}C, ^{15}N-labeld, α-^{15}N-Gln labeled samples revealed no formation of C=N stretch and disappearance of C=O stretch. This result shows that the Keto-enol tautomerism reaction does not take place in the Gln63 contrary to the previous proposal. From these data, possible model for the photoreaction of BLUF domain will be proposed.

3D0936 励起移動を記述する変分マスター方程式の改良および PSII への適用
Improvement of variational master equation describing excitation energy transfer, and its application to PSII

Yuta Fujihashi, Akihiro Kimura (*Department of Physics, Graduate School of Science, Nagoya University*)

The excitation energy transfer (EET) is an essential process in the light-harvesting system. EET interaction J between Chlorophylls (Chl) and coupling λ between Chl and protein are comparable in the light-harvesting system. Recently, Nazir et al. constructed theory of quantum master equation (QME) based on variational principle in order to adequately describe EET that both interactions are comparable. We improved theory of Nazir et al. They determined the variational parameter by the free energy minimization based on the Bogoliubov inequality. We used the generalized Bogoliubov inequality derived by Decoster instead of original one for free energy minimization. This inequality can provide value close to the true free energy than the original Bogoliubov inequality. We estimated rate constants of EET by the QME with variational parameter determined by this procedure. Our calculation of rate of λ dependence by our theory was closer to the result by the non-perturbative numerical approach than that by theory of Nazir et al.
We investigated extent of the delocalized excited state within Photosystem II (PSII) by using the character of perturbation terms of above theory. From our results, it is found that at 300 K excited states are localized unless J is at least 90 cm^{-1}. This result suggests that many of excited states of Chls in PSII are localized at 300 K unlike the theoretical model of Renger et al. which were determined to extent of the delocalized excited state in PSII based on only magnitude relationship between J and λ.

3D0948 光化学系 II コア複合体での非光化学的消光の可能性
Possible non-photochemical quenching mechanism within pohotosystem II core complex

Yutaka Shibata[1], Shunsuke Nishi[2], Keisuke Kawakami[3], Jian-Ren Shen[4], Thomas Renger[5] ([1]*Grad. Sch. Sci., Tohoku Univ.*, [2]*Grad. Sch. Sci., Nagoya Univ.*, [3]*Adv. Res. Inst., Osaka City Univ.*, [4]*Grad. Sch. Sci., Okayama Univ.*, [5]*JKU Linz*)

Non-photochemical quenching (NPQ) has been known to be an important mechanism to protect the phososystems from the damage by high light. The peripheral antennae of photosystem II (PS II) have been considered to play a major role in NPQ. On the other hand, there has been few study which proposed an NPQ component operating within the PS II core complex. We have studied the ultrafast fluorescence dynamics of PS II to characterize the “red chlorophylls (Red Chls)”, which have the excited-state energies lower than the primary donor. Although the thermal fluctuation ensures the up-hill energy transfer from Red Chl to the primary donor, they seem to have no productive contribution to increase the light-harvesting efficiency. Since the exciton energy is accumulated into Red Chl, transient formation of a quencher in vicinity to Red Chl can be an effective NPQ pathway within the PS II core complex. In order to validate the above scenario, the molecular identity of Red Chl is indispensable. Recent theoretical modeling based on the structure of PS II has offered a great opportunity to clarify the exciton energy flow in PS II. We have combined our ultrafast fluorescence studies of PS II with the theoretical modeling and assigned the Chl29 (nomenclature of Loll et al. 2005) to Red Chl. Chl29 was found to be located close to ChlZ, whose oxidized form was suggested to operate as a transient quencher. Carotenoid molecules also lie proximally, implying their quenching roles. The quenching mechanism through Chl29 will be discussed in the presentation.

3D1010 低温光化学系 II における多重光還元 $Mn_4CaO_5H_x$ クラスター分布: 時間平均 XRD 構造の照射 X 線量依存性
X-ray dose dependence of time-averaged XRD structure of multi-photoreduced $Mn_4CaO_5H_x$ clusters in photosystem II at low temperature

Masami Kusunoki (*Department of Physics, School of Science Technology, Meiji University*)

The XRD structure of a light-driven water-oxidation enzyme, photosysytem II (PSII), was very recently revealed its electron density image at resolution of 1.9 Å. However, it is critically inconsistent with EXAFS data in the dark stable S1-state. To evaluate the x-ray radiation damage, we present the potoreduction kinetics for the X-ray photoelectric effect followed by the photoionization processes leading to multiple photoreductions of the water-splitting Mn_4CaO_5 cluster, which is directly proportional to the X-ray dose. This kinetics is based on the fact that solvated photoelectrons can rapidly diffuse into and out from the manganese cluster through H-bonding water channel(s) to realize a quasi-

steady distribution under x-ray irradiation. This theory was applied to analyze two relevant photoreduction data by x-ray absorption near edge spectroscopy (XANES) at the manganese K-edge of PSII samples at low temperatures. Thus, we could establish the universal E_{edge} vs K_1t relationship of OEC in PSII together with the reduction rate constants, {K_j, j=0, -1, . . , -5}, as well as the most-likely manganese valence models of the Mn4 clusters in these photoreduced S_j-states, to show that the 1.9 Å. resolution XRD image of the Mn_4CaO_5 cluster in PSII crystal would be a result of integrated contributions mainly from S_0 and S_{-1} states. Using UDFT/B3LYP method, we also show X-ray dose dependence of its time averaged atomic structure is in line with the observed $Mn_4CaO_5(H_2O)_4$ structure.

3D1022 光化学系 II 酸素発生系 S_2状態における Mn 間磁気的相互作用の解明

Determination of magnetic couplings of S_2 state Mn-cluster in Photosystem II studied by PELDOR measurement

Mizue Asada[1], Hiroki Nagashima[1], Faisal Hammad Mekky Koua[2], Jian-Ren Shen[2], Hiroyuki Mino[1] ([1]*Grad. Sch. Sci., Univ. Nagoya*, [2]*Grad. Sch. Natl. Sci. & Tech., Univ. Okayama*)

Oxygen evolution is carried out by Mn-cluster in Photosystem II (PS II). Mn-cluster is consisted of four Mn, five O and one Ca, and is oxidized through a cycle of five redox states labeled S_n (n = 0-4). In the S_2 state, an EPR signal, called S_2 multiline signal, was detected at g = 2 with about 60 mT width. It is derived from mix valent Mn ions with one Mn(III) and three Mn(IV), coupled with exchange interactions. Recently, the PS II structure with 1.9 Å resolutions was revealed by X-ray analysis [1]. However, the magnetic structure of the Mn-cluster has not associated to the molecular structure derived by X-ray crystallography.
Pulsed electron-electron double resonance (PELDOR) is a well-established method for measuring distance between electronic spins by detecting dipole interactions. We measured the PELDOR signals between Y_D and Mn-cluster in S_2 state in the *spinach* and *T. vulcanus* PS II membranes. Based on the anisotropy of the PELDOR signal in the oriented PS II, the spin projections of each Mn atom were determined by using coordinates in the crystal structure. The results show that the Mn ion coordinated by H332, D342 and E189, has a valence of Mn(III) in the S_2 state. The signs of the exchange interactions between four Mn atoms were determined.
[1] Umena Y. et al. *Nature*, 473, 55-U65 (2011)

3D1034 光化学系 II におけるキノン電子受容体の酸化還元電位制御機構

Mechanism of controlling the redox potentials of the quinone electron acceptors in photosystem II

Ryota Ashizawa[1], Takuya Iwasa[1], Miwa Sugiura[2], Takumi Noguchi[1] ([1]*Division of Material Science, Graduate School of Science, Nagoya University*, [2]*Division of Material Science, Graduate School of Science, Nagoya University*)

Photosystem II (PS II) in plants and cyanobacteria withdraws electrons from water using light energy and transfer them to the primary quinone electron accepter Q_A and then to the secondary quinone acceptor Q_B. Although the chemical identity of Q_A and Q_B is both plastoquinone-9 (PQ-9), the redox potential of Q_B is higher than that of Q_A, facilitating an electron flow from Q_A to Q_B. The interactions of PQ with proteins should play a major role in determining the redox potentials of these quinone electron acceptors; however, the details remain to be clarified. In this study, we have investigated the mechanism of controlling the redox potentials of Q_A and Q_B using density functional theory calculations and Fourier transform infrared spectroscopy. Energy levels of neutral and anion forms of various H-bonded complexes of PQ with water or amino acids as H-bond donors were calculated and the redox potentials were estimated. It was shown that the redox potential of PQ linearly increased with the number of H-bond by +165 mV/H-bond at ε = 4.9. Thus, the higher redox potential of Q_B than Q_A by ~+80 mV can be attributed to more H-bonds in Q_B (three H-bonds) compared with Q_A (two H-bonds) as have been revealed by X-ray crystallography. We also calculated the frequencies and the 13C-isotope shifts of the C=O stretching vibrations of PQ in the model H-bond complexes. The calculated frequencies were compared with the experimental ones in relevance to the H-bond interactions of Q_A and Q_B in PSII proteins.

3D1046 光合成バクテリア反応中心の電子移動経路解析

Electron Transfer Pathway Analysis in Bacterial Photosynthetic Reaction Center

Hirotaka Kitoh-Nishioka, Koji Ando (*Grad. Sch. Sci. Kyoto Univ.*)

We have recently developed a novel approach [1] to describe long-distance electron transfer (ET) reaction in large systems by using the fragment molecular orbital (FMO) method. With use of the molecular orbitals (MO) from the FMO-LCMO method [2] that are properly delocalized over the entire system, we compute the electronic coupling energy of ETs by the generalized Mulliken-Hush and the bridge Green function methods. Moreover, the tunneling current analysis is carried out at the fragment resolution, which has advantages both conceptual and computational.
In this study [3], we have applied our approach to the ETs in photosynthetic reaction center of *Blastochloris viridis*. For the ET from menaquinone to ubiquinone, a major pathway via the Fe^{2+} ion and a histidine ligand (His L190) is observed. When the metal ion is replaced by a Zn^{2+}, another pathway involving two His ligands (His M217 and His L190) opens. These two His residues take up the central role when the metal ion is depleted. The computed values of electronic coupling are found to be consistent with experiments.
[1] H. Nishioka and K. Ando, *J. Chem. Phys.* **134** (2011) 204109. [2] S. Tsuneyuki et al., *Chem. Phys. Lett.* **476** (2009) 104. [3] H. Kitoh-Nishioka and K. Ando, submitted.

3D1058 光合成細菌 Rhodopseudomonas の遺伝子発現パターンの電気化学制御

Electrochemical regulation of gene expression profiles of Rhodopseudomonas, a photosynthesis bacterium

Yue Lu[1], Syoichi Matsuda[1], Shuji Nakanishi[2], Kazuhito Hashimoto[1] ([1]*The Univesity of Tokyo, School of Engineering, Department of Applied Chemistry*, [2]*Research Center for Advanced Science and Technology*)

Photosynthetic bacteria are able to synthesize organic compounds directly from CO2 and water by using energy from sun light. The amounts of CO2 reduced by such microorganism are so considerable that can significantly contribute to the carbon cycle on the earth. Recently, production of useful organics or bioenergy from CO2 by photosynthesis microorganisms has attracted a lot of attentions. Most of the studies conducted so far are based on molecular biological techniques such as construction of various mutants. Although these methods are very powerful, they also possess a couple of problems with respect to safety and cost. We are trying to enhance CO2 fixation ability of wild types of photosynthetic bacterium via electrochemical tuning of the intracellular redox environment which deeply involved in expressions of genes related to photosynthesis. As a first step, we successfully regulate the expression level of genes encoding chlorophyll, which is an extremely important biomolecule allowing bacteria to absorb light energy, of model bacteria Rhodopseudomonas by electrochemical method.

3E0900 核膜孔複合体構造変化による核移行制御機構の構造基盤

Structural basis for nuclear import regulated by molecular rearrangements in the nuclear pore complex

Junya Kobayashi[1], Yoshiyuki Matsuura[1,2] ([1]*Div. Biol. Sci., Grad. Sch. Sci., Nagoya Univ.*, [2]*Strl. Biol. R. Ctr., Grad., Nagoya Univ.*)

In all eukaryotes, precise regulation of the bidirectional transport of macromolecules between the nucleus and the cytoplasm is essential for many cellular processes, including gene expression, signal transduction, cell cycle progression and differentiation. Nuclear transport occurs through nuclear pore complexes (NPCs) that form aqueous channels across the nuclear envelope. Altering the structure of NPCs is emerging as a novel mechanism to control nuclear transport. In this study, we focus on a nuclear import pathway that is regulated by a cell-cycle dependent interaction between a nuclear import receptor and a nucleoporin. Here we report crystal structures of the import receptor in isolation, and also in complex with either its import cargoes or the nucleoporin or RanGTP. Our new structures establish the structural basis for recognition of a novel nuclear localization signal (NLS), cargo-displacement by RanGTP, and import regulation triggered by cell-cycle dependent NPC rearrangements.

3E0912 NADH シトクロム b_5還元酵素超高分解能結晶構造解析による水素と外殻電子の観察

Visualizing hydrogens and outer-shell electrons of NADH cytochrome b_5 reductase by ultra-high resolution crystallography

Kiyofumi Takaba[1], Kazuki Takeda[1], Masayuki Kosugi[1], Taro Tamada[2], Ryota Kuroki[2], Kunio Miki[1] ([1]*Grad. Sch. Sci., Univ. Kyoto*, [2]*JAEA*)

NADH cytochrome b_5 reductace (b5R) is an enzyme transferring electrons from NADH to cytochrome b_5, and it has an FAD molecule in the active center as a cofactor for reduction. To understand the molecular mechanism of b5R, it is indispensable to determine the accurate position of hydrogen atoms and the distribution of the outer-shell electrons. Ultra-high resolution X-ray crystallography better than 1Å resolution enables us to visualize such details of distribution of electrons. We determined an oxidized structure of porcine b5R at 0.78Å resolution by ultra-high resolution crystallography with high energy X-rays from SPring-8. The model structure includes about 90% of all hydrogen atoms. Considering the resolution-dependent feature of atomic scattering factors, some corrections in the reciprocal space was performed, which produced clear visualization of the electrons of hydrogens of FAD and the residues interacting with FAD, and outer-shell electrons such as lone pairs of carbonyl oxygens and imino nitrogens and covalent bond electrons of these groups in the electron density map. These detailed electron distribution revealed the hydrogen bond network in the active center of b5R, which provided significant clues for understanding its ability in transferring electrons.

3E0924 最新の各種固体 NMR 法を用いた絹の構造解析

Silk Structure studied by Newly-developed Solid-state NMR

Keiko Okushita, Koji Yazawa, Akihiro Aoki, Tetsuo Asakura (*Grad. Sch. of Eng., Tokyo Univ. Agr. Tech.*)

Recently, silk fibroins from silkworms have been used as excellent biomaterials as well as excellent textiles. In order to develop such an excellent biomaterial, the detailed structural information is required. Newly-developed solid-state NMR has been applied to clarify the silk fibroin structure. Ultra-high field NMR (930 MHz) coupled with ultra high speed MAS probe (80 kHz speed) have been used to clarify the inter-molecular structures of silk model peptides through ^{1}H solid-state NMR. In addition, ^{13}C labeling of silk fiber and ^{13}C solid-state NMR such as DARR or PDSD has been also used for studying the inter-molecular structure.

3E0936 Interaction of human calcitonin with curcumin as an inhibitor of fibrillation as revealed by NMR and docking simulation

Ken Takeuchi[1], Hikari Watanabe[1], Javkhlantugs Namsrai[1], Hiroshi Hirota[2], Akira Naito[1] ([1]*Yokohama National University Graduate School of Engineering*, [2]*Riken*)

Human calcitonin (hCT) is known to form an amyloid fibril precipitate in concentrated aqueous solution and is associated with medullary carcinoma of the thyroid, although calcitonin (CT) is a peptide thyroid hormone in mammals, and plays a central role in calcium-phosphorus metabolism. Therefore, CT has been studied not only for therapeutic use with long stability but also as a model peptide to clarify the fibrillation process and mechanism of amyloid fibril formation. In the TOCSY NMR experiments, the lyophilized preparation were dissolved in 20 mM phosphate buffer containing the 100 mM salt at pH 7.4 and added DMSO with the volume ratio be 15%. A freeze-dried sample was dissolved in this solution. TOCSY NMR was measured right after the mixing of the sample with the solution. Next, we measured TOCSY spectrum in the addition of 1.1 mM of Curcumin. It was noted that a peak of Phe16 did not disappear in the spectrum. This result indicates that the core part of hCT does not form fibril. It is therefore expected that Phe16 signal will disappear after the fibril formation. Thus, it is concluded that curcumin interacts with hCT to inhibit the fibril formation. The interactions of curcumin tautomers with hCT peptide were revealed by using docking simulation. The structures of curcumin tautomers and hCT were first determined in water solution and used for the initial conformations of the docking simulation until the stabilized structures were obtained. Detailed simulation results will be presented in the meeting.

3E0948 単粒子クライオ電子顕微鏡解析によるサポウイルスキャプシドの 8-Å 構造

8-Å structure of sapovirus capsid by single particle electron cryomicroscopy

Naoyuki Miyazaki[1], David Taylor[1], Grant Houseman[2], Kosuke Murakami[2], Kuniaki Nagayama[1], Kazuhiko Katayama[2], Kazuyoshi Murata[1] ([1]*National Institute for Physiological Sciences*, [2]*National Institute of Infectious Diseases*)

The caliciviruses are a family of small non-enveloped viruses of 27 to 40 nm in diameter, and can be classified into five genera: Vesivirus, Lagovirus, Norovirus, Sapovirus and Nebovirus. Among them, noroviruses and sapoviruses are well known to cause gastroenteritis in a range of mammals, including humans. However, study of the sapoviruses is far behind compared with noroviruses. For example, the capsid structures of noroviruses and vesiviruses have been determined at atomic resolution, while no structure is available for sapoviruses. Therefore, we determined the capsid structure of the sapovirus at about 8-Å resolution by conventional cryo-electron microscopy and single particle reconstruction to get structural insights into the host specificity. Furthermore, we performed homology modeling with the cryo-EM map. The sequence of the capsid protein of sapovirus was aligned with the related sequences of noroviruses and vesiviruses by using information of predicted secondary structures and electron microscopically determined three-dimensional structures due to their low sequence similarities. Then, homology model was created and refined after fitting into the cryo-EM map. To get more accurate model, we have tried to improve the resolution by Zernike phase contrast cryo-electron microscopy with a direct detection device (DDD) detector for electrons. These progresses will be discussed.

3E1010 Structural analysis of the 26S proteasome by cryo-electron microscopy and Single-Particle Analysis

Zhuo Wang[1], Yasuo Okuma[1], Daisuke Kasuya[2], Kaoru Mitsuoka[3], Yasushi Saeki[4], Yasunaga Takuo[1] ([1]*Department of Bioscience and Bioinformatics, Faculty of Computer Science and Systems Engineering, Kyushu Institute of Technology*, [2]*Biomedicinal Information Research Center, Japan Biologycal Information Consortium (JBIC)*, [3]*Biomedicinal Information Research Center, National Institute of Advanced Industrial Science and Technology*, [4]*Laboratory of Protein Metabolism, Tokyo Metropolitan Institute of Medical Science*)

The 26S proteasome is the key enzyme in eukaryotic homeostasis and it plays an important role by undertaking highly controlled degradation of a wide range of proteins, including cellular regulators such as those controlling cell-cycle progression and apoptosis. The 26S proteasome is composed of one 20S core particle (CP) and two 19S regulatory particles (RPs). According to fragile nature and dynamics of the 26S proteasome, RPs cannot bind to the CP tightly, which makes structural analysis of the 26S proteasome more difficult. Although the basic organization of the RP in the Schizosaccharomyces pombe 26S proteasome has been determined with a 9. 1Å resolution by cryo-electron microscopy (cryo-EM), the detailed localization of the RP subunits have not revealed yet. In our study, for preventing RPs from releasing, 10% glycerol has been added in the specimen and micrographs were acquired by cryo-EM at the liquid helium temperature, Thus it was found that the photograms of Rpn10-eliminated mutants have low contrast and so their 'picking up' was more difficult than usual. To solve this problem, CTF compensation using Wiener filter has been used in image processing considering spatial frequency-dependent SN ratio. After that, Rpn10-eliminated mutant particles have been visible and easily picked up only RP-bound CPs in the photograms. The 3D maps of Rpn10-eliminated mutant by single-particle analysis after classification and averaging will be reported here.

3E1022 大気圧電子顕微鏡（ASEM）によるタンパク質微結晶とマイコプラズマの液中観察

Direct electron microscopy of protein crystals and Mycoplasma cells in solution using the Atmospheric SEM

Yuusuke Maruyama[1], Tatsuhiko Ebihara[1], Daisuke Nakane[2], Hidetoshi Nishiyama[3], Takayuki Nishizaka[4], Miki Senda[5], Kazuhiro Mio[1], Mitsuo Suga[3], Toshiya Senda[1], Makoto Miyata[2], **Chikara Sato**[1] ([1]*AIST*, [2]*Univ. Osaka City*, [3]*JEOL*, [4]*Univ. Gakushuin*, [5]*JBIC*)

High-resolution, quick visualization of biological sample in solution is an important theme, especially in the field of diagnosis and screening. Protein microcrystals and Mycoplasmas are the samples not easy to observe by optical microscopy. The nanometer-to-sub-nanometer resolution range of electron microscopy (EM) would be appropriate for this; however, to avoid electron scattering, usual SEM (Scanning EM) and TEM (Transmission EM) require the electron pathway, including sample holder, to be essentially vacuum. This necessitates the time-consuming pretreatment of biological samples for preservation in extremely low pressure. In response to this difficulty, we have developed the advanced version of SEM, an atomospherice SEM (ASEM). This is an electron microscope with an inverted configuration, allowing samples to be viewed in open atmosphere. This system can be applied not only to examine cells and tissues, but also non-biological samples; salt crystal growth, nano-particle self-organization, electrochemical deposition, and the changes occurring during of solid / liquid phase transition of metal (1. We applied this microscopy to protein microcrystals and Mycoplasma, an important creature in medicine and in biology(2. [1] Ultramicroscopy 111, 1650-58, 2011. [2] BBRC 417, 1213-18, 2012.

3E1034 粗視化 Go モデルを用いた Ferredoxine-like fold タンパクのフォールディング機構の解析

Analyses of folding processes on the Ferredokin-like fold proteins by means of a coarse grained Go model

Masatake Sugita, Takeshi Kikuchi (*Dept. Bioinf., Coll. Life Sci., Ritsumeikan Univ.*)

It has been recognized that analysis of proteins with a same native topology is efficient strategy for comprehending protein folding mechanisms. In particular, proteins sharing Ferredoxin-like fold are widely studied experimentally. It has been reported that these proteins exhibit various φ value patterns. These profiles are interpreted that stability of the two competing foldons regulates folding mechanisms. We are currently studying Ferredoxine-like fold proteins by analyzing amino acid sequence information. Our data also indicate that a significant segment for a folding is different among Ferredoxin-like fold proteins. For detailed elucidation of folding mechanisms with higher resolution including extensive free energy profiles, we have to conduct simulation approach. In this study, we analyze the folding processes of Ferredoxin-like fold proteins using coarse grained Go model. We use protein S6, U1A and ADA2h as target proteins. While we couldn't distinguish individual folding pathway using a topology-only model, we discern the difference of heights of free energy barrier. On the other hand, we got inherent folding process respect to each target protein using the model including sequence colors.

3E1046 異なる参照状態を用いた統計ポテンシャルによるタンパク質モデル構造の最適化

Optimization of protein model structures according to statistical potentials with different reference states

Matsuyuki Shirota[1,2], Kengo Kinoshita[1,2,3] ([1]*GSIS, Tohoku Univ.*, [2]*ToMMo, Tohoku Univ.*, [3]*IDAC, Tohoku Univ.*)

Prediction of the 3D structure of a protein molecule from its amino acid sequence is an important challenge in computational biophysics. One of the bottlenecks is to select the most native-like structure among the model structures generated in the prediction process. Statistical potentials derived from protein structure database are widely used for this purpose. In principle, they are developed by counting the conformations in the database of native protein structures under the assumption that frequently observed conformations are energetically favorable ones. To quantify the significance of the counts of conformations in the database, the reference state, a virtual state in which all atomic interactions are random, is required. Previously, we demonstrated that the definition of the reference state of distance-dependent atomic pair statistical potentials can be theoretically variable and in practice statistical potentials with various reference states show different advantages, such as specificity for the native structures or the correlation to the native-likeness. To further explore the problem of reference states, here we developed an optimization method of protein model structures under several statistical potentials based on distinct reference states. In addition, we also employed several statistical potentials in a linear combination to improve the performance. Our results showed that various reference states have different advantages in both model evaluation and model optimization.

3E1058 クーロンレプリカ交換法を用いた A β フラグメントに関する研究

Studies on a Aβ fragment by the Coulomb replica-exchange method

Satoru Itoh[1,2], Hisashi Okumura[1,2] ([1]*Institute for Molecular Science*, [2]*The Graduate University for Advanced Studies*)

Effective samplings in the conformational space are necessary to predict the native structures of proteins. The replica-exchange method (REM) is one of the most well-known methods among the generalized-ensemble algorithms which realize effective samplings in the conformational space for biomolecular systems. However, REM has a difficulty for large systems that many replicas are needed to realize such effective samplings. In other words, huge amount of computer time is required in the replica-exchange method for the large systems. In order to overcome this difficulty, we proposed a new replica-exchange method, which we refer to as the Coulomb replica-exchange method (CREM), recently. In this CREM, electrostatic charges are exchanged among replicas although the temperatures are exchanged in conventional replica-exchange method. By exchanging the electrostatic charges, the free-energy barrier come from the electrostatic interactions are reduced. Moreover, the number of replicas can be decreased by exchanging the electrostatic charges only of solute atoms. Consequently, the CREM simulations realize effective samplings in the conformational space with small number of replicas. I will show the effectiveness of this method through applications to a amyloid-beta fragment.

3E1110 レプリカ交換インターフェースプログラム(REIN)

Replica-exchange interface program (REIN)

Naoyuki Miyashita[1,2,3], Suyong Re[4], Yuji Sugita[1,2,3,4] ([1]*RIKEN QBiC*, [2]*RIKEN CSRC*, [3]*RIKEN AICS*, [4]*RIKEN ASI*)

In the recent decade, replica-exchange molecular dynamics (REMD) method [1] has attracted much attention as an enhanced conformational sampling method. In REMD, ensembles consist of non-interacting copies (replicas) of an original system with different conditions. The pair of replicas are exchanged every few steps by metropolis criteria to enhance the sampling efficiency.
We have developed replica-exchange Interface program (REIN) to facilitate REMD simulations. Currently, the multi-dimensional REMD can be performed [2] using the highly parallelized conventional MD (NAMD2 [3] and MARBLE [4]). The other conventional MD programs can be easily combined as well. REIN is also tested for use in supercomputer systems, enabling us to simulate substrate binding or conformational changes in large proteins with high precision. The detail of program and some recent applications will be presented.
[1] Y. Sugita and Y. Okamoto, Chem. Phys. Lett., 314,141(1999)
[2] Y. Sugita, A. Kitao, and Y. Okamoto, J. Chem. Phys., 113, 6042 (2000)
[3] J. C. Philip et al., J. Comp. Chem., 26, 1781 (2005)
[4] M. Ikeguchi, J. Comp. Chem., 25, 529 (2004)

3F0900 サポーテット膜を用いた膜タンパク質の顕微鏡下でのイオン輸送活性計測

Evaluation of ion-pump activity of membrane proteins reconstituted on supported membrane under optical microscope

Jyunan Ki, Rikiya Watanabe, Kazuhito Tabata, Hiroyuki Noji (*Department of Applied Chem., Univ. Tokyo*)

Supported membrane is the experimental platform in which a lipid bilayer is tethered on a solid surface. Owing to the mechanical stability, it allows us to investigate physicochemical properties of membranes and also membrane proteins reconstituted in the membrane. In this study, to enhance the versatility of this method, we developed a novel supported membrane system that enables to measure the ion-pump activity of membrane proteins under an optical microscope. As a model ion pump, we reconstituted F_oF_1-ATP synthase (F_oF_1) in liposomes. The supported membrane was prepared on a glass surface from the reconstituted liposome with a buffer containing a pH indicator dye (pHrodo) and caged-ATP. By introducing the evanescent illumination of 405 nm light for uncaging of ATP from the bottom of the glass surface, ATP was supplied only in the illumination area. The local pH of the membrane-surface space was monitored with the fluorescent signal of pHrodo excited with the evanescent illumination of 532 nm. Only after the illumination for uncaging, the intensity of pHrodo evidently increased, suggesting the acidification between the membrane-surface space. Furthermore, the degree of the acidification was proportional to the amount of uncaged ATP. These results showed that this systems allowed us to successfully monitor the H^+-pumping activity of F_oF_1 reconstituted in the supported membrane.

3F0912 Catalytic activity of MsbA reconstituted in nanodisc particles is modulated by remote interactions with the bilayer

Takeaki Kawai[1], Jose Caaveiro[1,2], Toyomasa Katagiri[3], Hisashi Tadakuma[1], Takuya Ueda[1], Kouhei Tsumoto[1,2,4] ([1]*Grad. Sch. of Front. Sci., Univ. of Tokyo*, [2]*Inst. Med. Sci., Univ. of Tokyo*, [3]*Inst. Gen. Res., Univ. of Tokushima*, [4]*Dep. Chem. Bio., Univ. of Tokyo*)

ATP-binding cassette (ABC) transporters couple hydrolysis of ATP with vectorial transport across the cell membrane. We have reconstituted ABC transporter MsbA in nanodiscs of various sizes and lipid compositions to test whether ATPase activity is modulated by the properties of the bilayer. ATP hydrolysis rates, Michaelis-Menten parameters, and dissociation constants of substrate analog ATP-γ-S demonstrated that physicochemical properties of the bilayer modulated binding and ATPase activity. This is remarkable when considering that the catalytic unit is located ~50 angstrom from the transmembrane region. Our results validated the use of nanodiscs as an effective tool to reconstitute MsbA in an active catalytic state, and highlighted the close

relationship between otherwise distant transmembrane and ATPase modules.

3F0924 線虫イネキシン 6 ギャップ結合チャネルの単離と機能特性

Isolation and characterization of C. elegans innexin-6 gap junction channels

Atsunori Oshima[1], Tomohiro Matsuzawa[2], Kouki Nishikawa[1], Yoshinori Fujiyoshi[1] ([1]*CeSPI, Nagoya Univ.*, [2]*Grad. Sch. of Sci., Kyoto Univ.*)

Invertebrates possess gap junction channels composed of innexins that evolved independently from vertebrate connexins. Only limited information is, however, available on the innexin channel structure. Here we successfully expressed and purified *C. elegans* innexin-6 (INX-6, 45kDa) gap junction channels, and characterized the structural properties and channel permeability using electron microscopy and microinjection of fluorescent dye tracers, respectively. The INX-6 proteins formed gap junction plaques with a loosely packed hexagonal lattice. Channel distance, based on the reflection spots of the INX-6 gap junction plaques, was longer than that of connexin-26 (Cx26, 26 kDa). Thin-section electron microscopy revealed that the INX-6 junction was thicker than the Cx26 junction. The purified INX-6 channels in dodecylmaltoside solution generally ran slower than Cx26 channels in gel filtration analysis, suggesting that the purified INX-6 channels were mostly hemichannels, which was supported by electron microscopy and native gel electrophoresis. Dye transfer experiments showed that 3-kDa dextran-Texas red and 10-kDa dextran-Texas red passed through INX-6 channels at rates of approximately 50% and 10%, respectively, while no significant amounts passed through connexin-43 channels. These results have implications regarding the dimensions and overall structure of the INX-6 channels, and provide insight into the wider pore diameter of INX-6 channels compared with that of connexin channels.

3F0936 ATR-FTIR 法を用いた KcsA 野生型と不活化しない変異体に対するカチオン誘起構造変化の赤外分光分析

Cation-induced structural changes in the WT and non-inactivating mutant KcsA studied by ATR-FTIR

Chikako Muramatsu[1], Masayo Iwaki[1], Tetsuya Fukuda[1], Yusuke Asai[1], Yuji Furutani[1,2], Hideki Kandori[1] ([1]*Grad. Sch. Tech., Nagoya Inst. Tech.*, [2]*Inst. Mol. Sci.,*)

The bacterial potassium channel KcsA is a membrane protein complex of homotetramer. The channel is gated by high concentration of intracellular protons, and transports cations through the filter that permeates K^+selectively over Na^+. In the wild type (WT) KcsA, the filter can be in both open and inactivated (collapsed) structures depending on ionic/pH conditions, whereas the filter remains open in the non-inactivating mutants such as E71A, E71V and F103A. In this study, we investigate the mechanism of ion selectivity coupled with gating process using attenuated total reflection Fourier transform infrared (ATR-FTIR) spectroscopy. WT and mutant proteins of KcsA of *Streptmyces lividans* were expressed in *E. coli*, and purified proteins were reconstituted in liposomes and deposited on an ATR-prism. K^+- or Na^+-induced difference FTIR spectra were measured by switching perfusion buffers with and without cation. At pH 7, the gate of the WT was closed and the selectivity filter was presumably open. K^+-induced spectrum showed different IR features from Na^+-induced one, indicating different ionic interactions of K^+ and Na^+ to the protein. The IR spectra obtained at pH 4 were different from those at pH 7. The corresponding spectra measured in the non-inactivating mutants were compared to those in the WT. Conformational changes in peptides upon the binding of cations to KcsA are discussed based on the obtained IR data in the light of atomic structures available from X-ray crystallography.

3F0948 黄色ブドウ球菌の 2 成分性膜孔形成毒素の分子機構

Molecular basis of staphylococcal bi-component pore forming toxin

Yoshikazu Tanaka[1], Daichi Yamashita[2], Keitaro Yamashita[2], Yuka Kawai[2], Jun Kaneko[3], Noriko Tomita[4], Makoto Ohta[4], Yoshiyuki Kamio[5], Min Yao[1], Isao Tanaka[1] ([1]*Fac. of Adv. Life Sci., Hokkaido Univ.*, [2]*Grad. Schl. of Life Sci., Hokkaido Univ.*, [3]*Grad. Schl. of Agri. Sci., Tohoku Univ.*, [4]*Inst. of Fluid Sci., Tohoku Univ.*, [5]*Grad. Schl. of Life Sci., Tohoku Univ.*)

Pathogenic bacteria secrete various pore-forming toxins (PFTs) to kill host cells. PFTs are expressed as water-soluble monomeric proteins that oligomerize into nonlytic prepore intermediates on the membrane of the target cells, and then form bilayer-spanning pores.

Staphylococcus aureus, a ubiquitous and pernicious human pathogen, secretes several PFTs including α-hemolysin (αHL), γ-hemolysin (γHL), leukocidin (LUK), and Panton-Valentine leukocidin (PVL). αHL consists of a single polypeptide, whereas the others are bi-component PFTs that require the synergistic association of a class F component and a class S component. Extensive experiments have been carried out for more than two decades, and the crystal structures of the monomeric forms of bi-component PFTs have been determined. However, the structures of the prepore and pore forms have not been reported at atomic resolution, which has hindered detailed discussion of the complicated molecular mechanism.

In the present study, we determined the crystal structure of the prepore and pore form of bi-component PFT, γHL. This is the first report of the crystal structure of a heterocomponent β-barrel-type transmembrane protein. This is also the first PFT of which all of monomer-, prepore-, and pore-form structures have been determined by X-ray crystallography. Based on the structural differences between pore and monomer forms in combination with biological data accumulated over the past two decades, we propose a mechanism of pore formation by PFTs.

3F1010 分子動力学法によるグラミシジン A を含んだ脂質二重層膜の構造と圧力特性

Structure and lateral pressure profile of lipid bilayer containing gramicidin A by molecular dynamics simulation

Hiroaki Saito, Masashi Iwayama, Megumi Nishimura, Hiroyuki Takagi, Kazutomo Kawaguchi, Hidemi Nagao (*Kanazawa University*)

The molecular dynamics (MD) simulations of DMPC (diC14:0-PC) and DSPC (di18:0-PC) lipid bilayers in the absence and presence of gramicidin A (GA) peptide dimer were carried out to investigate the GA effect on these membrane structure and the lateral structure. The observed hydrophobic thickness and order parameter increased, and the gauche conformation reduced in the presence of GA, and these results are consistent with the experimental measurements. Due to the hydrophobic mismatch between the GA and surrounding lipid bilayer, the hydrophobic thickness of the DSPC membrane largely decreased to fit the length of hydrophobic core region of the GA peptide dimer, resulting in a distortion of the membrane surface around the GA. The surface tension around the polar headgroup region decreased due to the decrease of electrostatic interaction between headgroups. Since the DSPC lipid bilayer has a larger hydrophobic length, the larger positive lateral pressure appears around the GA channel entrance region in the membrane. The larger lateral pressure in the hydrophobic region of the DSPC/GA membrane results in the reduction of pore radius around the GA channel entrance, suggesting the decrease of ion accessibility to the GA channel entrance.

3F1022 代謝型グルタミン酸受容体の膜貫通領域における 1 アミノ酸変異がアゴニストをインバースアゴニストに変える

Single amino acid substitution in the transmembrane domain of metabotropic glutamate receptor changes an agonist into an inverse agonist

Masataka Yanagawa, Takahiro Yamashita, Yoshinori Shichida (*Department of Biophysics, Graduate School of Science, Kyoto University*)

Metabotropic glutamate receptors (mGluRs) are prototypical family 3 G protein-coupled receptors (GPCRs) that function as a constitutive homo dimer. They have a large extracellular ligand-binding domain (ECD) on the N-terminal side of seven-transmembrane domain (TMD). Upon binding of an agonist, an intersubunit relocation of the dimeric ECDs induces a mutual rearrangement of TMDs, which was observed by our previous fluorescence resonance energy transfer (FRET) analyses. However, the conformational change within each protomer of mGluR is largely unknown. Here we report that a single amino acid mutation at a threonine residue conserved in helix VI of mGluRs caused elevation of a basal activity, whereas the glutamate binding to the mutant partially suppressed the basal activity. Namely, original “agonist” works as an “inverse agonist” on this mutant. The comparative FRET analysis of wild-type and the mutant demonstrated that the glutamate-dependent dimeric rearrangement of the mutant is similar to that of wild-type. Therefore, alteration of the ligand character in the mutant should be originated from a conformational change within each protomer. Double mutation analyses revealed that an additional mutation in helix VII restored the “agonist”-dependent increase of the activity. In conclusion, the proper packing between helices VI and VII around the threonine residue within each protomer is a key determinant of the activation of mGluRs.

3F1034 non-detergent sulfobetaine (NDSB)による G 蛋白質共役型受容体 (GPCR)の熱安定化

Thermal stabilization of G protein-coupled receptor by non-detergent sulfobetaines (NDSBs)

Toshihide Yamai, Layla Takahashi, Masato Nakajima, Naoki Yamashita, Takeshi Ishii, Shigeki Takeda, Kaori Wakamatsu (*Gunma Univ.*)

Structural analyses of G protein-coupled receptors (GPCRs) are expected to facilitate drug development since more than a half of pharmaceutical drugs target at GPCRs. Thermal stabilization of GPCRs will be beneficial for the structural analyses because GPCRs generally heat labile.
Non-detergent sulfobetaines (NDSBs) are known to stabilize many proteins, and we have found that NDSBs, in particular NDSB-256, potently stabilize m2 muscarinic acetylcholine receptor (m2-R). Here we analyzed the mechanisms whereby NDSB-256 stabilizes m2-R.
The apparent dissociation constant Kd of NDSB-256 and m2-R, as determined by the NDSB-256 concentration dependence of the denaturation time constant of m2R at 50 degree, was smaller than the inhibition constant Ki of NDSB-256, as determined by competitive inhibition of [3H]QNB-binding to m2R. These observations suggest that NDSB-256 stabilizes m2R by two mechanisms: binding to the orthosteric site and stabilization of the whole protein.
Because the orthosteric sites of many amine receptors (including m2R) contain both an acidic aspartic acid residue and aromatic residues, amine receptors are expected to be stabilized in general by NDSB-256, which has both an ammonium moiety and an aromatic ring.

3F1046 固体 NMR を用いた熱および圧力により誘起されるバクテリオロドプシンの構造と運動性変化の解析

Thermal and Pressure induced structural and dynamics changes of bacteriorhodopsin as studied by solid-state NMR

Izuru Kawamura[1], Miyako Horigome[1], Hirohide Nishikawa[1], Kana Tajima[1], Takashi Okitsu[2], Akimori Wada[2], Satoru Tuzi[3], Tatsuo Iwasa[4], Akira Naito[1] ([1]*Grad. Sch. Eng., Yokohama Natl. Univ.*, [2]*Kobe Pharm. Univ.*, [3]*Univ. Hyogo*, [4]*Muroran Inst. Tech.*)

Bacteriorhodopsin (BR) has a light-driven proton pump function triggered by photoisomerization of retinal. In the dark adapted BR, the retinal configuration coexists as a mixture of all-*trans* and 13-*cis*, 15-*syn* states with the isomeric ratio close to 1. We have revealed that two major NMR signals of [1-^{13}C]Tyr-labeled BR is assigned to the protein structures with two retinal states in the dark at room temperature by the solid-state NMR experiments. In this study, thermal and pressure effects on structure of BR were investigated by solid-state NMR. Overall peak intensity of [1-^{13}C]Tyr-BR was higher at a lower temperature and the plot of signal intensity showed a discontinuity at 260K. It is indicated that dynamical transition of protein occurred at the freezing temperature of bulk water. The ratio of relative signal intensity of two major peaks of [1-^{13}C]Tyr-BR at 213K obviously increased compared with that at room temperature. In contrast, the relative signal intensity of [20-^{13}C] retinal-BR did not change significantly at 213K. This result was attributed to structural change from disorder to α-helix at a lower temperature. Next, we applied pressure to BR using fast sample spinning in NMR. The signal intensity of 13-*cis* retinal at 22.0 ppm was increased as the pressure increased. The signal of Tyr185 corresponding to 13-*cis* retinal was increased more pronouncedly. It is indicated that the isomerization from all-*trans* to 13-*cis*, 15-*syn* state and change of protein state from all-*trans* to 13-*cis* were occurred under the pressure condition.

3F1058 OBSERVATION OF TRANSMEMBRANE PROTEIN BY HIGH SPEED ATOMIC FORCE MICROSCOPY: BACTERIORHODOPSIN D85S MUTANT, A CHLORIDE PUMP

Maxime Ewald[1], Mikihiro Shibata[2], Takayuki Uchihashi[1,3], Hideki Kandori[4], Toshio Ando[1,3] ([1]*School of Mathematics & Physics, Institute of Science & Engineering, Kanazawa University*, [2]*Department of Neurobiology, Duke University Medical Center*, [3]*Bio-AFM Frontier Research Center, College of Science and Engineering, Kanazawa University*, [4]*Department of Frontier Materials, Nagoya Institute of Technology*)

Bacteriorhodopsin (BR) is a light-driven proton pump that is found in halobacterium salinarum. Photoisomerization of the all-trans retinal chromophore, covalently attached to Lys216 through a protonated Schiff base, to the 13-cis, 15-anti configuration initiates ion translocation across the cell membrane, and establishes an electrochemical gradient for ATP synthesis and other energy requiring in membrane processes. It is well known that some helices on the cytoplasmic surface change their conformation during the proton pumping. We have recently succeeded in visualizing the photo-induced conformational changes of the D96N mutant using high-speed atomic force microscopy (AFM).1 On the other hand, it is known that substituting serine for Asp85 converts bR to a halorhodopsin-like chloride pump, actively transporting chloride ions in the direction opposite from the proton pump.2 The crystal structure of the halide-bound and halide-free states of D85S reveals that helical movements occur on the extracellular side of the protein. Here we have applied high-speed AFM to directly visualize the conformational change of D85S mutant activated by illumination. The AFM movies showed that the molecules change their conformation only on the extracellular surface as expected and this molecular motion seemed completely different from that observed on the cytoplasmic surface for the proton pumping WT and D96N mutant. 1. M. Shibata et al, Nature Nanotechnology 5, 208-212(2010). 2. I.V Kalaidzidis and A.D Kaulen, FEBS Lett., 418, 239-242 (1997).

3G0900 好熱性 *Meiothermus ruber* H328 株が産生放出する高耐性ケラチン分解性プロテアーゼ複合体のフリーズレプリカ電子顕微鏡観察

Freeze-replica observation of keratinolytic protease complex produced and released from *Meiothermus ruber* H328

Kazunori Kawasaki[1], Maachi Kataoka[2], Keiji Nomura[2], Yasushi Shigeri[1], Kunihiko Watanabe[2] ([1]*AIST*, [2]*Grad. Sch. Kyoto Pref. Univ.*)

A moderately thermophilic bacterium *Meiothermus ruber* H328 produces peerlessly strong keratinolytic protease. Cultivation of strain H328 with intact chicken feather induces degradation of more than 55% of total keratin proteins (Matsui *et al., Appl Microbiol Biotechnol* 82, 941-950, 2009). Moreover, the keratinolytic activity of the protease is extraordinarily stable against denaturizing agents: detergents such as SDS and organic solvents such as acetone, methanol and ethanol. Molecular structural basis for the high activity and stability of the protease is the subject of the current study.
Supernatant of medium after cultivation of strain H328 with 3% (w/v) chicken feather at 60°C for 37hr was concentrated with ultrafiltration (MWCO 500kDa), and passed through gel-filtration column (Sephacryl S-1000). The first-peak fraction from the column was applied to 20-60% sucrose density gradient ultracentrifugation, and fraction with keratinolytic activity recovered from around 45% sucrose was examined with transmission electron microscopy.
Observation by negative staining method showed the fraction contained particles of about 100nm diameter. Images obtained using freeze-fracture replica method, on the other hand, revealed fractured hydrophobic faces of membrane fragments about 100nm wide, those bearing a high density of intramembrane particles of several nanometers wide. These morphological evidence suggested the keratinolytic protease would be a membrane-bound, possibly an integral membrane protein.

3G0912 Effects of model peptides for late embryogenesis abundant (LEA) proteins on the thermal properties of liposomes

Takao Furuki, Minoru Sakurai (*Center for Biol. Resources and Informatics, Tokyo Inst. Tech.*)

LEA proteins are one of the key molecules to acquire desiccation tolerance abilities for plant species and animals. The primary structure of almost all of LEA proteins from animals discovered so far consists more or less in repeat of the 11-mer motif sequence characteristic to its origin. Previously, we reported that the 22-mer peptides with two tandem repeats of the 11-mer motif such as AKDGTKEKAGE (PvLEA-22) had conformational and thermal natures in support of several proposed roles of LEA proteins in desiccated cells[1]. The interest is now in the interactions between the model peptide and cellular membrane, particularily in the dried states. Here effects of the 22-mer peptide, PvLEA-22, were studied on the thermal properties of liposomes as a model of cellular membrane.
Results of dried DPPC liposomes will be outlined. By DSC measurements, in the presence of PvLEA-22, the gel-to-liquid crystalline transition temperature Tm was found to be clearly lowered as compared to pure liposome. In FT-IR spectra of the tested dry liposomes on heating, the peak position of the CH_2 stretching vibration in hydrocarbon chains shifted monotonously from ca. 2850 cm^{-1} to 2854 cm^{-1}. The P=O stretching band shifts from pure liposome are suggestive of the direct interactions between the 22-mer peptide and the membrane polar headgroups. PvLEA-22 suppressed the desiccation-induced aggregation of liposomes. Taken together, PvLEA-22 is capable of playing as a role of protectant for dried liposomes.

1. T. Furuki et al. *Biochemistry* **50**, 7093-7103 (2011).

3G0924 微細パターン化モデル生体膜における膜結合タンパク質の濃縮の空間的制御

Spatially controlled accumulation of membrane-bound protein in a micro-patterned model biological membrane

Fumiko Okada[1], Kenichi Morigaki[1,2] ([1]*Grad. Sch. Agr., Univ. Kobe*, [2]*Res. Cent. Env. Genomi., Univ. Kobe*)

Lipid rafts play a key role to regulate many cellar functions by recruiting membrane proteins. In a model system, liquid-ordered (*lo*) phases have been used as a model of lipid raft. We previously developed a micro-patterned model membrane on a solid support that can control the size and spatial distribution of *lo* phases (1). The model membranes comprised polymerized and fluid lipid bilayers. They induced phase separation of *lo* and liquid-ordered (*ld*) domains in a designed geometry because *ld* domains preferentially localized at the polymeric bilayer boundaries. The controlled phase separation should provide a means to purposefully concentrate membrane-bound proteins in defined regions. In the present work, we evaluated the accumulation of membrane-bound proteins in spatially defined areas. We used cholera toxin subunit B (CTB) as a model protein. The degree of CTB accumulation was correlated with the progress of phase separation, the ratio of polymeric/ fluid lipid bilayers, the geometries of polymerized bilayer regions, and the composition of fluid lipid bilayer. Spatially controlled accumulation of proteins should provide a novel approach to study lipid raft by separating membrane-bound proteins according to their affinities to lipid rafts. This technique should also pave a way toward sensitive bioassay and biosensor owing to the fact that protein molecules are accumulated in pre-defined regions.

(1) Okazaki et al. Langmuir 2010, 26, 4126

3G0936 圧力摂動熱量法によるジミリストイルホスファチジルコリン二分子膜の緩和挙動の解明への試み

An attempt to reveal the relaxation behavior of dimyristoylphosphatidylcholine bilayer by pressure perturbation calorimetry

Nobutake Tamai, Sayuri Kakibe, Saeko Tanaka, Masaki Goto, Hitoshi Matsuki (*Dept. Life System, Inst. Technol. & Sci., Univ. of Tokushima*)

Pressure perturbation calorimetry (PPC) is a relatively new calorimetric technique, which allows us to directly quantify the thermal expansion coefficient for solute molecules and colloidal particles in solution. In a PPC scan, the flow of the heat that occurs when a small isothermal pressure change (~ 5 bar) is applied to a sample solution is recorded as a function of time, and the expansion coefficient can be obtained from the total heat quantity transferred into the sample solution during the relaxation process by applying several thermodynamic relations. Therefore, the temperature dependence of the thermal coefficient is easily obtained by performing a series of PPC scans at different temperatures. Usually, this technique is used to study thermotropic volume behavior of solutes and dispersed particles and to estimate the relative volume changes of them with thermotropic physical transformations, such first-order phase transitions and conformational changes, on the basis of the temperature dependence of the thermal expansion coefficient. On the other hand, the time dependence of the heat flow measured in a PPC scan can provide us with the information about the relaxation dynamics of solutes and dispersed particles. On the basis of this idea, we have recently started the investigation on the relaxation process of a phospholipid bilayer membrane using the PPC technique. In this presentation, we will report on our recent results about the relaxation behavior of dimyristoylphosphatidylcholine bilayer membrane.

3G0948 リン脂質二重膜の圧力誘起指組み構造形成：疎水鎖長依存性と形成限界

Pressure-induced interdigitation of phospholipid bilayer membranes: dependence of acyl-chain length and limitation of the formation

Hitoshi Matsuki, Masaki Goto, Nobutake Tamai (*Institute of Technology and Science, The University of Tokushima*)

Bilayer membranes of diacylphosphatidylcholines (CnPC) are known to induce the interdigitated gel phase under high pressure. Since the interdigitated gel phase is extended into the low-pressure region with increasing the acyl-chain length, it is expected that the bilayers of CnPC with longer acyl chains induce the interdigitated gel phase under atmospheric pressure. In this study, we investigated the bilayer interdigitation of CnPC with long acyl chains (Cn = 19-22). The temperature-pressure phase diagrams of four CnPC bilayers were constructed by differential scanning calorimetry and high-pressure light transmittance technique. We observed the interdigitation of the C19PC, C20PC and C21PC bilayers under high pressure, and the interdigitation was induced at lower pressures with the chain elongation. On the other hand, the C22PC bilayer showed the peculiar behavior: there exist two transitions under atmospheric pressure while one transition under high pressure. In order to confirm what the low-temperature phase of the C22PC bilayer is like, we performed measurements of the small angle neutron scattering and fluorescence spectroscopy under atmospheric pressure. These results proved that the phase is the interdigitated one. Therefore, it turned out that the maximum acyl-chain length required for the pressure-induced interdigitation is 21. Present results definitely indicate that the bilayer interdigitation is governed by the hydrophobic interaction as well as the hydrophilic interaction of the PC molecule in the bilayer.

3G1010 均一でないリン脂質単分子膜における崩壊現象について

Collapse of nonuniform phospholipid monolayers

Masahiro Hibino, Ken Hashimoto, Takuya Fujisawa (*Div. Appl. Sci., Muroran Inst. Technol.*)

The behavior in the stochastic collapse of lipid monolayers of a mixture of dipalmitoylphosphatidylcholine and palmitoyloleoylphosphatidylglycerol, a model system of pulmonary surfactant assembly, has been studied extensively by using experimental techniques and theoretical models. The monolayers at the air-water interface appear to be phase separated under compression and retain the continuous liquid-expanded phase network surrounding islands of condensed phase even at a surface pressure approaching 70 mN/m. When the two-dimensional monolayers are compressed beyond the equilibrium surface pressure, they collapse and assume a three-dimensional formation. However, these phenomena have been observed under a condition of uniform monolayers. In fact, monolayer is not always uniform at the interface. We can rarely observe that the areas with the coexistence of LE-C phases are contiguous to each other, but distinct from each other by using fluorescence microscopy. The nonuniform surface density in the monolayer has an influence on the collapse. Here we investigate the collapse of compressed nonuniform binary phospholipid monolayers using Langmuir-isotherms, fluorescence microscopy and atomic force microscopy. The monolayers at the air-water interface underwent fast collapse by folding within 100 ms or slow collapse by the formation of Baumkuchen-like structure at high surface pressure. They were composed of bilayers that remained suspended beneath the film.

3G1022 脂質分子の電荷が引き起こす膜構造変化：2 次元相分離と 3 次元曲率

Charge-induced transition in membrane mesoscopic structures: lateral domains and vesicular shapes

Hiroki Himeno, Tsutomu Hamada, Masahiro Takagi (*1Shool of Materials Science, Japan Advanced Institute of Science and Technology*)

Living cells exhibit various 2D and 3D structural dynamics of lipid membranes. These structural changes are recognized as “membrane dynamics”. The 2D membrane structures are represented by phase separation named “lipid raft”. The 3D membrane structures are morphological changes, such as endocytosis and intercellular vesicular traffic. The intrinsic properties of constituent lipids should play an important role on such membrane dynamics.

Giant unilamellar vesicles (GUVs) are often used as a model of biological membranes, because they are large enough to be observed directly by optical microscope. Previously, using GUVs, we succeeded in reproducing 2D and 3D membrane dynamics such as phase separation (Hamada et al., Soft Matter, 7, 220-224, 2011) and vesicular formation (Hamada et a., J. Am. Chem. Soc., 132, 10528-10532, 2010) by changing the molecular structure of membrane constituents.

To advance our understanding, we here focused on the effect of electric charges of lipid molecules, which is one of intrinsic properties of membrane lipids, on 2D (lateral phase separation) and 3D (membrane curvature) membrane mesoscopic structures.

3G1034 油中水滴エマルション遠心沈降法を用いたミクロスフェア内包型ジャイアントベシクル

Microsphere-containing giant vesicles prepared by water-in-oil emulsion centrifugation method

Yuno Natsume[1], Taro Toyota[1,2] ([1]*Grad. Art. Sci., Univ. Tokyo*, [2]*JST PRESTO*)

In cells, biological macromolecules are contained at a volume fraction of 20-30 vol %. Recently, this situation has much drawn attention as a crucial factor of the crowding effect of the cytosol. To construct cell models, giant vesicles (GVs) confining macromolecules, microspheres, or both have been adopted. However, in the conventional methods such as the natural swelling method, the inner state (concentration, number density and so on) of macromolecules or microspheres is scarcely controlled and non-uniform among the GVs. To form microsphere-containing GVs as desired, we employed the water-in-oil (W/O) emulsion centrifugation method reported by Pautot et al. (Langmuir 2003, 19, 2870), because this method is based on W/O emulsion droplet as a template of GV. By using polystyrene microspheres (diameter = 1 μm) dispersions of 2.0–25 vol % to form W/O emulsions in liquid paraffin, we obtained GVs that encapsulate microspheres with volume fractions in the range of 0–50 vol % and their diameters were in range of 4–40 μm. Although the distribution of the volume fraction of GVs was broad, it should be noted that the highest volume fraction of GV was higher than that of W/O emulsion droplets. It is the advantage that we can achieve GVs confining microspheres at high number density rather than that of microspheres dispersion we prepared initially. This technique can be applied to the GV encapsulation of other microspheres or macromolecules that exhibit entropy-driven effects, such as the crowding effect.

3G1046 オイルフリー GUV に封入された分子演算システム RTRACS

Molecular computing system RTRACS encapsulated in oil-free giant unilamellar vesicle

Koh-ichiroh Shohda, Tadashi Sugawara, Akira Suyama (*Grad. Sch. Arts Sci., Univ. Tokyo*)

RTRACS (Reverse-transcription-and-TRanscription-based Autonomous Computing System) is a molecular computing system in which RNA molecules work as input and output.[1,2] RTRACS is a reaction network system which consists of modularized molecular logic gates containing the Boolean gate such as AND, OR, etc. We intend to construct a giant unilamellar vesicle (GUV) encapsulating RTRACS as a minimal model of living cell. At present, the best preparation method of GUV is the w/o emulsion centrifuge method.[3] However the GUV prepared with the centrifuge method potentially contains the oil which surrounded the water droplet in the w/o emulsion. The oil changes the membrane properties, such as thickness, permeability, dynamics, etc. Hence we developed an oil-free GUV preparation method based on the lipid film gentle hydration method in the presence of mono- and di-valent metal cations. The inner water pool of GUV is stained with TMRA-dextran (M.W. 10,000) as a volume marker. The FAM-labeled molecular beacon probe which hybridizes with the output RNA molecule of RTRACS was used as a reaction marker. The dual-labeled GUV in which RTRACS runs was analyzed by optical microscopy and flow cytometry.

[1] N. Nitta, and A. Suyama *Lect. Note. Comput. Sc.*, **2004**, *2943*, 203-212.
[2] M. Takinoue, D. Kiga, K. Shohda, and A. Suyama *Phys. Rev. E*, **2008**, *78*, 041921.
[3] S. Pautot, B. J. Frisken, and D. A. Weitz *Langmuir*, **2003**, *19*, 2870-2879.

3G1058 低い pH が誘起する DOPS/MO 膜の液晶相からキュービック相への相転移の初期過程

Initial Step of Low pH-Induced Lamellar to Bicontinuous Cubic Phase Transition in Dioleoylphosphatidylserine/Monoolein

Toshihiko Oka[1], Tomoki Takahashi[1], Taka-aki Tsuboi[1], Masahito Yamazaki[2] ([1]*Fac. Sci., Shizuoka Univ.*, [2]*Grad. Sch. Sci. Tech., Shizuoka Univ.*)

The modulation of electrostatic interactions due to surface charges of lipid membranes induces transitions between the L_α phase and the inverse bicontinuous cubic (Q_{II}) phase [1]. Using time-resolved small angle X-ray scattering (TR-SAXS) and a home-made rapid mixing method, we investigated the kinetics of low pH-induced L_α to Q_{II}^D phase transition in MLVs of dioleoylphosphatidylserine (DOPS)/monoolein(MO) in the presence of PEG-6K, and found that the H_{II} phase appeared after the pH change (the initial step), and then the H_{II} phase slowly converted into the Q_{II}^D phase (the second step) [2]. However, we could not follow the initial step due to the limited time-resolution of the method.

In this report, we investigated the initial step of the low pH-induced L_α to Q_{II}^D phase transition in DOPS/MO in the absence of PEG-6K using TR-SAXS with a stopped flow apparatus. We succeeded in following structural changes in the membranes after 100 ms of the mixing of DOPS/MO-MLV in a neutral buffer with a low pH buffer with a time-resolution of 100 ms. We observed that at the initial step the peak intensity of the L_α phase gradually decreased but at the same time that of the H_{II} phase gradually increased, indicating that the L_α phase directly converts into the H_{II} phase without formation of any intermediates. The rate constant of the initial step greatly depended on final pH and DOPS concentrations in DOPS/MO membranes.

[1] Adv. Planar Lipid Bilayers Liposome, 9, 163, 2009; Langmuir, 24, 3400, 2008, [2] J. Chem. Phys. 134, 145102, 2011

3G1110 X 線及び電子線回折法を用いた皮膚角層の構造解析

Breakthrough for Unresolved Structural Problems in Skin Function by Combined Use of X-ray and Electron Diffraction Methods

Hiromitsu Nakazawa[1], Ichiro Hatta[2], Satoru Kato[1] ([1]*Sch. Sci. Tech. kwansei Gakuin Univ.*, [2]*Nagoya Industrial Science Research Inst.*)

The outermost layer of the human skin, stratum corneum (SC), consists of terminally differentiated keratinocytes and highly ordered intercellular lipid layers. The SC serves as a physicochemical barrier between the inner body and the outer external environment. Notwithstanding the extensive studies on structure of intercellular lipids which plays a crucial role for the skin barrier properties, owing to lack of the structural evidence under functioning lot of unresolved problem are left open. Using X-ray and Electron diffraction methods we deepened understanding the healthy skin state and developing the percutaneous drugs.

Both synchrotron X-ray diffraction (XD) and electron diffraction (ED) methods are the very powerful tool to analyze the intercellular lipid organization in SC. The XD has higher resolution than the ED, but requires invasive operation because a large amount of skin sample is necessary to obtain reliable data. On the other hand, the ED makes it possible to analyze the structures of the SC noninvasively, but radiation damage by electron beam must be suppressed.

By best use of these methods we will report here a fundamental structural change of SC in the skin permeation of chemical agents, the effect of temperature in the skin permeation, and the regional structural differences on the body. We will present these results and future perspective for the SC structural study.

3H0900 GTP 結合状態と GDP 結合状態の微小管分子構造における大きな構造変化

Large Conformational Changes in Tubulin in the GTP- and GDP-States Microtubules Observed by Cryo Electron Microscopy

Hiroaki Yajima[1], Toshihiko Ogura[2], Ryo Nitta[1], Yasushi Okada[1], Chikara Sato[2], Nobutaka Hirokawa[1] ([1]*Grad. Sch. Med., Univ. Tokyo*, [2]*Biomedical Research Inst., AIST*)

Microtubules are dynamic polymers that stochastically switch between growing and shrinking phases and their dynamics is regulated by GTP hydrolysis by β-tubulin, but its mechanism remains elusive because high-resolution microtubule structures have only been revealed for the GDP-bound state. Here we solved the cryo-EM structure of microtubule stabilized with a GTP analogue guanylyl 5'-α, β-methylenediphosphonate (GMPCPP) at 8.8 Å resolution by developing a novel cryo-EM image reconstruction algorithm. In contrast to the crystal structures of GTP-bound tubulin relatives such as γ-tubulin and bacterial tubulins, significant changes were detected between GTP- and GDP-bound states at the contacts between tubulins both along the protofilament and between neighboring protofilaments, contributing to the stability of the microtubule lattice. These findings are consistent with the structural plasticity or lattice model, and suggest the structural basis not only for the regulatory mechanism of microtubule dynamics, but also for the recognition of the nucleotide state of microtubule by several microtubule-binding proteins, such as EB1 or kinesin.

3H0912 紡錘体は一方の極から他方へ構造変化を伝搬することで対称形状を維持する

Meiotic spindles maintain the symmetrical shape by propagating structural changes to the opposite side

Kazuya Suzuki[1], Jun Takagi[1], Takeshi Itabashi[1], Shin'ichi Ishiwata[1,2] ([1]*Dept. Phys., Adv Sci. Eng., Waseda Univ.*, [2]*WABIOS*)

A microtubule-based spindle is designed for proper chromosome segregation. Recent studies have demonstrated that bipolar spindle formation requires the force balance sustained by molecular motors. However, it remains unclear

whether and how the mechanical properties of the two spindle poles are symmetrically balanced. Here, we quantitatively measured the mechanical stiffness, the microtubule density, and the response to the deformation of spindle poles by micromanipulation techniques and 3D analysis. To directly deform the spindle self-assembled in Xenopus egg extract, we inserted two glass micro-needles into a pole region and widened it perpendicularly to the pole-to-pole axis. We found that the stiffness and the microtubule density in the manipulated pole region reduced upon widening. Surprisingly, this reduction propagated to the other side, which resulted in the formation of a symmetrical defocused barrel-like shape of the unmanipulated pole region. On the other hand, it is known that inhibition of the dynein function causes the defocusing of pole regions, such that the barrel-shaped structure is formed. We compressed one side by the micro-needles and found that the stiffness and the microtubule density in the compressed region increased, and this effect propagated to the other side, resulting in the bipolar shape formation. Our results suggest that the symmetrical spindle shape is maintained by propagating the structural change from one side to the other via the communication through the central region.

3H0924 高圧負荷によって誘導されるクラミドモナス非運動性変異株鞭毛の屈曲運動

Resurrection of flagellar bending movements in *chlamydomonas* paralyzed mutants at high pressure

Toshiki Yagi[1], Masayoshi Nishiyama[2] ([1]*Grad. Sch. Medicine, Univ. Tokyo*, [2]*The Hakubi Center, Kyoto Univ.*)

Application of hydrostatic pressure modulates the activities of organisms. To examine the effect of the pressure on ciliary and flagellar motility, here we observed the flagellar movements of *chlamydomonas* under high-pressure conditions. Wild type cell movements were inhibited by the application of pressure; the swimming velocity and the percentage of moving cells decreased with the pressure increased, and the movements stopped under the pressure of >80 MPa at 25 °C. Surprising, however, paralyzed mutants lacking the central structures of the flagellum (central pair microtubule: CP, or radial spokes: RS) displayed vigorous beating under the pressure of 40 to 60 MPa, but the movements stopped under the pressure of ＞80 MPa at 25 °C. Axonemes (isolated and demembranated flagella) of the mutants did not display beating in the presence of 1 mM ATP, but they displayed beating under the pressure of 40 to 60 MPa. This suggests that the application of pressure modulates the functional activities of some axonemal components. The motility analysis of the double mutants lacking both of CP (RS) and various species of dyneins showed that outer-arm dynein is indispensable for the movements. Previous studies showed that the microtubule-sliding movements powered by dynein were reduced in the axonemes of the CP/RS-deficient mutants. We suggest that the application of pressure directly or indirectly activates the outer arm dynein and increases the sliding movements, which induces bending movements in the paralyzed mutants.

3H0936 走化性誘因物質の進行パルス刺激によって誘発された一方向細胞運動

Directed cell migration induced by travelling waves of chemoattractant

Akihiko Nakajima[1], Satoshi Sawai[1,2] ([1]*Grad. Sch. Arts & Sci., Univ. Tokyo*, [2]*Res. Cent. for Complex Systems Biology, Univ. Tokyo*)

Mirgration of Dictyostelium cells is mediated by chemotaxis toward the chemoattractant cAMP. It is believed that cells determine their direction of motion by comparing the concentration difference between the head and rear of the cell. However in aggregating Dictyostelium, concentration profile of chemoattractant is not static, but takes the form of traveling waves. Because reversal of spatial gradient occurs repeatedly after each passing wave, cells could potentially move in the reverse direction in the wake of a passing wave. This problem is referred to as ‘chemotactic wave paradox’. To address this problem, we designed and constructed a microfluidics system to generate traveling cAMP pulses of user-specified wave-length and propagation speed. Using this system, we studied chemotactic responses towards the traveling cAMP pulses and found that the migratory direction depends on the speed of pulse propagation. Cells migrate toward the in-coming cAMP pulse for waves with passage time of 3 ~ 10 min. In contrast, when the stimulus duration is less than 2 min, cells come almost to a halt. When stimulus duration is longer than 10 min, cells reversed their direction of motion at the back of the wave. These results indicate that cells are able to move towards the correct orientation only when stimulus duration time matches the cell response time. We will show how cytosolic signaling such as phosphatidyl inositol and actin localization is related to directed cell migration under the traveling cAMP pulses.

3H0948 極性を持つアメーバ細胞の走化性運動に関する理論

Theory on the chemotaxis of an amoeboid cell with the cell polarity

Tetsuya Hiraiwa, Tatsuo Shibata (*Kobe, Riken*)

Chemotactic amoeboid migration is an ubiquitous kind of cell motility, which is important for the immunological response, wound healing and developmental processes. In this presentation, we would like to explain our recent theory on the chemotactic migration of an amoeboid cell with the cell polarity, and share with you our results for the observable statistical quantities about the migrating direction based on the theoretical model in which we assume the following facts; 1. The cell has the polarity which is spontaneously organized. 2. The polarity is reoriented to the gradient direction the cell estimates from the binding states of chemoattractants to receptors. 3. The cell migrates to the direction of the polarity with a constant speed. 4. Chemotaxis is realized by the bias of the direction in which more chemoattractants bind to the receptors according to the chemical gradient. Using this model, firstly, we confirme our theory by comparison with the experimental data for the chemoattractant-concentration dependence of the correlation time of the spontaneous migrating direction. It should be noted that the spontaneous migration can also be discussed by our model as the case that the magnitude of the chemical gradient is zero. The results agree with the experimental data for Dictyostelium discoideum. Secondly, we derive the probability distribution of migrating directions and chemotaxis index. We find that the chemotaxis index is incremented by introducing the cell polarity. The details will be discussed on the day.

3H1010 Controlled cell migration with ultrasound

Shinya Murakami[1], Yo Otsuka[1], Manabu Sugimoto[1], Toshiyuki Mitsui[2] ([1]*Grad. Sci. Eng., Aogaku Univ.*, [2]*Assoc Prof., Aogaku Univ.*)

Ultrasound is not only used for ultrasound imaging but also used for ultrasound healing therapy to recover from bone fracture recently while the mechanism for healing is not known surprisingly. Since it is reported that aggregation of cells is enhanced by ultrasound on a microscopic scale, it may be possible that ultrasound can control cell behavior closely related to the cell aggregation which could be one of main causes for enhancing bone fracture healing. To clarify cell aggregation by ultrasound irradiations, we have observed cell migration under optical microscopy with or without the irradiations directly. Ultrasound is generated from a homemade ultrasound needle made of tungsten wire with the diameter at 1.0 mm. The frequency of the ultrasound is near 1.5 MHz. The power intensity of the irradiations is near 24 mW/cm2. In this conference, we will show the cell migration under ultrasound irradiation and discuss the result, converging cells on ultrasound exposure area. Finally, we will discuss the influence of ultrasound on cell migration.

3H1022 筋肉と異なるストレスファイバーの収縮特性

Contractile properties of stress fibers are distinct from those of muscles

Shinji Deguchi, Tsubasa Matsui, Daiki Komatsu, Masaaki Sato (*Tohoku University*)

Actin stress fibers play essential roles in cell adhesion regulation and tensional homeostasis. Here we measured the contractile properties of single stress fibers isolated from vascular smooth muscle cells. Cells were deroofed with low ionic strength buffers to extract basal stress fibers. Western blotting analysis and negative staining electron microscopy indicated that the extracted stress fibers were intact with regard to structure and function. Individual stress fibers were isolated from the substrate using two glass needles. Mg-ATP solutions were added to induce contractile activity of the stress fibers, and forces were measured from the deflection of one of the glass needles with a known spring constant. We obtained a convex form of contractile forces as a function of sarcomere distance, which was similar to that of myofibrils. Interestingly, the shortening rate of the stress fibers drastically decreased when an external load was applied. Thus, the shortening rate-loading relationship was sharply different from that of muscles typically having a parabolic curve. We speculate that a recently reported load-dependent decrease in ADP release rate of nonmuscle myosin II may be responsible for this unique contractile property of stress fibers.

3H1034 Smooth muscle differentiation related transcription factor CRP2 directly regulates physical properties of actin filaments

Takanori Kihara[1], Satoko Shinohara[1], Yasunobu Sugimoto[2], Jun Miyake[1] ([1]*Grad. Sch. Eng. Sci., Osaka Univ.*, [2]*Nagoya Univ. Synchrotron Radiat. Res. Center*)

Actin filaments form many types of structures and dynamically regulate the cell morphology and movement, and furthermore, they play a mechanosensory role for extracellular stimuli. Thus, actin filaments are the most important physical components of a cell and their modulation factors have the potential to directly regulate the cell fate. In this study, we clarified that smooth muscle related transcription factor, CRP2 (cysteine-rich protein 2), directly bound to actin filaments and regulated their physical properties. The CRP2 molecule has a dumbbell-like structure with 3 tandem clots as indicated by SAXS (small angle X-ray scattering) analysis. CRP2 is directly associated with F-actin through its N-terminal LIM domain and Gly-rich region. CRP2-bound actin filaments showed higher persistent length as compared with unmodified actin filaments. By induction of smooth muscle cells differentiation, intracellular CRP2 localizes to actin stress fibers as they are formed. Furthermore, smooth muscle cells with active CRP2 expression showed higher mechanical stiffness. Now we speculate that actin-bound CRP2 plays direct roles in the stabilization of smooth muscle cells differentiation by regulation of the physical properties of actin filaments. This study was supported by KAKENHI (24700454).

3H1046 細胞接着班における p130Cas と Src の動的相互作用を介した遊走制御機構の解明

A distinct role for the dynamics of p130Cas at focal adhesion via interaction with Src in the regulation of cell migration

Hiroaki Machiyama[1,2], Hiroaki Hirata[1], Yasuhiro Sawada[1,2] ([1]*Mechanobiology Inst., Nat. Univ. Singapore*, [2]*Dept. Biol. Sci., Nat. Univ. Singapore*)

Cell migration is involved by the orchestrated regulation of remodeling of actin cytoskeleton, actomyosin contraction and continuous focal adhesion turnover. The phosphorylation of a focal adhesion protein p130Cas (Cas) has been reported to regulate cell migration through the modulation of focal adhesion turnover. However, it is still unclear how individual Cas molecules contribute to the regulation of cell migration. The fluorescence recovery after photobleaching (FRAP) method was used to spatiotemporally analyze the dynamics of various forms Cas mutants at focal adhesion in migrating cells. We find that displacement of Cas molecules from adhesion sites is accelerated by their phosphorylation but hampered by association with Src, although the Src-binding of Cas at focal adhesion promotes Cas phosphorylation. Genetically-engineered stabilization of Cas association with Src using the bimolecular fluorescence complementation (BiFC) method, which sustain Cas phosphorylation but mitigate Cas displacement from adhesion complexes, result in retarded cell migration. Myosin II inhibition that impedes displacement of Cas molecules from adhesion sites also decreases cell migration, despite sustained Cas phosphorylation. Our findings indicate that both association with Src and dissociation from Src are the key elements for Cas to activate Cas-phosphorylation signaling and thereby to drive cell migration.

3H1058 Spatiotemporal regulation of signaling by active cytoskeletal remodeling

Bhaswati Bhattacharyya[1], Abhishek Chaudhuri[3], Kripa Gowrishankar[4], Satyajit Mayor[5], Madan Rao[4] ([1]*iCeMS, Kyoto University*, [2]*Rudolf Peierls Centre for Theoretical Physics, University of Oxford, UK*, [3]*Raman Research Institute, Bangalore, India*, [4]*NCBS-TIFR, Bangalore, India*)

Biochemical reactions performed by signaling and sorting complexes, both on the surface and within the living cell, is often subject to the local regulation by the active cytoskeleton. We have recently proposed that in many cases, this spatiotemporal regulation is due to the the interplay between active contractility and remodeling of the cytoskeleton which results in transient `asters', focusing of passive molecules to form clusters inside its core. This mechanism of clustering gives rise to a significant increase in the local concentration of signaling proteins, which enhances reaction efficiency and output signal. The dynamic cytoskeletal elements that drive focusing behave as quasi-enzymes catalyzing the chemical reaction. These ideas are applicable to the cortical actin dependent clustering of cell surface proteins such as lipid-tethered GPI-anchored proteins, Ras-proteins as well as many proteins that have domains to interact with the actin-cytoskeleton. We discuss the implications of actin dynamics by introducing an `activity temperature', which can work as a regulatory parameter for signaling replacing the details of cytoskeletal dynamics. We show this using time-temperature-transformation (TTT) and Arrhenius plots while `activity temperature' facilitate and/or inhibit(slow down) chemical reactions.

3H1110 Arp2/3 とアクチンを内包した油中液滴のフィロポディア様変形

Filopodia-like protrusions in water-in-oil droplets induced by Arp2/3 and actin polymerization

Masataka Chiba[1], Makito Miyazaki[1], Takashi Ohki[1], Shin'ichi Ishiwata[1,2] ([1]*Dept. of Phys., Waseda Univ.*, [2]*WABIOS, Waseda Univ.*)

When cell moves, cytoplasmic protrusions called filopodia spread out in the direction of movement. Filopodia consist mainly of bundled actin filaments and are elongating by the actin polymerization. In the initial growth, the following mechanism has been proposed. First, Arp2/3 complex is anchored to the cell membrane via the VCA domain of WASP, which activates Arp2/3 and nucleates actin polymerization. Arp2/3 transmits the force of actin polymerization to the membrane, protruding it. To verify this hypothesis, many experiments have been carried out using cells, however, the minimal components and physical conditions indispensable for the membrane protrusion are still unclear. In this study, we used purified proteins and cell-sized water droplets, surrounded by a phospholipid monolayer, in water-in-oil emulsions. Inside the droplets we encapsulated fluorescently labeled G-actin, Arp2/3, and VCA, which was designed to bind to the inner surface. After the promotion of actin polymerization, distribution of actin became inhomogeneous, and filopodia-like protrusions were occasionally observed. In the absence of Arp2/3, water droplets maintained a spherical shape. To understand the mechanism of such deformations, we plan to visualize Arp2/3 and VCA in addition to actin and clarify the relationship between the deformation and the localization of these three proteins. From these results, we will discuss the mechanism of filopodia formation and regulation.

3I0912 ヘモグロビンのアロステリック平衡のリアルな描像

A realistic picture of allosteric equilibrium of hemoglobin

Naoya Shibayama[1], Sam-Yong Park[2] ([1]*Biophysics, Jichi Med. Univ.*, [2]*Protein Design Lab., Yokohama City Univ.*)

In general, the molecular mechanism of protein allostery has been explained by assuming an equilibrium between the T (tense) and R (relaxed) states within the framework of the two-state allosteric model. However, it has long been recognized by hemoglobin (Hb) experts that such a simple two-state model fails to represent the relationship between structure and function in Hb in quantitative terms. To overcome this situation, some researchers including us continue to pursue the elusive “intermediate allosteric states” for decades. Here, we present crystallographic evidence that the Hb molecule assumes many kinds of distinct quaternary conformations that exist in equilibrium. In this study, we have utilized a novel Hb crystal form, which contains three independent Hb molecules with different quaternary structures. Significantly, this crystal allows large-scale conformational changes of the containing three molecules in response to the changes in ligation state and solution conditions. By using a series of three isomorphous crystals obtained from different conditions, nine distinct Hb conformations can be characterized by X-ray crystallography and oxygen equilibrium measurements. Notably, the nine conformations are distributed continuously over the whole conformational space of Hb, ranging from T to R2 through R, with various intermediate forms also present. These results suggest a mechanism for the allosteric control of a protein’s function by changing the delicate balance among the multiple states on its energy landscape.

3I0924 ヘムをヘム垂線のまわりに 90° 回転した時の共鳴ラマンスペクトル変化：ヘムオキシゲネース

Effects of Heme Rotation around the Heme Normal by 90° on Resonance Raman Spectra of Heme Proteins; Observation for Heme Oxygenase

Sachiko Yanagisawa[1], Hiroshi Fujii[2], Saburo Neya[3], Takashi Ogura[1], Teizo Kitagawa[1] ([1]*University of Hyogo*, [2]*Okazaki Inst. Integrative Biosci.*, [3]*Chiba University*)

To understand the protein effects on resonance Raman spectra of heme proteins further, we report here the resonance Raman spectra of two proteins in which their heme orientations are different with regard to the rotation around the heme normal by 90° in the same protein pocket. We employed heme oxygenase (HO)

as a model protein; one is wild type (WT HO) and the other is a mutant (KDMY HO) which involves replacements of four residues (K16N, D27A, M31K, Y112F). Their X-ray structures indicated that the 4-vinyl of WT HO seems to have the same environments as that of 2-vinyl of KDMY in crystal. The NMR spectra confirmed the 90° rotation of the heme in solution, and their catalytic activities demonstrated the corresponding differences in the α and δ cleavages of the heme. The resonance Raman spectra of WT HO and KDMY HO are alike regarding major heme skeletal modes, whereas some modes involving heme side chains vary in frequencies and behaviors. To characterize such bands, we reconstituted the two proteins with vinyl- or propionate-deuterated hemes and compared their resonance Raman spectra in their oxidized, reduced, and CO-bound forms. The vinyl associated modes exhibited frequency shifts between the two proteins.

3I0936 ヘムオキシゲナーゼにおける CO 光解離後の構造変化および CO の放出経路

Protein motions and CO migration following CO photolysis in heme oxygenase

Masakazu Sugishima[1,2], Keith Moffat[2,3], Masato Noguchi[1] ([1]*Dept. Med. Biochem., Kurume Univ. Sch. Med.*, [2]*Dept. Biochem. & Mol. Biol., Univ. Chicago*, [3]*BioCARS, Univ. Chicago*)

Heme oxygenase (HO) catalyzes the physiological degradation of heme using dioxygen and reducing equivalents to produce biliverdin, ferrous ion, and CO. The HO reaction proceeds without severe product inhibition by CO generated in the second step of the HO reaction, even though CO is known to be a potent inhibitor of HO and other heme proteins. Therefore HO must have an efficient mechanism for discriminating between dioxygen and CO.

To explore protein motions and CO migration in HO following CO photolysis which mimics CO generation during the HO reaction, we collected X-ray diffraction data on the CO-heme-HO complex before and after continuous illumination by CW laser at temperatures below 160 K. The weighted difference Fourier map shows that CO was partially photolyzed from the heme iron, and photodissociated CO had migrated to a hydrophobic cavity, as observed in previous results at 35 K. In contrast to previous results, motions of the distal helix, water, and heme were observed which are the reverse of motions observed in CO binding. Notably, similar motions were absent in dioxygen binding and photolysis. These results imply that the CO-bound form is severely constrained by steric hindrance between the distal helix and CO bound to the heme iron, and that steric hindrance contributes to discrimination between binding of CO and dioxygen. Further, another putative CO trapping site, more polar than previous sites, was found. Combining these studies with previous results, we will discuss CO migration pathways in HO.

3I0948 多様な生物種によるヘムオキシゲナーゼ反応の微調整戦略：オキシヘムの安定化

Strategy of a variety of organisms for the fine-tuning of heme oxygenase reactions: Stabilization of the oxyheme intermediate

Sayuri Takada, Taiko Migita (*Dep. Biol. Chem., Fac. Agr., Yamaguchi Univ.*)

Heme oxygenase (HO) catabolizes regioselective heme-ring opening to produce biliverdin, free iron, and carbon monoxide. In a variety of biological species, the HO reactions participate in recycling of iron, signaling, supplying resources of photoreceptive-molecule production, or generating anti-oxidants. To attain their own requirements for HO, each organism seems to take unique fine-tuning strategy. The HO reaction proceeds successively by consuming oxygen molecules and electrons, so that their constant supply is essential. In addition, formation of the first reactive species, hydroperoxy hemin, requires proton as well as electron transfer to the oxyheme. In different species, HO functions in different milieu, thereby regulated finely and differently by respective active sites. Our HO study is focused on such fine-tuning modes taken in different HOs from different species. In this study, stability of oxyheme, the first converted form of hemin in HO, was compared among the five HO complexes: rat HO1, puffer-fish HO1, cyanobacterial HO1, soybean HO1, and pathogenic-bacterial HO. The auto-oxidation rates of the oxyheme complexes showed unexpectedly big difference, which correlate with pKa of the heme-bound water as well as with g-agisotropy of the hydroxide-coordinated heme. Based on the crystal structures of three heme-HO complexes out of the five, very-well conserved Gly residue in the distal helix, closest to the heme iron, is proposed as the HB donor to stabilize the oxyheme in the heme pockets.

3I1010 Ultraviolet Resonance Raman Study on Indoleamine 2, 3-Dioxygenase

Masayuki Hara[1], Sachiko Yanagisawa[1], Hiroshi Sugimoto[2], Yoshitsugu Shiro[2], Takashi Ogura[1] ([1]*Grad. Sch. Sci., Univ. Hyogo*, [2]*Harima Inst., Riken*)

Indoleamine 2, 3-Dioxygenase (IDO) catalyzes incorporation reaction of two oxygen atoms into L-tryptophan (Trp), generating N-formylkynurenine, which is in the major catabolic pathway of Trp in mammals. Visible resonance Raman (RR) studies identified a key intermediate of ferryl-oxo (Fe=O) species. This suggested that two oxygen atoms were transferred to substrate one by one. The Fe=O species seemed to lie in the compound II oxidation level and a question arose whether such an intermediate could perform oxo-transfer reaction, since no example had been reported. Such a reaction might be possible if the substrate intermediate is unusually reactive. In the present study, we have adopted ultraviolet (UV) RR spectroscopy to characterize the substrate bound to IDO, since the technique selectively enhances vibrational spectra of aromatic molecules. UVRR scattering was excited at 229 nm for the ferrous state of IDO. UVRR spectrum of substrate-free IDO was primarily contributed by Trp and Tyr residues. In the spectrum of the substrate-bound IDO, intensity of the W3 band of Trp was increased. This was ascribed either to bound-Trp or Trp residue in IDO. In the latter case, binding of Trp induced structural change of intrinsic Trp in IDO. In order to distinguish these possibilities, we utilized indole-2-^{13}C- and indole-D_5-labeled Trp. The results showed that bound-Trp and not the intrinsic Trp exhibited the intensity change. The present study provides a new method to study the structure of the bound-substrate to IDO.

3I1022 An Intermediate Conformation of Cytochrome Oxidase in the Ligand-Free State Identified by Time-Resolved Resonance Raman Spectroscopy

Izumi Ishigami, Takeshi Nishigaki, Kyoko Shinzawa-Itoh, Shinya Yoshikawa, Satoru Nakashima, **Takashi Ogura** (*Grad. Schl. Life Sci., U. Hyogo*)

Cytochrome *c* oxidase (CcO) reduces dioxygen to water by heme a_3 and drives proton pump by heme *a*. In the present study, we applied green-pump and violet-probe time-resolved resonance Raman (TRRR) spectroscopy to monitor the dynamics of hemes after CO-photolysis with a time resolution of 10 ns. The green and violet light were used for CO-photolysis and resonance Raman excitation, respectively. TRRR spectra after CO-photolysis were measured at delay time = 10 ns - 5 ms. The Fe-His stretching mode was located at 221 wavenumbers at delay time between 10 ns and 100 ns, and then decreased exponentially with time with a time constant of 600 ns and at 5 ms reached 215 wavenumbers, which was the same value for equilibrium ligand-free form. This behavior was similar to that reported earlier. In this study, we found that intensity of the same mode decreased to two thirds at 100 ns relative to that at 10 ns and remained constant up to 5 ms, but was significantly smaller than the intensity for equilibrium ligand-free form. Results indicate that an intermediate conformation exists after ligand dissociation at delay time = 0.002 to 5 ms. This conformation might have a significantly smaller affinity to dioxygen compared with the conformation seen at 10 - 100 ns as judged from the Fe-His stretching frequency. The affinity control should be important to adjust the timing of dioxygen binding appropriately relative to the timing of proton loading for an efficient proton pumping.

3I1034 ポンプ・プローブレーザーと同期したパルスフローシステムの開発とそれを用いたタンパク質の時間分解赤外分光解析

Time-Resolved IR Analyses of Proteins Using a Novel Pulse Flow System Synchronized with Pump/Probe Lasers

Minoru Kubo[1], Satoru Nakashima[1], Masao Mochizuki[1], Kyoko Shinzawa-Itoh[2], Shinya Yoshikawa[1,2], Takashi Ogura[1,2] ([1]*Picobiology Inst., Grad. Sch. Life Sci., Univ. Hyogo*, [2]*Dept. Life Sci., Grad. Sch. Life Sci., Univ. Hyogo*)

IR spectroscopy is a method to analyze structures and reactivities of functional groups, and powerful to reveal protein reaction mechanisms. This spectroscopy, however, has the crucial shortcoming that the application to aqueous solution is practically impossible in most cases because of strong IR absorption of water, which has prevented time-resolved (TR) IR measurements using a flow cell. Recently, we developed a new pump-probe TRIR spectrometer based on the femtosecond IR technology and using a spinning cell. Our spectrometer can detect a 30 μOD protein signal even in the presence of ~2 OD water background in 50 sec of data accumulation, and is promising for flow-flash TRIR measurements. Here, we developed a novel flow system that can be coupled

with the pump-probe TRIR spectrometer. A flow cell was composed of two CaF_2 windows and a 50-μm-thick Teflon spacer that has a 500-μm-wide observation channel. A syringe pump delivered protein solution to the cell by triggering with a pulse generator at 1 kHz (or less). The pulse generator was also used to trigger the pump/probe lasers at 1 kHz with an appropriate delay. The repetition rate of pump illumination can be prescaled with an optical chopper when needed to see slow protein dynamics. The system was tested on CO-bound cytochrome *c* oxidase (0.5 mM) at a flow rate of 1 ml/min. High performance of our flow system was shown through the observation of nanosecond-TR Fe_{a3}-CO and Cu_B-CO signals upon CO photolysis. Details will be discussed at the meeting.

3I1046 チトクロム *c* 酸化酵素のヘム *a* 側鎖に由来する共鳴ラマン線の帰属

The assignment of the resonance Raman bands of heme *a* peripheral substituents in cytochrome *c* oxidase

Miyuki Sakaguchi[1], Yukie Katayama[2], Hiroshi Fujii[3], Hideo Shimada[2], Takashi Ogura[1,2] ([1]*Grad. Sch. Life. Sci., Univ. Hyogo*, [2]*Picobiol. Inst., Grad. Sch. Life. Sci., Univ. Hyogo*, [3]*Okazaki Inst. Integr. Biosci.*)

Proton-pumping process coupled to the O_2 reduction reaction in cytochrome *c* oxidase (CcO) generates the electrochemical potential of proton across the membrane. The putative proton-pumping pathway in bovine heart CcO has H-bond with heme *a* substituents, namely, the formyl, the 7-propionate and the hydroxyfarnesylethyl (HFE) groups, and the proton-pumping mechanism driven by heme *a* is proposed. The functions of heme peripheries are remained to be elucidated and the structural changes of them are needed to be observed. Resonance Raman (RR) spectroscopy has a potential to do it and assignments of the vibrational modes are necessary.

RR band of the formyl group has already been assigned and those of the 7-propionate and the HFE groups are investigated in this study using bacterial mutants. Although another proton-pumping pathway is proposed in bacterial CcO, the structure of the redox centers and the RR spectra are almost identical to the bovine heart CcO. Y406 and T50 have hydrogen bonds with the 7-propionate and the HFE groups, and Y406F and T50A mutants show frequency shifts of the RR bands at 364 and 1251 cm^{-1}, respectively. These mutants have normal absorption spectra and cytochrome *c* oxidation activities, suggesting minimal effects of the mutations. The former band is assigned to the bending mode of the 7-propionate group and we propose an assignment of the vibrational mode of the HFE group to the 1251 cm^{-1} band. The present study would enable us to monitor the heme peripheral groups during proton-pumping process.

3I1058 シアン結合型構造から推察される一酸化窒素還元酵素の反応機構

Functional Implications from Structural Characterization of CN-bound Nitric Oxide Reductase

Takehiko Tosha, Nozomi Sato, Norihiro Okada, Hiroshi Sugimoto, Yoshitsugu Shiro (*Harima Inst., RIKEN*)

Denitrification, conversion of nitrate to N_2, is an example of anaerobic respiration. Nitric oxide reductase (NOR) catalyzes reduction of NO to N_2O; $2NO + 2H^+ + 2e^- => N_2O + H_2O$, a key step for denitrification. NOR is supposed to share the same progenitor with aerobic cytochrome c oxidase (COX) catalyzing four electron reduction of O_2, based on the structural similarity. While we know the structures of NOR and COX, structural factors determining their catalytic properties are still unknown. Here, we characterized the detailed structure of NOR, and compared the results with that of COX, to elucidate the structural elements controlling the function of NOR. The X-ray structure of oxidized NOR indicated that the active site structures of NOR and COX are similarly composed of heme iron and non-heme metal, while the non-heme metal is different between NOR and COX; Fe in NOR is replaced with Cu in COX. To get insights into the structural property of NOR, we utilized CN-bound form as a model for the substrate, NO, bound form. Spectroscopic data showed that CN-bound to heme did not interact with non-heme iron in oxidized NOR, contrasted with CN bridging heme and Cu in COX. Since binding of two NO to the active site is required for the NOR catalysis, contrary to one O_2 binding in COX, the CN ligand for heme in NOR avoid to interact with non-heme Fe to keep second substrate binding site. We will present the X-ray structure of CN-bound NOR and further discuss the determinants for the functional difference between NOR and COX.

1PS001 アクチンの Tyr143 変異による生化学的性質の変化

Changes of biochemical properties of *Dictyostelium* actin induced by mutation of tyrosine-143

Yuki Gomibuchi[1], Taro Uyeda[3], Takeyuki Wakabayashi[2] ([1]*Teikyo Uni.Grad. Scienceand Engineering*, [2]*Teikyo Uni. Dept. Judo Therapy*, [3]*AIST*)

The frontal region of actin around Tyr143 has been proposed to be involved in the binding of myosin. It also changes its conformation during the polymerization (Murakami et al., 2010). Thus we introduced mutation to Tyr143 and examined the biochemical properties, such as polymerizability and the activation of myosin ATPase. In polymerization assay, it turned out that actin with Tyr143Phe mutation showed poorer polymerizability in the presence of NaCl compared with the wild-type actin. Tyr143Ile mutation showed, however, only small decrease in polymerizability. In the presence of phalloidin Tyr143Ile-actin showed almost normal polymerizability irrespective of the added monovalent cations, whereas Tyr143Phe showed the somewhat decreased polymerizability. The interaction with myosin moiety was compared with that of the wild-type actin. The rate of hydrolysis of ATP by rabbit skeletal heavy meromyosin (HMM) was determined by measuring the release of inorganic phosphate in the presence of phalloidin and low concentration (4 uM) of actin. Both of these mutant actins showed weaker ATPase activation. At higher actin concentrations (6-10 uM), Tyr143Ile-actin showed also poorer activation, whereas Tyr143Phe-actin showed the comparable activation. These data indicate the importance of Tyr143 for the activation of myosin ATPase and for the polymerization.

Reference
Murakami et al. (2010) Cell 143, 275-287.

1PS002 誘電緩和分光法によるアクチンフィラメントの水和特性の温度依存性

Temperature dependence of hydration properties of F-actin by dielectric relaxation spectroscopy

Yuichiro Okazaki, Asato Imao, Noriyoshi Ishida, **George Mogami**, Tetsuichi Wazawa, Makoto Suzuki (*Grad. Sch. Eng., Univ. Tohoku*)

Polymerization of G-actin into F-actin is known to be endothermic reaction as shown by Oosawa et al., and thus it thought to be entropy driven. Our previous studies by microwave dielectric relaxation spectroscopy (DRS) revealed that F-actin has a dual hydration shell composed of constrained water (CW, dielectric relaxation (DR) frequency $f_c < f_{cw}$(bulk water)) layer and hyper-mobile water (HMW, $f_c > f_{cw}$) layer which may be formed to a greater extent in an F-actin solution than in a G-actin solution. In this study we examined a temperature dependence of hydration properties of F-actin to understand the mechanism of HMW formation around F-actin. DR spectra of F-actin aqueous solutions were measured at 5, 10, 15 and 20 °C. At every temperature the spectrum was successfully fitted with two DR components, i.e. CW and HMW, in addition to the bulk water component around actin. Assuming that the DR amplitude of the each DR component is proportional to the number of hydration water, the amount of HMW decreased and that of CW increased, with increasing temperature. We estimated the van't Hoff enthalpy of transformation from bulk water to HMW to be +13 kJ/mol, and from bulk water to CW -24 kJ/mol. These results are consistent to the endothermic nature of actin polymerization, and suggest that this is due to the change in the water structure around actin.

1PS003 アクチン重合における水和変化の誘電緩和分光解析

Dielectric analysis of hydration change of actin by polymerization

Asato Imao, Yuichiro Okazaki, Noriyoshi Ishida, Tetsuichi Wazawa, George Mogami, Makoto Suzuki (*Grad. Sch. Eng., Tohoku. Univ*)

Actin is a major protein in cell and plays crucial roles in cellular functions. At low salt concentrations (e. g., less than several mM KCl), actin adopts a monomeric form, G-actin, whereas at higher salt concentrations (e.g., 50 mM KCl) and in the presence of adenosine triphosphate (ATP), actin polymerizes to a filamentous form, F-actin. This polymerization reaction is endothermic and occurs above a critical concentration. These endothermic reactions are believed to involve structural and dynamical changes in the surrounding water.

This paper introduces recent results on the rotational mobility of water around actin filaments (F-actin, a polymerized form of G-actin). Microwave dielectric relaxation spectroscopy (DRS) was employed. The DRS measurements showed that F-actin exhibits dual hydration properties as a structure-maker and a structure-breaker. Thus, in addition to the water molecules with lowered rotational mobility that form a constrained hydration shell around the F-actin, there exist water molecules with rotational relaxation frequencies higher than those of bulk water, which are here referred to as hyper-mobile water. Thus, the present study revealed a significant increase of hyper-mobile water around F-actin. This could be a clue to understanding the endothermic reactions of actin polymerization and constructing the energetics of adenosine-triphosphate-driven protein functions.

1PS004 アクチンの水和状態に及ぼすハライドイオンの効果

Effects of halide ions on the hydration properties of F-actin

Noriyoshi Ishida, Asato Imao, Yuichiro Okazaki, Tetsuichi Wazawa, George Mogami, Makoto Suzuki (*Grad. Sch. Eng., Tohoku. Univ.*)

Actin is a cytoskeletal protein and polymerizes into filaments (F-actin) in high salt condition. We investigated the effects of potassium halides (KCl, KBr, KI) on the hydration properties of F-actin. Actin was taken from chicken pectoral muscle, and purified by a method of Spudich & Watt (1971). The dielectric relaxation (DR) spectra of F-actin solutions (c = 6~7 mg/mL, 50mM KX, 2mM $MgCl_2$, 10mM HEPES (pH7.8), 1mM DTT, 0.1mM ATP ; X=Cl, Br and I) by using high-resolution DR spectroscopy in the frequency range from 0.2 GHz to 26 GHz at 20.0 ± 0.01 °C. With a fixed volume fraction analysis at φ/c = 0.005 mL/mg, the extracted spectrum for the fixed volume including an actin filament and a surrounding water layer was obtained by the Wagner mixture theory. The DR spectrum of the fixed volume around an actin filament for every KX was successfully fitted with two Debye components with DR frequencies, 20 GHz and ~5 GHz. The total DR amplitude for each salt was similar and around 73 and composed of three parts assigned to be constrained water (f_c ~5GHz), hyper-mobile water (HMW, f_c ~20 GHz), and bulk water (f_c = 17 GHz). As a result, the amount of constrained water appeared to be not sensitive to halide ions, and the amount of HMW was found to increase slightly from Cl to I, suggesting some absorption of large halide ions at the surface of actin.

1PS005 ミオシン S1 の水和に及ぼす共溶媒の影響

Cosolvent effects on the hydration state and the enzymatic activity of skeletal myosin

Takuya Nakagawa, Shin-ichiro Yasui, Tetsuichi Wazawa, George Mogami, Makoto Suzuki (*Grad. Sch. Eng., Tohoku. Univ.*)

Cosolvents such as urea and potassium halides are known to affect the hydration state of protein, and in turn cause changes in the conformation and enzymatic activity of protein. Myosin interacts with F-actin and generates mechanical work by ATP hydrolysis reaction. In this study, we have investigated effects of the cosolvents on the hydration state and enzymatic activity of myosin.

Myosin subfragment-1 (S1) and heavy meromyosin (HMM) were prepared from chicken skeletal myosin by papain and chymotrypsin, respectively. By our high-precision dielectric relaxation spectroscopy (DRS), dielectric spectra of aqueous solutions of myosin were measured to derive the hydration properties of myosin. In this study, cosolvents of urea, 1,3-diethylurea (DEU), KBr, or KI were used with a reference aqueous solvent containing 30 –50 mM KCl, 10 mM HEPES (pH 7.8) and 2 mM $MgCl_2$.

The effects of urea at 0.3 M on the sliding speed of F-actin were modest. DEU decreased the sliding speed of F-actin to 1/20 in the gliding assay using myosin, but had little effect on the V_{max} of acto-HMM ATPase, indicating that DEU uncouples the linkage between the ATPase and the mechanical work. DRS of S1 solution showed that the hydration shell of S1 consists of constrained water of a dielectric frequency of 3.8 –5.0 GHz. The content of the constrained water around S1 decreased by ~10%, when DEU was added or KCl was substituted for KI in the solvent.

1PS006 蛍光性カルモジュリンを用いた血管平滑筋ミオシン I および足場タンパク質によるアクチン繊維の組織化メカニズム

Actin filament organization of smooth muscle and possible roles of myosin I and scaffolding protein visualized by fluorescent calmodulin

Yoh Okamoto, Kai Sunada, Syougo Tokuda (*Muroran Institute of Technology, Division of Applied Science*)

In contrast to the architecture of contractile apparatus of striated muscle, smooth muscle has dynamic nature with respect to both of actin and myosin filaments. It should be noticed that a significant decrease of G-actin pool was observed upon the contractile stimulation of vascular smooth muscle according to Zang, W. et al.(2005). We have identified the presence of myosin I, a single headed myosin

with lipid binding short tail in both porcine aorta smooth muscle and A10 cell. An appreciable proportion of the myosin I existed in the cytosol of the A10. (Hasegawa,Y. et al; 1996,1998) We have attempted to find out the role of the cytosolic myosin I with respect to the actin filament organization in vascular smooth muscle cell. During the study of binding between the aorta myosin I and F-actin, an appreciable proportions of F-actin has been sedimented with small amounts of myosin I under physiological ionic strength. This phenomena was attributed to the occurrence of myosin I induced F-actin bundling. During the studies on myosin I, we have also found IQGAP1 in aorta smooth muscle. IQGAP1 has been known as a scaffolding protein of F-actin along with small GTPase, calmodulin. Both myosin I and IQGAP1 in aorta smooth muscle can be key players for actin reorganization during contraction and relaxation cycles of vascular smooth muscle. We have made a fluorescently labeled calmodulin for further characterization of F-actin bundling with myosin I or F-actin gel forming with IQGAP1.

1PS007 ホッキ牽引筋 NAM Mg-ATPase 活性に対する 2 種類の TM (TM1,TM2) の影響

The effects of two kinds TM(TM1,TM2) to Mg-ATPase activity of hokki retractor muscle NAM

Yoichi Yazawa

We have studied Hokki clam, *spisula sachalinensis*, protein components of muscle natural actomyosin (NAM) and Mg-ATPase activities (= Ca-senditivities).
In autumn(october and november), Ca sensitivity of hokki clam retractor muscle NAM ATPase activites showed low values (15~50%). Them of NAM prepared in other three seasons were higher than autumn(88~97%).
SDS-PAGE patterns of two kinds of NAM.
We was different from TM(TM1 and TM2). The difference between TM1 and TM2 is the first report about two types of TM function to Mg-ATPase activity.

1PS008 クライオ電子顕微鏡法を用いたアクチンーミオシン硬直複合体の高分解能構造への試み

Approach to higher-resolution structure of actin-myosin rigor complex by electron cryo-microscopy

Norihiro Shimizu[1], Yoshihiro Tsukada[1], Yakuo Yasunaga[1,2] ([1]*Kyushu Inst. of Tech*., [2]*JST*)

Actin-myosin interaction is involved in muscle contraction, cell motion, and intercellular transport, and the interaction mechanism in detail is not figured out yet. We convince it necessary to obtain high-resolution structure of the rigor complexes to elucidate the mechanism to produce strong binding between actin and myosin. The previous studies have reported their 13 Å resolution density maps but their resolution isn't good enough to discuss the rigor structure at the atomic level. We also have been challenging to obtain high resolution maps beyond 4 Å by cryo-electron microscopy and helical particle analysis. The obtained filaments formed arrowhead every 36 nm. It is due to the behavior of actin-myosin rigor complex: actin filaments take double-helical architecture with a half pitch of 36 nm, and actin molecule bind to myosin molecule in pairs. Therefore, those filaments were obtained as full-decoration. This time, we could get to about 30 filaments (~2000 units) in addition to existing 5500 units from earlier study (Tsukada, 2010), but need 10000 units or more number of units in order to get high-resolution structure beyond 4 Å. We calculated that it is important to increase the number of better quality complex filament.

1PS009 In vivo マウス心臓におけるサルコメア長のリアルタイム計測

Real-time measurement of sarcomere length in the mouse heart in vivo by using α-actinin-GFP

Akari Mizuno[1], Fuyu Kobirumaki-Shimozawa[2], Kotaro Oyama[1], Takako Terui[2], Erisa Hirokawa[2], Togo Simozawa[3], Shin'ichi Ishiwata[1], Norio Fukuda[2] ([1]*Department of Physics, Waseda University*, [2]*Department of Cell Physiology, The Jikei University School of Medicine*, [3]*Department of Physics, Gakushuin University*)

The heart is a unique organ in which cardiomyocytes repeat contraction and relaxation in response to electrical stimulation, thereby ejecting blood. Despite numerous studies conducted thus far under various experimental settings, the molecular mechanisms of contraction and relaxation of cardiomyocytes till remain elusive in vivo. In the present study, we expressed GFP at sarcomeric Z-discs (α-actinin) by using the adenovirus vector system in adult mice, and conducted real-time imaging of the movement of single sarcomeres in cardiomyocytes in the left ventricle under fluorescence microscopy at 10 nm precision (at 100 fps). First, we found that sarcomere length (SL) was ~2.0 μm in the isolated heart when perfused with 30 mM BDM (hence during diastole). This value is close to what was obtained previously by other investigators in rats using various experimental techniques. When perfused with Tyrode's solution containing 1 mM Ca2+, the heart started to exhibit beating with the diastolic and systolic SLs ~2.2 and ~1.7 μm in the left ventricle, respectively. Finally, we attempted to visualize single sarcomeres in vivo in open chest mice under anesthesia. We found that SL was ~2.0 and ~1.7 μm during diastole and systole, respectively, but varied by ~300 nm even in the same left ventricular cell. We also found that sarcomere contraction occurred at the T-wave end point on the electrocardiogram, followed by an in crease in the left ventricular pressure. At the meeting, we discuss these findings at the molecular level.

1PS010 チャネルロドプシンを発現した骨格筋管細胞における筋収縮と成熟の光操作

Optogenetic manipulation of myogenic contraction and maturation in channelrhodopsin-expressing skeletal muscle myotubes

Toshifumi Asano[1,2], Toru Ishizuka[1,3], Hiromu Yawo[1,3,4] ([1]*Grad. Sch. of Life Sci., Tohoku Univ.*, [2]*JSPS*, [3]*JST, CREST*, [4]*Center for Neurosci., Tohoku Univ. Grad. Sch. of Med.*)

Traditionally, neuron and muscle have been electrically stimulated to be induced the artificial activity and examined the specific functions. Although, this technique is simple and convenient, it is often nonuniform, nonspecific and invasive with the electrical field stimulation using metal electrodes placed in the extracellular space. In this study, to improve the spatiotemporal resolution and to reduce the invasiveness, mouse muscle cell lines, C2C12 myoblasts were genetically introduced a variant of light-gated ion channel, channelrhodopsin-green receiver (ChRGR), and subsequently induced into multi-nucleated myotubes according to the standard differentiation conditions. The LED light pulses depolarized the membrane potential of a ChRGR-expressing myotube and eventually evoked action potentials dependent on the intensity and duration of the illumination. The light-activated contraction of the photosensitive myotube was obvious in synchronous to the light pulses of the given frequency and the pattern (1-10 Hz, 20-100 ms). We also found that the optical stimulation using pulsed flash light promoted the sarcomere assembly and the contractile ability of the ChRGR-expressing myotubes. It is suggested that the myogenic contraction and the maturation of skeletal muscle cells can be manipulated by light using optogenetics. This technique could facilitate the studies such as the fundamental biological processes during myogenic development, the stem cell therapy for muscular disorder, and the bioengineering using the muscle-powered actuator.

1PS011 軟体動物横紋筋のコネクチン様タンパク質

Connectin-like protein in molluscan striated muscle

Yulong Bao[1], Akira Hanashima[1], Fumiaki Sodeyama[2], Sumiko Kimura[1] ([1]*Department of Biology, Graduate School of Science, Chiba University*, [2]*Department of Biology, Graduate School of Science, University of Tokyo*)

Connectin is an elastic muscle protein in vertebrate striated muscle. Invertebrate striated muscle is also known to possess several connectin-like proteins. Because the results of our SDS PAGE and immunoblot analyses have suggested the presence of a connectin-like protein in molluscan muscle, we examined its primary structure and compared it with those of some known connectin and connectin-like proteins.
Using the genome information of Lottia gigantea, we searched for a connectin-like protein and determined its sequence by RT-PCR. As a result, the connectin-like protein of the limpet was estimated to be 54 kbp and have a molecular weight of 2,020,000. The domain structure of this protein was similar to that of vertebrate connectin in that it possessed tandem Ig domains, a PEVK region at the N-terminus and a kinase domain at the C-terminus. However, the protein had characteristics substantially different from those of the already known connectin and connectin-like proteins. In particular, it was found to possess a tandem Fn region consisting of 45 repeated Fn domains at the C-terminus and to lack a super-repeat region.
Immunoblot analysis using a polyclonal antibody for the recombinant protein showed that the antibody against the PEVK region reacted with a 3000-kDa band of the limpet heart muscle. Furthermore, the observation with fluorescence microscopy revealed that the PEVK region of limpet connectin-like protein is localized in the I-band of the striated muscle sarcomere.

1PS012　環形動物斜紋筋のコネクチン様 4000K タンパク質の 47 アミノ酸リピート

47 amino acids repeat of connectin-like 4000K-protein in obliquely striated muscle of Annelida

Yui Nomiya[1], Shuji Kanamaru[2], Fumio Arisaka[2], Sumiko Kimura[1] ([1]*Department of Biology, Graduate School of Science, Chiba University*, [2]*Department of Life Science, Graduate School of Bioscience and Biotechnology, Tokyo Institute of Technology*)

Connectin that exists in the striated muscle of vertebrates is an elastic protein with a molecular mass of approximately 3000 kDa. Invertebrates are also known to possess various connectin-like proteins, one of which is a connectin-like 4000 kDa protein that is present in the obliquely striated muscle of Annelida. We have determined the nucleotide sequence of the gene which encodes a connectin-like 4000 kDa protein using a cDNA library of the body wall muscle of Neanthes sp. In the deduced a.a. sequence from the nucleotide sequence, we discovered a sequence in which a unit of 47 amino acids was repeated 11 times. This 47-amino acid sequence repeat contained a high proportion of E and Q, and no significantly homologous protein was found in the database. After preparing a recombinant protein corresponding to this repeat sequence, we performed analytical ultracentrifugation and measured far-UV CD spectrum to estimate its secondary structure content. The sedimentation velocity experiment revealed that the protein had an extremely asymmetric shape, and 48% of the whole structure assumed beta-structure. It was thus demonstrated that this protein could cover a longer distance than other ordinary proteins with the same size. The fact that the connectin-like 4000 kDa protein of the obliquely striated muscle of Annelida has a distinct structure with the 47-amino acid repeat sequence may be related to the resting length of a sarcomere in the Annelida obliquely striated muscle, which is about twice as long as that in the vertebrate striated muscle.

1PS013　プラナリアのコネクチン様タンパク質の配列

Sequential analysis of Planarian connectin-like protein

Kouhei Sasano[1], **Masayoshi Kurasawa**[1], Akira Hanashima[1], Yulong Bao[1], Yuni Nakauchi[2], Sumiko Kimura[1] ([1]*Grad. Sch. Sci., Chiba Univ.*, [2]*Fac. Sci., Yamagata Univ.*)

The striated muscle of vertebrates contains connectin, an elastic protein with a molecular weight of approximately 3,000,000 that functions to maintain the structure of sarcomeres. In addition to Ig, Fn3 and kinase domains, connectin has a PEVK elasticity-relating region. On the other hand, invertebrates possess connectin-like proteins some of whose domain structure are similar to those of vertebrate connectin.

Because connectin antibodies has reacted with 550 kDa band in planarian (Platyhelminth) electrophoresis sample, the planarian is suspected to possess connectin-like protein. Therefore, we searched for a possible candidate based on the genome information, thereby revealing a tentative sequence of the planarian (Platyhelminth) connectin-like protein. The total length of the tentative sequence was about 48 kb, and its molecular mass was estimated to be approximately 1820 kDa if the sequence was fully expressed. Based on the abundance of Ig and Fn3 domains and the presence of a kinase domain, this tentative sequence is considered to be that of connectin-like protein. In this tentative sequence, we observed a repeat sequence of 39-amino acids was repeated 34 times and a tandem Fn3 domain.

Based on this tentative sequence, we performed RT-PCR and determined the partial sequence of the 8.4 kbp region, including the tandem Fn3 domain. The results of the analyses revealed that the tentative sequence is expressed as mRNA in planarian muscle.

1PS014　*in vitro* 運動におけるアクチン束の自発的形成

Spontaneous formation of moving actin bundles *in vitro*

Masayuki Hoshida, Yuuto Maruko, Hajime Honda (*Nagaoka University of Technology*)

Actin filaments are forming both static and dynamic structures fulfilling their cellular functions *in vitro*. Some ones are supported by many kinds of actin binding proteins but some others are spontaneously formed according just to their physical properties. Understanding the formation mechanism of dynamic structures of actin filament with respect to their dynamic property might be important for biophysical researches.

Frequently used assay for actin filament gliding under fluorescent microscope are usually composed of myosin-coated glass slide and buffer mediums sandwiched with another glass slide. The concentration of actin filament should be reduced to below 1.0 mcg/mL in order to observe single filaments separately. We introduced un-labeled actin filament at the concentration of 0.1 mg/mL mixed with labeled filaments. After several ten minutes, bundles of moving actin filaments are spontaneously emerged. The width of bundle is about 0.1 mm winding to form a meshwork structures with the size of about 1.0 mm. Within the bundle of actin, filaments were moving bi-directionally with about 10 nm spacing. This mesh-like structure was formed when the actin concentration was over 0.1 mg/mL. At lower concentration, the structure was formed in the limited area but the shapes and the sizes are essentially the same in all cases. Therefore, these geometrical parameters of this structure should be determined by the physical properties of actin and myosin molecules on the glass side.

1PS015　異なる滑り運動を持つ 2 種類のアクチン分子は独立したフィラメントを形成する

Independent formation of actin filament with two actin species with different sliding velocities

Syunsuke Kinoshita, Kouhei Iwase, Hajime Honda (*Nagaoka University of Technology*)

G145V mutant of actin from dictyosterium was reported to slide about half to its wild type along skeletal muscle myosin molecules on the glass slide. To understand why the velocity was slow even driven by the same myosin, we tried to co-polymerize these two actin molecules in the various ratios. Surprisingly, polymerized portion of filaments were composed of same actin species of either mutant or intact actin molecules. In addition, some filaments were tandemly attached to each other to form a block copolymer. The block copolymers did not attached to skeletal myosin molecules on the glass slide in the presence of ATP in spite of the filament composed entirely from the same apiece did bind and slide along the glass surface at the same conditions.

The reason why these actin species polymerize independently might be caused from the difference in the velocity of polymerization. However, the difference in the binding constants between two molecules could not completely explain the reason why the block copolymers did not bind to myosin molecules. We are investigating the reason with respect to the difference of sliding velocity of each species of actin molecules. Sliding property of the block copolymers will be discussed in the meeting.

1PS016　ヒト心筋 SPOC に対する疾患と加齢の影響

The effects of disease and aging on human myocardial SPOC

Tatsuya Kagemoto[1], Mitsunori Yamane[1], Cristobal G. Dos Remedios[2], Norio Fukuda[3], Shin'ichi Ishiwata[1] ([1]*Department of Physics, Faculty of Science and Engineering, Waseda University*, [2]*Bosch Institute, The University of Sydney*, [3]*Department of Cell Physiology, The Jikei University School of Medicine*)

SPOC (SPontaneous Oscillatory Contraction) is a phenomenon observed in the contractile system of striated (skeletal and cardiac) muscle at an intermediate level of activation between contraction and relaxation. We previously reported that the period of the resting heart rate in various animal species is well correlated with that of sarcomere length oscillation under SPOC conditions (for review, see Ishiwata et al., Prog. Biophys. Mol. Biol. (2011) 105: 187-198). Recently, we reported the SPOC properties of human cardiac muscle fibers, such as SPOC period and propagation velocity of SPOC wave, in various samples prepared from human hearts (47th Ann. Meeting of Biophys. Soc. Japan: S122). In the present study, we examined the SPOC properties by using single human cardiac myofibrils prepared from non-failing hearts aged 19 to 65 years and failing hearts (dilated cardiomyopathy (DCM)) aged 15 to 63 years. The use of single myofibrils allowed us to observe the movements of individual sarcomeres with no influence of connective tissues or intercalated discs. Our preliminary results show that the SPOC period in human cardiac myofibrils is similar to that observed in myocardial fibers. At the meeting, we will discuss the effects of DCM and aging on human myocardial SPOC. This research has been approved by Human Ethics Committee at Waseda University.

1PS017　弛緩状態との境界領域における骨格筋筋原線維の自励振動状態（SPOC）

Characteristics of auto-oscillation (SPOC) for skeletal myofibrils observed near the boundary region with relaxation conditions

Kaori Sato[1], Shin'ichi Ishiwata[2] ([1]*Science and Engineering, Waseda Univ.*, [2]*Waseda Bioscience Research Institute in Singapore (WABIOS)*)

The contractile system of striated (skeletal and cardiac) muscle has the auto-oscillation state called SPOC (SPontaneous Oscillatory Contraction) state in addition to contraction and relaxation states (Ishiwata, S., Shimamoto, Y., Fukuda, N. (2011) Prog. Biophys. Mol. Biol.. 105, 187-198.). This is observed at the intermediate levels of activation between contraction and relaxation. In the SPOC state, the sarcomere length (SL) shows oscillation with a saw-tooth waveform consisting of slow shortening and rapid lengthening. On the other hand, the SPOC theory (Sato, K., Ohtaki, M., Shimamoto, Y., Ishiwata, S. (2011) Prog. Biophys. Mol. Biol. 105, 199-207.) predicted that, as the activation level is lowered approaching to the relaxation, the amplitude of SL oscillation decreases and its waveform tends to become a triangular one. In this study, we aimed to experimentally examine this theory. We analyzed the oscillation properties of skeletal myofibrils in the boundary conditions between relaxation and SPOC (ADP-SPOC; SPOC induced at the coexistence of MgATP, MgADP and Pi in the absence of Ca2+). As a result, we observed that myofibrils showed a transition from a general SPOC state to a weak oscillation state by lowering the ADP concentration (lowering the activation level), and the amplitude, the period and the waveform of SL oscillation became similar to those predicted by the theory. Therefore, it is concluded that the theoretical prediction has been experimentally confirmed. We will also report the other properties of weak oscillation.

1PS018 Force transmission and anisotropic stiffening of reconstituted cytoskeletons

David Head[1], Emi Ikebe[2], Akiko Nakamasu[2], Peijuan Zhang[2], Shoji Ando[3], Daisuke Mizuno[2] ([1]*University of Leeds*, [2]*Kyushu University*, [3]*Sojo University*)

Stresses transmit from force generators in living cells induce a non-linear cytoskeletal response which affects range of cell behaviors. Here we employ microrheology to apply physiological-strength point forces to intermediate filament (vimentin) networks and measure the transmission of 2D response at an anterior point. We observe both pronounced stiffening and a marked anisotropy, with a largerstiffness parallel to the force. This is intuitively and quantitatively explained in terms of the properties of individual filaments by an affine continuum model. We argue that deviations from the theoretical model at low frequencies is due to non-affine network deformation modes, rather than distributed inter-crosslink separations.

1PS019 高圧下におけるαアクチン構造安定性の理論的解析

Theoretical Analysis of α-Actin Stability at High Pressure

Nobuhiko Wakai[1], Kazuhiro Takemura[2], Takami Morita[3], Akio Kitao[2,4] ([1]*Grad. Sch. of Fron. Sci., Univ. of Tokyo*, [2]*IMCB, Univ. of Tokyo*, [3]*NRIFS*, [4]*JST, CREST*)

One of the main components of muscle fiber is α-actin, which plays many important roles in cellular functions. Monomeric actin proteins can polymerize into a filament with ATP hydrolysis. The amino acid sequences of actins are highly conserved across species. Deep-sea fish actins have specific amino acid substitutions, Q137K/V54A or Q137K/L67P. Since only Q137K substitution is located near the active site, this residue is expected to contribute to the pressure tolerance. Although some experiments showed the effects of substitutions at high pressure, the detailed mechanism of the pressure tolerance is still unclear. Therefore, we analyzed high pressure effects on monomeric actins using molecular dynamics simulations. Notable differences of excluded volume and solvent-accessible surface area were not observed at high pressure. However, the deep-sea fish actins form a salt bridge between K137 and ATP at the active site. This salt bridge may stabilize ATP at the active site even under high pressure. The orientations of the 137th residue are different between the deep-sea fish actins and other species, which shows a possibility of different reaction mechanism of ATP hydrolysis. In addition, the total number of the salt bridges in the deep-sea fish actins increased due to the formation of several salt bridges connecting pairs of the secondary structures and subdomains. These salt bridges are suggested to be a key for the pressure tolerance.

1PS020 ミオシンのレバーアーム・スイングの自由エネルギー計算とアクチンフィラメントの影響

Free energy calculation of lever-arm swing of myosin and the effect of actin filament

Jun Ohnuki, Takato Sato, Koji Umezawa, Mitsunori Takano (*Grad. Scl. of Adv. Sci. & Eng., Waseda Univ.*)

Myosin utilizes the free energy obtained from ATP hydrolysis for generating the force which drives the unidirectional motion on an actin filament. Lever-arm model, in which the swinging motion of the lever-arm region of myosin (called the power-stroke) is the driving force, gains widespread support as this force-generation mechanism. However, the model is deduced mainly from structural studies, and the energetic aspect in aqueous solution remains unclear. Therefore it is critical to evaluate the free energy change associated with the lever-arm swing. To do this, we calculated the free energy change accompanying the lever-arm swing by using the explicit-water all-atom model and the enhanced sampling method. In the single myosin molecule system, we found that the power stroke is accompanied by the unfavorable free energy change (to which the electrostatic energy dominantly contributed). This result, however, apparently conflicts with the lever-arm model. One possible reason is that the free-energy change is favorable but is not so large that the statistical error due to the sampling insufficiency might lead us to the conflicting result. Therefore, we improve the sampling efficiency by using better starting structures and reaction coordinate. The effect of the amino-acid sequences should also be examined. Another possible reason is the effect of the actin filament, so we recalculate the free energy change accompanying the power-stroke in the presence of the actin-filament.

1PS021 ATP 合成酵素の結晶化

Crystallization of ATPsynthase

Yasuo Shirakihara[1], Hiromi Tanikawa[1], Satoshi Murakami[2] ([1]*National Institute of Genetics*, [2]*Tokyo Institute of Technology*)

ATP synthase is responsible for ATP production in living cells, and is a membrane protein located in the energy conversion membrane. We crystallized ATP synthase from a thermophilic bacterium PS3, got diffraction patterns extending to 7 A resolution but with a very high mosaicity. In the course of improvement of those crystals, we suddenly got unable to reproduce them.
The problem was cured only partially, in spite of lots of efforts. Then we isolated 27 strains living in unusual environments like hot springs as ATP synthase source. We hoped, from a consideration of limited temperature range where those bacteria are viable, that our new strains carefully isolated may be suited to structural study. We purified ATP synthase from 27 such strains and to them applied crystallization screening test using conditions including the best ones for PS3 ATP synthase. However, the results were discouraging.
We are now back to PS3, and are examining conditions for getting back good old crystals. Those efforts are mainly on the PS3 ATP synthase preparation. Examined points are: test of available different bacterial stocks, culture conditions(temperature, airation, nutrition, and so on), membrane preparation methods (lysozyme lysis, French press, sonication), preparation temperature and Mg concentration in the buffer. Though definite answers are yet to come, we have a feeling that we have to use a good strain stock, and that culture conditions are very important. Details will be presented on why we think so.

1PS022 TF1 β E190D 変異体の外部トルクに対する影響

Effect of external torque on the rotation of TF1 βE190D mutant

Tomohiro Kawakami[1], Shoici Toyabe[2], Hiroshi Ueno[1], Seishi Kudo[3], Eiro Muneyuki[1] ([1]*Dept. Phys., Faculty of Science and Engineering, Chuo Univ.*, [2]*Faculty of Physics, LMU Munich*, [3]*Dept. Appl. Phys., Sch. Eng., Tohoku Univ.*)

The F0F1 ATP synthesizes ATP from ADP and inorganic phosphate (Pi) by proton motive force across the membrane. When isolated, F1 portion works as a motor, hydrolyzing ATP to ADP and Pi. Furthermore, F1-motor converts free energy change derived from ATP hydrolysis into the kinetic energy of the rotation of γ subunit. Recently, Toyabe examined the external torque dependency of the rotation rate of wild type F1-ATPase. He found that the maximum work estimated from the stall torque coincided well with the free energy change of ATP hydrolysis, reached the conclusion of high energy transduction efficiency. So, the next stage of the study is to elucidate the mechanism of this high efficiency. For this purpose, comparison of WT to mutant is a potent approach and we used a mutant βE190D which rotates slower than WT due to low catalytic activity. For applying torque, we adopt electrorotation method. We found different external torque dependence of the rotation of βE190D from that of WT. In case of WT, rotation rate changes sharply around stall torque under our experimental condition. But the torque

dependence of βE190D around stall point was rather small. Distant from the stall point, the rotation rate showed dramatic external torque dependency. We will discuss torque generation source of F1 motor based on the observation.

1PS023 Effect of nucleotide structure on nucleotide binding and rotation of F_1-ATPase

Yohsuke Kikuchi[1], Masaike Tomoko[2], Shoichi Toyabe[3], Hiroshi Ueno[1], Eiroh Muneyuki[1] ([1]*Dept. of Phys., Univ. Chuo*, [2]*Dept. of Phys., Univ. Gakushuin*, [3]*Fac. of Phys., LMU Munich*)

F_1-ATPase is a molecular motor in which the central γ subunit rotates 120° against the $\alpha_3\beta_3$ ring while hydrolyzing an ATP. This 120° step rotation consists of 80° substep and 40° substep. The 80° substep is triggered by the nucleotide binding to catalytic site which is located on each β subunit. The 40° substep is triggered by the phosphate release from the β subunit. Thus nucleotide binding plays an essential role in the rotation of the γ subunit. To study the coupling mechanism of the rotation and nucleotide binding to catalytic site, we compared the affinity of nucleotide binding to catalytic site of F_1 and a single β subunit by fluorescence quenching of genetically engineered βY341W with or without β E190Q mutation. The single β subunit, separated from F_1 complex, has ATP binding activity but does not hydrolyze ATP. For complex, we measured the K_{d3} and thermodynamic parameters such as enthalpy of the nucleotide binding. The K_{d3} of ATP binding to F_1 was bigger than ADP at all temperature range (4-50 degrees) and ΔH^0 of ATP (-28 kJ/mol) was smaller than ADP (-18 kJ/mol). But K_d and ΔH^0 of ATP or ADP binding to single β subunit were almost the same. A comparison between (G, I)TP and (G, I)DP showed a similar tendency. The results indicate the effect of complex formation on the nucleotide binding. To discuss the mechanism of the rotation and the nucleotide binding, we estimated torque of F_1 utilizing ATP, GTP or ITP hydrolysis. We will present the results of nucleotide binding and rotation of F_1.

1PS024 F_1-ATPase の P-loop 変異体に対するリン酸の阻害効果
Inhibitory effect of Pi on F_1-ATPase P-loop mutant

Hikaru Yoshida[1], Ayumi Ito[1], Jotaro Ito[1,3], Syoichi Toyabe[1,2], Hiroshi Ueno[1], Eiro Muneyuki[1] ([1]*Dept, of Physics. Chuo Univ.*, [2]*Faculty of Physics, LMU Munich*, [3]*School of Engineering, The University of Tokyo*)

F_1 -ATPase is an ATP-driven rotary molecular motor. Single molecular observation revealed γ subunit rotates 120° against $\alpha_3\beta_3$ ring. This 120° step consists of 80° substep and 40° substep. The former substep is triggered by ATP binding and ADP release. The latter substep is triggered by ATP hydrolysis and Pi release. In a previous study, two schemes of F_1 rotation were proposed (Adachi et al. Cell, 130 (2007) 309-321). The difference between these schemes was whether Pi releases before or after ADP. Because we cannot observe Pi release, the experiment on its Pi release has been difficult. Recently, Watanabe et al proposed that F1 released Pi after ADP (Nat Chem Biol. 2010 Nov; 6 (11) 794-5). In order to obtain another clue as to this problem, a mutant which releases Pi slowly will be useful. In the present study, we made a P-loop mutant (βG158S) based on (Sanjay et al. Biochemistry 2002, 41.14421-14429). We measured inhibitory effect of Pi on ATPase activity and single molecule rotation. 1 mM KPi decreased ATPase activity of the mutant about 20% at 200 uM ATP. On the other hand, 1 mM KPi did not affect turnover of wild type. In rotation assay, 1 mM KPi decreased the rotation rates of the mutant about 40% at 200 uM ATP. These results suggest that the P-loop mutant has strong affinity for Pi and releases Pi slowly.

1PS025 Conformational changes in the β subunits of F_1-ATPase revealed by FRET measurements during the rotation of the γ subunit

Mitsuhiro Sugawa, Masaru Kobayashi, Takashi Matsui, Tomoko Masaike, Takayuki Nishizaka (*Department of Physics, Gakushuin University*)

F_1-ATPase is a rotary molecular motor in which a central γ subunit rotates against hexagonally arranged subunits $\alpha_3\beta_3$, hydrolyzing ATP sequentially in three β subunits. It remains challenging to uncover the conformational changes of the F_1 complex during the rotation. Previous study has proposed sets of the β subunit conformations during the rotation (Masaike *et al.*, Nat. Struct. Mol. Biol. 2008). Here we performed single-pair FRET measurement to detect distance changes between two β subunits having a FRET pair (Cy3 and Cy5). Transition between high (0.8) and low (0.5) FRET efficiencies was observed, using F_1(βE190D). Given the crystal structures, low FRET efficiency indicates one β subunit in the open form but another in the closed form. On the other hand, high FRET efficiency indicates both of the β subunits in the closed form. Next, we performed a simultaneous measurement of FRET between two fluorescently labeled β subunits and the rotation of the γ subunit. Although the results were preliminarily, relationship between FRET efficiency and the rotation angle was revealed. High FRET efficiency was occurred in one of the three catalytic dwells. In other dwells, other two catalytic dwells and three ATP-waiting dwells, FRET efficiency was lower. These results suggest that in the ATP-waiting dwell two of three β subunits would not take the closed form as in the catalytic dwell. We are performing further experiments.

1PS026 F_1-ATPase におけるトルクの入出力
Torque input/output profiles of F_1-ATPase

Eiichiro Saita[1,2], Kazuhiko Kinosita[3], Masasuke Yoshida[1,2] ([1]*Dept. Mol. Bio., Kyoto Sangyo Univ.*, [2]*ICORP, JST*, [3]*Dept. Phys., Waseda Univ.*)

F_1 -ATPase is an ATP-driven rotary motor, which generates torque by consuming the chemical energy of ATP hydrolysis. Inversely, it can synthesize ATP from ADP and P_i by using reverse torque applied externally. Average output of the torque during ATP hydrolysis reaction is reported to be 40-50 pNnm. However, the detailed torque profile as a function of rotor angle remains unknown. To know it, we have been measuring the torque by using magnetic tweezers. A magnetic bead under a magnetic field can be approximated as a spring in the rotational motion, which allows us to measure the torque on a magnetic bead attached to the motor in a conservative manner. We note that this method can be applied to the torque measurement during ATP synthesis as well as during ATP hydrolysis.

One of primary findings is that the torque output during ATP hydrolysis is not constant but varies with the bead angle. A gradual decrease followed by a steep jump in torque repeats at least three times per 120 degree rotation, indicating that F_1-ATPase rotates with the transitions between at least three states. This is also the case for the torque input profile during ATP synthesis, and each of the two profiles of both reactions is almost identical under various substrates conditions. In addition, the amount of mechanical work calculated from the torque profiles is almost equal to that of calculated free energy change of ATP hydrolysis. The detailed torque profiles obtained possibly explain how F_1-ATPase attains very efficient energy conversion.

1PS027 H^+/ATP ratio of F_oF_1-ATP synthase from the thermophilic *Bacillus* PS3

Naoki Soga[1], Kazuya Kimura[1], Yuzo Kasuya[1], Toshiharu Suzuki[2], Masasuke Yoshida[2], Kazuhiko Kinosita[1] ([1]*Dept. of Phys., Waseda Univ.*, [2]*Molecular Bioscience, Kyotosangyo Univ.*)

F_oF_1-ATP synthase converts the energy of transmembrane proton flow into the high-energy bond between ADP and phosphate. The proton motive force that drives this reaction consists of two components, the pH difference (ΔpH) across the membrane and transmembrane electrical potential (Δψ). The H^+/ATP ratio and the standard Gibbs free energy of ATP synthase are important parameters of coupling between proton translocation and ATP synthesis. Here, to determine the H^+/ATP ratio and the free energy of ATP synthesis for the thermophilic Bacillus PS3 ATP synthase, we examined how the proton motive force is balanced by counteracting ATP hydrolysis. We measured the rates of ATP synthesis and hydrolysis with luciferin/luciferase system as a function of the proton motive force, which was formed by acid-base transition and valinomycin-mediated K^+ diffusion potential. For various nucleotide conditions we determined the proton motive force at which F_oF_1 neither synthesized nor hydrolyzed ATP. The shift of the equilibrium proton motive force as a function of [ATP]/[ADP][Pi] indicated the H＋/ATP ratio of 3.0 ± 0.4 and the standard Gibbs free energy of ATP synthesis of 36 ± 4 kJ/mol for this thermophilic enzyme.

1PS028 新ステップ解析アルゴリズムの F_1－ ATPase への応用
Application of New step finding algorithm to F_1-ATpase

Akihiko Seino, Takeshi Nakagawa, Kazuo Sasaki, Kumiko Hayashi (*Dept. Appl. Phys., Sch. Eng., Tohoku Univ.*)

Kerssemakers and coworkers proposed the step finding algorithm and their algorithm has been used in single-molecule experiments, because the distribution of step size and dwell time makes it possible to obtain important information about the molecule [J.W.J. Kerssemakers *et al.,* Nature 442, 709 (2006)]. In order to improve the performance of the algorithm in the presence of noise, we proposed a new step finding algorithm [Nakagawa et al. The 49th Annual Meeting of the Biophysical Society of Japan, 3M1036]. In this

algorithm, the candidate steps, which are found by the first stage of the Kerssemakers algorithm, are tested by Student's *t*-test. Thus, we came to be able to detect steps which could not be found in Kerssemakers algorithm. Besides, its performance was almost equal to that of Kalafut and coworkers algorithm, which developed recently [Kalafut & Visscher, Compt. Phys. Comm. 179, 716 (2008)]. We implemented the algorithm by using LabVIEW and applied it to single-molecule experiments on F_1-ATPase (F_1). Note that F_1 is a rotary protein which rotates hydrolyzing ATP and the time course of its rotary angle is a stepwise manner with the step size 120°. As an additional improvement of the algorithm, we did a tilt step fitting analysis to 120° rotation of F_1. This result enabled us to get real-time measurement of rotary torque of F_1.

1PS029 回転電場を用いた F_1-ATPase の一分子計測による拡散の Giant Acceleration の観察

Giant Acceleration of diffusion in single-molecule experiments

Ryunosuke Hayashi[1], Syuichi Nakamura[1], Seishi Kudo[1], Kazuo Sasaki[1], Hiroyuki Noji[2], Kumiko Hayashi[1] ([1]*Dept. Appl. Phys., Sch. Eng., Tohoku Univ.*, [2]*Dept. Appl. Chem., Sch. Eng., Univ. Tokyo*)

The diffusion coefficient is one of parameters that are often measured in small biological system to characterize their fluctuation. Giant acceleration of diffusion by use of tilted periodic potentials is one of the many theories on diffusion in the field of non-equilibrium statistical mechanics. According to the theory [1], when we apply a constant force to the colloidal particle in a periodic potential, the diffusion may be greatly enhanced, as compared to free thermal diffusion with an enhancement of up to 14 orders of magnitude for a realistic experimental set up [1]. The diffusion coefficient as a function of the force exhibits the resonance peak at the force value near the critical tilt, which gets more and more pronounced as the environmental temperature decreases [1]. Because the structure of F_1 has three-fold symmetry, the rotary potential is periodic with a period of 120°. It has been found that a constant torque can be applied to F_1 by using an electric rotating field [2]. When we measured the diffusion coefficient as a function of the external torque, we observed the giant acceleration of diffusion in F_1. We show the torque value at the resonance peak corresponds to the critical tilt in the rotary potential of F_1, which is estimated by the fluctuation theorem.

[1] P. Reinmann et al., Phys. Rev. Lett. 87, 010602 (2001).
[2] T. Watanabe-Nakayama et al., Biochem. Biophys. Res. Commun. 366, 951-957 (2008).
[3] K. Hayashi et al., Phys. Rev. Lett. 104, 218103 (2010).

1PS030 バネでつながれたモーター分子による ATP 合成

ATP synthesis by elastically coupled nanomotors

Yasuhiro Imafuku[1], **Nils Gustafsson**[2], Neil Thomas[2] ([1]*Department of Biology, Kyushu University*, [2]*School of Physics and Astronomy, University of Birmingham*)

We have studied a simplified analogue of ATP synthase, consisting of two elastically coupled nanomotors pulling against each other in a molecular 'tug of war'. When one of the nanomotors is driven strongly enough by an external free-energy source, it pulls the other ATP-driven nanomotor backwards so that it synthesizes ATP. Monte-Carlo simulations of the molecular tug of war allow us to study the dependence of the ATP synthesis rate on the free-energy drive ΔG and on the stiffness λ of the spring coupling the two motors. The model reproduces the experimentally observed dependence of ATP synthesis rate on free energy at two crucial points, the maximum ATPase velocity and the thermodynamic equilibrium where the velocity of the ATPase is zero. We have also investigated the variation of ATPase velocity with both ΔG and λ. There are three distinct phases of operation: (*i*) a forward ATP-synthesis phase, (*ii*) a backward ATP- hydrolysis phase, and (*iii*) a locked phase where the ATPase velocity is close to zero. The locked phase becomes more extensive with increasing stiffness λ. Its presence demonstrates the key role that elastic energy plays in the operation of ATP synthase.

1PS031 回転モーター F_1-ATPase の強制回転における長短ヌクレオチド結合の解釈

The interpretation of long and short bindings of nucleotides to rotary motor of F_1-ATPase during forced rotation

Kengo Adachi[1], Kazuhiro Oiwa[2], Masasuke Yoshida[3], Kazuhiko Kinosita, Jr.[1] ([1]*Waseda Univ.*, [2]*Adv. ICT Res. Inst., NICT*, [3]*Kyoto Sangyo Univ.*)

F_1-ATPase is a rotary molecular motor in which a central γ subunit rotates against hexagonally arranged subunits $\alpha_3\beta_3$. Three β-subunits, each hosting a catalytic site, bind ATP sequentially and hydrolyze it to power the rotation of γ, whereas they synthesize ATP from ADP and inorganic phosphate (Pi) when γ rotates in reverse under an external force. The chemical reactions that occur in three catalytic sites are tightly coupled to the mechanical rotation. Recently we have succeeded in determining the angle dependence of nucleotide affinity by directly observing binding/release of fluorescently (Cy3) labeled nucleotides during the forced rotation, revealing the entire reaction pathway of ATP synthesis/hydrolysis.

In that study under the condition of uni-site catalysis (at most one of the three catalytic sites is occupied), there are two types of nucleotide binding: short binding for <120° and long binding for ~240°. We interpreted the result as follows: the long binding is regular pathway and when a site that is to accommodate a nucleotide for ~240° happens to be vacant, due to failure in the initial binding (during open to closed conformational changes) or to early release the bound nucleotide, the site allows another chance of binding toward the end of the ~240° period (in re-opening process). To confirm the interpretation, here we attempt to identify the sites that are binding a Cy3-nucleotide by employing defocus imaging technique which resolves the three-dimensional orientation of a single fluorophore from the diffraction pattern.

1PS032 プラズモン増強電場を利用した蛍光 ATP と回転分子モーターの回転の同時観察

Simultaneous observation of fluorescent-nucleotides and rotation of rotary molecular motor on plasmonic metal nanostructures

Hiroshi Ueno[1], Shoichi Toyabe[1,2], Eiro Muneyuki[1] ([1]*Dept. of Phys., Fac. of Sci. & Eng., Univ. Chuo*, [2]*Sys. Biophys., Fac. of Phys. Munich Univ.*)

We have previously developed the simultaneous observation system of dark-field and fluorescence images using gold nanoparticle as both an optical probe with a low frictional load and a plasmonic nanoparticle for fluorescence enhancement. Metal nanostructures interact strongly with specific wavelength of light, which causes a localized surface plasmon resonance. The plasmonic nanostructures generate large electric field near its surface which enhances the fluorescence of dyes. Actually, we have succeeded in a simultaneous observation of Cy3-ATP binding/release and rotation of F_1-ATPase at 10ms temporal resolution and found an enhancement of Cy3-ATP fluorescence without increasing background noise. In addition, we found a change in fluorescence with 40° substep from 200° to 240°. Our results suggest that conformational change of nucleotide-binding region of β subunit occurs with 40° substep at 200°. However, we cannot rule out the possibility that this change is an artifact resulting from the inhomogeneity of the enhanced-electric field caused by rotation. So, we redesigned the layout of the nanostructures in which the plasmonic nanostructures were fabricated on the glass surface by direct immobilization of nanoparticles or nanosphere lithography to form nanostructure array. Our improved system may afford a versatile experimental platform for sensitive measurements of single molecule fluorescence and surface enhanced Raman scattering in the future.

1PS033 / 1YS1115 F_oF_1-ATP 合成酵素のプロトン駆動力による回転運動の直接観察

Direct observation of H^+-driven rotation of F_oF_1-ATP synthase

Rikiya Watanabe, Kazuhito V. Tabata, Ryota Iino, Hiroyuki Noji (*School of Engineering, The University of Tokyo*)

The synthesis of ATP, the key reaction of biological energy metabolism, is accomplished by the rotary motor protein; F_oF_1-ATP synthase (F_oF_1). *In vivo*, F_oF_1, located on the cell membrane, carries out ATP synthesis by coupling to the rotary motion driven by the proton motive force (*pmf*) across the membrane. F_oF_1 consists of two molecular motors; ATP-driven motor (F_1) and proton-driven motor (F_o). In 1997, we for the first time observed the ATP-driven rotation of F_1, and have thoroughly elucidated its operating principle as a rotary motor protein in this decade. In contrast, despite more than 10 years was elapsed, the proton-driven rotation of F_o or whole enzyme; F_oF_1, has not been observed yet. This is mainly due to the defects of the experimental system; *i.e.* the damage on the membrane, the instability of *pmf* generation system, and its interference with the detection system for rotary motions. In this year, to resolve these technical issues, we fixed these defects one by one, and eventually developed the experimental system which enabled to observe the proton-driven rotation of F_oF_1 under the optical microscope. By using this experimental

system, we directly observed the proton-driven rotation of F_oF_1 in clockwise, which is the reverse direction of ATP-driven rotation, and also obtained various information related to the "dynamics", such as the stepwise rotary motion coupled with the proton transport and ATP synthesis, which provided a clue for understanding the rotary catalysis mechanism of F_oF_1 in the physiological condition.

1PS034 分子動力学計算を用いて明らかにするγ 16° 回転前後の Yeast F1-ATPase の構造的特徴

Molecular Dynamics Simulation on Structural Characteristics of Yeast F1-ATPase before and after 16-degree Rotation of Gamma Subunit

Yuko Ito[1], Takashi Yoshidome[1,2], Nobuyuki Matsubayashi[3], Masahiro Kinoshita[2], Mitsunori Ikeguchi[1] ([1]*Yokohama-city univ. Nanobioscience*, [2]*Kyoto univ. Institute of Advanced Energy*, [3]*Kyoto univ. Institute of Chemical Research*)

We performed molecular dynamics simulations for crystal structures of yeast F1-ATPase whose crystallographic unit contains two different states. One complex binds Pi in the βE subunit, and the other liberated it. In the latter structure, the position of central stalk is also rotated +16 degree in the hydrolysis direction. Because single molecule experiments have proven that Pi release occurs at the βE subunit, and the γ subunit is rotated after ATP hydrolysis and Pi release, these structures are supposed to represent snapshots before and after Pi releases for the 40 degree substep, respectively. From their motional trajectories, we describe how the F1-ATPase complex changes the structure after Pi release. Then, we propose a possible mechanism of the 40 degree rotation of the γ subunit.

1PS035 Single-molecule analyses of the rotation and regulation of human F1-ATPase

Toshiharu Suzuki[1,2,3], Tanaka Kazumi[1,2], Chiaki Wakabayashi[1], Eiichiro Saita[1,2], Shou Furuike[4], Kazuhiko Kinosita Jr[5], Masasuke Yoshida[1,2] ([1]*ATP-synthesis regulation project, ICORP, JST*, [2]*Dept of Mol Bioscience, Kyoto Sangyo Univ*, [3]*Chemical Resources Laboratories, Tokyo Inst of Tech*, [4]*Dept of physics, Osaka Med College*, [5]*Dept of Physics, Faculty of Science and Engineering, Waseda Univ*)

F_1-ATPase (F_1) is the smallest rotary motor in life. The rotation and regulation mechanisms have been deeply investigated by using bacterial enzymes, especially Bacillus PS3 F_1(TF_1). One hydrolysis reaction of ATP makes 120°-rotation and during the 120°, two kinds of dwelling events, named ATP-binding dwell and catalytic dwell, are observable by single molecule microscopic analyses. Although researchers have desired to precisely compare the experimental results to structural information from X-ray crystal study to understand the rotary catalysis mechanism, available structural information is only from eukaryotic enzymes. Additionally, bacterial F_1s have no sensitivity toward most of chemical and protein factors affecting eukaryotic F_1, especially human F_1. To overcome the difficulties, we have established systems for recombinant human F_1.

Single molecule analyses showed counterclockwise rotation of the human F_1 by the energy of ATP as seen in bacterial F_1, but its rotation was remarkably fast, 705 ± 75 rps at 26°C and over 1,366 ± 43 rps at human body temperature, which was roughly 3-folds faster than TF_1. Slow hydrolysable ATP-analogue, ATP-γS, clarified the presence of catalytic dwell in it, although the angle was different from that of TF_1. Rotation analyses using several factors, such as inhibitory factor-1, revealed that another novel 3rd dwelling position is present in human F_1. These results suggest that rotation in mammalian F_1 is not necessarily same to that of bacterial enzymes.

1PS036 一分子 FRET 法によるキネシン頭部のヌクレオチド依存的な構造変化の観察

Single molecule FRET observation of the nucleotide-dependent conformational changes of the kinesin motor domain

Ryosuke Komiyama, Michio Tomishige (*Department of Applied Physics, School of Engineering, The University of Tokyo*)

Kinesin-1 is a motor protein that moves along microtubules by alternately exchanging two motor heads. Our lab recently showed that ATP hydrolysis cycles of trailing and leading heads are differently regulated depending on the direction of the neck linker extension, although it is still unknown how the tension posed to the neck linker affects the nucleotide-binding site distal from the neck linker. Based on the recently solved crystal structure which revealed nucleotide-dependent rotational motion within the motor domain, we hypothesized that ATP binding/hydrolysis can be regulated by the neck linker tension through restricting the subdomain rotation. To test this hypothesis, we developed a single-molecule FRET probe to detect the rotational motion in the kinesin head. We labeled a residue in the rotating subdomain and a residue in the microtubule-interface in kinesin monomer with donor and acceptor dyes. The FRET efficiency distribution in nucleotide-free and AMPPNP states showed distinct peaks separated by about 10%, indicating that the conformational difference before and after rotation can be distinguishable. Then, we labeled with this probe the leading head of the heterodimeric kinesin in which trailing head is a immotile mutant head, and showed that the leading head mainly takes pre-rotating conformation even in the presence of ATP. These results are consistent with the idea that ATP binding in the leading head is prohibited because the backward tension on the neck linker suppresses the rotation in the head.

1PS037 キネシンのヘッド間張力がヌクレオチド結合部位に与える影響 (分子シミュレーションによる調査)

The effect of the internal tension between two heads on the nucleotide binding site of kinesin-1 studied by All-atom MD

Ryo Kanada[1], Tsukasa Makino[2,3], Michio Tomishige[3], Shoji Takada[1] ([1]*Grad. Sch. Sci., Univ. Kyoto*, [2]*BSI, Riken*, [3]*Dept. of Appl. Phys., Univ. Tokyo*)

The dimeric motor protein kinesin-1 walks along microtubules (MT) in a hand-over-hand manner by alternately hydrolyzing ATP and moving two heads. The internal tension between two heads may be related to the regulation for the coordinated walking of kinesin, although the detail mechanism remains unknown. In this study, we focus on the mechanism how the internal tension imposed on the neck-linker region affects the nucleotide binding site in motor domain allosterically. To address this problem, we constructed the dimeric kinesin models bound on MT at on-path way "Tatp-Lapo" state (where the trailing head is ATP bounded state and the leading head is in nucleotide-free) and the monomeric model on MT at apo-state by using the new resolved x-ray structures. We performed all-atom MD and compared the structures and fluctuations at nucleotide binding sites between the dimeric (with internal-tension) and the monomeric model (without tension). Based on the comparison, we will discuss the validity of "front-head gating" mechanism which proposes ATP binding to the leading head is prohibited due to the internal-strain.

1PS038 スピンラベル ESR によるキネシンのネックリンカードッキング、リンカー間歪み、ヌクレオチドーリンカーサイト間伝達の動的構造解析

Structural dynamics of necklinker docking, interlinker strain and nucleotide-to-linker transmission in kinesin probed by spin-label ESR

Satoshi Yasuda[1], Shinji Takai[1], Masafumi D. Yamada[2], Shinsaku Maruta[2], Toshiaki Arata[1] ([1]*Grad. Sch. Sci., Osaka Univ.*, [2]*Grad. Sch. Eng., Soka Univ.*)

We have used site-directed spin label (SDSL) ESR to explore 3 structural events in kinesin monomer (KM) and dimer (KD) at atomic resolution; neck linker (NL) motion, the NL strain by 2 motor heads (MHs) and intersite transmission or communication. 1) We directly measured the distance between 2 SLs at motor domain (MD) (at C223) and NL (at C336), by availing spectral broadening. The NL-MD distance of KM on MTs was 1-2 nm (dock) in AMPPNP state whereas >2 nm (undock) in the no nucleotide (NN) or ADP state. 2) The distance between the C336s of NLs close to an NL-stalk junction of KD on MT was 1-2 nm (unstrained) in NN state whereas >2 nm (strained) in AMPPNP or ADP state. Using ESR, we for the first time detected the stress imposed by 2 docked NLs of front and rear MHs in AMPPNP state or by the dissociated and mobile MH in ADP state. 3) α-1 helix spans between nucleotide (nuc) and NL sites. We estimated steric hindrance, from SL mobility, around SL-cys residue 61, 62, 66, 67, 70, or 72 of α-1 in KM on MT. In NN state, the mobility of C66 and C67 was changed reversely; the mobility of C66 decreased, whereas that of C67 increased. Therefore, it is likely that nuc and NL sites communicate with each other through "rotation" of this helix that induces structural changes in both sites to regulate nuc affinity or NL docking to MD. We would discuss the structural transmission mechanism in KD by combining these data with the previous data on undock-dock transition and the length of NLs in the KD (Sugata et al. BBRC '04, JMB '09).

1PS039 The role of electrostatic interaction in binding-site selectivity of KIF1A on microtubule

Yukinobu Mizuhara, Kyohei Yamamoto, Jun Narita, Mitsunori Takano (*Grad. Scl. of Adv. Sci. & Eng., Waseda Univ.*)

KIF1A, a well-studied kinesin superfamily motor protein, functions as a monomer, where the biased binding to MT, which leads to force-generation, has been observed both in vitro and in silico experiments. Cryo-electron microscopy indicated that KIF1A binds to the α-β contact region within the dimmer (intra-dimer binding site), although there is another almost equivalent potential binding site between the adjacent dimmers (inter-dimer binding site). It has been indicated that the binding-site selectivity is achieved by the difference in the KIF1A-MT electrostatic interaction between the intra- and inter-dimer binding sites. On the other hands, binding of KIF1A to the inter-dimer binding site was also observed in our previous simulation study using a residue-based coarse-grained. However, it is possible that the binding-site selectivity was smeared in our simulation due to the coarse-graining of the protein model. Therefore, in this study, we examined this possibility by using the all-atom model, and calculated the binding energy between KIF1A and the αβ tubulin dimmer. We found that the binding energy for KIF1A binding to the intra-dimer binding site is lower than that to the inter-dimer binding site. We then analyzed the binding energy at the residue level, and examined whether the observed binding-energy difference is originated from the electrostatic interactions (including the critical role of loop 7 of KIF1A as has been suggested).

1PS040 Regulation of motor activity of kinesin-6 by phosphorylation of the N-terminal extension domain

Akihiko Sato[1], Tim Davis[2], Shin Yamaguchi[1], Masanori Mishima[2], Junichiro Yajima[1] ([1]*Graduate School of Arts and Sciences, Univ. Tokyo*, [2]*Centre for Mechanochemical Cell Biology Warwick Medical School University of Warwick*)

Kinesin-6 is a microtubule-based motor protein localized at centralspindle in anaphase. It has been demonstrated that phosphorylation of the motor domain of kinesin-6 on a conserved site within a N-terminal extension destabilised the interaction between microtubules and kinesin-6. Furthermore, deletion of the N-terminal extension also reduced its affinity for microtubules. The molecular mechanism in which the N-terminal extension domain controls the interplay between microtubule and kinesin-6 is unknown. Here, we investigate the influence of the N-terminal extension domain on motor activity. To do this, we have engineered *C.elegans* kinesin-6 motor domain construct with the mutation of one residue to asparatic acid (T9D) in its N-terminal region predicted to mimic phosphorylation of the conserved threonin. Using a microtubule sliding assay in which a quantum dot is attached to the microtubule (Yajima J. *et al.* Nat. Struct. Mol. Biol. 2008), we found that microtubules sliding over wildtype kinesin-6 underwent short-pitch rotation around their longitudinal axes, as revealed by the tracking of the quantum dot in 3D, which has not been previously seen for kinesin-6. In the case of T9D, sliding velocity decreased to 10% of wildtype kinesin-6 and rotations of sliding microtubules could not be observed. This result suggests that phosphorylation in the N-terminal extension domain will regulate torsional force as well as axial sliding force in kinesin-6.

1PS041 カーボンナノチューブを用いたキネシン運動の局所加熱

Local heating of kinesin motors on carbon nanotubes

Yuichi Inoue, Mitsunori Nagata, Akihiko Ishijima (*IMRAM, Tohoku Univ.*)

We demonstrated that single carbon nanotubes (CNTs) can be used as a heat conductor to induce local temperature change for skeletal muscle myosin (Annual meeting, 2011). However, adsorption of myosin on CNTs required very high concentration of myosin as 30 mg/ml to observe continuous sliding of actin filaments. To reduce number of motors on CNTs toward single molecular level, here we used kinesin as a typical processive motor.

Multiwall CNTs (~170 nm diameter, ~10 μm length) were coated with kinesin (~0.1 mg/ml) purified from a bovine brain to observe sliding of fluorescently-labeled microtubules in the presence of 1 mM ATP. During the sliding, a local point of the CNT was temporarily heated with a laser irradiation (645 nm, φ ~2 μm, 2.7 mW) to supply external heat.

Microtubules moved on the kinesin-coated CNTs at a speed of ~0.80 μm/s. By the local heating with laser, the speed increased to ~18.0 μm/s, indicating temperature jump over 10°C as observed for the myosin-coated CNTs.

Our results suggest that the local heating using CNTs can be applied to kinesin motors and processibity of kinesin provides a good reference for the CNTs as a nano heater at single molecular level for future applications of various proteins *in vitro* and *in vivo*.

1PS042 多分子キネシン間の協調性は運搬物を効率的に長距離輸送するのに重要である

Multiple kinesin molecules coordinate to ensure the long-distance walking: a DNA-kinesin hybrid nanomachine study

Yuya Miyazono[1], Masayuki Endo[2], Takuya Ueda[3], Hiroshi Sugiyama[2], Yoshie Harada[2], Hisashi Tadakuma[3] ([1]*Grad. Sch. Appl. Phys., Univ. Tokyo*, [2]*iCeMS, Univ. Kyoto*, [3]*Grad. sch. of Frontier Sci., Univ. Tokyo*)

Kinesin drives cellular transport using energy derived from ATP. However, how multiple kinesin affect the vesicle transport remains elusive. Here we created a hybrid nanomachine (DNA-tile-kinesin) using DNA-origami-tile as the skeletal structure and kinesin as the functional module. Single molecule imaging of DNA-tile-kinesin hybrid, on which 1 to 9 kinesin molecules were attached, allowed us to evaluate the effects of number of kinesins participating in vesicle transport. Our results show that the number of kinesin involving movement affects run length but not velocity of the DNA-tile-kinesin. Furthermore, disturbing the coordination of multiple kinesins, by replacing 1 molecule of 9 molecules to defect kinesin, revealed that coordination is crucial for efficient transport. Thus, the intermolecular coordination facilitates high processive movement of transport complex.

1PS043 フォトクロミック阻害剤を用いた有糸分裂キネシン Eg5 の光制御

Photo-regulation of mitotic kinesin Eg5 using photochromic inhibitors

Kumiko Ishikawa[1], Hideo Seo[1], Kanako Touyama[2], Shinsaku Matuta[1] ([1]*Div. Bioinfo., Grad. Eng., Soka Univ.*, [2]*Dept. Bioinfo., Fac. Eng., Soka Univ.*)

Kinesin Eg5, a member of the kinesin-5 family, is essential for formation of bipolar spindle during cell division. Eg5 is overexpressed in tumor cell and induce significant cell multiplication. Monastrol and Strityl-L-cysteine (STLC), potent inhibitor specific for kinesin Eg5 ATPase activity shut off mitotic division and results in apoptosis. Therefore, these inhibitors are attracting attention as an anti-cancer drug. In this study, we have tried to design and synthesize Monastrol and STLC analogues composed of photochromic molecules (azoboenzen and spiropyran derivatives) as kinesin Eg5 inhibitors, and their photo-reversible inhibitory effects for Eg5 were examined upon ultra-violet (UV) and visible (VIS) light irradiations. STLC analogue, PAM-Cys was synthesized by coupling reaction of 4-phenylazophenyl maleimide with SH-group of cysteine. PAM-Cys showed reversible absorption spectral changes upon UV-VIS light irradiations suggesting the cis-trans isomerization of azobenzen moiety of PAM-cys. Preliminary experiments revealed that the Microtubules dependent ATPase activity of EG5 was inhibited by PAM-Cys reversibly upon UV-VIS light irradiation. We also examined inhibitory effect of spiropyran derivative, 1', 3', 3' -Trimethylspiro [1 (2H) -benzopyran-2, 2'-indoline] (TMSBI) for Eg5. TMSBI inhibited ATPase activity of Eg5 upon UV light irradiation more effectively than VIS light irradiation.

1PS044 フォトクロミック阻害剤を利用したキネシン Kif18A の光制御

Photo-regulation of kinesin Kif18A using photochromic inhibitor

Hideo Seo[1], **Kumiko Ishikawa**[1], Kanako Touyama[2] ([1]*Div. Bioinfo., Grad., Eng., Soka Univ.*, [2]*Dept. Bioinfo., Fac. Eng., Soka Univ.t*)

The shape and function of the mitotic spindle depends on the cooperation action of various kinesins. Recently, it was demonstrated that the kinesin Kif18A is a central component for the correct alignment of chromosomes at the spindle equator. BTB-1 is a small molecule potent inhibitor for Kif18A. BTB-1 inhibits ATPase activity of Kif18A but not of other mitotic kinesins. BTB-1 also inhibits the motility of Kif18A in a reversible manner. BTB-1 inhibits Kif18A in an ATP competitive but microtubule -uncompetitive manner and slows down the progression of cells through mitosis. Azobenzen is one of the photochromic molecules that change their shapes and properties drastically upon ultra-violet (UV) and visible (VIS) light irradiation. Previously, we have incorporated azobenzen derivative into functional region of ATP driven motor protein and succeeded to control microtubule dependent ATPase activity reversibly by UV-VIS light irradiation. Interestingly, BTP-1 shows structural similarity to azobenzen derivatives. In this study, we examined photo-reversible inhibitory effects of various azobenzen derivatives for ATPase activity of Kif18A. Cis

isomer of 4-(phenylazo)-phenol (4-PAP) generated by UV irradiation inhibited ATPase activity of Kif18A more effectively than trans isomer of 4-PAP. Other azobenzen derivatives were also examined.

1PS045 RAD54, A CHROMATIN REMODELER, TRANSLOCATES ALONG DNA BY TRACKING THE DNA HELIX

Ichiro Amitani, Christopher Dombrowski, Ronald Baskin, Stephen Kowalczykowski (*Department of Microbiology, University of California, Davis*)

Rad54 is a member of the Snf2/Swi2 family of chromatin remodeling proteins. The members of this family belong to the superfamily2 helicase. Nevertheless, they do not show helicase activity. Instead they translocate on DNA. Rad54 plays various roles during repair of DNA double strand breaks with Rad51. In the initial phase of recombination, Rad54 binds to Rad51-ssDNA complex, stabilizes the nucleoprotein filament and stimulates the homology search by Rad51-ssDNA. Interestingly, in the late phase of recombination, Rad54 disrupts the Rad51 nucleoprotein filament formed on dsDNA, which is inhibitory in the following steps. Alteration of protein-DNA interaction is one of the important roles of Rad54. In eukaryotes, the access to the target DNA is limited since the DNA is wrapped around a histone octamer. Therefore the DNA has to be exposed to allow the DNA repair machinery to gain the access to the DNA. It has been reported that Rad54 has the ability to slide nucleosomes along DNA. However, the molecular mechanism is not yet understood. Here, we report that Rad54 generates 6-8 pN force and translocates along DNA by tracking the DNA helix. Our observations suggest that Rad54 conforms to the twist diffusion model when it slides nucleosomes. In this model, when Rad54 encounters a nucleosome, Rad54 pulls and twists the nucleosomal DNA. The twist defect generated by the action of Rad54 propagates along the histone surface, disrupting the DNA-histone contacts and re-establishing new contacts. As a result, the nucleosome's position is changed.

1PS046 DNA を分解中の RecBCD の高速 AFM 観察

Structural dynamics of RecBCD enzyme during DNA degradation processes studied by high-speed atomic force microscopy

Yusuke Moriguchi[1], Naofumi Handa[2], Noriyuki Kodera[3], Toshio Ando[1,3] ([1]*Sch. Math. & Phys., Int. Sci. & Eng., Kanazawa Univ.*, [2]*Dept. Microbiology, UC Davis*, [3]*Bio-AFM Frontier Research Center, Inst Sci. & Eng., Kanazawa Univ.*)

RecBCD, a heterotrimeric protein complex of the E. coli, is a highly processive DNA helicase and nuclease that is involved in the seemingly conflicting functions of recombinational DNA repair and the degradation of DNA. These biological activities are regulated by a recombination-activating Chi-sequence coded on DNA, in which RecBCD digests away DNA until the Chi-sequence is recognized. At the Chi-sequence, RecBCD pauses, reduces the nuclease activity, and then switches its polarity to initiate the recombination process. Although these properties have been extensively studied by biochemical and biophysical methods, little is known about the detailed mechanism at the nanometer level. In this study, we applied high-speed atomic force microscopy (HS-AFM) to directly observe structural dynamics of RecBCD at work. Last year, we reported successful direct visualization of DNA degradation processes by RecBCD, from which we obtained kinetic parameters of the ATP hydrolysis similar to those reported previously. However, the detail structure of RecBCD was not seen in the AFM movies due to the positional fluctuations of the molecules. This time, we developed a new experimental setup in which Ni-NTA-containing lipid bilayers were used as a substrate on which the His-tagged RecBCD was specifically immobilized. This setup enabled us to distinguish the domain structures of RecBCD. In the presentation, we will show the obtained results together with the HS-AFM movies.

1PS047 高密度昆虫細胞によるアクチン発現

Expression of recombinant beta-actin in the high-density insect cell culture

Takashi Ohki[1], Shin'ichi Ishiwata[1,2] ([1]*Dept. of Phys., Waseda Univ.*, [2]*WABIOS, Waseda Univ.*)

Actin is the most abundant protein in the cytoplasm of eukaryotic cells, which plays important roles in such processes as muscle contraction, cell division, morphogenesis, organelle positioning, and vesicle trafficking. In our previous study, we reported the expression method of recombinant beta-actin at high cell density in a shaking Erlenmeyer flask. In the insect cell culture at stationary phase (10-12 x 10^6 cells per ml), additional nutrients or medium exchange at time of infection restored the expression level of beta-actin per cell equivalent to that in the cell culture at early exponential phase (1 x 10^6 cells per ml). Therefore, the volumetric yield of recombinant beta-actin, which was determined by the maximal cell density and the yield of recombinant protein per cell, was at least ten-fold higher than compared to the manufacturer's protocol. The present study further developed the expression method of recombinant beta-actin at the density of 30 x 10^6 cells per ml, which is ~30-fold higher than the cell density at stationary phase. This method requires medium exchange plus additional nutrients and air ventilation after infection. The volumetric yield of recombinant beta-actin reached 350 mg per liter of insect cell culture. Here we report in detail the effective method for the production of recombinant beta-actin and the biological and the biochemical properties of recombinant beta-actin.

1PS048 ATP、ADP と無機リン酸存在下での運動するアクチン繊維の変形

Deformations of moving actin filaments on myosin molecules in the presence of ATP, ADP, and inorganic phosphate

Satoru Kikuchi, Kuniyuki Hatori (*Grad. Sch. Sci. Eng., Yamagata Univ*)

Deformations of actin filaments were evaluated by an analysis of fluorescence images of short filaments, in which displacement (DP), peak intensity (PI), and spreading (SD) of fluorescence of dyes bound to actin filaments were measured and the correlations between them were calculated. Using this approach with labeling of rhodamine-phalloidin (Rh-ph), we have previously shown that actin filaments perform the sliding movement with filamental deformations along heavy meromyosin molecules and an increase of velocity occurs after protractions of actin filaments (Kikuchi, S. and Hatori, K., BSJ annual meeting, 2011). In order to examine this further, we tested whether changes of fluorescence are distinct in single actin filaments that were directly labeled with IC3-PE-maleimide (Cy3 analog supplied by Dojido). Fluorescence intensity of actin filaments in labeling of IC3 was greater than that in Rh-ph. However, no difference between IC3 and Rh-ph was observed in correlation values between PI, SD, and DS. The presence of 4 mM ADP induced a decrease of DP, but not PI and SD. On the other hand, DP and SD for IC3-labeled actin filaments were increased by 50% when 10 mM inorganic phosphate was added to the solution with 1 mM ATP. This result shows that the presence of inorganic phosphate facilitates the protraction of the filaments during sliding movement and the increase of their velocity.

1PS049 生体分子モーターのストレインセンサー機構の発見とエネルギー変換への寄与の定量化 1YS0900

Discovery of strain-sensor mechanism in motor protein and the quantification for the energy conversion

Mitsuhiro Iwaki[1,2,3], Keisuke Fujita[2], Atsuko Iwane[2], Lorenzo Marcucci[2], Toshio Yanagida[1,2] ([1]*QBiC, RIKEN*, [2]*Grad. Sch. Biosci., Osaka Univ.*, [3]*Harvard Med. Sch.*)

It is believed that biological linear molecular motors (myosin, kinesin, dynein, etc.) generate force by dominantly structural changes in their composition. Myosin's swinging lever-arm model is a typical hypothesis, where the tilting of the lever-arm domain is strongly coupled to the force generation. On the other hand, random diffusion and forward catch of myosin head to actin is also directly visualized during the directional motion. Myosin-V and -VI are appropriate target in that both (1) lever-arm swing and (2) Brownian search-and-forward catch can be directly visualized during the directional motion. Remaining mystery is which process is critical for the force generation? And how is the mechanism for rectifying random Brownian motion? Here, we answered the questions by improving single molecule measurement techniques (Iwaki *et al., Nat. Chem. Biol.* , 2009; Fujita and Iwaki *et al., Nat. Commun.* , 2012).

We report the strain-sensor mechanism to realize the rectification of random Brownian motion and the quantification for the force generation. Also, we'll discuss the physiological meaning of the dual function (lever-arm swing and the Brownian seach-and-catch) in myosin transporters.

1PS050 統計処理による素過程推定手法の開発（分子マシンを例として）

Construction of statistical method for estimating elementary processes and their characteristics

Hiroto Tanaka, Hiroaki Kojima (*NICT*)

Bio molecular machines generally express macroscopic outputs (MOs) via cyclical and/or multiple microscopic elementary events (MEEs). For example, some bio molecular motors develop sliding or rotating movement (as MO) via cyclical unitary stepping events (as MEE). It is important to reveal such MEEs for understanding working mechanism of bio machines. However, such MEEs are often difficult to observe directly, while expressed MOs are often easy to observe. Therefore, a method that enables us to model MEEs and to estimate their characteristics (size of unitary step, stepping ratio, rate constants, etc. for molecular motors) from "easily observable" MOs, would be a powerful tool to overcome difficulties of direct observation and help understanding working mechanism of bio nano machines. We propose widely suitable method and procedure to model elementary events, and to estimate their characteristic in this study. We theoretically formulated statistical relation between MEEs and MOs for general motion and propose a estimation method (procedure) of characteristics of MEEs with non-linear fitting of "observable" MOs .
As a result of our tests for application, our method showed its potential to determine model of MEEs and their characteristics successfully. Our method and procedure proposed in this study can be a powerful tool to tackle more detail characteristics of bio molecular machines, and to improve apparent spatial and time resolutions of measurement system by using statistical analysis.

1PS051 Photo-control of microtubule flexibility using photochromic nucleotide analogue entrapped within GTP binding site of tubulin

Nozomi Furutani-Umezu[1], Takeshi Itaba[2], Shinsaku Maruta[1,2] ([1]*Dep. Bioinfo., Fac. Eng., Soka Univ.*, [2]*Div. Bioinfo., Grad. Sch. Eng., Soka Univ.*)

Azobenzene is a photochromic molecule that undergoes rapid and reversible isomerization between the cis- and trans-form in response to ultraviolet (UV) and visible (VIS) light irradiation, respectively. Previously, we have incorporated azobenzen derivative into functional region of ATP driven motor protein and succeeded to control microtubule dependent ATPase activity reversibly by photo-irradiation. The results suggested that the photo-control system using photochromic molecules might be applicable to other functional biomolecules. It is known that tubulin utilize GTP to polymerize and the GTP is entrapped within the site of tubulin. Interestingly, it was demonstrated the structure of the microtubules composed of GTP analogue GMP-PCP is more flexible than that composed regular GTP. In the present study, we have employed photochromic nucleotide analogue, Phenylazobenzoyl-iminoethyl-Tri-Phosphate (PABITP) in order to photo-control flexibility of microtubules. The microtubules composed of PABITP showed much more flexible shape change during gliding on in-vitro motility assay than that composed of regular GTP. The effect of photoisomerization of photochromic PABITP entrapped within the site of microtubules induced by UV and VIS light irradiation for flexibility of microtubules was examined.

1PS052 ヌクレオチドを利用する生体分子機械へのフォトクロミックヌクレオチドアナログの応用

Possible application of photochromic nucleotide analogue to the nucleotide required bio-molecular machines

Takeshi Itaba, Shinsaku Maruta (*Div. of Bioinfo., Grad. Sch. of Eng., Soka Univ.*)

Previously, we have synthesized photochromic nucleotide analogues Phenylazobenzoyl-iminoethyl-Tri-Phosphate (PABITP) that change its structure reversibly by light irradiation in order to photo-regulate the function of myosin II. PABITP was hydrolyzed by skeletal muscle myosin and induced dissociation of acto-myosin. X-ray small angle solution scattering analysis of myosin interacting with PABITP showed that the radius of gyration values of S1·PABITP(trans) and S1·PABITP(cis) are identical to those of S1·ATP and S1·ADP respectively. The results suggested that the photo-isomerization of the PABITP induce conformational change of myosin head, which may reflect energy transduction. In this study, we examined the possible application of PABITP to other nucleotide required bio-molecular machines, smooth muscle myosin, myosin V, conventional kinesin, Kif18A, Eg5, tubulin and small G-protein Ras. PABITP was hydrolyzed by these kinesin and myosin ATPase. PABITP induced microtubule gliding on conventional kinesin and polymerization of tubulin to microtubules. We also examined the effect of reversible photo-isomerization of PABITP for the nucleotide required bio-molecular machines.

1PT001 タンパク質ドッキング過程における溶媒和自由エネルギー変化

Solvation free energy in protein dochking process

Taku Mizukami[1], Hiroaki Siato[2], Hidemi Nagao[2] ([1]*Materials Science, JAIST*, [2]*Natural Science and Technology, Kanazawa Univ.*)

Hydration water is believed to play an important role in the process of protein functional expression, for example in protein structural change, or in folding, or in the ligand binding process. The series of intense studies on the water hydration has been done through last several decades. It showed the characteristic chemical/physical parameters, that is, low diffusion constant, vectorial or anisotropic motion, and protein dynamics controlled by water motion. These results suggest a strong correlation mechanisms between water and protein dynamics.
Recently, we have established a methodology to estimate the excess chemical potential or the solvation free energy in the use of trajectory data from MD simulation. In the case of a single globular protein, the protein structural changes caused ~10 [3] kcal/mol solvation free energy change which strongly correlated with the density of the first hydration and the second hydration shell water.
In this study, under the motivation to investigate the solvation effect in the course of protein docking process, we calculate the solvation free energy of Barnase-barstar complex. From MD trajectory performed on each configuration, a solvation free energy was estimated by means of the classical MD simulation and the energy representation method. We investigated the correlation between the solvation free energy depending on the distance and the configuration among two protein, the hydration water density. These results suggest that the hydration water mediates the protein docking process.

1PT002 ミオシン周囲の水の密度揺らぎ

Density fluctuation of water around myosin

Takato Sato, Jun Ohnuki, Koji Umezawa, Mitsunori Takano (*Grad. Scl. of Adv. Sci. & Eng., Waseda Univ.*)

Association and dissociation between myosin and actin are essential for force generation of the actomyosin molecular motor. However, the origin of the intermolecular interaction involved in these processes is complicated due to the coexistence of the electrostatic and hydrophobic interactions. In the previous report, by conducting an extensive explicit-water all-atom molecular dynamics (MD) simulation, we showed that the ATP-induced dissociation of myosin from the actin filament is likely to be caused by the allosteric response of myosin in the actin-binding loops (such as loop 2) and in the residues on the actin-binding surface, which are electrostatically-controlled by the ATP charge. We also found that the water density around the actin-binding surface slightly increases upon ATP-binding (the orientation of water is also affected by the ATP binding). In this study, we further investigated the hydration state of myosin from the viewpoint of water density fluctuation around the myosin surface, because the water fluctuation is closely related to the hydrophobic interaction (Acharya, et al. 2010). We found that some regions with large water-density fluctuation coincide with the actin-binding hydrophobic regions, and mobile regions including surface loops generally exhibit large water-density fluctuations. By placing hydrophobic small probes in the system, we directly examine whether those regions with large water-density fluctuation actually cause intermolecular attraction.

1PT003 中性子散乱による F-アクチン周辺水分子のダイナミクスの研究

Dynamics of Water around F-actin in Solution Studied by Neutron Scattering

Satoru Fujiwara[1], Marie Plazanet[2], Toshiro Oda[3] ([1]*QuBS, JAEA*, [2]*Univ. Fourier*, [3]*RIKEN SPring8 Center*)

Proteins are constantly fluctuating under the influence of surrounding aqueous environment. These thermal fluctuations, or dynamics, of the protein are indispensable for the structural changes that make the protein function. Ultimate understanding of the protein functions thus requires understanding of the dynamics of the proteins including the hydration water. We have been investigating the dynamics of F-actin. How the dynamics of water around F-actin affects the internal dynamics of F-actin is particularly interesting because the water around F-actin shows unusual behavior such that it has higher mobility than bulk water (the hyper-mobile water). Here we employed quasi-elastic neutron scattering (QENS) to characterize the dynamics of the hydration water as well as the internal dynamics of F-actin. The QENS spectra of the concentrated solutions of F-actin in D_2O and H_2O were measured with the instrument IN5 in the Institut Laue-Langevin, Grenoble, France. The spectra arising from the dynamics of the hydration water and those from the internal dynamics of F-actin were extracted from the obtained spectra. The dynamics of the hydration water around the protein in the "solution" samples is characterized

for the first time here, and it is shown that translational diffusion constant of water around F-actin has a similar value to that of the bulk water (2.8×10^{-5} cm^2/s) but longer residence time (3.3 ps compared to 0.6 ps of the bulk water). The results of the detailed analysis will be presented.

1PT004 Mean Exit Time Analysis about Water Molecules around Membrane Surfaces

Eiji Yamamoto[1], Takuma Akimoto[1], Yoshinori Hirano[2], Masato Yasui[3], Kenji Yasuoka[4] ([1]*Department of Mechanical Engineering, Keio University*, [2]*The Institute of Physical and Chemical Research (RIKEN)*, [3]*Department of Pharmacology, School of Medicine, Keio University*, [4]*Department of Mechanical Engineering, Keio University*)

The structures and dynamics of water molecules in the hydration layer of membranes are known to be different from those in bulk. In order to investigate the diffusivity around the surface of the membrane, we performed molecular dynamics simulations of a 1-palmitoyl-2-oleoyl-phosphatidylethanolamine (POPE) bilayer and water molecules at temperatures ranging from 250-350 K. The diffusion coefficient cannot properly characterize the diffusivity of water molecules on membrane surfaces because water molecules do not remain attached to the surface for all time. To characterize translational motion of the water molecules near membrane surfaces, we introduce the concept of mean exit time and show that translational motions of water molecules around the surface of the membrane are slower than those in bulk. Furthermore, we find that the distribution of trapping times of water molecules on membrane surfaces obeys a power law distribution, and the power-law exponent depends on temperature. These results imply that power-law trappings enhance the viscosity of water molecules around the surface of membranes.

1PT005 アルギニンによるカフェ酸の可溶化とそのダイナミクス
Solubilization and Its Dynamics of Caffeic Acid Induced by Arginine

Daisuke Shinozaki[1], Atsushi Hirano[2], Tomoshi Kameda[3], Tsutomu Arakawa[4], Kentaro Shiraki[1] ([1]*Facul. of Pure and Appl. Sci., Univ. of Tsukuba*, [2]*NRI, AIST*, [3]*CBRC, AIST*, [4]*Alliance Protein Lab.*)

Poor aqueous solubility of low molecular weight drug substances hampers their broader applications. We have shown that arginine increases the solubility of small organic compounds as well as proteins. Here we examined the molecular mechanism of arginine on the solubility of caffeic acid that also has a low aqueous solubility. The solubility of caffeic acid increased with increasing pH in the aqueous solutions. At a given pH, arginine further enhanced its solubility. Ratio of the solubility of caffeic acid in arginine solution to that in water was almost constant over the wide range of pH. The interaction between two caffeic acid molecules in the presence or absence of arginine was investigated by molecular dynamic simulation. Our simulation showed arginine decreases binding free energy between the caffeic acid molecules, which suggested the increased solubility of caffeic acid by arginine was attributable to stabilization of the dissociated state.

1PT006 Single molecule analysis for the energy conversion of actomyosin in the presence of osmolyte

Keisuke Fujita[1], Koji Itoh[2], Atsuko Iwane[1], Toshio Yanagida[1,3], Mitsuhiro Iwaki[1,3] ([1]*Grad. Sch. Front. Biosci., Osaka Univ.*, [2]*Fac. Sci., Chiba Univ.*, [3]*QBiC, RIKEN*)

Actomyosin is a biological molecular machine of nanoscopic size that converts the chemical free energy of ATP into mechanical work. Recent single molecule measurements enabled us to detect the mechanical motion at a phenomenological level. However, the energy transduction at the substantial level is still unsolved. It is expected that the majority of free energy of ATP to be used is originated from hydration and dehydration of surrounding water molecules. Here, we modulated the hydration of actomyosin during an energy transduction using osmolyte, Sucrose. From a viewpoint of osmotic pressure, the pressure at 0.5- 1 M sucrose is comparable with that in cell. In a cell, various biological molecules exist and is crowding. This is far from conventional in vitro environment. Our experiment would teach us to predict the energy transduction in a cell.

1PT007 低分子周囲の水のダイナミクスおよび電荷計算：MD および QM 計算
Calculation of dynamics and charges of water around small solute molecules: MD and QM calculations

Takuya Takahashi (*College of Life Sciences, Ritsumeikan Univ.*)

The physico-chemical properties during enzymatic reaction such as ATP hydrolysis are affected by solvent conditions, where the solvent ions and water around biomolecules seem to play important roles. To elucidate the properties, classical MD simulations of water molecules around several types of solutes (poly-phosphates, AMP, and monovalent ions) were done with several water models. The hydrating water molecules around mono-phosphate and di-phosphate molecules with a moderate negative charge showed increased mobility of water compared with bulk water and the results were consistent with the experimental results of the dielectric relaxation spectroscopy although no HMW was observed around tri-phosphate molecules where both the SPCE and TIP5P models were tried. As well as the classical MD, the QM calculations of water around phosphate molecules and other polar and non-polar small molecules were done with Gaussian software. In case of the tri-phosphate molecules (H5P3O10 ~ P3O10) with various protonated states (i.e., the net charge of the molecule varies from neutral to -5 e), the calculated absolute charge of water oxygen atom was smaller as the solute charge became negative and the tendency was not changed in several calculation conditions such as different system size, basis function and chemical model. The details of other QM results will be shown in the meeting.

1PT008 力場パラメタが溶媒和ダイナミクスに及ぼす影響の探索
Investigation of force field parameter effect on solvation dynamics

Yoshito Kondo, Takuya Takahashi (*College of Life Sciences, Ritsumeikan Univ*)

Ions and water are important players in most of the biological phenomena. The anomalous behavior of water around ions would indirectly affect dynamics of biomacromolecules. In addition, hyper-mobile water (HMW) which has higher dielectric relaxation frequency than bulk water is observed around most of the solutes called water structure breakers. NMR experiments also show the existence of water molecules whose translational self-diffusion coefficient is larger than that of pure water around the structure breaker solutes. In our previous studies, molecular dynamics (MD) simulations of water molecules were done around monatomic ion solutes by using conventional water models (TIP3P, TIP4P, TIP5P, SCP etc.). Then, the self-diffusion coefficients and rotational relaxation times in all simulations were calculated to examine the motility change of water molecules due to the solute molecule. As the HMW was not reproduced with the conventional water models, we developed the modified TIP5P water model which force field parameters were optimized with quantum mechanical calculations. After that, we could partly reproduce the HMW. In this study, we tried a variety of parameters of force field to find the most suitable one that reproduces the dynamics of water more quantitatively. The mobility change of water molecules in ionic solutions by the conditions of the appropriate force field parameters from the analysis results will be shown.

1PT009 蛋白質水和の物理的特性．IV. 水和サイト動力学の定量解析
Physical Properties of Protein Hydaration. IV. Quantitative Analysis of Hydration-Site Dynamics

Kunitsugu Soda[1], Yudai Shimbo[1], Yasutaka Seki[2], Makoto Taiji[1] ([1]*Lab. Comp. Molec. Des., QBiC, RIKEN*, [2]*Lab. Struc. Biol., Sch. Pharmacy, Iwate Med. Univ.*)

[Background and Objective] In a series of studies on protein hydration, we have newly defined the hydration site (HS) of proteins to report on static and dynamic properties of HSs and detailed molecular michanism of the dynamics of internal hydration water (HW). These studies showed that HSs of a protein are classified into Single HSs (SHS) and Clustered HSs (CHS) composed of one and more than one polar groups (PGs) respectively. They confirmed that, in any of SHSs, external CHSs and internal CHSs, HWs are very dynamic entity. Quite different from that given by X-ray crystallography, the real view of HWs is far from static. The aim of this study is to characterize quantitatively dynamics of the HW of lysozyme (Lzm).
[Method and Results] Performing MD simulation on an aqueous solution of Lzm, we obtained data on the fluctuation of the hydration state of Lzm. Analysis of the data led to the conclusion as follows: (1) Fluctuations of the hydration state of all the SHSs relax very rapidly within a few tens of ps. (2) In CHSs, HWs H-bonding to their respective PGs fluctuate in mutually correlated manner. Temporal fluctuations of HWs in the largest internal CHS, 'Hg', can be

approximately divided into 11 independent relaxational modes, about half or five of which with larger amplitudes contribute to 76% of the whole fluctuation. (3) Each of these major modes originates in correlated fluctuations of the hydration states of several specific PGs. Their relaxation times range widely from 10 ps to several tens of ns.

1PT010 誘電緩和分光測定によるオリゴリン酸塩の水和解析

Hydration study of oligophosphates by dielectric relaxation spectroscopy

Kazuki Ishimori, George Mogami, Nobuyuki Morimoto, Makoto Suzuki (*Grad. Sch. Eng., Univ. Tohoku*)

Adenosine triphosphate (ATP) is an energy mediator in biological systems. Recently, the importance of the hydration effects on ATP hydrolysis free energy is being realized widely. In this study, we performed high-resolution dielectric relaxation spectroscopy (DRS) for oligophosphates aqueous solution (orthophosphate, pyrophosphate and triphosphate; ≤20mM) as a model of adenosine oligophosphates. The present DRS analysis can divide dielectric properties of the solution into multiple relaxation components. Experiments were performed by microwave network analyzer on 0.2-26 GHz frequency range with the sample solution controlled at 20.0 ± 0.01 °C.

Firstly, we found two types of water that have different relaxation frequency (5 GHz, 20 GHz) from bulk water (17 GHz) around solute ions. The 5-GHz component was attributed to the constrained water, and the 20-GHz component to the hyper-mobile water; HMW.

Secondly, with increasing valence of solute ions, the dispersion intensity of HMW increased significantly. It suggested that the hydration state of oligophosphates was strongly influenced by the valence rather than the polymerized structure of phosphate unit.

1PT011 ATP，ADP，Pi の水溶液から脂肪酸アミン / オクタノール溶媒への移行：その熱力学特性とメカニズム

Thermodynamics and mechanism of transfer of ATP, ADP and Pi from aqueous solution to fatty acid amine/octanol solvent

Hideyuki Komatsu (*Dept. Bioscience & Bioinformatics, Kyushu Inst. Tech.*)

ATP hydrolysis is an important exergonic reaction driving the thermodynamically unfavorable reactions in living systems. Although hydration is considered to contribute significantly to energy profiles of chemical reactions in aqueous condition, the extent of its contribution to ATP hydrolysis remains to be experimentally assessed. In order to evaluate the effect of hydration on the thermodynamics of ATP hydrolysis, ATP hydrolysis in non aqueous condition (i.e., organic solvent) has been studied. For this purpose, fatty acid amine-containing octanol was used as a model solvent, in which ATP, ADP and Pi are highly dissolved. Approximate hydration energies were estimated from the partition coefficients as Gibbs energy changes (ΔG) for transfer of ATP, ADP and Pi from aqueous solution to the fatty acid amine-containing octanol, and compared to ΔG for hydrolysis in the solvent. ΔG for the transfer was smaller than that for hydrolysis in the solvent. Thus, the hydration energy may modestly modulate the Gibbs energy of ATP hydrolysis in aqueous solution.

This energy profile is going to be refined by consideration of the enthalpy changes for the transfers, which can be estimated from van't Hoff plots of temperature-dependencies of the partition coefficients. In addition, in order to elucidate how ATP, ADP and Pi are stabilized in the solvent, ionizations of ATP, ADP and Pi and reversed micelle formation will be investigated by pH titration and dynamic light scattering, respectively.

1PT101 リガンド結合状態及び非結合状態のケナガマンモスヘモグロビンの結晶構造

The crystal structures of hemoglobin from the woolly mammoth in liganded and unliganded states

Hiroki Noguchi[1], Satoru Unzai[1], Kevin L. Campbell[2], Chien Ho[3], Sam-Yong Park[1], Jeremy R. H. Tame[1] ([1]*Protein Design Laboratory, Yokohama City University, Japan*, [2]*Department of Biological Science, University of Manitoba, Canada*, [3]*Department of Biological Sciences, Carnegie Mellon University, USA*)

We have recreated the hemoglobin (Hb) of the extinct woolly mammoth using artificial genes expressed in *Escherichia coli*. The globin sequences were previously determined using DNA recovered from frozen cadavers. Although highly similar to the Hb of existing elephants, the woolly mammoth protein shows rather different responses to chloride ions and temperature. In particular, the heat of oxygenation is found to be much lower in the mammoth than in the elephant protein, which appears to be an adaptation to the harsh Siberian winter. Many Arctic animals such as reindeer show a similarly low temperature dependence of oxygen affinity in order to ensure oxygen transport to the limbs, which may experience much lower temperatures than the body core, even in large, active and fur-covered mammals. In order to discover the structural basis for the altered heterotropic effect we have determined the crystal structures of the Hb in the deoxy, carbonmonoxy and aquo-met forms. These models, the first protein structures from any extinct species, show many features reminiscent of human Hb, but underline how delicate control of oxygen affinity relies on much more than overall quaternary structure changes.

1PT102 HIV-1 プロテアーゼによるダルナビル耐性の分子機構の解明

Structural change at the flap region of HIV-1 protease associated with darunavir resistance

Hirotaka Ode[1], Koji Suzuki[1,2], Masayuki Fujino[3], Masami Maejima[1], Yuki Kimura[1,2], Takashi Masaoka[1], Junko Hattori[1], Yoshiyuki Yokomaku[1], Atsuo Suzuki[2], Nobuhisa Watanabe[2], Yasumasa Iwatani[1,4], Wataru Sugiura[1,4] ([1]*Clin. Res. Center, Nagoya Med. Center*, [2]*Grad. Sch. Eng., Nagoya Univ.*, [3]*AIDS Res. Center, NIID*, [4]*Grad. Sch. Med., Nagoya Univ.*)

Darunavir (DRV) is the most potent protease (PR) inhibitor (PI) currently available for anti-HIV therapy. It has a higher genetic barrier to resistance development than the other PIs. However, it has been reported that DRV is vulnerable to the resistance acquisition, especially for the patients who have previously failed the PI-containing treatments. Here, in order to understand the basis of DRV-resistance, we analyzed structures of the DRV-resistant PR.

We first induced DRV-resistant virus in the culture system with the DRV concentration increased over 154 days. On day 154, we isolated the DRV-resistant virus with 55.5 times higher IC50 against DRV than the wild-type (WT) clone. The analysis of the viral sequences revealed that the escape mutant with five mutations in PR was dominantly induced during the viral replications. Next, we determined a high-resolution (1.8 Å) crystal structure of the DRV-resistant PR. It turns out that the DRV-resistant PR has an open configuration at its flap region, which has not been observed in WT PR. Furthermore, the motional properties and DRV-binding modes of the PR were analyzed by molecular dynamics (MD) simulations. MD simulations showed that the flap region of DRV-resistant PR is more flexible than WT, and that the DRV-interaction modes are distinct. The results suggest that structural change at the flap region is involved in the resistance development of HIV-1 PR. Our findings will provide useful information to develop effective PIs even to the DRV-resistant HIV-1.

1PT103 P2X 受容体の ATP 認識機構およびチャネル活性化機構
1YS1030 Mechanism of ATP binding and channel activation in P2X receptors

Motoyuki Hattori[1], Eric Gouaux[1,2] ([1]*Vollum Institute, Oregon Health & Science University*, [2]*Howard Hughes Medical Institute*)

ATP is known as the vital energy source involved in energy metabolism, biosynthetic reactions and active transport. It is also an essential extracellular signaling molecule that activates two distinct families of ATP receptors: ionotropic P2X and G-protein-coupled P2Y receptors.

P2X receptors are trimeric ATP-activated ion channels permeable to Na^+, K^+ and Ca^{2+}, expressed throughout the human body including the nervous, cardiovascular and immune systems and are implicated in various physiological processes such as synaptic transmission, smooth muscle contraction, taste and pain sensing and inflammation.

A recent crystal structure of zebrafish P2X4 receptor in an apo, closed state, revealed the chalice-shaped trimeric architecture of P2X receptors. However, due to the lack of a crystal structure in complex with ATP, the ATP binding site and the mechanism of channel activation remained unclear.

Here we report the crystal structures of zebrafish P2X4 receptor in the presence and absence of ATP at 2.8 and 2.9 Å resolution, respectively. The agonist-bound structure reveals a novel ATP binding motif and an open channel pore conformation. A structural comparison of two states suggests that ATP binding induces cleft closure in an intersubunit agonist binding site, which expands the region of the receptor proximal to the transmembrane domain, causing an iris-like opening of the channel pore. This work provides the first structural insights into how ATP binding activates P2X receptors based on atomic resolution structures.

1PT104 20S プロテアソームの機能阻害と X 線結晶構造解析

Crystal structure of the yeast 20S proteasome in complex with new inhibitor

Takuma Maekawa[1], Kazuya Nishio[2], Bahrudin Udin[3], Ichiro Hisatome[3], Yasushi Saeki[4], Keiji Tanaka[4], Hiroshi Yamaguchi[1], Yukio Morimoto[2] ([1]*Grad. Sch. Sci&Tec, Univ. Kangaku*, [2]*Grad. Sch. Physi, Univ. Kyoto*, [3]*Grad. Sch. Med., Univ. Tottori*, [4]*Tokyo Inst., Rinshoken*)

Proteasome is a multi-catalytic compound and has function for degrades unfold or nonfunctional proteins. The function of proteasome involves ubiqutin proteasome system that plays important role in living organism. We found a new proteasome inhibitor that has no side effect in normal cell, but effect for the tumor cell degradation. To reveal the precise structure of the inhibitor-binding site and to obtain the fundamental date for development of more effective inhibitor for anticancer reagent, we have determined the crystal structure of the yeast 20S proteasome in complex with the inhibitor.

Yeast 20S proteasome was prepared by over expression in yeast (Saccharomyces cerevisiae), and was purified by each chromatographies. Isolated 20S proteasome was co-crystallized with small molecule inhibitor by using sitting drop vapor diffusion method. The solution of 0.1 M MES-NaOH (pH 6.5), 15% MPD, 50 mM magnesium acetate was used as reservoir solution, and protein solution of 10 mg/ml proteasome was used as droplet. Diffraction images were recorded at BL44XU, SPring-8, Japan, and analysed by using HKL2000 and Refmac.

The inhibitor was bond to the S1 pocket at subunit β5. Three-dimensional orientation of amino acid residues around S1 pocket are available for occupation of one molecule of the inhibitor; TYR(135) and GLY(128) interact with -OH and -C=O groups by hydrogen bond. It is considered that the inhibitor rather than a bortezomib reagent has slightly weak binding-abilities in the S1 pocket and hence induces no side effect for a human being.

1PT105 Ⅳ型分泌系構成蛋白質、DotI の構造

Structure of DotI, a core component of the Type IVB secretion system

Takuya Kuroda[1], Yumiko Uchida[1], Tomoko Kubori[2], Hiroki Nagai[2], Katsumi Imada[1] ([1]*Grad. Sch. Sci. Osaka Univ.*, [2]*RIMD Osaka Univ.*)

Type IV secretion systems (T4SSs) are bacterial molecular machines that directly translocate virulence effecter proteins or DNA into the target cells. Many pathogenic Gram-negative bacteria utilize the T4SSs for infection of their hosts. The T4SSs are evolutionarily related to bacterial conjugation systems, and are divided into two subgroups, type IVA (T4ASS) and type IVB (T4BSS). The Dot/Icm system of *Legionella pneumophila* is classified as a T4BSS and closely related to conjugation systems of IncI plasmids. T4BSS is a multi-protein complex that form a channel spanning the inner and the outer membrane of bacteria. The core complex consists of, at least, six distinct proteins. DotI is one of the core components. DotI is an inner membrane protein composed of a small N-terminal region, a single transmembrane helix and a C-terminal periplasmic domain. Here, we report the crystal structure of periplasmic fragments of DotI and its homologue TraM in IncI plsmid conjugation system. DotI and TraM share a same folding topology and their structures are similar to that of VirB8, which is an inner membrane protein located most inside of the core complex of VirB/D4 T4ASS of *Agrobacterium tumefaciens*, suggesting that DotI and TraM are present at the inside of the core complex of T4BSS. DotI forms an octamer ring with an internal diameter of 30Å and an external diameter of 120Å in the crystal. This ring structure is detected under certain conditions in solution, implying that the ring is also formed in the core complex in vivo.

1PT106 枯草菌細胞壁溶解酵素阻害タンパク質 IseA の立体構造解析：特徴的な阻害ループを持つ弓鋸型新規構造の解明

Solution structure of an autolysin inhibitor IseA from *Bacillus subtilis*: a novel hacksaw-like fold with a characteristic inhibitory loop

Sadaharu Fukui[1], **Ryoichi Arai**[1,2], Naoya Kobayashi[1], Hua Li[3], Satoru Watanabe[3], Junichi Sekiguchi[1] ([1]*Appl. Biol., Fac. Tex. Sci. Tech., Shinshu Univ.*, [2]*YREC, Shinshu Univ.*, [3]*SSBC, RIKEN*)

In *Bacillus subtilis*, LytE, LytF, CwlS and CwlO are vegetative peptidoglycan hydrolases, DL-endopeptidases, which cleave the D-glutamic acid-meso-diaminopimelic acid linkage, and they play important roles in cell separation and growth. IseA is a proteinaceous inhibitor against the DL-endopeptidases. Here we report the solution structure of IseA determined by NMR spectroscopy. (All NMR data were measured and analyzed at RIKEN NMR Facility.) The structure of IseA comprises a single domain consisting of three α-helices, one 3_{10} -helix and eight β -strands, which is a novel "hacksaw-like" fold. A noteworthy region in the IseA structure is a flexible loop between β4 and 3_{10}-helix, which looks like a blade of a hacksaw. Electrostatic potential distribution of IseA shows that most surface charges positively but the surface around the loop region charges negatively. In contrast, an active-site cleft of DL-endopeptidase, LytF, is expected to charge positively. NMR chemical shift perturbation of IseA, interacting with LytF, indicates that the potential interaction sites are located around the loop region, the end region of α-helix, and C-terminal region. These results suggest that IseA inhibits DL-endopeptidase through direct interaction of the loop and around the region with the active-site cleft of the enzyme.

1PT107 4.1 蛋白質 FERM domian と calmodulin の結合解析

Unique structural changes in calcium-bound calmodulin upon interaction with a peptide of protein 4.1R

Wataru Nunomura[1,2], Noriyoshi Isozumi[3], Shigeyoshi Nakamura[4], Shinya Ohki[3], Shun-Ichi Kidokoro[4], Yuichi Takakuwa[5] ([1]*Dept. of Life Sci., Grad. Sch. Eng. & Resource Sci., Akita Univ.*, [2]*Cent. for Geo-Environment. Sci., Grad. Sch. Eng. & Resource Sci., Akita Univ.*, [3]*Cent. for Nano Mat. & Tech., JAIST*, [4]*Dept. of Bioeng., Nagoka Univ. of Tech.*, [5]*Dept. of Biochem., TWMU*)

Calmodulin (CaM) binds to the FERM domain of 80kDa erythrocyte protein 4.1R (R30) independently of Ca^{2+} but, paradoxically, regulates R30 binding to transmembrane proteins in a Ca^{2+} -dependent manner. We have previously mapped a Ca^{2+} -independent CaM binding site, pep11 (A^{264} KKLWKVCVEHHTFFRL), in R30 and demonstrated that, when saturated by Ca^{2+}, CaM (Ca^{2+}/CaM) interacts simultaneously with pep11 and with S^{185}, the binding affinity of Ca^{2+}/CaM for S^{185} increasing dramatically in the presence of pep11. Based on these findings, we hypothesized that pep11 induced key conformational changes in the Ca^{2+}/CaM. Using nuclear magnetic resonance spectroscopy (NMR) and differential scanning calorimetry (DSC) analyses, we established that apo-CaM was more stable when bound to pep 11 and that pep11 bound to apo-CaM through amino acid residues V^{108}, M^{145} and A^{147} in the C-lobe of CaM. Surprisingly, pep11 interacted with both N- and C-lobes of Ca^{2+} /CaM. FTIR analysis revealed that these changes in binding features upon interaction of Ca2+/CaM with pep11 were accompanied by a dramatic increase in CaM β-sheet structures, but not α-helix structures, and by conformational changes of the carboxyl side chain of E^{141} in CaM, a key residue in CaM interaction with Ca^{2+}. We propose that these unique properties may account in part for the previously described Ca^{2+} /CaM-dependent regulation of R30 binding to membrane proteins.

1PT108 真空紫外円二色性分光により予測されたβ2-Microglobulin フラグメントの Steric Zipper 構造

Steric-Zipper Structures of β2-Microglobulin Fragment in Amyloid Fibrils Revealed by Vacuum-Ultraviolet Circular Dichroism Spectroscopy

Koichi Matsuo[1,2], Hirotsugu Hiramatsu[3], Kunihiko Gekko[4], Robert W. Woody[2] ([1]*Synch. Radi., Hiroshima Univ.*, [2]*Biochem. Mol. Biol., Colorado State Univ.*, [3]*Grad. Sch. Pharm. Sci., Tohoku Univ.*, [4]*Inst. Sust. Sci. Devel., Hiroshima Univ.*)

The 21-29 region of β 2-microglobulin (β_2-$m_{21\text{-}29}$) was suggested as the core fragment of β_2-m amyloid fibrils, but its detailed structure in solution remains unclear. Vacuum-ultraviolet (VUV) circular dichroism (CD) spectroscopy using synchrotron radiation has a great advantage for the structure analysis of amyloid fibrils and recently the experimental protein CD was successfully calculated from the 3D coordinates by CD theory with the matrix method. In this study, we combined the theoretical method with a VUVCD spectroscopy to reveal the steric-zipper structures of β_2-$m_{21\text{-}29}$ [21NFLNCYVSG29] fibrils. The VUVCD spectrum of β_2-$m_{21\text{-}29}$ fibrils exhibited negative peaks at 285, 250, 222, and 185 nm, and a positive peak at 202 nm. Two steric-zipper models, in which two parallel β-sheets are linked with disulfide bonds and face in parallel or anti-parallel directions, were constructed and simulated by molecular dynamics for 20 ns. We calculated the VUVCD spectra of the simulated model structures by CD theory and found that the spectra are significantly affected by the orientations of aromatic side-chain of Phe and Tyr residues. Four steric-zipper models composed of six β-sheets were constructed by varying the aromatic stacking. One simulated model, in which all six β-sheets face in the anti-parallel

direction, reproduced well the experimentally observed spectrum, suggesting that β_2-m_{21-29} fibrils form three types of steric-zipper structures with different aromatic stacking between Phe and Tyr residues.

1PT109 どのようにβ-strnad はβ-sheet 中でその位置を決めるのか？

How do β-strands determine their positions in β-sheets ?

Hiromi Suzuki (*Sch. Agri., Meiji Univ.*)

We analyzed the role of amino acid pairing propensity for β-sheet formation. Statistical scores were computed from the frequency of the inter-strand amino acid pairs based on experimental protein structure data, taking the existence of hydrogen bond formation into account. These scores suggested that residues on a strand tend to avoid inconvenient residues on the other strand as partners (negative selection) rather than to select convenient residues (positive selection). Prediction accuracies for alignment order of adjacent strands in the sheets from one edge to the other (Order) in the β-sheets were 77, 57, 39 and 22% for 3-, 4-, 5- and 6-strand sheets, respectively, by using these pairing scores with two restrictions: i) Strands form anti-parallel pairs if a loop region is shorter than 12 residues long, ii) All residues on β-strands have at least one pairing partner(s). H-bond formation was almost completely predicted when Order, direction and register were correctly predicted. Analysis of prediction results showed that in more than half mis-predicted cases for 5-strand sheets, one of edge strands was predicted as a middle strand. If two edge strands were correctly selected among β-strands, accuracies of Order prediction can be over 70 and 40 % for 5- and 6-strand sheets, respectively. Such increase of accuracies may reflect important factors, convenient strand pairing and discrimination between edge and middle strands, for β-sheet formation.

1PT110 X 線小角散乱法による酵母 26S プロテアソームの構造研究

Structural investigation of the yeast 26S proteasome in an aqueous solution by a small-angle X-ray scattering

Yuya Morita[1,2], Takashi Matsumoto[3], Akihito Yamano[3], Yukio Morimoto[1,2] ([1]*Graduate School of Science, Kyoto University*, [2]*Research Reactor Institute, Kyoto University*, [3]*TX-ray Research Laboratory, Rigaku Corporation*)

The 26S Proteasome is a large multiprotein complex involved in a regulated degradation of ubiquitinated protein in the cell. The 26S proteasome is composed of two kinds of three sub-complexes, one core particle (CP, 20S) and two regulatory particles (RP, 19S). CP is formed by axial stacking of four heptameric rings: two inner β-rings and two outer α-rings. Capping at each end of the CP is the RP that regulates the proteolytic function of the protease core. The RP can be further divided into base and lid subcomplexes.
It has not been the way itself how the 26S proteasome degrades ubiquitinated proteins. We have experimented that degradation process and/or particle forming by a small angle X-ray scattering (SAXS). Scattering intensities were collected by use of a BioSAXS-1000 installed FR-E X-ray generator with a protein concentration of 1mg/mL. We have calculated a liberal structure of the 26S component by SAXS without any constraints on shapes of components.
In the session, we will compare our 26S SAXS model with the 26S electron microscopy image, and present characteristic structure of our model.

1PT111 Bombyx mori 液状絹の溶液 NMR 構造解析

NMR Study of Bombyx mori liquid silk

Yu Suzuki[1], Toshimasa Yamazaki[2], Akihiro Aoki[1], Tetsuo Asakura[1] ([1]*Tokyo Univ. of Agri. and Tech.*, [2]*NIAS*)

A *Bombyx mori* Silkworm larve keeps silk in silkglnad at high concentrated (~20% w/w) aqueous solution state before spinning. Liquid silk is expected to form some ordered structure since liquid silk transforms to B-sheet riched silk fiber with high strength in a moment under normal temperature and pressure. In fact, observation of α-helix like pattern in the CD spectra of liquid silk at the concentrated state was reported. On the other hand, the ^{13}C chemical shift of liquid silk indicate random coil although liquid silk extracted from a different kind of silkworm, *S.c.ricini*, which has polyalanine sequences $(Ala)_{12}$ clearly shows α-helix in the three carbons of Ala residues. In this study, atomic-leveled conformation of *Bombyx mori* liquid silk was analyzed with several solution NMR techniques.
^1H and ^{13}C resonance assignments were achieved with ^1H- ^1H NOESY, TOCSY, ^{13}C HSQC and ^{13}C HSQC-NOESY. The assignments revealed that the Gly and Ala residues have several chemical shifts mainly due to forward and backward amino acids. NOE signals between Ha-HN(i, i+2) which indicates repeated type II B-turn conformation observed in ^1H- ^1H NOESY spectra. The intensity of those signals are stronger for liquid silk than regenerated silk aqueous solution with same concentration as liquid silk. From these experiments, it was confirmed that repeated type II B-turn like conformation was generated in *Bombyx mori* liquid silk.

1PT112 Solution stucture of the alternatively folded state of ubiquitin

Soichiro Kitazawa[1], Tomoshi Kameda[2], Maho Yagi[3,4], Kenji Sugase[5], Nicky Baxter[6], Koichi Kato[3,4], Michael P. Williamson[6], Ryo Kitahara[1] ([1]*Ritsumeikan, univ*, [2]*Computational Biology Research Center, AIST*, [3]*Okazaki Institute for Integrative Bioscience and Institute for Molecular Science*, [4]*Nagoya City univ.*, [5]*Suntory Foundation for Life Sciences*, [6]*University of Sheffield*)

Although significant progress has been made in understanding the basic folded state of proteins, atomic coordinates of high-energy states, which are marginally populated high free-energy states, remain largely unexplored by traditional structural experiments. Here, We demonstrate a rational design for the high-energy conformer N_2 of ubiquitin based on the high-pressure NMR study and structure determination of the N_2 by solution NMR spectroscopy. Using a single amino acid replacement method, we created the ubiquitin mutant Q41N that favors the population of N_2. High pressure NMR spectroscopy showed that the N_2 is significantly populated in the mutant sample (~80%) at 1 bar than in the wild-type sample (~15%). The atomic details of the N_2 showed that the α1-helix, the following loop, the β 3-strand, and the β 5-strand change their orientations relative to the remaining regions. Conformational fluctuation on the microsecond to millisecond time scale, characterized by ^{15}N spin relaxation NMR analysis, is remarkably increased for these regions of the mutant. These structure and dynamic characteristics of Q41N are similar to those of the N_2 of the wild-type protein under high pressure. The rational mutation based on the structure and dynamic characteristics of proteins derived by pressure experiments is crucial for amplifying the particular fluctuations in proteins.

1PT113 加圧による IPMDH への水分子の侵入と深海微生物由来タンパク質の圧力適応

High-pressure-induced water penetration into IPMDH and pressure-adaptation mechanism of the proteins from deep-sea bacteria

Takayuki Nagae[1], Yuki Hamajima[2], Takashi Kawamura[3], Ken Niwa[1], Masashi Hasegawa[1], Chiaki Kato[4], Nobuhisa Watanabe[1,3] ([1]*Grad. Sch. of Eng., Nagoya Univ.*, [2]*Grad. Sch. of Life Sci., Rikkyo Univ.*, [3]*Synchrotron Res. center, Nagoya Univ.*, [4]*Inst. of Biogeosci., JAMSTEC*)

Several organisms have been found in deep-sea environments such as the Mariana Trench, and their proteins are known to be adapted to high-pressure environments. However, the pressure-adaptation mechanism of proteins from deep-sea bacterium is not well understood. For example, 3-isopropylmalate dehydrogenase (IPMDH) from a deep-sea bacterium *Shewanella benthica* DB21MT-2 (SbIPMDH) is more tolerant towards high-pressure stress than the same enzyme from a land bacterium *S. oneidensis* MR-1 (SoIPMDH). To elucidate the pressure-adaptation mechanism of IPMDHs, we have initiated structural studies on these proteins by a high-pressure protein crystallography method using a diamond-anvil cell. Crystal structures of SoIPMDH were determined at 2 Å resolution at room temperature under pressures up to about 600 MPa. In the high-pressure structure of SoIPMDH, a new cleft is formed together with water penetration, which is not observed in the structure under atmospheric-pressure [1]. Interestingly, several residues at the cleft vary between SoIPMDH and SbIPMDH. Those residues could be the regions responsible for pressure-adaptation of SbIPMDH. Results of high-pressure structure analysis of IPMDHs will be reported. [1] T. Nagae, T. Kawamura, L. Chavas, K. Niwa, M. Hasegawa, C. Kato & N. Watanabe. (2012), *Acta Cryst*. D68, 300-309.

1PT114 Amyloid-Fibrillation of Lysozyme Is Enhanced by C64-C80 and C76-C94 Disulfide Bonds

Ryohei Kono[1,3], Kaoru Shinohara[2], Yutaro Fujita[2], Hideki Tachibana[2,3] ([1]*Med. Univ. Wakayama*, [2]*Dep. Biotech., School of BOST, Univ. Kinki*, [3]*HPPRC, Institute of Advanced Technology, Univ. Kinki*)

Effect of presence or absence of specific disulfide bonds on the amyloid-fibrillation reaction of hen lysozyme was investigated by using a set of disulfide-variant proteins: 0SS, an all-disulfide-deficient variant; 1SS, single-disulfide-retaining variants (four molecular species); 2SS, double-disulfide-retaining variants (two species employed); 3SS, triple-disulfide-retaining

variants (four molecular species); and 4SS (WT). The extent of monomolecular folding covered by this set of proteins ranges from global unfolding, through local folding/unfolding, to global folding. Fibrillation reaction was carried out with the addition of sonicated WT lysozyme fibril fragments as seeds, at various incubation temperatures and periods, and was monitored with thioflavine T fluorescence, CD spectroscopy, and scanning probe microscopy. All the data showed that the presence of the disulfide bonds C64-C80 and/or C76-C94 enhanced amyloid-fibrillation when compared with the all-disulfide-deficient variant, 0SS, indicating that these native disulfide bonds have a positive role in the misfolding into regular intermolecular beta-structures. The presence of the other native disulfide bond, C6-C127 or C30-C115, had no direct effect compared with 0SS under strongly unfolding conditions, but had an indirect effect against fibrillation through protein stabilization under folding conditions.

1PT115 Structural analysis of hNck2 SH3 domain at various pH: non-native α-helix-rich monomer and native dimer

Masaji Shinjio[1], Yoshitaka Matsumura[1], Kaoru Ichimura[1], Jianxing Song[2], Kihara Hiroshi[3] ([1]*Kansai Medical Univ.*, [2]*Department of Biochemistry, Yong Loo Lin School of Medicine and Department of Biological Sciences*, [3]*SR Center, Ritsumeikan University*)

hNck2 SH3 is a protein which takes β-structure at the native state. On the other side, Liu and Song reported[1)] that the protein forms non-native α-helix-rich structure below pH2 based on NMR spectroscopy. We have done X-ray solution scattering study of hNck2 SH3 at various pH. hNck2 SH3 lost its tertiary structure below pH2, judging from Kratky plots. That is, the non-native α-helix-rich intermediate, found by Liu and Song[1)], is not compact. We also found that monomer- dimer transition occurred from pH2 to pH4 by X-ray solution scattering. Below pH2, the protein is monomer and above pH4, the protein forms dimer, resulting from I(0) analyses. Structural calculations were done by using DAMMIN[2)] program. Elongated structure was obtained at pH2 and ellipsoidal structure was obtained at pH8. The volume of the structure at pH8 is found to be almost twice as large as that at pH2, which also supports the structure below pH2 is monomer and the structure above pH4 is dimer. 1) Liu & Song (2008) Biophys. J., 95, 4803-4812 2) D.Svergun (1999) Biophys. J., 76, 2879-2886

1PT116 Crystal structure of the fatty acid binding protein 3 (FABP3) with or without fatty acid

Mika Hirose[1,2], Shigeru Sugiyama[1,2], Mayumi Niiyama[1,2], Hanako Ishida[2,3], Tsuyoshi Inoue[2,3], Shigeru Matsuoka[1,2], Michio Murata[1,2] ([1]*Grad Sch. of Sci., Osaka Univ.*, [2]*JST, ERATO, Lipid Active Structure Project*, [3]*Appl. Chem., Grad Sch. of Eng., Osaka Univ.*)

Recently, in biological membrane, it revealed that lipids were not only the component of the membrane but also influenced the nature of membrane, and lipids were involved in various intracellular signaling affecting differentiation, regulation, of growth, and gene expression. Thereby, lipids have been proposed as a potential drug target. The structural studies of lipids are helpful to investigate the precise functions of lipids.

However, so far as we know, they show no clear and well separated electron densities corresponding to individual atoms of a lipid molecule. To obtain well-defined lipids, we focused on the structure of fatty acid binding protein 3 (FABP3) previously determined at 1.4 Å resolution.

In cell, long-chain fatty acids (FA) are insoluble molecules, therefore, binding with FABP is essential for intracellular trafficking. Fatty acid binding proteins (FABPs) are 14-15 kDa cytosolic proteins found in different cell types and their amino acid sequences exhibit considerable tissue specific variation.

We tried to purify and crystallize apo-FABP3 by conventional methods for structure comparison of FABP3 with or without FA. However, it was difficult to remove endogenous fatty acids from FABP3 and impossible to obtain clear electron densities of a lipid molecule. It was assumed that the binding affinity of FABP3 to fatty acid was higher than other FABPs.

We will report a removal of endogenous fatty acids from FABP3 and structure analyses of FABP3 with or without FA at high resolution.

1PT117 結晶構造に基づくグラム陰性菌多剤排出ポンプ阻害剤開発に向けた研究

Structural study on inhibitor specifity of bacterial multidrug efflux pumps

Katsuhiko Hayashi[1,2], Ryosuke Nakashima[1], Keisuke Sakurai[1], Seiji Yamasaki[1,2], Chikahiro Nagata[3], Kazuki Hoshino[3], Yoshikuni Onodera[3], Kunihiko Nishino[1], Akihito Yamaguchi[1,2] ([1]*ISIR, Osaka Univ.*, [2]*Grad. Sch. Pharm. Sci., Osaka Univ.*, [3]*DAIICHI SANKYO COMPANY, LIMITED*)

Pseudomonas aeruginosa highly expresses intrinsic resistance against various antibiotics. Resistance in *P. aeruginosa* is mainly caused by two RND type multidrug efflux pumps, MexB and MexY. Compound A (CA) inhibits both MexB and AcrB of the major RND pump in *Escherichia coli*, but CA can't obstruct MexY. There is no useful inhibitor of MexY, which is impediment for overcoming of *P. aeruginosa* infection. CA derivative has great potential to be a universal inhibitor for RND pumps.

First, in order to clarify the interaction manner between CA and AcrB/MexB, we made AcrB-CA and MexB-CA co-crystals. With X-ray analyses, we find the interaction between CA and F178 residue in AcrB and in MexB. MexY homology model was constructed from AcrB and MexB crystal structure. The corresponding position of F178 in AcrB/MexB is W177 in MexY, which suggests that the voluminous side chain of Trp may have the steric hindrance rather than interaction with CA.

To verify this hypothesis, we exchanged F178 in AcrB and the W177 in MexY each other, and checked whether CA inhibits or not. The result is remarkable, and MexY W177F is inhibited but AcrB F178W isn't obstructed by CA. Furthermore, the crystal structure of AcrB F178W certifies that AcrB mutant has normal folding and that there is no space for interaction around the W178 residue.

This result can be not only the indicator of the way to make a universal inhibitor of AcrB, MexB and MexY but also the good example for structure based drug design.

1PT118 STEM トモグラフィー法を用いた細菌および真核細胞内超分子複合体の可視化

Structural visualization of supramolecules in bacterial and eukaryotic cells using STEM tomography

Masafumi J. Koike[1,3], Shiho Minakata[2], Akihiro Narita[3], Michio Homma[4], Jiro Usukura[2,5], Yuichiro Maeda[3] ([1]*RIMD, Osaka Univ.*, [2]*Grad. Sch. Eng., Nagoya Univ.*, [3]*Structural Biology Research Center, Nagoya Univ.*, [4]*Grad. Sch. Sci., Nagoya Univ.*, [5]*EcoTopia Sci. Inst., Nagoya Univ.*)

In order to form hypotheses on the functions on protein complexes in living cells, it is essential to visualize the structures of these complexes. Electron tomography is a powerful tool for structural analyses of supramolecules inside cells. However, this technique does not work well for thick specimens, which limits the area that can be visualized. To overcome this problem, we used STEM (scanning transmission electron microscopy) for tomography analysis. Although this technique is not commonly used in the field of biology, it provides high-contrast images of thick specimen. Using STEM we obtained high-contrast structural images of supramolecules in both bacterial and eukaryotic cells. We imaged the bacterial flagellar motor complex in *Vibrio alginoliticus*. The flagellar basal body and ring structures were clearly recognized in the STEM images we obtained. However, the cytoplasmic part of this motor structure was not visualized due to the method of sample processing. In eukaryotic cells we utilized STEM to show for the first time images of the thin actin network structure juxtaposed with the nucleus. Due to the increased thickness of the cell in this area, imaging was not possible using electron microscopy. By image processing filaments *in silico*, the spatial location of the actin network was visualized three dimensionally. We show that STEM tomography is useful tool for imaging of supramolecular structures in the cell, and is particularly useful for imaging of thick specimens not amenable to conventional techniques.

1PT119 EM Data Bank と Protein Data Bank の低分解能 3D 電子顕微鏡構造データの類似構造検索システム

Similarity search system for low-resolutin 3D-EM strcutre data in EM Data Bank and Protein Data Bank

Hirofumi Suzuki[1,2], Haruki Nakamura[1,2] ([1]*IPR, Osaka-univ.*, [2]*PDBj*)

More than 1800 structure data by 3D electron microscopy (3D-EM) are deposited on the Protein Data Bank (PDB) and the EM Data Bank (EMDB). Extensive and indiscriminate comparison of such 3D-EM data was difficult for some reasons: 1) EMDB data are not atomic coordinates but 3D maps which are not able to be compared by existing tools for coordinates. 2) Various quality values of the 3D maps such as resolutions and CTF-correction accuracies must be unified for each comparison. We have been developing a structure comparison system for 3D-EM data, in which dependencies of data types and

resolutions were limited by comparing distance profiles of coarse-grained models made by vector quantization of the structures instead of the structure data themselves. Therefore, 1707 structures from 3D-EM data in PDB and EMDB were compared mutually by very low computational costs. In the comparison, most of 70S ribosome structures were distinguished from 80S ribosomes. And also, distinguishment of 30S ribosome subunits from 50S subunits and of group I chaperonins from group II were achieved. Using this method, we will provide a web service for similarity search of low-resolution 3D-EM structure data.

1PT120 Residues contributing to the stability of bovine β lactoglobulin elucidated by comparing with a chimera protein, Gyuba

Ryo Imaizumi, Hideaki Ohtomo, Masamichi Ikeguchi (*Soka Univ.*)

A chimeric β lactoglobulin, Gyuba is composed of the amino acid sequences from bovine β lactoglobulin (BLG) in the secondary-structured regions and those from equine β lactoglobulin (ELG) in the loop regions. Previously, the crystal structure of Gyuba was determined and clarified that the three-dimensional structure of Gyuba was very similar to that of BLG. However, thermal denaturation experiments revealed that the stability of Gyuba was dramatically decreased as compared with that of BLG. Additionally, at pH 1.5, BLG maintain its native structure, whereas Gyuba was denatured. The comparison of the crystal structures between BLG and Gyuba suggested that the residue 81 and 126 were responsible for the destabilization of Gyuba.
In this study, we characterized two mutants of Gyuba (E81V and Q126P), in which the residues 81 or 126 of Gyuba were replaced with those of BLG, respectively. At pH 7.0, near- and far-UV circular dichroism spectra of the two mutants were similar to those of Gyuba, indicating that the substitutions did not affect with the structure. Thermal denaturation experiments at pH 7.0 showed T_m of mutants were 5-6ºC higher than that of Gyuba. Additionally, E81V and Q126P maintained their native structure at pH 1.5. These results suggest that the interaction of Cγ1 of V81 with Cδ of K91 and Cδ1 of L93 and the stacking between side chains of P126 and Y20 stabilize BLG structure.

1PT121 X-ray crystallographic analysis of a chemoreceptor protein of Vibrio cholerae, Mlp24

Kazumasa Sumita[1], Yumiko Utida[1], So-ichiro Nishiyama[2], Ikuro Kawagishi[2], Katsumi Imada[1] ([1]*Grad. Sch. Sci. Osaka Univ.*, [2]*Dept. Front. Biosci. Sci., Hosei Univ.*)

Vibrio cholerae is a pathogenic Gram-negative bacterium that causes the human diarrhoeal disease cholera. V. cholerae actively swims in liquid environment using a single polar flagellum. In nutrient-poor aquatic environments, the bacteria do not produce toxin. However, in nutrient-rich environment, such as the lumen of the human small intestine, they begin to form colonies and express pathogenic proteins. Thus, sensing of nutrient is the crucial for pathogenicity of V. cholerae. Mlp24 is a chemoreceptor for multiple amino acids, including serine, arginine and asparagine, which stimulate the expression of several virulence factors. Interestingly, Mlp24 is required for the production of cholera toxin upon mouse infection. These facts suggest that chemotaxis toward a set of amino acids mediated by Mlp24 plays a crucial role in pathogenicity. To elucidate the molecular mechanism of multiple amino acid recognition and pathogenicity of V. cholerae, we expressed, purified and crystallized the ligand binding domain of Mlp24. Static light scattering measurement indicated that the purified Mlp24 domain is in equilibrium between monomer and dimmer. After several days of incubation, rod-shaped crystals were grown from a solution containing PEG400 as precipitant. Structure analysis of the crystal is underway.

1PT122 時計タンパク質 KaiB の KaiABC 複合体形成における構造変化

Structural change of the clock protein KaiB on the formation of the KaiABC clock oscillator complex

Ryosuke Tajika[1], Risa Mutoh[3], Hiroyuki Mino[1], Masahiro Ishiura[1,2] ([1]*Grad. Sch. Sci., Nagoya Univ.*, [2]*Center for Gene Research, Nagoya Univ.*, [3]*Inst. Prot. Res., Osaka Univ.*)

Circadian rhythms, biological oscillations with a period of 24 h in various metabolic and behavioral activities, are observed ubiquitously from procaryotes to eucaryotes. In cyanobacteria, three clock proteins, KaiA, KaiB and KaiC, form the KaiABC clock oscillator complex, which plays essential roles in generating circadian oscillations. KaiA enhances KaiC autophosphorylation whereas KaiB suppresses it. We believe that those functions are associated with structural change of the KaiABC complex. We have previously demonstrated that the structural changes of KaiB occur on the formation of a complex with KaiA and KaiC. However, it is not clear how and when the protein complexes are formed.
Pulsed electron-electron double resonance (PELDOR) is a well-established method to determine the distance between radicals with high accuracy. In order to measure the distance between proteins, the site-directed spin labeling method was used. We prepared a KaiB mutant, which has a Cys residue substitution at the 22nd Val residue ($KaiB_{V22C}$), attached maleimide spin label (MSL) to the cysteine residue (MSL-$KaiB_{V22C}$). PELDOR result showed that the inter-distance between the spin labels in MSL-$KaiB_{V22C}$ was calculated to be about 30 Å. In addition, the longer distance was obtained in the co-presence of KaiA and KaiC. We are now investigating the time course of the formation and structural modification of the KaiABC complex.

1PT123 分裂酵母由来 SpHsp16.0 のシャペロン機能における N 末領域のフェニルアラニン残基の重要な役割

Phenylalanine residues of the N-terminus region play a crucial role in regulating chaperone activity of SpHsp16.0 from fission yeast

Yuya Hanazono[1], Yoshiki Aikawa[1], Nobuhiko Akiyama[1], Tetsuya Abe[2], Kazuki Takeda[1], Toshihiko Oka[3], Masafumi Yohda[2], Kunio Miki[1] ([1]*Grad. Sch. Sci., Kyoto Univ.*, [2]*Dept. Biotech. Life Sci., Tokyo Univ. Agricult. Tech.*, [3]*Grad. Sch. Sci. Tech., Shizuoka Univ.*)

Small heat shock proteins (sHsps), which are widely found in all domains of life, bind and stabilize denatured proteins to prevent aggregation. The sHsps exist as large oligomers that are composed of 9-40 subunits and control their chaperone activity by the transition of the oligomeric state. The sHsps have a globular α-crystallin domain from which the peripheral N-terminal and C-terminal regions protrude. In order to elucidate how sHsps recognize substrates and transit the oligomeric state, we performed crystallographic and biochemical studies by use of SpHsp16.0 from fisson yeast, *Schizosaccharomyces pombe*.
We performed mutational analysis at well-conserved phenylalanine residues of the N-terminal region. Size exclusion chromatography at elevated temperatures and thermal aggregation measurements indicate that Phe6, Phe7 and Phe9 are probably involved in oligomeric stability and interaction with substrates. Moreover, we have determined the crystal structure of SpHsp16.0 at 2.4 angstrom. SpHsp16.0 forms a 16-meric oligomer with 422 symmetry. The SAXS analysis supports this oligomeric assembly. The crystal structure indicates that the three phenylalanine residues (Phe6, Phe7 and Phe9) form a hydrophobic cluster at the center of the oligomer.

1PT124 Staphylococcal nuclease の触媒活性におけるループの役割

The role of the flexible loop in Staphylococcal nuclease on its catalytic activity

Rumi Shiba, Hironari Kamikubo, Yoichi Yamazaki, Mariko Yamaguchi, Mikio Kataoka (*Graduate School of Materials Science, Nara Institute of Science and Technology*)

The molecular control mechanism of enzymatic catalysis is a fundamental problem in protein science.
We have generated the mutant of Staphylococcal nuclease that takes a stable native structure but loses enzymatic activity. The mutant maintains all of active site residues but lacks a flexible loop (Δ44-49). The deletion mutant also keeps substrate binding ability. In order to clarify how enzymatic activity is controlled, we carried out X-ray crystal structure analysis of the mutant with and without an inhibitor, prAp, as well as the WT. While the flexible loop (44-49) of WT takes an open form in the absence of prAp, the loop shows large movement in the presence of prAp to bring a closed form. Accompanying the motion, the residue E43 which acts as a general base catalyst moves to point to the phosphate group of prAp. The mutant Δ44-49 does not show such a large movement because it lacks the flexible loop. E43 of Δ44-49 slightly moves to the similar position to that of WT. However, the flexibility of E43 is apparently lost. Furthermore the movement upon binding prAp of the loop (76-90) which contains another catalytic residue R87 is larger for Δ 44-49 than WT, although the final configuration of R87 is identical. The motions of the loops are closely coupled with each other. We assume that the loop flexibility is an important factor of catalytic activity and that the 44-49 loop controls the flexibility.

1PT125 Athermal Fluctuations in Active Cytoskeletal Networks Follow Truncated Levy Distribution

Heev Ayade, Syou Yamamoto (*kyushu University*)

A reconstituted active cytoskeletal networks consisting of an actin filament network coupled to myosins (motor proteins) have been shown to display rich in dynamical and mechanical behaviors that is often in contrast to passive, equilibrium system. The motor proteins, which spontaneously generate forces, kept the active cytoskeletal network out of equilibrium. The athermal fluctuations observed in the network are linked to the active force generation by motor proteins which give more relevant information including the interaction with the surrounding materials. In prior studies, only the second moment of the athermal fluctuations has been investigated. There is no reason a priori to expect Gaussian statistics in nonequilibrium systems. Indeed, the full displacement distribution of the athermal fluctuations in active cytoskeleton recently probed using video microrheology is found to be far from Gauss. In this study, we investigated the nonequilibrium statistics and dynamics of the active network by analyzing the athermal fluctuations. The model developed here is based on Levy statistics which is generally observed for the effectors whose impacts decays as 1/r2. It was found that the displacement distribution is obtained as a convolution of truncated Levy distribution due to the finite-size of probe particles. The truncation of Levy becomes less and power-law tail is enhanced as the probe particle gets smaller.

1PT126 Atoms in molecules 法によるタンパク質αヘリックス、βシートの水素結合相互作用の理論解析

Atoms in molecules analysis of hydrogen-bond interactions in α- helix, and β-sheets of protein

Hideki Yamasaki, Haruki Nakamura (*IPR, Osaka Univ.*)

Hydrogen-bond interactions (HBIs) between biomolecular systems play an important role in physics, chemistry, and biology, and affect many biological processes, such as molecular recognition. In this study, HBIs of α-helix (AH), and parallel and antiparallel β-sheets (PBS and APBS) were investigated in terms of both energetics and topological points of view, using the electron density analyses of atoms in molecules (AIM) (Yamasaki & Nakamura, 2012) in conjunction with quantum chemical calculations. The secondary structures were built such that the numbers of peptide bonds of AH, and PBS and APBS were increased from 2 to 12 or 16, respectively, in addition to extended models, followed by refining and analyzing with DFT-M062X/6-31+G* calculations. For BS, the interaction energies (Ecp) were estimated with difference in total energy between dimer and the sum of each monomer. The basis sets superposition error was corrected by counterpoise-correction method. For AH, the correlation between total energy differences between AH and extended peptide and the sums of electron density over the bond critical points (Σinterρb) were found with r2 of 0.99. For PBS and APBS, the correlations between Ecps and Σinterρb of HBIs were also found with r2 of 0.99 and 0.97, respectively, implying that Ecp were well reproduced with Σinterρb. Interestingly, while Ecps were monotonically increased for PBS as the numbers of peptide bonds increased, the stepwise increase of Ecps was found for APBS, implying the cooperative HBI effect in APBS.

1PT127 Go モデルによるフォールディングシミュレーションに対する天然構造の差異の影響について

Analysis of the influence of differences in native structures of a protein on its folding simulations with a Go model

Shuji Abe, Masatake Sugita, Takeshi Kikuchi (*Dept. Bioinf., Coll. Life Sci., Ritsumeikan Univ.*)

Go model is a simple model with inter-atomic potentials between only native contacts in a given protein. The native structure of a protein is determined by X-ray crystallography or NMR spectroscopy. Although the 3D structures of a protein determined by these methods show the same structures at the level of the backbone fold, it has been reported that differences in the folding mechanisms predicted by a Go model are observed depending on whether its 3D structure has been determined by X-ray of NMR, or which structure in the NMR models has been used as a native structure. That is, we have to clarify the following points; 1) the extent of the influence of the definition of the native structure on the results of folding simulations by a Go model, 2) How can fruitful information on the folding mechanisms of a protein be extracted using NMR structural ensemble. In this study, this problem is treated by performing simulations using a coarse grained Go model which we have developed. Protein G, Protein L and α-spectrin SH3 domain are used for tests. Our results show that the differences appeared in the folding simulations in Protein L is especially large and specific. We will show the detailed results.

1PT128 光駆動性陽イオンチャネルであるチャネルロドプシンの結晶構造解析
1YS0930 Crystal Structure of a light-gated cation channel, channelrhodopsin

Hideaki E. Kato[1], Feng Zhang[2], Ofer Yizhar[2], Charu Ramakrishnan[2], Tomohiro Nishizawa[1], Kunio Hirata[3], Jumpei Ito[4], Yusuke Aita[4], Tomoya Tsukazaki[1], Shigehiko Hayashi[5], Peter Hegemann[6], Andres D. Maturana[4], Ryuichiro Ishitani[1], Karl Deisseroth[2], Osamu Nureki[1] ([1]*Dept. of Biophys. and Biochem., Grad. Sch. of Sci., Univ. of Tokyo*, [2]*Dept. of Bioengineering, Stanford Univ.*, [3]*Harima Inst., Riken*, [4]*Bioengineering Dept., Nagaoka Univ, of Tech.*, [5]*Dept. of Chem., Grad. Sch. of Sci., Kyoto Univ.*, [6]*Inst. of Biol., Experimental Biophys., Humboldt-Univ.*)

Channelrhodopsin (ChR) is a light-gated cation channel derived from algae that conducts cations, including sodium ions, in a light-dependent manner. Because the inward flow of sodium ions changes the electrochemical gradient and triggers neuron firing, neurons expressing ChRs can be optically controlled with high temporal precision within systems as complex as freely moving mammals. Although ChR has been broadly applied to neuroscience research, little is known about its molecular mechanism. Here, we present the crystal structure of ChR at 2.3 angstrom resolution, showing its basic architecture and molecular mechanism, and give the long-awaited answer to the question, “Where is the cation conducting pathway?” The integration of structural and electrophysiological analyses provides insight into the molecular basis for the remarkable function of ChR, and paves the way for the precise and principled design of ChR variants with novel properties.

1PT129 DNA ポリメラーゼηによるホスホジエステル結合形成を観察する
1YS1000 Watching DNA polymerase η make a phosphodiester bond

Teruya Nakamura[1], Ye Zhao[2,3], Yuriko Yamagata[1], Yue-jin Hua[3], Wei Yang[2] ([1]*Grad. Sch. of Pharmaceut. Sci., Kumamoto Univ.*, [2]*NIDDK, NIH*, [3]*INAS, Zhejiang Univ.*)

A DNA polymerase catalyzes a nucleotidyl-transfer reaction with Mg^{2+}, and a new bond is formed between the 3'-OH of the primer strand and the α-phosphate of dNTP and the phosphodiester bond between α and β-phosphates of dNTP is broken. Until now, a number of structural and kinetic studies of DNA polymerases proposed the catalytic mechanism of the nucleotidyl-transfer reaction. However, the actual reaction mechanism remains unknown. In this study, we have visualized the nucleotidyl-transfer reaction process catalyzed by human DNA polymerase η (Polη) using X-ray crystallography. Polη, DNA and dATP were co-crystallized at pH 6.0 without Mg^{2+}. The reaction was initiated by exposing crystals to 1 mM Mg^{2+} at pH 7.0 and stopped at various time points by freezing. The substrates and two Mg^{2+} are aligned for reaction within 40 sec, but the new bond begins to form at 80 sec. Structures at reaction times from 80 to 300 sec reveal a mixture of decreasing substrate and increasing product of the nucleotidyl-transfer reaction. In sequence, the nucleophile 3'-OH is deprotonated, the deoxyribose at the primer end converts from C2'-endo to C3'-endo, and the nucleophile and the α-phosphate of dATP approach each other to form the new bond. A third Mg^{2+} ion, which arrives with the new bond and stabilizes the intermediate state, may be an unappreciated feature of the two-metal-ion mechanism. Here we show a chemical bond formation at atomic resolution and in real time.

1PT130 Endo-1,3-β-glucanase・オリゴ糖複合体の MD シミュレーション

Molecular dynamics simulations of endo-1,3-β-glucanase and oligosaccharide complex

Nobutaka Komichi[1], Narutoshi Kamiya[2], Haruki Nakamura[2], Masayuki Oda[1] ([1]*Grad. Sch. of Life and Environ. Sci., Kyoto Pref. Univ.*, [2]*Inst. for Protein Res., Osaka Univ.*)

Endo-1,3-β-glucanase from *Cellulosimicrobium cellulans* DK-1, is composed of catalytic domain and carbohydrate-binding module. The catalytic domain belongs to glycoside hydrolase family 16, and catalyzes the hydrolysis of β-1,3-glucans such as laminarin and laminarioligosaccharides. We have determined the crystal structure of catalytic domain, and analyzed its interactions with β-1, 3-glucans using isothermal titration calorimetry. The catalytic domain would have six subsites for the binding of glucose units, four subsites (-4 to -1) being on the non-reducing end from the scissile glucosidic bond and two subsites (+1 and +2) on the reducing end. In this study, we carried out molecular dynamics simulations to clarify the complex structure with laminarioligosaccharides whose degrees of polymerization are 2 to 7. Each oligosaccharide was modeled

and docked into the crystal structure of catalytic domain. Then, a spherical box of water molecules was placed around the subsites. Molecular dynamics simulations in explicit water were carried out at 300 K, and stable structures were chosen from the trajectories by using the cluster analysis. The key residues for the oligosaccharide recognition based on the subsite theory were identified. In the bound oligosaccharide, the glucose unit on the non-reducing end was more fluctuated than that on the reducing end. Taken together with the experimental results of binding thermodynamics, the energetic contribution on the respective subsites could be elucidated.

1PT131 αヘリックス・βストランドレプリカ交換分子動力学シミュレーション法の開発と応用

Development and application of the helix-strand replica-exchange molecular dynamics method

Hisashi Okumura[1,2], Satoru G. Itoh[1,2] ([1]*Inst. Mol. Sci.*, [2]*SOKENDAI*)

Biomolecules such as proteins have complicated free energy surfaces with many local minima. Conventional molecular dynamics (MD) and Monte Carlo (MC) simulations tend to get trapped in these local-minimum states. One of the powerful techniques to avoid this difficulty is the replica-exchange method. We propose helix-strand replica-exchange molecular dynamics method. We apply this method to a design peptide and show the results.

1PT132 PDB データベースによるアミノ酸ごとに最適化した主鎖二面角力場

Development of a force field of backbone dihedral angles for each amino acid using Protein Data Bank

Yoshitake Sakae[1,2], Yuko Okamoto[1,3,4] ([1]*Dept. of Phys., Nagoya Univ.*, [2]*IMS*, [3]*Structural Biology Research Center, Nagoya Univ.*, [4]*Center for Computational Science, Nagoya Univ.*)

A force field is widely used in the field of molecular simulations for biomolecular systems and is determined by an atomic model based on classical mechanics. Many commonly used force fields for protein systems such as AMBER, CHARMM, GROMACS, OPLS, and ECEPP have amino-acid-independent force-field parameters of main-chain torsion-energy terms. Here, we propose a new type of amino-acid-dependent torsion-energy terms in the force fields. As an example, we applied this approach to AMBER ff03 force field and determined new amino-acid-dependent parameters for φ and φ' angles for each amino acid by using our optimization method, which is based on the minimization of some score functions by something in the force-field parameter space, where the score functions are derived for the protein coordinate data in the Protein Data Bank (PDB) [1-3]. In order to test the validity of the new force-field parameters, we then performed folding simulations of α-helical and β-hairpin peptides, using the optimized force field. The results showed that the new force-field parameters gave structures more consistent with the experimental implications than the original AMBER ff03 force field.

[1] Y. Sakae and Y. Okamoto, Chem. Phys. Lett. 382, 626-636 (2003).
[2] Y. Sakae and Y. Okamoto, J. Theo. Comput. Chem. 3, 339 (2004).
[3] Y. Sakae and Y. Okamoto, J. Theo. Comput. Chem. 3, 359 (2004).

1PT133 コフィルアクチンフィラメントの分子動力学モデルの構築

Molecular dynamics model of cofilactin filament

Tetsuya Fujii[1], Yasuhiro Inoue[2], Taiji Adachi[3] ([1]*Grad. Sch. Eng., Dept. of Micro Eng., Kyoto Univ.*, [2]*Dept. of Biomechanics, Inst. Frontier Med. Sci., Kyoto Univ.*, [3]*Dept. of Biomechanics, Inst. Frontier Med. Sci., Kyoto Univ.*)

Cofilin is an actin regulatory protein which dissembles and severs actin filaments. The binding affinity of cofilin to actin filament is regulated via biochemical pathways. In addition, it has been pointed out that tension in actin filament prevents cofilin from binding to the filament. Because cofilin binding put a twist on the helix of the actin filament that might be incompatible filament conformation caused by the tension, we suppose that structural change of actin filament is related to the mechanism on tension-induced inhibition of cofilin binding. In order to obtain better understanding the mechanism at molecular level, we need to investigate energetic and structural effects on binding domains of actin and cofilin caused by the conformational change of the filament.

To achieve the research mentioned above, in this study, we construct molecular dynamics (MD) model of cofilin-decorated actin (cofilactin) filament. First, we placed cofilins in the vicinity of their binding domains on actin along the filament based on the PDB data of actin-cofilin complex. Second, MD simulation for 20ns was conducted to obtain an equilibrium structure of cofilactin filament. Because this equilibrium structure has included thermally-induced various twist angles, a cofilin-bound actin trimer with a moderate angle has been extracted from the equilibrium structure as a sample of cofilactin complex. In this way, we succeeded to construct MD models of cofilactin complexes with distinct twist angles.

1PT134 ロボット機構の運動学に基づくタンパク質の内部運動解析

Internal Motion Analysis of Proteins based on Robot Kinematics

Keisuke Arikawa (*Fcl. Eng., Kanagawa Inst. of Tech.*)

From the perspective of robot kinematics, we investigated a method for predicting the internal motions of proteins using data from PDB. The protein model used in this method is simple; it comprises main chains and linear springs between the alpha carbons. The main chains are considered to be robot manipulators that control the positions of the alpha carbons or the distances between them, where the dihedral angles on the main chains correspond to the joint angles of robot manipulators. We apply forces in static equilibrium to the model and evaluate the deformation caused by them. The deformation magnitude differs depending on the direction of the force, despite the magnitude of applied forces being the same. It can be concluded that deformations of a large magnitude occur easily. Here, forces are applied in two different manners. One is the application of forces at the alpha carbons in the residues interacting with other molecules and the other is the application of forces at the centroids of the atomic groups (e. g., secondary structures, domains, and subunits). The formulation of basic equations for this method is similar to that for kinematic analysis of robot manipulators. We applied this method to data from PDB of some proteins (e.g., calmodulin, lactoferrin, and aspartate transcarbamoylase). Despite being a simple model, the results are almost consistent with the actual internal motions.

1PT135 コンピュータシミュレーションによる 4-helix bundle タンパク質を基にしたタンパク質分子間相互作用面の設計

Simulation study for designing protein-protein interaction interfaces based on a four-helix bundle protein

Masaki Fukuda[1], Yu Komatsu[2], Ryota Morikawa[1], Takeshi Miyakawa[1], Masako Takasu[1], Satoshi Akanuma[1], Akihiko Yamagishi[1] ([1]*Dept. of Mol. Biol., Tokyo Univ. of Pharm. Life Sci.*, [2]*Grad. Sch. of Pure Appl. Sci., Univ. of Tsukuba*)

Some proteins have the ability to self-assemble and form fibers. The purposes of our study are: i) designing binding interfaces on two proteins which specifically interact to each other; ii) inducing self-assembly through the intermolecular interaction between the two proteins; and iii) forming co-polymers. A four-helix bundle structure is chosen as a model for designing the binding interface. Using the four-helix bundle as the scaffold, we designed the binding interfaces on the target protein YciF involving charged and hydrophobic amino acid residues. To evaluate the designed binding interfaces, we performed molecular dynamics (MD) simulation of the variants of YciF proteins with the designed binding interface using GROMACS [1]. For the initial state, two protein molecules with the designed interface were placed with appropriate distance, and their binding interfaces faced each other. After 5ns simulation, we calculated the distance between centroid of binding interface of the molecules, and visualized the structures using Pymol[2]. The details will be presented at the conference.

[1] Berendsen, et al. Comput. Phys. Commun. 91 (1995) 43. [2] http://www.pymol.org

---

1PT136 透明で柔軟性を持った実用性の高いタンパク質分子模型

A Soft and Transparent Handleable Protein Model

Masaru Kawakami (*Sch. Mat. Sci.*)

The field of molecular and structural biology currently relies on computer-generated graphical representations of three-dimensional (3D) structures to conceptualize biomolecules. As the size and complexity of the molecular structure increases, model generation and peer discussions become more difficult. It is even more problematic when discussing protein-protein interactions wherein large surface area contact is considered. This report demonstrates the viability of a new handleable protein molecular model with a soft and transparent silicone body similar to the molecule's surface. A full-color printed main chain structure embedded in the silicone body enables users to simultaneously feel the molecular surface, view through the main chain structure, and manually simulate molecular docking. The interactive, hands-on

experience deepens the user's understanding of the complicated 3D protein structure and elucidates ligand binding and protein-protein interactions. This model would be an effective discussion tool for the classroom or laboratory that stimulates inspired learning in this study field.

1PT137　蛋白質熱安定性に及ぼす糖の影響

Effects of sugars on the thermal stability of proteins

Hiraku Oshima[1], Ken-ichi Amano[2], Masahiro Kinoshita[1] ([1]*Inst. Adv. Energy, Kyoto Univ.*, [2]*Dep. Chem., Kobe Univ.*)

It is experimentally known that the heat-denaturation temperature of a protein T_m is raised by the sugar addition. The magnitude of this effect stabilizing the protein depends on the sugar species [1]. In earlier work, we proposed a measure of the thermal stability of a protein, which is defined as the solvent-entropy gain at 298 K upon protein folding S normalized by the number of residues [2,3]. S was calculated using a hybrid of the angle-dependent integral equation theory combined with the mulipolar water model and the morphometric approach. Here we show that S can be calculated using the hard-sphere solvent whose number density and molecular diameter are set at those of water. We then investigate the effects of sugar addition on the thermal stability by considering water-sugar solution modeled as a binary mixture of hard spheres. The three-dimensional integral equation theory is employed. The thermal stability is determined by a complex interplay of the molecular size of the sugar D and the total packing fraction of the solution η. D is estimated from the volume per molecule in the sugar crystal, and η is calculated using the experimental data of the solution density. We find that the thermal stability is considerably enhanced by addition of sucrose. In the presentation, we will discuss the effects of addition of not only sugars other than sucrose but also osmolytes.

[1] J. F. Back, Biochemistry 18 (1979) 5191.
[2] K. Amano *et al.*, Chem. Phys. Lett. 474 (2009) 190.
[3] K. Oda *et al.*, J. Chem. Phys. 134 (2011) 025101.

1PT138　ヒトカルシトニンアミロイド線維形成阻害機構の解析

Amyloid fibril inhibition mechanism of human calcitonin

Naoharu Kouduki[1], Hironari Kamikubo[1], Tomoyasu Aizawa[2], Yoko Ogawa[3], Yoichi Yamazaki Yoichi Yamazaki[1], Mariko Yamaguchi[1], Mikio Kataoka[1] ([1]*Grad. Sch. Mat. Sci., NAIST*, [2]*Graduate School of Life Science, Hokkaido University*, [3]*Osaka University of Pharmaceutical Sciences*)

Human calcitonin (hCT) is a 32-residue peptide hormone. hCT is used as a medicine for osteoporosis, but it easily forms amyloid fibrils under physiological condition, which is a problem on medication. Salmon calcitonin (sCT) is known to inhibit amyloid formation of hCT. Combinational use of hCT and sCT is expected to improve the pharmacological activity. While the N-terminal region (9-19) of sCT takes an α-helix, the C-terminal half of the helix is disordered in hCT. Although an interaction between the disordered region and the C-terminal tail of hCT is proposed to play a role on the amyloid formation, the detailed mechanism of the inhibition of the amyloid formation by sCT has not been revealed. In this study, we investigated amyloid fibril formation of hCT in the presence of each of two chimera peptides, which are comprised of the 1-15residues of hCT and the 16-32residues of sCT and, the reverse combination. The former region (1-15) contains the stable α-helix and the latter the flexible region in hCT. Amyloid fibril formation was monitored by fluorescence intensity from Thioflavin T. While the fluorescence intensity raised about 30~40 hours after incubation of hCT alone, the amyloid fibril formation was inhibited in the presence of sCT, or each of the two chimera peptides, indicating that each of the N-terminal and the C-terminal regions of sCT possesses the inhibitory ability. From these results, we conclude that both the C-terminal region and the N-terminal stable α-helix are engaged in the inhibition of the amyloid formation.

1PT139　ダブル pH ジャンプによるアミロイド線維のほぼ可逆的な構造変化の解析

Analysis of Almost Reversible Conformational Change of Amyloid Fibrils by Double pH-jump

Keiichi Yamaguchi[1], Yuji O. Kamatari[2], Mayuko Fukuoka[1], Reiji Miyaji[3], Kazuo Kuwata[1] ([1]*Unit. Grad. Sch. of Drug Dis. and Med. Inf. Sci., Gifu Univ.*, [2]*Life Sci. Res. Center, Gifu Univ.*, [3]*Sup. and Dev. Center for Tech. Ed., Fac. of Eng., Gifu Univ.*)

To obtain insights into the mechanism of amyloid fibril conversion, pH-jump experiments were performed using a H2 peptide of mouse prion protein. Previously, we reported that H2 peptide formed ordered amyloid fibrils with an immensely large minimum at 207 nm on CD spectrum at pH 2.9 (named pH2.9 fibrils), but aggregate-like fibrils with a minimum at 220 nm were formed at pH 7.5 (named pH7.5 fibrils) near its isoelectric point. In this study, firstly single pH-jump from 2.9 to 7.5 was performed. As a result, the CD spectrum showed that the pH2.9 fibrils instantly changed to pH7.5-like fibrils with a minimum at 218 nm, but the ellipticities were certainly distinct between pH7.5-like and pH7.5 fibrils, implying that the conformation of pH2.9 fibrils partially remains even at pH 7.5. Moreover, the pH7.5-like fibrils almost returned to the pH2.9 fibrils by restoring the solution pH from 7.5 to 2.9. FT-IR spectra indicated that these conformational changes were caused by the disruption of highly ordered β -sheet and β-turn conformations, and the subsequent their reconstructions. In addition, kinetic conformational changes of the fibrils after the single and double pH-jumps were examined using ANS fluorescence stopped-flow. As a result, these conversions of the fibrils composed of a few phases were accomplished within several seconds. Thus, amyloid fibrils can be changed readily between the distinct conformations separated by a low energy barrier almost reversibly.

1PT140　金属結合によるヒトプリオンタンパク質のペプチド断片の構造変化

Conformation change in peptide fragments of human prion protein caused by metal binding

Kazuya Iwama[1], Takahito Imaki[1], Masahiro Yagi[2], Wakako Hiraoka[2] ([1]*Grad. Sch.Sci,Univ.Meiji*, [2]*Sch.Sci,Univ.Meiji*)

Prion diseases are transmissible spongiform encephalopathies (TSE) and lethal infectious diseases caused by misfolding of prion protein (PrP). Human prion protein (huPrP) binds metal ion at the residues 60-91 (His61, His69, His77, His85) and residues 90-126 (His96,His111) in N-terminal. Histidine residue are known as high-affinity sites to metal binding. Metal binding to PrP is considered as an important process for misfolding of PrP. This report aims to investigate conformation change in huPrP caused by metal binding. huPrP Peptide fragments conteining His96 and/or His111 were examined for binding metal such as Cu^{2+}, Ni^{2+} and Co^{2+}. p*K*a values were determined with electro titrimetric analysis (Metrohm, 848 titrino plus). Metal binding to peptide fragment was observed using visible absorption spectra (Hitachi, U-2800 Spectrophotometer) and Circular Dichroism (CD)(JASCO,J-820). Secondary structure of peptide fragment was observed using Far-UV CD. Addition of Cu^{2+} and Ni^{2+} to huPrP (93-102:GGTHSQWN) showed the shift of p*K*a value. Vis absorption and Vis CD indicated the characteristic spectra resulting from metal binding. It was derived from imidazole N bound to metal ion and from d-d transition of metal ion. Far-UV CD spectrum showed the conformational change of secondary structure induced by metal binding. We will also investigate metal binding to peptide fragments of huPrP containing His111 by using UV/Vis spectroscopy, CD and electron spin resonance (ESR) to further understand about metal binding to huPrP.

1PT141　ユビキチンの温度-圧力-自由エネルギー地形図

Temperature-pressure-free energy landscape of ubiquitin

Tsubasa Yamamoto[1], Minoru Kato[2] ([1]*Graduate school of Life Science, Ritsumeikan University*, [2]*Department of Pharmacy, Ritsumeikan University*)

To understand the change of packing and/or solvation of protein denaturation from quantitative point, volume change ΔV and isothermal compressibility change $\Delta\beta_T$, and thermal expansion coefficient change Δα are needed. These thermodynamic parameters at given temperature and pressure are determined from temperature(T)- pressure(p)- free energy change(ΔG) landscape,which is obtained fraom combined series of pressure/temperature variable denaturation experiments.

In this study, we explore the (T, p, ΔG) landscape of ubiquitin. FTIR spectra of ubiquitin was reversibly changed by temperature/pressure perturbation at pD 2.0 and pD 5. 5. To determined ΔG at given temperature and pressure, temperature/pressure transition curves were obtained from change in FTIR peak intensity at 1673 cm^{-1} which is assigned to native β-strand structure. Three-dimensional (T, p, ΔG) landscapes and thermodynamic parameters (ΔV, $\Delta\beta_T$, Δα, entropy change ΔS and heat capacity change ΔC_p,) at ambient temperature and pressure (298K, 0.1MPa) were obtained.

1PT142　X 線小角散乱によるフェリチンアセンブリ反応の追跡

Ferritin assembly kinetics followed by small-angle X-ray scattering

Daisuke Sato[1], Masayoshi Inoue[1], Ayumi Sunato[1], Yoshiteru Yamada[2], Hideaki Ohtomo[1], Seiichi Tukamoto[1], Kanako Nakagawa[1], Masamichi Ikeguchi[1] ([1]*Soka university*, [2]*JASRI/SPring-8*)

Non-heme ferritin (Ftn) from Escherichia coli forms a spherical shell-shape with 4/3/2 symmetry of 24 subunits. It stores Fe(III) as ferrihydrite mineral within the protein shell. Ftn dissociates into 12 dimers at acidic pH, and it is able to reassemble into the native 24-mer when pH is returned to a neutral one. The circular dichroism (CD) spectrum and small angle X-ray scattering (SAXS) have shown that the acid-dissociated Ftn dimer maintains native-like secondary and tertiary structures. To clarify the assembly mechanism of apo-Ftn the reassembly of acid-dissociated apo-Ftn dimers was initiated by stopped-flow mixing with appropriate buffers and monitored by synchrotron radiation at SPring-8 (Beamline 45XU) and a photon-counting two-dimensional detector PILATUS. The reassembly rate depended on pH; it was too rapid to measure at pH 6.4 and slowed down at higher pHs. At pH 8, we succeeded to observe an overall change from the initial scattering identical to that of acid-dissociated dimer to the final scattering identical to the native apo-Ftn. The process consisted of at least two kinetic phases. A native-like radius gyration was attained in the faster phase and the zero-angle scattering intensity increased in both the fast and slow phases. The rate of the fast phase depended on the protein concentration, suggesting that this phase corresponds to the assembly of dimers.

1PT143 GroEL-GroES 複合体形成の熱力学的解析
THERMODYNAMIC PARAMETERS ASSOCIATED WITH THE GroEL-GroES BINDING

Toshio Takenaka, Takashi Nakamura, Jin Chen, Kunihiro Kuwajima (*Okazaki Institute for Integrative Bioscoence*)

The tetradecameric chaperonin GroEL forms a complex with its co-chaperonin GroES and mediates the refolding of substrate proteins in the cell. Despite a large body of studies to elucidate the underlying mechanism of the chaperone-assisted refolding of substrate proteins, the thermodynamic parameters associate with the GroEL-GroES binding have not yet been determined. We therefore combined NMR spectroscopy and isothermal titration calorimetry (ITC) to quantitatively estimate the GroEL-GroES binding constant in solution. In 2-D HSQC NMR measurements, by monitoring amide hydrogen signal intensities of cross peaks in a mobile loop region of 15N labeled GroES as a function of concentration of single-ring of GroEL (SR1), we obtained the equilibrium binding constants between GroES and SR1 at different temperatures in 20 mM Tris-HCl , 100 mM KCl, 10 mM MgCl2, and 3 mM ADP (pH 7.5), and the values were compared with those obtained by ITC under the conditions.

1PT144 Local and Global Structural Analysis of Denatured Protein by CW and pulsed ESR

Jun Abe[1], Munehito Arai[2], Satoshi Takahashi[1], Seigo Yamauchi[1], Yasunori Ohba[1] ([1]*IMRAM*, [2]*Grad. Sch. Art and Sci, Univ. Tokyo*)

Details of structural information of unfolded proteins are limited despite the active investigations in the past. As a structural model, a random coil has been assumed. However, recent researches have revealed that denatured protein has residual structures similar to secondary structures: helices and β sheet[1]. In our study, we analyzed the structure of unfolded protein based on electron spin resonance (ESR) methods (CW-ESR and pulsed ESR) with the site-directed spin labeling. We introduced the spin labels to 22 and 55th residue to measure the distance between the helices H2 and H3 in the B domain of protein A (BDPA). ESR signals were measured for the unfolding state by adding guanidinium chloride (GdmCl) as denaturant in the folded and unfolded states. CW-ESR reveals that the rotational correlation time in the folded state (GdmCl 0 M) is faster than that in the unfolded state (GdmCl 5 M) for single labeled BDPA. This result indicates that the motion of main chain in denatured protein become faster. For doubly labeled BDPA, we found that the well-defined H2-H3 distance for the folded state. In contrast, a broad distribution of the H2-H3 distance is observed for unfolded BDPA. We will compare the obtained distance distribution with that obtained by numerical calculation which is based on assumption of the random coil behaviors. [1] Shortle, D. and Ackerman, M.S., Science, 293, 487-489 (2001)

1PT145 β_2ミクログロブリン部分ペプチドの運動性とアミロイド線維形成能との相関
Correlation of the dynamics of β_2-microglobulin fragments with their amyloidogenicity

Mahoshi Takeda[1], Kazumasa Sakurai[1], Takahisa Ikegami[1], Hironobu Naiki[2], Yuji Goto[1] ([1]*Inst. Protein Res., Osaka Univ.*, [2]*Med. Sci., Univ. Fukui.*)

The tendency of the amyloid fibril formation of a peptide depends on its sequence. Recently, several programs which can predict amyloidogenicity of a given sequence have been presented. Although these programs predict well the amyloidogenicity of individual sequence, they do not provide information about the dynamics of the corresponding peptide in solution. Thus, in our study, we investigated dynamics of various peptides and correlated them with their amyloidogenicity. We previously reported that β_2 -microglobulin (β2m) is digested by Achromobacter protease I into 9 fragments (denoted as K1-K9). Among them, K3 and K6 were found to form amyloid fibrils, consistent with the prediction by Aggrescan, one of the prediction algorithms for amylodiogenic sequences. We investigated the urea-concentration-dependent transverse relaxation rates (R_2) of K2, K3, K5, K6, K7 and K9. It was found that non-amyloidogenic peptides showed only slight increase in R_2 as the urea concentration increased, indicating expansion of the peptide chain with an enhanced solvation. K3 also showed the same dependency at high urea concentrations. However, at lower urea concentrations, it showed an abrupt increase in R_2 at the amyloidogenic portion of the sequence, indicating a formation of a hydrophobic cluster. From these results, we propose that an amyloidogenicity is related to the ability of hydrophobic cluster formation. The prediction algorithm is assumed to identify specifically such sequences.

1PT146 タウタンパク質の凝集の初期段階の解析
In vitro analysis of the early stage of aggregation of tau protein

Teikichi Ikura, Nobutoshi Ito (*Medical Research Institute, Tokyo Medical and Dental University*)

Tau protein is essential to assembly of microtubules, which mainly consist of two types of tubulins. Hyperphosphorylation of tau protein abolishes its ability to bind tubulin and promote microtubule assembly. When it is released from tubulin, phosphorylated tau protein aggregates into paired helical filaments, which are characterized as the neuropathological hallmarks of Alzheimer's disease. The mechanism of aggregation of tau protein is still unsolved, though great efforts have been made to elucidate it. The early stage of aggregation is especially poorly understood because of difficultly of its detection. Here we synthesized various peptides including microtubule binding domains, which showed high aggregation propensity, and then investigated their in-vitro aggregation under various conditions by fluorescence and dynamic light scattering measurements. As a result, the tau peptides quickly aggregated into the oligomeric forms even in the absence of inducers. Their critical concentration of unpolymerization was less than 1 micro-molar in the absence of inducers. Increase in the concentration accelerated the velocity of aggregation. Ionic strength and phosphorylation state also affected the velocity of aggregation. The mechanism of aggregation of tau protein at the early stage will be discussed on the basis of these results.

1PT147 MSES 法によるタンパク質間相互作用の解析
Multiscale enhanced sampling simulation of protein interaction

Kei Moritsugu[1], Tohru Terada[1,2], Akinori Kidera[1,3] ([1]*CSRP, RIKEN*, [2]*Grad. Sch. of Agri. and Life Sci., Univ. of Tokyo*, [3]*Grad. Sch. of Nanobiosci., Yokohama City Univ.*)

Protein interaction plays a fundamental role for biological processes such as transcription, signal transduction and immune response. Simulating protein association dynamics will be challenging beyond the conventional computational studies such as predicting protein complex structures and calculating free energy differences via residual mutations at the complex interface. Since protein complex formation involves atomistic interaction and desolvation process, in this study, we aim to achieve a conformational sampling of protein interaction on atomistic resolution and under physiological condition including explicit solvent using multiscale enhanced sampling (MSES) simulation.

The MSES simulation allows an enhanced sampling of the full-dimensional, all-atom model in explicit solvent, by coupling with the accelerated dynamics of the coarse-grained degrees of freedom. Here, this method has been applied to barnase-barster complex which has been studied in extensive experiments and computations. The sampling of the relative configuration of the two proteins has been enhanced via coupling to a Ca-atom coarse-grained model which moves freely around the complex structure. The interaction process at the interface has been characterized by formation of the hydrogen bonds and desolvation in atomic detail. The MSES has also been applied to the same system with a site-

directed mutation at the barster interface to demonstrate the role of the hydrogen bonds at the mutated residue during the complex formation.

1PT148 原子間力顕微鏡を用いたβ-カテニンの力学的挙動解析

Analysis of the mechanical behavior of β-catenin using AFM

Koichiro Maki[1,2], Sung-Woong Han[1], Taiji Adachi[1,2] ([1]*Department of Biomechanics, Institute for Frontier Medical Sciences, Kyoto University, Japan*, [2]*Department of Microengineering, Kyoto University, Japan*)

In cellular activities, mechanical stimuli are functionally converted into biochemical signals. This process called mechanotransduction has an essential role in cell-cell communication through mechanical interaction. Cells communicate with each other through mechanotransduction which is induced by adherens junctions (AJs)-mediated intercellular tension. According to recent studies, AJs adapting modulate its intensity to the intercellular tension to which the mechanical behaviors of its components contribute. However, the mechanical behaviors of the components such as β-catenin and α-catenin are unclear. In this study, we focused on β-catenin, which interestingly forms a superhelical structure, and analyzed its mechanical behaviors using atomic force microscope (AFM). AFM cantilever was modified using a NHS-PEG-Maleimide for the glutathione modification. The N-terminus GST-tagged β-catenin was then modified using a GST-glutathione affinity. The AFM-tip was approached and made contact to the NHS-ester modified substrate to allow outside amine of β-catenin and NHS-ester binding. Then we obtained force-extension curves for β-catenin and found a linear-elastic region in both loading and unloading processes under small tension less than 120 pN without any relaxation. Moreover, relaxation event was not observed under high tension more than 1000 pN, that is, β-catenin was not unfolded. These results indicate that β-catenin exhibits stiff mechanical behaviors and can be a molecule which stably transmits the intercellular tension.

1PT149 PPC, DSC のコンビネーション解析により明らかになったシトクロム c の新規多状態熱転移

A combination analysis of PPC and DSC revealed novel multi-state thermal transitions of cytochrome c

Shigeyoshi Nakamura, Shun-ichi Kidokoro (*Nagaoka University of Technology*)

Molten globule, MG, state is known as the equilibrium and/or kinetic intremediate state which has a key role on the stability and folding mechanizum of proteins. The thermal transition of the MG state of cytochrome c at extreme acidic pH and high salt condition showed the complicated transition rather than the simple two-state transition. We performed differential scanning calorimetry (DSC) and pressure perturbation calorimetry (PPC) analysis of thermal transition of the MG state at pH 2.5 with 500 mM KCl. By DSC measurements, the protein concentration dependence of the thermal transition was clearly observed in the range of 0. 25~18 mg/ml cytochrome c. The transition temperature of the MG state shifted to lower temperature by increasing cytochrome c concentration. In all cases, the thermal transition of the MG state showed full reversibility. It strongly suggests that the thermal transition of the MG state at pH 2.5 with 500mM KCl is the complicated transition including the reversible oligomerization process of the disordered molecules. By PPC measurements, the thermal expansion coefficient showed the complicated shape composed by the broad positive peak at lower temperature and a broad negative peak at higher temperature. It indicates that the positive and negative volume changes are occurred at lower and higher temperature in this transition. The results of the multi-state analysis with self-dissociation/association process will be discussed.

1PT150 蛍光共鳴エネルギー移動を用いたスタフィロコッカルヌクレアーゼのフォールディングにおける特異的凝縮過程の研究

Site-specific collapse of staphylococcal nuclease during the folding followed by Förster resonance energy transfer

Takuya Mizukami[1], Ming Xu[2], Heinrich Roder[2,3], Kosuke Maki[1] ([1]*Grad. Sch. Sci., Nagoya Univ.*, [2]*Fox Chase Cancer Center*, [3]*Dep. Biochem. Biophys., Univ. Penn.*)

Many proteins form compact intermediates in the early stages of folding. However, whether the condensation of the polypeptide chain is driven by non-specific hydrophobic interactions or by specific local interactions remains elusive. Staphylococcal nuclease consists of an N-terminal β-barrel and a C-terminal α-helical domains. Previous pulsed H/D exchange studies showed that some amide protons in the β-barrel domain are protected from exchange within 10 ms of the refolding. In addition, previous studies using a series of single tryptophan variants showed that a hydrophobic core comprising a large fraction of the β-barrel domain is formed in 100 μs time range.
In the present study, the collapses within the β-barrel domain and between the two domains were monitored by the time-dependent change in the apparent efficiency of Förster resonance energy transfer. Variants with single donor/acceptor pairs within the β-barrel domain showed an increase in the efficiency in 100 μs time range. In contrast, a variant with a single donor/acceptor pair in the α-helical/β-barrel domains, respectively, showed virtually no change in the efficiency in the submillisecond time range but an increase only after 100 ms time range. These results indicate that the collapse within the β-barrel domain occurs in 100 μs time range, while the α-helical domain is recruited to the rest of the molecule in the rate-limiting step of the folding. Thus the condensation is suggested occurring in the specific and cooperative manner.

1PT151 蛍光相関分光法を用いた網羅的 *in vivo* 酵母タンパク質動態解析

Global analysis of protein dynamics in living yeast cells using fluorescence correlation spectroscopy

Takafumi Fukuda[1], Chan-Gi Pack[2], Yasushi Sako[2], Shigeko Kawai-Noma[1], Hideki Taguchi[1] ([1]*Grad. Sch. of Biotech., Tokyo Tech*, [2]*RIKEN ASI*)

In the cell, the majority of proteins does not work alone, but interacts with other proteins or themselve, to maintain the cellular function, constituting a so-called “protein community” in the cell. Previous efforts on mass spectrometry-based protein interaction networks, interactomes, have provided a picture on the protein community. However, those were “static” information after cells were disrupted. For a better understanding of the protein community, it is important to obtain “dynamic” information in living cells, such as how proteins behave in the cell, how large they are, how fast they diffuse, what portions of proteins interact with others. Therefore, we have started a large-scale analysis on dynamic aspects of proteins in living cells using fluorescence correlation spectroscopy (FCS), which is a technique to investigate the diffusion properties of fluorescence molecules in cells. Using a budding yeast GFP clone collection, which is a *Saccharomyces cerevisiae* strain collection expressing GFP tagged open reading frames, we have evaluated i) diffusion constant, ii) the population of fast components and slow components, iii) abundance and iv) tendency for self-assembly, of ~200 kinds of yeast proteins in living yeast cells.

1PT152 マイクロ秒分解一分子 FRET 測定による蛋白質折り畳み運動の追跡

Microsecond-resolved traces of protein folding by single-molecule FRET measurements

Hiroyuki Oikawa[1], Yuta Suzuki[2], Kiyoto Kamagata[1], Munehito Arai[3], Satoshi Takahashi[1] ([1]*IMRAM, Tohoku Univ.*, [2]*Grad. Sch. Sci., Tohoku Univ.*, [3]*Grad. Sch. Arts. Sci., Univ. Tokyo*)

High-speed measurements of fluorescence signals from single molecules are expected to reveal the detailed information of protein folding. However, the time resolution of single-molecule measurements is usually limited to a few milliseconds. To improve the time resolution, we developed a line-confocal microscope with two-color detection system that was combined with the sample flow system. By using the developed device, we can trace a time evolution of fluorescence intensity and FRET efficiency from single molecules with the time resolution of 30 μs. We investigated the equilibrium unfolding transition of B domain of protein A (BdpA). The two cysteine residues were introduced into BdpA and labeled by a FRET pair of Alexa 633 and Alexa 488. The labeled sample shows a typical two-state unfolding upon the guanidium chloride (GdmCl) titration. The microsecond-resolved FRET efficiency time series from the single BdpA molecules revealed a significant conformational heterogeneity in the chemically unfolded state. The heterogeneity of the unfolded BdpA is substantiated by calculating the FRET efficiency histograms at the different GdmCl concentrations. The distribution obtained in the absence of denaturant consists of single peak for the native protein. In contrast, the distributions obtained in the presence of higher concentration of denaturants are broad. The data demonstrate the presence of multiple substates, which are separated by sizable energy barriers.

1PT153 エレメントを用いた人工酵素の設計と機能解析

Element-based molecular design can reproduce an artificial protein with an expected enzymatic activity

Hironari Kamikubo, Eri Sakai, Yoichi Yamazaki, Mariko Yamaguchi, Mikio Kataoka (*NAIST/MS*)

We have revealed that proteins are comprised of structure and function elements, and linkers connecting each of the elements [1]. We are proposing that the elements act as building blocks responsible for structure and function. Here, we are focusing on the concept of the function element as a building block realizing a function. Assuming that our hypothesis is correct, it can be expected that a complete set of the function elements alone reproduces its defining function. Using the function elements of staphylococcal nuclease (SNase) extracted before, we designed an artificial enzyme, in which the complete set of the function elements are connected with appropriate linkers extracted from the other protein, TSN domain of human p100, which structurally resemble the linkers of SNase. The resultant artificial enzyme showed the enzymatic activity for the hydrolysis reaction seen in SNase. The enzymatic reaction by SNase is known to require a Ca ion. The designed enzyme also clearly exhibited the Ca2+ requirement for its hydrolytic activity, indicating that the enzymatic mechanism of the designed enzyme remains to be that of SNase. The present results support our concept of the element as a building block, and also suggests the usefulness of function elements in designing functionally modified protein. [1] R. Shiba et al. "Systematic alanine insertion reveals the essential regions that encode structure formation and activity of dihydrofolate reductase" Biophysics 7, 1-10 (2011)

1PT154 水及び非水環境におけるタンパク質の立体構造安定性

Structural stability of a protein in aqueous and nonaqueous environments

Satoshi Yasuda[1], Hiraku Oshima[2], Masahiro Kinoshita[2] ([1]*Graduate School of Energy Science, Kyoto University*, [2]*Institute of Advanced Energy, Kyoto University*)

A protein folds into its native structure having the secondary structures such as α -helices and β-sheets in aqueous solution. The relative content of them largely differs from protein to protein. Such structural variability, however, is not always exhibited in nonaqueous environment. For example, it is known that alcohol induces proteins to form α-helices [1]. Many membrane proteins in the lipid bilayer possess only α -helices [2]. Here we investigate the structural stability of a protein in aqueous and nonaqueous environments using our free-energy function F and its energetic and entropic components, Λ and S. Λ is a measure of intramolecular hydrogen bonds. -S represents the efficiency of the backbone and side-chain packing brought by the entropic effect arising from the translational displacement of solvent molecules or nonpolar chains of lipid molecules. The α-helices and β-sheets are very advantageous with respect to Λ and -S [3]. In terms of Λ, the α-helices are even more stable. We find the following. In aqueous solution, the entropic effect is so strong that the β-sheets are often chosen especially for the close packing of side chains. In nonaqueous environment, by contrast, the entropic effect is considerably weaker and Λ becomes more imperative in the structural stability. As a consequence, there is a strong tendency that the α-helices are exclusively chosen. [1] M. Kinoshita et al., J. Am. Chem. Soc. 122 (2000) 2773. [2] J. U. Bowie, Nature 438 (2005) 581. [3] S. Yasuda et al., J. Chem. Phys. 132 (2010) 065105.

1PT155 抗プリオン化合物のプリオンタンパク質への結合特性による分類

Characterization of anti-prion compounds according to the binding properties to the prion protein

Yuji O. Kamatari[1], Yosuke Hayano[2], Keiichi Yamaguchi[2], Junji Hosokawa-Muto[2], Kazuo Kuwata[2] ([1]*Life Sci. Res. Center, Gifu Univ.*, [2]*Unit. Grad. Sch. Drug Dis. Med. Info. Sci., Gifu Univ.*)

To date, a variety of anti-prion compounds have been reported that are effective in ex vivo and also in vivo treatment experiments. However the molecular mechanisms of most of these compounds remain unknown. Here we classified anti-prion mechanisms into four categories; I: conformational stabilization, II: interference with the interaction between the cellular form of prion protein (PrPC) and the scrapie form (PrPSc), III: precipitation of prion proteins, and IV: interaction with proteins other than PrPC. To characterize the anti-prion compounds according to this classification, we determined their binding affinities to PrPC and their binding sites in PrPC using the surface plasmon resonance and NMR spectroscopy, respectively. GN8 and GJP49 bind specifically to the hot spot in PrPC, and act as 'medicinal chaperones' to stabilize the native conformation and interfere with the interaction between PrPC and PrPSc. Thus mechanism I & II are predominant. While quinacrine and epigallocathechin bind to PrPC rather non-specifically. They may mainly interfere with the intermolecular interaction, and mechanism II may be applied. On the other hand Congo red and pentosan polysulfate bind to PrPC and cause its precipitation reducing the effective concentration of prion protein. So, mechanism III is appropriate. The proposed characterization of diverse anti-prion compound would help understanding their anti-prion activities as well as facilitating further effective anti-prion drug discovery.

1PT156 糖タンパク質 A の変性温度、可逆性及び熱によって誘起される重合体の解析

Conformational stability, reversibility and heat-induced aggregation of glycoprotein A

Takafumi Iwura, **Fumio Arisaka** (*Graduate School of Bioscience and Biotechnology, Tokyo Institute of Technology*)

In order to elucidate the relationship of conformational stability, reversibility of heat-induced denaturation and aggregation of protein, the conformation, T_m and reversibility of denaturation of glycoprotein A were measured by circular dichroism (CD) and differential scanning micro-calorimetry (DSC) in aqueous solutions at a number of pH values. Under the same pH conditions, solutions of glycoprotein A were incubated at 37° C and analyzed by size exclusion chromatography (SEC), SDS-PAGE, fluorescence from di-tyrosine, CD, and SEC in the presence of 4,4'-dianilino-1,1'-binaphthyl-5,5'-disulfonic acid (Bis-ANS) to quantitate and characterize heat-induced aggregation of glycoprotein A. It was observed that the conformational stability of glycoprotein A was lowered at lower pH based on the lower T_m with endothermic ΔH, whereas the reversibility of the protein was decreased at higher pH. Glycoprotein A formed some fractions of large non-covalent aggregates during incubation at lower pH, whereas incubation at higher pH tended to cause formation of covalent dimers including disulfide bond and di-tyrosine without forming larger aggregates. These results indicated that lower conformational stability caused non-covalent aggregation, whereas the covalent aggregation resulted in lower reversibility. Thus the evaluation of both stability and reversibility is necessary to develop optimal formulations and to predict the kinds of aggregation which could be induced during storage.

1PT157 Structural properties and folding process of hNck2 SH3 domain

Yoshitaka Matsumura[1], Masaji Shinjo[1], Tsutomu Matsui[2], Kaoru Ichimura[1], Jianxing Song[3], Hiroshi Kihara[4] ([1]*Dept. Phys., Kansai Med. Univ.*, [2]*Bio-SAXS, SSRL*, [3]*Dept. Biochem., Yong Loo Lin School of Medicine, Dept. Biol. Sci., Facul. Sci., National Univ. Singapore*, [4]*SR center, Ritsumeikan Univ.*)

Liu and Song (1) reported that hNck2 SH3 domain takes equilibrium non-native alpha-helix intermediate at acidic pH, though the protein takes native beta structure at neutral pH. To elucidate the structure in more depth, we did CD and X-ray slolution scattering of this protein at various pH. First, we did concentration dependence of the protein at neutral pH by X-ray scattering, and found that this protein forms monomer at low concentration, but dimer at relatively higher concentration at pH 6. We also did pH titration of the protein at c. a. 1 and 3 mg/mL, monitored by CD and X-ray solution scattering, respectively. I(0) shows the protein takes monomer below pH 2, and dimer above pH 4. Kratky plots show that the shape of hNck2 SH3 domain at acidic pH is not so compact as molten globule state is. According to these findings, the protein seems to take like C-state. We have also done kinetic refolding experiments by cryo-stopped-flow monitored by CD. The results show that there were no burst phases even at low temperatures. We will discuss the relationship of kinetic intermediate onf the refolding process and equilibrium intermediate at acidic pH of hNck2 SH3 domain, and the relationship of the folding process of hNck2 SH3 and other SH3 domains at the poster. (1) Liu and Song (2008) Biophys. J. 95, 4803-4812

1PT158 天然変性蛋白質 p53 TAD による CBP TAZ2 への極めて速い結合反応

Extremely rapid binding of the intrinsically disordered p53 transactivation subdomain with the TAZ2 domain of CBP

Munehito Arai[1,2,3], Josephine C. Ferreon[2], Peter E. Wright[2] ([1]*Dept. Life Sci., Univ. Tokyo*, [2]*Dept. Mol. Biol., The Scripps Res. Inst.*, [3]*PRESTO, JST*)

The tumor suppressor activity of p53 is regulated by interactions with the general transcriptional coactivator, CREB-binding protein (CBP). We previously showed that the AD2 region of the intrinsically disordered N-terminal transactivation domain of p53 tightly interacts with the TAZ2 domain of CBP.

To study the detailed structure of the TAZ2:p53 AD2 complex, here we perform NMR HSQC titrations in which the unlabeled p53 AD2 peptide was added incrementally to ^{15}N-labeled TAZ2. The cross peaks in the spectrum of the TAZ2 domain shift in fast exchange and exhibit curvature, indicating the presence of two binding sites. Global fitting of the titration curves show that dissociation constants for primary and secondary binding are 32 nM and 10.2 μM, respectively. This small K_d in nM range is amazing, because the HSQC cross peaks show fast-exchange shifts, which indicate rapid dissociation. To estimate the association and dissociation rates, k_{on1} and k_{off1}, respectively, we perform global fitting of lineshapes of a series of titrations. We find a k_{on1} of 1.7×10^{10} M^{-1} s^{-1}, which is extremely fast but not beyond the diffusion-controlled limit. k_{off1} is estimated to be 540 s^{-1}, which is reasonably fast to show fast-exchange shifts. We suggest complementary electrostatics between AD2 (-8) and TAZ2 (+14) plays a major role in determining the very rapid binding kinetics of the AD2 motif. It is plausible that a large net charge causes both intrinsic disorder and rapid binding, suggesting that fast association is an intrinsic nature of IDPs.

1PT159 STABILITY OF FOLDING INTERMEDIATE AFFECTS THE AMYLOIDOGENIC PROPENSITY OF IMMUNOGLOBULIN LIGHT CHAIN VARIABLE DOMAIN

Yuta Kobayashi[1], Yuki Tashiro[2], Kyohei Ikeda[2], Tetsuyuki Abe[2], Daizo Hamada[1] ([1]*Grad. Sch. Med., Univ. Kobe*, [2]*Sch. Med., Univ. Kobe*)

Immunoglobulins (Ig) consist of a set of heavy (HCs) and light chains (LCs), and both chains contain variable and constant domains belonging to Ig fold. Intrinsic sequence variation in the variable domains provides Ig the variation in molecular recognitions for these anti-pathogenic agents. However, this also provides a risk to generate the aggregation-prone Ig domains to cause diseases such as AL amyloidosis.

Here we analysed folding and unfolding kinetics of isolated variable domains (V_L) from amyloidogenic BRE and nonamyloidogenic REI *k*LCs which were originally isolated from patients of AL amyloidosis and multiple myeloma, respectively. Although these proteins share 85% of sequence identity, the native state of BRE V_L is significantly decreased due to the increased unfolding and the decreased refolding rates compared to REI V_L, suggesting the destabilisation of the native state play important role in amyloid formation by BRE V_L. A close analysis on the folding/unfolding rates, thermal stability of the native states and aggregation propensity of several chimeric mutants between REI and BRE V_L suggested that the stability of folding intermediates is one of the most important factors to determine the aggregation propensity of V_L, and the stability of unfolded state ralative to the native state may be less relevent.

1PT160 Recognition of a TAR nucleic acid by HIV-1 Tat, an intrinsically disordered protein

Kohei Sodeyama[1], Yuuki Hayashi[1], Takashi Nakamura[2], Koki Makabe[2], Kunihiro Kuwajima[2], Munehito Arai[1] ([1]*Dept. Life Sci., Univ. Tokyo*, [2]*Okazaki Inst. Integr. Biosci.*)

Previously, native protein has been considered to have one rigid tertiary structure and exerts its function associated with its structure. Therefore, proteins which have no defined structures have been considered less important. Recently, however, it has been discovered that intrinsically disordered proteins (IDPs) are functional and structured when they recognize their target molecules. Human immunodeficiency virus (HIV-1) transcriptional activator Tat is known as an IDP, and binds to the trans-activating responsive element (TAR) of HIV-1 RNA. Because Tat-TAR interaction is essential for virus gene expression and replication, Tat has been a target for anti-HIV drug development. However, the mechanism of TAR recognition by Tat remains elusive. To address this problem, we study the Tat-TAR binding reaction by thermodynamic, spectroscopic, and kinetic approaches. As a model protein, Tat(37-72)C37W including the TAR recognition site is used. Fluorescence titration and isothermal titration calorimetry measurements reveal the dissociation constant at 4 nM. The association and dissociation rate are measured by stopped-flow fluorescence experiments. We also measure the Tat-TAR binding by NMR titration. Detailed results will be presented in the poster.

1PT161 NRSF/REST の競合誘起天然変性による mSin3 の構造安定性制御
Control of Structure Stability of mSin3 by Frustration-Induced Intrinsic Disorder of NRST/REST

Katsuyoshi Matsushita[1,2], Macoto Kikuchi[1,3,4] ([1]*Cybermedia Center, Osaka University*, [2]*Institute for Protein Research, Osaka University*, [3]*Graduate School of Science, Osaka University*, [4]*Graduate School of Frontier Biosciences, Osaka University*)

Protein intrinsic disorder has various biological roles [1]. In particular, hydrophobic intrinsic disorder region (HIDR) exhibits a peculiar coupled binding and folding with a target protein. Much effort has been devoted to the investigation of HIDR in the last decade. However, understanding of biological roles of HIDR seems not to be sufficient. In order to gain deep insight into the roles, we have theoretically investigated NRSF/REST (neuron-restrictive silencer factor / RE1-Silencing Transcription factor) [2]. Recently, on the basis of calculation results of a model of NRSF/REST binding mSin3, we suggested the possibility that intrinsic disorder of HIDR is induced by structural frustration [3]. In the present work, we further investigated the stabilization of mSin3 in the binding. Evaluating change in structural order parameter of mSin3 with increasing chemical potential of the binding, we showed that the structure of mSin3 is sharply stabilized at a specific value of the chemical potential. In contrast, the stabilization of the structure of mSin3 is comparatively gradual in the case without the frustration, namely without the intrinsic disorder. From this result, we concluded that the frustration-induced intrinsic disorder enhances response sensitivity of mSin3 to concentration change of NRSF/REST. [1] P. E. Wright and R. J. Dyson J. Mol. Bio. 293 (1999) 321. [2] M. Nomura et al., J. Mol. Bio. 354 (2005) 903; J. Higo et al., J. Am. Chem. Soc. 133 (2011) 10448. [3] Seibutsu Butsuri Supplement 1 51 (2011) S133.

1PT162 リゾチームの乾燥誘導凝集に対する G3LEA タンパク質及びモデルペプチドの抑制効果
Measurement of the association constant of a G3LEA protein or its model peptide with lysozyme in aqueous solution

Kentaro Yamakawa[1], Takao Furuki[1], Rie Hatanaka[2], Hiroyuki Furusawa[3], Takahiro Kikawada[2], Yoshio Okahata[3], Alan Tunnacliffe[4], Minoru Sakurai[1] ([1]*Center for Biological Resources and Informatics, Tokyo Inst. Tech.*, [2]*National Institute of Agrobiological Sciences*, [3]*Department of Biomolecular Engineering, Graduate School of Tokyo Inst. Tech.*, [4]*University of Cambridge, Department of Chemical Engineering and Biotechnology*)

Group3 Late Embryogenesis Abundant (G3LEA) proteins are responsible for the occurrence of desiccation tolerance in many anhydrobiotic organisms, but the functional mechanism remains unclear. The major part of the primary amino acid sequence of a G3LEA protein is composed of several times repeats of characteristic 11-mer motif. In our previous studies (T. Shimizu, et al., Biochemistry 49 (2010) 1093, T. Furuki, et al., Biochemistry 50 (2011) 7093), we synthesized several kinds of 22-mer peptides (LEA peptides), each of which has two tandem repeats of the 11-mer motif, and studied their structural and thermodynamic properties in detail. Recently, we have investigated to what extent these peptides reduce aggregation of proteins (e.g. lysozyme) during dehydration and compared the result with that from the similar experiment using a native LEA protein (*A. Avenae* G3LEA protein, AavLEA1) (T. Furuki, et al., BBA 1824 (2012) 891). As a result, it was found that the LEA peptide reduced the aggregation of lysozyme during dehydration, whereas AavLEA1 promoted the aggregation. In this study, we tried to measure the association constant (K_a) between AavLEA1 and lysozyme using the Quartz Crystal Microbalance (QCM) method. The interaction between lysozyme and AavLEA1 was moderately strong with the Ka value of 3.2×10^6 M^{-1}. In the case of the lysozyme-LEA peptide system, a change of the QCM frequency was observed but the K_a value was too small to be quantified. These results were interpreted from the pI value differences between the proteins studied.

1PT163 表面力測定によるシグナル伝達タンパク質間相互作用の研究
Interactions between signal transduction proteins studied by surface force measurement

Hitomi Fujiwara[1], Taizo Umemura[1], Masaya Fujita[2], Kazue Kurihara[1,3] ([1]*Institute of Multidisciplinary Research for Advanced Materials (IMRAM) Tohoku*, [2]*University of Houston*, [3]*World Premier International-Advanced Institute for Materials Research*)

Spoluation in Bacillus subtilis is controlled by phosphorelay signal transduction. KinA and Spo0F are involved in this sporulation initiation process. In the first step of this series of phosphorylation reactions, KinA binds ATP and autophosphorylates at a histidine residue. The phosphoryl moiety on KinA is then transferred to a single-domain response regulator Spo0F. We have studied interactions between these signal transduction proteins (KinA and Spo0F) using

colloidal probe atomic force microscopy (AFM). KinA and Spo0F were immobilized on a glass substrate and a glass sphere using Langmuir Blodget films of a chelate amphiphile. The conditions of adsorbing proteins were determined using quartz crystal microbalance and AFM. Surface force profiles for KinA and Spo0F showed only repulsive force in the buffer solution with/without ATP. Adding cofactor Mg2+ and Ca2+ to buffer solution with ATP, attractive forces and adhesive forces were observed on approach and in retraction process. These forces were not observed without ATP . These results demonstrated the specific interaction between KinA and Spo0F only in the presence of a substrate ATP and cofactor divalent ions.

1PT164 GroEL 円順列変異体 CP86 のストップトフロー機能解析

Functional and Stopped-flow analysis of circularly permutated GroEL mutant CP86

Toshifumi Mizuta[1], Tatsuya Uemura[2], Takuma Hirayama[1], Kunihiro Hongo[1,2], Yasushi Kawata[1,2], Tomohiro Mizobata[1,2] ([1]*Dept. of Chem. and Biotech., Grad. Sch. of Eng., Tottori Univ*, [2]*Dept. of Biomed. Sci., Grad. Sch., Tottori Univ*)

Escherichia coli GroEL is a member of the chaperonins, a well-conserved protein folding assistant necessary for cell growth. The GroEL subunit consists of three different functional domains. The apical domain contains GroES and substrate protein binding sites, the equatorial domain contains the ATPase binding site which controls the overall functional cycle, and these domains are linked by the intermediate domain.
We have used random circular permutation to study the structural and functional characteristics of the GroEL subunit. In a previous study, we constructed a circularly permuted mutant of GroEL (GroEL CP86) that relocated the N terminus and C terminus from its original position to a new site in the vicinity of the ATPase binding site. This mutant was characterized by a ~50% decrease in its basal ATPase activity and, interestingly, a change in specificity toward substrate proteins in refolding assays.
To probe the effects of this circular permutation in more detail, we introduced a fluorescent tryptophan residue to monitor the dynamic movements of the CP86 apical domain (GroEL CP86 R231W). Stopped-flow fluorescence experiments that probed movements of the apical domain showed that almost all of the large domain movements that were detected in the wild-type protein were lost in the mutant. In spite of this, CP86 was able to assist the folding of MDH efficiently. Functional assays provided details regarding a possible functional mechanism for this mutant.

1PT165 Design of functional miniature peptides acting like the lipase

Yoshihiro Iida, Atsuo Tamura (*kobe university*)

Obesity has become a huge problem in modern life. It is a condition that the lipid droplet enlarges in cell. To avoid obesity, we should hydrolyze triglyceride (neutral lipid) in lipocyte. As a candidate for an anti-obesity drug, we tried to design peptides having enzyme activity like the lipase to expose and hydrolyze triglyceride. As a strategy for the design, we make the peptide to have the catalytic triad composed of histidine, asparagine acid and serine. When the molecule forms the dimer, the two serine residues coming from each molecule hold the triglyceride together. We make use of alpha-helical peptides that form coiled-coil when dimerized. Based on the strategy, we synthesized peptides me1-4. CD (Circular Dichroism) measurements show that the conformations of me2, me3, and me4 are alpha helical coiled-coil. DLS (Dynamic Light Scattering) measurements indicate that the particle sizes of designed peptides are around 4nm, suggesting that they are dimers. The calcein leakage experiment showed that me3 and me4 hydrolyzed the membrane. The hydrolysis of p-nitrophenyl acetate (pNPA) showed that me4 had been conferred esterase activity. Based on these result, we conclude that the designed peptide can be regarded as a lipase mimic which is capable of hydrolyzing the lipid droplets.

1PT166 異なるリガンドと結合した DHFR の構造転移のカメレオンモデルによる比較

Comparison of the conformational transitions of DHFR bound to the different ligands using the chameleon model

Toru Kimura[1], Masaki Sasai[2], Tomoki P. Terada[2] ([1]*Dept. of Applied Physics, Grad. Sch. of Engineering, Nagoya Univ.*, [2]*Dept. of Computational Science and Engineering, Grad. Sch. of Engineering, Nagoya Univ.*)

A well-characterized protein, dihydrofolate reductase (DHFR), has the enzymatic reaction rates that are correlated with the conformational changes of the protein (Boehr et al., Science 313, 1638 (2006)). Its reaction cycle consists of five chemical steps, which can be described as the conformational switches between roughly two structures, the occluded and closed structures. Among those five steps, we here focus the two steps connecting the similar pair of protein structures in the opposite directions. Since different ligands are bound to DHFR in these two reactions, the difference in the two reaction rates should be intrinsically related to the difference in the ligand-protein interactions. To calculate the free energy landscape with the different ligands, we have extended the chameleon model to include the ligand-protein interactions, so that the interactions between ligand and protein is dependent on their local environments, as is the case of intraprotein interactions. Here, using this extended model, we examine the conformational transitions of DHFR in both directions. From the calculated free energy landscapes, we discuss the transition state structure and changes in thermodynamic parameters accompanying these two conformational transitions. Furthermore, we will examine the mutational effect on the chemical reaction rate of DHFR, which is experimentally measured recently (Bhabha et al., Science 332, 236 (2011)).

1PT167 DHFR のフォールディング過程の多次元自由エネルギー曲面

Multidimensional free energy landscape of folding of DHFR

Takashi Inanami, Tomoki Terada, Masaki Sasai (*Dept. of Comp. Sci. Eng., Univ. of Nagoya*)

Free energy landscape is a useful theoretical tool to analyze pathways and intermediates of protein folding. Multiple folding pathways or multiple intermediates, however, are overlapped with each other to become indisting-uishable in the one-dimensional landscape drawn with a single order parameter. In this study, in order to analyze the distributions of multiple intermediates, we construct the two- and three-dimensional landscapes by using multiple order parameters of folding. As an example, we calculate the multidimensional free energy landscape of folding of dihydrofolate reductase (DHFR) and discuss the folding intermediate recently observed by M. Arai et al. (J Mol Biol (2011) 410: 329-342). For this simulation, we develop the extended Wako-Saito-Munoz-Eaton model which correctly describes the tendency that regions near the N- and C- termini have the ordered structures to some extent at the early phase of folding.

1PT168 Effect of flexibility and electrostatic interaction on rapid binding and unbinding of an intrinsically disordered protein

Koji Umezawa[1], Kohei Nishimura[1], Junichi Higo[2], Haruki Nakamura[2], Mitsunori Takano[1] ([1]*Grad. Scl. of Adv. Sci. & Eng., Waseda Univ.*, [2]*IPR, Osaka Univ.*)

It is now well known that there are a large number of proteins that are disordered under a physiological condition. The intrinsically disordered proteins (IDPs), which are generally highly charged, are thus more flexible than ordered proteins (OPs). One of the interesting features of IDP is as the so-called “coupled folding and binding”, which implies that IDP may adopt different bound conformations depending on its partner proteins, leading to the “hub” property of IDP. The coupled folding and binding of IDP also implies the chain-entropy loss upon binding is greater than OP. Furthermore, IDP can capture distant partners via its extended conformation and long-range electrostatic interaction. To examine these potential capabilities of IDP, in this study, we focused on the effect of flexibility and electrostatic interaction upon binding of KID, a well-studied IDP, to its binding partner KIX, by using a combination of coarse-grained model and an enhanced sampling technique. The potential of mean force (PMF) showed that increased flexibility destabilizes the final complex but stabilizes the encounter complex, which is suitable for rapid binding and unbinding. The electrostatic interaction also contributed to the stability of the encounter complex. In addition, we address the possible role of the phosphorylation of KID (pKID), which has stronger binding affinity for KIX, in terms of the competition of the intra- and intermolecular electrostatic interactions.

1PT169 Calculation of local dielectric constants of proteins using dipole-dipole correlations

Asahi Konno, Jun Narita, Kentaro Fukunaga, Koji Umezawa, Mitsunori Takano (*Grad. Scl. of Adv. Sci. & Eng., Waseda Univ.*)

In a classical dielectric model of the protein systems, the dielectric constants are usually assumed to be homogeneous inside and outside the protein, respectively. However, it is obvious that this assumption is the zero-th order approximation of

reality. The dielectric constant is expected to vary depending on the local electrostatic environments and the structural constraints imposed on the system. In this study, we calculated the local dielectric environments of protein-water systems by employing the theoretical framework proposed by Guest et al. (PCCP, 2011) where the dipole-dipole correlations are properly taken into account. We used long molecular dynamics simulation trajectories of the three systems (solvated myosin, solvated actin, and F_o in the solvated lipid bilayer systems) to evaluate the dipole-dipole correlations. From the local dielectric constant map, we found that the regions around the flexible loops tend to exhibit a large dielectric constant. The regions with a large dielectric constant are supposed to respond well to the approaching charges of the binding partner and stabilize the electrostatic self-energy of the charges. Similarly, we will discuss the ion translocation path in F_o portion of ATP synthase in terms of the local dielectric constant map. We also point out a technical problem that calculated dielectric constants sometimes become too large or even negative, and discuss a possible solution to this problem.

1PT170 シグナル伝達に関与する PDZ ドメインの分子動力学データに対する時系列解析

The time series analysis of molecular dynamics data about PDZ domain in synapse

Naoko Kishida[1], Hiroshi Fujisaki[2], Mikito Toda[3] ([1]*Graduate School of Humanities and Science, Nara Women's University*, [2]*Nippon Medical School*, [3]*Faculty of Science Nara ,Women's University*)

The functions of a protein are supposed to have relation to its structures. We study the relationship between its functions and movement from data of molecular dynamics(MD) simulation. We analyse the protein called the PDZ domain. For human being,we can find them in a synapse of the nervous system. In particular, these proteins exist mainly in postsynaptic cells as domains of recepters. They play an important role in signaling in the nervous systems[1]. We chose one of the PDZ, and its PDB code is 1BE9. It is the third domain of PSD-95, where PSD-95 is a recepter which is in the center of the postsynaptic cell. For the signaling,the clustering of domain is essential, and is caused by interaction with other proteins. Here, we pay our attention to the mechanism of signaling. It is shown that it has a path within the domain and signals are transduced along this path[2]. We study its motion with wavelet transform and canonical correlation analysis. First, by wavelet transform,we can find the time-dependent spectra and find which parts of the secondary structure move with large amplitude. Second, in order to find whether we can see the flow of thermal energy along this path at room temperature, we compare the correlations between amino acids by canonical correlations analysis.

[1]E.Kim and M.Sheng.2004.Nature review neurosience,5,771-781
[2]N.Ota and D.A.Agard.2005.J.Mol.Bio.351,345-354
[3]A.Dyle,et al.1996.Cell,85,1067-1076

1PT171 粗視化シミュレーションによる 3 ドメインタンパク質 suf1 のコ・トランスレーショナルフォールディングの研究

Co-translation folding of a three-domain protein surf1 studied by coarse-grained molecular simulations

Tomohiro Tanaka, Naoto Hori, Syoji Takada (*Dept. of Biophys., Kyoto Univ.*)

Proteins are synthesized linearly from N-terminus in ribosome and gradually extruded from it. The native interactions of extruded polypeptide chain may be initiated before the protein synthesis is completed. Protein folding which proceeds during the synthesis is termed co-translational folding. Because total conformation space of a polypeptide chain under translation is smaller than that of the full-length polypeptide chain of the protein, co-translational folding could be facilitated kinetically. In addition, the rate of translation is not uniform, but is affected by tRNAs abundance. Recently, it was found that the correct folding of suf1, a three-domain protein, is maintained by the particular use of rare codons. When the rare condos were replaced with codons by synonymous mutations, successful folding yield substantially decreased. However, the detailed mechanism of this phenomenon is unclear. To understand the mechanism, we developed a coarse-grained (CG) model and simulated suf1 co-translational folding as well as post-translational folding as a control. The CG model is a mixture of Go like atomic interaction based CG (AICG) model and generic hydrophobic interactions which makes correct folding and misfolding possible. Via comprehensive simulations, we address the difference between co- and post- translational folding.

1PT172 粗視化シュミレーションによるサテライトタバコモザイクウィルスの安定性とダイナミクス

Stability and dynamics of satellite tobacco mosaic viruses studied by coarse-grained simulations

Koji Ono, Naoto Hori, Shoji Takada (*Dept of Biophys, Kyoto Univ*)

Satellite tobacco mosaic virus (STMV) is one of the smallest (about 170 angstrom diameter) and icosahedral virus (T = 1). The virus consists of 60 copies of single proteins to make a icosahedral capsid and a 1058-base RNA genome. The existence and importance of the viral genome for its stability have been acknowledged. Recently, STMV was analyzed by an all-atom MD simulation. The research indicated that their RNA is important to stable their capsid structure. All-atom simulation is, however, limited of the system size and the time scale. To overcome them, we used coarse-grained simulation (CafeMol developed by Our lab) to simulate STMV virus for longer time that all-atom MD could do. In this simulation, each amino acid is represented as a CG bead and interactions are modeled with structure-based potential. We first carried out simulation of STMV without their RNA in various environments to investigate the STMV particle stability and dynamics. For example at low ion strength or high temperature, how the virus is deformed has been studied. We discuss importance of the RNA genome for the stability of this virus.

1PT173 エピレギュリンー抗体の分子動力学シミュレーション

Molecular dynamics simulation of epiregulin and its antibody

Keiko Shinoda, Hideaki Fujitani (*Laboratory for Systems Biology and Medicine, Research Center for Advanced Science and Technology,University of Tokyo*)

We present a molecular dynamics study of protein target for cancer, epiregulin and its antibody. Epiregulin is a member of the epidermal growth factor family and stimulates EGFR-driven cancer cell growth such as pancreatic cancer. To investigate the structural stability and thermodynamic property of the epiregulin-antibody complex, we have performed 1-μs molecular dynamics simulations and free energy calculations. In this meeting, we discuss the results of the simulations and compare with experimental results.

1PT174 Molecular Dynamics Simulation of Protein Using Robot Dynamics Algorithm

Yu Yamamori[1,2], Kazuhiro Takemura[1], Akio Kitao[1,2] ([1]*Institute of Molecular and Cellular Biosciences The University of Tokyo*, [2]*Department of computational biology Graduate school of frontier science, University of Tokyo*)

In the simulation study of biophysical phenomena, the gap between the time scale of the simulation and that of the target process is a major bottleneck of Cartesian Molecular Dynamics (CMD). High frequency motions in proteins prohibit CMD from enlarging the simulation time step beyond 1.0-2.0 fs. To overcome this limitation, we adopted a strategy to consider the torsion angles as the only degrees of freedom (DOF) which enables us to employ a method developed originally in robotics, namely Articulated-Body Algorithm (ABA), which can solve the equations of motion of internal coordinates with the small computational cost that linearly depends on the number of DOF. The program of Molecular Dynamics in Torsion Angle space (TAMD) is equipped with an extended version of ABA, so-called Freed-end ABA developed by the authors. The program can treat the AMBER and ECEPP force field and with NVE and NVT ensembles. To evaluate our program, we compared the spectra of 20 distinct dipeptides calculated by TAMD to the results of the normal mode analysis in torsion angle space. From good agreements in this comparison, we confirmed that the program can give reasonable results. We also searched the maximum time step length to give reasonable energy conservation based on the simulations of three proteins, villin head piece subdomain, BPTI and ubiquitin. We concluded that time step 4.0 fs can be employed with the original force field, and 6.0 fs can be employed if we scale the torsion energy terms of the terminal chemical groups.

1PT175 4 量体型サルコシン酸化酵素の酵素-基質複合体の分子動力学的解析

Analysis of enzyme-substrate complex of heterotetrameric sarcosine oxidase by molecular dynamic simulation

Akinori Hiroshima, Haruo Suzuki, Shigetaka Yoneda (*Grad. Sch. Sci., Kitasato Univ.*)

Heterotetramic sarcosine oxidase [SO, EC 1.5.3.1] catalyses the oxidative demethylation of sarcosine to generate glycine, hydrogen peroxide, and formaldehyde or 5,10-methylene-tetrahydrofolate, depending on the availability of tetrahydrofolate. SO was first purified from *Corynebacterium* sp. U-96 [SO-U96], and then from various sources. SO-U96 comprises four non-identical subunits (α, 110 kDa; β, 44 kDa; γ, 21 kDa; δ, 10 kDa) and one FAD, one FMN, and one NAD^+. The 3D structure of the SO-U96-complex with dimethylglycine [DMG] has been determined from X-ray crystallography. The structural and biochemical analyses gave new insight into the cavity, conformational change, and channeling of oxygen, sarcosine, and products through the cavity. The authors performed the free energy perturbation molecular dynamics simulations in which the bound DMG was mutated by the coupling parameter approach into sarcosine, and analysed the simulated enzyme-substrate complex from the structural and energetic viewpoints. The mobility of substrate was also analyzed to examine the possibility of realistic simulations of channeling of substrate and products. The GROMACS program, the GROMOS 53a6 energy parameters, and the SPC water parameters, and the particle mesh Ewald method were used. The numbers of the atoms were from 130 000 to 160 000, depending on the number of the water molecules included in the simulations.

1PT176 アデニル酸キナーゼ反応機構に関する ONIOM 法による研究

Study on the reaction mechanism of adenylate kinase with ONIOM method

Kenshu Kamiya (*Department of Physics, School of Science, Kitasato university*)

Adenylate kinase catalyzes the reaction: ATP + AMP + Mg2+ -> ADP + ADP + Mg2+ . In order to elucidate the nature of the reaction, we have been studying the theoretical model using MM/QM. We constructed the complex structure of enzyme and substrates, ATP and AMP with Mg ion, based on the PDB data of complex with inhibitor. After the full optimization of the whole molecule in vacuo with MM, we put TIP3P water molecules arround catalytic center Mg ion with spherical boudary condition, and harmonic constraint potentials on the surrounding atoms in the boudary region. Some model structures were sampled from 900 K MD simulation followed by structural nergy minimizations. In order to obtain the resonable initial model of the transition state, we performed the molecular mutation calculation from the reactant to the product. Further truncated models were used for the calculations with ONIOM method, the reactant, product, transition structures were optimized. In these calculations, small barrier (several kcal/mol) shown in the low level model (19/834 atoms in QM/MM, HF/6-31G(d):AMBER) vanishes with higher level, and the present highest model (89/764 atoms in QM/MM, B3LYP/6-31+G(d):AMBER, embed model) gives the reaction barrier of 19 kcal/mol, and 10 kcal/mol exothermicity. For further discussion, however, more qualitative consideration as well as free energies on the conformational effects of the surrounding atoms is necessary.

1PT177 酵素の多機能性に関する解析

Analysis of enzyme promiscuity

Chioko Nagao, Kenji Mizuguchi (*NIBIO*)

For a long time, enzymes are believed to catalyze specific reactions with specific substrates. Specificity is essential for enzymes to work in the crowded environment of a cell. However, recent experimental studies have shown that many enzymes can catalyze more than one reaction or have broad substrates (i. e., enzyme promiscuity). It is becoming recognized that enzyme promiscuity is related to functional evolution, drug metabolism and protein engineering [1]. Although molecular mechanisms of promiscuity of each enzyme have been investigated, there have only been a few attempts to define the general properties that characterize promiscuous enzymes, and no comprehensive analysis using reaction constants have been made [2]. Moreover, a good measure for describing promiscuity has not been established.

In order to elucidate how widespread the substrates and reactions are that an enzyme can bind and catalyze, we performed a systematic analysis of the enzyme data in the BRENDA database [3]. The enzymes 1) for which UniProt ids were obtained from BRENDA or through PubMed ids and NCBI Entrez links, and 2) which have Michaellis constants or turnover numbers for at least ten different substrates were selected for the analysis. At the fourth level of Enzyme Commission Number and within an orthologous enzyme group, the relationships among sequence identities, reaction constants and substrate similarities are discussed.

1. Nat Biotechnol 2009;27:157. 2. Biochemistry 2008;47:157. Bioinformatics 2010;26:2012. 3. Nucleic Acids Res 2009;37:D588.

1PT178 Folding of topologically complex proteins by an atomic interaction based coarse grained model

Wenfei Li[1,2,3], Tsuyoshi Terakawa[2], Wei Wang[1], Shoji Takada[2,3] ([1]*National Laboratory of Solid State Microstructure and Department of Physics, Nanjing University*, [2]*Graduate School of Science, Kyoto University*, [3]*CREST, Japan Science and Technology Agency*)

While fast folding of small proteins has been relatively well characterized by experiments and theories, much less is known for slow folding of larger proteins. Recent progress of experimental works on the folding of large proteins revealed a number of new features arising from the topological complexity, which poses new challenges to the current protein folding theories. Reasonably describing the folding of such topologically complex proteins needs more sophisticated theoretical models. In this presentation, we introduce a new model, i. e., AICG model, developed within the framework of the energy landscape theory. The features of this new model include: i) contact interactions are delicately weighted according to the atomic interactions via a multiscale protocol; ii) a realistically flexible energy function is used for the local interactions. We applied this model to a number of topologically complex proteins, including multi-domain proteins and knotted proteins, and it reproduced all the major features of folding revealed experimentally. Our results suggest that the structure-based model can capture the essential features of the folding of proteins with complex topologies after delicately weighting the contact interactions, and including realistic local flexibilities.

1PT179 多様な分子コンホメーションを取り得る溶質の小角 X 線散乱プロフィルの近似計算法

A new approximation method for estimating SAXS profiles of solutes with multiple molecular conformations

Yasutaka Seki[1], Shigeyoshi Nakamura[2], Shun-ichi Kidokoro[2], Takamasa Nonaka[1], Kunitsugu Soda[3] ([1]*Sch. of Pharm., Iwate Med. Univ.*, [2]*Dept. of Bioeng., Nagaoka Univ. of Technol.*, [3]*High Perform. Molec. Simula. Team, ASI, RIKEN*)

Small-angle X-ray scattering (SAXS) has long been used as an important means for determining global-structure parameters of biopolymers in solution. It can be applied not only to natively globular proteins with a practically single global structure but also to natively unfolded proteins with many available conformations such as intrinsically disordered proteins (IDP). In the latter case, however, we need to evaluate a large number of SAXS profiles for averaging them, because the IDP consists of an ensemble with diverse conformations. The program CRYSOL (Svergun, D. et al., *J Appl. Cryst.*, 1995) has been commonly used to calculate SAXS profiles of IDPs. We found that the calculated profiles contain a non-negligible amount of error caused by the approximation taken in estimating the contribution of protein hydration-layer. Though it is possible in principle to use the method combined with MD simulation (Seki, Y. et al., *Biophys. Chem.*, 2002) for removing the error, the computational cost would go impractically high for IDPs. We present here a new approximation method for estimating SAXS profiles applicable to solutes with multiple molecular conformations. Though the accuracy of this method is lower than that of the MD-combined method in the large-K region, it gives sufficient accuracy in small-K region with low computational cost. In the meeting, we will report on the detail of approximation and its applicable range of scattering angle.

1PT180 極低温電子顕微鏡による 26S プロテアソームの単粒子解析

Single particle analysis of 26S proteasome by cryo-electron microscopy

Kaoru Mitsuoka[1], Daisuke Kasuya[2], Yasushi Saeki[3], Takuo Yasunaga[4] ([1]*BIRC, AIST*, [2]*BIRC, JBIC*, [3]*Tokyo Metropolitan Institute of Medical Science*, [4]*KITEC*)

The eukaryotic 26S proteasome functions to degrade a large fraction of intracellular proteins. The 26S proteasome is composed of at least 33 different subunits in 20S core particle (CP) and one or two 19S regulatory particles (RPs). Proteins destined for degradation are marked by poly-ubiquitin, a degradation signal that is recognized by the RPs. The proteolytic sites are sequestered inside the CP and are accessible only thorough a narrow channel. Thus the RP deconjugates ubiquitin chains, unfolds substrate proteins, and translocates them into the catalytic CP. The CP was amenable to structure determination by X-ray crystallography but the 26S holocomplex with 1 or 2 RPs has so far resisted all crystallization attempts. Here we optimized the single particle analysis methods by cryo-electron crystallography for the structural analysis of the 26S proteasome.

In the EM preparation, the RPs tend to dissociate from the holoenzyme and so we applied chemical fixation in density gradient centrifugation (GraFix) to the complex. For the optimal contrast of the images, we used energy-filter to estimate the thickness of the ice layer. For the easier pickup of the particles, we used the defocus pairs. By these improvements, now we can collect suitable images for the single particle analysis, which can deduce the three-dimensional architecture of macro-molecules without crystallization. We would like to discuss the structural implications by the single particle analysis, too.

1PT181 Free energy decomposition and functional sites of proteins

Mami Saito, Shoji Takada (*Grad.Sch.Sci.,Kyito Uni.*)

Prediction of functional sites of proteins has long been studied, but still has room to improve. A major way of predicting functional sites of proteins relies on sequence and/or structure alignments. When a target protein has a novel function or motif or under 30% homology, however, alignment-based methods do not work well. For overcoming this problem, someone have paid attention to free energy analysis because it should mirrors sequence and structure. In particular, it was reported that free energy of residues in functional sites tends to be higher than that in non-functional sites. Here, based on these observation, we extend free energy analysis of functional sites using some standard molecular mechanics force field. We choose MMPBSA.PY script in AMBER11, which automates post-processing of MD trajectories, to analyze energetics using continuum solvent models. It can be used to break energies into "pieces" arising from different residues. It can also calculate contribution of energy component (electrostatic energy or so). Using them, we survey free energy of residues in functional sites and non-functional sites for an ensemble of enzyme set.

1PT182 時間分解蛍光偏光法によるタンパク質周囲の水和層の局所粘性測定

Measurement of the local viscosity of the hydration shell around protein by time-resolved fluorescence anisotropy spectroscopy

Tetsuichi Wazawa, George Mogami, Nobuyuki Morimoto, Noriyoshi Ishida, Makoto Suzuki (*Dept of Material Processing, Grad Sch of Engin, Tohoku Univ*)

Hydration water is vital for the function, dynamics, and conformation of protein, and analysis of how the hydration states of protein change during the molecular processes would give better understandings of the molecular mechanisms. In this study, we have investigated time-resolved fluorescence anisotropy of a fluorophore tethered to a protein in order to apply the technique to the analysis of hydration states of protein.

Cy3, a fluorophore, was tethered to Cys-374 of actin, as a model protein, through a flexible linker so that the dye underwent rotational Brownian motion in the hydration shell. The rotational motion was anticipated to be subject to the local viscosity of the hydration shell. A time-correlated single photon counting method was used to measure the time-resolved fluorescence anisotropy of Cy3 tethered to actin.

The fluorescence anisotropy of Cy3 tethered to G-actin was investigated at room temperature. The anisotropy decay was decomposed into two components, which showed the time constants of >40 ns and ~200 ps with anisotropy amplitudes of 0.29 and ~0.04, respectively. The slow component reflects the tumbling motion of G-actin molecules. The fast decay component would be attributed to the rotational Brownian motion of Cy3. Now, the response of the fast decay component to solvent viscosity is being investigated to establish the technique to detect changes in the hydration state of protein.

1PT183 Highly accurate statistical pickup method for single particle 3D analysis using electron microscope

Masaaki Kawata[1], Chikara Sato[2] ([1]*ITRI, AIST*, [2]*BRI, AIST*)

Single particle analysis is an information technology-based structure determination method of biological macromolecules. Among data processing in the three-dimensional (3D) reconstruction, particle pickup from micrographs is of critical importance for the final resolution. Quality of the image library also seriously affects the processing time using the following sub-algorithms, i.e., classification, alignment and 3D reconstruction. We found a new approach based on classification of local similarity (LC method), and compares its performance with other various pickup methods. We further developed an extension of the LC method using statistical particle recognition techniques to increase reliability of particle recognition. The recognition- and computation-efficiency of this method was superior to those of other methods; the modified LC method was especially robust against noise and independent of parameter settings. We demonstrate the performance both with synthetic micrographs and cryo-micrographs. The new method is a key for fully automated cropping of high quality particle images from micrographs, and a step for a fully automated single particle reconstruction algorism.

1PT184 中程度傾斜撮影した電子顕微鏡画像からの単粒子 3 次元再構築

Single Particle Reconstruction with Medium Tilt Images by Electron Microscopy

Yutaka Ueno, Emiko Kobayashi, Shouhei Mine, Kazunori Kawasaki (*AIST Kansai*)

In three dimensional reconstruction of single particle molecules taking tilted pairs of the same specimen in different angles greatly contributes reliability of the reconstruction of the volume data from projection images. While the random conical tilt method has been widely employed for a specimen with the same face up, a more general method for randomly oriented particles was studied. We have introduced medium tilt by plus-minus 20 degrees that comprises 40 degrees tilted pairs. The method relays on the fact: the images in the same orientation are found in both tilted images and they are grouped into unified clusters in terms of viewing directions. Once a major group of images of the particle in a certain viewing angles exist in images from different tilt angles, these tilted pair gives additional tilted view of the particle beyond the major tilt observation. They contribute to cover wider projection angles minimizing loss of projection information known as the missing cone situation. The method was first examined by simulated reconstruction with a theoretical model phantom. As with the case with traditional tilting observation data collection requires adjusting the viewing scope to locate the same as another tilted pair. Introducing recent electron microscope with CCD camera and the tilting stage controller greatly facilitated data collection. Possible automation for this tedious task will be discussed together with our preliminary results with our single particle analysis of deacetylase from Archaea.

1PT185 拘束付き分子動力学法を適用した、電子顕微鏡法のための原子モデル構築ツールの開発

Development of atomic modelling tool for Electron Microscopy, applying steered Molecular Dynamics method

Risa Yamashita, Ryota Nakao, Hiroshi Sakamoto, Takuo Yasunaga (*Kyushu Institute of Technology*)

In most of studies of proteins using electron microscopy (EM), it is difficult to discuss detail at the atomic level because three-dimensional electron microscopic maps (3D-EM maps) are mostly low or medium resolution and the typical resolution of the 3D-EM map of proteins is about 1 to 4nm. Thus we have developed an atomic modelling tool based on a 3D-EM map under an image processing package of Eos , which we called SRMD and planed atomic models constructed even from the typical resolutions of EM maps. The SRMD method is one of the extensions of steered molecular dynamics (MD) simulation techniques, in which EM maps are used as a potential for MD and constrain each atoms within a target protein. This SRMD method tool did not have GUI yet: When we use SRMD method tool, we need to use an editor to set temperatures for simulated annealing and conditions of constraints from EM-maps. Furthermore, we cannot watch atomic models during modelling in real time. To construct an atomic model precisely, there are two planning points. One is embedding of SRMD into a model viewer with GUI to monitor models and change modeling conditions easily during calculation. The other is to change molecular conditions by a pointing device like IMD. Thus, it will be possible to make atoms stacked unnaturally by 3D-EM map potentials rescued. Here, we will report our progress of the SRMD techniques and examples for a complex map of heme oxygenase and cytochrome P450 redutase, which is reconstructed from EM images.

1PT186 Comparative survey of image processing packages for electron computed tomography

Nan Shen, Mingyue Jin, Takuo Yasunaga (*Dep. Biosci. Bioinf., Inst. Tech. Kyushu*)

Electron computed tomography (ECT) is one of the most widely applicable methods for obtaining the three-dimensional (3D) reconstruction of organelles or cell components. First, tilt series of two-dimensional (2D) projection images of the specimen are recorded in electron microscope, and then 3D structure is computed from the tilt series using some softwares. A common problem

encountered in this ECT is alignment accuracy of tilted projection images. Here, three ET software packages (IMOD, Inspect3D and TEMography) are well known and applied to tilt series alignment in different ways. In our previous work, we have acquired tilt series from axonemes by cryo-transmission electron microscopy (cryo-TEM), and reconstructed the 3D structure using IMOD, Inspect3D and Eos we have developed, mainly. IMOD can automatically determine tilt axis by using fiducial marker, while Inspect3D needs to manually determine tilt axis but gave us more precise alignment than that of IMOD, judging from obtained 3D. Thus we decided to compare them systematically, i. e., our present purpose is to evaluate the quality of 3D reconstruction and the usability of these software packages, show the pros and cons of them systematically and then make our developed Eos more convenient with higher analysis ability. We acquired tilt series of model structure (phantom data) and axonemes by cryo-TEM, and computed the 3D structure using IMOD, Inspect3D, TEMography and Eos from each of them, respectively. Comparison between them will here be reported and discussed.

1PT187 Gibbs energies of secondary structures for α-Chymotrypsinogen A investigated by FT-IR spectroscopy

Koichi Murayama (*Grad. Sch. Med., Gifu Univ.*)

FT-IR spectra were measured over a temperature range of 25-90 degree, to investigate difference in Gibbs energies of secondary structures for α-Chymotrypsinogen A (a-ctg). The curve fitting method combined with Fourier self-deconvolution technique allowed us to explore details of the secondary structure. The spectra of a-ctg in the amide I' region reveal eight bands for anti-parallel β-sheet, turn, α-helix, β-sheet, intermolecular β-sheet and side chain vibration below 70 degree. Additional band for disordered appears over 70 degree in the spectra. Then, Gibbs energies for secondary structures and their transition temperatures (T_m) were calculated. The T_m for the four bands due to the α-helix, turn and disordered structures are found to be around 60 degree. Corresponding values for anti-parallel β-sheet and side chain are higher by about 67 degree, and those for β-sheet, inter-molecular β-sheet structures were around 63-64 degree. The Gibbs energies were obtained about 11-16 $kJmol^{-1}$ for α-helix, β-sheet and turn. The value for intermolecular β-sheets was much higher than others, suggesting that intermolecular β-sheets formation need more energy than other secondary structures. In this study, I will discuss Gibbs energy and T_m values for secondary structures of a-ctg obtained from FT-IR spectroscopy in details.

1PT188 TIP3P モデルおよび Generalized Born モデルを併用した分子動力学計算によるタンパク質の構造サンプリング

Improvement of sampling efficiency through combined use of molecular dynamics simulations with implicit and explicit solvent models

Hiroko Kondo[1,2], Noriaki Okimoto[2], Makoto Taiji[1,2] ([1]*Department of Computational Biology, the University of Tokyo*, [2]*Laboratory for Computational Molecular Design, Quantitative Biology Center (QBiC), RIKEN*)

Various experimental and computational studies have indicated that the protein conformation and its function are closely linked. Investigating their dynamical properties is consequently important to understand their functional properties. The molecular dynamics (MD) simulation is powerful tool for these analyses because we can observe the kinetics of protein at the atomic revel. It is however that the time scale of the simulation is not enough for examining the significant event including protein folding, domain movement, and so on. Therefore the enhanced sampling methods to overcome this computational limitation are so important.

In this study we aim at the improvement of sampling efficiency, reduction in actual simulation time by combining the results from implicit solvent simulations and those of explicit one; the former is used for reducing the sampling space and the latter for correcting the conformational distribution sampled by the former simulation. The replica exchange method was adopted for rough conformational sampling with implicit solvent followed by the explicit solvent simulation. Here, we performed conformational sampling of a mini protein, chignolin to examine the efficiency of our method. The results show that our new method covered a wider region of conformational space as compared with the conventional MD simulation with the explicit solvation model.

1PT189 生体分子の分子動力学に対する時系列解析ー集団運動の揺らぎと構造変化の関係を探るー

Time-series analysis of molecular dynamics: Conformational change and dynamics of collective behavior

Kana Fuji[1], Masakazu Sekijima[2], Hiroshi Fujisaki[3], Mikito Toda[4] ([1]*Graduate of school Humanities and Sciences, Nara Women's Univ.*, [2]*GSIC, Tokyo Tech*, [3]*Phys., Nippon Medical School*, [4]*Sci. , Nara Women's Univ.*)

Our study aims to analyze time series data of molecular dynamics simulation for proteins to extract collective behavior involving side chains and water molecules. Our methodology consists of the following two steps: (1) conformational analysis (dihedral principal conponent analysis) (2) dynamical analysis (the wavelet transformation and singular value decomposition(SVD)). The wavelet transformation enables us to investigate time-varying features of oscillatory motions, and SVD extracts collective variables involving multiple amino residues[1].

Our system is chignolin. In our previous work, we analyzed time series data using implicit solvent method for dynamics simulation. Here, we study data using explicit solvent method and will conpare these two cases.

In particular, we aim to extract collective behavior involving not only the main chain but also the side chain. By analyzing relationship of collective behavior between the main chain and the side chains, we can understand to what extent collective behavior involving the main chain provides us with information concerning collective behavior with the side chains. Furthermore, we expect that the study of collective behavior involving the side chain will give us an important clue to understand molecular functions for other proteins.

[1]M.Kamada,et. al,Chem.Phys.Lett.502(2011)241-7.

1PT190 イオンモビリティ質量分析と分子動力学シミュレーションを用いた気相中におけるヒストン多量体の構造解析

Characterization of histone multimers in the gas phase by ion mobility mass spectrometry and molecular dynamics simulation

Kazumi Saikusa[1], Sotaro Fuchigami[1], Kyohei Takahashi[1], Yuuki Asano[1], Aritaka Nagadoi[1], Hiroaki Tachiwana[2], Hitoshi Kurumizaka[2], Mitsunori Ikeguchi[1], Yoshifumi Nishimura[1], Satoko Akashi[1] ([1]*Yokohama City Univ.*, [2]*Waseda Univ.*)

Nucleosome core particle (NCP) is the basic structural unit of eukaryotic chromatins. In order to understand the mechanism of the NCP assembly and disassembly, structural characterization of the histone multimers, H2A/H2B dimer and H3/H4 tetramer, should be of great help. However, these atomic-level structures have not been determined. In the present study, human histone multimers were prepared and characterized by electrospray ionization ion mobility mass spectrometry (ESI-IM-MS) and molecular dynamics (MD) simulation. Experimentally obtained arrival times of these histone multimer ions showed rather wide distributions, which suggested that histone multimers had various conformations. To probe the conformers' structures, several MD simulations of the histone multimers were carried out in solution and in vacuo, and it was identified that the histone multimers had a variety of structure. In addition, the simulation showed that the conformers with smaller CCS values had more compact tail regions than those with larger CCS values. On the other hand, the CCS values of the folded core structure were almost kept identical in the analyzed conformers. This implies that the disordered regions brought about the structural variety of histone multimers. This paper presents that the combination of IM-MS and MD simulation enables comprehensive characterization of the gas-phase structures of biomolecular complexes containing disordered regions.

1PT191 カーネル正準相関分析と離散ウェーブレット変換を用いたタンパク質立体構造の時系列解析

Time-series analysis for protein dynamics using discrete wavelet transform with kernel canonical correlation analysis

Mayumi Kamada[1], Mikito Toda[2], Tatsuya Akutsu[1] ([1]*Inst. Chem. Res., Kyoto University*, [2]*Phys. Dept., Nara Womens Univ.*)

Structural dynamics of proteins play an important role in expression of protein functions. In particular, slow collective motions of proteins make a large contribution to performing its functions. To understand a correlation between protein functions and structural dynamics, we need a method to extract slow collective motions from structural dynamics without losing important information, and correctly characterize them. For this purpose, we use the discrete wavelet transformation (DWT) for the time-series data of protein structures obtained from molecular dynamics (MD) simulation. DWT is one of time-frequency analysis methods used for denoising and data composition, and

opens a door to extract compact datasets keeping the features of both time and frequency. In other words, it enables us to perform trend analysis of time-series data for protein structural dynamics. In this work, we apply DWT to trajectory data obtained by all-atoms MD simulation of Myoglobin[1,2], and analyze them concerning a ligand pathway problem of Myoglobin. For a correlation analysis of structural motions involving ligand pathway, we apply, to the data transformed by DWT, the kernel canonical correlation analysis (kCCA), which is useful to analyze an association between two variables even when they have non-linear association. We discuss the result of correlation analysis and usefulness of our strategy.

[1] Scorciapino MA et al., J Am Chem Soc. 131(33):11825-32 (2009)
[2] Scorciapino MA et al., J Am Chem Soc. 132(14):5156-63 (2010).

1PT192 生体分子における原子レベルでのストレステンソル解析
Atomic stress tensor analysis in biomolecules

Takakazu Ishikura, Tatsurou Hatano, Takahisa Yamato (*Grad. Sch. Sci., Nagoya Univ.*)

In 1985, Frauenfelder and co-workers proposed the “protein quake” concept to illustrate the molecular function of myoglobin, which experiences an allosteric conformational change triggered by the dissociation of CO from heme iron. Although the concept is intuitively appealing, only a limited number of theoretical studies have addressed the protein-quake-model [1].
One of the possible ways to characterize the model is to introduce atomic stress tensors. However, any of the conventional methods considered only two-body interatomic potential terms for stress tensors, which is not convenient because the force field functions for molecular dynamics simulation contain multi-body potentials such as angle, torsion and improper terms. To address the issue, we derived complete pair-wise expression for interatomic forces in biomolecules. Then we have developed a computer program, CURP, for the atomic stress tensor analysis of molecules and performed test calculations for small polypeptides [2]. As a result, we calculated the contribution to the stress from each component, and found out that the contribution from multi-body potential terms was larger than non-valence potential terms. This means that the analysis of atomic stress tensor must be performed with all of potential terms. In this presentation, we will introduce the results obtained by stress tensor analysis method for some systems.

[1] K. Koike, K. Kawaguchi, and T. Yamato, Phys. Chem. Chem. Phys. 10, 1400 (2008).
[2] T. Ishikura, T. Hatano, T. Yamato, Chem. Phys. Lett. (in press)

1PT201 細胞環境における蛋白質の構造安定性とダイナミクス
1YS1100 Protein stability and dynamics under cellular environments

Ryuhei Harada[1], Yuji Sugita[1,2,3], Michael Feig[3,4] ([1]*RIKEN AICS*, [2]*RIKEN ASI*, [3]*RIKEN QBiC*, [4]*Michgan state university*)

The effect of crowding on the stability and dynamics of protein was examined from explicit solvent molecular dynamics simulations of a series of protein G and protein G/villin systems at different protein concentrations.
In these simulations, the native state was found to be significantly destabilized under crowded environments. Especially, for the villin systems, where induced extensive unfolding to extended structures. This finding is entirely contrary to what is predicted from excluded volume effects but can be explained again through stabilizing interactions with other proteins. These simulations are the clearest evidence so far that enthalpic interactions due to protein-protein interaction can in fact overcome the entropic cost of extension under crowded environments.
Hydration structure was further analyzed through radial distribution functions, three-dimensional hydration sites and preservation of tetrahedral coordination. Analysis of hydration dynamics focused on self-diffusion rates and dielectric constants as a function of crowding. The results show significant changes in both structure and dynamics of water under crowded environments. The structure of water is altered mostly beyond the first solvation shell. Diffusion rates and dielectric constants are significantly reduced following linear trends as a function of crowding reflecting highly constrained water. The reduced dynamics of diffusion is expected to be strongly related to hydrodynamic properties of crowded cellular environments.

1PT202 マクロファージ細胞株における LPS 活性化時の遺伝子発現の細胞間ゆらぎに細胞間相互作用が与える影響
Effects of the cell-cell communication on the populational variability of mRNA levels among clonal macrophages after LPS stimulation

Mai Yamagishi[1], Yoshitaka Shirasaki[1], Nanako Shimura[1,2], Nobutake Suzuki[1], Osamu Ohara[1,3] ([1]*RCAI, RIKEN*, [2]*Grad. Sch. Med. Pharm., Chiba Univ.*, [3]*KAZUSA DNA Res. Inst.*)

Macrophages are activated by lipopolysaccharide (LPS) to start expressing various kinds of cytokines/chemokines. In the previous studies, single cell analyses using the AmpliGrid system and the BioMark system revealed that a population distributions of mRNA level varied quite widely from gene to gene and changed in a gene-specific manner; some genes were activated after LPS stimulation with a narrow populational distribution, but some with a broad one. To understand the mechanism to produce such a wide populational variation in mRNA levels in spite of the genetic homogeneity of a clonal macrophage-like cell line, RAW264.7. We here examine whether or not cell-cell communication has some impacts on this cell-to-cell variation. In the first experiment, we examined the dependence of cell density on the populational variations of cytokine mRNA profiles. The results indicated that only CXCL10 gene showed a decrease in the standard deviation of populational distribution of mRNA levels with increase of the cell density while the other responding genes seemed little affected. Because the cell density employed was not so high that cell-cell contact plays a major role in cell-cell interaction, it is very likely that the cell density effect is exerted by humoral factor(s). Analysis and characterization of the humoral factor(s) will be presented.

1PT203 小腸絨毛下線維芽細胞における各種刺激による ATP 放出
ATP-releases with various stimuli in subepithelial fibroblasts in intestinal villi

Kishio Furuya[1], Sonoko Furuya[2], Masahiro Sokabe[3] ([1]*FIRST Research Center for Innovative Nanobiodevice, Nagoya Univ*, [2]*National Institute for Physiological Science*, [3]*Dept. Physiol., Grad. Sch. Med., Nagoya Univ*)

Subepithelial fibroblasts of the intestinal villi, which form a contractile network under the epithelium, are in close contact with epithelial cells, neurons, capillaries, smooth muscles and immune cells. Developing a primary culture of these cells, we revealed unique characteristics such as: cAMP-dependent cell-shape changes between flat and stellate, cell-shape dependent mechano-sensitivity with ATP release as a paracrine mediator, and expression of various receptors for endothelins (ETs) (ETA, ETB), ATP (P2Y1), substance-P (SP) (NK1), etc. From these features, we proposed that subepithelial fibroblasts work as a mechano-sensor and signal transduction machinery in the intestinal villi. Here, we show that, in addition to the mechanical stimulation, receptor stimulations by ET1 and SP, and hypo-osmotic stimulation induce ATP-release from the subepithelial fibroblasts, using a real time ATP-imaging system. ATP is released sparsely from a limited number of stimulated cells and the ability of ATP-release is cell shape dependent. Peak concentration of released ATP reaches to 1-10 microM, being enough to propagate the Ca2+ waves to neighbor cells or whole colonies. Differences of the effects of various blockers for ATP-release and difference of the ATP-releasing kinetics suggest the existence of several mechanisms of ATP-release in subepithelial fibroblasts. These mechanisms may concomitantly regulate villous functions such as villous movement, nutrient absorption and intestinal maturation.

1PT204 An optimal heterogeneity in a cell population maximizes the effects of growth factors directing stochastic PC12 cell fate decisions

Kazunari Mouri, Yasushi Sako (*Adv. Sci. Inst., Riken*)

Recently, the heterogeneity arising from the stochastic fate decisions of clonal cells in the same environmental conditions has been reported for several cell types. Here we focused on the stochasticity in PC12 cell fate decisions. PC12 is a cell line derived from rat pheochromocytoma, and is a model system of the differentiation of sympathetic neurons. In general, PC12 cells are stimulated proliferation in the presence of a growth factor EGF, while extension of neuritis to differentiate into neuron-like phenotype in the presence of another growth factor NGF. In our work, however, we found that cells spontaneously induced cell fates without any external induction stimuli, which resulted in heterogeneity in a population. Serum contained in the culture medium suppresses spontaneous differentiation and cell death. Stochasticity in cell fate decisions affected by the spontaneity makes it difficult to predict the responses of cells to external stimuli of growth factors. In our experiments, for example, EGF (NGF) stimulus stochastically went so far as to induce differentiation (proliferation) depending

on the environmental serum concentrations. Careful quantification of the response rates for growth factors suggested that under an appropriate environmental condition to bring optimal heterogeneity caused by the stochasticity of cell fate decisions, the effects of the growth factors become maximum, i.e., suppressing cell death, NGF directs PC12 cell fates efficiently to differentiation and EGF directs to proliferation.

1PT205 蛍光相関分光法を用いた単一細胞内グルココルチコイド受容体のホモダイマー形成の解析

Quantification of Glucocorticoid Receptor of homo-dimer in single cell by using Fluorescence Correlation Spectroscopy

Sho Oasa[1], Akira Sasaki[1], Shintaro Mikuni[1,2], Masataka Kinjo[1] ([1]*Grad. Life Sci., Hokkaido Univ.*, [2]*Grad. Med. Department of Advanced Optical Imaging Reasarch., Hokkaido Univ.*)

The dimerization of GR (Glucocorticoid Receptor) in single cell is analysed. It is known that GR is dimerized by adding Dex (Dexamethasone) in living cell. However, when and where the dimerization of GR is occurred is still controversial. Moreover, many previous studies of GR processing have been carried out by using trangent-expressed cell. When the heterogeneous amounts of target protein is estimated in each cell such as trangent-expressed cell, the single-cell measurement might be better than conventional biochemical methods and required for better understanding of GR activity. In our laboratory, to assess protein contents in single cell, the small cavity (MicroWell) on the PDMS (polydimethylsiloxane) chip was constructed [1, 2]. Single cell was easily isolated in MicroWell and target protein was extracted and kept into the MicroWell. FCS (Fluorescence Correlation Spectroscopy) was performed to obtain number and concentration of target protein in MicroWell and protein complex information from CPM (count per molecule). EGFP-GR dimerized by adding Dex is analysed by using CPM and the ratio between monomeric and dimeric EGFP-GR is estimated with different concentraton of EGFP-GR in trangent-expressed cell.

[1] Sasaki, A, Kinjo, M, Curr Pharm Biotechnol., 2010, 11, 117-121
[2] Oasa, S, Sasaki, A, Kinjo, M, Biophysic Society meething, 2011

1PT206 マスト細胞と後根神経節初代培養細胞の相互作用における接着分子の研究

Cell adhesion molecule 1 (CADM1) on mast cells promotes interaction with dorsal root ganglion neurites by heterophilic binding to nectin-3

Tadahide, Furuno[1], Miho, Sekimura[2], Keisuke, Okamoto[2], Man, Hagiyama[3], Akihiko, Ito[3], Ryo, Suzuki[2], Naohide, Hirashima[2], Mamoru, Nakanishi[1] ([1]*Sch. Pharm., Aichi Gakuin Univ.*, [2]*Grad. Sch. Pharm. Sci., Nagoya City Univ.*, [3]*Fac. Med., Kinki Univ.*)

Functional interaction between mast cells and sensory nerves has been shown to occur in various physiological and pathological situations. We previously showed that an immunoglobulin superfamily adhesion molecule, cell adhesion molecule 1 (CADM1), on both mast cells and sympathetic superior cervical ganglia (SCG) promoted their attachment and communication via the homophilic binding using in vitro coculture approach. Here we have studied the role of CADM1 in the interaction between sensory dorsal root ganglia (DRG) and mast cells. Though CADM1 was hardly expressed in DRG, CADM1 on bone marrow-derived mast cells (BMMCs) accumulated in contact region with DRG neurites. CADM1-deficient IC-2 mast cell line was defective in attachment to DRG, while it was recovered in CADM1-transfected IC-2 cells (IC-2^{CADM1} cells) to the similar level to BMMCs. Searching adhesion molecules known as heterophilic binding partner of CADM1, DRG expressed nectin-3 but not Necl-1, Necl-5, and class-I-restricted T-cell-associated molecule. CADM1 on mast cells and nectin-3 on DRG neurites were colocalized in their attached region in coculture. The efficiency in calcium response of attached IC-2CADM1 cells after specific activation of DRG was significantly higher than that of IC-2 cells and was as similar as BMMCs. A neutralizing antibody to nectin-3 inhibited both mast cell attachment and subsequent calcium responses. This suggests that heterophilic binding between CADM1 and nectin-3 mediates functional DRG-mast cell interactions in vitro.

1PT207 Duration of CaMKII activation required for plasticity of dendritic spines revealed by photo-activatable CaMKII inhibitor

Hideji Murakoshi[1,2], Ryohei Yasuda[3] ([1]*National Institute for Physiological Sciences*, [2]*PRESTO, JST*, [3]*Dept of Neurobiology, Howard Hughes Medical Institute, Duke University Medical Center*)

Ca2 + /Calmodulin-dependent kinase II (CaMKII) is required for long-term potentiation (LTP) and associated spine enlargement, which underlies learning and memory in the mammalian forebrain. Previously, it has been demonstrated that exogenous CaMKII activity lasts for ~1 min during induction of spine-specific LTP and spine enlargement. Here, to determine the duration of endogenous CaMKII activation required for CaMKII-dependent synaptic plasticity, we developed a genetically encoded light-inducible inhibitor of CaMKII activation by fusing autocamtide inhibitory peptide 2 (AIP2) to LOV2-Jα derived from phototropin1. We applied it to the study of structural plasticity of single dendritic spines by using 2-photon glutamate uncaging, and found that ~10 s of CaMKII activation is sufficient for inducing transient spine enlargement, while ~60 s is required for sustained spine enlargement. The different temporal requirement between these two phases must be due to differences in the integration properties of downstream signaling. The design of the light-inducible CaMKII inhibitor shown here should be applicable to the design of similar light-inducible inhibitors for many different proteins.

1PT208 TPO 受容体の二量体安定化によるシグナルの正のフィードバック制御

Positive feedback control of thrombopoietin signaling by stabilization of its receptor dimers revealed through single-molecule imaging

Akihiko Sakamoto[1], Takashi Kato[2], Takashi Funatsu[1] ([1]*Grad. Sch. of Pharm. Sci., The Univ. of Tokyo*, [2]*Fac. of Ed. and Int. Arts. and Sci., Waseda Univ.*)

The thrombopoietin (TPO) receptor, Mpl, is a single transmembrane cytokine receptor which stimulates differentiation of platelet progenitor cells and maintains hematopoietic stem cells. Like other cytokines, TPO induces phosphorylation of Mpl, which recruits various adaptor proteins regulating cell proliferation and differentiation. Although dimerization of cytokine receptors is necessary for their phosphorylation, the regulatory mechanism is poorly understood. Here, we describe the regulatory mechanism of Mpl dimerization by single-molecule fluorescence imaging in living cells. Fluorescently labeled Mpl molecules associated and dissociated repeatedly on the plasma membrane. As a result, Mpl molecules resided in monomers, dimers, and oligomers. TPO increased the ratio of Mpl dimers or oligomers, which was resulted from stabilization of Mpl dimers. Surprisingly, stabilization of Mpl dimers was resulted from their phosphorylation rather than TPO binding itself. Furthermore, TPO-induced stabilization of Mpl dimers was dependent on an adaptor protein, Shc, suggesting that phosphorylated Mpl dimers were crosslinked by Shc. By contrast, a monomeric Mpl mutant inhibited TPO-induced phosphorylation of Mpl and downstream cell proliferation. In addition, cholesterol depletion reduced the stability of Mpl dimers, resulting in inhibition of their phosphorylation. Thus, we propose positive feedback control of TPO signaling by stabilization of Mpl dimers.

1PT209 Rac1 recruitment to the archipelago structure of focal adhesion through the fluid membrane as revealed by single-molecule analysis

Akihiro Shibata[1], Chen Limin[1], Nagai Rie[1], Fumiyoshi Ishidate[1], Yoshihiro Miwa[2], Keiji Naruse[3], Takahiro Fujiwara[1], Akihiro Kusumi[1] ([1]*Institute for Frontier Medical Sciences, Kyoto University*, [2]*Department of Pharmacology, Institute of Basic Medical Sciences, University of Tsukuba*, [3]*Cardiovascular Physiology, Okayama University Graduate School of Medicine, Dentistry, and Pharmaceutical Sciences*)

The small G protein Rac1 has been shown to regulate actin reorganization and polymerization at the focal adhesions (FA), an integrin-based architecture of the plasma membrane (PM), mechanically linking the extracellular matrix with the termini of actin stress fibers, providing the scaffold for cell migration. Previously, we found that the FA is not a single entity of massive protein assembly, but rather consists of many protein islands sparsely scattered in the fluid PM (archipelago architecture), and membrane molecules undergo rapid diffusion in the PM even within the FA zone. Here, using single fluorescent-molecule imaging, we examined how Rac1 and its upstream activator GEFs, alphaPIX and betaPIX, are recruited to the FA. We found that almost all of the PIX molecules were directly recruited to the FA zone from the cytoplasm. Meanwhile, 81% of Rac1, which has a geranylgeranyl (+ possibly a palmitoyl) hydrophobic anchoring chains, first landed on the general inner surface of the PM from the cytoplasm and then

entered the FA zone via lateral diffusion in-on the PM, continuing diffusion even within the FA zone (diffusion coefficient is 1/3 of that outside the FA). 11% Of Rac1 molecules that entered the FA zone exhibited temporary or long-term immobilization in the FA zone, suggesting the binding to the FA island proteins. 19% Of Rac1 arrived at the FA zone directly from the cytoplasm and immobilized, suggesting that Rac1 is recruited to the FA protein islands both directly from the cytoplasm and via the general PM area.

1PT210 ERK リン酸化・脱リン酸化反応再構成系の ERK 濃度に依存した応答特性

Response characteristics of reconstructed ERK phosphorylation and dephosphorylation depending on ERK concentration

Masahiro Takahashi[1], Toshio Yanagida[2], Yasushi Sako[1] ([1]*RIKEN ASI*, [2]*Graduate School of Frontier Biosciences, Osaka University*)

ERK, the mitogen-activated protein kinase (MAPK) in the Raf-MEK-ERK cascade, has two phosphorylation sites which are phosphorylated by a kinese, MEK (MAPKK) and dephosphorylated by a phosphatase, MKP. Some theoretical studies have shown that two enzymes with opposing effect (e.g. kinase and phosphatase) can lead to zeroth-order ultrasensitivity which is an ultrasensitive response at the steady-states depending on the substrate concentration (Goldbeter, A. and Koshland, D., PNAS: 78 1981).
To show this type of ultrasensitivity experimentally, we reconstructed the ERK phosphorylations and dephosphorylations in *E. coli* cells, in which concentrations of ERK, MEK and MKP were independently controllable using extracellular chemicals. The attained protein concentrations were estimated by fluorescence intensities of Cerulean (a cyan fluorescent protein variant), Venus (a yellow fluorescent protein variant), and mCherry (a red fluorescent protein variant) each fused on ERK, MEK and MKP, respectively.
We investigated the dependence of ERK phosphorylation on MEK and MKP expression level. The ERK phosphorylation increased by the increase of MEK concentration and/or the decrease of MKP concentration. Thus, the response curve for ERK phosphorylation depended on the ratio of MEK to MKP concentration and could be described by the Hill equation. When the ERK expression decreased by a factor of 0.29, the Hill coefficient decreased by a factor of 0.69. This response is consistent with the theoretical prediction by the zeroth-order ultrasensitivity.

1PT211 マウス胚盤胞における細胞内カルシウム濃度とメカニカルストレス負荷の同時計測

Simultaneous investigation of intracellular calcium concentration and mechanical stimuli to mouse blastocysts

Koji Matsuura[1], Yuka Asano[1], Ikuyo Sugimoto[1], Mieko Kodama[1], Keiji Naruse[2] ([1]*Research Core for Interdisciplinary Sciences, Okayama University*, [2]*Cardiovascular Physiology, Graduate School of Medicine, Dentistry and Pharmaceutical Sciences, Okayama University*)

Mammalian embryos are transported to the uterine cavity through the fallopian tube during cell cleavage and blastocyst development. Fertilized oocytes may be subjected to a mechanical influence. Dynamic embryo culture systems have been developed to generate and apply mechanical stimuli (MS) similar to those generated within the oviduct affecting the mammalian embryo. To investigate the responses of the mammalian embryos to MS, we developed an dynamic air actuation system to apply MS in a microfluidic channel by deforming a 0.1-mm membrane, and investigated changes of intracellular calcium ion concentration ($[Ca^{2+}]_i$) in mouse blastocyst applied MS. Both MS and ($[Ca^{2+}]_i$) were quantified in the microfluidic channel. ($[Ca^{2+}]_i$) was measured in a stained mouse embryo with Fluo-4 AM using confocal fluorescence microscopy. We captured a z-series stack of sections encompassing the entire embryo. When blastocysts were compressed, fluorescence intensity (FI) in the blastocyst also increased in response to the applied MS. Compressive force estimated from the shape of the blastocysts was approximately 0.5-2.0 μN according to a force deformation curve for the mouse embryo. The sum of FIs increased by a factor of 1.1-1.2 times compared with those observed before MS. The increase in the sum of FI indicated that enhancement of ($[Ca^{2+}]_i$) would be induced by these MS. Molecular mechanosensing systems such as mechanosensitive ion channels (MSIs) would play an important role in responses to these MS.

1PT212 バイセクティング GlcNAc とフコースの導入が水中 N 型糖鎖の構造多様性に及ぼす影響

Effect of Bisecting GlcNAc and Core Fucosylation on Conformational Properties of Biantennary Complex-Type N-Glycans in Solution

Wataru Nishima[1], Naoyuki Miyashita[2], Yoshiki Yamaguchi[1], Yuji Sugita[1,2,3], Re Suyong[1] ([1]*ASI, Riken*, [2]*QBiC, Riken*, [3]*AICS, Riken*)

The introduction of bisecting GlcNAc and core fucosylation in N-glycans is essential for fine functional regulation of glycoproteins. In this presentation, the effect of these modifications on the conformational properties of N-glycans is examined at the atomic level by performing replica-exchange molecular dynamics (REMD) simulations. We simulate four biantennary complex-type N-glycans, namely, unmodified, two single-substituted with either bisecting GlcNAc or core fucose, and disubstituted forms. By using REMD as an enhanced sampling technique, five distinct conformers in solution, each of which is characterized by its local orientation of the Manα1-6Man glycosidic linkage, are observed for all four N-glycans. The chemical modifications significantly change their conformational equilibria. The number of major conformers is reduced from five to two and from five to four upon the introduction of bisecting GlcNAc and core fucosylation, respectively. The population change is attributed to specific inter-residue hydrogen bonds, including water-mediated ones. The experimental NMR data, including nuclear Overhauser enhancement and scalar J-coupling constants, are well reproduced taking the multiple conformers into account. Our structural model supports the concept of "conformer selection", which emphasizes the conformational flexibility of N-glycans in protein-glycan interactions.

1PT213 新規フォトクロミック HDAC 阻害剤の設計・合成ならびに阻害作用

Design and synthesis of a novel photochromic HDAC inhibitor and its inhibitory effect

Keiko Tanaka, Shinsaku Maruta (*Dept. of Bioinfo., Fac. Eng., Soka Univ.*)

Histone acetylation-deacetylation is one of the epigenetic regulations of gene expression in eukaryotes. Histone deacetylase (HDAC) catalyze deacetylation of lysine residues in N-terminal domain of core histones and regulates gene transcription and expression. Inhibition of them induces transcriptionally active chromatin, causing arrest of growth, differentiation and apoptosis. HDAC inhibitors are thought to be effective for neurodegenerative disorders, cardiac hypertrophy, inflammation and cancer. In this study, we designed and synthesized novel photochromic HDAC inhibitor, composed of photochromic region (azobenzene), linker, and zinc-interacting thiol, for photo-regulation of differentiation or apoptosis. Azobenzen moiety is placed in hydrophobic interacting region of inhibitor, therefore, light-induced structural change were thought to be affect affinity against HDACs. Synthesized photochromic HDAC inhibitor showed light-induced isomerization. Photochromic HDAC inhibitor showed micro-molar order HDAC inhibitory effect in vitro. The inhibitor composed of trans isomer azobenzene generated by visible-light irradiation inhibited deacetylase activity of HDAC with higher Ki than that composed of cis isomer azobenzene induced by ultraviolet-light irradiation. Development of photochromic HDAC inhibitor is thought to be useful for site-directed inhibition of HDACs.

1PT214 PC12 細胞シグナル伝達系における PLS 回帰を用いた解析

PLS regression analysis of Signal transduction network and phenotypes in PC12 cell

Yuki Akimoto, Katsuyuki Yugi, Shinsuke Uda, Shinya Kuroda (*University of Tokyo*)

PC12 cells, an adrenal chromaffin cell line, are a well-characterized model of nerve cells. This cell line exhibit several characteristic phenotypes such as differentiation, proliferation and apoptosis in response to different external stimuli. Previous studies reported that these various stimuli are redundantly mediated by a few common signal transduction factors such as Akt, CREB and MAPKs, which increase expression levels of some proteins known as Immediate Early Genes (IEGs). However, quantitative relationships between these factors and cell phenotypes are yet to be well characterized. To elucidate this underlying relationship between the temporal patterns of the signaling factors, IEGs and phenotypes we focus a statistical analysis. Statistical models are constructed to predict temporal patterns of IEGs/phenotypes from those of signaling factors such as Akt, CREB and MAPKs using Partial Least Squares (PLS) regression analysis. The expression patterns of signal transduction factors and IEGs were measured by QIC method previously developed by our group and the cell phenotypes are measured by some molecular biological experiments. Using these data a regression equation was calculated in terms of

PLS regression. Finally, we obtained four principal component dimensions characterizing characterize some phenotypes. This data driven approach is effective to identify undefined aspects of complex temporal signal transduction networks.

1PT215 幹細胞様のふるまいを示す人工遺伝子ネットワークの構築

Synthetic biology of stem cells: creating artificial gene network of "differentiation"

Sumire Ono[1], Reiko Okura[1], Yuichi Wakamoto[2,3] ([1]*Grad. Sch. Arts and Sci., Univ. Tokyo*, [2]*Research Center for Complex Systems Biology, Univ of Tokyo*, [3]*JST PRESTO*)

Stem cells can differentiate spontaneously and irreversibly, producing a variety of differentiated cells in context-dependent manners. It remains to be resolved what kind of fundamental characteristics of intracellular network enable such remarkable attributes of stem cells. Recently, Goto and Kaneko have proposed a dynamical systems model of stem cells that can explain spontaneous bifurcation of cellular states using two-gene regulatory network. In this model, a “diffusible inducer” causes cellular interaction, leading to coexistence of two cellular states. The simplicity of the regulation proposed in the model should allow us to synthesize such regulatory network artificially and thereby test the hypothesis regarding the stem cell gene networks.

Inspired by this theoretical study, we aim to construct an *Escherichia coli* strain that possesses an artificial gene regulatory network equivalent to the scheme presented in the model. To realize cellular interaction through diffusible inducer, we utilized the lux operon of *Vibrio fischeri*. However, the original lux operon has positive regulation whereas the inducer acts negatively in the proposed model. For this reason, we designed the actual network with three genes instead of two in a manner that tet operon mediates the lux operon's function. T7 RNA Polymerase system and the lac operon were also used for regulation. RFP and YFP were also introduced as reporters for the activities of the sub-networks. The results and the perspective will be discussed in this meeting.

1PT216 カタユウレイボヤ初期胚におけるラマン顕微鏡による細胞内分子の検出

Detection of bio-molecules localized in specific cells of *Ciona intestinalis* embryo by Raman spectroscopy

Mitsuru Nakamura, Kohji Hotta, Kotaro Oka (*Graduate School of Science and Technology, Keio University*)

Localization of bio-molecules plays central roles in the specification of cell fates and morphogenesis in the embryogenesis. For this reason, to trace the distribution of bio-molecules, especially, mRNAs and proteins, is one of the major issues in developmental biology. In current study, genetic manipulation can be used to observe molecular distribution through the use of fluorescein-labeling molecules. This technique, however, can result in phenotypic changes, need prior identification of target molecules, and the number of labels applicable is limited. Raman spectroscopy, in contrast, is a low-invasive and “label-free” technique, allowing imaging of the distribution of the number of bio-molecules, including molecules without prior identification. In this study on the *Ciona intestinalis* embryogenesis, we explore the application of Raman spectroscopy within the developmental process to investigate the distribution of bio-molecules without labeling. We applied Raman spectroscopy to collect the spectra scattered from *Ciona* embryo at single-cell resolution for early developmental stages. After the spectral analysis, we succeeded to detect vegetal hemisphere-specific localization of some bio-molecules and its localization is similar to maternal factors. This result suggests that Raman spectroscopic imaging in low-invasive and label-free manner on the spatial distribution of bio-molecules is feasible to investigate for developmental studies in *Ciona intestinalis*.

1PT217 細胞分化のエピジェネティック動力学の平均場理論

Mean field theory of epigenetic dynamics of cell differentiation

Takaya Koshii[1], Tomoki P. Terada[2], Masaki Sasai[2] ([1]*Department of Applied Physics, Nagoya University*, [2]*Department of Computational Science and Engineering, Nagoya University*)

Expression of the marker genes of cell differentiation is regulated by the epigenetic modifications of histones, and such epigenetic modifications are regulated by the expression of genes which encode transcription factors (TFs). We analyzed this entangled dynamics of gene expression and epigenetic modification by developing a mean field model of the simplified gene network. In this model the network of three genes is assumed; the network is composed of gene A which maintains the pluripotent state, gene B which induces the differentiation to one lineage, and gene C which induces the differentiation to the other lineage. Each TF synthesized from each of gene A, B, and C is assumed to mutually represses the expression of other genes. We analyze how the difference between the rate of the TF binding/unbinding and the rate of the histone methylation/demethylation affects the process of transitions among the cell states.

1PT218 細胞分化の力学系モデル：安定な発生過程と細胞リプログラミングの理解へ向けて

A dynamical system modeling of cell differentiation for understanding of robust development and cell reprogramming

Chikara Furusawa[1], Kunihiko Kaneko[2] ([1]*QBiC, RIKEN*, [2]*Dept. Basic Sci., Univ. Tokyo*)

Two important problems in stem cell biology are how to characterize the difference in cellular states between undifferentiated stem cells and terminally differentiated cells, and how to understand the dynamics of cell reprogramming from terminally differentiated cells to undifferentiated cells. In this study, to answer these questions, we have carried out a dynamical systems modeling of interacting cells with a gene regulatory network to reveal stem cell differentiation triggered by the cell-cell interactions. We have simulated cellular dynamics using gene regulatory networks with a small number of genes (e.g, less than 10), and screened regulatory networks that can generate cell-type heterogeneity through cell-cell interaction by using genetic algorithm simulations. The results revealed that expression dynamics of cells that have potential to differentiate (i.e. stem cells) generally show irregular (chaotic) oscillation, whereas such complex oscillation is lost for terminally differentiated cell types. Furthermore, we found that, to reprogram terminally differentiated cells to undifferentiated cells, a perturbation to genes which are positively auto-regulated by its products is important. The emergence of stable cellular states that are not chosen by normal development and its relevance to cancer cells will also be discussed.

1PT219 リバーシブル・ネットワーク・リコネクションモデルによる形態形成過程の組織大変形シミュレーション

Simulations of large deformation during tissue morphogenesis using reversible network reconnection model

Satoru Okuda[1], Yasuhiro Inoue[1], Mototsugu Eiraku[2], Yoshiki Sasai[2], Taiji Adachi[1] ([1]*Inst. Frontier Med. Sci., Kyoto Univ.*, [2]*Riken CDB*)

Tissue morphogenesis is accompanied by large three-dimensional (3D) deformations, in which mechanical interactions among multiple cells are spatiotemporally regulated. To reveal the deformation mechanisms, in this study, we newly propose the reversible network reconnection (RNR) model. The RNR model is developed on the basis of 3D vertex models, which express a multicellular aggregate as a network composed of vertexes. 3D vertex models have successfully simulated morphogenetic dynamics by expressing cellular rearrangements as network reconnections. However, in cases simulating large deformations during dynamic tissue morphogenesis, a 3D vertex model can possibly induce unphysical results and failures. We found this is because of geometrical irreversibility, energetic inconsistency, and topological irreversibility in network reconnections. Mathematical and numerical analyses suggested that these problems can be resolved in the RNR model. In addition, to demonstrate the applicability of the RNR model, we simulated tissue deformation of growing cell sheets and showed that the proposed model can simulate large tissue deformations, in which large changes occur in the local curvatures and layer formations of tissues. Thus, the proposed RNR model enables *in silico* recapitulation of complex tissue morphogenesis.

1PT220 細胞体位置と神経突起の伸長方向を制御した 3 次元脳回路再構成技術の開発

Development of Three-dimensional reconstruction brain circuit controlling the direction of neurite elongation and cell body position

Aoi Odawara, Ikuro Suzuki, Masao Gotoh (*Tokyo University of Technology*)

3D reconstruction techniques in biological tissues have been expected to be beneficial in validation of drug candidates and an effective transplant technology in regeneration medicine. Recently, 3D reconstruction techniques using cells combined with biocompatible materials have been developed. In

particular, cell sheet transplantation techniques applied to heart and retina. However, the 3D reconstruction of biological tissues that has an orientation as the brain nerve tissues is still not developed.The aim of this study is to develop a 3D reconstruction technique of brain circuit, controlling the spatial arrangement of neuronal cells. We have developed a 3D neuronal circuit culturing technique by controlling the position of nerve cell body and the direction of neurite elongation using collagen fiber orientation techniques and poly dimethylsiloxane (PDMS) micro-processing. As a result, we observed that the neurite grow in one direction along the collagen fiber with cell body position fixed. In addition, by observing neurite configuration in Z axis using confocal microscope, we confirmed that neurite in 3D gel matrix are elongated in one way. Furthermore, a multilayer structure that mimics the six-layer structure of the cerebral cortex was successfully created. We were able to confirm that neurite are elongated in one way among three layers. Finally, to confirm the function of the 3D reconstructed neuronal circuit, we were able to obtain the propagation of action potential between two cell body layers using multielectrode arrays (MEAs).

1PT221　3 次元ネットワーク再構成のための神経組織の脱細胞化条件

Decellularized conditions of neuronal tissue for the reconstruction of 3D neuronal network

Shota Amano, Ikuro Suzuki, Masao Gotoh (*Tokyo University of Technology*)

Artificial heart and joints has been translated into the medical field. In recent years, transplantation techniques used by these artificial tissues have been expected. Cell transplantation using cell sheet such as in epidermal tissue, corneal epithelium, and the heart, has been successful. The discovery of iPS cell made it an important tool in creating a variety of tissues, but in cell culture, the use of decellularized cellular components such as scaffold has been of interest because of its ability to keep the three-dimensional tissue structure and extracellular matrix (ECM) stable. Until now, changes in decellularization conditions and ECM evaluation in liver, lung, heart tissues, and muscles has been investigated, but not in nerve tissue. Therefore, the aim of this study is to investigate the changes in decellularization conditions and ECM evaluation of nerve tissue. Using rat brain, nerve tissue decellularization was performed using de-sodium dodecyl sulfate (SDS), Trypsin/EDTA, and TritonX-100, decellularized tissues were stained using hematoxylin and eosin (H&E). In addition, the processing of each decellularized nerve tissue's ECM was evaluated. Together all the results of nerve tissue decellularization, will be reported at the conference.

1PT222　一分子蛍光ソーティングを目指したマイクロ流体システムの構築

Construction of a microfluidic system for fluorescence-based single-molecule sorting

Sho Saitoh[1], Hiroyuki Oikawa[2], Kiyoto Kamagata[2], Satoshi Takahashi[2] ([1]*Grad. Sch. Life Sci., Tohoku Univ.*, [2]*IMRAM, Tohoku Univ.*)

Techniques of sorting micro-particles such as cells have found wide applications in biological sciences; however, sorting of biological molecules with relatively small molecular weights including proteins and nucleic acids is still difficult. This is mainly because of the lack of the method to discriminate molecules sensitively at the single molecule level. We are currently constructing a fluorescence-based single-molecule sorting device, which is composed of an optical system for the detection of fluorescence from fluorophores labeled to sample molecules and the microfluidic system for the sorting of molecules after the fluorescence detection. As the optical system, we utilized a light correction system based on a spherical mirror, which achieves a large detection area and high numerical aperture at the same time. As the microfluidic system, we constructed a silica-based chip, in which an inlet channel and two outlet channels for waste and collection were carved. The sample was introduced to the inlet channel, and its fluorescence intensity was detected at the observation point. Based on the detected fluorescence intensity, the flow was controlled to direct sample either to the waste channel or the collection channel. We utilized miniature solenoid valves to switch the sample flow. We confirmed that the system can be used to sort a mixture of two kinds of microbeads with different colors. To further examine the performance of the developed system, we are currently conducting sorting experiments of DNAs with different lengths.

1PT223　電子顕微鏡画像分類の利便化のためのツール開発

Development of a convenient tool for making processes of particle clustering and averaging in 3D reconstruction from electron micrographs

Tatsuya Kihara, Takuo Yasunaga (*Dept. of Biosc. and Bioinfo., Grad. of Comp. Sc. and System Eng., Kyushu Inst. of Tech.*)

Eos (Extensible object-oriented system for macromolecular imaging), we have been developing, has many tools to process electron micrographs and environment for software development. Some tools provide GUI (Graphical User Interface) -based one in Eos but others not. A group of program for classification and averaging has been also implemented as only CUI (Character User Interface)-based ones. Therefore, we tried to develop a convenient tool with GUI. This was implemented by an integration of different programs under Eos and so only a few simple steps using mouse were necessary for processing to be executed. I succeeded in developing the tool with GUI and it was evaluated in actual analyses by some researchers. At the last meeting, we reported the evaluations of the tool using model data sets, phantoms. We here report evaluations for actual electron micrographs in these analyses. Actually, the tests showed some problems from the researchers such as limits of image number, no function for resetting zooming size and so on. At present we solved some of the problems, added to new functions and modified the tool to be more convenient. However some still remain. Furthermore, we try to test the tools iteratively and add functions and parameters for more precise image analysis and refinement.

1PT224　高重力を利用した非球形構造を持つマイクロハイドロゲル粒子の作製法

High-gravity-based synthesizing method for hydrogel microparticles with non-spherical structures

Masayuki Hayakawa[1], Hiroaki Onoe[3], Ken H. Nagai[4], Masahiro Takinoue[1,2] ([1]*Interdisciplinary Grad. Sch. Sci. and Eng., Tokyo Tech.*, [2]*PRESTO, JST*, [3]*IIS, Univ. of Tokyo*, [4]*Dept. Phys, Univ. of Tokyo*)

In recent years, hydrogel-based anisotropic microparticles have attracted much attention due to their various applications including micrometer-scaled self-assembly, tissue engineering, drug delivery, and artificial cell models. By three-dimensionally organizing such anisotropic microparticles encapsulating some functional molecules, it will become possible to construct self-assembled systems with higher-order functions as living cells and living tissues. However, constructing such three-dimensional structures from anisotropic microparticles is now difficult because it is unable to synthesize three-dimensionally complex anisotropic particles such as colorful beach balls, gears, etc. due to the use of two-dimensional microfluidic channels in the synthesis of microparticles. Thus, it is desired to develop a method to generate three-dimensionally anisotropic microparticles.

In this presentation, we report a method for generating three-dimensionally anisotropic microparticles such as hemispherical microparticles. This method was based on Centrifuge-based Droplet Shooting Device (CDSD) [1]; it is a device to synthesize monodisperese microparticles with multiple compartments. Here, we constructed three-dimensionally anisotropic microparticles by removing a part of the multiple compartments of the microparticles. We believe that our method will contribute to the study of more complex self-assembled systems of microparticles.

[1] Maeda et al., Adv. Mater. (2012)

1PT225　ハイドロゲルマイクロファイバー内での血管内皮細胞の管構造形成

Tube Formation of Endothelial Cells in the Hydrogel Microfiber

Hiroaki Onoe[1,2], Shoji Takeuchi[1,2] ([1]*IIS, The University of Tokyo*, [2]*ERATO Takeuchi Biohybrid Innovation Project, JST*)

Creating vascular network in a macroscopic artificial tissue has been stated as an essential element for constructing long-life artificial tissues having nutrient/metabolite circulation. Various attempts have been made to create blood vessels in an artificial tissue though, the arrangement of vascular network in a designed 3D configuration have still been a challenging issue.

Recently, we have proposed a cell-encapsulating core-shell hydrogel fiber, named "cell fiber". One important feature of our "cell fiber" is that we can freely manipulate the fibers with keeping cellular activities and assemble them into designed 3D configurations. Here we present the tube formation of endothelial cells in the collagen/alginate core-shell hydrogel microfiber. We found that encapsulated MS1 (mouse pancreatic endothelial cell line) and HUVEC (human umbilical vein endothelial cell) spontaneously create tube-like monolayer cell structures along the axial direction of the fiber at meter-length scale. Because the produced endothelial tubes are free-standing and can be manipulated in a culture medium with the support of the alginate shell, our

endothelial cell fibers would be a fundamental tissue unit for constructing three-dimensional (3D) macroscopic tissues with vascular network and for analyzing cellular behaviors (ex. vasculogenesis or angiogenesis) under intercellular/chemical/mechanical/fluidic interactions.

1PT226 分子ロボットによる人工パンスペルミア

Artificial Panspermia by Molecular Robots

Masahiro Endo[1], Kei Fujiwara[1,2], Syougo Hamada[1,3], Satoshi Murata[1,4], Shin-ichiro. M Nomura[1,5] ([1]*Undergrad. Sch. Eng., Tohoku Univ.*, [2]*JSPS. Postdoc., Tohoku Univ.*, [3]*Assi Prof. Tohoku Univ.*, [4]*Prof. Tohoku Univ.*, [5]*Assoc Prof. Tohoku Univ.*)

Molecular robotics is an emerging research field aiming at development of a systematic methodology to design complex molecular machines, which have a potential to overcome difficult problems that natural living system cannot solve. Recently, owing to the rapid progress in DNA nanotechnology, many types of molecular devices have been proposed. Those devices, usually made of several artificially synthesized DNA, have shapes and functions designed by humans. However, these devices work only in test tubes. Extending their operation to the wider conditions, such as in vivo, in low temperature and in high/low pH, is one of the important research targets of molecular robotics. An example of such extreme environment is the space, where not only the zero pressure but intensive radiations surround the molecules. Here, we think artificial pansperimia* is a good target for molecular robotics, and focus on environmental resistance of molecular devices against cosmic radiation and freeze-dry treatment. As a test piece, we have designed a DNA nanostructure and evaluated its functionality (in this case, the shape) after re-hydration. Atomic force microscopy observation showed that the structure well maintains the designed shape throughout the treatment. *"Panspermia" is a hypothesis about the origin of life, assuming interstellar travel of living organisms.

1PT227 細胞膜上の分子ロボットの作成に向けて

Prototype molecular robots working on cellular membrane

Yusuke Sato[1], Kei Fujiwara[2], Shogo Hamada[3], Satoshi Murata[4], Sin-ichiro Nomura[5] ([1]*Undergrad. Sch. Eng., Tohoku Univ*, [2]*JSPS. Research Fellow. Tohoku Univ*, [3]*Assi Prof. Tohoku Univ*, [4]*Prof. Tohoku Univ*, [5]*Assoc Prof. Tohoku Univ*)

Recent progress of micro-nano technology enables us to design "molecular robots" [1,2,3]. Molecular robot is a system of molecular devices in which DNA nanostructures, DNA devices and modified proteins are combined as a coordinated system. They are in the scale of up to several tens nanometer, and huge number of the same robot can be produced in a test tube by self-assembly. We are investigating interaction between such molecular robots and living cells. In the operations of the molecular robots, the following features are important: 1) target cell specificity and 2) launching/landing back to/from the target. Here, we present a design of prototype robot working on cellular membrane. The robot has hydrophobic "legs" that holds onto the membrane. Because of diffusion of lipid molecules in the membrane, the robot is also expected to show lateral diffusive behavior. To verify this, single molecular tracking experiment with fluorescent-tagged robot has been conducted. The data obtained by total internal reflection fluorescence (TIRF) microscopy clearly showed lateral diffusion of the robot in several seconds. In the future applications, these robots floating on the membrane will protect cells from virus infection, or will used to control the specific receptors on the cell.

[1] G. M. Churchet al. Science 2012, 335, 831-834 [2]W. Winfree et al. PNAS 2012, vol.109, no.17, 6405-6410 [3]H. Sugiyama et al. JACS 2010, 132, 1592-1597

1PT228 分子ロボティクス：リモコン分子クロラ・プロトタイプの構築

Molecular robotics: Construction of a remote control molecule crawler prototype

Daiki Komatsu, Kei Fujiwara, Shin-ichiro M. Nomura (*Tohoku University*)

Molecular robotics is a new research field to develop an artificial molecular system. The major methodology, self-organization of biomacromolecules, is quite suitable for biological applications. Thus, designing smart drag delivery system (DDS) is strongly expected in the future. Here we aim to create a "remote-controllable" molecular system. We constructed the prototype with water-in-oil droplet (10 to 50 micrometer in diameter), incorporated magnetic nano particles. The magneto-droplets showed three-dimensional motion induced by external magnetic field. It was predicted that the accumulation pattern of the magnetic particles is strongly effect the whole droplet movement. The droplet can easily transfer the structure into giant liposome by passing through the lipidic oil/water surface. Thus, we are now designing a "movable" molecular system on using this chassis. The result will be reported.

1PT229 バクテリア駆動マイクロギアの構築とトルク計測

Building and torque measurement of bacteria driven micro gear

Masaru Kojima[1,2], Tatsuya Miyamoto[2], Masahiro Nakajima[3], Michio Homma[4], Toshio Fukuda[2,3] ([1]*Present address: Grad. Sch. Eng. Sci., Osaka Univ.*, [2]*Dept. Micro-Nano Sys. Eng., Nagoya Univ.*, [3]*Center for Micro-Nano Mech., Nagoya Univ.*, [4]*Div.Bio. Sci., Nagoya Univ.*)

Bio-hybrid system has been attracting attention in recent years. The biological macromolecule and living organism are worked as very small and highly effective actuator and these bio-actuators are expected as next generation motivity. Especially, several bio motors were reported. However, the research field of bio-actuator is in advance, many unsolved problem are exist. For example, biological reaction is not well known, evaluation of bio actuator is not enough, therefore developing control method for such kind of reaction is important. In this study, to realize the new bio motor, which can be applied to micro-nano systems power source (built-in mechanical factor), we used Vibrio alginolyticus, some kind of marine bacteria, specific motile mode "Surface swarming" as actuator. At first, we tried to drive micro beads on surface swarming of V. alginolyticus. Furthermore, we succeeded in controlling movement of surface swarming by ratchet shape micro channel and then driving the micro gear in the closed micro channel. As a next step, to transmit power of rotational movement, we fabricated the open micro channel and micro object (floating pillar, micro gear etc.) and succeeded in driving the object in the open micro channel. In addition, we revealed that rotational power of floating pillar by deformation of nano probe. Finally, we assembled the micro gear with shaft like crank. Therefore, it became possible transmitting the power from rotational movement to outside. Thus, we achieved to construct base of bio-motor.

1PT230 Evaluation of microtubule deformation by live cell imaging and image analysis

Ryosuke Tanaka, Takeomi Mizutani, Hisashi Haga, Kazushige Kawabata (*Grad. Sch. Life. Sci., Univ. Hokkaido*)

Deformation of cytoskeleton is thought to be a converter of mechanical stimulus into chemical activity in living cells. Although recent reports showed that actin fiber, one of cytoskeleton, acts as a converter, contribution of other cytoskeletons is still unclear. As a first step to elucidate this question, we began to evaluate deformation of other cytoskeletons.

We evaluated microtubule deformation by live observation of GFP-tagged tubulin expressing cells and image analysis. We observed microtubules dynamically bent in contrast to straight actin fiber. Therefore, longitudinal deformation of microtubule is difficult to evaluate by using actin fiber deformation analysis. To overcome this problem, we developed image analysis software aimed to extract fluorescent intensity profile along curved microtubule and identify the same points on the fiber from a set of time course images. Microtubule deformation was evaluated by time change of distance between the identical points. We successfully evaluated deformation of curving microtubule. The next step of our study is to evaluate validity of our analysis. In this annual meeting, we will also report microtubule deformation under cell deformation. Besides, we will discuss roll of microtubule deformation as a cellular sensor.

1PT231 マイクロファイバーゲルマトリックスの弾性パターニングによる三次元細胞運動のメカニカル制御

Mechanical control of 3-D cell movement in elastically-micropatterned matrix of micro-fiber gels

Aya Ogata[1], Satoru Kidoaki[2] ([1]*Grad. Sch. Eng., Univ. Kyushu*, [2]*IMCE, Univ. Kyushu*)

The cell movements are critically affected by the stiffness of extracellular surroundings of 2-D substrate surfaces or 3-D matrices. To scrutinize the mechanobiology of the cell motility, systematic design of the extracellular mechanical surroundings is quite essential. In this study, we have developped the novel methodology of microelasticity-design of 3-D cell culture matrix which consists of nonwoven mesh of swollen micro-fiberous gels with well-tuned different elasticity, in order to clarify the effect of matrix stiffness on the 3-D cell movement. Nanofiber mesh of photocurable styrenated gelatin (StG)

including radical generator camphoquinone was prepared by electrospinning, cross-linked in ethanol media, and swollen in aqueous solution, which successfully produced swollen micro-fiber gel matrix. By regulating the photocuring conditions, elastic modulus of fiber gel sheet was well-tuned. Assessment of movement of 3T3 fibroblasts on the prepared gel sheets with different stiffness showed that cells extended well on the surface of the sheet and did not enter the inside of soft matrix (1.4 kPa), whereas cells got into the hard sheet (15.8 kPa) and finally reached to the bottom of the sheet 6 hours after seeding. This result suggested that 3-D cell mechanotaxis can be driven by matrix-stiffness dependent manner as well as the 2-D mechanotaxis. Mechanism of such 3-D mechanotaxis and possible manipulation of 3-D cell movement by the design of stiffness of gel sheet are discussed.

1PT232 微視的弾性境界の曲率設計による細胞メカノタクシスの高効率誘導

Efficient manipulation of cell mechanotaxis: effect of the curvature of micro-elasticity boundary

Ayaka Utsumi[1], Satoru Kidoaki[2] ([1]*Grad. Sch. Eng., Univ. Kyushu*, [2]*IMCE, Univ. Kyushu*)

The directional cell movements induced by a mechanical gradient on a substrate surface, so-called mechanotaxis, are useful model phenomenon to investigate the mechanobiology of cell motility. So far, we have established the elasticity boundary conditions required to induce mechanotaxis of fibroblasts with certain reproducibility; sharp linear boundary with enough narrow width and enough high elasticity jump in the single-cell adhered interface on cell culture gels. However, the induction efficiency of mechanotaxis was significantly affected by the shape of moving cells, suggesting the importance of a shape interaction between cells and elasticity boundary. In this study, to assess the effect of the shape interactions on the induction efficiency of mechanotaxis, a curvature of the elasticity boundary was systematically designed with a custom-built mask-free photolithography using elasticity-tunable photocurable styrenated gelatin. Fixing the elastic gradient strength as 30-40 kPa/ 50 μm, the radius of curvature of boundary was designed as 50, 100, 250, 500, 750, and 1000 μm in both convex and concave shapes. Migration of 3T3 fibroblasts was observed on these boundaries and efficiency of induction of mechanotaxis was analyzed. As the result, highly efficient mechanotaxis was induced on the convex boundary with 100 μm in radius and on the concave boundary with 750 μm in radius. Interestingly, directional cell migration toward a softer region emerged on the concave boundary with 50 μm in radius for the first time.

1PT233 線虫内部への蛍光ナノビーズの選択的導入

Selective Injection of Fluorescent Nanobeads into *Caenorhabditis elegans*

Masahiro Nakajima[1], **Hirotaka Tajima**[2], Masaru Kojima[2], Naoya Nakanishi[2], Naoki Hisamoto[3], Michio Homma[3], Toshio Fukuda[1,2] ([1]*Cent. For Micro-nano Mechatro., Grad. Sch. of Engineer., Nagoya Univ.*, [2]*Dept. of Micro-Nano Sys. Engineer., Grad. Sch. of Engineer., Nagoya Univ.*, [3]*Div. of Biol. Sci., Grad. Sch. of Sci., Nagoya Univ.*)

We present a novel selective injection of fluorescent nanobeads into *Caenorhabditis elegans* (*C. elegans*) based on bio-nanomanipulation technique for in-vivo single cell analysis.

The nanomanipulation system was constructed under hybrid microscope. The hybrid microscope consists of the optical microscope (OM) and environmental-scanning electron microscope (E-SEM). It realizes detail analyses of biological specimens by fluorescent imaging by the OM, and nano-scale manipulation by the imaging of the E-SEM.

Based on the bio-nano manipulation system, we propose a nanoinjection method by the nanoprobe insertion for embeddedness of nanobeads. The nanoprobe was designed to have the four tips to fix single nanobead. It was fabricated by focused ion beam (FIB) process. The nano-scale probe size is considered to be important for minimal damage to the biological specimens.

In this work, as a biological specimen, the *C. elegans* was used, because it is one of the important model organisms for various biological analysis. The nanoinjection technique was applied to embed a fluorescent nanobead into a specific cell inside *C. elegans* for in-vivo analysis. We inserted the nanoprobe into the body of *C. elegans* at a depth in approximately 6 μm. The size of fluorescent nanobeads was 500 nm in diameter. The proposed system is considered to be important as future nano-surgery system for life innovation using model organism.

1PT234 W/O ドロップレット内での酵母を用いた G タンパク質共役受容体のリガンドアッセイシステム

Yeast-based ligand assay system for detecting G protein-coupled receptor activation in water-in-oil droplets

Takashi Sakurai[1], Ryo Iizuka[1], Yasuyuki Tanigaki[2], Rui Sekine[3], Dong H. Yoon[3], Tetsushi Sekiguchi[4], Jun Ishii[5], Akihiko Kondo[6], Naoto Nemoto[2], Shuichi Shoji[3], Takashi Funatsu[1] ([1]*Grad. Sch. of Pharm. Sci., The Univ. of Tokyo*, [2]*Grad. Sch. of Sci. and Eng., Saitama Univ.*, [3]*Major in Nanosci. and Nanoeng., Waseda Univ.*, [4]*Nanotech. Research Center, Waseda Univ.*, [5]*Org. of Advanced Sci. and Tech., Kobe Univ.*, [6]*Grad. Sch. of Sci. and Tech., Kobe Univ.*)

G protein-coupled receptors (GPCRs) are involved in many different cellular processes, and are targets of many therapeutic drugs. We developed a yeast-based ligand assay system for detecting GPCR activation in water-in-oil (W/O) droplets. Our system is based on linking between the genotype and the phenotype using W/O droplets. DNA library encoding peptides, in vitro transcription-translation system, and budding yeast cells expressing target GPCR are co-encapsulated into droplets using a microchannel. Yeast cells are genetically engineered to express GFP in response to ligand stimulation. The generated droplets were collected into a microcentrifuge tube and incubated to allow the gene translation and ligand stimulation. The droplets would be fluorescent when synthesized peptides stimulate GPCRs, enabling easy identification of ligand candidates. Using this system, we firstly demonstrated cell-free GFP synthesis in the presence of yeast cells in W/O droplets, indicating the presence of yeast cells did not inhibit protein expression. Next, we encapsulated yeast cells expressing Ste2p (an endogenous GPCR) and the gene of α-factor (ligand of Ste2p) in the droplets. After incubation, GFP-expressing cells were clearly observed in response to α-factor stimulation. The α-factor synthesized from the five-molecule DNA template in the droplets successfully induced GFP expression. Our system will provide an effective approach for the high-throughput screening of peptide ligands targeted at mammalian GPCRs by evolutionary molecular engineering.

1PT235 フロー型乳酸バイオセンサの開発とその脳内乳酸測定への応用

Development of a flow-type lactate biosensor and its application to the measurement of lactate in the mouse brain

Kaoru Yamazaki[1], Mai Ichikawa[1], Ryo Shimazaki[1], Hideo Mukai[2], Minoru Saito[1] ([1]*Graduate School of Integrated Basic Sciences, Nihon University*, [2]*Faculty of Medicine, Saitama Medical University*)

Lactate biosensors which enable us to measure lactate concentration in blood and other body fluids are applicable to some medical fields such as sports medicine. We fabricated a lactate biosensor by a flow-type sensing system, in which the injected sample flows into an immobilized enzyme (lactate oxidase; LOD) column. The column was fabricated by packing an immobilized enzyme support into a 30 mm long column. The support was obtained by immobilizing LOD on silica particles (particle size: 30-60 mesh). The immobilization was performed by loading LOD onto the aminoalkyl-bonded particles with glutaraldehyde. The column was kept at a constant temperature (37°C). The generated H_2O_2 or consumed O_2 in the column was detected by the H_2O_2 electrode or O_2 electrode. The fabricated biosensor could measure lactate concentration up to 10 mM. By using it, we next measured lactate levels of the mouse brain. The samples were prepared by homogenizing the brain slices in ACSF. The results showed the differences of lactate levels among each part of the brain and among each age of the mouse.

1PT236 マイクロチャンバー内でのβ-グルコシダーゼ 1 分子の酵素活性のモニタリング

Monitoring the single-molecule enzymatic activity of β-glucosidase in a microchamber array chip

Kentaro Tahara[1], Ryo Iizuka[1], Takao Ono[2], Kiyohiko Igarashi[3], Masahiro Samejima[3], Takanori Ichiki[2,4], Takashi Funatsu[1,4] ([1]*Grad. Sch. of Pharm. Sci., The Univ. of Tokyo*, [2]*Grad. Sch. of Eng., The Univ. of Tokyo*, [3]*Grad. Sch. of Agri. and Life Sci., The Univ. of Tokyo*, [4]*JST-CREST*)

β-glucosidase (BGL), which catalyzes the hydrolysis of cellobiose to glucose, is one of the important enzymes in bioethanol production. We aim to obtain BGL mutants with improved hydrolytic activity by directed evolution. To screen many potential mutants easily and precisely, we are trying to develop the single-

molecule assay for BGL activity in a microchamber array chip.
The microchamber array chips were fabricated by micromolding processes with polydimethylsiloxane polymer. BGL1B from the basidiomycete *Phanerochaete chrysosporium* was confined with fluorogenic substrate [Fluorescein di-β-D-glucopyranoside (FD-Glu), TokyoGreen-βGlu (TG-Glu) or Resorufin β-D-glucopyranoside (R-Glu)] in microchambers with a volume of 50 fL. The enzyme produced a large number of fluorescent molecules by hydrolyzing fluorogenic substrates, leading to fluorescence increase in microchambers. However, in the absence of BGL1B, TG-Glu was found to be hydrolyzed spontaneously in microchambers, whereas the others not. We also proved that R-Glu is more adequate for the enzymatic assay than FD-Glu. Unlike FD-Glu that requires a two-step hydrolysis to generate maximum fluorescence, R-Glu requires only a single-step hydrolysis reaction to attain full fluorescence, thereby affording a higher rate of fluorescence increase and ensuring the linear relationship between the fluorescence intensity and the BGL activity. Hence, using R-Glu, we are trying to monitor the single-molecule enzymatic activity of BGL1B in microchambers.

1PT237 フェリチン空洞内でのレアアース(Eu、Tb、Tm、Y)ナノ粒子合成

Synthesis of rear earth (Eu, Tb, Tm and Y) nanoparticles in apoferritin cavity

Tomoaki Harada, Hideyuki Yoshimura (*Meiji Univ.*)

Eu, Tb, Tm and Y nanoparticles were fabricated in the cavity of a cage shaped protein, recombinant apoferritin (fer0). Apoferritin is a spherical protein of 13 nm diameter with a cavity of 7 nm diameter. It is known to mineralize several metal ions in the cavity. Eu nanoparticles were synthesized by mixing 0.1 mg/ml apoferritin with 100 mM MOPS (pH 6.8) and 1 mM $Eu(NO_3)_3$ $6H_2O$ and kept standing for 24 hours at room temperature. This solution was centrifuged for 3 minute at 12000 rpm to remove small amount of precipitation. The supernatant was dialyzed with 20 mM NH_3 acetate, whose pH was adjusted to 8.0 by adding NH_3, to stabilize core in the ferritin cavity. Tb, Tm and Y nanoparticles were prepared as the same method, except 100 mM MOPS (pH 7.0) was used for Y nanoparticles. The nanoparticles formation was confirmed with transmission electron microscopy (TEM) with and without aurothioglucose negative staining. The lattice structure of the cores was observed by high resolution TEM (HRTEM). Some of cores were showed lattice structure, however most of cores were amorphous. These nanoparticles were analyzed with an EDX and the specific peaks of expected elements were observed. The solution of Eu nanoparticles was applied to gel-filteration (Sephadex G-25) with elution buffer of 5 mM NH3 acetate (pH 8.0) and was dried at 60℃. Subsequently, it was sintered at 800℃ for 4 hours in the air. The sintered specimen showed electronic diffraction pattern corresponding to the lattice spacing of Eu_2O_3.

1PT238 カゴ状蛋白質アポフェリチンを使用したガドリニウムナノ粒子の作成

Synthesis of gadolinium-based nanoparticles using the protein cage of apoferritin

Hiroko Fukano, Hideyuki Yoshimura (*Physics. Univ. Meiji*)

Gadolinium-based nanoparticles are expected as a better contrast agent for magnetic resonance imaging (MRI), since their effect for the relaxation rate is much higher than those of chelated gadolinium (III) complexes used in the medical field. Here we report the synthesis of gadolinium oxide nanoparticles in the apoferritin cavity which is known to reserve metals as oxide or oxy-hydroxide state. The apoferritin coated-gadolinium nanoparticles were synthesized by the following simple procedure; the mixture solution of 0.1 mg/mL recombinant apoferritin, 1 mM $Gd(NO_3)_3$ $6H_2O$, and 0.1 M MOPS (pH 7.0) was just incubated for overnight at 4 ºC. The synthesized nanoparticles were characterized by TEM and EDS. Homogeneous and spherical nanoparticles coated with protein shell were confirmed by TEM. The average diameter of them was determined to be 5.8 ± 0.5 nm by evaluating 900 particles. According to the high-resolution TEM images, the nanoparticles showed single-crystal, multi-crystal, or amorphous state. With EDS analysis, the peaks of gadolinium (Lα; 6.06 keV, Lβ; 6.71 keV, Mα; 1.19 keV) were detected only at the synthesized nanoparticles. The electron diffraction pattern suggested that the nanoparticles were gadolinium oxide. However further investigation of crystal identification is needed because the electron diffraction image was broad and weak.

2PS001 タンデム PomA を固定子とする Na^+駆動型キメラべん毛モーターの回転計測

Rotation Measurement of Na^+-driven Chimeric Flagellar Motor with Tandem PomA

Yong-Suk Che, Yoshiyuki Sowa (*Department of Frontier Bioscience, Hosei University*)

Four PomA and two PomB, homologs of MotA and MotB in the H^+-driven flagellar motor of *Escherichia coli*, form a stator complex in the Na^+-driven flagellar motor of *Vibrio alginolyticus*. The motor torque is generated by the interaction between the cytoplasmic domain of PomA and the C-terminal domain of FliG, a component of the rotor. It was shown that a tandem fused PomA is functional as a torque generator in *V. alginolyticus* (Sato and Homma, JBC 2000). Furthermore, a chimeric stator (which consists of PomA and the chimeric fusion protein PotB) works as a Na^+-driven flagellar motor in *E.coli* (Asai et al., JMB 2003). In the last annual meeting, we demonstrated that tandem PomA dimer was expressed as a single polypeptide in *E. coli* and swimming speed of *E.coli* cells with tandem PomA was about half of that with the monomeric PomA, suggesting that tandem PomA functions as a torque generator in *E.coli*.

Here, in order to characterize the details of tandem PomA, we carried out rotation measurements of single flagellar motors in *E. coli* cells expressing tandem PomA using 1 μm beads attached to truncated flagellar filaments. Maximum motor speed with tandem PomA was 80 Hz, similar to that with monomeric PomA. However, the motor speed with tandem PomA distributed broadly compared to that with monomeric PomA. We also measured motor speeds with tandem PomA with several combinations of mutants in the cytoplasmic charged residues, which are thought to be crucial for torque generation. Details of these results will be discussed.

2PS002 枯草菌べん毛モーターの異なる 2 種類の固定子 MotA サブユニットと MotP サブユニットの細胞質内ループの荷電アミノ酸残基の機能的役割

The functional role of the charged residues of two different stators: MotA subunit and MotP subunit in *B. subtilis* flagellar motor

Yuka Takahashi, Masahiro Ito (*Grad. Sch. Life., Univ. Toyo*)

The flagellar motor is energized by either H^+ or Na^+ motive force. MotAB-type stators use H^+, while MotPS-type and PomAB-type stators use Na^+ as coupling ions. The MotAB-type stator flagellar motor torque in *E. coli* is considered to be generated by electrostatic interactions at the interface between rotor and stator as indicated by previous studies. There are conserved charged residues in the cytoplasmic loop of MotA, which probably interact with the conserved charged residues of the C-terminal domain of rotor FliG. However, it is not clear whether the electrostatic interaction between the rotor and the Na^+-type stator PomAB is required. Here we studied a flagellar motor that consists of two different stators, MotAB and MotPS, in *B. subtilis* and tried to identify critical charged residues for torque generation in each MotA and MotP subunit. We identified the conserved charged residues in the cytoplasmic loop of MotA and MotP. *B. subtilis* with mutations in conserved charged residues and several other charged residues were measured for swarming and stator subunit protein expression levels. These charged residues in the cytoplasmic loop of stators can be divided into two types: those important to torque generation by interaction between rotor and stators, and those involved in stabilization of the structure of stators. Thus, important charged residues for motility in the H^+-driven MotAB and Na^+-driven MotPS were identified in this study.

2PS003 べん毛モーターの回転と GFP 標識固定子の同時観察

Simultaneous observation of the rotation of flagellar motor and GFP-labeled stator unit in a functioning flagellar motor

Mizuki Nakajima[1], Hajime Fukuoka[2], Yuichi Inoue[2], Hiroto Takahashi[2], Akihiko Ishijima[2] ([1]*Grad.Sch.Life.Sci.,Tohoku Univ.*, [2]*IMRAM.Tohoku Univ.*)

The bacterial flagellar motor is driven by the influx of coupling ions, and the interaction between stators and a rotor is thought to generate the motor rotation. It have been estimated the number of stators in a motor from the stepwise increment of rotational speed or the bleaching steps derived from GFP-labeled stator units. However, it is not quantified how many stator units are required for each step of speed-increment, and the timing of stator assembly in the step of speed-increment is not measured. To clarify these questions, the rotational speed of motor and stator assembly should be measured simultaneously. To observe stator assembly, we newly designed GFP-fused stator units based on PomAPotB, which functions as the Na^+-driven stator units in an *Escherichia coli* cell. When we observe the tethered cell expressing GFP-PomAPotB, the stepwise increment of rotational speed was detected when the motility medium without Na^+ was replaced to the medium containing 85 mM of Na^+. Next, we developed the microscopic system to simultaneously obtain the bright field image (wavelength more than 600 nm, taking by high speed camera) for the measurement of rotational speed and the fluorescence image (wavelength 500 - 560 nm, taking by EMCCD camera) for the observation of stator assembly. We would like to discuss this simultaneous measuring result in the annual meeting.

2PS004 蛍光観察による細菌鞭毛モーターの解析

Imaging of fluorescently-tagged motor components of bacterial flagella

Yoshiyuki Sowa, Yong-Suk Che (*Department of Frontier Bioscience, Hosei University*)

Bacteria, such as *Escherichia coli*, can swim by rotating their helical flagella, protruding from the cell body. Rapid rotation of each filament (up to several hundreds hertz) is driven by a motor located in the cell envelope at the base of the filament. This motor is powered by the flux of ions across the cytoplasmic membrane. We have measured its rotation by a bead assay, in which we attach a small s bead onto the flagellar filament or hook of the motor and detect its motion. This assay is very useful for measuring the basic properties of the motor and detecting elementary steps in flagellar rotation. However, we can detect motor rotation only via the filament or hook, although the rotational torque is generated at the cytoplasmic side of the motor components, FliG, FliM, FliN, MotA and MotB. To understand how the motor works, direct observation of motor movements at the site of torque generation is required. In this study, we aim at developing the assay to detect motor dynamics by fluorescent microscopy at single-molecule level. To track movements of single fluorescent dyes with nanometer accuracy, we have built total internal reflection fluorescence (TIRF) microscope and are currently optimizing it. We also have succeeded in labeling MotB with rhodamine dyes, which are more suitable for single-molecule tracking than fluorescent proteins such as GFPs. We confirmed the rhodamine labeled MotBs function in a motor and currently observe them by TIRF microscopy.

2PS005 べん毛輸送装置構成タンパク質 FliP ペリプラズム領域の構造機能解析

Structural and functional analyses of a periplasm region of FliP, a component of the flagellar protein export apparatus

Takuma Fukumura[1], Yukio Furukawa[1], Yumiko Saijo-Hamano[1], Katsumi Imada[2], Keiichi Namba[1,3], Tohru Minamino[1] ([1]*Grad. Sch, Frontier Biosci., Osaka Univ.*, [2]*Grad. Sch. Sci. Osaka Univ.*, [3]*QBiC, RIKEN*)

Most of flagellar proteins are transported by a specific export apparatus from the cytoplasm to the growing distal end of the flagellum where they self-assemble. The export apparatus consists of a water-soluble ATPase complex and a proton-driven export gate made of six membrane proteins FlhA, FlhB, FliO, FliP, FliQ, and FliR. The ATPase complex escorts flagellar proteins from the cytoplasm to the export gate. It has been reported that FlhA plays a role in energy transduction along with the ATPase complex. However, the structure and function of other gate proteins still remain unknown. FliP is the only protein that has a signal peptide in its N terminus. FliP has a molecular weight of about 26 kDa and is predicted to have four transmembrane helices (TM). FliP has a relative large periplasmic domain (FliPp) with ca. 8.5 kDa between TM-2 and TM-3. A deletion of FliPp results in a loss-of-function phenotype. We focused on FliPp to elucidate the role of FliP in flagellar protein export. Alanine-substitution of highly conserved residues of FliPp indicated that Glu-178 is critical for the export function. We constructed an E. coli expression system of FliPp from Thermotoga maritima for structural analysis. The results of size exclusion chromatography, static light scattering and analytical ultracentrifugation indicated that purified FliPp forms homo-tetramer. Far-UV CD spectra showed that the secondary structure is mostly α-helix. Crystallization for X-ray structural analysis is now in progress.

2PS006 2 種類の異なる固定子から構成されるべん毛モーターのトルク特性の解析

Torque-speed relationship of the flagellar motor consisting of two distinct stators

Naoya Terahara[1], Yukina Noguchi[2], Syuichi Nakamura[1], Nobunori Kamiike[1], Masahiro Ito[2], Keiichi Namba[1] ([1]*Graduate School of Frontier Biosciences, Osaka University*, [2]*Graduate School of Lifescience, Toyo University*)

The bacterial flagellum is an organelle for cell locomotion and consists of a helical propeller and a rotary motor at its base. The rotary motor is powered by electrochemical potential difference of ions across the cytoplasmic membrane. Rotational energy is mediated by inward ion flux through the channel of the stator complexes. Most bacterial flagellar motors are driven by the electrochemical gradient of H^+, and their stator complexes consist of MotA and MotB. It has been found recently that the Na^+-dependent stator required for the motility of alkaliphilic *Bacillus* is expressed from a pair of genes, *motPS*. Furthermore, *Bacillus subtilis*, which belongs to neutrophile, has not only *motAB* but also *motPS* on its genome. We have shown that *B. subtilis* MotPS plays a major role at an elevated pH, Na^+ concentration and viscosity, and that both MotAB and MotPS contribute in motility of *B. subtilis*. However, there has been no direct evidence to date that these two stator complexes coexist in the flagellar motor. We therefore measured the rotation speed of single motors by bead assay under various conditions to see whether these two stators actually work together in a motor. A spherical bead was attached to the sheared flagellar filament, and the rotation of the bead was followed by a photo-detector. Motor torque was calculated from the rotational speed, bead size and radius of the bead rotation. The details of the analyses will be reported at the conference.

2PS007 べん毛特異的分子シャペロン FlgN から紐解くⅢ型蛋白質輸送制御

Reading of the flagellar type III protein export regulation from a flagellar specific chaperone FlgN

Akira Hida (*Graduate School of Frontier Biosciences, Osaka University*)

The bacterial flagellum is a rotary motor for motility. It builds up with basal body, hook and filament. Most of flagellar component proteins are transported to outside the cell from inside by the flagellar type III protein export apparatus. It consists of six integral membrane protein (FlhA, FlhB, FliO, FliP, FliQ, FliR) and three soluble proteins (FliH, FliI, FliJ). In addition, FlgN, FliS, FliT and FliA act as flagellar specific chaperones. The export apparatus is considered to regulate the protein export.

FlgN binds to the hook-filament junction protein, FlgK and FlgL. FliS binds to the flilament protein FliC. FliT binds to the flilament cap protein FliD. These chaperones act as bodyguard to prevent their premature aggregation. Not only that, FlgN interacts with FliI, FliJ and FlhAC. Through FlgN interacting with FliI and $FlhA_C$, FlgN facilitates the export of FlgK and FlgL. Thus, FlgN seems to have many functions for the protein export regulation. In the same way, FliS and FliT too. However, most of the regulatory mechanism and chaperone's functions remains unknown in detail.

In previous time, to investigate the regulatory mechanism, we carried out genetic analysis of a Salmonella Δ*fliH-fliI flhB*(P28T) Δ*flgN* mutant and its suppressor mutants which have FlhA(D456V, T490M) and FliS(I7V, L114stop, W122stop). We are continuing its analysis. As a result, We thought that FlgN is the most important key protein to clarify the regulatory mechanism.

2PS008 Controlling Bacterial Flagellar Motor Rotation by Optical Spanner

Tsai-Shun Lin, Chien-Jung Lo (*National Central University*)

Bacterial Flagellar Motor (BFM) is a powerful molecular machine that can propel bacterium to swim in low Reynolds number environment. Many studies have focused on the mechanical properties of the BFM using electro-rotation and optical tweezers. However, due to the rotational nature of the motor motion, it's not easy to control the rotation by a symmetry external potential such as optical tweezer. The external torque can be applied to a micron size birefringent particle through circular-polarized light. We synthesize uniform vaterite micro particles with surface coating that can be attached to the bacterial flagella. While the motor rotates, we can apply external torque to accelerate/decelerate the motor. We will show our latest result of the torque speed relationship of single bacterial flagellar motor.

2PS009 Insights into myosin V stepping mechanism using point mutations in the converter

Sergey V. Mikhailenko[1], Takashi Ohki[1], Jun-ichi Yoshimoto[1], Shin'ichi Ishiwata[1,2,3] ([1]*Sch. Adv. Sci. Eng., Waseda Univ., Japan*, [2]*Org. Univ. Res. Initiatives, Waseda Univ., Japan*, [3]*WABIOS, Waseda Univ., Singapore*)

Dimeric myosin V is an intracellular transporter, which moves cargoes towards the barbed end of actin filaments in cells. Its ability to perform as individual molecules implies that the ATPase cycles in two head domains must be coordinated to ensure the efficient unidirectional motility. The kinetics of nucleotide binding to myosin V is directionally modulated by load, suggesting that the head-head communication may be achieved via intramolecular load generated when both heads are bound to actin. Here we used point mutations in the converter domain to directly test the effect of the intramolecular load on the processive stepping of myosin V. The converter is a compact structure, which transmits tiny conformational changes at the nucleotide-binding site to the lever arm. To disturb the transmission mechanism, we replaced with alanines, one at a time, two phenylalanine residues that form a hydrophobic cluster with the C-terminus of the relay helix. These mutations are inferred to reduce intramolecular load but affect neither the nucleotide binding nor actin affinity. We found that the F697A mutation, which completely eliminates intramolecular load, abolishes the motility of myosin V motors. At the same time, the F749A mutation, which only partly reduces intramolecular load, significantly increases the proportion of backward steps, providing strong experimental evidence that the efficient unidirectional processive stepping of myosin V is ensured by the head-head communication based on the intramolecular load.

2PS010 負荷存在下におけるアクチンーミオシン VI 相互作用の自由エネルギーランドスケープ解析

Free energy landscape analysis of the actin-myosin VI interaction under the applied force

Masahito Ikeo[1], Masaki Sasai[2], Tomoki P. Terada[2] ([1]*Dept. of Applied Physics, Grad. Sch. of Engineering, Nagoya Univ.*, [2]*Dept. of Computational Science and Engineering, Grad. Sch. of Engineering, Nagoya Univ.*)

Myosin VI moves toward the minus end of an actin filament, oppositely to the motions of myosin II and myosin V. Besides, the large step size (~36nm) of myosin VI, which has the short lever arms, suggests that the Brownian motion in the weakly bound state plays an important role in the search for the strong binding position on the actin filament.

A single molecule measurement using the single headed myosin VI (Iwaki *et al.*, *Nat. Chem. Biol.* 5, 403 (2009)) has shown that the probability of strong binding of myosin VI to the actin filament is dependent on the direction of the applied force. We here simulate this experimental situation by extending the methods which we previously used for simulating the Brownian movement of myosin II in the weakly bound state along the actin filament (Takano *et al.*, *PNAS* 107, 7769 (2010)). Using the coarse-grained model of the actin-myosin VI system, we performed Langevin molecular dynamics simulations to obtain the effective free energy landscape in the presence of the different forces applied to myosin VI. We examine the difference of actin-myosin interface between forward and backward pulling conditions and correlate this difference with the obtained effective free energy landscape. Finally, we also discuss on the importance of this difference in the context of reaction cycle of the myosin VI.

2PS011 ミオシン 6 の双機能性とレバーアーム構造の関係

Relation between myosin VI's dual functionality and its lever arm structures

Keigo Ikezaki[1,2], Tomotaka Komori[1], **Toshio Yanagida**[1,2,3,4] ([1]*Graduate School of Frontier Biosciences, Osaka University*, [2]*Quantitative Biology Center (QBiC), RIKEN*, [3]*Center for Information and Neural Networks (CiNet)*, [4]*WPI, Immunology Frontier Research Center*)

Myosin VI is a molecular motor which walks along actin filaments using the energy of ATP hydrolysis in a dimmer state. Myosin VI has unique aspects differ from other myosin families. As one of the functional aspects, myosin VI has two different rolls, a transporter and an anchor, in a cell. Recently, we performed simultaneous observations of myosin VI during steps which revealed that myosin VI has unique stepping mechanism taking both distant and adjacent binding states to the actin filament. We assume that this stepping mechanism is important for enabling its dual function. We also assume that myosin VI's lever arms, which has only two light chains, decrease a steric hindrance between them and enable to take the adjacent binding state for its dual function. Currently, to confirm this point, we are investigating the stepping behaviors of recombinant myosins which have modified lever arms.

2PS012 アクトミオシン活性に対する尿素とトリメチル N オキシドの中和効果

Counteractive effect of urea and trimethylamine N-oxide on the activity of the actomyosin motor

Kuniyuki Hatori, Ryusei Kumemoto (*Grad. Sch. Sci. Eng. Yamagata Univ.*)

It is known that urea induces unfolding of proteins with solvation whereas trimethylamine N-oxide (TMAO) stabilizes their structure due to peripheral hydration. In addition, deleterious effect of urea on the structure of certain proteins is completely counteracted by the presence of TMAO. We examined whether their counteraction is effective in actomyosin functions. CD spectroscopy showed that urea decreased unfolding transition temperature (Tm) of heavy meromyosin (HMM), on the other hand, TMAO increased its Tm. The decrease of Tm by 0.6 M urea was recovered by 0.3 M TMAO. Both urea and TMAO in the concentration range of 0-1.0 M considerably decreased the sliding velocity of actin filaments on HMM molecules under in vitro motility assay. Similarly, actin-activated ATPase activity was decreased by urea and TMAO although the ATPase activity of HMM alone was not suppressed. The urea-induced decrease of ATPase activation was further reduced by the addition of TMAO. Meanwhile, urea and TMAO were found to have counteractive effects on motility at concentrations of 0.6 M and 0.2 M, respectively. The difference of counteractive effects on HMM structure and on the motility suggest that water-related action in addition to the structural dynamics of HMM structure contributes to actomyosin activity.

2PS013 アクチン線維が滑走中のミオシン線維トラックからの ADP 遊離速度計測

Measurement of ADP release from bipolar myosin filament track along which actin filament slides

Takahiro Maruta, Hiroyuki Okubo, Takahiro Kobatake, Shigeru Chaen (*Department of Integrated Sciences in Physics and Biology, College of Humanities and Sciences, Nihon University*)

The motility assays have shown that along myosin thick filament, actin filaments moved at a fast speed towards the central bare zone and at a slower speed away from the bare zone. The force and displacement of myosin crossbridges interacting with actin filament in the backward direction was smaller than that in the forward direction. Sellers and Kachar speculated that myosin heads in the backward movement might rotate 180 degrees so as to face the actin in the right configuration, and might be constrained so that the detachment of the rotated heads from actin would occur at slower rate. Recently, we have found that the thermal activation energy of the backward movement was significantly higher than that of the forward movement, suggesting that the backward movement causes the myosin heads to be constrained, and increases the energy required for the ADP release step. However, there is no direct evidence for the slow ADP release rate in the backward movement. Here, in order to examine whether rate of ADP release step depends on the direction of the actin movement, we measured nucleotide turnover rates of bipolar myosin thick filament along which actin filament slides by monitoring the displacement of prebound fluorescent ATP analog, Cy3-EDA-ATP on flash photolysis of caged ATP.

2PS014 細胞性粘菌ミオシン II の SH1 ヘリックス領域の変異がその運動特性に与える影響

Effect of mutation of the SH1 helix region of Dictyosterium myosin II on the motile characteristics

Tsubasa Koyama[1], Takahiro Maruta[1], Sosuke Iwai[2], Shigeru Chaen[1] ([1]*Department of Integrated Sciences in Physics and Biology, College of Humanities and Sciences, Nihon University*, [2]*Department of Biology, Faculty of Education, Hirosaki university*)

A human myopathy has been reported to be caused by a point mutation in a fast myosin heavy chain gene. The mutation, glutamic acid to lysine at the 706th amino acid, is located at the SH1 helix region of the myosin II motor domain. The SH1 helix region acts as a linker for transmitting the structural changes of ATP-binding site in the catalysis domain to the lever arm. To investigate the effect of the mutation on the actin-myosin motility, we have introduced a corresponding mutation into the SH1 helix of Dictyosterium myosin II (E683K). The mutation resulted in a decrease in the actin-myosin sliding velocity (about 1/8 of the wild type), a decrease in thermal stability and the thermal aggregation of the myosin, which might be implicated in the disease process. This suggests that SH1 helix has an important function in the motor activity.

2PS015 ミオシン首振り運動の分子動力学シミュレーション

Molecular dynamics simulation for the swinging lever-arm motion of a myosin molecular motor

Tadashi Masuda (*Symbiotic Sys. Sci., Fukushima Univ.*)

I have proposed a theory called "Driven by Detachment (DbD)" mechanism for the working principle of myosin molecular motors. In this theory, the power stroke of myosin is not directly caused by the hydrolysis energy of ATP, but is produced by distortion in a myosin molecule, which is generated during the docking of myosin against an actin filament.

To verify the validity of this theory, a series of molecular dynamics (MD) simulation have been conducted. However, it was found that very long calculation time is necessary to generate the distortion in a myosin molecule during the docking process. Therefore, instead of directly producing the pre-power stroke configuration, external force was applied to the end of neck domain of a myosin molecule.

The MD software used was Gromacs code with its default Gromos96-43a1 force field and SPC water model. The initial structure of myosin was taken from PDB file 1M8Q. The AFM pull function of Gromacs was used to apply external force to the end of the neck domain toward the minus-end direction of an actin filament. The residues assumed to be engaged in the docking were fixed to the space.

When the applied force was 17 pN (10 kJ/(mol*nm^2)), the neck domain bent about 60 degrees around the junction between the head and neck domains after 48 nm. If the applied force was removed, the neck domain returned to the initial position. As shown in these simulations, the junction between the head and neck domains works as an elastic element that can produce the power stroke of myosin molecular motors.

2PS016 Movement of cortical actin cables is driven by type V myosins in fission yeast cells during interphase

Jun Kashiwazaki, Issei Mabuchi (*Dept. of Life Sci., Faclt. of Sci., Gakushuin Univ.*)

Actin cytoskeleton is involved in various cellular activities such as cell morphogenesis, membrane traffic, polarized growth and cytokinesis. In the fission yeast *Schizosaccharomyces pombe*, actin filaments form three major structures; patches, cables and contractile rings. During interphase, actin cables extend from the growing ends toward the cell equator. Although actin cables have been shown to be important for establishment of cell polarity, their detailed behavior has still not been clear. We found that thick actin bundles were formed 15 min after addition of the actin stabilizer, Jasplakinolide (Jasp), in interphase fission yeast cells. Interestingly, these actin bundles showed an oscillatory movement along the long axis of the cell. We aimed to elucidate the mechanism of this movement. Most of the actin bundles moved along cell cortex at a maximum speed of 0.14 ± 0.04 μm/sec. To identify factors which are involved in the movement of the actin bundles, we treated various mutant cells with Jasp. We found that type V myosins and the formin For3 are required for the rapid movement of actin bundles. Especially, Myo51/Myo5 (Win et al., 2001; Motegi et al., 2001), which is one of the two type V myosins in fission yeast, colocalized with actin cables at the cell cortex. These results suggest that actin cables elongating from ends of interphase cells are guided toward the mid-region by cortical type V myosins.

2PS017 Contribution of the conformational change of myosin II in the coupled sliding and binding process of the force-generation

Qing-Miao Nie[1,2,3], Masaki Sasai[1], Tomoki P. Tereda[1] ([1]*Dept. of Comp. Sci. Eng., Nagoya Univ., Chikusa-Ku, Nagoya 464-8603, Japan*, [2]*Institute for Molecular Science, Okazaki 444-8585, Japan*, [3]*Dept. of Applied Physics, Zhejiang Univ. of Tech., Hangzhou 310023, China*)

The mechanism of the actomyosin motor is still under debate. In the most widely believed lever-arm model, it has been hypothesized that the mechanical force is generated by the conformational change of the myosin head which is strongly bound to the actin filament. In contrast, a single molecule observation has shown that the unidirectional Brownian motion of the myosin head, while keeping weakly bound to the actin filament (Kitamura et al., Nature (1999)). Furthermore, a molecular dynamics simulation study has suggested that the unidirectional Brownian motion is indeed possible due to the asymmetric slope of the energy landscape arising from the electrostatic interaction between actin and myosin (Takano et al., PNAS (2010)). In that simulation, however, the

contribution of the large conformational change of the myosin head has not been investigated in depth. In the present study, to resolve the controversy between the lever-arm model and the unidirectional Brownian motion model, we study the contribution of the conformational change of myosin head during the coupled sliding/binding motion of myosin on the actin filament. The structural ensemble of actin-myosin complex is sampled with a coarse-grained model with Go-like interactions, and the free energy landscapes of the three different chemical states of myosin are calculated. The coupling of the conformational change of the myosin head and the process of the weak-to-strong binding to the actin filament is also investigated using a double-well structure-based model of myosin head.

2PS018 コフィリンと HMM のアクチンフィラメントへの相互排他的な協同的結合はアクチンフィラメントの協同的構造変化に依存する

Cooperative conformational changes of actin filaments drive mutually exclusive cooperative binding of cofilin and HMM to the filaments

Nobuhisa Umeki, Taro Uyeda (*Advanced Industrial Science and Technology*)

Cofilin and HMM of myosin II both bind to actin filaments cooperatively. There is ample evidence that HMM or S1 causes cooperative conformational changes of actin filaments, but corresponding biochemical evidence for cofilin-induced cooperative conformational changes was lacking. Thus, we made copolymers of cofilin-actin fusion protein and actin, and found that fluorescence of pyrene attached to actin was quenched, and DNase loop of actin became more susceptible to subtilisin cleavage, demonstrating cooperative conformational changes induced by cofilin. Cosedimentation assay showed that copolymerization with cofilin-actin increases affinity of actin to cofilin, indicating that conformational changes induced by cofilin attracts further cofilin binding through a domino effect. In contrast, copolymerization with acto-S1 fusion protein decreased the affinity of actin for cofilin while increased the affinity for HMM in 1 mM ADP + 0.1 mM ATP. These results indicate that cooperative conformational changes induced by cofilin or S1 is the basis for cooperative binding of cofilin and HMM to actin filaments. Furthermore, these data as well as those of fluorescence microscopy (Nishikawa et al., this meeting) indicate that cooperative binding of cofilin and HMM for actin filaments is mutually exclusive. We suggest that these positive and negative effects that the binding of a specific actin binding protein exerts on the binding of the same or other actin binding proteins is involved in functional differentiation of actin filaments in vivo.

2PS019 分子数を制御したキネシンとダイニンの綱引きによる積極的な両方向性運動の再構成

Reconstitution of tug-of-war between defined numbers of kinesin and dynein as active bidirectional transport

Kazuyuki Yamamoto[1], Ken'ya Furuta[2], Hajime Honda[1], Hiroaki Kojima[2] ([1]*Department of Bioengineering, Nagaoka University of Technology*, [2]*Bio ICT lab, NICT*)

Microtubule-based intracellular transport is fundamental for many biological processes. The transport is typically achieved by the cooperation of oppositely directed motor proteins, kinesins and dyneins that are engaged to the same cargo. Strikingly, many cargos move bidirectionally, alternating frequently between plus end- and minus end-directed motion. Because this property appears ineffective in delivering a cargo, many researchers are now asking how such active fluctuations of the cargo contribute delivery to its destination via the complex microtubule network. In the cell, it is extremely difficult to identify the number and class of engaging motor on moving cargos, much less the presence of various regulatory factors. To circumvent this problem, we constructed minimal assemblies containing defined numbers of kinesin and dynein on single DNA scaffolds, so that we can clearly quantify the effect of linking oppositely directed motor proteins together in vitro. To construct the motor assemblies, we linked recombinant human kinesin-1 and cytoplasmic dynein 1 by DNA scaffolds containing up to 5 binding sites. Using a total internal reflection fluorescence microscope, we show that dynein-kinesin assemblies displayed stochastic, bidirectional motion along microtubules, which was reminiscent of typical intracellular transport. Further analysis to evaluate the performance of these assemblies on an artificial microtubule network will be presented.

2PS020 Ascaris 精子をもちいたアメーバ運動装置の in vitro 再構成
1YS0945 Simultaneous reconstitution of MSP-based protrusion and retraction in the amoeboid sperm of Ascaris

Katsuya Shimabukuro[1,2], Naoki Noda[3], Masasuke Yoshida[2,4], Murray Stewart[5], Thomas M. Roberts[6] ([1]*Ube Nat. Colg. Tech.*, [2]*ICORP, JST*, [3]*MBL*, [4]*Kyoto Sangyo Univ.*, [5]*MRC*, [6]*Florida St. Univ.*)

Crawling movement in eukaryotic cells requires coordination of the force for leading edge protrusion with that for cell body retraction. In Ascaris sperm, protrusion and retraction are powered by a motility system comprised of major sperm protein (MSP) in place of the actin apparatus typically associated with cell migration. By adjusting the concentration of cell-free sperm extracts, we reconstituted protrusion and retraction simultaneously in MSP filament meshworks, called fibers, that assemble behind plasma membrane-derived vesicles. As polymerization of filaments at the growing end of the fiber pushed the vesicle ahead (protrusion), filament rearrangement and disassembly pulled the rear of the fiber forward (retraction). Because nematode sperm do not use motor proteins to power retraction, we used these fibers to explore the mechanism of retraction by focusing on the cytoskeletal dynamics that occur during the transition from protrusion to retraction. Using a combination of fluorescent speckle microscopy, electron tomography, and advanced polarization microscopy, we found that although fibers progressively lost filaments during retraction the average length of the filaments did not change. The surviving filaments were able to move and reorient so that their packing density was conserved. To do so, fewer filaments packed into a smaller volume and this rearrangement appears to provide the driving force for retraction.

2PS021 Identification of leg and crank proteins of Mycoplasma mobile on gliding machinery by electron microscopy

Hiroki Yamamoto, Makoto Miyata (*Graduate School of Science, Osaka City University*)

Mycoplasma mobile, a fish pathogen, glides by a unique mechanism based on three huge proteins unrelated to conventional motor proteins. To date, the “leg” structure on the surface of the gliding machinery and the molecular shapes of isolated component proteins have been clarified, by freeze-fracture electron microscopy and rotary-shadowing electron microscopy, respectively. However, the whole structure of the machinery or the assignment of component proteins in the machinery has been unknown. In the annual meeting of last year, we reduced background by using volatile buffer and digested scaffold proteins, and then succeeded in visualizing the machinery by negative-staining electron microscopy. In this year, we achieved higher contrast images by (i) rotary-shadowing and (ii) negative-staining in the absence of scaffold proteins. The observation of each mutant lacking one of Gli349, Gli521 or Gli123 suggested that Gli349, a “leg” protein is sticking flexibly and irregularly from the machinery surface with 2-3 nm thickness and 30-80 nm length, and Gli521, a crank protein is aligned in 5 nm parallel to the cell membrane with 3 nm diameter.

2PS022 ヒト肺炎 *Mycoplasma pneumoniae* の滑走運動装置と構成タンパク質の構造解析

Structural analysis of gliding machinery and component proteins of *Mycoplasma pneumoniae*

Yoshito Kawakita[1], Daisuke Nakane[1], Lisa Matsuo[1], Tsuyoshi Kenri[2], Makoto Miyata[1] ([1]*Osaka City University*, [2]*National Institute of Infectious Diseases*)

Mycoplasma pneumonia, a human pathogenic bacterium glides with repeated catch and release of sialylated oligosaccharides on host cell surfaces. At a pole, this organism forms a membrane protrusion, the attachment organelle which is composed of a surface receptor, named P1 adhesin, and the internal rod structure. The rod structure can be devided into three parts, Terminal button, Paired plates, and Wheel complex from the tip. In the present study, we identified two novel component proteins of the rod structure, and assigned eleven component proteins onto the organelle, based on the data of peptide mass fingerprinting, YFP fusion, and electron microscopy. Next, we expressed and purified four Wheel complex proteins coded by MPN311, MPN312, MPN387 and MPN526, a Terminal button protein coded by MPN309 and P1 adhesin coded by MPN141, for crystallization. We used chemically synthesized genes to solve the codon problems and induced these genes in *Escherichia coli* at a low temperature, and obtained pure proteins, of which the proteins of MPN311 and MPN387 showed high solubility and yields.

2PS023 *Mycoplasma mobile* の滑走運動に方向性を持たせる“あし”の結合

Directed binding of *Mycoplasma mobile* may cause directed displacement in gliding

Akihiro Tanaka[1], Daisuke Nakane[1], Takayuki Nishizaka[2], Makoto Miyata[1] ([1]*Graduate School of Science, Osaka City University*, [2]*Faculty of Science, Gakushuin University*)

Mycoplasma mobile, a pathogenic bacterium forms membrane protrusion, the gliding machinery, and glides on solid surface smoothly up to 4.5 μm/s and 27 pN in the direction of protrusion. *M. mobile* is thought to glide by repeated catch-pull-release of sialylated oligosaccharide fixed on solid surface by hundreds of 50 nm flexible legs sticking out from the gliding machinery. However, the directed displacement of cell is difficult to explain, because the legs are flexible. To elucidate this mystery, we examined a starved cell binding to sialylated oligosaccharide, by pulling forward and backward at a speed of 160 nm/s, using a bead manipulated by a laser trap. Tension was generated at similar rate for forward and backward, 0.09 ± 0.03 pN/nm. In these processes, the tension occasionally shifted down, suggesting temporal detachment of legs from sialylated oligosaccharide fixed on solid surface, namely "slippage". The slippage occurred at tension of averages, 22.5 ± 13.9 pN and 48.4 ± 28.0 pN for forward and backward, respectively, whereas no significant difference was found in the occasional decrease in tension between both directions. The tension at slippage did not differ significantly between directions, when two types of non binding mutants lacking valid legs were artificially bound to glass. These results suggest that *M. mobile* binds to solid surface in a direction dependent manner, and this directed binding may cause the directed gliding.

2PS024 Leg movements suggested from inhibition of mycoplasma gliding by free sialylated oligosaccharid

Taishi Kasai[1], Daisuke Nakane[1], Hideharu Ishida[2], Hiromune Ando[2,3], Makoto Kiso[2,3], Makoto Miyata[1] ([1]*Graduate School of Science, Osaka City University*, [2]*Faculty of Applied Biological Sciences, Gifu University*, [3]*iCeMS, Kyoto University*)

Mycoplasmas, known as a pathogen of human pneumonia, bind to solid surfaces and glide to one direction. In gliding, mycoplasmas catch sialylated oligosaccharides, the common target of many pathogens. In previous studies, we analyzed the inhibitory effects of synthesized sialylated oligosaccharide on binding of gliding mycoplasmas and concluded the affinity, the cooperativity, and the recognized structure. In the present study, we analyzed the effects of those compounds to the gliding of *M. mobile* cells, to know the relationship between sialylated oligosaccharide binding and the gliding mechanism. Gliding speed was reduced by the addition of sialylated oligosaccharide with time, and the decrease appeared accelerated with time after the decrease became obvious. The decrease in gliding speed should be caused by the decrease in the working legs in the addition of free sialylated compound. The acceleration in decrease may suggest that the binding inhibition of a leg affect the affinity of neighboring legs. The cells showed pivoting around the gliding machinery before the detach. The shortage of propelling force caused by the free sialylated oligosaccharide may induce remaining of legs after stroke on glass, some of which form the center of cell pivoting. All of these results support our assumption that the leg after stroke should be removed by the continuous cell movement caused by other legs in the gliding mechanism.

2PS025 Swarm Dynamics of Vibrio alginolyticus

Szu-Ning Lin, Chien-Jung Lo (*Department of Physics and Institute of Biophysics, National Central University, Taoyuan County 32001, Taiwan*)

Swarming is an important step for bacterial colonization and spreading. We investigate the swarming dynamics of the dual flagellated bacterium, Vibrio alginolyticus, in different growing stages and external conditions. While growing on agar surface, Vibrio alginolyticus elongate and synthesize lateral flagella that can move rapidly in the thin liquid layer above agar. The cell motion is constrained by the cell to cell interaction and hydro-dynamical interaction with the liquid boundary conditions. We measured the colony spreading speed and the single cell motility in different growing stages and agar concentrations. The cells lengths are widely distributed. The cell density is higher in the colony edge. Edge-cells show parallel alignments while interior-cells show swirling motion with different time and length scale. We found the edge-cells shows waving while the interior-cells shows turbulent like collective motion. Far behind the spreading edge, cell density reduced down to single-cell layer. We exam the collective motion and cluster size distribution in this condition. Vibrio alginolyticus shows different motility dynamics in different growing stage. We aim to build up a simply model to explain the collective motion of Vibrio alginolyticus.

2PS026 表面タンパク質のらせん流で動くバクテリア

Helical Flow of Surface Protein Required for Bacterial Locomotion

Daisuke Nakane[1], Keiko Sato[1], Hirofumi Wada[2], Mark J. McBride[3], Koji Nakayama[1] ([1]*Grad. Sch. Biomedical Sci., Univ. Nagasaki*, [2]*Dept. Phys., Univ. Ritsumeikan*, [3]*Dept. Biological Sci., Univ. Wisconsin-Milwaukee*)

A large group of bacteria belonging to the phylum *Bacteroidetes* show a characteristic rapid surface movement known as gliding motility. Bacteroidetes gliding motility is different from other motility systems, but its mechanism is unknown. Here, we visualized the dynamics of cell adhesin SprB, and proposed "helical loop track" to explain the motility.

A soil bacterium, *Flavobacterium johnsoniae* has a 669 kDa cell-surface adhesin, SprB, which is responsible for the gliding motility and cell adhesion. Electron microscopic experiments revealed that SprB formed 150 nm long filaments, and dynamic movements of SprB were observed by fluorescence microscopy. SprB was located dispersedly on a long pitch of helical loop along the membrane, and moved on the cell surface along an apparent right-handed helical closed loop. When the apparent velocities of SprB signals were determined with respect to the glass substratum, about half of the SprB signals moved with velocities of 3.4 μm/s and the other half moved with velocities of -0.5 μm/s. Taking the velocity of cells (1.9 μm/s) into consideration, SprB signals migrating in opposite directions appeared to move at the similar speeds with respect to the cell. The results suggest a model for Flavobacterium gliding, supported by mathematical analyses, in which adhesins always moved on an endless right-handed helical track at a constant speed, while some SprB tightly bound to the solid surface, generating rotation and translation of the cell.

2PS027 Gene manipulation of gliding bacterium, *Mycoplasma mobile*

Isil Tulum, Atsuko Uenoyama, Makoto Miyata (*Graduate School of Science, Osaka City University*)

Mycoplasma mobile, a pathogenic bacterium, glides on solid surfaces with a unique mechanism, not related to known bacterial motility systems or conventional motor proteins. The gliding machinery is composed of three huge surface proteins and more than ten internal proteins. To elucidate the gliding mechanism and the roles of component proteins, the genetic manipulation including homologous recombination should be a powerful tool. However, this organism has not been transformed so far by standard procedures used for other *Mycoplasma* species. In this study, we examined and improved the steps of transformation as follows. (i) The electroporation conditions have been adjusted to fit to the *M. mobile* cells which are much tougher than the other species. (ii) The recovery time after electroporation was elongated from 2 h to 12 h. (iii) The growth medium was modified to get clearer colony shapes. Then, we achieved the transformation of *M. mobile* with efficiencies ranging 10^{-5} to 10^{-7} per competent cells by 10 μg of vector DNA, and also fluorescence labeling of cells by using enhanced yellow fluorescent protein (EYFP). We are constructing special vectors allowing us gene expression and homologous recombination.

2PS028 低温電子線トモグラフィーによって明らかとなった細菌べん毛蛋白質輸送装置の構造と機能

Structure and function of bacterial flagellar protein export apparatus revealed by electron cryotomography of *Salmonella* minicells

Akihiro Kawamoto[1,2], Yusuke V. Morimoto[1,2], Takayuki Kato[2], Kelly T. Hughes[3], Toshio Yanagida[1,2], Keiichi Namba[1,2] ([1]*QBiC., RIKEN*, [2]*Grad. Sch. of Frontier Biosci., Osaka Univ*, [3]*Dept. Med. Sci., Univ. Fribourg*)

The bacterial flagellum is a motility organelle composed of a basal body that functions as a rotary motor and a long helical filament that works as a propeller. Most of flagellar axial proteins are translocated into the central channel of the growing flagellum for self-assembly at the distal end by the flagellar protein export apparatus. A structural study on many different types of intact flagellar basal bodies by electron cryotomography (ECT) has suggested that the export apparatus is highly conserved in their structures across species. However, soluble components of the export apparatus have not yet been clearly observed in the basal body of *Salmonella entrica* because the wild-type cell is about 1 μm in diameter, which is too thick to visualize the intracellular structures by ECT in detail. To visualize the structure of the export apparatus in the cell, we constructed *Salmonella* minicell by overproducing FtsZ to make the cell small enough for a high-resolution ECT analysis and carried out the structural analysis

of intact flagellar basal body. Comparison with the structure of a purified basal body revealed the density of the export platform and the ring structure derived from FliI within and below the C ring. The flagellar basal body of the Δ*fliH-fliI*-bypass mutant, which maintaines flagellar protein export and motility in the absence of FliH and FliI showed that the two densities within and below the C ring were completely lost,suggesting that the platform structure is not essential for flagellar protein export.

2PS029 細菌べん毛モーターの固定子組込み機構に対する MotB(D33N)点変異の影響

Effect of the D33N mutation in MotB on stator assembly of the bacterial flagellar motor

Shuichi Nakamura[1], Tohru Minamino[2], Nobunori Kami-ike[2], Seishi Kudo[1], Keiichi Namba[2,3] ([1]*Department of Applied Physics, Tohoku University*, [2]*Graduate School of Frontier Bioscience, Osaka University*, [3]*Riken Quantitative Biology Center*)

The bacterial flagellar motor converts the energy of proton translocation across the membrane through the proton-channel stator complex into torque. The MotA/B proton channel complex is firmly anchored to the peptidoglycan (PG) layer through the PG-binding domain of MotB to act as the stator of the motor. The stator units dynamically associate with and dissociate from the motor during flagellar motor rotation, and an electrostatic interaction between MotA and a rotor protein FliG is required for efficient stator assembly. However, the association and dissociation mechanism of the stator units still remains unclear. In this study, we analyzed the speed fluctuation of the flagellar motor of Salmonella enterica wild-type cells carrying a plasmid encoding a nonfunctional stator unit, MotA/MotB(D33N), which lost the proton conductivity. The wild-type motor rotated stably but the motor speed fluctuated considerably when the expression level of the MotA/B(D33N) stator was increased. Rapid accelerations and decelerations were also observed. These results suggest that the MotA/B(D33N) stator retains the ability to associate with the motor but rapidly dissociates from it as well. We propose that the stator dissociation process depends on the proton translocation through the proton channel.

2PS030 MS リングに突然変異が生じたサルモネラ菌べん毛モータの構造安定性と出力特性

Structural stability and rotational characteristics of the flagellar motor of Salmonella MS-ring mutant

Shun Taga[1], Akira Asaumi[1], Shuichi Nakamura[1], Fumio Hayashi[2], Kenji Oosawa[2], Seishi Kudo[1] ([1]*Department of Applied Physics Tohoku University*, [2]*Department of Chemistry and Chemical Biology Gunma University*)

The bacterial flagellar motor is a rotary nanomachine fueled by the proton motive force. Two ring structures, MS ring and C ring, together act as a rotor, and responsible for torque generation by interacting with a stator complex consisting of MotA and MotB. It has been known that the flagella of a Salmonella FliF mutant are fragile as compared with those of wild-type strain, suggesting that the MS ring plays an important role in keeping stability of the motor structure. In this study, the mechanical strength and the rotational characteristics of the FliF mutant motor were analyzed to understand how MS ring is involved in the structural stability. Quantitative measurement of the strength revealed that the mechanical strength of the FliF mutant motor decreases up to a half of wild-type motor. However, both the swimming speed and the motor speed of the FliF mutant were almost same with those of wild-type strain. These suggest that the defect of MS ring can decrease the structural stability of flagellar motor without impairment of torque generation.

2PS031 The role of the flagellar C ring in hook-length control by FliK

Kaoru Uchida, Tatsuya Yamasaki, Shin-Ichi Aizawa (*Grad. Sch. Pref. Univ. Hiroshima*)

The flagellar hook has an average length of 55 nm, which is controlled mainly by FliK. We previously demonstrated that mutations of any one of the fliG, fliM, and fliN genes gave rise to short hooks in Salmonella enterica serover Typimurium. FliG, FliM, and FliN form the cytoplasmic ring (C ring) at the flagellar base, which is a multifunctional structure necessary for flagellar protein secretion, torque generation, and switching of the motor rotation. We also showed that hook length of the C-ring deficient mutants broadly distributes around 55 nm, suggesting a tight length-control by the C ring. In order to elucidate the role of the C ring in hook-length control, we introduced two modified fliK constructs into C-ring mutants. A recombinant FliK with the size of 373 a.a. produced short hooks and the other recombinant FliK with the size of 570 a.a. produced long hooks, suggesting that FliK is dominant in hook length control even in the C ring mutants. However, the hook length in C-ring mutants varied in wider range than that of the wild type. We will be discussing the interaction between the C ring and FliK.

2PS032 べん毛モーターのトルク発生器における帯電残基の性質

Characterization of the electrically-charged residues in the torque-generating unit of the flagellar motor

Satoshi Inaba, Shin-Ichi Aizawa (*Prefectural University of Hiroshima*)

FliG is one of the rotor components of the flagellar motor in *Salmonella enterica serovar Typhimurium*. It is said that five conserved charged residues (K264, R281, D288, D289, R297) in the C-terminal domain of FliG are directly involved in torque generation. These five charged residues formed a ridge on the surface of the domain. Among these residues, R281, D288 and D289 are belonging to the same α-helix. R281X and D288X/D289X gave rise to motility-defective mutants by substitution with either Thr or Ala. In order to examine the functional roles in detail of the residues R281 and R288/R289, we substituted these residues with all 20 amino acids.

Among variants of R281X, four (R281D, E, G, and P) were Mot$^-$, and the rest swam at various speeds. Distribution of their rotational speeds continuously dispersed in a wide range, indicating that torque generated in the motor may change according to changes in conformation near the R281 site. Among D288X/D289X pair variants, three pairs (D288E/D289E, S/S, Y/Y) swam, while the rest were Mot$^-$. To fill the gap between R281 and D289, we chose D284 and I285 and substituted them with 20 a.a. The variants I285D, R, T swarmed. The variants D284E, F, R, and V swarmed. These results indicate that D284 and I285 at the middle of the α-helix are not directly involved in torque generation. In summary, a pair of D288/D289 residues might be the major element of the torque generator, and that R281 residue might play a subsidiary role in the torque generator.

2PS033 Meaning of HAP1 in the length measurement of the hook

Kohei Dono, Kaoru Uchida, Sin-Ichi Aizawa (*Grad. Sch., Pref. Univ. Hiroshima*)

In the bacterial flagella, the hook occupies a region between the rod and HAP1 in an average length of 55 nm to connect the filament to the basal body. The hook is composed of FlgE. We analyzed the hook in a temperature-sensitive flgE mutant of Salmonella enterica seover Typhimurium. The mutant cells produced wild-type flagella when grown at 30 ℃ but short hooks without filaments at 37℃. We found by electron microscopy that the mutant hooks produced at 30℃ had wild-type length (average length: 55 nm) in intact flagella, whereas they were shorter (45 nm) in the hook basal body (HBB) obtained by acid treatment of intact flagella. SDS-PAGE showed that the HBB preparation did not contain HAP1 that is supposedly attached on the distal end of wild-type hook, indicating that interaction between the mutant hook and HAP1 might becoma weaker by a mutation of the hook protein. As a consequence, we learned that the hook length that we have so far measured was length of the hook region including HAP1, and that authentic hook length was about 45 nm and HAP1 length was about 10 nm in the wild-type "hook". The HAP region (HAP1 and HAP3) in intact flagella is distinguishable from the hook and filament by its appearance and thin width. However, surface appearance of the HAP region resembles that of the hook than the filament, which led us to measure hook length including HAP1. We will show length distribution of HAP region in wild type and mutants.

2PS034 コフィリンのアクチン線維への協同的結合の直接観察

Direct observation of cooperative binding of cofilin to actin filaments

Kimihide Hayakawa[1], Hitoshi Tatsumi[2], Takafumi Goto[2], Masahiro Sokabe[1,2] ([1]*FIRST Research Center for Innovative Nanobiodevice, Nagoya Univ.*, [2]*Dept. of Physiol., Nagoya Univ. Grad. Sch. of Med.*)

ADF/cofilin proteins are ubiquitously distributed actin severing proteins in eukaryotic cells. Several biochemical and electron microscopic studies have suggested that cofilin binds to the actin filament in a cooperative manner. We directly observed the binding of single Alexa-labeled cofilin molecules to actin filaments in solution by a single molecule imaging technique. We analyzed the non-contiguous (isolated, non-cooperative) cofilin binding to an actin filament

using low concentration of cofilin (10 nM-100 nM), in which measurement of the binding was made on a short segment (600 nm in length) in the filament The rate constant of cofilin binding to the actin filament was estimated at 0.06/ μM^-1s^-1, which agrees with the value obtained with biochemical techniques. The rate constant elevated to 0.18/ μM^-1s^-1 when the concentration of cofilin was increased to 10 μM. This result indicates that our single molecule measurements could detect the process of the cooperative binding of cofilin in solution. In low cofilin concentrations (10 nM-100 nM), long lasting cofilin bindings followed by a subsequent cofilin binding in the same segment (600 nm) of the filament were observed. While the rate constant of the preceding cofilin binding was 0.06/ μM^-1s^-1, the rate constant of the subsequent cofilin binding was elevated to 0.18/ μM^-1s^-1. This result suggests the binding of cofilin to the actin filament accelerates the binding of another cofilin to the neighboring (less than 600 nm) binding site on the actin filament.

2PS035 微小管結合蛋白質 4 を介したアクチンフィラメントと微小管の相互作用の解析

Analysis of microtubule-associated protein 4-mediated interaction between actin filaments and microtubules

Shoma Saito[1], Ayumu Kuramoto[1], Tsuyoshi Yamasaki[2], Taro Q.P. Noguchi[2], Yurika Hashi[3], Susumu Kotani[3], Kiyotaka Tokuraku[1] ([1]*Grad. Sch. Appl. sci., Muroran Inst.*, [2]*Miyakonojo Nation. Col. Tech.*, [3]*Kanagawa Univ.*)

Microtubule-associated protein (MAP) 4 is a non-neural MAP that plays important role in the intracellular organization of microtubules. Recent study revealed that MAP4 also binds to actin filaments, but not actin monomer, at the C-terminal part of the Proline-rich region in the microtubule-binding domain (Matsushima et al., J.Biochem., 2012). Since the binding affinity of MAP4 for actin filaments was the same order with that for microtubules, we believed that the interaction of MAP4 to actin filaments was physiologically significant. In this study, we examined MAP4 functions when both actin filaments and microtubules (or unpolymerized tubulin) coexisted in a sample. To distinguish actin filaments and microtubules under fluorescence microscopy, these filaments were labeled with different fluorescent dyes. When microtubules were mixed with actin filaments that preincubated with MAP4, bundles consisted of both microtubules and actin filaments were observed. Moreover, when unpolymerized tubulin instead of microtubules was mixed with actin filaments that preincubated with MAP4, elongation of microtubules along the actin filaments was observed. These results suggest that MAP4 bound to actin filaments retain microtubule binding and microtubule assembly-promoting activities. On the other hand, when actin filaments were mixed with microtubules that preincubated with MAP4, bundles containing both actin filaments and microtubules were not observed, suggesting that MAP4 bound to microtubules lost actin filament-binding activity.

2PS036 血管平滑筋細胞から単離したストレスファイバの収縮特性の計測

Measurement of contractile properties of stress fibers isolated from vascular smooth muscle cells

Tsubasa S. Matsui[1], Daiki Komatsu[2], Masaaki Sato[3], Shinji Deguchi[2] ([1]*Grad. Sch. Life Sci., Tohoku Univ.*, [2]*Grad. Sch. Eng., Tohoku Univ.*, [3]*Grad. Sch. Biomed. Eng., Tohoku Univ.*)

Several lines of evidence have suggested a critical involvement of nonmuscle myosin II in the fundamental cellular functions of proliferation, differentiation, and apoptosis. In nonmuscle cells, nonmuscle myosin II forms stress fibers (SFs) along with actin filaments and exerts contractile forces on the extracellular matrix. Compared to increasing reports studied at the whole cell level, the contractile properties intrinsic to SFs themselves remain poorly understood. In the present study, we characterized the contractile properties of single SFs isolated from cultured vascular smooth muscle cells. SFs were extracted from the cells treated with hypotonic buffers and detergents. Western blotting showed that main constituents of SFs were maintained in the isolated materials. We manipulated the isolated SFs by using two fine glass needles and measured their contractile forces under physiological MgATP concentrations. The results showed that SFs could generate forces of several tens of nano-Newtons. SFs suddenly relaxed at high MgATP concentrations, and some fragments of F-actin were dissociated from the SFs. Interestingly, we observed rotational motions of SFs under passive stretch as well as active contraction conditions. These results may be useful in the understanding the biophysical roles of SFs in cell behavior.

2PS037 IQGAP confines myosin-II to the cytokinetic contractile ring

Masak Takaine, Osamu Numata, Kentaro Nakano (*Grad. Sch. Life & Env. Sci., Univ. Tsukuba*)

During cytokinesis, myosin-II concentrates at the equatorial cortex with actin filaments (F-actin) and is supposed to generate forces to divide the cell into two, which is called the contractile ring (CR) hypothesis. Several lines of evidence indicate F-actin-independent recruitment of myosin-II and its specific interaction with the equatorial F-actin, although their details are still unknown. We investigate the dual regulation of myosin-II localization using the fission yeast S. pombe. IQGAP Rng2 is implicated both in the F-actin-independent recruitment of myosin-II to cortical dots and in its sufficient concentration on CR F-actin. Rng2 is required for the dot localization of Myo2 (the essential myosin-II) via its tail. Rng2 shows a slower exchange rate and lower mobility than Myo2. Myo2 is inhomogenous and unstable in CR of the rng2 mutant and preferably associates with ectopic F-actin induced by overexpression of the actin-modulating moiety of Rng2, Rng2Ns. Biochemically, Rng2Ns slows actin-activated Mg-ATPase of myosin-II. These results suggest that Rng2 tethers the Myo2 tail to cortical dots and accumulates myosin-II to CR F-actin by modulating its ATPase-coupled turnover.

2PS038 キネシン Eg5 に対するフォトクロミック阻害剤を用いた細胞分裂の光制御

Photo-regulation of cell division using photochromic inhibitors for kinesin Eg5

Kei Sadakane[1], Kumiko Ishikawa[1], Hideo Seo[1], Banri Yamanoha[2], Shinsaku Maruta[1] ([1]*Division of Bioinfomatics, Graduate school of engneering, Soka University*, [2]*Department of development of environmental engineering , Faculty of engineering, Soka University*)

Previously it has been demonstrated that some ATP driven motor proteins kinesins are directly involved in regulation of the cell division cycle. Eg5 is one of the kinesin and its biochemical properties and structure were well studied. Interestingly Eg5 is activated in M phase of cell cycle and performs stabilizing and positioning of spindle. It is also known that Eg5 is overexpressed in tumor cell and induce significant. Monastrol and STLC, which are potent inhibitor specific for kinesin Eg5 ATPase activity, shut off mitotic division and result in apotosis. Therefore, these inhibitors are attracting as anti-cancer drug. Azobenzene and spiropyran, a widely studied photochromic compound, can be reversibly isomerized between the cis and trans forms by ultra-violet (UV) and visible (VIS) light irradiation, respectively. We have recently demonstrated the Monastrol and STLC analogues composed of photochromic molecules inhibit ATPase activity Eg5 reversibly upon UV and VIS light irradiation in vitro. Therefore, it is strongly expected that the photochromic inhibitors are applicable to reversible photo-regulation of cell mitosis. In this study, we have examined the effects of the photochromic inhibitors for mammalian cells. Effects of the photo-chromic inhibitors were evaluated by survival number of mammalian cells, HeLa cells or A172 cells. The experimental results suggested that the effects of photo-chromic inhibitor for cell division were controlled by UV and VIS light reversibly.

2PS039 蛍光顕微鏡観察による細胞性粘菌由来のコフィリン、HMM と F-actin の協同的相互作用の解析

Analysis of cooperative interaction of Dictyostelium-derived cofilin and HMM to F-actin using fluorescence microscopy

Yusuke Nishikawa[1], Ayumi Satoh[1], Taro Q.P. Ueda[2], Kiyotaka Tokuraku[1] ([1]*Grad. Sch. Appl. Sci., Muroran Inst.*, [2]*Nation. Inst. Adv. Indust. Sci. Tech.*)

In crawling cells, cofilin and myosin II are localized in the anterior and posterior regions, respectively. It has not been understood the molecular mechanism of the differential localization so far. In the last meeting, we reported that cooperative binding of cofilin and HMM for F-actin was mutually exclusive, and concluded that the mutually exclusive binding might contribute to the differential localization of cofilin and myosin II. However, since the cooperative binding was analyzed by use of proteins derived from different origins, such as human cofilin, Dictyostelium HMM, and rabbit actin, it has been remained a concern that the cooperative interaction containing the mutually exclusive binding is not a physiological phenomenon. In this study, therefore, we used proteins derived from only Dictyostelium to analyze the cooperative interaction. To visualize cofilin and HMM, we prepared recombinant Dictyostelium cofilin (D-cofilin) and HMM (D-HMM) fused with mCherry and GFP, respectively. Actin was purified from Dictyostelium (D-actin) or rabbit (R-actin), and was labeled with fluorescent-phalloidins. The cooperative binding for 40 nM F-D-actin was observed in the range of 100-150 nM D-cofilin. The cooperative

binding of D-cofilin was also observed for F-R-actin, suggesting that the cooperative binding of cofilin was not origin-dependent phenomenon. We are now examining the cooperative binding of D-HMM to F-D-actin. We will present detailed data of the cooperative interactions containing mutually exclusive binding at this meeting.

2PS040 棘皮動物コラーゲン性のキャッチ結合組織における可逆的な硬さ変化の分子機構

Molecular mechanisms of reversible changes in stiffness of echinoderm collagenous 'catch' connective tissues

Akira Yamada[1], Yasuhiro Takehana[2], Masaki Tamori[2], Tatsuo Motokawa[2] ([1]*Adv. ICT Res. Inst., NICT*, [2]*Grad. Sch. Biosci. Biotech., Tokyo Inst. Tech.*)

'Catch' connective tissues shown in echinoderm animals such as sea urchins, sea stars, and sea cucumbers can extensively and reversibly change their stiffness in a few minutes under the regulation of the nervous system. Neurotransmitters such as acetylcholine, adrenaline, and some oligopeptides cause changes in the stiffness of the living pieces dissected from these tissues. They are no more effective, however, after the treatment with detergent solubilizing cell membranes. There are some granule-containing cells in the tissues, which are assumed to secret some factors under the regulation of nerves causing changes in the tissue stiffness. The tissues contain a large amount of the extracellular matrix mainly consisting of collagen fibrils. It seems that cross-linking between the fibrils are formed or broken during the change of the stiffness of the tissues. Its molecular mechanisms are, however, not yet fully understood. We isolated a protein factor called 'tensilin' from an extract of sea cucumber body wall dermis, one of the known 'catch' connective tissues. It stiffens the detergent-treated dermal pieces and induces aggregation of collagen fibrils isolated from the tissue. We also isolated a crude extract solution which softens the detergent-treated dermal pieces. It is possible that there are other factors affecting on interactions among dermal fibrils and the stiffness of the tissues. Molecular mechanisms of the stiffness changes of the 'catch' connective tissues should be clarified by purifying and characterizing these factors.

2PS041 Cooperative function of raft domains and actin skeleton utilized for anthrax toxin assembly and internalization: a single-molecule study

Yukihiko Kudo[1,2], **An-An Liu**[1,2,3], Shihui Liu[4], Kenichi Suzuki[1,5], Takahiro Fujiwara[1], Dai-Wen Pang[3], Stephen Leppla[4], Akihiro Kusumi[1,2] ([1]*Institute for Integrated Cell-Material Sciences, Kyoto University, Japan*, [2]*Institute for Frontier Medical Sciences, Kyoto University, Japan*, [3]*College of Chemistry and Molecular Sciences,Wuhan University*, [4]*Division of Intramural Research, NIAID, NIH, USA*, [5]*The National Centre for Biological Science/The Institute for Stem Cell Biology and Regenerative Medicine (inStem), Bangalore, India*)

How raft domains and cortical actin filaments (actin-based membrane skeleton) collaboratively work in the plasma membrane (PM) is one of the key issues in understanding the functions of the raft domains and internalization of raft-associable receptors. To address this question, we examined the mechanism by which a component of anthrax toxin, called protective antigen (PA), bound to the cell surface receptor (PA-receptor complex, called PARC) form heptamers in the PM and internalized. The lethal and edema protein components of the toxin are known to only bind to PARC heptamers, and after internalization, cross the endosomal membrane to enter the cytoplasm. The process for the PARC heptamer formation has not been totally understood, because, previously, only PARC monomers and heptamers were detectable due to methodological limitations. Here, by using CHO cells stably expressing the PA receptor, CMG2, and the PA specifically labeled with a fluorescent dye precisely at a 1:1 mole ratio, we succeeded in observing intermediate PARC clusters and the recruitment of a specific lipid to those clusters by simultaneous dual-color single-molecule tracking. With an increase of the cluster size, the residency time of the raft lipid at the clusters was prolonged. Furthermore, the PARC intermediate clusters induced actin polymerization, which is enhanced with an increase of the cluster size. How these events are correlated and lead to heptamer formation and the subsequent internalization is under investigation.

2PS042 核内を運動する粒子の分子同定と、可視化、トラッキング解析

Imaging, tracking and analysis on the intranulclear moving particles

Soyomi Uchibori[1], Maiko Kuramochi[1,2], Saori Mimatsu[1,2], Emiko Kobayashi[1,2], Kaoru Katoh[1,2] ([1]*Biomed. Res. Inst, AIST*, [2]*Grad. Sch. Live & Env. Sci., Univ. Tsukuba*)

Cell nucleus is a site of gene expression. The expression process should require dynamic change in architectural framework of nuclear structures and active transport of many kinds of molecules and subcellular components. Many researchers microinjected fluorescently labeled molecules into the nucleus and showed high mobility of the molecules in nucleoplasm. Moreover, advaned in fluorescently tagged protein leads to more precise analysis on dynamics of nulceoplasm. However not so many studies were reported in the living unstained nucleus. We, therefore, used pupil projection apodized phase contrast (PPAPC) microscopy, (external phase contrast with special frequency filtering). The PPAPC revealed many moving particles in living cell nucleus, which were unable to observe with conventional phase contrast microscopy. We reported cell cycle dependent movement of the intranuclear particles. The particles were identified by interactive observation of optical (PPAPC) and electron microscopy. Here, we identified the molecules involved in the moving particles, with immunofluorescence method. Moreover, we tracked the moving particles and analyzed the trajectory. Motile mechanisms of the particle and biological meaning of the movements were discussed in the presentation.

2PS043 クライオトモグラフィーによる動的生細胞内イメージングの開発

Development for dynamic Live Cell imaging by cryo-electron tomography

Atsuko H. Iwane[1,2], Ruriko Ogawa[2], Rina Nagai[1], Akihiro Kawamoto[1,2], Kazuhiro Aoyama[1,3] ([1]*Osaka Univ. Grad. Sch. of Front. Biosci. Speci. Res. Promotion Group*, [2]*RIKEN Quantitative Biol. Center Cell Dynamics Res.*, [3]*FEI JAPAN Application Lab.*)

Cryo-electron tomography of intact cells is an emerging technology that compliments crystallography, NMR and single molecule imaging techniques. Its strength is in that it reveals the spatial arrangements of key proteins and complexes during intracellular signaling and mechanical events like motility and division. In this meeting, we describe dynamical Live Cell imaging by cryo-electron tomography using the Titan Krios microscope. Observed living cells were grown directly on Holey Carbon Support Film, 200 mesh molybdenum EM specimen grids (Quantifoil R2/2). We analysed normal cell movement and cell division on Quantifoil using Image J and compared these properties with those of cells grown on a normal cell culture plastic plate. After phosphate-buffered saline washing and rapid freezing, the specimen grids were transferred onto the microscope immediately while keeping the environment under liquid N2. Cells were imaged over an angular range from -70 degrees to 70 degrees at 2 degrees x cosθ tilt increments automatically and analyzed with Amira software to provide 3D images. We will present several 3D images in several types of Live Cell and would like to discuss them with everyone.

2PS044 Live cell imaging of the growth factor-induced nuclear translocation of ERK in PC12 cells

Yuki Shindo[1,2,3], Kazunari Mouri[4], Kayo Hibino[3], Masaru Tomita[1,2], Yasushi Sako[4], Koichi Takahashi[1,3] ([1]*Inst. Adv. Bio. Sci., Keio Univ.*, [2]*Syst. Biol. Prog. Grad. Sch. Media & Governance, Keio Univ.*, [3]*RIKEN QBiC.*, [4]*RIKEN ASI.*)

ERK (extracellular signal-regulated kinase) is one of the most major MAPKs and its dynamic activation regulates cell fate such as the growth and differentiation in PC12 cells. Specifically, nuclear translocation of ERK after the activation of Raf/MEK/ERK cascade leads to further activation of proteins in the nucleus such as the transcription factor, resulting in cell fate decisions. However dynamics of the ERK translocation within individual cells have not been well characterized. For further understanding and quantitative modeling of this signal transduction system, dynamical behavior of ERK in response to extracellular signals in single cells should be addressed. EGFP-tagged ERK was transfected into PC12 cells, and visualized in living cells using confocal laser microscopy, which allows quantitative measurement of the dynamics of ERK nuclear translocation induced by growth factor stimuli. The results revealed that the amount and time course of the translocation were varied among individual cells. To investigate the mechanism to induce such heterogeneity, translocation of Raf, the MAPKKK in the ERK cascade, to the cell membrane upon growth factor stimuli are being investigated, using TagRFP-tagged Raf. Thus, we will discuss the relation between dynamics of ERK and Raf, and further perspectives toward single molecule measurement and modeling.

2PS045 Live-cell imaging and analysis of cAMP-induced cAMP response in *Dictyostelium* using microfluidics chambers

Fumihito Fukujin[1], Keita Kamino[1], Satoshi Sawai[1,2,3] ([1]*Graduate School of Arts and Sciences, University of Tokyo*, [2]*Research Center for Complex Systems Biology, University of Tokyo*, [3]*PRESTO, Japan Science and Technology Agency*)

Transient synthesis and secretion of cyclic AMP (cAMP) induced by extracellular cAMP mediates intercellular signaling during aggregation of *Dictyostelium*. The response is characterized by a fast initial peak that appears about 1min after exposure to an increase in extracellular cAMP followed by dose-dependent attenuation to the pre-stimulus level. There is also a fast oscillatory component of about 3 min periodicity during this prolonged response. However, biochemical pathways responsible for each of these properties are not revealed. Analyzing sensitivity of the response to variations in activity of the biochemical components is helpful to this end. We developed continuous flow microfluidics chambers that allow fast switching of the stimulus and drug application. We found that the overall dose dependence of cAMP-induced cAMP response is similar to those observed in a larger macroscopic chamber reported earlier. To take advantage of the current setup, we studied cells continuously bathed with inhibitors of PI3Kinase and actin polymerization. We will discuss implications of our observations to the topology of underlying biochemical networks.

2PS046 高密度な集団中におけるサルモネラ菌の走化性応答の解析

Chemotactic response of Salmonella in high cell density

Takahiro Abe, Shuichi Nakamura, Seishi Kudo (*Depertment of applied physics, graduate school of engineering, Tohoku University*)

Many bacteria can swim by rotating flagella, and migrate to favorable environments for growth. When cell density is low, the chemotactic response in which smooth swimming (running) and change of direction (tumbling) are repeated has been known as a biased random walk. However, it still remains unknown how increase of cell density influences the chemotaxis. In this study, we analyzed chemotactic responses of Salmonella by a capillary assay under an optical microscope with changing cell density to characterize the chemotaxis in high cell density. As a result, we found that chemotactic responses to concentration gradient of attractant were significantly affected by cell density. At least three distinct states were observed in the collecting process, which are a gentle collecting state, a fast collecting state and a stationary state. Duration time of the gentle state in high cell density were shorter than those in low cell density, implying that hydrodynamic interactions among cells generate oriented flows and improve the efficiency of chemotaxis.

2PS047 円弧パターンを用いた *Navicula pavillardii* の運動解析

Trajectory analysis of *Navicula pavillardii* cells by using an arc pattern

Kazuo Umemura[1], Takahiro Haneda[1], Yoshikazu Kumashiro[2], Kazuyoshi Itoga[2], Teruo Okano[2], Shigeki Mayama[3] ([1]*Fac. Sci, Tokyo Univ Sci*, [2]*Tokyo Women's Medical Univ*, [3]*Fac. Edu, Tokyo Gakugei Univ*)

Some types of diatom cells actively glide on a solid surface. The actin-myosin system has been proposed to explain the movement of diatoms. Although motility studies on diatom cells have been performed since 1950, single-cell analysis using a microchamber has not been performed for this purpose. In 2011, we reported trajectory analysis of *Navicula* sp. diatom cells that were shut in a hole (diameter, 600 μm). In that study, we found that the diatom cells moved freely in the center of the hole and that movement was prohibited at the edge of the hole . In the current study, we fabricated a polydimethylsiloxane (PDMS) micro pattern involving arc grooves (width, 40 μm; depth, 25 μm) in order to observe single *Navicula pavillardii* cells. The diatom cells glided along the edge of the grooves while repeating inversion. Consequently, the velocity of the cells was not affected by the curvature radius of the arc groove. Furthermore, the velocities for the clockwise and counterclockwise directions were almost the same as expected. In contrast, the velocity of each cell was obviously accelerated when N,N-dimethyl-p-toluidine (DT) was injected into the culture medium. The average velocities were 10.2 and 13.0 μm/s in the absence and presence of DT, respectively. However, the maximum velocity among 150 cells was almost 18 μm/s in both absence and presence of DT, which suggests that the value represents the mechanical limit of the cell motility.

2PS048 基質伸縮に対する運動性細胞毎の応答の違い

Difference of migrating directions among fast crawling cell types on a substratum with cyclic stretch-shrinkage

Chika Okimura[1], Takafumi Mizuno[2], Katsuya Sato[3], Yuta Nakashima[4], Kazuyuki Minami[4], Hitomi Nakashima[1], Yoshiaki Iwadate[1] ([1]*Grad. Sch. Med., Yamaguchi Univ.*, [2]*Biomedical Research Institute, AIST*, [3]*Inst. Tech. Sci., Grad. Sch., The Univ. Tokushima*, [4]*Grad. Sch. Sci. Eng., Yamaguchi Univ.*)

Living cells are constantly subjected to various mechanical stimulations. They must sense the mechanical aspects of their environment and respond appropriately for proper cell function.

Cells adhering to substrata must receive and respond to mechanical stimuli from the substrata in order to decide their shape and/or migrating direction. In response to cyclic stretch-shrinkage of the elastic substratum, intracellular stress fibers in slowly crawling cell types, such as fibroblasts and endothelial cells, are rearranged perpendicular to the stretch-shrinkage direction, and then the shape of those cells becomes extended in the same direction.

On the other hand, in the case of *Dictyostelium* cells, a kind of fast crawling cell types, not the shape but the direction of migration is regulated by the cyclic stretch-shrinkage. They migrate perpendicular to the stretch-shrinkage. Fan-shaped keratocytes, isolated from fish epidermis, are also known as fast crawling cell types. It is well known that treatment with staurosporine induces fragmentation of lamellipodia of keratocytes, which is followed by formation of motile cytoplasts. We observed the migration in keratocytes and their motile cytoplasts on the substratum with cyclic stretch-shrinkage. They showed the directional migration different from *Dictyostelium* cells, i.e. migrated parallel to the stretch-shrinkage direction. We will discuss how different the reaction in cell migration in response to the cyclic stretch-shrinkage of substratum among the fast crawling cell types.

2PS049 コレラ菌走化性因子ホモログの局在制御機構の解析

Localization control of chemotaxis-related signaling components of *Vibrio cholera*

Hiroki Okabe[1], Tomoyuki Nakamura[2], Hiremath Geetha[3], Ikuro Kawagishi[1,2,3] ([1]*Dept. Frontier Biosci., Fac. Biosci. Appl. Chem., Hosei Univ*, [2]*Dept. Frontier Biosci., Grad. Sch. Eng., Hosei Univ*, [3]*Res. Cen. Micro-Nano Tech., Hosei Univ*)

Vibrio cholera, the causative agent of cholera, has three sets of chemotaxis-related signaling proteins, but only System II is directly involved in chemotaxis. System II components localize constitutively to a cell pole. By contrast, System I and III components show clustering at a pole and lateral membrane in cells cultured with standing (microaerobic conditions) but not with shaking (aerobic conditions), suggesting that System I and III functions under oxygen-limiting conditions. The addition of NaN_3 upon shaking incubation induces localization of these proteins, suggesting that it is not limitation of oxygen itself but some change in energy metabolism that triggers the localization of these components. In this study,we examined the effects of NaN_3 on localization of System I, II and III histidine kinases, CheA1, CheA2 and CheA3, under various conditions. At 30℃, CheA2-GFP localize to a cell pole with any concentration of NaN_3 tested, but at 37℃, it localized to a cell pole and lateral membrane regions with 0.2% NaN_3. Fractions of cells with polar and lateral localization of CheA1-GFP NaN_3 and CheA3-GFP increased with increasing concentrations of NaN_3 at 30℃ At 37℃, localization of CheA1-GFP was observed at lower concentrations of NaN_3. CheA3-GFP localized to the pole at 37℃ even in the absence of NaN_3. Immunoblotting demonstrated that NaN_3 did not affect the expression levels of the GFP fusions to CheA1, CheA2 and CheA3. These results suggest that Che systems I and III of *V. cholera* may be active in the host.

2PS050 クラミドモナスにおける走光性符号のレドックス調節

Redox-regulated switching of the phototactic sign in Chlamydomonas

Shota Mochiji[1], Norikazu Ohnishi[2], Jun Minagawa[2], Ritsu Kamiya[3], Ken-ichi Wakabayashi[1] ([1]*Dept. Biological Sciences, Grad. School of Science, Univ. Tokyo*, [2]*Div. Environmental Photobiology, National Institute for Basic Biology*, [3]*Dept. Life Science, Faculty of Science, Gakushuin Univ.*)

The unicellular green alga Chlamydomonas shows positive or negative phototaxis depending on the light intensities, circadian rhythms, etc. Switching of direction (or “sign”) of phototaxis is important for the cells to stay under proper light conditions for photosynthesis. However, its mechanism has been

unclear. Recently, we showed that the cellular redox (reduction-oxidation) poise determines the phototactic sign: cells show positive phototaxis after treatment with reactive oxygen species (ROS), whereas they show negative phototaxis after treatment with ROS quenchers. This finding raised two questions of 1) how cellular redox poise changes in vivo and 2) what is the molecular basis for the redox-regulated switching of the phototactic sign. Regarding 1), we focused on state transitions of photosynthesis, because the ROS generation has been suggested to greatly change depending on the state of photosynthesis. Low-temperature fluorescence spectroscopy revealed that cells showing positive phototaxis are in State 1, whereas those showing negative phototaxis are in State 2. We propose a model that changes in the intracellular ROS amount, caused by state transitions, function as a signal for the phototactic sign switching. Regarding 2), we found that two previously isolated phototaxis-deficient mutants have defects in redox sensing. We also isolated a new mutant that responds to the treatment with redox reagents in an opposite manner to that of wild type. We will present the results of phenotypic analyses.

2PS051 細胞性粘菌で探る細胞運動ダイナミクスと走電性応答の関係性

Cell migration dynamics and its relevance to electrotaxis in Dictyostelium cells

Hiroaki Takagi[1,3], Masayuki J. Sato[2,3], Masahiro Ueda[2,3,4,5] ([1]*Sch. Med., Nara Med. Univ.*, [2]*Grad. Sch. Front. Biosci., Osaka Univ.*, [3]*JST, CREST*, [4]*Grad. Sch. Sci., Osaka Univ.*, [5]*QBiC, Riken*)

Directional cell migration is a fundamental process associated with many physiological phenomena. On the signaling process realizing directional cell migration, the dominant view is that cells respond to external signals passively and digitally. Recently, however, a complementary view in which cellular spontaneous dynamics without external signals plays an important role to produce cellular behaviors attracts considerable attention. In order to verify the latter view, a relationship between spontaneous random cell migration and directional cell migration with external guidance cues (direct current electric field) was extensively investigated in Dictyostelium discoideum. It was confirmed that a generalized Langevin model with asymmetry for cellular polarity could successfully reproduce the statistical characteristics of spontaneous cell migration. Also, it was shown that the Langevin model extended with additional velocity bias in accordance with the electric field strength could describe directional cell migration under electrotaxis quantitatively. Based on these results, the hypothesis that electrotaxis is realized by biasing spontaneous cell migration properly, and velocity memory is relevant to cellular flexible response for uncertain environment was proposed and tested through a series of electric field reversal experiments and the model simulations.

2PS052 細胞運動のための力と生化学の相互作用

Force-biochemical interaction for cell migration

Yuichi Sakumura[1], Yoshiaki Iwadate[2] ([1]*Sch. Info. Sci., Aichi Pref. Univ.*, [2]*Grad. Sch. Sci., Yamaguchi Univ.*)

Motile cell generates traction force to show crawling migration. Although biochemical signals such as Rho family small GTPases have been well studied, it is still unclear how the migrating cell manages and integrates the traction force and biochemical signals. Our experiment using force microscopy shows that migrating Dictyostelium cell generates a small traction force at the front relative to the other directions. Keratocyte also migrates by generating relatively small traction force at the front direction. In addition, our experiment using GFP-myosin II revealed that the cell accumulates myosin II at the intracellular space where force was added from extracellular side, suggesting that the cell transduces extracellular force to a biochemical signal through myosin II accumulation. How the cell integrates intra- and extracellular interactions for migration? To examine the mechanism of the cell migration based on the experimental observations, we developed a simple computational model cell which has a hexagonal shape with a spring-dumper system and contains force-biochemical interactions. The model cell migrates on the adhesive substrate where the cell repeats adhesion and exfoliation. Using the model cell, we show that the cell can migrate to the direction at which it generates small traction force relative to the other directions. This suggests that exfoliation facilitated by myosin II accumulation not at the front side plays key role for cell migration.

2PS053 歩行中ミオシン X の高速 AFM 観察

Direct observation of walking behavior of myosin X by high-speed atomic force microscopy

Yusuke Sakiyama[1], Noriyuki Kodera[2], Osamu Satou[3], Mitsuo Ikebe[3], Toshio Ando[1,2] ([1]*Sch. Math. & Phys., Int. Sci. & Eng., Kanazawa Univ.* [2]*Bio-AFM Frontier Research Center, Inst Sci. & Eng., Kanazawa Univ.* [3]*Dept. Physiology, Univ. Massachusetts Med. Sch.*)

Double-headed myosin X, one of the actin-based motors, is involved in filopodia formation and intrafiropodial transport. Structurally, each head of myosin X is comprised of a motor domain, an ~11 nm long neck domain (lever-arm domain) consisting of three IQ motifs bound to calmodulins or calmodulin-like light chains, and a proximal tail of a stable alpha-helix which is hypothesized to extend the working stroke of myosin X. The head is followed by a coiled-coil domain for possible dimerization and then by two unique globular tail domains. Recently, single molecule fluorescent microscopy revealed that the artificially dimerized tail-truncated myosin X can move processively on single actin filaments with a large step size of ~34 nm [Y. Sun *et al., Nat. Struct. Mol. Biol.* (2010)]. This large step size can be explained by the hypothesis of the stable alpha-helix extension to the lever arm domain [*i.e.*, total lever arm length is estimated to be ~26 nm (~11 nm + ~15 nm)]. However, this structural evidence on the functioning molecule is still missing. Thus, here we have been performing high-speed atomic force microscopy imaging to directly observe behaviors of myosin X moving along an actin filament. We established an appropriate motility assay condition in which phospholipid bilayers were used as a substrate. Using this assay condition, we successfully visualized myosin X molecules that were moving with a large step size of ~36 nm. The details of the structural dynamics are now under investigation.

2PT001 独立してフォールドする構造ドメインデータベースの構築

I-StDom: A dataset of Independently foldable Structural Domains automatically delineated from protein structures

Yuki Umezawa[1,2], Teppei Ebina[2], Yutaka Kuroda[1] ([1]*Dept of Biotech. & Life Sci., Tokyo University of Agriculture & Technology*, [2]*Brain Science Inst., RIKEN*)

Protein domains that can fold in isolation (structural domains) are significant targets in diverse areas of proteomics research as they are often readily analyzed by high-throughput methods. In this process, the ability to identify sequence regions corresponding to structural domains in novel proteins with unknown structures is an essential step. Computational methods for predicting domain regions from sequence information only are thus becoming valuable. In developing such predictors, reliable structural domain datasets are necessary as learning data.

In this study, we constructed I-StDom, a dataset of **St**ructural **Dom**ains that can fold **I**ndependently and in isolation (ISDs). We identified ISDs from multi-domain proteins cataloged in SCOP and CATH by assuming that they form little inter-domain interactions, such as H-bonds and hydrophobic cores, and which we calculated from the protein's atomic coordinates. We parameterized interactions, and optimized them so as to select the maximal number of protein domains cataloged in PDB. 48089 ISDs were selected using the optimal parameters (less than 11 MC-MC, 9 MC-SC, and 7 SC-SC H-bonds, and 7 hydrophobic cores) with 29.7% of them having sequence similarity to a domain cataloged in PDB. This is more than 10% higher than for the unfiltered SCOP and CATH domains, which strongly suggested that domains in I-StDom can fold in isolation. I-StDom is available at http://domserv.lab.tuat.ac.jp/i-stdom.html.

2PT002 ADS 仮説に基づくタンパク質のデノボ立体構造予測法の開発

Development of a de novo protein structure prediction method based on the antecedent domain segment(ADS) hyphothesis

Kota Nakamori, Shintaro Minami, Kengo Sawada, George Chikenji (*Grad. Sch. of Eng. Univ. of Nagoya*)

Protein structure prediction is one of the most important and fundamental problems of biology. In particular, the prediction of novel protein structures, for which we cannot use template, is a very significant from the viewpoint of biophysics. Currently, one of the most successful method for predicting novel protein structures is the fragment assembly (FA) method. The success of the method is, however, limited to low contact order (CO) proteins, probably because the FA method emphasizes local interaction too much. (R.Bonneau. Protein Sci. 2002;11:1937-1944). In order to predict novel protein structures with high CO, we developed a method for novel protein structures prediction. The idea of the medhod is based on the antecedent domain segment(ADS) hyphothesis, which was originally proposed by Lupas et al. In this hypothesis, ancient protein structures were formed by self-assembling aggregates of short polypeptides. Our method mimick this aggregation processes for protein tertialy

structure assembly. Thus, the method enphasises non-local interactions rather than local ones. One of the advantage of the method is that the method can directly be applied to oligomer targets. We will report the detailed description of the method and the results of benchmark tests.

2PT003 配列順序に依存しない構造関係性を用いた長い挿入配列の構造モデリング

Modeling structure of large insersion regions in homology modeling bu utilizing non-sequential structure relationship

Yuki Nakagawa, Shintaro Minami, Kengo Sawada, George Chikenji (*Grad. Sch. of Engineering, Nagoya Univ.*)

Homology modeling is a powerful method for predicting protein structures by using a template structure having a similar amino-acid sequence to the target protein. However, in the region where the amino acid sequence is very different between the target and the template or large insertions exit, the predicted structure for such a region remains unreliable.If such an unreliable region is so large that three or four secondary structures have to be constructed, de novo modeling is needed. Currently, such de novo modeling, however, does not always provide an accurate prediction. Here, we propose a new homology modeling method that can effectively generate reasonable structure candidates of such unreliable regions. The idea of the method is based on the observation that if we search similar structures of the reliable region of the target protein in PDB by a non-sequential structure alignment program, we almost always find good structure candidates of such unreliable regions. In the presentation, we will report the detailed description of method and results of benchmark tests.

2PT004 Common structural / sequence features of proteins that share non-sequential structural similarity

Kengo Sawada, Shintaro Minami, Geroge Chijenji (*Dept. of eng., Nagoya Univ.*)

Recently, many researchers have reported interesting examples of non-sequential alignments such as circular permutations and domain or region swaps. For example, Alexj et al. conducted a comprehensive large-scale study of non-sequential alignments between available protein structures in Protein Data Bank (PDB) and found that 35.2% of all significant alignments are non-sequential [1]. Furthermore, Aysam et al. identified significant non-sequential structural similarity between some new folds and existing structures in PDB [2]. These observations suggest that appropriately utilizing non-sequential template enables us to predict new fold targets.

The goal of this research is to identify the structural and sequence features of proteins that share non-sequential structural similarity, in order to predict new folds utilizing non-sequential templates. In this work, we collected structures sharing non-topological similarity with one of the super-folds such as Ferredoxin-like fold, and found common features among them. We will report detailed description of the method and the results in the presentation.

[1]Alexej Abyzov and Valentin A Ilyin. 2007. BMC Structural Biology 7:78
[2]Aysam Guerler and Ernst-walter Knapp. 2008. Protein Science. 17:1374-1382

2PT005 PoSSuM: タンパク質の既知及び潜在的基質結合部位類似性検索のためのデータベース

PoSSuM: a database for searching similar pairs of known and potential ligand-binding sites in proteins

Jun-ichi Ito[1,2,4], Yasuo Tabei[3], Kana Shimizu[1], Koji Tsuda[1,3], **Kentaro Tomii**[1,2] ([1]*CBRC, AIST*, [2]*Department of Computational Biology, Graduate School of Frontier Sciences, The University of Tokyo*, [3]*Minato Discrete Structure Manipulation System Project, JST*, [4]*National Institute of Biomedical Innovation*)

We proposed a fast alignment-free method that can enumerate similar pairs from millions of ligand-binding sites in the Protein Data Bank (PDB). In our method, ligand-binding sites are first encoded as feature vectors based on their physicochemical and geometric properties of amino acid residues. Once feature vectors representing ligand-binding sites are converted to bit strings, called structural sketches, which is obtained by random projections of the vectors, a multiple sorting method is applied to the enumeration of all similar pairs in terms of the Hamming distance.

We have developed our new database, called Pocket Similarity Search using Multiple-sketchsorts (PoSSuM) to compile all similar pairs detected using our method as a relational database. In the latest version of our database, we used the following two datasets: 226,630 small ligand-binding sites obtained from protein-ligand complexes in the PDB, and 3,134,413 potential ligand-binding sites identified using an existing pocket detection algorithm, ghecom. We applied our method to all-pair similarity searches for the 3.4 million known and potential ligand-binding sites. Consequently, we discovered ca. 24 million similar binding sites. Here we report those results including all the discovered pairs. Our database is expected to be useful for predicting protein functions and rapid screening of target proteins in drug design. The PoSSuM database is available at http://possum.cbrc.jp/PoSSuM/.

2PT006 サポートベクターマシンを用いた糖鎖結合部位予測手法の開発

Development of method for predicting carbohydrate binding site using support vector machine

Masaki Banno, Kentaro Shimizu (*Grad Sch Agricul. life sci., Univ Tokyo*)

Carbohydrate play an important roles in molecular recognition mechanism. Especially, carbohydrate-protein interaction are associated with important biological process such as cell to cell communication, cellular immunity and cell recognition.Recently, the number of carbohydrate binding proteins were achived over 4000 structures. It is desired to extract new biological findings from these large amount of structual data. In this study, We have carried out data mining of the Protein Data Bank (PDB) to collecting carbohydrate binding proteins, and construct the prediction model of carbohydrate binding site in protein sequence using support vector machine. We analyzed binding site propensity for each types of carbohydrate. We also evaluated this prediction model for 5-fold cross validation.The sensitivity and specificity are achieved an 81% specificity of prediction at 64% sensitivity. Area Under Curve (AUC) were achieved 0.81.

2PT007 タンパク質における部位間での同時的補償的置換に基づく隣接残基対予測

Prediction of Contact Residue Sites Based on Concurrent and Compensatory Substitutions Between Sites in Protein Evolution

Sanzo Miyazawa (*Gunma Univ., Grad. Sch. Eng.*)

Structural and functional constraints originating in residue-residue interactions act on each amino acid in a protein, because a protein must fold into a unique three-dimensional structure and play a specific function. Selective constrains on amino acids in proteins are recorded in amino acid orders in homologous protein sequences and also in the evolutionary trace of amino acid substitutions. Thus, statistical analyses of amino acid orders and of the evolutionary trace of amino acid substitutions can provide information on residue pair couplings. A challenge is to extract direct dependencies between residue sites by excluding indirect correlations that originate from indirect interactions through other residues within a protein or even through other molecules. Recent attempts of disentangling direct from indirect dependencies of amino acid types between residue positions in multiple sequence alignments of proteins have revealed that the strength of inferred residue couplings is an excellent predictor of residue-residue proximity in folded structures. Here, we report an alternative attempt of inferring site couplings from concurrent and compensatory substitutions between sites at each branch of a phylogenetic tree. Accuracy of contact prediction based on the present method is comparable to that of the maximum entropy method.

2PT008 3DMET 構築のためのキュレーション支援システム

Supporting system for manual curation of the 3DMET database

Miki Maeda (*National Institute of Agrobiological Sciences*)

We have developed the 3DMET database, a three-dimensional structure database of natural metabolites. Automatic conversion from 2D- to 3D-structures causes conversion errors especially for chiral information. Thus, we applied automatic confirmation and manual curation to each 3D-structure. During the work, we need some supporting system and have developed.

"Structure-Checker" is a supporting system for self-judge of the conservation between two structures. The user interface is web browser and two MOL files are sent to the web server. In the server, the structures are converted to InChI and each columns are compared. If a column does not correspond to one structure, the color of the column is changed. Curators judged manually based on the results. To understand the results, curators need basic knowledge for the InChI description.

"Molecular Viewer" is a system for manual check of 3D-structures and literatures, developed for chemists not familiar to computer. The user interface of this system is also web browser. Book name, pages, and chemical name are

selected in order; a 3D-structure of the molecule is shown. For this 3D-visualization, J-mol is used as a plug-in program for web browsers.
The 3DMET is now available as Release 2.1. The Release 2.2 will be opened to access until this presentation. The recent development and changes of 3DMET will be also reported.

2PT009 配列順序を無視したタンパク質構造アライメントの性質

Some characteristic features of non-sequential structural alignment: difference between sequential and non-sequental alignments

Tatsuo Mukai, Kengo Sawada, Shintaro Minami, George Chikenji (*Grad. Sch. of Eng. Univ. of Nagoya*)

Recently, a number of interesting examples that show non-sequential structure similarity have been reported, where non-sequential structural similarity is the structural similarity in which structurally equivalent regions are aligned in different order in the sequence of the compared proteins. For example, Minami et al. demonstrated that the usage of a non-sequential structure alignment program yielded many structure alignments with significant similarities between proteins of known three-dimensional structure and newly determined protein structures that possess a new fold. This finding suggest that many new folds can be modeled by permutating old folds.
In order to develop a new prediction method for new fold targets utilizing the non-sequential structure relationship, we first must clarify characteristic features of non-sequenttial structural relationship. As a first step towards the goal, we performed a large scale non-sequential alignment between protein pairs deposited in PDB and compare their features with those of sequential alignments. We found several characteristic features found only in non-sequential alignment. For example, protein size and solvent accessibility were largely not conserved in non-sequentially similar pairs. These finding may be usefull for developing a new De Novo prediction method. In the presentation, we will report detailed description of the method and the results.

2PT010 Prediction of the types of carbohydrate-binding proteins

Zhenyi Ge, Wei Cao, Kazuya Sumikoshi, Shugo Nakamura, Kentaro Shimizu (*Department of Biotechnology, Graduate School of Agricultural and Life Sciences, The University of Tokyo*)

Carbohydrate-binding proteins or lectins, which are defined as carbohydrate-binding complexes which are not directly modified by carbohydrate, are important complexes that participate in many biological processes as intercellular information transfer and cell recognition. Though there are a variety of methods to classify lectins, classifying lectins based on structural and evolutionary sequence similarities is more popular because of some highly conserved amino acid sequence motifs in CRD (Carbohydrate Recognize Domain). Depending on this way, lectins could be classified into C-type lectins (require calcium for recognition), S-type lectins (also known as Galectins, which require free thiols for stability), L-type lectins (have a feature structure called “jelly roll fold”) and so on. We developed a tool to detect and classify lectins by HMM (Hidden Markov Models). Several corresponding profile HMMs are composed and are prepared for scoring entry sequences. Sequences in low score section are regarded as NOT lectins and sequences in the corresponding range of scores are classified into fitting types of lectins.

2PT011 Analysis of DNA-binding sites using novel amino acid index for molecular recognition (MR-index)

Katsutoshi Hibino[1], Yasunori Yokoyama[2], Shigeki Mitaku[2] ([1]*Dept. of Computational Science and Engineering, Grad. Sch. of Engineering, Nagoya Univ.*, [2]*Dept. of Applied Physics, Grad. Sch. of Engineering, Nagoya Univ.*)

Protein-DNA interaction plays an important role in many biological processes. However, the mechanism of protein-DNA interaction is still not clear. Prediction of DNA-binding sites in DNA-binding proteins using their physical properties is very useful for understanding mechanism of protein-DNA interaction. There are many experimentally determined structures in Protein Data Bank database, but only a few protein-DNA complexes are available. In addition, it is very expensive and time-consuming process to solve the structure of a protein-DNA complex through experimental methods. Therefore, a sequence-based computational prediction of DNA-binding sites in DNA-binding proteins is required. In this work, we used a novel amino acid index for molecular recognition (MR-index) to develop a system for predicting DNA-binding sites in DNA-binding proteins. Although MR-index was originally developed for predicting allergen-unique fragments (AUFs), it is found that most proteins have MR-index peaks at a constant rate. Also, MR-index peaks locate at positions with large structural fluctuations such as loop regions, and those sites tend to interact with other molecules. We took account of physical properties around MR-index peaks and aimed to develop the system for predicting DNA-binding sites in DNA-binding proteins. The discrimination analysis showed that the MR-index peaks around DNA-binding sites have characteristic distribution of physical properties.

2PT101 アミノ酸保存度と相互作用エネルギーを組み合わせたタンパク質ーリガンド結合部位予測手法の開発

Protein-Ligand Binding Site Prediction by Using Energy-based Method with Amino Acid Conservation Scores

Hiroto Tsujikawa, Yusuke Umeda, Mizuki Morita, Shugo Nakamura, Kentaro Shimizu (*Grad. Sch. Agric. Life Sci., Univ. Tokyo*)

Protein-ligand interaction is one of the most important steps for expression of protein functions. Identifying ligand binding sites helps protein function analysis and structure-based drug design. Recently, a variety of computational methods for predicting ligand binding sites are proposed. Among these methods, the energy-based method which calculates protein-ligand interaction energy on a three-dimensional protein structure is shown to realize high precision. In this study, we developed a new method which combines the energy-based method with amino acid sequence conservation scores. Our method locates methyl probes around the protein surface and calculates van der Waals interaction energy between each probe and the protein. In addition, we calculate amino acid conservation scores by constructing position-specific scoring matrix (PSSM) and add their weighted scores to the interaction energy. It is considered that highly conserved amino acid residues are expected to be closely related to protein function and appear in functional sites. Probes with energetically favorable for binding sites and within a short distance are clustered and they are ranked according to their total interaction energies. As a result, in 80% proteins, at least one site in top three predicted sites predicts ligand binding sites correctly. We will evaluate the performance of our method and compare it with other existing methods, and show the importance of amino acid sequence conservation in ligand binding sites prediction.

2PT102 蛋白質・蛋白質相互作用ネットワークにおけるドメイン及び非ドメイン間相互作用の解析

Analysis of Domain and Non-Domain Interactions in Protein-Protein Interaction Network

Komori Satoshi, Sarai Akinori, Fujii Satoshi (*Kyusyu Institute of Technology*)

The analysis of protein-protein interactions and their network has been usually based on protein chains and domains. However, non-domain regions are often involved in the interactions and serve function as well. Here, we have considered non-domains as well as domains in the protein-protein interactions. The information of domains within the individual chains was obtained from Pfam, and sequence-based clustering was carried out. Non-domains were defined as the regions outside the domains, within certain length threshold. We have examined physical contacts among all pairs of domains and non-domains within each complex structure of PDB, and identified 15,742 domain-domain interactions, 15,218 domain-non-domain interactions and 12,804 non-domain-non-domain interactions. Then, we constructed the interaction network. These pieces of information on domains and non-domains and their interactions were implemented into PDBnet, which enables users to examine protein interaction network in terms of domain and non-domain interactions. We have compared characteristics of interactions due to domains and non-domains, such as amino acid composition, interaction type and packing. We will also make systematic analysis on the relationship among various properties at molecular structure, interaction and network levels, in order to get insight into the function of proteins. Furthermore, we will apply the present analysis to the systematic predictions of protein-protein interactions based on the catalog of interacting domains and non-domains.

2PT103 進化的に保存されたタンパク質間相互作用の複合体立体構造の予測

3D complex structure assignment for evolutionary conserved protein-protein interactions

Takeshi Kawabata, Haruki Nakamura, Akira Kinjo (*Institute of Protein Research, Osaka University*)

A huge amount molecular interaction data are accumulated to elucidate entire landscape of cellular activities. 3D complex structures of interacting proteins can add their physical mechanisms, such as interacting residues and driving binding forces. The goal of this study is to gather all the reported molecular interactions, and to predict their 3D structures using homology modeling as many as possible. Another goal is to propose biologically important interacting protein sets to be solved their 3D complex structures in the future. However, current experimental molecular interaction data are not comprehensive and reliable. To overcome these problems, we compare interactions of several different organisms, and consider conserved interactions to be highly reliable. As the preliminary study, we analyzed yeast and human interactromes. The INTACT database stored 70,000 and 40,000 two-body protein-protein interactions for yeast and human, respectively. Among these interactions, 3D complex structures for 1.5 % yeast and 6 % human pairs can be modeled using homologies for known 3D complexes. To reduce false positive data, we extracted conserved interactions (*interologs*) between the two species. Number of the *interologs* are about 5,000, they may be more reliable and should be biological important. 3D complex structures can be assigned for 11 % and 24 % of the interlogs for yeast and human, respectively. The remaining 4,000 protein pairs are good candidates protein pairs to be solved their 3D complex structures.

2PT104 相互作用プロファイルを使った正解相互作用部位の絞込みによる再ドッキング法の研究

Development of re-docking method by obtaining native interaction pattern

Nobuyuki Uchikoga[1], Yuri Matsuzaki[2], Masahito Ohue[2], Yutaka Akiyama[2], Takatsugu Hirokawa[3] ([1]*Dept. Phys., Sch. Sci. & Eng., Chuo Univ*, [2]*Grad. Sch. Comput. & Sci., Tokyo Inst. Tech.*, [3]*CBRC, AIST*)

In a study of protein-protein Interaction network, it is important to predict which pairs of proteins interact in living cell and how these bind each other. We approach to these problems using rigid-body docking algorithm, generating many decoys including false positives. Although this docking method is popular and useful, there are some cases with no near-native decoys. In previous work, we developed a method of generated Profile of Interaction FingerPrints (P-IFP) rather than generating near-native decoys. Then, we applied a profile method to obtaining region including native interacting residue pairs for re-docking process.

We have been developed Interaction FingerPrints (IFP) for the post-docking analysis of protein-protein rigid-body docking. IFP is composed of binary states of interacting amino acid residues of each proteins, as a scale for measuring unique similarities between the complex structures. Then, IFP can be used more easily to evaluate similarities between decoys than RMSD method, which depends on methods of superposing their structures. Additionally, IFP can be useful to assemble interaction profiles from various decoys.

In this work, we examined re-docking process after generating P-IFP for rigid-body docking decoys. As results, we could obtain a set of decoys with higher similarities than that of decoys generated in the initial docking process. Re-docking method using IFPs is expected to improve cases without near-native decoys in an initial docking process.

2PT105 タンパク質-低分子リガンド相互作用における結合様式の網羅的比較解析

Comprehensive comparisons of interactions in small-ligand recognitions by proteins at the atomistic level

Kota Kasahara[1], Kengo Kinoshita[1,2,3] ([1]*Grad. Sch. Information Sci., Tohoku Univ.*, [2]*ToMMo, Tohoku Univ.*, [3]*IDAC, Tohoku Univ.*)

Illuminating molecular mechanisms of ligand recognitions by proteins is a long-standing problem in the biophysics. Toward this, the 3D structural data of protein-ligand complexes provide fruitful information and recent continuous innovation of experimental techniques has been skyrocketing the structural data. However, it is not straightforward to mine information and knowledge from the complicated data, consisting of the Cartesian coordinates of atoms.

Here, we developed a method to extract information about molecular interactions form structural data of protein-ligand complexes and comprehensive comparisons of their interactions were performed. In this study, the interacctions in a protein-ligand complex was described as a network, nodes of which indicates amino acid residues or ligand atoms, and edges of which indicates interactions. The similarity between a pair of complex was calculated by alignment of these networks. We performed all-against-all comparisons of binding modes on a dataset consisting of 35,338 protein-ligand complexes. Further, similarities in the SCOP classification and ligand 2D structure were also calculated and consistency among these three similarity measures was evaluated.

As a result, basically, pairs with similar protein folds had similar ligands and interactions. However, there were many exceptions, i.e., dissimilar interactions with similar folds and ligands, and similar interactions with dissimilar folds and ligands. Novel relationships among proteins and ligands were mined by our study.

2PT106 分子ネットワークにおける構造情報と相互作用情報の統合

Integration of Structural and Biochemical Information into Protein Interaction Network

Yuji Kawakami, Akinori Sarai, Satoshi Fujii (*Kyushu Institute of Technology*)

Interactions among proteins have been mostly studied by structural and biochemical methods. Both kinds of interaction data have advantages and disadvantages, and complement with each other. Thus, the integration of these data will be useful for research. On the other hand, the quality of these experimental data is not necessarily uniform, making it more difficult to analyze them. Here, we try to integrate the structural and biochemical information of protein-protein interactions. The structural information is based on PDB. We used DIP, BOND, HPRD, IntAct and Mint databases for biochemical interaction data. We first evaluated the quality of the experimental data, and add the information along with the interaction data. We unified the biochemical data by using Uniprotkb ID and removed the data redundancy among them. Then we integrated the data into PDBnet by using Uniprotkb ID and PDB chain ID. Owning to this integration, PDBnet now contains more comprehensive interaction network. Many biochemical interactions are not present in the structural interactions. This would help researchers working on structures to identify missing potential interactions for structural analysis. On the other hand, some interactions are present only in the structural information. The integration of structural information into the biochemical network also helps researchers to understand the molecular mechanism of protein interactions and to develop potential drugs.

2PT107 酵素反応の分類と代謝パスウェイ検索への応用

A classification of enzymatic reactions and its application to metabolic pathway search

Susumu Goto, Masaaki Kotera, Toshiaki Tokimatsu, Yuki Moriya, Zen-ichi Nakagawa, Ai Muto, Minoru Kanehisa (*Inst. Chem. Res., Kyoto Univ.*)

Enzymatic reactions are key components in the metabolic pathway and have been classified by the Enzyme Nomenclature Committee of the International Union of Biochemistry and Molecular Biology. This classification (EC number system) is based on six classes: oxidoreductases, transferases, hydrolases, lyases, isomerases, and ligases, and each class is further subdivided according to more detailed reaction mechanisms such as bond types and functional groups. While quite useful, the system also has some limitations. For example, similar (resp. totally different) reactions in terms of mechanisms of chemical transformation are sometimes classified into different classes (resp. a same class). We, therefore, developed a new classification system for enzymatic reactions based on chemical transformation mechanisms and functional groups of chemical compounds.

First, we defined substrate-product pairs of enzymatic reactions. Each pair was structurally aligned, from which reaction centers and different and matched parts were extracted (RPAIR database). Reaction (chemical transformation) patterns were then defined using the extracted parts and stored in RCLASS database. This can be considered as a classification of substrate-product pairs and their associated reactions by the reaction patterns. As of June 2012, 2,516 RCLASS entries have been registered and further classified into 384 groups based on functional group conversions. This resource including some pathway tools utilizing RCLASS is available on the GenomeNet (http://www.genome.jp/reaction/).

2PT108 アポリポプロテインにおける疾患感受性のある点変異付近のアミノ酸配列断片の物性的特徴

Physical characteristics of amino acid fragments around point mutation with disease susceptibility in apolipoproteins

Ryouta Masai, Yasunori Yokoyama, Shigeki Mitaku (*Dept. Applied Physics, Grad. Sch. of Engineering, Nagoya Univ*)

Apolipoproteins are proteins that bind lipids to form lipoproteins. They serve as enzyme cofactors, receptor ligands, and lipid transfer carriers that regulate the

metabolism of lipoproteins and their uptake in tissues. Some mutations in apolipoproteins are related to inheritable disease. In this work, we studied physical properties of amino acid mutations in two groups: mutations with and without disease susceptibility in apolipoproteins. The analysis was carried out by two steps: First, we enumerated peaks of MR-index plots from amino acid sequences, and the mutations which changed the position of the MR-index peak were used for further analysis. Second, we calculated the average hydrophobicity and charge density of seven residues, and changes in the magnitude as well as the position of MR-index peaks. MR-index is an index that estimates allergen-specific amino acid sequence and binding site. The result indicated that the properties were significantly different between the mutations with and without disease susceptibility. The results will be useful for the prediction of inheritable diseases of multi-factors.

2PT109 L-リシン酸化酵素の X 線結晶構造解析

Structure of L-lysine α-oxidase from *Trichoderma viride*

Tadahisa Sano[1], Tatsuya Kawaguchi[1], Marie Amano[2], Kengo Shinyashiki[2], Haruka Nakata[2], Takashi Tamura[2], Kenji Inagaki[2], Hitoshi Kusakabe[3], Katsumi Imada[1] ([1]*Grad. Sch. Sci. Osaka Univ*, [2]*Grad. Sch. Env. & Life. Sci. Okayama Univ*, [3]*Enzyme Sensor Co. Ltd.*)

L-amino acid oxidase (LAO) is a dimeric flavoenzyme that catalyzes oxidative deamination of an L-amino acid to produce a 2-oxo acid with ammonia and hydrogen peroxide. Most of known LAOs show wide substrate specificity, but almost no activity for L-lysine oxidation. Unlike other LAOs, L-lysine α-oxidase (LysOX) from *Trichoderma viride*, which is found during the search for antitumor agents, exhibits strict substrate specificity for L-lysine. Thus, LysOX is an attractive candidate for an enzyme-based amino acid sensor. Moreover, LysOX has broad antitumor activity. To understand the strict substrate recognition mechanism of LysOX, structural information is essential. Here we report the crystal structure of LysOX from *T. viride* at 1.9 Å resolution. Since no active enzyme was expressed in E. coli, we purified LysOX from wheat bran culture of *T. viride*, and used it for crystallization. The diffraction data were collected at Spring-8 beamline BL41XU and the structure was determined by molecular replacement using the structure of L-amino acid oxidase from *Vipera ammodytes* as a search model. LysOX is composed of three domains and forms a tetramer in the crystal. The structural refinement is now in progress.

2PT110 Differences between key amino acid residues for the transitions L- to R- and R- to L-protofilaments of Salmonella flagellar filament

Fumio Hayashi, Hidetoshi Tomaru, Eiji Furukawa, Kanami Ikeda, Kenji Oosawa (*Department of Chemistry and Chemical Biology, Graduate School of Engineering, Gunma University*)

Salmonella cell swims by rotating its flagellar filaments. The filament (~ 10 μm) is composed of ~30,000 molecules of a single protein flagellin and forms left-handed helical structure under physiological conditions. The cell repeats swim-and-tumble and consequently move toward their favorite environments and away from unfavorites. The swim-and-tumble is caused by the change of the filament shape introduced by reversal of flagellar rotation, and the change of the filament shape is called polymorphic transformation. To elucidate the transformation mechanisms of flagellar filaments, we applied genetic suppressor analysis within flagellin molecule against SJW1655 producing R-type straight filament and SJW1660, HFG180, and HFG195 producing L-type straight filament. We isolated about 100 revertants from every mutant, determined the second mutation sites, investigated the localization of the amino acid residues on L- and R-type flagellin molecules, measured their swimming and swarming speeds, and observed their flagellar filaments. From these results, we propose that S106, A416, A427, and R431 are key residues involved in transitions from L- to R-type protofilaments, whereas D107 and G426, and S448 are keys from R- to L-type protofilaments. From the differences in the key residues, we suggest that L to R (R to L) transition is not just the inverse reaction of R to L (L to R) transition.

2PT111 アミロイドベータペプチドのオリゴマー形成メカニズムに関する構造学的解析

Structural analysis of the oligomerization mechanism of amyloid beta peptide

Hitomi Yamauchi[1], Shigeto Iwamoto[1], Takashi Saito[2], Toshiyuki Kohno[3], Takaomi Saido[2], Hiroaki Terasawa[1] ([1]*Facul. of Life Sci., Kumamoto Univ.*, [2]*RIKEN BSI*, [3]*Sci. of Med., Kitasato Univ.*)

Amyloid beta peptides (Aβ) form senile plaques following oligomerization in the brain. Aβ oligomers are thought to be neurotoxic and to play a key role in Alzheimer's disease (AD). Aβ40, 42 and 43 are major species of Aβ. It is known that Aβ42 and 43 are more prone to aggregation than 40. Thus, the length of the C-terminus is assumed to promote Aβ oligomerization and neurotoxicity.
This study aims to investigate the structure of Aβ oligomers and the oligomerization mechanism associated with AD.
To examine the influence of the C-terminus on Aβ properties, we compared the oligomerization propensity of Aβ by PICUP (Photo-Induced Cross-linking of Unmodified Proteins). All species formed dimers, however, large oligomers (trimers and tetramers) were formed at higher rate by Aβ42 and 43. Further, NMR analyses suggested that the C-terminal structure of Aβ42, 43 differs from that of 40. Besides, the flexibility of the C-terminus was higher in Aβ40 than in 42 and 43 revealed by NMR. The results showed that the interaction between the C-terminus of Aβ42 and 43 is stronger than that of 40.
To investigate the cross-linking sites, we used ESI-TOF MS to analyze for tryptic decomposition product of Aβ dimer stabilized by PICUP. It was found that H6-K16 fragments were cross-linked. In Aβ dimers, this region may exist in close proximity to the corresponding region on the other molecule.
In conclusion, our data suggested that Aβ forms parallel dimers. Moreover, a difference in C-terminal structure is important in the formation of large oligomers.

2PT112 Role of the Tyr residue stacked on the si-face of the isoalloxazine ring moiety in ferredoxin-NADP$^+$ oxidoreductase from *Bacillus subtilis*

Daisuke Seo, Hiroshi Naito, Erika Nishimura, Takeshi Sakurai (*Division of Material Science, Graduate School of Natural Science and Technology, Kanazawa University*)

Ferredoxin-NADP$^+$ oxidoreductase (FNR, [EC 1.18.1.2], [EC 1.18.1.3]) from the low-GC gram-positive bacterium *Bacillus subtilis* (BsFNR) is similar to bacterial thioredoxin reductases (TdRs) in amino acid sequence. The crystal structure analysis of BsFNR revealed the presence of the aromatic residue Tyr50 stacked on the si-face of the isoalloxazine ring of the FAD prosthetic group within a distance of approximately 3.5 Å. This conformation has been often found among the flavoprotein super family including FNR from plastid, but TdRs lack such the residue. To investigate the role of Tyr50 in catalysis with NADPH and ferredoxin (Fd), we performed site specific mutation analysis. While Tyr50Trp mutant retained reactivities with NADPH and Fd of ~20 and ~40%, against those of the wild type respectively, replacements to nonaromatic Gly and Ser residues drastically decreased the reactivities with both NADPH and Fd.

2PT113 アミロイド構造の決定におけるタンパク質揺らぎの役割の解析

NMR study on the role of protein fluctuation in determining the amyloid conformation

Yumiko Ohhashi, Motomasa Tanaka (*Brain Science Institute, RIKEN*)

Aggregation-prone proteins often misfold into multiple distinct amyloid conformations. Although amyloid conformation is crucial factor to determine its toxicity or infectivity, the formation mechanism of diverse conformation remains unclear. Yeast prion Sup35, the [PSI+] ptotein determinant, forms several types of amyloid with different conformations. Sup35 is translation termination factor composed of three domains (N, M, and EF). An EF is globular domain carrying translation termination function. N and M are intrinsically disordered domains required for amyloid formation, however, biological function is unknown. In the present study, we elucidate the role of protein fluctuation in determining the amyloid conformation using NMR spectroscopy. We found that the Sup35-NM mutant, S17R, dramatically altered the amyloid core region. The S17R-type amyloid conformation can propagate to wild-type Sup35-NM easily. These results raised an intriguing possibility that there are (more than) two non-overlapping amyloid core regions in the Sup35-NM sequence and one of the regions is selected depending on the condition under which Sup35-NM amyloid is formed. NMR analysis with CLEANEX-PM and STD revealed that the amino acid residues in both amyloid core regions showed fast exchange rates and their transient interactions in the oligomers might act as a nucleus for amyloid growth.

2PT114 抗真菌活性をもつ DUF26 タンパク質 Gnk2 の構造と機能

Structure and function of Gnk2, a DUF26 protein with antifungal activity

Takuya Miyakawa[1], Yoriko Sawano[1], Ken-ichi Hatano[2], Masaru Tanokura[1] ([1]*Grad. Sch. Agric. Life Sci., Univ. Tokyo*, [2]*Fac. Eng., Gunma Univ.*)

Plants have a variety of potent defense mechanisms against pathogens, including the synthesis of secondary metabolites and antimicrobial proteins. We found that the endosperm of Ginkgo biloba seeds contains ginkbilobin-2 (Gnk2), a novel antifungal protein. Gnk2 consists of 108 amino acids and inhibits growth of plant and human pathogenic fungi. Gnk2 also belongs to DUF26 protein family in plants and has a homology (28-31% identical) to the extracellular domain of cysteine-rich receptor-like kinases (CRKs) from *Oryza sativa* and *Arabidopsis thaliana*. The CRKs are involved in the hypersensitive reaction, which is cell death reaction caused by infection of plant pathogens. Here, we present the structure and function of Gnk2 to provide the first insights into the biochemical properties of DUF26 protein family. Crystal structure showed that the conserved motif of DUF26 protein family considerably contributed to maintain the overall structure of Gnk2 by forming three disulfide bonds. In addition, NMR experiments showed that Gnk2 recognized D-mannose using a binding site surrounded by the residues, Asn11, Gly91, Ala92, Arg93 and Glu104. Their hydrophilic side-chains probably contribute to binding of D-mannose by hydrogen bonds with the free hydroxyl groups of the monosaccharide. The growth-inhibitory assay against a yeast variant lacking mannose chain on cell surface showed that the interaction with mannose chain was an essential event in antifungal mechanism of Gnk2.

2PT115 The short α2-helix of the phospholipase C-δ1 pleckstrin homology domain contributes to stable IP_3 binding

Michikazu Tanio, Katsuyuki Nishimura (*Institute for Molecular Science*)

The phospholipase C (PLC) -δ1 pleckstrin homology (PH) domain has a characteristic short α-helix (α2) from residues 82-87. The contributions of the α2-helix toward the inositol 1, 4, 5-trisphosphate (IP_3) binding activity and thermal stability of the PLC-δ1 PH domain were investigated. Native-PAGE analyses indicated that disruption of the α-helical conformation by replacement of Lys-86 with proline resulted in reduced affinity for IP_3 and in thermal destabilization of the IP_3-binding state. Although the mutant protein with replacement of Lys-86 with alanine showed a slight reduction in thermal stability, the IP_3-binding affinity was similar to that of the wild-type protein. Replacement of Phe-87 with alanine, but not with tyrosine, also resulted in reduced affinity for IP_3 and in thermal instability. The ^1H-^{15}N HSQC NMR study of the selectively [α-^{15}N]Lys-labeled PLC-δ1 PH domain indicated that the conformation of the α2-helix couples with the IP_3-binding activity of the PLC-δ1 PH domain. These results indicated that the helical conformation of the α2-helix and the phenyl ring of Phe-87 play important roles in the IP_3-binding activity and thermal stability of the PLC-δ1 PH domain. Based on these results, the biological role of the α2-helix of the PLC-δ1 PH domain is discussed in terms of membrane binding.

2PT116 ヒト心臓脂肪酸結合蛋白質(FABP3)の脂肪酸結合メカニズムに関する研究

Study of the Fatty Acid Binding Mechanism to Human Heart Fatty Acid Binding Protein (FABP3)

Daisuke Matsuoka[1,2], Shigeru Matsuoka[1,2], Mika Hirose[1,2], Mayumi Niiyama[1,2], Hanako Ishida[1,3], Fuminori Sato[1], Shigeru Sugiyama[1,2], Michio Murata[1,2] ([1]*JST ERATO*, [2]*Grad. Sch. of Sci., Osaka Univ.*, [3]*Grad. Sch. of Eng., Osaka Univ.*)

Understanding the interaction modes between a protein and a small molecule is essential to explain a ligand binding to a protein and to elucidate how water molecules and lipid molecules contribute to the stabilization of proteins. However, unlike water molecules and hydrophilic substrates, hydrophobic molecules interact with proteins mainly through van der Waals interactions, and it is hard to characterize clearly the ambiguous interaction mode.

We are now studying the binding modes of fatty acids to a human heart fatty acid protein (FABP3) through molecular dynamics (MD) simulation, isothermal titration calorimetry and cryogenic X-ray crystallography. We first performed MD simulations of native and mutant FABP3 binding a stearic acid (C18:0 fatty acid). When the residues lining the binding cavity are mutated to smaller amino acids *in silico*, the conformations of the fatty acids and positions of water molecule in the binding cavity are different from ones observed in the native. Then we performed MD simulations of native FABP3 binding lauric (C12:0), myristic (C14:0), and palmitic (C16:0) acids. Within the simulation runs, the palmitic and stearic acids keep the U-shape conformation in the binding cavity, but the myristic and lauric acids show L-shape conformation.

In addition to the computational study, the calorimetric experiment also suggests the interaction modes are different between these fatty acids. From these results and our high resolution crystal structure, we want to discuss the binding modes of fatty acids to FABP3.

2PT117 Actinin-4 変異体の機能解析

The prediction of three dimensional structure for mutants of actinin-4

Nami Miura[1], Miho Banno[2], Kazufumi Honda[1], Akihiko Miyanaga[1], Tesshi Yamada[1] ([1]*Div. Chem. Clin., Natl. Cancer Ctr. Res. Ins.*, [2]*Mitsui Knowledge Industry Co., Ltd.*)

Actinin-4, an actin-bundling protein previously identified by our laboratory, is closely associated with cell motility and cancer metastasis. Three mutations in the *ACTN4* gene encoding the actinin-4 protein are associated with dysfunction of podocytes due to familial focal segmental glomerulosclerosis. We recently identified a novel alternative splice-variant of ACTN4 (ACTN4-sp) that was specifically expressed in high-grade neuroendocrine tumor of the lung (HGNT). The expression of ACTN4-sp, which differs from ACTN4 by three amino acids, was correlated with poor prognosis of patients with HGNT.

ACTN-4 consists of four spectrin repeats, a pair of C-terminal EF-hands, and an actin-binding domain (ABD), which itself consists of a tandem pair of calponin homology (CH) subdomains (CH1 and CH2). All of the mutations in three familial mutations and ACTN4-sp were restricted to the CH2 subdomain of the ABD. Moreover, these mutations were located on the side of the helix, facing the helix-helix interface between CH1 and CH2.

These findings suggest that the three-dimensional structures of the mutations and ACTN4-sp differ from actinin-4, and that these changes were responsible for differences in the biological characteristics of the disease.

2PT118 蛋白質濃度感受性蛍光蛋白質の開発

New fluorescent protein indicator for intracellular protein concentration

Takamitsu Morikawa[1], Katsumi Imada[2], Keiko Yoshizawa[3], Toshio Yanagida[1,3], Takeharu Nagai[4], Tomonobu Watanabe[1,3] ([1]*Graduate School of Frontier Biosciences, Osaka University*, [2]*Department of Macromolecular Science, Graduate School of Science, Osaka University*, [3]*RIKEN Quantitative Biology Center (QBiC)*, [4]*The Institute of Scientific and Industrial Research, Osaka University*)

Typical intracellular protein concentration of cell is about 350mg/mL, which makes the cell a very crowded environment. Recently, it was reported that such molecular crowding could alter enzyme activation. To observe the effects of local protein concentrations inside a cell, we developed a new protein concentration indicator by using YFP.

YFP is sensitive to protein concentration such that an increasing protein concentration causes its fluorescence intensity to decrease. To enhance this sensitivity, we inserted several glycine residues at beta-strand 7.

We next took advantage of CFP being insensitive protein concentration by combining it and a YFP with one glycine insert (hereafter called YFP1G) via a flexible linker. The ratio of the 480nm (CFP) and 525nm (YFP) fluorescent light intensity depended on the protein concentration. Increasing the protein concentration caused the fluorescence intensity of CFP to increase and that of YFP1G to decrease. These results suggest our CFP-YFP1G chimera can act as a protein concentration sensitive FRET probe.

2PT119 Interactions of SicP with SptP subdomains in SicP-binding domain

Yurie Kawashima, Fumio Hayashi, Kenji Oosawa (*Department of Chemistry and Chemical Biology, Graduate School of Engineering, Gunma University*)

Many of Gram-negative bacteria cause infectious diseases. Some of the bacteria construct nano-size of syringe-like structures and export virulence proteins “effector proteins” into host cells using the syringes. Each effector required the most appropriate chaperone for efficient export of the effector. *Salmonella* effector protein SptP, which is involved in cytoskeletal remodeling of the host cell, interacts with SptP-specific chaperone SicP at its N-terminal domain, and the atomic structure of the complex (SicP-$SptP_{1\text{-}158}$) is revealed. According to the complex structure, $SptP_{36\text{-}136}$ seems to be totally involved in SicP-interaction, and the two helices, $SptP_{77\text{-}86}$ and $SptP_{93\text{-}105}$, seem to interact with SicP directly. Thus, the subdomains are responsible for SicP-SptP interactions. To quantitatively reveal the effects of the subdomain on their interactions, we

prepared several truncated SptPs and SicP and examined whether the truncated SptPs interact with SicP in vitro by Native-PAGE and western blotting as the first step.
We constructed pET3c-based plasmids expressing $SptP_{1-136}$, $SptP_{1-105}$, and $SptP_{1-86}$, and the three kinds of the truncated SptPs were individually prepared under denaturing conditions. We also constructed pET3c-based SicP expression plasmid and prepared SicP under native conditions. Thus, we prepared the truncated SptPs and SicP individually, and then we examined whether the truncated SptPs interact with SicP. In this meeting, we will show the results and discuss further efforts.

2PT120 Purification and characterization of glycine-proline-fused type of InvC involved in Salmonella type III secretion system

Aya Watanabe, Fumio Hayashi, Kenji Oosawa (*Department of Chemistry and Chemical Biology, Graduate School of Engineering, Gunma University*)

Some of Gram-negative bacteria export virulence proteins “effector proteins” into host cells using type III secretion systems (T3SS). *Salmonella* T3SS consists of syringe-like structures, effector-specific chaperones, T3SS-specific ATPase, and so on. InvC is the T3SS-specific ATPase in *Salmonella*, and the importance of its ATPase activity is demonstrated by mutant analyses. To reveal the detailed properties of InvC, InvC having a long extra amino acid sequence at the N-terminal end had been examined. In this study, we aimed to prepare InvC whose extra sequence was as short as possible. For this purpose, we used pET50b as an expression vector, because a target protein is expressed as a highly soluble His-Nus-tag fusion protein and the tag is removed by HRV3C protease, which has highly sequence-specific endoprotease activity at 4 °C. We cloned *invC* into the SmaI site by in-fusion method, and then transferred the plasmids into *E.coli* BL21(DE3) cells. The crude extract including His-Nus-InvC was prepared from the culture of the cells, and His-Nus-InvC was prepared using Ni-NTA agarose column. After that, His-Nus-InvC was cleaved by HRV3C protease. As the result of the sequential procedure, we prepared InvC having two amino acid residues, glycine and proline, as the extra sequence. Here, we termed the glycine-proline-fused type of InvC as GP-InvC. We applied GP-InvC to several column chromatography steps for further purification and then examined ATPase activities of GP-InvC under various conditions.

2PT121 X 線 1 分子追跡法による II 型シャペロニン協同性評価

Cooperative Motion Analysis of group II chaperonin at Single-molecule Level using Diffracted X-ray Tracking

Hiroshi Sekiguchi[1,2], Ayumi Nakagawa[4], Kazuki Moriya[4], Mayuno Arita[4], Yohei Yamamoto[4], Kouhei Ichiyanagi[2,3], Masafumi Yohda[4], Naoto Yagi[1], Yuji Sasaki[3] ([1]*Research Utilization Div., JASRI*, [2]*JST CREST Sasaki Team*, [3]*Grad. School Frontier Sci., Univ. Tokyo*, [4]*Dept. Biotech. Life Sci., Tokyo Univ. Agricult. Tech.*)

Group II chaperonin, found in archaea and in the eukaryotic cytosol, is an indispensable protein that captures an unfolded protein and refolds it to the correct conformation in an ATP dependent manner. ATP-induced structural changes are essential for chaperonin foldase activity; the closure and opening of the chamber are the focus of group II chaperonin studies. We had previously reported that the diffracted X-ray tracking method (DXT) could trace ATP induced twisting motion of group II chaperonin ring at single molecule level with high accuracy. In DXT, gold nanocrystal immobilized on one side of chaperonin-ring is used as tracer for structural change of chaperonin. The timing, speed and direction of twising motion of chaperonin-ring after ATP binding could be analyzed by DXT method in detail. In this study, we checked how ATPase deficient mutant subunits modulate the speed or frequency of twisting motion. We controlled the number of ATPase deficient mutant within one chaperonin ring, constructed the ATP deficient hetero-ring using circular permutated connected mutants, and evaluated the effects of those mutants to chaperoning-ring's twisting motion. We will discuss intra- and inter-ring cooperativity of group II chaperonin from such motion analysis view at single molecule level.

2PT122 PAP の酵素活性制御因子としてのトリプトファン残基近傍のコンフォメーションとダイナミクス

The dynamics and conformation of Trp208 and Trp237 as regulating factor of enzymatic activity of Pokeweed Antiviral Protein

Hiromichi Nakashima[1], Yukihiro Fukunaga[2], Keiichi Watanabe[3], Shoji Yamashita[4], Etsuko Nishimoto[4] ([1]*Institute of Biophysics, Faculty of Agriculture, Graduate School of Kyushu University*, [2]*Interdisciplinary Graduate School of Engineering Sciences Kyushu University*, [3]*Department of Applied Biological Sciences, Saga University*, [4]*Molecular Biosciences, Bioscience and Biotechnology, Kyushu University*)

Pokeweed Antiviral Protein (PAP) belongs to a family of Ribosome Inactivating Proteins (RIPs) and works as N-glycosidase to remove a specific adenine residue from ribosomal RNA. We have focused on Trp208 andTrp237 uniquely arranged in PAP as the activity regulating factor. Trp208 locates at the entrance lid of active site and Trp237 is arranged at the C-terminal domain. We have shown that enzymatic activity of PAP is dramatically affected by substitution of Trp208 and Trp237. Additionally, changes of dynamics of Trp208 and the distance between Trp237 and Tyr172 were observed when PAP bound with N-acetylglucosamine, and these changes induced the enhancement of enzymatic activity of PAP. These results demonstrate that dynamics motilities and conformations of Trp208 and Trp237 play important roles in regulating PAP activity. In the present study, we investigated in detail the correlation between the conformation and dynamics near the active site, dynamics in the C-terminal domain and the enzymatic activity of PAP based on the fluorescence spectroscopic data. To analyze the conformational changes, we measured time resolved anisotropy decay and FRET between Tyr and Trp by sub-pico second laser based TCSPC method. Results suggest that Trp208 approached closer nearest neighboring Tyr at the active site as temperature increasing. Then, the internal rotational motion of Trp208 was not observed. Other properties on the dynamics and conformation near the active site will be also discussed compared the enzymatic activity of PAP.

2PT123 フォトンファクトリーの小角散乱ビームラインの現状

Current Status of Small-Angle X-ray Scattering Beamlines at Photon Factory

Nobutaka Shimizu[1], Noriyuki Igarashi[1], Takeharu Mori[1], Ohta Hiromasa[2], Yasuko Nagatani[1], Takashi Kosuge[1], Kenji Ito[1] ([1]*KEK, Photon Factory*, [2]*Mitsubishi Electric SC*)

BL-6A and BL-10C at Photon Factory (PF) has been dedicated for small-angle X-ray scattering (SAXS) experiment. BL-6A is a bending magnet beamline and was moved from the previous BL-15A last summer. This beamline is optimized for measuring samples of various forms, such as a solution, a fiber, and a membrane. CCD detectors (C7300, C4880, Hamamatsu photonics) have used for the time-resolved measurement in a sub-second region. Moreover fast speed (200Hz framing rate) pixel-array detector PILATUS 300K (Dectris) will be installed in this September. BL-10C is also bending magnet beamline and is optimized for measuring a biological solution sample. The data in the broad angle region can be measured with an imaging plate detector R-AXIS VII (Rigaku). We are upgrading BL-10C especially for high-throughput measurement of Bio-SAXS experiment, and developed and installed an automatic solution mixing machine which is a part of a solution-sample changer. Construction of new BL-15A, which light source is a short-gap undulator, is planned for SAXS filed, this will be opened from the autumn of 2013. Moreover, the national project for structure life science research has been started from this April for 5 years, and the SAXS beamlines, BL-10C and new BL-15A will be opened to this project from April in 2013. In this presentation, we will introduce not only the current status of these beamlines, the construction plan of new BL-15A and the upgrade plan based on this project but our results of protein solution structure analysis.

2PT124 *Legionella* DotI and DotJ form a multimeric subcomplex associated with the core complex of the Dot/Icm type IVB secretion system

Tomoko Kubori[1], Takuya Kuroda[2], Katsumi Imada[2], Hiroki Nagai[1] ([1]*RIMD, Osaka Univ.*, [2]*Grad. Sch. Sci., Osaka Univ.*)

Type IV secretion systems (T4SSs) play a central role in the pathogenicity of many bacterial pathogens, including *Agrobacterium tumefaciens, Helicobacter pylori*, and *Legionella pneumophila*. *L. pneumophila* utilizes a protein transport system categorized as a type IVB secretion system (T4BSS), which is a sophisticated supramolecular complex composed of Dot/Icm proteins, to translocate a large array of “effector proteins” into the cytosol of host cells. Due to interact with host cellular systems, effector proteins play pivotal roles for the establishment of infection. Composed of five component proteins, the core complex of the *Legionella* Dot/Icm T4BSS spans the bacterial inner and outer

membrane and is anticipated to form a protein-transport channel. However, the molecular structures of the core complex and potential peripheral subcomplexes have not yet been revealed. We report here that two inner membrane spanning proteins, DotI and DotJ, form a multimeric complex that associates with the inner-membrane components of the core complex. DotI and DotJ show a mutual dependency to maintain their protein levels in bacteria. From these results and other evidence, we hypothesize that DotI and DotJ form a ring like structure that associates with the core complex to function as a transport conduit on the inner membrane.

2PT125 基質及び阻害剤によって誘起される ABC トランスポーター ABCB1 の構造・ダイナミクス変化

Dynamics and Structural Changes of ABCB1 transporter induced by binding of substrates and inhibitors

Wei-Lin Hsu, Yurika Watanabe, **Tadaomi Furuta**, Minoru Sakurai (*Center for Biol. Res. & Inform., Tokyo Tech*)

ATP-binding cassette (ABC) transporters form one of the largest protein families. ABC transporters translocate a number of substrates across cellular membrane by coupling with ATP hydrolysis. Several of these membrane proteins are clinically important in causing, as example, multidrug resistance to cytotoxic pharmaceuticals.
The crystal structures of some ABC transporters have recently been determined. They reveal similar arrangements of the conserved ATP-hydrolyzing nucleotide-binding domains (NBD), but various architectures of the transmembrane domains (TMD), with the exception of common coupling helices that are necessary for transmitting conformational changes. Despite the fact that a wealth of research has been conducted on these structures to resolve the mechanistic problems about how ABC transporters couple with ATP hydrolysis in cytosolic domains to translocate substrates through the transmembrane pore, the specific process about how substrates bind to the proteins and the resultant protein structural change still remains elusive.
Our present study focuses on the mechanism of protein structure changes induced by binding of ATP, substrates or inhibitors in the mouse ABCB1 transporter with an inward-facing conformation. The structure fluctuation simulated by the GROMACS package (version 4.0.7) shows the atomic-level description of the protein structural changes. The result sheds light on the mechanism about the drug translocation process of ABC transporter and the molecular design of inhibitors.

2PT126 核磁気共鳴法による DNA ミスマッチ修復蛋白質 MutL の解析

NMR study on DNA mismatch repair protein MutL

Ryota Mizushima[1,2], Tomoyo Takai[2], Young-Ho Lee[2] ([1]*Grad. Sch. Frontier Biosciences, Osaka Univ.*, [2]*IPR, Osaka Univ.*)

DNA mismatch repair (MMR) works in the last process of gene repair system, enhancing the DNA replication fidelity up to 100 - 1000 folds. Familial non-polyposis colon cancers called Lynch-Syndrome (LS) caused by mutations of genes coding MMR proteins occupies 2 - 5 % of total colon cancers. About 80 % of those who hold such genetic mutations suffered from colon cancers in their life. I am currently engaged in studying one of the MMR proteins called MutL in terms of structural biology by the method of NMR and other biophysical techniques. MutL homologs can be divided into two groups: E coli. and Eukaryotic MutL. The former does not possess endonuclease activity (MutH does instead) and the latter does. In this research, I deal with the latter. MutL is comprised of three parts: dimerized and endonuclease C-terminal domain (CTD), ATPase N-terminal domain transiently dimerized thorough ATP-binding and hydrolytic cleavage and the linker region connecting CTD and NTD. Inter-domain configuration between CTD and NTD is thought to be regulated thorough ATP hydrolysis cycle. Moreover, this configuration dynamics regulates endonuclease activity of MutL and interaction with other MMR proteins. No NMR study has been officially published on both E coli. and eukaryotic MutL so far. The purpose of this research is to elucidate the regulatory mechanisms of MtuL endonuclease activity through analyzing the interaction between CTD and NTD at the residue level by means of NMR.

2PT127 選択的スプライシングによる新規タンパク質アイソフォームの機能・構造予測情報を得るためのツールの開発と公開

Development of a functional and structural annotation tool of novel protein isoforms produced by alternative splicing

Masafumi Shionyu[1], Ken-ichi Takahashi[1], Mitiko Go[1,2] ([1]*Fac. Bio-Sci., Nagahama Inst. Bio-Sci. Tech.*, [2]*ROIS*)

Alternative splicing (AS) is thought to be a major mechanism for diversifying transcriptome and proteome in metazoans. Especially, more than 90% of multi-exon genes in human genome are shown to undergo AS using a next-generation sequencing method. Although the accumulation of novel transcript data produced by AS are accelerated by new experimental technologies, a large portion of proteins encoded by the transcripts (termed "AS isoforms") is not known in their 3D structures and functions. Therefore, information whether AS events affect 3D structures and/or functional sites is expected to be useful for studies of novel AS isoforms. For this purpose, we have developed a pipeline that automatically annotates users' uploaded transcript sequences. Given a transcript sequence, the pipeline identifies regions altered by AS events (termed "AS regions") in a putative protein sequence encoded by the transcript, and assigns functional information such as domains and inter-molecular interaction sites obtained by the 3D structure information. Furthermore, the pipeline predicts the possible 3D structure of the AS isoform using structural constraints of hydrophobic core residues mainly. Based on the pipeline, we have been developing a web tool, named AS-EAST (Alternative Splicing Effects ASsessment Tools). Using our web tool, users can inquire whether their own transcripts encode a novel AS isoform and infer the impact of AS on its molecular function. AS-EAST is a freely available at http://as-alps.nagahama-i-bio.ac.jp/ASEAST/.

2PT128 EGFR 分子 C-末端の天然変性ドメインの 1 分子 FRET 時系列計測

Single-molecule FRET measurement of a intrinsically disordered C-tail domain of an epidermal growth factor receptor

Kenji Okamoto, Yasushi Sako (*RIKEN*)

Structural dynamics of biomolecules, especially proteins, has been known to have indispensable roles in living systems. While conventional X-ray crystallography or NMR is powerful tools to investigate a molecular structure, single-molecule FRET (smFRET) measurement has advantages in observing its dynamics. smFRET can investigate structures of, for example, the intrinsically disordered proteins (IDP) and its time resolution enables realtime observation of structural changes. Epidermal growth factor receptor (EGFR), which is a membrane protein and triggers cellular signal transduction pathways, has the intrinsically disordered (ID) C-tail domain in its intracellular part. The C-tail domain has several phosphorylation sites, one of which binds a protein Grb2 after phosphorylation. Years ago, Grb2-binding kinetics was found to be nonlinear system and it has been suggested that structural dynamics of this ID domain plays an important role. We introduce smFRET measurement of EGFR C-tail domain using recently developed apparatus and statistical data analysis, which is based on the hidden Markov model and the variational Bayes. Time series of 2ch fluorescence signals are obtained from single EGFR C-tail molecules immobilized *in vitro*. Obtained data are analyzed to reconstruct the state transition trajectory (STT) while the number of states is also estimated from data. Further analysis on those STTs gives us details of dynamics, such as possible paths or rates of state transitions.

2PT129 タンパク質の変性及びクロスベータ転移に対する浸透圧効果

Effect of osmotic pressure on protein unfolding and cross-beta transition

Kazuki Takeuchi, Mitsuhiro Hirai (*Grad. Sch. Eng., Gunma Univ.*)

[Introduction]
Proteins are designed to function in crowded environments. However, how a protein folds into its native structure under crowed macromolecular condition is still ambiguous. To clarify the crowding effect on the thermal stability of proteins, we carried out synchrotron radiation wide-angle and small-angle X-ray scattering (WAXS, SAXS) experiments. We employed so-called "osmotic stress" method by using a high molecular weight neutral polymer (osmolyte) in solutions.
[Experimental]
Polyvinylpyrrolidone (PVP) with Mt. 40,000 was used as an osmolyte. The proteins were myoglobin (MY) from horse skeletal muscle and hemoglobin (HM) form bovine blood. The proteins were dissolved in 10 mM HEPES buffers at pH 7.4 with different PVP concentration (0 % to 25 % (w/v)). WAXS and SAXS measurements were performed both at SPring-8 and PF. The temperature of the samples were controlled from 25°C to 85°C.
[Results]
The radius of gyration of the protein at 25 °C showed a minimum at a low PVP

concentration (~15 % for MY; 5 % for HM), which is similar to that of lysozyme [1], where the osmotic pressure induces change of hydration shell. Both proteins show cross-beta transition by the elevation of temperature. The presence of PVP descends the transition temperature of the whole structure, suggesting the destabilization of the native structures. The cross-beta transition was also influenced by PVP addition. The detailed results and discussion will be given.

[Reference]
1. M. Hirai, K. Takeuchi, et al., Thermochimica Acta 532 (2012) 15.

2PT130 Motion Tree 法で解析された SERCA の大規模な構造変化

Large-scale conformational changes of SERCA analyzed by Motion Tree method

Chigusa Kobayashi[1], Ryotaro Koike[2], Motonori Ota[2], Yuji Sugita[1,3,4] ([1]*RIKEN, ASI, Theoretical molecular science*, [2]*Graduation school for information science, Nagoya University*, [3]*RIKEN, AICS*, [4]*RIKEN, QBiC*)

Sarcoplasmic reticulum Ca^{2+}-ATPase (SERCA) is structurally and functionally the best studied member of P-type ATPases. To uptake Ca^{2+} from the cytoplasm to sarcoplasmic reticulum lumen against a large concentration gradient, SERCA undertakes rearrangements of the transmembrane helices coupled with large-scale cytoplasmic domain movements. Although atomic structures of SERCA in different physiological states have been determined by X-ray crystallography, the differences between two crystal structures are significantly large, leaving the molecular mechanisms underlying the structural transitions elusive. In this study, we develop an approach to analyze such large-scale conformational changes of SERCA or other proteins, based on the motion tree algorithm originally developed by Koike et al. (manuscript in preparation). Using the method, we characterize structural transition pathways computed by Climber, a morphing software, and 100ns molecular dynamics (MD) trajectories starting from E2 and E2.Pi states. We conclude that the method is useful to observe intermediate structures for describing large-scale conformational transitions in more detail.

2PT131 H-ras GTP 複合体と H-ras GDP 複合体の分子動力学シミュレーションにおける水分子の解析

Analysis of water molecules in molecular dynamics simulations of H-ras GTP and GDP complexes

Takeshi Miyakawa[1], Ryota Morikawa[1], Masako Takasu[1], Kimikazu Sugimori[2], Kazutomo Kawaguchi[3], Hiroaki Saito[3], Hidemi Nagao[3] ([1]*Sch. Life Sci., Tokyo Univ. Pharm. and Life Sci.*, [2]*Dept. Phys. Therapy, Faculty Health Sci., Kinjo Univ.*, [3]*Inst. Sci. and Eng., Kanazawa Univ.*)

We study the structures of H-ras GTP complex and H-ras GDP complex in solution by molecular dynamics (MD) simulations in order to understand the hydrolysis of the GTP to GDP in the H-ras complex, which play a key role in overcoming human cancer. We have derived the potentials and the atomic charges around Mg^{2+} in H-ras GTP complex and H-ras GDP complex by quantum chemical calculations using hybrid B3LYP functional with 6-31G** basis set. We performed MD simulations using potential parameters of AMBER03 and our parameters around Mg^{2+}. And we analyzed the properties of water molecules around GTP and GDP in each complex. Our analysis shows that the diffusion of water molecules around GTP and GDP is nearly equal to the diffusion of ordinary water molecules. The distance of the closest water molecule from one of P or O atoms in GTP or GDP depends on the species of this atom in GTP or GDP. The probabilities that the water closest to one of P or O atoms in guanine nucleotide is the same water closest to another P or O atom in guanine nucleotide have large value for bonded P-O pairs. We also found that the probabilities in GTP are higher than the probabilities in GDP. This implies that these high probabilities in GTP make the water molecule come to the appropriate position to activate GTP hydrolysis in H-ras-GTP complex.

2PT132 T4 ゲノムパッケージングモーターの分子ダイナミクス

Molecular Dynamics of T4 Genome Packaing Motor

Kazuhiro Takemura[1], Akio Kitao[1,2] ([1]*IMCB, Univ. of Tokyo*, [2]*JST,CREST*)

Almost all bacteriophages have a process of packaging genome into vacant procapsids. The packaging of DNA is powered by ATP hydrolysis and the packaging motor. T4 genome packaging motor consists of gp20, gp17, and gp16. The cryo-EM reconstruction study reported that gp17 forms pentamer and that the X-ray crystal structure of monomeric gp17 could not be fitted into cryo-EM image which is expected to be related to its function. Molecular dynamics simulations were performed to model the atomic structure of pentameric gp17 and to investigate the mechanism of the DNA packaging. Gp17 is composed of N-terminal (1-360) and C-terminal (361-610) domains. A domain motion was detected as the first mode of the principal component analysis for the gp17 monomer in solution which contributes 50 percent of its molecular fluctuation. The observed domain motion might be related to its function and the structural difference between the cryo-EM image and the X-ray crystal structure. To model the gp17 structure close to the EM image from the X-ray crystal structure, we used the recently developed sampling method, PArallel Cascade Sampling MD (PACS-MD, R. Harada and A. Kitao in preparation) in which the snapshots close to the target structure are selected and velocities are redistributed. Using PACS-MD, we successfully obtained the structure of monomeric gp17 which is close to the structure of EM image. Starting from the obtained structure of monomeric gp17, we are currently modeling the atomic structure of pentameric gp17 using PACS MD.

2PT133 タンパク質へのリガンド結合過程の粗視化シミュレーション：タンパク質の立体構造変化の影響の解析

Coarse-grained MD simulations of ligand binding to proteins: Effect of the conformational changes of the proteins

Tatsuki Negami[1], Tohru Terada[2], Kentaro Shimizu[1,2] ([1]*Department of Biotechnology, Graduate School of Agricultural and Life Sciences, The University of Tokyo*, [2]*Agricultural Bioinformatics Research Unit, Graduate School of Agricultutal and Life Sciences, The University of Tokyo*)

Clarifying the mechanism of protein-ligand interactions is one of the most important research subjects in the field of biophysics. However, most of the research efforts have been devoted to predicting the docked structure. The process of ligand binding remains to be clarified. We have demonstrated that coarse grained simulations with the MARTINI force field can reproduce the processes of ligand binding to proteins. However, this method is not directly applicable to proteins that change their conformations upon binding to ligands because elastic network is used to conserve protein structures in the simulation with the MARTINI force field. Since conformational changes of proteins often occur upon ligand binding, it is necessary to extend the method to enable the conformational change of a protein in the coarse grained simulation. Here, we combined a double-well network model with the MARTINI force field for this purpose. First, we constructed Elnedyn elastic network potentials for the ligand-free and ligand-bound structures, and then connected them smoothly to make a double-well potential. We observed frequent conformational transitions between the two states during coarse grained simulations with the double-well potential for several proteins. Furthermore, we performed a few-microsecond simulation randomly arranging ligand molecules around these proteins. We found that the ligands correctly bound to the ligand-binding sites. We will discuss the coupling between the conformational change and the ligand binding affinity.

2PT134 分子動力学シミュレーションによるリジン 48 結合型ジユビキチンのコンパクト構造の解析

Molecular dynamics simulation study of Lys48-linked diubiquitin in compact conformation

Sotaro Fuchigami[1], Mitsunori Ikeguchi[1], Akinori Kidera[1,2] ([1]*Grad. Sch. of Nanobioscience, Yokohama City Univ.*, [2]*CSRP, RIKEN*)

Protein ubiquitination is a post-translational modification involved in regulation of diverse cellular processes, including protein degradation, cell signaling, DNA damage response and transport processes. Ubiquitin can be conjugated not only to a target protein but also to another ubiquitin via one of its seven lysine residues, resulting in formation of polyubiquitin chains with diverse types of linkages. The most examined is Lys48-linked polyubiquitin chain, which acts as a tag for protein degradation by 26S proteasome. Several studies have shown that Lys48-linked diubiquitin is in the compact conformation, in which the hydrophobic patches of both ubiquitins interact with each other. It is considered that the Lys48-linked diubiquitin changes its conformation to interact with its receptors, whereas its mechanism is not well understood. In the present study, we performed molecular dynamics simulation of the Lys48-linked diubiquitin in the compact conformation and investigated its conformation stability. More than one microsecond simulations revealed that the compact conformation was fairly stable even though interaction between the hydrophobic patches was partially disrupted by local conformational changes of ubiquitins. We attributed the high stability of the diubiquitin to main-chain hydrogen bonds between ubiquitins and confirmed this by mutant simulations.

2PT135 粗視化モデルによる PPAR γの基質依存的な活性変化の考察

Coarse-grained molecular dynamics study of ligand-dependent reaction activity of PPARγ

Akinori Awazu (*Dept. of Mathematical and Life Sciences, Hiroshima University*)

Peroxisome proliferator-activated receptors γ (PPARγ) is one of the nuclear receptors of transcription factors controlling genes implicated in energy, carbohydrate, and lipid metabolism. Recent experimental studies reported that PPARγ can bind with several ligands and show its activity. These ligands are classified by Full agonist and Partial agonist depend on the activity of the transcriptional response, where the binding with Full agonists induces much higher molecular activity than that with Partial agonists. On the other hand, the recent X-ray crystal structure analysis implies the structure of PPARγ is obtained almost the same independent of the types of agonists. This fact seems the difference of transcriptional activity is originated by the difference of molecular motion and the motion inducing effective molecular structure, which are encoded in the mechanical network consists of amino acids and the binding ligand.

In the present study, we perform the Brownian dynamics simulation of the coarse-grained model of PPARγ to unveil the biding ligand shape dependency of the molecular dynamical properties. Through the statistical analysis of the results of GO-like model simulation, we extract the ligand-dependent effective interaction network and compare the contribution of these networks to the molecular function.

2PT136 多剤排出トランスポーター AcrB の全原子分子動力学シミュレーションによる解析

All-atom molecular dynamics simulation of multidrug transporter AcrB

Tsutomu Yamane, Mitsunori Ikeguchi (*Grad. Sch. Bio-nano sci. Yokohama City Univ.*)

In E. coli, the multi drag transporter AcrB resides in the inner membrane region. Recently, x-ray structures provided that AcrB forms trimeric protein where each protomer is different conformation, “binding”, “extrusion” and “access” state, which are different from the shape of drug binding region (porter domain). In addition, extrusion state protomer has the unique side chain conformations of residues which are essential for the proton transfer, “proton translation site” (Asp407, Asp408 and Lys940). These results suggest that AcrB exported drugs outside of the cell by a three-step structural change involved in the proton motive force which related with the conformational change in protonation sites. In the present study, we performed all-atom molecular dynamics (MD) simulations of AcrB-membrane-water system. Our simulations with the different protonation states of the titratable residues in the proton translation site revealed the correspondence between the specific protonation states and the side-chain configurations observed in the crystal structure. Changing the protonation state of one aspartate induced a spontaneous structural transition, suggesting that the stoichiometry of proton translocation might be one proton per step of the functional rotation. Furthermore, our simulations demonstrate that alternating the protonation states in the transmembrane domain induces functional rotation in the porter domain that is primarily responsible for drug transport.

2PT137 キサンチン酸化還元酵素とリガンド複合体に関する分子動力学計算と結合自由エネルギー解析

Molecular dynamics simulations and binding free energy analysis of xanthine oxidoreductase-ligand complexes

Hiroto Kikuchi[1], Hiroshi Fujisaki[1,3], Tadaomi Furuta[2], Ken Okamoto[4], Takeshi Nishino[5] ([1]*Dept. of Phys., Nippon Med. Sch.*, [2]*Grad. Sch. of Biosci. & Biotech., Tokyo Inst. of Tech.*, [3]*Wako, Riken*, [4]*Dept. of Biochem., Nippon Med. Sch.*, [5]*Grad. Sch. of Agri. & Life Sci., Univ. Tokyo*)

Xanthine oxidoreductase (XOR) is an enzyme which is found in a wide range of organisms from bacteria to man and plays an important role in the catabolism of purine substrates. In mammals and birds, XOR physiologically catalyzes the hydroxylation of hypoxanthine to xanthine, followed by the catalysis of the hydroxylation of xanthine to uric acid. As the excessive production of uric acid leads to gout and hyperuricemia, the inhibitors for XOR can be effective as the drugs for these diseases. Febuxostat, which fills up most of the cavity of mammalian XOR without being covalently bound to it, has been developed as a non-purine selective inhibitor of XOR, showing a more potent and longer-lasting urate-lowering effect than allopurinol which is another XOR inhibitor, widely prescribed as a treatment of gout and hyperuricemia for more than 40 years. Clinical efficacy and tolerance to febuxostat have been confirmed, and the drug is available as Adenuric (EU), Uloric (US), or Feburic (Japan). In our previous work [H. Kikuchi et al., Sci. Rep. **2**, 331 (2012)], we studied the binding interaction between febuxostat and two (mammalian and bacterial) XORs, and clarified the role of the molecular details of the drug-enzyme interaction using both molecular dynamics simulations and enzymological experiments. In the present work, we further investigate the binding mechanism using free energy calculations, employing different types of drugs and mutated XORs.

2PT138 Features of Amino Acids Changes Determining the Glycan Specificities of Influenza Hemagglutinins: Interaction Energy Profiles

Katsumi Omagari (*Nagoya City University*)

The interaction between hemagglutinin (HA) and glycan receptors exposed on the host cell is a kernel in the study of host adaptation of influenza A viruses. Receptor binding, the initial event in virus infections, is major determinant of virus transmissibility. HA's of avian viruses prefer sialic acid in α2,3-linkage to galactose, the avian receptor, while those of human viruses prefer sialic acid in α2,6-linkage, the human receptor. A conversion to human receptor specificity is believed to be one of the changes required for the introduction of new HA subtypes to the human population, which can lead to pandemics. Extensive crystal structural studies have revealed that the human or avian receptors adopt a very similar conformation in both human and avian HA-receptor complexes. Those structures revealed no preferential binding of avian receptor over that of human receptor. In this poster, to understand the detailed interaction profile of the HA-receptor complex, I will describe why/how HA's recognize two type of receptor through those HA's bind receptors in similar fashion, using molecular dynamics and MM-GBSA/PBSA methods. The examined systems comprise explicitly solvated form of three H1 human virus HA's, avian and swine H1 HA in complex with avian and human receptors, respectively. Effects of substitutions at key positions on the HA and their possible contribution to specificities were investigated too. Those results suggested the differences of interaction energy profiles between HA's in spite of similar binding conformation.

2PT139 筋小胞体カルシウムポンプの ATP 結合状態の分子動力学計算

Molecular dynamics simulations of SR Ca2+-pump in the ATP bound forms

Yasuaki Komuro[1,2], Chigusa Kobayashi[2], Eiro Muneyuki[1], Yuji Sugita[2,3,4] ([1]*Grad. Dept. Phys., Chuo Univ.*, [2]*RIKEN ASI*, [3]*RIKEN QBiC*, [4]*RIKEN AICS*)

Sarcoplasmic reticulum (SR) Ca2+-pump is a P-type ATPase that transports two Ca2+ ion across the SR membrane against a large concentration gradient, utilizing chemical energy released in ATP hydrolysis. This protein consists of ten transmembrane helices as well as three large cytoplasmic domains: A (actuator), N (nucleotide-binding), and P (phosphorylation) domains. In an enzymatic reaction cycle, SR Ca2+-pump rearranges six out of ten transmembrane helices and thereby changes the affinity for Ca2+ at the binding sites. In classical E1/E2 theory, the E1 state is defined as the high affinity state for Ca2+, whereas the affinity is low in the E2 state. In this study, we focus on the ATP or ADP bound states (E1ATP and E1PADP) for the SR Ca2+-pump and perform atomistic molecular dynamics (MD) simulations with explicit solvent and DOPC lipid bilayer, starting the X-ray crystal structures. Although the X-ray structure for the ATP bound form is almost the same as that for the ADP bound form, the differences of physiological conditions between these two states have been pointed out. By performing the MD simulations, we investigate the global conformational flexibilities of the pump as well as the Ca2+-binding affinities at the transmembrane binding sites.

2PT140 Computational design of small peptide inhibotrs of protein-protein interactions in intracellular signaling

Junya Yamagishi[1,2], Noriaki Okimoto[2], Takuma Kasai[3], Mariko Okada[3], Akira Imamoto[4], Makoto Taiji[1,2] ([1]*Grad. Sch. of Fron. Sci., Univ. of Tokyo*, [2]*QBiC, RIKEN*, [3]*Yokohama Inst., RIKEN*, [4]*Ben May Dept., Chicago Univ.*)

A CRK SH2 domain preferentially binds to peptides having the pYXXP motif

(where pY is a phosphotyrosine and X is any amino acids). CRK have been considered to be indispensable for malignant features of human cancers, so that it is important to develop novel inhibitors of CRK mediated protein-protein interactions for new cancer therapies. In this work, we performed docking-based screening of small peptides against the CRK SH2.
Conventional docking programs have been developed to design small molecules and cannot be applied for peptide design because of their following characteristics. (1) Peptides have many rotatable bonds, which makes difficult to predict binding mode in a peptide-protein complex. (2) Peptides also have more polar functional moieties than small molecules and no proper scoring functions are available for peptide docking. Rescoring of docking poses using MM (molecular mechanics) is a useful approach to estimate binding affinities of peptides to their target protein. But the problem of inaccuracy of docking poses still remains.
In this work, we developed our docking program using MM and the generalized born (GB) solvent. For large computational requirements of MM and GB, we accelerated our program using GPU. After docking, a MM-PBSA rescoring was conducted to estimate binding affinities. Furthermore, we performed additional conformational search of peptides in unbound states to take account of ligand's reorganization effects. Our methods showed high performances in discrimination of known binding sequences.

2PT141 タンパク質（DHFR）における局所変異が引き起こす運動性の変化に関する理論的考察

Theoretical study of change of motility by local mutation in DHFR

Tomo Matsubara, Masashi Fujii, Hiraku Nishimori, Akinori Awazu (*Dept. of math and Life Sci, Hiroshima Univ*)

The dihydrofolate reductase (DHFR) is composed of some secondary structures and fluctuating loops called Met20 loop, CD loop, FG loop, GH loop. The recent experimental study indicates that the dynamical properties encoded by such molecular structure provide the dominant contribution to the function of DHFR, where a small mutation of CD loop which does not give structual variation of the molecule and far from the reaction site (around Met20 loop) gives a drastic change in intra-molecular global motion and its reaction activity. In the present study, we perform the normal mode analysis of an all-atom model of DHFR and discuss the general features of the relations among the local and global motions of such molecules.
We employ the elastic network model as all-atom model of protein dynamics.In this model, each atom is described as beads and each pair of beads connected by virtual bonds with the natural length that equals to the native distance between the corresponding atoms. We obtained the atomic coordinates from Protein Data Bank (PDB code:1rx2, 1rx6) to construct the structure of DHFR. By the normal mode analysis of this model, we investigate the correlation of motility among characteristic local structures and discuss the mechanism of the suppression of the reaction activity by the minor local mutation observed in the experiment.

2PT142 Theoretical evaluation of structural stability of the active site of T1 lipase: cation-π vs. water-π interactions

Atsushi Nakamura, Jiyoung Kang, Masaru Tateno (*Grad. Sch. Sci., Univ. Hyogo*)

Crystallographic data obtained by Matsumura, H., et al. (Osaka Univ.) suggested that the sphere electron density that was found in the active site of T1 lipase is corresponding to the interaction of Na+ and the aromatic ring of a Phe residue (i.e., cation-π interaction). However, it was also augured that a water molecule can interact with π electrons (i. e., water-π interaction). Thus, experimental approaches could not dismiss the possible presence of water instead of Na+ in the active site of T1 lipase. We theoretically evaluated these two types of interactions, employing molecular dynamics (MD) simulations.
The current force fields cannot estimate the cation-π interaction correctly, requiring *ab initio* quantum mechanical calculations. So, we developed a novel efficient scheme to calculate the potential energy of cation-π interaction, with the high accuracy at the CCSD(T) level and the low calculation cost comparable to the standard force field. Our MD calculations showed that a large enthalpy gain of the Na＋-π interaction can preserve the catalytic core structure. In contrast, water-π interaction seriously induced the structural instability. Thus, the possible presence of water may be excluded [1-2]. Our novel scheme is currently the only way to perform long-time MD simulations involving cation-π interaction, with reasonable calculation cost. In the session, the functional roles of cation-π interactions in T1 lipase will be discussed.
[1] JCTC 7 (2011) 2593
[2] JACS 132 (2010) 2751

2PT143 分子動力学シミュレーションによる緑色蛍光タンパク質の切断位置と蛍光回復の研究

Research of Split Point and Fluorescent Recovery of Green Fluorescent Protein by Molecular Dynamics Simulation

Mashiho Ito[1,2], Shoji Takada[2], Takeaki Ozawa[1] ([1]*Dep. Chem., Sch. Sci., Univ. Tokyo*, [2]*Dep. Bio., Grad. Sch. Sci., Kyoto Univ.*)

Split Green Fluorescent Protein (Split GFP) is a useful tool for investigating protein-protein interaction *in vivo*. Each fragment of Split GFP are reconstruct chromophore by binding and recover fluorescence. However, less is known about the mechanism of folding and reconstructing of Split GFP. In particular, the reason why fluorescence depends on the position of split point. To reveal this, we performed molecular dynamics simulation of Split GFP, Coarse-Grain simulation and All-Atom simulation. From Coarse-Grain simulation of Split GFP, here we report three points about Split GFP Folding. First, N-terminal fragment in Split GFP is folding earlier than C-terminal at all events. Second, the folding of C-terminal fragment and whole GFP are at the same time. Finally, the stability of N-terminal fragment is related to the speed of folding of whole Split GFP. From these data we devised a model of Folding of Split GFP that first N-terminal fragment becomes core structure of GFP, and then it will covered by C-terminal fragment. From All-Atom simulation, we evaluate the stability of Split GFP of each split point and show the difference of split point in loop regions or β-strand regions. These results provide a new perspective on split protein folding.

2PT144 SlyD 融合による人工三本鎖ベータヘリックスの可溶化の試み

Solubilization approaches of artificial three-stranded beta-helix by fusing SlyD protein

Kaname Nishijo[1], Shuji Kanamaru[2], Fumio Arisaka[1] ([1]*Dept of LifeScience, Grad Sch of Biosci&Bioeng, Tokyo Institute of Technology*, [2]*Dept of Bioengineering, Grad Sch of Biosci&Bioeng, Tokyo Institute of Technology*)

The C-terminal domain of gp5 of bacteriophage T4 has a unique three-stranded parallel beta-helix and forms a triangular prism. The amino acid sequence of this domain has the characteristic 12 repeats of 8 amino acids VXGXXXXX. We aim to create artificial triple beta-helix proteins whose length is controlled by tandemly connecting the building block of 6 repeats of VXGXXXXX ($(VXG)_6$).
In our previous studies of tandemly connected $(VXG)_6$ by genetic engineering, we were able to create and purify the artificial triple beta-helix which was expected to consist of one or two building blocks. However, large amounts of larger oligomers as well as the dimer of beta-helix were formed. Those larger oligomers are formed by association the artificial three-stranded beta-helix.
In order to avoid the dimer formation of the beta-helix, we fused ^{His}SlyD at the N-terminus of the three-stranded beta-helix. SlyD is known to have the ability to solubilize fused proteins. Sedimentation velocity analysis of the purified proteins indicated that the main product was still the dimer of the beta-helix. In addition, size exclusion chromatography of the products indicated the presence of partially unfolded beta-helices. Thus we concluded that the dimerization of the beta-helix spontaneously occurred at the N-terminus of the beta-helices which is partially unfolded.

2PT145 Fluorescence Titration for finding the binding sites of Peptide Aptamers on Calmodulin

Yasodha Manandhar, Wei Wang, Takanori Uzawa, Yoshihiro Ito, Toshiro Aigaki (*RIKEN, Advanced Science Institute*)

Aptamers are in vitro selected nucleic acids or peptides which specifically bind to various target molecules. Although aptamers modified with a fluorescent molecule are often used for diagnoses to signal out its target binding, such modifications sometimes interfere the specific binding. To avoid this we previously selected signaling peptide aptamers from a library of random sequenced peptides including a non-natural fluorogenic amino acid, 7-Nitro-2,1,3-benzoxadiazole modified aminophenylalanine (NBD-aa). We choose a multifunctional intermediate messenger protein, calmodulin (CaM), as a target. CaM transduces calcium signals by binding calcium ions on its two approximately symmetrical globular C and N domains. We found that one of the selected peptides, C5 (YWDKIKD*IGG; *NBD-aa) has a strong binding affinity (Kd= 2) with the C domain of CaM. However the binding sites of the other selected peptides have not been clarified yet. Thus motivated here we investigated the binding sites of those peptides from the titrations with the CaM-

C5 complex.
The titration of B4' with CaM-C5 exhibited signal increase in a similar way as the titration with CaM, implying that the primary binding site of this peptide is N domain of CaM. In contrast the titration of other peptides with CaM-C5 did not exhibited significant signal change, implying that the primary binding site of those peptides are C domain of CaM where C5 occupies already. We further examine the B4' binding site by employing NMR.

2PT146 Characterization of norovirus RNA replicase *in vitro* for the autonomous protein evolution using *in vitro* virus

Hidenao Arai[1], Manish Biyani[2], Yuzuru Husimi[3] ([1]*Grad. Sch. Sci. Eng., Saitama Univ.*, [2]*Inst. of Engineering Innovation, Grad. Sch. Eng., Univ. of Tokyo*, [3]*Innovation Research Organization, Saitama Univ.*)

We have been trying to construct an autonomous protein evolution system, combining the *in vitro* virus (IVV) and the one-pot isothermal RNA replication reaction. In our system, the norovirus RNA replicase ($3D^{pol}$) is planned to be displayed on the IVV.
In this work, we evaluated the activity of $3D^{pol}$, which was synthesized in cell-free protein synthesis system. As indicated in the previous report, when a ss (single-stranded) RNA was incubated with $3D^{pol}$, it was replicated to a ds (double-stranded) RNA in a primer-independent manner. And the isothermal amplification of the dsRNA by eight-fold was realized. In the primer-independent replication reaction, the presence of C-stretch at the 3'-terminus increased the replication efficiency by six-fold. Contrary to the previous report, $3D^{pol}$ also replicated RNA in a primer-dependent manner and a self-primed (small stem-loop) manner. Moreover, the initiation of replication was severely dependent on the 3'-terminal structure of RNA, and especially, $3D^{pol}$ preferred the very small self-primed structure than the single- or double-stranded structure. And the initiation form may be dependent on the divalent ions (Mg^{2+} or Mn^{2+}). From these results, we were able to draw a scheme of the *in vitro* primer-independent RNA replication by $3D^{pol}$.
Using the IVV displaying $3D^{pol}$, we designed the one-pot isothermal replication reaction system, in which the IVV can amplify itself, and evolve autonomously. This reaction system will evolve not only the RNA replicase but also the amplification algorithm itself.

2PT147 *In vitro* selection of a protease using cDNA display

Shingo Ueno[1,3], Yuka Mashio[2,3], Takanori Ichiki[1,3], Naoto Nemoto[2,3] ([1]*Grad. Sch. Eng., Univ. Tokyo*, [2]*Grad. Sch. Sci. and Eng., Saitama Univ.*, [3]*CREST, JST*)

The artificial evolution of enzymes is one of the ultimate goals of evolutionary molecular engineering. *In vitro* display technologies, such as phage display, ribosome display, mRNA display and cDNA display have been widely used for affinity selection against various targets in the last two decades[1]. Conversely, although some groups have been able to evolve enzymes using phage display[2], there are only a few examples describing mRNA display[3] and ribosome display[4].
Recently, we have started the challenge to evolve enzymes *in vitro* using cDNA display, which is more stable and easy-to-use than mRNA display[5]. We designed a selection system with a new puromycin linker of cDNA display for *in vitro* selection of a protease. The linker was designed to release the cDNA coding the gene of a displayed protease, from a solid-phase support when a peptide substrate was cleaved by the displayed protease.
In this study, we demonstrated a model selection of subtilisin, one of well identified protease. We will discuss the model screening experiments and present some results.

References
1. Ullman CG, Frigotto L, Cooley RN (2011) *Brief Funct Genomics* **10**: 125-134.
2. Fernandez-Gacio A, Uguen M, Fastrez J (2003) *Trends Biotechnol* **21**: 408-414.
3. Seelig B, Szostak JW (2007) *Nature* **448**: 828-831.
4. Yanagida H, Matsuura T, Kazuta Y, Yomo T (2011) *Chembiochem* **12**: 962-969.
5. Yamaguchi J, et al. (2009) *Nucl Acids Res* **37**: e108.

2PT148 ヒトレチノイン酸結合蛋白質をスカッフォールドとする蛋白質のスクリーニング

Screening of mutant proteins scaffolding human cellular retinoic acid binding protein 2

Hinako Nakada, Nobuya Itoh, Yoshihide Makino (*Grad. Sch. Eng., Toyama Pref. Univ.*)

Proteins have ability to bind other molecule specifically. The creation of artificial specificity of proteins has been studied. The proteins developed by these studies are expected to be applied to pharmaceuticals or drug carriers. Our objective is to create the library mutant human retinoic acid binding protein 2 (HCRABP2), and to screen novel binding ability to vascular endothelial growth factor (VEGF). Sixteen amino acid mutations were introduced into HCRABP2 at the side surface of beta-barrel. Phage display library of the mutants were constructed. Display phage clones were selected through three rounds of affinity panning. The affinity of concentrated display phages was analyzed; and the positive signals were obtained by ELISA analysis. This result suggests existence of clones which might bind to VEGF. Detailed analysis of VEGF-binding affinity and sequence of mutant clones is in progress.

2PT149 マイクロ波照射下での PCR 反応の DNA ポリメラーゼの特異性

The DNA Polymerase Specificity on Microwave Assisted PCR

Hiroya Osoegawa[1], Seiji Higa[1], Takaya Takei[1], Kaori Tanaka[1], Takeo Yoshimura[2], Shokichi Ohuchi[1] ([1]*Dept. Biosci. Bioinform., Kyushu Inst. Technol.*, [2]*Dept. Appl. Bio. Sci., Tokyo Univ. Sci.*)

Microwave has shown its various features in various chemical reactions, the time shortening, the reduction of reaction temperature, and so on. The microwave effect can be also applied to biocatalysts and enzyme reactions. We have studied to take advantage of the microwave heating to the field of chemical biology and biotechnology. Among them, the polymerase chain reaction (PCR) for gene amplification under microwave irradiation was obtained as a unique result. In PCR method, the three processes are repeated, (1) the thermal denaturation to the single-stranded DNA from the double strand DNA, (2) the hybridization by annealing between the primer and the single-strand DNA, (3) the enzymatic DNA elongation from the primer by DNA polymerase. So that, we demonstrated the microwave heating for the processes of the thermal denaturation and the enzymatic elongation reaction. The Vent DNA polymerase and ExTaq DNA polymerase were used in this study. The ExTaq polymerase was decreased the fluorescence intensity by the microwave irradiation. On the other hand, the Vent polymerase was shown same intensity of fluorescence between the microwave irradiation and the conventional condition. The ExTaq polymerase showed the different phenomena between the microwave irradiation and the conventional heating in spite of same temperature. It is seems that the protein structure is changed under the microwave irradiation. This fact might mean a new state of protein denaturation, what we would call "Microwave Denaturation".

2PT150 モルテングロビュール状態の蛋白質を利用した新規抗腫瘍複合体の作製

Development of novel anti-tumor complexes made from a protein in the molten globule state

Takashi Nakamura[1,2], Ryusho Kariya[3], Seiji Okada[3], Kunihiro Kuwajima[1,2,4] ([1]*Okazaki Inst. Integr. Biosci.*, [2]*Inst. Mol. Sci.*, [3]*Center for AIDS Reseach, Kumamoto Univ.*, [4]*Dept. of Funct. Mol. Sci., Grad. Univ. Adv. Studies*)

Human α-lactalbumin (α-LA)-oleic acid complex, named HAMLET (human alpha-lactalbumin made lethal to tumor cells), induces apoptosis-like death of tumor cells, and α-LA in the HAMLET is in a molten globule (MG)-like conformation. Our previous studies have suggested that α-LA in the anti-tumor complex may act as a carrier and that oleic acid in the complex may act as an apoptosis inducer in tumor cells. We have thus asuumed that α-LA in the MG state can be used as a delivery carrier of anti-cancer drugs to tumor cells. To investigate this possibility, first, we attempted to make complexes between α-LA and various anti-cancer drugs. As a results, certain anti-cancer drugs form a complex with α-LA in the MG state at pH 2.0, and these complexes were stable under physiological conditions (pH 7.4). Next, we tested cell toxicity of these complexes against various cells. Interestingly, these α-LA-anti-cancer drug complexes exhibited stronger toxicity against tumor cells, but weaker toxicity against normal fibroblast cells than the free drugs. This finding demonstrates that α-LA in the MG state may be a potential drug carrier for cancer therapy.

2PT151 計算化学と実験から考察した，黄色ブドウ球菌のヘム鉄結合・輸送機構解析

Computational and experimental studies on heme-binding and heme-transport mechanisms of Isd proteins of *Staphylococcus aureus*

Yoshitaka Moriwaki[1], Tohru Terada[1], Jose M. M. Caaveiro[2], Yousuke Takaoka[3], Itaru Hamachi[3], Kouhei Tsumoto[2], Kentaro Shimizu[1] ([1]*Dept. of Biotech., Grad Sch. of Agri. Life Sci., Univ. of Tokyo*, [2]*Ins. of Med. Sci., Univ. of Tokyo*, [3]*Dept. Syn., Chem. & Biol. Chem., Kyoto Univ.*)

Iron is an absolute requirement for nearly all organisms. Bacterial pathogens have evolved the iron acquisition systems because iron is not readily available in human body. *Staphylococcous aureus* employs the iron-regulated surface determinant (Isd) system as its primary heme-iron uptake pathway. In other words, this system is a promising target to battle *S.aureus*. Heme molecule is first extracted from humans' hemoglobin and captured by IsdH or IsdB. IsdA and IsdC relays heme to IsdE on the plasma membrane. Although the crystal structures of Isd proteins have been solved with and without heme, the mechanism of the one-way transport is still unclear because of the close similarity of these structures. We examined the heme-binding and heme-transport mechanisms of Isd proteins not only in vitro, but also using in silico methodologies. Isothermal titration calorimetry (ITC) experiments showed that the downstream Isd proteins have higher affinities against heme than the upstream proteins. Qualitatively consistent results were obtained from the free-energy calculations with the MM-PBSA method, which revealed enthalpic contributions of the residues to the affinity to heme for each Isd protein. Based on these results, we designed and synthesized a heme derivative. We will examine its growth inhibition activity in vivo. In addition, the QM/MM (ONIOM) calculation is being performed for a model of a heme-transport complex composed of two Isd proteins and one heme. We will discuss the transport mechanism between the Isd proteins.

2PT152 ヒトヘモグロビンの酸素親和性の制御における本質：四次構造、三次構造変化に共通して起こる Fe-His 結合の変化

Essence in oxygen affinity regulation of human adult hemoglobin: Change of Fe-His bond length by quaternary or tertiary structure change

Shigenori Nagatomo, Yasuhisa Yamamura, Kazuya Saito (*Dept. Chem., Univ. Tsukuba*)

Human adult hemoglobin (HbA) possessing $\alpha_2\beta_2$ tetramer structure exhibits cooperativity in oxygen binding. X-ray crystallographic studies have demonstrated the presence of two distinct quaternary structures, called T (tense) and R (relaxed) states, which correspond to the low- and high- O_2 affinity forms, respectively. Both the quaternary structures of T and R exhibit different Fe-His bond lengths: they are shorter in R state than T state in both the α and β subunits.

Extensive examinations of HbA in the presence of the allosteric effector bezafibrate (BZF) showed a reduction of the oxygen affinity of oxyHbA in the R structure and the importance of tertiary structure change for oxygen affinity is stressed. Recently, one of authors reported that the decrease in oxygen affinity of oxyHbA upon BZF addition accompanies the elongation of Fe-His bond in α subunit [1]. Our finding is consistent with the molecular dynamics calculation of Yonetani and Laberge [2], in which the main chain in E and F helices of HbA fluctuates more in the presence than in the absence of BZF. This enhanced fluctuation in the E and F helices results in weakening of the Fe-His bond.

Thus, the longation of Fe-His bond length is caused by not only quaternary structure but also tertiary structure change. This suggests that the elongation of Fe-His bond is essential in oxygen affinity regulation of human adult hemoglobin. [1] S. Nagatomo, H. Hamada and H. Yoshikawa, *J. Phys. Chem.* **B 115**, 12971 (2011). [2] T. Yonetani and M. Laberge, *Biochim. Biophys. Acta* **1784**, 1146 (2008).

2PT153 Structural fluctuation and change around heme pockets of liganded Hb induced by L35 binding

Kenji Kanaori[1], Yusuke Tajiri[1], Antonio Tsuneshige[2], Takashi Yonetani[3] ([1]*Grad. Sch., Kyoto Inst. of Tech.*, [2]*Hosei Univ.*, [3]*Univ. Pennsylvania*)

Hemoglobin (Hb) takes two structures, depending on oxygen binding; T-quaternary structure with low oxygen-affinity and R-quaternary structure with high oxygen-affinity. Heterotropic effectors decrease the oxygen-affinity and its cooperativity. In the presence of two potent effectors, L35 and inositol hexaphosphate (IHP) at pH 6.8, 1H-NMR spectra of human adult Hb showed oxy-T-quaternary structure. The NMR signals around heme pockets of the oxy-T structure were rather broad, indicating that some structural fluctuations occur around the heme, and the fluctuations may be related with the reduction of the oxygen-affinity. In order to clarify the structural fluctuations in the heme-pocket induced by L35 and IHP, NMR spectra of liganded met-Hbs were measured in the presence of the effectors. It has been known that the N3-metHb shows some IHP-induced hyper fine shifted (hfs) signals besides the heme methyl signals around 15-35 ppm. The addition of L35 to the N3-metHb with IHP showed that the heme signals were shifted and broadened, but the IHP-induced hfs signals were increased. The pH dependence of the hfs signals was also examined and the pH increase from 6 to 8 showed that the IHP-induced signals disappeared, suggesting that the spectral change should be related to the change in the oxygen affinity. The quaternary structural change of metHb will be discussed based on hydrogen bond signals around 12-13 ppm.

2PT154 ヒトヘモグロビンのβ 145Tyr の Thr または Leu への置換が機能と構造に与える影響

Effects of the substitutions of Thr or Leu for β145 Tyr on the structure and oxygen binding properties of human hemoglobin

Momoko Ichii[2], Yukifumi Nagai[1], Kiyohiro Imai[1,2], Masako Nagai[1] ([1]*Res. Center for Micro-Nano Tech.Hosei Univ.*, [2]*Frontier Biosci. and Applied Chem. Hosei Univ.*)

In all the vertebrate hemoglobins and myoglobins, the penultimate position (HC2) is invariably occupied by tyrosine (Tyr). The natural and artificial mutants of β145Tyr studied so far, show the extremely high oxygen affinity and low cooperativity. To examine the role of β145Tyr on the structure and oxygen binding properties, we expressed two new artificial mutant Hbs in *E. coli*, rHb(βY145L) and rHb(βY145T) and purified them as described previously [1]. These mutant Hbs exhibited a markedly high oxygen affinity and diminished cooperativity (P_{50}=0.6-0.9 mmHg, Hill's n=1.3-1.4). In the presence of inisitol hexaphosphate (IHP), however, oxygen affinity of these mutant Hbs decreased and exhibited significant cooperativity; P_{50} = 1. 7 mmHg, n = 1. 9 for Hb (βY145T); P_{50}=2.4 mmHg, n=2.2 for Hb(βY145L). From the oxygen binding properties of these mutant Hbs, the replacement of β145Tyr by Leu seems to stabilize the T-conformation more than that of Thr. DeoxyHb (βY145L) exhibited a smaller negative CD band at 286 nm (a T-state marker band) than that of deoxyHbA, but exhibited an increase in intensity of the negative CD band upon the addition of IHP. These results indicate that the residue at HC2 of β subunits contributes to stabilization of the T-conformation through hydrophobic interactions with the surroundings in addition to hydrogen bonding to βFG5Val corbonyl group. [1]Nagai,M., Nagai,Y., Aki,Y., Imai,K., Wada, Y., Nagatomo,S., and Yamamoto,Y. *Biochemistry, 47*, 517-525 (2008).

2PT155 *cbb*$_3$型チトクロム酸化酵素の酸素消費活性

Oxygen consumption activity of *cbb*$_3$-type cytochrome c oxidase

Yui Iwamoto[1], Yuriko Ando[1], Kazumasa Muramoto[1], Robert Gennis[2], Yoshitsugu Shiro[1,3] ([1]*Grad. Sch. Sci., Univ. Hyogo*, [2]*Univ. Illinois*, [3]*Harima Inst., Riken*)

Terminal oxidases of the aerobic respiratory chain in inner mitochondrial membrane and bacterial cell membrane catalyze oxygen reduction to water coupling to electron and proton transfer. Terminal oxidases containing heme and copper atom at catalytic sites are called as heme-copper oxidases, which are classified into A-, B-, C- and several types of subfamilies. Although structures of the oxygen reduction sites are similar between subfamilies, structures of the proton pathways and energy transduction efficiency are different. To understand energy transduction mechanism, in this study, we compared oxygen consumption activity of cytochrome *aa*$_3$ (A-type) and *cbb*$_3$ (C-type) oxidases purified from bovine heart mitochondria and *Vibrio cholera* cells, respectively.

The measurement was performed by using ascorbate as electron donor and TMPD as mediator. In the presence of *aa*$_3$ or *cbb*$_3$, oxygen concentration was almost linearly decreased. When the enzyme concentration was changed, the rate varied as *aa*$_3$ up to 5uM and *cbb*$_3$ up to 0.2uM. The rate increased with increasing concentration TMPD, indicating that electron transfer from TMPD to the enzyme is rate limiting step. In ascorbate/TMPD system, the specific activity of *cbb*$_3$ was estimated to be 50 to 60 times higher than that of *aa*$_3$. Inhibitory effect by nitric monoxide was measured. Addition of nitrite decreased oxygen consumption rate of both *aa*$_3$ and *cbb*$_3$, but in the case of *cbb*$_3$ the rate was dependent on the oxygen concentration suggesting change of rate limiting step.

2PT156 *cbb*$_3$型チトクロム酸化酵素の精製

Purification of *cbb*$_3$-type cytochrome c oxidase

Yuriko Ando[1], Yui Iwamoto[1], Kazumasa Muramoto[1], Hideo Shimada[1,2], Robert Gennis[3], Yoshitsugu Shiro[1,4] ([1]*Graduate school of Life Science, University of Hyogo*, [2]*Picobiology Institute, University of Hyogo*, [3]*University of Illinois*, [4]*RIKEN, SPring-8 Center*)

The terminal oxidases of the aerobic respiratory chains in mitochondria and bacteria catalyze the oxygen reduction coupled to proton pumping, which generates the proton-motive force. The terminal oxidases containing heme and copper at the catalytic site form the heme-Cu oxidase (HCO) super family. Although conformations of the catalytic sites are similar in HCOs, the proton transfer pathways are not conserved and the energy transducing efficiencies are different. To identify structurally important elements and clarify common mechanism on the energy transduction, we aim to investigate cbb_3 -type cytochrome c oxidase from *Vibrio cholera* by X-ray crystallographic analysis. In previous study, we have examined culture condition for *V. cholera* cells carrying His-tagged cbb_3 oxidase expression plasmid and then performed purification by metal affinity chromatography. We have obtained cbb3 oxidase showing enough oxygen consumption activity, but SDS-PAGE showed the preparation still contained some impurity. In this study, to improve purity and yield, we examined the conditions of metal ion resin and solution composition on the chromatography. By using Ni ion resin, 5mg of cbb_3 oxidase was obtained from 30g cells. Purity was significantly improved by increasing salt concentration in charge and wash solution on the chromatography. Currently, we collect many preparations by this method for crystallization.

2PT157 水素原子レベルでの酸化還元に伴う構造変化同定を目的としたウシ心筋チトクロム酸化酵素の X 線結晶構造解析

X-ray structural analysis of bovine heart cytochrome *c* oxidase to clarify redox coupled structural changes at H atom level

Naomine Yano[1], Kazumasa Muramoto[1], Kyoko Shinzawa-Itoh[1], Tomoko Maeda[1], Eiki Yamashita[2], Tomitake Tsukihara[2], Shinya Yoshikawa[3], Yoshitugu Shiro[1,4] ([1]*Dept. of Life Sci., Univ. of Hyogo*, [2]*Inst. for protein Res., Osaka Univ*, [3]*Picobio. Inst., Univ. of Hyogo*, [4]*Harima Inst., Riken*)

Cytochrome *c* oxidase (CcO) catalyzes the molecular oxygen reduction coupling to the proton transfer across the inner membrane. To understand proton transfer mechanism in detail, it is necessary to determine orientations and protonation states of amino acid residues (imidazole and carboxyl group etc.) and waters in the proton pathways in both oxidized and reduced states. For this purpose, we are currently carrying out high resolution X-ray structural analysis of bovine CcO.

To reduce X-ray damage and increase data accuracy, many data from isomorphous crystals were collected. Low quality images whose R_{merge} or mosaicity were larger than 0.3 were removed from data set. At present, data of the oxidized state showed $I/\sigma(I)$ of 1.6 at 1.42 to 1.40 Å resolution range. As a result of structural analysis, many multi-conformations (Met residue etc.) were found. Electron density map of phospholipids, waters and peroxide at the O_2 binding site were improved. To determine H atom positions, residual density of F_o-F_c map must be reduced. 1) about 2800 waters and 36 hydrocarbons were added, 2) 88 multi-conformations were introduced to amino acids, 3) individual anisotropic B-factor were introduced 50% amino acid residues. As a result, residual density of hydrophilic region was removed. R and R_{free} values were also reduced from 0.199 to 0.154 and 0.213 to 0.177, respectively. Structural refinement of reduced state carries out as well as oxidized state.

2PT158 有機薄膜電極上での P450 反応の電気化学制御と応用

Electrochemically-driven cytorhcome P450 reactions at organic films and its bioprocess application

Yasuhiro Mie, Emi Tateyama, Yasuo Komatsu (*AIST*)

Cytochrome P450 enzymes catalyze a vast array of oxidative biotransformations that are potentially useful for pharmaceutical synthesis. Generally, P450s require reducing power in the form of expensive cofactors such as NADPH and one or two additional redox proteins to transfer electrons to the P450 active site to limit their technological applications. Replacing the conventional electron supply system with an electrode is a promising approach to develop inexpensive P450-driven systems. Recently, we found that nanostructured gold electrode is useful for the purpose. In the present study, we prepared several organic films on nanostructured electrodes to investigate the effect of surface features of electrodes on the electrochemical P450 reactions. Nanostructured surfaces of gold electrodes were modified with some thiolates by dip treatment. Immobilizations of P450s on the thiolate films were examined. CYP modified electrodes were investigated with voltammetry of a normal three-electrode configuration. CYPs on hydrophobic electrode surfaces coated with aromatic thiolates showed clear non-turnover signal, indicating rapid direct electron transfer between P450 heme and electrode and gave the largest catalytic current. On the other hand, electrode surfaces with coating materials containing hydrophilic functional groups were found to be mostly not suitable for the rapid electron transfer, and poorer P450-catalytic currents were obtained, indicating the importance of electrode surface nature for electrochemically-driven P450 reaction.

2PT159 ヒトヘモグロビンα鎖の近位ヒスチジンのグリシンへの置換が構造と酸素結合機能に与える影響

Substitution effects of Gly for the proximal His of α subunits on the structure and oxygen binding function of human hemoglobin

Yayoi Aki[1], Yukifumi Nagai[2], Kiyohiro Imai[2], Shigenori Nagatomo[3], Takashi Ogura[4], Teizo Kitagawa[4], Masako Nagai[2] ([1]*Med., Kanazawa Univ.*, [2]*Res. Center for Micro-Nano Tec.*, [3]*Chem., Univ. Tsukuba*, [4]*Life Sci., Univ. Hyogo*)

It has been proposed that the proximal histidine (His) in human adult hemoglobin (HbA) plays a pivotal role in the transmission of oxygenation-induced conformational changes in one subunit to another and in the resultant triggering of cooperativity [1]. We synthesized a mutant Hb in which the proximal His of α subunits was replaced by glycine (G), and examined its quaternary structure change upon ligand binding by means of near-UV circular dichroism (CD) and UV resonance Raman (UVRR) spectroscopy as well as its oxygen binding function. Mutant Hb(α87His->Gly) (αH87G) was produced in *E. coli*, and purified as previously described [2]. Oxygen equilibrium curve (OEC) was measured by an automatic OEC recording apparatus or by a tonometer method. The OEC of Hb(αH87G) showed an unusual shape having two components with a very high oxygen affinity and a distinctly low oxygen affinity without cooperativity. In near-UV region, a small positive CD band was observed for oxyHbA while a distinct negative CD for deoxyHbA. The negative CD of deoxyHbA at 287 nm, called "a T-state marker band", was observed in oxyHb(αH87G), indicating that the substitution of Gly for the proximal His failed to undergo the T-to-R quaternary structure transition. Changes of UVRR spectrum upon ligand binding of Hb(αH87G) also suggested lack of quaternary structure transition.

[1] Perutz, M. F., *Nature*, **228**, 725-734 (1970).
[2] Nagai, M., Nagai, Y., Aki, Y., Imai, K., Wada, Y., Nagatomo, S., and Yamamoto, Y. *Biochemistry*, **47**, 517-525 (2008).

2PT160 細菌 Vibrio alginolyticus 由来呼吸鎖末端酸化酵素の遺伝子クローニングと同定

Gene cloning and identification of terminal oxidase of respiratory chain in Vibrio alginolyticus

Naomine Yano[1], **Kazumasa Muramoto**[1], Seiji Kojima[2], Michio Homma[2], Yoshitsugu Shiro[1,3] ([1]*Dept. of Life Sci., Univ. of Hyogo*, [2]*Dept. of Biol. Sci., Nagoya Univ.*, [3]*RIKEN, Harima*)

The terminal oxidase of the aerobic respiratory chain catalyzes reduction of molecular oxygen to water molecule. The terminal oxidases containing heme and copper at the catalytic site are classified into several types which form the heme-Cu oxidase superfamily. Although conformations of the catalytic sites are similar between different types, the proton transfer pathways are not conserved and the energy transducing efficiencies are different. In many bacteria, the cell is known to expresses multiple terminal oxidases in different types depending on growth environment. Genome sequence of *Vibrio alginolyticus* indicates that there are several gene homologs of terminal oxidases, one of which is aa_3-type homolog. Primary sequence of core subunit I shows about 47% homology to bovine mitochondrial aa_3-type and 46-47% homology to *Paracoccus denitrificans* or *Rhodobacter sphaeroides* aa_3-type, these are well studied ones. Structural modeling suggests that hemes *a* and a_3 can be built into the subunit I. To identify the aa_3-type terminal oxidase in *V. alginolyticus*, we cloned possible aa_3-type genes and constructed His-tagged expression system in *V. alginolyticus* cell. Absorption spectrum of cultured cell suspension showed absorption peak at cytochrome *a* region, although its height was much lower than those of cytochromes *b* and *c* regions. Partially purified sample showed absorption peak at cytochrome *a* region in the reduced minus oxidized difference spectrum. These results indicate that the aa_3-type terminal oxidase is in *V. alginolyticus* cell.

2PT161 硬骨魚類の祖先型ヘモグロビン遺伝子の設計・合成および大腸菌内発現

Design and construction of ancestral Osteichthyes hemoglobin genes and its expression in *Escherichia coli*

Sho Sugiyama[1], Takatoshi Matsuo[2], Kazuha Seki[3], Taro Nakagawa[4], Kiyohiro Imai[1,2,3] ([1]*Department of Frontier Bioscience, Graduate School of Engineering, Hosei University*, [2]*Research Center for Micro-Nano Technology, Hosei University*, [3]*Department of Frontier Bioscience, Faculty of Bioscience and Applied Chemistry, Hosei University*, [4]*Department of Bioscience, Nagahama Institute of Bio-Science and Technology*)

The hemoglobin (Hb) of vertebrates including Osteichthyes is tetrameric composed of two α chains and two β chains. Hbs from some Osteichthyes species show the Root effect in which the oxygen capacity of Hb is halved upon lowering of blood pH to an acidic range. We intended to learn by a reverse phylogenetic analysis how those species acquired the Root effect and cooperativity in oxygen binding through molecular evolution of Hb. In this present study, we designed and constructed Node296α and Node203β genes which are the globin genes of a common ancestor of Osteichthyes, and cloned them into pET-22b(+). The resultant pET- Node296α and pET- Node203β were expressed in *E.coli.*, yielding a definite quantity of the ancestral Hbs.

2PT162 Exclusion of the active site waters by substrate in cytochrome P450cam

Ayaka Kishimoto[1], Keisuke Sakurai[2], Kenji Takagi[1], Tsunehiro Mizushima[1], Takashi Hayashi[3], Hideo Shimada[1] ([1]*Grad. Sch. Sci., Univ. Hyogo*, [2]*Inst. Sci. Ind. Res., Osaka Univ.*, [3]*Grad. Sch. Eng., Osaka Univ.*)

Waters occupying the substrate-binding site of enzymes are expelled by substrate. Mechanistic study on the water exclusion is limited by difficulty in monitoring the waters. Cytochrome P450cam, a heme *b* containing monooxygenase of D-camphor, is a good model for such study because the water exclusion accompanied by spin change of heme iron could be monitored by UV/Vis spectroscopy. We have proposed a water-expelling pathway with gate formed by Asp297, the heme-7-propionate, Glu322, and Arg299. Here, we report binding reactions of Asp297Leu-mutant enzyme with D-camphor and the X-ray structures. Leu297 mutation dramatically retarded camphor binding; at 25 °C, bound form was ca 20% of the enzyme at 24 hrs after exposure to 1mM camphor (*K*d value of wild type is ca 1μM). Binding still proceeded at a month later (Under the same conditions wild type enzyme showed denaturation). Binding, however, was greatly facilitated by glycerol, PEG4000, and sucrose and by temperature over 5 and 45 °C; At 65% (V/V) glycerol ca 75 % bound form was rapidly formed, while in wild type, glycerol lowered the affinity. In wild type, temperature does not change *K*d for camphor between 10 and 30 °C (temperature higher than 30 °C denatured the protein). X-ray structure of camphor-free Leu297-mutant showed opened substrate channel that closed by camphor binding, suggesting normal substrate channel. The present results strongly suggest retardation of camphor binding by the mutation is caused by slow exclusion of the waters, supporting the water-expelling pathway.

2PT163 ヘモグロビンの自動酸化速度に対する糖類の効果
The effect of saccharide on autoxidation rate of hemoglobin

Wataru Uehara, Kiyohiro Imai (*Department of Frontier Bioscience, Graduate School of Engineering, Hosei University*)

Hemoglobin (Hb) is a tetrameric heme protein composed of two α and two β subunits. The ferrous heme iron of each subunit is capable of reversible oxygen binding which becomes irreversible when the heme iron is oxidized to the ferric state (met form). OxyHb is apt to autoxidize gradually to metHb. Recently it was reported that aquometHb with trehalose and glucose added underwent heat-induced reduction at 70-80 ℃. In the present study we measured autoxidation rate for horse oxyHb at 50 ℃ in the presence and absence of glucose, trehalose, sucrose and glucose-trehalose mixture. It was suggested that saccharide is effective in preventing autoxidation of Hb.

2PT164 Norcamphor binding to cytochrome P450cam with a mutation to block pathway for the active site waters excluded by substrate

Natsumi Kitamura[1], **Aya Amano**[1], Ayaka Kishimoto[1], Keisuke Sakurai[2], Kenji Takagi[1], Tsunehiro Mizushima[1], Takashi Hayashi[3], Hideo Shimada[1] ([1]*Grad. Sch. Sci., Univ. Hyogo*, [2]*Inst. Sci. Ind. Res., Osaka Univ.*, [3]*Grad. Sch. Eng., Osaka Univ.*)

Active site waters of cytochrome P450cam, a heme *b* containing monooxygenase of D-camphor, are excluded by camphor. We have proposed that the waters are expelled to bulk waters through a pathway with gate formed by Asp297, heme-7-propionate, Glu322, and Arg299. Mutation of Asp297 to Leu seems to block the water exodus, thereby interfering substrate bindings. Here, we studied binding reaction between the Leu297-mutant and norcamphor, which lacks two methyl groups at C8 and C9 positions of camphor. Norcamphor binding was dramatically retarded. However, high concentration of polyol such as glycerol, PEG4000, and sucrose greatly facilitated binding, while in the wild type protein polyol lowered the affinity for norcamphor. X-ray structures of norcamphor bound wild type and Leu297 mutant proteins were determined at 1.6 and 1.8 Å resolution, respectively. Norcamphor at the active site of the both proteins exhibited multiple conformations where the Tyr96-bound conformation was not evident, contradicting to the X-ray structure by Poulos et al. where only norcamphor H-bonded to Tyr96 was reported. When we compare norcamphor bound mutant-structure with the previously determined camphor-free one, norcamphor provides no repulsive effect on Leu297. However, Leu297 sidechain exhibited the same conformation with that of previously determined camphor-bound form. Thus, sidechain conformation of Leu297 would not be resulted from repulsive effects from C8 methyl group of camphor. The present results support the proposed water-expelling pathway.

2PT165 ヒトヘモグロビンの複数酸素分子侵入経路の計算的解析
Computational analysis of multiple oxygen migration pathways in human hemoglobin

Masayoshi Takayanagi[1,2], Ikuo Kurisaki[1,2], Masataka Nagaoka[1,2] ([1]*Graduate School of Information Science, Nagoya University*, [2]*CREST, Japan Science and Technology Agency, Japan*)

Hemoglobin expresses the function upon its binding to the ligand molecules at the heme site. The ligand binding site of hemoglobin is buried in the interior of the protein, indicating that the ligand must migrate inside of hemoglobin. However, it is still under debate to clarify the ligand migration pathway. We examined multiple ligand migration pathways in human hemoglobin and identified the dominant ones. We executed 128 independent molecular dynamics (MD) simulations of tetramer human hemoglobin with the time length of 8 ns under oxygen-rich condition and obtained the migration pathways inside hemoglobin subunits. With the help of the clustering analysis, we visualized the multiple ligand migration pathways. The obtained rate of ligand entry into the binding site is consistent with those observed by CO geminate recombination experiments.

2PT166 Theoretical analysis of fully-hydrated structures of human adult hemoglobin exploiting molecular dynamics simulations

Tetsuhiko Itagaki, Jiyoung Kang, Masaru Tateno (*Grad. Sch. Sci., Univ. Hyogo*)

Molecular dynamics (MD) simulations of human adult hemoglobin (HbA) were performed employing the highest resolution crystal structures (1.25 Å) of the R(oxy)- and T(deoxy)-forms, to compare the resultant fully-hydrated structures (1000-ns MD calculations) with the spectroscopic data obtained using the previous NMR and infrared analyses. Previously, Perutz proposed the stereo chemical mechanism of the O2 affinity regulation by comparing the crystal structures in both forms of HbA. This is widely accepted. However, recent experiments have shown that several heterotoropic effectors (e.g. L35) can modulate the O2 affinity without significant structural changes of HbA. Yonetani, et al. postulated that entropic/dynamical properties contribute to this modulation. We found that the hydrated structures in both forms obtained using the MD simulations are consistent with the spectroscopic data, some of which are inconsistent with the crystallographic data. As a result of the analysis, the solution structure of the T-form may be different from the crystal structure, while the R-form is conserved in the solution and crystal structures. The hydration/entropic properties could be closely relevant to this difference between the solution and crystal structures of the T-form. Thus, our MD simulations can be a solid basis to analyze the roles of the heterotoropic effectors.

2PT167 Theoretical analysis of the electronic structure of CuB site of bovine cytochrome c oxidase

Toru Matsuoka, Jiyoung Kang, Masaru Tateno (*Grad. Sch. Sci., Univ. Hyogo*)

Cytochrome c oxidase (CcO), which is the terminal enzyme of the electron transfer system, reduces an oxygen molecule to two water molecules ($4H^+ + O2 \rightarrow 2H_2O$). The trigger of this reaction is the binding of an oxygen molecule to the bi-nuclear center (BNC), which is composed of Cu_Bsite and heme a_3 site). Experimentally, to obtain the geometric structure of the complex with an oxygen molecule is currently difficult; recently, the crystal structures of several

complexes with CO, NO, and CN ligands were revealed by Muramoto et al. In this study, employing these crystal structures, we performed hybrid *ab initio* quantum mechanics/molecular mechanics (QM/MM) simulations, and analyzed the geometric and electronic structures of the BNC.
As a result of the analysis, we found that the configuration of CO ligand in the crystal structure is different from that of the theoretically-optimized structure. We investigated this discrepancy by mapping the potential energy values of various positions of CO ligand in the BNC. The obtained potential field revealed the major two types of configurations, for which the energy values are close to each other, although the corresponding electron densities obtained by the crystallographic analysis cannot be separated into the two CO configurations. So, we calculated the IR spectrums, and found that they are consistent with the experimental data. In the session, the roles of the Cu_B site in the reaction will be discussed.

2PT168 In-situ 光照射固体 NMR を用いた D96N-bR の M 中間体で生じる構造変化の解析

Conformational change in M-intermediate of D96N-bR as studied by in-situ photo-irradiated solid-state NMR

Ryota Miyasa[1], Izuru Kawamura[1], Satoru Tuzi[2], Akira Naito[1] ([1]*Graduate School of Engineering, Yokohama National University*, [2]*Department of Life Science, University of Hyogo*)

Bacteriorhodopsin (bR) is the membrane protein of *H. salinarum*. When bR is photo irradiated, retinal in bR is photoisomerized and bR transfer proton from cytoplasmic side to extracellular side during photo cycle starting from all-*trans* retinal via K, L, M, N and O-intermediates. When M-intermediate generate, Schiff base is deprotonated and occurred large dynamic conformational changes. Since these conformational changes play a key role for proton pump mechanism, we aim to detect the conformational changes occurred in M-intermediate by applying in-situ photo-irradiated solid state NMR (P-SS-NMR) to D96N-bR that has long life time of M-intermediate.
We measured ^{15}N P-SS-NMR spectrum of [ε -^{15}N] Lys-D96N-bR at the temperature range from 0℃ to -60℃. As a result, we assigned new peaks appeared with photo-irradiation at 300 ppm and, 201 and 399 ppm (first spinning side bands) to deprotonated Schiff base of M-intermediate in D96N-bR. In contrast, we assigned the peaks decreased significantly with photo-irradiation at 154 and 147 ppm to the protonated Schiff bases of 13-*cis*, 15-*syn* and all-*trans* retinals in D96N-bR, respectively.
Additionally, we measured ^{13}C P-SS-NMR spectrum of [3-^{13}C]Ala, [1-^{13}C]Val doubly labeled D96N-bR. We observed the changes of ^{13}C NMR signal intensities from dark adapted state to photo activated state. Consequently, we detected local conformational changes in the protein side at M-intermediate of D96N-bR.

2PT169 LOV2 ドメインの中間体揺らぎの時間分解検出

Transient fluctuation of phototropin LOV2 domain

Kunisato Kuroi[1], Francielle Sato[2], Yusuke Nakasone[1], Kazunori Jikihara[3], Satoru Tokutomi[3], Masahide Terazima[1] ([1]*Univ. of Kyoto*, [2]*Univ. of Maringa*, [3]*Osaka Prefecture University*)

For biological function of proteins, their structural fluctuations could play an important role. Recently we succeeded in detecting such transient volume fluctuations by using TG and TrL techniques for a blue light sensor protein, PixD. Here, we studied the fluctuation of reaction intermediates of phototropoin LOV2 domain, which is one of the most versatile blue-light sensor domain. Although the reaction have been investigated extensively so far, it remains still unknown how LOV2 domain transmits its light signal toward the effector domain linked with usually the C-terminal of LOV2 domain, because only a minor structural change around its chromophore is observed upon the blue-light excitation. For example, it has been reported that the LOV2 domain except the chromophore region does not undergo a remarkable structural change upon the light excitation, but it causes the unfolding of the C-terminal linker-helix domain. We consider that the intermediate structural fluctuation of LOV domain should be involved in this step. Therefore in the present study, we detected and compared the intermediate fluctuation of the LOV2-linker and LOV2 domains by extending the TG and TrL measurements. For the LOV2-linker domain, we succeeded in observing the enhanced fluctuation for the unfolding event of the linker-helix. By comparison of the fluctuation between the LOV2 domain and LOV2-linker, we discuss the functional role of the fluctuation of the LOV2 domain in the signal transmission step.

2PT170 Photoactive Yellow Protein 中に存在する低障壁水素結合近傍のアルギニン 52 のプロトン化状態

Protonation State of Arginine 52 near the Low Barrier Hydrogen Bond in Photoactive Yellow Protein

Kento Yonezawa[1], Hironari Kamikubo[1], Keito Yoshida[1], Shigeo Yamaguchi[1], Tarou Tamada[2], Kazuo Kurihara[2], Yoichi Yamazaki[1], Mariko Yamaguchi[1], Mikio Kataoka[1] ([1]*Grad. Sch. Mat. Sci., NAIST*, [2]*Japan Atomic Energy Agency*)

Low Barrier Hydrogen Bond (LBHB) is a special type of hydrogen bonds (HBs), in which a proton locates near the center between donor and acceptor atoms. Although the bond energy of LBHB (ΔH_{LBHB}) is generally higher than that of a normal HB, ΔH_{LBHB} in a protein has not been evaluated. To estimate ΔH_{LBHB}, we carried out pH titration experiments at various temperatures upon Photoactive Yellow Protein. We clarified that the HB between the chromophore (pCA) and E46 is LBHB. The LBHB is converted to an ordinary HB (NH-O) in E46Q. Neither the LBHB nor the HB can be formed in E46A. Therefore, ΔpKa (WT-E46A) and ΔpKa (E46Q-E46A) is assumed to reflect bond free energies of LBHB and HB, respectively. From the temperature dependence of ΔpKa values, ΔH_{LBHB} and ΔH_{HB} were estimated to be 8 kcal/mol and 7 kcal/mol, respectively. ΔH_{LBHB} is rather smaller than the expected value. We found the substantial difference in Hill's coefficients. The Hill's constant for WT is about 2, while those of E46Q, and E46A are close to 1, suggesting that there exist another protonation site in WT than pCA. To identify the presumed protonation site, we performed the neutron crystallographic analysis on E46Q, revealing that R52 in E46Q is partly protonated. Together with the fact that R52 is deprotonated in WT, it can be proposed R52 was cooperatively protonated upon the protonation of the pCA in WT. The apparent ΔH_{LBHB} reflects both of the energy gain of LBHB and the energy loss due to deprotonation of R52 at the physiological pH, resulting in the relatively small value.

2PT171 PYP Phytochrome Protein Related (Ppr) に存在する PYP ドメインによるフィトクロムドメインの光反応構造変化の制御

Photoreaction of PYP domain regulates the structural change during the photoreaction of phytochrome domain of Ppr

Keito Yoshida, Hironori Kamikubo, Kento Yonezawa, Yoichi Yamazaki, Mariko Yamaguchi, Mikio Kataoka (*Graduate school of Materials Science, Nara Institute of Science Technology*)

PYP-Phytochrome Related protein (Ppr) is a multi-domain protein comprised of a PYP domain, a bacteriophytochrome domain (Bph), and a histidine kinase domain. We previously reported that the pohoto-reactions of PYP and Bph are closely coupled, where the intermediate state of PYP influences the photo-reaction rates of Bph. To investigate the molecular mechanism of the interdependency, we prepared holo-holo-Ppr and apo-holo-Ppr, and performed solution x-ray scattering experiments. The scattering profiles of the holo-holo and apo-holo Pprs were nearly identical, indicating that the overall molecular shapes of holo-holo and apo-holo Pprs are indistinguishable. Red light absorption brings that holo-holo-Ppr changes in the scattering profile, holo-holo-Ppr does not. It can be suggested that the structural change is suppressed by the holo-PYP domain despite that holo-PYP does not absorb red light. Blue light irradiation to holo-holo-Ppr causes the formation of PYP_M. The photointermediate of Bph was slowly accumulated by the following red light irradiation. The scattering profile of the final product is largely different from the original state, the change of which is similar to that of apo-holo-Ppr by red light absorption. From these results, we propose that the photoreaction of PYP domain regulates the domain rearrangement during the Bph photoreaction. The unphotolyzed PYP domain suppresses the structural change, but the PYP_M state enables Ppr to undergo the large structural change.

2PT172 PYP の構造形成に対する N 末端領域の効果

Effect of N-terminal region to the structure formation of PYP

Mitsuhiro Sakonji, Yoichi Yamazaki, Hironari Kamikubo, Mariko Yamaguchi, Mikio Kataoka (*Grad. Sch. Mat. Sci., NAIST*)

Structure element is defined as an uninterruptable region on the amino acid sequence which is required for the structure formation of a protein [1]. Photoactive yellow protein (PYP) is a water soluble light absorbing protein. PYP can be separated into the N-terminal region and the chromophore binding region. Upon absorption light, large disorder is brought to the N-terminal region. The deletion of the N-terminal region, however, does not affect the

structure of the chromophore binding region. The N-terminal lacking PYP is also photoactive. These facts suggest that the N-terminal region of PYP does not contain structure element. In order to analyze the effect of N-terminal region to structure formation of PYP as well as the effect of the chromophore binding, we applied systematic alanine insertion to the N-terminal region of PYP.
Wild type apo-PYP takes a unique tertiary structure, although its CD spectrum is slightly different from that of holo-PYP, indicating that the further structure formation by chromophore binding. In apo-form, CD intensities of some alanine insertion mutants decreased from that of wild type. The CD increase upon chromophore binding is commonly observed, even though the CD spectra of holo-form are slightly different from that of wild type. These results indicate that the N-terminal region does not contain structure element, although the effect of chromophore binding to the structure formation is affected by insertion.
[1] R. Shiba, et.al. Biophysics 7, 1-10 (2011)

2PT173 Rc-PYP の相互作用における発色団周辺水素結合の寄与

The role of hydrogen bonding network around the chromophore for the interaction of Rc-PYP

Yoichi Yamazaki, Mayu Shimada, Hironari Kamikubo, Mikio Kataoka (*Grad. Sch. Mat. Sci., NAIST*)

Photoactive Yellow Protein (PYP) is a blue light receptor firstly isolated from purple photosynthetic bacterium, *Halorhodospira halophila* (Hh-PYP), which has a *p*-coumaric acid as a chromophore. The PYP photoreaction and structural information has been analyzed in detail, but there has been little progress in the analysis of signal-transduction mechanism, since the target protein of Hh-PYP has not been identified. PYP from *Rhodobacter capsulatus* (Rc-PYP) is the only protein that the interaction protein is identified so far. Therefore, Rc-PYP is more suitable for the research of PYP signal-transductions. Rc-PYP shows two absorption maxima at around 370 and 440 nm, and shows reactivity to UV-A light. Rc-PYP's reaction with its interaction protein is light dependent. UV-A illuminated Rc-PYP binds its interaction protein. At the formation of the Rc-PYP complex the absorption maximum of cis-chromophore shows red-shift, this is indicating chromophore environment changes in the complex state.

To verify relationship between the chromophore environment and complex formation, we examined spectral difference and complex formation about several amino-acid residues mutants around the chromophore which construct hydrogen bond network and Rc-PYP re-constituted by chromophore analog which lacks chromophore hydrogen bond. All the mutants kept their interaction ability, even though spectral features were different from that of wild-type. But the Rc-PYP in which chromophore substituted with cinnamic-acid did not show complex formation.

2PT174 桂皮酸導入 Photoactive Yellow Protein の発色団由来水素結合の欠損効果

Roles of hydrogen bonds around chromophore in Photoactive Yellow Protein studied by OH-defficient cinnamic acid

Masatoshi Narumi, Yoichi Yamazaki, Mariko Yamaguchi, Hironari Kamikubo, Mikio Kataoka (*Grad. Sch. Mat. Sci., NAIST*)

Photoactive Yellow Protein (PYP) is a water-soluble photosensor protein isolated from *Halorhodospira halophila*. It has a covalently attached chromophore, *p*-coumaric acid (*p*CA). Oxygen atom of *p*CA phenol group forms hydrogen bonds with the E46 and Y42. These two hydrogen bonds play crucial roles in the structure formation and photoreaction of PYP. In order to clarify the roles of these hydrogen bonds, we have attempted to remove these hydrogen bonds by using a cinnamic acid as a chromophore(CA-PYP). CA-PYP was successfully reconstituted. Although free cinnamic acid showed its absorption maximum at 265nm, it shifted to 316nm in CA-PYP, suggesting that the importance of hydrogen bonds for visible light absorption. Absorption intensity of CA-PYP decreased by UV illumination, but intensity never recovered to its original state by shutting of the light. CA-PYP is light reactive but not cyclic. FT-IR difference spectrum showed chromophore vibational mode changes of *trans-cis* photoisomerization by UV-light illumination in CA-PYP. In addition, back bone changes and carboxyl group changes were also observed in FT-IR difference spectrum. CA-PYP did not show radius of gyration change and secondary structural change. These results suggest that hydrogen bonds constructed from phenolic oxygen of *p*CA, Y42 and E46 are required for the proper photoreaction of PYP accompanying with the substantial structural change, although the hydrogen bonds are not essential for the chromophore attachment.

2PT175 青色光センサータンパク質 YtvA の LOV と LOV-linker の光化学反応の比較

Comparison of the photochemical reaction between the LOV domain and the LOV-linker domain of a blue light sensor protein YtvA

Seokwoo Choi[1], Yusuke Nakasone[1], Klaas Hellingwerf[2], Masahide Terazima[1] ([1]*Department of Chemistry, Graduate school of Science Kyoto University*, [2]*University of Amsterdam, Swammerdam Inst Life Sci*)

YtvA is a blue light sensor protein which consists of the N-terminal LOV (Light-Oxygen-Voltage) domain and the C-terminal STAS (Sulphate Transporter and Anti Sigma factor antagonists) domain, linked by the linker helix. Physiological studies have reported that YtvA is involved in the initiation of environmental stress response (light, salt, heat etc.) by regulating an activity of transcriptional factor σB. However, the molecular mechanism of its signal transduction process has not been revealed yet. For understanding this signal transduction mechanism, the photochemical reaction dynamics has to be elucidated. In this study, we investigated the photochemical reaction dynamics of the LOV and LOV-linker domains of YtvA using the time-resolved transient grating (TG) method. In particular, by comparing the photochemical reactions dynamics of the LOV and LOV-linker domain, we try to find the importance of linker domain in the signal transduction. From the concentration dependence, we found that the LOV domain in the ground state exists in the equilibrium between the dimer and the tetramer, whereas the equilibrium is between the dimer and the higher oligomeric form for the LOV-linker domain. For both cases, it was shown that the photoreaction of dimer seemed to be important; that is, the dimer of the LOV domain associates into the tetramer, whereas the dimer of the LOV-linker domain occurs structural change without oligomerization. We will discuss the reaction in more detail in the poster presentation.

2PT176 *Natronomonas pharaonis* 由来のセンサリーロドプシン II の光誘起プロトン移動における塩化物イオンの役割

The role of chloride in the photo-induced proton transfer in sensory rhodopsin II from *Natronomonas pharaonis*

Jun Tamogami[1], Katsunori Iwano[2], Atsushi Matsuyama[1], Takashi Kikukawa[2], Makoto Demura[2], Kazumi Shimono[1], Toshifumi Nara[1], Naoki Kamo[2] ([1]*College of Pharmaceutical Sciences, Matsuyama University*, [2]*Faculty of Advanced Life Science, Hokkaido University*)

Natronomonas pharaonis has a sensory rhodopsin II (NpSRII, or called *pharaonis* phoborhodopsin) which functions as a negative phototaxis receptor. This protein has a retinal as a chromophore and illumination induces the photochemical reaction (photocycle) accompanied by the photo-induced proton uptake and release. Previously, it was reported that the early proton release originated from Asp193 in phospholipid-reconstituted NpSRII occurs in the presence of chloride [1, 2]. In this study, the effect of Cl^- on this proton release from Asp193 was investigated by detail experiments with the indium-tin oxide (ITO) electrode. With increasing of Cl^- concentration in the medium, the p*K*a's of Asp193 in both of the dark and excited state increased. From these Cl^--dependence of the p*K*a's in Asp193, *K*d values in both of the photolyzed and unphotolyzed state were estimated. In the unphotolyzed state, two *K*d's were estimated. One was estimated to ~24 mM, while the other was estimated to > ~1 M which indicates very weak Cl^- binding affinity. On the other hand, *K*d was estimated to ~244 mM in the photolyzed state. This implies that the Cl^- binding affinity becomes about 10-fold weaker by the conformational change in the excited state. In addition to these estimations, we verified the position of putative Cl^- binding sites. Finally, the role of Cl^- in the photo-induced proton transfer was discussed.
[1] Iwamoto *et al*. (2004) *Biochemistry* **43**, 3195-3203. [2] Kitade *et al*. (2009) *Biochemistry* **48**, 1595-1603.

2PT177 アナベナセンサリーロドプシンの光誘起プロトン移動反応の解析

Photo-induced proton transfer of *Anabaena* sensory rhodopsin

Takatoshi Hasemi[1], Takashi Kikukawa[1], Masakatsu Kamiya[1], Tomoyasu Aizawa[1], Keiichi Kawano[1], Kwang-Hwan Jung[2], Naoki Kamo[1,3], Makoto Demura[1] ([1]*Grad. Sch. Life Sci.,Hokkaido Univ.*, [2]*Dept. Life Sci. & Inst. Biol. Interfaces, Sogang Univ.*, [3]*College Pharm. Sci., Matsuyama Univ.*)

Anabaena sensory rhodopsin (ASR), found from freshwater cyanobacterium, is a novel photosensing rhodopsin, which activates the soluble transducer for the

chromatic adaptation. Unlike the most microbial rhodopsins, the cytoplasmic (CP) half of ASR is unusually hydrophilic due to many polar residues and water molecules. Basically, ASR lacks electrogenic proton transport. However, unusual proton transfer was observed: the Schiff base proton is transferred to Asp217 in the CP domain upon the formation of M photo-intermediate (Shi *et al.*, *J. Mol. Biol.* 2006). Thus, ASR has a potential to move proton in the direction opposite to that of proton-pumping rhodopsins.
In this study, we examined the proton transfer reactions of ASR by using indium-tin oxide electrode, which enables the time-dependent measurements of local pH changes by flash-activated ASR. At the neutral pH, ASR induces the transient alkalization of the local medium, indicating that photolyzed ASR accepts proton from the medium and then releases it at the same side. On the other hand, above pH 8, the sequence of the proton movement is reversed: proton release occurs first, followed by uptake. This suggests that a certain residue acts as proton releasing residue in the alkaline condition. These proton transfers were greatly modified by the mutations of Asp217 and Glu36 locating at the CP domain. Thus, the proton transfers mainly occur through this hydrophilic channel. Based on this analysis, we will discuss the proton transfer reactions of ASR.

2PT178　ウシロドプシンの構造に関する理論研究

A theoretical study on the structure of bovine rhodopsins

Motoshi Kamiya, Shigehiko Hayashi (*Grad. Sch. Sci., Kyoto Univ.*)

Rhodopsin is a photoreceptor in the retina. It consists of the protein moiety opsin and an all-trans-retinal which is derived from Vitamin A. The photoisomerzation of the retinal induces the structural change of the protein and eventually activates the associated G-protein, transducin. The purpose of this study is to elucidate the structures of early intermediates during the photoreactions such as lumirhodopsin. Computationally, the structure around Schiff base of the retinal is difficult to be described with the classical forcefield, although accurate description of the structure around the retinal is critically important for the calculations of vibrational frequencies and the excitation energy. Therefore, QM/MM calculations must be involved to obtain reasonable structure. On the other hand, structural rearrangements/relaxations at finite temperature (not only fluctuations) of the system, which are usually not involved in QM/MM methods, shall not be ignored for the structural relaxation which takes more than nanoseconds. In order to fulfill these two requisites, in this study, we employed QM/MM-RWFE-SCF method [Kosugi and Hayashi, JCTC, 2011]. The structures and vibrational frequencies of the Schiff base in rhodopsin, bathorhodopsin, and lumirhodopsin will be discussed.

2PT179　グロエオバクターロドプシンの三量体形成に関する研究

Homo-trimeric assembly of a cyanobacterial ion-pump *Gloeobacter* rhodopsin

Takashi Tsukamoto[1], Takashi Kikukawa[1,2], Masakatsu Kamiya[1,2], Tomoyasu Aizawa[1,2], Keiichi Kawano[1,2], Kwang-Hwan Jung[3], Naoki Kamo[2,4], Makoto Demura[1,2] ([1]*Grad. Sch. Life Sci., Hokkaido Univ.*, [2]*Fac. Adv. Life Sci., Hokkaido Univ.*, [3]*Dept. Life Sci. & Inst. Biol. Interfaces, Sogang Univ.*, [4]*College Pharm. Sci., Matsuyama Univ.*)

Rhodopsin-like molecules in microorganisms (microbial rhodopsins) play roles as an ion-pump or a photosensor. The four microbial rhodopsins from halophilic archaea have been investigated well so far; bacteriorhodopsin (BR), halorhodopsin (HR), sensory rhodopsin I (SRI) and sensory rhodopsin II (SRII, also called phoborhodopsin). These proteins form intrinsic oligomers depending on their function. The phototaxis sensors SRI and SRII form a tetramer which is composed of two units of receptor-transducer hetero-dimer. On the other hand, the ion-pumps BR and HR form a homo-trimer. This is a unique structural property of them and recent studies have revealed several factors for the trimer formation and stabilization (Tsukamoto *et al.*, *Biophys. J.* 2012). Other than BR and HR, however, little is known about the trimer formation of the ion-pumping rhodopsins.
We have started to investigate the oligomeric structure of *Gloeobacter* rhodopsin (GR), which is an ion-pumping protein discovered from freshwater cyanobacterium, by means of size-exclusion chromatography (SEC) and circular dichroism (CD) spectroscopy. The analysis of SEC gave us a conclusion that GR formed a trimer as well as BR and HR. However, the CD spectrum of GR ((+) 500 nm/(-) 567 nm, crossover point; 540 nm) indicated that the trimeric state of GR was different from that of BR and HR. Interestingly, the trimeric state of GR altered in a pH-dependent manner. Based on these analyses, we will discuss the homo-trimeric structure of GR.

2PT180　パルミトイル修飾とロドプシンのラフト親和性の関係

Relationship between palmitoylations and raftophilicity of rhodopsin

Keiji Seno[1], Fumio Hayashi[2] ([1]*Hamamatsu Univ. Sch. Med.*, [2]*Grad. Sch. Sci., Kobe Univ.*)

As we reported in the last meeting of BPSJ, we have found that rhodopsin forms dimer in the complex of retinal G protein transducin (G_t). The rhodopsin dimer favors l_o lipids and distributes in the detergent-resistant membrane (DRM) prepared from vertebrate (bovine and frog) rod photoreceptor outer segment membranes. Our single molecule observation of rhodopsin and transducin revealed that the increased affinity to raft of rhodopsin upon dimerization hinders the diffusion of rhodopsin. Here, we studied the contribution of tandem palmitoyls at the C terminal end of helix-8 of rhodopsin to the raftophilicity of rhodopsin dimer. We examined the effect of depalmitoylation of rhodopsin by reducing agent (20 mM dithiothreitol) on the distribution of rhodopsin-transducin complex or IgG-crosslinked (artificially dimerized) rhodopsin to the DRM of frog rod photoreceptor outer segments. Depalmitoylation was confirmed by MALDI-TOF MS. Rhodopsin-transducin complex in DRM fraction was reduced to almost half by depalmitoylation. When we artificially dimerized rhodopsin by anti-rhodopsin monoclonal antibody, significant portion of anti-rhodopsin IgG, which means rhodopsin dimer, was detected in DRM fractions, however, when we used depalmitoylated rhodopsin, much less IgG was detected in DRM fractions. These data support our idea that the palmitoyl modifications on rhodopsin are indispensable for raftophilicity of rhodopsin dimer.

2PT181　海洋性細菌におけるプロテオロドプシンの生理的役割および分子特性

Physiological role and molecular properties of proteorhodopsin from marine bacterium

Rei Abe-Yoshizumi[1], Keiichi Inoue[1], Susumu Yoshizawa[2], Kazuhiro Kogure[2], Hideki Kandori[1] ([1]*Dept. of Frontier Materials, Nagoya Inst. Tech.*, [2]*AORI, Univ. Tokyo*)

Nature created two kinds of light-driven ion pumps, bacteriorhodopsin (BR) and halorhodopsin (HR), functioning as outward proton and inward chloride pumps, respectively [1]. Then, thousands of proteorhodopsin (PR) have been discovered and are widely distributed among marine prokaryotes [2]. But its physiological role was unclear, because very few strains carrying the PR gene have been cultured. Recently, we demonstrated light-driven proton pump activity of PR in native *Flavobacteria* cells [3].
Here we studied the molecular mechanism and the physiological role of PR from *Krokinobacter* sp. in *Flavobacterium* that codes two microbial rhodopsin genes in their genome. We first examined their pump activity in native cells. It was found that PR is expressed in stationary phase, suggesting that PR-mediated electrochemical proton gradient is use to ATP synthesis when nutrition is depleted. We then studied the spectral and photochemical properties of recombinant PR from *Krokinobacter* (KroPR). KroPR shows λmax at 525 nm (pH 7.0), being similar to GPR. On the other hand, pKa of the counterion (4.3) is lower than that of GPR (6.9), although the amino acid identity between KroPR and GPR is 41 % and His75 (GPR) is conserved. Flash photolysis measurement of KroPR is in progress and the molecular mechanism of KroPR will be discussed.
[1] Kandori, *Mol. Sci.* 5, A0043 (2011).
[2] Beja et al. *Science* 289, 1902 (2000).
[3] Yoshizawa et al. *Environ. Microbiol.* 14, 1240 (2012).

2PT182　時間分解赤外分光法によるファラオニスハロロドプシンの機能発現過程での水の水素結合ダイナミクス

Water hydrogen-bonding dynamics in the function of *pharaonis* halorhodopsin studied by time-resolved FTIR spectroscopy

Kuniyo Fujiwara[1,2], Tetsunari Kimura[1,2,3], Takashi Kikukawa[4], Makoto Demura[4], Hideki Kandori[5], Yuji Furutani[1,2,6] ([1]*SOKENDAI*, [2]*IMS*, [3]*JST CREST*, [4]*Grad. Sch. Life Sci., Hokkaido Univ.*, [5]*Grad. Sch. Eng. , NITech*, [6]*JST PRESTO*)

pharaonis Halorhodopsin (*p*HR) is an inward chloride ion pump protein. pHR has a retinal as the chromophore, which is bound through the protonated Schiff base and all-*trans* to 13-*cis* photoisomerization triggers conformational changes of the protein moiety for pumping a chloride ion. The ion transportation is performed through the sequential formation of some intermediates which are named K, L_1, L_2, N and O. The structural detail of each intermediate state is still

unclear, and especially, it is open question how water molecules involve in the translocation of a chlorine ion inside protein during the photocyclic reaction. To analyze the hydrogen-bonding dynamics of water and protein, we performed the time-resolved Fourier transform infrared (TR-FTIR) spectroscopy in the whole mid-infrared region. The measurement was performed under the condition of hydration with H_2O or $H_2{}^{18}O$, which allow us to assign the water O-H stretching bands. As a result, we observed a water band at 3626 cm^{-1} which exhibited down shift to 3605cm^{-1} upon the formation of the N and O states. We also analyzed the dependency on the chloride concentration to discriminate whether the water change occurs in the N or O intermediates, which are related to release and uptake of chloride ion. Anion dependency (Br^-, NO_3^- and SO_4^{2-}) was investigated as well. By comparing these experimental data, the relationship between the water hydrogen-bonding dynamics and the conformational changes of protein will be discussed.

2PT183 全反射赤外分光法によるキメラチャネルロドプシンの構造変化解析

Structural changes in the chimeric Channelrhodopsins revealed by ATR-FTIR spectroscopy

Asumi Inaguma[1,2], Hisao Tsukamoto[1], Tetsunari Kimura[1,3], Toru Ishizuka[3,4], Hiromu Yawo[3,4], Yuji Furutani[1,2] ([1]*Inst. Mol. Sci.*, [2]*JST PREST*, [3]*JST CREST*, [4]*Grad. Sch. Life Sci., Tohoku Univ.*)

Channelrhodopsin 1 and 2 (ChR1 and ChR2) can function as light-gated cation channels which were discovered from *Chlamydomonas reinhardtii*. Recently, ChR2 and its derivatives have been utilized as a useful tool to control the neural circuit by light. ChR1/2 chimera such as ChR-wide receiver (ChR-WR) and ChR-fast receiver (ChR-FR) have improved characters as the electrophysiological tool. ChR-WR is sensitive to the light in the wider range of wavelength compare to the wild type. ChR-FR exhibits faster ON/OFF kinetics in the photocurrent. However, the molecular mechanisms behind these useful properties have not been understood well. Nowadays, the crystal structure of ChR has been reported, but the structural changes connecting the closed and open conformation have not been answered well. In this research, we applied attenuated total reflection Fourier transform infrared (ATR-FTIR) spectroscopy to reveal the structural changes of the chimeric ChRs during the formation of the open/photostationary state and return to the closed state. The light-induced difference FTIR spectra of ChR-WR and ChR-FR were very similar to each other, suggesting that the structural changes are mostly same. Interestingly, the recovery from the photostationary state of ChR-FR was faster than ChR-WR. We will discuss the relationship between the structural changes and the photocurrent properties of these chimera ChRs.

2PT184 Crystal Structure of deltarhodospin from Haloterrigena Thermotolerans

Jin Zhang, **Katsuhide Mizuno**, Mizuno Kouyama (*Nagoya University*)

Deltarhodopsin, a new member of the microbial rhodopsin family, functions as a light-driven proton pump. In this study, we investigated the crystal structure of deltarhodopsin (dR3) from Haloterrigena thermotolerans, a thermo-tolerant archaeon isolated from a solar saltern in Puerto Rico. For preparation of a large quantity of the target protein, the gene encoding deltaopsin-3 was transformed into a bR-deficient host strain of Halobactrium salinarum. When the membrane fusion method was applied, the purified sample of dR3 was crystallized into trigonal crystals belonging to space group R32. In this crystal form, dR3 forms a trimeric assembly as observed for bR and other archaeal rhodopsins. It is demonstrated that the inner part of the protein (the retinal binding pocket and the proton release and uptake pathways) is similar to that of bR and other microbial rhodopsins. One of major differences is observed in the protein-protein contact regions. Interestingly, the carotenoid bacterioruberin binds to the crevice between the AB helices of one subunit and the DE helices of a neighboring subunit. Another peculiar property of dR3 is a highly crowded distribution of positively charged residues on the cytoplasmic surface. Structural comparison of dR3 with other archaeal rhodopsins allows us to recognize the structural motif that is relevant to the proton pumping activity, while also offering insight into the formation mechanism of the trimeric structure and the recognition mechanism of specific lipid components.

2PT185 The chroride ion uptake mechanism in *pharaonis* halorhodopisin as studied by the energy representation method

Hiroyuki Tamura[1], Shuntaro Chiba[1], Shun Sakuraba[2], Nobuyuki Matsubayasi[2], Minoru Sakurai[1] ([1]*Center for Biol. Res. & Inform, Tokyo Tech*, [2]*ICR, Kyoto Univ*)

Halorhodopsin (hR) is a light-driven chloride ion pump exist in halophilic archaea. hR uses the light energy to move chloride ions from extracellular side to cytoplasmic side. The process is thought to be divided into the two steps: (i) a chloride ion passively enters the binding site near retinal Schiff base linkage in the protein from the extracellular medium with a high NaCl concentration (~4M), and (ii) the chloride ion is transported into the cytoplasmic side after the photoisomerization of retinal. The purpose of this work is to clarify the mechanism of the first step by calculating the free energy of a chloride ion in the following two cases: it is located in the extracellular side (bulk) and at the binding site. The free energies were calculated using the method of energy representation combined with molecular dynamics simulations. First, we calculated the free energy of a chloride ion in the aqueous solution of NaCl. As a result, the free energy decreased from -88.6 to -122.0 kcal/mol as the NaCl concentration was increased from 0M to 4M. Next, we calculated the free energy of a chloride ion at the binding site: the result was -120.3 kcal/mol, which is equal to that in the aqueous solution of 3.4 M NaCl. These results indicate that a chloride ion in bulk passively enters the binding site if the NaCl concentration in bulk is lower than 3.4 M. The largest contributor to the stabilization of a chloride ion at the binding site is the chromophore (-49.3 kcal/mol) and the next is the nearby water molecule (-20.5 kcal/mol).

2PT186 ATP ショットと caged-ATP の光分解により開始されるホタル生物発光の時間発展及びその pH 依存性

Time Dependent Characteristics of Firefly Bioluminescence Initiated by Two Methods with Usual ATP Injection and Photolysis of Caged-ATP

Yuki Yanagisawa[1], Takeshi Kageyama[1], Masatoshi Tanaka[1], Shin-ya Ohno[1], Naohisa Wada[2] ([1]*Faculty of Engineering, Yokohama National University*, [2]*Department of Life Sciences, Toyo University*)

The time-resolved spectrum and the rise time course of firefly bioluminescence initiated by ATP injection into the HEPES buffer containing luciferin, luciferase, and Mg^{2+} were first measured with time resolution of 10 ms, and compared with those of the bioluminescence triggered by photolysis of caged-ATP. The time course is significantly dependent on pH; both time constants of rise and decay increase with decreasing pH from 7.8 to 6.8. The observed time course is constituted by two components; the diffusion-controlled reaction follows the homogenization of reactants. The usual ATP injection may prevent ATP^{4-} from falling into the catalytic center of Luc. Contrarily, in the case of the bioluminescence triggered by photolysis of caged-ATP, the intrinsic reaction dominates the time course not correlative with pH [1]. The time-resolved spectra can be decomposed into two Gaussians peaked at 2.0 eV and 2.2 eV. The intensity of 2.2 eV component decreases with decreasing pH, being consistent with previous report [2]. Spectral shapes do not change from the initiation of the enzymatic reaction up to 200 s for both methods of ATP addition. After 200 s, the 2.0 eV component decays slower than the 2.2 eV component in the case of the photolysis of caged-ATP, which may be caused by the product of photolysis. Interestingly, above results are not influenced regardless of the concentration ratio [Ln]/[Luc].

[1] T. Kageyama, et al., Photochem. Photobiol. 87 (2011) 653-658.
[2] Y. Ando, et al., Nature Photonics 2 (2008) 44-47.

2PT187 水溶液中のホタルルシフェリン蛍光スペクトルの理論的研究

Theoretical Analysis of Fluorescence Spectra of Firefly Luciferin in Aqueous Solutions

Miyabi Hiyama[1], Hidefumi Akiyama[2], Kenta Yamada[3], Nobuaki Koga[1] ([1]*Grad. Sch. Info. Nagoya Univ.*, [2]*ISSP Univ. Tokyo*, [3]*Grad. Sch. Nanobio. Yokohama City Univ.*)

To understand the mechanism of firefly bioluminescence, researchers have investigated the spectroscopic properties of firefly luciferin as an analog of oxyluciferin [1-6]. Despite the previous experimental and theoretical studies, some peaks in the fluorescence spectra of firefly luciferin still remain unassigned. To elucidate the origin of fluorescence spectra of firefly luciferin, the excited states of firefly luciferin and its conjugate acids and bases were investigated by performing the density functional theory calculations (DFT). Time-dependent DFT calculations were performed for the excited states of these molecules. The solvent effect in aqueous solution was taken into account by the polarizable continuum model. We obtained the energies and oscillator strengths of excitation of firefly luciferin and its conjugate acids and bases [7]. Although the wavelengths of energies in theoretical fluorescence spectra are approximately 40 nm lower than those in the experimental data, the relative

theoretical energies are in good agreement with the experimental ones.
[1] Seliger et al., Proc. Natl. Acad. Sci. U.S.A. 47, 1129 (1961) [2] Morton et al., Biochem. 8, 1598 (1969)[3] White et al., Bioorg. Chem. 1, 92 (1971) [4] Jung et al., J. Am. Chem. Soc. 98, 3949 (1976) [5] Gandelman et al., J. Photochem. Photobio. B: Biol. 19, 187 (1993) [6] Ando et al., Jpn. J. Appl. Phys. 49, 117002 (2010) [7] Hiyama et al., Photochem. Photobio. (2012) In press

---

2PT188 シアノバクテリア由来のフィトクロム様光受容体「PixJ1」における短波長シフトした光反応の分子基盤

Molecular Basis for the Blue-shifted Photoconversion of PixJ1, Phytochrome-like Photoreceptor in Cyanobacterium, Studied by FTIR

Kazunori Zikihara[1,2], Shizue Yoshihara[1], Takahiro Kitano[1], Hitomi Katsura[1], Takayuki Kohchi[3], Satoru Tokutomi[1] ([1]*Grad. Sch. Sci., Osaka Pref. Univ.*, [2]*Grad. Sch. Med., Osaka Univ.*, [3]*Grad. Sch. Bio., Kyoto Univ.*)

Plant phytochrome binds a linear tetrapyrrole, phytochromobilin (PΦB), as a chromophore covalently to a conserved Cys residue (1st Cys) in the GAF domain forming a thioether bond and has two absorption forms, named red light-absorbing (Pr) and far-red light-absorbing (Pfr) forms, between which they are photoconvertible by red and far-red light, respectively. Recently, a phytochrome-like chromoprotein, PixJ1, was found in cyanobacterium Synechocystis sp. PCC 6803 that binds a tetrapyrrol chromophore to the 1st Cys in the GAF2 domain and shows a photoconversion between blue light-absorbing (Pb) and green light-absorbing (Pg) forms instead between Pr and Pfr. To uncover the molecular basis for the blue-shifted photoconversion, Fourier transform infrared (FTIR) spectra of the PixJ1-GAF2 domain were measured and analyzed in reference to that of the photosensory domain of Arabidopsis phytochromeB (PhyB-N651).
Both the PixJ1-GAF2 and the PhyB-N651 showed light-induced changes in the fingerprint region of the FTIR difference spectra that are reproducible upon successive photoconversions. Notably, Pg minus Pb and Pg minus Pb difference spectra of PixJ1 showed positive and negative peaks, respectively, in the S-H stretching region indicating an association and a dissociation of H in a S-H group, possibly of the 2nd Cys in PixJ1-GAF2. On the other hand, neither Pfr minus Pr nor Pfr minus Pr difference spectra of the PhyB-N651 showed them. The details of the molecular basis for the blue shift in PixJ1-GAF2 will be discussed.

2PT189 視物質の熱雑音発生メカニズム

Mechanism of thermal activation of visual pigments in the dark

Daiki Kawata[1], Kota Katayama[1], Hiroo Imai[2], Hideki Kandori[1] ([1]*Department of Frontier Materials, Nagoya Institute of Technology*, [2]*Primate Research Institute, Kyoto University*)

Visual pigments possess an 11-*cis* retinal as the chromophore, and its photoisomerization to the all-*trans* form initiates our vision. Highly sensitive vision originates from efficient photoisomerization and little thermal isomerization. In fact, the cis-trans isomerization coordinate suggests high thermal activation barrier (> 180 kJ/mol), which is supported by the tightly packed chromophore in the crystal structure of rhodopsin. However, the reported activation enthalpy of the dark noise is 80-110 kJ/mol, and mechanism of such low thermal activation has been a paradox in vision. We recently challenged this paradox using FTIR spectroscopy and H/D exchange. Thr118 is located in contact with the chromophore and isolated from hydrogen-bonded network connecting to the outside of rhodopsin. We reported that the O-H group is not deuterated in D_2O at ambient temperature [1]. Nevertheless, we found that H/D exchange occurs at 50-70 ℃, suggesting that protein fluctuation drives the retinal binding pocket transiently open. We proposed a quantitative two-step model that can explain the observed low thermal activation in rhodopsin [2]. In this study, we extend this analysis to other visual pigments. Temperature-dependent H/D exchange measurements of the O-H group are in progress for 9-*cis* rhodopsin and monkey green-sensitive pigment, and molecular origin of dark noise in vision will be discussed.
[1] Nagata et al. *J. Phys. Chem. A* 106, 1969-1975 (2002).
[2] Lorentz-Fonfria et al. *J. Am. Chem. Soc* 132, 5693-5703 (2010).

2PT190 クモにおけるピンぼけ像を用いた新規距離知覚メカニズム
1YS1015 A novel depth perception mechanism based on image defocus in a spider

Takashi Nagata[1], Mitsumasa Koyanagi[2], Hisao Tsukamoto[2], Shinjiro Saeki[3], Kunio Isono[3], Yoshinori Shichida[4], Fumio Tokunaga[5], Michiyo Kinoshita[1], Kentaro Arikawa[1], Akihisa Terakita[2] ([1]*Dept Evol Stud Biol Sys, Sokendai-Hayama*, [2]*Grad. Sch. Sci., Osaka City Univ.*, [3]*Grad. Sch. Information Sci., Tohoku Univ.*, [4]*Grad. Sch. Sci., Kyoto Univ.*, [5]*Grad. Sch. Sci., Osaka Univ.*)

A pair of eyes of jumping spiders has a unique retina with four-tiered photoreceptor layers, on each of which light of different wavelength is focused due to chromatic aberration of the lens. Because the absorption spectrum of visual pigments is in general adaptively tuned to maximize visual information, the visual pigment in each layer was thought to be sensitive to the wavelength of the light focused on the layer. However, interestingly, we previously found that all photoreceptors in both the deepest and second-deepest layers contain a green-sensitive pigment, although green light is only focused on the deepest layer, indicating that the second-deepest layer always receives defocused images. Given that defocused images contain distance information of the scene in optical theory, we hypothesized that jumping spiders perceive distance from the amount of defocus in the second-deepest layer. In the present study, to test the hypothesis, we conducted detailed behavioral analysis of distance perception of the spiders under monochromatic illumination by measuring distances of jumps toward preys. Under red illumination, which generates a larger amount of defocus in the second-deepest layer than green light, jumping spiders exhibited shorter jumps than under green illumination. This result was in good agreement with theoretical predictions of our model based on experimentally determined optical parameters of the lens, strongly supporting our hypothesis that jumping spiders perceive distance based on how much the retinal image is defocused.

2PT191 酵母におけるニワトリクリプトクロム 4 の大量発現と特異的抗体を用いた精製

Overexpression of chicken cryptochrome4 in a budding yeast and its purification using a specific monoclonal antibody

Hiromasa Mitsui, Toshinori Maeda, Chiaki Yamaguchi, Yusuke Tsuji, Yoko Kubo, Keiko Okano, Toshiyuki Okano (*Dept. Eng. and Biosci., Grad. Sch. Adv. Sci. and Eng., Waseda Univ.*)

A wide variety of living organisms on the earth have developed several photoreceptive proteins for photosynthesis, visual perception, circadian photoentrainment, seasonal reproduction, and so on. Cryptochromes (CRYs), which are flavoproteins and are likely function as blue-light photoreceptor, have been found in bacteria, plants, and animals. Although CRYs are known to work as central components in the circadian oscillator in mammals, many CRYs in all kingdoms of life are considered to work as photosensors. The photochemistry and photocycle of CRYs have been studied in plants and flies, but little is known about the photoreception mechanism of vertebrate CRYs partly due to the lack of the expression and purification system of vertebrate CRY. We have tried to express vertebrate (chicken or zebrafish) CRYs in various host cells such as *Escherichia coli*, insect cell line, mammalian cell line, and yeast, and here we report a novel expression system for chicken CRY4 (cCRY4) using a budding yeast, *Saccharomyces cerevisiae*. In this system, cCRY4 was constitutively expressed and the expression level was approximately 500 μg per liter, which is comparable to a conventional system using *E. coli.* We also established a purification system of cCRY4 without any tag by immunoaffinity chromatography using a monoclonal antibody to C-terminal region of cCRY4. The purified cCRY4 was subjected to UV-visible absorption spectroscopy to analyze its photocycle.

2PT192 青色光により誘起される転写因子 AUREO1 の構造変化

Blue-light induced conformational change of a transcription factor, AUREO1

Osamu Hisatomi[1], Ken Takeuchi[1], Youichi Nakatani[1], Fumio Takahashi[2], Hironao Kataoka[3] ([1]*Graduate School of Science, Osaka University*, [2]*PRESTO, JST*, [3]*Botanical Gardens, Tohoku University*)

Aureochrome 1 (AUREO1) found in *Vaucheria* has one basic region/leucine zipper (bZIP) domain and one light-oxygen-voltage sensing (LOV) domain, and is believed to play a role as a blue light (BL)-regulated transcription factor[1]. To clarify the molecular mechanisms of AUREO1, we prepared recombinant AUREO1 proteins, containing full coding sequence (FL), bZIP and LOV domains (ZL), and LOV domain. Recombinant AUREO1s showed absorption and emission spectra typical of flavoproteins, and selectively bound to the target sequence (TGACGT). The absorption around 450 nm decreased immediately after the BL illumination, and was recovered to its original level with a half-life of about 6 min at pH 7 in the dark. Dynamic light scattering (DLS)

measurements demonstrated that the BL-induced change of the hydrodynamic radius (R_H) of LOV domain was slight. However, the R_H of FL and ZL in the light-adapted states were about 5% larger than those in the dark-adapted states. The R_H values were reverted to the dark-adapted level when illuminated FL and ZL were kept in the dark. Our results suggested that FL and ZL underwent a reversible conformational change upon illumination. Furthermore, the non-reducing SDS-PAGE assay indicated that ZL existed as dimers through intermolecular disulfide bonds in bZIP domains. The conformational change and dimer formation may play a crucial role for AUREO1 function.

1. Takahashi, F., et al. *Proc. Natl. Acid. Sci. USA* 104, 19625-19630 (2007).

2PT201 インシリコハイブリダイゼーション：新しい原核生物種の分類手法

In silico hybridization: A new tool for the classification of prokaryotic cells

Kunio Ihara[1], Tomomi Kitajima-Ihara[1], Masahiro Kamekura[2], Akinobu Echigo[3] ([1]*Nagoya Univ.*, [2]*Halophiles Lab.*, [3]*Toyo Univ.*)

What does species mean in prokaryotic cell? We, now, know even a single mutation might cause a drastic phenotypic or biochemical changes. Therefore, it is very difficult to delineate the species by comparing two prokaryotic cells only in phenotypic or biochemical point of view. At present, further including of DNA-DNA hybridization (DDH) studies should be essential for establish the species concept. However, DDH studies are laborious and their reproducibility among different laboratory would be marginal. Recently, it comes to easy to make complete genome sequencing by using next generation sequencer. We have tried to make a quick and simple method for classification of prokaryotes using SOLiD (Sequencing by Oligonucleotide Ligation and Detection) sequencing system. For the first trial, we have investigated the genus *Haloarcula*, because of our interesting of rhodopsin patchy distribution. We have sequenced 7 *Haloarcula* strains including the type strain *Haloarcula marismortui*. Several millions of 50bp short reads produced by the SOLiD sequencer were *de novo* assembled using the software velvet to produce thousands of contigs. Total short reads from one strain were mapped against assembled contigs. Mapping process is to search for the closely related region from the total genome, what we call, ***in silico* hybridization (ISH)**. The mapping values obtained in ISH were compared with the experimental DDH values and their correlation constant was 0.97. We will present in detail in the meeting.

2PT202 Homologous proteins with different fold: how were they raised ?

Shintaro Minami[1], Kengo Sawada[1], George Chikenji[2] ([1]*Grad. Sch. Eng., Nagoya Univ.*, [2]*Dept. Eng., Nagoya Univ.*)

Currently some examples of protein pairs with evidence for evolutionary relationships that fold into topologically different but share the same secondary structure packing arrangement have been known. One of the most interesting examples of such protein pairs is that of KH domains of hnRNP K and ribosomal protein S3 [1]. They show statistically significant sequence similarity (38% identity) implying homology. However, their structures are quite different in topology while converging to the same architecture.

Such examples suggest that proteins have changed their folds by segment shuffling or rearrangment events while conserving the same core packing arrangements. Further investigation of such protein pairs would give us a hint as to how proteins can change their fold in the course of evolution.

In this work, we performed comprehensive database search for all possible pairs which was classified into same superfamily in SCOP to encompass such interesting pairs of homologous protein. After the comprehensive search, we found a number of homologous protein pairs which show non-topological structural similarity. These pairs were investigated at a level of structure, amino acids, and DNA, and we found some clues as to how these proteins can arise in the course of evolution.

[1]N. V. Grishin, J. Str. Biol. (2001) 134:167-85

2PT203 全生物共通祖先以前のタンパク質のアミノ酸組成に実験的に迫る

Experimental approach to the amino acid usage of pre-last universal ancestor

Masami Shimada, **Satoshi Akanuma**, Kozue Shinozaki, Yoshiki Nakajima, Akihiko Yamagishi (*Dept. of Mol. Biol., Tokyo Univ. of Pharm. Life Sci.*)

Little is known about the nature of ancient proteins hosted by primitive organisms that lived before the last universal common ancestor emerged. However, it has been argued that primordial protein synthesis was much simpler and involved less than 20 amino acids. Given simpler protein synthesis system, the primitive proteins, which might have comprised a reduced set of amino acids, must have had a sufficiently adequate structure for functional interactions and catalysis. To address this issue experimentally, we used “protein simplification engineering (1)” to examine whether a protein composed of less than 20 types of amino acids can retain its stable structure and biological function. Using a thermally stable, ancestral-designed nucleoside diphosphate kinasase (Arc1) as the starting molecule, we constructed two reduced amino acid set variants, Arc1-s1 and Arc1-s2, in which non-conserved M, Q, K, Y and N and all of the five amino acid letters were replaced by other amino acids, respectively. Because cysteine is absent from Arc1, Arc1-s2 consists of only 14 amino acid letters. Arc1-s1 and Arc1-s2 retain thermal stability similar to that of Arc1. Arc1-s1 shows catalytic efficiency similar to that of Arc1; whereas, no detectable level of catalytic activity was observed for Arc1-s2. Therefore, the fourteen amino acid types are sufficient to encode a thermally stable protein but more amino acid types may be required for its function.

(1) Akanuma et al., PNAS 99, 13549 (2002)

2PT204 cDNA display 法による 4 種類のアミノ酸からなる機能ペプチドの創出

Generation of Functional Peptides Consisting of 4 Types of Amino Acids by cDNA Display Method

Shigefumi Kumachi[1], Miho Suzuki[1], Koichi Nishigaki[1], Yuzuru Husimi[2], Naoto Nemoto[1] ([1]*Grad. Sch. Sci. & ENG., Saitama Univ.*, [2]*Innovation Research Organization, Saitama Univ.*)

In general, proteins are composed of the 20 natural amino acids. However, how many type of amino acids required for the creation of a functional protein remains unresolved. Thus, we tried to design an experiment to examine the function of primitive proteins composed of a limited set of amino acids by in vitro selection approach. Interestingly, it has been postulated by two different approaches that the most primitive protein could consist of 4 types of amino acids (i.e., glycine, alanine, aspartic acid and valine): 1) Eigen *et al* . (RNA world hypothesis); and 2) Ikehara *et al* . (protein sequences analysis). So what function would a primitive protein have in an early translation system? The first primitive protein would most likely be associated with the enhancement of Ribozyme. Furthermore, in the early stages of protein synthesis, the genotype-phenotype linking strategy, which is essential for molecular evolution, could become a virus-type, because this strategy is the most efficient for protein evolution of a single function. If this strategy is adopted, the interaction between RNA and protein is indispensable. Thus, we investigated the possibility of whether peptides consisting of these 4 amino acids could interact with RNA by cDNA display technology. Then, some peptides were selected to interact with tRNA with low affinity. This shows that a primitive protein consist of 4 types of amino acids could evolve by the virus-type strategy in the early stage of emerging translation system.

2PT205 Directed evolution of a self-encoding system using giant liposome

Takeshi Sunami[1,2], Norikazu Ichihashi[1,2], Takehiro Nishikawa[1], Yasuaki Kazuta[1], Tomoaki Matsuura[1,3], Hiroaki Suzuki[1,2], Tetsuya Yomo[1,2,4] ([1]*ERATO, JST*, [2]*Grad. Sch. Info., Univ. Osaka*, [3]*Grad. Sch. Eng., Univ. Osaka*, [4]*Grad. Sch. Biosci., Univ. Osaka*)

Evolvability is a common property of living organisms, and gene replication system is essential to allow the living system to evolve. We have constructed a simplified system, in which the genetic information is replicated by self-encoded replicase in liposomes. For the self-encoding system to evolve, the genes must be compartmentalized and only a small number of them should be present in each compartment for genotype-phenotype linkage. The translated replicase needs to amplify only the gene encoding itself. Here we demonstrate the directed evolution of the self-encoding system by screening replicase mutants. Cell-sized giant liposomes were used as a micro reactor, and fluorescence-activated cell sorter (FACS) was used to analyze and sort the reacted liposomes. The antisense of the beta-galactosidase gene was inserted into the template DNA as a reporter gene. Beta-galactosidase was transcribed from the minus strand RNA replicated from plus strand RNA, and the green fluorescence from the hydrolyzed products by beta-galactosidase was evaluated as self-replication activity. Fluorescent liposomes with higher active replicase gene were sorted by FACS. The DNA templates for next selection round were amplified from the selected plus strand RNA in a test tube. After 69 rounds of selection, the self-replication activity of the selected mutants was evaluated in liposomes, and the mutants were higher active than wild-type replicase. The result indicates that the simplified gene replication system has evolvability as well as extant cells.

2PT206 枯葉に擬態した蛾・蝶の翅模様に実装された正確な擬態をもたらすモジュールデザイン

Modular spatial stabilization of leafy moth/butterfly wing pattrns for precise mimesis

Takao K. Suzuki, Hideki Sezutsu (*NIAS TG_SilkwormUnit*)

In nature, where *yuragi* is pervasive, many features of animal's structures are assumed to be so perfectly suited to their function that they seem unlikely to have arisen by chance. Among these features, mimetic patterns, resemblance to natural objects such as leaves, seem to be a typical example implementing a specific design to deal with yuragi. However, how the mimetic leafy patterns are established to manage yuragi has been poorly understood. Here, we developed a novel method, morphometrical network analysis, to reveal how the leafy moth/butterfly wing patterns are spatially coordinated. As model organisms, we used two leafy wing patterns: a moth, *Oraesia excavata*, and a butterfly, *Kallima inachus*. Our quantitative analysis indicated that in both organisms the constituent components of the leafy patterns are tightly coupled as modules, each of which corresponds to each component of the leaf venation pattern (i.e., the main, right-hand, and left-hand venation patterns). Interestingly, phylogenetic analysis showed that the modules detected in two organisms evolved independently, strongly suggesting that the modules of two leafy patterns were needed for mimetic performance. The establishment of modules allows within-module components to be put together, suggesting that the leafy pattern is precisely stabilized by implementing the spatially-synchronized arrangement of its subordinate leaf-venation components. Our results may suggest that the modular design likely improve the visual trick of leafy mimesis for predator avoidance.

2PT207 巨大化大腸菌(GP)からの大腸菌再生過程の観察

Observation of reproducing process the E. coli bacterium from a giant protoplast

Kazuhito Tabata[1], Takao Sogo[1], Shoji Takeuchi[2], Hiroyuki Noji[1] ([1]*App. chem. Univ. Tokyo*, [2]*IIS Univ. Tokyo*)

We report to reproduce into the original bacteria from a giant protoplast (GP), having a diameter in excess of 10 μm and prepared from a single *Escherichia coli* bacterium. Bacteria have long been known to be capable of gigantism. When ampicillin is added after a lysozyme treatment in an isotonic solution for culturing *E. coli*, cell wall synthesis is inhibited and division does not occur; this results in gigantism and the relatively easy formation of a GP with a diameter larger than 10 μm. A GP formed through such abnormal gigantism is believed to have already lost the ability to divide and proliferate. However, when this GP was confined in a microchamber and observed for more than 10h, we found that the spherical GP deformed and divided. This result may indicate that *E. coli* maintains its life system and is in a functional state even after becoming a GP and experiencing an extreme change in its intracellular environment. We showed that the GP have an ability to divide and return to its original bacteria cell using the miriochamber. We investigated the extent to which the gene expression system inside the GP was stable with respect to the duration of GP transformation culturing and found that protein expression ceased approximately 10 h after culturing. This finding is consistent with the fact that *E. coli* also stopped increasing in size in approximately 10 h, suggesting that 10 h is the critical line for the *E. coli* life system.

2PT208 天然のタンパク質のアミノ酸配列における隠れた局所的な反復性についての考察

An investigation on local pseudo-periodicity in the amino-acid sequences of native proteins

Koji Inai, **Masahito Oka** (*Osaka Prefecture University*)

In the previous work, we tried to investigate the repetitive amino-acid sequences in proteins by using currently available protein data base. A total of 8286132 proteins have the repetitive amino-acid sequences among whole 12619557 proteins, suggesting that repetitive amino-acid sequences are generally found in the native proteins. Then, using autocorrelation function method, we also tried to investigate the cryptic periodicity of amino-acid sequence, which cannot be found in the usual method aimed at the strict amino-acid sequence. It was shown that many proteins have quasi-repetitive sequences by these analyses. In this work, it is further tried to investigate on local pseudo-periodicity which was failed to notice in the full sequence analysis because its autocorrelation coefficient is usually underestimated. It was shown that many quasi-repetitive sequences were locally found in proteins in addition to those found in the previous work. These results would be a supporting data for our hypothesis on the amino-acid sequences of the earliest proteins.

2PT209 人工共生系の実験進化

Experimental evolution of a synthetic symbiosis

Kazufumi Hosoda[1], Akihiro Asao[2], Shingo Suzuki[1], Tetsuya Yomo[1,2,3] ([1]*IST, Osaka-u*, [2]*FBS, Osaka-u*, [3]*ERATO, JST*)

Most organisms belong to some mutually beneficial symbioses (mutualisms) in nature. Despite their ubiquity, mutualisms are evolutionarily vulnerable, because they are based on cooperative behaviors which do not necessarily provide direct benefit to the own fitness. Roughly speaking, if organisms only optimize their own fitness, mutualisms seem to collapse due to the emergence of "selfish" one that abandons the cooperative behavior. Various theories based on the natural selection (ultimate factor) have been proposed to fill the gap between the ubiquity and the vulnerability, but little is known about the insight into the physical/structural property of organisms (proximate factor) that affects the evolution of mutualism. As it is very challenging to follow the evolution of natural mutualisms at the molecular level, studying experimental evolution of a synthetic symbiosis, which is composed of previously non-interacting different populations, is effective to gain an understanding of the structural insight (Momeni et al. 2011). Here we show that a synthetic mutualism composed of two genetically engineered Escherichia coli strains did not collapse but developed in ~1,000 generation. The strains actually increased their own growth ability in the evolution, but they did not lose their cooperative ability. With the results of comprehensive analyses showing how their intracellular state changed, we want to discuss why they developed, not being too selfish.

2PT210 束論を用いた種の遷移における頑健性と最適性の研究

The robust and the optimal adaptation in species-transition network from the perspective of the lattice theory

Takayuki Niizato, Yukio Gunji (*Grad. Sch. Sci., Univ. Kobe*)

We investigate the adaptive behavior of species to a given environment. We here focus on two contradictory aspects of the adaptive process in evolution. The one is the optimization implying that species increase their own fitness as much as possible in a given environment. The other one is robustness implying that species sustain the inherent diversity despite changing environments. We address this issue to construct a model by using a lattice theory. A crucial point in our model relies on the novel idea of "multiplicity of fitness" which can cover malfunctioned individuals. This idea is partly taken in nature of exaptation. The multiplicity of fitness, in our model, would emerge as an overestimation of the fitness (each individual tends to overestimate own fitness compared with underlying fitness). This overestimation is not random, but context-dependent, represented by a lattice structure. We here show that species in our model demonstrate the power law of the lifespan distribution and 1/f fluctuation for the adaptive process without any parameter tuning. We also discuss essential difference between the behavior for adapting process and stochastic parameter-tuned process. Using a lattice theory enables us to construct a simple model of the adaptation equipped with the multiplicity of fitness, because we can address a complex fitness landscape by an algebraic ordered set. Furthermore, we provide new approach to the network theory by using lattice theory.

2PT211 Study on competitive reaction between enzymes with different diffusivity

Kenta Yashima[1], Jun Nakabayashi[2], Akira Sasaki[3] ([1]*Meiji Univ.*, [2]*Yokohama City Univ.*, [3]*The Graduate University for Advanced Studies*)

Diffusion process of molecules within heterogeneous medium shows a peculiar behavior termed anomalous diffusion. Here the motions of molecules are hindered by the obstacles, which constitute the heterogeneity of the environment. Accordingly, compared to homogeneous medium, the area that a molecule moves for a given time is smaller for heterogeneous medium. This affects the reaction process deeply (especially for diffusion limited reactions) and the classical formulation based on mass action law fails to describe the process and a formulation based on the Fractal reaction theory is necessary [Kopelman, Science 1988]. In this study we analyzed the competitive reaction between enzymes with different sizes. We assume that for larger enzymes obstruction due to molecular crowding makes the environment heterogeneous to it. On the other hand for smaller enzymes the environment is assume to be

homogeneous due to smaller obstruction effects from the molecular crowding. Accordingly there is a difference in the diffusivity, one with normal diffusivity and the other with anomalous diffusivity. We would like to discuss the physiological implications of this effect using Lattice Monte Carlo simulation and theoretical analysis based on the Fractal reaction theory.

2PT212 Counting statistics for genetic switches

Jun Ohkubo (*Grad. Sch. Informatics, Kyoto Univ.*)

The number of switching between activate and inactivate states in a genetic switch is investigated. Counting statistics is a scheme to study the number of specific transitions in a stochastic system. While the counting statistics has been studied a lot for a stochastic system with a finite number of states, the genetic switches are formulated as a system with an infinite number of states. Hence, it is needed to check the applicability of the counting statistics for the genetic switches. Actually, it immediately becomes clear that a straightforward application of the scheme derives intractable non-closed equations. We here use an effective interaction approximation, and it is shown that the switching problem can be treated as a simple two-state model approximately, which indicates that the switching obeys non-Poisson statistics.

2PT213 分化多能性を持つ細胞の分化初期段階における状態遷移
Transitions of the cell state in the early stage of differentiation from the pluripotent cell

Kou Makishi, Tomoki P. Terada, Masaki Sasai (*Dept. of Computational Science and Engineering, Nagoya Univ.*)

Embryonic stem (ES) cells have the ability to differentiate into all three germ layers, mesoderm, endoderm and ectoderm. This capability of ES cells is called pluripotency, and it has been shown that Sox2, Oct4, and Nanog (SON) are the important genes for maintaining pluripotency. We built a model of the network of core genes including SON, and performed the stochastic simulation of the early stage of differentiation starting from the pluripotent ES cells. We take into account three types of processes to regulate the gene expression in the model; binding/unbinding of transcription factors (TF), formation of the transcription apparatus (TA), and the modification of epigenetic histone code. The simulated population of pluripotent cells becomes phenotypically heterogeneous showing the different patterns of gene activity in individual cells when the rate of forming TA is slower than the rate of change in the copy number of TF. We will discuss the diversity of patterns of gene activity arising from the difference in the time scale among the processes to regulate the gene expression.

2PT214 シロイヌナズナにおける植物ホルモンの制御ネットワーク解析
Regulation network analysis of plant hormones in Arabidopsis thaliana

Mariko Miyamoto, Hiraku Nishimori, Akinori Awazu (*Dept. of Mathematical and Life Sciences, Hiroshima University*)

The plant hormone is low-molecular-weight chemical that is produced in the plant body and affects the plant activity in minute amounts. The plant produces several kinds of plant hormones and hormone-like substances which play the roles of the signaling molecules for gene expressions related to the growth, stress response, etc... In general, each of these hormones and hormone-like substances does not work independently but works cooperatively or competitively with each other, and the production of them are mutually regulated.
In this study, we extrapolate the regulation network among several plant hormones and hormone-like substances by the statistical analysis of the database of gene expression levels of microarray. We analyze the data set released in the Internet produced by “At Gen Express” project through the statistical methods such as Gaussian graphical modeling. Based on this analysis, we also construct the dynamical system model of the plant hormone regulation network of Arabidopsis thaliana to unveil physiological mechanism of the stress response and adaptation against the environmental fluctuation.

2PT215 Toward simulation of epidermal growth factor (EGF) pathway at the molecular resolution for K computer

Kazunari Iwamoto, Kazunari Kaizu, Koichi Takahashi (*Laboratory for Biochemical Simulation, QBiC, RIKEN*)

Cellular environment consists of the localization of various proteins, clustering of membrane molecules and cytoskeleton. Recently, the simulation at the molecular resolution indicated that characteristic of molecular network such as bistable and ultrasensitivity under such environment was different from prediction by conventional non-space simulation, which was supported by in vitro experiments. Therefore, the simulation at the molecular resolution is useful to understand the characteristic of cellular signaling pathways. In this study, we will implement the simulation at the molecular resolution of epidermal growth factor (EGF) signaling pathway which regulated cell proliferation and differentiation, and elucidate the characteristic.
The simulation software at the molecular resolution, Spatiocyte, was developed by Arjunan et al. (2010). However, it was difficult to execute the cellular-scale simulation at the molecular resolution using Spatiocyte. Thus, we are developing new software for supercomputer, especially K computer, based on the algorithm of Spatiocyte. On the other hand, prototype model of EGF pathway was constructed and preliminary simulation at one hundredth scale of actual cell was implemented. The simulated results showed heterogeneity of ERK activation, which qualitatively agreed with observed data. Further analysis suggested that this heterogeneity resulted from the minority of specific species in EGF pathway.

2PT216 Emergence of a spatial structure with a minority molecule in a catalytic reaction network

Atsushi Kamimura, Kunihiko Kaneko (*Dept. of Basic Science, The Univ. of Tokyo*)

It is crucial to explain the emergence of primitive cellular structure from a set of chemical reactions to unveil the origin of life and to experimentally synthesize protocells. Recently, we considered a hypercycle with two mutually-catalyzing chemicals to demonstrate that the reproduction of a protocell with a growth-division process occurs when the replication and degradation speeds of one chemical are, respectively, slower than those of the other chemical, and molecules are crowded as a result of replication. In this presentation, we discuss the effects of the crowding molecule in details on the formation of primitive structure and also show results when we consider more complex reaction networks.

2PT217 Complex biological networks from the standpoint of the category theoretical duality

Taichi Haruna (*Kobe University*)

In general, there are two pictures on directed biological networks. The first picture is structural one: a network is a collection of passages on which something flows. In the second picture, networks are seen as more functional entities: a network is a collection of local workings of the biological system which the network represents glued together. In our previous work, we showed that these two pictures can be described as a category theoretical duality and two path notions corresponding to each picture emerge as a result of a category theoretical universality. Conventional directed path and a path notion called lateral path correspond to the first and second pictures, respectively. Here, to examine how this duality is embedded in real directed biological networks, we introduce lateral betweenness centrality and directed betweenness centrality of arcs based on the corresponding path notions. Both centralities measure importance of a given arc by counting the number of shortest paths in each path notion that pass through the arc. We found that there exists a significant trade-off relationship between them in real biological networks. We show that the trade-off relationship can emerge mainly from an optimization process maximizing efficiency with respect to lateral path by numerical simulations. We also found that the optimized networks have similar qualitative features with real biological networks in the view of standard network analysis.

2PT218 分子混み合いが小胞内反応系に与える影響の理論的考察
Theoretical study of influence of molecular crowding to enzyme reaction system in vesicle

Masashi Fujii, Hiraku Nishimori, Akinori Awazu (*Grad. Sch. Sci., Hiroshima Univ.*)

Several living systems contain a variety of macromolecules, and the large number of such molecules is confined in small internal spaces of cells or intracellular organs. Some recent studies pointed out that the reactions and diffusions of these molecules are extremely restricted by their excluded volume. In this study, we investigate the effects of the excluded volume of densely confined molecules, commonly called `molecular crowding' effects, to the biochemical reaction. In order to consider this issue, we propose a coarse-

grained model of the enzyme reaction in a small vesicle, where the reaction process is inspired by the sugar-chain scission reaction of the lysozyme.
In this model, the enzyme/substrate is constructed by five/two large particles constructing the chain-like molecular form with three small particles playing the role of binding sites to the substrate/enzyme. We assume when the each binding site of an enzyme binds to that of the substrate, the substrate becomes the products.
By the Brownian dynamics simulation of the present model, the rate of the product formation in the initial stages is obtained as a bell-shaped function of the initial substrate density. We also observe that the reaction progresses intermittently like "stick-slip motion" when the initial substrate density is high, while the reactions occur smoothly when the initial substrate density is low. These results indicate that the molecular crowding provide the glassy state of the biochemical reaction in vivo.

2PT219 Temporal Decoding of MAP Kinase and CREB Phosphorylation by Selective Immediate Early Gene Expression

Takeshi Saito[1], Shinsuke Uda[1], Yu-ichi Ozaki[1,2], Shinya Kuroda[1] ([1]*Department of Biophysics and Biochemistry, Graduate School of Science, University of Tokyo*, [2]*Laboratory for Cell signaling Dynamics, Quantitative Biology Center, RIKEN*)

A wide range of growth factors encode information into specific temporal patterns of MAP kinase (MAPK) and CREB phosphorylation, which are further decoded by expression of immediate early gene products (IEGs) to exert biological functions. However, the IEG decoding system remain unknown. We built a data-driven model based on time courses of MAPK and CREB phosphorylation and IEG expression in response to various growth factors to identify systems. We found that IEG expression uses common decoding systems regardless of growth factors and expression of each IEG differs in upstream dependency, switch-like response, and linear temporal filters. Pulsatile ERK phosphorylation was selectively decoded by expression of EGR1 rather than c-FOS. Conjunctive NGF and PACAP stimulation was selectively decoded by synergistic JUNB expression through switch-like response to c-FOS. Thus, specific temporal patterns and combinations of MAPKs and CREB phosphorylation can be decoded by selective IEG expression via distinct temporal filters and switch-like responses.

2PT220 ショウジョウバエ翅原基における成長制御メカニズム
Growth control mechanism in the Drosophila wing disc

Ken-ichi Hironaka[1,2], Yoh Iwasa[2], Yoshihiro Morishita[1] ([1]*CDB, RIKEN*, [2]*Grad. Sch. of Sys. Life Sci., Kyushu Univ.*)

In the Drosophila wing disc, whereas BMP-homolog Dpp directs Antero-Posterior patterning, it also functions as a growth factor for the tissue. But underlying mechanism of Dpp-dependent growth control is not considered a simple concentration-dependent manner, because tissue grows uniformly under graded Dpp profile and grows nonuniformly under uniform Dpp profile. Recently, Wartlick et al. (2011) proposed that cell division is triggered by temporal change in Dpp concentration. We test the validity of this hypothesis by a constructive approach. In this presentation, we report that some combination of network motifs can realize the hypothetical growth control mechanism of Wartlick et al.(2011).

2PT221 ミドリゾウリムシの細胞内共生における最適行動
Optimal Behavior in Endosymbiosis in Green Paramecium

Sosuke Iwai (*Faculty of Education, Hirosaki Univ.*)

Paramecium bursaria, or green paramecium, is a unicellular ciliate that contains several hundreds of chlorella-like green algae in its cytoplasm as endosymbionts. It is generally believed that the symbiosis is mutualism, in which the host paramecium provides the symbiont alga with nitrogen sources such as amino acids, while the symbiont provides the host with photosynthetic products. To gain insights into mutualistic endosymbiosis, here we have constructed a simple model for the endosymbiosis in *Paramecium bursaria* and determined optimal behavior both for the host and for the symbiont. Assuming that the fitness of both of two organisms is linearly related to the amounts of carbon and nitrogen sources gained by two organisms, we revealed the optimal behavior of both of two organisms and also the conditions that allow the mutualistic endosymbiosis. The experimental verification of the model will be discussed.

2PT222 2 次元セルオートマトンモデルによる細胞の自己形成及び自己複製のシミュレーション
Two-dimensional cellular automata simulation of the self-assembly and self-reproduction phenomenon of cell

Takeshi Ishida (*Nippon Institute of Technology*)

Understanding the generalized mechanism of self-assembly and self-reproduction phenomenon of cell. is considered to be fundamental for application in various fields such as mass-production of molecular machines of nanotechnology and artificial synthetic of biology (synthetic biology). Thus we have to elucidate not only the details of the real cellular reaction network but also the necessary conditions for self-organized, self-replicating cells.
We developed a model for simulating cellular self-organization in two-dimensional cellular automaton. We demonstrated that the following 3 functions can be realized. (1) Emergence of cell (emergence of border (like cell membrane) and information carrier (like DNA). (2) Self-replication is achieved while maintaining a carrier containing information. (3) The division of the cell membrane is achieved while maintaining the total structure.
The previous self-reproduction models were two types, first is Neumann model that was very complicated one, second is Langton model that was very simple shape. Our study was able to show a self-reproduction phenomenon of the shape that was nearer to a living cell for the first time. This is not study to clarify all the necessary and sufficient conditions of the self-reproduction. It is thought that it can simulate the self-replication phenomena in real dynamic, chemical reaction environment applying the transition rules that became clear by this study.

2PT223 神経細胞の過渡的ダイナミクスにより神経情報コーディングがどのように制限されるか
Restriction of the information-coding scheme in the nervous system based on transient dynamics of neuronal activity

Takanobu Yamanobe[1,2] ([1]*Sch. Med., Hokkaido Univ.*, [2]*PRESTO, JST*)

In digital circuits, information is encoded on the basis of pulse patterns. To this end, pulse generation is independent of previous device activity. The rise and fall times of a pulse corresponding to the duration of its transient regime should be sufficiently short to achieve this independence. Otherwise, pulse generation will be dependent on previous activity because the transient regime affects the generation of other pulses. If the nervous system uses spike patterns to transmit information, as in the case of pulses in digital circuits, spike generation should be independent of previous neuronal activity. Thus, understanding the transient dynamics of a single neuron is crucial to elucidating the information carrier. In this study, we analyze the transient dynamics of a stochastic neuron model. First, we introduce a linear Markov operator that relates the density evolution between two consecutive input impulses. We show that the products of the operators (also linear Markov) reproduce the dynamics of the entire phase space of the neuron model in response to impulses. Next, we introduce a stochastic rotation number of the neuron model, which makes it possible to relate the density evolution of the neuron model to the number of generated spikes. Furthermore, the dynamics of the products of the operators is decomposed into invariant and transient parts. Thus, we evaluate the amount of the transient component, and we discuss the possible information carrier on the basis of its properties.

2PT224 Spontaneous and Evoked Neural Activities Shaped through A Sequential Learning Process

Tomoki Kurikawa, Kunihiko Kaneko (*Univ. Tokyo, Grad. Sch. Arts. Scis.*)

In neural science, neural response activities to external stimuli are generally recorded in order to understand neural computation. In this scheme, spontaneous activity in the absence of an input is disregarded as a back ground noise. However, recent experimental studies have suggested that the spontaneous activity plays a role in information processing and this role is not unclear. In order to uncover the role, in our previous study, we proposed a novel memory view and introduced a neural network model in which network structure is given. We found that when a neural network responds to a memorized input significantly, the spontaneous activity wanders among the memorized patterns, which is similar to the behavior typically observed in the neural system. In this study, we introduce a model with a simple learning rule. By this rule, we can analyze the spontaneous and evoked (memorized) activities for larger class of network structures than the given structure in the previous model. As results, we found that two types of behaviors are shaped: One behavior shows a stationary

activity both in the absence and presence of the learned input and does not respond to the input. The other behavior shows chaotic behavior wandering among the memorized patterns in the absence of the input and responds significantly to the input. Remarkably, the network structure for the latter is similar to that in the previous given model. It suggests that wandering spontaneous behavior is helpful to respond to external familiar stimuli.

2PT225 大腸菌の複数の鞭毛モーターの回転方向の協調的な切り換え現象の理論

A theory of the coordinated switching in the rotational direction of multiple flagellar motors in a single bacterium

Toshinori Namba[1,2], Tatsuo Shibata[2] ([1]*Department of Mathematical and Life Sciences, Hiroshima University*, [2]*RIKEN CDB*)

Many living organisms have systems to respond to the change in external environments, such as signal transduction systems. Such systems responsible for many important processes consist of complex interaction of molecular components. In these systems, molecular signals need to propagate in the cytoplasm. Terasawa et al. have recently reported a coordinated switching in the rotational direction of the multiple flagellar motors in an *E.coli* [1], suggesting that signaling molecules could propagate in cytoplasm to coordinately regulate the motors. The bacteria regulate the swimming behavior by controlling the rotational direction of flagellar motors to respond to extracellular stimuli. Thus, this coordination in the motor rotation may be important for the efficient regulation of the swimming behavior. This coordinated motor behavior can be explained by a spatial propagation of response regulator molecule. In this presentation, we propose a mathematical model of spatial regulation of response regulator molecules. We show possible behaviors of the signal molecules in the cytoplasm, such as wavelike propagation. Based on such a theoretical results, we will discuss the condition of the coordinated motor behaviors.

[1] S. Terasawa et al. (2011) Biophys. J. 100, 2193-2200.

2PT226 走化性真核細胞の変形と勾配認識

Gradient sensing of deformed eukaryotic chemotactic cells

Akinori Baba, Tetsuya Hiraiwa, Tatsuo Shibata (*CDB, Riken*)

Eukaryotic chemotactic cells sense the gradient of ligand molecules from the noisy input of the ligand binding/unbinding of the receptors distributed around the surface. For example, Dictyostelium Discoideum cells are possible to sense a shallow (about 1-2% of) gradient. To understand the eukaryotic chemotaxis, a theoretical model has been studied in terms of the maximum likelihood estimation of the chemical gradient from the noisy input. If the gradient is sufficiently shallow and/or the ligand concentration is sufficiently dilute, it is hard for a cell to find the correct direction from the ligand binding/unbinding of the receptors. In this case, the estimated direction of the gradient is strongly affected by the input noise. We consider the cell deformation to an elliptical shape in this model. For the shallow limit of the gradient, the estimated direction for an elliptical cell is anisotropic due to the anisotropic distribution of the receptors. We will discuss the comparison between the two scenarios of the gradient estimation: the simultaneous estimation of the steepness and the direction, and the estimation of only the direction with knowing the correct steepness.

2PT227 アメーバ運動による 3 次元経路探索の理論的考察

A theoretical study for three-dimensional path finding by amoeboid migration

Shin I. Nishimura (*Hiroshima University*)

Amoeboid cells such as lymphocytes migrate within collagen web matrix and pass through narrow channels between cells. It is known that T lymphocytes inhabiting lymph nodes migrate with searching antigen presenting cells (APC) that present acceptable antigens. Neutrophils appearing from vessels should find and catch external microbes within the body. Amoeboid cells in our body should migrate within complex structure. It is not well known how those cells arrive at appropriate positions through complex maze-like substrata. Even if external signal guides them, amoebae sometimes turn their direction to avoid obstacles. How they keep persistent migration even in such obstacle-rich space? To answer those questions, I construct a model for a three-dimensional amoeba and obstacles. The model cell has membrane, actin and control factor (CF) that prevent actin polymerization. CF is assumed to accumulate by retraction but become diluted by protrusion. This mechanism amplifies fluctuation of CF distribution and leads to directional migration of the cell. The simulated cell shows amoeboid-like migration not only on plane surface but also in a three-dimensional jungle gym that imitates complex structure within organs. This result implies that the strategy of amoeboid migration is versatile for any environment.

2PT228 一細胞分布解析を用いた大腸菌運動性の非遺伝的な影響評価

Single cell distribution analysis of motility reveals the heterogeneity of Escherichia coli

Daisuke Takagi, Kazumi Hakamada, Jun Miyake (*Osaka university*)

Genotype does not always agree with the phenotype, though cells can maintain their function. Such inconsistency leads us the idea that the system is made robust. In recent study, many reports try to elucidate their robustness and stable of the system using single cell analysis. Taniguchi et al. reported the distribution of gene expression follow gamma distribution, and Ozbudak et al. reported the multi-stability of bacterial system. These suggest it is difficult to elucidate the systems without understanding their distribution. In this study, four deletion mutants of Escherichia coli (Δ*flhC*, Δ*yhjH*, Δ*yfiN*, and Δ*ycgR*) and their parental strain BW2513 were selected and distributions of motility of single cells were observed. The peaks of their logarithmic distributions were observed 3. 7 (BW25113), 3. 2 (Δ*flhC*), 3. 5 (Δ*yhjH*), 4. 3 (Δ*yfiN*), and 5. 5 (Δ*ycgR*), respectively and they had statistical significance (p <0.001). The peaks of order corresponds to the function of genes. In the case of using Δ*ycgR*, the bimodal distribution of was given and it means this system has multi-stability. On the contrary, unimodal distribution was given in the case of using BW25113. This result suggests *ycgR* plays important role of giving stability of the system of flagella. It is necessary to construct mathematical model to elucidate the system.

2PT229 時計タンパク質 KaiB-KaiC 相互作用間の ATP による制御

The regulation of cyanobacterial circadian clock proteins KaiB-KaiC interaction by ATP

Risa Mutoh[1], Atsuhito Nishimura[2], So Yasui[2], Kiyoshi Onai[2], Masahiro Ishiura[2] ([1]*Institute for Protein Research*, [2]*Center for Gene Research*)

The cyanobacterial circadian clock oscillator is composed of three clock proteins called KaiA, KaiB and KaiC. The oscillator generates circadian oscillations in the phosphorylation level, ATPase activity of KaiC and complex formation among the three Kai proteins in the presence of ATP. KaiC is a homohexameric ATP-binding protein with autokinase activity and very weak temperature-independent ATPase activity. The KaiC subunit has a duplicated structure, which is composed of N-terminal and C-terminal domains, and each domain has a series of ATPase motifs (a Walker's motif A, a Walker's motif B and a catalytic glutamate (CatE)).

In the absence of ATP, KaiC was monomeric and formed a complex with KaiB. In the presence of Mg^{2+} and ATP (Mg-ATP), KaiC became a homohexameric ATPase with bound Mg-ATP and formed a complex with KaiB, whereas the KaiCs hexamerized by unhydrolyzable substrates such as ATP and Mg-ATP analogs did not. KaiC N-terminal domain protein formed a complex with KaiB, whereas its C-terminal one did not, indicating that KaiC associates with KaiB via its N-terminal domain. A hexameric KaiC mutant lacking N-terminal ATPase activity did not form a complex with KaiB, whereas that lacking C-terminal ATPase activity formed the complex. Thus, the hydrolysis or release of KaiC-bound ATP by N-terminal ATPase motifs is required for the complex formation.

2PT230 時計タンパク質 KaiC の ATP 放出

ATP release from cyanobacterial circadian clock protein KaiC

Keita Iwata[1,2], Risa Mutoh[3], Kiyoshi Onai[1], **Masahiro Ishiura**[1] ([1]*Center for Gene Research, Nagoya Univ.*, [2]*Sch. of Sci., Nagoya Univ.*, [3]*Institute for Protein Research*)

Cyanobacteria are the simplest organisms that exhibit circadian rhythms. The cyanobacterial circadian clock oscillator is composed of three clock proteins called KaiA, KaiB, and KaiC. KaiC has autokinase and ATPase activities. KaiC subunit has a duplicated structure, which is composed of N-terminal and C-terminal domains, and each domain has a series of ATPase motifs (a Walker's motif A, a Walker's motif B, and a catalytic glutamate (CatE)). KaiC subunit has two phosphorylation sites, Ser431 and Thr432, on its C-terminal domain. In the presence of ATP, ATP binds to the ATPase motifs of KaiC and induces the hexamerization of KaiC.

Here, we investigated ATP release from KaiC by the real time monitoring of bioluminescence using firefly luciferase. We measured the amount of ATP released from KaiC, using wild-type KaiC and mutant KaiCs with a mutation in the phosphorylation sites and ATPase motifs. We observed different ATP

releasing patterns between with and without KaiB, suggesting that KaiB may enhance ATP release from KaiC.

2PT231 概日周期の温度 / 栄養補償性に関する理論的研究

Theoretical study of temperature and nutrient compensation of circadian clock

Tetsuhiro Hatakeyama, Kunihiko Kaneko (*Graduated school of Arts and Science, Univ. of Tokyo*)

The circadian clock satisfies three criteria: persistence in constant conditions, phase resetting by light/dark signals, and temperature/nutrient compensation of the period, which is our concern here. In general, the period of chemical oscillator is very much sensitive to kinetic rate constants, which increase strikingly with temperature. Thus, the temperature compensation is an uncommon property of biochemical oscillators. Here, we propose a novel mechanism for this temperature compensation. Kondo and his colleagues recently demonstrated that the period of circadian oscillation of Kai-proteins indeed is temperature compensated. By simulating a model with phosphoration/dephosphoration cyclic reactions (extended from van Zon, et al., 2007), we first demonstrated the temperature compensation of the period indeed works over a broad range of temperatures, without the need for tuning parameters in the reactions. We then unveiled the mechanism for it as " enzyme-limited competition". We also showed that the nutrient compensation for ATP/ADP ratio is achieved by same mechanism as temperature compensation.

2PT232 シアノバクテリアの概日時計は低温で Hopf 分岐を介して消失する

Cyanobacterial circadian clock is nullified by low temperature through Hopf bifurcation

Yoriko Murayama[1], Hiroshi Kori[2,3], Takao Kondo[4,5], Hideo Iwasaki[1,3], Hiroshi Ito[2,6] ([1]*Grad. Sch. Sci. Eng., Waseda Univ.*, [2]*Fac. Sci., Ochanomizu Univ.*, [3]*PRESTO JST*, [4]*Grad. Sch. Sci., Nagoya Univ.*, [5]*CREST JST*, [6]*Fac. Design, Kyushu Univ.*)

Physiological rhythms with a period of approximately 24 hours are called circadian rhythms. One of the key characteristics of all circadian rhythms is that the free-running period remains stable under a relatively broad range of ambient temperatures, referred to as “temperature compensation” of the period. Outside of the range of temperature compensation, circadian clocks stop running and are arrested at a certain phase.

Dynamics of self-sustained oscillator such as circadian clocks has been studied in the field of nonlinear physics. Qualitative changes in the dynamics as parameters of a system are varied are called “bifurcations”. Based on the bifurcation theory, Hopf bifurcation and saddle-node bifurcation are plausible scenarios of circadian arrhythmia at low temperature.

The cyanobacterial circadian timing in *Synechococcus elongatus* PCC 7942 requires neither *de novo* transcription nor translation, and the posttranslational oscillation can be reconstituted in a test tube using only three clock proteins, KaiA, KaiB, and KaiC. The KaiC phosphorylation rhythm *in vitro* is best to observe directly and precisely dynamics of circadian oscillator. We found that the phenomena of nullification of KaiC phosphorylation rhythm by low temperature were explained by theory of Hopf bifurcation. We will report interesting phenomena predicted from the theory, and discuss fitness and physiological implications of circadian clock under lower temperature condition.

2PT233 チャコウラナメクジ嗅覚神経系に見られる時空間活動パターンとその非線形解析

Spatiotemporal Patterns of Neural Activities in the Olfactory Center of the Land Slug and the Nonlinear Analysis

Tomoya Shimokawa[1], Yuuta Hamasaki[1], Yoshimasa Komatsuzaki[2], Minoru Saito[1] ([1]*Graduate School of Integrated Basic Sciences, Nihon University*, [2]*College of Science and Technology, Nihon University*)

Rhythmic patterns of electrical activity are a ubiquitous feature of nervous systems. The modulation of oscillatory activity plays an essential role in the processing of sensory information. In the present study, we examined the odor responses of the oscillatory activity in the olfactory center (procerebrum; PC) of the land slug *Limax valentianus* by extracellular recording, and analyzed them by wavelet analysis. The local field potential (LFP) of the PC showed an oscillation of about 1 Hz, and the oscillatory activity was changed by various odor stimuli to the tentacle. Prior to the odor stimuli, the wavelet energy was distributed into some frequency ranges. After the aversive odor stimuli, the wavelet energy concentrated mainly into two ranges and the wavelet entropy decreased. These results suggest that the activities of neurons in the PC became more coherent in response to the aversive odor stimuli. To confirm it, we then examined the spatiotemporal patterns of neural activities in the PC by fluorescent voltage imaging technique. The PC preparation was stained with a voltage-sensitive dye, Di-4-ANEPPS. The stained preparation was illuminated by a LED (530 nm; LEX2-G, Brain Vision), and the 705 nm fluorescent images were acquired through a CCD camera (iXon X3 897, Andor). As a result, an oscillation of fluorescent intensity was observed in the PC, and the oscillation had a phase delay along the distal-proximal axis. After aversive odor stimuli, the phase delay disappeared, which showed more coherent activities of neurons in the PC.

2PT234 Motion analysis of collective soldier crab swarms

Hisashi Murakami[1], Yuta Nishiyama[1], Takayuki Niizato[1], Koichiro Enomoto[2], Masashi Toda[2], Toru Moriyama[3], Kojiro Iizuka[3], Yukio Gunji[1] ([1]*Kobe University*, [2]*Hakodate Future University*, [3]*shinshu University*)

Previously, collective behavior just as bird flock, fish school and insect swarm is explained by numerical model such as BOID (Bird-andrOID) and SPP (Self-Propelled Particle). These models can make collective motion by matching velocity of agent to neighbors in neighborhood, coupling well-turned noise externally. Yet, there is a little field data that should be compared with the models. We have observed the soldier crabs in Iriomote Island, Okinawa, Japan, which live in tideland, making big swarm. By using video camera, we recorded their swarms from above, and analyzed their collective motion by reconstructing their positions on two-dimensional coordinates. The results of this analysis show that the fluctuation of their motion positively contributes to maintenance and/or formation of a swarm, standing in contrast to the fluctuation of classical model, which is given as just random noise.

2PT235 Analysis of lateral connectivity in networks based on a lattice theory

Takenori Tomaru, Yukio Gunji (*Kobe University*)

In studying networks, there are many useful toolkits to analyze the properties. However, most of ways of analysis focus on an amount and distribution of vertices and/or edges to estimate structural properties of networks. We here propose a novel method to analyze a network structure as a whole in a term of algebraic structure, lattice structure. A directed network is expressed as a lattice by using a formal context based on a relation between edges and vertices. Through applying this method to some real networks, we show that a generated lattice can reflect original structure well. In addition, we can extract a particular structure called "overlapped lateral connection" of a network by the structure of a lattice and/or the number of generated elements by completion. The overlapped lateral connection can be related to robustness based on parallel functionality. In biological networks, such as food webs, it is important that networks evolve and maintain with diversity having overlapped target. This notion was missed by previous analytical toolkits based on existence of redundant pathways although it can play an essential role in a network evolving with respect to quality.

2PT236 真性粘菌モデルを用いた感性の計算

Computation of emotional information by using numerical model of true slime mold

Iori Tani, Yukio-Pegio Gunji (*Department of Earth and Planetary Sciences, Graduate School of Science, Kobe University*)

True slime mold *Physarum polycephalum* plasmodium is a unicellular cenocytic amoebic organism which is used as model organism in the field of biocomputation. Our numerical model of *Physarum* is able to construct various morphological pattern of real plasmodium and we have tried to apply this model to the emulation of visual perception. We already showed that the behaviors of our model for two-valued ambiguous figures were similar to human’s ones in figure-ground sense (I. Tani, et al., 2011). We treat more simpler figure like Kanizsa triangle and show our model can construct subjective contour of Kanizsa triangle. In addition, we discuss relationship of emotional information and biocomputation.

2PT237 Hill 式による非線形自励力学系の近似計算

Numerical investigation with Hill equation on approximated nonlinear autonomous dynamical systems

Eisuke Chikayama[1,2] ([1]*Niigata University of International and Information Studies*, [2]*RIKEN*)

We have shown that arbitrary nonlinear autonomous dynamical systems for chemical systems can be approximately expressed by using combinations of Hill equations or sigmoid functions. The numerical aspect of the theory, however, have not been demonstrated enough. We thus report that the results of the investigation of numerical calculations between exact and approximated nonlinear autonomous dynamical systems. As preliminary results for dynamical systems in one variable, of which the right-hand sides are X, squared X, and sine X, we set the intervals, 1, 0.1, and 0.01 along each X axis for step functions. They resulted in errors of -0.74, -0.0082, and -0.00010, respectively, for X; -5.9, -0.16, and -0.0017, respectively, for squared X; and 0.011, 0.015, and -0.00036, respectively for sin X. We further investigated the interval 1 with sigmoid functions and it resulted in errors of -0.70, -0.31, and 0.94, respectively, which were relatively good. We will offer further investigation including nonlinear dynamical systems with two variables.

2PT238 非平衡人工細胞モデルのための油中水滴マイクロ流体システム
Droplet-based microfluidic system for nonequilibrium artificial cells

Masahiro Takinoue[1,2], Haruka Sugiura[1] ([1]*Interdisciplinary Grad. Sch. Sci. and Eng., Tokyo Tech.*, [2]*PRESTO, JST*)

Understanding the essential mechanism of life systems is one of the most important issues in biophysics. Although biological sciences and technologies have clarified the molecular basis of life systems, the whole picture of life systems as autonomous integrated molecular systems has not been revealed yet. In recent years, biophysical technologies to construct artificial cells as simplified models of natural living cells have been proposed, and they help us to characterize life systems as the autonomous integrated molecular systems. However, most of them have limitations caused by the difficulty in transporting exterior/interior biomolecules through the membrane interface of artificial cell vesicles. Therefore, it is difficult to achieve experiments of dynamic nonequilibrium reaction systems in the artificial cell vesicles [1].
Here, we demonstrate a novel method for artificial cell study based on picoliter-sized water-in-oil (W/O) microdroplets (named "Cell-sized CSTR"). The cell-sized CSTR can control influx and efflux of biomolecules into and out of the artificial cell vesicles by microfluidic and electric manipulations of molecular interfaces of W/O microdroplets [2]. In this presentation, we show experimental investigations of the cell-sized CSTR and discuss the possibilities of nonlinear chemical reactions in the cell-sized CSTR. We believe that our method will promote the construction of nonequilibrium artificial cells in future.
[1] Takinoue et al., Anal. Bioanal. Chem. (2011)
[2] Takinoue et al., Small (2010)

2PT239 Phase response of the collective cAMP oscillations in Dictyostelium discoideum and its implication to the adaptive properties

Daisuke Imoto[1], Satoshi Sawai[1,2,3] ([1]*Graduate School of Arts and Sciences, University of Tokyo*, [2]*Research Center for Complex Systems Biology, University of Tokyo*, [3]*PRESTO, Japan Science and Technology Agency*)

Oscillatory phenomena are widely found in biological systems such as heart beating, flashing of fireflies, and development of Dictyostelium and Myxococcus. In most of these phenomena, it is important that the timing of pulsing of each element is synchronized. Characterizing the responses of the systems experimentally by the phase response curve (PRC) helps one identify the underlying instability that gives rise to the periodic activity (T. Tateno et al. (2007)). Earlier works on this aspect in cAMP oscillations in Dictyostelium have been fragmentary. Gerisch predicted Type 0 PRC (discontinuous type) to relatively strong cAMP stimuli in his theoretical model (Gerisch et al. (1979)). Experimentally, pH measurements on cell suspension also reported Type 0 PRC (Nanjundiah (1998)). However, PRC has not been obtained directly from measurements of cAMP. Moreover, there have been no work on measurement of Type 1 PRC (continuous type), thus it is still unclear how much stimuli are needed for the onset of cAMP oscillations.
Here we report PRC obtained by direct measurements of intracellular cAMP using a FRET sensor (Nikolaev et al. (2004)). By studying PRCs obtained at various concentrations of extracellular cAMP stimuli, we explored the relationship between the group-level PRCs and the single-cell input-output relation (Gregor et al. (2010)). We also examined mutant cells harboring a non-phosphorylatable form of the cAMP receptor and discuss the relationship between the PRC property and the adaptive properties of cAMP oscillations.

2PT240 Feedback-enhanced active-passive microrheology in cells

Hiroshi Arimatsu, Marcel Bremerich, Daisuke MIzuno, Heev Ayade, Peijuan Zhang (*Univ.Kyushu*)

The cytoskeleton is responsible for mechanics and various mechanical functions of cells. Mechanics of intracellular environments are, however, still elusive since living cells indicate a further complication due to the active force generation mostly governed by molecular motors. Here we investigate the non-equilibrium mechanical properties of cells using optical-trapping-based active-passive microrheology. By combining "active" micromanipulation of phagocytosed probe particles with an optical trap with high-resolution tracking of thermal(passive) motions of the very same particles by laser interferometry, we can both measure the mechanical properties of and, at the same time, identify nonequilibrium forces in biological materials as a violation of flluctuation-dissipation theorem. In cells, however, stable microrheology experimetns are hampered due to the active athermal fluctuations which easily drives the probe particles out of the laser foci. We therefore compensated the 3D active motion by implementing a PID-controlled feedback to reposition the sample chamber with a 3D-piezo stage. The piezo-control signal together with the optical trap measurement recover the complete bead trajectory. This way we performed active and passive microrheology in fibroblasts and analyzed the full distribution of probe particle displacements, the lag-time dependent van Hove correlation function, and discuss the results by comparing with those obtained from active reconstituted cytoskeletons in vitro (actin/myosin gel).

3PS001 IC138 リン酸化によるクラミドモナスダイニン-f テールの形態変化

Configuration changes of *Chlamydomonas* dynein-f tail coupled with IC138 phosphorylation

Hitoshi Sakakibara, Kazuhiro Oiwa, Hiroaki Kojima (*KARC, Nat. Inst. Inf. Com. Tech.*)

Inner-arm dynein-f of *Chlamydomonas* is a hetero-dimeric dynein which has two heavy chains (α and β), three intermediate chains and light chains on the tail. It has been shown that an axonemal casein kinase I phosphorylates the 138K intermediate chain (IC138) and that this phosphorylation is involved in regulation of flagellar activity. To elucidate the regulation mechanisms of dynein-f functions through the IC138 phosphorylation, we examined molecular configuration changes of dynein-f coupled with IC138 phosphorylation by negative-staining EM and following single-particle analyses. For the analyses, we picked up a dynein-f density map from the tomogram of axoneme, prepared projections of the map from various angles, and used tail parts of the projections as the templates for alignments. First, we found that the distribution of the two heads' positions spread and distance between the α and β heads became closer coupled with IC138 phosphorylation. Second, in ~10% classes, we found that the tail showed forked structure which consisted of thick stem and the thin branch linking to the beta head. This thin branch became smearing in phosphorylation conditions, suggesting that the branch positioning became unstable. From these observations, we suppose that the IC138 phosphorylation could first affect the thin branch positioning, then the β-head position should be shifted. In axonemes, position shift of the β head could affect the interactions of dynein-f and adjacent microtubule to change their operation mode.

3PS002 鞭毛・繊毛運動の研究に向けたヒト軸糸ダイニンの発現系の開発

Expression and purification of human axonemal dynein for studying cilia/flagella beating

Akane Furuta, Ken'ya Furuta, Misako Amino, Hiroaki Kojima (*Bio ICT lab, NICT*)

Motile cilia and flagella are crucial component for wide variety of cells. Previous studies have shown that the mutation in axonemal dyneins often impairs beating of cilia, leading to serious diseases known as primary ciliary dyskinesia. Normal axonemal dyneins in the cilia and flagella generate force that is highly regulated in time and space to generate regular waveform. Given the timescale of the regulation which is much shorter than that of signal transductions, it is natural to expect that individual dynein molecules act as a mechanical sensor for external loads, forming feedback loop to generate the oscillations. However, how dynein responds to external loads is unclear. To address this problem, it is critical to measure the force of both normal and mutated axonemal dyneins upon an applied external load. These assays require specific probes and mutations at desired sites on the axonemal dynein. A limiting issue in the study of axonemal dynein is that the recombinant proteins are not available so far. Here we used a transient expression system in HEK293 cells to express human recombinant axonemal dyneins. We isolated full-length and truncated human inner arm dyneins (DNAH2 and DNAH7) in a soluble form. Currently, we are working with functional analysis of these recombinant axonemal dyneins.

3PS003 Tubulin polyglutamylation regulates axonemal motility by modulating the function of a specific inner-arm dynein species

Tomohiro Kubo[1], Toshiki Yagi[2], Ritsu Kamiya[1] ([1]*Department of Biological Sciences, Graduate School of Science, University of Tokyo*, [2]*Department of Cell Biology and Anatomy, Graduate School of Medicine, University of Tokyo*)

Tubulin polyglutamylation is a post-translational modification that affects various microtubule-dependent cellular functions. The tpg1 mutant of Chlamydomonas lacks a homologue of mouse TTLL9 (a tubulin polyglutamylase) and has a reduced level of polyglutamylated alpha tubulin in the outer-doublet B-tubule. It displays lowered flagellar motility because of deficient interaction between inner-arm dynein and doublet microtubules (Kubo et al. Curr. Biol. 20, 441-445, 2010). Chlamydomonas has seven major species of inner-arm dyneins, designated dynein a~g. Dynein f (dynein I1) is a two-headed dynein containing two heavy chains, while all others are one-headed. In the present study, we produced double mutants of tpg1 and various inner-arm-deficient mutants, and found that the tpg1 mutation did not affect the lowered motility of mutants lacking inner-arm dynein e, while it greatly reduced the motility of mutants lacking dyneins other than dynein e. This observation suggests that tubulin glutamylation most sensitively affects the function of dynein e. The exceptionally basic microtubule binding site (the stalk tip) of dynein e may account for its high sensitivity to the tpg1 mutation, which should greatly change the microtubule surface charge.

3PS004 高速 AFM による細胞質ダイニンの機能動態の観察

High-Speed-AFM Observation of Processive Movement of Cytoplasmic Dynein

Shuji Fujita[1], Karunakaran Aathi[2], Uchihashi Takayuki[1,3], Vale Ronald D.[2], Toshio Ando[1,3] ([1]*College of Science and Engineering, Kanazawa University*, [2]*Department of Cellular & Molecular Pharmacology, University of California, San Francisco*, [3]*Bio-AFM Frontier Research Center, College of Science and Engineering, Kanazawa University*)

Cytoplasmic dynein is a microtubule-based motor protein which transports a cargos toward microtubule minus end. So far, several studies based on structural analysis and single molecule observations have been reported to reveal dynein's mechanims[1-3]). For examples, the structural analyses revealed the manners in which the mechanical elements interacts with the ATPase ring and a long-range allosteric communication takes place between the primary ATPase site and the microtubule-binding site. The single molecule analysis revealed the step-wise motions during the processive movement and what the stepping behavior varied as a function of interhead separation. However, there is no study by which direct observation of the conformational state of the functional dynamic because of a lack of technique. While we have recently succeeded in directly visualizing hand-over-hand movement of myosin V.[4]) This observation provided straightforward and detailed information on how myosin V moves along an actin filament. Here, we applied to high-speed AFM to observation of cytoplasmic dynein moving along microtubules. In this presentation, we will discuss what information about the dynnein's mechanisms can be gained with high-speed AFM .

1) A. Carter, C. Cho, L. Jin and R. D. Vale, Science 331, 1159-1165 (2011).
2) M. A. DeWitt., A. Y. Chang, P. A. Combs, A. Yildiz, Science 335, 221-225 (2011).
3) T. Kon, T. Oyama et al., Nature 484, 345-350 (2012).
4) N. Kodera, D. Yamamoto et al., Nature 468, 72-76 (2010).

3PS005 鞭毛軸糸ダイニンによって駆動される微小管配列の振動運動

Oscillation of a microtubule array driven by axonemal dynein

Susumu Aoyama, Yuichi Hiratsuka (*Sch. Matl. Sci., JAIST*)

Flagellar axoneme produces high speed oscillatory movements, which is essential for many eukaryotes to survive. Details of the mechanism of flagellar beating is not clearly elucidated, although some studies have shown that the minimal elements of oscillation is motor protein dynein and microtubules in an axoneme. To solve the mystery of flagellar movements, we tried to fabricate oscillatory units by arranging microtubules and dynein molecules with some accessory structures. In an axoneme, nine microtubules are arranged in the same polarity, and the minus ends of them are tightly bound with each other. We fabricated such microtubule arrays by polymerizing tubulin from polarity-arranged microtubules fixed on a glass surface. Polarity of microtubules was arranged by kinesin motility guided by a micro-track. A typical microtubule array was composed of five to fifteen microtubules. Next, we made microtubules on which axonemal dynein molecules were aligned, and incorporated them into microtubule arrays. In the microtubule array, dynein-bound microtubules interacted with polarity-arranged microtubules and displayed cyclical attachment and detachment. As a next step of this study, we are now trying to produce bending oscillation in our experimental system by loose cross-links between microtubules. We expect that the basis of flagellar beating can be produced in a simple microtubule-array system driven by dynein motors.

3PS006 Structural and Biochemical Properties of the Outer-Dynein-Arm Docking Complex (ODA-DC) in Chlamydomonas flagella

Mikito Owa[1], Takahiro Ide[1], Ritsu Kamiya[1,2], Kenichi Wakabayashi[1] ([1]*Dept. Biological Sciences, Grad. school of Science, Univ. Tokyo*, [2]*Dept. Life Science, Faculty of Science, Gakushuin Univ.*)

Outer dynein arms in cilia and flagella are bound to specific loci on outer-doublet microtubules with a regular spacing of 24 nm. Their binding to the doublet microtubules is mediated by the outer dynein arm docking complex (ODA-DC) present at the base of the outer arm. In Chlamydomonas, the ODA-DC is composed of three subunits, DC1 (ODA3), DC2 (ODA1) and DC3

(ODA14). ODA-DC binds to specific loci on the outer-doublets of mutant axonemes that lack outer arm dynein, suggesting that it is responsible for the binding of outer arm dyneins to specific sites. To understand the basis for this crucial function of the ODA-DC, we examined the structural and biochemical properties of ODA-DC using both recombinant and native proteins. Low-angle rotary shadowing indicated that the recombinant ODA-DC has an oval shape, ~25 nm in length. The recombinant ODA-DC binds to cytoplasmic microtubules in an all-or-none manner, suggesting a cooperative binding event. Chemical crosslinking of axonemes from a mutant lacking outer-arms revealed that the native ODA-DCs associate with each other on the doublet microtubules. These data suggest that the periodic and cooperative binding of the ODA-DC molecules on the doublet microtubules is based on an end-to-end association of the ODA-DCs. Furthermore, chemical crosslinking also revealed that the ODA-DC is associated with three uncharacterized novel proteins on the axoneme. These proteins possibly specify the binding site of the ODA-DC on the outer doublet microtubules.

3PS007 クラミドモナス軸糸微小管上の外腕ダイニンの組み立てに必要なタンパク質間相互作用の解析

Analysis of protein-protein interactions required for the assembly of outer arm dyneins on the axonemal microtubules in Chlamydomonas

Takahiro Ide[1], Mikito Owa[1], Kaoru Yoshida[3], Manabu Yoshida[2], Ritsu Kamiya[4], Ken-ichi Wakabayashi[1] ([1]*Dept. Biological Sciences, Grad. School of Science, Univ. Tokyo*, [2]*Misaki Marine Biological Station, Graduate School of Science, University of Tokyo*, [3]*Biomedical Engineering Center, Toin University of Yokohama*, [4]*Department of Life Science, Graduate School of Science, Gakushuin University*)

Outer arm dynein (OAD) in cilia and flagella are bound to specific loci on outer-doublet microtubules with a regular spacing of 24 nm. Previous studies showed that OAD has two sites for binding to microtubules: intermediate chain 1 (IC1) and the outer dynein arm docking complex (ODA-DC) located at the base of OAD. Studies using Chlamydomonas mutants have shown that OAD cannot bind to the microtubule at all without the ODA-DC, and the ODA-DC can bind to MTs only in a reduced amount without OAD. These data suggest that the two sites have weak binding affinities to microtubules, and therefore they possibly cooperate with each other to enable strong OAD attachment to microtubules. To test this idea, we quantified binding affinities of IC1, IC2 (the other intermediate chain located at the base of OAD) and the ODA-DC using recombinant proteins, and also tested whether there is a direct interaction between ICs and the ODA-DC. The recombinant IC1 and IC2 were found to form heterodimers, and the IC1-IC2 heterodimer further formed a complex with ODA-DC in vitro, in which IC2 was in contact with DC1 (an ODA-DC subunit). In addition, the binding affinities of ICs and ODA-DC to cytoplasmic microtubules, measured with a quartz crystal microbalance (QCM), were similar to each other. From these results, we propose a new model of protein-protein interactions for the docking of outer dynein arms to the axonemal microtubules.

3PS009 *In vitro* analyses on two adjacent inner-arm dyneins, subspecies e and c

Youské Shimizu, Hiroaki Kojima, Kazuhiro Oiwa, Hitoshi Sakakibara (*Advanced ICT Research Institute, NICT*)

Subspecies of inner-arm dyneins are aligned periodically and specifically in flagella. Though each of dynein subspecies “e” and “c” is able to be purified as monomer, these two dyneins are adjacent in flagella so that there may be interaction and/or cooperation between them. To study the properties, dynein e and c were highly purified. ATPase activity of dynein e (k_{cat} ~ 0.3) was low compared with that of dynein c (k_{cat} ~ 1.8). MT-binding affinity of nucleotide-sensitive binding domain of dynein e was higher than that of dynein c. *In vitro* motility assay indicated that dynein e was relatively slow (V_{max} ~ 2 μm/s) and dynein c was relatively fast (V_{max} ~ 17 μm/s) in MT-sliding. To obtain clues on the mechanism of spontaneous work of two dyneins, we analyzed properties of mixture. From the MT-sliding by the mixture of dyneins, it was suggested that slow dynein e did not cause a drag force on fast MT-sliding by dynein c. On the other hand, direct interaction between these dyneins was not confirmed, so the interaction was thought to be limited or weak. Dynein e and c may be working in flagella in cooperation with each other.

3PS010 生細胞内における温度分布のイメージング

1YS0915 Imaging of temperature distribution in a living cell

Kohki Okabe[1], Seiichi Uchiyama[1], Noriko Inada[2], Yoshie Harada[3], Takashi Funatsu[1] ([1]*Grad. Sch. Pharm. Sci., Univ. Tokyo*, [2]*NAIST*, [3]*iCeMs, Kyoto Univ.*)

Temperature is a fundamental physical quantity that governs every biological reaction within living cells, and temperature distribution reflects cellular thermodynamics and function. In medical studies, the cellular pathogenesis of diseases (e. g., cancer) is characterized by extraordinary heat production. Therefore, intracellular temperature imaging of living cells should promote better understanding of cellular events and the establishment of novel diagnoses and therapies. However, imaging of temperature distributions in living cells has never been achieved. Here we demonstrate the first intracellular temperature imaging based on a fluorescent polymeric thermometer and fluorescence lifetime imaging microscopy (FLIM). The spatial and temperature resolutions of our thermometry were at the diffraction limited level (200 nm) and 0.2 degree Celsius, respectively. The intracellular temperature distribution we observed indicated that the nucleus and centrosome of a COS7 cell both showed a significantly higher temperature than the cytoplasm and that the temperature gap between the nucleus and the cytoplasm differed depending on the cell cycle. The heat production from mitochondria was also observed as a proximal local temperature increase. These findings demonstrate an intrinsic connection between temperature and organelle function. Thus, our intracellular temperature imaging has a significant impact on the comprehension of cell function and will provide insights into the regulatory mechanisms of intracellular signaling.

3PS011 走査電子顕微鏡を用いた非染色生物試料の高コントラスト・低ダメージ観察方法

A high-contrast and low-damage observation method of the unstained biological samples by scanning-electron microscope

Toshihiko Ogura (*AIST Biomedical Research Institute*)

Scanning electron microscope (SEM) is a useful technique for the investigation of surface structure of biological samples. To allow observations under the high vacuum conditions of SEM, many preparations of biological samples have been developed, e. g., glutaraldehyde fixation, negative staining, the Sputter-Cryo technique, and coating with gold or osmium. These preparations have some positive effects on the biological samples; for instance, they enhance contrast, reduce damage, and are uncharged up by the electron beam. However, these preparations require many steps and/or special equipments. Therefore, a more convenient preparation method for biological samples is needed. Here, we show that the unstained biological samples under a thin film give a high contrast detected by the secondary electron (SE) signal at a low accelerating voltage. The unstained biological samples are attached to the lower surface of a 30-50 nm thin film. The high-contrast images are created from the SE signal under the thin film. These are very low damage to the samples, and the images are similar to the transmission image. Our novel method can be easily utilized to observe various biological samples of bacteria, viruses and protein complexes.

3PS012 低温電子顕微鏡による細菌べん毛キャップ連結部の 3 次元再構成

The structure of the flagellar cap-junction complex by electron cryomicroscopy

Fumiaki Makino, Takayuki Kato, Tomoko Miyata, Keiichi Namba (*Frontier Bioscience*)

The bacterial flagellum is a biological nanomachine for the locomotion of bacteria. The cap at the growing end of the bacterial flagellum is essential for its growth. Flagellar axial proteins travel through the central channel of the flagellum to the distal end where self-assembly occurs. After flagellar hook has reached its mature length, the two junction proteins FlgK and FlgL assemble to form the hook-filament junction, and then the filament cap protein FliD forms a cap structure at the distal end of the junction to form the cap-junction complex. When FliC molecules are exported to the distal end, the FliD pentamer works as the filament cap for filament growth. It has been revealed form the cap-filament structure that five leg-like anchor domains of the pentameric cap flexibly adjust their conformations to keep just one FliC binding site open at a time. This has suggested a cap rotation mechanism to promote FliC self-assembly. However, the boundary between the cap and the filament end has remained unclear.
In this study, we report 3D structure of the cap-junction complex, in which we

can see how the leg-like anchor domains of FliD bind to FlgL in a similar manner to the structure of the D0-D1 domain of FliC over the symmetry mismatch as well as the depression and space inside the cap complex for promoting assembly.

3PS013 バイメタルカンチレバーを用いた褐色脂肪細胞の発熱量の定量的解析

Quantitative analysis of heat production of brown adipocytes using bimetal cantilever

Masaaki Sato[1], Masaya Toda[2], Naoki Inomata[2], Yuichi Inoue[1], Takahito Ono[2], Akihiko Ishijima[1] ([1]*IMRAM, Tohoku Univ.*, [2]*Grad. Sch. Eng., Tohoku Univ.*)

Brown adipocyte is a cell specified for metabolic heat production. From a calorimetry using 10^8 numbers of the cells, the cell is thought to produce nW-ordered heat. However, the character of each cell cannot be investigated by the calorimetry. To reveal the character, the measurement technique for heat production of a single cell is needed. So we developed a bimetal cantilever (750 ×40 μm), which is composed of gold (100 nm in thickness) and silicon nitride (200 nm in thickness). When the cantilever senses heat, it bends due to the difference of the coefficient of thermal expansion of the metals. We tried to measure the heat produced by a small number of the cells using the cantilever. The displacement of cantilever was measured under a conventional microscope when the 5-6 cells reached about 2 μm away from the tip of cantilever. After the addition of norepinephrine (final 1 μM), the displacement of the cantilever increased as time passed on. After 60 min from the addition, the displacement of cantilever became maximum value (60 nm). If the heat which the cantilever detected has escaped only at the end of the cantilever, the value corresponds to that the temperature of the tip of the cantilever has increased 10 mK. After further 90 min, the displacement was not observed. We would like to discuss the activation and inactivation of heat production of the cell together with lipid consumption of the cell and expression level of protein which is involved in heat production.

3PS014 細胞シート 1 軸延伸測定法による時間依存力学測定

Time-dependetn Poisson's ratio and Power-law rheology of cell sheet in uniaxial stretching experiment

Masahiro Tsuchiya, Yusuke Mizutani, Takaharu Okajima (*Graduate School of Information Science and Technology, Hokkaido Univ.*)

Mechanical properties of living cells are strongly related to their physiological functions such as migration, division and restructuring of their intracellular structures. Rheological properties of living cells have been extensively investigated by various microbead techniques, atomic force microscopy and single cell stretching method. These studies showed the single cell exhibited a power-law behavior in frequency domains. The Poisson's ratio of living cells is one of the important modulus and related with some time dependent modulus. Moreover, studies regarding polymer materials revealed that the Poisson's ratio was a function of time. However, the time-dependent Poisson's ratio of cells has not been measured. In this study, we measured the Poisson's ratio of cells as a function of time during stress relaxation of cell sheet composed of NIH3T3 cells with a size of ca.500 × 400 μm. We found that the Poisson's ratio of cell increased with time and became time constant. As the actin filaments were disrupted, the time dependent Poisson's ratio reduction is rapidly changed. The results indicated that the time dependent Poisson's ratio was strongly related to the contraction of actin structures.

3PS015 原子間力顕微鏡を用いた単一細胞レオロジーの高速・精密測定法の開発

High-speed measurement of single cell rheology with an atomic force microscope

Ryosuke Takahashi, Satoshi Ichikawa, Takaharu Okajima (*Graduate School of Information Science and Technology, Hokkaido University*)

Single cell measurements of cell mechanics are crucial not only for understanding various cell functions such as migration and proliferation but also for distinguishing different types of cells. It has been reported that the elastic property of cancer cells is smaller than that of normal cells [1, 2]. We obviously observed that cancer cells are softer and more fluid than normal cells and found the difference of the ensemble distribution of rheological properties between normal and cancer cells such as human mammary epithelial cells (MCF-10A) as normal cell and human mammary adenocarcinoma cells (MCF-7) as cancer cell [7]. To improve throughput of cell measurements, we developed an AFM system for the measurement of rheological properties of a large number cells, the shape of which was controlled with micropatterned substrates [3], in the frequency domain [4, 5]. The observed AFM data could be analyzed using a power-law structural damping model [6]. We will present the detailed AFM system and discuss the ensemble distribution of power-law rheology parameters between normal and cancer cells.

[1] J. Guck, et al., Biophysical Journal. 88, 3689 (2005)
[2] S. E. Cross, et al., Nat. Nanotech. 2, 780 (2007)
[3] C. Y. Park, et al., Am J Physiol Cell Physiol 298, 1245 (2010)
[4] Y. Mizutani, et al., Jpn. J. Appl. Phys. 47, 6177 (2008)
[5] S. Hiratsuka, et al., Ultramicroscopy 109, 937 (2009)
[6] B. Fabry, et al., Phys. Rev.E, 68, 041914 (2003)
[7] R. Takahashi, et al., in preparation

3PS016 "ホッピングモード"高速原子間力顕微(HS-AFM)の開発

Development of "hopping-mode" high speed atomic force microscopy (AFM)

Hiroki Watanabe[1], Mikihiro Shibata[2], Takayuki Uchihashi[1,4], Ryohei Yasuda[3], Toshio Ando[1,4] ([1]*Department of Mathematics and Physics, Grad School of Natural Science and Technology, Kanazawa University*, [2]*Department of Neurobiology, Duke University Medical Center*, [3]*Max Planck Florida Institute*, [4]*Bio-AFM Frontier Research Center, College of Science and Engineering, Kanazawa University*)

High-speed AFM (HS-AFM) can directly visualize dynamic behaviors of single protein molecules in action and has recently been proven to be powerful in the elucidation of functional mechanisms of proteins[1, 2]. However, it is hard to observe large and soft biological samples such as live cells and organelles using our tapping-mode HS-AFM because the AFM cantilever tip exerts relatively large lateral forces to the sample during scanning and thus damages soft samples.

To overcome this problem, we attempt to combine a new operation mode of AFM called hopping mode[3] with the HS-AFM. In hopping-mode AFM, we no longer use continuous feedback operation. Instead, at each imaging point, the AFM tip approaches the sample from a starting position that is above any of the surface features. The cantilever is freely oscillating when the tip is well away from the surface. The tip then approaches until the amplitude is reduced to a predefined value. When the amplitude experiences this reduction, the position of the z-piezo is recorded as the sample height at this imaging point. Owing to this operation principle, the tip lateral forces applied to the sample can be significantly reduced even for tall samples. In this presentation, we will show the capability of this new AFM system by presenting captured images of HeLa cells.

1) M. shibata et al., Nature Nanotechnol. **5**, 208-212 (2010)
2) T. Ucihashi et al., Science **333**, 755-758 (2011).
3) P. Noval, C. Li et al., Nature Method **6**, 279-281 (2009).

3PS017 超音波高速 AFM の開発に向けた基礎研究

Pilot study for the development of high-speed ultrasonic AFM

Yasuto Nagashima[1], Tomofumi Saito[1], Noriyuki Kodera[2], Toshio Ando[1,2] ([1]*Sch. Math. & Phys., Inst. Sci. & Eng., Kanazawa Univ*, [2]*Bio-AFM Frontier Research Center, Inst. Sci. & Eng., Kanazawa Univ*)

We have developed high-speed AFM (HS-AFM) that enables us to directly visualize dynamic structural changes of protein molecules at high spatiotemporal resolution. So far, various biological processes performed by protein molecules have been directly filmed as molecular movies, which allowed us to gain insights into their functional mechanisms much more straightforwardly than other techniques [T. Ando, Nanotechnol (2012)]. However, the observations by HS-AFM are generally limited only to phenomena occurring on relatively hard surfaces, meaning that we can observe neither objects placed on a soft surface (e.g., protein molecules on mammalian cell surfaces) nor objects placed under a surface (e. g., organelles and cytoskeletons in the interior of cells).Ultrasonic techniques must be useful in breaking this limitation because they have been widely used for non-invasiveness imaging of objects lying on/under a surface, whereas their spatial resolution is limited by the wavelength of ultrasonic used. However, AFM which is combined with ultrasonic techniques is recently claimed to be able to perform subsurface imaging of objects in the interior of cells at nanometer resolution [GS. Shekhawat & VP. Dravid, Science (2005)]. Thus, we are currently attempting to find a way to combine our HS-AFM with ultrasonic techniques. In the presentation, we will report our pilot study on this subject.

3PS018 原子間力顕微鏡を用いたタンパク質界面膜の研究

AFM studies on the spread films of protein

Taiji Furuno (*Dept. Phys., Keio Univ. Sch. Med.*)

The spread films of protein at the air/water interface hold almost hundred years of research history. The surface properties of them have been mainly discussed based on the pressure-area isotherms. However, the study lacks the direct structural information on the state of the spread protein molecules.
The invention of atomic force microscope (AFM) has opened the avenue to study single proteins or protein assemblies in water if they were deposited on smooth solid surfaces. In the present study, a number of proteins have been directly spread on the water surface using a 10uL microsyringe with its needle end touching the water surface. The surface films were transferred onto hydrophobic silicon surface and imaged by tapping mode AFM under water. They were classified into three groups. Catalase, carbonic anhydrase, ferritin and apoferritin, which denatured gradually after spreading, formed two-dimensional random packing in the spread films. In the second group to which bovine serum albumin and thermally treated carbonic anhydrase belonged, the unfolding was very quick at the air/water interface, and almost no granular particles corresponding to the spread protein molecules were not found bound to or embedded in the film. The third group consisted of lysozyme and streptavidin, which resisted to be spread at the interface, and were mostly lost into the subphase. All these classifications were possible by AFM imaging of the transferred films.

3PS019 カーボンナノチューブ電極を用いた神経伝達物質の高感度記録法の開発

Development of Carbon Nanotube Electrode For High Sensitivity Recordings of Neurotransmitters

Mao Fukuda, Ikurou Suzuki, Masao Gotoh (*Department of Bionics, Graduate School of bionics, computer and media science Tokyo University of Technology*)

We have developed a microelectrode array chip and paste electrode that can measure neurotransmitters. In this study, we focused on using carbon nanotubes because they indicate high conductivity, and changeable in physical properties. A 64 planner electrodes were fabricated by etching an indium-tin oxide (ITO) layer on a glass slide, then covered with insulating film. The surface of recording terminals was formed by etching the insulating film to 50 μm in diameter and was then coated with single-wall carbon nanotube (SWCNT) and multi-wall carbon nanotube (MWCNT) of bamboo-type or HC-type by electroplating. On the other hand, the paste electrode was fabricated by filling it with mixed carbon nanotube dispersion. Using these carbon nanotube microelectrode array chip and paste electrodes, we successfully detected their response to (10nM) of dopamine, acetylcholine, and serotonin. These results suggest that the microelectrode array chip have the potential for real-time recordings of neurotransmitters.

3PS020 心毒性検査での細胞外電位記録における心筋細胞拍動周期制御のための電気刺激方法の最適化

Optimization of electrical stimulation protocol for cardiac beat control with extracellular potential measurement in cardiotoxicity test

Tomoyuki Kaneko, Fumimasa Nomura, Tomoyo Hamada, Kenji Yasuda (*Dept. Biomed. Inform., IBB, TMDU*)

The QT prolongation in electrocardiogram is recognized as a potential risk associated with the use for cardiotoxicity testing. Recently, cardiomyocytes derived from human embryonic stem cell (hESC) have been applied for in vitro cardiotoxicity testing, in which QT prolongation risk is estimated by the prolongation of drug-induced change of the field potential duration (FPD) in on-chip extracellular potential measurement assay. As this *in vitro* assay usually uses unstable spontaneous beating cardiomyocytes, the precise beat-to-beat correction procedure of *in vivo* QT_c measurement was not applied for this unstable FPD data. To overcome this problem, we have examined the effective electrical stimulation protocols for cardiomyocyte beating interval control with smallest influence to continuous extracellular potential measurement. First, by applying the simple bipolar stimulation with same amplitude of positive and negative voltages, the artifacts in electrical stimulation were too large and long to record the extracellular field potentials of cardiomyocytes after each stimulation. In contrast, the sequential short rectangular pulses with the balanced positive and negative pulses caused to record the sharp negative artifact only, which was little and short influence to measure the FPD of cardiomyocytes. The results indicate that the balanced applied voltages and pulse numbers are desirable to minimize the artifacts and to respond the hESC-derived cardiomyocyte clusters by electrical stimulation with extracellular potential measurement.

3PS021 イオン移動ボルタンメトリーに基づく微量ペプチドの物質量決定

Determination of mole number for trace amount of a peptide based on the ion transfer voltammetry

Yumi Yoshida, Yoshiro Morita, Shotaro Nakamura, Junya Uchida, Kohji Maeda (*Department of Chemistry and Materials Technology, Kyoto Institute of Technology*)

Most of quantitative analytical methods require a calibration curve made of the reference material of analyte, of which mole number is usually determined by weight measurement. For trace amount of biological compound such as peptides and proteins, its weight is too little to determine its mole number. Usually, these compounds are decomposed into short peptides, amino acids or N element, and these decomposition products are determined using a calibration curve of low molecular substances which is weighable. These procedures are complicate and should be carried out with respect to each compound. In contrast, electrochemical method is the most powerful method to determine mole number without weight measurement, in which mole number is estimated according to Faraday's law. In the present work, we propose mole number determination based on the ion transfer voltammetry, in which an ionic molecule transfer from aqueous sample, W, to organic phase, Org, by applying interfacial potential at the W|Org interface, and the ion transfer is detected as current. Total charge, Q, of current gives mole number, n, of the ionic molecule based on Faraday's low, $n = Q / zF$. Here, z and F are valence of the ionic molecule and Faraday constant. As an ionic molecule, we tried to determine mole number of some short peptides such as Lys-Leu-Val-Phe-Phe.

3PS022 リング状微小電極上の心筋細胞の環状細胞ネットワークを用いた心毒性検査技術

On-chip quasi-in vivo cardiac toxicity assay using ring-shaped closed circuit microelectrode with lined-up cardiomyocyte network

Fumimasa Nomura, Tomoyuki Kaneko, Tomoyo Hamada, Kenji Yasuda (*Inst. of Biomaterials & Bioengineering, Tokyo Medical & Dental Univ.*)

Re-entry of excitation in heart is one of the abnormal phenomena to cause the lethal arrhythmia and is thought to be induced by the looped structure of excitation conduction pathway. For adaptable preclinical strategies to evaluate global cardiac safety, an on-chip quasi-in vivo cardiac toxicity assay for lethal arrhythmia measurement using ring-shaped closed circuit microelectrode chip has been developed. The ventricular electrocardiogram (ECG) -like field potential data, which includes both the repolarization and the conductance abnormality, was acquired from the self-convolutied extracellular field potentials (FPs) of a lined-up mouse embryonic cardiomyocyte network on a circle-shaped microelectrode in an agarose microchamber. When E4031 (hERG blocker, positive control) and Astemizole (false-negative drug in vitro assay) applied to the closed-loop cardiomyocyte network, self-convoluted FP profile of normal beating changed into an early afterdepolarization (EAD) like waveform, and then showed ventricular tachyarrhythmias and ventricular fibrilations (VT/Vf). QT-prolongation-like self-convoluted FP duration prolongation and its fluctuation increase ware also observed according to the increase of Astemizole concentration. The results indicate that the convoluted FPs of the quasi-in vivo cell network assay includes both of the repolarization data and the conductance abnormality of cardiomyocyte networks has the strong potential to prediction lethal arrhythmia.

3PS023 細胞外電位解析と光学イメージング解析を組み合わせた心機能計測解析システムの開発

Development of Dual Recording Assay for Cardiac Function Measurement using Electrical Field Potential and Optical Image Analysis

Toru Shoji, Tomoyuki Kaneko, Fumimasa Nomura, Akihiro Hattori, Kenji Yasuda (*BMI, IBB, TMDU*)

In drug assessment of cardiac safety, development of mechanophysiological effects on cardiomyocytes caused by false positive/negative compounds has becoming more important to acquire more precise prediction of cardiotoxicity. For the evaluation of correlation between mechanophysiological effects and electrophysiological effects against drugs, we have developed a dual

measurement system that records the extracellular field potentials and the contractile motions in lined-up cardiomyocyte network simultaneously. Cardiomyocytes were isolated from embryonic mouse heart by collagenase treatment and seeded in rectangular microchambers fabricated on the multi electrode array (MEA) chip for field potential recordings. To detect contractility of cardiomyocytes, the cells were labeled with the fluorescent polystyrene beads and the motions of beads were treated with image-based analysis. Hence, electrophysiological properties (interspike intervals and field potential durations) and mechanophysiological properties (displacements and velocities of beads) were obtained simultaneously. In the presence of verapamil, typical L-type calcium channel blocker, beating rate decreased companying with shortening of field potential duration (FPD) and its fluctuation increase, and contractility was weakened significantly with its fluctuation increase. The results indicate that the fluctuation of force generation should also become a biomarker of cardiotoxicity risk more correctly in drug development, also might be used for the clarification of mechanisms.

3PS024 白色 X 線源を用いた X 線 1 分子計測法の開発

Development of Diffracted X-ray Tracking measurement system using various wide-band energy X-ray sources

Kouhei Ichiyanagi[1,2], Hiroshi Sekiguichi[2,3], Masato Hoshino[3], Kentaro Kajiwara[3], Shunsuke Nozawa[4], Tokushi Sato[4], Shin-ichi Adachi[4], Naoto Yagi[3], Yuji Sasaki[1,2] ([1]*Graduate School of Frontier Sciences*, [2]*JST CREST Sasaki team*, [3]*Japan Synchrotron Radiation Research Institute*, [4]*High energy acceralation research organization*)

Diffracted X-ray tracking (DXT) enable to measure milliradian resolved rotating and tilting motion of single protein molecules using high-brilliant and wide-band energy X-ray source. The tilting (θ) and rotating (χ) angle resolution and temporal resolution in this measurement are 0.9 mrad, 6 mrad and from 5 μs/frame to 36 ms/frame corresponding to the photon flux. Tracking the diffraction spot from gold nanocrystals attached functional group with protein was developed for revealing the detailed fluctuation and functionalized motions in protein reaction processes at the beamline BL28B2, and BL40XU at the SPring-8 and NW14A at the PF-AR, KEK. (1) We installed the X-ray toroidal mirror at the beamline BL28B2 because the wide-angle diffraction spot tracking of gold nanocrystal markers in the measurement range $\Delta\theta = 7.4°$ can be observed in this beamline. (2) The undulator beamline BL40XU (the measurement range, $\Delta\theta = 4.2°$) allows high speed DXT in microsecond time region using the CMOS CCD camera. (3)New DXT measurement system which was synchronized with pulse laser system (Nd: YAG laser, pulse-width 10 ns, 10 Hz, UV-Vis) has succeeded to observe the open-close motion of membrane protein in reaction process at the beamline NW14A (measurement range, $\Delta\theta = 2.1°$). Thus, the biological science applications of DXT can high profit from observation of the in-vivo functionalized motions of single protein molecules. Here, we will present the development of DXT measurement system and the future plan.

3PS025 CT 撮影用投影型 X 線顕微鏡の開発

Development of Projection X-ray Microscope for Micro-Tomography

Hideyuki Yoshimura (*Meiji Univ.*)

The projection X-ray microscope makes use of a very small X-ray light source excited by the focused electron beam on a thin metal target. If an object is placed just below the metal target, the expanding X-rays enlarge the shadow of the object with infinite focal depth. We have developed the microscope by modifying a scanning electron microscope (SEM) and achieved a resolution about 0.1 &mum. It is advantageous to investigate an opaque sample with better resolution than an optical microscope. And also has additional benefit to investigate three-dimensional structure of the thick specimen which can not studied by an electron microscopy. Taking these advantages, we have applied projection X-ray microscope for three-dimensional (3-D) structure analysis by means of cone-beam computed tomography (CT). To get higher resolution and better contrast, the choice of the metal target is important. The size of X-ray source determines the resolution, thus the electron beam should be focused as small as possible by condenser lens of SEM. And it should have a good balance to get enough strength of X-ray. The electron beam irradiated at the metal target is scattered in the metal and the scattered area is smaller in heavy metal. To get better contrast the wave length of X-ray should be longer utmost it penetrate the sample. In this case light metal target works better because of longer wavelength of Kα characteristic X-rays. By accounting these conditions we have optimized the metal target for biological specimens.

3PS026 XFEL を用いた 3 次元分子イメージングのための雑音下における 2 次元回折像の類似度自動同定

Automatic similarity identification of 2D diffraction patterns with noisy background for 3D coherent x-ray diffractive imaging

Atsushi Tokuhisa[1], Yasumasa Joti[2], Hidetoshi Kono[3], Nobuhiro Go[1] ([1]*Harima Inst., Riken*, [2]*JASRI*, [3]*KPSI,JAEA*)

We proposed a method for classifying and assembling two-dimensional diffraction patterns to reconstruct the three-dimensional diffraction intensity functions (A. Tokuhisa, et. al., Acta Crystallographica, A68, 366 (2012)).In the classification process, similarity of each pair of patterns is judged based on the correlation of corresponding pixels along the concentric circles When two diffraction patterns are similar to each other, a straight line with high correlations appears from the origin to a certain high scattering-angle region. Theoretically, the integrated value of the correlation value along this line is proportional to the extent of the similarity and can be used as threshold for the classification. This correlation line disappears with increasing scattering-angle due to the quantum noise and the structural irregularity. In our estimation, diffraction images of 10^6orders will be required to construct the 3D structure with 3 Å resolution for a molecule with a radius of 200 Å. In this case, the necessary number of pattern comparisons is ~ 10^{10}order. To achieve such a huge number of comparisons, we have to develop an automatic system. In this meeting, we will report how to deal with such a huge amount of data and our current status of the system.

3PS027 植物細胞の飛行時間型二次イオン質量分析法と多変量スペクトル分離法による評価

Evaluation of plant cells using time-of-flight secondary ion mass spectrometry and multivariate curve resolution

Satoka Aoyagi[1], Noriko Kodani[1], Katsushi Kuroda[2], Kazuhiko Fukushima[3], Isao Kayano[4], Seiichi Mochizuki[4], Akira Yano[1] ([1]*Facul. Life & Environmental Sci., Shimane Univ.*, [2]*Forestry & Forest Products Res. Institute*, [3]*Dept. Biosphere Resources Sci., Nagoya Univ.*, [4]*Dept. Medical Eng., Kawasaki Univ. Medical Welfare*)

Time-of-flight secondary ion mass spectrometry (TOF-SIMS) is one of the most sensitive surface analysis methods providing submicron-scale chemical mapping. It is, however, often difficult to interpret TOF-SIMS spectra of complex samples such as tissues and cells. In this study, multivariate curve resolution (MCR) was employed in order to extract less complex TOF-SIMS spectra from original TOF-SIMS data of plant tissue. As a result, components related to intracellular tissues and cell wall tissues, respectively, were extracted from both samples. By comparing the component of the main sample to that of the reference sample, peaks specific to the main sample were indicated.

3PS028 Shannon エントロピーの可視化による質量顕微鏡データの情報解析

Information analysis by visualizing Shannon entropy using Imaging Mass Spectrometric data

Noritaka Masaki, Mitsutoshi Setou (*Hamamatsu University School of Medicine, Department of Cell Biology and Anatomy*)

Microscopic Imaging Mass Spectrometry (MIMS), which we have developed cooperatively with Shimadzu Corporation and others, enables us to analyze spatial distribution of enormous molecules in the resolution of single cell level. MIMS has demonstrated its successful performance by revealing key molecules and their distribution in various research fields, e.g., medical development, agriculture, and material analysis. On the other hand, ageing and some inflammation are difficult to understand using a few key molecules. Principal component analysis and machine learning are also inadequate to elucidate such phenomena overlaying high-dimensional space. In this study, we try to figure out biological state in the framework of overall behavior of molecules, citing the famous argument by Erwin Schrödinger who first utilized entropy for biology to understand living organisms as system that autonomously maintaining their order against disruption.

In our previous presentation in this biophysical society, we visualized Shannon entropy in mouse brain to quantify *in situ* information held in molecular composition. Entropy image reveals characteristic distribution irrespective to anatomical representation. To confirm and discuss such spatial variation in information entropy, we propose a new data processing that takes advantage of

spatial distribution by binning mass spectrum. This bundle of mass spectrum corresponds to maximum likelihood estimation and entropy image calculated from bundled spectrum shows more distinct pattern than normal entropy image.

3PS029 シャペロニン GroEL フットボール型複合体を介したタンパク質フォールディングの直接観察

Direct observation of protein folding mediated by the football-shaped GroEL-GroES complex

Yodai Takei, Ryo Iizuka, Taro Ueno, Takashi Funatsu (*Grad. Sch. of Pharm. Sci., The Univ. of Tokyo*)

The chaperonin GroEL is an essential molecular chaperone that mediates protein folding together with its cofactor GroES in *Escherichia coli*. It has been commonly believed that GroES binds alternatively to each ring of GroEL, which is composed of two identical rings stacked back to back, during the functional cycle. In other words, an asymmetric GroEL-GroES complex (the bullet-shaped complex) is formed throughout the cycle, whereas a symmetric GroEL-$(GroES)_2$ complex (the football-shaped complex) is not formed. We have recently shown that the football-shaped complex coexists with the bullet-shaped complex during the functional cycle. However, how protein folding proceeds in the football-shaped complex remains poorly understood. Here, we used green fluorescent protein (GFP) as a substrate to visualize the folding in the football-shaped complex by single-molecule fluorescence techniques. First, we directly counted the number of refolded GFP molecules in the football-shaped complex, and showed that GFP can fold in both rings of the complex. Next, we performed the real-time imaging of GFP folding in the football-shaped complex. Remarkably, the folding was a sequential two-step reaction, and the kinetics was in excellent agreement with that in the bullet-shaped complex. These results demonstrate that the same reactions take place in both cavities of the football-shaped complex in the same manner to facilitate protein folding. These findings shed new light on the functional cycle including the football-shaped complex.

3PS030 等方性と偏光変調性の 2 つの全反射型蛍光顕微鏡を組み合わせる

Combining of isotropic TIRFM and polarization-modulation TIRFM

Shoko Fujimura[1], Yuh Hasimoto[1,2], Kengo Adachi[1,3], Rinako Nakayama[1], Tomoko Masaike[1], Takayuki Nishizaka[1] ([1]*Gakushuin Univ.,Dept.Physics*, [2]*Present Dept. Hamamatsu Photonics K.K.*, [3]*Present Dept. Waseda Univ.*)

Two different types of total internal reflection fluorescence microscopy, TIRFM, have been independently developed in our research group. The first one is an isotropic TIRFM, ***iTIRFM*** (Adachi *et al.*, *Cell* 2007), in which the hollow-cone light generated by a diffractive diffuser is parallelized and focused to the back focal plane of the objective. Single flurorephores at the sample plane are almost uniformly excited even when their orientation are randomly distributed, because the incident light comes from all directions and so the resultant evanescent field contains all (*X*, *Y* and *Z*) polarization-components. The second one is a polarization-modulation TIRFM, ***pmTIRFM*** (Nishizaka *et al.*, *Nat. Struct. Mol. Biol.*, 2004; Masaike *et al.*, *Nat. Struct. Mol. Biol.*, 2008), which enables us to detect orientation of single flurorephores in *XY*-plane by analyzing a phase of the oscillation of their intensity.
We here combined these two techniques on the same Nikon microscope equipped with a commercial 'perfect-focus system.' Two different illuminations are switchable in a second by translating two filter cubes, which are located at the different points on the optical axis, with electric motors. This experimental setup allows to characterize single fluorophores quantitatively in terms of intensity, orientation and anisotropy, which uncover the change in local environment of multiple catalytic sites in a single protein molecule, such as F_1-ATPase, by directly visualizing repetitive binding and hydrolysis of 2'-Cy3-EDA-ATP.

3PS031 炎症時におけるヒト単球サイトカイン分泌のライブセルイメージング

Live-cell secretion imaging assay of the inflammatory cytokine from human monocytes

Yoshitaka Shirasaki[1,2], Nanako Shimura[1,3], Nobutake Suzuki[1], Kazushi Izawa[4], Asahi Nakahara[1,2], Mai Yamagishi[1], Yoshie Harada[5], Shuichi Shouji[2], Ryuta Nishikomori[4], Osamu Ohara[1,6] ([1]*RCAI, RIKEN*, [2]*Grad. Sch. Adv. Sci. Eng., Waseda Univ.*, [3]*Grad. Sch. Med. Pharm., Chiba Univ.*, [4]*Grad. Sch. Med., Kyoto Univ.*, [5]*iCeMS, Kyoto Univ.*, [6]*KAZUSA DNA Res. Inst.*)

Inflammatory cytokines play a key role in the initiation of inflammation. However, their secretion dynamics especially at the single cell resolution still remain unclear. For example, IL-1β is a leaderless protein, lacking the signal peptide that typically directs secreted proteins through the classical endoplasmic reticulum-Golgi secretory pathway. Therefore the mechanisms of cellular release into the extracellular environment remain the subject of much investigation. To overcome this, we developed live-cell secretion imaging assay by total internal reflection fluorescence illumination with micro-fabricated well array chip. Here we tried to monitor the release dynamics of LPS activated human monocyte before and after additional ATP stimulation. Forty wells were observed every 1 minute for 4 hours. While little signals of IL-1β could observed before ATP stimulation, the fraction of the IL-1β secreting cells largely increased after ATP stimulation. Moreover they showed strong IL-1β signal and increased in their membrane permeability indicated with SYTOX dead cell staining reagent. This change seems to represent a "Terminal release", which is usually associated with cell death called "pyroptosis". This work thus succeeded in imaging of IL-1β secretion from living cells at a high temporal resolution, which will enable us to investigate acute-phase inflammatory reactions of monocytes at the single-cell level for the first time.

3PS032 大腸菌異物排出タンパク質複合体コンポーネントの細胞内動態解析

Intracellular dynamics of the xenobiotic efflux proteins in *Escherichia coli*

Kentaro Yamamoto[1], Takehiko Inaba[2,4], Yoshiyuki Sowa[2,3], Ikuro Kawagishi[1,2,3] ([1]*Dept. Frontier Biosci., Grad. Sch. Eng., Hosei Univ.*, [2]*Res. Cen. Micro-Nanotech., Hosei Univ.*, [3]*Dept. Frontier Biosci., Fac. Biosci. and Appl. Chem., Hosei Univ.*, [4]*Present: RIKEN Adv. Sci. Inst.*)

The rising occurrence of multidrug-resistant bacteria is a serious worldwide issue. One of the major causes of the multidrug resistance is the elevated expression of an RND-type xenobiotic efflux transporter complex, which consists of three components, the inner membrane transporter, the membrane fusion protein, and the outer membrane channel. Among the five inner membrane transporters of *Escherichia coli*, only AcrB, which forms a complex with the membrane fusion protein AcrA and the outer membrane channel TolC, is constitutively expressed. Interestingly, the other inducible transporters are also coupled to TolC. This raises an interesting question: does a newly synthesized inner membrane transporter replace the pre-existing transporter in complex with TolC or form a ternary complex *de novo*? In this study, we aim at visualization of the construction processes of the efflux protein complex. First, we constructed a strain expressing a chromosome-encoded fusion protein AcrB-GFP. We observed with total internal reflection fluorescence microscopy (TIRFM), most fluorescent foci of AcrB-GFP did not show lateral movement, whereas they were moving incessantly in the absence of TolC. Second, a residue in the extramembrane loop of TolC was replaced by Cys, and the resulting mutant was stained with the thiol-reactive fluorescent reagent to demonstrate co-localization of AcrB-GFP with labeled TolC. These results suggest that AcrB is fixed when it forms a complex with TolC, which penetrate through the peptidoglycan layer.

3PS033 1 分子蛍光イメージングを用いた転写活性化による Arp4 の動態変化の定量解析

Quantitative analysis of changes in molecular dynamics of Arp4 upon transcriptional activation using single-molecule fluorescence imaging

Katsuo Ichinomiya[1], Masahiko Harata[2], Kumiko Sakata-Sogawa[1,3], Makio Tokunaga[1,3] ([1]*Grad. Sch. Biosci. Biotech., Tokyo Inst. Tech.*, [2]*Grad. Sch. Agr. Sci., Tohoku Univ.*, [3]*RCAI, RIKEN*)

Actin-related protein 4 (Arp4) is a component of a chromatin-remodeling complex. Chromatin-remodeling is thought to occur with direct binding of Arp4 to histones, indicating that Arp4 is involved in transcription control. Consequently, molecular dynamics of Arp4 is expected to change in correlation with transcriptional activity. However, the details of relationship between molecular dynamics of Arp4 and transcriptional activity remain unclear. In this study, we performed quantification of molecular dynamics of Arp4 both before and after stimulation with the phorbol ester PMA, as a transcriptional activator. We carried out single-molecule fluorescence imaging of the nucleus of CHO cells expressing TagRFP-T fusion proteins of Arp4 at a low level. The residence time of individual Arp4 molecules, the time from appearance to disappearance of the fluorescence spot, was measured in the images. We found that a residence time after stimulation tends to become shorter than before. It means that transcriptional activation causes dissociation of Arp4-containing chromatin-remodeling complexes from the target sites. In yeast, the number of the

chromatin-remodeling complexes is estimated to be much less than that of the target sites. Upon transcriptional activation, Arp4 needs to cover the increased target sites with the limited number of the molecules. Our result may reflect this molecular mechanism. We will also discuss how Arp4 is involved in transcription with regard to RNA polymerase II.

3PS034 ATP 結合部位変異体 Arp4 βのイメージング解析

Imaging analysis of Arp4β mutants in ATP-binding site

Naomichi Inaba[1,2], Yuma Ito[1,2], Masahiko Harata[3], Makio Tokunaga[1,2], Kumiko Sakata-Sogawa[1,2] ([1]*Grad. Sch. Biosci. Biotech., Tokyo Inst. Tech.*, [2]*RCAI, RIKEN*, [3]*Grad. Sch. Agr. Sci., Tohoku Univ.*)

Actin related proteins (Arps) are evolutionarily and structurally similar with actin, and they have ATP binding activity like actin. Actin and Arp4β are critical components of ATP-dependent chromatin remodeling complex, which regulates the dynamic modification of chromatin architecture. Arp4β found to play a key role as a regulator of the activity. However, the detail of the regulatory mechanism remains unclear.

To clarify whether ATP binding to Arp4β handles the regulation, we planned to analyze dynamics of the Arp4β mutant which have the defect of ATP binding activity. We constructed GFP fusion protein of Arp4β (GFP-Arp4β) and GFP-Arp4 β -G173D by single nucleotide substitution to deprive ATP binding activity. We established CHO cell lines expressing GFP-Arp4β or GFP-Arp4β-G173D at a low level.

When we observed the cells with fluorescence microscopy, wild type Arp4β were localized mainly in the nucleus. In contrast, Arp4β-G173D was scarcely localized in the nucleus, and most of them were localized in the cytoplasm. To check the effect of nuclear export or actin polymerization to this cytoplasmic localization of the mutant protein, we observed the mutant under nuclear export inhibitor (LeptomycinB), or actin polymerization inhibitor (LatrunculinB) existence. However, the localization of the mutant did not change. It is suggested that ATP binding activity may regulate its localization in the nucleus.

3PS035 遺伝的にコードされたカルシウムインジケーターを用いた細胞内カルシウム分布の動態解析

Dynamics of intracellular Ca^{2+} distribution measured by genetically encoded Ca^{2+} indicators

Hirofumi Oyama[1,2], Yuma Ito[1,2], Satoshi Ikeda[1,2], Kumiko Sakata-Sogawa[1,2], Makio Tokunaga[1,2] ([1]*Grad. Sch. Biosci. Biotech., Tokyo Inst. Tech.*, [2]*RCAI, RIKEN*)

Ca^{2+} mediates the signal transduction pathways in cells as a second messenger. By stimulus, the distribution of intracellular Ca^{2+} changes dramatically. After Ca^{2+} is released to the cytoplasm from the endoplasmic reticulum, calcium influx occurs via calcium ion channel on the cell membrane to the cytoplasm. Ca^{2+} is thought to diffuse into nucleus from the cytosol through nuclear pores. Free calcium in the nucleus regulates important functions such as transcription of some genes. There could be some mechanism for precise regulation of Ca^{2+} concentration in the nucleus. Recently genetically encoded Ca^{2+} indicators have been developed. The fusion proteins of the indicator enable us to analyze the local Ca^{2+} concentration. To analyze the Ca^{2+} distribution after stimulation, we constructed fusion proteins of membrane protein or nuclear protein to Ca^{2+} indicator GCaMP3 and established the HeLa cells expressing these Ca^{2+} indicators. Upon stimulation with Histamine, We observed the propagation of Ca^{2+} over the cytoplasm and into the nucleus. We will discuss the difference of Ca^{2+} distribution pattern between in the cytoplasm and the nucleus.

3PS036 大腸菌二成分制御系センサーおよび応答調節因子の蛍光イメージング

Fluorescence imaging of histidine kinases and response regulators of *Escherichia coli*

Daigo Nakamura[1], Yuka Iritani[2], Mitsuyasu Fukushima[2], Akiko Yamakawa[1], Hiroyuki Sawaki[1], Takehio Inaba[3,5], Satomi Banno[4], Ikuro Kawagishi[1,2,3] ([1]*Dept. Frontier Biosci., Grad. Sch. Eng., Hosei Univ.*, [2]*Dept. Frontier Biosci., Fac. Biosci. Appl. Chem., Hosei Univ.*, [3]*Res. Cen. Micro-Nano. Tech., Hosei Univ.*, [4]*Natl. Inst. Infect. Dis.*, [5]*RIKEN Adv. Sci. Inst.*)

Escherichia coli has many two-component regulatory systems (TCS) that respond to specific environmental signals. Each TCS consists of a sensor histidine kinase (HK) and a response regulator (RR), together forming a signal transduction pathway via histidyl-aspartyl phospho-relay. We previously constructed GFP fusions to each HK and classified their localization patterns into six groups. In this study, to explore the physiological significance of localization of HKs, we constructed a series of plasmids encoding mCherry fusions to each RR. Unexpectedly, expression of mCherry fusions to some RRs resulted in occurrence of elongated cells. This appears to be due to overexpression because cell sizes were normal when the expression levels of the relevant RR-mCherry fusions were tightly controlled. Out of 24 RRs tested, mCherry fusions to AtoC that is involved in acetoacetate metabolism and TorR that is involved in regulation of anaerobic respiration showed (polar and/or lateral) dotted patterns of localization. These RR-mCherry fusions appeared to co-localize with the GFP fusions of the cognate HKs (AtoS and TorS, respectively). We next examined the effect of the cognate HKs (AtoS and TorS) on the localization of these RR-mCherry fusions. Localization of AtoC-mCherry was lost when the *atoS* gene was deleted, whereas TorR-mCherry retained its localization pattern in the *torS* deletion background. These results suggest that AtoC (and possibly TorR also) localize to a pole or lateral membrane regions by interacting with its cognate HK.

3PS037 ラマン分光顕微鏡を用いて細胞の分化状態を識別する

Raman microscopy distinguishes the status of differentiating cell

Muneki Yoshida[1], Taro Ichimura[1,2], Chiu Liang-da[3], Katsumasa Fujita[3], Tomonobu Watanabe[1,2,4], Hideaki Fujita[1,2] ([1]*Grad. Sch. FBS, Unive. Osaka*, [2]*QBiC, Riken*, [3]*Grad. Sch. Eng., Unive. Osaka*, [4]*Precursory Research for Embryonic Science and Technology*)

We demonstrate that Raman microscopy distinguishes the status of cell differentiation without any labeling. Raman scattering arises from molecular vibration of sample molecules. When a molecule is exposed to photons, a small fraction of photons are scattered with a different frequency from that of incident photons. The shift of the frequency is equal to the molecular vibration frequency. Spectra of Raman scattering are considered as “molecular fingerprints”, because one can reveal molecular species, structures, and surrounding environment by the shift. We expect that the Raman scattering spectrum of a cell can be considered as “cellular fingerprint”, and that we can distinguish, in particular, the status of cell differentiation without any labeling. In order to prove it, we observed the transition of the status of cells during differentiation by Raman microscopy. We built a confocal slit-scanning microscope with excitation wavelength of 532 nm, and continuously obtained Raman images of ES cells from the beginning of differentiation. In analyzing the spectra of nuclei of the ES cells, we found a significant difference between before and after differentiation. Furthermore, to analyze the spectra quantitatively, we employed principal component analysis. The plot of principal component scores showed the translation of the scores in the principal component hyperspace with progression of the differentiation. We believe this result verifies the applicability of Raman microscopy to monitoring of the transition of cellular status.

3PS038 VSFG 検出赤外超解像顕微鏡を用いた毛髪サンプルの分子構造解析

Molecular structure analysis of the human hair samples by using VSFG detected IR super-resolution microscope

Katsuya Kikuchi[1], **Takaki Sato**[1], Tomoki Tajima[1], Masaaki Fujii[1], Shinobu Nagase[2], Yuuji Hirano[2], Takashi Itou[2], Makoto Sakai[1] ([1]*Tokyo Tech*, [2]*Kao Corp*)

We have developed vibrational sum-frequency generation (VSFG) detected IR super-resolution microscope with a sub-micrometer spatial resolution until now, and have reported the applications to various biological samples such as onion root cell, A549 cultured cell, bio-cellulose, etc. In this study, we applied an IR super-resolution microscope to human hairs. Human hair is a complex biological material consisting of distinct morphological components and is well-known to compose of the medulla, cortex, and cuticle regions from inside to outside. At the cortex area occupying 90% of human hair, keratin protein, which is primary component of human hair, forms a line in the shape of fiber along the longitudinal direction of human hair, and controls physical properties such as flexibility, strength, softness and curliness. To understand the relationship between physical properties and the internal nanostructure, we attempted IR imaging at IR super-resolution in the 6-9 μm mid-IR region.

As a result, we succeeded in obtaining VSFG image in the amide III band at 1250 cm^{-1} with sub-micrometer spatial resolution, and clearly observed strong VSFG signals only from the cortex area. VSFG image seems to be contributed to the IR mapping of the distribution of α-helix structure at the cortex. This is supported by very weak emission from the cuticle and medulla, those do not have an α-helix structure. In the presentation, the internal nanostructure of human hairs will be discussed in detail.

3PS039 希土類材料を用いた膜蛋白質の高感度イメージング

Highly sensitive imaging of cell membrane proteins by using lanthanide materials

Tatsuya Nakamrua[1], Shin Mizukami[1,2], Kazuya Kikuchi[1,2] ([1]*Graduate school of Engineering, Osaka University*, [2]*Immunology Frontier Research Center, Osaka University*)

Since cell membrane proteins play important roles for membrane transport and signaling, it is important to analyze functions of cell membrane proteins. So far, fluorescent proteins have been utilized to study the protein behaviors. On the other hand, protein labeling technique with organic dyes and protein tags has been focused because it yields temporal labeling and excellent fluorescent properties. Our group developed protein labeling system based on a mutant β-lactamase (BL-tag), which specifically forms covalent binding with β-lactam compounds. We have developed the fluorogenic probes, which consist of organic fluorescent dyes and β-lactam compound.
In this study, we further developed new probes that utilize luminescent lanthanide complex with silica nanoparticles to achieve higher measurement sensitivity. Luminescent lanthanide complexes show long lifetime luminescence that reaches millisecond order. Since fluorescence lifetime of organic dyes is of the order of nanoseconds, luminescent lanthanide complexes enable time-resolved fluorescence measurement to eliminate short-lifetime fluorescence such as autofluorescence from biological samples. Silica nanoparticles are biocompatible materials and can include a large number of dyes. By combining lanthanide complex with silica nanoparticles, we developed highly luminescent lanthanide silica nanoparticles. Additionally, we attempted labeling of BL-tag expressed on cell surface.

3PS040 ストレス顆粒内 mRNA 微小構造体の超解像イメージング

Super-resolution imaging of mRNA nano-structures in stress granule

Ko Sugawara, Kohki Okabe, Akihiko Sakamoto, Takashi Funatsu (*Grad. Sch. Pha. Sci., Univ. Tokyo*)

mRNAs play critical roles in gene expression with various regulations. Under stress, cytoplasmic mRNAs assemble and form stress granules (SGs), where they are remodeled for repression of translation. However, the mechanisms of action remain elusive. The aim of this study was to visualize the fine structure of SGs and to investigate the detailed physiological role of them. Stochastic optical reconstruction microscopy (STORM) provided us super-resolution images with spatial resolution of ~20 nm in the lateral direction and of ~60 nm in the axial direction. Three-dimensional super-resolution imaging was performed using cylindrical lens. To visualize endogenous cytoplasmic mRNAs, we have microinjected Cy5-labeled linear antisense 2'-*O*-methyl probes into the cytoplasm of COS7 cells. After the injection, cellular stress was induced by addition of 0.5 mM arsenite in a culture medium. To examine the maturation of SGs, STORM images were captured at various time-points during SG formation. Three-dimensional super-resolution images showed that endogenous mRNAs located in spherical compartments with a diameter of 200 nm, which could not be observed in diffraction-limited imaging. We termed this structure "mini-granule". With stress duration, mini-granules increased in number, while they maintained the same size. The results demonstrated that the growing process of SGs was resulted from the assembly of mini-granules. The result of this study indicated that mini-granules were responsible for the physiological functions of SGs.

3PS041 位相変調型微分干渉顕微鏡を用いたミトコンドリアのイメージング解析

The imaging analysis of mitochondria with retardation mediated differential interference microscope (RM-DIC)

Keisuke Haseda, Keita Kanematsu, Yoshihiro Ohta (*Div. Biotechnology and Life sciences , Tokyo University of Agriculture and Technology*)

Mitochondria produce ATP by utilizing the membrane potentials. In this study, we measured the mitochondrial internal density with RM-DIC and examined the influence of the internal density on mitochondrial membrane potentials (MMP). Both the internal densities and the MMPs are heterogeneous in a single cell. Though it is considered that increase in the internal densities affects the MMPs through the concentration of proton pumps, the correlation between them remains to be clarified. To examine the effects of the mitochondrial internal densities on the MMPs, we have improved RM-DIC and examined each mitochondrion in terms of the optical length and TMRE fluorescence as measures of the internal density and MMP, respectively. To eliminate the effects of the mitochondrial size on the optical length and TMRE fluorescence intensity, we corrected these values with the mitochondrial sizes obtained from transmittance images of individual mitochondria. When we measured isolated mitochondria, the corrected optical length showed a close correlation with the corrected TMRE fluorescence. These results suggest that the increase in internal densities of mitochondria stimulates mitochondrial activity. Next we examined mitochondria in neurites but we did not observe the correlation between the internal density and the activity. These results indicate that the surrounding environments of mitochondria are more important for the mitochondrial activity than the internal density.

3PS042 ^{19}F MRI monitoring of Gene Expression in living cells

Hisashi Matsushita[1], Shin Mizukami[1,2], Yuki Mori[2,3], Fuminori Sugihara[1,2], Masahiro Shirakawa[4], Yoshichika Yoshioka[2,3], Kazuya Kikuchi[1,2] ([1]*Grad. Sch. Eng., Univ. Osaka*, [2]*Immunology Frontier Research Center, Univ. Osaka*, [3]*Grad. Sch. Frontier Biosci., Univ. Osaka*, [4]*Grad. Sch. Eng., Univ. Kyoto*)

It is highly significant to accurately determine spatiotemporal expression patterns of each gene in vivo for the establishment of new medical treatments, development of diagnostic methods, and discovery of pharmaceuticals. The development of ^{19}F MRI probes as a powerful in vivo imaging tool for monitoring biological phenomena has attracted increasing attention, since ^{19}F MRI has many advantages such as no detectable intrinsic MRI signals in biological samples and the relatively high sensitivity, which corresponds to 83% of ^{1}H sensitivity.
Recently, we successfully developed off/on switching ^{19}F MRI probes to detect enzyme activities on the basis of the paramagnetic relaxation enhancement (PRE) effect. In the previous study, we detected β-galactosidase activity as a reporter enzyme for gene expression in the cytosol using a specific ^{19}F MRI probe. However, the cells required fixation to image intracellularly expressed β-gal activity, because the probe molecules were not permeable through the intact plasma membrane. For the in vivo applications, it is necessary to detect gene expression in living cells. In this report, we describe a novel method for monitoring gene expression in living cells by measuring extracellularly expressed enzyme activity by ^{19}F MRI. We constructed a new imaging system by exploiting β-lactamase displayed on the plasma membrane as a reporter enzyme, a ^{19}F MRI probe was rationally developed to monitor β-lac activity.

3PS043 Development of nanocapsule probes for sensitive ^{19}F MRI

Hiroaki Mukai[1], Shin Mizukami[1,2], Yosuke Nakanishi[1], Fuminori Sugihara[2], Kazuya Kikuchi[1,2] ([1]*Grad. Sch. Engin., Osaka univUniv.*, [2]*iFReC*)

MRI is suitable for in vivo imaging because it can non-invasively visualize the living body with high spatial and temporal resolution. Thus, recently many smart ^{1}H MRI probes have been reported. However, such ^{1}H MRI signal enhancement needs to be discriminated from the background ^{1}H MRI signals of water, fatty acids, and other biomolecules. To avoid the limitation, we have focused on the use of ^{19}F MRI. Since almost no intrinsic ^{19}F MRI signals are observed in animal bodies, a high signal-to-noise ratio measurement of extrinsic ^{19} F-containing compounds could be achieved. Thus, we have developed the ^{19}F MRI probes to detect protease activity on the basis of PRE effect. [1)] However, further improvement of the sensitivity is still required for practical usage. Thus, we developed nanoparticles (NPs) containing perfluorocarbon as highly sensitive ^{19}F MRI contrast agents.
When the nanoparticles were injected into live animals, the ^{19}F NMR signals were clearly detectable and accumulation was observed in the liver after 1 day. Protein-tag ligands were modified on the surface of NPs, then specific cellular labeling was achieved. In summary, we developed a highly sensitive ^{19}F MRI nanoparticle that can be visualized in vivo, and this novel material would lead to novel molecular imaging method using ^{19}F MRI.
1) *J. Am. Chem. Soc*., **2008**, *130*, 794-795

3PS044 hiPSCs 細胞培養のための polydimethylsiloxane への細胞外基質コート

ECM coating on polydimethylsiloxane for hiPSCs culture

Ryosuke Yoshimitsu[1], Koji Hattori[2], Shinji Sugiura[2], Toshiyuki Kanamori[2], Kiyoshi Ohonuma[1] ([1]*Nagaoka University of Technology*, [2]*National Institute of Advanced Industrial Science and Technology*)

Human induced pluripotent stem cells (hiPSCs), which can be cultured in monolayers under a feeder- and serum-free condition, provide a good model for studying cell differentiation by imaging. However, cell differentiation on a conventional culture dish faces problems such as spatio-temporal unevenness of medium components caused by autocrine and paracrine factors and by intermittent medium change. To address such problems, we have developed a perfusion culture microchamber array chip that enables the control of culture conditions. Most previously reported microchips have been made of polydimethylsiloxane (PDMS). However, only limited cell types are cultivable on PDMS without extracellular matrix (ECM) coating. Here, we show that ECM coating (fibronectin, laminin, collagen, and gelatin) is determined by the adhesion, growth, and differentiation of hiPSCs on the PDMS surface under a feeder- and serum-free condition. The number of adhered cells and the growth rate of hiPSCs that were cultured on the PDMS surface coated with fibronectin and laminin were larger than that on the surface coated with collagen and gelatin. Flow cytometry analysis revealed that undifferentiated marker positive cells on the PDMS surface coated with fibronectin and laminin were larger than on the one coated with collagen and gelatin. These results suggest that the optimal ECM for culturing hiPSCs on a PDMS surface is fibronectin and laminin. This study enables the establishment of differentiation process imaging systems using hiPSCs on perfusion culture chips.

3PS045 Perfusion device to observe of single ES cells

Shougo Nakamura[1], Atushi Maruyama[4], Yuichi Wakamoto[2], Shin-ichi Sakai[3], Bayar Hexig[3], Toshihiro Akaike[3], Kiyoshhi Ohnuma[4] ([1]*Nagaoka university of Technology*, [2]*Grad. Sch. Arts. & Sci., Univ. Tokyo*, [3]*Grad. Sch. Biosci. & Biotech., Tokyo Inst of Tech*, [4]*TRI, Nagaoka Univ of Tech*)

ES and iPS cells characterized by both pluripotency and self-renewal are a promising source of regenerative medicine, as well as a good model for studying cell transition to multiple states. It is believed that cell population differentiation is a result of individual cell differentiated sub-population. To determine which hypothesis is more reasonable, we developed a single cell observation system, which we reported at the previous meeting. The system consists of three elements: GFP reporter mouse ES cells used to monitor the differentiation state, serum- and feeder-free culture conditions, and an E-Cad-Fc coated plate that enables us to dissociate cells into single cells. However, the number of data acquired is very small, because cells at seeding were heterogeneous in their state, and many cells were lost during the medium change. In this study, we developed a perfusion device for observing a single-cell reaction to medium stimulation to improve data acquisition efficiency. This device has two functions: to change the culture medium automatically by using a perfusion-culture system, and to seed the cells directly in the device using a cell sorter. This device may enable us to elucidate mechanisms of cell transtion to multiple states.

3PS046 アルギン酸シートを用いた初代培養細胞セルソーティング法の開発

A Non-destructive Culturing and Cell Sorting Method for Cardiomyocytes and Neurons Using an Alginate Layer

Hideyuki Terazono[1], Hyonchol Kim[1], Akihiro Hattori[2], Fumimasa Nomura[2], Tomoyuki Kaneko[2], Kenji Yasuda[1,2] ([1]*Yasuda "On-chip cellomics" project, KAST*, [2]*Biomed. Info., Biosys., Biomat. Bioeng., Tokyo Medical and Dental Univ.*)

It is proposed that a non-destructive collecting method of cultured cells after identifying their functional characteristics. Embryonic stem (ES) or induced Pluripotent stem (iPS) cells are widely expected to be used in clinical therapeutics for transplantation or as drug screening tools. For each passaging and collecting of cells, cultured cells are usually detached from the culture dish using collagenase or trypsin, which degrades the extracellular matrix or proteins. These methods are harmful to cells, so that fragile cells cannot be recultured. Alginate is a useful polymer for use as a culturing scaffold, because it is non-perturbing to cells. In our method, cells are cultivated on a thin alginate layer in a culture dish and released by spot application of a calcium chelate buffer that locally melts the alginate layer and allows collection of cultured cells at the single-cell level. Primary hippocampal neurons, beating human embryonic stem (hES) cell-derived cardiomyocytes, and beating hES cell-derived cardiomyocyte clusters cultivated on an alginate layer were successfully released and collected with a micropipette. The collected cells were recultured while maintaining their physiological function, including beating, and elongated neurites. The results suggest that this method may allow to sort cells that physiological properties are aligned, and eventually facilitate transplantation of matured ES- or iPS-derived cardiomyocytes and neurons differentiated in culture.

3PS047 様々な粒径の超常磁性ヤヌス微粒子の作製と非侵襲的細胞回収技術への応用

Fabrication of Superparamagnetic Janus Particles Having Various Sizes and Its Application for Non-Destructive Cell Sorting

Hyonchol Kim[1], Hideyuki Terazono[1], Hiroyuki Takei[1,2], Kenji Yasuda[1,3] ([1]*KAST*, [2]*Facul. Life Sci., Toyo Univ.*, [3]*Inst. Biomat. Bioeng., Tokyo Med. Dent. Univ.*)

Janus particles, which are composed of two chemically distinct hemispheres, are used for sensors, new devices, or for a model to study self-assembly physics. Fabrication of various Janus particles is therefore fundamental, and we propose a method for fabrication of superparamagnetic Janus particles and its application for target cell sorting without serious damages. Janus particles were fabricated using polystyrene spheres as casts. The sphere was placed on a substrate, and magnetic materials were deposited on the sphere by thermal evaporation. In addition, thin Au layer, typically 2 to 5 nm thick, was formed on the particle for easy immobilization of biomolecules. Janus particles whose half was composed of deposited metal and the other was polystyrene were then fabricated. By using this method, we fabricated superparamagnetic Janus particles with strict control of magnetic material thickness. One advantage of our method is easy fabrication of particles having various sizes using different polystyrene casts, which achieve particle size-dependent collection of target molecules. For a practical application of fabricated magnetic particles, a DNA aptamer was immobilized onto the particle to use it for specific cell sorting. The particle was reacted with cells and collected using magnet, then its target cell can be specifically collected. Moreover, the magnetic probe can be easily detached from the cell with nuclease treatment. These results indicate that fabricated magnetic particles can be used for non-destructive cell sorting.

3PS048 一細胞時系列解析を用いた定量的プロモータ活性評価法の開発

Event driven time lapse image analysis reveal the promoter activity

Kazumi Hakamada, Yusaku Somei, Jun Miyake (*Osaka University*)

Modeling and understanding cellular dynamics is the holy grail of biology. Many researchers addressed to this target and developed a lot of methods. It is still difficult to elucidate cellular dynamics quantitatively due to cellular heterogeneity. Here, using time lapse images of both phase-contrast and fluorescent images of single cell image analysis, we investigate the promoter activity. HeLa cells were transfected with AcGFP, which encodes AcGFP under the control of promoter of CMV, EF1-α, and SV40 by NanoJuice, respectively. After transfection of them, phase-contrast image and fluorescent images of cells in each well were recorded at interval of ten min for 24h by using Programmable Cellular image Tracer. By recording the timing of cell division by using phase contrast image and that of onset of fluorescent by using fluorescent image, we calculate the difference between cell division and onset of gene expression about three promoters. The fluorescent intensity was observed in order of CMV (248.5 min), EF1-α (461.3 min), SV40 (339.4 min), respectively and time periods between cell division and onset of three promoters had statistically significance ($p < 1.8 \times 10\text{-}20$, welch's t-test). Because these three vectors have the same genes (AcGFP) and they were expected to have the same translation period, those differences suggested the differences of promoter activities. By using single cell time lapse image analysis, we can quantitatively compare the promoter activity.

3PS049 画像認識型オンチップ・セルソーターによる形状認識に基づいた細胞分離法の定量的評価

Quantitative evaluation of cell separation method based on shape recognition using on-chip imaging cell sorter

Akihiro Hattori[1,2], Tomoyuki Kaneko[1], Fumimasa Nomura[1], Kenji Yasuda[1,2] ([1]*Dept. Biomedical Information, Div. Biosystems, Inst. Biomaterials and Bioengineering, Tokyo Medical ana Dental Univ.*, [2]*Yasuda "On-chip Cellomics" Project, Kanagawa Academy of Science and Technology*)

We have evaluated the method for the label-free optical microscopic image-based separation of cardiomyocytes from the mixture of collagenase-digested embryonic mouse heart cells using the on-chip imaging cell sorter system, in which real-time high-speed camera-based phase-contrast cell image recognition was performed. To separate the cardiomyocytes from other cells including

fibroblasts, we distinguished the roughness of the cell surface quantitatively as the index of sorting. The selected cells with smooth surface (roughness index not more than 1.1) for cardiomyocytes, and confirmed that the more than 80% of the collected and recultivated cells were self-beating and the 99.2% of them were identified as cardiomyocytes by immunostaining. The results indicates the potential of the label-free cell purification using imaging cell sorting system, especially for cardiomyocytes by the index of their cell surface roughness, which might be applicable for purification of cariomyocytes for regenerative medicine.

3PS050 マイクロ波照射下での微生物培養とプロテオーム解析

Microorganism cultivation under microwave irradiation and its proteomic analysis

Wataru Nagayoshi[1], Rintaro Hoshino[1], Yuki Kurita[1], Arata Shiraishi[1], Takeo Yoshimura[2], Toru Kodama[3], **Shokichi Ohuchi**[1] ([1]*Dept. Biosci. Bioinform., Kyushu Inst. Technol.*, [2]*Dept. Appl. Bio. Sci., Tokyo Univ. Sci.*, [3]*Vecell Inc.*)

We have studied to take advantage of the microwave heating to the field of chemical biology and biotechnology. In this study, we applied the microwave irradiation for microorganism cultivation. The bacteria such as Escherichia coli, Flavobacteria, and Bacillus subtilis were cultivated on various temperatures and microwave irradiations. The microwave culture system was composed of multimode microwave apparatus with electrical transformer, thermocouple, and air pump. The microwave apparatus by modified domestic microwave oven could be controlled the temperature by thermocouple at 2.45 GHz frequency. The air bubble was flowed to the culture medium instead of shaking the tube. Escherichia coli JM 109 was cultured at 37 degree C for 12 hours under microwave irradiation in LB and M9 culture media. Conventional culture with bubbling was incubated by water bath at 37 degree C. The culture medium was sampled to measure the optical density (OD660) at each time. A comparison of optical density between conventional and microwave cultivation showed that optical density remained unchanged. On the other hand, the expressed protein from cells of E. coli JM 109 was estimated by two-dimensional electrophoresis through the treatment for the proteomic analysis. As the results, several proteins under microwave cultivation were very different from conventional incubation. Their proteins from microwave culture was analyzed and identified by method of peptide mass fingerprint (PMF).

3PS051 PDMS 基盤表面上でのタンパク質混合物の吸着による hiPS 細胞のパターニング

Patterning for human iPS cells by adsorption mixture of proteins on PDMS surface

Ryotaro Yamada[1], Koji Hattori[2], Shinji Sugiura[2], Toshiyuki Kanamori[2], Kiyoshi Ohnuma[1] ([1]*Nagaoka University of Technology*, [2]*Agency of Industrial Science and Technology*)

Human induced pluripotent stem (hiPS) cells derived from human somatic cells have pluripotency, and they are therefore expected to be a suitable model for studying early development. Cell differentiation is affected by cell-cell interaction, which is difficult to control. A micro-patterning technique makes it possible to create cell patterns in order to control cell-cell interaction. However, fabrication of these micro-patterns generally requires a lot of time and labor, as well as expensive reagents and robotics. Here we report a simple micropatterning technique to create patterns of hiPS cells on a poly-dimethylsiloxane (PDMS) surface under a serum- and feeder-free culture condition. PDMS has translucency, gas permeability, low cytotoxicity, and can be molded easily, so it is therefore typically used as a substrate material for fabricating micro structures for cell cultures. We found that cell adhesion patterning was achieved by coating a mixture of proteins, rather than a single purified protein, on a PDMS patterned surface. This suggests the cell adhesion on a PDMS surface is controlled by multiple proteins. We coated the PDMS surfaces with a combination of purified proteins and succeeded in controlling hiPS cell adhesion. We will apply this coating on a PDMS surface treated with patterned plasma. This technique enables simple and low-cost patterning of hiPS cells.

3PT001 飢餓的ストレス下での 100S リボソーム形成による細菌の生存戦略

Survival strategy of bacteria under the starvation stress by 100S ribosome formation

Takayuki Kato[1], Masami Ueta[2], Tomoko Miyata[1], Hideji Yoshida[3], Akira Wada[3], Keiichi Namba[1] ([1]*Grad. Sch. of Frontier Biosci Osaka Univ*, [2]*Yoshida Biol. Lab.*, [3]*Dept. Phys., Osaka Med. Coll.*)

In most bacteria, protein biosynthesis is suppressed by the formation of 100S ribosome, a dimmer of 70S ribosome, under the starvation stress. In the case of gram-negative bacteria, such as Escherichia coli (E. coli), the 100S ribosome is promoted by ribosome modulation factor (RMF) and hibernation promoting factor (HPF) binding to 70S ribosome. On the other hand, a protein named SaHPF, which is a homolog of HPF, causes the formation of 100S ribosome in gram-positive bacteria, such as Staphylococcus aureus (S. aureus). To understand the suppression mechanisms of protein biosynthesis, we tried to analyze both structures by cryoEM image analysis. The numbers of particle images used for the structural analyses of 100S ribosome from E. coli and S. aureus were 11,889 and 15,885, respectively. We treated the images of two 70S ribosome particles individually for 3D image reconstruction, and the structures of 70S ribosome were solved at 18 Å and 15 Å, respectively. Then the atomic model of 70S ribosome was fitted into the 3D density map to build the models of 100S ribosomes. In both cases, 100S ribosome is formed by the face-to-face contacts between the 30S subunits of the two 70S ribosomes. Surprisingly, however, the binding interfaces are completely different between E. coli and S. aureus. We are now trying to determine the binding site and the structure of SaHPF on ribosome. I will discuss different mechanisms of 100S ribosome formation and the structural difference between RMF/HPF and SaHPF responsible for the different mechanisms.

3PT002 ラミノパチー発症に関する A 型ラミンの構造学的研究

Electron microscopy of oligomerization function of nuclear lamin A and the laminopathic mutants

Kazuhiro Mio[1], Toshihiko Sugiki[2], Muneyo Mio[1], Chie Matsuda[1], Yukiko Hayashi[3] ([1]*AIST*, [2]*Dep. Pharm, Musashino Univ.*, [3]*NCNP*)

The nuclear lamins are type V intermediate filament proteins that constitute lamina at the inner nuclear membrane, critically important for the structural properties of the nucleus. Mutations in A-type lamins (LMNA) cause a variety of diseases from muscular dystrophy and lipodystrophy to systemic diseases such as premature aging syndromes. The molecular basis of these diseases is still unknown. To understand the lamin-associated network at the inner nuclear membrane and the mechanisms of laminopathies onset, we analyzed the structures of lamin A ant its mutants using electron microscopy and other structure determining methods. We obtained wild type and mutant lamin A, that include R453W (Emery-Dreifuss muscular dystrophy; EDMD), R527P (EDMD) and R527H (mandibuloacral dysplasia; MAD) from recombinantly expressed E. Coli and analyzed their oligomerization function in terms of head-to-tail filamentous assembly and the paracrystal formation. NMR and biochemical analysis was performed for addressing the association modification of lamin A with LEM family proteins (Lap2, EMD, Man1).

3PT003 NMR 法による APOBEC3C デアミネース活性に関する研究

A study on deaminase activity of APOBEC3C by NMR

Ryo Iwaoka[1], Shingo Kitamura[2,3], Keisuke Kanba[1], Ayako Furukawa[1], Hideyasu Okamura[1], Wataru Sugiura[2,4], Takashi Nagata[1], Yasumasa Iwatani[2,4], Masato Katahira[1] ([1]*Inst. Of Adv. Energy, Kyoto Univ.*, [2]*CRC, NMC*, [3]*Biotech., Grad. Sch. Of Eng., Nagoya Univ.*, [4]*Prog. In Integ. Mol. Med., Grad. Sch. Of Med., Nagoya Univ.*)

APOBEC3 (A3) proteins are responsible for the restriction of exogenous viruses by its cytidine deaminase activity against minus strand DNA produced by reverse transcription of the virus genome. We have been focusing on A3G, a potent restrictor against HIV-1, and been analyzing its deaminase activity. Recently, we started analyzing cytidine deamination by A3C, another antiviral protein, which has different target with A3G. A3G prefers 5'-CCC-3' context on viral minus strand DNA, while A3C primarily recognizes 5'-TC-3' context. Detailed knowledge on the molecular mechanism of the deaminase activity of A3C together with that of A3G would contribute to better understanding of how A3 family proteins recognize and catalyze the different targets.

In this study, we have applied our established NMR method (EMBO J., 2009) to monitor the time-course of cytidine deamination by A3C. The length of the substrate single-strand DNA (ssDNA) reportedly affects the affinity and activity of A3G. A3G shows similar affinity against 10-mer and longer ssDNAs, however the affinity reduces against shorter ssDNAs. In addition, the activity of A3G is highly influenced by the neighboring nucleotides of the 5'-CCC-3'. Accordingly, we have carefully designed and synthesized two 11-mer ssDNAs, TTTTTCTTTTT and AAAATCAAAAA. Using these substrates, we have chased, respectively, the decreasing and increasing signals of cytidine and uridine with time. The comparison of the deaminase activity between A3C and A3G will be discussed.

3PT004 蛍光相互相関分光法を用いた転写因子-DNA 間相互作用の定量

Determination of dissociation constant between glucocorticoid receptor and DNA using FCCS

Shintaro Mikuni[1], Masataka Kinjo[2] ([1]*Research Center for Cooperative Projects, Graduated School of Medicine, Hokkaido University, Japan*, [2]*Laboratory of Molecular Cell Dynamics, Faculty of Advanced Life Science, Hokkaido University, Japan*)

Glucocorticoid receptor (GR) is a transcriptional factor that controls broad range of physiological gene networks. By stimulation of ligand, not only GR activates gene transcription by association to the specific genomic glucocorticoid response elements (GRE) as a dimer, but also GR represses transcription by association to negative GRE as a monomer in nucleus. Hence, it is important to understand quantitatively association of GR to GRE.

For measurement of affinity between DNA and DNA binding protein, such as a transcriptional factor, the electrophoresis mobility shift assay (EMSA) is well used in vitro. However, in EMSA, their interaction is enhanced by the cage effect of gel matrix. Therefore, it is difficult to discuss about the affinity acquired from EMSA as in living cells, although EMSA is excellent as a method for detecting their interaction.

So, we established the determination of the affinity (dissociation constant, Kd) between GR and DNA contained GRE sequence using fluorescence cross correlation spectroscopy (FCCS). For FCCS measurement, the full length human GR was expressed in insect cells as EGFP fused protein (EGFP-GR) and purified by using combination of His-tag and cation exchange column chromatography. By FCCS measurement of purified EGFP-GR with Alexa647-labeled GRE, the dissociation constant of GR-GRE was estimated as 2.71 μM. Furthermore, we will discuss the differences of affinity of GR to several different sequence of GRE.

3PT005 Quantitative study of Homo-Dimer Glucocorticoid Receptor interaction by using Fluorescence Cross Correlation Spectroscopy in living cell

Manisha Tiwari[1], Shintaro Mikuni[2], Masataka Kinjo[3] ([1]*Graduate School of Life Science, Hokkaido University, Japan*, [2]*Research Center for Cooperative Project, Graduate School of Medicine, Hokkaido University, Japan*, [3]*Faculty of Advanced Life Science, Hokkaido University, Japan*)

The Glucocorticoid Receptor (GR) is a member of a superfamily of ligand inducible transcription factors that control variety of physiological and metabolic processes. Upon ligand binding, GRs translocate from cytoplasm to nucleus, then associate with glucocorticoid response element (GRE) as a dimer. This dimerization involves in regulation of variety of genes; however it is not clear that GR dimerization takes place in cytoplasm or nucleus in living cell. To understand the dimerization mechanism of GR, Fluorescence Cross Correlation Spectroscopy (FCCS) was performed in living U2OS cells transiently expressed mCherry tandem dimer and EGFP fused GR wild type. The positive cross correlation was obtained after addition of Dexamethasone (Dex) which is an agonist for GR. Then, the Kd value of dimerization of GR wild type was estimated as 13.2 μM. Moreover, we measured A458T and C421G mutants which were mutated to disable for dimerization and DNA binding, respectively, for further understanding dimerization of GR. In nucleus after addition of Dex, almost no cross correlation was observed in A458T mutant. On the other hand, positive cross correlation was obtained in C421G mutant as wild type. Then, the Kd value of dimerization of C421G was estimated as 12.3 μM. These results suggest that DNA binding is unnecessary to dimerization for GR, and GR is dimerized before association with GRE. Furthermore, we will discuss the dimerization mechanism in cytoplasm by FCCS measurement of nuclear translocation deficiency mutant.

3PT006 Transcription factor p53 searching dynamics on nucleosomal DNA: Coarse-grained molecular dynamics simulation study

Tsuyoshi Terakawa, Shoji Takada (*Grad. Sch. Sci., Univ. Hyogo*)

Transcription factor p53 has to search its specific binding site on DNA to activate transcription of several proteins that are involved in tumor suppressing process. Two of four major domains of p53 [Core domain (Core) and C-terminal domain (CTD)] are known to bind to DNA non-specifically. The roles and interplay of these two DNA binding domains during the search have been controversial. Furthermore, the searching mechanism on nucleosomal DNA in which histone proteins bind to DNA has been largely unknown. In this work, we performed coarse-grained molecular dynamics simulations of tetrameric full-length p53 on duplex DNA with and without histone proteins to elucidate such searching mechanisms.

First, we conducted coarse-grained simulations of p53 on DNA without histone proteins at various ion concentrations. The result shows that only CTDs keep bound to DNA and the Cores frequently hop on DNA during the search. This is in perfect agreement with a recent single molecule experiment. The result also shows that the sliding via the CTD does not follow the helical pitch of DNA (rotation-uncoupled diffusion mechanism) at physiological ion concentration. This finding indicates that p53 can bypass the obstacles on DNA such as histone proteins.

Second, in order to get insight into how p53 bypasses the histone proteins, we conducted coarse-grained simulations of p53 on DNA with histone proteins. The result indicates the importance of rotation-uncoupled diffusion mechanism to bypass the obstacles on DNA.

3PT007 粗視化分子シミュレーションを用いた T4 sliding clamp の DNA 上での動きの解析

Movement of T4 sliding clamp on DNA studied by coarse-grained molecular simulations

Itaru Narihara, Tsuyoshi Terakawa, Hiroo Kenzaki, Shoji Takada (*Biophy, Grad Sch Sci, Kyoto Univ*)

DNA sliding clamp proteins increase enzymatic processivity of DNA polymerases during DNA synthesis. DNA sliding clamp also play a key role in controlling several reactions, such as DNA repair, translesion DNA synthesis, DNA methylation and chromatin remodeling, through the coordination and organisation of different proteins. DNA sliding clamp forms a closed circle around double stranded DNA and is able to move along DNA in a random walk, but the molecular nature of this diffusion process along DNA is poorly understood.

Then we studied movement of the DNA T4 sliding clamp (bacteriophage) on double strand DNA at different ion strength by using a coarse-grained molecular dynamics method of CafeMol. We used Clementi's Go model for proteins, de Pablo model for DNA and included electrostatic and excluded volume interactions between DNA and protein. From a series of simulations, we measured the diffusion constant of the DNA T4 sliding clamp, its dependence on the ion strength, coupling between the rotation around DNA and the diffusion. We also analyze the tilt angle toward DNA.

3PT008 分子シミュレーションと電子顕微鏡像を用いて解析された tRNA 転位の自由エネルギー地形

Free-energy landscape of tRNA translocation through ribosome analysed using MD simulations and cryo-EM density maps

Hisashi Ishida, Atsushi Matsumoto (*Quantum Beam Science Directorate, Japan Atomic Energy Agency*)

Ribosome is one of the supra-biomolecules used in the process of translating genetic information for the synthesis of polypeptides. In the course of its synthesis, two tRNA molecules move with mRNA through ribosome. This process, called translocation of tRNAs, is catalyzed by the elongation factor G (EF-G). Recent results from cryo-electron microscopy (cryo-EM) suggest that there are large-scale structural rearrangements of both ribosome and EF-G occur. However, the dynamic mechanism of translocation is unclear at the atomic level. We used all-atom molecular dynamics (MD) simulations including water molecules to direct 70S ribosome complexed with EF-G at the post-translocational state towards the pre-translocational states by fitting 70S ribosome into cryo-EM density maps. Additionally, the simulations were assisted by umbrella sampling simulations, in which biased potentials were imposed on the centers of masses of the protein molecules in the 70S ribosome, to relax the transitional conformations and to construct the free-energy landscape of the translocation. Multistep structural changes, such as a ratchet-like motion between the small and large ribosomal subunits were observed during the translocation. The free-energy landscape shows that there are semi-stable states between two stable states at the pre- and post-translational states. It was shown that a loop of nucleic acids from the small ribosomal subunit, which is located near the P- and E-sites, plays an important role in the translocation of P-tRNA and E-tRNA.

3PT009 粗視化シミュレーションによる単 / 多ヌクレオソーム系の構造ダイナミクス

Mono- and poly-nucleosome structural dynamics by coarse-

grained simulations

Hiroo Kenzaki[1], Shoji Takada[1,2] ([1]*Dept. of Biophysics, Graduate School of Science, Kyoto Univ*, [2]*CREST-JST*)

Nucleosome is a basic unit of chromatin structure in which DNA duplex wraps about 1 and 3/4 times around histone octamer. Poly-nucleosome takes higher order chromatin structure to store the very long genome into compact space. On the other hand, nucleosome is needed to be unstructured dynamically for function; recognized by transcription factor and transcription to mRNA. Recently, many experiments have investigated mono-nucleosome dynamics. Unwrapping of DNA duplex from histone octamer is observed by equilibrium and force unwrapping experiments. We simulate these nucleosome dynamics by using coarse-grained DNA-protein model, in which one amino acid is represented by one bead and one nucleotide is represented by three beads corresponding to phosphate, sugar, and base. Simulation results reproduce partial/full unwrapping of DNA. We also simulate model poly-nucleosome systems to investigate higher-order structure of chromatin.

3PT010 Zero-dipole summation 法を用いた Est1-DNA 複合体の分子動力学シミュレーション

Molecular Dynamics Simulations of Ets1-DNA complexes using Zero-Dipole Summation Method

Takamasa Arakawa[1,2], Masaaki Shiina[3], Kazuhiro Ogata[3], Narutoshi Kamiya[2], Ikuo Fukuda[4], Haruki Nakamura[2] ([1]*Dept. of Biol. Sci., Grad. Sch. of Sci., Osaka Univ.*, [2]*IPR, Osaka Univ.*, [3]*Dept. of Biochem., Yokohama City Univ. Sch. of Med.*, [4]*Riken*)

For understanding the phenomenon of life, it is important to investigate ingenious transcription mechanisms. Ets1 is a transcription factor, which has a highly conserved DNA binding domain, the Ets domain, and functions in various biological important procedures, such as the regulation of developmental processes in response to extracellular signals. The DNA binding activity of Ets1 is in an autoinhibited state enhanced by phosphorylation. This fact clearly suggests that phosphorylation of transcription factors plays a critical role linking signal transduction to transcriptional regulation. Here, we attempted to unravel how phosphorylation affects protein's DNA-binding ability by applying molecular dynamics (MD) simulations in explicit water molecules with small ions using zero-dipole summation method (Fukuda et al., 2011) to several transcription complexes having Ets1. Zero-dipole summation is a novel idea for calculations of long-ranged Coulombic interactions as a kind of truncation methods, and it achieved good accuracy and high parallelization efficiency in several biological systems even with highly charged DNA double-strands. In addition, this method is formally free from the periodicity assumption, and thus we can avoid the relevant artifacts. The effect of phosphorylation for DNA-binding will be discussed based on the results of long MD simulations.

3PT011 分子シミュレーションによる TFIIIA ジンクフィンガーの DNA 上の拡散

Diffusion of TFIIIA zinc fingers along DNA studied by molecular simulations

Yohei Miyoshi, Tsuyoshi Terakawa, Shoji Takada (*Dept Biophysics, Div Biology, Grad School Science, Kyoto University*)

TFIIIA is a transcription factor which recognizes a site-specific sequence of DNA. Generally, transcription factors search on DNA sequence by various diffusion mechanisms. As one of search mechanisms, one-dimensional diffusion along DNA, or sliding, is proposed. Sliding is that a transcription factor moves along DNA sequence by keeping contact with DNA. It has been suggested that one-dimensional diffusion coefficient is independent of ion concentration when a transcription factor slides on DNA. To investigate if this phenomenon is true or not, we performed a series of coarse-grained (CG) simulations. The system of simulations includes one zinc finger motif of TFIIIA and 200-bp DNA. We used Go model for proteins, de Pablo model for double-strand DNA, and electrostatic and excluded-volume interactions for protein-DNA interactions.

According to our simulation, the one-dimensional diffusion coefficient increases when ion concentration increases from 1 mM to about 200 mM. Moreover, the diffusion coefficient is constant when ion concentration is higher than 200 mM. Hence, it is realized that electrostatic interaction between a transcription factor and DNA influences the diffusion coefficient when ion concentration varies from diluted condition to physiological condition. This phenomenon suggests that experimental results often done at dilute solution are not necessarily the same as the results of physiological solution. The same tendency is observed in each of zinc fingers in TFIIIA, and thus this may be applied to other proteins.

3PT101 溶液環境が決定付ける単一 DNA 分子の凝縮速度

How dose Environmental Solution Conditions Determine the Compaction Velocity of Single DNA Molecules?

Ken Hirano[1], Ishido Tomomi[1], Katsuhisa Nakamichi[2], Naoki Ogawa[2], Masatoshi Ichikawa[3], Kenichi Yoshikawa[2] ([1]*Health Res. Inst., AIST*, [2]*Fac. Life Med. Sci., Doshisha Univ.*, [3]*Dep. Phys., Kyoto Univ.*)

Understanding the mechanisms of DNA compaction is becoming increasingly important for gene therapy and nanotechnology. The kinetics of the compaction velocity of single DNA molecules was studied using two non-protein condensation systems, poly (ethylene glycol) (PEG) with Mg2+ as a representative of crowding effect and spermine as a polycationic condensation agent. The compaction velocities of single tandem λ-DNA molecules were measured at various PEG and spermine concentrations with video fluorescent microscopy. Single DNA molecules were observed using a molecular stretching technique under microfluidic flow. The results show that the compaction velocity of a single DNA molecule was proportional to the PEG or spermine concentration to the power of a half. Theoretical considerations indicate that the compaction velocity is related to differences in the free energy of a single DNA molecule between the random coil and compacted states. In the compaction kinetics with PEG, acceleration of the compaction velocity occurred above the overlap concentration while considerable deceleration occurred during the coexistence state of the random coil and the compacted conformation. This study demonstrates quantitative approach to determine the kinetics of DNA compaction by use of environmental conditions as the control parameters. Further study on such kinetics on the change of the higher-order structure in genomic giant DNA molecules would exhibit of biological importance to understand the essential feature of living matter. [Ref] NAR,40(2012)284.

3PT102 新規なフォトクロミック ATP アナログによるキネシン / 微小管系の駆動と光可逆的な運動制御

Driving and Reversible Photo-control of Motility of a Kinesin/Microtubule System by a Novel Photochromic ATP Analogue

Takashi Kamei, Tuyoshi Fukaminato, Nobuyuki Tamaoki (*RIES, Hokkaido Univ.*)

Adenosine triphosphate (ATP) is a biogenic molecule that functions as an energy donor and interacts with various proteins, ATPases. Therefore an ATP analogue having the potential to artificially control the functions of ATPases would be a promising molecule to control various biochemical processes. In this regard, a photo-controllable ATP analogue has the advantage of using an external stimulus, light, with high spatiotemporal resolution.

We designed and synthesized novel nucleotide analogues, ATP-Azos, consist of ATP and photochromic compounds, azobenzene derivatives. It is confirmed with a spectrophotometer that ATP-Azos exhibit *trans*-to-*cis* and reverse *cis*-to-*trans* isomerizations in the azobenzene moieties through alternating irradiation with UV (λ = 365 nm) and visible (λ = 436 nm) lights, respectively.

Kinesin, an ATPase bio-nano-motor moving along a microtubule filament, is allowed to be driven by ATP-Azos without ATP molecules confirmed by an *in vitro* motility assay. Furthermore, in the presence of the ATP-Azo possessing *tert*-butyl group in the azobenzene moiety (ATP-tBuAzo), the gliding velocity (at ≤ 300 μM ATP-tBuAzo condition) and binding manner (1 mM ATP-tBuAzo) of the kinesin-microtubule system in the assay was reversibly photo-controlled by alternate irradiations with UV and visible lights.

We anticipate that ATP-Azos might find wide applicability in nanobio-technology using bio-motors and other ATPases. Furthermore, replacing ATP with other nucleotide might allow related systems to apply to other nucleotidases.

3PT103 ナノメートルサイズの軸で巻くことにより DNA の曲げ弾性を測定

Bending stiffness of double-stranded DNA measured by winding single-molecule on a nanometer-sized reel

Huijuan You, Ryota Iino, Rikiya Watanabe, Hiroyuki Noji (*Department of Applied Chemistry, School of Engineering, The University of Tokyo*)

The bendability of double-stranded DNA (dsDNA) with curvature radius of 2-20 nm is important in many cellular process such as genomic DNA packaging, transcriptional regulation, and also important in fabrication of DNA

nanostructures. Previous measurements were based on the analysis of thermal bending of dsDNA. However, sharp bending to curvature radius of 2-20 nm was rarely occurred thermally. Therefore, methodology that controls the bending curvature of dsDNA is required to explore the micromechanics of sharply bent dsDNA. For mechanically bent dsDNA to nanometer curvatures, we developed a molecular system of a nanometer-sized reel based on F_1-ATPase, a rotary motor protein. By combination with magnetic tweezers and optical tweezers system, single-molecule dsDNA was wound around the molecular reel. The bending stiffness of dsDNA was estimated based on the winding tension (0.9-6.0 pN) and the diameter of the wound loop (21.4-8.5 nm). Our results were in good agreement with the conventional worm-like chain model and were used to estimate a persistence length of 54 ± 9nm. This molecular reel system offers a new platform for single-molecule study of micromechanics of sharply bent DNA molecules and is expected to be applicable to the elucidation of the molecular mechanism of DNA-associating proteins on sharply bent DNA strands.

3PT104 1 分子機械的アンジッピングが示すエントロピー駆動的 DNA 構造安定性の GC と AT 塩基対における違い

GC and AT pairs show different entropic stabilization of DNA structures found in single-molecule mechanical unzipping

Akihiro Fukagawa[1], Michio Hiroshima[2], Makio Tokunaga[1,3] ([1]*Grad. Sch. Biosci. Biotech., Tokyo Inst. Tech.*, [2]*Adv. Sci. Inst. RIKEN*, [3]*RCAI, RIKEN*)

Unzipping of double-stranded DNA is involved in several biological processes. We have performed a quasi-static mechanical unzipping of single-molecule DNA using intermolecular force microscopy, modified atomic force microscopy with high resolution. We obtained force-extension (FE) curves of two oligonucleotides with a stem-loop containing six tandem repeats of a 6-bp sequence. To reduce noise, FE curves of the unzipping region were averaged using correlation analysis. FE curves showed a dependence on the ruptures of single hydrogen bonds.

To reveal the molecular mechanism of stabilization of DNA structures by hydrogen bonds, we have carried out the molecular dynamics (MD) simulations of mechanical unzipping of DNA. Cross-correlation analysis of FE curves showed the force-peaks of single hydrogen bonds more clearly than those by the unzipping experiments. Furthermore, we depicted the two-dimensional (2D) energy landscape, trajectory density map to visualize the behavior of DNA unzipping from MD simulations. Trajectories tended to escape the energetic mountain and took heterogeneous pathways on rugged energy landscape. We calculated entropy from trajectory densities and total energy. The entropy of the AT pair was negatively correlated with the number of hydrogen bonds. In contrast, not the entropy but the total energy of GC pair was correlated with the number of hydrogen bonds. The result suggests that the formation of GC pair is driven by mainly energy and that of AT pair is driven by not only energy but also entropy.

3PT105 Controllable adsorption-desorption of double-stranded DNA onto single-walled carbon nanotube functionalized with polyethylene glycol

Daisuke Nii, Takuya Hayashida, Kazuo Umemura (*Grad. Shc. Sci. univ of science. Tokyo*)

Since the discovery of the hybridization of DNA and the single-walled carbon nanotube (SWNT), various researches have been conducted on the mechanism of the interaction between single-stranded DNA (ssDNA) and SWNTs during the hybrid formation. However, the adsorption mechanism of double-stranded DNA (dsDNA) onto SWNTs has not yet been studied as comprehensively. Further, there are few reports on the detachment of DNA molecules from a DNA-SWNT hybrid, although it may be important to understand the desorption technique of ssDNA from the ssDNA-SWNT hybrids in order to employ the hybridization for medical applications such as biodevices or drug delivery. In this study, we employed an SWNT functionalized with polyethylene glycol (PEG SWNT) for controlling ssDNA adsorption and desorption onto the SWNT. Firstly, we achieved the hybridization of dsDNA and the PEG SWNT in aqueous solution for the first time. Secondly, we succeeded in the detachment of dsDNA from the PEG SWNT by annealing at 95°C; the desorption was not observed in the use of usual SWNT. Atomic force microscopy, electrophoresis, and Raman spectroscopy indicated the occurrence of dsDNA adsorption onto and desorption from the PEG SWNT. Our results demonstrated the potential of controlling the interaction between ssDNA and PEG SWNT in aqueous solutions.

3PT106 分子動力学シミュレーションによる dGMP、8-oxo-dGMP のコンフォメーション比較：イオンの影響

Comparison of dGMP and 8-oxo-dGMP conformation by molecular dynamics simulations: effect of ions

Shin-ichi Fujiwara, Takashi Amisaki (*Fac. Med., Tottori Univ.*)

8-oxo-7, 8-dihydroguanine (8-oxo-G) is produced by the oxidation at C8 position of G and is the most abundant species among bases in DNA modified by oxygen radicals. 8-oxo-G causes transversion as well as transition mutation. Human MutT homologue-1 (hMTH1) hydrolyzes oxidized 8-oxo-dGTP to 8-oxo-dGMP, thereby preventing the misincorporation of oxidized nucleotides during replication. Although the “syn” conformation predominates in 8-oxo-dGTP, the crystal structure of hMTH1 indicates that the protein binds the mononucleotide in the “anti” conformation with no direct interaction between hMTH1 and the 8-oxo position of the oxidized base. It is unclear how the protein structurally distinguishes 8-oxo-dGTP from dGTP. To elucidate the specific interaction of 8-oxo-dGTP by hMTH1 on the basis of mononucleotide conformation, molecular dynamics (MD) simulations were carried out for deprotonated/protonated dGMP and 8-oxo-dGMP in explicit water. The effect of ions on the mononucleotide conformation was specifically examined, by including Li^+, Na^+, Mg^{2+}, or Ca^{2+} in the system. In a series of MD simulations, dGMP took both the stable “anti” and “syn” conformation. Although 8-oxo-dGMP took the stable “syn” conformation in most cases, 8-oxo-dGMP with Mg^{2+} took the stable “anti” conformation as well as the stable “syn” conformation. We will discuss the “anti” conformational stability of 8-oxo-dGMP with ion in detail.

3PT107 粗視化モデル分子動力学法を用いた RNA 立体構造予測

RNA 3D structure prediction by using coarse-grained molecular dynamics simulation

Tomoshi Kameda (*CBRC, AIST*)

During the last two decades, significant developments have showed the importance of RNA in biological functions. To perform their functions, many RNA molecules adopt well defined tertiary structures. Hence, there is an interest in accurate *ab initio* prediction of three-dimensional (3D) structure of RNAs. However, RNA 3D structure prediction is not studied well, compared to protein three dimensional (3D) structure prediction. The one of reasons is that the size of nucleic acid is larger than amino-acid, which needs quite a long time for molecular dynamics (MD) simulation even if we deal with small RNA molecules. Hence, to predict RNA 3D prediction, we developed a simplified, coarse-grained RNA model for molecular dynamics simulation. In our model, one base consists of 3 beads (P; phosphate, S; sugar, B; base). When our model is applied to small RNA (<60bases), it takes only ~5 minutes for the structure prediction using single processor (1 core). The details will be shown in the presentation.

3PT108 分子動力学シミュレーションによる DNA 構造に対する溶媒条件の影響の研究

The influence of solvent condition on DNA structures studied by molecular dynamics simulations

Satoshi Fujii[1], Hidetoshi Kono[2], Akinori Sarai[1] ([1]*Dept. Bioscience and Bioinformatics, Kyushu Institute of Technology*, [2]*Computational Biology, JAEA*)

The conformational properties of DNA play important roles in various biological processes. For example, interactions of proteins with DNA sequences are known to be affected by the conformational properties of DNA. It has also been known that the transitions among various conformational states are induced by the change in environments: Variations in ionic strength and identity, sequence, water activity, and ligand/protein binding all can modulate DNA structure. In this study, we analyzed how the sequence and the environments such as water activity influence the DNA conformations. We have carried out a series of molecular dynamics (MD) simulations to explore the conformational preferences and dynamical behavior of DNA duplex. We prepared the initial structure models with two different sequences in two kinds of conformations; $d(CGCGTATACGCG)_2$ and $d(CGCGTATACGCG)_2$ in B- and A-forms. The MD simulations were carried out in four different environments: in only water solvent and in 75, 85 and 95 % (v/v) ethanol / water mixture solvent. We analyzed the differences of the DNA backbone conformation, the base-pair step parameter and the localization of water

molecules in the groove on each structure. The variability of the conformation was different depending on the solvation condition. The DNA conformation seemed to be influenced by the localization of the water molecules in the groove.

3PT109 Model for self-assembly of flexible DNA motifs using stacking interactions

Keitel Cervantes-Salguero, Shogo Hamada, Satoshi Murata (*Tohoku University*)

Molecular Clusters (MCs) with variable number of constituents seem to be possible if building units are properly designed. Recently, concentration-dependent self-assembly of MCs was demonstrated by utilizing both flexibility of DNA motifs and inter-molecular binding by sticky-ends (He, Y. et al., Nature 2008). Here we propose a cluster of DNA motifs by using DNA blunt-end stacking and flexibility introduced into the motif. First, we study an abstract model of flexible planar monomers (triangle with sticky sides A and B, and shrinkable side C. Angle between A and B is about 60 deg.) that move randomly on a surface colliding against each other. Sides A and B of different monomers can stack, thus forming a flexible dimer. Over time we expect to obtain clusters from dimers up to hexamers. We simulated the dynamics of the cluster formation based on chemical kinetics successfully applied to rigid monomers (Hosokawa, K. et al. Artificial life 1995). Our simulation shows that the amount of trimers overcomes the tetramers. However, contrary to the work of Hosokawa et al., dimers and pentamers seem to be equally formed. Second, to realize the concept, we have designed a DNA motif with blunt-end stacking interactions, which were proved to be a potential tool for self-assembling larger DNA structures (Woo, S. et al., Nature Chemistry 2011).

3PT110 A Growth mechanism of DNA tile array

Yuki Matsubara, Nao Otani, Miho Tagawa, Akira Suyama (*Univ Tokyo, Dept Life Sci*)

We report a growing mechanism of DXAB (DNA double-crossover AB-staggered) tile array known to form planar structures and grow to micro-scale. DXAB tile array is a kind of DNA tile arrays and can work as a scaffold to control positions of nano-particles. Growth mechanisms of the array are important information to set its properties, such as size, accuracy of position control, yield, or the required time of annealing. Here, we report that the growth of array is a co-operative phenomenon in narrow temperature range. This transition width is shorter than a prediction by model based on lengths of the sticky-ends. This has been visualized by fluorescence optical microscope, because, unlike the tiles' assembly, growth of the tile arrays cannot be observed in melting curve. From this knowledge we show two applications, making big isolated sheets and shortening the annealing time in protocol, as examples. These experimental results demonstrate that such knowledge about growth mechanisms is useful to control properties of DNA nanostructures.

3PT111 DNA ナノ構造を用いた DNA-RNA ポリメラーゼ・ハイブリッドナノマシンの構築と機能評価

Construction and functional analysis of DNA origami base DNA-RNAP hybrid nanomachine

Takeya Masubuchi[1], Hisashi Tadakuma[1], Masayuki Endo[2], Hiroshi Sugiyama[2], Yoshie Harada[2], Takuya Ueda[1] ([1]*Graduate School of Frontier Science, The University of Tokyo*, [2]*iCeMS, Kyoto University*)

DNA nanotechnology has recently developed a new nanoscale device called as DNA origami tile (DNA origami). DNA origami is a method for folding long single strand DNA into arbitrary two or three dimensional structures and can be used as a molecular platform which allows proteins and other molecules to place with precisely controlled patterns at nanometer order. Here, we applied DNA origami technology into transcription system. Transcription system is thought to couple to other system in E. coli (e. g. translation and replication). And reconstitution of such sequential reactions in vitro is important for science and engineering, for which the DNA origami technology may provide platform. As a first step, we assembled T7 RNA polymerase (T7-RNAP) on DNA origami. Rectangle DNA origami (90 x 60 nm) are prepared as reported (Rothemund Nature 2006), and SNAP-tag protein fused T7-RNAP (T7-RNAP-SNAP) were site-specifically anchored on DNA origami through its specific ligand (benzylguanine (BG)-ligand) included on the DNA origami. With the optimized assembly condition, we succeeded in measuring the activity of T7 assembled DNA origami (T7-Tile). We will check the effect of the number and the layout of T7-RNAP on the activity of T7-Tile.

3PT112 リポソームへの DNA リングの吸着

Adsorption of DNA ring onto Liposome

Yumiko Kumagai, Shogo Hamada, Shin-ichiro Nomura, Satoshi Murata (*Department of Bioengineering and Robotics, Graduate School of Engineering, Tohoku University, Japan*)

The various molecular devices made of biomolecules such as nucleic acid, protein and lipid are reported. We are now able to design each devices with certain complexity, although it is still difficult to combine multiple devices into one functional system. Embedding various molecular devices within a given-size compartment is one of the potential solutions to solve this problem and enable us to achieve programmed behavior of the system. A key component to realize this concept is a channel device integrated into the compartment, which allows materials pass through the compartment.

Here, we adopt a phospholipid as material for micron-sized compartment, and DNA nanostructure for the channel device embedded on the compartment surface. In the design of the DNA channel, we have been inspired by the macrocyclic resorcin channel, which is an artificial mimic of a natural ion channel. We have adopted the T-motif DNA ring that has a similar structure to this. The surface of the DNA ring is hydrophilic, therefore, has affinity to the lipid membrane surface. In order to integrate the ring into the membrane, hydrophobic groups are attached to the DNA rings. We adopt Cholesteryl-TEG as the hydrophobic groups and confirmed the formation of those DNA rings. We also found that DNA structures tend to rest on the lipid membrane surface by giving positive charge to the lipid. Currently, we are working on the optimization of the lipid composition to give an appropriate charge condition.

3PT113 脂質二重膜上での DNA ナノ構造の基板上成長

Substrate-Assisted Self-Assembly of DNA Nanostructure on lipid bilayer

Shogo Kudo, Shogo Hamada, Shin-ichiro Nomura, Satoshi Murata (*Department of Bioengineering and Robotics, Graduate School of Engineering, Tohoku University, Japan*)

Substrate-Assisted Self-Assembly (SASA) by Hamada *et al*. enables us to make large 2-D DNA nanostructures that are difficult for conventional self-assembly in free solution. So far, limited materials, e.g., cleaved mica, are known for suitable substrate for the method. It is necessary to extend the method to utilize various materials for the substrate. However, the process of SASA is very complex and not yet thoroughly understood.

To model SASA, we divide it into adsorption and self-assembly processes. The adsorption process is described by DLVO theory. Following Sushko, we can calculate energy of DNA adsorption by DLVO. We also measured minimal length of DNA, or equivalently energy per base pair, to be absorbed on mica substrate. In order to extend SASA to other materials, measured absorption energy between DNA and mica surface roughly indicates the feasible condition for SASA. Based on this consideration, we chose lipid bilayer (DOPG) for the substrate, because the calculated energy between 100 base pairs of DNA and the bilayer is enough to absorb when magnesium ion concentration is 12.5 mM. However, we haven' t confirmed DNA adsorption under this condition. Currently, we are working on experiments to search appropriate conditions for SASA.

3PT114 中性膜に結合した LFampinB の膜結合構造と膜親和性の固体 NMR と QCM による解析

Structure and affinity of bovine lactferrampin bind to neutral model membrane as studied by by solid state NMR and QCM

Masayoshi Imachi[1], Javkhlantugs Namsrai[1], Atsushi Kira[2], Izuru Kawamura[1], Akira Naito[1] ([1]*Graduate School of Engineering, Yokohama National University*, [2]*Reasearch and Development Division, ULVAC Inc.*)

Recently antimicrobial peptide is focus attention on a potential alternative for antibiotics. Analysis of membrane bound structure of peptide provides important information on efficiency and side effect of medicine.

Bovine lactoferrampin(LFampinB) is an antimicrobial peptide found in the N1-domain of bovine lactoferrin (268-284) and consists of 17 amino acid residues. Bovine lactoferrin (bLF) is an iron binding glyco protein with innate immunity factor in mammalian secretory fluid for example, tear saliva and milk.

In this study, the structure of LFampinB bound to the neutral membrane was determined using chemical shift oscillation analysis by observing the chemical

shift anisotropy of the carbonyl carbon of Leu4, Ala7, Gly12 amino acid residues. These results indicate that LFampinB forms α-helix in the N-terminal region inserting into the membrane and the α-helical axis rotates rapidly about the bilayer normal with the tilt angle of 12 degree to the axis
The association constant (Ka) of LFampinB with the neutral lipid was determined which was smaller than that with the acidic membrane. The difference of the Ka of LFampinB with neutral and acidic membrane explain the reason why the α-helical structure of LFampinB in neutral membrane is more distorted than that in acidic membrane. This also explain that LFampinB may selectively interact with the acidic bacterial membrane and shows the hemolytic activity to the neutral membrane.

3PT115 大腸菌異物排出タンパク AcrB のペリスタポンプ機構の解明

Structures of the multidrug exporter AcrB reveal a proximal multisite drug-binding pocket

Keisuke Sakurai[1], Ryosuke Nakashima[1], Seiji Yamasaki[1,2], Kunihiko Nishino[1], Akihito Yamaguchi[1,2] ([1]*Institute of Scientific and Industrial Research, Osaka University*, [2]*Graduate school of pharmaceutical sciences, Osaka University*)

AcrB and its homologues are the principal multidrug transporters in Gram-negative bacteria and are important in antibiotic drug tolerance. AcrB is a homotrimer that acts as a tripartite complex with the outer membrane channel TolC and the membrane fusion protein AcrA. Minocycline and doxorubicin have been shown to bind to the phenylalanine cluster region of the binding monomer. Here we report the crystal structures of AcrB bound to the high-molecular-mass drugs rifampicin and erythromycin. These drugs bind to the access monomer, and the binding sites are located in the proximal multisite binding pocket, which is separated from the phenylalanine cluster region (distal pocket) by the Phe-617 loop. Our structures indicate that there are two discrete multisite binding pockets along the intramolecular channel. High-molecular-mass drugs first bind to the proximal pocket in the access state and are then forced into the distal pocket in the binding state by a peristaltic mechanism involving subdomain movements that include a shift of the Phe-617 loop. By contrast, low-molecular-mass drugs, such as minocycline and doxorubicin, travel through the proximal pocket without specific binding and immediately bind to the distal pocket. The presence of two discrete, High-volume multisite binding pockets contributes to the remarkably broad substrate recognition of AcrB.

3PT116 エントロピー力による円筒状容器からの大球の放出

Entropic release of a big sphere from a cylindrical vessel

Hirokazu Mishima[1], Hiraku Oshima[1], Satoshi Yasuda[1], Ken-ichi Amano[2], Masahiro Kinoshita[1] ([1]*Inst. of Adv. Energy, Kyoto Univ.*, [2]*Dept. of Chem., Kobe Univ.*)

Insertion of a large solute into a vessel comprising biopolymers followed by release of the same solute from it is a fundamental function in biological systems. A typical example of such insertion/release processes is found in TolC. TolC is a cylindrical vessel possessing an entrance at one end and an exit at the other end for the solute. In earlier work [1], we showed that the solute-vessel potential of mean force (PMF) formed by the solvent plays imperative roles in the processes. The PMF can be decomposed into its entropic and energetic components denoted by Φ_S and Φ_E, respectively. Φ_S is insensitive to the solute and vessel properties (i.e., solvophobic or solvophilic) whereas Φ_E is largely dependent on them. A significant feature of TolC is that a variety of solutes are inserted into and released from the vessel, which is known as “multidrug efflux”. This feature can be exhibited when Φ_S with the insensitivity mentioned above is dominant. However, our earlier work [1] suggested that Φ_S acts only for the insertion. Here we explore the possibility of releasing the solute by Φ_S. We calculate the PMF between a big sphere and a cylindrical vessel with open ends immersed in small spheres using the three-dimensional integral equation theory [1] combined with rigid-body models. It is shown that the solute inserted through the entrance can entropically be released by a continuous variation of the vessel geometry to squeeze out the solute from the exit.
[1] K. Amano, H. Oshima, and M. Kinoshita, J. Chem. Phys. **135**, 185101 (2011).

3PT117 2 者タンパク質間を認識するライト抗体を利用したバンド 3-グリコフォリン A 複合体の精製

Use of a dual specificity Wright antibody for the purification of structurally unstable band 3-glycophorin A complex

Yohei Ikeda[1], Hinako Hatae[2], Hiroyuki Kuma[2], Naotaka Hamasaki[2], Teruhisa Hirai[1] ([1]*Harima Inst., RIKEN*, [2]*Fac. Pharm. Sci., Nagasaki International Univ.*)

Band 3 (also known as anion exchanger 1 or SLC4A1) and glycophorin A (GPA) are the most abundant membrane proteins in human erythrocyte and both present at ~1 × 106 copies per cell. Biochemical and genetic analyses suggested a close relationship between band 3 and GPA during and after biosynthesis (Auffray et al., Blood 97 pp.2872-2878, 2001, Telen and Chasis, Blood 96 pp. 842-848, 1990). Bruce et al. reported that band 3 and GPA were associated though an interaction residues Glu658 of band 3 and Arg61 of GPA (Bruce et al., Blood 85 pp.541-547, 1995). However, it was difficult to maintain their structure as a complex during purification, because of loose binding. In this study, we purified band 3 and GPA (B3-GPA) complex with Wright monoclonal antibody (or Fab fragment), which recognized Wright blood group antigens. We also characterized the biochemical properties of the complex.
After we confirmed the binding of Wright antibody Fab fragment against the erythrocyte membrane, we solubilized that erythrocyte membrane with C12E8 directly, then C12E8-solubilized membrane were loaded on a size-exclusion column. Elution peak of B3-GPA-Fab complex appeared at a position predicted for a dimeric form together with a small uncharacterized shoulder. Two dimensional polyacrylamide gel electrophoresis (blue native/SDS-PAGE) analysis showed that purified complex contains three subunits. We will discuss the polypeptide composition and stoichiometry of the complex.

3PT118 カルシウム活性化クロライドチャネルの *in vitro* でのイオン透過活性測定系の構築

Functional *in vitro* reconstitution of Calcium-activated Chloride channel, TMEM16A/anoctamin1

Hiroyuki Terashima[1,2], Alessandra Picollo[1], Alessio Accardi[1] ([1]*Department of Anesthesiology, Weill Cornell Medical College*, [2]*Department of Macromolecular Science, Graduate School of Science, Osaka University*)

Calcium-activated chloride channel is widely expressed and involved in various physiological functions, for example, electrolyte secretion in epithelia and grands, contraction of cardiac muscle, olfactory signal transduction and maintain/amplification of membrane potential in nervous system. At 2008, three of independence groups demonstrated TMEM16A/anoctamin1 is a component of calcium-activated chloride channel. TMEM16A protein is thought to have eight transmembrane segments and form at least dimer in vivo from results of chemical cross-linking and native PAGE. Although TMEM16A is activated intracellular calcium, there is no well-known calcium-binding motif (e.g., EF hand) in TMEM16 family protein. Recently, mutation of two other glutamate residues dramatically decreased calcium-sensitivity, implying that two glutamate residues are involved in calcium-binding or activation. We expressed the protein in insect cell and solubilized it by digitonin. The reconstituted liposomes showed chloride-conducting activity. The purified TMEM16A protein was activated at sub-micromolar of calcium concentration and inhibited by well-known chloride channel blocker. Chloride flux activity was changed depending on applied voltage, suggesting that it has voltage-dependency. From these results, we could construct in vitro flux assay system for TMEM16A.

3PT119 COS7 細胞と酵母細胞を用いた筋型 CPT1 の発現系の比較

Comparison of two expression systems using COS7 cells and yeast cells for expression of heart/muscle-type CPT1

Takuya Hada[1,2], Yumiko Kato[1,2], Eriko Obana[1], Naoshi Yamazaki[2], Takenori Yamamoto[1], **Yasuo Shinohara**[1,2] ([1]*Inst Genome Res, Univ Tokushima*, [2]*Fac Pharm Sci, Univ Tokushima*)

Carnitine palmitoyltransferase 1 (CPT1), catalyzing the transfer of the acyl group from acyl-CoA to carnitine to form acylcarnitine, is located at the outer mitochondrial membrane. Because it is easily inactivated by solubilization, expression systems using living cells are essential for its functional characterization. COS7 cells or yeast cells are often utilized for this purpose; however, the advantages/disadvantages of the use of these cells or the question as to how the CPT1 enzyme expressed by these cells differs are still uncertain. In this study, we characterized the heart/muscle-type isozyme of rat CPT1 (CPT1b) expressed by these two cellular expression systems. The mitochondrial fraction prepared from yeast cells expressing CPT1b showed 25% higher CPT1 activity than that obtained from COS7 cells. However, the expression level of CPT1b in the former was 3.8 times lower than that in the latter; and thus, under the present experimental conditions, the specific activity of CPT1b expressed in

yeast cells was estimated to be approximately five times higher than that expressed in COS7 cells. Possible reasons for this difference are discussed.

3PT120 紫膜表面の隆起構造およびバクテリオロドプシン分子構造に与える紫膜中の古細菌型脂質除去の影響

Effects of archaeal lipids removal in purple membrane upon bump structures of membrane surface and bacteriorhodopsin conformations

Kosuke Yamada, **Yasunori Yokoyama**, Shigeki Mitaku (*Department of Applied Physics, Graduate School of Engineering, Nagoya University*)

Purple membrane (PM) is a membrane patch found in cytoplasmic membrane of halophilic archaebacteria. Since PM consists of a two-dimensional crystal of membrane protein bacteriorhodopsin (bR) with some archaeal lipids, it is presumed that surface of PM is uniform planner. However, atomic force microscopy (AFM) observations for PM have revealed a lot of bump structures in the surface, showing that PM surface is not a uniform. The molecular packing of bR and the lipids, including the bump structure formation, should be determined by physicochemical interaction between bR molecules as well as bR and lipids. Our studies against the bump structures of PM have showed a large contribution of electrostatic interaction because bump curvatures were affected by pH and ionic concentrations of medium. In this work, we focus on the lipids in PM because of its highly negatively charged headgroups, and investigate removal effects of the lipids upon bump structures of membrane surface by AFM observations. AFM topography of delipidated PM demonstrated bump structures had larger curvature than those in native PM. A mean curvature was largest at 25 % delipidated PM samples, and decreased with increasing delipidation level. AFM analysis in the presence of KCl with various concentrations showed KCl concentration dependence of the bump curvature of delipidated PM was different from that of native PM. The removal effect of the lipids upon bump structures will be discussed together with theses results as well as delipidation effects on bR conformations.

3PT121 EGF 受容体の活性化機構：EGFR はリガンド結合前に 2 量体として存在する

Molecular mechanism underlying activation of the EGF receptor: preformed, inactive dimer and positive cooperativity

Hiraku Miyagi, Ichiro Maruyama (*OIST*)

Epidermal growth factor receptor (EGFR) is an integral membrane protein that has an extracellular ligand binding domain, a single-path transmembrane domain, and an intracellular kinase domain. The ‘dimerization model’ has widely been believed as a molecular mechanism underlying the activation of EGFR, in which ligand binding induces EGFR dimers from monomers. However, we have recently shown that EGFR and its family proteins exist as a preformed, yet inactive, dimers prior to ligand binding, and have proposed a “rotation/twist model”, in which ligand binding induces rotation/twist of the receptor’ s transmembrane domains. The rotation/twist breaks the inactive dimeric structure, and rearranges the domains to take active forms. To distinguish the two models, we examined the dimeric structure based on FLIM/FRET before ligand binding, and found that EGFR has a preformed dimeric structure. We also constructed a series of EGFR mutants in which a small point mutation or large deletion was introduced into the receptor molecule, and found that EGFR mutants with the deletion at its C-terminal region were spontaneously activated. In contrast to the wild-type EGFR with biphasic affinity for EGF, further, the mutant showed a single affinity for the ligand. These results are consistent with the ‘rotation/twist’ model for the mechanism of the EGFR activation. In the meeting, we shall report the results described above, and shall discuss about the positive cooperativity between the ligand-binding sites required for the activation of EGFR.

3PT122 表層ストレス応答における、PDZ ドメインによる RseP プロテアーゼ機能制御機構の解析

Analysis of a regulatory mechanism of the proteolytic function of RseP by the PDZ domains in extracytoplasmic stress response

Yohei Hizukuri, Yoshinori Akiyama (*Institute for Virus Research, Kyoto Univ.*)

The *Escherichia coli* σ^E extracytoplasmic stress response monitors and responds to folding stress in the cell envelope. A protease cascade directed at RseA, a membrane-spanning anti-σ that inhibits σ^E activity, controls this critical signal-transduction system. Stress cues activate the DegS proteases to cleave RseA; a second cleavage by the RIP protease releases RseA from the membrane, enabling its rapid degradation. Stress control of proteolysis requires that RseP cleavage is dependent on DegS cleavage. *In vitro* and structural studies found that RseP cleavage requires binding of RseP PDZ-C to the newly exposed carboxyl terminal residue (Val148) of RseA, generated by DegS-cleavage, explaining dependency (Li et al., 2009, Proc. Natl. Acad. Sci. U. S. A.). We tested this mechanism *in vivo*. Neither the C-terminal residue of DegS-processed RseA nor mutations in the putative PDZ ligand-binding regions or even deletion of entire RseP PDZ domains had significant effects on RseA cleavage *in vivo*. Indeed, strains with a chromosomal *rseP* gene deleted for either PDZ domain grew normally at all temperatures and exhibited almost normal σ^E-activation in response to stress signals. We conclude that recognition of the cleaved amino acid by the PDZ domain of RseP is unable to explain sequential cleavage *in vivo*. To explore the possibility that the PDZ domains are involved in regulation of the RseP functions through ligand-binding we are trying to identify a physiological ligand of RseP PDZ by using site-directed *in vivo* photo-cross-linking experiment.

3PT123 部分フッ素化ホスファチジルコリン小胞に再構成されたバクテリオロドプシンの液晶相における分子集合体

Molecular assembly of bacteriorhodopsin reconstituted into partially fluorinated phosphatidylcholine liposome in liquid crystalline phase

Masaru Yoshino[1], Kenji Kanayama[1], Takashi Kikukawa[2], Toshiyuki Takagi[3], Hiroshi Takahashi[1], Toshihiko Baba[3], Toshiyuki Kanamori[3], Masashi Sonoyama[1] ([1]*Grad. Sch. Eng., Univ. Gunma*, [2]*Grad. Sch. Sci., Univ. Hokkaido*, [3]*R.C. Stem Cell Eng., AIST*)

Fluorine-containing lipids are expected to be very useful in the research area of membrane proteins. Our recent studies on physical properties of a novel partially fluorinate phosphocholine, 1, 2-di (11, 11, 11, 12, 12, 13, 13, 14, 14-nonafluorotetradecanoyl) -sn-glycero-3-phosphocholine (diF4H10-PC), an analog of a common phosphatidylcholine DMPC, demonstrated that diF4H10-PC membrane shows the gel-to-liquid crystalline phase transition at ~5 ^oC and the fluidity in the interface region is higher than that of DMPC. We succeeded in reconstituting a photoreceptor membrane protein, bacteriorhodopsin (bR), into diF4H10-PC liposome. The reconstituted bR retained the trimeric structure even after the chain melting phase transition of lipid bilayers at least up 40 ^oC and showed a photocycle similar to native purple membrane, which is in a striking contrast with the previous studies on bR reconstituted in DMPC*. In order to address what is responsible for retaining the trimeric structure even in the fluid phase of diF4H10-PC, bR reconstituted in a binary immiscible membrane of diF4H10-PC and DMPC was investigated by some spectroscopic methods. It has been shown that most of bR molecules are selectively reconstituted into DMPC-rich domain, suggesting bR is mostly immiscible to diF4H10-PC. It is plausible that the immiscibility between bR and diF4H10-PC is essential for the formation of bR trimers.

*Sonoyama et al., (2009), Yokoyama et al., (2010)

3PT124 Elucidation of the membrane microdomain assembly mechanism via reconstituted artificial lipid membranes using high performance proteomics

Lumi Negishi[1], Satoshi Hosoya[1], Osamu Toda[1], Tsuyoshi Oosawa[1], Ken Hirosaki[1], Thanai Paxton[2], Nobuhiro Hayashi[1] ([1]*Grad. Sch. of Life Sci. and Biotech., Tokyo Inst. Tech.*, [2]*Solution Center, Nihon Waters K.K.*)

Plasma membrane microdomains are associated with a variety of biomolecules and considered to play an important role in effective response to external stimuli. The physicochemical basis controlling the association remains incompletely understood. In this work, we investigate the role of intermolecular interactions in the assembly of proteins and lipids into the microdomain using reconstituted membranes of varying composition and physiochemical properties. We carried out high performance proteomics of the membrane microdomain and identification of the proteins to investigate component proteins in the microdomain. Using a standard procedure, the membrane microdomain was extracted from Jurkat cells (Human T-cell lymphoblast cell line) because membrane microdomains play an important role in the recognition of antigen-presenting-cells in immune system. The results of the 2D-gel electrophoresis showed about 150 spots and of these approximately 60 proteins have so far been identified using in-gel tryptic digestion and LC-MS/MS measurements. Some identified proteins such as actin and V-type ATPase have already been reported as membrane microdomain components. However, original proteins such as interferon-induced GTP-binding protein, tumor necrosis factor and sphingolipid

desaturase have not yet been reported as microdomain components and they are possibly involved with the immune system. Finally, important factors in the antigen recognition system and the construction of the in vitro system using artificial membranes will also be discussed.

3PT125 無細胞膜タンパク質合成におけるリポソームのシャペロン機能

Liposomes as chaperone in cell-free membrane protein synthesis

Minato Akiyama[1], Jun-ichi Yasuoka[2,3], Shin-ichi Sawada[1,3], Kazunari Akiyoshi[1,3] ([1]*Grad. Sch. Eng., Kyoto Univ.*, [2]*Inst. Biomater. Bioeng., Tokyo Med. Dent. Univ.*, [3]*JST-ERATO*)

Membrane proteins play significant roles in organism, such as signal transduction and cellular communication. However, studies of membrane proteins are not enough established because most of them are water-insoluble and likely to aggregate in water. Recently, we reported direct reconstitution of membrane proteins into liposomes using cell-free protein synthesis system. In this study, we focused on a membrane protein, connexin-43 (Cx43), which form hexameric hemichannel named connexon. Two connexons on neighboring cells join and form gap junction that mediates intercellular communication. We report the synthesis of Cx43 using cell-free protein synthesis and chaperone-like function of liposome.

Cx43 was successfully synthesized with the reconstituted cell-free protein synthesis system (PURE system), as shown by western blotting analysis. Synthesized Cx43, however, was observed to completely aggregate in the absence of liposomes. In the presence of liposomes, a certain amount of synthesized Cx43 was detected in the soluble fractions containing liposomes. Aggregated Cx43 was removed by sucrose density gradient centrifugation. The supernatant was collected as Cx43-reconstituted liposome fraction. The chaperone-like function of liposomes prevents the aggregation of the water-insoluble membrane protein in solution and aids the oligomerization of Cx43 in the membrane. Hemichanel formation and the effect of concentration, size and lipid composition of liposome as a chaperone for the membrane protein synthesis were investigated.

3PT126 可溶化系における膜タンパク質ハロロドプシンとバクテリオルベリンの複合体形成

Formation of a complex between membrane protein halorhodopsin and carotenoid of bacterioruberin in the solubilized system

Takanori Sasaki, Nur Wahida Abdul Razak, Noritaka Kato, Yuri Mukai (*Sch. Sci. and Tech., Univ. Meiji*)

Halorhodopsin is a retinal protein with a seven-transmembrane helix and acts as an inward light-driven Cl^- pump. In this study, structural state of the solubilized halorhodopsin (NpHR) from the biomembrane of mutant strain KM-1 of *N. pharaonis* in non-ionic detergent was investigated. A gel filtration chromatography monitored absorbances at 280, 504 nm corresponding to the protein and a lipid soluble pigment of bacterioruberin (BR) respectively has clearly detected an oligomer formation of the NpHRs and a complex formation between the NpHR and BR in the solubilized system. From a BR titration experiment for the NpHR, a molar ratio of NpHR:BR in the solubilized complex was estimated to be close to 1:1. Further SDS-PAGE analysis of the solubilized NpHR cross-linked by glutaraldehyde has revealed that the NpHR forms homotrimer in detergent system. Although this trimeric structure was stable in the presence of NaCl, it was dissociated to the monomer by the heat treatment at 45 °C in the desalted condition. Interestingly, the trimer dissociation on the NpHR was accompanied by the complete dissociation of the BR molecule from the protein, indicated that the cavity formed by the NpHR protomers in the trimeric conformation is important for tight binding of the BR. The trimer dissociation ratio of the NpHR-BR complexes (about 25%) after heat treatment for 3h at 45 °C was much lower than that of the NpHRs not bound the BR (about 65%), suggested the physiological role of the BR to stabilize the trimeric structure.

3PT127 Structure, orientation and interactions of bovine lactoferrampin in membrane bilayers

Namsrai Javkhlantugs, Kazuyoshi Ueda, Akira Naito (*Department of Advanced Materials Chemistry, Graduate School of Engineering, Yokohama National University*)

One of the antibacterial peptide is bovine lactoferrampin (LFampinB) which found in the sequence of bovine lactoferrin (268-284), and consists of 17 amino acid residues. It is important to determine the orientation and the interactions of LFampinB with lipid molecules in acidic dimyristoylphosphatidylglycerol (DMPG) and zwitterionic dimyristoylphosphatidylcholine (DMPC) membranes to reveal the antibacterial mechanism. LFampinB formed alpha-helix at N-terminus region with the tilted angle of 42 degrees in DMPG and of 38 degrees in DMPC to the bilayer normal after the simulation. We analyzed the interaction energy between hydrophilic side chains of peptide and lipid head groups of membrane bilayers. It is found that the interaction energy between peptide and DMPG is higher than that of DMPC membrane. Structure of LFampinB in mimetic bacterial membrane was investigated by experimentally using solid-state NMR method. It showed that the LFampinB specifically interacts with acidic phospholipids and disrupts the bacterial membrane. Solid-state NMR clarified that peptide keeps helical structure and its helix were tilted to the membrane normal which is in good agreement with both methods.

3PT128 Laser flash photolysis study on the decay kinetics of the M photointermediate of bacteriorhodopsin in diheptanoylphosphocholine micelles

Masashi Sonoyama[1], Yumiko Kuwabara[1], Takashi Kikukawa[2] ([1]*Grad. Sch. Eng., Gunma Univ.*, [2]*Grad. Sch. Life Sci., Hokkaido Univ.*)

Diheptanoylphosphocholine (diC7-PC), a short chain phospholipid that has the same basic chemical structure as native long chain phospholipid in biomembrane, is a promising detergent available for solubilization of membrane proteins. We have recently reported that diC7-PC is actually a very powerful detergent for solubilization of a membrane protein bacteriorhodopsin (bR), and the solubilized bR was much more stable than that with other conventional detergents, especially in the functional state under illumination with visible light*. Interestingly, laser flash photolysis of the solubilized bR at neutral pH demonstrated that the decay curve of the M intermediate can be well expressed with two kinetically different components. In this study, further laser flash photolysis measurements were performed for bR in diC7-PC micelles in the wide pH range, in order to address the origin of the two kinetically different M species. The obtained experimental results that the ratio of the two components is highly dependent on pH of the surrounding media indicates that pKa of Asp 96 in the dark is perturbed by solubilization with diC7-PC and is estimated as ~8.5. Further works on the activation volume for the decay of the two M species are under progress by analyzing the hydrostatic pressure dependence of the decay at neutral pH. These results will be also discussed.

*M. Sonoyama, M. Fukumoto and Y. Kuwabara, Chem. Lett. 39, 876-877 (2010).

3PT129 Characterization by mutagenesis analysis of putative proton transfer pathway, D-pathway of bovine heart cytochrome *c* oxidase

Ryohta Aminaka[1], Mai Itoh[1], Kunitoshi Shimokata[2], Yukie Katayama[3], Tomitake Tsukihara[1], Shinya Yoshikawa[1], Hideo Shimada[1] ([1]*Grad. Sch. Life Sci., Univ. Hyogo*, [2]*WORLD INTEC CO., LTD.*, [3]*Grad. Sch. Agric. Life Sci., Univ. Tokyo*)

X-ray structures of the bovine heart and bacterial cytochrome *c* oxidase suggest three proton transfer pathways (D-, K-, and H-pathways), each homologous between the two. Glu242Gln and Asp91Asn mutations of the bacterial D-pathway (bovine numbering) abolish the O_2 reduction activity, while Asn98Asp and Asn163Asp abolish proton-pumping activity with keeping high O_2 reduction activity. These results support for a proposal that D-pathway transfer both water-forming and pumping protons. Conservation of amino acid residues essential to D-pathway functions suggests bovine D-pathway proton pumping, contradicting to our H-pathway proton-pumping proposal. Here, we analyzed bovine D-pathway by mutagenesis employing HeLa cell bovine/human hybrid enzyme expression system developed by us. The Asn98Asp and Asn163Asp mutations did not change the enzymatic activity. All subunit genes of the hybrid enzymes including isoform genes were found not to have any other mutations, eliminating possible back mutation to restore the enzymatic activity. Immunoblot analysis demonstrated that Glu242Gln and Asp91Asn mutant did not dominate over the endogenous human enzyme in contrast to expression of the wild type and other mutant hybrid enzymes. However, proton pumping and cytochrome *c* oxidation activities of the mitochondrial samples relative to those of the samples expressing only the human enzyme indicated the mutations abolished the enzymatic activity. The present results did not support D-pathway proton pumping but support the water forming proton transfer.

3PT130 陰溶媒膜モデルとレプリカ交換シミュレーションによるα-ヘリカル型膜タンパク質の構造予測

Prediction of α-helical membrane protein structures by replica-exchange simulations with implicit membrane model

Ryo Urano[1], Yuko Okamoto[1,2,3] ([1]*Dept. of Phys. Grad. Sch. of Sci. Nagoya Univ.*, [2]*Bio. Research Center Grad. Sch. of Sci. Nagoya Univ.*, [3]*Center for Comput. Sci. Grad. Sch. of Eng. Nagoya Univ.*)

Membrane proteins are essential for life. Their structures are related to their functions. Their 3-dimensional structures are typically in α-helical structures. Although the determination of the structures is usually done by x-ray diffraction, solid-state NMR, or electron microscope experiments, it takes a long time to prepare the samples. The purpose of the present work is to predict the 3-dimensional structure of α-helical membrane proteins by computer simulation. The procedure is as follows. At first, we extract trans-membrane amino acid residues from membrane proteins by prediction tools based on bioinformatics. Next, the ideal helix structure is formed for the trans-membrane helix regions. During simulations, the replica-exchange method and a simple implicit membrane model to represent restrictions of membrane proteins from membrane environment are applied. The Monte Carlo move sets include backbone torsion angles for the deformation of helix structures from ideal helix formation. This implicit membrane model represents the restriction of trans-membrane helices within the membrane regions. A principal component analysis is used to examine the simulation trajectory and divide structures into local- minimum free energy states. We applied our method to the prediction of the structures of small membrane proteins including bacteriorhodopsin. In this poster presentation, we show the results of these structure predictions.

3PT131 Homology modeling and molecular dynamics study of proton permeation pathway in a channel protein

Susumu Chiba[1], Kota Kasahara[1], Matsuyuki Shirota[1,2], Kengo Kinoshita[1,2,3] ([1]*Grad. Sch. of Information Sci., Tohoku Univ.*, [2]*Tohoku Medical Megabank Organization, Tohoku Univ.*, [3]*IDAC, Tohoku Univ.*)

Hv1, voltage sensitive proton channel is known as voltage sensor only protein (VSOP). In contrast to other voltage sensitive ion channels, VSOP doesn't have a pore domain but has only a voltage sensor domain (VSD), through which proton permeate. Recent simulation studies based on homology models of VSOP showed the possibility that proton permeation is caused by proton "hopping" (Grotthuss mechanism), from water to water in the crevice of transmembrane region, but details of permeation mechanism is still unclear. To analyze proton pathway, molecular dynamics (MD) simulation is powerful method. Since the proton pathway is formed by the interaction between water and the charged residues in transmembrane region, precise modeling of membrane region is important to simulate and estimate characteristic of proton permeation. VSD of voltage-gated potassium channel (Kv channel) was used for template of homology modeling in the preceding studies. On the other hand, voltage-gated sodium channel (Nav channel) NavAb, which was recently entered in PDB database, share higher sequence identity with VSOP than Kv channel. Therefore we made VSOP-NavAb alignment considering sequence of transmembrane regions, and subsequently we modeled structure based on the alignment. We performed the MD simulation of the predicted model embedded in POPE membrane for 200 ns. It was observed that a continuous pathway of water molecules exist in the crevice of the channel. Finally we discuss the behavior of waters and charged residues, and proton permeation mechanism.

3PT132 大腸菌機械受容チャネル MscL の開口過程におけるタンパク質と水との協調過程の役割の分子動力学的解析

Molecular Dynamics Analysis of the Role of Protein-Water Interplay in the Opening Process of E-coli Mechanosensitive Channel MscL

Yasuyuki Sawada[1], Masahiro Sokabe[1,2] ([1]*Dept. Physiol. Nagoya Univ. Grad. Sch. Med.*, [2]*FIRST Res. Ctr. for Innovative Nanobiodevice, Nagoya Univ.*)

The bacterial mechanosensitive channel MscL is constituted of homopentamer of a subunit with two transmembrane inner (TM1) and outer (TM2) α-helices. Neighboring TM1s cross and interact with each other near the cytoplasmic side through hydrophobic interaction, forming the most constricted hydrophobic part of the pore. The crossings stabilize the closed state of MscL with hydrophobic interactions, thus called gate. The major issue of MscL is to understand the gating (opening) mechanism driven by tension in the membrane. We performed molecular dynamics (MD) simulations of tension-driven opening of MscL, particularly focusing on the conformational change of MscL associated with water. Upon membrane stretch, Phe78 in TM2 helix, which is suggested to be a major tension sensor in our previous work, was dragged by lipids and TM1s were gradually tilted accompanied by outward sliding of the crossings between TM1 helices. While TM1s were tilted, a breakage of the helical structure around the gate was shown and an exposure of oxygen atoms of the backbone to the inner surface of the gate occurred, followed by formation of hydrogen bonds between water and the exposed oxygen. This allowed further access of water to the gate and weakened the hydrophobic interaction at the crossings, leading to a further opening of the gate. It is suggested that the combination of conformational changes of MscL by membrane stretch and following hydrogen bond formation forms a positive feedback cycle, which seems to be critical to induce rapid channel opening.

3PT133 ATP-Binding induced conformational change in CFTR as studied by MD simulation

Tomoka Hagiya[1], Tadaomi Furuta[1], Shuntaro Chiba[1], Yoshiro Sohma[2], Minoru Sakurai[1] ([1]*Grad. Sch. of Biosci. & Biotech., Tokyo Tech.*, [2]*Dept of Pharmacol., Sch. Med., Keio Univ.*)

The Cystic fibrosis transmembrane conductance regulator (CFTR, ABCC7) is a chloride channel and belongs to the ATP-binding cassette (ABC) protein superfamily that binds and hydrolyzes ATP to drive substrate transport across membranes. For the gating mechanism, the following hypothesis has been proposed: after phosphorylation of the regulatory domain, ATP molecules bind to the two nucleotide-binding domains (NBDs), which in turn induces the dimerization of the NBDs and the concomitant opening of the channel gate. To clarify its mechanism, we first built a homology model of CFTR (with an inward-facing conformation) by using several X-ray crystal structures of ABC transporters as templates. Subsequently we explored its stable conformations and dynamics using molecular dynamics (MD) simulations, which were performed for Mg and ATP-bound (MgATP) state and nucleotide-free (Free) state. Interestingly, in the MgATP state, NBD1 and NBD2 were dimerized so that the ATP molecules were sandwiched between Walker A and the signature motif. Additionally we found the closing of the TMDs internal cavity in the intracellular loop regions. On the other hand, the NBDs remained monomers in the Free state. This study suggests that ATP-binding not only causes the NBD dimerization, but also exerts a significant influence on the TMD structure.

3PT134 リポソームと機能性ペプチドを用いた酵素活性検出法の開発

Development of enzyme activity detection system using liposome and functional antimicrobial peptide

Masayoshi Kashibe[1], Shin Mizukami[1,2], Kazuya Kikuchi[1,2] ([1]*Graduate School of Engineering, Osaka University*, [2]*Immunology Frontier Research Center, Osaka Univ.*)

The development of enzyme activity detection system has attracted wide attention in the field of biology, pharmacology, and medicine. We developed a new system for enzyme activity assay by using anionic liposome and the derivatives of an antimicrobial peptide, temporin L (TL). It was reported that TL has membrane-damaging activity against anionic membranes of micro-organisms. Previously, we reported that modification of the Lys amino group of TL by a photosensitive protective group suppressed its membrane-damaging activity. Thus, we hypothesized the membrane-damaging activity of TL derivatives can be modulated also by modification of other amino acid residues.
We designed several TL derivatives modified with a phosphate group at the various amino acid residues. The membrane-damaging activities in some of the derivatives were suppressed and liposome disruption does not occur. When the peptides were treated with a phosphatase, these activities were recovered. This conversion induced the inclusion release from liposome, in which fluorophores were quenched, and the inclusion release induced the fluorescence enhancement. This result indicates that this system can be used for the detection of phosphatase activity.
Since various modifications of peptides for many types of enzyme assay is possible, it could lead to detection system for various enzyme activities. Moreover, since liposomes can include various compounds such as proteins, and drugs, this system would be applied not only to diagnosis but also to therapeutics.

3PT135　モデル細胞間に形成された脂質 2 分子膜の吸着力測定

Adhesive force of a lipid bilayer between contacted cell-sized droplets

Taka-aki Yoshida[1], Miyuki Furuta[2], Yui Matuda[2], Satoshi Nakata[2], Masayuki Tokita[1], Miho Yanagisawa[1] ([1]*Grad. Sch. Sci., Kyushu Univ.*, [2]*Grad. Sch. Sci., Hiroshima Univ.*)

Cell-sized water/oil droplet coated by a lipid monolayer has been shown to be a useful system for examining the interaction between lipid membrane and encapsulated proteins [1-2]. The droplets can easily connect with each other and form a continuous structure like a cell tissue where lipid bilayers bound them. In the case of adhesive two droplets, the adhesive force is calculated from $F = 2\gamma(1-\cos\theta)$, where θ and γ are contact angle and surface tension at the oil/water interface [3]. We have evaluated the lipid dependence on θ and γ independently by using three different types of lipids, unsaturated lipids: DOPE (dioleoylphosphatidylethanolamine), DOPC (dioleoylphosphatidylcholine), and a saturated DMPC (dimyristoylphosphatidylcholine). Then, the contact angle term $2(1-\cos\theta)$ differs among lipid species and fails in the order: DMPC < DOPC ~ DOPE, which might reflect the molecular structure of hydrophobic tails. On the other hand, γ follows the order: DOPC <DMPC <DOPE, which is consistent with non-lamellar PE unlike PC. Finally, we obtained the lipid dependence on F: DMPC <DOPC <DOPE. Based on these values, we elucidated the effects of membrane or cytoplasmic structures on F by the addition of polyethylene glycol (PEG) conjugated DOPE or encapsulation of gelatin gel. We believe that this system is useful to clarify the effects of proteins on adhesive lipid mono-layers.

[1] A. Kato, et al., 2012 Sci. Rep., 2:283.
[2] M. Yanagisawa, et al., 2011 J. Am. Chem. Soc., 133:11774.
[3] P. Poulin et al., 1997 Phys. Rev. Lett., 79:3290.

3PT136　ジェット流による細胞サイズリポソームの作製

Preparation of cell-sized liposomes by pulsed jet flow

Koki Kamiya[1], Ryuji Kawano[1], Toshihisa Osaki[1], Syoji Takeuchi[1,2] ([1]*Kanagawa Academy of Science and Technology*, [2]*Institute of Industrial Science, The University of Tokyo*)

Giant liposomes are composed of phospholipid membranes similar to those commonly found in living cells. A giant vesicle is typically ~10 μm in diameter, which is sufficient observation by optical microscopy. Therefore, such artificial liposomal systems have been used in biochemical and biophysical studies such as the microencapsulation of gene expression systems. To effectively form uniformly-sized giant vesicles and encapsulate biological molecules into giant vesicles, in our previous study, we created giant vesicles by the microfluidic-jetting-induced deformation of a planar lipid bilayer including an organic solvent. However, this method has limitations; for instance, the giant vesicle is a W/O/W emulsion having a thin shell of an organic solvent. Further, it is unstable and very large (over 300 μm in diameter). In the present study, we prepared cell-sized lipid vesicles using an improved double-well device and a pulsed jet flow. When the jet was applied for 4.2 ms at 250 kPa, vesicle formation could be observed using a high-speed camera. Vesicles of two different sizes were formed by the jet flow. The vesicles with a diameter of over 100 μm immediately collapsed in the glucose solution. However, the vesicles with the diameter of approximately 5 μm sank in the glucose solution and their shape was maintained. The average diameter of the vesicles formed immediately and after 24 h was 4.4 μm.

3PT137　タンパク質内包リポソームの熱安定性に関する小角・広角 X 線散乱研究

SWAXS study of thermal structural stability of liposomes entrapping proteins

Ryota Kimura, Mitsuhiro Hirai (*Grad. Sch. Eng., Gunma Univ.*)

[Introduction]
By using synchrotron radiation small-angle and wide-angle X-ray scattering (SR-SWAXS), we studied the structural characteristics of liposomes entrapping proteins. The aim of this study is to clarify the thermal stability of liposomes entrapping proteins that mimic an intracellular environment.
[Experimental]
Liposomes measured were large uni-lamellar vesicles (LUVs) of lipid-mixtures composed of glycosphingolipid, cholesterol and phospholipid lipids (egg-PC or DPPC). The protein occluded in liposmes was myoglobin. LUVs were prepared as follows. The lipid mixtures dissolved in protein solutions in 10 mM HEPES buffer at pH 7.5 were subjected to natural swelling, ultra-sonic dispersion, freeze-throw, extrusion using a extruder system, and spin-filtration, successively. SR-SWAXS experiments were done SPring-8 and at PF The temperature range of the samples was 25 - 85 °C.
[Results]
In the case of the empty DPPC-LUV, the bilayer structure changed evidently in the range from 40 °C to 45 °C due to the gel-to-liquid crystal transition, whereas, both the diameter and the radius of gyration were mostly unchanged. In the case of the filled DPPC-LUV, the transition temperature became higher in around 5 degrees, suggesting that the thermal stability of liposome was improved by the protein occlusion. Both the diameter and the radius of gyration increased once, and suddenly decreased. Above the transition temperature, both values were mostly constant. Further experimental results and analyses will be shown.

3PT138　溶質含有脂質フィルムから調製した巨大リポソームのサイズ、形態と膜多重度

Size, morphology and lamellarity of giant liposomes generated from solute-containing lipid films

Kanta Tsumoto, Shota Kimura, Masahiro Tomita (*Grad. Sch. Eng., Mie Univ.*)

Giant liposomes are adopted for studies on cell membrane and microcompartment models, and a lot of methods have been developed to improve various properties of them, including formation efficiency, size distribution, lamellarity, etc. Of course, all protocols are useful; however, the hydration methods, such as the gentle hydration (natural swelling) which is based on the Bangham method, and the electroformation, are often used for preparation of giant liposomes in a buffer saline. Especially, the natural swelling is still popular probably because it is so simple and reasonable. Previously, we and collaborators reported improvement of this method, in which hydration and swelling processes in liposome formation may be enhanced through promoted osmosis due to water- and methanol-soluble solutes such as NaI and monosaccharide sandwiched between lipid lamellae of films [1,2]. In the present work, we further studies detailed properties of such giant liposomes with respect to changes in size, morphology and lamellarity. Here, DOPC films with fructose in various molar ratios were hydrated, resulting in transition of liposome sizes from micron to submicron at the higher ratio of Fru/DOPC (60:1 and more). An NBD quenching assay showed the transition from multi- to unilamellar liposomes. We also tried to investigate if the liposome morphology would be dependent on the kind of solute, using polymer as a model.

[1] Yamada, N.L., et al. EPL, 80, 48002 (2007). [2] Tsumoto, K., et al. Colloids Surf. B, 68, 98-105 (2009)

3PT139　表面修飾ナノ粒子の巨大リポソームへのエンドサイトーシス様取込み

Endocytosis-like Uptake of Surface-Modified Nanoparticles into a Giant Liposome

Kohei Tahara[1,2,3], Satoshi Tadokoro[1], Yoshiaki Kawashima[2], **Naohide Hirashima**[1] ([1]*Grad. Sch. Pharmaceut. Sci., Nagoya City Univ.*, [2]*Sch. Pharm., Aichi Gakuin Univ.*, [3]*Gifu Pharmaceut. Univ.*)

Cell-sized giant unilamellar vesicles (GUVs) have been used as artificial cell systems that mimic various cellular events. We previously reported an artificial exocytosis model by encapsulating small unilamellar vesicles in a GUV.
In the present study, we observed the uptake of surface-modified nanoparticles (NPs). We prepared a cell-sized GUV that mimics a cell membrane to investigate the interaction between cell membranes and NPs. As NPs, we used poly (D,L-lactideco-glycolide) (PLGA) NPs modified with nonionic surfactant P80 or cationic polymer chitosan (CS) on their surface. To observe interaction between GUV and NPs with a fluorescence microscope, GUV was prepared with rhodamine-conjugated phosphatidylethanolamine, and NPs were labeled with 6-coumarin.
Average particle diameters of unmodified NPs, CS-modified NPs and P80-modified NPs were 221 ± 1.4 nm, 350 ± 17.1 nm, and 210 ± 5.1 nm, respectively. Zeta-potentials of unmodified NPs, CS-modified NPs and P80-modified NPs were -27.4 ± 0.6 mV, +27.5 ± 0.6 mV, and -28.3 ± 0.7 mV, respectively.
Endocytosis-like uptake of NPs into a GUV was observed when the NPs were modified with P80. In contrast, unmodified NPs and those modified with CS were not internalized into a GUV, although large number of NPs with CS adhered to the surface of GUV due to their positive charge. These results

suggest that surface properties of PLGA-NPs are important for endocytosis-like uptake into a GUV.

3PT140 トランスポータン 10 が DOPC 膜の巨大リポソームの膜透過性と構造に与える効果

Effects of Transportan-10 on Membrane Permeability and Structure of Single Giant Unilamellar Vesicles of DOPC membranes

Hirotaka Ariyama, Masahito Yamazaki (*Integrated Bioscience Section, Graduate School of Science and Technology, Shizuoka Univ.*)

Transportan 10 (TP 10) is one of the cell penetrating peptides. So far the permeation of TP 10 into cells and the interaction of TP 10 with lipid membranes using LUV suspension have been investigated. However, the detail characteristics and mechanism of the interaction and its permeation through membranes remain unclear. In this report, we have investigated the effect of TP 10 on membrane permeability of lipid membranes using the single giant unilamellar vesicle (GUV)method.
First, we investigated the interaction of TP 10 with single GUVs composed of dioleoylphosphatidylcholine (DOPC) and PEG2K-DOPE (molar ratio, 98: 2) containing the fluorescent dye, calcein, in a physiological buffer using phase contrast, fluorescence microscopy. The interaction of 0.8 μM TP 10 with single DOPC-GUVsinduced the rapid monotonous leakage of calcein from the inside of the most GUVs, but in some GUVs step-wise leakages were observed. During the calcein leakage, the size of most GUVs decreased a little (less than 5 %), but in some GUVs their radius decreased greatly and some small high-contrast particles appeared on the GUV membranes. The fraction of leaked GUVincreased with time, and also with an increase in TP 10 concentration. Second, the effect of cholesterol on the TP 10-induced leakage of calcein was investigated. 0.2 μM TP 10 did not induce calcein leakage from DOPC/chol (6/4)-GUVs. On the basis of these data, we discuss the mechanism of the interaction of TP 10 with DOPC-GUVs and DOPC/chol-GUVs.

3PT141 F-BAR によるリポソームのチューブレーションのリアルタイム観察

Real-time observation of liposome tubulation by F-BAR

Yohko Takiguchi[1], Toshiki Itoh[2], Kingo Takiguchi[1] ([1]*Grad. Sch. Sci., Univ. Nagoya*, [2]*Grad. Sch. Med., Univ. Kobe*)

The Fer-CIP4 homology-BAR (F-BAR) domain has been identified as a biological membrane-deforming module. The F-BAR domain has been reported to transform lipid bilayer membranes into tubules. However, the process of tubulation still remains unknown. Here we monitored the entire tubulation process induced by the F-BAR domains or by the full lengths of four different F-BAR domain proteins, PSTPIP1, FBP17, CIP4 and Pacsin2, using direct real-time imaging, and show that each F-BAR domain or protein induces tubules through a unique kinetics from model membranes.
FBP17 and CIP4 develop many projections simultaneously throughout the surface of individual liposomes, whereas PSTPIP1 and Pacsin2 develop only a few projections from a narrow restricted part of the surface of individual liposomes. The results provide striking evidence that a nucleation process is involved in the F-BAR-induced tubulation, and individual F-BAR domains have a unique nucleation rate and/or property even though essentially they have the same crescent-shaped structure. The differences in process of tubulation induced with those F-BAR domain proteins may reflect their unique physiological roles, and function favorably to build networks of various and robust membrane trafficking processes observed in cells.

3PT142 PEG 担持ジャイアントベシクルにおける膜組成と分裂様式の関係

Correlation between Membrane Composition and Mode of Division of PEG-grafted Giant Vesicles

Yumi Kan[1], Kensuke Kurihara[2], Taro Toyota[2,3], Masayuki Imai[4], Tadashi Sugawara[3,5] ([1]*Ochanomizu University*, [2]*The University of Tokyo*, [3]*Research Center for Complex Systems Biology*, [4]*Tohoku University*, [5]*Kanagawa University*)

Recently we realized a model protocell using a giant vesicle (GV) as a compartment, comprised of phospholipids, cationic synthesized membrane molecule (V) and an amphiphilic catalyst (C). Encapsulated DNA in GV was amplified by polymerase chain reaction, and then the GV grew and divided when the incorporated membrane-precursor was converted to V by the assistance of C. We also revealed that the attractive interaction between amplified DNA and the inner surface of the GV membrane accelerated the GV division. Here we prepared a new model protocell including 5 mol% of polyethylene glycol (PEG5000)-grafted phospholipid: a PEG-chain of the phospholipid not only increased the tolerance of GV to high ionic strength and high temperature but also affected the interaction between DNA and the GV membrane containing the cationic membrane molecule V. In order to elucidate the morphological change of the GV membrane throughout the self-reproduction process, we stained the membrane by Texas Red-tagged phospholipid and observed the dynamics in terms of a confocal laser scanning fluorescence microscope. Whereas the division mode of non PEG-grafted GV was a budding-type exclusively, the birthing-type deformation occurred mainly in the case of PEG-grafted GV. We speculated that the interaction between the amplified DNA and the PEG-grafted inner surface of the membrane influences the division mode of GV self-reproduction. In this symposium, we will discuss the effect of the length and the content of PEG-grafted phospholipid on the mode of GV division.

3PT143 静置水和法による均一径リポソームアレイ

Size-controlled Giant Liposome Array System with Gentle Hydration

Toshihisa Osaki[1], Koki Kamiya[1], Kaori Kuribayashi[2], Ryuji Kawano[1], Shoji Takeuchi[2] ([1]*Kanagawa Academy of Science and Technology*, [2]*Institute of Industrial Science, The University of Tokyo*)

This work presents a methodology that realizes size-controlled, solvent-free giant liposome arrays with simple gentle hydration technique. Gentle hydration and electroformation have been the most commonly used methods to prepare giant liposomes, yet they have difficulty controlling the size distribution of the formed liposomes as well as their shape and lamellarity. We therefore set the goal of developing an alternative method that allows the formation of uniform-size giant liposomes with high reproducibility. Our system consists of a dried lipid pattern on a substrate that is a micropatterned polymer thin film on an ITO glass slide. An electrospray deposition (ESD) method was applied to obtain the selective lipid-deposition at the polymer pattern where the ITO surface was exposed. With a simple hydration process of the dried lipid, we succeeded in formation of giant liposomes on top of the pattern. The diameter of the liposomes was similar to the patterned size, achieving a narrow range of size distribution. We also report the applicability of the system for various biological assays such as object encapsulation into the liposomes, buffer exchange during the assays, and reconstitution of membrane proteins into the liposome membranes.

3PT144 REMD シミュレーションによる粗視化された脂質膜の相転移の研究

Study on phase transition of coarse-grained lipid bilayer by REMD simulations

Tetsuro Nagai, Yuko Okamoto (*Grad. Sch. Sci., Nagoya Univ.*)

A replica-exchange molecular dynamics simulation of a lipid bilayer system was performed in order to study sol-gel phase transitions. The replica-exchange molecular dynamics method enables one to enhance conformational sampling efficiency and to study the system at a wide temperature range at once. We employed a coarse-grained model MARTINI. The results show abrupt changes in internal energy, bilayer thickness, and area of bilayer around 296 K. A peak in specific head capacity was also observed around this temperature. These suggested that the sol-gel phase transitions. The bilayer has two states in the gel state. One is a tilted gel state and the other is an un-tilted gel state. A previous work with MARTINI force filed reported only the un-titled gel state. This indicates that conformational sampling efficiency is not trivial even with coarse-grained model, which has smoother energy landscapes and reach longer time scales than atomistic model. The un-tilted gel phase is a little thicker than the tilted gel phase, while the area of lipid bilayer is quite similar. We will show more detail results in the presentation.

3PT145 長鎖リン脂質 DMPC と短鎖リン脂質 DHPC で構成される複雑な相挙動のダイナミクス

Dynamics of complicated phase behavior on the mixtures consisting of long-chain phospholipids DMPC and short-chain phospholipids DHPC

Ryota Kobayashi, Tetsuhiko Ohba (*Department of Physics, Tohoku University.*)

The binary phospholipid mixtures of long-chain DMPC and short-chain DHPC show a variety of complicated phase behavior, depending on the mixing ratio of two lipids, the total lipid concentration in water, and temperature. At low

temperature, the mixture is transparent and has a low viscosity, and its structure is thought to be disk-like micelles, which is often called "bicelles". At high temperature, the mixture is turbid and also has a low viscosity, and its structure is thought to be multi lamellar vesicles (MLV). In intermediate temperature range, the mixture has high viscosity. This phase is called nematic phase because the polarized optical microscopy observation exhibit optical anisotropy. The structure of nematic phase is not yet clear although some models, such as worm-like or disk-like aggregates, had been proposed.
We measured membrane fluidity and fluorescence anisotropy of DMPC/DHPC mixtures, using fluorescence GP imaging with Laurdan or fluorescence spectroscopy with DPH. The results support stability of the structure of bicelles at low temperature and mechanism of generating MLVs at high temperature. However, in intermediate temperature range, we obtained conflicting results between microscopic and macroscopic behavior.
Now, we are observing this system using Muller Matrix microscopy which was developed in our laboratory. Muller Matrix microscopy could detect, in principle, any change of polarization states induced by the sample and therefore it is expected to elucidate structural dynamics around the nematic phase.

3PT146 細胞毒性を有する酸化コレステロールのホスファチジルコリン膜分子充填への影響

Effect of cytotoxic oxysterols on the molecular packing of phosphatidylcholine membranes

Tatsuya Hoshino[1], Takaaki Hikima[2], Masaki Takata[2], Toshihide Kobayashi[3], Hiroshi Takahashi[1] ([1]*Grad. Sch. Eng., Gunma Univ.*, [2]*Harima Inst., Riken*, [3]*Wakou Inst., Riken*)

Oxidative stress induces the conversion from cholesterol (CH) to various oxysterols in biomembranes. Some oxysterols are cytotoxic. For example, 7 β-hydroxycholesterol (7 β-OH) and 25-hydroxycholesterol (25-OH) have been reported to be associated with neurodegenerative diseases and arteriosclerosis, respectively.
The oxysterol-related diseases presumably result from the difference between CH and oxysterols on ability to modulate the biophysical properties of the membrane bilayer. In this work, to gain fundamental insight into the effects of oxysterols on biophysical properties of biomembranes, we investigated the molecular packing of binary mixtures of dipalmitoylphosphatidylcholine (DPPC)/CH, DPPC/7 β-OH, and DPPC/25-OH.
The apparent specific volumes estimated by neutral flotation method were same for all three mixtures, at least, from 0 to 40 mol% sterol concentrations. Meanwhile, X-ray diffraction analysis of the mixtures containing 30 mol% sterols showed that the order of the bilayer thickness was DPPC/CH < DPPC/25-OH <DPPC/7 β-OH.
These results indicate that the addition of OH group by oxidation decreases CH's capacity of condensing the bilayer in the lateral direction and the OH group on the middle position more strongly perturbs the molecular packing of bilayers than that on the edge position.
We are also currently studying palmitoyloleoylphosphatidylcholine/oxysterol mixtures.

3PT147 ジヘキサデシルホスファチジルコリンの指組ゲル相二層膜間の氷点下温度における水和斥力

Hydration repulsive force of the interdigitated phase of dihexadecylphosphatidylcholine at subzero temperatures

Hiroshi Takahashi (*Grad. Sch. Eng., Gunma Univ.*)

The clarification on the interactions of lipid bilayers is one of the most important issue of membrane biophysics, however, many aspects of these interactions still remain mysterious. One of such examples is “hydration repulsive forces” and several different explanations on its origin have been proposed. Here we investigated the hydration repulsive force between the interdigitated ($L_{\beta}I$) phase bilayers of dihexadecylphosphatidylcholine (DHPC) at subzero temperatures. The number of headgoups per an unit area at the bilayer surface of the interdigitated phase is about twice as compared with normal gel ($L_{\beta'}$) phase. The measurement of the force was carried out by using our previously proposed method [1] based on the combination of ice formation free energy values and structural information obtained by X-ray diffraction. The estimated hydration repulsive force curve of DHPC in the $L_{\beta}I$ phase was different from that of dipalmitoylphosphatidylcholine (DPPC) in the $L_{\beta'}$ phase. This suggests that headgroup (dipole moment) density affects the hydration repulsive force profiles. In addition, we are planning to present the result of dipalmitoylphosphatidylethanolamine (DPPE) and will also discuss the effects of the difference of headgroup on the hydration repulsive forces.

[1] H. Takahashi & P.J. Quinn, *Mol.Cryst. Liql.Cryst.* **367** (2001) pp.427-434

3PT148 架橋脂質二分子膜における秩序液体相／液晶相の分離

Localization of Liquid-Ordered/Liquid-Crystalline Phase Separation at a Lipid Bilayer Suspended over Microwells

Koji Sumitomo[1], Yukihiro Tamba[2], Aya Tanaka[1], Touichiro Goto[1], Keiichi Torimitsu[1] ([1]*NTT Basic Research Labs.*, [2]*Suzuka Nat. Coll. of Tech.*)

The localization of liquid-ordered (Lo) and liquid-crystalline (L α) phase domains is investigated on a silicon substrate with a microwell array. The localization of Lo and Lα phase separation as a model of a lipid raft plays an important role regarding the arrangement and function of membrane proteins. When we fabricate a nanobiodevice that works with membrane proteins, controlling the function of proteins is a key technique. A microwell array with a sealing lipid bilayer, whose phase separation can be controlled, will be a promising platform for nanobiodevices.
Suspended lipid bilayers were formed by rupturing giant unilamellar vesicles (GUVs) on the substrate. The GUVs were prepared from ternary mixtures of DOPC, DPPC, and cholesterol. We found that the Lα phase is preferable at the suspended membrane over microwells because of its curvature. On the other hand, the Lo phase domain disappeared from the suspended membrane. Phase separation and localization are governed by the stiffness and line tension of the membrane. Lateral diffusion at the molecular level occurs quickly, although domain movement is restrained at the supported membrane by the interaction with the substrate. Unsaturated lipid is condensed at the suspended membrane, and saturated lipid and cholesterol are excluded. Additional phase transition and domain rearrangement occurs. By modification of surface roughness, charge, and/or chemical state, the localization of phase separation on the suspended lipid bilayer will be controlled.

3PT149 ラウリル硫酸ナトリウム(SLS)溶液塗布によるヒト皮膚角層の構造変化

Effect of sodium lauryl sulfate on the human stratum corneum structures

Hironori Yoshida[1], Satoe Azechi[2], Hiromitsu Nakazawa[1], Yasutami Shigeta[2], Satoru Kato[1] ([1]*Sch. Sci. Tech., Kwansei Gakuin Univ.*, [2]*SUNSTAR INC.*)

The stratum corneum (SC), a thin envelope surrounding our body, is known to be responsible for the skin barrier function. It consists of corneocyte cells filled with keratin filaments and intercellular lipid layers. In this study we examined the effect of a substance inducing rough skin on the SC structures by electron diffraction measurements to clarify its permeation path in the human SC. Layers of corneocyte cells were stripped off from the surfaces of human forearms of five subjects with glue-coated grids for electron microscopy after administration of a 1% sodium lauryl sulfate (SLS) aqueous solution on the skin surface. Control specimens were collected from the opposite forearms without the SLS treatment. Acquisition of electron diffraction patterns was carried out under very low electron dose conditions (~3 e/nm^2) with an electron microscope (JEM1400) equipped with a high-sensitivity CCD camera. One-dimensional diffraction profiles were calculated for analysis of the structural change induced by the SLS permeation. Our results suggested that the lipid packing structures remain intact during the SLS permeation though the transepidermal water loss increases significantly. Furthermore, the SLS treatment seemed to slightly reduce the diffraction intensity around 2.0 nm^{-1}, which comes from the structure other than the well-established orthorhombic or hexagonal domains in the intercellular lipid layers. We speculate that the applied SLS molecules penetrated into the corneocyte cell body to affect the keratin filament structure.

3PT150 高感度 DSC によって求めたジトリデカノイルホスファチジルコリン-コレステロール系の詳細な相図

Detailed Phase Diagram of Ditridecanoylphosphatidylcholine-Cholesterol System Determined by High-Sensitivity DSC

Yasushi Kamitani, Fumihiro Okazaki, Yasuo Saruyama, Haruhiko Yao (*Gra. Sch. Sci. Tech., Kyoto Inst. of Tech.*)

It was recently found that the L_x phase exists in ditridecanoyl-phosphatidylcholine (DC13PC)[1]. Besides, the L_x phase is the liquid-ordered phase reported in phosphatidylcholine-cholesterol system, because there is no phase line between the L_x phase of pure DC13PC and the liquid-ordered

phase of DC13PC-cholesterol mixtures in the binary phase diagram. However, our previous phase diagram was determined every 5 mol% cholesterol concentration. Thus, there is some risk that we might miss the phase line if it is nearly normal to the concentration axis. Therefore, we have performed heat capacity measurements on DC13PC-cholesterol binary mixtures to make the phase diagram more detailed using high-sensitivity DSC developed in our laboratory. As a result, it is confirmed that phase transition was not observed between the L_x and liquid-ordered phases, and that the L_x phase is the liquid-ordered phase. Moreover, it is found that the temperature range of the liquid-ordered phase drastically increases at cholesterol concentrations higher than 23 mol%. The detailed phase diagram will be presented.

[1] F. Okazaki, Y. Saruyama, H. Yao: *Abstracts of 46th Annual Meeting of the Japan Society of Calorimetry and Thermal Analysis,* (2010)2B1420.

3PT151 高感度 DSC によるヒト皮膚角層の熱容量測定

Heat Capacity Measurement of Human Stratum Corneum using High-Sensitivity DSC

Keisuke Oki[1], Ichiro Hatta[2], Yasuo Saruyama[1], Haruhiko Yao[1] ([1]*Gra. Sch. Sci. & Tech., Kyoto Inst. of Tech.*, [2]*Nagoya Ind. Sci. Res. Inst.*)

The outermost layer of skin called stratum corneum (SC) is composed of corneocytes and intercellular lipids. Intercellular lipids have the long and short lamellar structures (LSs). It has been proposed that the short LS plays an important role in control of water content in skin [1]. Therefore, we have performed DSC measurements of human SC at various water contents between 0-40wt% using high-sensitivity DSC developed in our laboratory. Human SC was dried under vacuum overnight. The water content of the dried SC was defined as 0 wt%. Disk-shaped pieces (3 mm diameter) were punched out from the dried SC and hydrated in a container where relative humidity was controlled with glycerol aqueous solution until they had reached a desired water content. Then, they were sealed into a gold pan. DSC measurements were performed in the temperature range of -20-130 °C. For human SC with a water content of 20 wt%, thermal anomalies were observed at 9, 20-60, 75 and 89 °C on 1st heating. The phase transition at 9 °C, that had not been reported previously, was observed at all water contents between 0-40 wt%. On 1st and successive cooling, thermal anomalies were observed at -2, 12, 32, and 70 °C. On 2nd and successive heating thermal anomalies were observed at 5, 15, 33, and 71 °C. At higher water content, it is found that the anomaly at 70-71 °C splits into two anomalies. To identify the phase transitions, we have performed x-ray diffraction measurements and the results will be presented.

[1] I. Hatta *et al., Biochim. Biophys. Acta* **1758** (2006) 1830.

3PT152 モデル細胞内における相分離とミクロゲルのパターン形成

Gel pattern formation in model cells coupled with phase separation

Shinpei Nigorikawa, Masayuki Tokita, Miho Yanagisawa (*Grad. Sch. Sci., Kyushu Univ.*)

It is known that huge amount and great variety of macromolecules are encapsulated in cells, and they maintain their appropriate spatial distribution inside of the cellular membranes. We used cell-sized water/oil droplet coated by a lipid layer as a cell model, and studied phase separation of binary polymer solution: gelatin and polyethylene glycol (PEG) aqueous system. This system shows phase separation and gelation of gelatin with decreasing temperature, however, the mechanism to bring the phase separation has been unclear. Using fluorescence-labeled gelatin, we observed the pattern formation of gelatin-rich domains upon phase separation by a fluorescence microscope. At first, the time development of domain size was analyzed in PC (phosphatidylcholine) droplets, and found that the growth rate was decreased with an increase in droplet size. Therefore, at a given time, the number of domains in small droplets <30μm is larger than that in large droplets > 100μm. This acceleration of domain growth in smaller droplets may be originated from the depletion effect between rigid gelatin and soft PEG molecules under micro-scale confinements. On the other hand, in the case of PE (phosphatidylethanolamine) droplets, a thin layer of gelatin gel was observed at the interface. It is illustrated that the negatively charged PE membrane has an electrostatic attractive force with electrolyte gelatin gel. Furthermore, shape deformation of droplets coupled with the gel patterns was observed, and was discussed from the Young-Laplace equation.

3PT153 脂質膜ヘテロ界面はナノ物質をサイズ依存的に識別する
1YS1045 Size-dependent selective localization of nano-particles on heterogeneous membrane surfaces

Tsutomu Hamada, Masamune Morita, Makiyo Miyakawa, Masahiro Takagi (*Japan Adv. Inst. of Sci. and Tech.*)

It is of biological importance that we understand the biophysical mechanisms that govern the interaction between nanoparticles (NPs) and heterogeneous cellular surfaces because of the possible cytotoxicity of engineered nanomaterials. In this study, we investigated the lateral localization of NPs within a biomimetic heterogeneous membrane interface using cell-sized two-phase liposomes. We found that lateral heterogeneity in the membrane mediates the partitioning of NPs in a size-dependent manner: small particles with a diameter of <200 nm were localized in an ordered phase, while large particles preferred a fluidic disordered phase. This partitioning behavior was verified by temperature-controlled membrane miscibility transition and laser-trapping of associated particles. In terms of the membrane elastic energy, we present a physical model that explains this localization preference of NPs. The calculated threshold diameter of particles that separates the particle-partitioning phase was 260 nm, which is in close agreement with our observation (200 nm). These findings may lead to a better understanding of the basic mechanisms that underlie the association of nanomaterials within a cell surface.

3PT154 UV irradiation driven deformation of photoresponsive molecule doped membrane

Kazunari Yoshida, Yasuhiro Fujii, Izumi Nishio (*Sci. and Eng., Aoyama Gakuin Univ.*)

The phospholipid bilayer has been widely studied as a model system of biological membrane since its structure is the main component of biomembrane. In particular, the deformation of the vesicles has been intensively investigated in relation to the exocytosis and endocytosis.

In the previous study, we doped the photoresponsive molecule *pseudogem*-Bis (diphenylimidazole) [2.2] paracyclophane (abbreviated as "*pseudogem*-BisDPI [2.2]PC" hereafter) to DOPC multilamellar vesicles, and performed UV light irradiation experiments. The *pseudogem*-BisDPI [2. 2] PC has one [2. 2] paracyclophane that bridges two diphenylimidazoles and one C-N bond that connects two imidazole rings. The C-N bond is easily cleaved by UV irradiation. It was found that the shape of the doped membrane began to change after about 10 seconds of UV irradiation, and its surface area per volume increased with time. Shape of the vesicle was changed into rippling form. We assumed that increasing of surface area per volume of the vesicle was caused by *pseudogem*-BisDPI[2.2]PC that excluded lipids of around the molecule with UV exposure.

In this study, we improved the experimental condition of forming vesicles so that the unilamellar structure became dominant because we can analyze unilamellar spherical vesicles easier than multilamellar vesicles with irregular-form. In this presentation, we discuss the membrane deformation of unilamellar vesicles.

3PT155 フリップフロップのダイナミクスの直接的観察

Direct observations of flip-flops in membranes

Takuma Akimoto[1], Noriyoshi Arai[2], Eiji Yamamoto[1], Kenji Yasuoka[1], Masato Yasui[3] ([1]*Department of Mechanical Engineering, Keio university*, [2]*Department of Mechanical Engineering and Intelligent Systems, University of Electro-Communications*, [3]*Department of Pharmacology, Keio university*)

How do lipid molecules in membranes perform a flip-flop? Flip-flop of a lipid molecule plays a crucial role in membranes. However, little is known regarding the way of flip-flop by experiments as well as molecular dynamics simulations. Here, we observe single molecules performing filip-flops in membranes using DPD simulations. There are three different ways of flip-flop, which can be clearly characterised by paths in a free energy surface. Furthermore, we find that interevent times of flip-flop are distributed according to the exponential distribution with cutoff. The rate of flip-flop depends on temperature.

3PT156 Low-frequency dynamics of phospholipid bilayers studied by terahertz time-domain spectroscopy

Tomoyo Andachi[1], Naoki Yamamoto[2], Atsuo Tamura[1], Keisuke Tominaga[1,2] ([1]*Grad. Sch. Sci., Univ. Kobe*, [2]*Molecular Photoscience Reserch Center, Univ. Kobe*)

Phospholipid is a main component of cell, which forms bilayers by self-assembling. Lipid bilayers, which are usually hydrated, continuously fluctuate due to thermal activation in the terahertz (THz; 1 THz ~ 33 cm^{-1}) frequency region. These fluctuations originate from delocalized vibrational motions of

lipid molecules and/or hydrogen-bond making and breaking dynamics with water molecules. Therefore, terahertz time-domain spectroscopy (THz-TDS) is a powerful tool to investigate lipid molecule dynamics. In this study, we focus on dependence of the low-frequency dynamics of lipid bilayers on hydration, temperature, and their structure by using THz-TDS. As a sample, we selected 1, 2-Dimyristoyl-*sn*-glycero-3-phosphoglycerol (DMPG), which is known to form several different structures like crystalline or gel phase states. We measured the temperature dependence of the low-frequency spectra of the DMPG under different hydration degrees and structures. The absorption coefficients of each sample were obtained in the frequency region from 10 cm^{-1} to 50 cm^{-1}. We discuss about the dynamics of DMPG from the changes of the absorption coefficients.

3PT157 表面張力レプリカ交換法による脂質二重膜の構造サンプリング

Surface tension replica exchange molecular dynamics method for an efficient sampling of lipid bilayer structures

Takaharu Mori[1], Yuji Sugita[1,2,3] ([1]*RIKEN Quantitative Biology Center*, [2]*RIKEN Advanced Institute for Computational Science*, [3]*RIKEN Advanced Science Institute*)

Generalized ensemble algorithm is one of the efficient sampling methods for biomolecular systems. Recently, various replica exchange molecular dynamics methods (REMD) in different parameter spaces have been developed. However, simulations for membranes or protein-membrane systems are still difficult with generalized ensemble algorithms, because the membrane can easily collapse in such enhanced sampling methods like temperature REMD. To overcome this problem, we propose a new replica exchange molecular dynamics method, where the surface tension of the system in an NPγT ensemble is exchanged (γ REMD). Exchanging the surface tension can moderately induce the deformation of lipid bilayers. We introduced γ REMD in our laboratory-developed MD program (GENESIS), and it was applied to a fully hydrated 1,2-di-palmitoyl-phosphatidylcholine (DPPC) lipid bilayers. We found that the area per lipid and membrane thickness can change significantly in the γ REMD simulation, compared to the single NPγT simulation. We believe that our method is useful for investigating structural properties of lipid bilayers, conformational changes of membrane proteins in membranes, and protein-lipid interactions.

3PT158 膜厚変化とゲル、アミノ酸、水素化アモルファスシリコンを用いたイオン伝導整流素子の特性

Film thickness and property of ion conductive rectification element using amino acids, gel and hydrogenated amorphous silicon

Takahiko Sano[1], Hideaki Sugawara[1], Takaaki Ichikawa[1], Yuuki Hiramitsu[1], Hiroshi Masumoto[2], Takashi Goto[3], Yutaka Tsujiuchi[1] ([1]*Department of Material Science and Engineering, Akita University*, [2]*Center for Interdisciplinary Research, Tohoku University*, [3]*Institute for Materials Research, Tohoku University*)

This report mainly focuses an electro-potential-current property correlated with film thickness on ion conductive rectification element using amino acids, gel and hydrogenated amorphous silicon. In general, ionic conduction, in solution as well as in intermediate states between a liquid and a solid, such as gels, is a phenomenon key to inter-conversion between light energy, chemical energy, and electric energy. As such, this phenomenon is essential for devices that store, generate, and convert electric energy, including batteries, photovoltaics, capacitors, and actuators. This report secondly focuses on ionic conduction in nontoxic materials to discuss the creation of elements coated with multi-layer functional thin-films using a combination of different technologies, such as the rectification property of ionic conduction, photo-induction control, and the use of wavelength conversion materials, and the potential application of these materials to biological tissue. Ion conductive behaviors of neutral, acidic, or basic amino acid dispersed in agarose gel are characterized. We report an attempt of measuring a photo-controlled effect of a-Si:H film on ion conducting behavior of bio-molecules in detail, comparing several thickness of a-Si:H film.

3PT159 BLM を介したイオン性蛍光プローブの膜透過性―電流と蛍光に基づいた動的解析―

Permeability of an ionic fluorescent probe through a BLM - dynamic analysis based on an electric current and a fluorescent change-

Yasuhiro Naka, Yumi Yoshida, Megumi Shimazaki, Kazunari Sakai, Kohji Maeda (*Department of Chemistry and Materials Technology, Kyoto Institute of Technology*)

Transport of an ionic species through a bilayer lipid membrane, BLM, is influenced not only by its hydrophobicity but also by a coexisted counter ion, and the transport mechanism has been considered to be complicated. Recently, new opinion for the BLM transport of an ion has been reported by Shirai et al. [1, 2]. In the opinion, a BLM was recognized as like a thin liquid membrane with two aqueous/membrane interfaces. The transferring ion distributes to a BLM with coexisted counter ion and transports across the BLM keeping electroneutrality in the BLM. Electrochemical results were given as experimental evidences for the transport mechanism, but not enough for supporting the cotransport mechanism which is not detected by electrochemical measurement. In the present work, an ionic fluorescent probe was employed as the transferring ion through a BLM. Transport of the probe was detected not only as the ion transfer current but also as fluorescent change near to the BLM induced by the ion transport. Comparing the transport current with the fluorescent change, whether the transferring species is ionic or neutral was estimated. According to the observation, the mechanism of ion transport through a BLM was discussed. [1] O. Shirai, S. Kihara, Y. Yoshida, M. Matsui: J. Electroanal. Chem., 389, 61-70 (1995) [2] O. Shirai, Y. Yoshida, M. Matsui, K. Maeda, S. Kihara: Bull. Chem. Soc. Jpn., 69, 3151-3162 (1996)

3PT160 ABC トランスポーターのヌクレオチド結合ドメインに対する ATP 結合自由エネルギー計算

Calculation of the binding free energy of ATP to the nucleotide binding domain of an ABC transporter

Yusuke Kaneta, Shuntaro Chiba, Tadaomi Furuta, **Minoru Sakurai** (*Center for Biol. Res. & Inform., Tokyo Tech*)

ABC (ATP-binding Cassette) transporters exist in almost all kinds of living things and use ATP as an energy source to transport a wide range of substrates across the membrane. ABC transporters have the common 3D structural architecture: the whole molecule is divided into two domains, that is, Transmembrane Domain (TMD) and Nucleotide-Binding Domain (NBD). NBD has two highly conserved ATP binding sites (Walker A&B and LAGGQ). It has been proposed that binding of ATPs to these sites induces the dimerization of two NBDs, eventually leading to a large structural change from the inward- to outward-facing conformation of TMD.

Our study is to elucidate this structural change mechanism from energetic aspects. In this study, as a first step, we evaluated the free energy gain obtained from binding of the ATP to NBD. We examined this for NBDs in the maltose transporter ($MalFGK_2$) from *Escherichia coli*. For this purpose, molecular dynamics (MD) simulations were performed starting from the crystal structure of the NBD dimer and subsequently the above free energy was calculated according to the MM/PBSA method.

We first evaluated the binding energy of one ATP molecule to an NBD monomer. The resultant values were -37.6 and 4.1 kcal/mol when ATP binds to the Walker A&B motif or the LSGGQ one, respectively. Next, the NBD dimerization energy was evaluated to be -5.91 kcal/mol. We are now calculating the binding free energies of ADP and inorganic phosphate (Pi) to an NBD to elucidate the role of ATP hydrolysis in the substrate transportation process.

3PT161 パターン化モデル生体膜へのロドプシンの再構成

Reconstitution of rhodopsin into micropatterned model biological membrane

Keisuke Okada[1], Kenichi Morigaki[1,2], Fumio Hayashi[3] ([1]*Grad. Sch. Agr., Univ. Kobe*, [2]*Res. Cent. Env. Genomi., Univ. Kobe*, [3]*Grad. Sch. Sci., Univ. Kobe*)

Rhodopsin (Rh) is a photoreceptor that forms a complex with transducin (G_t) upon activation by light. It has been reported that the affinity of Rh*-G_t complex to lipid rafts (raftophilicity) was higher than that of Rh (Hayashi et al. ARVO meeting (2011)). We are developing a methodology to evaluate the raftophilicity quantitatively with a supported phospholipid bilayer (SPB). Micropatterned SPBs composed of photo-polymerized lipid bilayer and fluid lipid bilayer. By changing the compositions of polymeric and fluid bilayers, liquid ordered (l_o) domains and liquid disordered (l_d) domains in the fluid bilayer were separated into a pre-determined pattern. To measure the localization of Rh and Rh*-G_t in l_o regions, we incorporated Rh into SPB by rapid dilution of Rh/ octylglucoside micelles. We confirmed single Rh molecules in SPB by TIRF-microscopy. Furthermore, we observed binding of fluorescently labeled α-subunit of G_t ($G_{\alpha t}$) upon activation of Rh and changes in

the mobility of Rh*-G_t upon subsequent addition of GTP. Hence, we concluded that Rh and G_t in SPB were active. At the same time, we also observed some immobile Rh molecules in SPB, which could interfere with the analysis of raftophilicity. We discuss on the reconstitution strategies of Rh to establish the means to measure the raftophilicity in micropatterned l_o domains.

3PT162 カリウムチャネル KcsA の開閉によるリン脂質の flip-flop 誘起能の評価

Induction of phospholipid flip-flop by KcsA channel gating

Hiroyuki Nakao[1], Masaki Wakabayashi[1], Yasushi Ishihama[1], Minoru Nakano[2] ([1]*Grad. Sch. Pharm. Sci., Kyoto. Univ*, [2]*Grad. Sch. Med. Pharm. Sci., Fac. Pharm. Sci., Univ. Toyama*)

Regulation of phospholipid flip-flop is important for homeostasis of biological membranes. Flip-flop of phospholipids in the endoplasmic reticulum (ER) is very fast, compared to that in other membranes. However the flippases that govern the fast flip-flop in the ER have not been identified, and the mechanism by which the flip-flop is induced is still unknown. It has been reported that KcsA induces flip-flop of phospholipids. KcsA is a pH-dependent potassium channel, activated by acidic pH. Conformational change of transmembrane region during channel gating was recently observed at a single channel level. We therefore hypothesized that the fluctuation of transmembrane region influences flip-flop of phospholipids.
Dithionite reduction assay was used to measure flip of C_6 -NBD-phosphatidylcholine (C_6-NBD-PC) in proteoliposomes, composed of PC and KcsA. KcsA was found to induce flip of phospholipids at acidic pH, while less affected at neutral pH. To confirm whether the fluctuation of transmembrane region of KcsA induce flip, we measured flip of C_6-NBD-PC at acidic pH in the presence of tetrabutylammonium, which locks KcsA in the open state. The results showed that KcsA mediates flip of phospholipids even in the open-locked state. These results suggest that KcsA enhances flip of phospholipids not by the fluctuation of transmembrane region, but by the open structure or the change of charged state of amino acids in transmembrane region.

3PT163 人工細胞膜アレイを用いた全自動イオンチャネル計測システム

Automated Drug Screening System for Ion Channel Proteins using Artificial Cell Membranes

Ryuji Kawano[1], Yotaro Tsuji[1,4], Koki Kamiya[1], Toshihisa Osaki[1], Minako Hirano[3,5], Toru Ide[3,5], Norihisa Miki[1,4], Shoji Takeuchi[1,2] ([1]*Kanagawa Academy of Science and Technology (KAST)*, [2]*IIS, Univ. of Tokyo*, [3]*Riken*, [4]*Keio Univ.*, [5]*The Graduate School for the Creation of New Photonics Industries*)

This paper describes an automated drug screening system for Ca2+-activated K + channel (BK channel). BK channels are pharmacological targets for the treatment of stroke. We have been developing multiple lipid bilayer membranes (BLMs) system for reconstituting the membrane proteins. In this study, we are succeeded in simultaneous reconstitution of BK channels in the BLMs array using an injection robot, and the channel inhibition behavior was examined using K+ channel blocker. Our system can be applied to a high-throughput screening (HTS) system for drug discovery. Membrane proteins account for approximately 25% of the polypeptides encoded within the human genome. Of these, ion channels are an important class of proteins that mediate ion flow across cellular membranes and which, among other things, are responsible for the excitability of neurons. In the drug discovery, the high-throughput screenings of the ion channels are highly desirable. We have been developing the lipid bilayer membrane array for the HTS of the ion channels using MEMS technology. BK channels are essential for the regulation of several key physiological processes including smooth muscle tone and neuronal excitability. We have therefore attempted to reconstitute BK channel within the artificial lipid bilayers. In this study, BK channels were automatically reconstituted in the BLMs array device by using an injection robot, and also the channel activity was examined using its inhibitor.

3PT164 KcsA カリウムチャネル活性に影響を及ぼすリン脂質作用部位の同定

Identification of the interaction site with the effective phospholipids for the KcsA potassium channel activity

Masayuki Iwamoto, Shigetoshi Oiki (*Dept. Mol. Physiol. Biophys., Univ. Fukui Facult. Med. Sci.*)

Membrane lipids are known to affect the function and activity of ion channels. Specific lipid molecules are indispensable for some ion channels to become active. How the specific lipids regulate the ion channel activity is essential to understand the structure-function relationship of ion channels in the membrane environment. For the KcsA potassium channel, anionic phospholipids such as phosphatidylglycerol (PG) have been thought to play an essential role in its activity as the KcsA channel exhibits quite low open probability in the absence of these lipids. Our previous study revealed by means of single-channel current recordings in the asymmetric lipid bilayer that the KcsA channel requires PG molecules in the inner leaflet to exhibit high open probability. In this study we tried to identify the interaction site with PG within the KcsA molecule for further understanding of lipid-mediated regulation of the KcsA channel activity. Potential positive charges such as Arg, Lys and His were expected to be candidates for the interaction site with PG. We found that mutation of several sites out of 24 potential positive charges in the monomeric KcsA molecule were sensitive to the PG effect on the KcsA channel activity. Mechanism underlie PG-mediated regulation of the KcsA channel opening will be discussed.

3PT165 Kv1.2 チャネルでの選択的イオン透過

Selective Ion Permeation though the Kv1.2 Channel

Takashi Sumikama[1], Shinji Saito[2], Shigetoshi Oiki[1] ([1]*University of Fukui*, [2]*Institute for Molecular Science*)

Ion selectivity is a crucial function for ion channels. So far, it has been considered the K^+ channels discriminate for K^+ over Na^+ more than a thousand-fold due to the destabilized binding of Na^+ at the selectivity filter. However, several recent researches showed that Na^+ can enter into the selectivity filter and permeate: the x-ray crystallographic structure of the K^+ channel with Na^+ was resolved, where Na^+ ions form six-coordination structure in the selectivity filter. Its structure was then supported by theoretical calculations. The electrophysiological measurement also suggested that a certain amount of Na^+ ions can permeate through the K^+ channel by punch-through mechanism. Thus, there still exists controversial arguments concerning the ion selectivity. Here we observed the efflux of ion in the mixed ion solution, 200 mM KCl and 200 mM NaCl, through the Kv1.2 channel by the molecular dynamics simulation. It is found that K^+ ions permeate at rates at about five times higher than Na^+ ions, which is approximately the same ratio the punch-through mechanism reported. We also found that once ions, regardless of ion species, enter into the central cavity, they cannot return to the cytoplasmic side solution. This means the selectivity is caused by the free energy barrier at the entrance of the channel. Therefore, the selectivity is a part of ion permeation issues rather than the stability of ions in the channel; kinetics, instead of thermodynamics, determines the ion selectivity.

3PT166 Controlling an ion channel's voltage sensing domain without voltage

Morten Bertz, Kazuhiko Kinosita (*Waseda University, Dpt. of Physics*)

Voltage gating - the opening and closing of ion channels on response to changes in membrane potential - is fundamental to signal transduction in living organisms. Voltage gating is achieved by four voltage sensing domains (VSDs) that surround the ion-conducting pore of the channel protein. In these VSDs, conserved positively charged residues located in the S4 transmembrane helix move according to the transmembrane electrical field, and the resulting conformational change is transmitted to the channel pore. Up to date, however, direct structural information on the deactivated, closed state of a channel has remained elusive. Consequently, the extent and direction of the VSD movement remain controversial, with both small translations and large-scale movements reported in the literature depending on the technique used in the investigation. Here, we attempt the manipulation of voltage sensor conformation using engineered probes as a substitute for voltage to shed light on the transitions involved in voltage gating.

3PT167 ガラス針による人工平面膜へのイオンチャネルの再構成

Reconstitution of ion channel into lipid bilayer using glass needle

Daichi Okuno[1], Minako Hirano[2], Yukiko Onishi[1], Toshio Yanagida[1], Toru Ide[2] ([1]*Quantitative Biology Center, Riken*, [2]*The Graduate School for the Creation of New Photonics Industries*)

Ion channels are membrane proteins that regulate cell functions by controlling ion flow through cell membrane. To elucidate the molecule mechanism of the regulation for the ion flow, it is necessary to investigate the relationship between the conformation and function and interaction with some factors. To aim this task, ion channel is kept suppressing lateral diffusion in the membrane for

detecting conformational change, ligand desorption and current at the same time and it is preferable to fix ion channel to solid support in the lipid bilayer. We have previously reported that the reconstitution of ion channel fixed onto the solid support such as agarose bead and the tip of AFM cantilever into lipid bilayer. In this study, we conducted reconstitution of ion channel into lipid bilayer using glass needle as a solid support. The tip of glass needle (<100 nm) was modified with Ni-NTA and ion channel (KcsA) was fixed on it through interaction between His-tag and Ni-NTA. It was also available for reconstitution of ion channel into lipid bilayer as well as AFM cantilever. There is possibility that simultaneous optical and electrical recording system for single ion channel may be built without complicated optics when using optical fiber instead of glass needle.

3PT168 生物物理学的解析を目指した、哺乳培養細胞を用いた哺乳類カリウムイオンチャネルの大量発現の試み

Trials of large amount expression of mammalian potassium ion channels using cultured mammalian cells for biophysical analyses

Hisao Tsukaoto[1], Koichi Nakajo[2], Yoshihiro Kubo[2], Yuji Furutani[1] ([1]*Institute for Molecular Science*, [2]*National Institute for Physiological Sciences*)

Ion channels are very important membrane-spanning proteins, which regulate permeability of ions between outside and inside of living cells. Thus, it is important to understand how ion channels function using various biophysical techniques. For example, infra-red (IR) spectroscopy on ion channels is expected to reveal how the channels discriminate different ions and undergo conformational changes in the channel functions. In fact, IR spectroscopy is applicable to analyses of a bacterial potassium channel KcsA, and the ion-protein interactions at the selectivity filter (1). It is natural to suppose that you could do similar studies on other ion channels, in particular mammalian ones. However, there is a problem on studies of mammalian ion channels. IR spectroscopy requires only several μg of purified proteins for the measurement, but in general, even such amount of mammalian ion channels cannot be expressed in E. coli. In this study, we tried to prepare sufficient amount of mammalian potassium channels using mammalian cultured cells. We made a series of constructs for expression of GFP-tagged ion channels. Based on profiles of fluorescence-detected size-exclusion chromatography (FSEC), we screened various potassium channels derived from human and mouse, and selected channels that can be highly expressed in the cultured cells. Currently, we are trying to purify large amount of the screened channel proteins.
(1) Furutani et al., submitted., please see his presentation in this meeting.

3PT169 テトラエーテル型人工リン脂質とアポリポタンパク質からの膜ディスク形成

Membrane disc formation from tetraether-type artificial phospholipids and apolipoproteins

Teruhiko Baba[1], Toshiyuki Takagi[1], Toshiyuki Kanamori[1], Daisuke Handa[2], Tatsuya Oka[3], Hiroyuki Saito[2,3] ([1]*Res. Center Stem Cell Eng., AIST*, [2]*Fac. Pharm. Sci., Univ. Tokushima*, [3]*HBS, Univ. Tokushima Grad. Sch.*)

Plasma apolipoprotein A-I (apoA-I) molecules form a membrane disc in which a straight-chained phosphatidylcholine (PC) bilayer is accommodated. In order to apply this unique structure to membrane-protein reconstitution matrices, we tried to prepare membrane discs by employing a tetraether-type artificial PC (PTEPC), which forms stable monolayer membranes, and obtained the optimal molar ratio of lipid to apoA-I yielding relatively homogeneous membrane discs. The size distribution of membrane discs was examined by GPC and TEM techniques, and the average diameter of PTEPC membrane discs was 10-12 nm. The helices content of apoA-I in PTEPC membrane discs was comparable to those in bilayer-forming PC (*e.g.*, egg yolk PC and diphytanoyl-PC) membrane discs. By evaluating membrane disc stability from the viewpoint of guanidine-induced denaturation of apoA-I, PTEPC was found to form more stable membrane discs than straight-chained egg yolk PC. We will also discuss the usefulness of PTEPC membrane discs for membrane-protein reconstitution matrices.

3PT170 AFM Probing Opioid Signalosome on Neuroblastoma

Lara Villaruz[1], Junhua Li[1], Catherine Tardin[2], Daisuke Mizuno[1] ([1]*Kyushu Universiy*, [2]*IPBS/CNRS*)

Opioid receptors responsible for sensing pain signals are the major target of pain treatment. The opioid and other proteins confined in domains could play the role of signalosome that permits the encounter of various proteins involved in the fast response of receptor signaling to extracellular activation. Thus it is likely that the receptor function would coincide with dynamic physical properties of the signalosome. Geared towards this motivation, we aim to detect and quantify the interaction of the AFM probe modified with antiT7 and the T7-tagged receptor on SHSY5Y neuroblastoma. Forces between the tip and receptor were monitored by indenting and retracting the tip at different points. Molecular recognitions were evident from the attractive signals of a unique shape during the retract phase which increase from stretching the linker after binding until the bond breaks. In a single event, several bonds may be formed so that the unbinding force is a multiple of the elementary bond strength. To obtain a good statistical value in estimating the fundamental force, the force volume mode was used to conveniently record successive force curves in one file. The data analyzed with fuzzy logic for the event detection showed that single unbinding force is 123 pN. Since this is in the range consistent with those reported in literature, this indicates the potential of the sensor for localizing receptor sites in future studies on the effect of agonist stimulation on the receptor distribution and its association to changes in biophysical properties.

3PT171 Analysis of protein translocation in a reconstituted *Dictyostelium* cell membrane on a solid substrate

Kei Takahashi[1], Nao Shimada[1], Taro Toyota[1,2], Satoshi Sawai[1,2,3] ([1]*Grad. Sch. Arts Sci.,Univ. Tokyo*, [2]*Res. Center as Complex Sys. Bio., Univ. Tokyo*, [3]*PRESTO, Japan Science and Technology Agency*)

Rigorous analysis of spatio-temporal dynamics of cell motion, membrane deformation and their underlying biochemical reactions remain to be a challenge due to their complexity. From yeast to human, localized signaling at the plasma membrane such as activation of cdc42, rac and phosphatidylinositols signaling breaks the intracellular symmetry and plays a crucial role in generating polarized membrane extension and retraction. In an attempt to clarify and evaluate some of the critical dynamics involved in these processes, we developed a two-dimensional reconstituted membrane on a glass-substrate using lipid extracted from *Dictyostelium discoideum*. We have tested whether the solid-supported membrane in a microchamber containing extracted cytosol provides an appropriate microenvironment for localized signaling by observing translocation of PH-domain protein and PTEN which were tagged with RFP and GFP respectively. Signal intensities were analyzed by a confocal laser scanning fluorescence microscopy. We found that both the PH-domain protein and PTEN attached to the membrane within 20 seconds after application of the cytosol containing these proteins. Localization of these proteins appeared as transient reciprocal patches of micrometer order indicating that there was heterogeneity of phosphatidylinositols in our reconstituted membrane. We will discuss implications of our present observations to the *in vivo* dynamics of cell signaling during cell movement and chemotaxis of *Dictyostelium*.

3PT172 ラフト親和性 GPI アンカー型分子プリオンタンパク質の神経細胞膜でのダイナミクス

Dynamics of normal prion protein, a raft-associated GPI-anchored molecule, in the live neuronal plasma membrane

Yuri L. Nemoto[1], Chieko Nakada[1], Hiroko Hijikata[1], Takahiro K. Fujiwara[1], Rinshi S. Kasai[1], Yoshiro Ishikawa[1], Akihiro C. E. Shibata[1], Ankita Chadda[1], Roger J. Morris[2], Akihiro Kusumi[1] ([1]*Institute for integrated Cell-Material Sciences (WPI-iCeMS), Institute for Frontier Medical Sciences, Kyoto University*, [2]*Wolfson Centre for Age Related Disease, King's College London*)

The prion protein (PrP) is a glycosylphosphatidylinositol (GPI) -anchored protein located in the outer leaflet of the plasma membrane (PM) of neuronal cells in the brain. Misfolded forms of PrP cause prion diseases, such as Creutzfeldt-Jakob disease, by inducing abnormal folding of other normal PrP molecules and the subsequent clustering of the misfolded PrP molecules, which creates brain damage. The behaviors of these normal PrP in the PM and their functions remain unknown. Since GPI-anchored proteins are generally believed to be raft-associated, one of the general hypotheses for the propagation of misfolding involves concentration of both misfolded and normal PrP in raft domains, which enhances their close and prolonged interactions, somehow generating more misfolded molecules. Here, we investigated PrP dynamics in the neuronal PM. Using single fluorescent-molecule imaging, we found that: (1) the diffusion coefficient of PrP (0.22 square microns/s) was 2.4-times smaller than that of a control GPI-anchored protein Thy1 (0.53 square microns/s) in 1-week-old rat neurons, (2) this difference is unchanged in older neurons (2-week-old) or in CHO-K1 cells, and (3) immobilized fractions of these molecules represent 29% and 19% for PrP and Thy1, respectively. In addition, live PALM

observation revealed that some areas in the PM excluded PrP or Thy1 in the neuronal PM. These results suggest that there are two different-types of raft domains, dynamically concentrating PrP or Thy1 in the PM of non-stimulated cells.

3PT173 マガイニン 2 が誘起するポア形成の初期過程

The Initial Stage of Magainin 2-Induced Pore Formation in Lipid Membranes

Victor Levadny[1,2], Tomoki Takahashi[3], Jahangir Md. Alam[1], **Masahito Yamazaki**[1,3] ([1]*Int. Biosci., Grad. Sch. Sci. Tech., Shizuoka Univ.*, [2]*Rus. Acad. Sci.*, [3]*Dept. Phys., Fac. Sci., Shizuoka Univ*)

Antimicrobial peptide magainin 2 (M2) forms pores in lipid membranes to induce leakage of internal contents of cells, which is a main cause of its bactericidal activity. However, the mechanism of its pore formation remains unclear. In this report, to reveal the mechanism of the initial stage of the M2-induced pore formation in lipid membranes, first we examined the area change of lipid membranes during the interaction of GUVs of dioleoylphosphatidylglycerol (DOPG) and dioleoylphosphatidylcholine (DOPC) mixture with M2 solution using the micropipet aspiration method. The areas of 40%DOPG/60%DOPG- and 30%DOPG/70%DOPC-GUVs increased with an increase in M2 conc. in buffer. After the conversion from the M2 conc. in buffer to the M2 surface conc. in GUVs, we found that the fractional changes of the area of these GUVs were almost proportional to the M2 surface conc. Next we developed a simple theoretical model that describes the variations in the free energy of the system upon the binding of M2 into the outer monolayer of GUVs. Assuming that M2 molecules don't transfer into the inner monolayer of GUVs before the pore formation, the inner monolayer is stretched to produce tension, resulting in production of a local rarefaction in the lateral density of the inner monolayer, i.e., half-pores. When a half-pore attains a critical size, it transforms into a transmembrane pore. The lifetimes of intact GUVs were determined using the mean first passage time concept, which agreed with experimental data [1].

[1] *J. Phys. Chem. B.* 113, 4846, 2009

3PT174 外力が誘起する脂質膜の張力によるポア形成の速度定数

Rate constants of constant tension-induced pore formation in single GUVs

Taka-aki Tsuboi[1], Victor Levadny[2,3], Masahito Yamazaki[1,3] ([1]*Dept. Phys. Fac. Sci. Shizuoka Univ.*, [2]*Rus. Acad. Sci.*, [3]*Grad. Sch. Sci. Tec. Shizuoka Univ.*)

When external forces are applied to cells or liposomes, tension is induced in biomembranes or lipid membranes. It is considered that above a critical value of the intensity of tension a pore formation occurs to cause rupture of cells or liposomes. On the other hand, antimicrobial peptide, magainin 2 (M2), induces pore formation in single giant unilamellar vesicles (GUVs) at and above a critical surface concentration of M2 [1]. To compare the tension-induced pore formation with the M2-induced pore formation, we investigated the constant tension-induced pore formation in GUVs of dioleoylphosphatidylglycerol (DOPG) and dioleoylphosphatidylcholine (DOPC) mixture using the micropipet aspiration method.

First we applied aspiration pressure on a 40%DOPG/60%DOPC-GUV using a micropipet to produce a constant tension of 5.5 mN/m and kept this state for a long time. Suddenly a pore was formed to cause rupture of the GUV. When we made same experiments using many single GUVs, we found that the pore formation occurred stochastically. The time course of the fraction of intact GUV without rupture, $P_{intact}(t)$, was well fitted by a single exponential decay function. By this fitting, we obtained the rate constant of the pore formation, k_p, which was 6.3×10^{-3} s^{-1}. We made the same kinds of experiments under different constant tensions, and found that k_p increased with tension. We analyzed these results theoretically, and compared them with the M2-induced pore formation [1,2].

[1]*J. Phys. Chem. B*, 113, 4846, 2009, [2]*ibid*, 114, 12018, 2010

3PT175 ミトコンドリアの密集が ATP 合成に及ぼす影響

Effects of the crowding of mitochondria on their ATP production

Daiki Yoshimatsu, Yoshihiro Ohta (*Dept. of Biotech. and Lifesci.,Tokyo Univ. of Agric. and Tech.*)

Mitochondria are organelles which produce ATP through the transport of H^+ across the membrane. They are considered to locate at the regions where ATP is required. Intracellular distribution of mitochondria is non-uniform. Since the crowding of mitochondria will lead to the local increase in ATP concentration and the lack of substrates around mitochondria, the mitochondrial crowding might be unfavorable for ATP production. In the present study, to investigate the effects of mitochondrial crowding on their ATP production, we adsorbed isolated mitochondria on cover slips in different densities and measured ATP production and membrane potentials of mitochondria. Membrane potential of each mitochondrion was measured with TMRE fluorescence. To investigate ATP production rate of single mitochondria, ATP content in the supernatant and the number of mitochondria on a cover slip were measured. Interestingly, when we adsorbed mitochondria in the higher density, each mitochondrion produced ATP at a higher rate. Oligomycin, an inhibitor of F_oF_1-ATPase, negated the effects of mitochondrial crowding on their ATP production. In addition, mitochondrial crowding induced the polarization of mitochondria. When mitochondria were suspended in the buffer, we did not observe the dependence of ATP production on the mitochondrial concentration. The mechanism by which mitochondrial crowding stimulates their ATP production on cover slips will be discussed.

3PT176 Promotion of DNA delivery into nucleus dramatically enhances the transfection efficiency mediated by biosurfactant -containing liposomes

Yoshikazu Inoh[1], Tadahide Furuno[1], Naohide Hirashima[2], Dai Kitamoto[3], Mamoru Nakanishi[1] ([1]*Sch. Pharm., Aichi Gakuin Univ.*, [2]*Grad. Sch. Pharm. Sci., Nagoya City Univ.*, [3]*AIST*)

Gene transfection using cationic liposomes is a promising approach for the safe gene therapy. However, transfection efficiency by cationic liposomes has not been equal to those of by viral vectors yet. For successful gene transfection, there are several barriers to be overcome, such as process that the foreign gene passes through the plasma membrane, escapes from lysosomal degradation, and translocates into the nucleus. We previously showed that the biosurfactant mannosylerythritol lipid-A (MEL-A) -containing cationic liposomes could deliver foreign gene into the target cells through the membrane fusion between liposomes and plasma membrane. Using MEL-A-containing cationic liposomes, the foreign gene was rapidly and efficiently delivered into the nucleus because it was released into the cytosol directly and could escape from lysosomal degradation. Here, we investigated the effect of pre-condensation of plasmid DNA by a cationic polymer protamine on gene transfection. The pre-condensation of plasmid DNA significantly increased the transfection efficiency by cationic liposomes. The promotion was more effective in cationic liposomes with MEL-A than without MEL-A because MEL-A could accelerate greatly the delivery of pre-condensed plasmid DNA into the nucleus. Our findings indicate that combination of MEL-A-containing cationic liposomes and pre-condensed DNA might be a useful system for gene delivery to non-dividing cells and for clinical application.

3PT177 マスト細胞の開口放出様の膜融合におけるカルシウムの役割

Effects of Ca2+ on liposomal membrane fusion that mimics mast cell exocytosis

Satoshi Tadokoro, Yumiko Nagai, Hiroki Sakiyama, Naohide Hirashima (*Graduate School of Pharmaceutical Sciences, Nagoya City University*)

Mast cells involved in allergic reactions. Antigen stimulation causes elevation of the intracellular Ca(2+) concentration, which triggers the exocytotic release of inflammatory mediators. Recent researches have revealed that SNARE (soluble N-ethylmaleimide-sensitive factor attachment protein receptor) proteins such as syntaxin-3, -4, SNAP-23, and VAMP-8 are involved in mast cells exocytosis. Although mast cells exocytosis is Ca(2+) dependent, the role of Ca(2+) is not clear. Synaptotagmins are candidates of Ca(2+) sensor for exocytosis. Since synaptotagmin 2 is the most abundant isoform of synaptotagmins expressed in mast cells, in this study, we focused on the role of Ca(2+) in mast cell exocytosis by a liposome-based fusion assay. SNARE proteins (SNAP-23, syntaxin-3, VAMP-8) and synaptotagmin 2 were expressed in E. coli and purified as GST-tagged or His-tagged fusion proteins. These SNARE proteins were incorporated into liposomes by a detergent dialysis method. Membrane fusion between liposomes was monitored by fluorescence resonance energy transfer between fluorescent-labeled phospholipids. Ca2+ did not show any significant effects on SNARE mediated membrane fusion by itself, however, in the presence of synaptotagmin 2, Ca2+ induced membrane fusion. This action of synaptotagmin 2 required phosphatidylserine as a membrane component. These results suggest that Ca2+ regulates SNARE dependent membrane fusion in mast cells, and that this regulation is dependent on synaptotagmin 2 and phosphatidylserine.

3PT178 脂質二重膜上における Def6 PH ドメインの高次構造の解析

Conformational properties of the Def6 PH domain located at the lipid bilayer surface

Naomi Tokuda[1], Michikazu Tanio[2], Katsuyuki Nishimura[2], Toshiyuki Kohno[3], Daisuke Yokogawa[4], Takahisa Ikegami[5], **Satoru Tuzi**[1] ([1]*Grad. Sch. Life Sci., Univ. Hyogo*, [2]*Inst. Mol. Sci.*, [3]*Kitasato Univ., Sch. Med.*, [4]*Grad. Sch. Sci., Nagoya Univ.*, [5]*Inst. Prot. Res., Osaka Univ.*)

Conformations of the pleckstrin homology (PH) domain of SWAP-70-like adapter of T-cells (SLAT, also known as Def6) in solution and at the membrane surface were investigated by using circular dichroism (CD), fluorescence and NMR spectroscopy. Previously, we reported that the switch-associated protein (SWAP) -70 PH domain undergoes conformational alteration including the α-helix to random coil transition at the lipid bilayer surface. The random coil transition of the C-terminal α-helix was expected to allow water-exposed conformation of nuclear localization signal (NLS) sequence located in the C-terminal α-helix, and consequently regulates intracellular relocalization of SWAP-70. The Def6 PH domain shares high sequence homology with the SWAP-70 PH domain, but lacks NLS in the C-terminal α-helix. The CD and NMR spectra show that the β-sandwich core of the Def6 PH domain undergoes similar conformational change to that of the SWAP-70 PH domain at the lipid bilayer surface. On the contrary, the random coil transition of the C-terminal α-helix was not observed for the Def6 PH domain. The difference in the conformational properties of the C-terminal α-helices of the Def6 and SWAP-70 PH domain would related to the absence and presence of the functional NLS in the C-terminal α-helix.

3PT179 ErbB シグナル伝達過程において Shc と Grb2 は個別に反応する

Independent response of Shc and Grb2 in the ErbB signaling revealed by FCS/FCCS and single molecule analysis

Chang-Gi Pack, Yuko Saeki, Michio Hiroshima, Mariko Okada, Yasushi Sako (*RIKEN, ASI*)

The signaling pathway of ErbB receptors including ErbB1 - 4 is involved in diverse physiological processes such as cell proliferation, differentiation, apoptosis, and carcinogenesis. Systems-level analyses have been recently carried out for this pathway, combining conventional biochemical methods in vitro with computational simulation. However, information about spatiotemporal dynamics and reaction-kinetics of related proteins are largely lacking. It will be worthwhile to directly quantify the changes of localization, diffusion, and interaction of related proteins during the process in living cells. We have established a live cell FCS/FCCS and single molecule (SM) analysis of the proteins in the ErbB networks. Firstly, we focused on the behavior of diffusions of Shc52 and Grb2 and direct interaction between them. Complex formation between them is known to be necessary for activating Ras in the EGF (ErbB1 ligand) and HRG (ErbB3, 4 ligand) signaling process. Our analysis using live cells indicates that diffusoinal responses of the two cofactors to ligand stimulations were very different. Moreover, direct interaction between them was hardly found in living cells, even though interactions with ErbBs were detected for the factors. These results suggest that spatiotemporal responses of Shc52 and Grb2 with ErbB receptors are independently regulated in living cells, even details of the independent response have not been described until now. Our study will pave the way toward a new insight for the true role of Shc52 in the ErbB signaling.

3PT180 クロストークを利用したべん毛回転制御系の構築

Control of bacterial flagellar rotation via crosstalk from a non-cognate histidine kinase to the response regulator CheY

Tohru Umemura[1], Chiho Hara[2], Yoshiyuki Sowa[1,3], Ikuro Kawagishi[1,2,3] ([1]*Res. Cen. Micro-Nano Tech., Hosei Univ*, [2]*Dept. Frontier Biosci., Fac. Eng., Hosei Univ*, [3]*Dept. Frontier Biosci., Fac. Biosci. Appl. Chem., Hosei Univ*)

Escherichia coli has various two-component regulatory systems (TCS), typically consisting of a histidine kinase (HK) and a response regulator (RR) for responses to environmental changes. For instance, the chemotaxis of E. coli employs, as a central processing unit, a TCS consisting of CheA (HK) and CheY (RR). The activity of CheA is regulated but the four chemoreceptors in the cytoplasmic membrane in response to environmental stimuli. CheA autophosphorylates at its histidine residue and then donates its phosphoryl group to an aspartate residue of CheY. Binding of phospho-CheY to the flagellar motor induces its clockwise (CW) rotation. An *in vitro* study showed that 22 out of 30 HKs of E. coli transfer their phosphoryl groups to non-cognate RRs (Yamamoto et al., 2005). In this study, we examined *in vivo* whether the activity of CheY can be regulated by non-cognate HK, BaeS. We first established a CheY expression system under the control of the arabinose-controllable promoter. In a strain (HCB437), in which all the chemotaxis genes are deleted, the more CheY is expressed, the more population of cells tumbled. We then co-expressed BaeS with CheY in the same strain. The tumbling frequency of cells co-expressing BaeS and CheY was significantly higher than that of cells expressing only CheY. Furthermore, the addition of indole enhanced tumbling frequency of cells co-expressing BaeS and CheY, but not those expressing CheY only. Thus, crosstalk between BaeS and CheY appears to occur *in vivo*, providing a system to regulate flagellar rotation.

3PT181 T 細胞活性化におけるカルシウムシグナリングと細胞内構造変化の時空間定量解析

Spatial-temporal dynamics of calcium signaling and organelles in T cell activation

Masahiro Shimozawa[1,2], Yuma Ito[1,2], Makio Tokunaga[1,2], Kumiko Sakata-Sogawa[1,2] ([1]*Grad. Sch. Biosci. Biotech., Tokyo Inst. Tech*, [2]*RCAI, RIKEN*)

When cells are subjected to the specific signals, Ca^{2+} is released from the endoplasmic reticulum (ER) resulting store-operated calcium entry (SOCE) via calcium-release activated calcium (CRAC) channels in the plasma membrane. These channels are opened by STIM1, ER-resident calcium sensor, after depletion of intracellular Ca^{2+} stores. In T cell, the duration of this cytoplasmic Ca^{2+} increases controls the efficiency and specificity of the transcription of immune-related genes. STIM1 and Orai1, an essential pore subunit of the CRAC channel, accumulate in the area of contact between T cell and antigen presenting cells. Recently mitochondria are reported to translocate to the contact area and allow sustained Ca^{2+} entry. As STIM1 resides in ER membrane, the accumulation can cause the translocation of ER. Actually, we reported last year that ER redistributed in T cell activation. However, the relationship between Ca^{2+} release from ER, SOCE, and local cytosolic Ca^{2+} elevations in T cell activation is not known in detail. Here aiming to analyze the relationship between ER redistribution and local Ca^{2+} elevations, we visualized CRAC channels or ER redistribution using GFP fusion proteins. In addition, we visualized local Ca^{2+} entry via CRAC channels or Ca^{2+} dynamics in ER using genetically encoded calcium indicator. We will discuss spatial regulation of Ca^{2+} signaling by structural changes in T cell.

3PT182 低分子量 G タンパク質 Ras のフォトクロミック分子 PAM を用いた光制御

Photo-regulation of small G protein Ras using photochromic molecule

Seigo Iwata[1], Shinsaku Maruta[2] ([1]*Division of Bioinformatics, Graduate school of Engineering, Soka University*, [2]*Department of Bioinformatics, Faculty of Engineering, Soka University*)

Ras is one of small G-proteins known as a molecular switch. Ras performs intracellular signal transduction. Interestingly, the core nucleotide-binding motif is considerably conserved in Ras and the ATP driven motor proteins: myosin and kinesin. Therefore, it is believed that these bio-molecular machines share common molecular mechanism utilizing nucleotide hydrolysis cycle. Previously, we have incorporated photochromic molecules, 4-phenylazophenyl maleimide (PAM), into the functional site of kinesin as a photo-switching device and succeeded to regulate kinesin ATPase activities reversibly upon VIS and UV light irradiation.

In this study, we performed basic study to control the Ras function reversibly by light using photochromic molecules. First, to observe the nucleotide exchange reaction of Ras GTPase, we synthesized a new fluorescent GTP analogue, NBD-GTP that changes its fluorescent intensity along the formation of Ras-GTP, Ras-GDP-Pi and Ras-GDP states. Experimental data suggested that NBD-GTP bind to the nucleotide-free Ras with burst kinetics and subsequently the Ras-GTP transit to Ras-GDP-Pi state slowly. Second, to photo-regulate the GTPase activity of Ras, we designed the Ras mutants, which have an additional reactive cysteine residue at the functional region. In the preliminary experiment, the GTPase activity of Ras mutants modified with PAM was reversibly alternated upon ultra-violet and visible light irradiation.

3PT183 Gradient sensing limit in Dictyostelium discoiduem cell

Masaki Watabe, Kazunari Kaizu, Koichi Takahashi (*RIKEN*)

Dictyostelium discoideum cell can sense local gradient in cAMP concentration across the cell body, and move with directional preference toward or away from the source of cAMP in a wide concentration range from 10 pM to 10 uM. In shallow gradient less than 10^-3 nM/um, the cells showed no directional response and exhibit a constant basal motility. In the steeper gradient, the cells can spatially integrate information about 1-2% increase in cAMP concentration on the cell surface, but their directional response is largely fluctuated in the range of 60 to 180 degrees. Here we simulate single particle-based cellular dynamic model and quantitatively analyze the simulated data to determine threshold response of sensing the gradient signals at an upper-stream part of the chemotactic signaling pathway.

3PT184 3-クロロ安息香酸による 3-クロロ安息香酸分解細菌 *Burkholderia* sp. NK8 外膜ポリン遺伝子の転写促進

Enhanced transcription of a porin gene in a 3-chlorobenzoate degrading bacterium, *Burkholderia* sp. NK8, with 3-chlorobenzoate

Kimiko Yamamoto[1,2], Ikuro Kawagishi[2], Takeshi Fujii[1] ([1]*Natl. Inst. Agro-Environ. Sci.*, [2]*Dept. Frontier Biosci., Grad. Sci. Eng., Hosei Univ.*)

Chlorobenzoates are the major intermediate products of aerobic catabolism of polychlorinated biphenyls (PCBs). In most PCB-degrading microorganisms, however, chlorobenzoates are not further metabolized. Therefore, chlorobenzoate degradation is important for the complete degradation of PCBs. *Burkholderia* sp. NK8 can utilize 3-chlorobenzoate (3CB) as a sole source of carbon and energy. The (chloro)benzoate dioxygenase of strain NK8 converts 3CB to 3- and 4-chlorocatechols, and then the resulting chlorocatechols may be decomposed into β -ketoadipate by the products of the chlorocatechol degradation genes *tfdT-CDEF* on the catabolic megaplasmid (pNK8) of strain NK8. We demonstrated by capillary assay that cells of strain NK8 show chemotaxis toward 3CB and the degradation compounds. We also found that the chemotaxis toward β-ketoadipate was lost in the absence of pNK8, and was recovered by the introduction of a plasmid carrying a porin gene, located next to the *tfdT-CDEF* gene cluster of pNK8. By contrast, 3CB-taxis was not complemented by the porin gene, named omp_{NK8}. RT-PCR analyses demonstrated that the transcription of the omp_{NK8} gene was enhanced when cells were grown in the presence of 3CB or β-ketoadipate. These findings indicate that the outer membrane permeability and chemotaxis of strain NK8 may be regulated in response to the presence of 3CB or β-ketoadipate.

3PT185 ペリプラズム領域を欠失した走化性受容体 Tar の温度受容能

Thermosensing abilities of the mutant aspartate chemoreceptor Tar lacking the periplasmic domain

So-ichiro Nishiyama[1,2], Masaaki Jinguji[1], Ikuro Kawagishi[1,2] ([1]*Dept. Frontier Biosci., Hosei Univ.*, [2]*Res. Cent. Micro-nano Tech., Hosei Univ.*)

The aspartate chemoreceptor Tar of *Escherichia coli* can mediate thermoresponses: attractant and repellent responses to increases and decreases in temperature. When methylated upon adaptation to a chemoattractant, it mediates thermoresponses with opposite polarity: repellent and attractant responses to increases and decreases in temperature. Tar is an integral membrane protein with two transmembrane (TM) helices as well as the periplasmic sensing and the cytoplasmic signaling/adaptation domains. Our previous studies suggest that the second TM region and the adaptation domain are involved in temperature sensing, regulation of signal output or both. However, whether there is a specific region of the chemoreceptor for thermosensing, is still unclear. Here we examined thermosensing ability of a mutant version of Tar [Δ (44-183), named Tar^o], which lacks the entire periplasmic domain [Pham & Parkinson (2011) *J. Bacteirol.* 193: 6597-6604]. Tar^o did not mediate any chemotactic or thermotactic response. However, Tar^o derivatives (S272L, T264I), when expressed in an otherwise receptor-less strain, mediated repellent responses to glycerol, suggesting that they retained sufficient activities to regulate the receptor-coupled histidine kinase CheA. Tar^o-S272L mediated thermoresponses with opposite polarity. Tar^o-S272L showed elevated methylation without any stimuli, which can account for the inverted thermoresponse. These results suggest that the periplasmic domain of the chemoreceptor is not essential for its function as a thermosensor.

3PT186 大腸菌アスパラギン酸走性受容体 Tar による忌避物質 Ni^{2+}感知機構の解析

Exploring the mechanism underlying sensing of the repellent Ni^{2+} by the aspartate chemoreceptor Tar of *Escherichia coli*

Takaya Inui[1], Hirotaka Tajima[2], Yosiyuki Sowa[3,4], Ikuro Kawagishi[1,3,4] ([1]*Dept. Frontier Biosci., Grad. Sch. Eng., Hosei Univ.*, [2]*Dept. Micro-Nano Systems Eng., Grad. Sch. Eng. Nagoya Univ.*, [3]*Dept. Frontier Biosci., Fac. Biosci. Appl. Chem., Hosei Univ.*, [4]*Res. Cen. Micro-Nano Tech., Hosei Univ.*)

In the chemotaxis of *Escherichia coli*, four methyl-accepting chemotaxis proteins (Tsr, Tar, Trg and Tap) mediate attractant responses to some amino acids, sugars and other organic compounds, and repellent responses to some metal ions and organic compounds. In contrast to attractant sensing, repellent sensing by the chemoreceptors is poorly understood in terms of ligand recognition and structural changes triggered by ligand binding. In this study, we focused on the ability of the aspartate chemoreceptor Tar to sense Ni^{2+} as a repellent. Taking advantage of the fact that the serine chemoreceptor Tsr, though closely related to Tar, does not mediate a response to Ni^{2+}, we tried to determine the residues responsible for Ni^{2+} sensing by examining a series of chimeras between Tar and Tsr. Responses of otherwise receptor-less cells expressing each chimera to Ni^{2+} and amino acids, and methylation patterns of each chimera in the presence or absence of Ni^{2+} and amino acids indicate that the region 157-256 of Tar is critical for Ni^{2+} sensing.Iso-thermal calorimetry measurements demonstrated direct binding of Ni^{2+} to the periplasmic domain of Tar. However, we also found that a mutant version of Tar [Δ(44-183), named Tar°], which lacks the entire periplasmic domain [Pham & Parkinson (2011) J. Bacteirol. 193: 6597-6604] can mediate a response to Ni^{2+} and becomes less methylated in the presence of Ni^{2+}. To understand these apparently contradictory data, further analyses are in progress.

3PT187 走化性受容体 Tcp によるクエン酸と金属-クエン酸複合体の識別機構の解析

Characterization of the bacterial chemoreceptor Tcp that discriminates citrate and the citrate-metal ion complex as distinct attractants

Tetsuya Shiroi[1], Ikuro Kawagishi[1,2,3], Hirotaka Tajima[4] ([1]*Dept of Frontier Biosci., Grad. Sch. Eng., Hosei Univ.*, [2]*Res. Cen. Micro-Nano. Tech., Hosei Univ.*, [3]*Dept of Frontier Biosci., Fac. Biosci. Appl. Chem., Hosei Univ.*, [4]*Dept. Micro-Nano Systems Eng., Grad. Sch. Eng. Nagoya Univ.*)

The chemoreceptor Tcp of *Salmonella enterica* mediates chemotactic responses to citrate as well as a metal ion-citrate complex by recognizing them as different attractants. Mutant Tcp receptors with substitutions for residue Asn67 fell into either of the four possible phenotypes in terms of their abilities to mediate responses to citrate and metal-citrate (referred to as Cit and Mec, respectively): (i) Cit^+ Mec^+; (ii) Cit^+ Mec^-; (iii) Cit^- Mec^+; (iv) Cit^- Mec^-. This lead to a proposal of two models for the mechanism of discrimination; (a) citrate binding to one of the two binding pockets would alter the shape of the other binding pocket, the induced conformation of which accommodates metal-citrate but not citrate alone; (b) a metal ion binds to citrate that is already bound to one of the two binding sites to modify the conformation of the bound citrate, which would then trigger a conformational change of the ligand-binding domain to generate an attractant signal. In this study, we aimed at testing these models by examining binding of citrate and metal ions to Tcp. Direct binding of citrate to Tcp was suggested previously by our chemical modification assay. Here wecarried out isothermal calorimetry measurements of a periplasmic fragment of wild-type Tcp or its derivative with a cysteine residue at the dimer interface. Neither fragment bound citreate or Mg^{2+}. However, membrane vesicles of an otherwise receptor-less strain of Escherichia coli expressing full length Tcp appeared to bind citrate. Further analyses are in progress.

3PT188 コレラ菌新規アミノ酸走性トランスデューサーの同定と機能解析

Identification and characterization of novel *Vibrio cholerae* transducers for amino acid chemotaxis

Tetsuya Kawaguchi[1], Kimiko Yamamoto[1,2], So-ichiro Nishiyama[3,4], Ikuro Kawagishi[1,3,4] ([1]*Dept. Frontier Biosci., Grad. Sci. Eng., Hosei Univ.*, [2]*Natl. Inst. Agro-Environ. Sci.*, [3]*Dept. Frontier Biosci., Fac. Biosci. Appl. Chem., Hosei Univ.*, [4]*Res. Cen. Micro-Nano Tech., Hosei Univ.*)

The chemotaxis of *Vibrio cholerae*, the causative agent of cholera, has been implicated in pathogenicity and survival in various environments. A classical biotype strain of *V. cholerae* has 44 homologs of methyl-accepting chemotaxis protein (MCP), which we name MCP-like proteins (MLPs). Our previous studies showed that Mlp24 and Mlp37, which have two periplasmic PAS-like domains, are major chemoreceptors that mediate attractant responses to amino acids. However, the mutant lacking *mlp24* and *mlp37* (Δ*mlp24* Δ*mlp37*) showed weak but significant responses to amino acids, suggesting the presence of

additional amino acid chemoreceptor(s). None of the other MLPs with tandem PAS-like domains appeared to mediate amino acid taxis. We then turned our attention to MLPs with a single PAS-like domain. The overproduction of two members of this family, Mlp2 and Mlp3, in the Δ*mlp24* Δ*mlp37* strain enhanced taxis to serine in capillary assays, suggesting that these MLPs mediate attractant responses to serine. Interestingly, the expression of Mlp3, but not Mlp2, enhanced taxis to alanine, cysteine, glycine and threonine, implying the difference in specificity between these MLPs. However, we failed to detect direct binding of serine to these MLPs in isothermal titration calorimetry measurements with periplasmic fragments of Mlp2 and Mlp3, as well as membrane vesicles of an otherwise receptor-less strain of *Escherichia coli* expressing Mlp2 or Mlp3. This raises the possibility that these MLPs sense serine via periplasmic serine-binding protein(s).

3PT189 アミノ酸変異による苦味受容体 TAS2R16 機能の多様化

Functional diversity of bitter taste receptor TAS2R16 by amino acid substitution

Hiroo Imai[1], Nami Suzuki[1], Yoshiro Ishimaru[2], Takanobu Sakurai[2], Lijie Yin[3], Wenshi Pan[3], Keiko Abe[2], Takumi Misaka[2], Hirohisa Hirai[1] ([1]*Primate Research Institute, Kyoto University*, [2]*Graduate School of Agricultural and Life Sciences, The University of Tokyo*, [3]*School of Life Sciences, Peking University*)

In mammals, bitter taste is mediated by TAS2Rs, which belong to the large family of seven transmembrane G protein-coupled receptors. Since TAS2Rs are directly involved in the interaction between mammals and their dietary sources, it is likely that these genes evolved to reflect species' specific diets during mammalian evolution (1, 2). Here, we investigated the sensitivities of TAS2R16s of various primates by using a cultured cell expression system in combination with behavioral tests (3). We found that the sensitivity of each primate species varied according to the ligand. Especially, the sensitivity of TAS2R16 of Japanese macaques to salicin, a bitter compound contained in the bark of Salicaceae (willow) plants, was much lower than that of human TAS2R16, which was supported by behavioral tests. The replacement of amino acid residue at position 86 caused dynamic changes in the sensitivities of TAS2R16s. These results suggest the possibility that bitter taste sensitivities evolved independently by replacing specific amino acid residues of TAS2Rs in different primate species to adapt to accessible food items they use. The amino acid residues responsible for the specificities of each ligand would be discussed in the presentation.

References
1. Suzuki N. et al., Primates 51, 285-289 (2010)
2. Sugawara T. et al., Mol. Biol. Evol. 28, 921-931 (2011)
3. Imai H. et al., Biol. Letters in press (2012)

3PT190 弾性ネットワークモデルを利用したβ_2アドレナリン受容体のアンサンブルドッキング

Ensemble Docking Simulation for β_2 Adrenergic Receptor Using Elastic Network Models

Tomoyuki Iwamoto[1], Hiroshi Wako[2], Shigeru Endo[3], Haruki Nakamura[4] ([1]*Department of Biological Sciences, Graduate School of Science, and Faculty of Science Osaka University*, [2]*School of Social Sciences, Waseda University*, [3]*Department of Physics, Faculty of Science, Kitasato University*, [4]*Institute for Protein Research, Osaka University*)

G protein-coupled receptors (GPCRs) are membrane proteins involved in signal transduction and participate in many diseases. Therefore, the receptors are important targets in the field of drug discovery.

Protein structural information is useful to understand their function and enable us to develop new therapeutic molecules. However, these membrane proteins are not easy to crystallize. And it sometimes happens that rigid-body protein docking simulation for GPCR based on one ligand-receptor complex structure to discovery new drugs lead to inefficient results with own flexible conformation. In this study, GPCR's conformational polymorphism into the virtual screening of β_2 adrenergic receptor (ADRB2) using elastic network model (ENM) and normal mode analyses (NMA). First, we build the ENM of ADRB2 and performed NMA. Next, we make virtual models based on ADRB2's elastic network normal mode analysis data. And we do docking simulation for the virtual model group to make up for the above shortcoming.

According to the results, the screening efficiency of virtual model group is improved by over 20% against that of the initial model.

3PT191 大腸菌走化性受容体 Tar システイン置換シリーズの化学架橋によるクラスター構造推定

Characterization of receptor clustering by cross-linking a series of cysteine-substituted mutants of the aspartate chemoreceptor Tar

Tsuyoshi Watanabe[1], Kosuke Jintori[1], Hiroki Irieda[2], Ikuro Kawagishi[1,3,4] ([1]*Dept. Frontier Biosci., Grad. Sch. Eng., Hosei Univ.*, [2]*Div. Biol. Sci., Grad. Sch. Sci., Nagoya Univ.*, [3]*Res. Cen. Micro-Nano. Tech., Hosei Univ.*, [4]*Dept. Frontier Biosci., Fac. Biosci. Appl. Chem., Hosei Univ.*)

In the chemotaxis of *Escherichia coli*, the bacterium can respond to a wide range of attractant concentrations. The chemoreceptors, which exist as homodimers regardless of ligand binding, form complexes with the adaptor protein CheW and the histidine kinase CheA. The chemoreceptors form "trimers of dimers" with their cytoplasmic tips in contact with each other, which are supposed to be organized into a hexagonal array. To account for high sensitivity of the chemotaxis system, it has been proposed that attractant binding to a receptor dimer affects neighboring receptor dimers. Receptor clustering has also been implicated in signal gain control by methylation of specific glutamate residues that is responsible for adaptation to persisting stimuli. However, molecular mechanisms underlying such interactions between receptor dimers remain to be elucidated. In this study, we carried out *in vivo* chemical cross-linking assay to probe changes in the receptor array by using divalent maleimide cross-linkers and a series of site-directed mutant proteins of the aspartate chemoreceptor Tar with single cysteine residues on the surface of the dimer. The pattern of cross-linking was generally in agreement with our previous results of disulfide-crosslinking assay without a chemical cross-linker. Efficiencies of cross-linking were affected when an attractant or a repellent was added. We propose a plausible model of the receptor array, in which three trimers of dimers are in contact with each other in the periplasmic spacer.

3PT192 コレラ菌走化性解析のためのスウォームアッセイ法の開発

Development of a system for swarm assays to evaluate chemotaxis of *Vibrio cholera*

Ryosuke Iwazaki[1], Nakagawa Tsubasa[2], So-ichiro Nishiyama[3], Ikuro Kawagishi[1,2,3,4] ([1]*Dept. Frontier Biosci., Grad. Sci. Eng., Hosei Univ.*, [2]*Dept. Frontier Biosci., Fac. Eng., Hosei Univ.*, [3]*Res. Cen. Micro-Nano Tech., Hosei Univ.*, [4]*Dept. Frontier Biosci., Fac. Biosci., Appl. Chem., Hosei Univ.*)

Vibrio cholerae, the causative agent of cholera, shows chemotaxis, which has been implicated in pathogenicity and survival in various environments. A classical biotype strain of *V. cholerae* has 44 homologs of methyl-accepting chemotaxis protein (MCP), which are named MCP-like proteins (MLPs). Among them, Mlp24 and Mlp37 are major chemoreceptors for amino acid taxis in *V. cholerae*. A mutant strain lacking *mlp24* and *mlp37* (Δ *mlp24* Δ *mlp37*) shows significantly weaker attractant responses to amino acids than the wild-type strain in capillary assays. However, in swarm assays, no detectable difference is observed between the double mutant and the wild-type strains. The swarm assay is not only easier than the capillary assay but also suited for screening of mutants. In this study, we aimed at developing a system for swarm assays to evaluate chemotaxis of *V. cholerae*. We deleted the *mlp32* gene (previously named *are-2*), which encodes a homolog of the redox sensor Aer for aerotaxis of *Escherichia coli*. The resulting triple mutant strain (Δ *mlp24* Δ *mlp37* Δ *mlp32*) showed significantly slower spreading than the wild-type and the double mutant strains in tryptone swarm plates. Introduction of a plasmid carrying the *mlp32* gene complemented the defect of the triple mutant strain in swarming. Furthermore, introduction of a plasmid carrying the *mlp24* or *mlp37* gene significantly enhanced swarming of the triple mutant strain, demonstrating that this strain can be used as a plasmid host to evaluate amino acid taxis of *V. cholerae* by the swarm assay.

3PT201 Seeking molecular and neural mechanisms of temperature response and resistance in C. elegans

Tomoyo Ujisawa, Satoru Sonoda, Yukie Ohkubo, Hitomi Mizutani, Hiromi Nagaya, Naoto Kuwahara, Akane Ohta, Atsushi Kuhara (*Sch. Sci., Univ. Konan*)

Animals have adaptation mechanisms against environmental temperature changes. To understand the molecular mechanism of temperature response, we are using simple model animal, nematode C. elegans. We recently found that C. elegans shows cultivation temperature-dependent cold-resistance, which is regulated through neural pathway. After cultivation at 25 degree, wild-type

animals isolated from U.K. were destroyed by cold stimuli, 2℃ for 48 hours. By contrast, most of wild-type animals can survive for 48 hours at 2℃, after cultivation at 15 degree. Detailed temperature-changes experiments revealed that the cold-resistance is established by temperature memory at adult stage. We measured cold-resistance in various mutant animals defective in sensoryneurons. Abnormal enhancement of cold-resistance is found in the mutant animals defective in TAX-4 cGMP-gated channel, which is expressed in 10 pairs of sensoryneurons including thermo-sensoyneuron AFD and chemo-sensoryneurons. Developmental defect of AFD that is caused by mutation in OTX transcriptional factor did not affect cold-resistance. These results suggest that cold-resistance is controlled by sensory neurons excepting AFD, and that sensoryneurons transmit inhibitory signaling for cold resistance. To determine molecular pathway for cold resistance, we referred previous DNA microarray analysis (Sugi et al., Nature neurosci., 2011). So far, at least 10 genes such as endonuclease, tubulin kinase and phosphatase PP1 are involved in cold-resistance.

3PT202 Inhibitory effect of glutamate-stimulated astrocytes on action potentials evoked by bradykinin in cultured dorsal root ganglion neurons

Kazuo Suzuki, Kenji Tonaka, Minehisa Ono (*Dept. Biomedical Engr. Tokai Univ.*)

The patch-clamp and Ca^{2+} -imaging techniques have revealed that astrocytes have dynamic properties including ion channel activity, neurotransmitter release, such as adenosine triphosphate (ATP) and glutamate. Our previous study demonstrated that free nerve endings of cultured neuron from dorsal root ganglion (DRG) are activated by bradykinin (BK). We study whether ATP and glutamate can modulate the BK-response of the neuron cultured with the astrocyte in the mouse DRG, and enunciate the role of the astrocyte in the nociceptive signal transmission using patch-clamp technique. The astrocytes were identified using fluorescent antibody, anti-GFAP. The membrane potential of the astrocyte was about -39 mV. The application of glutamic acid (GA) to the bath evoked the opening of two kinds of Cl^- channel of the astrocyte membrane with unit conductance of about 380 pS and 35 pS in the cell-attached mode, respectively. ATP application evoked the opening of two kinds of K^+ channel of the astrocyte with unit conductance of about 60 pS and 29 pS, respectively. Application of BK to the neuron evoked an action potential (spike). The BK-application of concomitantly with ATP increased the frequency of BK-evoked spike of the neuron. Stimulation of BK with GA inhibited the BK-evoked spike. The application of furosemide, a potent cotransporter (Na^+ -K^+ -Cl^-) inhibitor, prior to the stimulation of BK with GA blocked the inhibition of the spike. It is thought that the inhibition of the spike is related to Cl^- movement from the astrocyte.

3PT203 マウス脳ホモジネートにおける一酸化窒素（NO）の測定

Nitric oxide measurement in mice brain homogenate

Yoshiichiro Kitamura, Akira Hirai, Toshihiko Nishio, Yutaka Kirino (*Kagawa Sch. Pharm. Sci., Tokushima Bunri Univ.*)

It is known that nitric oxide (NO) plays important roles in a number of physiological processes over various animal species of vertebrate and invertebrate, such as neurotransmission, vasodilation and immune response. Especially in recent years, relationship between nitric oxide (NO) and aging has been received a lot of attention. However down-regulation of NO signaling during aging process is strongly suggested, NO dynamics in brain have not been studied in detail. Therefore, in this study, NO production in mice brain homogenate was measured using NO-specific electrode. Brain homogenates (cerebral cortex, cerebellum and hippocampus) were prepared from male wild-type mice (8 and 120 weeks). After oxidation current of the NO electrode stabilized in the saline, each brain homogenate was added for estimation of basal NO production. To confirm specificity of the electrode, brain homogenate was stimulated with calcium ion (Ca^{2+}). When brain homogenate was added, NO concentration increased and was stabilized at constant level. Ca^{2+} accelerated the basal NO production in a concentration-dependent manner. However concentration of basal NO production did not so different in region and age, Ca^{2+}-induced NO production in aged mice significantly decreased in every region compared with young mice. From these results, NO production from mice brain homogenate was successfully measured with the NO-specific electrode. We also examined that aging induced down-regulation of Ca^{2+}/NO signaling in mice brain.

3PT204 線虫 AIY 介在神経細胞での局在した神経活動：蛍光イメージングによる研究

Localized neural activities in AIY interneuron of Caenorhabditis elegans: fluorescent imaging study

Hisashi Shidara, Junya Kobayashi, Ryo Tanamoto, Kohji Hotta, Kotaro Oka (*Grad. Sch. Sci and Tech., Keio Univ*)

The neural activities of subcellular regions are important for understanding the relationship between the cellular morphology and the function in single neurons. From this view, AIY interneuron of *Caenorhabditis elegans* has a very unique feature of Ca^{2+} dynamics; Ca^{2+} change is observed only on the specific region of neurites, but not on soma during odor and temperature stimulation. To investigate this dynamics in subcellular regions of AIY in detail, we visualized the membrane potential and showed that its dynamics is different from the Ca^{2+} one.

For visualization of neural activities on specific neurons in *C. elegans*, we have developed a specific micro-fluidic device to fix the worm. The worm was applied to 10^{-4} dilution of isoamyl alcohol as the controlled odor stimulation during 50 sec. The genetic Ca^{2+} indicator (YC3.60) expressed in AIY has revealed the subcellular neural activities to the external environmental change. To compare membrane potential change with the dynamics, we also used voltage-sensitive fluorescent protein (VSFP) 2.42 (Akemann et al., 2010). VSFP2.42 revealed that the odor stimulation depolarized membrane potential both on the neurite and soma. In addition, the membrane potential showed oscillation with attenuation of the amplitude during odorant stimulation. These results suggest that AIY has the diversity of biophysical characteristics in the single cell and it is necessary for understanding its function.

3PT205 コルチコステロンは、シナプス局在の GR-kinase 系を介して、海馬神経シナプスを増やす

Corticosterone induced GR/kinase network-driven rapid spinogenesis in rat hippocampus

Yoshimasa Komatsuzaki[1,2,3], Masatoshi Kasuya[2,3], Yasushi Hojo[2,3], Suguru Kawato[2,3] ([1]*Dept of Physics, CST, Nihon Univ*, [2]*Grad Sch of Arts and Sci, Univ of Tokyo*, [3]*Bioinformatics Project, JST*)

Modulation of hippocampal synaptic plasticity by corticosterone (CORT) has been attracting much attention, due to its importance in stress responses. Many studies have investigated the chronic effect of CORT, but rapid effect of CORT in hippocampus is unclear. Here, we investigated effect of CORT, a major glucocorticoid in rat, on density and morphology of dendritic spine which is essential for memory storage processes, in adult male rat hippocampus. The application of 1 μM CORT induced a rapid increase in the total density of spines of CA1 pyramidal neurons within 1 h from 0.98 spines/μm to 1.24 spines/μm. CORT increased the density of large-head (0.5-1.0 μm) and middle-head spines (0.4-0.5 μm), but not small-head (0.2-0.4 μm) spines. Co-presence of RU486, an antagonist of glucocorticoid receptor (GR), completely abolished the effect of CORT. Blocking ionotropic glutamate receptors with MK-801 inhibited the CORT effect. This result suggests that Ca2+ homeostasis via NMDA receptors is necessary to CORT-induced spinogenesis. Blocking various kinases shows that CORT enhances spinogenesis via MAPK, PKA, PKC, PI3K and calcineurin signaling pathways. In particular, the contribution of Erk MAPK and PKA is essential. Inhibition of protein synthesis reduced the CORT-induced spinogenesis but inhibition of transcription. These results indicate that CORT drives the signaling pathway including synaptic GR and multiple kinase pathways in hippocampal CA1 neurons. (Komatsuzaki et al., 2012 PLoS-ONE)

3PT206 IP_3/Ca^{2+} シグナリングによる GABA 作動性シナプスの制御

Regulation of GABAergic synapses by IP_3/Ca^{2+} signaling

Hiroko Bannai[1], Fumihiro Niwa[1], Mark W. Sherwood[1], Misa Arizono[1], Akitoshi Miyamoto[1], Kotomi Sugiura[1], Sabine Levi[2], Antoine Triller[3], Katsuhiko Mikoshiba[1] ([1]*RIKEN BSI*, [2]*Institut du Fer a Moulin*, [3]*IBENS, ENS Paris*)

The number of GABA-A receptors ($GABA_AR$) clustering at the inhibitory synapse is a crucial determinant of GABAergic synaptic transmission efficacy. Ca^{2+} influx in response to excitatory neuronal activity results in the dispersal of synaptic $GABA_AR$ clusters. In addition to Ca^{2+} influx, Ca^{2+} release from the intracellular Ca^{2+} store also plays various roles in neurons. However, the impact of Ca^{2+} release on the inhibitory synapse remains to be elucidated. Here, we

examined whether the inositol 1,4,5-trisphosphate (IP_3)-induced Ca^{2+} release (IICR) is involved in the regulation of the synaptic clustering of $GABA_A$Rs. In hippocampal neurons from mice lacking intracellular Ca^{2+} releasing channel IP_3 receptor type 1 (IP_3R1), clusters of $GABA_A$R and those of its scaffold protein gephyrin were significantly smaller than in wild type neurons. In wild type neurons, the inhibition of IICR by specific inhibitors resulted in the decrease in $GABA_A$R and gephyrin cluster size, without reducing the amount of $GABA_A$R on the cell surface. Single particle tracking with quantum dot (QD-SPT) revealed that the loss of IP_3R1 and inhibition of IICR enhanced the lateral diffusion of $GABA_A$Rs. The increase of $GABA_A$R lateral mobility resulting from the loss of IICR was completely prevented by an inhibitor of calcineurin. Our results suggest that IP_3/Ca^{2+} signaling contributes to the stabilization of synaptic $GABA_A$ R clusters through the regulation of $GABA_A$ R lateral diffusion, possibly through phosphorylation.

3PT207 海馬でのアクチビンによるシナプス可塑性の急性制御

Acute Modulation of Synaptic Plasticity of Pyramidal Neurons by Activin in Adult Hippocampus

Yoshitaka Hasegawa, Hideo Mukai, Makoto Asashima, Yuki Ooishi, Suguru Kawato (*Life sciences, The University of Tokyo*)

Activin is known as a sex-hormone in mammalian. We attempt to reveal the role of activin as a neuromodulator in the adult hippocampus. Activin is a homodimer of inhibin β, and activin belong to the superfamily of transforming growth factor-β (TGF-β). We showed endogenous/basal expression of activin in the hippocampal neurons. Localization of activin receptors in spines was demonstrated by immunoelectron microscopy. The incubation of hippocampal acute slices with activin A altered the density and morphology of spines in CA1 pyramidal neurons. The total spine density was increased by activin treatments. Activin increased the head diameter of spines. Blocking of MAPK, PKA or PKC prevented the activin-induced spinogenesis by reducing the density of spines. We also demonstrated that activin induced the long term potentiation (LTP) of the hippocampal neurons.

3PT208 カエル神経筋接合部シナプスでの細胞外 Ca^{2+}濃度変化による神経伝達物質放出量増加の二項分布解析

Binomial distribution analysis of increase of transmitter release depending on $[Ca^{2+}]_e$ at the frog neuromuscular junction

Taisuke Matsuda, Naoya Suzuki (*Dept. Phys., Sch. Sci., Univ. Nagoya*)

To investigate the action of Ca^{2+} to induce the transmitter release, we analyzed the dependency of quantal release parameters on extracellular Ca^{2+} concentration ($[Ca^{2+}]_e$). Binomial distribution analysis with two parameters, release probability (**p**) and number of releasable synaptic vesicles (**n**) having that release probability was applied to the release induced by single stimulations at frog neuromuscular junction. Endplate potentials (EPPs) and miniature endplate potentials (MEPPs) were electrically recorded with an intracellular glass microelectrode under five different $[Ca^{2+}]_e$ changed from 0.55mM to 0. 95mM at intervals of 0.10mM. The averaged size of EPPs was proportional to the about 3.0-3.5 power of $[Ca^{2+}]_e$. The binominal analysis of EPPs distribution with using MEPPs distribution as single unit event gave values of **p** about 0.1-0. 5 and **n** about 10-50. Detail analysis of the change of two parameters, **p** and **n**, showed **p** was approximately proportional to $[Ca^{2+}]_e$ and **n** was proportional to the about square of that. It suggests that increase of **n** contributed largely and increase of **p** contributed slightly to increase of transmitter release with change of $[Ca^{2+}]_e$.

3PT209 アミロイドβペプチドが及ぼす神経活動への影響とチモキノンによる保護効果の検討

Thymoquinone, the Nigella sativa Bioactive Compound, Prevents β amyloid neurotoxicity in cultured rat primary neurons

Amani Alhibshi, Ikuro Suzki, Masao Gotoh (*Tokyo University of Technology*)

Alzheimer disease (AD) is a neurodegenerative disease characterized by extracellular abnormal accumulation and extensive deposition of amyloid beta peptide (A β). This accumulation is associated with oxidative damage, inflammatory reactions, synaptic function impairment, synaptic loss and finally leads to neuronal death, and the use of antioxidants and anti-inflammations could reduce this risk. Thymoquinone (TQ), the abundant essential oil compound of Nigella sativa L. seeds, known to be the active principle responsible for many of the seed's antioxidant and anti-inflammatory effects, was used in this study. In every experience, rat cultured embryonic hippocampal and cortical neurons were treated simultaneously with Aβ1-42 and TQ for 72 h. The results showed that co-treatment with TQ efficiently attenuated Aβ1-42-induced neurotoxicity, as evidenced by the improved cell viability. In addition, TQ inhibited the mitochondrial membrane potential depolarization and reactive oxygen species generation caused by Aβ1-42. TQ also restored synaptic vesicle recycling inhibition, partially reversed the loss of spontaneous activity, and inhibited Aβ1-42 aggregation. These beneficial effects may contribute to the protection against Aβ-induced neurotoxicity. Together, our results suggest that the natural antioxidant TQ has potential for neuroprotection and therefore, may be a promising candidate for AD treatment.

3PT210 インスリンを介した神経シグナルによって制御される線虫 *C. elegans* の温度適応の解析

Insulin-mediated neural signals negatively regulate temperature tolerance in *C. elegans*

Akane Ohta, Tomoyo Ujisawa, Yukari Kinoshita, Hitomi Mizutani, Takurou Inoue, Naho Inoue, Atsushi Kuhara (*Dept. Biol., Facul. Sci. Engin., Konan Univ.*)

Temperature is one of the most critical environmental stimuli and cause biochemical change in the body. Therefore, animals have adaptation mechanisms against environmental temperature changes, however, its molecular mechanisms are still poorly understood. Here we show that *C. elegans* has a cultivation temperature-dependent cold resistance, which is regulated by insulin-mediated pathway. 25℃-grown wild-type animals isolated from U.K. were destroyed by cold stimuli, 2℃ for 48hr. By contrast, most of 15℃-grown wild-type animals can survive for 48 hours at 2℃. These facts suggests that C. elegans has cold resistance with changes in environmental temperature. To reveal the molecular mechanisms underlying the cold resistance, we measured cold-resistance in the various mutant animals defective in temperature sensation and temperature-controlled hormonal signaling. We found that the mutants defective in insulin-like molecule DAF-28, insulin receptor DAF-2 and its downstream molecules showed enhancement in cold resistance. These results suggest that insulin-mediated neural signals negatively regulate cold resistance. In another approach, we focused on the natural variation of wild-type strains isolated from different areas. We so far found that British strain showed weaker phenotypes in cold resistance than California or Vancouver strains, respectively. We are also using artificial evolution approaches and forward genetic screening to isolate the mutation in cold resistance.

3PT211 海馬での年齢依存的な性ホルモン受容体・合成酵素遺伝子の発現変動解析

Age-related changes in the expression of mRNAs encoding for sex steroidogenic enzymes and sex hormone receptors in the hippocampus

Tetsuya Kimoto, Masahiko Wakabayashi, Suguru Kawato (*Dept. Biophys. Life Sci., Grad. Sch. Art. Sci., Univ. Tokyo*)

Although sex steroids play a crucial role in the development/maintenance of brain function, the age-related changes in the hippocampal sex steroidogenesis remain largely unknown. We examined the mRNA expression levels of sex steroidogenic enzymes and sex steroid receptors in the hippocampus of aged (24 month-old) male rats compared with those of young adult (3 month-old) male rats by means of semi-quantitative RT-PCR. The levels of mRNAs for cytochrome P45017 α, 17 β -HSD3 and 5 α -reductase2 reduced in the hippocampus of aged rats to approx. 45%, 76% and 75% of young adult rats, respectively. On the other hand, the levels of 17β-HSD1, 5α-reductase1 and P450aromatase were almost the same between aged and young adult hippocampus. The levels of estrogen receptor β and androgen receptor reduced in aged hippocampus to approx. 84% and 55% of young adult hippocampus, respectively, while almost no change was observed in the mRNA expression of estrogen receptor α between aged and young adult hippocampus. These results indicate that the hippocampal sex steroidogenic properties are substantially altered between aged and young animals.

3PT212 NMDA 受容体と相互作用することにより CaMKII は分子メモリとして機能する － *in vitro* 実験系による実証－

CaMKII functions as a molecular memory through interaction with NMDA receptors - validation in *in vitro* experiments -

Hidetoshi Urakubo[1,2], Shin Ishii[2], Shinya Kuroda[1] ([1]*Dept. Biophys. Biochem., Grad. Sch. Sci., U. Tokyo*, [2]*Dept. Syst. Sci., Grad. Sch. Info, Kyoto U.*)

In the process of long-term potentiation (LTP) at synapses, calcium-calmodulin (CaM) dependent protein kinase II (CaMKII) is interacted with NMDA receptors, and the interaction leads to Ca^{2+} /CaM-induced, but CaM-independent CaMKII activity (Bayer 2001, Nature 411, pp. 801-805). This sustained activity is considered as a part of mechanisms of LTP maintenance; however, additional mechanisms are needed to explain reversibility of LTP, and stable basal CaMKII activity even with spontaneous Ca^{2+} increase at synapses. Here, in an *in vitro* experimental system, we found that CaMKII autophosphorylation at T286 shows hysteresis through interaction of a NMDA receptors-derived peptide. This indicates that CaMKII activity can work as a molecular memory for LTP maintenance. The hysteresis was regulated by protein phosphatase 1 (PP1), and canceled by high PP1 application, corresponding to reversal of LTP (Depotentiation). Ca^{2+} -concentration dependence of the hysteresis showed that the hysteresis is robust against spontaneous Ca^{2+} increase. This can provide a mechanism of reversible LTP and stable basal CaMKII activity at synapses.

3PT213 新規な神経スパイン解析プログラム

Novel program and its applications for spines in neurons

Hideo Mukai[1,2,3], Yuusuke Hatanaka[2], Kenji Mitsuhashi[2], Gen Murakami[2,3], Yasushi Hojo[2,3], Suguru Kawato[2,3] ([1]*Dept. Biochem., Fac. Med., Saitama Med. Univ.*, [2]*Dept. Biophys. & Life Sci., Grad. Art & Sci., Univ. Tokyo*, [3]*BIRD, JST*)

Dendritic spines in the brain are substrates of synaptic contacts that may be involved in neuronal computational processes. Visualization and analysis of dendritic spines is of critical importance to elucidate physiological changes of morphological plasticity, as well as effects of various hormones and pharmacological agents. Advent of laser-scanning confocal microscopy / 2-photon microscopy and fluorescent dye allowed us to collect large body of neuronal image data, namely tens of dendrites and several tens of thousands of spines residing on each dendrite of single neurons. Conventional methods using manual tracing software need time-consuming efforts by researchers and not suitable to handle large data. Therefore introduction of protocol for a new automatic analysis of neuronal structure including spines will greatly enhance progress of research in the area. Here we developed a new software, Spiso-3D, to extract spines as well as dendrites and in neuronal image based on their geometrical features. Our "geometric method" utilises scale-free, shape-dependent analysis, making less dependent on brightness in the image. Because Spiso-3D is a Java-based program, it will readily work on a PC with a relatively limited resource.
Using the Spiso, we analyzed the effect of activin, an endogenous sex hormone in the mammalian brain, on spines of hippocampal neurons. Ref. Mukai et al., Cerebral Cortex, 21, (12): 2704-2711. (2011)

3PT214 高速ビデオカメラ法および筋電位法によるサル瞬目反射条件付けシステムの開発

Evaluation of eyeblink classical conditioning in monkey by using high-speed video sensing and electromyogram signal

Yasushi Kishimoto[1], Shigeyuki Yamamoto[2], Kazutaka Suzuki[2], Toyoda Haruyoshi[2], Hideo Tsukada[2], Yutaka Kirino[1] ([1]*Lab. Neurobiophysics, Kagawa Sch Pharmaceut Sci, Tokushima Bunri Univ.*, [2]*Central Research Lab., Hamamatsu Photonics Co., Ltd.*)

Classical eyeblink conditioning is one of the best-characterized behavioral models of associative learning in mammals. Especially, standard delay paradigm has been used for assessing the motor learning or cognitive performance in a variety of mammalian species including, rabbit, rat, human and mouse. In the present study, we first developed the system for evaluating the delay eyeblink conditioning in monkey (*Macaca mulatta*). The eye blinking of a monkey was measured and evaluated by eyelid electromyogram (EMG) method and a 1khz high-speed image processing (Intelligent Vision Sensor, C8201; Hamamatsu Photonics K. K.), simultaneously. Within the conditioning procedure, a 1-kHz tone served as the CS while an air-puff was used as the US. The EMG-based analysis indicated that monkeys exhibited over 60 % of conditioned response (CR) frequency during 5-days acquisition session (100 trials per day), and rapid extinction of CRs during 2-days extinction session. Also in the high-speed image processing analysis, the monkeys exhibited similar results of both in acquisition and extinction of CRs. Hence, we have concluded that both methods of the EMG-based and video-based analysis are effective in measuring eyeblink conditioning in monkey. Our results indicated that the conventional delay conditioning procedure can also effective in conditioning monkeys. The novel multi-measuring system of eyeblink CRs in monkeys will provide useful tools for elucidating the neural mechanism underling motor learning in higher mammals.

3PT215 視床下部室傍核の吻側部位に存在するヒスタミン H1 受容体発現ニューロンは摂食抑制作用をもつ

Histamine H1 receptor-expressing neurons in the anterior part of the hypothalamic paraventricular nucleus inhibit food intake

Shuhei Horio (*Institute of Health Biosciences, The University of Tokushima Graduate School*)

Food intake in mammals is controlled by neurons in the hypothalamus. To suppress food intake, the information from the periphery is conveyed to the hypothalamus via two distinct pathways; one is a humoral pathway that transmit satiety information to hypothalamic paraventricular nucleus (PVH) via arcuate nucleus (ARC) that lies adjacent to blood circulation, and the other is a neuronal pathway that send information to PVH via nucleus solitarius (NTS). Thus satiety information converges in PVH, which is now considered as a center for suppressing food intake. Thus far, several neurons in PVH including CRH (corticotropin-releasing hormone) neurons, oxytocin neurons, and melanocortin neurons are found to suppress food intake.
We studied the role of histamine H1 receptor (H1R)-expressing PVH neurons in food intake. H1R is highly expressed in murine PVH in both the anterior and posterior parts. We developed gene-targeted mice that expressed human IL-2Rα selectively in H1R-expressing neurons. Injection of immunotoxin to PVH selectively ablated these neurons (the toxin binds to IL-2Rα and disrupts the cell). The ablation of these neurons caused a 30% increase in food intake. The body weight was also increased approximately 30% compared to control. The ablation of the posterior part of H1R-expressing PVH neurons had no effect on food intake.
These results indicate that H1R-expressing neurons in the anterior PVH have a crucial role in the regulation of food intake. It is probable that these neurons constantly suppress food intake.

3PT216 記憶・学習中枢海馬の性差は海馬で合成されるホルモンによるものである

Sex difference in profile of hippocampal hormones generates sex difference in hippocampal function

Yasushi Hojo[1,2], Masahiko Wakabayashi[1], Kotaro Yoshida[1], Tetsuya Kimoto[1,2], Suguru Kawato[1,2] ([1]*The University of Tokyo*, [2]*BIRD, JST*)

Sex difference in the brain is a very attractive problem. For example, the hypothalamus, the brain region responsible for reproductive behavior, exhibits a clear sex difference in the size of nerve nucleus.
In contrast, the hippocampus, a center for learning and memory, does not have sex difference at the anatomical level including the volume and the number of neurons. Nevertheless, the significant sex difference in the performance of hippocampus-dependent task such as spatial memory using Morris water maze or radial arm maze task.
What is the cause of sex difference in the performance of learning and memory depending on hippocampus? So far, sex difference in the hippocampus had been attributed to the level of sex hormones in the blood.
However, we revealed that the hippocampal level of sex hormones is much higher than the blood level. Surprisingly, hippocampal estradiol (E2), the most potent female hormone, in the male is 7-fold higher than female whereas female E2 in the blood is much higher than male. Moreover, the density of spines (postsynapses) as well as the level of E2 in female hippocampus flucutuates with a period of 4 days (estrous cycle), whereas those in male are retained at a constant level.
This clear sex difference in hormonal profile in hippocampus may generate the sex difference in the hippocampal structure at more subtle level, that is, synaptic level, resulting in the sex difference in the performance of hippocampus-dependent task.

3PT217 老化に伴う海馬神経シナプスの密度の減少と記憶の劣化

Age-related changes in spine density and morphology of hippocampal neurons in relation to memory impairment

Suguru Kawato, Koren Li, Yasushi Hojo (*Grad Sch of Arts& Sci, Univ Tokyo*)

We have investigated the spine density and morphology of neurons in

hippocampal CA1 region which regulates spatial memory. Spine is a postsynapse. We observed a significant decrease in the spine density by going from young rat (3 month old, ~20 years in human) to aged rat (24 month, ~70 years in human). The density of spine as well as the head diameter are analyzed with Spiso-3D software (mathematical and automated software developed by Bioinfomatics Project of our group, now commercially available). Spine morphology is classified into three categories according to the head diameter; (1) small-head spine (0.2-0.4 μm) (2) middle-head spine (0.4-0.5 μm) (3) large-head spine (0.5-1.0 μm). In aged rats, dendrites had significantly less spines (1.7 spines/μm) than young rat (2.3 spines/μm). The density of large-head spine and middle-head spine was significantly decreased in aged rats. From many studies, surprisingly, the number of neurons is not decreased and the dendritic atrophy does not occur upon aging in the hippocampus. Therefore, the observed decrease in spine density may be essential for loss of memory capacity. It is well known that sex-hormone replacement therapy rescues memory loss in humans, rats and mice, probably by restoration of synaptic density. Therefore, we have been investigation a correlation between the decrease in spine density and reduction of sex hormone levels in aged rat hippocampus (not only in blood circulation), using mass spectrometric determination.

3PT218 オプトジェネティクスを用いた光によるウィスカへの触覚刺激

Whisker photostimulation induces spike and LFP responses in barrel cortex of ChR2 transgenic rat

Tatsuya Honjoh[1,2], Zhi-Gang Ji[1,2], Toru Ishizuka[1,2], Hiromu Yawo[1,2,3] ([1]*Tohoku Univ. Grad.Sch. Lif Sci, Sendai, Japan*, [2]*CREST, JST*, [3]*Tohoku Univ. Center for Neuroscience*)

In one of thy1.2-channelrhodopsin 2 (ChR2)-Venus transgenic rat lines, W-TChR2V4, the ChR2-Venus conjugate was expressed exclusively in the mechanoreceptive, not in the nociceptive subpopulation of trigeminal ganglion neurons (Ji et al., poster of the 35th annual meeting of the Japan Neuroscience Society). As the sensory nerve endings are densely innervating each whisker follicle, its photostimulation is well expected to induce a whisker-related sensory perception.
The rats were anesthetized with urethane (1.2g/kg body weight). All whiskers of right side were trimmed to photo-stimulate the trigeminal nerve endings innervating the hair follicles. For extracellular recording, a 1.4-mm diameter craniotomy was performed over the barrel cortex of left hemisphere. Glass electrodes filled with 0.5M Na acetate were inserted into the cortex through an opening of the dura. Right whisker pad was illuminated broadly with a 50ms light pulse of blue LED.
We found that the whisker photostimulation could induce the spike and LFP responses of neurons in somatosensory barrel field. It is suggested that the whisker photostimulation could activate the whisker-barrel cortex pathway of mechanoreceptive signaling. The optogenetic actuation of the whisker mechanoreception would facilitate detailed studies of the rodents' whisker-barrel sensory system.
All animal procedures were conducted in accordance with the guiding principles of Physiological Society of Japan and NIH.

3PT219 軟体動物ナメクジの嗅覚中枢における長期活動ダイナミクス

Dynamics of long-term activities of the olfactory center in the land slug

Yuichi Tanaka[1], Kouya Katou[1], Minoru Saito[3], Yoshimasa Komatsuzaki[2] ([1]*Grad. Sch. Sci. and Tech., Nihon Univ.*, [2]*Dept Phys, CST, Nihon Univ*, [3]*Grad Sch Integ Basic Sci, Nihon Univ*)

Spontaneous oscillation of activity in olfactory system is commonly observed in various species and is thought to be important for odor-information processing. However, the functions of the oscillatory activity are not well understood. The land slug *Limax valentianus* has a highly developed olfactory center, the procerebrum (PC), which exhibits oscillation of local field potential (LFP) at about 1 Hz. Because the application of conditioned odor changes the frequency of the LFP oscillation in slug PC, odor information is thought to be represented as the temporal pattern of the oscillation. Here, we investigated the statistical property of spontaneous oscillation in the PC over an extended timescale. To analyze the autocorrelation of the time series of interspike intervals, we performed a detrended fluctuation analysis (DFA), which is a scaling analysis technique used to provide a quantitative parameter (scaling exponent, α). We found that the fluctuation of spike timing of the PC possessed a long-term correlation and can be characterized as 1/*f* noise at timescales larger than 10^2 spikes (α~1.10). Furthermore, to investigate the contribution of innervations to spontaneous oscillation, we measured the LFP following the tentacle amputation. In the scaling region for small n ($n < 10^2$ spikes), the scaling exponent α decreased from 0.73 to 0.58, indicating that the fluctuations of spike timings are uncorrelated under this experimental condition. These results suggest that the innervations to PC maintain the intrinsic dynamics.

3PT220 ヨーロッパモノアラガイの中枢神経系における神経活動の膜電位イメージング

Fluorescent Voltage Imaging of the Neural Activities in the Central Nervous System of the Pond Snail

Shogo Nakada[1], Makoto Hosoi[1], Yosimasa Komatuzaki[2], Minoru Saito[1] ([1]*Graduate School of Integrated Basic Sciences, Nihon University*, [2]*College of Science and Technology, Nihon University*)

The brain or ganglia forms a complex network composed of so many neurons which communicate with one another. We have found that a regulatory neuron (cerebral giant cell; CGC), which is involved in feeding responses, in the cerebral ganglion of the pond snail *Lymnaea stagnalis* shows regular beating, regular bursting and irregular bursting discharges depending on the d.c. current through the cell membrane. In the present study, we examined how the activities of CGC affect the neural activities of the buccal ganglion by using fluorescent voltage imaging technique. After the central nervous system was isolated from the body, it was stained with a voltage-sensitive dye, Di-4-ANEPPS. The stained preparation was illuminated by a LED (530 nm; LEX2-G, Brain Vision), and the 705 nm fluorescent images were acquired through a CCD camera (iXon X3 897, Andor or ORCA-Flash 4.0, Hamamatsu Photonics). The activities of CGC were measured simultaneously by intracellular recording using a glass electrode. The d. c. current was injected into CGC through the electrode to control the activities. The fluorescent images showed that some neurons in the buccal ganglion fired coherently, and the firing patterns were affected by the discharge of CGC.

3PT221 マウス海馬スライスの CA1 領域における様々な時空間活動パターンのレーザー共焦点イメージング

Laser confocal imaging of various spatiotemporal activity patterns in the CA1 region of mouse hippocampal slices

Hiromi Osanai[1], Akiyoshi Suzuki[2], Sachiko Matsumura[2], Hideo Mukai[3], Minoru Saito[2] ([1]*College of Humanities and Sciences, Nihon University*, [2]*Graduate School of Integrated Sciences, Nihon University*, [3]*Faculty of Medicine, Saitama Medical University*)

The brain forms a complex network composed of so many neurons which communicate with one another. In addition, even a single neuron shows very complex activities, and some neurons spontaneously fire due to nonlinear characteristics. Recently, Ikegaya et al. have developed functional multineuron calcium imaging which enables us to access brain function with single-neuron resolution. In the present study, we observed spatiotemporal activity patterns in the CA1 region of mouse hippocampal slices by a similar technique. The slices (350 μm) were prepared from 1-week-old male ddY mouse. The slice preparation was stained with a Ca^{2+}-sensitive dye, oregon green. The stained slice was illuminated by an Ar laser (488 nm; 532-BS-A04, Melles Griot), and the 520 nm fluorescence images were acquired through a Nipkow confocal unit (CSU-10, Yokogawa) and a CCD camera (iXon X3 897, Andor). As a result, some dozens of neurons fired incoherently in some slices, while they exhibited a completely coherent activity pattern in other slices. The coherent pattern occurred more frequently under the existence of penicillin and a higher K^+ concentration which are often used to induce the epilepsy-like state. Interestingly, we also observed the irregular switching between the coherent and incoherent activity patterns in other slices. This phenomenon may be explained by the dynamics of itinerancy among quasi-stable states reported in some neural network models.

3PT222 QM/MM 法による同化型亜硝酸還元酵素の反応機構についての理論的研究

A QM/MM study on the reaction mechanism of assimilatory nitrite reductase

Mitsuo Shoji[1,2], Kyohei Hanaoka[1], Daiki Kondo[1], Hiroaki Umeda[2], Megumi Kayanuma[2], Katsumasa Kamiya[1], Kenji Shiraishi[1], Shogo Nakano[3], Katsuo Katayanagi[3] ([1]*Grad. Sch. Pure & Appl. Sci., Univ. Tsukuba*, [2]*CCS, Univ. Tsukuba*, [3]*Grad. Sch. Sci., Hiroshima Univ.*)

Assimilatory nitrite reductase (aNiR) catalyzes a multi-electron reduction reaction of nitrite to ammonia, which is a fundamental process for the biological synthesis of

nitrogen-containing cellular constituents such as plant. Although this multi-electron reaction is a novel type of biological catalysis for the reaction specificity and regulation, the reaction mechanism is not fully understood yet because of the complicated reaction process. In this study, the mixed quantum mechanical/classical mechanical (QM/MM) method was applied to investigate the reaction mechanism of aNiR. We discuss the reaction efficiency of Nii3, one of the aNiR, based on the calculated intermediate states and the reaction energy profile.

3PT223 RNase H の RNA 加水分解反応機構の理論的研究

Computational study of the phosphodiester hydrolysis of RNA by RNase H

Yu Takano, Makoto Kita, Haruki Nakamura (*IPR, Osaka University*)

The phosphate diester hydrolysis is an important reaction in biology. The ribonuclease H (RNase H) catalyzes the nonspecific hydrolysis of RNA in RNA/DNA hybrids, yielding a 3'-hydroxyl and a 5'-phosphate at the hydrolysis site. This enzyme is found that the Mg^{2+} ion is essential for the enzymatic reaction and that aspartate and glutamate are coordinated the Mg^{2+} ion in the active site. This catalytic mechanism is ubiquitous among nucleic acid processing enzymes and ribozymes. In particular, RNases H has emerged as important therapeutic targets because RNase H activity is absolutely required for proliferation of HIV and other retroviruses. Although the X-ray crystallographic structures of RNase H are determined, there are controversies about the catalytic mechanism of RNase H, the number of Mg^{2+} ions, the proton transfer pathway, and the protonation states of the active site residues.
In the present study, we have explored the hydrolysis of the phosphate diester group of RNA by RNase H, using density functional theory to elucidate how many Mg^{2+} ions are required for the catalysis of RNase H. Our computation demonstrates that both one- and two-metal models show the step-wise hydrolysis pathway and lower the activation barriers, compared to the non-enzymatic hydrolysis of phosphate diester. However, the activation barrier of the two-metal model is smaller than that of the one-metal model by about10 kcal mol^{-1}.

3PT224 First principles molecular simulation with a generalized-ensemble algorithm for studying chemical reactions of biomolecular systems

Yoshiharu Mori[1], Yuko Okamoto[2,3,4] ([1]*IMS*, [2]*Dept. of Phys., Nagoya Univ.*, [3]*Structural Biology Research Center, Nagoya Univ.*, [4]*Center for Computational Science, Nagoya Univ.*)

It is important to study chemical reactions by molecular simulations because we have to treat a chemical reaction to understand an interesting chemical system such as biomolecular systems including enzymes. We can perform a first principles molecular simulation to understand these systems. However the time scale of a first principles molecular simulation is limited because its computational cost is much higher than a simulation with some force fields.
In order to overcome such a difficulty, we need to use generalized-ensemble algorithms, which enhance conformation sampling in molecular simulations. In this study, we used a simulated tempering method, Simulated Tempering Umbrella Sampling (STUS). Molecular simulations with this method can enhance a chemical reaction in reaction coordinate space. As a result, we can obtain the free energy of the chemical reaction accurately.
We performed first principles molecular dynamics simulations with the simulated tempering method for the system of malonaldehyde in water. The reaction coordinate fluctuated in large conformational space. As a result, we were able to calculate the potential of mean force of the reaction coordinate accurately. We found that molecular simulations with STUS also allow us to understand chemical reactions of biomolecular systems.

3PT225 大規模量子化学計算(FMO 法)による HIV-1 糖鎖認識抗体 2G12 と糖鎖間の相互作用解析

Interaction Analysis of HIV-1 Antibody 2G12 and Glycans by Large-Scale Quantum Chemical Calculations based on FMO method

Kaori Noto[1], Yuka Koyama[2], Keiko Takano[2] ([1]*Kitasato University*, [2]*Ochanomizu University*)

Human antibody 2G12 is capable of recognizing the high-mannose glycans on the HIV-1 surface glycoprotein, gp120. Doores et al. found that Fab-2G12 is bound to D-fructose stronger than the original ligand, D-mannose. Details of the neutral carbohydrate-antibody interaction remain unclear. To elucidate the differences in the ligand-binding, we carried out ab initio fragment molecular orbital (FMO) calculations at MP2/6-31G (d) level for Fab-2G12 with D-mannose/D-fructose complexes using their crystal structures (PDB ID: 1OP3, 3OAY). The interaction energy between Fab-2G12 and D-fructose was smaller than that between Fab-2G12 and D-mannose excluding the effects of water, which was not consistent with the experimental result. We further investigated the interaction involving water molecules observed in the crystal structures and found notable pair interaction energies among D-fructose, waters, and several amino acid residues. In addition, we constructed a model glycan ligand without a side chain group of the D-fructose and studied its interaction with the antibody to evaluate the effect of the substituent of the ligand on the interaction. The obtained results indicated a significant role of C2-OH group of D-fructose in the ligand-antibody interaction.

3PT226 FTIR 法による光合成酸素発生マンガンクラスター近傍の水素結合ネットワークの構造解析

FTIR analysis of the hydrogen bonding network around the O_2-evolving Mn_4CaO_5 cluster

Kai Ota, Takumi Noguchi (*Grad. Sch. Sci., Univ. Nagoya*)

Photosynthetic O_2 evolution is performed at the Mn_4CaO_5 cluster in photosystem II (PSII) through five intermediates called S states (S_0-S_4). Recent X-ray structure of PSII showed that two water molecules are bound to the Ca^{2+} and form a hydrogen-bond network between the Mn_4CaO_5 cluster and Y_Z. To clarify the roles of the water molecules and the hydrogen-bond network around the Ca^{2+}, we have investigated the effect of the replacement of Ca^{2+} with Ba^{2+} on these structures using Fourier transform infrared (FTIR) difference spectroscopy. S_2/S_1 FTIR difference spectra of moderately hydrated films of NaCl-washed PSII membranes of spinach were recorded at 283 K in the presence of either Ca^{2+} or Ba^{2+}. The weakly hydrogen-bonded OH bands of water at 3617/3587 cm^{-1} observed in Ca^{2+}-PSII were absent in Ba^{2+}-PSII. A broad feature at 2900-2600 cm^{-1}, which arises from strong hydrogen bonds with high proton polarizability, also disappeared in Ba^{2+}-PSII. These results strongly suggest that the above bands of water OH and strong hydrogen bonds originate from the water molecules bound to Ca^{2+} and the surrounding hydrogen bond network, respectively, and the replacement of Ca^{2+} with Ba^{2+} with a larger ion radius changed or destructed these structures. The data support the idea that either of the water molecules attached to the Ca^{2+} functions as a substrate and that the hydrogen-bond network from the Ca^{2+} to Y_Z plays an important role in proton transfer in the $S_2 \rightarrow S_3$ transition, which is blocked by Ba^{2+} substitution.

3PT227 QM/Langevin-MD と振動モード解析を用いた光合成初期過程における光化学系 II の理論的研究

A study of QM/Langevin-MD simulation and vibrational analysis for photosystem II in early process of photosynthesis

Waka Uchida[1], Yoshiro Kimura[1], Taichi Yuki[1], Makoto Hatakeyama[1], Koji Ogata[3], Satoshi Yokojima[2,3], Shinichiro Nakamura[3] ([1]*Graduate School of Tokyo Institute of Technology*, [2]*Tokyo University of Pharmacy and Life Sciences*, [3]*RIKEN Research Cluster for Innovation*)

In the early process of photosynthesis in photosystem II (PSII) protein, the oxidation reaction, evolving one oxygen molecule by oxidizing two water molecules, occurs in oxygen-evolving complex (OEC) forming oxo-bridged cluster consisting of four manganese and one calcium ions (Mn4O5Ca). This reaction goes through the five oxidation states denoted Sn (n=0-4), called Kok cycle. Here we have performed a QM/Langevin-MD simulation and FTIR spectrum calculation for OEC and residues surrounding it. The structure of PSII solved by X-ray crystallography at 1.9 Å was used in this study (PDB entry 3ARC). The structure was optimized using QM/MM calculations. And by changing Mn oxidation numbers at the same as S2 state ones, the structure satisfying four Mn oxidation numbers in the S2 state was predicted using QM/MM calculation from the structure of S1 state. For these optimized structures, QM/Langevin-MD and vibrational frequency were performed in many variation of four Mn oxidation numbers. From the experimental evidences, one Mn ion in the cluster is oxidized during going through S1 to S2 states, and meanwhile the spectra of Ala344 and Glu354 show the clear peak shift in IR spectra. We have observed the same peak shift in our vibrational frequency calculation. And the trajectory of QM/Langevin-MD simulation reveals the most stable Mn oxidation numbers of S1 state in the thermal fluctuation. In addition, based on the trajectory of the S1 state, we will discuss about four Mn oxidation numbers in the S2 state.

3PT228 コケ植物におけるそれぞれ異なる 3 つの消光機構

Three different mechanisms of energy dissipation of a desiccation-tolerant moss to protect reaction centres against photo-oxidation

Hisanori Yamakawa[1], Yoshimasa Fukushima[1], Shigeru Itoh[1], Ulrich Heber[2] ([1]*Grad. Sch. Sci., Univ. Nagoya*, [2]*Bio. Sci., Univ. Wurzburg*)

Three different types of non-photochemical de-excitation of absorbed light energy protect photosystem II of the sun- and desiccation-tolerant moss Rhytidium rugosum against photo-oxidation. The first mechanism, which is light-induced in hydrated thalli, is sensitive to inhibition by dithiothreitol. It is controlled by the protonation of a thylakoid protein. Other mechanisms are activated by desiccation. One of them permits exciton migration towards a far-red band in the antenna pigments where fast thermal deactivation takes place. This mechanism appears to be similar to a mechanism detected before in desiccated lichens. A third mechanism is based on the reversible photoaccumulation of a radical that acts as a quencher of excitation energy in reaction centres of photosystem II. On the basis of absorption changes around 800 nm, the quencher is suggested to be an oxidized chlorophyll. The data show that desiccated moss is better protected against photo-oxidative damage than hydrated moss. Slow drying of moss thalli in the light increases photo-protection more than slow drying in darkness.

3PT229 光化学系 II と金ナノ粒子の結合による人工光水分解ナノデバイスの開発

Development of artificial light-driven water splitting nanodevice using gold nanoparticles and photosystem II

Kousuke Kawahara[1], Tatsuya Tomo[2,3], Takumi Noguchi[1] ([1]*Grad. Sch. Sci., Nagoya Univ.*, [2]*Faculty of Sci., Tokyo Univ. of Sci.*, [3]*JST PRESTO*)

Development of efficient artificial photosynthetic systems is crucial to solve the energy and environmental crisis. We have recently developed a light-driven water-splitting nanodevice by conjugation of photosystem II (PSII) protein complexes with gold nanoparticles (GNPs) (Noji et al., J. Phys. Chem. Lett., 2011). However, O_2 evolution activity of this PSII-GNP conjugate was only 23% of free PSII. In this study, we have improved the preparation method of the PSII-GNP conjugates to increase the O_2 evolution activity and further detected light-induced electron transfer in PSII-GNP using attenuated total reflection (ATR)-Fourier transform infrared spectroscopy (FTIR). The previous decrease in the O_2 evolution activity in PSII-GNP was found to be caused by a low Ca^{2+} concentration (30 μM) in the buffer adopted to prevent aggregation of GNP. To address this problem, the incubation time for binding PSII with GNP in the 30 μM Ca^{2+} buffer was shortened from 120 min to 10 min, and then the resultant PSII-GNP was suspended in a buffer with 1 mM Ca^{2+}. The PSII-GNP conjugates were stable in the 1 mM Ca^{2+} buffer, whereas free GNP was aggregated in the same buffer. The O_2 evolution activity of the PSII-GNP increased by a factor of two compared with the previous study. A light-induced ATR-FTIR difference spectrum of the PSII-GNP conjugates in the presence of DCMU showed typical signals of the semiquinone anion of Q_A, providing evidence that light-driven electron transfer took place in this nonodevice.

3PT230 光化学系 II 酸素発生中心の暗所安定状態における電子スピン状態とプロトン化状態の理論的研究

Theoretical Study on the Protonation and Electronic Spin State of the O2-Evolving Complex in Photosystem II at the dark stable S1 state

Makoto Hatakeyama[1], Waka Uchida[1], Kouji Ogata[2], Satoshi Yokojima[2,3], Shinichiro Nakamura[2] ([1]*Grad. Sch. Bio., Titech*, [2]*Harima Inst., Riken*, [3]*Sch. Pharm., Tokyo Univ. Pharm.*)

An oxygen evolving complex (OEC) of photosystem II protein has been known as the catalyst for water splitting and oxygen evolving reactions of photosynthesis. The structure and catalytic capability of OEC have been investigated extensively by both experimental and theoretical studies, in order to learn how the water splitting proceeds in nature. The latest X-ray diffraction (XRD) analysis has revealed that the OEC contains the multi-nuclear Mn4Ca cluster with the five oxo bridges. Nonetheless, the XRD analysis has not indicated two indispensable factors for the water splitting mechanism; i.e. (i) coordinate of hydrogen atoms and (ii) electronic spin state of the Mn4Ca cluster. The coordinate of hydrogen atoms is necessary to analyze the strength of the Mn ion ligand field and to identify the oxidation Mn site during the water splitting. Although the Mn4Ca cluster has been elucidated to involve two Mn(III) and two Mn(IV) ions in the dark stable steady state (S1), the locations of Mn(III)/Mn(IV) ions in the latest crystal structure has been not yet determined in considering the coordinate of hydrogen atoms. Taking account on those arguments, we investigated the electronic spin state of the Mn4Ca cluster at the dark stable state, by respecting the latest crystal structure and by changing the protonation state of the coordinating O atoms around the Mn4Ca cluster.

3PT231 光合成酸素発生の S 状態サイクルにおける NH_4^+阻害のメカニズム

Mechanism of NH_4^+ inhibition in the S-state cycle of photosynthetic oxygen evolution

Takashi Kobayashi, Takumi Noguchi (*Grad.Sch.Sci.,Univ.Nagoya*)

Photosynthetic O_2 evolution by plants and cyanobacteria is performed at the Mn cluster in photosystem II (PSII). O_2 is released as a result of four-electron oxidation of two water molecules through a light-driven cycle of five intermediates called S states (S_0-S_4). We recently found that NH_4^+ works as an effective inhibitor of O_2 evolution. However, the detailed mechanism of NH_4^+ inhibition has not been understood yet. In this study, we investigated the mechanism of NH_4^+ inhibition in the O_2 evolving S-state cycle using Fourier transform infrared (FTIR) spectroscopy. PSII membranes from spinach in the presence of 200 mM NH_4Cl were subjected to12 successive flashes and FTIR difference spectra upon individual flashes were obtained. It was shown that the amplitude of the caroboxylate stretching bands was significantly reduced at the third flash, indicating that specific inhibition took place in the $S_3 \rightarrow S_0$ transition. The overall intensity of the FTIR signals was also smaller with NH_4Cl than with NaCl as a control, suggestive of irreversible inactivation of the Mn cluster. The O_2 evolution activity, however, was unchanged when the sample was incubated with 1 M NH_4Cl in the dark for 1 h and then washed. Flash-induced S_2/S_1 FTIR difference spectra repeatedly measured every five minutes showed a signal decrease as the flash number increases. These results suggest that NH_4^+ inhibition of O_2 evolution is caused by mixed effects of inhibition in the $S_3 \rightarrow S_0$ transition and irreversible inactivation of the Mn cluster in the S_2 state.

3PT232 光合成膜蛋白質 PSII の分子動力学シミュレーション

A study of molecular dynamics simulation on Photosystem II protein

Koji Ogata[1], Makoto Hatakeyama[2], Taichi Yuki[2], Waka Uchida[2], Shinichiro Nakamura[1] ([1]*RIKEN Research Cluster for Innovation*, [2]*Tokyo Institute of Technology*)

Photosystem II (PSII) protein, which governs the initial process of the photosystem in the plant, is transmembrane protein consisting of 20 subunits. This protein plays an important role of yielding O2 molecules by oxidizing water molecules. The structure of PSII has been solved by X-ray cystography techniques and publicly accessed from Protein Data Bank (PDB) and clearly shows the detail of structure in the active center for photosynthesis and statical structure can be observed. Here, to observe the dynamical structure of PSII protein, we have performed molecular dynamic simulation on a dimer PSII protein on the thylakoid membrane. The composition of phospholipids and galactolipids in the modeling thylakoid membrane were built as close as the native one. The parameters of four lipids (MGDG, DGDG, SQDG and PG) and the other ligands (Chlorophyll, Plastoquinone, etc.) were assigned in GAFF atomic types combining the charges obtaining by the quantum chemistry calculation. A trajectory of 10 ns simulation was analyzed. From the analysis of the trajectory, water molecules went through into the Mn4CaO5 cluster, which is important part for the O2 oxidation, using three pathways but not so fast movements near the Mn4CaO5 cluster. And the two monomer conformations of PSII showed the correlated motions with each other, the thylakoid membrane and the other ligands. We will discuss on the influences of the vibrations of PSII and its surroundings to the mechanism of the oxygen evolution in PSII protein.

3PT233 好熱性紅色硫黄細菌 Thermochromatium tepidum 由来 cytochrome c' における耐熱化メカニズムの検討

Molecular mechanisms for the thermostabilization of cytochrome c' from the thermophilic purple sulfur bacterium Thermochromatium tepidum

Sachiko Kasuga[1], Yukihiro Kimura[1,2], Kei Furusawa[3], Takashi Ohno[2], Seiu Otomo[3] ([1]*Grad. Sch. Agri. Sci., Kobe Univ.*, [2]*OAST, Kobe Univ.*, [3]*Fac. Sci., Ibaraki Univ.*)

Cytochrome (Cyt) c' purified from thermophilic purple sulfur photosynthetic

bacterium, Thermochromatium (Tch.) tepidum, exhibits enhanced thermal stability as compared with that of the mesophilic counterpart, Allochromatium (Alc.) vinosum despite 82% of sequence homology between two species. Recently, it was proposed that several factors including numbers of hydrogen bonds, flexibility and compactness of the structure enhance the thermal stability of Tch. tepidum Cyt c'. To understand more details of the thermostabilization, we focused on the amino acid residues at D131 or R129 position in the C-terminal region of Tch. tepidum Cyt c', and introduced single mutation using the E. coli expression system. The Cyt c' mutants were examined by differential scanning calorimetry (DSC) or resonance Raman spectroscopy to reveal the effects of C-terminal residues on the thermal stability or the heme environment of Cyt c'. The D131K and D131G mutants in the air-oxidized forms exhibited the denaturing temperatures, significantly lower than that of control Cyt c'. In contrast, R129K and R129A mutants denatured at the temperatures comparable to that of control Cyt c'. The resonance Raman bands of the control Cyt c' at 1635 and 1625 cm-1 for the intermediate-spin and high-spin states, respectively, were also affected by the mutations. Based on the results presented here and other finidngs, possible roles of the C-terminal residues of the Tch. tepidum Cyt c' are discussed.

3PT234 好熱性紅色硫黄細菌 Thermochromatium tepidum 由来光捕集 1 複合体における BChl-a と Trp 残基間の水素結合相互作用

Hydrogen-bonding interactions between BChl-a and Trp residues in the light-harvesting1 complexes from Thermochromatium tepidum

Yong Li[1], Yukihiro Kimura[1,2], Tomoko Numata[3], Yuta Inada[1], Teruhisa Arikawa[1], Seiu Otomo[4], Takashi Ohno[1] ([1]*Grad. Sch. Agri. Sco, Kobe Univ.*, [2]*OAST, Kobe Univ.*, [3]*HORIBA Co., Ltd.*, [4]*Fac. Sci., Ibaraki Univ.*)

The light-harvesting 1 reaction center (LH1-RC) from Thermochromatium (Tch.) tepidum exhibits an unusually red-shifted Qy absorption at 915 nm (B915) and the enhanced thermal stability in the presence of Ca ions. To access further details, thermal and spectroscopic properties of the LH1-RCs from wild-type and Sr-substituted Tch. tepidum were investigated by near infrared Raman spectroscopy and differential scanning calorimetry (DSC). The LH1-RCs purified from the Sr-substituted Tch. tepidum exhibited the Qy maximum at 888 nm (B888), blue-shifted by 27 nm from the native position. The B915 exhibited C3-acetyl/C13-keto νC=O bands at 1637/1675 cm-1, which were shifted to ~1643/1673 cm-1 when Ca was biosynthetically replaced with Sr. The removal of the original metal cations from B915 and B888 resulted in marked band shifts of the C3-acetyl/C13-carbonyl νC=O modes to ~1645/~1670 cm-1, supporting the metal cations to be involved in the fine-tuning of the hydrogen-bonding between the BChl-a and LH1-polypeptides. The hydrogen-bonding interactions were almost identical between the Ca2+-depleted B915 and Sr-depleted B888 and between B915 and Ca-substituted B888, despite the significant differences in their LH1 Qy positions and the DSC denaturing temperatures. Effects of the metal-depletion/-substitution on the hydrogen-bonding interactions strongly indicate that some factors besides the hydrogen-bondings between BChl-a and LH1-polypeptides are also responsible for the unusual Qy red-shift of the Tch. tepidum LH1-RC complexes.

3PT235 緑色硫黄細菌のホモダイマー光合成反応中心において部位特異的変異が一次電子供与体周辺の構造に与える影響

Local Structural Modifications around the Primary Electron Donor of the Green Sulfur Bacterial Photosynthetic Reaction Center

Chihiro Azai[1], Yuko Sano[1], Takumi Noguchi[1], Hirozo Oh-oka[2] ([1]*Div. Mat. Sci., Grad. Sch. Sci., Nagoya Univ.*, [2]*Dept. Biol. Sci., Grad. Sch. Sci., Osaka Univ.*)

Green sulfur bacteria are obligatory anaerobic photosynthetic bacteria. Their photosynthetic reaction center (RC) has a unique homodimeric core-protein, which consists of two identical core-polypeptides, while any other kinds of RCs have heterodimeric core-proteins. The homodimeric structure is considered as a primitive character from the view of molecular evolution, and the green sulfur bacterial RC is expected to be a model for the ancestral RC. However, the structure and the function of green sulfur bacterial RC are barely unknown because of difficulties in biochemical manipulation arisen from its anaerobic property. Therefore, molecular biological approach such as analyses using site-directed mutants is strongly desired to break through the present situation.
This is the first report of site-directed mutants of green sulfur bacterial RC. First, based on the X-ray structural information of Photosystem I, a homologue of green sulfur bacterial RC, we predicted the amino acid residues nearby the primary electron donor P840, a special dimer of bacteriochlorophyll *a*. Then, we constructed the amino acid substitution mutant RC for each residue, and studied its effect on the P840 with light-induced FTIR spectroscopy. As a result, the structural modification was clearly observed as a shift of a keto C=O band of bacteriochlorophyll *a* attributable to the P840

3PT236 Light-harvesting Antenna Phosphorylation Enhances Protein Mobility in Thylakoid Membranes

Masakazu Iwai[1,2], Changi Pack[2], Yoshiko Takenaka[3], Yasushi Sako[2], Akihiko Nakano[2,4] ([1]*JST PRESTO*, [2]*RIKEN ASI*, [3]*AIST*, [4]*University of Tokyo*)

Phosphorylation of chloroplast light-harvesting antenna complex II (LHCII) is essential for the energy balance between photosystem I (PSI) and photosystem II (PSII) in photoadaptation. However, molecular details of how LHCII phosphorylation causes to switch the energy flow between the two photosystems are still unclear. Single molecule measurements by using fluorescence correlation spectroscopy reveals that LHCII phosphorylation enhances protein mobility in a certain subfraction of thylakoid membranes in a unicellular green alga Chlamydomonas reinhardtii. Studies on a mutant of LHCII kinase, stt7, also revealed that the lack of LHCII phosphorylation slowed protein mobility in the thylakoid membrane. Our working model illustrates the possible function of LHCII phosphorylation that affects the molecular crowding in thylakoid membranes to counterbalance the energy levels between PSI and PSII.

3PT237 Essential role of NADPH oxidase in vitamin D3- and PMA-induced monocytic differentiation of PLB-985 cells

Hiroyuki Kato, Omi Nawa, Asuka Kato, Wakako Hiraoka (*Meiji University*)

Peripheral cellular differentiation is an important process for keeping homeostasis especially immune response and development. We have studied the role of reactive oxygen species (ROS) from NADPH oxidase in the process of monocytic differentiation of myeloid leukemia PLB-985 cells. Exposure to both or either tumor promoter Phorbol 12-myristate 13-acetate (PMA) and bioactive secosteroid 1 α, 25-dihydroxyvitamin D3 (vitamin D3) for a few days led the cells to acquire monocytic properties such as phagocytosis and adhesion activity. Both ESR spin-trapping and chemiluminescence revealed that NADPH oxidase was activated also in immature state of PLB-985 cells, in which OH- and O2- were detected. In order to clarify the role of NADPH oxidase and ROS, we employed NADPH oxidase gp91phox knockout X-CGD cells, whose response to PMA and VitD3 were compared to that of normal PLB-985 cell. In normal cells, VitD3 showed an intense adhesion to dishes, on the other hand PMA produced the adhesion property of cell-to-cell. These results indicate that the function of vitamin D3 was not identical to that of PMA in the process of monocytic differentiation. The antigen expression of surface molecule upon phagocytosis was measured with flow cytometry. The degree of expression of Mac-1α (leukocyte surface antigen :CD11b) and ICAM-1 (CD54) depended on stimulants and cells. Our result shows that there is some important role of NADPH oxidase in vitamin D3- and PMA-induced monocytic differentiation of PLB-985 cells.

3PT238 Effects of inositol hexaphosphate apatite cements on human cells and a biological implication between the cements and ROS

Asuka Kato, Mamoru Aizawa, Wakako Hiraoka (*Sch. Sci.&Tec, Univ. Meiji*)

Inositol hexaphosphate (IP_6), phytic acid, is a potent metal chelator, and is known as an anti-cancer reagent. Recently, IP_6 has received a lot of attention as ingredient in Hydroxyapatite ($Ca_{10}(PO_4)_6(OH)_2$; HAp) material of artificial bones and teeth. In this report, we examined the antioxidant effects of IP_6 and HAp-IP_6 cements, which are created by mixing the HAp powder modified with IP_6, on cell-free and cell culture systems. The enzymatic superoxide (O_2^-) from Hypoxanthine-xanthine oxidase (XO) and hydroxyl radical (HO·) from a fenton reaction (Fe(II)-H_2O_2) were employed for antioxidant assay using electron spin resonance (ESR) combined with spin-trapping. In vitro systems, in the case of IP_6, O_2^- and HO· were suppressed at neutral pH. In contrast, the effect of HAp-IP_6 was so sensitive to pH fluctuation as far as HO· is concerned. For the biological assay, human leukemia PLB-985 and X-CGD (NADPH oxidase knockout cell) cultures were utilized. Cells were incubated with 1-10 mM of IP_6 (pH7.4) for 24 hours. Both the inhibition of cell proliferation and the induction of apoptosis were detected in the cells treated with a concentration higher than 4 mM of IP_6. When the effect of HAp-IP_6 to cell survival at pH 7.4 was examined, there was a distinct difference between PLB-985 and X-CGD. It is possible that there' s some biological effect between HAp-IP_6 and ROS. These results

suggested that HAp-IP_6 has a potential to activate osteoblastic and osteoclastic cells in bone formation.

3PT239 MHz ultrasound inhibits leukemia cells

Risa Fuji, Yusuke Kobayashi (*Grad.Sch. Sci.&Tec, Univ. Meiji*)

Recently, ultrasound has been a lot of attention in medical field because of its widely usage in diagnosis and therapeutic treatment. However, the information about the therapeutic treatment mechanism and its safety of MHz ultrasound is insufficient. Therefore we have studied the biological effect of MHz ultrasound on human lymphoma U937 cells in order to properly evaluate the therapeutic effect of ultrasound. For an ultrasound apparatus, ceramic resonators of 1.0 MHz and 2.4 MHz were used and placed in the bottom of water tank made of brass. A glass tube containing 2.0 ml cell suspension was set above the transducer on the water. The frequency of ultrasound was 1.0 MHz, 2.4 MHz, 3.4 MHz, 5.7 MHz and 7.9 MHz. The intensity of ultrasound was determined with calorimetric method. The cells were irradiated with ultrasound for 10 seconds. Because the ultrasonic irradiation to the cells leads to excessive cell death of normal cells, we examined the survival rate of cells. The reproductive cell death was measured for three days after irradiation. In addition, we examined the induction of apoptosis one day after irradiation by flow cytometer. As a result, the cell growth of U937 was inhibited and the induction of apoptosis was observed in 1.0 MHz and 2.4 MHz. On the other hand, the effect of ultrasound on the cell growth was not seen in 7.9 MHz.

Name Index (索引)

名字（Family Name）のアルファベット順にソートしています。すべて、オンラインで入力されたデータのまま、表示しています。

Ando, Toshio (安藤 敏夫) 2PS053 (S119)
Aathi, Karunakaran (Aathi Karunakaran) 3PS004 (S146)
Abdul Razak, Nur Wahida (Abdul Razak Nur Wahida) 3PT126 (S162)
Abe, Jun (阿部 淳) **1PT144 (S93)**
Abe, Keiko (阿部 啓子) 3PT189 (S174)
Abe, Shuji (阿部 修治) **1PT127 (S90)**
Abe, Takahiro (阿部 貴寛) **2PS046 (S118)**
Abe, Tetsuya (阿部 哲也) 1PT123 (S89)
Abe, Tetsuyuki (阿部 哲之) 1PT159 (S96)
Abe-Yoshizumi, Rei (吉住 玲) 1B1424 (S21)
2F1412 (S47)
2I1448 (S54)
2PT181 (S136)
Accardi, Alessio (アッカーディ アレッシオ) 3PT118 (S160)
Adachi, Kengo (足立 健吾) **1PS031 (S79)**
3PS030 (S151)
Adachi, Shin-ichi (足立 伸一) 3PS024 (S150)
Adachi, Shinichi (足立 伸一) 1H1610 (S35)
Adachi, Taiji (安達 泰治) 1PT133 (S91)
1PT148 (S94)
1PT219 (S105)
Aigaki, Toshiro (敏郎 相垣) 2PT145 (S129)
Aihara, Kazuyuki (合原 一幸) 1SC-04 (S4)
Aihara, Ryuzo (相原 龍三) 1H1546 (S34)
Aihara, Tomoki (相原 朋樹) 2H1412 (S52)
Aihara, Yusuke (相原 悠介) 2F1510 (S48)
Aikawa, Yoshiki (相川 佳紀) 1PT123 (S89)
Aita, Yusuke (相田 雄亮) 1PT128 (S90)
1YS0930 (S90)
Aizawa, Mamoru (相澤 守) 3PT238 (S181)
Aizawa, Shin-Ichi (相沢 慎一) 2PS031 (S115)
2PS032 (S115)
Aizawa, Sin-Ichi (相沢 慎一) 2PS033 (S115)
Aizawa, Tomoyasu (相沢 智康) **1C1400 (S23)**
1PT138 (S92)
2PT177 (S135)
2PT179 (S136)
Akaike, Toshihiro (赤池 敏宏) 1D1400 (S25)
3PS045 (S154)
Akanuma, Satoshi (赤沼 哲史) 1PT135 (S91)
2PT203 (S139)
Akasaka, Kazuyuki (赤坂 一之) **1SB-03 (S2)**
1B1400 (S21)
2E1448 (S46)
2E1522 (S46)
Akashi, Satoko (明石 知子) 1PT190 (S101)
Aki, Yayoi (安藝 弥生) **2PT159 (S132)**
Akimoto, Takuma (秋元 琢磨) 1PT004 (S84)
3PT155 (S167)
Akimoto, Yuki (秋元 勇輝) **1PT214 (S104)**
Akinori, Sarai (皿井 明倫) 2PT102 (S121)
Akitaya, Tatsuo (秋田谷 龍男) **3C0924 (S60)**
Akiyama, Hidefumi (秋山 英文) 2PT187 (S137)
Akiyama, Minato (秋山 源) **3PT125 (S162)**
Akiyama, Nobuhiko (秋山 信彦) 1PT123 (S89)
Akiyama, Shuji (秋山 修志) 3B1110 (S59)
Akiyama, Yoshinori (秋山 芳展) 3PT122 (S161)
Akiyama, Yutaka (秋山 泰) 2PT104 (S122)
Akiyoshi, Kazunari (秋吉 一成) 3PT125 (S162)
Akutsu, Tatsuya (阿久津 達也) 1PT191 (S101)
Alam, Jahangir Md. (ALAM Jahangir Md.) 3PT173 (S171)
Alam, Jahangir Md. (Alam Jahangir Md.) **2G1424 (S50)**
Alhibshi, Amani (あるひぶし あまーに) **3PT209 (S176)**
Amano, Aya (天野 亜耶) **2PT164 (S133)**
Amano, Ken-ichi (天野 健一) 1PT137 (S92)
3PT116 (S160)
Amano, Marie (天野 万里) 2PT109 (S123)
Amano, Shota (天野 翔太) **1PT221 (S106)**
Amemiya, Takayuki (Amemiya Takayuki) 1I1436 (S35)
Amemiya, Takayuki (雨宮 崇之) **1I1424 (S35)**
Aminaka, Ryohta (網中 良太) **3PT129 (S162)**
Amino, Misako (網野 美紗子) 3PS002 (S146)
Amisaki, Takashi (網崎 孝志) 3PT106 (S158)
Amitani, Ichiro (網谷 一郎) **1PS045 (S82)**
Andachi, Tomoyo (安達 知世) **3PT156 (S167)**
Ando, Genki (安藤 元気) **1I1510 (S36)**
Ando, Hiromune (安藤 弘宗) 2PS024 (S114)
Ando, Joji (安藤 譲二) 2SH-06 (S16)
Ando, Koji (安藤 耕司) 3D1046 (S63)
Ando, Shoji (安藤 祥司) 1PS018 (S77)
Ando, Toshio (ANDO TOSHIO) 3F1058 (S67)
Ando, Toshio (Ando Toshio) 1H1522 (S34)
Ando, Toshio (安藤 敏夫) 2SB-03 (S10)
1H1510 (S34)
2G1534 (S51)
1PS046 (S82)
3PS004 (S146)
3PS016 (S148)
3PS017 (S148)
Ando, Yuriko (安藤 友里子) 2PT155 (S131)
2PT156 (S131)
Ando, Yuta (安藤 優太) 2D1448 (S44)
Aoki, Akihiro (青木 昭宏) 3E0924 (S64)
1PT111 (S87)
Aoki, Hiroyoshi (青木 弘良) 1I1610 (S37)
Aoki, Yoshimitsu (青木 義満) 2SH-01 (S16)
Aonuma, Hiroka (青沼 宏佳) 1I1546 (S36)
Aoyagi, Satoka (青柳 里果) **3PS027 (S150)**
Aoyama, Kazuhiro (青山 一弘) 2A1400 (S38)
2PS043 (S117)
Aoyama, Susumu (青山 晋) **3PS005 (S146)**
Arai, Hidenao (新井 秀直) **2PT146 (S130)**
Arai, Hidenobu (新井 秀信) **3A0936 (S56)**
Arai, Munehito (新井 宗仁) 1PT144 (S93)
1PT152 (S94)
1PT158 (S95)
1PT160 (S96)
Arai, Noriyoshi (荒井 規允) 3PT155 (S167)
Arai, Ritsuko (荒井 律子) 1SD-04 (S4)
Arai, Ryoichi (新井 亮一) **1PT106 (S86)**
Arai, Yoshihiro (新井 善博) 1H1534 (S34)
1H1546 (S34)
Arakawa, Takamasa (荒川 貴将) **3PT010 (S157)**
Arakawa, Tsutomu (荒川 力) 1PT005 (S84)
Araki, Tsutomu (荒木 勉) 1H1558 (S34)
Aramaki, Shinji (荒牧 慎二) **2A1400 (S38)**
Arata, Toshiaki (荒田 敏昭) **2H1412 (S52)**
3B1046 (S59)
1PS038 (S80)
Arata, Yukinobu (荒田 幸信) **1D1424 (S25)**
Arikawa, Keisuke (有川 敬輔) **1PT134 (S91)**
Arikawa, Kentaro (蟻川 謙太郎) 2PT190 (S138)
1YS1015 (S138)
Arikawa, Teruhisa (有川 曜央) 3PT234 (S181)
Arimatsu, Hiroshi (有松 寛) **2PT240 (S145)**
Arisaka, Fumio (有坂 文雄) 1PS012 (S76)
1PT156 (S95)
2PT144 (S129)
Arita, Mayuno (有田 真優乃) 2PT121 (S125)
Ariyama, Hirotaka (有山 弘高) **3PT140 (S165)**
Arizono, Misa (有薗 美沙) 3PT206 (S175)
Asada, Mizue (浅田 瑞枝) **3D1022 (S63)**
Asai, Yusuke (浅井 佑介) 3F0936 (S66)
Asai, Yusuke (浅井 祐介) 2G1610 (S51)
Asakawa, Yoshinori (浅川 義範) 1D1610 (S26)
Asakura, Tetsuo (朝倉 哲郎) 3E0924 (S64)
1PT111 (S87)
Asano, Ryutaro (浅野 竜太郎) 1C1448 (S23)
Asano, Toshifumi (浅野 豪文) **1PS010 (S75)**
Asano, Yuka (浅野 友香) 1PT211 (S104)
Asano, Yuuki (浅野 裕輝) 1PT190 (S101)
Asao, Akihiro (浅尾 晃央) 2PT209 (S140)
Asashima, Makoto (浅島 誠) 3PT207 (S176)
Asaumi, Akira (浅海 光) 2PS030 (S115)
Ashida, Masaaki (芦田 昌明) 1H1558 (S34)
Ashizawa, Ryota (芦沢 竜壮) **3D1034 (S63)**
Ataka, Kenichi (安宅 憲一) **1F1546 (S30)**
Atomi, Tomoaki (跡見 友章) 1SB-04 (S2)
1SB-05 (S2)
1SB-06 (S2)
Atomi, Yoriko (跡見 順子) **1SB-04 (S2)**
1SB-05 (S2)
1SB-06 (S2)
Atsumi, Tatsuo (渥美 龍男) 2I1610 (S55)
Awazu, Akinori (粟津 暁紀) **2PT135 (S128)**
2PT141 (S129)
2PT214 (S141)
2PT218 (S141)
Ayade, Heev (Ayade Heev) **1PT125 (S90)**
2PT240 (S145)
Azai, Chihiro (浅井 智広) **3PT235 (S181)**
Azechi, Satoe (疇地 里衣) 3PT149 (S166)
Azuma, Ryuzo (我妻 竜三) **2D1412 (S44)**
Azuma, Takachika (東 隆親) 3B0924 (S58)
Baba, Akinori (馬場 昭典) **2PT226 (S143)**
Baba, Reisuke (馬場 玲輔) 1C1424 (S23)
Baba, Teruhiko (馬場 照彦) **3PT169 (S170)**
Baba, Toshihiko (馬場 俊彦) 3PT123 (S161)
Baigl, Damien (ベイグル ダミアン) 2G1436 (S50)
Bannai, Hiroko (坂内 博子) **3PT206 (S175)**
Banno, Masaki (番野 雅城) **2PT006 (S120)**
Banno, Miho (阪野 美穂) 2PT117 (S124)
Banno, Satomi (坂野 聡美) 3PS036 (S152)
Bao, Yulong (包 玉龍) **1PS011 (S75)**
1PS013 (S76)
Baskin, Ronald (Baskin Ronald) 1PS045 (S82)
Baxter, Nicky (Baxter Nicky) 1PT112 (S87)
Berry, Richard (Berry Richard) 1A1534 (S20)
Bertz, Morten (Bertz Morten) **3PT166 (S169)**
Bhattacharyya, Bhaswati (Bhattacharyya Bhaswati) **3H1058 (S71)**
Biyani, Manish (ビヤニ マニッシュ) 2PT146 (S130)
Blair, D. (Blair David) 2SA-02 (S9)
Bloquel, David (Bloquel David) 1H1522 (S34)
Bremerich, Marcel (Bremerich Marcel) 2PT240 (S145)
Caaveiro, Jose (カーベイロ ホセ) 3F0912 (S65)
Caaveiro, Jose M. M. (Caaveiro Jose M. M.) 2PT151 (S131)
Campbell, Kevin L. (Kevin L. Campbell) 1PT101 (S85)
Cao, Wei (曹 巍) 2PT010 (S121)
Carlton, Peter (Carlton Peter) **2SC-05 (S11)**
Cervantes-Salguero, Keitel (Cervantes-Salguero Keitel) **3PT109 (S159)**
Chadda, Ankita (チャダ アンキタ) 3PT172 (S170)
Chaen, Shigeru (茶圓 茂) 2PS013 (S112)
2PS014 (S112)
Chandak, Mahesh (CHANDAK MAHESH) **1B1412 (S21)**
Chang, Le (常 楽) **2E1558 (S47)**
Chatani, Eri (茶谷 絵理) **1E1424 (S27)**
Chaudhuri, Abhishek (Chaudhuri Abhishek) 3H1058 (S71)
Che, Yong-Suk (蔡 栄淑) **2PS001 (S110)**
2PS004 (S110)
Chen, Jin (CHEN Jin) 1B1412 (S21)
Chen, Jin (陳 進) 1PT143 (S93)
Chiba, Masataka (千葉 雅隆) **3H1110 (S71)**
Chiba, Shuntaro (千葉 峻太朗) 2PT185 (S137)
3PT133 (S163)
Chiba, Shuntaro (千葉 峻太郎) 3PT160 (S168)
Chiba, Susumu (千葉 奏) **3PT131 (S163)**
Chijenji, Geroge (千見寺 浄慈) 2PT004 (S120)
Chijimatsu, Reiko (千々松 伶子) **2A1424 (S38)**
Chikayama, Eisuke (近山 英輔) **2PT237 (S145)**
Chikenji, George (千見寺 浄慈) 2PT002 (S119)
2PT003 (S120)
2PT009 (S121)
2PT202 (S139)
Chiwata, Ryohei (千綿 亮平) **3A1022 (S57)**
Choi, Seokwoo (崔 錫宇) **2PT175 (S135)**
Christie, John M. (Christie John M) 2F1558 (S49)
Crane, Brian R. (Crane Brian R.) **2SA-02 (S9)**
Dasgupta, Bhaskar (Dasgupta Bhaskar) **2B1436 (S40)**
David von, Stetten (デヴィッド フォン ステッテン) 2SH-01 (S16)
Davis, Tim (Davis Tim) 1PS040 (S81)
Dedachi, Kenichi (出立 兼一) 2B1400 (S40)
Deguchi, Shinji (出口 真次) **3H1022 (S70)**
2PS036 (S116)
Deisseroth, Karl (Deisseroth Karl) 1PT128 (S90)
1YS0930 (S90)
Demura, Makoto (出村 誠) **1SH-01 (S7)**
1C1400 (S23)
3C0924 (S60)
2PT176 (S135)
2PT177 (S135)
2PT179 (S136)
2PT182 (S136)
Dewa, Takahisa (出羽 毅久) 2G1558 (S51)
Dhara, Koushik (Dhara Koushik) **1C1424 (S23)**
Ding, Da-Qiao (丁 大橋) 2SG-06 (S15)
Dombrowski, Christopher (Dombrowski Christopher) 1PS045 (S82)
Dono, Kohei (道野 宏平) **2PS033 (S115)**
Dora, Sujit Kumar (Dora Sujit Kumar) **1H1522 (S34)**
Dos Remedios, Cristobal G. (dos Remedios Cristobal G.) 1PS016 (S76)

Ebihara, Tatsuhiko (海老原 達彦) 3E1022 (S64)
Ebina, Teppei (蝦名 鉄平) 2PT001 (S119)
Ebisuya, Miki (戎家 美紀) **2SG-04 (S15)**
Echigo, Akinobu (越後 輝敦) 2PT201 (S139)
Eiraku, Mototsugu (永楽 元次) 1PT219 (S105)
Ejima, Daisuke (江島 大輔) 2H1534 (S53)
Endo, Masahiro (遠藤 将弘) **1PT226 (S107)**
Endo, Masayuki (遠藤 政幸) 1PS042 (S81)
3PT111 (S159)
Endo, Shigeru (猿渡 茂) 3PT190 (S174)
Enoki, Sawako (榎 佐和子) **3A0924 (S56)**
Enomoto, Koichiro (榎本 洸一郎) 2PT234 (S144)
Ewald, Maxime (EWALD MAXIME) **3F1058 (S67)**
Feig, Michael (Feig Michael) **2SD-01 (S12)**
Feig, Michael (Michael Feig) 1PT201 (S102)
1YS1100 (S102)
Ferreon, Josephine C. (Ferreon Josephine C.)
1PT158 (S95)
Fuchigami, Sotaro (渕上 壮太郎) 1PT190 (S101)
2PT134 (S127)
Fuji, Kana (冨士 香奈) **1PT189 (S101)**
Fuji, Risa (藤 里砂) **3PT239 (S182)**
Fujihashi, Yuta (藤橋 裕太) **3D0936 (S62)**
Fujii, Hiroshi (藤井 浩) 3I0924 (S71)
3I1046 (S73)
Fujii, Masaaki (藤井 正明) 3PS038 (S152)
Fujii, Masashi (藤井 雅史) 2PT141 (S129)
2PT218 (S141)
Fujii, Satoshi (藤井 聡) 1C1534 (S24)
2PT106 (S122)
3PT108 (S158)
Fujii, Takashi (藤井 高志) **2SB-05 (S10)**
Fujii, Takasi (藤井 高志) 2SE-01 (S12)
Fujii, Takeshi (藤井 毅) 3PT184 (S173)
Fujii, Tetsuya (藤井 徹矢) **1PT133 (S91)**
Fujii, Yasuhiro (藤井 康裕) 3PT154 (S167)
Fujimoto, Eriko (藤本 恵理子) 2I1610 (S55)
Fujimura, Shoko (藤村 章子) **3PS030 (S151)**
Fujino, Masayuki (藤野 真之) 1PT102 (S85)
Fujisaki, Hiroshi (藤崎 弘士) **2B1412 (S40)**
1PT170 (S98)
1PT189 (S101)
2PT137 (S128)
Fujisawa, Masao (藤澤 雅夫) 2B1510 (S41)
Fujisawa, Takuya (藤澤 拓也) 3G1010 (S68)
Fujita, Eri (藤田 恵理) 1SB-04 (S2)
1SB-06 (S2)
Fujita, Hideaki (藤田 英明) 3PS037 (S152)
Fujita, Katsumasa (藤田 克昌) 3PS037 (S152)
Fujita, Keisuke (藤田 恵介) 1PS049 (S82)
1YS0900 (S82)
1PT006 (S84)
Fujita, Masaya (藤田 昌也) 1PT163 (S96)
Fujita, Shuji (藤田 嵩治) **3PS004 (S146)**
Fujita, Yutaro (Fujita Yutaro) 1PT114 (S87)
Fujita-Yanagibayashi, Sari (柳林(藤田) 彩理)
1F1436 (S29)
Fujitani, Hideaki (藤谷 秀章) 1PT173 (S98)
Fujiwara, Hitomi (藤原 瞳) **1PT163 (S96)**
Fujiwara, Kei (藤原 慶) **1E1448 (S27)**
1PT226 (S107)
1PT227 (S107)
1PT228 (S107)
Fujiwara, Kuniyo (藤原 邦代) **2PT182 (S136)**
Fujiwara, Satoru (藤原 悟) 2H1400 (S51)
1PT003 (S83)
Fujiwara, Shin-ichi (藤原 伸一) **3PT106 (S158)**
Fujiwara, Takahiro (藤原 敬宏) 1H1448 (S33)
1PT209 (S103)
2PS041 (S117)
Fujiwara, Takahiro K. (藤原 敬宏) 1G1412 (S31)
3PT172 (S170)
Fujiyoshi, Satoru (藤芳 暁) **2SI-03 (S17)**
Fujiyoshi, Yoshinori (藤吉 好則) 3B0900 (S57)
3F0924 (S66)
Fukada, Harumi (深田 はるみ) 2E1522 (S46)
Fukagawa, Akihiro (深川 暁宏) **3PT104 (S158)**
Fukaminato, Tuyoshi (深港 豪) 3PT102 (S157)
Fukano, Hiroko (深野 弘子) **1PT238 (S109)**
Fukuchi, Satoshi (Fukuchi Satoshi) 1I1436 (S35)
Fukuchi, Satoshi (福地 佐斗志) 1I1424 (S35)
Fukuda, Ikuo (福田 育夫) 3PT010 (S157)
Fukuda, Mao (福田 真生) **3PS019 (S149)**
Fukuda, Masaki (福田 真己) **1PT135 (S91)**
Fukuda, Norio (福田 紀男) 2H1510 (S52)
2H1546 (S53)
1PS009 (S75)
1PS016 (S76)
Fukuda, Shingo (福田 真悟) **1H1510 (S34)**
Fukuda, Takafumi (福田 隆文) **1PT151 (S94)**
Fukuda, Tetsuya (福田 哲也) 2G1610 (S51)
3F0936 (S66)
Fukuda, Toshio (福田 敏男) 1PT229 (S107)
1PT233 (S108)
Fukui, Sadaharu (福井 貞晴) 1PT106 (S86)
Fukujin, Fumihito (福神 史仁) **2PS045 (S118)**
Fukumori, Yoshihiro (福森 義宏) **2SE-02 (S13)**
Fukumura, Takuma (福村 拓真) **2PS005 (S110)**
Fukunaga, Kentaro (福永 謙太郎) 1PT169 (S97)
Fukunaga, Yukihiro (福永 幸裕) 2PT122 (S125)
Fukuoka, Hajime (福岡 創) 2I1546 (S55)
2I1558 (S55)
2PS003 (S110)
Fukuoka, Mayuko (福岡 万佑子) 1PT139 (S92)
Fukushima, Kazuhiko (福島 和彦) 3PS027 (S150)
Fukushima, Mitsuyasu (福島 光鎮) 3PS036 (S152)
Fukushima, Yoshimasa (福島 佳優) 3PT228 (S180)
Funatsu, Takashi (船津 高志) 3C1058 (S61)
1PT208 (S103)
1PT234 (S108)
1PT236 (S108)
3PS010 (S147)
1YS0915 (S147)
3PS029 (S151)
3PS040 (S153)
Funayama, Tomoo (舟山 知夫) 1G1510 (S31)
Furuike, Shou (古池 晶) 3A1022 (S57)
1PS035 (S80)
Furukawa, Ayako (古川 亜矢子) **3C1034 (S61)**
3PT003 (S155)
Furukawa, Eiji (古川 英嗣) 2PT110 (S123)
Furukawa, Taichi (古川 太一) 1H1558 (S34)
Furukawa, Yoshiaki (古川 良明) **2B1534 (S41)**
2B1546 (S41)
2B1558 (S41)
2B1610 (S41)
3C0900 (S59)
Furukawa, Yukio (古川 進郎) 2PS005 (S110)
Furuki, Takao (古木 隆夫) 1PT162 (S96)
Furuki, Takao (古木 隆生) **3G0912 (S67)**
Furuno Tadahide (古野 忠秀) **1PT206 (S103)**
Furuno, Tadahide (古野 忠秀) 2D1558 (S45)
3PT176 (S171)
Furuno, Taiji (古野 泰二) **3PS018 (S149)**
Furusawa, Chikara (古澤 力) **1PT218 (S105)**
Furusawa, Hiroyuki (古澤 宏幸) 1PT162 (S96)
Furusawa, Kei (古澤 敬) 3PT233 (S180)
Furuta, Akane (古田 茜) **3PS002 (S146)**
Furuta, Ken'ya (古田 健也) **1SI-04 (S8)**
2PS019 (S113)
3PS002 (S146)
Furuta, Masakazu (古田 雅一) 2I1610 (S55)
Furuta, Miyuki (古田 美由紀) 3PT135 (S164)
Furuta, Tadaomi (古田 忠臣) **2PT125 (S126)**
2PT137 (S128)
3PT133 (S163)
3PT160 (S168)
Furutani, Yuji (古谷 祐詞) 1C1546 (S24)
1C1558 (S24)
1F1400 (S29)
2G1610 (S51)
3F0936 (S66)
2PT182 (S136)
2PT183 (S137)
3PT168 (S170)
Furutani-Umezu, Nozomi (梅津 のぞみ) **1PS051 (S83)**
Furuya, Kishio (古家 喜四夫) **1PT203 (S102)**
Furuya, Sonoko (古家 園子) 1PT203 (S102)
Futaki, Shiro (二木 史朗) 2SB-02 (S10)
Ge, Zhenyi (葛 臻翼) **2PT010 (S121)**
Geetha, Hiremath (Geetha Hiremath) 2PS049 (S118)
Gekko, Kunihiko (月向 邦彦) 1PT108 (S86)
Gennis, Robert (Gennis Robert) 2PT155 (S131)
2PT156 (S131)
Getzoff, Elizabeth (Getzoff Elizabeth) 2F1546 (S49)
Getzoff, Elizabeth D. (Getzoff Elizabeth D)
2F1558 (S49)
Getzoff, Elizabeth D. (ゲトゾフ エリザベス)
2F1534 (S49)
Go, Mitiko (郷 通子) 2PT127 (S126)
Go, Nobuhiro (郷 信広) 3PS026 (S150)
Gohara, Kazutoshi (郷原 一寿) 1D1522 (S26)
Gohara, Mizuki (郷原 瑞樹) **1B1424 (S21)**
2I1448 (S54)
Golestanian, Ramin (Golestanian Ramin) 1SF-03 (S6)
Gomibuchi, Yuki (五味渕 由貴) **1PS001 (S74)**
Gonzalez-Bonet, G. (Gonzalez-Bonet Gabriela)
2SA-02 (S9)
Goto, Masaki (後藤 優樹) 3G0936 (S68)
3G0948 (S68)
Goto, Susumu (五斗 進) **2PT107 (S122)**
Goto, Takafumi (後藤 孝文) 2PS034 (S115)
Goto, Takashi (後藤 孝) 2G1522 (S50)
3PT158 (S168)
Goto, Touichiro (後藤 東一郎) 3PT148 (S166)
Goto, Yuji (後藤 祐児) 1E1436 (S27)
1PT145 (S93)
Gotoh, Masao (後藤 正男) 1PT220 (S105)
1PT221 (S106)
3PS019 (S149)
3PT209 (S176)
Gouaux, Eric (Gouaux Eric) 1PT103 (S85)
1YS1030 (S85)
Gowrishankar, Kripa (Gowrishankar Kripa)
3H1058 (S71)
Gruet, Antoine (Gruet Antoine) 1H1522 (S34)
Guerin, Laurent (ゲラン ロラン) 2SH-01 (S16)
Gunji, Yukio (郡司 幸夫) 2PT210 (S140)
2PT234 (S144)
2PT235 (S144)
Gunji, Yukio-Pegio (郡司 ペギオ-幸夫) 2PT236 (S144)
Guo, Hao (Guo Hao) **1C1546 (S24)**
Gustafsson, Nils (Gustafsson Nils) **1PS030 (S79)**
Habchi, Johnny (Habchi Johnny) 1H1522 (S34)
Hada, Takuya (秦 拓也) 3PT119 (S160)
Haga, Hisashi (芳賀 永) 1PT230 (S107)
Hagiwara, Yohsuke (萩原 陽介) 1B1610 (S22)
Hagiya, Tomoka (萩谷 朋佳) **3PT133 (S163)**
Hagiyama Man (萩山 満) 1PT206 (S103)
Hagiyama, Man (萩山 満) 2D1558 (S45)
Hakamada, Kazumi (袴田 和巳) 2PT228 (S143)
3PS048 (S154)
Hakoshima, Toshio (箱嶋 敏雄) 1B1448 (S21)
Hamachi, Itaru (浜地 格) 2PT151 (S131)
Hamada, Daizo (浜田 大三) 1PT159 (S96)
Hamada, Hiroshi (濱田 博司) 1SF-02 (S6)
Hamada, Shogo (浜田 省吾) 1PT227 (S107)
3PT109 (S159)
3PT112 (S159)
3PT113 (S159)
Hamada, Syougo (浜田 省吾) 1PT226 (S107)
Hamada, Tomoyo (浜田 智代) **2D1510 (S44)**
3PS020 (S149)
3PS022 (S149)
Hamada, Tsutomu (濱田 勉) **3PT153 (S167)**
1YS1045 (S167)
Hamada, Tsutomu (濱田 勉) 3G1022 (S68)
Hamaguchi, Hiro-o (浜口 宏夫) 2SH-03 (S16)
Hamajima, Yuki (濱島 裕輝) 1PT113 (S87)
Hamasaki, Naotaka (濱崎 直孝) 3PT117 (S160)
Hamasaki, Yuuta (浜崎 雄太) 2PT233 (S144)
Han, Sung-Woong (韓 成雄) 1PT148 (S94)
Han, Yong-Woon (韓 龍雲) **1SD-01 (S4)**
Hanaoka, Kyohei (花岡 恭平) 3PT222 (S178)
Hanashima, Akira (花島 章) 1PS011 (S75)
1PS013 (S76)
Hanazono, Yuya (花園 祐矢) **1PT123 (S89)**
Handa, Daisuke (半田 大祐) 3PT169 (S170)
Handa, Naofumi (半田 直史) 1PS046 (S82)
Haneda, Takahiro (羽子田 貴広) 2PS047 (S118)
Hara, Chiho (原 千穂) 3PT180 (S172)
Hara, Masayuki (原 雅行) **3I1010 (S72)**
Hara, Noritaka (原 典孝) 2I1424 (S54)
Hara, Yukari (原 ゆかり) 3C0936 (S60)
Harada, Kouji (原田 耕治) **2C1558 (S43)**
Harada, Ryuhei (原田 隆平) **1PT201 (S102)**
1YS1100 (S102)
Harada, Tomoaki (原田 知明) **1PT237 (S109)**
Harada, Yoshie (原田 慶恵) 1SD-01 (S4)
3C1046 (S61)
1PS042 (S81)
3PS010 (S147)
1YS0915 (S147)
3PS031 (S151)
3PT111 (S159)
Haraguchi, Tokuko (原口 徳子) 2SG-06 (S15)
Harata, Masahiko (原田 昌彦) 3PS033 (S151)
3PS034 (S152)
Haruna, Taichi (春名 太一) **2PT217 (S141)**
Haruyoshi, Toyoda (豊田 晴義) 3PT214 (S177)
Haseda, Keisuke (長谷田 圭亮) **3PS041 (S153)**
Hasegawa, Katsuya (長谷川 克也) 1SB-04 (S2)
1SB-06 (S2)
Hasegawa, Koji (長谷川 浩司) 1H1610 (S35)
Hasegawa, Masashi (長谷川 正) 1PT113 (S87)
Hasegawa, Yoshitaka (長谷川 賢卓) **3PT207 (S176)**
Hasemi, Takatoshi (長谷見 崇俊) **2PT177 (S135)**
Hashi, Yurika (橋 友理香) 2PS035 (S116)
Hashikami, Kentaro (階上 健太郎) 1C1448 (S23)
Hashimoto, Kazuhito (橋本 和仁) 1I1558 (S36)
3D1058 (S63)
Hashimoto, Ken (橋本 健) 3G1010 (S68)
Hashimoto, Mamoru (橋本 守) 1H1558 (S34)
Hasimoto, Yuh (橋本 優) 3PS030 (S151)
Hata, Hiroaki (畑 宏明) **3C0912 (S60)**
Hata, Tomonori (秦 智紀) 2A1448 (S38)
Hatae, Hinako (波多江 日成子) 3PT117 (S160)
Hatakeyama, Makoto (畠山 允) 3PT227 (S179)
3PT230 (S180)

3PT232 (S180)
Hatakeyama, Tetsuhiro (畠山 哲央) **2PT231 (S144)**
Hatanaka, Rie (畑中 理恵) 1PT162 (S96)
Hatanaka, Yuusuke (畑中 悠介) 3PT213 (S177)
Hatano, Ken-ichi (秦野 賢一) 2PT114 (S124)
Hatano, Tatsurou (波多野 達朗) 1PT192 (S102)
Hatori, Kuniyuki (羽鳥 晋由) 1PS048 (S82)
2PS012 (S112)
Hatta, Ichiro (八田 一郎) 3G1110 (S69)
3PT151 (S167)
Hattori, Akihiro (服部 明弘) 3PS023 (S149)
3PS046 (S154)
3PS049 (S154)
Hattori, Junko (服部 純子) 1PT102 (S85)
Hattori, Koji (服部 浩二) 3PS044 (S153)
3PS051 (S155)
Hattori, Motoyuki (服部 素之) **1PT103 (S85)**
1YS1030 (S85)
Hattori, Yoshikazu (服部 良一) 1B1424 (S21)
Hayakawa, Kimihide (早川 公英) 2B1448 (S40)
2PS034 (S115)
Hayakawa, Masayuki (早川 雅之) **1PT224 (S106)**
Hayakawa, Yoshinori (早川 慶紀) **2C1436 (S42)**
Hayakawa, Yoshinori (早川 美徳) **1SC-02 (S3)**
Hayano, Yosuke (早野 陽介) 1PT155 (S95)
Hayashi, Fumio (林 史夫) 2PS030 (S115)
2PT110 (S123)
2PT119 (S124)
2PT120 (S125)
Hayashi, Fumio (林 文夫) 2PT180 (S136)
3PT161 (S168)
Hayashi, Katsuhiko (林 克彦) **1PT117 (S88)**
Hayashi, Kumiko (林 久美子) **2SI-04 (S17)**
1PS028 (S78)
1PS029 (S79)
Hayashi, Nobuhiro (林 宣宏) 3PT124 (S161)
Hayashi, Ryunosuke (林 龍之介) **1PS029 (S79)**
Hayashi, Shigehiko (林 重彦) 3B1034 (S59)
1PT128 (S90)
1YS0930 (S90)
2PT178 (S136)
Hayashi, Takashi (林 高史) 2PT162 (S133)
2PT164 (S133)
Hayashi, Tomohiko (林 智彦) **2F1400 (S47)**
Hayashi, Yukiko (林 由起子) 3PT002 (S155)
Hayashi, Yuuki (林 勇樹) **1C1436 (S23)**
1PT160 (S96)
Hayashida, Takuya (林田 拓也) 3PT105 (S158)
Hazemoto, Norio (櫨本 紀夫) 3C0924 (S60)
Head, David (Head David) **1PS018 (S77)**
Heber, Ulrich (Heber Ulrich) 3PT228 (S180)
Heberle, Joachim (Heberle Joachim) 1F1546 (S30)
Hegemann, Peter (Hegemann Peter) 1PT128 (S90)
1YS0930 (S90)
Hellingwerf, Klaas (Hellingwerf Klaas) 2PT175 (S135)
Hexig, Bayar (賀喜 白乙) 1D1400 (S25)
3PS045 (S154)
Hibino, Katsutoshi (日比野 勝俊) **2PT011 (S121)**
Hibino, Kayo (日比野 佳代) **1G1558 (S32)**
2PS044 (S117)
Hibino, Masahiro (日比野 政裕) **3G1010 (S68)**
Hida, Akira (肥田 哲) **2PS007 (S111)**
Hidaka, Tetsurou (日高 徹郎) 1F1558 (S30)
Higa, Seiji (比嘉 世滋) 2PT149 (S130)
Higo, Junichi (肥後 順一) 1PT168 (S97)
Higuchi, Hideo (樋口 秀男) 1SI-01 (S8)
1H1412 (S33)
2A1522 (S39)
2A1558 (S39)
Higuchi, Yoshiki (樋口 芳樹) 3B0912 (S57)
Hiiragi, Takashi (柊 卓志) **2SF-05 (S14)**
Hijikata, Hiroko (土方 博子) 3PT172 (S170)
Hikima, Takaaki (引間 孝明) 2D1522 (S45)
3PT146 (S166)
Himeno, Hiroki (姫野 泰輝) **3G1022 (S68)**
Hira, Riichiro (平 理一郎) 2SH-05 (S16)
Hirai, Akira (平井 彰) 3PT203 (S175)
Hirai, Hirohisa (平井 啓久) 3PT189 (S174)
Hirai, Mitsuhiro (平井 光博) **1C1610 (S25)**
1F1412 (S29)
2PT129 (S126)
3PT137 (S164)
Hirai, Teruhisa (平井 照久) 3PT117 (S160)
Hiraiwa, Tetsuya (平岩 徹也) **3H0948 (S70)**
2PT226 (S143)
Hiramatsu, Hirotsugu (平松 弘嗣) **2E1424 (S46)**
1PT108 (S86)
Hiramitsu, Yuuki (平光 佑基) 3PT158 (S168)
Hirano, Atsushi (平野 篤) 1PT005 (S84)
Hirano, Ken (平野 研) **3PT101 (S157)**
Hirano, Minako (平野 美奈子) **2G1546 (S51)**
3PT163 (S169)
3PT167 (S169)
Hirano, Yoshinori (平野 秀典) 1PT004 (S84)
Hirano, Yuuji (平野 祐司) 3PS038 (S152)
Hiraoka, Wakako (平岡 和佳子) 1PT140 (S92)
3PT237 (S181)
3PT238 (S181)
Hiraoka, Yasushi (平岡 泰) **2SG-06 (S15)**
Hirashima Naohide (平嶋 尚英) 1PT206 (S103)
Hirashima, Naohide (平嶋 尚英) **3PT139 (S164)**
3PT176 (S171)
3PT177 (S171)
Hirashima, Tsuyoshi (平島 剛志) **1G1400 (S31)**
Hirata, Hiroaki (平田 宏聡) 3H1046 (S71)
Hirata, Kunio (平田 邦生) 1PT128 (S90)
1YS0930 (S90)
Hiratsuka, Yuichi (平塚 祐一) 3PS005 (S146)
Hirayama, Takuma (平山 卓磨) 1PT164 (S97)
Hiroaki, Hidekazu (廣明 秀一) 2SB-02 (S10)
1I1424 (S35)
Hirokawa, Erisa (広川 恵里沙) 1PS009 (S75)
Hirokawa, Nobutaka (廣川 信隆) 3H0900 (S69)
Hirokawa, Takatsugu (広川 貴次) 2PT104 (S122)
Hiromasa, Ohta (大田 浩正) 2PT123 (S125)
Hironaka, Ken-ichi (廣中 謙一) **2PT220 (S142)**
Hirosaki, Ken (廣崎 賢) 3PT124 (S161)
Hirosawa, Koichiro M. (廣澤 幸一朗) 1G1412 (S31)
Hirose, Mika (廣瀬 未果) **1PT116 (S88)**
2PT116 (S124)
Hirose, Noboru (廣瀬 昇) 1SB-04 (S2)
1SB-05 (S2)
1SB-06 (S2)
Hiroshi, Kihara (木原 裕) 1PT115 (S88)
Hiroshima, Akinori (広島 明宣) **1PT175 (S98)**
Hiroshima, Michio (廣島 通夫) 1D1424 (S25)
1G1610 (S32)
3PT104 (S158)
3PT179 (S172)
Hirota, Hiroshi (廣田 洋) 3E0936 (S64)
Hirota, Shun (廣田 俊) **1SE-04 (S5)**
Hirotsune, Shinji (広常 真治) 2A1436 (S38)
Hisamoto, Naoki (久本 直毅) 1PT233 (S108)
Hisatome, Ichiro (久留 一郎) 1PT104 (S86)
Hisatomi, Osamu (久冨 修) **2PT192 (S138)**
Hisatomi, Osamu (久富 修) 2F1436 (S48)
Hitomi, Kenichi (人見 健一) 2F1534 (S49)
Hitomi, Kenichi (人見 研一) 2F1546 (S49)
2F1558 (S49)
Hiyama, Miyabi (樋山 みやび) **2PT187 (S137)**
Hizukuri, Yohei (檜作 洋平) **3PT122 (S161)**
Ho, Chien (Chien Ho) 1PT101 (S85)
Hoerning, Marcel (Hoerning Marcel) **1SB-07 (S3)**
2C1534 (S43)
Hojo, Eri (北條 江里) 1C1400 (S23)
Hojo, Yasushi (北条 泰嗣) 3PT217 (S177)
Hojo, Yasushi (北條 泰嗣) 3PT205 (S175)
3PT213 (S177)
3PT216 (S177)
Homma, Michio (本間 道夫) 1A1546 (S20)
1A1610 (S20)
1B1424 (S21)
2I1448 (S54)
2I1510 (S54)
2I1522 (S55)
2I1534 (S55)
1PT118 (S88)
1PT229 (S107)
1PT233 (S108)
2PT160 (S132)
Honda, Hajime (本多 元) **1SB-08 (S3)**
1PS014 (S76)
1PS015 (S76)
2PS019 (S113)
Honda, Kazufumi (本田 一文) 2PT117 (S124)
Hongo, Kunihiro (本郷 邦広) 1PT164 (S97)
Honjoh, Tatsuya (本城 達也) **3PT218 (S178)**
Honma, Michio (本間 道夫) 2I1400 (S53)
Hori, Naoto (堀 直人) **3C0948 (S60)**
1PT171 (S98)
1PT172 (S98)
Hori, Yuichiro (堀 雄一郎) 1C1424 (S23)
Horigome, Miyako (堀籠 美也子) 3F1046 (S67)
Horio, Shuhei (堀尾 修平) **3PT215 (S177)**
Hoshi, Takahiko (星 貴彦) 2D1522 (S45)
Hoshida, Masayuki (星田 政行) **1PS014 (S76)**
Hoshino, Kazuki (星野 一樹) 1PT117 (S88)
Hoshino, Masato (星野 真人) 3PS024 (S150)
Hoshino, Rintaro (星野 倫太朗) 3PS050 (S155)
Hoshino, Tatsuya (星野 達也) **3PT146 (S166)**
Hosoda, Kazufumi (細田 一史) **2PT209 (S140)**
Hosoda, Kazuo (細田 和男) 1I1424 (S35)
Hosoi, Makoto (細井 誠) 3PT220 (S178)
Hosokawa, Chie (細川 千絵) 1D1546 (S26)
Hosokawa, Yoichiroh (細川 陽一郎) 1G1400 (S31)
2D1558 (S45)
Hosokawa-Muto, Junji (武藤 淳二) 1PT155 (S95)
Hosoya, Satoshi (細谷 悟史) 3PT124 (S161)
Hotta, Kohji (堀田 耕司) 1PT216 (S105)
3PT204 (S175)
Houseman, Grant (Houseman Grant) 3E0948 (S64)
Hsu, Wei-Lin (許 維麟) 2PT125 (S126)
Hua, Yue-jin (Hua Yue-jin) 1PT129 (S90)
1YS1000 (S90)
Hughes, Kelly T. (Hughes Kelly T.) 2PS028 (S114)
Husimi, Yuzuru (伏見 譲) 2PT146 (S130)
2PT204 (S139)
Ichihashi, Norikazu (市橋 伯一) **1G1534 (S32)**
2PT205 (S139)
Ichii, Momoko (一居 桃子) **2PT154 (S131)**
Ichikawa, Mai (市川 麻衣) 1PT235 (S108)
Ichikawa, Masatoshi (市川 正敏) 3PT101 (S157)
Ichikawa, Muneyoshi (市川 宗厳) **2A1448 (S38)**
2A1546 (S39)
Ichikawa, Satoshi (市川 論) 3PS015 (S148)
Ichikawa, Satoshi (市川 諭) 2D1546 (S45)
Ichikawa, Takaaki (市川 貴章) 2G1522 (S50)
3PT158 (S168)
Ichiki, Takanori (一木 隆範) 1PT236 (S108)
2PT147 (S130)
Ichimiya, Masayoshi (一宮 正義) 1H1558 (S34)
Ichimura, Kaoru (市村 薫) 1PT115 (S88)
1PT157 (S95)
Ichimura, Taro (市村 垂生) 3PS037 (S152)
Ichinomiya, Katsuo (一宮 勝雄) **3PS033 (S151)**
Ichiyanagi, Kouhei (一柳 光平) 2PT121 (S125)
3PS024 (S150)
Ide, Takahiro (井手 隆広) 3PS006 (S146)
3PS007 (S147)
Ide, Toru (井出 徹) 2G1546 (S51)
3PT163 (S169)
3PT167 (S169)
Igarashi, Kiyohiko (五十嵐 圭日子) 1PT236 (S108)
Igarashi, Noriyuki (五十嵐 教之) 2PT123 (S125)
Ihara, Kunio (井原 邦夫) 1F1522 (S30)
2I1400 (S53)
2PT201 (S139)
Iida, Yoshihiro (飯田 禎弘) **1PT165 (S97)**
Iijima, Giichi (飯島 義市) 1H1546 (S34)
Iino, Ryota (飯野 亮太) 1A1436 (S19)
3A0924 (S56)
1PS033 (S79)
1YS1115 (S79)
3PT103 (S157)
Iino, Takanori (飯野 敬矩) 1G1400 (S31)
2D1558 (S45)
Iizuka, Kojiro (飯塚 浩二郎) 2PT234 (S144)
Iizuka, Ryo (飯塚 怜) 3C1058 (S61)
1PT234 (S108)
1PT236 (S108)
3PS029 (S151)
Ikebe, Emi (池辺 詠美) 1PS018 (S77)
Ikebe, Mitsuo (池辺 光男) 2PS053 (S119)
Ikeda, Kanami (池田 佳奈美) 2PT110 (S123)
Ikeda, Kyohei (池田 京平) 1PT159 (S96)
Ikeda, Satoshi (池田 諭史) 3PS035 (S152)
Ikeda, Yohei (池田 洋平) **3PT117 (S160)**
Ikegami, Koji (池上 浩司) 3A0912 (S56)
Ikegami, Takahisa (池上 貴久) 1C1412 (S23)
1PT145 (S93)
3PT178 (S172)
Ikeguchi, Masamichi (池口 雅道) 1PT120 (S89)
1PT142 (S93)
Ikeguchi, Mitsunori (池口 満徳) 1F1534 (S30)
1PS034 (S80)
1PT190 (S101)
2PT134 (S127)
2PT136 (S128)
Ikeo, Masahito (池尾 眞人) **2PS010 (S111)**
Ikeuchi, Akinori (池内 暁紀) 1C1510 (S24)
Ikezaki, Keigo (池崎 圭吾) 2PS011 (S111)
Ikura, Teikichi (伊倉 貞吉) 1C1522 (S24)
1PT146 (S93)
Imachi, Masayoshi (井町 昌義) **3PT114 (S159)**
Imada, Katsumi (今田 勝己) 2SE-05 (S13)
Imada, Katsumi (今田 勝巳) **1SA-07 (S2)**
2I1424 (S54)
1PT105 (S86)
1PT121 (S89)
2PS005 (S110)
2PT109 (S123)
2PT118 (S124)
2PT124 (S125)
Imafuku, Yasuhiro (今福 泰浩) 1PS030 (S79)
Imai, Hiroo (今井 啓雄) 1F1400 (S29)
2PT189 (S138)
3PT189 (S174)
Imai, Kiyohiro (今井 清博) 2PT154 (S131)
2PT159 (S132)

2PT161 (S133)
2PT163 (S133)
Imai, Masayuki (今井 正幸) 3PT142 (S165)
Imaizumi, Ryo (今泉 亮) **1PT120 (S89)**
Imaki, Takahito (今木 貴仁) 1PT140 (S92)
Imamoto, Akira (今本 公) 2PT140 (S128)
Imamoto, Yasushi (今元 泰) 1F1424 (S29)
3B0936 (S58)
Imanishi, Miki (今西 未来) **1SE-03 (S5)**
Imao, Asato (今尾 麻人) 2H1424 (S52)
1PS002 (S74)
1PS003 (S74)
1PS004 (S74)
Imoto, Daisuke (井元 大輔) **2PT239 (S145)**
Imoto, Seiya (井元 清哉) 2SD-04 (S12)
Inaba, Naomichi (稲葉 直道) **3PS034 (S152)**
Inaba, Satomi (稲葉 理美) **2E1522 (S46)**
Inaba, Satoshi (稲葉 敏) **2PS032 (S115)**
Inaba, Takehiko (稲葉 岳彦) 3PS032 (S151)
Inaba, Takehio (稲葉 岳彦) 3PS036 (S152)
Inada, Noriko (稲田 のりこ) 3PS010 (S147)
1YS0915 (S147)
Inada, Yuta (稲田 勇太) 3PT234 (S181)
Inagaki, Kenji (稲垣 賢二) 2PT109 (S123)
Inagaki, Kouya (稲垣 宏弥) **1B1436 (S21)**
Inaguma, Asumi (稲熊 あすみ) **2PT183 (S137)**
Inai, Koji (稲井 公二) 2PT208 (S140)
Inanami, Takashi (稲波 崇) **1PT167 (S97)**
Inoh, Yoshikazu (伊納 義和) **3PT176 (S171)**
Inomata, Kohsuke (猪股 晃介) **2SB-02 (S10)**
Inomata, Naoki (猪股 直生) 3PS013 (S148)
Inoue, Keiichi (井上 圭一) 1F1448 (S29)
2PT181 (S136)
Inoue, Masayo (井上 雅世) **2C1424 (S42)**
Inoue, Masayoshi (井上 正義) 1PT142 (S93)
Inoue, Naho (井上 奈穂) 3PT210 (S176)
Inoue, Rintaro (井上 倫太郎) 1E1424 (S27)
Inoue, Takurou (井上 琢朗) 3PT210 (S176)
Inoue, Tsuyoshi (井上 豪) 1PT116 (S88)
Inoue, Yasuhiro (井上 康博) 1PT133 (S91)
1PT219 (S105)
Inoue, Yuichi (井上 裕一) 1A1412 (S19)
2I1546 (S55)
2I1558 (S55)
1PS041 (S81)
2PS003 (S110)
3PS013 (S148)
Inui, Takaya (乾 貴矢) **3PT186 (S173)**
Irie, Katsumasa (入江 克雅) **3B0900 (S57)**
Irieda, Hiroki (入枝 泰樹) 3PT191 (S174)
Iritani, Yuka (入谷 有香) 3PS036 (S152)
Iseki, Mineo (伊関 峰生) 1H1610 (S35)
3D0924 (S62)
Ishibashi, Munenori (石橋 宗則) 1G1412 (S31)
Ishida, Hanako (石田 英子) 1PT116 (S88)
2PT116 (S124)
Ishida, Hideharu (石田 秀治) 2PS024 (S114)
Ishida, Hisashi (石田 恒) **3PT008 (S156)**
Ishida, Nobuhiro (石田 亘広) 1C1510 (S24)
Ishida, Noriyoshi (石田 誠宜) 2H1424 (S52)
1PS002 (S74)
1PS003 (S74)
1PS004 (S74)
1PT182 (S100)
Ishida, Takeshi (石田 武志) **2PT222 (S142)**
Ishidate, Fumiyoshi (石館 文善) 1PT209 (S103)
Ishido, Satoshi (石戸 聡) 3B1022 (S58)
Ishigami, Izumi (石上 泉) 3I1022 (S72)
Ishihama, Yasushi (石濱 泰) 2G1448 (S50)
2G1510 (S50)
3PT162 (S169)
Ishihara, Jun-ichi (石原 潤一) **2C1510 (S43)**
Ishihara, Shuji (石原 秀至) **1SF-04 (S6)**
1SI-06 (S9)
1D1436 (S25)
Ishii, Jun (石井 純) 1PT234 (S108)
Ishii, Kentaro (石井 健太郎) **3B1046 (S59)**
Ishii, Shin (石井 信) 3PT212 (S177)
Ishii, Shuya (石井 秀弥) **3B0948 (S58)**
Ishii, Takeshi (石井 毅) 3F1034 (S67)
Ishijima, Akihiko (石島 秋彦) **1SA-04 (S1)**
1A1412 (S19)
2I1558 (S55)
1PS041 (S81)
2PS003 (S110)
3PS013 (S148)
Ishikawa, Kumiko (石川 久美子) **1PS043 (S81)**
1PS044 (S81)
2PS038 (S116)
Ishikawa, Takuji (石川 拓司) 1SF-02 (S6)
Ishikawa, Yoshiro (石川 慶郎) 3PT172 (S170)
Ishikita, Hiroshi (石北 央) **3D0912 (S62)**
Ishikura, Takakazu (石倉 孝一) **1PT192 (S102)**
Ishikura, Zen (石倉 禅) 2D1546 (S45)
Ishimaru, Yoshiro (石丸 喜朗) 3PT189 (S174)
Ishimori, Kazuki (石杜 和希) **1PT010 (S85)**
Ishitani, Ryuichiro (石谷 隆一郎) **1SH-02 (S7)**
1PT128 (S90)
1YS0930 (S90)
Ishiura, Masahiro (石浦 正寛) 3B1046 (S59)
1PT122 (S89)
2PT229 (S143)
2PT230 (S143)
Ishiwata, Shin'ichi (石渡 信一) **2SG-05 (S15)**
2H1546 (S53)
3B0948 (S58)
3H0912 (S69)
3H1110 (S71)
1PS047 (S82)
2PS009 (S111)
Ishiwata, Shin’ ichi (石渡 信一) 2H1510 (S52)
1PS009 (S75)
1PS016 (S76)
1PS017 (S77)
Ishizuka, Toru (石塚 徹) 1PS010 (S75)
2PT183 (S137)
3PT218 (S178)
Isjijima, Akihiko (石島 秋彦) 2I1546 (S55)
Islam, Mohammad M (Islam Mohammad M)
2E1546 (S47)
Islam, Mohammad, M (Islam Mohammad, M)
2E1534 (S47)
Isojima, Hiroshi (磯島 広) **1A1436 (S19)**
Isomura, Yoshikazu (礒村 宜和) 2SH-05 (S16)
Isono, Kunio (磯野 邦夫) 2PT190 (S138)
1YS1015 (S138)
Isozumi, Noriyoshi (五十棲 規嘉) 1PT107 (S86)
Itaba, Takeshi (板場 武史) 1PS051 (S83)
1PS052 (S83)
Itabashi, Takeshi (板橋 岳志) 3H0912 (S69)
Itagaki, Tetsuhiko (板垣 哲彦) **2PT166 (S133)**
Ito Akihiko (伊藤 彰彦) 1PT206 (S103)
Ito, Akihiko (伊藤 彰彦) 2D1558 (S45)
Ito, Ayumi (伊藤 亜由美) 1PS024 (S78)
Ito, Daisuke (伊東 大輔) **1D1522 (S26)**
Ito, Etsuro (伊藤 悦朗) **1D1534 (S26)**
Ito, Hiroshi (伊藤 浩史) 2PT232 (S144)
Ito, Jotaro (伊藤 丈太郎) 1PS024 (S78)
Ito, Jumpei (伊藤 順平) 1PT128 (S90)
1YS0930 (S90)
Ito, Jun-ichi (伊東 純一) 2PT005 (S120)
Ito, Kenji (伊藤 健二) 2PT123 (S125)
Ito, Kentaro (伊藤 賢太郎) 1SF-06 (S7)
Ito, Masahiro (伊藤 政博) 2PS002 (S110)
2PS006 (S111)
Ito, Mashiho (伊藤 真志保) **2PT143 (S129)**
Ito, Nobutoshi (伊藤 暢聡) 1C1522 (S24)
1PT146 (S93)
Ito, Shota (伊藤 奨太) **2F1436 (S48)**
3D0924 (S62)
Ito, Yoshihiro (伊藤 嘉浩) 2PT145 (S129)
Ito, Yuko (伊藤 祐子) **1PS034 (S80)**
Ito, Yuma (伊藤 由馬) **1H1424 (S33)**
3PS034 (S152)
3PS035 (S152)
3PT181 (S172)
Ito, Yutaka (伊藤 隆) 2SB-02 (S10)
1B1448 (S21)
Itoga, Kazuyoshi (糸賀 和義) 2PS047 (S118)
Itoh, Hideki (伊藤 秀城) 2H1510 (S52)
Itoh, Koji (伊藤 光二) 1PT006 (S84)
Itoh, Mai (伊藤 真衣) 3PT129 (S162)
Itoh, Nobuya (伊藤 伸哉) 2PT148 (S130)
Itoh, Satoru (伊藤 暁) **3E1058 (S65)**
Itoh, Satoru G. (伊藤 暁) 1PT131 (S91)
Itoh, Shigeru (伊藤 繁) 3PT228 (S180)
Itoh, Toshiki (伊藤 俊樹) 3PT141 (S165)
Itoh, Toshiyuki (伊藤 俊幸) 1H1534 (S34)
Itou, Takashi (伊藤 隆司) 3PS038 (S152)
Iwadate, Yoshiaki (岩楯 好昭) 2PS048 (S118)
2PS052 (S119)
Iwai, Hidenao (岩井 秀直) 2D1424 (S44)
Iwai, Masakazu (岩井 優和) **3PT236 (S181)**
Iwai, Shigenori (岩井 成憲) 2F1534 (S49)
2F1546 (S49)
Iwai, Sosuke (岩井 草介) 2PS014 (S112)
2PT221 (S142)
Iwaki, Masayo (岩城 雅代) 3F0936 (S66)
Iwaki, Mitsuhiro (岩城 光宏) **1PS049 (S82)**
1YS0900 (S82)
1PT006 (S84)
Iwaki, Takafumi (岩城 貴史) 3C1110 (S61)
Iwama, Kazuya (岩間 和也) **1PT140 (S92)**
Iwamoto, Hiroyuki (岩本 裕之) **2H1610 (S53)**
Iwamoto, Kazunari (岩本 一成) **2PT215 (S141)**
Iwamoto, Masayuki (岩本 真幸) 2SH-01 (S16)
2G1558 (S51)
3PT164 (S169)
Iwamoto, Shigeto (岩本 成人) 2PT111 (S123)
Iwamoto, Tomoyuki (岩本 知之) **3PT190 (S174)**
Iwamoto, Yui (岩本 唯) **2PT155 (S131)**
2PT156 (S131)
Iwane, Atsuko (岩根 敦子) 1PS049 (S82)
1YS0900 (S82)
1PT006 (S84)
Iwane, Atsuko H. (岩根 敦子) **2PS043 (S117)**
Iwano, Katsunori (岩野 亮宗) 2PT176 (S135)
Iwaoka, Michio (岩岡 道夫) **2B1400 (S40)**
Iwaoka, Ryo (岩岡 諒) **3PT003 (S155)**
Iwasa, Takuya (岩佐 拓也) 3D1034 (S63)
Iwasa, Tatsuo (岩佐 達郎) 1F1412 (S29)
3F1046 (S67)
Iwasa, Yoh (巌佐 庸) 2PT220 (S142)
Iwasaki, Hideo (岩崎 秀雄) 2C1510 (S43)
2PT232 (S144)
Iwasaki, Kenji (岩崎 憲治) **1H1610 (S35)**
Iwase, Kouhei (岩瀬 航平) 1PS015 (S76)
Iwata, Keita (岩田 慶太) 2PT230 (S143)
Iwata, Seigo (岩田 聖悟) **3PT182 (S172)**
Iwata, Tatsuya (岩田 達也) 2F1436 (S48)
2F1448 (S48)
2F1546 (S49)
3D0924 (S62)
Iwatani, Yasumasa (岩谷 靖雅) 1PT102 (S85)
3PT003 (S155)
Iwayama, Masashi (岩山 将士) 1E1400 (S27)
3F1010 (S66)
Iwazaki, Ryosuke (岩崎 良祐) **3PT192 (S174)**
Iwura, Takafumi (井浦 貴文) 1PT156 (S95)
Izawa, Kazushi (井澤 和司) 3PS031 (S151)
J. McBride, Mark (J. McBride Mark) 2SE-05 (S13)
Javkhlantugs, Namsrai (ジャブクラントゥクス ナムスライ)
3PT127 (S162)
Ji, Zhi-Gang (姫 志剛) 3PT218 (S178)
Jikihara, Kazunori (直原 一徳) 2PT169 (S134)
Jin, Mingyue (金 明月) **2A1412 (S38)**
2A1424 (S38)
1PT186 (S100)
Jinguji, Masaaki (神宮司 将晃) 3PT185 (S173)
Jintori, Kosuke (陣取 孝輔) 3PT191 (S174)
Johmura, Masae (城村 雅恵) 2SB-01 (S10)
Jolley, Craig (Jolley Craig) **2C1522 (S43)**
Joti, Yasumasa (城地 保昌) 3PS026 (S150)
Ju, Jungmyoung (朱 正明) 1I1610 (S37)
Jung, Kwang-Hwan (Jung Kwang-Hwan)
1F1510 (S30)
2PT177 (S135)
2PT179 (S136)
Kagemoto, Tatsuya (影本 達也) **1PS016 (S76)**
Kageyama, Takeshi (景山 健志) 2PT186 (S137)
Kai, Noriko (甲斐 憲子) 1H1534 (S34)
Kainosho, Masatsune (甲斐荘 正恒) 1B1424 (S21)
Kaizu, Kazunari (海津 一成) 2SI-04 (S17)
2C1412 (S42)
2PT215 (S141)
3PT183 (S172)
Kajiwara, Kentaro (梶原 健太郎) 3PS024 (S150)
Kakibe, Sayuri (柿部 小百合) 3G0936 (S68)
Kalay, Ziya (Kalay Ziya) **2C1400 (S42)**
Kamada, Mayumi (鎌田 真由美) **1PT191 (S101)**
Kamagata, Kiyoto (鎌形 清人) **2E1412 (S45)**
1PT152 (S94)
1PT222 (S106)
Kamatari, Yuji O. (鎌足 雄司) 1PT139 (S92)
1PT155 (S95)
Kambara, Taketoshi (神原 丈敏) **2A1522 (S39)**
Kameda, Tomoshi (亀田 倫史) 1PT005 (S84)
1PT112 (S87)
3PT107 (S158)
Kamei, Takashi (亀井 敬) **3PT102 (S157)**
Kamekura, Masahiro (亀倉 正博) 2PT201 (S139)
Kami-ike, Nobunori (上池 伸徳) 2I1436 (S54)
2PS006 (S111)
2PS029 (S115)
Kamikubo, Hironari (上久保 裕成) 2PT173 (S135)
Kamikubo, Hironari (上久保 裕生) 2F1424 (S48)
1PT124 (S89)
1PT138 (S92)
1PT153 (S95)
2PT170 (S134)
2PT172 (S134)
2PT174 (S135)
Kamikubo, Hironori (上久保 裕生) 2PT171 (S134)
Kamimura, Atsushi (上村 淳) 2SF-02 (S14)
2PT216 (S141)
Kamino, Keita (神野 圭太) 2PS045 (S118)
Kamio, Yoshiyuki (神尾 好是) 3F0948 (S66)
Kamioka, Tetsuya (上岡 哲矢) 1C1412 (S23)
Kamitani, Yasushi (紙谷 泰史) **3PT150 (S166)**

Kamiya, Katsumasa (神谷 克政) 3PT222 (S178)
Kamiya, Kenshu (神谷 健秀) **1PT176 (S99)**
Kamiya, Koki (神谷 厚輝) **3PT136 (S164)**
3PT143 (S165)
3PT163 (S169)
Kamiya, Masakatsu (神谷 昌克) 1C1400 (S23)
2PT177 (S135)
2PT179 (S136)
Kamiya, Motoshi (神谷 基司) **2PT178 (S136)**
Kamiya, Narutoshi (Kamiya Narutoshi) 2B1436 (S40)
Kamiya, Narutoshi (神谷 成敏) **3B1010 (S58)**
1PT130 (S90)
3PT010 (S157)
Kamiya, Ritsu (神谷 律) 2A1412 (S38)
2PS050 (S118)
3PS003 (S146)
3PS006 (S146)
3PS007 (S147)
Kamiya, Yukiko (神谷 由紀子) 1B1436 (S21)
Kamo, Naoki (加茂 直樹) 1F1558 (S30)
2PT176 (S135)
2PT177 (S135)
2PT179 (S136)
Kan, Yumi (菅 悠美) **3PT142 (S165)**
Kanaba, Teppei (金場 哲平) **1B1448 (S21)**
Kanada, Ryo (金田 亮) **1PS037 (S80)**
Kanada, Soun (金田 創運) 1F1522 (S30)
Kanamaru, Shuji (金丸 周司) 1PS012 (S76)
2PT144 (S129)
Kanamori, Toshiyuki (金森 敏幸) 3PS044 (S153)
3PS051 (S155)
3PT123 (S161)
3PT169 (S170)
Kanaori, Kenji (金折 賢二) 1C1522 (S24)
2PT153 (S131)
Kanaya, Toshiji (金谷 利治) 1E1424 (S27)
Kanayama, Kenji (金山 賢治) 3PT123 (S161)
Kanba, Keisuke (神庭 圭祐) 3PT003 (S155)
Kanbe, Toshio (神戸 俊夫) 3C0924 (S60)
Kandori, Hideki (KANDORI HIDEKI) 3F1058 (S67)
Kandori, Hideki (神取 秀樹) 1F1400 (S29)
1F1448 (S29)
1F1510 (S30)
2F1412 (S47)
2F1436 (S48)
2F1448 (S48)
2F1534 (S49)
2F1546 (S49)
2G1610 (S51)
3D0912 (S62)
3D0924 (S62)
3F0936 (S66)
2PT181 (S136)
2PT182 (S136)
2PT189 (S138)
Kanehisa, Minoru (金久 實) 2PT107 (S122)
Kaneko, Jun (金子 淳) 3F0948 (S66)
Kaneko, Kunihiko (金子 邦彦) **1SC-05 (S4)**
1PT218 (S105)
2PT216 (S141)
2PT224 (S142)
2PT231 (S144)
Kaneko, Tomoyuki (金子 智行) 2D1510 (S44)
3PS020 (S149)
3PS022 (S149)
3PS023 (S149)
3PS046 (S154)
3PS049 (S154)
Kanematsu, Keita (兼松 啓太) 3PS041 (S153)
Kaneta, Yusuke (金田 祐輔) 3PT160 (S168)
Kang, Jiyoung (Kang Jiyoung) **1B1610 (S22)**
1I1448 (S35)
2PT142 (S129)
2PT166 (S133)
2PT167 (S133)
Kano, Hideaki (加納 英明) **2SH-03 (S16)**
Kano, Masanobu (狩野 方伸) 2SH-05 (S16)
Kanuka, Hirotaka (嘉糠 洋陸) 1I1546 (S36)
Karino, Yasuhito (狩野 康人) **1E1522 (S28)**
Kariya, Ryusho (刈谷 龍昇) 2PT150 (S130)
Kasahara, Kota (笠原 浩太) **2PT105 (S122)**
3PT131 (S163)
Kasai, Haruo (河西 春郎) 2SH-05 (S16)
Kasai, Rinshi (笠井 倫志) **1H1448 (S33)**
Kasai, Rinshi S. (笠井 倫志) 1G1412 (S31)
3PT172 (S170)
Kasai, Taishi (笠井 大司) **2PS024 (S114)**
Kasai, Takuma (葛西 卓磨) 2PT140 (S128)
Kashibe, Masayoshi (樫部 順美) **3PT134 (S163)**
Kashima, Risa (鹿島 理沙) 2E1412 (S45)
Kashiwazaki, Jun (柏崎 隼) **2PS016 (S112)**
Kasuga, Sachiko (春日 章千子) **3PT233 (S180)**
Kasuya, Daisuke (糟屋 大介) 3E1010 (S64)
1PT180 (S99)
Kasuya, Masatoshi (粕谷 昌寿) 3PT205 (S175)
Kasuya, Yuzo (粕谷 有造) **3A1046 (S57)**
1PS027 (S78)
Katagiri, Toyomasa (片桐 豊雅) 3F0912 (S65)
Katahira, Masato (片平 正人) 3C0936 (S60)
3C1034 (S61)
3PT003 (S155)
Kataoka, Hironao (片岡 博尚) 2F1436 (S48)
2PT192 (S138)
Kataoka, Maachi (片岡 真亜知) 3G0900 (S67)
Kataoka, Mikio (片岡 幹雄) 1E1534 (S28)
2F1424 (S48)
1PT124 (S89)
1PT138 (S92)
1PT153 (S95)
2PT170 (S134)
2PT171 (S134)
2PT172 (S134)
2PT173 (S135)
2PT174 (S135)
Kataoka, Yuto (片岡 悠人) 2SD-04 (S12)
Katayama, Kazuhiko (片山 和彦) 3E0948 (S64)
Katayama, Kota (片山 耕大) **1F1400 (S29)**
2PT189 (S138)
Katayama, Yukie (片山 幸江) 3I1046 (S73)
3PT129 (S162)
Katayanagi, Katsuo (片柳 克夫) 3PT222 (S178)
Kato, Asuka (加藤 あす香) 3PT237 (S181)
3PT238 (S181)
Kato, Chiaki (加藤 千明) 1PT113 (S87)
Kato, Hideaki E. (加藤 英明) **1PT128 (S90)**
1YS0930 (S90)
Kato, Hiroyuki (加藤 博之) **3PT237 (S181)**
Kato, Koichi (KATO Koichi) 1B1412 (S21)
Kato, Koichi (加藤 晃一) 1B1436 (S21)
1PT112 (S87)
Kato, Mikio (加藤 幹男) **2I1610 (S55)**
Kato, Minoru (加藤 稔) 2B1510 (S41)
1PT141 (S92)
Kato, Noritaka (加藤 徳剛) 3PT126 (S162)
Kato, Satoru (加藤 知) 3G1110 (S69)
3PT149 (S166)
Kato, Shoichi (加藤 翔一) 2D1522 (S45)
Kato, Takashi (加藤 尚志) 1PT208 (S103)
Kato, Takayuki (加藤 貴之) 2SE-01 (S12)
2PS028 (S114)
3PS012 (S147)
3PT001 (S155)
Kato, Yoshitaka (加藤 善隆) **1F1510 (S30)**
Kato, Yumiko (加藤 弓子) 3PT119 (S160)
Katoh, Kaoru (加藤 薫) 2PS042 (S117)
Katou, Kouya (加藤 功弥) 3PT219 (S178)
Katsura, Hitomi (桂 ひとみ) 2PT188 (S138)
Katsurada, Yuki (桂田 悠基) 1SB-06 (S2)
Kawabata, Kazushige (川端 和重) 1PT230 (S107)
Kawabata, Takeshi (川端 猛) **2PT103 (S121)**
Kawagishi, Ikuro (川岸 郁朗) 1PT121 (S89)
2PS049 (S118)
3PS032 (S151)
3PS036 (S152)
3PT180 (S172)
3PT184 (S173)
3PT185 (S173)
3PT186 (S173)
3PT187 (S173)
3PT188 (S173)
3PT191 (S174)
3PT192 (S174)
Kawaguchi, Kazutomo (川口 一朋) **1E1400 (S27)**
3F1010 (S66)
2PT131 (S127)
Kawaguchi, Tatsuya (川口 辰也) 2PT109 (S123)
Kawaguchi, Tetsuya (川口 徹也) **3PT188 (S173)**
Kawahara, Kousuke (河原 弘典) **3PT229 (S180)**
Kawai, Takeaki (河合 武揚) **3F0912 (S65)**
Kawai, Yuka (河合 優香) 3F0948 (S66)
Kawai-Noma, Shigeko (河合 繁子) 1PT151 (S94)
Kawakami, Keisuke (川上 恵典) 3D0948 (S62)
Kawakami, Masaru (川上 勝) 2E1400 (S45)
1PT136 (S91)
Kawakami, Tomohiro (河上 知広) **1PS022 (S77)**
Kawakami, Tomoya (川上 智也) 3A1022 (S57)
Kawakami, Yuji (川上 祐司) **2PT106 (S122)**
Kawakita, Yoshito (川北 祥人) **2PS022 (S113)**
Kawamoto, Akihiro (川本 晃大) **2PS028 (S114)**
2PS043 (S117)
Kawamoto, Shuhei (川本 周平) **2G1400 (S49)**
Kawamura, Izuru (川村 出) 1F1558 (S30)
3F1046 (S67)
2PT168 (S134)
3PT114 (S159)
Kawamura, Takashi (河村 高志) 1PT113 (S87)
Kawanabe, Akira (川鍋 陽) 1F1510 (S30)
Kawano, Keiichi (河野 敬一) 1C1400 (S23)
2PT177 (S135)
2PT179 (S136)
Kawano, Ryuji (川野 竜司) 2G1412 (S49)
3PT136 (S164)
3PT143 (S165)
3PT163 (S169)
Kawasaki, Kazunori (川崎 一則) **3G0900 (S67)**
1PT184 (S100)
Kawashima, Yoshiaki (川島 嘉明) 3PT139 (S164)
Kawashima, Yurie (川島 有里恵) **2PT119 (S124)**
Kawata, Daiki (川田 大輝) **2PT189 (S138)**
Kawata, Masaaki (川田 正晃) **1PT183 (S100)**
Kawata, Yasushi (河田 康志) 1PT164 (S97)
Kawato, Suguru (川戸 佳) 3PT205 (S175)
3PT207 (S176)
3PT211 (S176)
3PT213 (S177)
3PT216 (S177)
3PT217 (S177)
Kaya, Motoshi (茅 元司) **1SI-01 (S8)**
2A1522 (S39)
2A1558 (S39)
Kayama, Yoko (香山 容子) 1H1534 (S34)
Kayano, Isao (茅野 功) 3PS027 (S150)
Kayanuma, Megumi (栢沼 愛) 3PT222 (S178)
Kazama, Toshiya (風間 俊哉) 1SF-06 (S7)
Kazumi, Tanaka (田中 一巳) 1PS035 (S80)
Kazuta, Yasuaki (数田 恭章) 2PT205 (S139)
Ken'ya, Furuta (古田 健也) 2A1546 (S39)
Kenmoku, Hiromichi (兼目 裕充) 1D1610 (S26)
Kenri, Tsuyoshi (見理 剛) 2PS022 (S113)
Kenzaki, Hiroo (検崎 博生) 3PT007 (S156)
3PT009 (S157)
Khan, Alam, M (Khan Alam, M) 2E1534 (S47)
Khan, Monsur A (Khan Monsur A) **2E1546 (S47)**
Ki, Jyunan (紀 十男) **3F0900 (S65)**
Kidera, Akinori (木寺 詔紀) 1F1534 (S30)
2B1412 (S40)
1PT147 (S93)
2PT134 (S127)
Kidoaki, Satoru (木戸秋 悟) 1PT231 (S107)
1PT232 (S108)
Kidokoro, Shun-Ichi (城所 俊一) 1PT107 (S86)
Kidokoro, Shun-ichi (城所 俊一) 1PT149 (S94)
1PT179 (S99)
Kihara, Hiroshi (木原 裕) 1PT157 (S95)
Kihara, Takanori (木原 隆典) **3H1034 (S71)**
Kihara, Tatsuya (木原 達也) **1PT223 (S106)**
Kijima, Saku (貴嶋 紗久) 2SE-03 (S13)
Kikawada, Takahiro (黄川田 隆洋) 1PT162 (S96)
Kikuchi, Hiroto (菊地 浩人) **2PT137 (S128)**
Kikuchi, Katsuya (菊地 克也) 3PS038 (S152)
Kikuchi, Kazuya (菊地 和也) 1C1424 (S23)
3PS039 (S153)
3PS042 (S153)
3PS043 (S153)
3PT134 (S163)
Kikuchi, Macoto (菊池 誠) 1B1534 (S22)
1PT161 (S96)
Kikuchi, Satoru (菊池 覚) **1PS048 (S82)**
Kikuchi, Takeshi (菊地 武司) 1I1400 (S35)
3E1034 (S65)
1PT127 (S90)
Kikuchi, Yohsuke (菊池 洋輔) **1PS023 (S78)**
Kikukawa, Takashi (菊川 峰志) 1C1400 (S23)
2PT176 (S135)
2PT177 (S135)
2PT179 (S136)
2PT182 (S136)
3PT123 (S161)
3PT128 (S162)
Kikushima, Kenji (菊島 健児) **1H1412 (S33)**
Kim, Do-myoung (金 渡明) 1C1510 (S24)
Kim, Hyonchol (金 賢徹) 3PS046 (S154)
3PS047 (S154)
Kimoto, Tetsuya (木本 哲也) **3PT211 (S176)**
3PT216 (S177)
Kimura, Akatsuki (木村 暁) 1SD-04 (S4)
1SI-05 (S9)
Kimura, Akihiro (木村 明洋) 3D0936 (S62)
Kimura, Hiroshi (木村 宏) **2SG-01 (S15)**
Kimura, Kazuya (木村 和哉) 1PS027 (S78)
Kimura, Kenjiro (木村 建次郎) **2SI-05 (S18)**
Kimura, Masako (木村 雅子) 2H1558 (S53)
Kimura, Ryota (木村 亮太) 1C1610 (S25)
3PT137 (S164)
Kimura, Shota (木村 彰太) 3PT138 (S164)
Kimura, Sumiko (木村 澄子) 1PS011 (S75)
1PS012 (S76)
1PS013 (S76)
Kimura, Tetsunari (木村 哲就) 1C1546 (S24)

1C1558 (S24)
2PT182 (S136)
2PT183 (S137)
Kimura, Toru (木村 徹) **1PT166 (S97)**
Kimura, Yoshiro (木村 嘉朗) 3PT227 (S179)
Kimura, Yuki (木村 雄貴) 1PT102 (S85)
Kimura, Yukihiro (木村 行宏) 3PT233 (S180)
3PT234 (S181)
Kinbara, Kazushi (金原 数) 2I1546 (S55)
Kinjo, Akira (Kinjo Akira) 2B1436 (S40)
Kinjo, Akira (金城 玲) 2PT103 (S121)
Kinjo, Masataka (Kinjo Masataka) 3PT005 (S156)
Kinjo, Masataka (金城 政孝) **1SD-05 (S5)**
1G1546 (S32)
1H1400 (S33)
1PT205 (S103)
3PT004 (S156)
Kinoshita, Kengo (木下 賢吾) 3E1046 (S65)
2PT105 (S122)
3PT131 (S163)
Kinoshita, Masahiro (木下 正弘) 1PS034 (S80)
1PT137 (S92)
1PT154 (S95)
3PT116 (S160)
Kinoshita, Michiyo (木下 充代) 2PT190 (S138)
1YS1015 (S138)
Kinoshita, Miki (木下 実紀) 2I1424 (S54)
Kinoshita, Syunsuke (木下 俊祐) **1PS015 (S76)**
Kinoshita, Yukari (木下 ゆかり) 3PT210 (S176)
Kinosita Jr, Kazuhiko (木下 一彦) 1PS035 (S80)
Kinosita, Jr., Kazuhiko (木下 一彦) 1PS031 (S79)
Kinosita, Kazuhiko (木下 一彦) 3A1046 (S57)
1PS026 (S78)
1PS027 (S78)
3PT166 (S169)
Kinosita, Kazuhiko Jr. (木下 一彦) 3A1022 (S57)
Kinosita, Yoshiaki (木下 佳昭) **3A1058 (S57)**
Kira, Atsushi (吉良 敦史) 3PT114 (S159)
Kirino, Yutaka (桐野 豊) 3PT203 (S175)
3PT214 (S177)
Kishi, Takaaki (岸 孝亮) **2I1522 (S55)**
Kishida, Naoko (岸田 直子) **1PT170 (S98)**
Kishimoto, Ayaka (岸本 彩花) **2PT162 (S133)**
2PT164 (S133)
Kishimoto, Yasushi (岸本 泰司) **3PT214 (S177)**
Kiso, Makoto (木曽 真) 2PS024 (S114)
Kita, Makoto (喜多 真琴) 3PT223 (S179)
Kita, Sayaka (喜多 清) 1H1412 (S33)
Kitagawa, Daiju (北川 大樹) **2SB-04 (S10)**
Kitagawa, Teizo (北川 禎三) 3I0924 (S71)
2PT159 (S132)
Kitahara, Ryo (北原 亮) 1PT112 (S87)
Kitahata, Hiroyuki (北畑 裕之) 2C1448 (S42)
Kitajima-Ihara, Tomomi (北島一井原 智美) 2PT201 (S139)
Kitamoto, Dai (北本 大) 3PT176 (S171)
Kitamura, Kazuo (喜多村 和郎) 2SH-05 (S16)
Kitamura, Natsumi (北村 奈津美) 2PT164 (S133)
Kitamura, Shingo (北村 紳悟) 3PT003 (S155)
Kitamura, Yoshiichiro (北村 美一郎) **3PT203 (S175)**
Kitano, Takahiro (北野 貴寛) 2PT188 (S138)
Kitao, Akio (北尾 彰朗) 1A1522 (S20)
1PS019 (S77)
1PT174 (S98)
2PT132 (S127)
Kitaoka, Maya (北岡 麻耶) 2I1400 (S53)
Kitayama, Hiroki (北山 寛貴) 1E1436 (S27)
Kitazawa, Soichiro (北沢 創一郎) **1PT112 (S87)**
Kitoh-Nishioka, Hirotaka (鬼頭一西岡 宏任)
3D1046 (S63)
Klumpp, Stefan (クランプ ステファン) 2I1412 (S54)
Ko, Jong Soo (Ko Jong Soo) 1I1610 (S37)
Kobatake, Takahiro (小畑 貴広) 2PS013 (S112)
Kobayashi, Asako (小林 麻子) 1I1522 (S36)
Kobayashi, Chigusa (小林 千草) **2PT130 (S127)**
2PT139 (S128)
Kobayashi, Emiko (小林 恵美子) 1PT184 (S100)
2PS042 (S117)
Kobayashi, Junya (小林 純也) **3E0900 (S63)**
3PT204 (S175)
Kobayashi, Masaru (小林 大) 1PS025 (S78)
Kobayashi, Naoya (小林 直也) 1PT106 (S86)
Kobayashi, Ryo (小林 亮) **1SF-06 (S7)**
Kobayashi, Ryota (小林 亮太) **3PT145 (S165)**
Kobayashi, Shiori (小林 詩織) 1B1424 (S21)
2I1448 (S54)
Kobayashi, Takashi (小林 聖) **3PT231 (S180)**
Kobayashi, Takuya (小林 琢也) **2A1558 (S39)**
Kobayashi, Tetsuya (小林 徹也) 1D1424 (S25)
Kobayashi, Tetsuya J. (小林 徹也) **2SF-02 (S14)**
Kobayashi, Toshihide (Kobayashi Toshihide)
2G1424 (S50)
Kobayashi, Toshihide (小林 俊秀) 3PT146 (S166)
Kobayashi, Yasuhiko (小林 泰彦) 1G1510 (S31)
Kobayashi, Yusuke (小林 裕亮) 3PT239 (S182)
Kobayashi, Yuta (小林 祐太) **1PT159 (S96)**
Kobirumaki-Shimozawa, Fuyu (小比類巻 生)
1PS009 (S75)
Kodama, Mieko (兒玉 美恵子) 1PT211 (S104)
Kodama, Toru (児玉 亮) 3PS050 (S155)
Kodani, Noriko (小谷 紀子) 3PS027 (S150)
Kodera, Noriyuki (古寺 哲幸) **2SB-03 (S10)**
1PS046 (S82)
2PS053 (S119)
3PS017 (S148)
Koga, Nobuaki (古賀 伸明) 2PT187 (S137)
Kogure, Kazuhiro (木暮 一啓) 2F1412 (S47)
2PT181 (S136)
Kohchi, Takayuki (河内 孝之) 2PT188 (S138)
Kohno, Toshiyuki (河野 俊之) 2PT111 (S123)
3PT178 (S172)
Kohori, Ayako (小堀 綾子) 3A1022 (S57)
Koike, Masafumi J. (小池 雅文) **1PT118 (S88)**
Koike, Ryotaro (小池 亮太郎) **1B1546 (S22)**
1I1424 (S35)
2PT130 (S127)
Kojima, Chojiro (児嶋 長次郎) 1B1424 (S21)
Kojima, Hiroaki (小嶋 寛明) 1PS050 (S82)
2PS019 (S113)
3PS001 (S146)
3PS002 (S146)
3PS009 (S147)
Kojima, Keiichi (小島 慧一) **1F1424 (S29)**
Kojima, Masaru (小嶋 勝) **1PT229 (S107)**
1PT233 (S108)
Kojima, Seiji (小嶋 誠司) 1A1546 (S20)
1A1610 (S20)
2I1400 (S53)
2I1448 (S54)
2I1510 (S54)
2I1522 (S55)
2I1534 (S55)
2PT160 (S132)
Komatsu, Daiki (小松 大貴) 3H1022 (S70)
1PT228 (S107)
2PS036 (S116)
Komatsu, Hideyuki (小松 英幸) **1PT011 (S85)**
Komatsu, Yasuo (小松 康雄) 2PT158 (S132)
Komatsu, Yu (小松 勇) 1PT135 (S91)
Komatsuzaki, Yoshimasa (小松崎 良将) 2PT233 (S144)
3PT205 (S175)
3PT219 (S178)
Komatuzaki, Yosimasa (小松崎 良将) 3PT220 (S178)
Komeda, Tadahiro (米田 忠弘) 2E1412 (S45)
Komichi, Nobutaka (小道 信孝) **1PT130 (S90)**
Komiya, Ken (小宮 健) **1I1522 (S36)**
Komiyama, Ryosuke (小見山 亮祐) **1PS036 (S80)**
Komori, Tomotaka (小森 智貴) 2PS011 (S111)
Komuro, Yasuaki (小室 靖明) **2PT139 (S128)**
Kon, Takahide (昆 隆英) **1SI-02 (S8)**
3B1010 (S58)
Kondo, Akihiko (近藤 昭彦) 1PT234 (S108)
Kondo, Daiki (近藤 大生) 3PT222 (S178)
Kondo, Hiroko (近藤 寛子) **1PT188 (S101)**
Kondo, Jiro (近藤 次郎) **3C1010 (S60)**
Kondo, Takao (近藤 孝男) 3B1058 (S59)
3B1110 (S59)
2PT232 (S144)
Kondo, Yoshito (近藤 嘉人) **1PT008 (S84)**
Konno, Asahi (昆野 朝陽) **1PT169 (S97)**
Kono, Hidetoshi (河野 秀俊) 1SD-03 (S4)
1B1522 (S22)
3PS026 (S150)
3PT108 (S158)
Kono, Ryohei (河野 良平) 2B1510 (S41)
1PT114 (S87)
Kori, Hiroshi (郡 宏) 2PT232 (S144)
Koshii, Takaya (越井 貴也) **1PT217 (S105)**
Kosuge, Takashi (小菅 隆) 2PT123 (S125)
Kosugi, Masayuki (小杉 正幸) 3E0912 (S63)
Kotani, Susumu (小谷 享) 2PS035 (S116)
Kotera, Masaaki (小寺 正明) 2PT107 (S122)
Koua, Faisal Hammad Mekky
(Koua Faisal Hammad Mekky) 3D1022 (S63)
Kouduki, Naoharu (上月 尚治) **1PT138 (S92)**
Kouyama, Mizuno (神山 勉) 2PT184 (S137)
Kouyama, Tsutomu (神山 勉) 1SH-06 (S8)
1F1522 (S30)
Kowalczykowski, Stephen (Kowalczykowski Stephen)
1PS045 (S82)
Koyama, Masako (小山 昌子) **2SB-06 (S10)**
Koyama, Tsubasa (小山 翼) **2PS014 (S112)**
Koyama, Yuka (小山 裕佳) 3PT225 (S179)
Koyanagi, Mitsumasa (小柳 光正) 2PT190 (S138)
1YS1015 (S138)
Koyasako, Kotaro (小屋迫 光太郎) 2A1412 (S38)
2A1436 (S38)
Koyasu, Kazuma (小安 司馬) **3A1010 (S56)**
Kubo, Koji (久保 康児) 3C0924 (S60)
Kubo, Minoru (久保 稔) **3I1034 (S72)**
Kubo, Tomohiro (久保 智広) **3PS003 (S146)**
Kubo, Yoko (久保 葉子) 2PT191 (S138)
Kubo, Yoshihiro (久保 義弘) 3PT168 (S170)
Kubori, Tomoko (久堀 智子) 1PT105 (S86)
2PT124 (S125)
Kubota, Chihiro (久保田 千尋) **1I1412 (S35)**
Kubota, Hiroaki (久保田 寛顕) 3B0948 (S58)
Kubota, Kenshuke (久保田 健介) 2F1522 (S48)
Kudo, Seishi (工藤 成史) **2SI-01 (S17)**
2SI-02 (S17)
1PS022 (S77)
1PS029 (S79)
2PS029 (S115)
2PS030 (S115)
2PS046 (S118)
Kudo, Shogo (工藤 翔吾) **3PT113 (S159)**
Kudo, Yukihiko (工藤 恭彦) 2PS041 (S117)
Kudoh, Suguru N. (工藤 卓) 1D1546 (S26)
Kuhara, Atsushi (久原 篤) 3PT201 (S174)
3PT210 (S176)
Kuma, Hiroyuki (隈 博幸) 3PT117 (S160)
Kumachi, Shigefumi (熊地 重文) **2PT204 (S139)**
Kumagai, Izumi (熊谷 泉) 1C1448 (S23)
1C1510 (S24)
Kumagai, Yumiko (熊谷 裕美子) **3PT112 (S159)**
Kumaki, Yasuhiro (熊木 康裕) 1C1400 (S23)
Kumashiro, Yoshikazu (熊代 善一) 2PS047 (S118)
Kumemoto, Ryusei (久米本 龍生) 2PS012 (S112)
Kuramochi, Maiko (倉持 麻衣子) 2PS042 (S117)
Kuramoto, Ayumu (倉本 歩) 2PS035 (S116)
Kurasawa, Masayoshi (倉沢 正義) **1PS013 (S76)**
Kuribayashi, Kaori (栗林 香織) 3PT143 (S165)
Kuribayashi-Shigetomi, Kaori (栗林(繁富) 香織)
1I1546 (S36)
Kurihara, Kazue (栗原 和枝) 1PT163 (S96)
Kurihara, Kazuo (栗原 和男) 2PT170 (S134)
Kurihara, Kensuke (栗原 顕輔) 3PT142 (S165)
Kurikawa, Tomoki (栗川 知己) **2PT224 (S142)**
Kurisaki, Ikuo (栗崎 以久男) **2E1436 (S46)**
2PT165 (S133)
Kurisu, Genji (栗栖 源嗣) 3B1010 (S58)
Kurita, Yuki (栗田 祐輝) 3PS050 (S155)
Kuroda, Katsushi (黒田 克史) 3PS027 (S150)
Kuroda, Shinya (黒田 真也) **2SF-03 (S14)**
1PT214 (S104)
2PT219 (S142)
3PT212 (S177)
Kuroda, Takuya (黒田 琢弥) **1PT105 (S86)**
2PT124 (S125)
Kuroda, Yutaka (Kuroda Yutaka) 2E1546 (S47)
Kuroda, Yutaka (黒田 裕) 1C1412 (S23)
2E1534 (S47)
2PT001 (S119)
Kuroi, Kunisato (黒井 邦巧) **2PT169 (S134)**
Kuroki, Ryota (黒木 良太) 3E0912 (S63)
Kurosawa, Masaru (黒沢 大) 2B1558 (S41)
Kuroyanagi, Shigehide (畔柳 成秀) 1B1610 (S22)
Kurumizaka, Hitoshi (胡桃坂 仁志) **2SG-03 (S15)**
1PT190 (S101)
Kusakabe, Hitoshi (日下部 均) 2PT109 (S123)
Kusumi, Akihiro (楠見 明弘) 1G1412 (S31)
1H1448 (S33)
1PT209 (S103)
2PS041 (S117)
3PT172 (S170)
Kusunoki, Masami (楠 正美) **3D1010 (S62)**
Kuwabara, Yumiko (桑原 由美子) 3PT128 (S162)
Kuwahara, Naoto (桑原 直人) 3PT201 (S174)
Kuwajima, Kunihiro (KUWAJIMA Kunihiro)
1B1412 (S21)
Kuwajima, Kunihiro (桑島 邦博) 1PT143 (S93)
1PT160 (S96)
2PT150 (S130)
Kuwata, Kazuo (桑田 一夫) 1PT139 (S92)
1PT155 (S95)
Lee, Sang Min (Lee Sang Min) 1I1610 (S37)
Lee, Young-Ho (李 映昊) 1E1436 (S27)
2PT126 (S126)
Leppla, Stephen (Leppla Stephen) 2PS041 (S117)
Levadny, Victor (LEVADNY Victor) 3PT173 (S171)
Levadny, Victor (Levadny Victor) 3PT174 (S171)
Levi, Sabine (LEVI Sabine) 3PT206 (S175)
Li, Hua (李 華) 1PT106 (S86)
Li, Junhua (Li Junhua) 3PT170 (S170)
Li, Koren (李 香蓮) 3PT217 (S177)
Li, Na (李 な) 1A1546 (S20)
Li, Pai-Chi (Li Pai-Chi) **3B1022 (S58)**
Li, Wenfei (Li Wenfei) **1PT178 (S99)**
Li, Yong (永 麗) **3PT234 (S181)**
Liang-da, Chiu (Liang-da Chiu) 3PS037 (S152)

Libchaber, Albert (リップシャーバー アルバート) 2SC-06 (S11)
Limin, Chen (陳 莉敏) 1PT209 (S103)
Lin, Szu-Ning (Lin Szu-Ning) **2PS025 (S114)**
Lin, Tsai-Shun (Lin Tsai-Shun) **2PS008 (S111)**
Lin, Yuxi (林 雨曦) 1E1436 (S27)
Liu, An-An (刘 安安) **2PS041 (S117)**
Liu, Feng (Liu Feng) 1SE-02 (S5)
Liu, Huan (劉 歓) 1I1558 (S36)
Liu, Shihui (Liu Shihui) 2PS041 (S117)
Lo, Chien-Jung (Lo Chien-Jung) 2PS008 (S111)
2PS025 (S114)
Lo, Chien-Jung (羅 健榮) **1A1534 (S20)**
Longhi, Sonia (Longhi Sonia) 1H1522 (S34)
Lu, Yue (魯 ゆえ) **3D1058 (S63)**
Mlzuno, Daisuke (水野 大介) 2PT240 (S145)
Mabuchi, Issei (馬渕 一誠) 2PS016 (S112)
Machiyama, Hiroaki (町山 裕亮) **3H1046 (S71)**
Maeda, Kohji (前田 耕治) 3PS021 (S149)
3PT159 (S168)
Maeda, Miki (前田 美紀) **2PT008 (S120)**
Maeda, Munetoshi (前田 宗利) 1G1510 (S31)
Maeda, Ryo (前田 亮) 1F1424 (S29)
Maeda, Tomoko (前田 友子) 2PT157 (S132)
Maeda, Toshinori (前田 俊徳) 2PT191 (S138)
Maeda, Yuichiro (前田 雄一郎) 1B1546 (S22)
1PT118 (S88)
Maeda, Yusuke (前多 裕介) **2SC-06 (S11)**
Maejima, Masami (前島 雅美) 1PT102 (S85)
Maekawa, Takuma (前川 拓摩) **1PT104 (S86)**
Maeno, Akihiro (前野 覚大) **2E1448 (S46)**
2E1522 (S46)
Maesaki, Ryoko (前崎 綾子) 1B1448 (S21)
Maeshima, Kazuhiro (前島 一博) **1SA-05 (S1)**
Makabe, Koki (MAKABE KOKI) 1B1412 (S21)
Makabe, Koki (真壁 幸樹) 1PT160 (S96)
Maki, Koichiro (牧 功一郎) **1PT148 (S94)**
Maki, Kosuke (槇 亙介) 1PT150 (S94)
Maki-Yonekura, Saori (眞木 さおり) 2D1522 (S45)
Makino, Fumiaki (牧野 文信) **3PS012 (S147)**
Makino, Tsukasa (牧野 司) 1PS037 (S80)
Makino, Yoshihide (牧野 祥嗣) 2PT148 (S130)
Makino, Yoshiteru (槙野 義輝) 1F1558 (S30)
Makishi, Kou (牧志 洸) **2PT213 (S141)**
Manandhar, Yasodha (Manandhar Yasodha)
2PT145 (S129)
Marathe, Rahul (マーラー ラウール) 2I1412 (S54)
Marcucci, Lorenzo (マルクッチ ロレンツォ)
1PS049 (S82)
1YS0900 (S82)
Maruko, Yuuto (丸子 勇人) 1PS014 (S76)
Marunaka, Yoshinori (丸中 良典) 2C1546 (S43)
Maruta, Shinsaku (丸田 晋策) 1PS038 (S80)
1PS051 (S83)
1PS052 (S83)
1PT213 (S104)
2PS038 (S116)
3PT182 (S172)
Maruta, Takahiro (丸田 隆広) **2PS013 (S112)**
2PS014 (S112)
Maruyama, Atsushi (丸山 篤史) 1D1400 (S25)
Maruyama, Atushi (丸山 篤史) 3PS045 (S154)
Maruyama, Ichiro (丸山 一郎) 3PT121 (S161)
Maruyama, Yuusuke (丸山 雄介) 3E1022 (S64)
Masai, Ryouta (政井 良太) **2PT108 (S122)**
Masaike, Tomoko (政池 知子) 2H1448 (S52)
3A0912 (S56)
3A1034 (S57)
1PS025 (S78)
3PS030 (S151)
Masaki, Noritaka (正木 紀隆) **3PS028 (S150)**
Masaoka, Takashi (正岡 崇志) 1PT102 (S85)
Mashima, Tsukasa (真嶋 司) 3C0936 (S60)
Mashimo, Tadaaki (真下 忠彰) 3B1010 (S58)
Mashio, Yuka (眞塩 由佳) 2PT147 (S130)
Masubuchi, Takeya (増渕 岳也) **3PT111 (S159)**
Masuda, Shinji (増田 真二) 2F1522 (S48)
Masuda, Tadashi (増田 正) **2PS015 (S112)**
Masumoto, Hiroshi (増本 博) 2G1522 (S50)
3PT158 (S168)
Matsubara, Tomo (松原 倫) **2PT141 (S129)**
Matsubara, Yuki (松原 佑記) **3PT110 (S159)**
Matsubayashi, Nobuyuki (松林 伸幸) 1PS034 (S80)
Matsubayasi, Nobuyuki (松林 伸幸) 2PT185 (S137)
Matsuda, Chie (松田 知栄) 3PT002 (S155)
Matsuda, Shoichi (松田 翔一) **1I1558 (S36)**
Matsuda, Syoichi (松田 翔一) 3D1058 (S63)
Matsuda, Taisuke (松田 泰祐) **3PT208 (S176)**
Matsuda, Tomoki (松田 知己) 1C1412 (S23)
Matsudaira, Paul T. (Matsudaira Paul T.) **2SA-03 (S9)**
Matsueda, Ryohei (松枝 遼平) **2D1448 (S44)**
2G1522 (S50)
Matsui, Takashi (松井 貴志) 1PS025 (S78)
Matsui, Tsubasa (松井 翼) 3H1022 (S70)
Matsui, Tsubasa S. (松井 翼) **2PS036 (S116)**
Matsui, Tsutomu (松井 つとむ) 1PT157 (S95)
Matsuki, Hitoshi (松木 均) 3G0936 (S68)
3G0948 (S68)
Matsumoto, Atsushi (松本 淳) 3PT008 (S156)
Matsumoto, Hideki (松本 英樹) 1G1510 (S31)
Matsumoto, Takashi (松本 崇) 1PT110 (S87)
Matsumoto, Takashi (松本 貴之) 1C1400 (S23)
Matsumura, Sachiko (松村 佐智子) 3PT221 (S178)
Matsumura, Yoshitaka (松村 義隆) 1PT115 (S88)
1PT157 (S95)
Matsunaga, Sachihiro (松永 幸大) 2D1522 (S45)
Matsunaga, Yasuhiro (松永 康佑) 2B1412 (S40)
Matsunami, Hideyuki (松波 秀行) 2SE-01 (S12)
Matsuo, Koichi (松尾 光一) **1PT108 (S86)**
Matsuo, Lisa (松尾 里紗) 2PS022 (S113)
Matsuo, Takatoshi (松尾 高稔) 2PT161 (S133)
Matsuo, Tatsuhito (松尾 龍人) **2H1400 (S51)**
Matsuoka, Daisuke (松岳 大輔) **2PT116 (S124)**
Matsuoka, Masanari (松岡 雅成) **1I1400 (S35)**
Matsuoka, Shigeru (松岡 茂) 1PT116 (S88)
2PT116 (S124)
Matsuoka, Toru (衆岡 亨) **2PT167 (S133)**
Matsushita, Hisashi (松下 尚嗣) **3PS042 (S153)**
Matsushita, Katsuyoshi (松下 勝義) **1PT161 (S96)**
Matsushita, Mitsugu (松下 貢) **1SC-03 (S3)**
Matsutaka, Hiroshi (松鷹 宏) 1A1412 (S19)
Matsuura, Azuma (松浦 東) 2F1400 (S47)
Matsuura, Koji (松浦 宏治) **1PT211 (S104)**
Matsuura, Tomoaki (松浦 友亮) 1C1534 (S24)
2PT205 (S139)
Matsuura, Yoshiyuki (松浦 能行) 2SB-06 (S10)
3E0900 (S63)
Matsuyama, Atsushi (松山 淳) 2PT176 (S135)
Matsuyama, Take (松山 武) 3B0936 (S58)
Matsuzaki, Masanori (松崎 政紀) **2SH-05 (S16)**
Matsuzaki, Yuri (松崎 由理) 2PT104 (S122)
Matsuzawa, Tomohiro (松澤 朋寛) 3F0924 (S66)
Matubayasi, Nobuyuki (松林 伸幸) 1E1522 (S28)
Matuda, Yui (松田 唯) 3PT135 (S164)
Maturana, Andres D. (Maturana Andres D.)
1PT128 (S90)
1YS0930 (S90)
Matuta, Shinsaku (丸田 晋策) 1PS043 (S81)
Matuyama, Takashi (松山 崇) 1C1510 (S24)
Mayama, Shigeki (真山 茂樹) 2PS047 (S118)
Mayanagi, Kota (真柳 浩太) 2A1400 (S38)
2A1412 (S38)
Mayor, Satyajit (Mayor Satyajit) 3H1058 (S71)
McBride, Mark J. (McBride Mark J.) 2PS026 (S114)
Michiue, Tatsuo (道上 達男) 1D1400 (S25)
Mie, Yasuhiro (三重 安弘) **2PT158 (S132)**
Migita, Taiko (右田 たい子) 3I0948 (S72)
Mikhailenko, Sergey V. (Mikhailenko Sergey V.)
2PS009 (S111)
Miki, Kunio (三木 邦夫) 3E0912 (S63)
1PT123 (S89)
Miki, Masao (三木 正雄) 2H1412 (S52)
Miki, Norihisa (三木 典尚) 3PT163 (S169)
Mikoshiba, Katsuhiko (御子柴 克彦) 3PT206 (S175)
Mikuni, Shintaro (Mikuni Shintaro) 3PT005 (S156)
Mikuni, Shintaro (三國 新太郎) 1PT205 (S103)
3PT004 (S156)
Mimatsu, Saori (三松 さおり) 2PS042 (S117)
Mimura, Yasumasa (三村 泰昌) **1SC-01 (S3)**
Minagawa, Jun (皆川 純) 2PS050 (S118)
Minakata, Shiho (南方 志帆) 1PT118 (S88)
Minami, Kazuyuki (南 和幸) 2PS048 (S118)
Minami, Shintaro (南 慎太朗) 2PT004 (S120)
2PT009 (S121)
2PT202 (S139)
Minami, Shintaro (南 慎太郎) 2PT002 (S119)
2PT003 (S120)
Minamino, Tohru (南野 徹) 1SA-07 (S2)
2SE-01 (S12)
2I1424 (S54)
2I1436 (S54)
2PS005 (S110)
2PS029 (S115)
Mine, Shouhei (峯 昇平) 1PT184 (S100)
Minezaki, Toshiya (峯崎 俊哉) 2B1400 (S40)
Mino, Hiroyuki (三野 広幸) 3D0900 (S61)
3D1022 (S63)
1PT122 (S89)
Mio, Kazuhiro (三尾 和弘) 2G1534 (S51)
3E1022 (S64)
3PT002 (S155)
Mio, Muneyo (三尾 宗代) 2G1534 (S51)
3PT002 (S155)
Misaka, Takumi (三坂 巧) 3PT189 (S174)
Mishima, Hirokazu (三嶋 浩和) **3PT116 (S160)**
Mishima, Masaki (三島 正規) 1B1448 (S21)
Mishima, Masanori (Mishima Masanori) 1PS040 (S81)
Mitaku, Shigeki (美宅 成樹) 2PT011 (S121)
2PT108 (S122)
3PT120 (S161)
Mitaku, Sigeki (美宅 成樹) 1A1400 (S19)
Mitarai, Namiko (御手洗 菜美子) 2C1424 (S42)
Mitomi, Yasushi (三冨 康司) **2B1558 (S41)**
Mitsuhashi, Kenji (三橋 賢司) 3PT213 (S177)
Mitsui, Hiromasa (三井 広大) **2PT191 (S138)**
Mitsui, Toshiyuki (三井 敏之) 1G1448 (S31)
1I1510 (S36)
2D1436 (S44)
3H1010 (S70)
Mitsuoka, Kaoru (光岡 薫) 3E1010 (S64)
1PT180 (S99)
Mitsutake, Ayori (光武 亜代理) **2B1424 (S40)**
Miura, Nami (三浦 奈美) **2PT117 (S124)**
Miura, Takashi (三浦 岳) 2C1448 (S42)
Miwa, Yoshihiro (三輪 佳宏) 1G1412 (S31)
1PT209 (S103)
Miyagi, Hiraku (宮城 拓) **3PT121 (S161)**
Miyaji, Reiji (宮地 礼司) 1PT139 (S92)
Miyakawa, Makiyo (宮川 真紀代) 3PT153 (S167)
1YS1045 (S167)
Miyakawa, Takeshi (宮川 毅) 1PT135 (S91)
2PT131 (S127)
Miyakawa, Takuya (宮川 拓也) **2PT114 (S124)**
Miyake, Jun (三宅 淳) 3H1034 (S71)
2PT228 (S143)
3PS048 (S154)
Miyamori, Takaaki (宮森 一彰) **2F1558 (S49)**
Miyamoto, Akitoshi (宮本 章歳) 3PT206 (S175)
Miyamoto, Keita (宮本 恵太) **2H1522 (S52)**
Miyamoto, Mariko (宮本 万理子) **2PT214 (S141)**
Miyamoto, Tatsuya (宮本 達也) 1PT229 (S107)
Miyanaga, Akihiko (宮永 晃彦) 2PT117 (S124)
Miyano, Satoru (宮野 悟) 2SD-04 (S12)
Miyanoiri, Yohei (宮ノ入 洋平) 1B1424 (S21)
Miyasa, Ryota (宮佐 亮太) **2PT168 (S134)**
Miyashita, Naoyuki (宮下 尚之) 3B1022 (S58)
3E1110 (S65)
1PT212 (S104)
Miyata, Makoto (Miyata Makoto) 2PS027 (S114)
Miyata, Makoto (宮田 真人) **2SE-04 (S13)**
3A1058 (S57)
3E1022 (S64)
2PS021 (S113)
2PS022 (S113)
2PS023 (S114)
2PS024 (S114)
Miyata, Tomoko (宮田 知子) **2SE-01 (S12)**
2I1436 (S54)
3PS012 (S147)
3PT001 (S155)
Miyawaki, Atsushi (宮脇 敦史) **2SH-07 (S17)**
Miyazaki, Makito (宮崎 牧人) 3H1110 (S71)
Miyazaki, Naoyuki (宮崎 直幸) **3E0948 (S64)**
Miyazaki, Naoyuli (宮崎 直幸) 1H1610 (S35)
Miyazawa, Sanzo (宮澤 三造) **2PT007 (S120)**
Miyazono, Yuya (宮薗 侑也) **1PS042 (S81)**
Miyoshi, Hiromi (三好 洋美) **1I1610 (S37)**
Miyoshi, Yohei (三吉 洋平) **3PT011 (S157)**
Mizobata, Tomohiro (溝端 知宏) 1PT164 (S97)
Mizuguchi, Kenji (水口 賢司) 1PT177 (S99)
Mizuhara, Yukinobu (水原 志暢) **1PS039 (S81)**
Mizukami, Shin (水上 進) 3PS039 (S153)
3PS042 (S153)
3PS043 (S153)
3PT134 (S163)
Mizukami, Taku (水上 卓) **1PT001 (S83)**
Mizukami, Takuya (水上 琢也) **1PT150 (S94)**
Mizuno, Akari (水野 紅理) 2H1510 (S52)
1PS009 (S75)
Mizuno, Daisuke (水野 大介) **2SC-03 (S11)**
1PS018 (S77)
3PT170 (S170)
Mizuno, Katsuhide (水野 克秀) **2PT184 (S137)**
Mizuno, Takafumi (水野 敬文) 2PS048 (S118)
Mizushima, Ryota (水島 良太) **2PT126 (S126)**
Mizushima, Tsunehiro (水島 恒裕) 2PT162 (S133)
2PT164 (S133)
Mizuta, Toshifumi (水田 敏史) **1PT164 (S97)**
Mizutani, Hitomi (水谷 仁美) 3PT201 (S174)
3PT210 (S176)
Mizutani, Kana (水谷 佳奈) 3A1058 (S57)
Mizutani, Takeomi (水谷 武臣) 1PT230 (S107)
Mizutani, Yusuke (水谷 祐輔) 2D1546 (S45)
3PS014 (S148)
Mochiji, Shota (持地 翔太) **2PS050 (S118)**
Mochizuki, Atsushi (望月 敦史) 1G1436 (S31)
2C1436 (S42)
2C1510 (S43)
Mochizuki, Masao (望月 正雄) 3I1034 (S72)

Mochizuki, Seiichi (望月 精一) 3PS027 (S150)
Moffat, Keith (Moffat Keith) 3I0936 (S72)
Mogami, George (最上 譲二) 1E1558 (S28)
2H1424 (S52)
1PS002 (S74)
1PS003 (S74)
1PS004 (S74)
1PS005 (S74)
1PT010 (S85)
1PT182 (S100)
Mori, Takaharu (森 貴治) **3PT157 (S168)**
Mori, Takeharu (森 丈晴) 2PT123 (S125)
Mori, Tomoyuki (森 智行) 1B1448 (S21)
Mori, Toshiaki (森 利明) 3C1110 (S61)
Mori, Yoshiharu (森 義治) **3PT224 (S179)**
Mori, Yuki (森 勇樹) 3PS042 (S153)
Morigaki, Kenichi (森垣 憲一) 3G0924 (S68)
3PT161 (S168)
Moriguchi, Yusuke (森口 雄介) **1PS046 (S82)**
Morii, Hisayuki (森井 尚之) 2E1522 (S46)
Morikawa, Mika (森川 美佳) 1D1534 (S26)
Morikawa, Ryota (森河 良太) 1PT135 (S91)
2PT131 (S127)
Morikawa, Takamitsu (森川 高光) **2PT118 (S124)**
Morimatsu, Fumiki (森松 文毅) 1C1400 (S23)
Morimoto, Jumpei (森本 淳平) 1C1436 (S23)
Morimoto, Nobuyuki (森本 展行) 1E1558 (S28)
1PT010 (S85)
1PT182 (S100)
Morimoto, Wakako (森本 和加子) 1A1610 (S20)
Morimoto, Yukio (森本 幸生) 1PT104 (S86)
1PT110 (S87)
Morimoto, Yusuke (森本 雄祐) 2SE-01 (S12)
Morimoto, Yusuke V. (森本 雄祐) **2I1436 (S54)**
2PS028 (S114)
Morino, Kai (森野 佳生) 1SC-04 (S4)
Morishita, Naoki (森下 直樹) 1C1400 (S23)
Morishita, Ryo (森下 了) 3C1034 (S61)
Morishita, Yoshihiro (森下 喜弘) 2PT220 (S142)
Morita, Masamune (森田 雅宗) 3PT153 (S167)
1YS1045 (S167)
Morita, Mizuki (森田 瑞樹) 2PT101 (S121)
Morita, Shin-ichi (盛田 伸一) 1D1412 (S25)
Morita, Takami (森田 貴己) 1PS019 (S77)
Morita, Yoshiro (森田 恭朗) 3PS021 (S149)
Morita, Yuya (森田 有哉) **1PT110 (S87)**
Moritsugu, Kei (森次 圭) **1PT147 (S93)**
Moriwaki, Yoshitaka (森脇 由隆) **2PT151 (S131)**
Moriya, Kazuki (守谷 和騎) 2PT121 (S125)
Moriya, Yuki (守屋 勇樹) 2PT107 (S122)
Moriyama, Toru (森山 徹) 2PT234 (S144)
Morotomi-Yano, Keiko (諸冨 桂子) 1G1424 (S31)
Morris, Roger J. (モリス ロジャー) 3PT172 (S170)
Motojima, Fumihiro (元島 史尋) **1E1412 (S27)**
Motojima-Miyazaki, Yuko (元島(宮崎) 優子)
1E1412 (S27)
Motokawa, Tatsuo (本川 達雄) 2PS040 (S117)
Mouri, Kazunari (毛利 一成) 2SI-04 (S17)
1PT204 (S102)
2PS044 (S117)
Mukai, Hideo (向井 秀夫) 1PT235 (S108)
3PT207 (S176)
3PT213 (S177)
3PT221 (S178)
Mukai, Hiroaki (向井 大陽) **3PS043 (S153)**
Mukai, Tatsuo (向 辰朗) **2PT009 (S121)**
Mukai, Yuri (向井 有理) 3PT126 (S162)
Mukaiyama, Atsushi (向山 厚) **3B1110 (S59)**
Muneyuki, Eiro (宗行 英朗) **2SI-02 (S17)**
1PS022 (S77)
1PS024 (S78)
1PS032 (S79)
2PT139 (S128)
Muneyuki, Eiroh (宗行 英朗) 1PS023 (S78)
Murakami, Gen (村上 元) 3PT213 (S177)
Murakami, Hisashi (村上 久) **2PT234 (S144)**
Murakami, Kosuke (村上 耕介) 3E0948 (S64)
Murakami, Midori (村上 緑) **1SH-06 (S8)**
1F1522 (S30)
Murakami, Satoshi (村上 聡) 1PS021 (S77)
Murakami, Seiko D. (村上 聖子) 1I1424 (S35)
Murakami, Shinya (村上 真也) 1G1448 (S31)
2D1436 (S44)
3H1010 (S70)
Murakoshi, Hideji (村越 秀治) **1PT207 (S103)**
Muramatsu, Chikako (村松 知可子) **3F0936 (S66)**
Muramoto, Kazumasa (村本 和優) 2PT155 (S131)
2PT156 (S131)
2PT157 (S132)
2PT160 (S132)
Muraoka, Takahiro (村岡 貴博) 2I1546 (S55)
Murata, Kazuyoshi (村田 和義) 1H1534 (S34)
3E0948 (S64)
Murata, Michio (村田 道雄) 1PT116 (S88)
2PT116 (S124)
Murata, Satoshi (村田 智) 1PT226 (S107)
1PT227 (S107)
3PT109 (S159)
3PT112 (S159)
3PT113 (S159)
Murata, Shizuaki (村田 静昭) 3C0924 (S60)
Murayama, Koichi (村山 幸市) **1PT187 (S101)**
Murayama, Shuhei (村山 秀平) 2SB-02 (S10)
Murayama, Takashi (村山 尚) **2A1610 (S40)**
Murayama, Yoriko (村山 依子) **2PT232 (S144)**
Muto, Ai (武藤 愛) 2PT107 (S122)
Mutoh, Risa (武藤 梨沙) 1PT122 (S89)
2PT229 (S143)
2PT230 (S143)
Nagadoi, Aritaka (長土居 有隆) 1PT190 (S101)
Nagae, Takayuki (永江 峰幸) **1PT113 (S87)**
Nagai, Hiroki (永井 宏樹) 1PT105 (S86)
2PT124 (S125)
Nagai, Ken (永井 健) **2SC-02 (S11)**
Nagai, Ken H. (永井 健) 1PT224 (S106)
Nagai, Masako (長井 雅子) 2PT154 (S131)
2PT159 (S132)
Nagai, Rina (永井 里奈) 2PS043 (S117)
Nagai, Takeharu (永井 健治) **1SA-03 (S1)**
2PT118 (S124)
Nagai, Tetsuro (永井 哲郎) **3PT144 (S165)**
Nagai, Toshiki (長井 俊樹) 2B1424 (S40)
Nagai, Yukifumi (長井 幸史) 2PT154 (S131)
2PT159 (S132)
Nagai, Yumiko (永井 弓子) 3PT177 (S171)
Naganawa, Tatsuya (永縄 達也) **2H1448 (S52)**
Nagao, Chioko (長尾 知生子) **1PT177 (S99)**
Nagao, Hidemi (長尾 秀実) 1E1400 (S27)
3F1010 (S66)
1PT001 (S83)
2PT131 (S127)
Nagaoka, Masataka (長岡 正隆) 1E1510 (S28)
2E1436 (S46)
2PT165 (S133)
Nagasaki, Akira (長崎 晃) 2SE-03 (S13)
Nagasaki, Masao (長崎 正朗) 2SD-04 (S12)
Nagase, Shinobu (長瀬 忍) 3PS038 (S152)
Nagashima, Hiroki (長嶋 宏樹) **3D0900 (S61)**
3D1022 (S63)
Nagashima, Yasuto (長嶋 泰人) **3PS017 (S148)**
Nagata, Chikahiro (永田 親弘) 1PT117 (S88)
Nagata, Kumiko (永田 久美子) **1F1448 (S29)**
Nagata, Mitsunori (永田 光範) **1A1412 (S19)**
1PS041 (S81)
Nagata, Taashi (永田 崇) 3C1034 (S61)
Nagata, Takashi (永田 崇) 3C0936 (S60)
2PT190 (S138)
1YS1015 (S138)
3PT003 (S155)
Nagata, Tomohiro (永田 智啓) 1H1558 (S34)
Nagatani, Akira (長谷 あきら) 2F1510 (S48)
Nagatani, Yasuko (永谷 康子) 2PT123 (S125)
Nagatani, Yukinori (永谷 幸則) 1H1534 (S34)
1H1546 (S34)
Nagatomo, Shigenori (長友 重紀) **2PT152 (S131)**
2PT159 (S132)
Nagaya, Hiromi (長屋 ひろみ) 3PT201 (S174)
Nagayama, Kuniaki (永山 國昭) **1H1534 (S34)**
1H1546 (S34)
3E0948 (S64)
Nagayama, Masaharu (長山 雅晴) 1G1400 (S31)
2C1448 (S42)
Nagayoshi, Wataru (永吉 航) 3PS050 (S155)
Naiki, Hironobu (内木 宏延) 1E1436 (S27)
1PT145 (S93)
Naito, Akira (内藤 晶) **1F1558 (S30)**
3E0936 (S64)
3F1046 (S67)
2PT168 (S134)
3PT114 (S159)
3PT127 (S162)
Naito, Hiroshi (内藤 洋) 2PT112 (S123)
Naito, Tatsuya (内藤 達也) **3A1034 (S57)**
Naka, Yasuhiro (仲 泰嘉) **3PT159 (S168)**
Nakabayashi, Jun (中林 潤) 2PT211 (S140)
Nakada, Chieko (中田 千枝子) 3PT172 (S170)
Nakada, Hinako (中田 比奈子) **2PT148 (S130)**
Nakada, Kyoko (中田 恭子) 1E1510 (S28)
Nakada, Shogo (仲田 正吾) **3PT220 (S178)**
Nakagaki, Toshiyuki (中垣 俊之) 1SF-06 (S7)
Nakagawa, Ayumi (中川 あゆみ) 2PT121 (S125)
Nakagawa, Hiroshi (中川 洋) **1E1534 (S28)**
Nakagawa, Kanako (中川 香奈子) 1PT142 (S93)
Nakagawa, Takeshi (中川 健) **1A1424 (S19)**
1PS028 (S78)
Nakagawa, Takuya (中川 卓哉) **1PS005 (S74)**
Nakagawa, Taro (中川 太郎) 2PT161 (S133)
Nakagawa, Yuki (中川 裕規) **2PT003 (S120)**
Nakagawa, Zen-ichi (中川 善一) 2PT107 (S122)
Nakahara, Asahi (中原 旭) 3PS031 (S151)
Nakahara, Naoya (中原 直哉) 2H1558 (S53)
Nakajima, Akihiko (中島 昭彦) **3H0936 (S70)**
Nakajima, Masahiro (中島 正博) 1PT229 (S107)
1PT233 (S108)
Nakajima, Masato (中島 正人) 3F1034 (S67)
Nakajima, Mizuki (中嶋 瑞樹) **2PS003 (S110)**
Nakajima, Yoshiki (中島 慶樹) 2PT203 (S139)
Nakajo, Koichi (中條 浩一) 3PT168 (S170)
Nakaki, Ryo (仲木 竜) 1I1448 (S35)
Nakamasu, Akiko (中益 朗子) 1PS018 (S77)
Nakamichi, Katsuhisa (中道 勝久) 3PT101 (S157)
Nakamori, Kota (中森 弘太) **2PT002 (S119)**
Nakamrua, Tatsuya (中村 竜也) **3PS039 (S153)**
Nakamura, Atsushi (中村 淳志) **2PT142 (S129)**
Nakamura, Daigo (中村 大吾) **3PS036 (S152)**
Nakamura, Haruki (Nakamura Haruki) 2B1436 (S40)
Nakamura, Haruki (中村 春木) 1C1412 (S23)
3B1010 (S58)
1PT119 (S88)
1PT126 (S90)
1PT130 (S90)
1PT168 (S97)
2PT103 (S121)
3PT010 (S157)
3PT190 (S174)
3PT223 (S179)
Nakamura, Mitsuru (中村 允) **1PT216 (S105)**
Nakamura, Shigeyoshi (中村 成芳) 1PT107 (S86)
1PT149 (S94)
1PT179 (S99)
Nakamura, Shinichiro (中村 振一郎) 3PT227 (S179)
3PT230 (S180)
3PT232 (S180)
Nakamura, Shogo (中村 昇吾) 1D1400 (S25)
Nakamura, Shotaro (中村 祥太郎) 3PS021 (S149)
Nakamura, Shougo (中村 昇吾) **3PS045 (S154)**
Nakamura, Shugo (中村 周吾) 2PT010 (S121)
2PT101 (S121)
Nakamura, Shuichi (中村 修一) 2SE-01 (S12)
2PS029 (S115)
2PS030 (S115)
2PS046 (S118)
Nakamura, Syuichi (中村 修一) 1PS029 (S79)
2PS006 (S111)
Nakamura, Takashi (NAKAMURA Takashi)
1B1412 (S21)
Nakamura, Takashi (中村 敬) 1PT143 (S93)
1PT160 (S96)
2PT150 (S130)
Nakamura, Teruya (中村 照也) **1PT129 (S90)**
1YS1000 (S90)
Nakamura, Tomoyuki (中村 知幸) 2PS049 (S118)
Nakamura, Yuki (中村 由樹) **1H1436 (S33)**
Nakane, Daisuke (中根 大介) 2SE-05 (S13)
3A1058 (S57)
3E1022 (S64)
2PS022 (S113)
2PS023 (S114)
2PS024 (S114)
2PS026 (S114)
Nakanishi Mamoru (中西 守) 1PT206 (S103)
Nakanishi, Mamoru (中西 守) 3PT176 (S171)
Nakanishi, Naoya (中西 直哉) 1PT233 (S108)
Nakanishi, Shuji (中西 周次) 1I1558 (S36)
3D1058 (S63)
Nakanishi, Taichi (中西 太市) **1F1522 (S30)**
Nakanishi, Takeshi (中西 猛) 1C1448 (S23)
Nakanishi, Yosuke (中西 陽介) 3PS043 (S153)
Nakano, Akihiko (中野 明彦) 3PT236 (S181)
Nakano, Kentaro (中野 賢太郎) 2PS037 (S116)
Nakano, Masahiro (中野 雅裕) 3A0948 (S56)
Nakano, Minoru (中野 実) 2G1448 (S50)
2G1510 (S50)
3PT162 (S169)
Nakano, Shogo (中野 祥吾) 3PT222 (S178)
Nakao, Hiroyuki (中尾 裕之) **3PT162 (S169)**
Nakao, Ryota (中尾 亮太) 1PT185 (S100)
Nakasako, Masayoshi (中迫 雅由) **2D1522 (S45)**
2D1534 (S45)
Nakashima, Hiromichi (中嶋 寛倫) **2PT122 (S125)**
Nakashima, Hitomi (中嶋 仁珠) 2PS048 (S118)
Nakashima, Ryosuke (中島 良介) 1PT117 (S88)
3PT115 (S160)
Nakashima, Satoru (中島 聡) 3I1022 (S72)
3I1034 (S72)
Nakashima, Yuta (中島 雄太) 2PS048 (S118)
Nakasone, Yusuke (中曽根 祐介) **2F1510 (S48)**
2F1558 (S49)
2PT169 (S134)

2PT175 (S135)
Nakata, Haruka (中田 春香) 2PT109 (S123)
Nakata, Satoshi (中田 聡) 3PT135 (S164)
Nakatani, Youichi (中谷 陽一) 2PT192 (S138)
Nakauchi, Yuni (中内 祐二) 1PS013 (S76)
Nakayama, Koji (中山 浩次) 2SE-05 (S13)
2PS026 (S114)
Nakayama, Rinako (中山 莉奈子) 3A0912 (S56)
3PS030 (S151)
Nakazato, Kenichi (中里 研一) 1D1424 (S25)
Nakazawa, Hikaru (中澤 光) **1C1510 (S24)**
Nakazawa, Hiromitsu (中沢 寛光) **3G1110 (S69)**
3PT149 (S166)
Nakazumi, Taichi (中住 太一) 1C1400 (S23)
Namba, Keiichi (難波 啓一) 2SE-01 (S12)
2I1424 (S54)
2I1436 (S54)
2PS005 (S110)
2PS006 (S111)
2PS028 (S114)
2PS029 (S115)
3PS012 (S147)
3PT001 (S155)
Namba, Toshinori (難波 利典) **2PT225 (S143)**
Namsrai, Javkhlantugs (ナムスライ ジャブクラントゥス)
3E0936 (S64)
Namsrai, Javkhlantugs (ナムズライ ジャフカラントゥクス)
3PT114 (S159)
Nara, Toshifumi (奈良 敏文) 2PT176 (S135)
Narihara, Itaru (成原 格) **3PT007 (S156)**
Narita, Akihiro (成田 哲博) 1H1610 (S35)
2H1436 (S52)
1PT118 (S88)
Narita, Jun (成田 純) 1PS039 (S81)
1PT169 (S97)
Narumi, Masatoshi (鳴海 正寿) **2PT174 (S135)**
Naruse, Keiji (成瀬 恵治) 1PT209 (S103)
1PT211 (S104)
Natali, Francesca (Natali Francesca) 2H1400 (S51)
Natsume, Yuno (夏目 ゆうの) **3G1034 (S69)**
Nawa, Omi (名和 臣) 3PT237 (S181)
Negami, Tatsuki (根上 樹) **2PT133 (S127)**
Negishi, Lumi (根岸 瑠美) **3PT124 (S161)**
Nemoto, Naoto (根本 直人) 1PT234 (S108)
2PT147 (S130)
2PT204 (S139)
Nemoto, Yuri L. (根本 悠宇里) 1G1412 (S31)
3PT172 (S170)
Neya, Saburo (根矢 三郎) 3I0924 (S71)
Nie, Qing-Miao (Nie Qing-Miao) **2PS017 (S112)**
Nigorikawa, Shinpei (濁川 慎平) **3PT152 (S167)**
Nii, Daisuke (二井 大輔) **3PT105 (S158)**
Niida, Atsushi (新井田 厚司) 2SD-04 (S12)
Niioka, Hirohiko (新岡 宏彦) **1H1558 (S34)**
Niisato, Naomi (新里 直美) 2C1546 (S43)
Niitani, Yamato (新谷 大和) **1A1448 (S19)**
Niiyama, Mayumi (新山 真由美) 1PT116 (S88)
2PT116 (S124)
Niizato, Takayuki (新里 高行) **2PT210 (S140)**
2PT234 (S144)
Nishi, Shunsuke (西 俊介) 3D0948 (S62)
Nishida, Koji (西田 幸次) 1E1424 (S27)
Nishigaki, Koichi (西垣 功一) 2PT204 (S139)
Nishigaki, Takehiko (西垣 岳彦) **2I1400 (S53)**
Nishigaki, Takeshi (西垣 武) 3I1022 (S72)
Nishihara, Yasutaka (西原 泰孝) **1A1522 (S20)**
Nishijo, Kaname (西條 要) **2PT144 (S129)**
Nishikata, Koro (西方 公郎) **1F1534 (S30)**
Nishikawa, Hirohide (西川 大英) 3F1046 (S67)
Nishikawa, Kouki (西川 幸希) 3F0924 (S66)
Nishikawa, Takehiro (西川 雄大) 2PT205 (S139)
Nishikawa, Yoshihiro (中村 真梨子) 3A0948 (S56)
Nishikawa, Yusuke (西川 雄亮) 2SE-03 (S13)
2PS039 (S116)
Nishikomori, Ryuta (西小森 隆太) 3PS031 (S151)
Nishima, Wataru (二島 渉) **1PT212 (S104)**
Nishimori, Hiraku (西森 拓) 2PT141 (S129)
2PT214 (S141)
2PT218 (S141)
Nishimoto, Etsuko (西本 悦子) 2E1610 (S47)
2PT122 (S125)
Nishimura, Atsuhito (西村 篤人) 2PT229 (S143)
Nishimura, Erika (西村 恵里夏) 2PT112 (S123)
Nishimura, Katsuyuki (西村 勝之) 2PT115 (S124)
3PT178 (S172)
Nishimura, Kohei (西村 航平) 1PT168 (S97)
Nishimura, Megumi (西村 めぐみ) 1E1400 (S27)
3F1010 (S66)
Nishimura, Shin I. (西村 信一郎) **2PT227 (S143)**
Nishimura, Takahiro (西村 隆宏) **1I1534 (S36)**
Nishimura, Yoshifumi (西村 善文) 1PT190 (S101)
Nishino, Kunihiko (西野 邦彦) 1PT117 (S88)
3PT115 (S160)
Nishino, Takeshi (西野 武士) 2PT137 (S128)
Nishino, Tomohide (西野 伴英) 2E1424 (S46)
Nishio, Izumi (西尾 泉) 3PT154 (S167)
Nishio, Kazuya (西尾 和也) 1PT104 (S86)
Nishio, Toshihiko (西尾 俊彦) 3PT203 (S175)
Nishioka, Noriko (西岡 典子) 2I1400 (S53)
Nishiyama, Hidetoshi (西山 英利) 3E1022 (S64)
Nishiyama, Masayoshi (西山 雅祥) **1A1558 (S20)**
3H0924 (S70)
Nishiyama, So-ichiro (西山 宗一郎) 1PT121 (S89)
3PT185 (S173)
3PT188 (S173)
3PT192 (S174)
Nishiyama, Yuta (西山 雄太) 2PT234 (S144)
Nishizaka, Takayuki (西坂 崇之) 2H1448 (S52)
3A0912 (S56)
3A1034 (S57)
3A1058 (S57)
3E1022 (S64)
1PS025 (S78)
2PS023 (S114)
3PS030 (S151)
Nishizawa, Tomohiro (西澤 知宏) 1PT128 (S90)
1YS0930 (S90)
Nitta, Ryo (仁田 亮) 3H0900 (S69)
Niwa, Fumihiro (丹羽 史尋) 3PT206 (S175)
Niwa, Ken (丹羽 健) 1PT113 (S87)
Niwa, Tatsuya (丹羽 達也) **1B1510 (S21)**
Nobe, Yukiko (野辺 由紀子) 1I1424 (S35)
Noda, Naoki (野田 直紀) 2PS020 (S113)
1YS0945 (S113)
Noda, Sigeho (野田 繁穂) 2SD-03 (S12)
Noguchi, Hiroki (野口 大貴) **1PT101 (S85)**
Noguchi, Masato (野口 正人) 3I0936 (S72)
Noguchi, Takumi (野口 巧) 3D1034 (S63)
3PT226 (S179)
3PT229 (S180)
3PT231 (S180)
3PT235 (S181)
Noguchi, Taro Q.P. (野口 太郎) 2SE-03 (S13)
2PS035 (S116)
Noguchi, Yukina (野口 有希奈) 2PS006 (S111)
Noji, Hiroyuki (野地 博之) 3A0936 (S56)
Noji, Hiroyuki (野地 博行) **1SA-02 (S1)**
1A1436 (S19)
3A0924 (S56)
3A0948 (S56)
3A1010 (S56)
3F0900 (S65)
1PS029 (S79)
1PS033 (S79)
1YS1115 (S79)
2PT207 (S140)
3PT103 (S157)
Noji, Sumihare (野地 澄晴) 1F1436 (S29)
Nomiya, Yui (野宮 唯) **1PS012 (S76)**
Nomura, Fumimasa (野村 典正) 2D1510 (S44)
3PS020 (S149)
3PS022 (S149)
3PS023 (S149)
3PS046 (S154)
3PS049 (S154)
Nomura, Keiji (野村 圭史) 3G0900 (S67)
Nomura, Shin-ichiro (野村 慎一郎) 3PT112 (S159)
3PT113 (S159)
Nomura, Shin-ichiro M. (野村 M. 慎一郎) 1E1448 (S27)
1PT228 (S107)
Nomura, Shin-ichiro. M (野村 慎一郎) 1PT226 (S107)
Nomura, Sin-ichiro (野村 慎一郎) 1PT227 (S107)
Nomura, Takao (野村 尚生) 2B1558 (S41)
Nonaka, Takamasa (野中 孝昌) 1PT179 (S99)
Noriyuki, Kodera (Noriyuki Kodera) 1H1522 (S34)
Noto, Kaori (能登 香) **3PT225 (S179)**
Nozawa, Shunsuke (野澤 俊介) 3PS024 (S150)
Nozoe, Takashi (野添 嵩) **2C1610 (S43)**
Nukina, Nobuyuki (貫名 信行) 2B1558 (S41)
Numata, Osamu (沼田 治) 2PS037 (S116)
Numata, Tomoko (沼田 朋子) 3PT234 (S181)
Nunomura, Wataru (布村 渉) **1PT107 (S86)**
Nureki, Osamu (濡木 理) 1SH-02 (S7)
1PT128 (S90)
1YS0930 (S90)
Oasa, Sho (大浅 翔) **1PT205 (S103)**
Oba, Tetsuya (大羽 哲也) **2I1510 (S54)**
Obana, Eriko (尾華 絵里子) 3PT119 (S160)
Oda, Masayuki (織田 昌幸) 1C1522 (S24)
2E1522 (S46)
3B0924 (S58)
1PT130 (S90)
Oda, Toshiro (小田 俊郎) 1PT003 (S83)
Odawara, Aoi (小田原 あおい) **1PT220 (S105)**
Ode, Hirotaka (大出 裕高) **1PT102 (S85)**
Ogata, Aya (緒方 彩) **1PT231 (S107)**
Ogata, Kazuhiro (緒方 一博) 3PT010 (S157)
Ogata, Koji (緒方 浩二) 3PT227 (S179)
3PT232 (S180)
Ogata, Kouji (緒方 浩二) 3PT230 (S180)
Ogawa, Naoki (小川 直輝) 3PT101 (S157)
Ogawa, Ruriko (小川 瑠里子) 2PS043 (S117)
Ogawa, Yoko (小川 洋子) 1PT138 (S92)
Ogawa, Yutaka (小川 泰) 2SB-01 (S10)
Ogi, Hirotsugu (荻 博次) 1E1436 (S27)
Ogura, Takashi (小倉 尚志) 3I0924 (S71)
3I1010 (S72)
3I1022 (S72)
3I1034 (S72)
3I1046 (S73)
2PT159 (S132)
Ogura, Toshihiko (小椋 俊彦) 3H0900 (S69)
3PS011 (S147)
Ogura, Yusuke (小倉 裕介) 1I1534 (S36)
Oh-oka, Hirozo (大岡 宏造) 3PT235 (S181)
Ohara, Masahiro (小原 正裕) 1H1534 (S34)
Ohara, Osamu (小原 收) 1PT202 (S102)
3PS031 (S151)
Ohba, Tetsuhiko (大場 哲彦) 3PT145 (S165)
Ohba, Yasunori (大庭 裕範) 1PT144 (S93)
Ohhashi, Yumiko (大橋 祐美子) **2PT113 (S123)**
Ohkawa-Nishiwaki, Taeko (大川(西脇) 妙子)
3B1058 (S59)
Ohki, Shinya (大木 進野) 1PT107 (S86)
Ohki, Takashi (大木 高志) 3B0948 (S58)
3H1110 (S71)
1PS047 (S82)
2PS009 (S111)
Ohkubo, Fuki (大久保 文貴) 2SH-05 (S16)
Ohkubo, Jun (大久保 潤) **2PT212 (S141)**
Ohkubo, Yukie (大久保 幸恵) 3PT201 (S174)
Ohmae, Eiji (大前 英司) 2E1448 (S46)
Ohnishi, Norikazu (大西 紀和) 2PS050 (S118)
Ohno, Shin-ya (大野 真也) 2PT186 (S137)
Ohno, Takashi (大野 隆) 3PT233 (S180)
3PT234 (S181)
Ohno, Tetsuo (大野 哲生) 2H1558 (S53)
Ohnuki, Jun (大貫 隼) **1PS020 (S77)**
1PT002 (S83)
Ohnuma, Kiyoshhi (大沼 清) 3PS045 (S154)
Ohnuma, Kiyoshi (大沼 清) **1D1400 (S25)**
3PS051 (S155)
Ohonuma, Kiyoshi (大沼 清) 3PS044 (S153)
Ohta, Akane (太田 茜) 3PT201 (S174)
3PT210 (S176)
Ohta, Makoto (太田 信) 3F0948 (S66)
Ohta, Noboru (太田 昇) 1C1610 (S25)
Ohta, Yoshihiro (太田 善浩) 3PS041 (S153)
3PT175 (S171)
Ohtomo, Hideaki (大友 秀明) 1PT120 (S89)
1PT142 (S93)
Ohtsuki, Ryuji (大槻 隆司) 1C1400 (S23)
Ohuchi, Hideyo (大内 淑代) 1F1436 (S29)
Ohuchi, Shokichi (大内 将吉) 2PT149 (S130)
3PS050 (S155)
Ohue, Masahito (大上 雅史) 2PT104 (S122)
Oikawa, Hiroyuki (小井川 浩之) **1PT152 (S94)**
1PT222 (S106)
Oiki, Shigetoshi (老木 成稔) 2SH-01 (S16)
2G1558 (S51)
2G1610 (S51)
3PT164 (S169)
3PT165 (S169)
Oiwa, Kazuhiro (大岩 和弘) 2SC-02 (S11)
1PS031 (S79)
3PS001 (S146)
3PS009 (S147)
Oka, Kotaro (岡 浩太郎) 1PT216 (S105)
3PT204 (S175)
Oka, Masahito (岡 勝仁) **2PT208 (S140)**
Oka, Tatsuya (岡 辰也) 3PT169 (S170)
Oka, Toshihiko (岡 俊彦) **3G1058 (S69)**
1PT123 (S89)
Okabe, Hiroki (岡部 紘輝) **2PS049 (S118)**
Okabe, Kohki (岡部 弘基) **3PS010 (S147)**
1YS0915 (S147)
3PS040 (S153)
Okada, Fumiko (岡田 文子) **3G0924 (S68)**
Okada, Kaoru (岡田 薫) 3A1034 (S57)
Okada, Keisuke (岡田 佳祐) **3PT161 (S168)**
Okada, Mariko (岡田 眞理子) 2PT140 (S128)
3PT179 (S172)
Okada, Norihiro (岡田 昇大) 3I1058 (S73)
Okada, Ryuichi (岡田 龍一) 1D1534 (S26)
Okada, Seiji (岡田 誠治) 2PT150 (S130)
Okada, Takeru (岡田 健) 1A1412 (S19)
Okada, Taketo (岡田 岳人) 1D1610 (S26)
Okada, Yasushi (岡田 康志) 2SI-04 (S17)
3H0900 (S69)

Okada-Hatakeyama, Mariko (岡田 眞理子) 1G1610 (S32)
Okahata, Yoshio (岡畑 恵雄) 1PT162 (S96)
Okajima, Koji (岡島 公司) 2F1510 (S48)
Okajima, Takaharu (岡嶋 孝治) **2D1546 (S45)**
3PS014 (S148)
3PS015 (S148)
Okamoto Keisuke (岡本 恵佑) 1PT206 (S103)
Okamoto, Ken (岡本 研) 2PT137 (S128)
Okamoto, Kenji (岡本 憲二) **2PT128 (S126)**
Okamoto, Tetsuaki (岡本 哲明) 2SI-02 (S17)
Okamoto, Yoh (岡本 洋) **1PS006 (S74)**
Okamoto, Yuko (岡本 祐幸) 1PT132 (S91)
3PT130 (S163)
3PT144 (S165)
3PT224 (S179)
Okamura, Hideyasu (岡村 英保) 3PT003 (S155)
Okano, Keiko (岡野 恵子) 2PT191 (S138)
Okano, Teruo (岡野 光夫) 2PS047 (S118)
Okano, Toshiyuki (岡野 俊行) 2PT191 (S138)
Okazaki, Fumihiro (岡崎 文洋) 3PT150 (S166)
Okazaki, Yuichiro (岡崎 裕一郎) 1PS002 (S74)
1PS003 (S74)
1PS004 (S74)
Oki, Keisuke (沖 佳祐) **3PT151 (S167)**
Okimoto, Noriaki (沖本 憲明) 1PT188 (S101)
2PT140 (S128)
Okimura, Chika (沖村 千夏) **2PS048 (S118)**
Okitsu, Takashi (沖津 貴志) 1F1558 (S30)
3F1046 (S67)
Okubo, Hiroyuki (大久保 宏之) 2PS013 (S112)
Okuda, Satoru (奥田 覚) **1PT219 (S105)**
Okuma, Yasuo (大熊 康夫) 3E1010 (S64)
Okumura, Hisashi (奥村 久士) 3E1058 (S65)
1PT131 (S91)
Okuno, Daichi (奥野 大地) 2G1546 (S51)
3A0948 (S56)
3PT167 (S169)
Okuno, Masanari (奥野 将成) 2SH-03 (S16)
Okura, Reiko (大倉 玲子) 2C1610 (S43)
1PT215 (S105)
Okushita, Keiko (奥下 慶子) **3E0924 (S64)**
Okuta, Akiko (奥田 明子) 1D1534 (S26)
Omagari, Katsumi (尾曲 克己) **2PT138 (S128)**
Onai, Kiyoshi (小内 清) 2PT229 (S143)
2PT230 (S143)
Onishi, Yukiko (大西 幸子) 2G1546 (S51)
3PT167 (S169)
Ono, Koji (小野 晃司) **1PT172 (S98)**
Ono, Minehisa (小野 巌久) 3PT202 (S175)
Ono, Sumire (小野 すみれ) **1PT215 (S105)**
Ono, Takahito (小野 崇人) 3PS013 (S148)
Ono, Takao (小野 尭生) 1PT236 (S108)
Ono, Yukiko (小野 友紀子) **2F1448 (S48)**
Onodera, Yoshikuni (小野寺 宜郷) 1PT117 (S88)
Onoe, Hiroaki (尾上 弘晃) 1I1546 (S36)
1PT224 (S106)
1PT225 (S106)
Onoue, Yasuhiro (尾上 靖宏) 3B1110 (S59)
Ooishi, Yuki (大石 悠貴) 3PT207 (S176)
Oosawa, Kenji (大澤 研二) 2PS030 (S115)
2PT110 (S123)
2PT119 (S124)
2PT120 (S125)
Oosawa, Tsuyoshi (大澤 剛) 3PT124 (S161)
Oroguchi, Tomotaka (笠口 友隆) 2D1522 (S45)
2D1534 (S45)
Osaki, Toshihisa (大崎 寿久) 2G1412 (S49)
3PT136 (S164)
3PT143 (S165)
3PT163 (S169)
Osako, Masato (大迫 政人) 3B1110 (S59)
Osanai, Hiromi (小山内 裕美) **3PT221 (S178)**
Oshima, Atsunori (大嶋 篤典) **3F0924 (S66)**
Oshima, Hiraku (尾嶋 拓) **1PT137 (S92)**
1PT154 (S95)
3PT116 (S160)
Osoegawa, Hiroya (小副川 博也) **2PT149 (S130)**
Ota, Hiroki (大田 啓貴) 2A1610 (S40)
Ota, Kai (大田 該) **3PT226 (S179)**
Ota, Motonori (Ota Motonori) 1I1436 (S35)
Ota, Motonori (太田 元規) 1B1546 (S22)
1I1424 (S35)
2PT130 (S127)
Otani, Nao (大谷 直) 3PT110 (S159)
Otomo, Seiu (大友 征宇) 3PT233 (S180)
3PT234 (S181)
Otsuka, Kensuke (大塚 健介) 1G1510 (S31)
Otsuka, Yo (大塚 陽) **1G1448 (S31)**
2D1436 (S44)
3H1010 (S70)
Owa, Mikito (大和 幹人) **3PS006 (S146)**
3PS007 (S147)
Oyama, Hirofumi (大山 浩史) 1H1424 (S33)
3PS035 (S152)
Oyama, Kotaro (大山 廣太郎) **2H1510 (S52)**
2H1546 (S53)
1PS009 (S75)
Ozaki, Yu-ichi (尾崎 裕一) 2PT219 (S142)
Ozaki, Yukihiro (尾崎 幸洋) 1D1412 (S25)
Ozaki, Yuya (尾崎 裕哉) **2F1412 (S47)**
Ozawa, Katsuya (小澤 克也) 2SH-05 (S16)
Ozawa, Takeaki (小澤 岳昌) 2PT143 (S129)
P. Terada, Tomoki (寺田 智樹) 1PT166 (S97)
P.N., Sunilkumar (P.N. Sunilkumar) 2E1448 (S46)
Pack, Chan-Gi (白 燦基) 1PT151 (S94)
Pack, Chan-gi (白 燦基) 1D1424 (S25)
Pack, Chang-Gi (白 燦基) **3PT179 (S172)**
Pack, Chang-gi (白 燦基) 2SI-04 (S17)
Pack, Changi (白 燦基) 3PT236 (S181)
Pan, Wenshi (Pan Wenshi) 3PT189 (S174)
Pang, Dai-Wen (庞 代文) 2PS041 (S117)
Park, Sam-Yong (朴 三用) 3I0912 (S71)
1PT101 (S85)
Paul, Koushik (Paul Koushik) 2SA-02 (S9)
Paxton, Thanai (Paxton Thanai) 3PT124 (S161)
Picollo, Alessandra (ピッコロ アレサンドラ) 3PT118 (S160)
Pilizota, Teuta (Pilizota Teuta) 1A1534 (S20)
Plazanet, Marie (Plazanet Marie) 1PT003 (S83)
Ramakrishnan, Charu (Ramakrishnan Charu) 1PT128 (S90)
1YS0930 (S90)
Rao, Madan (Rao Madan) 3H1058 (S71)
Re, Suyong (李 秀栄) 3E1110 (S65)
Renger, Thomas (レンガー トーマス) 3D0948 (S62)
Rie, Nagai (理恵 永井) 1PT209 (S103)
Roberts, Thomas M. (Roberts Thomas M.) 2PS020 (S113)
1YS0945 (S113)
Roder, Heinrich (Roder Heinrich) 1PT150 (S94)
Ronald D., Vale (Ronald D. Vale) 3PS004 (S146)
Royant, Antoine (ロヤン アントン) 2SH-01 (S16)
Ryo, Akihide (梁 明秀) 3C1034 (S61)
Sadakane, Kei (貞包 慧) **2PS038 (S116)**
Sadamoto, Hisayo (定本 久世) **1D1610 (S26)**
Saeki, Shinjiro (佐伯 真二郎) 2PT190 (S138)
1YS1015 (S138)
Saeki, Yasushi (佐伯 泰) 3E1010 (S64)
1PT104 (S86)
1PT180 (S99)
Saeki, Yuko (佐伯 夕子) 1G1610 (S32)
3PT179 (S172)
Sagawa, Takashi (佐川 貴志) **2I1546 (S55)**
2I1558 (S55)
Saido, Takaomi (西道 隆臣) 2PT111 (S123)
Saijo-Hamano, Yumiko (西條 由見子) 2PS005 (S110)
Saikusa, Kazumi (七種 和美) **1PT190 (S101)**
Sainoo, Yasuyuki (道祖尾 恭之) 2E1412 (S45)
Saita, Eiichiro (税田 英一郎) **1PS026 (S78)**
1PS035 (S80)
Saito, Ayumu (斉藤 あゆむ) 2SD-04 (S12)
Saito, Hiroaki (齋藤 大明) 1E1400 (S27)
3F1010 (S66)
2PT131 (S127)
Saito, Hiroyuki (斎藤 博幸) 3PT169 (S170)
Saito, Kazuya (齋藤 一弥) 2PT152 (S131)
Saito, Kei (斎藤 慧) 2A1448 (S38)
Saito, Keisuke (斉藤 圭亮) 3D0912 (S62)
Saito, Mami (齋藤 真美) **1PT181 (S100)**
Saito, Minoru (斎藤 稔) 1PT235 (S108)
2PT233 (S144)
3PT219 (S178)
3PT220 (S178)
3PT221 (S178)
Saito, Shinji (斉藤 真司) 3PT165 (S169)
Saito, Shoma (齊藤 翔馬) **2PS035 (S116)**
Saito, Takashi (斉藤 貴志) 2PT111 (S123)
Saito, Takeshi (斎藤 健) 2SF-03 (S14)
Saito, Takeshi (齊藤 健) **2PT219 (S142)**
Saito, Tomofumi (齋藤 智文) 3PS017 (S148)
Saitoh, Sho (斉藤 翔) **1PT222 (S106)**
Saitoh, Zenpei (斎藤 善平) 1H1534 (S34)
Sakae, Yoshitake (榮 慶丈) **1PT132 (S91)**
Sakaguchi, Miyuki (坂口 美幸) **3I1046 (S73)**
Sakai, Chihiro (坂井 ちひろ) 1C1400 (S23)
Sakai, Eri (坂井 絵厘) 1PT153 (S95)
Sakai, Kazumi (酒井 佳寿美) 1F1436 (S29)
Sakai, Kazunari (坂井 一成) 3PT159 (S168)
Sakai, Makoto (酒井 誠) **2SH-02 (S16)**
3PS038 (S152)
Sakai, Shin-ichi (坂井 慎一) 1D1400 (S25)
3PS045 (S154)
Sakakibara, Hitoshi (榊原 斉) **3PS001 (S146)**
3PS009 (S147)
Sakakibara, Manabu (榊原 学) 1D1534 (S26)
Sakakibara, Shotaro (榊原 正太郎) **2B1448 (S40)**
Sakamoto, Akihiko (坂本 明彦) **1PT208 (S103)**
3PS040 (S153)
Sakamoto, Hiroshi (坂本 寛) 1PT185 (S100)
Sakamoto, Shigetaka (坂本 盛宇) 1I1424 (S35)
Sakata-Sogawa, Kumiko (十川 久美子) **2SG-02 (S15)**
1H1424 (S33)
3PS033 (S151)
3PS034 (S152)
3PS035 (S152)
3PT181 (S172)
Sakiyama, Hiroki (崎山 裕紀) 3PT177 (S171)
Sakiyama, Yusuke (崎山 雄介) **2PS053 (S119)**
Sako, Yasushi (佐甲 靖志) 1D1412 (S25)
1D1424 (S25)
1G1558 (S32)
1G1610 (S32)
1PT151 (S94)
1PT204 (S102)
1PT210 (S104)
2PS044 (S117)
2PT128 (S126)
3PT179 (S172)
3PT236 (S181)
Sakonji, Mitsuhiro (左近司 充洋) **2PT172 (S134)**
Sakumura, Yuichi (作村 諭一) **2PS052 (S119)**
Sakuraba, Shun (櫻庭 俊) 2PT185 (S137)
Sakurai, Kazumasa (櫻井 一正) 1E1436 (S27)
1PT145 (S93)
Sakurai, Keisuke (櫻井 啓介) 1PT117 (S88)
2PT162 (S133)
2PT164 (S133)
3PT115 (S160)
Sakurai, Minoru (櫻井 実) 2F1400 (S47)
3G0912 (S67)
1PT162 (S96)
2PT125 (S126)
2PT185 (S137)
3PT133 (S163)
3PT160 (S168)
Sakurai, Takanobu (桜井 敬展) 3PT189 (S174)
Sakurai, Takashi (櫻井 孝司) 2D1424 (S44)
Sakurai, Takashi (櫻井 貴志) **1PT234 (S108)**
Sakurai, Takashi (櫻井 隆) 2A1610 (S40)
Sakurai, Takeshi (櫻井 武) 2PT112 (S123)
Sakurai, Yasuyuki (櫻井 靖之) **2B1546 (S41)**
Sakurai, Yu (櫻井 佑) 3C0936 (S60)
Samejima, Masahiro (鮫島 正浩) 1PT236 (S108)
Sannomiya, Takumi (三宮 工) 1H1546 (S34)
Sano, Masaki (佐野 雅己) **1SF-01 (S6)**
Sano, Tadahisa (佐野 宰久) **2PT109 (S123)**
Sano, Takahiko (佐野 貴彦) **3PT158 (S168)**
Sano, Yuko (佐野 裕子) 3PT235 (S181)
Sarai, Akinori (皿井 明倫) 2PT106 (S122)
3PT108 (S158)
Saruyama, Yasuo (猿山 靖夫) 3PT150 (S166)
3PT151 (S167)
Sasahara, Kenji (笹原 健二) **2B1522 (S41)**
Sasai, Masaki (笹井 理生) **1SE-01 (S5)**
1G1522 (S32)
1PT166 (S97)
1PT167 (S97)
1PT217 (S105)
2PS010 (S111)
2PS017 (S112)
2PT213 (S141)
Sasai, Yoshiki (笹井 芳樹) 1PT219 (S105)
Sasaki, Akira (佐々木 章) **1H1400 (S33)**
1PT205 (S103)
Sasaki, Akira (佐々木 顕) 2PT211 (S140)
Sasaki, Kazuo (佐々木 一夫) 1A1424 (S19)
2H1522 (S52)
1PS028 (S78)
1PS029 (S79)
Sasaki, Takanori (佐々木 貴規) **3PT126 (S162)**
Sasaki, Yuji (佐々木 裕次) 2PT121 (S125)
3PS024 (S150)
Sasaki, Yuji C. (佐々木 裕次) 3B0924 (S58)
Sasamoto, Kouhei (笹本 浩平) **2C1546 (S43)**
Sasano, Kouhei (佐々野 耕平) 1PS013 (S76)
Sato, Akihiko (佐藤 秋彦) **1PS040 (S81)**
Sato, Chikara (佐藤 主税) **3E1022 (S64)**
3H0900 (S69)
1PT183 (S100)
Sato, Daisuke (佐藤 大輔) **1PT142 (S93)**
Sato, Francielle (佐藤 フランシエーレ) 2PT169 (S134)
Sato, Fuminori (佐藤 文憲) 2PT116 (S124)
Sato, Hiroyuki (佐藤 博之) 2F1400 (S47)
Sato, Kaori (佐藤 香) **1PS017 (S77)**
Sato, Katsuya (佐藤 克也) 2PS048 (S118)
Sato, Keiko (佐藤 啓子) **2SE-05 (S13)**
2PS026 (S114)
Sato, Koji (佐藤 幸治) 2G1412 (S49)

Sato, Masaaki (佐藤 政秋) 2SI-04 (S17)
3PS013 (S148)
Sato, Masaaki (佐藤 正明) 3H1022 (S70)
2PS036 (S116)
Sato, Masayuki J. (佐藤 雅之) 2PS051 (S119)
Sato, Nozomi (佐藤 希美) 3I1058 (S73)
Sato, Takaki (佐藤 孝樹) **3PS038 (S152)**
Sato, Takato (佐藤 昂人) 1PS020 (S77)
1PT002 (S83)
Sato, Tokushi (佐藤 篤志) 3PS024 (S150)
Sato, Yusuke (佐藤 佑介) **1PT227 (S107)**
Satoh, Ayumi (佐藤 歩美) 2PS039 (S116)
Satoh, Tadashi (佐藤 匡史) 1B1436 (S21)
Satoshi, Fujii (藤井 聡) 2PT102 (S121)
Satoshi, Komori (小森 慧) **2PT102 (S121)**
Satou, Osamu (佐藤 治) 2PS053 (S119)
Sawabu, Yusuke (澤武 裕輔) **2C1448 (S42)**
Sawada, Kengo (澤田 賢吾) 2PT002 (S119)
2PT003 (S120)
2PT004 (S120)
2PT009 (S121)
2PT202 (S139)
Sawada, Shin-ichi (澤田 晋一) 3PT125 (S162)
Sawada, Yasuhiro (澤田 泰宏) 3H1046 (S71)
Sawada, Yasuyuki (澤田 康之) **3PT132 (S163)**
Sawai, Satoshi (澤井 哲) 1SF-04 (S6)
3H0936 (S70)
2PS045 (S118)
2PT239 (S145)
3PT171 (S170)
Sawaki, Hiroyuki (澤木 浩之) 3PS036 (S152)
Sawano, Yoriko (澤野 頼子) 2PT114 (S124)
Segawa, Hiroki (瀬川 尋貴) 2SH-03 (S16)
Seino, Akihiko (清野 晶彦) **1PS028 (S78)**
Seki, Kazuha (関 一葉) 2PT161 (S133)
Seki, Yasutaka (関 安孝) 1PT009 (S84)
1PT179 (S99)
Sekiguchi, Hiroshi (関口 博史) 3B0924 (S58)
2PT121 (S125)
Sekiguchi, Junichi (関口 順一) 1PT106 (S86)
Sekiguchi, Tetsushi (関口 哲志) 1PT234 (S108)
Sekiguchi, Yuki (関口 優希) 2D1522 (S45)
Sekiguichi, Hiroshi (関口 博史) 3PS024 (S150)
Sekijima, Masakazu (関嶋 政和) 1PT189 (S101)
Sekimura Miho (関村 美穂) 1PT206 (S103)
Sekine, Rui (関根 瑠威) 1PT234 (S108)
Senda, Miki (千田 美紀) 3E1022 (S64)
Senda, Toshiya (千田 俊哉) 3E1022 (S64)
Seno, Keiji (妹尾 圭司) **2PT180 (S136)**
Seo, Daisuke (瀬尾 悌介) **2PT112 (S123)**
Seo, Hideo (瀬尾 英雄) 1PS043 (S81)
1PS044 (S81)
2PS038 (S116)
Serizawa, Takahiro (芹澤 隆博) 2H1510 (S52)
Setou, Mitsutoshi (瀬藤 光利) **2SH-04 (S16)**
3A0912 (S56)
3PS028 (S150)
Sezutsu, Hideki (瀬筒 秀樹) 2PT206 (S140)
Shaevitz, Joshua W. (Shaevitz Joshua W.)
2SE-06 (S13)
Shaji, Divya (Shaji Divya) **1I1436 (S35)**
Shen, Jian-Ren (沈 建仁) 3D0948 (S62)
3D1022 (S63)
Shen, Nan (沈 楠) **1PT186 (S100)**
Sherwood, Mark W. (SHERWOOD Mark W.)
3PT206 (S175)
Shiba, Rumi (芝 るみ) **1PT124 (S89)**
Shibafuji, Yusuke (柴藤 佑介) 1F1558 (S30)
Shibata, Akihiro (柴田 明裕) **1PT209 (S103)**
Shibata, Akihiro C. E. (柴田 明裕) 3PT172 (S170)
Shibata, Keitaro (柴田 桂太朗) 2A1448 (S38)
2A1510 (S39)
Shibata, Mikihiro (SHIBATA MIKIHIRO) 3F1058 (S67)
Shibata, Mikihiro (柴田 幹大) 3PS016 (S148)
Shibata, Tatsuo (柴田 達夫) **2SF-04 (S14)**
1D1424 (S25)
3H0948 (S70)
2PT225 (S143)
2PT226 (S143)
Shibata, Yutaka (柴田 穣) **3D0948 (S62)**
Shibayama, Naoya (柴山 修哉) **3I0912 (S71)**
Shichida, Yoshinori (七田 芳則) 1F1424 (S29)
1F1436 (S29)
3B0936 (S58)
3F1022 (S66)
2PT190 (S138)
1YS1015 (S138)
Shidara, Hisashi (設樂 久志) **3PT204 (S175)**
Shigeri, Yasushi (茂里 康) 3G0900 (S67)
Shigeta, Yasutami (繁田 泰民) 3PT149 (S166)
Shiina, Masaaki (椎名 政昭) 3PT010 (S157)
Shima, Tomohiro (島 知弘) 2A1522 (S39)
Shimabukuro, Katsuya (島袋 勝弥) **2PS020 (S113)**
1YS0945 (S113)
Shimad, Mayu (島田 麻由) **2F1424 (S48)**
Shimada, Hideo (島田 秀夫) 3I1046 (S73)
2PT156 (S131)
2PT162 (S133)
2PT164 (S133)
3PT129 (S162)
Shimada, Masami (島田 真実) 2PT203 (S139)
Shimada, Masato (島田 万里) **2H1534 (S53)**
Shimada, Mayu (島田 麻由) 2PT173 (S135)
Shimada, Nao (島田 奈央) 3PT171 (S170)
Shimamoto, Yuta (島本 勇太) **2SC-01 (S11)**
Shimamura, Teppei (島村 徹平) 2SD-04 (S12)
Shimazaki, Megumi (嶋崎 恵) 3PT159 (S168)
Shimazaki, Ryo (島崎 亮) 1PT235 (S108)
Shimbo, Yudai (新保 雄大) 1PT009 (S84)
Shimizu, Hirofumi (清水 啓史) **2SH-01 (S16)**
2G1610 (S51)
Shimizu, Kana (清水 佳奈) 2PT005 (S120)
Shimizu, Kentaro (清水 謙多郎) 2PT006 (S120)
2PT010 (S121)
2PT101 (S121)
2PT133 (S127)
2PT151 (S131)
Shimizu, Miho (清水 美穂) 1SB-04 (S2)
1SB-05 (S2)
1SB-06 (S2)
Shimizu, Nobutaka (清水 伸隆) **2PT123 (S125)**
Shimizu, Norihiro (清水 則宏) **1PS008 (S75)**
Shimizu, Youské (清水 洋輔) **3PS009 (S147)**
Shimobayashi, Shunsuke (下林 俊典) **3C1110 (S61)**
Shimokata, Kunitoshi (下方 国稔) 3PT129 (S162)
Shimokawa, Tomoya (下川 智也) **2PT233 (S144)**
Shimomura, Takushi (下村 拓史) 3B0900 (S57)
Shimono, Kazumi (下野 和実) 2PT176 (S135)
Shimosato, Taku (下里 卓) 2B1400 (S40)
Shimozawa, Masahiro (下沢 将啓) **3PT181 (S172)**
Shimozawa, Togo (下澤 東吾) 2H1448 (S52)
Shimura, Nanako (志村 七子) 1PT202 (S102)
3PS031 (S151)
Shindo, Yuki (新土 優樹) **2PS044 (S117)**
Shinjio, Masaji (新庄 正路) **1PT115 (S88)**
Shinjo, Masaji (新庄 正路) 1PT157 (S95)
Shinoda, Keiko (篠田 恵子) **1PT173 (S98)**
Shinoda, Wataru (篠田 渉) 2G1400 (S49)
Shinohara, Kaoru (Shinohara Kaoru) 1PT114 (S87)
Shinohara, Kyosuke (篠原 恭介) 1SF-02 (S6)
Shinohara, Satoko (篠原 聡子) 3H1034 (S71)
Shinohara, Yasuo (篠原 康雄) **3PT119 (S160)**
Shinozaki, Daisuke (篠崎 大将) **1PT005 (S84)**
Shinozaki, Kozue (篠崎 梢) 2PT203 (S139)
Shintani, Seine (新谷 正嶺) 2H1510 (S52)
2H1546 (S53)
Shinyashiki, Kengo (新屋敷 健悟) 2PT109 (S123)
Shinzawa-Itoh, Kyoko (伊藤・新澤 恭子) 2PT157 (S132)
Shinzawa-Itoh, Kyoko (新澤-伊藤 恭子) 3I1034 (S72)
Shinzawa-Itoh, Kyoko (新澤伊藤 恭子) 3I1022 (S72)
Shionyu, Masafumi (塩生 真史) **2PT127 (S126)**
Shirai, Natsuki (白井 菜月) 2SB-06 (S10)
Shirai, Nobu C. (白井 伸宙) **1B1534 (S22)**
Shirai, Tadao (白井 忠雄) 1H1546 (S34)
Shiraishi, Arata (白石 新) 3PS050 (S155)
Shiraishi, Kenji (白石 賢二) 3PT222 (S178)
Shirakawa, Masahiro (白川 昌宏) 2SB-02 (S10)
3PS042 (S153)
Shiraki, Kentaro (白木 賢太郎) 2H1534 (S53)
1PT005 (S84)
Shirakihara, Yasuo (白木原 康雄) **1PS021 (S77)**
Shirasaki, Yoshitaka (白崎 善隆) 1PT202 (S102)
3PS031 (S151)
Shiro, Yoshitsugu (城 城宜嗣) 2PT160 (S132)
Shiro, Yoshitsugu (城 宜嗣) 3I1010 (S72)
3I1058 (S73)
2PT155 (S131)
2PT156 (S131)
Shiro, Yoshitugu (城 宜嗣) 2PT157 (S132)
Shiroguchi, Katsuyuki (城口 克之) 3A1022 (S57)
Shiroi, Tetsuya (城井 哲也) **3PT187 (S173)**
Shirota, Matsuyuki (城田 松之) **3E1046 (S65)**
3PT131 (S163)
Shohda, Koh-ichiroh (庄田 耕一郎) **3G1046 (S69)**
Shoji, Mitsuo (庄司 光男) **3PT222 (S178)**
Shoji, Shuichi (庄子 習一) 1PT234 (S108)
Shoji, Toru (庄司 亨) **3PS023 (S149)**
Shomura, Yasuhito (庄村 康人) **3B0912 (S57)**
Shouji, Shuichi (庄子 習一) 3PS031 (S151)
Siato, Hiroaki (齋藤 大明) 1PT001 (S83)
Simozawa, Togo (下澤 東吾) 1PS009 (S75)
Sircar, R. (Sircar Ria) 2SA-02 (S9)
Sneppen, Kim (Sneppen Kim) 2C1424 (S42)
So, Masatomo (宗 正智) 1E1436 (S27)
Soda, Kunitsugu (曽田 邦嗣) **1PT009 (S84)**
1PT179 (S99)
Sodeyama, Fumiaki (袖山 文彰) 1PS011 (S75)
Sodeyama, Kohei (袖山 浩平) **1PT160 (S96)**
Soga, Haruka (曽我 遥) **1C1534 (S24)**
Soga, Naoki (曽我 直樹) 3A1046 (S57)
1PS027 (S78)
Sogo, Takao (十河 孝夫) 2PT207 (S140)
Sohma, Yoshiro (相馬 義郎) 2G1534 (S51)
3PT133 (S163)
Sohya, Shihori (惣谷 志保里) 1C1412 (S23)
Sokabe, Masahiro (曽我部 正博) 2B1448 (S40)
1PT203 (S102)
2PS034 (S115)
3PT132 (S163)
Somei, Yusaku (染井 悠作) 3PS048 (S154)
Somiya, Takayasu (宗宮 孝安) 2H1412 (S52)
Song, Jianxing (Song Jianxing) 1PT115 (S88)
1PT157 (S95)
Sonoda, Satoru (園田 悟) 3PT201 (S174)
Sonoyama, Masashi (園山 正史) 3PT123 (S161)
3PT128 (S162)
Sowa, Yoshiyuki (Sowa Yoshiyuki) 1A1534 (S20)
Sowa, Yoshiyuki (曽和 義幸) 1A1558 (S20)
2PS001 (S110)
2PS004 (S110)
3PS032 (S151)
3PT180 (S172)
Sowa, Yosiyuki (曽和 義幸) 3PT186 (S173)
Stasevich, Timothy J. (スタセビッチ ティモシー)
2SG-01 (S15)
Stewart, Murray (Stewart Murray) 2PS020 (S113)
1YS0945 (S113)
Sudo, Yuki (須藤 雄気) 1F1558 (S30)
Suga, Hiroaki (菅 裕明) 1C1436 (S23)
Suga, Mitsuo (須賀 三雄) 3E1022 (S64)
Sugase, Kenji (菅瀬 謙治) 3C1034 (S61)
1PT112 (S87)
Sugase, Kenjji (菅瀬 謙治) 2E1510 (S46)
Sugawa, Mitsuhiro (須河 光弘) **1PS025 (S78)**
Sugawara, Hideaki (菅原 英明) 3PT158 (S168)
Sugawara, Ko (菅原 皓) **3PS040 (S153)**
Sugawara, Tadashi (菅原 正) 3G1046 (S69)
3PT142 (S165)
Sugawara, Takeshi (菅原 武志) **1SD-04 (S4)**
Sugihara, Fuminori (杉原 文徳) 3PS042 (S153)
3PS043 (S153)
Sugihara, Minoru (杉原 稔) 1SH-06 (S8)
Sugiki, Toshihiko (杉木 俊彦) 3PT002 (S155)
Sugimori, Kimikazu (杉森 公一) 2PT131 (S127)
Sugimoto, Hiroshi (杉本 宏) 3I1010 (S72)
3I1058 (S73)
Sugimoto, Ikuyo (杉本 育代) 1PT211 (S104)
Sugimoto, Manabu (杉本 学) 1G1448 (S31)
2D1436 (S44)
3H1010 (S70)
Sugimoto, Yasunobu (杉本 泰伸) 3H1034 (S71)
Sugimura, Kaoru (杉村 薫) **1SI-06 (S9)**
1D1436 (S25)
Sugishima, Masakazu (杉島 正一) **3I0936 (S72)**
Sugita, Masatake (杉田 昌岳) **3E1034 (S65)**
1PT127 (S90)
Sugita, Yuji (杉田 有治) 3B1022 (S58)
3E1110 (S65)
1PT201 (S102)
1YS1100 (S102)
1PT212 (S104)
2PT130 (S127)
2PT139 (S128)
3PT157 (S168)
Sugiura, Haruka (杉浦 晴香) 2PT238 (S145)
Sugiura, Kotomi (杉浦 琴美) 3PT206 (S175)
Sugiura, Miwa (杉浦 美羽) 3D1034 (S63)
Sugiura, Shinji (杉浦 慎治) 3PS044 (S153)
3PS051 (S155)
Sugiura, Wataru (杉浦 亙) 1PT102 (S85)
3PT003 (S155)
Sugiyama, Hiroshi (杉山 弘) **2SI-06 (S18)**
1PS042 (S81)
3PT111 (S159)
Sugiyama, Shigeru (杉山 成) 1PT116 (S88)
2PT116 (S124)
Sugiyama, Sho (杉山 将) **2PT161 (S133)**
Sumi, Tomonari (墨 智成) **2I1412 (S54)**
Sumikama, Takashi (炭竈 享司) 2G1558 (S51)
3PT165 (S169)
Sumikoshi, Kazuya (角越 和也) 2PT010 (S121)
Sumino, Ayumi (角野 歩) **2G1558 (S51)**
Sumino, Yutaka (住野 豊) 2SC-02 (S11)
Sumita, Kazumasa (住田 一真) **1PT121 (S89)**
Sumitomo, Koji (住友 弘二) **3PT148 (S166)**
Sunada, Kai (砂田 海) 1PS006 (S74)
Sunaga, Yasuhiro (須永 泰弘) 2SD-03 (S12)
Sunami, Takeshi (角南 武志) **2PT205 (S139)**
Sunami, Tomoko (角南 智子) **1B1522 (S22)**

Sunato, Ayumi (砂戸 歩美) 1PT142 (S93)
Sutoh, Kazuo (須藤 和夫) 3A1022 (S57)
Suwa, Makiko (諏訪 牧子) **1SH-06 (S8)**
Suyama, Akira (陶山 明) 3C0912 (S60)
3G1046 (S69)
3PT110 (S159)
Suyong, Re (李 秀栄) 1PT212 (S104)
Suzki, Ikuro (鈴木 郁朗) 3PT209 (S176)
Suzuki Ryo (鈴木 亮) 1PT206 (S103)
Suzuki, Akihiro (鈴木 明大) 2D1522 (S45)
Suzuki, Akiyoshi (鈴木 章義) 3PT221 (S178)
Suzuki, Atsuo (鈴木 淳巨) 1PT102 (S85)
Suzuki, Haruo (鈴木 春男) 1PT175 (S98)
Suzuki, Hiroaki (鈴木 宏明) 2PT205 (S139)
Suzuki, Hirofumi (鈴木 博文) **1PT119 (S88)**
Suzuki, Hiroki (鈴木 博己) **2G1522 (S50)**
Suzuki, Hiromi (鈴木 博実) **1PT109 (S87)**
Suzuki, Ikuro (鈴木 郁郎) 1PT220 (S105)
1PT221 (S106)
Suzuki, Ikurou (鈴木 郁郎) 3PS019 (S149)
Suzuki, Kazuo (鈴木 和夫) **3PT202 (S175)**
Suzuki, Kazutaka (鈴木 一隆) 3PT214 (S177)
Suzuki, Kazuya (鈴木 和也) **3H0912 (S69)**
Suzuki, Kenichi (鈴木 健一) 2PS041 (S117)
Suzuki, Kenichi G. N. (鈴木 健一) **1G1412 (S31)**
Suzuki, Koji (鈴木 康二) 1PT102 (S85)
Suzuki, Madoka (鈴木 団) 2H1510 (S52)
Suzuki, Makoto (鈴木 誠) 1E1558 (S28)
2H1424 (S52)
1PS002 (S74)
1PS003 (S74)
1PS004 (S74)
1PS005 (S74)
1PT010 (S85)
1PT182 (S100)
Suzuki, Miho (鈴木 美穂) 2PT204 (S139)
Suzuki, Nami (鈴木 南美) 3PT189 (S174)
Suzuki, Naoya (鈴木 直哉) 3PT208 (S176)
Suzuki, Nobutake (鈴木 信勇) 1PT202 (S102)
3PS031 (S151)
Suzuki, Shingo (鈴木 真吾) 2PT209 (S140)
Suzuki, Takao K. (鈴木 誉保) **2PT206 (S140)**
Suzuki, Toshiharu (鈴木 俊治) 3A1046 (S57)
1PS027 (S78)
1PS035 (S80)
Suzuki, Yo (鈴木 陽) **3C0900 (S59)**
Suzuki, Yu (鈴木 悠) **1PT111 (S87)**
Suzuki, Yuta (鈴木 雄太) 1PT152 (S94)
Tabata, Kazuhito (田端 和仁) 3F0900 (S65)
2PT207 (S140)
Tabata, Kazuhito V. (田端 和仁) 1PS033 (S79)
1YS1115 (S79)
Tabei, Yasuo (田部井 靖生) 2PT005 (S120)
Tachibana, Hideki (橘 秀樹) **2B1510 (S41)**
1PT114 (S87)
Tachikawa, Masashi (立川 正志) 1D1424 (S25)
1G1436 (S31)
2C1510 (S43)
Tachiwana, Hiroaki (立和名 博昭) 1PT190 (S101)
Tadakuma, Hisashi (多田隈 向史) 3PT111 (S159)
Tadakuma, Hisashi (多田隈 尚史) 3F0912 (S65)
1PS042 (S81)
Tadokoro, Satoshi (田所 哲) 3PT139 (S164)
3PT177 (S171)
Taga, Shun (多賀 瞬) **2PS030 (S115)**
Tagaki, Seiji (高木 清二) 2C1534 (S43)
Tagawa, Miho (田川 美穂) 3PT110 (S159)
Taguchi, Hideki (田口 英樹) 1B1510 (S21)
1PT151 (S94)
Taguchi, Takahisa (田口 隆久) 1D1546 (S26)
Tahara, Kentaro (田原 健太朗) **1PT236 (S108)**
Tahara, Kohei (田原 耕平) 3PT139 (S164)
Taiji, Makoto (泰地 真弘人) 1PT009 (S84)
1PT188 (S101)
2PT140 (S128)
Tajika, Ryosuke (田鹿 良介) **1PT122 (S89)**
Tajima, Hirotaka (田島 寛隆) **1PT233 (S108)**
3PT186 (S173)
3PT187 (S173)
Tajima, Kana (田島 可奈) 3F1046 (S67)
Tajima, Tomoki (田島 朋樹) 3PS038 (S152)
Tajiri, Yusuke (田尻 祐介) 2PT153 (S131)
Takaba, Kiyofumi (高場 圭章) **3E0912 (S63)**
Takada, Sayuri (高田 さゆり) **3I0948 (S72)**
Takada, Shoji (Takada Shoji) 1PT178 (S99)
Takada, Shoji (高田 彰二) **1SE-05 (S5)**
2E1558 (S47)
3C0948 (S60)
1PS037 (S80)
1PT172 (S98)
1PT181 (S100)
2PT143 (S129)
3PT006 (S156)
3PT007 (S156)
3PT009 (S157)
3PT011 (S157)
Takada, Syoji (高田 彰二) 1PT171 (S98)
Takagi, Daisuke (高木 大輔) **2PT228 (S143)**
Takagi, Hiroaki (高木 拓明) **2PS051 (S119)**
Takagi, Hiroyuki (高木 啓行) 1E1400 (S27)
3F1010 (S66)
Takagi, Jun (高木 潤) 3H0912 (S69)
Takagi, Kenji (高木 賢治) 2PT162 (S133)
2PT164 (S133)
Takagi, Masahiro (高木 昌宏) 3G1022 (S68)
3PT153 (S167)
1YS1045 (S167)
Takagi, Toshiyuki (高木 俊之) 3PT123 (S161)
3PT169 (S170)
Takahashi, Chisato (高橋 知里) **2G1510 (S50)**
Takahashi, Fumio (高橋 文雄) 2F1436 (S48)
2PT192 (S138)
Takahashi, Hironobu (高橋 宏暢) 1D1610 (S26)
Takahashi, Hiroshi (高橋 浩) 3PT123 (S161)
3PT146 (S166)
3PT147 (S166)
Takahashi, Hiroto (高橋 泰人) 2I1546 (S55)
2I1558 (S55)
2PS003 (S110)
Takahashi, Kei (髙橋 慧) **3PT171 (S170)**
Takahashi, Ken-ichi (高橋 健一) 2PT127 (S126)
Takahashi, Koichi (高橋 恒一) **2SD-02 (S12)**
2C1412 (S42)
2PS044 (S117)
2PT215 (S141)
3PT183 (S172)
Takahashi, Kouichi (高橋 恒一) 2SI-04 (S17)
Takahashi, Kyohei (高橋 恭平) 1PT190 (S101)
Takahashi, Layla (高橋 玲羅) 3F1034 (S67)
Takahashi, Masahiro (高橋 正裕) **1PT210 (S104)**
Takahashi, Ryosuke (高橋 亮輔) **3PS015 (S148)**
Takahashi, Satoshi (高橋 聡) 2E1412 (S45)
1PT144 (S93)
1PT152 (S94)
1PT222 (S106)
Takahashi, Seiya (高橋 聖弥) 2E1412 (S45)
Takahashi, Takuya (高橋 卓也) 1PT008 (S84)
Takahashi, Takuya (髙橋 卓也) **1PT007 (S84)**
Takahashi, Tomoki (高橋 智樹) 3G1058 (S69)
3PT173 (S171)
Takahashi, Yuka (高橋 優嘉) **2PS002 (S110)**
Takahashi, Yukio (高橋 幸生) 2D1522 (S45)
Takai, Eisuke (高井 英輔) 2H1534 (S53)
Takai, Shinji (高井 進二) 1PS038 (S80)
Takai, Tomoyo (高井 朋代) 2PT126 (S126)
Takaine, Masak (高稲 正勝) **2PS037 (S116)**
Takakuwa, Yuichi (高桑 雄一) 1PT107 (S86)
Takamatsu, Atsuko (高松 敦子) **1SF-02 (S6)**
Takanezawa, Sota (高根沢 聡太) **1D1412 (S25)**
Takano, Hiroshi (高野 宏) 2B1424 (S40)
Takano, Keiko (鷹野 景子) 3PT225 (S179)
Takano, Mitsunori (高野 光則) 1PS020 (S77)
1PS039 (S81)
1PT002 (S83)
1PT168 (S97)
1PT169 (S97)
Takano, Yu (鷹野 優) 3B1010 (S58)
3PT223 (S179)
Takaoka, Yousuke (高岡 洋輔) 2PT151 (S131)
Takaori, Akifumi (高折 晃史) 3C1034 (S61)
Takasu, Masako (高須 昌子) 1PT135 (S91)
2PT131 (S127)
Takata, Masaki (高田 昌樹) 3PT146 (S166)
Takayama, Yuki (高山 裕貴) 2D1522 (S45)
Takayanagi, Masayoshi (高柳 昌芳) 2E1436 (S46)
2PT165 (S133)
Takayuki, Uchihashi (内橋 貴之) 3PS004 (S146)
Takeda, Kazuki (竹田 一旗) 3E0912 (S63)
1PT123 (S89)
Takeda, Mahoshi (武田 真星) **1PT145 (S93)**
Takeda, Shigeki (武田 茂樹) 3F1034 (S67)
Takeda, Shuichi (武田 修一) 1B1546 (S22)
Takehana, Yasuhiro (竹花 康弘) 2PS040 (S117)
Takei, Hiroyuki (竹井 弘之) 3PS047 (S154)
Takei, Takaya (竹井 敬哉) 2PT149 (S130)
Takei, Yodai (武井 洋大) **3PS029 (S151)**
Takekawa, Norihiro (竹川 宜宏) **2I1534 (S55)**
Takemori, Shigeru (竹森 重) **1SB-09 (S3)**
2H1558 (S53)
Takemura, Kazuhiro (竹村 和浩) 1PS019 (S77)
1PT174 (S98)
2PT132 (S127)
Takenaka, Toshio (TAKENAKA Toshio) 1B1412 (S21)
Takenaka, Toshio (竹中 健朗) **1PT143 (S93)**
Takenaka, Yoshiko (武仲 能子) **1SB-02 (S2)**
3PT236 (S181)
Takeshita, Daijiro (竹下 大二郎) **3C1022 (S61)**
Taketani, Hiroshi (竹谷 寛司) 2SI-02 (S17)
Takeuchi, Hideo (竹内 英夫) 2E1424 (S46)
Takeuchi, Kazuki (竹内 一樹) 1C1610 (S25)
2PT129 (S126)
Takeuchi, Ken (竹内 健) **3E0936 (S64)**
2PT192 (S138)
Takeuchi, Shoji (竹内 昌治) 1I1546 (S36)
2G1412 (S49)
1PT225 (S106)
2PT207 (S140)
3PT143 (S165)
3PT163 (S169)
Takeuchi, Syoji (竹内 昌治) 3PT136 (S164)
Takigami, Satoshi (滝上 慧) 1D1534 (S26)
Takiguchi, Kingo (滝口 金吾) 3PT141 (S165)
Takiguchi, Yohko (滝口 陽子) **3PT141 (S165)**
Takinoue, Masahiro (瀧ノ上 正浩) 1PT224 (S106)
2PT238 (S145)
Takuo, Yasunaga (安永 卓生) 3E1010 (S64)
Tamada, Taro (玉田 太郎) 3E0912 (S63)
Tamada, Tarou (玉田 太郎) 2PT170 (S134)
Tamada, Yoshinori (玉田 嘉紀) **2SD-04 (S12)**
Tamai, Nobutake (玉井 伸岳) **3G0936 (S68)**
3G0948 (S68)
Tamaoki, Nobuyuki (玉置 信之) 3PT102 (S157)
Tamashiro, Tomonari (玉城 智成) **1C1522 (S24)**
Tamba, Yukihiro (丹波 之宏) 3PT148 (S166)
Tame, Jeremy R.H. (Jeremy R.H. Tame) 1PT101 (S85)
Tamogami, Jun (田母神 淳) **2PT176 (S135)**
Tamori, Masaki (田守 正樹) 2PS040 (S117)
Tamura, Atsuo (田村 厚夫) 1E1546 (S28)
1PT165 (S97)
3PT156 (S167)
Tamura, Hiroyuki (田村 浩之) **2PT185 (S137)**
Tamura, Koichi (田村 康一) **3B1034 (S59)**
Tamura, Takashi (田村 隆) 2PT109 (S123)
Tanabe, Yoichi (田邊 陽一) 1C1522 (S24)
Tanaka, Akihiro (田中 晃弘) **2PS023 (S114)**
Tanaka, Aya (田中 あや) 3PT148 (S166)
Tanaka, Gouhei (田中 剛平) **1SC-04 (S4)**
Tanaka, Hiroto (田中 裕人) **1PS050 (S82)**
Tanaka, Isao (田中 勲) 3F0948 (S66)
Tanaka, Kaori (田中 香織) 2PT149 (S130)
Tanaka, Keiji (田中 啓二) 1PT104 (S86)
Tanaka, Keiko (田中 啓子) **1PT213 (S104)**
Tanaka, Masatoshi (田中 正俊) 2PT186 (S137)
Tanaka, Motomasa (田中 元雅) 2PT113 (S123)
Tanaka, Ryosuke (田中 良昌) **1PT230 (S107)**
Tanaka, Saeko (田中 佐江子) 3G0936 (S68)
Tanaka, Tomohiro (田中 智大) **1PT171 (S98)**
Tanaka, Yoshikazu (田中 良和) **3F0948 (S66)**
Tanaka, Yoshimi (田中 良巳) 1SF-06 (S7)
Tanaka, Yuichi (田中 裕一) **3PT219 (S178)**
Tanaka, Yusuke (田中 裕介) **3B0924 (S58)**
Tanamoto, Ryo (棚元 亮) 3PT204 (S175)
Tang, Chao (Tang Chao) **2SA-04 (S9)**
Tani, Iori (谷 伊織) **2PT236 (S144)**
Tani, Yoshiaki (谷 芳明) 2A1522 (S39)
Tanida, Jun (谷田 純) 1I1534 (S36)
Tanigaki, Yasuyuki (谷垣 保幸) 1PT234 (S108)
Tanigawara, Mizue (谷川原 瑞恵) 3A1010 (S56)
Taniguchi, Daisuke (谷口 大相) 1SF-04 (S6)
Taniguchi, Mieko (谷口 美恵子) **1A1400 (S19)**
Taniguchi, Yuichi (谷口 雄一) **2SB-01 (S10)**
Tanikawa, Hiromi (谷川 ひろみ) 1PS021 (S77)
Tanio, Michikazu (谷生 道一) **2PT115 (S124)**
3PT178 (S172)
Tanizawa, Hideki (谷沢 英樹) 1A1400 (S19)
Tanokura, Masaru (田之倉 優) 2PT114 (S124)
Taoka, Azuma (田岡 東) 2SE-02 (S13)
Tardin, Catherine (Tardin Catherine) 3PT170 (S170)
Tashiro, Yuki (田代 裕己) 1PT159 (S96)
Tate, Shin-ichi (楯 真一) 2E1448 (S46)
Tateno, Masaru (舘野 賢) 1B1610 (S22)
1I1448 (S35)
2PT142 (S129)
2PT166 (S133)
2PT167 (S133)
Tateyama, Emi (館山 絵美) 2PT158 (S132)
Tatsumi, Hitoshi (辰巳 仁史) 2B1448 (S40)
2PS034 (S115)
Taylor, David (Taylor David) 3E0948 (S64)
Terada, Tohru (寺田 透) 1PT147 (S93)
2PT133 (S127)
2PT151 (S131)
Terada, Tomoki (寺田 智樹) 1PT167 (S97)
Terada, Tomoki P. (寺田 智樹) 1PT217 (S105)
2PS010 (S111)
2PT213 (S141)
Terahara, Naoya (寺原 直矢) **2PS006 (S111)**
Terakawa, Tsuyoshi (Terakawa Tsuyoshi)
1PT178 (S99)

Terakawa, Tsuyoshi (寺川 剛) **1SD-02 (S4)**
3PT006 (S156)
3PT007 (S156)
3PT011 (S157)
Terakita, Akihisa (寺北 明久) **1SH-05 (S7)**
2PT190 (S138)
1YS1015 (S138)
Terasawa, Hiroaki (寺沢 宏明) 2PT111 (S123)
Terashima, Hiroyuki (寺島 浩行) **3PT118 (S160)**
Terashita, Masahiro (寺下 匡大) 2D1448 (S44)
Terazima, Masahide (寺嶋 正秀) 2F1510 (S48)
2F1558 (S49)
2PT169 (S134)
2PT175 (S135)
Terazono, Hideyuki (寺薗 英之) **3PS046 (S154)**
3PS047 (S154)
Tereda, Tomoki P. (寺田 智樹) 2PS017 (S112)
Terui, Takako (照井 貴子) 1PS009 (S75)
Teshima, Tetsuhiko (手島 哲彦) **1I1546 (S36)**
Thomas, Neil (Thomas Neil) 1PS030 (S79)
Tirtom, Naciye Esma (Tirtom Naciye Esma)
3A0948 (S56)
Tiwari, Manisha (Tiwari Manisha) **3PT005 (S156)**
Toba, Shiori (鳥羽 栞) 2A1436 (S38)
Tochio, Hidehito (杤尾 豪人) 2SB-02 (S10)
Toda, Masashi (戸田 真志) 2PT234 (S144)
Toda, Masaya (戸田 雅也) 3PS013 (S148)
Toda, Mikito (戸田 幹人) 1PT170 (S98)
1PT189 (S101)
1PT191 (S101)
Toda, Osamu (戸田 収) 3PT124 (S161)
Togashi, Yuichi (冨樫 祐一) **1SA-01 (S1)**
Toichi, Keisuke (東一 圭祐) **2B1610 (S41)**
Tokimatsu, Toshiaki (時松 敏明) 2PT107 (S122)
Tokino, Takashi (時野 隆至) 2E1412 (S45)
Tokita, Masayuki (鴇田 昌之) 3PT135 (S164)
3PT152 (S167)
Tokuda, Naoko (徳田 直子) **1G1522 (S32)**
Tokuda, Naomi (徳田 尚美) 3PT178 (S172)
Tokuda, Syougo (徳田 昇悟) 1PS006 (S74)
Tokuhisa, Atsushi (徳久 淳師) **3PS026 (S150)**
Tokunaga, Fumio (徳永 史夫) 2PT190 (S138)
1YS1015 (S138)
Tokunaga, Makio (徳永 万喜洋) 2SG-02 (S15)
1H1424 (S33)
3PS033 (S151)
3PS034 (S152)
3PS035 (S152)
3PT104 (S158)
3PT181 (S172)
Tokuraku, Kiyotaka (徳楽 清孝) 2SE-03 (S13)
2PS035 (S116)
2PS039 (S116)
Tokutomi, Satoru (徳富 哲) 2F1510 (S48)
2PT169 (S134)
2PT188 (S138)
Tomaru, Hidetoshi (都丸 英敏) 2PT110 (S123)
Tomaru, Takenori (都丸 武宜) **2PT235 (S144)**
Tomii, Kentaro (富井 健太郎) **2PT005 (S120)**
Tominaga, Keisuke (富永 圭介) 1E1546 (S28)
3PT156 (S167)
Tominaga, Takashi (冨永 貴志) **1D1558 (S26)**
Tominaga, Yoko (冨永 洋子) 1D1558 (S26)
Tomisawa, Satoshi (冨澤 聡) 1C1400 (S23)
Tomishige, Michio (富重 道雄) 1A1436 (S19)
1A1448 (S19)
1PS036 (S80)
1PS037 (S80)
Tomita, Kozo (富田 耕造) 3C1022 (S61)
Tomita, Masahiro (冨田 昌弘) 3PT138 (S164)
Tomita, Masanori (冨田 雅典) **1G1510 (S31)**
Tomita, Masaru (冨田 勝) 2PS044 (S117)
Tomita, Noriko (冨田 典子) 3F0948 (S66)
Tomo, Tatsuya (鞆 達也) 3PT229 (S180)
Tomoko, Masaike (政池 知子) 1PS023 (S78)
Tomomi, Ishido (石堂 智美) 3PT101 (S157)
Tomonaga, Yuya (友永 雄也) 1F1558 (S30)
Tomonari, Sayuri (友成 さゆり) 1F1436 (S29)
Tonaka, Kenji (渡仲 健仁) 3PT202 (S175)
Tonooka, Taishi (外岡 大志) **2G1412 (S49)**
Torii, Jumpei (鳥井 淳平) **2E1610 (S47)**
Torimitsu, Keiichi (鳥光 慶一) 3PT148 (S166)
Torisawa, Takayuki (鳥澤 嵩征) 2A1448 (S38)
2A1510 (S39)
2A1546 (S39)
Tosha, Takehiko (當舎 武彦) **3I1058 (S73)**
Touyama, Kanako (當山 奏子) 1PS043 (S81)
1PS044 (S81)
Toyabe, Shoichi (鳥谷部 祥一) 2SI-02 (S17)
1PS023 (S78)
1PS032 (S79)
Toyabe, Shoici (鳥谷部 祥一) 1PS022 (S77)
Toyabe, Syoichi (鳥谷部 祥一) 1PS024 (S78)
Toyama, Yusuke (遠山 祐典) **1D1448 (S25)**
Toyoshima, Yoko (豊島 陽子) 1A1510 (S19)
2A1448 (S38)
2A1510 (S39)
2A1534 (S39)
2A1546 (S39)
Toyota, Taro (豊田 太郎) 3G1034 (S69)
3PT142 (S165)
3PT171 (S170)
Triller, Antoine (TRILLER Antoine) 3PT206 (S175)
Trusina, Ala (Trusina Ala) 2C1424 (S42)
Tsubasa, Nakagawa (中川 翼) 3PT192 (S174)
Tsuboi, Taka-aki (坪井 駿明) 3G1058 (S69)
3PT174 (S171)
Tsuchiya, Masahiro (土屋 雅博) **3PS014 (S148)**
Tsuda, Koji (津田 宏治) 2PT005 (S120)
Tsuji, Yotaro (辻 祐太郎) 3PT163 (S169)
Tsuji, Yusuke (辻 悠佑) 2PT191 (S138)
Tsujikawa, Hiroto (辻川 寛人) **2PT101 (S121)**
Tsujiuchi, Yutaka (辻内 裕) 2D1448 (S44)
2G1522 (S50)
3PT158 (S168)
Tsukada, Hideo (塚田 秀夫) 3PT214 (S177)
Tsukada, Yoshihiro (塚田 祥弘) 1PS008 (S75)
Tsukamoto, Hisao (塚本 寿夫) 2PT183 (S137)
2PT190 (S138)
1YS1015 (S138)
Tsukamoto, Takashi (塚本 卓) **2PT179 (S136)**
Tsukaoto, Hisao (塚本 寿夫) **3PT168 (S170)**
Tsukazaki, Tomoya (塚崎 智也) 1PT128 (S90)
1YS0930 (S90)
Tsukihara, Tomitake (月原 冨武) 2PT157 (S132)
3PT129 (S162)
Tsukiji, Yuuki (築地 祐樹) 2F1522 (S48)
Tsumoto, Kanta (凄元 幹太) **3PT138 (S164)**
Tsumoto, Kouhei (津本 浩平) 2E1510 (S46)
3F0912 (S65)
2PT151 (S131)
Tsuneshige, Antonio (常重 アントニオ) 2PT153 (S131)
Tukamoto, Seiichi (塚本 精一) 1PT142 (S93)
Tulum, Isil (Tulum Isil) **2PS027 (S114)**
Tunnacliffe, Alan (Tunnacliffe Alan) 1PT162 (S96)
Tuzi, Satoru (辻 暁) 3F1046 (S67)
2PT168 (S134)
3PT178 (S172)
Uchibori, Soyomi (内堀 そよみ) **2PS042 (S117)**
Uchida, Junya (内田 潤也) 3PS021 (S149)
Uchida, Kaoru (内田 薫) **2PS031 (S115)**
2PS033 (S115)
Uchida, Nariya (内田 就也) **1SF-03 (S6)**
Uchida, Waka (打田 和香) **3PT227 (S179)**
3PT230 (S180)
3PT232 (S180)
Uchida, Yumiko (内田 裕美子) 1PT105 (S86)
Uchihashi, Takayuki (UCHIHASHI TAKAYUKI)
3F1058 (S67)
Uchihashi, Takayuki (内橋 貴之) 2SB-03 (S10)
1H1510 (S34)
2G1534 (S51)
3PS016 (S148)
Uchikoga, Nobuyuki (内古閑 伸之) **2PT104 (S122)**
Uchiyama, Seiichi (内山 聖一) 3PS010 (S147)
1YS0915 (S147)
Uda, Shinsuke (宇田 新介) 2SF-03 (S14)
1PT214 (S104)
2PT219 (S142)
Udin, Bahrudin (Udin Bahrudin) 1PT104 (S86)
Ueda, Asami (植田 朝美) 1C1448 (S23)
Ueda, Hiroki (上田 泰己) **1SA-06 (S1)**
2C1522 (S43)
Ueda, Kazuyoshi (上田 一義) 3PT127 (S162)
Ueda, Keisuke (植田 啓介) 2H1412 (S52)
Ueda, Masahiro (上田 昌宏) 1G1558 (S32)
2PS051 (S119)
Ueda, Takuya (上田 卓也) 1B1510 (S21)
3F0912 (S65)
1PS042 (S81)
3PT111 (S159)
Ueda, Taro Q.P. (上田 太郎) 2PS039 (S116)
Ueda, Yusuke (植田 悠介) **1D1546 (S26)**
Uehara, Wataru (上原 航) **2PT163 (S133)**
Ueki, Shoji (植木 正二) 2H1412 (S52)
Uekusa, Yoshinori (植草 義徳) 1B1436 (S21)
Uemura, Tatsuya (植村 達也) 1PT164 (S97)
Ueno, Hiroshi (上野 博史) 2SI-02 (S17)
1PS022 (S77)
1PS023 (S78)
1PS024 (S78)
1PS032 (S79)
Ueno, Shingo (上野 真吾) **2PT147 (S130)**
Ueno, Takamasa (上野 貴将) 2E1510 (S46)
Ueno, Taro (上野 太郎) 3PS029 (S151)
Ueno, Yutaka (上野 豊) **1PT184 (S100)**
Uenoyama, Atsuko (Uenoyama Atsuko) 2PS027 (S114)
Ueta, Masami (上田 雅美) 3PT001 (S155)
Ujisawa, Tomoyo (宇治澤 知代) **3PT201 (S174)**
3PT210 (S176)
Umeda, Hiroaki (梅田 宏明) 3PT222 (S178)
Umeda, Yusuke (梅田 祐介) 2PT101 (S121)
Umeki, Nobuhisa (梅木 伸久) 2SE-03 (S13)
2PS018 (S113)
Umemura, Kazuo (梅村 和夫) **2PS047 (S118)**
3PT105 (S158)
Umemura, Taizo (梅村 太三) 1PT163 (S96)
Umemura, Tohru (梅村 徹) **3PT180 (S172)**
Umetsu, Mitsuo (梅津 光央) **1C1448 (S23)**
1C1510 (S24)
Umezawa, Koji (梅澤 公二) 1PS020 (S77)
1PT002 (S83)
1PT168 (S97)
1PT169 (S97)
Umezawa, Yuki (梅澤 祐貴) **2PT001 (S119)**
Unno, Masashi (海野 雅司) **2F1522 (S48)**
Unzai, Satoru (雲財 悟) 1PT101 (S85)
Urakubo, Hidetoshi (浦久保 秀俊) **3PT212 (S177)**
Urano, Ryo (浦野 諒) **3PT130 (S163)**
Urisu, Tsuneo (宇理須 恒雄) **1SH-03 (S7)**
Usukura, Jiro (臼倉 治郎) 1PT118 (S88)
Utida, Yumiko (内田 裕美子) 1PT121 (S89)
Utsumi, Ayaka (内海 彩香) **1PT232 (S108)**
Utsumi, Yui (内海 唯) 2A1510 (S39)
Uyeda, Taro (上田 太郎) 1PS001 (S74)
2PS018 (S113)
Uyeda, Taro Q.P. (上田 太郎) **2SE-03 (S13)**
Uzawa, Takanori (鵜澤 尊規) 2PT145 (S129)
Villaruz, Lara (Villaruz Lara) **3PT170 (S170)**
Wada, Akimori (和田 昭盛) 1F1558 (S30)
3F1046 (S67)
Wada, Akira (和田 明) 3PT001 (S155)
Wada, Hirofumi (和田 浩史) **2SC-04 (S11)**
2SE-05 (S13)
2PS026 (S114)
Wada, Naohisa (和田 直久) 2PT186 (S137)
Wada, Yuji (和田 侑士) 2E1448 (S46)
Wakabayashi, Chiaki (若林 千晃) 1PS035 (S80)
Wakabayashi, Ken-ichi (若林 憲一) 2PS050 (S118)
3PS007 (S147)
Wakabayashi, Kenichi (若林 憲一) 3PS006 (S146)
Wakabayashi, Masahiko (若林 正彦) 3PT211 (S176)
3PT216 (S177)
Wakabayashi, Masaki (若林 真樹) 2G1448 (S50)
2G1510 (S50)
3PT162 (S169)
Wakabayashi, Takeyuki (若林 健之) 1PS001 (S74)
Wakai, Nobuhiko (若井 信彦) **1PS019 (S77)**
Wakamatsu, Kaori (若松 馨) 3F1034 (S67)
Wakamoto, Yuichi (若本 祐一) **2SF-01 (S14)**
1D1400 (S25)
2C1610 (S43)
1PT215 (S105)
3PS045 (S154)
Wako, Hiroshi (輪湖 博) 3PT190 (S174)
Wang, Wei (Wang Wei) **1SE-02 (S5)**
1PT178 (S99)
2PT145 (S129)
Wang, Yangtian (王 楊天) **1E1558 (S28)**
Wang, Yaolai (Wang Yaolai) 1SE-02 (S5)
Wang, Zhuo (王 卓) **3E1010 (S64)**
Watabe, Masaki (渡部 匡己) **3PT183 (S172)**
Watanabe, Aya (渡辺 綾) **2PT120 (S125)**
Watanabe, Hajime (渡邉 肇) 1C1534 (S24)
Watanabe, Hikari (渡邊 ひかり) 3E0936 (S64)
Watanabe, Hiroki (渡辺 大輝) **3PS016 (S148)**
Watanabe, Keiichi (渡邊 啓一) 2PT122 (S125)
Watanabe, Kunihiko (渡部 邦彦) 3G0900 (S67)
Watanabe, Masakatsu (渡辺 正勝) 1H1610 (S35)
3D0924 (S62)
Watanabe, Nobuhisa (渡邊 信久) 1PT102 (S85)
1PT113 (S87)
Watanabe, Rikiya (渡邊 力也) 3A1010 (S56)
3F0900 (S65)
1PS033 (S79)
1YS1115 (S79)
3PT103 (S157)
Watanabe, Rikiya (渡邊 力也) 3A0936 (S56)
Watanabe, Satoru (渡部 暁) 1PT106 (S86)
Watanabe, Shingo (渡辺 真悟) **1F1412 (S29)**
Watanabe, Tomonobu (渡邊 朋信) 2PT118 (S124)
3PS037 (S152)
Watanabe, Toshiyuki (渡辺 敏行) 1SB-06 (S2)
Watanabe, Tsuyoshi (渡邊 剛) **3PT191 (S174)**
Watanabe, Yurika (渡辺 百合香) 2PT125 (S126)
Watanabe, Yuta (渡辺 裕多) 2A1448 (S38)
Watanabe-Nakayama, Takahiro (中山 隆宏)
2SI-02 (S17)
Wazawa, Tetsuichi (和沢 鉄一) 1E1558 (S28)

2H1424 (S52)
1PS002 (S74)
1PS003 (S74)
1PS004 (S74)
1PS005 (S74)
1PT182 (S100)
Wijaya, I Made Mahaputra (ウィジャヤ イ マディ マハプトラ)
2F1534 (S49)
Williamson, Michael P. (Williamson Michael P.)
1PT112 (S87)
Woody, Robert W. (Woody Robert) 1PT108 (S86)
Wright, Peter E. (Wright Peter E.) 1PT158 (S95)
Wu, Nan (呉 楠) **1C1412 (S23)**
Wulff, Michael (ウルフ ミカエル) 2SH-01 (S16)
Xu, Ming (Xu Ming) 1PT150 (S94)
Yagi, Hisashi (八木 寿梓) 1E1436 (S27)
Yagi, Maho (矢木 真穂) 1PT112 (S87)
Yagi, Masahiro (八木 正浩) 1PT140 (S92)
Yagi, Naoto (八木 直人) 2H1610 (S53)
2PT121 (S125)
3PS024 (S150)
Yagi, Takeshi (八木 健) **2SF-06 (S14)**
Yagi, Toshiki (八木 俊樹) **3H0924 (S70)**
3PS003 (S146)
Yajima, Hiroaki (矢島 孔明) **3H0900 (S69)**
Yajima, Junichiro (矢島 潤一郎) **1SI-03 (S8)**
1A1510 (S19)
2A1534 (S39)
1PS040 (S81)
Yamada, Akira (山田 章) **2PS040 (S117)**
Yamada, Daichi (山田 大智) **2F1546 (S49)**
Yamada, Kazuteru (山田 一輝) 1I1510 (S36)
Yamada, Kenji (山田 憲嗣) 1I1534 (S36)
Yamada, Kenta (山田 健太) 2PT187 (S137)
Yamada, Kosuke (山田 浩輔) 3PT120 (S161)
Yamada, Makiko (山田 麻紀子) 2G1510 (S50)
Yamada, Masafumi D. (山田 正文) 1PS038 (S80)
Yamada, Ryotaro (山田 遼太郎) **3PS051 (S155)**
Yamada, Tesshi (山田 哲司) 2PT117 (S124)
Yamada, Yoshiteru (山田 好輝) 1PT142 (S93)
Yamagata, Yuriko (山縣 ゆり子) 1PT129 (S90)
1YS1000 (S90)
Yamagata, Yutaka (山形 豊) 1I1610 (S37)
Yamagishi, Akihiko (山岸 明彦) 1PT135 (S91)
2PT203 (S139)
Yamagishi, Junya (山岸 純也) **2PT140 (S128)**
Yamagishi, Mai (山岸 舞) **1PT202 (S102)**
3PS031 (S151)
Yamagishi, Masahiko (山岸 雅彦) **1A1510 (S19)**
Yamaguchi, Akihito (山口 明人) 1PT117 (S88)
3PT115 (S160)
Yamaguchi, Chiaki (山口 千秋) 2PT191 (S138)
Yamaguchi, Hideaki (山口 秀明) 3C0924 (S60)
Yamaguchi, Hiroshi (山口 宏) 1PT104 (S86)
Yamaguchi, Keiichi (山口 圭一) **1PT139 (S92)**
1PT155 (S95)
Yamaguchi, Maki (山口 眞紀) 2H1558 (S53)
Yamaguchi, Mariko (山口 真理子) 2F1424 (S48)
1PT124 (S89)
1PT138 (S92)
1PT153 (S95)
2PT170 (S134)
2PT171 (S134)
2PT172 (S134)
2PT174 (S135)
Yamaguchi, Rui (山口 類) 2SD-04 (S12)
Yamaguchi, Shigeo (山口 繁生) 2PT170 (S134)
Yamaguchi, Shin (山口 真) **2A1534 (S39)**
1PS040 (S81)
Yamaguchi, Yoshiki (山口 芳樹) 1PT212 (S104)
Yamai, Toshihide (山井 俊英) **3F1034 (S67)**
Yamakawa, Akiko (山川 明来子) 3PS036 (S152)
Yamakawa, Hisanori (山川 壽伯) **3PT228 (S180)**
Yamakawa, Kentaro (山川 賢太郎) **1PT162 (S96)**
Yamamori, Yu (山守 優) **1PT174 (S98)**
Yamamoto, Akie (山本 晃衣) 2H1412 (S52)
Yamamoto, Eiji (山本 詠士) **1PT004 (S84)**
3PT155 (S167)
Yamamoto, Hiroki (山本 泰生) **2PS021 (S113)**
Yamamoto, Hirotsugu (山本 裕紹) 1I1534 (S36)
Yamamoto, Johtaro (山本 条太郎) **1G1546 (S32)**
Yamamoto, Junpei (山元 淳平) 2F1534 (S49)
2F1546 (S49)
Yamamoto, Kazuyuki (山本 和志) **2PS019 (S113)**
Yamamoto, Kentaro (山本 健太郎) **3PS032 (S151)**
Yamamoto, Kimiko (山元 季実子) **3PT184 (S173)**
3PT188 (S173)
Yamamoto, Kimiko (山本 希美子) **2SH-06 (S16)**
Yamamoto, Kyohei (山本 恭平) 1PS039 (S81)
Yamamoto, Masahide (山本 雅英) 1E1424 (S27)
Yamamoto, Masaki (山本 雅貴) 2D1522 (S45)
Yamamoto, Naoki (山本 直樹) **1E1546 (S28)**
3PT156 (S167)
Yamamoto, Shigeyuki (山本 茂幸) 3PT214 (S177)
Yamamoto, Syou (山本 匠) 1PT125 (S90)
Yamamoto, Takenori (山本 武範) 3PT119 (S160)
Yamamoto, Tsubasa (山本 翼) **1PT141 (S92)**
Yamamoto, Yohei (山本 陽平) 2PT121 (S125)
Yamamura, Masayuki (山村 雅幸) 1I1522 (S36)
Yamamura, Yasuhisa (山村 泰久) 2PT152 (S131)
Yamanaka, Akihiro (山中 章弘) **1SH-04 (S7)**
Yamane, Mitsunori (山根 光智) 1PS016 (S76)
Yamane, Tsutomu (山根 努) **2PT136 (S128)**
Yamano, Akihito (山野 昭人) 1PT110 (S87)
Yamanobe, Takanobu (山野辺 貴信) **2PT223 (S142)**
Yamanoha, Banri (山之端 万里) 2PS038 (S116)
Yamaoki, Yudai (山置 佑大) **3C0936 (S60)**
Yamasaki, Hideki (山崎 秀樹) **1PT126 (S90)**
Yamasaki, Seiji (山崎 聖司) 1PT117 (S88)
3PT115 (S160)
Yamasaki, Tatsuya (山崎 達哉) 2PS031 (S115)
Yamasaki, Tsuyoshi (山崎 剛) 2PS035 (S116)
Yamashita, Daichi (山下 大智) 3F0948 (S66)
Yamashita, Eiki (山下 栄樹) 2PT157 (S132)
Yamashita, Hayato (山下 隼人) **2G1534 (S51)**
Yamashita, Keitaro (山下 恵太郎) 3F0948 (S66)
Yamashita, Naoki (山下 直樹) 3F1034 (S67)
Yamashita, Risa (山下 理沙) **1PT185 (S100)**
Yamashita, Shoji (山下 昭二) 2E1610 (S47)
2PT122 (S125)
Yamashita, Takahiro (山下 高廣) 1F1424 (S29)
1F1436 (S29)
3F1022 (S66)
Yamashita, Takefumi (山下 雄史) **1B1558 (S22)**
Yamashita, Yutaka (山下 豊) 2D1424 (S44)
Yamato, Takahisa (倭 剛久) 1PT192 (S102)
Yamauchi, Hitomi (山口 瞳) **2PT111 (S123)**
Yamauchi, Seigo (山内 清語) 1PT144 (S93)
Yamauchi, Toyohiko (山内 豊彦) **2D1424 (S44)**
Yamazaki, Kaoru (山崎 薫) **1PT235 (S108)**
Yamazaki, Masahito (Yamazaki Masahito)
2G1424 (S50)
Yamazaki, Masahito (山崎 昌一) 3G1058 (S69)
3PT140 (S165)
3PT173 (S171)
3PT174 (S171)
Yamazaki, Naoshi (山崎 尚志) 3PT119 (S160)
Yamazaki, Toshimasa (山崎 俊正) 1PT111 (S87)
Yamazaki, Yoichi (山崎 洋一) 2F1424 (S48)
1PT124 (S89)
1PT153 (S95)
2PT170 (S134)
2PT171 (S134)
2PT172 (S134)
2PT173 (S135)
2PT174 (S135)
Yanagawa, Masataka (柳川 正隆) **3F1022 (S66)**
Yanagida, Toshio (柳田 敏雄) 1PS049 (S82)
1YS0900 (S82)
1PT006 (S84)
1PT210 (S104)
2PS011 (S111)
2PS028 (S114)
2PT118 (S124)
3PT167 (S169)
Yanagisawa, Haru-aki (柳澤 春明) 2A1412 (S38)
Yanagisawa, Miho (柳澤 実穂) **2G1436 (S50)**
3PT135 (S164)
3PT152 (S167)
Yanagisawa, Sachiko (柳澤 幸子) **3I0924 (S71)**
3I1010 (S72)
Yanagisawa, Yuki (柳沢 祐樹) **2PT186 (S137)**
Yanaka, Saeko (谷中 冴子) **2E1510 (S46)**
Yang, Wei (Yang Wei) 1PT129 (S90)
1YS1000 (S90)
Yang, Zhuohao (楊 倬皓) **3C1058 (S61)**
Yano, Akira (谷野 章) 3PS027 (S150)
Yano, Ken-ichi (矢野 憲一) **1G1424 (S31)**
Yano, Naomine (矢野 直峰) **2PT157 (S132)**
2PT160 (S132)
Yao, Haruhiko (八尾 晴彦) 3PT150 (S166)
3PT151 (S167)
Yao, Min (姚 閔) 3F0948 (S66)
Yashima, Kenta (八島 健太) **2PT211 (S140)**
Yasuda, Kenji (安田 賢二) 2D1510 (S44)
3PS020 (S149)
3PS022 (S149)
3PS023 (S149)
3PS046 (S154)
3PS047 (S154)
3PS049 (S154)
Yasuda, Ryohei (安田 涼平) 1PT207 (S103)
3PS016 (S148)
Yasuda, Satoshi (安田 哲) **1PS038 (S80)**
Yasuda, Satoshi (安田 賢司) **1PT154 (S95)**
3PT116 (S160)
Yasui, Masato (安井 正人) 2G1534 (S51)
1PT004 (S84)
3PT155 (S167)
Yasui, Shin-ichiro (安居 慎一郎) 1PS005 (S74)
Yasui, So (安井 聡) 2PT229 (S143)
Yasunaga, Takuo (安永 卓生) 2A1400 (S38)
2A1412 (S38)
2A1424 (S38)
2A1436 (S38)
2D1412 (S44)
1PT180 (S99)
1PT185 (S100)
1PT186 (S100)
1PT223 (S106)
Yasunaga, Yakuo (安永 卓生) 1PS008 (S75)
Yasuoka, Jun-ichi (安岡 潤一) 3PT125 (S162)
Yasuoka, Kenji (泰岡 顕治) 1PT004 (S84)
3PT155 (S167)
Yawo, Hiromu (八尾 寛) 1PS010 (S75)
3PT218 (S178)
Yawo, Hiromu (八尾 寛) 2PT183 (S137)
Yazawa, Koji (矢澤 宏次) 3E0924 (S64)
Yazawa, Yoichi (矢沢 洋一) **1PS007 (S75)**
Yildiz, Ahmet (YILDIZ Ahmet) **2SA-01 (S9)**
Yin, Lijie (Yin Lijie) 3PT189 (S174)
Yizhar, Ofer (Yizhar Ofer) 1PT128 (S90)
1YS0930 (S90)
Yohda, Masafumi (養王田 正文) 1PT123 (S89)
2PT121 (S125)
Yoichi Yamazaki, Yoichi Yamazaki (山崎 洋一)
1PT138 (S92)
Yokogawa, Daisuke (横川 大輔) 3PT178 (S172)
Yokojima, Satoshi (横島 智) 3PT227 (S179)
3PT230 (S180)
Yokomaku, Yoshiyuki (横幕 能行) 1PT102 (S85)
Yokomizo, Shunnya (横溝 駿矢) 2H1558 (S53)
Yokota, Hideo (横田 秀夫) **2SD-03 (S12)**
Yokota, Hiroaki (横田 浩章) **3C1046 (S61)**
Yokota, Yuichiro (横田 裕一郎) 1G1510 (S31)
Yokoyama, Hirokazu (横山 弘和) **2G1448 (S50)**
Yokoyama, Keiko (横山 慶子) 1D1522 (S26)
Yokoyama, Ken (横山 謙) 3A0948 (S56)
Yokoyama, Yasunori (横山 泰範) 2PT011 (S121)
2PT108 (S122)
3PT120 (S161)
Yomo, Tetsuya (四方 哲也) 1C1534 (S24)
1G1534 (S32)
2PT205 (S139)
2PT209 (S140)
Yoneda, Shigetaka (米田 茂隆) 1PT175 (S98)
Yoneda, Takuro (米田 拓郎) **1A1610 (S20)**
Yonekita, Taro (米北 太郎) 1C1400 (S23)
Yonekura, Koji (米倉 功治) 2D1522 (S45)
Yonetani, Takashi (米谷 隆) 2PT153 (S131)
Yonetani, Yoshiteru (米谷 佳晃) **1SD-03 (S4)**
Yonezawa, Kento (米澤 健人) **2PT170 (S134)**
2PT171 (S134)
Yoon, Dong H. (Yoon Dong H.) 1PT234 (S108)
Yoshida, Aya (吉田 文) **2E1400 (S45)**
Yoshida, Hideji (吉田 秀司) 3PT001 (S155)
Yoshida, Hikaru (吉田 光) **1PS024 (S78)**
Yoshida, Hironori (吉田 浩典) **3PT149 (S166)**
Yoshida, Hiroshi (吉田 寛) **1D1510 (S26)**
Yoshida, Kaoru (吉田 薫) 3PS007 (S147)
Yoshida, Kazunari (吉田 一也) **3PT154 (S167)**
Yoshida, Keito (吉田 桂人) 2PT170 (S134)
2PT171 (S134)
Yoshida, Kotaro (吉田 広太郎) 3PT216 (S177)
Yoshida, Manabu (吉田 学) 3PS007 (S147)
Yoshida, Masasuke (吉田 賢右) 1E1412 (S27)
3A1022 (S57)
3A1046 (S57)
1PS026 (S78)
1PS027 (S78)
1PS031 (S79)
1PS035 (S80)
2PS020 (S113)
1YS0945 (S113)
Yoshida, Muneki (吉田 宗生) **3PS037 (S152)**
Yoshida, Ryo (吉田 亮) **2SD-05 (S12)**
Yoshida, Taka-aki (吉田 貴亮) **3PT135 (S164)**
Yoshida, Yumi (吉田 裕美) **3PS021 (S149)**
3PT159 (S168)
Yoshidome, Takashi (吉留 崇) 1PS034 (S80)
Yoshihara, Shizue (吉原 静恵) 2PT188 (S138)
Yoshikawa, Kenichi (吉川 研一) 2C1534 (S43)
2G1436 (S50)
3C0924 (S60)
3C1110 (S61)
3PT101 (S157)
Yoshikawa, Shinya (吉川 信也) 3I1022 (S72)
3I1034 (S72)
2PT157 (S132)

3PT129 (S162)
Yoshimatsu, Daiki (吉松 大輝) **3PT175 (S171)**
Yoshimitsu, Ryosuke (吉満 亮介) **3PS044 (S153)**
Yoshimoto, Jun-ichi (吉本 順一) 2PS009 (S111)
Yoshimura, Hideyuki (吉村 英恭) 1PT237 (S109)
1PT238 (S109)
3PS025 (S150)
Yoshimura, Takeo (吉村 武朗) 2PT149 (S130)
3PS050 (S155)
Yoshimura, Yuichi (吉村 優一) **1E1436 (S27)**
Yoshinaga, Natsuhiko (義永 那津人) **1SF-05 (S6)**
Yoshino, Masaru (吉野 賢) **3PT123 (S161)**
Yoshioka, Yoshichika (吉岡 芳親) 3PS042 (S153)
Yoshizawa, Keiko (慶澤 景子) 2PT118 (S124)
Yoshizawa, Susumu (吉澤 晋) 2F1412 (S47)
2PT181 (S136)
You, Huijuan (游 慧娟) **3PT103 (S157)**
Yu, Isseki (優 乙石) **1E1510 (S28)**
Yugi, Katsuyuki (柚木 克之) 1PT214 (S104)
Yuki, Taichi (由木 太一) 3PT227 (S179)
3PT232 (S180)
Yura, Kei (由良 敬) 1I1412 (S35)
Zaccai, Giuseppe (Zaccai Giuseppe) 2H1400 (S51)
Zhang, Feng (Zhang Feng) 1PT128 (S90)
1YS0930 (S90)
Zhang, Jin (張 進) 2PT184 (S137)
Zhang, Peijuan (Zhang Peijuan) 1PS018 (S77)
2PT240 (S145)
Zhang, You (張 宇) 2F1436 (S48)
Zhang, Yu (張 宇) 2F1534 (S49)
2F1546 (S49)
Zhao, Chenchao (Zhao Chenchao) 2H1412 (S52)
Zhao, Ye (Zhao Ye) 1PT129 (S90)
1YS1000 (S90)
Zhu, Shiwei (朱 世偉) **1A1546 (S20)**
Zikihara, Kazunori (直原 一徳) **2PT188 (S138)**
Zinchenko, Anatoly (ジンチェンコ アナトーリ)
3C0924 (S60)

GE Healthcare
Life Sciences

日本生物物理学会第50回年会

GEヘルスケア・ジャパン株式会社 ランチョンセミナー

9月22日(土)　12:00〜12:50　A会場(理学南館「平田・坂田ホール」)

「熱」がもたらす生体分子相互作用の新しい理解

〜生体分子における熱分析の現状と今後〜

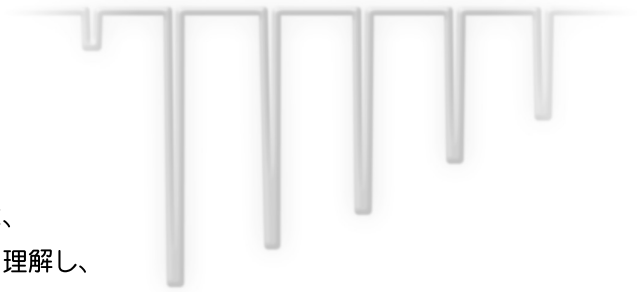

東京大学 医科学研究所

教授 津本 浩平 先生

生体分子の相互作用を物理化学的に解釈することは、
タンパク質や核酸などの物質から構成される生命を理解し、
応用するうえでますます重要になってきています。
本セミナーでは、物理化学的指標の中でも基本となる「熱」に注目し、生体分子相互作用解析において、熱がどのように測定、理解、応用されているのか、そして創薬への適用を実例を通してご紹介します。
熱分析を用いて生命現象を物理化学的に読み解くおもしろさと今後の展望をお伝えします。

本ランチョンセミナーでは、東京大学 津本先生のご講演に加え、ITCを使用した医薬品候補化合物のエンタルピーランキング法 (competitive SITE法) などのアプリケーションをご紹介いたします。ぜひご参加ください。

演者紹介

津本先生は生体高分子、特にタンパク質の分子認識機構や凝集メカニズムなどを物理化学的に読み解き、それを基盤に新たな分子設計、創薬の分野に適用されています。

GE imagination at work

GEヘルスケア・ジャパン株式会社
ライフサイエンス統括本部
〒169-0073
東京都新宿区百人町 3-25-1 サンケンビルヂング
お問合せ：バイオダイレクトライン
TEL : 03-5331-9336　FAX : 03-5331-9370
e-mail : Tech-JP@ge.com
Home Page　**http://www.gelifesciences.co.jp**

日本生物物理学会第50回年会

浜松ホトニクス株式会社
ランチョンセミナー

◇ 日時：2012年9月22日（土）12:00 ～ 12:50

◇ 会場：B会場（多元数理科学棟「講義室 509」）

演題 1

CMOSカメラによるライブイメージング ～1分子から個体まで～

岡田 康志 先生

（ 独立行政法人理化学研究所　生命システム研究センター　細胞極性統御研究チーム ）

【 要旨 】

カメラはイメージングで最も重要な素子の一つである。バイオイメージングでは、CCDとくにEMCCDカメラが急速に発達して広く使用されているが、たとえば携帯電話やデジカメの撮像素子としては、CCDからCMOSへと急速に世代交代が進んでいて、最近のスマートフォン内蔵カメラのほとんどは背面照射型CMOSを搭載している。CMOSカメラはCCDに比べて高速性・画素数・サイズ・価格などの点で優位性があるためだ。しかし、バイオイメージング、特に微弱蛍光用のカメラとして用いるには様々な問題があった。この数年、scientific CMOS(sCMOS)という呼び方でバイオイメージングに適したCMOSカメラが市販されるようになり、状況が変わりつつある。私自身、これまで主にEMCCDカメラを用いてきたが、ごく最近、いわゆるsCMOSカメラを使い始めて以来、主にそちらを用いるようになってきている。本講演では、1分子イメージングや超解像イメージング、多点ライブセルイメージング、in vivo イメージングなどの様々なイメージングでの実際の作例を紹介しつつ、sCMOSの特徴をEMCCDカメラとの比較でユーザーとしての視点から論じてみたい。

演題2

EM-CCDを超えるGEN-ⅡsCMOS ～ 設計者が語る ～

戸田 英児

（ 浜松ホトニクス株式会社　システム事業部　第１設計部　第14部門 ）

浜松ホトニクス株式会社　URL： http://jp.hamamatsu.com

システム事業部 システム営業推進部

〒431-3196　静岡県浜松市東区常光町812

TEL：（053）431-0150　FAX：（053）433-8031

E-mail： sales@sys.hpk.co.jp

Ryoka Systems Inc.

第 50 回日本生物物理学会年会

株式会社菱化システム ランチョンセミナー

3D-RISM 法による溶媒解析

日時： 9 月 22 日（土） 12:00～12:50

場所： E 会場（多元数理科学棟 「講義室109」）

MOEの3D-RISMによる水和解析例：KcsAチャネルフィルター部位の水和構造の解析 -フィルター機能の理解を目指して-

滋賀医科大学 麻酔学講座 瀬戸 倫義

イオンや薬物がタンパク質と複合体形成し、チャネル機能や薬物作用をおこす。複合体形成による機能修飾の解析には、結合部位、リガンド-受容体相互作用、相互作用による機能修飾の解明が必要である。結合部位の探索にはドッキング計算が用いられるが、水和エネルギーの精度に限界があった。3D-RISM 理論は水和をあらわに取り扱い、分布密度、水和自由エネルギーを含めて評価することができる。水和エネルギーマッピングから水和有利・脱水和有利の分布を観察することができる。KcsA は閉構造が明らかとなっている K^+チャネルである。チャネルのソルトブリッジや水素結合と水和密度分布の関連を調べれば、リガンド結合による水和変化がソルトブリッジ・水素結合に及ぼす影響を知ることができる。KcsA のフィルター部位の水和分布について紹介する。

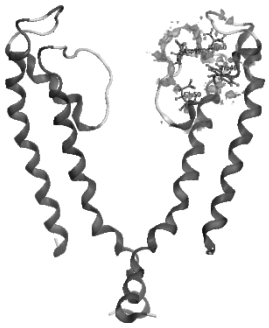

KcsA(WSK3)フィルター部位の水素結合・ソルトブリッジ周りの水和水酸素原子分布

MOE-Solvent Analysisによる溶媒解析の応用事例

株式会社菱化システム 科学技術システム事業部 東田 欣也

MOE-Solvent Analysis は、3D-RISM 法に基づき、タンパク質周辺における水溶媒、塩、疎水性溶媒の確率密度分布や、水の溶媒和エネルギー値を可視化します。この機能により、タンパク質-リガンド複合体において水分子を媒介した相互作用が重要な位置や、溶媒和エネルギーが有利/不利に働く部分を明らかにすることができます。本セミナーでは、3D-RISM 法によるタンパク質-リガンド相互作用解析の応用事例についてご紹介します。

株式会社菱化システム 科学技術システム事業部
〒104-0033 東京都中央区新川 1-28-38 東京ダイヤビル 3 号館 3 階
TEL: 03-3553-9206 FAX: 03-3553-9207
E-mail: support@rsi.co.jp URL: http://www.rsi.co.jp/

第50回日本生物物理学会年会ランチョンセミナー

Correlative Microscopy Different flavors

光学顕微鏡と電子顕微鏡をつなぐ新たなアプリケーション

■ 日　時: 2012年9月22日 (土) 12:00 – 12:50
■ 会　場: F会場（理学部B館　講義室501）
■ 演　題: Correlative Microscopy – Different flavors
■ 講演者: Wim Voorhout (FEI Company, Eindhoven, The Netherlands)

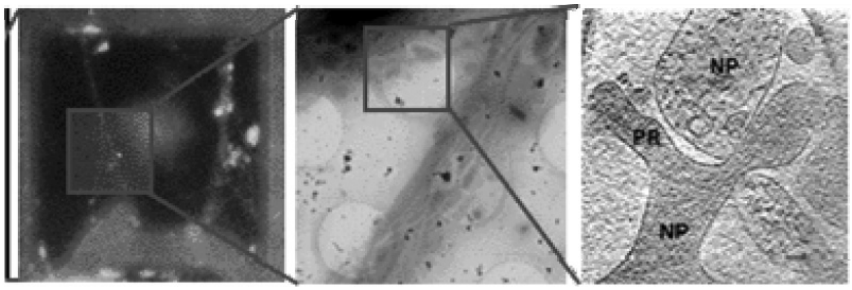

■ 要旨:

Over the last decade electron microscopy techniques have evolved from delivering 2D information to 3D information with a main focus on the architecture of organelles on a subcellular level. These techniques have yielded important new insights in intracellular architecture and connectivity of organelles.

However, understanding complex biological systems requires knowing how this high resolution 3D Electron microscopy data correlates with the situation in-vitro, or even better in-vivo. To obtain more complete and meaningful information about the biological processes within a cell developments have taken place to combine light microscopy data with electron microscopy data.

In this seminar we will present two techniques that enable the correlation of these two microscopy domains: one where both techniques are combined in one instrument and the other where the data of these techniques can be combined in an easy and intuitive way.

The first part will be about ILEM (Integrated Light and Electron Microscope) where we address FEI's developments in integrating a fluorescent light microscope into our Transmission Electron Microscope (TEM). The second part will address FEI's Maps product where data from arbitrary (Light microscopy) source can be imported, scaled and aligned in an intuitive way.

Both methods aim to correlate the light and Electron microscopy domain with the maximum ease of use, but with different pro's and con's which will be addressed in this seminar.

日本エフイー・アイ株式会社
〒108-0075　東京都港区港南2-13-34　NSSIIビル4F
TEL: 03-3740-0970（代）
FAX: 03-3740-0975

日本生物物理学会第50回年会

オリンパスランチョンセミナー

「これから」の光学イメージング技術

日　時

9月23日 [日]　**12:00〜12:50**

場　所

名古屋大学 東山キャンパス B会場（多元数理科学棟「講義室509」）

演　者

渡邉 朋信 先生
独立行政法人 理化学研究所 生命システム研究センター
先端バイオイメージング研究チーム

近10年に、生物学研究・基礎医学研究が飛躍的に発展したのは、疑う余地がない。その立役者の一つに、光学顕微鏡の技術革新が挙げられる。蛍光蛋白質技術を初めとする蛍光標識技術の進展も伴って、生きた細胞の中での蛋白質の機能や振る舞いが、明らかになりつつある。今や、蛋白質、細胞、個体、各層における生命のメカニズムを解明するために、顕微鏡は無くてはならないツールとなった。一方で、生命研究は、各層での振る舞いのみならず、層を繋ぐ研究へとパラダイムシフトを見せている。顕微鏡を用いたイメージング技術もまた、上記のニーズに答えるべく、発展している。本ランチョンセミナーでは、これからの生命研究のために開発された、顕微鏡の命とも言える対物レンズ、長期間観察用の顕微鏡システム、および、新しい蛍光蛋白質プローブと、少しずつではあるが、幅広く紹介する。

演題：オリンパス新倒立顕微鏡 IX3 シリーズ 特長のご紹介
演者：田村恵祐（オリンパス株式会社　開発本部）

NEW
倒立型リサーチ顕微鏡「IX3 Series」新発売

OLYMPUS®
Your Vision, Our Future

PDBj
Protein Data Bank Japan

http://pdbj.org/

PDBj：Protein Data Bank Japan
（日本蛋白質構造データバンク）

演者１：中村　春木（大阪大学蛋白質研究所）
『 Big data 時代に向けた wwPDB と PDBj の役割 』

2012 年 3 月に米国による Big Data initiative の立ち上げと巨額の予算投資が発表され、Data Driven Science に対する関心が国内外で急速に高まっている。生体高分子の立体構造情報は、ゲノム情報ほどの Big さは無いものの、既に 8 万件を越える生体分子の原子分解能の構造情報が蓄積され、さらに増大している。この構造情報については、wwPDB（worldwide PDB）による国際的な枠組みのもとで、大阪大学・PDBj、米国・RCSB-PDB、欧州・PDBe-EBI、BMRB (BioMagResBank) 、EMDB が協力して、Big Data の基本となる品質の高い構造情報と関連するメタデータとをデータベース化し、世界中に無償で公開をしている。本セミナーでは、Big Data 時代に対応した wwPDB と PDBj の活動の概要と提供するサービスについて紹介し、より良いデータベースにするために、利用者の皆様からのご意見やご質問を伺う機会にしたいと考えている。

演者２：小林　直宏（大阪大学蛋白質研究所）
『 仮想化技術を用いた NMR データの統合的解析環境 』

近年、進歩の目覚しい計算機、IT 技術により我々の解析環境は大きく変わりつつある。特に仮想化技術、クラウドコンピューティングなどの新世代の技術の進歩はデータベースなどに蓄積された既存のデータに基づく解析支援を強力なものにしてきている。

NMR を始めとする生体高分子を扱う実験データの構造もそれに伴い複雑化し、それらを利用するためのワークステーションやソフトウエアなどの環境設定、解析操作は年々煩雑化する傾向がある。このような状況において、少人数体制の研究グループによるデータや解析環境の管理は益々困難になってきている。

本セミナーでは、NMR データ解析環境の運用を効率化するために、仮想化技術を使ったシステムの構築に関するノウハウ、複数の解析プラットフォームを統合した解析支援システムについて紹介、解説する。

PDBj：Protein Data Bank Japan

〒565-0871　大阪府吹田市山田丘 3－2 大阪大学蛋白質研究所・附属蛋白質解析先端研究センター内
PDBj 事務局：TEL(06)6879-4311、FAX(06)6879-8636
PDBj データベース登録業務事務局：TEL(06)6879-8634、FAX(06)6879-8636
http://pdbj.org/

日本生物物理学会 ランチョンセミナー

マルバーン ランチョンセミナー

マルチ検出器GPC/SECシステムによる タンパク質の絶対分子量測定および構造解析

日時　：2012年 9月23日(日) 12:00 ～ 12:50
会場　：H 会場(理学部 C館「講義室 517」)
講演者：スペクトリス株式会社 マルバーン事業部
プロダクトスペシャリスト
池田 英幸

サイズ排除クロマトグラフィー(size-exclusion chromatography: SEC)またはゲル浸透クロマトグラフィー(gel permeation chromatography: GPC)は、しばしば生命科学の研究において精製タンパク質、または組み換えタンパク質の特性評価に使用される。従来の方法では、標準的な球状タンパク質で検量線を作成し、未知の試料の溶出時間を検量線と比較することでその分子量を導き出す。この方法は、分子量とサイズ、形状、流体力学的体積が、常に不変の関係にあるという仮定に基づいている。この関係は、タンパク質間で大きく異なるため、この方法による計測値には、数量化できない不正確さが伴う。最新のマルチ検出器分析システムを用いることで、従来とは異なる原理により、正確な分子量の測定が可能である。また、屈折率(refractive index: RI)検出器、紫外線(UV)検出器、光散乱(light scattering: LS)検出器、粘度検出器(viscometry: IV)など複数の検出器を組み合わせることで、より多くの情報を得ることが出来る。光散乱検出器は絶対分子量の測定に使用され、粘度検出器は、構造変化の指標となる試料の固有粘度を測定する。また、屈折率検出器と紫外線検出器を組み合わせることで、複合体の成分比分析を行うことができる。本講演では、いくつかの事例をもとに、マルチ検出器GPC/SECシステムのタンパク質科学への応用を紹介する。

Malvern

スペクトリス株式会社 マルバーン事業部
〒650-0047神戸市中央区港島南町5-5-2 神戸国際ビジネスセンター北館511
電話:078-306-3806　Fax:078-306-3807
東京支社
〒101-0048東京都千代田区神田司町2-6司町ビル5F
電話:03-5207-3461　FAX:03-3258-1160
フリーダイアル:0120-57-17-14
http://www.malvern.jp/

日本生物物理学会第50回年会 共催ランチョンセミナー

血管新生の新規スイッチ制御分子BAZFの機能と核内局在

― 超解像顕微鏡Nikon SIMイメージングからわかること

東山 繁樹 先生
愛媛大学プロテオ医学研究センター　細胞増殖・腫瘍制御部門
愛媛大学大学院医学系研究科　生化学・分子遺伝学分野

日 時 2012年9月24日（月）12:00～12:50

会 場 名古屋大学東山キャンパス A会場
（理学南館「平田・坂田ホール」）

血管新生は固形腫瘍増殖や組織損傷時の修復過程には必須であり、その制御は血管内皮細胞の増殖促進と抑制のバランス制御で成立している。私どもは血管内皮細胞の増殖促進（VEGFシグナル）と抑制（Notchシグナル）のバランスを制御する分子を探索し、Zn-フィンガータンパク質BAZFを新規に同定した。 BAZFはVEGFシグナル下で誘導され、Notchシグナル下流分子CBF1に結合し、これを分解に導くことでNotchシグナルを遮断する。さらに、CBF1分解の本体としてユビキチンE3 リガーゼCullin3(CUL3)を同定し、CUL3-BAZF複合体が、CBF1特異的なユビキチンリガーゼとして機能することを明らかにした。また、超解像顕微鏡 Nikon SIM による時空間局在解析の結果、CUL3-BAZF-CBF1複合体が核内ドメインのPML bodyに局在する事を示唆してくれた。

****

本学会の連絡先は下記の通りです.

1. 会長室
   〒 565-0871 大阪府吹田市山田丘 1-3
   大阪大学大学院　生命機能研究科内
   TEL 06-6879-4625　FAX 06-6879-4652
   E-mail bpsjp@biophys.jp
2. 正会員(学生会員を含む), 機関会員および賛助会員の入会, 退会, 会費納入, 住所変更などの手続き, 会誌発送
   〒 113-0033 東京都文京区本郷 5-29-12-906
   中西印刷株式会社東京事務所内　日本生物物理学会事務支局
   TEL 03-3816-0738　FAX 03-3816-0766　E-mail bsj@nacos.com
3. 会誌の広告
   〒 101-0051 千代田区神田神保町 3-2-8
   昭文館ビル 3F　株式会社エー・イー企画
   TEL 03-3230-2744　FAX 03-3230-2479
4. 学会ホームページニュース欄の原稿（無料および有料), その他学会の運営に関すること
   〒 565-0871 大阪府吹田市山田丘 1-3
   大阪大学大学院　生命機能研究科内
   TEL 06-6879-4625　FAX 06-6879-4652
   E-mail bpsjp@biophys.jp
5. 学会誌の編集に関連する業務（投稿を含む）
   〒 602-8048 京都市上京区下立売通小川東入ル
   中西印刷株式会社内　日本生物物理学会編集室
   TEL 075-441-3155　FAX 075-417-2050
6. 日本生物物理学会の www ホームページ
   http://www.biophys.jp

本誌記事の動物実験における実験動物の扱いは,
所属機関のルールに従っています.

生物物理 SEIBUTSU BUTSURI
日本生物物理学会 THE BIOPHYSICAL SOCIETY OF JAPAN

Vol.52 SUPPLEMENT 1　2012 年 8 月 15 日発行

編集発行　日本生物物理学会
制作　中西印刷株式会社編集室
〒 602-8048　京都市上京区下立売通小川東入ル
TEL 075-441-3155　FAX 075-417-2050
デザイン　齋藤知恵子

広告　INDEX

㈱ニコン　インステック	S1-1	インフォコム㈱	S1-14
日本エフイー・アイ㈱	S1-2	㈱菱化システム	S1-15
オリンパス㈱	S1-3	大陽日酸㈱	S1-16
共立出版	S1-4	シュレーディンガー㈱	S1-17
エルゼビア・ジャパン㈱	S1-5	ブレインビジョン㈱	S1-18, 19
WDB ㈱	S1-6	バイオリサーチセンター㈱	S1-20
遠藤科学㈱	S1-7	アンドール・テクノロジー PLC	S1-21
理科研㈱	S1-8	フォトニックインストゥルメンツ㈱	S1-22
㈱木下理化	S1-9	和光純薬工業㈱	S1-23
キコーテック㈱	S1-10	橋本電子工業㈱	S1-24
㈱島津製作所	S1-11	ブルカー・オプティクス㈱	S1-25
㈱ JCC ギミック	S1-12	ブルカー・バイオスピン㈱	S1-26
㈱日立製作所	S1-13		

※ 直接連絡される場合には，必ず「生物物理を見て」とお付け加え下さい.

【PLEASE COPY】

広告製品資料請求は下記宛E-mailか, この用紙をコピーしFAXでご請求下さい。

希望項目 / 請求番号	1	2	3	4	5	使用目的・知りたい仕様など, ご要望事項があればお書き下さい
No.						
No.						
No.						
No.						
No.						

1. 購入希望　2. サンプル希望　3. 価格表希望　4. 担当者訪問希望　5. カタログ希望

住所変更（あり・なし） ※○印をつけて下さい	お名前（フリガナ）
勤務先名	ご所属
所在地（フリガナ） （〒　　）　TEL.　　FAX.	

ご研究内容をわかりやすくご記入下さい

E-mail: adinfo@aeplan.co.jp
FAX to 03(3230)2479
株式会社　エー・イー企画

日本生物物理学会第50回年会 附設展示会

◆ 展示会期：2012年 9月22日（土）～ 24日（月）　◆ 展示会場：名古屋大学 豊田講堂

出展社一覧

アンドール・テクノロジー PLC
㈱インターメディカル
SIサイエンス㈱
オリンパス㈱
公益財団法人 高輝度光科学研究センター
GEヘルスケア・ジャパン㈱
シグマ光機㈱
シュレーディンガー㈱
スペクトリス㈱ マルバーン事業部
㈱生体分子計測研究所
㈱セルフリーサイエンス
ソーラボジャパン㈱
ティー・エイ・インスツルメント・ジャパン㈱
㈱ディジタルデータマネジメント
テガサイエンス㈱
㈱デジタルマイクロシステムズ
㈱ニコンインステック
独立行政法人 日本原子力研究開発機構 JPR-3 ユーザーズオフィス
㈱日本レーザー
㈱日本ローパー
パーク・システムズ・ジャパン㈱
バイオリサーチセンター㈱
橋本電子工業㈱
浜松ホトニクス㈱
ピーアイ・ジャパン㈱
深江化成㈱
ブルカー・エイエックスエス㈱
プロメガ㈱
モレキュラーデバイス ジャパン㈱
文部科学省・HFSP
文部科学省「創薬等支援技術基盤プラットフォーム事業」事務局
㈱ユニソク
㈱菱化システム
㈱渡商会

※50音順 敬称略 作成：2012年 6月29日

展示即売会　＆　サイン会

「大沢流　手づくり統計力学」

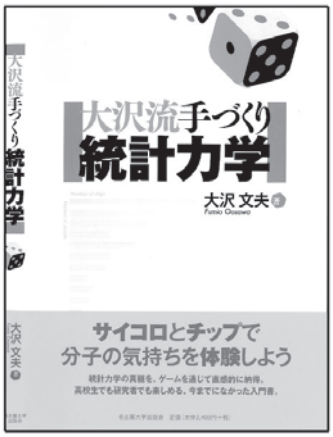

大沢文夫 著

定価 2520 円を
特別価格

統計力学の真髄をサイコロとチップを使ったゲームで紹介した、
物理を学んでいない学生にも理解できる入門書。
関連する最新の様々な生物物理の話題も取り上げる。

著者サイン会開催！

9 月 23 日 (日)
午後 2 時～3 時
豊田講堂ロビー 1F

都合により予定が変更になることがあります
あらかじめご了承ください

展示即売会　豊田講堂ロビー 1F

9 月 22 日（土）10:00 ～ 17:00
23 日（日）10:00 ～ 17:00
24 日（月）10:00 ～ 16:00

細胞の物理生物学

ダイナミックな学問の変化を伝える一冊！

Rob Phillips，Jane Kondev，Julie Theriot［著］

笹井理生・伊藤一仁・千見寺浄慈・寺田智樹［訳］

B5判・上製ハードカバー・992頁・定価13,650円（税込）

物理生物学（Physical Biology）は，伝統的な生物物理学（Biophysics）の立場からさらに一歩踏み込んで，物理学の考え方と方法が生物学の中核となったことを表す新しい言葉である。これまで物理学の方法を用いてタンパク質や核酸などの生体分子が研究されてきたが，学問の進歩とともに，生体分子の複合体，ネットワーク，細胞小器官，細胞，そして進化までが物理学の対象となり，物理学的アプローチが生物学の中核となる段階にまで発展してきた。本書は，この発展を担う研究現場の息吹を，分かり易く読者に伝える現代的な教科書である。現象を捉える出発点となる重要な物理量の見積もり，そしてモデル作りの発想と狙いが丁寧に説明されており，理論と実験の結果が分かり易く定量的に比較されていて，本書を読むことで“物理学的アプローチとは何か”が自然に理解できるように書かれている。

計算科学講座

全10巻

金田行雄・笹井理生 監修

日進月歩の急速なコンピュータ技術の進歩により，シミュレーションやデータ解析など，コンピュータを使って研究することのできる対象は大きく拡がりつつある。特に，いまだかつて無いような超多自由度を持つシステムを，計算によって理解，予測，設計することができるようになり，基礎科学から応用科学，そして社会的実践にいたるまで，深くて広いインパクトが生まれている。また，将来の科学と技術の大きな牽引力になると予想されている。このとき，従来の個別分野ごとのシミュレーションツールとしての枠を超えて計算とは何か，何をどのように計算すべきか，という問題に系統的に取り組む計算科学の発展に強い期待が寄せられている。本講座は，計算科学の基盤分野と応用展開分野の密接な連携を軸にして計算科学を体系的に解説し，その最前線を展望する講座である。

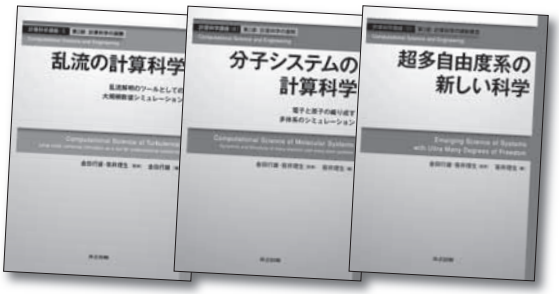

【各巻】 A5判・上製ハードカバー・260～400頁

【第1部　計算科学の基盤】

①計算科学のための基本数理アルゴリズム
張　紹良編……続　刊

②20世紀のトップテンアルゴリズム
張　紹良編……続　刊

③統計・多変量解析とソフトコンピューティング
古橋　武編……近　刊

④計算科学のための並列計算
石井克哉編……続　刊

【第2部　計算科学の展開】

❺乱流の計算科学
金田行雄編……268頁・定価3,990円（税込）

❻分子システムの計算科学
笹井理生編……390頁・定価4,620円（税込）

⑦ゲノム系計算科学
美宅成樹編……続　刊

⑧プラズマの計算科学
荻野瀧樹編……続　刊

【第3部　計算科学の横断概念】

⑨超多自由度系の最適化
古橋　武・笹井理生編……続　刊

⑩超多自由度系の新しい科学
笹井理生編……336頁・定価4,200円（税込）

〒112-8700 東京都文京区小日向4-6-19
TEL 03-3947-2511／FAX 03-3947-2539

共立出版

http://www.kyoritsu-pub.co.jp/
≪共立ニュースメール会員募集中≫

＜資料請求番号 S1-5＞

＜資料請求番号 S1-6＞

〔研究・開発機器の総合商社〕

取扱い品目

電子計測器・理化学器械・試験機・光学機器・バイオニクス関連機器・コンピュータ関連機器。　（1,000社を超すメーカーを取り扱っております）

計測制御システムの設計・開発。

・最新の機器情報をいち早くお届けいたします。

・最適の機種の選定のお手伝いをいたします。

・特殊仕様のシステムアップもいたします。

・アフターサービスは完璧を期します。

＊ISO9001 ・ ISO14001 認証取得

遠藤科学は、東はつくばから西は安城まで計15営業所

お問合せは最寄の営業所へ

つくば営業所 029-852-6560	千葉営業所　043-254-2211
横浜営業所　045-471-5422	平塚営業所　0463-54-1121
厚木営業所　046-297-7877	御殿場営業所 0550-84-1141
三島営業所　055-973-3211	富士営業所　0545-51-5311
静岡営業所　054-283-5222	島田営業所　0547-38-3900
袋井営業所　0538-43-5151	浜松営業所　053-464-3400
湖西営業所　053-577-4111	豊橋営業所　0532-55-6655
安城営業所　0566-75-6010	

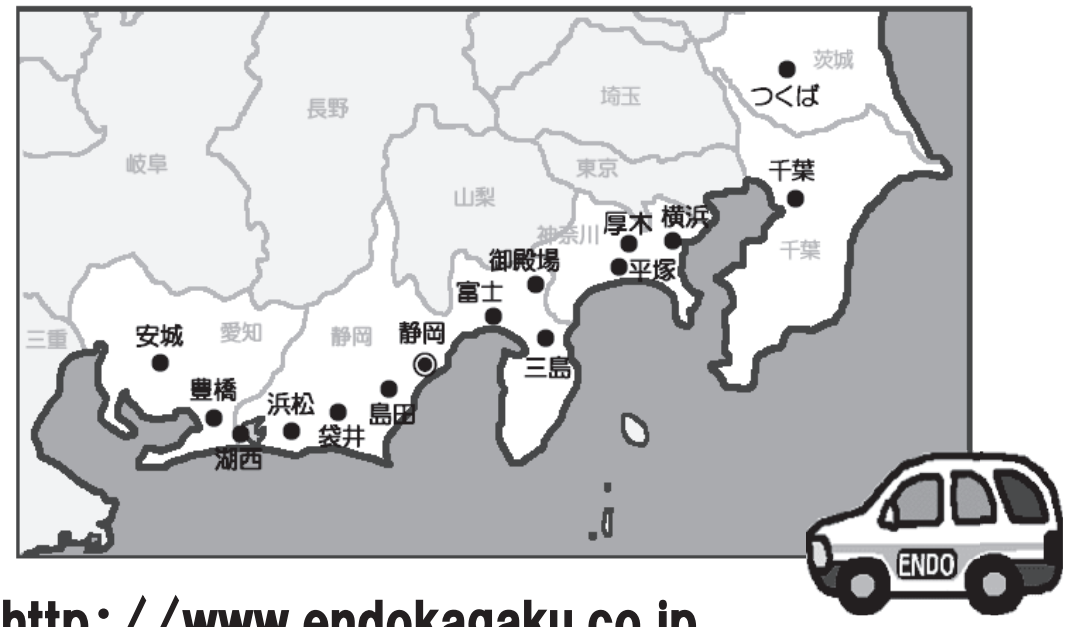

URL　http://www.endokagaku.co.jp

ENDO Kagaku K.K

遠藤科学株式会社

本社：静岡市駿河区西脇1294　　電話　054-283-6222

＜資料請求番号 S1-7＞

生命を構成するＤＮＡ。それは宇宙の誕生から現在まで途切れることなく、全ての生命に受け継がれてきました。
しかし、もとをたどれば全宇宙に存在する虫も、動物も、そしてヒトも、全て同じものから創られているのです。
そこにはまだ、未知なる宇宙の神秘として医療・研究・開発者の前に立ちはだかり、
様々な難問を解かれることを待っています。
私たち「理科研」が、この問題へ向かう人々を真心でお手伝い出来るのは、
設立当初から受け継がれてきた社訓、「誠意」が遺伝子として組み込まれているから。
理科研は、「バイオ研究」に欠かすことのできない機器・試薬の販売を通じ、
人類の幸せと豊かな社会の実現を願っています。

理科研株式会社

体内宇宙への挑戦。

■本　　社　名古屋市守山区元郷二丁目107番地
〒463-8528　TEL 052-798-6151(代)　FAX 052-798-6157

■岡 崎 営業所　愛知県岡崎市明大寺町字西長峰50番
〒444-0864　TEL 0564-57-1751(代)　FAX 0564-57-1757

■福 井 営業所　福井県福井市開発3丁目3010
〒910-0842　TEL 0776-52-1651(代)　FAX 0776-52-1653

■岐 阜 営業所　岐阜県岐阜市岩地2丁目25番2号
〒500-8225　TEL 058-240-0721(代)　FAX 058-240-1082

■津　営 業 所　三重県津市丸之内養正町20番地14号
〒514-0036　TEL 059-224-6661(代)　FAX 059-224-6671

■四日市営業所　三重県四日市市桜町2129番の1
〒512-1211　TEL 059-326-0231(代)　FAX 059-326-3577

■静 岡 営業所　静岡市駿河区広野3丁目29番8号
〒421-0121　TEL 054-256-3751(代)　FAX 054-256-3755

■東 京　支 店　東京都文京区本郷3丁目44番2号
〒113-0033　TEL 03-3815-8951(代)　FAX 03-3818-3186

■つくば営業所　茨城県つくば市高野台三丁目16-2
〒305-0074　TEL 029-856-2151(代)　FAX 029-856-5071

■柏　営 業 所　千葉県柏市若柴197番地17
〒277-0871　TEL 04-7135-6651(代)　FAX 04-7135-6751

■神奈川営業所　横浜市緑区十日市場町901-31
〒226-0025　TEL 045-989-6551(代)　FAX 045-989-6701

■鶴 見 営業所　横浜市鶴見区朝日町一丁目49番地
〒230-0033　TEL 045-500-4551(代)　FAX 045-500-4571

■三 島 営業所　静岡県駿東郡長泉町下土狩217番地1
〒411-0943　TEL 055-980-1101(代)　FAX 055-980-1105

関連会社／株式会社　片　岡　〒920-1155　石川県金沢市田上本町71-7　TEL 076-263-2011(代)　FAX 076-263-2051
並木薬品株式会社　〒930-0834　富山県富山市問屋町3-11-3　TEL 076-451-4545(代)　FAX 076-451-0085

＜資料請求番号 S1-8＞

研究設備・分析機器・光学機器・分析器具

主要特約代理店

オ　リ　ン　パ　ス	パナソニック ヘルスケア
ヤ　マ　ト　科　学	ＧＥヘルスケア・ジャパン
ト　ミ　ー　精　工	ライフテクノロジーズジャパン
旭　　硝　　子	ア　ズ　ワ　ン

株式会社 木下理化

〒466-0035
名古屋市昭和区松風町１丁目３２番地の３
TEL（０５２）８５９－２１３２
FAX（０５２）８５９－２１３６

＜資料請求番号 S1-9＞

理化学機器・試薬・消耗品　販売

バイオ・ライフサイエンス　その先端研究へのサポート
良きパートナーを目指して

キコーテック株式会社

本　　社　大阪府箕面市船場西三丁目10番3号
〒562-0036　TEL 072(730)6790　FAX 072(730)6795

東京支社　東京都世田谷区駒沢二丁目11番1号集花園ビル3階
〒154-0012　TEL 03(5787)3323　FAX 03(5787)3324

つくば営業所　茨城県つくば市筑穂二丁目4番2号ＫＭＳＳ101
〒300-3257　TEL 029(864)3811　FAX 029(864)3816

神奈川営業所　神奈川県藤沢市藤が岡一丁目8番14号田中ビル1F
〒251-0004　TEL 0466(55)4110　FAX 0466(55)4120

神戸営業所　神戸市中央区港島南町一丁目5番2号神戸ｷﾒｯｸｾﾝﾀｰﾋﾞﾙ6F
〒650-0047　TEL 078(302)5978　FAX 078(302)5993

＜資料請求番号 S1-10＞

SHIMADZU
Excellence in Science

Spectrophotometer for Life Science

BioSpec-nano

島津ライフサイエンス分光光度計

簡単・迅速な
核酸定量を実現します。

Power of small.

小さくても、パワフル。小さいからこそ、扱いやすい。
私たちは、そんなラボツールをラインアップしていきます。

ドロップ & クリック分析

サンプルを滴下位置（ターゲット）にドロップし、ボタンをクリックするだけで分析が行えます。測定とワイピングは装置が自動で行います。

1～2μLでの核酸定量

1μL（光路長0.2mm）、2μL（光路長0.7mm）のサンプル量で分析が可能です。

シンプル & クイック操作

ブランク測定、サンプル測定、レポートのPDF出力、CSV出力などの基本操作はボタンをクリックするだけで、シンプル & クイックに行えます。

株式会社 島津製作所　分析計測事業部

東京 (03) 3219-5685　北関東 (048) 646-0081　神戸 (078) 331-9665
関西 (06) 6373-6556　横浜 (045) 311-4615　岡山 (086) 221-2511
札幌 (011) 205-5500　静岡 (054) 285-0124　四国 (087) 823-6623
東北 (022) 221-6231　名古屋 (052) 565-7531　広島 (082) 248-4312
郡山 (024) 939-3790　京都 (075) 823-1603　九州 (092) 283-3334
つくば (029) 851-8515

http://www.an.shimadzu.co.jp/

＜資料請求番号 S1-11＞

＜資料請求番号 S1-12＞

＜資料請求番号 S1-13＞

United Innovation
infocom group

SCORPION

An Exploration of Network Hotspots and Cooperativity in Protein-Ligand Recognition

Scorpion は独自のネットワークモデルにより Protein-Ligand 複合体の相互作用を解析する最新ツールで、Ligand 設計に応用できます。
～Binding Sites解析とLigandデザインに！～

＊Scorpion によるアプローチ

1) Protein-Ligand の Binding sites 内の各種相互作用を識別、クラス分け
2) 共有結合と favorable 相互作用を単一ネットワークに結合
3) リガンド原子を含むネットワーク・パスをネットワーク記述子により記述
4) プロテイン構造の reduced グラフ表現を定義
5) 高品質なデータセットに対して遺伝的アルゴリズムを用いてパラメータ化

ネットワーク・モデル

Protein-Ligand 複合体をネットワークモデルを用いて表すことにより、複合体の協調効果を把握することができます。

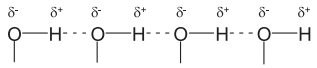

＜協調効果の例＞

水素結合の相関により、個々の水素結合の総和より、自由エネルギーが低下します。

スコア関数

高品質の構造データと複合体の実験値を用いて、遺伝的アルゴリズムによりパラメータの最適化を行い、スコア関数を決定します。

$$S = \sum_{n} f(Int) \quad \text{(ネットワーク項なし)}$$

$$S_{Scorpion} = \sum_{n} f(Int) + \sum_{m} g(Int\_nw)$$

リガンド原子へのスコア表示

→ リガンド設計への *Hint!*

各原子のスコアを表示し、大きさを色別に示します。 各原子のスコアへの寄与を知ることで、リガンド設計の*Hint* とすることができます。

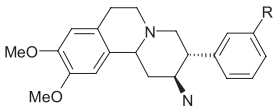

R	K_d (nM)	$S_{Scorpion}$	network
H	200	7.9	0.8
CH_3	4.6	10.8	1.6
CH_2F	0.5	11.3	1.7

論文情報

Kuhn, B.; Fuchs, J. E.; Reutlinger, M.; Stahl, M.; Taylor, N. R. Rationalizing tight ligand binding through cooperative interaction networks. J. Chem. Inf. Model. 2011, 51, 3180-3198

DesertSci社製品ラインナップ

- **Proasis2**
  Protein および Protein-Ligand 複合体の構造情報DB構築
- **Proasis3**
  Priasis2 のインターフェース。優れた操作性と可視化機能
- **ViewContacts**
  Protein-Ligand 複合体の非共有結合性相互作用解析、結合水の取扱い

infocom インフォコム株式会社
ケム＆バイオインフォマティクス部
〒150-0001東京都渋谷区神宮前二丁目34番17号住友不動産原宿ビル
TEL：03-6866-3860　FAX：03-6866-3055
E-mail：info-science@infocom.co.jp　URL：http://infocom-science.jp/

DesertSci
"Something Different"

◎Interaction type の分類

原子タイプを自動アサインし、各種相互作用を認識

有利な相互作用
1. hydrogen bond
2. metal bonding
3. ionic
4. cation-dipole
5. cation-pi
6. dipolar
7. halogen
8. h_donor-pi
9. pi-pi
10. van der Waals

不利な相互作用
11. close contacts of wrongly matched atom types
12. clashes of atom pairs
13. polar-nonpolar desolvation penalties

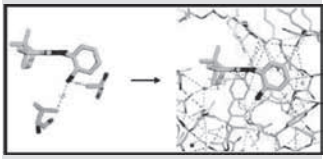

◎Hardware and Software Requirements:

Industry standards:

・Scorpion server software runs under Linux
Linux version supported
RHEL 4, 5 ... 32- , 64-bit
CentOS 4, 5...32- , 64-bit
SUSE 10, 11 ... 32- , 64-bit

•ViewContacts™ software runs on Linux, with Python 2.4 or above

•clients using VCWeb can use MS Windows, Mac and Linux, and any of the major browsers

•PyMol required for visualizations, version 0.99rc6 or above (MOE and Benchware 3D Explorer also soon to be supported)

•Openbabel (or OpenEye's Babel) needed for pdb to mol file format conversions

＜資料請求番号 S1-14＞

CHEMICAL COMPUTING GROUP INC.

統合計算化学システム

MOE

Molecular Operating Environment

創薬・生命科学研究に最適な分子設計環境

- 分子モデリング・シミュレーション
  Molecular Modeling and Simulations
- ケムインフォマティクス
  Cheminformatics and High Throughput Discovery
- タンパク質モデリング
  Protein Modeling and Bioinformatics
- 立体構造に基づく分子設計
  Structure-Based Drug Design
- ファーマコフォア解析
  Pharmacophore Modeling
- 開発環境
  Development Environment

PSILO

タンパク質立体構造データベースシステム

3D相互作用検索
類似ポケット構造検索
リガンド結合部位の3D/2D表示
タンパク質の重ね合わせ

お問い合せはこちらまで

Ryoka Systems Inc.

Chemical Computing Group社 日本総代理店
株式会社 菱化システム
科学技術システム事業部
〒104-0033 東京都中央区新川1-28-38東京ダイヤビル3号館3階

TEL: 03-3553-9206
FAX: 03-3553-9207
URL: http://www.rsi.co.jp/ e-mail: support@rsi.co.jp

＜資料請求番号 S1-15＞

安定同位体標識化合物
Stable Isotope for Structural Biology

大陽日酸は多次元NMRでの構造解析に必須な安定同位体標識化合物を
高い品質・お求め易い価格で販売しております。

1 安定同位体標識無細胞タンパク質合成キット 新発売!!

独立行政法人理化学研究所の無細胞タンパク質合成技術をキット化いたしました。

● 無細胞くん Quick

タンパク質合成キット
無細胞® くん Quick

■ キット内容

名 称	容 量	保温温度	製品番号
クイック液	1mL(50μL×20回相当分)	-80℃	A29-0058
コントロールDNA (pUC-CAT)**	50μL(10μg/mL)		

**クロラムフェニコールアセチルトランスフェラーゼ(CAT)を発現します。

■ 特徴

大腸菌抽出液を用いたタンパク質発現確認用キットです。クイック液には非標識アミノ酸をはじめ、必要な成分がすべて含まれておりますので、**テンプレートDNAを添加**して**1時間**インキュベートするだけで**簡単にタンパク質を合成できます。**

● 無細胞くん SI

安定同位体標識タンパク質合成キット
無細胞® くん SI

■ キット内容

名 称	容 量	保温温度	製品番号
内液	1mL(1回分)	-80℃	A29-0059
外液	10mL(1回分)		

■ 特徴

大腸菌抽出液を用いた安定同位標識タンパク質発現専用キットです。透析膜に内液とテンプレートDNAを添加し、外液に浸してインキュベートするだけで**大量の安定同位体標識タンパク質**を得ることができます(CATタンパク質最大合成量5mg/mL)。より大量のタンパク質が必要な場合には、複数のキットをまとめてスケールアップしてご使用ください。

2 標識アミノ酸

- 無細胞くん用安定同位体標識アミノ酸
- L-Amino Acids-UL-(^{15}N), (^{13}C, ^{15}N), (^{15}N, d)
- Algal Amino Acids Mixture-UL-(^{15}N), (^{13}C, ^{15}N), (^{15}N, d), (^{13}C, ^{15}N, d)

3 標識培地用

- D-Glucose-(UL-$^{13}C_6$), (C-d_7), (UL-$^{13}C_6$, d_7)
- Ammonium-^{15}N Chloride／Ammonium-$^{15}N_2$ Sulfate

4 安定同位体標識 DNA/RNA

- dNTPs-UL-^{13}C, ^{15}N／rNTPs-UL-^{13}C, ^{15}N
- オリゴマー受託合成

大陽日酸
The Gas Professionals
メディカル事業本部 SI事業部

〒142-8558 東京都品川区小山1-3-26 東洋Bldg.
TEL. 03-5788-8550(代表) FAX. 03-5788-8710

●資料のご請求は、大陽日酸(株)までお気軽にご用命下さい。
メールアドレス Isotope.TNS@tn-sanso.co.jp
ホームページアドレス http://stableisotope.tn-sanso.co.jp

New Product Release !

A comprehensive modeling package for biologics

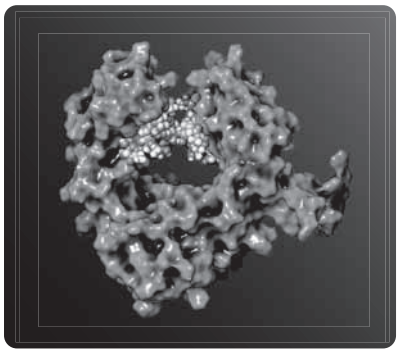

BioLuminate

BioLuminate is the first product designed from the ground up, with significant user input, to specifically address all the key questions associated with the molecular design of biologics. BioLuminate embeds industry-leading simulations within an easy-to-use interface that logically organizes tasks and workflows.

Schrödinger Software Solutions For Drug Discovery

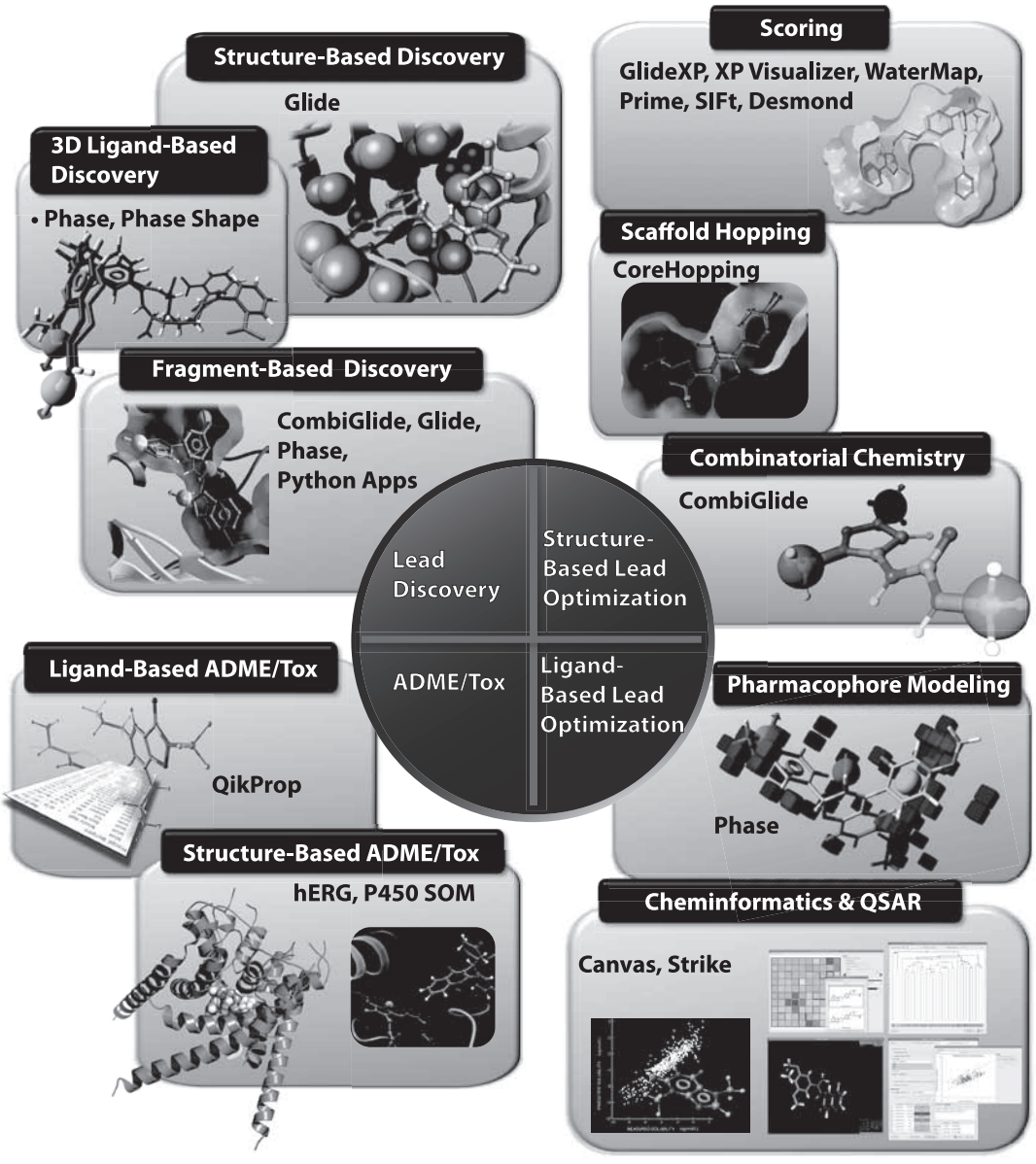

日本国内お問い合わせ先

SCHRÖDINGER K.K.
シュレーディンガー株式会社

シュレーディンガー株式会社
〒100-0005 東京都千代田区丸の内1-8-1
丸の内トラストタワーN館　17階
Tel: 03-6860-8316 Fax: 03-6273-4722
Email: info-japan@schrodinger.com URL: http://www.schrodinger.com/jp

開発・販売元

SCHRÖDINGER
Schrödinger LLC
101 S.W. Main Street Suite 1300,
Portland, OR, U.S.A
Tel: +1-503-299-1150 Fax: +1-503-299-4532
Email: info@schrodinger.com URL: http://www.schrodinger.com

＜資料請求番号 S1-17＞

Brainvision
www.brainvision.co.jp

ブレインビジョンは理化学研究所　脳科学総合研究センター発のベンチャー企業として1998年に設立され、今年で15年目を迎えました。
神経・心臓の膜電位変化を蛍光で捉える高速イメージングシステムとその周辺機器を中心に開発し、世界中の大学、研究所へ販売しています。

自社開発製品

高速イメージングシステム

CMOSイメージセンサー

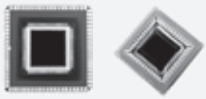

高輝度・高安定光源

データ解析ソフトウェア

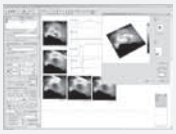

マクロ光学系

水浸対物レンズ

電気刺激装置

カスタム CMOSセンサー　高速カメラ

特注品製作の相談も承ります！！

豊富な自社製品の開発実績により培われた技術力・開発ノウハウをもとに、市販品には無い特注品や様々な使用目的に合わせた標準品のカスタマイズにも対応いたします。

お気軽にお問い合わせください

蛍光寿命測定装置　LED光源　刺激装置　データ解析ソフトウェア

新製品

TOF方式 距離画像カメラ BV-TOF

BV-TOFカメラ
（寸法W50xH50xD63mm）

距離画像
（対象物までの距離を擬似カラーで表示）

輝度画像
（通常の白黒画像）

TOF（Time of Flight）方式 距離計測法の原理

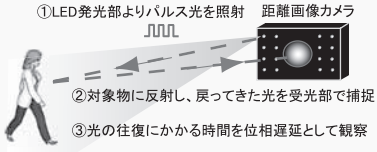

カメラ両側に搭載された高輝度IR-LEDで10MHzの高周波で変調したパルス光を対象物に照射します。対象物で反射した光は距離に比例した遅れ時間をもってセンサー受光部に到達します。この遅れ時間と光の速度から対象物までの距離を算出します。

ブレインビジョン株式会社

〒101-0052 東京都千代田区神田小川町2-2 UIビル7F
TEL: 03-5280-7108　FAX: 03-5280-7109
E-mail: info@brainvision.co.jp
URL: http://www.brainvision.co.jp/

＜資料請求番号 S1-18＞

LED光源

高出力 300 mW/cm²
高安定 <0.05% ドリフト

LEX2

High-Powered / Highly Stabilized LED Light Source

主な仕様

品番	LEX2-B	LEX2-G	LEX2-R
中心波長	465 nm	530 nm	625 nm
100%出力時輝度（注1）	300 mW/cm²	150 mW/cm²	170 mW/cm²
150%出力時輝度（注1）	400 mW/cm²	180 mW/cm²	220 mW/cm²
出力安定時間	3ミリ秒		
光出力雑音（注2）	<±0.015%		
ドリフト	<±0.05%(2秒間点灯時：注2) <±0.1% (20秒間点灯時：注2)		
輝度安定化回路	PDフィードバック回路		
点灯制御	手動制御：フロントパネルのスイッチのON/OFF 外部制御：1.5V以上の電圧入力による		
調光制御	手動制御：フロントパネルのスイッチのON/OFF 外部制御：電圧値により0-100%制御		
輝度設定モニター出力	電圧信号出力（100%設定時、3.3V出力）		
価格	367,500（税込）		

（注1）ストレートライトガイド（ガラス素材、結束径10mm、ファイバ長2200mm）接続時の出射口の値です。
（注2）100%出力時。高速/高感度イメージング装置MiCAM02-HRによる計測の結果です（100fpsで30秒間、4回加算測定）。

波長特性

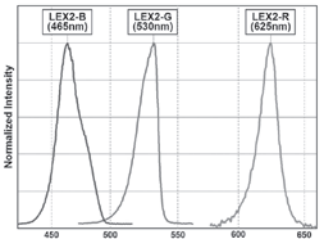

フィードバック制御による輝度安定性

輝度100%設定で2秒間点灯時には0.05%未満の輝度変化

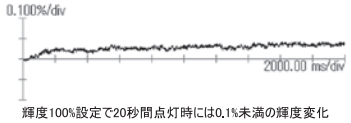

輝度100%設定で20秒間点灯時には0.1%未満の輝度変化

アプリケーション

- 膜電位感受性色素・カルシウム色素などの蛍光指示薬や、蛍光タンパクなどの光遺伝学的プローブを用いた高速蛍光イメージングの励起用光源として
- チャネルロドプシン2（ChR2）、ハロロドプシン（NpHR）の光刺激用光源として
- ハロゲン、水銀、キセノン光源の代替光源として
- その他、高輝度が必要とされる撮影用の光源として

ブレインビジョン株式会社

〒101-0052 東京都千代田区神田小川町2-2 UIビル7F
TEL: 03-5280-7108 FAX: 03-5280-7109
E-mail: info@brainvision.co.jp
URL: http://www.brainvision.co.jp/

＜資料請求番号 S1-19＞

オートパッチクランプ / バイレイヤーシステム

nanion
Nanion Technologies GmbH

世界最小のセットアップで，誰でも簡単にパッチクランプ実験が行えます！
細胞だけではなく，リポソームを使用したバイレイヤー研究にも応用できます。

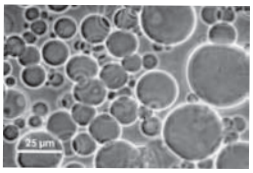

GUV (Giant Unilamellar Vesicle) を自動で簡単に作製できます！

Port-a-Patch

顧客評価，販売台数 **No.1**

50 データ / 日	ガラスチップ
全アンプに接続可能	Current Clamp 可能
常時灌流（細胞外液 / 細胞内液）	ホールセル記録 :70 ～ 90%
化合物投与量，回数，灌流量無制限	温度制御

Port-a-Patch は、世界初のオートパッチユーザーへの実態調査(英 HTStec 社「Ion Channel Trends 2005,2006」)でほぼ最高の評価を頂きました。

Vesicle Prep Pro

リポソーム自動作製装置	単層リポソーム
温度コントロール	高安定性リポソーム
高再現性	リアルタイムで観察可能
蛍光封入リポソームの作製	バイレイヤー研究への応用

hERG

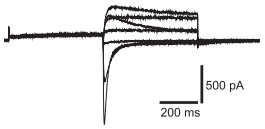

GABA

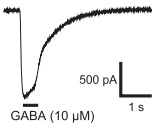

Current Clamp

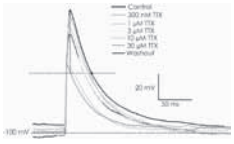

Bilayer

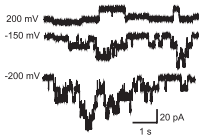

TRPV1

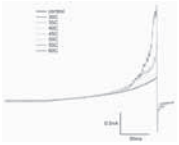

internal solution exchange

DNA hairpin translocation through a porin

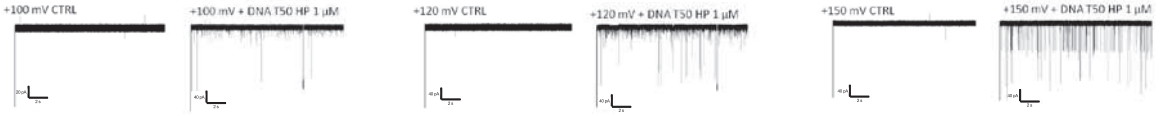

新製品！ Orbit 16

タンパク質を添加するだけで，簡単にハイスループットバイレイヤー記録が行えます。

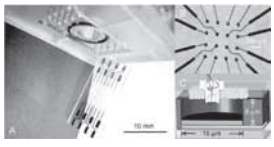

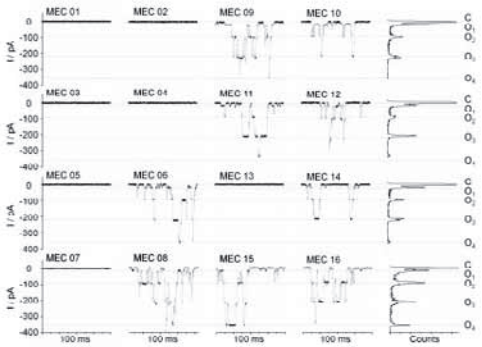

16 ch バイレイヤー同時記録	低ノイズ
既存アンプが使用可能	ペインティング or リポソーム

バイオリサーチセンター株式会社

http://www.brck.co.jp

本社　〒461-0001　名古屋市東区泉2-28-24 ヨコタビル4F　TEL : 052-932-6421　FAX : 052-932-6755
東京　〒101-0032　東京都千代田区岩本町1-7-1 瀬木ビル2F　TEL : 03-3861-7021　FAX : 03-3861-7022
大阪　〒532-0011　大阪市淀川区西中島6-8-8　花原第8ビル2F　TEL : 06-6305-2130　FAX : 06-6305-2132
福岡　〒813-6591　福岡市東区多の津1-14-1 FRCビル6F　TEL : 092-626-7211　FAX : 092-626-7315

＜資料請求番号 S1-20＞

Ander's Supercharged iXon Ultra EMCCD

Accelerated!

iXon Ultra EMCCD and OptoMask

Achieve up to 595 fps from a 128 x 128 ROI

Bundle Offer

Limited time offer ...
Purchase:
- *iXon Ultra 512x512(56fps) back-illuminated EMCCD camera*
- *Receive a FREE OptoMask*

Andor's new 'supercharged' iXon Ultra 897 back-illuminated EMCCD is now overclocked to 17 MHz, performing more than 60% faster.

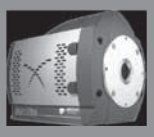

iXon Ultra

Combine with the OptoMask accessory to operate in Cropped Sensor Mode, boosting Region of Interest acquisition to unparalleled speeds, for example achieving up to 595 fps from a 128 x 128 ROI.

OptoMask

東京Office:〒101-0064 東京都千代田区猿楽町2-7-6
Tel:03-3518-6488　Fax:03-3518-6489
大阪Office:〒564-0051 大阪府吹田市豊津町1-34
Tel:06-6387-0900　Fax:06-6387-0955

ANDOR™ TECHNOLOGY

＜資料請求番号 S1-21＞

PHOTONIC
INSTRUMENTS

顕微鏡下で光刺激

MicroPoint/Mosaic

■既存の正立・倒立光学顕微鏡へ取り付けて、
光刺激とイメージングを同時に行うことが可能です。
■波長、照射エリアは自由に選択可能です。

●アプリケーション
- Uncaging
- Photoactivation
- Photobleaching
- Photoconversion
- ChR2、NpHR
- Ablation

●刺激光源
- 水銀、キセノン
- 405nmDiodeレーザ
- 488nmArgonレーザ
- その他光源対応可能

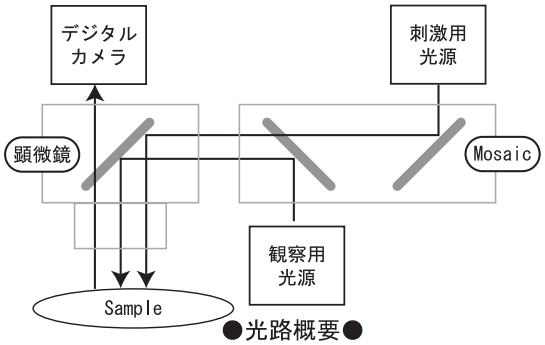

●光路概要●
光学顕微鏡の蛍光投光管に取り付けます。
共焦点システムとの組合せも可能です。

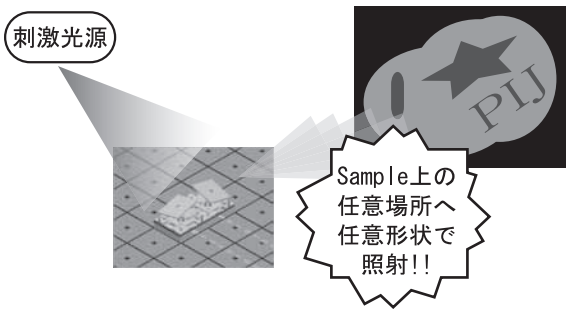

●デジタル・マイクロミラー・デバイス●
視野内に複数のマスクを指定し時差なしに
すべての箇所を光刺激することが可能です。

●光学顕微鏡周辺機器を取り扱っています。ご要望に沿ったシステムの構築をお手伝い致します。

MÄRZHÄUSER WETZLAR

自動ステージ

●独国メルツホイザー社●
◆電動スキャニングステージ
◆電動マイクロマニピュレータ
・抜群の操作性能。
・1台からカスタム対応。
・高精度Closed loop制御タイプも
ございます。

VISTEK INCORPORATED

除振台

●米国ビステック社●
◆卓上型除振プラットフォーム
机上に設置するだけで使用可能!!
・高い除振効果
・省スペース
・電気、エアの供給不要
・メンテナンスフリー

PHOTONIC INSTRUMENTS
フォトニックインストゥルメンツ株式会社

●お問い合わせください!!
〒215-0025　川崎市麻生区五力田2-2-1-102
電話　044-981-0025　　FAX　044-981-0026
E-mail info@pij.co.jp　http://pij.co.jp/

＜資料請求番号 S1-22＞

Wako

高性能300万画素CCDカメラ搭載イメージャー

OptimaShot OS-300 シリーズ

OptimaShotイメージャーはDNAアガロース電気泳動ゲルの撮影に最適なCCD蛍光イメージングシステムです。300万画素CCDカメラを搭載し、解像度の高い画像の取得を低価格で実現します。UVトランスイルミネーターと画像取得ソフトウェアは標準付属で、専用パソコン付属モデルとパソコンなしのモデルをご用意しています。

特　長

■低価格、省スペース
■高解像度300万画素CCDカメラ搭載
■20cm×20cmの広い画像取得エリア
■スライド式トレイにより、ゲルへのアクセスが容易
■UVトランスイルミネーター（標準付属）により、EtBr／SYBR染色DNAゲルに対応
■画像取得ソフトウェアを標準付属
■LED白色光源（標準搭載）により、CBB染色や銀染色ゲルなど様々なサンプルに対応
■LEDトランスイルミネーター「ゲルみえーる」（オプション）搭載可能

仕　様

モデル名	OS-300UVPC （専用パソコン付属モデル）	OS-300UV
コードNo	298-34671	295-34681
希望納入価格（円）	750,000	600,000
CCD カメラ	カメラ解像度　：300万画素 A/D 変換　：16ビット レンズ　：ズームレンズ（6.5-39mm, f=1.4）	
フィルター	EtBr／CBB兼用フィルター（標準付属）	
光源	白色LED光源（標準搭載） UVトランスイルミネーター（標準付属）	
画像エリア	最大20×20cm	
ソフトウェア	画像取り込み 加工ソフトウェア GeneSys Image Capture（標準付属）	
専用パソコン	付属	なし
サイズ	400W×375D×620H（mm）　※CCD部を含む。	
重量	15.6kg	

※専用パソコンを搭載したOS-300UVPCとパソコンが付属しないOS-300UVの2種類のモデルをラインナップしています。

和光純薬工業株式会社

本　　社　〒540-8605　大阪市中央区道修町三丁目1番2号　TEL: 06-6203-2759 （機器システム部）
東 京 支 店　〒103-0023　東京都中央区日本橋本町四丁目5番13号　TEL: 03-3270-8124 （機器システム部）
URL：www.wako-chem.co.jp　お問い合わせ：www.wako-chem.net/bms　機器お見積もり：www.wako-chem.net/estimate/index.php

＜資料請求番号 S1-23＞

リポソーム自動製造装置

多機能リポソーム自動製造装置

&プログラマブルバイオリアクター

―― 特長 ――

・７種類のリポソーム自動製造
MLV, SUV, LUV, GV,
物質封入リポソーム、
機能性リポソーム、
リポソームワクチン

・製法はオーソドックスな常法ベース
LUV, GVもボルテックス処理のみで作製可

・タッチパネルによるマニュアルレス操作

・全自動生産による良好な再現性と省力化

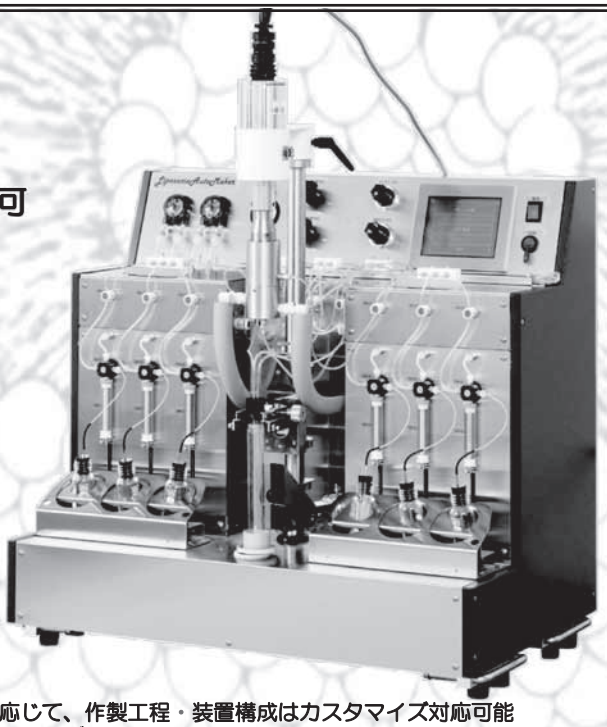

＜製作例＞

Giant Vesicle (GV)

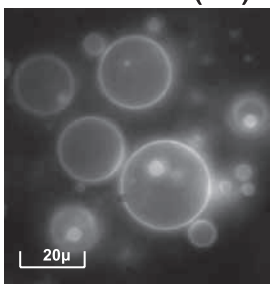

ご要望に応じて、作製工程・装置構成はカスタマイズ対応可能
装置詳細カタログ：http://www.hashimoto-inc.co.jp/product/pdf/lipo.pdf

Auto Extruder

―― 特長 ――

- 全自動で5段階（5種類）のフィルター処理を自動実行
- 多機能リポソーム自動製造装置と連動し、簡単操作で整粒化されたリポソームの作製可能

外形寸法：500mm(W)×362mm(D)×520mm(H)

脂質薄膜自動製造装置

―― 特長 ――

- 多機能リポソーム自動製造装置のエバポレータ機能付きボルテックスミキサー機構に特化し、サイズダウン
- 試料の自動注入が可能
（任意のタイミングでの、手動注入も可能）

補足：超音波破砕機はオプションになります。

外形寸法：500mm(W)×468mm(D)×520mm(H)
(超音波処理部含まず)

経済産業省　新連携認定事業　「研究開発向けリポソーム等多機能リポソーム自動製造装置の製造・販売事業」（平成21年6月26日認定）

コア企業

橋本電子工業株式会社

：装置の研究開発、製造、メンテナンス

〒515-0104 三重県松阪市高須町3866-12
Tel:0598-51-3111　Fax:0598-52-4300
E-mail: hdk@hashimoto-inc.co.jp
http://www.hashimoto-inc.co.jp

連携企業　**お問い合わせ先**

株式会社リポソーム工学研究所

：各種リポソームの作製及び応用技術開発
リポソーム受託開発作製・市場開拓・品質評価

〒514-8507 三重県津市栗真町屋町1577(三重大学内)
Tel:059-231-5326　Fax:059-231-5328
E-mail: info@lel.co.jp
http://www.lel.co.jp

三重大学：研究協力

CONFOCHECK タンパク質解析用 FT-IR

赤外分光法によるタンパク水溶液解析

- タンパクの定量（水溶液 0.03 ～ 100 mg/ml）
- タンパク二次構造の測定
- コンフォメーション変化の動的解析
- 熱変性、凝集、沈降、結晶化過程など

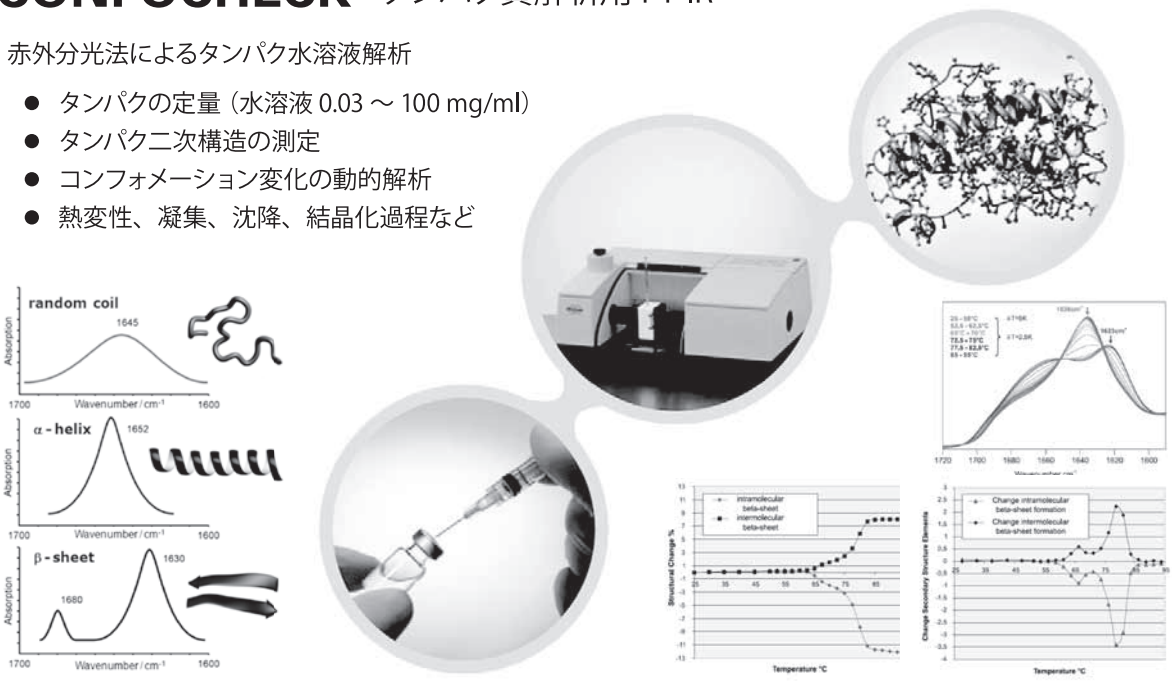

ブルカー・オプティクス株式会社　www.bruker.jp/optics

MultiMode 8 AFM (原子間力顕微鏡) による膜分子の機械特性測定

分子レベルの 3 次元形状と弾性率の同時測定

- バクテリアの細胞膜タンパク観察
- プロトンポンプの構造変化観察

  説明 : 弾性率の高い部分がαヘリックスで、低い部分がインターヘリカルループに相当

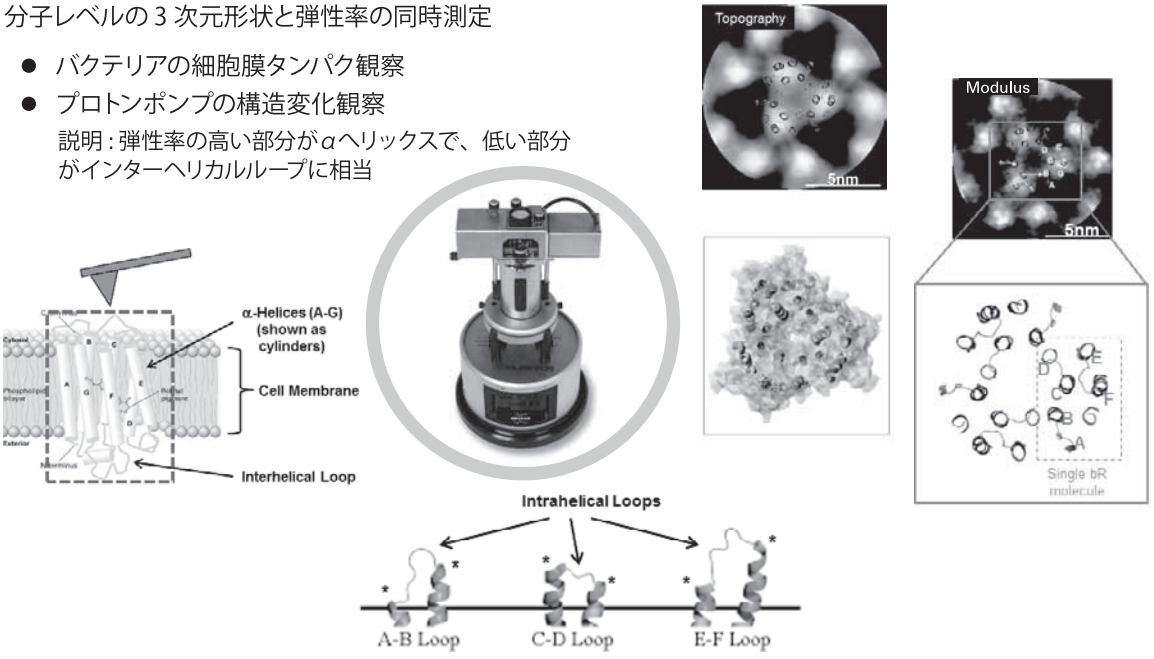

ブルカー・エイエックスエス株式会社　www.bruker.jp/axs/nano

＜資料請求番号 S1-25＞

NEW

BRUKER

Bruker NMR Thermometer

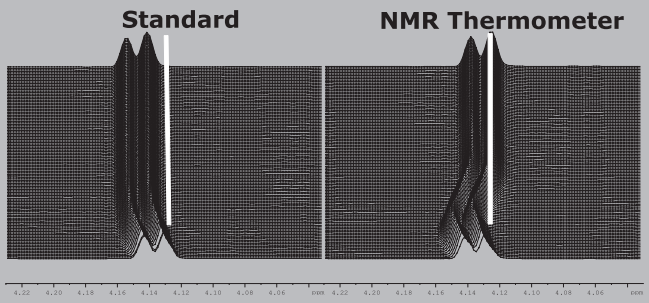

Mission:

サンプル温度をロックせよ！

実際の試料温度を如何に検知し、制御し、安定させるか。
種々の RF パルスにより、また MAS 試料回転の空気摩擦により、水溶液中の蛋白質や膜蛋白質などの試料の温度は上昇します。従来の NMR 装置では試料管外の外部センサーによって温度検知および温度制御をしており、検出された温度はサンプル自体の温度と誤差が生じていました。
この度、Bruker 社は、第 2 世代重水素デジタルロック “2G-Digilock™” *によって、正確かつ短時間に行える全く新しい温度可変システムを実現致しました。
このシステムでは、実際の試料内の温度を計測している為、測定装置、プローブ、またはパルスプログラムによる温度の違いを生じません。 実験ごとに得られるスペクトルにおいて、温度の差による化学シフトのずれがない為、スペクトルの解析を容易に行うことができます。

主な応用範囲 ： 蛋白質 NMR、BioSolids、メタボロミクス、IVD リサーチなど

＊2G-Digilock™ は新型 NMR 分光計 “AVANCEⅢ HD” に搭載されています。

測定試料 ：10 mM raffinose in D_2O with ～ 50 mM NaAc-d3

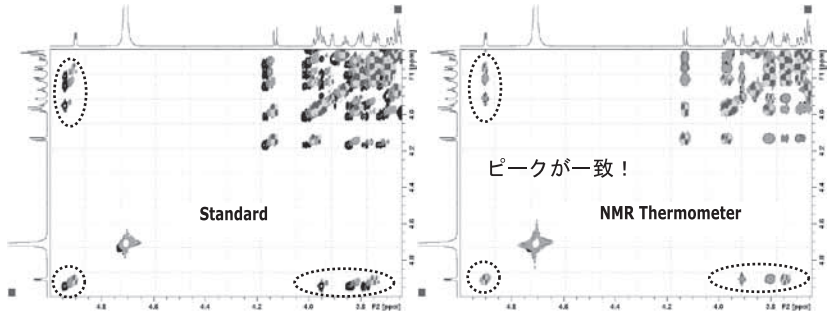

RF パルス励起効果による、温度上昇の影響

DQF COSY / TOCSY with MLEV mixing with 9.6 kHz rf field for 40 msec, 80 msec and 160 msec 4 種のスペクトル重ね合わせ（右が 2D－Digilock）

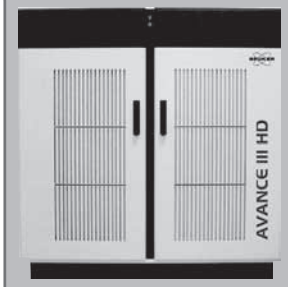

新型 NMR 分光計
AVANCE III HD

〒２２１－００２２
神奈川県横浜市神奈川区守屋町3-9
ブルカー・バイオスピン株式会社 本社
TEL: 045-444-1390 FAX: 045-453-2457
E-Mail : info@bruker-biospin.jp

〒５３２－０００４
大阪府大阪市淀川区西宮原1-8-29
ブルカー・バイオスピン株式会社 大阪営業所
TEL: 06-6394-8989 FAX: 06-6394-9559
HP : www.bruker-co.jp

Innovation with Integrity

NMR Solutions

＜資料請求番号 S1-26＞

Bridge the resolution gap between Light Microscope and Electron Microscope

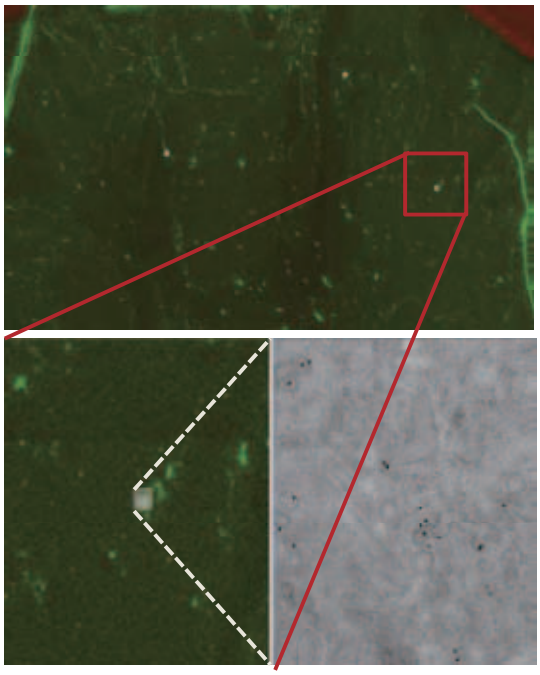

光学顕微鏡と電子顕微鏡をつなぐ Tecnai iLEM™

- 蛍光顕微鏡像と同一視野を電顕で拡大して観察
- 動的な生命現象をナノスケールで捉える
- 標識タンパク質の極在を高分解能で観察
- 蛍光モードと電顕モードを素早く切替え
- 蛍光退色による低レベルの蛍光シグナルも検出
- クライオ電子顕微鏡法の適用可能

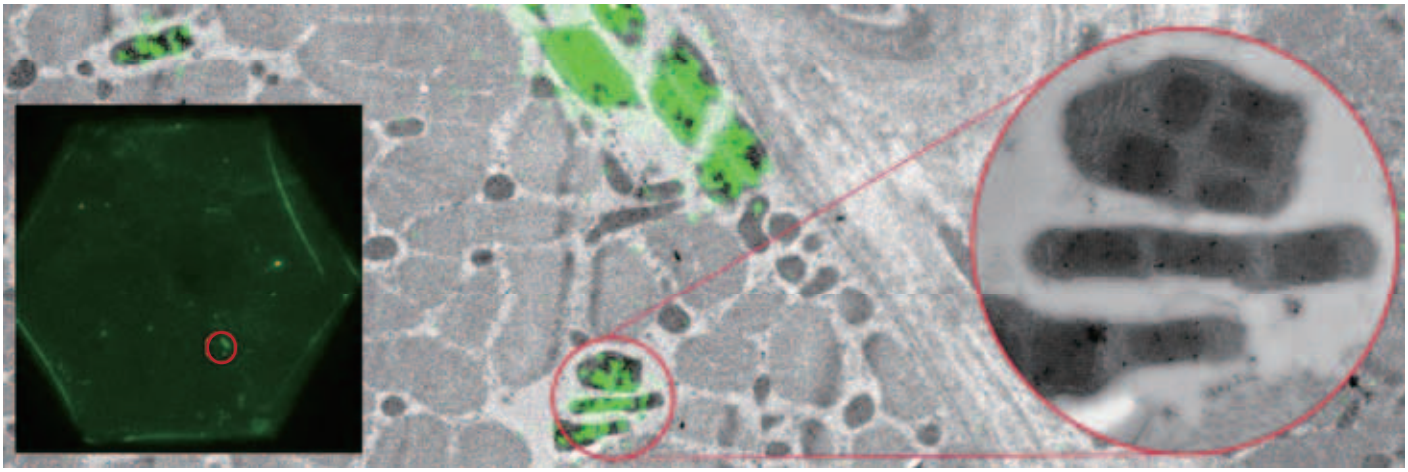

筋ジストロフィーの症状を示す筋細胞と蛍光標識をしたクレアチンキナーゼ
Samples provided by Matthia Karreman and Elly van Donselaar (Utrecht University)

See beyond at FEI.com/Life Sciences

日本エフイー・アイ株式会社
〒108-0075　東京都港区港南2-13-34　NSSIIビル4F
TEL: 03-3740-0970(代)
FAX: 03-3740-0975

FEI™ Explore. Discover. Resolve.

＜資料請求番号　S1-2＞

定価 3,500円

＜資料請求番号 S1-3＞

昭和42年8月1日 国鉄大局特別扱承認雑誌第216号
平成24年8月15日 増刊号